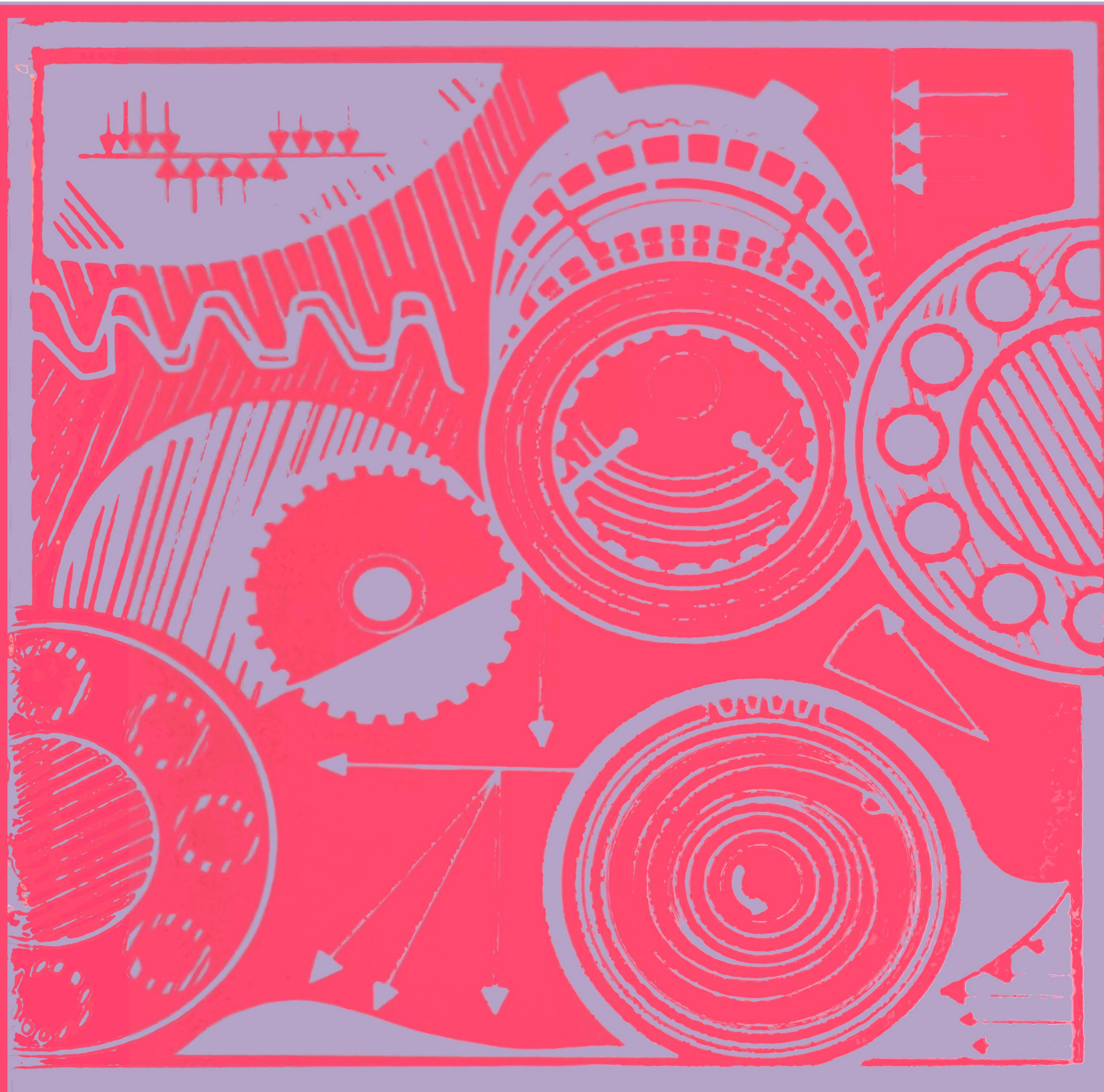


V. DOBROVOLSKY  
K. ZABLONSKY  
S. MAK  
A. RADCHIK  
L. ERLIKH

# MACHINE ELEMENTS











V. DOBROVOLSKY

K. ZABLONSKY

S. MAK

A. RADCHIK

L. ERЛИKH

# MACHINE ELEMENTS

**A TEXTBOOK**

---

---

FOREIGN LANGUAGES PUBLISHING HOUSE  
Moscow



**В. А. ДОБРОВОЛЬСКИЙ, К. И. ЗАБЛОНСКИЙ,  
С. Л. МАК, А. С. РАДЧИК, Л. Б. ЭРЛИХ**

**ДЕТАЛИ МАШИН**

**Translated from the Russian by  
А. ТРОИТСКИЙ**

# CONTENTS

Introduction . . . . .	9
------------------------	---

## PART ONE

### FUNDAMENTALS OF DESIGNING MACHINE ELEMENTS

<i>Chapter I.</i> Criteria of Operating Capacity and Calculation of Machine Elements . . . . .	15
Strength of Machine Elements . . . . .	17
Volume Strength . . . . .	18
Surface Strength . . . . .	46
Rigidity of Machine Elements . . . . .	56
Resistance to Vibration of Machine Elements . . . . .	58
Heating of Machine Elements . . . . .	59
<i>Chapter II.</i> Selection of Material . . . . .	60
Comparative Evaluation of Various Materials by Weight . . . . .	63
The Principle of "Local Quality" and Its Utilisation in the Selection of Materials . . . . .	64
Reduction in the Range of the Materials Employed . . . . .	69
<i>Chapter III.</i> Standardisation of Machine Elements . . . . .	69
<i>Chapter IV.</i> Production Soundness of Machine Elements . . . . .	74

## PART TWO

### JOINTS OF MACHINE ELEMENTS

<i>Chapter V.</i> Types of Joints and Their Principal Features . . . . .	79
Types of Joints . . . . .	79
Strength of Joints . . . . .	81
Tightness of Joints . . . . .	84
Stiffness of Joints . . . . .	85
<i>Chapter VI.</i> Riveted Joints . . . . .	86
The Functioning of Rivets in a Seam . . . . .	89
Strength of Riveted Joint Elements . . . . .	94
Calculation of Riveted Seams . . . . .	97
Strong Seams . . . . .	97
Tight-Strong Seams . . . . .	99

<i>Chapter VII. Welded Joints</i> . . . . .	101
Calculation of Welds . . . . .	107
Welded Joints Designed for Static Load . . . . .	107
Strength of Welds at Varying Load . . . . .	111
<i>Chapter VIII. Joints Formed by Interference Fits</i> . . . . .	115
<i>Chapter IX. Threaded Joints</i> . . . . .	120
Types and Causes of Thread Failure . . . . .	127
Strength under Static Load . . . . .	128
Joints Designed without Initial Stress . . . . .	128
Joints Designed with Initial Stress . . . . .	133
Strength at Varying Loads (Endurance of Bolted Joints) . . . . .	141
Calculation of Strength . . . . .	141
Temperature Stresses in Threaded Joints . . . . .	147
Load Distribution Between Threaded Parts in a Group Joint (Determination of Design Load in a Group Joint) . . . . .	149
<i>Chapter X. Cottered Fastenings</i> . . . . .	153
Cottered Joints . . . . .	153
Pin Joints . . . . .	158
<i>Chapter XI. Key, Splined and Serrated, and Keyless (Shaped and Other) Joints</i> . . . . .	160
Keys . . . . .	161
Calculation of Unstrained Joints . . . . .	163
Calculation of Strained Joints . . . . .	164
Multiple Splines . . . . .	169
Keyless Joints . . . . .	172

### PART THREE

### POWER TRANSMISSION

<i>Chapter XII. Power Transmission Systems and Their Principal Features</i> . . . . .	174
Types of Drives . . . . .	175
Drives with a Constant Velocity Ratio . . . . .	177
Velocity Ratio . . . . .	178
Peripheral Velocity . . . . .	178
Transmitted Horse Power . . . . .	179
Loss of Horse Power and Efficiency . . . . .	180
Weight, Size and Cost of Drives . . . . .	181
Drives with a Variable Velocity Ratio . . . . .	183
<i>Chapter XIII. Friction Drives</i> . . . . .	185
Fundamentals of the Theory and Operation of Friction Drives . . . . .	189
Slip and Creep in Friction Drives . . . . .	189
Pressure . . . . .	190



Parts of Friction Drives . . . . .	194
Calculation of Friction Drives . . . . .	196
Design for Strength . . . . .	196
Shaft Loads . . . . .	199
Losses and Efficiency of Drives . . . . .	199
Design for Heating . . . . .	200
<i>Chapter XIV. Belting</i> . . . . .	202
Fundamentals of the Theory and Operation of Belt Drives . . . . .	204
Tension in a Flexible Cord Embracing a Cylinder . . . . .	204
Elastic Creep . . . . .	204
Velocity Ratio . . . . .	206
Pull Factor . . . . .	207
Tension Due to Centrifugal Forces . . . . .	208
Stresses in Belts . . . . .	209
Losses in Transmission . . . . .	210
Components of Belt Drives . . . . .	211
Belts . . . . .	211
Pulleys . . . . .	217
Belt Tension Adjusters . . . . .	225
V-Belt Variable-Speed Drives . . . . .	229
Calculation of Belt Drives . . . . .	234
Geometry of Belt Drives . . . . .	234
Calculating Belt Pull . . . . .	235
Calculating Belt Service Life . . . . .	238
Loads Carried by Shafts . . . . .	240
Transmitted Horse Power and Efficiency of Belt Drives . . . . .	241
<i>Chapter XV. Gearing</i> . . . . .	244
Basic Rack . . . . .	245
Accuracy of Gears . . . . .	248
Components of Toothed Gears . . . . .	249
Materials . . . . .	249
Design of Pinions and Wheels . . . . .	252
Types of Failure in Gear Teeth . . . . .	256
Design of Straight-Tooth Spur Gears . . . . .	262
Main Geometrical Proportions . . . . .	263
Forces Acting in a Gear . . . . .	264
Design Load . . . . .	265
Calculation of Teeth for Surface Strength . . . . .	274
Calculation of Teeth for Beam Strength . . . . .	279
Lubrication and Efficiency . . . . .	289
Design of Helical and Herringbone Spur Gears . . . . .	290
Main Geometrical Proportions . . . . .	290
Forces Acting in a Gear . . . . .	291
Design Load . . . . .	293

Calculation of Teeth for Surface Strength . . . . .	296
Calculation of Teeth for Beam Strength . . . . .	297
Design of Bevel Gears . . . . .	299
Main Geometrical Proportions . . . . .	299
Forces Acting in a Gear . . . . .	301
Calculation of Teeth for Surface Strength . . . . .	304
Calculation of Teeth for Beam Strength . . . . .	305
<i>Chapter XVI. Screw, Hypoid, Worm and Globoidal Gears</i> . . . . .	307
Screw Gears . . . . .	310
Hypoid Gears . . . . .	311
Worm Gears . . . . .	312
Materials . . . . .	312
Design of Worms and Wheels . . . . .	313
Accuracy of Gears . . . . .	314
Failures of Worm Wheel Teeth . . . . .	316
Main Geometrical Proportions . . . . .	317
Forces Acting in a Gear . . . . .	321
Design Load . . . . .	323
Design for Surface Strength . . . . .	326
Design of Teeth for Bending . . . . .	329
Lubrication and Efficiency . . . . .	331
Globoidal Gears . . . . .	334
Materials . . . . .	334
Design of Worms and Wheels . . . . .	336
Main Geometrical Proportions . . . . .	337
Calculation of the Gear for Wear . . . . .	339
Lubrication and Efficiency . . . . .	342
<i>Chapter XVII. Toothed and Worm Reduction Gears</i> . . . . .	343
Main Types of Reduction Gears . . . . .	343
Designs of Reduction Gears . . . . .	349
Lubrication and Calculation for Heating . . . . .	354
<i>Chapter XVIII. Chain Drives</i> . . . . .	364
Velocity Ratio . . . . .	367
Chain Tension . . . . .	368
Components of Chain Drives . . . . .	370
Chains . . . . .	370
Sprockets . . . . .	372
Chain Housings and Slack Adjusters . . . . .	373
Design of Drives . . . . .	374
Kinds of Failure in Chain Drives . . . . .	374
Determining Chain and Sprocket Proportions . . . . .	375
Lubrication and Efficiency . . . . .	379

<i>Chapter XIX. Power Screws</i> . . . . .	382
Materials and Design of Screws and Nuts . . . . .	383
Calculation of Power Screws . . . . .	385

## PART FOUR

## SHAFTS AND AXLES, BEARINGS AND COUPLINGS AND CLUTCHES

<i>Chapter XX. Shafts and Axles</i> . . . . .	391
Straight Shafts and Axles . . . . .	392
Design . . . . .	392
Kinds and Causes of Failure in Shafts and Axles and Defects in Operation . . . . .	397
Materials for Shafts and Axles . . . . .	398
Calculation for Strength . . . . .	399
Calculation for Stiffness . . . . .	406
Methods of Increasing the Endurance of Shafts and Axles . . . . .	408
Transverse Vibrations of Shafts. Critical Shaft Velocity . . . . .	410
Flexible Wire Shafts . . . . .	412
<i>Chapter XXI. Sliding Contact Bearings</i> . . . . .	419
Materials for Sliding Radial and Thrust Bearings . . . . .	423
Metals . . . . .	423
Nonmetallic Materials . . . . .	425
Lubricants . . . . .	425
Radial Bearings . . . . .	428
Design . . . . .	428
Calculation of Sliding Bearings . . . . .	432
Thrust Bearings . . . . .	442
Design . . . . .	442
Calculation of Thrust Bearings . . . . .	444
Lubricating Devices for Bearings . . . . .	447
Methods of Increasing the Operating Capacity of Sliding Bearings . . . . .	448
<i>Chapter XXII. Rolling Contact Bearings</i> . . . . .	451
Fundamentals of the Theory of Antifriction Bearings . . . . .	459
Load Distribution between Balls or Rollers . . . . .	459
Stresses at Points of Contact of Bearing Components . . . . .	461
Operating Capacity of Antifriction Bearings . . . . .	465
Calculation of Antifriction Bearings . . . . .	467
Calculation of Statically Loaded Bearings . . . . .	467
Calculation of Dynamically Loaded Bearings . . . . .	468
Mounting, Lubrication and Sealing of Antifriction Bearings . . . . .	471
Methods of Increasing the Operating Capacity of Antifriction Bearings . . . . .	475
<i>Chapter XXIII. Couplings and Clutches</i> . . . . .	477
Couplings . . . . .	479



c) the course of metallography, which provides necessary information on the rational choice of materials;

d) methods of casting, forging and welding, heat treatment, machining and assembly, which make their own—production—demands on the design of machine elements;

e) technical drawing.

In the curricula of Soviet higher engineering schools the course "Machine Elements" completes a series of general engineering subjects and links these with a series of special subjects which outline the fundamentals of the theory, design and operation of machines used in practice.

The development of the design of machine elements is closely bound up with the development of machines.

**Main Trends in the Development of Machine Design.** Machines are means of production which utilise the forces of nature for the benefit of society, facilitate the labour of the workers and increase its productivity. The level of machine production and its technical standards clearly illustrate the industrial development of a country.

Machine designs are being continuously improved as new demands are made on them by the conditions of operation and production, and new potentialities are opened up by the development of science, the appearance of new materials and new methods for giving these materials the required forms and properties.

The following are the main requirements of operation and production which determine the design of modern machines: higher productivity of the machine and greater power and efficiency; simple servicing requiring no concentrated attention or considerable muscular effort on the part of the worker; high reliability—the continuous functioning of the machine without failure; the possibility of producing the designed machine in the quantities required by the national economy with a minimum expenditure of labour, materials and other resources.

The higher productivity of machines and greater engine power are most effectively attained by increasing their velocity and automatising labour processes. Comprehensive automatisisation freeing the operator from arduous work involved in auxiliary operations (switching over, erecting and removing parts, handling the operating tools, etc.), higher rates of production processes and increased pressures (of steam, gas and liquid) and temperatures are the most characteristic tendencies in the development of present-day mechanical engineering. The achievements in this sphere can be evaluated from the following data borrowed from various branches of mechanical engineering.

During the last seventy years the speed of automobiles has changed as follows:

	1895- 1900	1900- 1915	1915- 1930	1930- 1945	1945- 1955
Maximum attained speed in km/hr . . . . .	105.9	210.9	372.4	594.8	634.5
Maximum cruising speed in km/hr . . . . .	15-20	30-40	55-75	90-110	130—150

The speed of cutting steel during the last 100 years has changed as follows:

	Before 1850	1864	Early 20th century	1927	1950
Material of cutting tools	Carbon steel	Chrome- tungsten steel	High- speed steel	Hard alloys	
Cutting speed in m/min	5	7-8	30	70-80	400 and more

The speeds of cold rolling of strip steel have increased in the last twenty-five years as follows:

	1925-1930	1940	1945	1950
Rolling speed in m/sec	0.3-0.5	5	20	30

A similar increase in speed can be observed in machines employed for other processes. For example, the average speed of machines producing corrugated cardboard has risen from 3 m/min in 1895 to 165 m/min today; the speeds of sewing machines have increased from 600-800 rpm in 1915 to 3,500 rpm in 1947, etc.

These figures give an idea of the rates of growth in the speeds of various machines and of the future prospects.

These general tendencies have predetermined the following important features in the development of the design of various machines:

1. *The use of mechanisms with uniform rotary motion instead of those with reciprocating motion.* At the beginning of machine-building the extensive employment of mechanisms with reciprocating motion was quite natural; it could be accounted for by the fact that man strove to imitate by means of a mechanism the movements of arms used for identical processes. At the same time reciprocating motion inevitably involves the loss of time on idle strokes and overruns and also dynamic loads which restrict the speed of manufacturing processes. It is quite natural therefore that all modern machines should preferably employ continuous rotary motion instead of periodic reciprocating motion. Illustrations of this tendency are: steam and gas turbines which are used for higher speeds and powers than piston engines; centrifugal, gear and wing pumps as well as turbo-

compressors which have ousted piston reciprocating pumps and compressors; rotary boring drills which have replaced percussion drills; rotary printing machines instead of flat types, etc. The development of design in this direction is far from completed. For example, in earth-moving works a power shovel with one bucket is as yet the main machine employed and in the weaving industry it is a loom with a reciprocating shuttle. There are many such machines. However, specialists in all branches of mechanical engineering are keenly aware of the necessity of replacing machines with periodic operation by continuously operating machines with the result that an experimental earth-digging machine and a circular weaving loom have been recently developed.

2. *The application of block designs.* Machines have long been made in separate parts for convenient servicing, or even manufacture, assembly and conveyance. However, during the last twenty-five years the division of machines into parts, which earlier was dictated exclusively by the above motives, has become an independent and important way of improving the economical indices of production and operation. Designs of machines split into rational units from the considerations outlined below are called *aggregate designs* (machine-tool building, aircraft industry) or *block designs* (crane building). They offer the following advantages.

a) When setting up a machine from independent units, the elaboration of various versions or modifications, their testing and putting into serial production can be limited only to one unit at a time. This greatly simplifies the process of carrying out improvements.

b) Unit design allows the design of machines for various purposes, using only a small number of units (blocks).

c) Splitting into units shortens the time of assembly operations, because all units can be assembled and tested simultaneously and brought together for erection ready-made.

d) Unit design facilitates the maintenance of machines, since this can be reduced to the replacement of one unit by another—either reconditioned or new.

Examples of splitting machines into assemblies are shown in Fig. 25.

3) *The employment of various drives.* Until recently power was transmitted from the prime mover to the driving mechanisms almost exclusively by shafts, toothed wheels, belts, pushers, levers and other similar devices. Modern machines are characterised by the wide use also of electric, hydraulic and pneumatic drives. The wide use of these drives considerably facilitates the control of mechanisms, which can even be made completely automatic, mechanisms being remotely controlled to carry out a programme of any complexity (see also p. 174).



4. *The reduction of the weight of machines* together with the improvement of their quality is an important trend in the development of designs of modern machines. A reduction in weight is important in several respects.

a) The weight of a machine  $G$  together with the factor accounting for the consumption of metal  $\eta_{con}$  determine the weight of metal needed to manufacture the machine. Economy of metal is of prime national importance. With the same amount of metal produced in the country, after curtailing unproductive expenditure, the quantity of machines and other items produced can be materially increased. Besides, expenditure on metal comprises a considerable part of the cost price of machines. For example, in machine-tool building it amounts to 30-40% of the total production expenditure; on an average it is 3.5 times larger than the labour costs.

b) The weight of transport machines, besides its importance in the sense of the amount of metal required, is important in other respects too. For example, the cost per ton of transit of passenger waggons amounts to 5-6 thousand rubles annually.

An index of a rational design from the point of view of metal consumption is its specific weight—the ratio between the weight of the machine and the useful load which it is intended to carry.

Thus, for engines this index equals the weight in kg per 1 h. p. (or 1 kw). The specific weight of gasoline engines is:

aircraft engines . . . . .	0.6-1.1 kg/h.p.
car engines . . . . .	2.5 kg/h.p.
lorry engines . . . . .	6-15 kg/h.p.
tractor engines . . . . .	10-40 kg/h.p.

For railway passenger cars this index is the factor accounting for the ratio between the weight of the car in tons and the number of passengers. The average values of this factor are:

for suburban two-axle cars . . . . .	0.30-0.40
for four-axle cars . . . . .	0.45-0.5
for sleeping cars . . . . .	3-3.4

An index analogous in structure may serve for estimating the rationality of the use of metal in individual units. For example, for gearboxes and reduction gears it equals the ratio between the weight of the gearbox (reduction gear) and the maximum transmitted torque. For the gearboxes of some lorries the values of this index are given in Table 1.

As the speeds increase and the machine designs are improved the specific weight is reduced. For example, the following figures are characteristic for the development of screw-cutting lathes with a centre height of 225 mm and centre distance of 1,000 mm (Table 2).

Table 1

Ratio between the Weight of Gearboxes and the Maximum Transmitted Torque for Some Lorries

Model	Maximum load-carrying capacity in tons	Maximum torque on the gearbox in kgm	Weight of the gearbox in kg	Specific weight in kg/kgm
ГАЗ-51 . . . . .	2.5	134.5	59	0.4
ЗИЛ-150 . . . . .	4.0	190.9	110	0.6
МАЗ-200 . . . . .	7.0	296.0	224	0.8

Table 2

Change in the Specific Weight of Screw-Cutting Lathes

Parameters of the lathe	Year of manufacture		
	1875	1934	1949
Power in kw . . . . .	1.1	7.4	14.5
Weight in kg . . . . .	750	2,350	3,500
Specific weight in ton/kw . .	0.68	0.32	0.24

PART ONE

# FUNDAMENTALS OF DESIGNING MACHINE ELEMENTS

---

CHAPTER I

## CRITERIA OF OPERATING CAPACITY AND CALCULATION OF MACHINE ELEMENTS

A machine under design should satisfy various requirements outlined in specifications. These are, first of all, its output capacity and operating velocity, its cost—initial and operational, its weight and expected (guaranteed) life. In certain cases additional requirements are made concerning overall dimensions and transportability (in transit by rail, the machine, loaded onto a freight flat-car, should have proportions in conformity with the loading gauge), uniformity of rotation, noiseless operation, simple and easy control, styling, etc.

For these reasons individual components should have adequate strength and rigidity and effectively resist vibration (oscillations of high intensity); they should also allow the use of common cheap materials for their manufacture.

Some of these requirements are so essential that the normal operation of a machine becomes impossible if they are not satisfied; these requirements are regarded therefore as the *main criteria of operating capacity*. They are first and foremost the necessary and sufficient strength (volume and surface) and rigidity; for many components vibration and thermal resistance are also important.

To ensure these main criteria of operating capacity appropriate calculations (for strength, rigidity, elastic oscillations, etc.) are required and this is an integral part of the process of designing machine elements.

This process is usually carried out in the sequence outlined below.

1. A design scheme is worked out in which the design of the component and its conjunction with other components are greatly simplified and the forces applied to it are assumed to be either concentrated or distributed in conformity with the given or arbitrary regularities.

2. The magnitudes of loads acting upon the component are determined.

During operation machine elements are subjected primarily to the action of varying loads. The nature of variation of these loads may depend on a number of systematic or occasional factors. Thus, for machines which perform definite technological functions in the production process the nature of load variation for one production cycle remains nearly constant. In other cases, for example for automotive vehicles, the nature of force variation depends on a number of fortuitous factors (resistance arising in motion due to the terrain and the roadbed, the effects of inertia and the wind, etc.). It is, therefore, an extremely complex and important task to determine and assign the loads which will act on the machine components.

In calculations use is made of *rated* and *design* loads.

A *rated* load is an arbitrary constant load chosen from among the operating loads; usually it is the maximum or the most continuously operating load; sometimes it is the mean load.

A *design* load is a load constant in time, which can be used instead of the actual operating varying load, on the assumption that by their effect with respect to the corresponding criteria of operating capacity the design and actual loads are equivalent.

3. Material is selected on the basis of its physico-mechanical properties, including machinability, taking into account the economical factors—cost, accessibility, etc.

4. Some of the most characteristic dimensions of the component are determined by calculation according to those criteria of operating capacity which are most important in the given case and these dimensions are coordinated with the standards in force. As a rule, these calculations are *preliminary*, since they are based on the simplified schemes mentioned above, which do not allow the precise evaluation of the actual operating capacity of the component. Besides, with the loads usually met with in mechanical engineering practice, which cause alternating stresses to develop in cross-sections of machine elements, the mechanical characteristics of strength (for example, limit of endurance) are not constant for a given material for they depend on the absolute dimensions and on the form of the component together with some other factors.

Therefore, a reliable calculation is possible only when the forms and absolute dimensions of the component and some other factors are already known. For this reason these calculations are used to find only the initial dimensions for designing a unit; it is only in the simplest cases that they are also final, in which case they are called *design* calculations.

5. A general sketch of the assembly is drawn followed by a detailed elaboration and indication on the working drawing of all the

dimensions, tolerances, classes of surface finish, special production requirements, kinds of service, etc.

6. Calculations are then done using the main criteria of operating capacity, i. e., margins of safety in dangerous cross-sections, deformations (deflections, angles of twist), critical velocities (rpm), etc., are determined, and compared with the allowable values. When the required conformity between these values cannot be ensured, the design should be altered and revised calculations carried out again. This method of consecutive approximation helps to arrive at the required conformity between the design and allowable values of margins of safety, deflections, etc.

Since in the process of designing optimal solutions are to be found, which must meet the various, sometimes contradictory, requirements to the best advantage, such solutions can be arrived at usually only after the elaboration of several versions, properly compared and evaluated.

### STRENGTH OF MACHINE ELEMENTS

During operation, loads applied to elements of inadequate strength may cause impermissibly high remanent deformations in them and their failure.

The development of remanent deformations should be in many instances avoided since the change in the form and size of the component can violate the normal interaction of machine parts and alter their required conjunction.

In engineering practice most failures are due to breakage and the disintegration of the working surfaces of parts of machines: pitting, wear (abrasion), etc.

Breakage, occurring before the specified life has expired, and failure of the working surfaces of machines are impermissible if they develop progressively.

Therefore, the problem of the strength of machine elements should be considered in connection with the time factor—the service life of these elements. The proper consideration of this circumstance is primarily dictated by the fact that the task of a continuous improvement of production processes, mechanisation and automation requires periodic replacement of obsolete designs by improved up-to-date machines.

It is clear that for machines of different design the expected service life will be different. For example, the life of an aircraft engine amounts to only several hundred flying hours, for mine winders it is 10,000 hours and for metal-cutting machine tools—50,000 hours.

On the other hand, since the components of any one machine are stressed differently, it is important to know how to control the processes of wear and other kinds of surface failure to prevent the parts

from being put out of commission prematurely and to ensure definite intervals between repairs. For some components therefore the expected service life should be specified in advance. Thus, for anti-friction bearings employed in metal-cutting machine tools it amounts to 5,000 hours.

Hence, in order to ensure the required and adequate strength, such forms and proportions of the machine elements must be found which will prevent very high remanent deformations, premature failure and surface defects.

The most widespread method of evaluating the strength of machine elements in use today is the comparison of the stresses ( $\sigma$ ,  $\tau$ ) developing under load with the safe *allowable stresses* ( $[\sigma]$ ,  $[\tau]$ ). The strength condition is written thus

$$\sigma \leq [\sigma] \text{ or } \tau \leq [\tau] \quad (1)$$

where

$$[\sigma] = \frac{\sigma_{lim}}{n} \text{ or } [\tau] = \frac{\tau_{lim}}{n} .$$

In these formulae  $\sigma_{lim}$  and  $\tau_{lim}$  are the limit normal and, correspondingly, limit tangential stresses on attaining which the component is put out of commission either due to an impermissibly high remanent deformation or due to failure;  $n$  is the margin of safety.

The strength condition (1) of the elements of a designed machine depends on the accurate determination of the *acting* stresses and the correct assignment of *allowable* stresses.

During recent years a tendency has arisen to reject the method of evaluating strength by stresses and to calculate it by the *limit states* of components, by which are meant those states when further normal operation becomes impossible. According to this method, characteristic limit states can be established for various elements and the condition found for each limit state which will preclude its development. Thus, for example, the condition of integrity of a component in a limit state as regards carrying capacity can be formulated thus: *possible maximum loads acting on the component during operation should be below the minimum load at which the carrying capacity of this component is impaired.*

The method of calculation by limit states has been successfully used in civil engineering. It also possesses considerable interest for mechanical engineering but is inadequately elaborated for the calculation of machine elements.

In certain cases this method gives the same results as stress calculations.

**Volume Strength.** The calculation by rated stresses found from the formulae of the theory of the strength of materials, which do not take into detailed account the component form, does not allow the

determination of the actually existing stressed state in the dangerous zones of the designed component.

As a rule, the forms of machine elements are very complex. The presence of abrupt changes of cross-section, grooves, holes (boreholes), force-fitted parts and other *stress concentration points* develops *stress concentration*, a phenomenon involving a local increase in stress and variation in the stressed state in the area where the component abruptly changes in form. In this case: a) the maximum local stress may materially exceed the rated stress; b) local stresses quickly decrease as they are removed from the stress concentration point which caused them; in other words these stresses are characterised by a high gradient.

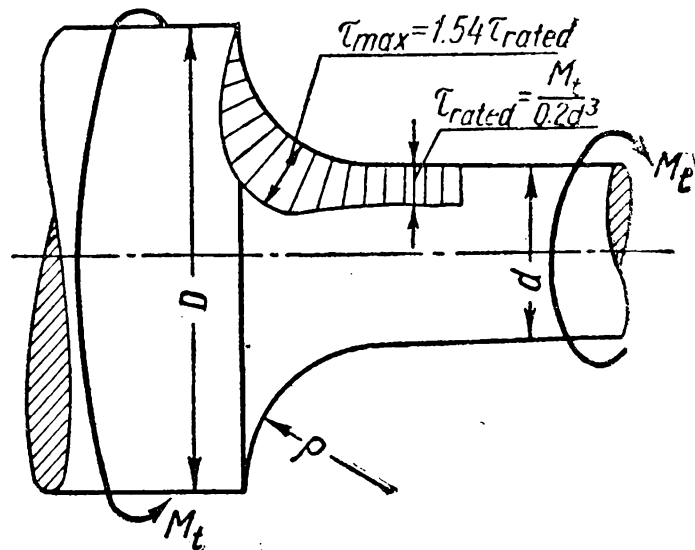


Fig. 1

By way of example, Fig. 1 shows how tangential stress is distributed over the length of the fillet of a stepped shaft subject to the torque  $M_t$ .

The relation of the maximum local stress to the rated stress is called the *stress concentration factor* found in the elastic zone:

$$\alpha_\sigma = \frac{\sigma_{\max}}{\sigma_{\text{rated}}}; \quad \alpha_\tau = \frac{\tau_{\max}}{\tau_{\text{rated}}}. \quad (2)$$

The magnitude of the factor  $\alpha$ , which characterises the effect of the component form on stress distribution in the zone of operation of the stress concentration point, can by no means be regarded as a criterion of the decrease in strength due to local stresses. The actual decrease in strength depends in these cases not only on the form of the concentration point but also on the properties of the material of the component, which manifest themselves differently depending on the load conditions, and is evaluated by the *effective stress concentration factor* ( $k$ ), which is understood to mean the limit stresses ratio, at the same nature of loading, in a smooth sample and in a sample with a stress concentration point having the same absolute dimensions as the smooth sample.

Thus, at static load

$$(k_\sigma)_{st} = \frac{\sigma_{ul}}{\sigma'_{ul}} \quad \text{and} \quad (k_\tau)_{st} = \frac{\tau_{ul}}{\tau'_{ul}} \quad (3,a)$$

where  $\sigma_{ul}$ ,  $\tau_{ul}$ ,  $\sigma'_{ul}$ ,  $\tau'_{ul}$  are the magnitudes of the ultimate strength for smooth samples ( $\sigma_{ul}$ ,  $\tau_{ul}$ ) and for samples with concentration points ( $\sigma'_{ul}$ ,  $\tau'_{ul}$ ).

At loads causing stresses varying in time

$$k_{\sigma} = \frac{\sigma_r}{\sigma_r'} \quad \text{and} \quad k_{\tau} = \frac{\tau_r}{\tau_r'} \quad (3,b)$$

where  $\sigma_r$ ,  $\tau_r$ ,  $\sigma_r'$ ,  $\tau_r'$  are the limits of endurance for a smooth sample and for a sample of the same size but with a stress concentration point.

The effective stress concentration factor found in this manner takes account of the effect of smoothing out local stresses (equalising of stresses) which depends on the plastic properties of the materials. The more plastic is the material, the greater is the reduction in stress concentration and the more pronounced is the difference between the actual maximum local stresses and their values calculated by theoretical methods and, consequently, the greater is the difference between  $\alpha$  and  $k$ .

The ability of various materials to manifest this effect is evaluated by a factor accounting for the *sensitivity of the material* to stress concentration ( $q$ ), which is understood to mean the relation between the actual magnitude of the maximum increment in stress in the concentration zone and the theoretically calculated value:

$$q_{\sigma} = \frac{k_{\sigma}\sigma_{rated} - \sigma_{rated}}{\alpha_{\sigma}\sigma_{rated} - \sigma_{rated}} = \frac{k_{\sigma} - 1}{\alpha_{\sigma} - 1} \quad \text{for normal stresses;}$$

$$q_{\tau} = \frac{k_{\tau} - 1}{\alpha_{\tau} - 1} \quad \text{for tangential stresses.}$$

When  $\alpha$  and  $q$  are known we can determine the values of the effective stress concentration factors:

$$k_{\sigma} = 1 + q_{\sigma}(\alpha_{\sigma} - 1); \quad k_{\tau} = 1 + q_{\tau}(\alpha_{\tau} - 1). \quad (4)$$

If the material is not sensitive to stress concentration ( $q_{\sigma}=0$  and  $q_{\tau}=0$ ) then  $k_{\sigma}=1$  and  $k_{\tau}=1$ . For materials exhibiting complete sensitivity to stress concentration ( $q_{\sigma}=1$  and  $q_{\tau}=1$ ),  $k_{\sigma}=\alpha_{\sigma}$  and  $k_{\tau}=\alpha_{\tau}$ .

*Strength at static stress.* When the loads cause static stresses to arise in the component cross-sections the strength condition (1) changes depending on the state of the material (plastic or brittle).

For plastic materials the limit stress is understood to mean the corresponding yield points. Establishment of the values of allowable stress, as part of the yield point, limits the remanent deformations to allowable, and usually very low, values and ensures integrity of the component.



For brittle materials of heterogeneous structure, such as cast iron, the ultimate strength should be taken as the limit stress.

Under static load stress concentration does not decrease the carrying capacity of components made from plastic materials; this is explained by the fact that the local plastic deformations help redistribute and equalise the stresses in the component cross-sections. In this case the concentration zone is strengthened and the effective stress concentration factor proves to be below unity.

In this connection the strength calculations at static loads for parts made from plastic materials are carried out according to the rated stresses, which increases the margin of safety.

For materials of low plasticity with a homogeneous structure (alloy steels, steels operating at low temperatures, etc.) the calculation should be according to the maximum local stresses, since stress concentration accounted for by the factor  $k$  [formula (3, a)] decreases the component strength.

For brittle materials with a heterogeneous structure (cast iron) the calculations are done according to the rated stresses because of their low sensitivity to stress concentration.

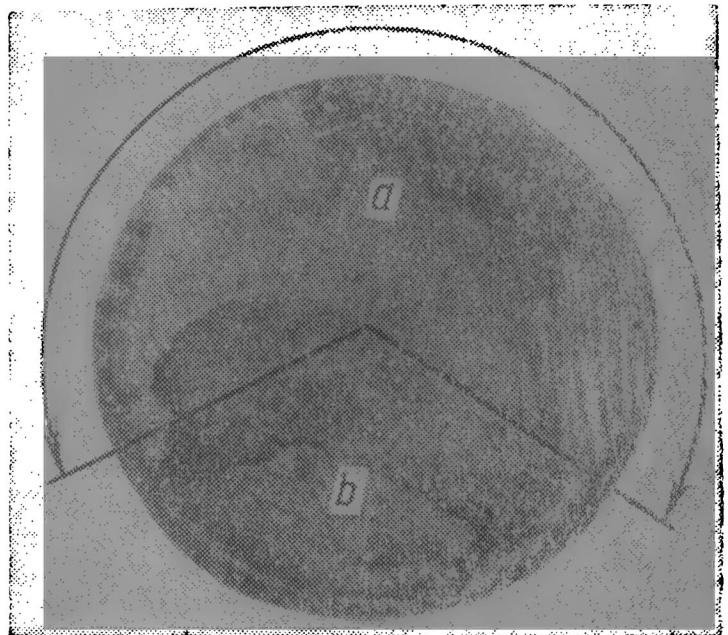


Fig. 2

*Strength at alternating stresses.* Loads which cause stresses varying in time to arise in the cross-sections are most typical for machine elements. Failure of machine elements at such loads occurs at stresses below the ultimate strength and even below the yield point if these variations of stress are repeated sufficiently frequently. For this reason, failure due to fatigue of parts made even from plastic materials does not usually involve any external manifestation of plastic deformation and is therefore in the nature of sudden breakage.

A typical fracture due to fatigue (Fig. 2) has two zones: the zone of fatigue failure (*a*)—a fine-granular almost smooth surface where the fatigue crack has gradually penetrated into the cross-section and the zone of static failure (*b*)—a large-crystal structure along which the final (brittle) failure occurred.

A fatigue failure may begin at several points simultaneously.

A broken axle with three foci of failure is shown in Fig. 3; two foci had merged together before the zone of static failure developed.

The shape of zones of fatigue failure depends on the number of load cycles during which the crack developed since in the process of cyclic loading there occurs a mutual compression and abrasion of the broken surfaces accompanied by cold hardening.

At an *insignificant cyclic overload* the fatigue failure will develop slowly. In this case, before the final—brittle—failure occurs the component will endure many load repetitions and the effect of the mutual compression and abrasion of the crack surfaces will be considerable; these surfaces will appear finely polished and the zones will differ sharply. In this case the crack will have penetrated

to a greater depth, due to which the zone of static failure will be comparatively small.

The surface of the zone of fatigue failure often displays in this case traces of the gradual development of cracks in the form of distinctively curved lines—steps. The development of these traces is connected with the selectivity of the crack development—they appear when the development of the crack stops or changes its direction because of the varying strength of various microvolumes of the component, possible changes in the process of operation of the loads acting on the component and frequent stopping of the machine.

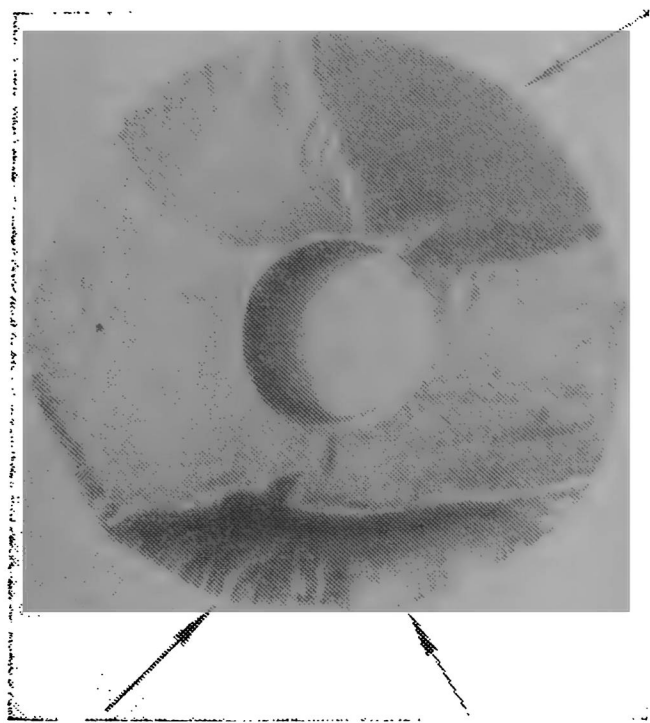


Fig. 3

The study of the distribution of cold hardening on the surface of a fracture shows that it reaches its maximum where the number of cycles of contact is the greatest, i. e., in the zone of the fracture origin.

When the *degree of cyclic overload is increased* the zones are more alike in appearance, since the number of stress repetitions before failure sets in is less the higher the acting stresses are. In this case the area of penetration of the fatigue fracture diminishes and the area of static failure increases.

Since as the fracture penetrates more deeply, the magnitude of local stresses grows at its base, a phenomenon accompanied by an increase in the plastic deformation (cold hardening) in the same zone, the maximum degree of cold hardening will be at the points where one zone passes into another. When the fracture penetrates quickly this effect is more prominent than that of mutual compression and wear of the surfaces. Thus, the value of cold hardening will be opposite to that examined above.

The size and form of a static fracture depend on the conditions of loading, the magnitude of rated stresses at which failure occurs and the value of the stress concentration factor.

Diagrams illustrating fatigue fractures are shown in Table 3; some of them are also shown in Fig. 4.

Fig. 4, *a* shows a photograph of a fracture in a shaft (symmetric flexure in rotation). The failure occurred at a high rated stress and a high stress concentration factor. At smaller rated stresses with a high stress concentration factor the fracture is shaped as an ellipse displaced relative to the centre (Fig. 4, *b*). A decrease in the stress concentration factor at moderate rated stresses for the same case of

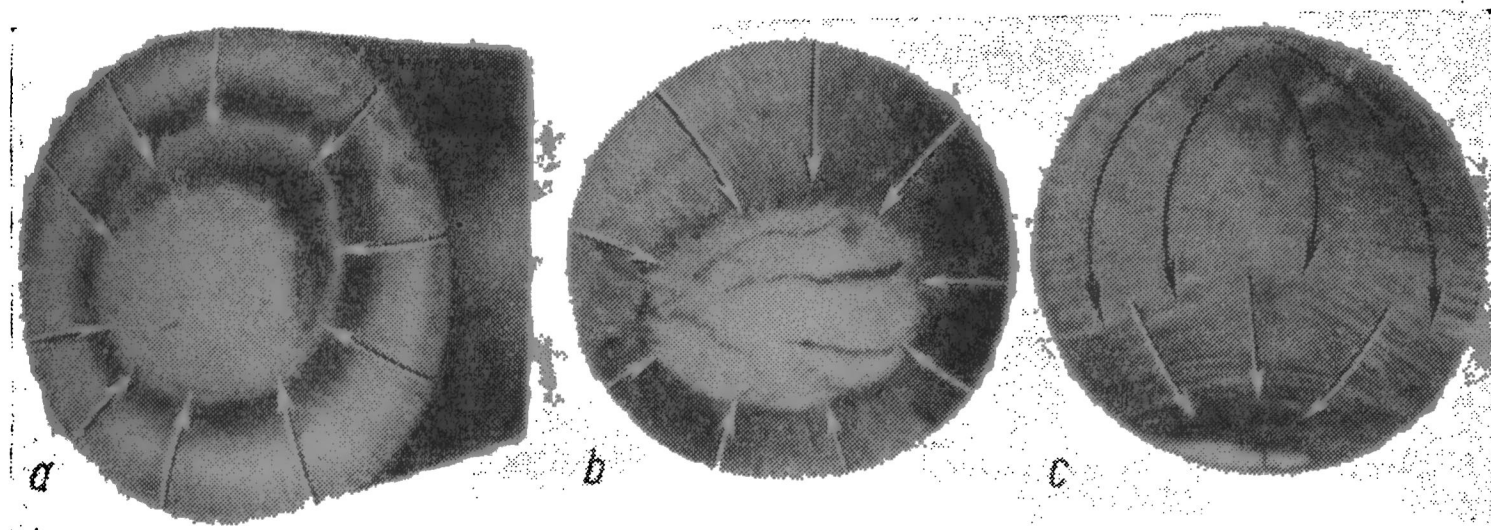


Fig. 4

a symmetric flexure in rotation is illustrated by the fracture in Fig. 4, *c*.

At cyclic twisting fatigue failures may occur: on the surfaces on which the maximum normal stresses act (at an angle of  $45^\circ$  to the axis of torsion)—at a comparatively low cyclic overload (Fig. 5); on the plane perpendicular to the axis (Fig. 6, *a*) or passing through the axis (Fig. 6, *b*) in which the maximum tangential stresses operate—at a considerable cyclic overload; the direction of the fracture development often depends on the presence of surface machining traces along the axis or round the circumference or of any other concentration points.

These examples show that the structure of the fracture surface often allows conclusions to be drawn as to the causes of failure. Study of fractures makes it possible to determine conditions which will preclude the appearance of similar faults.

*Endurance curves and diagrams of limit stresses.* The relations between the number of cycles before failure and the stresses causing failure are established by means of experimentally obtained *endurance curves* (Fig. 7) plotted in coordinates  $\sigma$ ,  $N$  or  $\sigma$ ,  $\log N$ .

Table 3

Diagrams of Fatigue Failure

	Without macroscopic stress concentration point		Low stress concentration factor		High stress concentration factor	
	At moderate cyclic overload	At high cyclic overload	At moderate cyclic overload	At high cyclic overload	At moderate cyclic overload	At high cyclic overload
Cyclic tension-compression						
Cyclic unilateral flexure						
Cyclic bilateral flexure						
Symmetric flexure in rotation						

The curve makes it possible to determine the maximum cycle stress—the *limit of endurance* at which the component will resist failure at a very high (arbitrary) number of stress variations. As

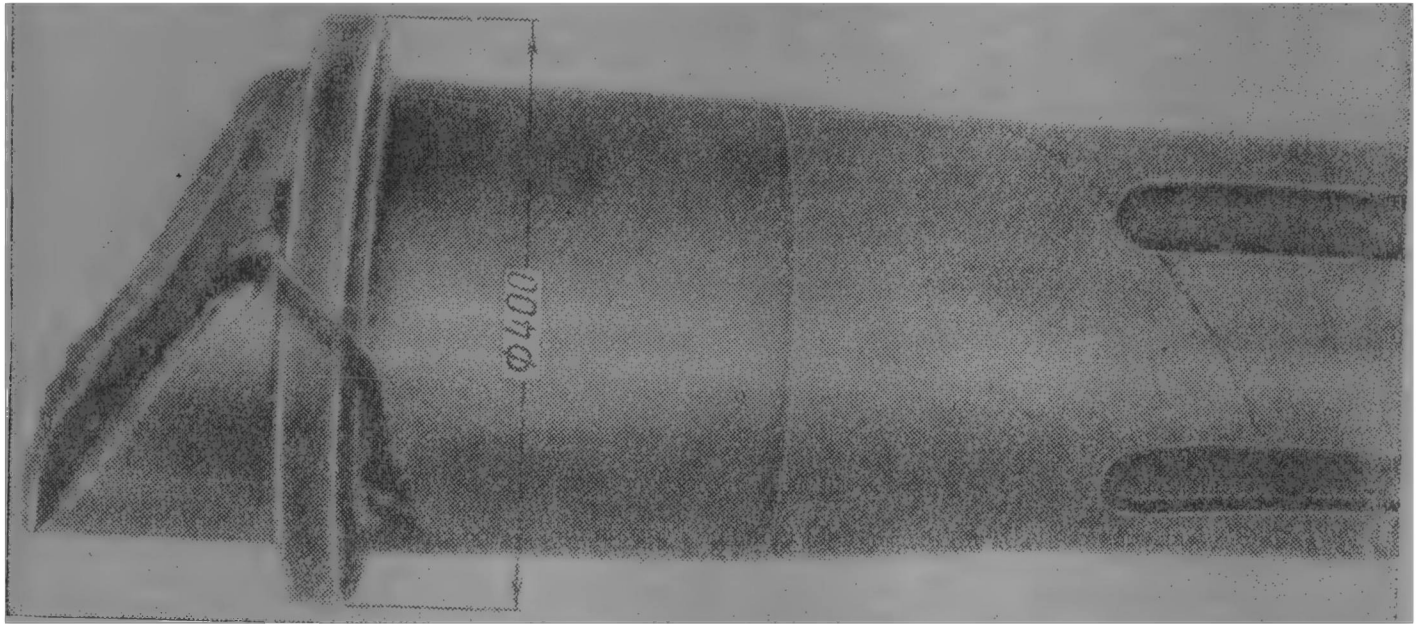


Fig. 5

a rule, for ferrous metals, it is sufficient to find this stress on the basis of the number of cycles  $N_{base} = 5 \times 10^6$ ; sometimes it is brought to  $N_{base} = 10^7$  and more. In this case it is assumed that if the

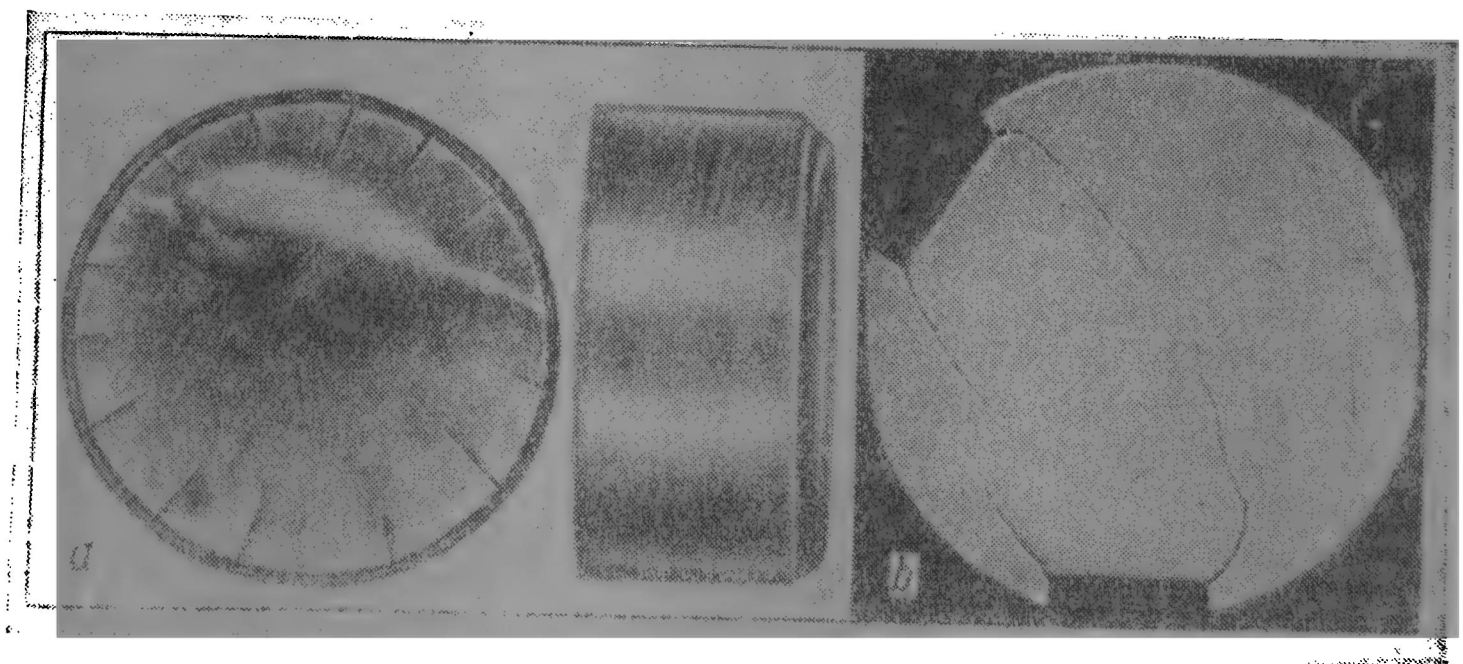


Fig. 6

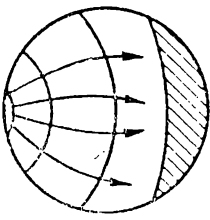
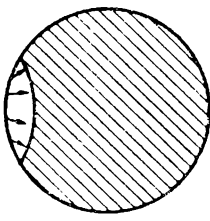
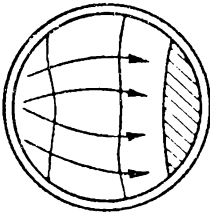
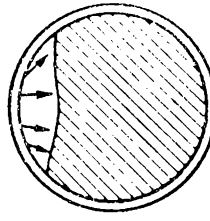
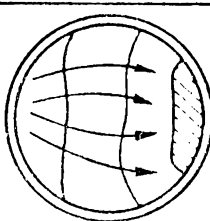
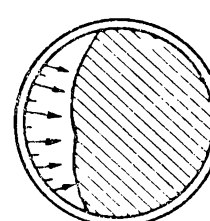
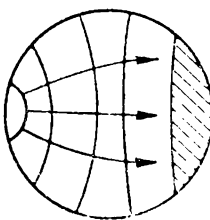
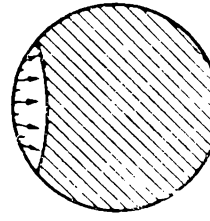
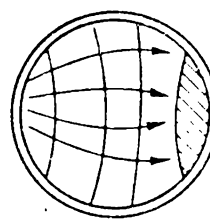
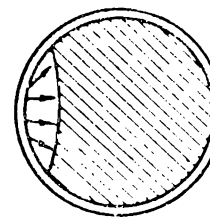
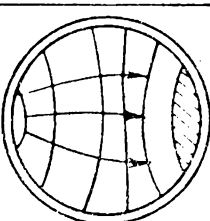
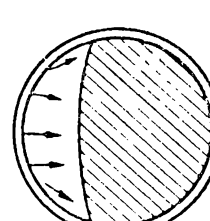
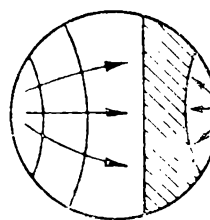
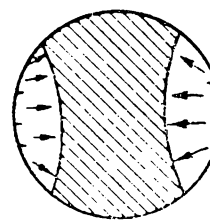
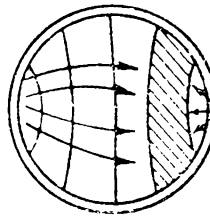
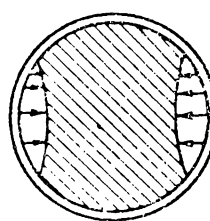
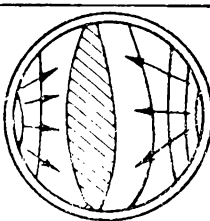
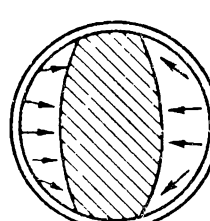
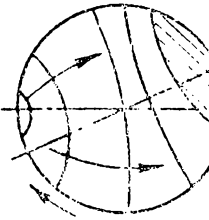
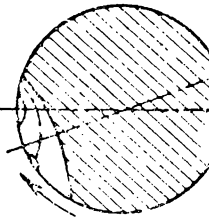
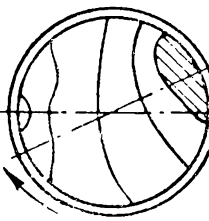
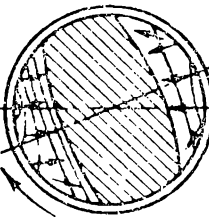
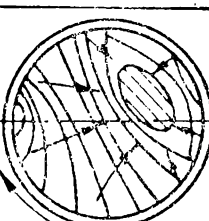
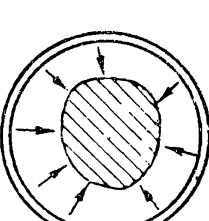
sample has not failed when the base number of stress variations is reached during testing, it will also remain integral if these tests are continued.

If the required service life of a component is limited to a number of cycles ( $N_1$ ,  $N_2$ , etc.) smaller than the base number, the *restricted*



Table 3

Diagrams of Fatigue Failure

	Without macroscopic stress concentration point		Low stress concentration factor		High stress concentration factor	
	At moderate cyclic overload	At high cyclic overload	At moderate cyclic overload	At high cyclic overload	At moderate cyclic overload	At high cyclic overload
Cyclic tension-compression						
Cyclic unilateral flexure						
Cyclic bilateral flexure						
Symmetric flexure in rotation						

The curve makes it possible to determine the maximum cycle stress—the *limit of endurance* at which the component will resist failure at a very high (arbitrary) number of stress variations. As

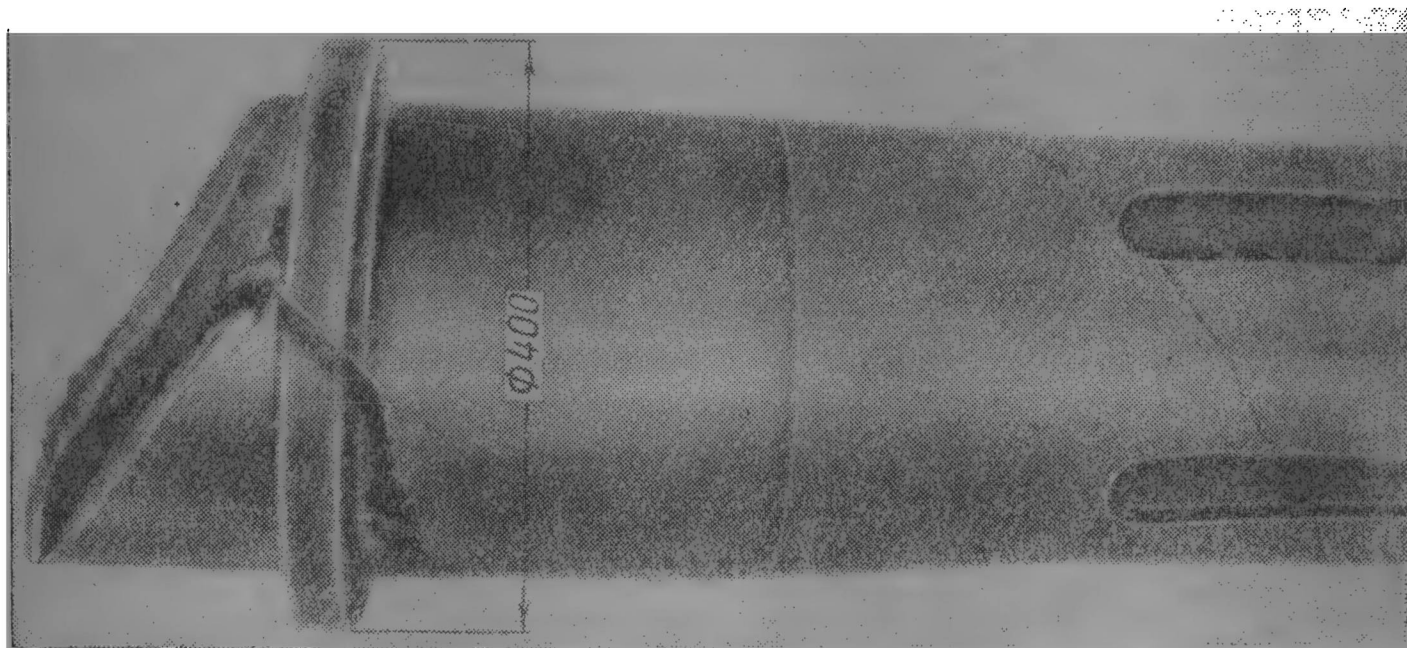


Fig. 5

a rule, for ferrous metals, it is sufficient to find this stress on the basis of the number of cycles  $N_{base} = 5 \times 10^6$ ; sometimes it is brought to  $N_{base} = 10^7$  and more. In this case it is assumed that if the

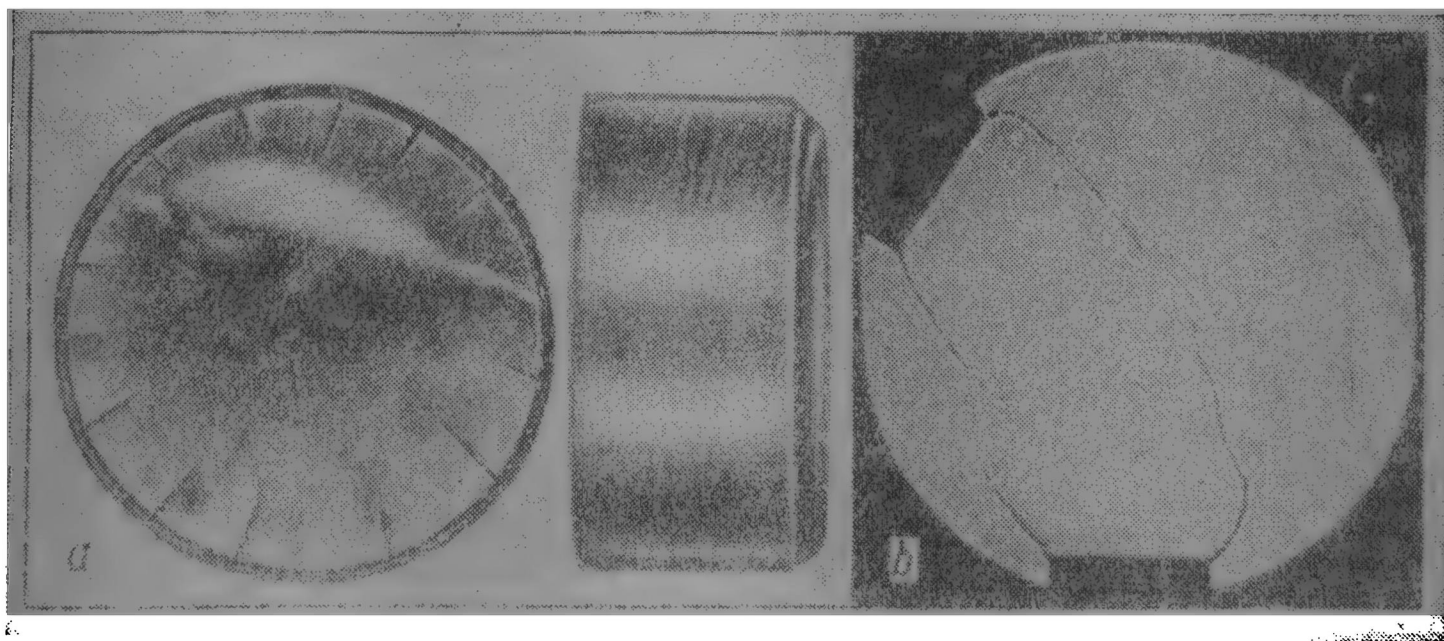


Fig. 6

sample has not failed when the base number of stress variations is reached during testing, it will also remain integral if these tests are continued.

If the required service life of a component is limited to a number of cycles ( $N_1$ ,  $N_2$ , etc.) smaller than the base number, the *restricted*

*limit of endurance* should be used for calculations; this is the maximum stress of the cycle which the sample can endure at a corresponding number of stress variations  $N_1, N_2$ , etc. ( $\sigma_{-1N_1}; \sigma_{-1N_2}$ , etc.); in this case if  $N_1 > N_2$  then  $\sigma_{-1N_2} > \sigma_{-1N_1}$ , etc. The limit of endurance

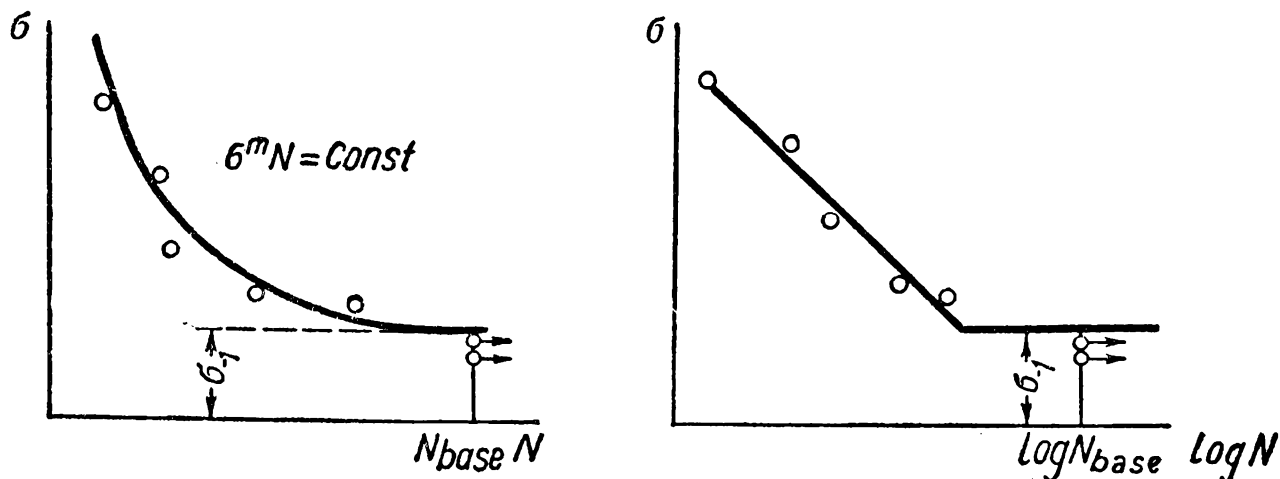


Fig. 7

depends both on the nature of stress variations in time—the degree of the cycle asymmetry, and on the kind of the stressed state.

The effect of the degree of the cycle asymmetry is determined by means of diagrams of limit stresses plotted in the coordinates  $\sigma_m(\tau_m)$  and  $\sigma_a(\tau_a)$  or  $\sigma_m(\tau_m), \sigma_{max}(\tau_{max})$  and  $\sigma_{min}(\tau_{min})$ .

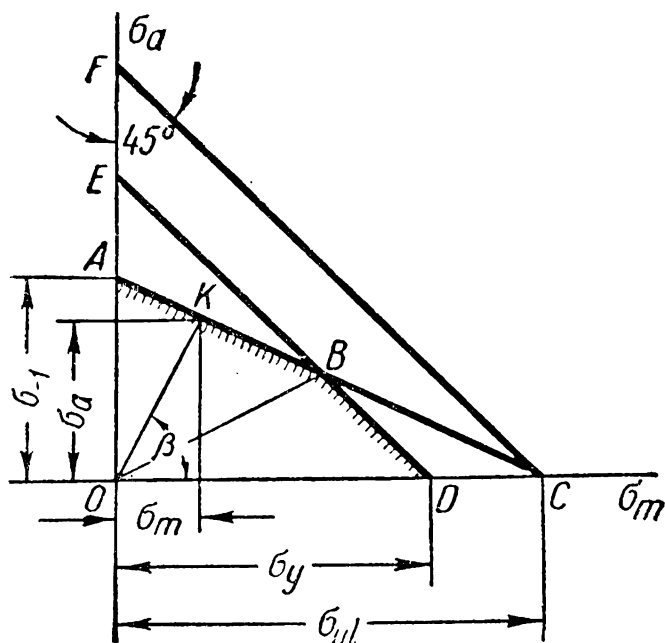


Fig. 8

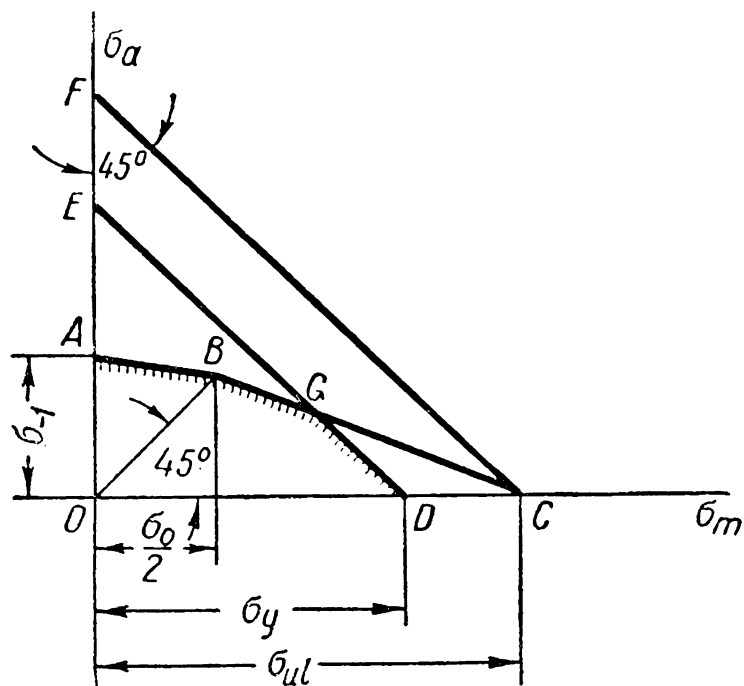


Fig. 9

Fig. 8 shows a simplified diagram plotted with two characteristics of static strength  $\sigma_y$  and  $\sigma_{ul}$  and the limit of endurance  $\sigma_{-1}$ .

In calculations use is frequently made of the diagram drawn by the method suggested by S. V. Serensen and R. S. Kinasoshvili which specifies more accurately the magnitudes of the limits of endurance in the region of cycles with the asymmetry factor  $r =$



$= -1.0$ ; to draw such a diagram the values of  $\sigma_{-1}$ ,  $\sigma_0$ ,  $\sigma_y$  and  $\sigma_{ul}$  should be known (Fig. 9).

Fig. 10 shows by way of example a typical diagram of limit stresses in tension-compression for structural steel plotted in the coordinates  $\sigma_m$ ,  $\sigma_{\max}$  and  $\sigma_{\min}$ .

Diagrams of limit stresses for cases of varying pure shear are drawn in the same manner.  $\tau_{-1}$ ,  $\tau_y$ ,  $\tau_{ul}$ , etc., are taken as initial values.

When diagrams of limit stresses are not available, the approximate values of the limits of endurance  $\sigma_{-1}$  and  $\sigma_0$  for steel can be determined from empirical relations which establish the connection between the static and fatigue characteristics of metal (Table 4).

Table 4

Relation Between the Fatigue and Static Characteristics of Metals

Deformation	Symmetric cycle	Intermittent cycle
Bending . . . . .	$\sigma_{-1b} = 0.43\sigma_{ul}$	$\sigma_{0b} = 0.60\sigma_{ul} \leq \sigma_y^b$
Tension-compression . . . . .	$\sigma_{-1t} = 0.36\sigma_{ul}$	$\sigma_{0t} = 0.50\sigma_{ul} \leq \sigma_y$
Torsion . . . . .	$\tau_{-1} = 0.22\sigma_{ul}$	$\tau_0 = 0.3\sigma_{ul} \leq \tau_y$

For cast iron, approximately,  $\sigma_{-1b} = 0.45\sigma_{ult}$ .

A very accurate idea of the actual strength of machine elements can be obtained by testing these elements on machines which fully reproduce the operating conditions of loading (the kind of stressed state, load conditions, etc.).

It is difficult, however, to obtain such data, because in mechanical engineering a great variety of components are employed and the operating conditions of loading are difficult to simulate on testing machines.

Therefore data on the resistance offered by materials to alternating stresses are obtained as a rule from tests carried out on standard samples.

When evaluating the strength of machine elements the values of limits of endurance obtained from the tested samples should be

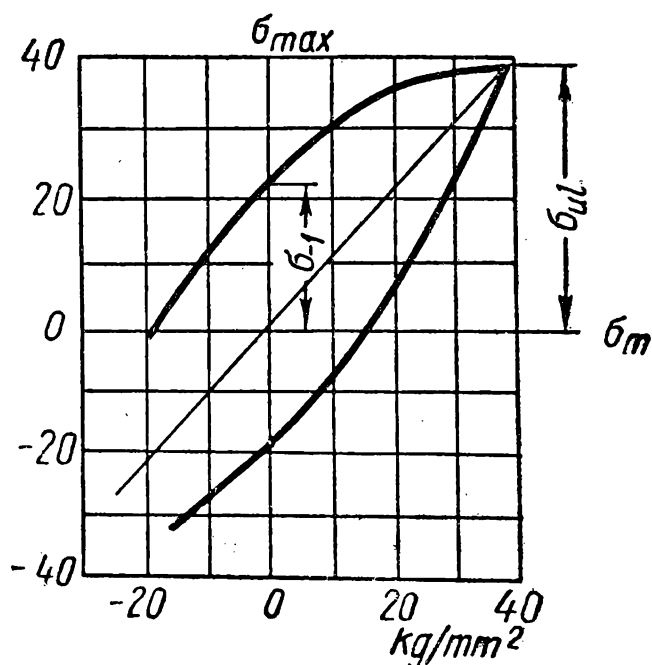


Fig. 10

corrected, because strength is affected by the following main factors: the form and absolute dimensions of the component; the state of the surface and the properties of the surface layer; variations in load conditions.

*The effect of design forms of machine elements on their endurance.* Design forms materially affect the ability of machine elements to resist the action of alternating stresses.

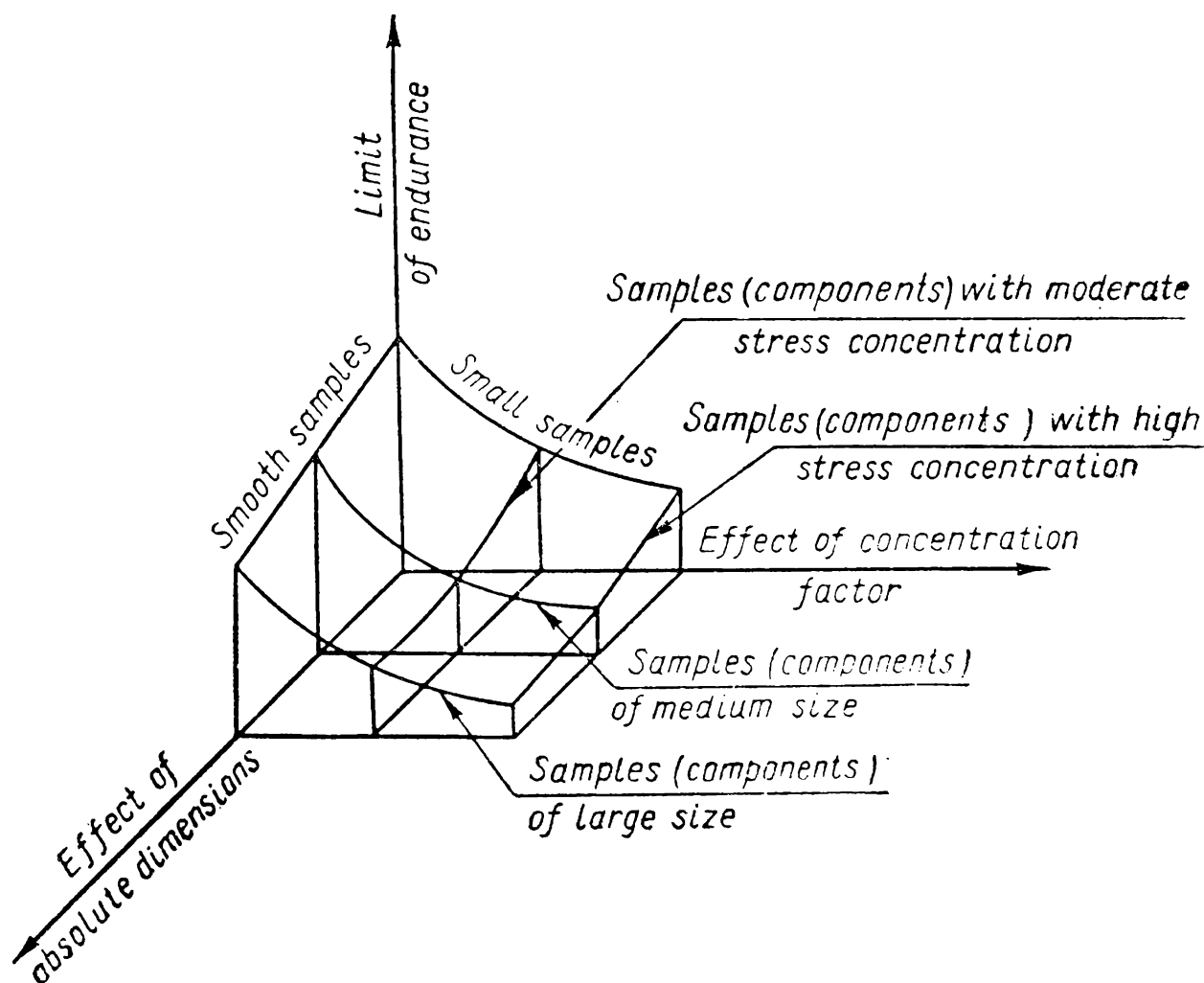


Fig. 11

Comparison of the results of testing for strength of machine elements (real) and smooth samples of a small diameter cut out from the same elements shows that the strength of metal is utilised inadequately and that for many components the reduction in strength due to the form and absolute dimensions is considerable. Thus, the relationship between the limit of endurance of the component and the limit of endurance of the sample amounts to  $\sim 0.3-0.4$  for crankshafts; to  $\sim 0.37$  for railway car axles; and to  $\sim 0.13$  for bolts, etc.

A diagram showing the effect of the form and absolute dimensions of machine elements on their endurance is shown in Fig. 11.

The effect of form is accounted for by the effective stress concentration factor calculated by the formula (3, b).

As distinct from the behaviour of materials under static load, under the load conditions examined here stress concentration should

be also taken into account if the components are made from plastic materials: under alternating stresses the effect of equalising (smoothing out the peaks) the stresses cannot manifest itself to full measure because the zone to which the processes of plastic deformation extend is restricted. For this reason, fatigue failure of components occurs when there are peak stresses in individual granules and not when the stresses are equalised in the cross-section.

The factor accounting for the sensitivity of the material to stress concentration  $q$  depends primarily on the properties of the material. This factor was introduced on the assumption that it did not depend on the form of the concentration point and was constant for a given material. Subsequently it was proved that it also depended on the type of concentration point: the sensitivity of the material to stress concentration diminished as the radius of curvature in the concentration point decreased.

The effect of the type of concentration point on the value of  $q$  is also confirmed by the fact that  $q$  depends on the ratio between two factors— $k_\sigma$  and  $\alpha_\sigma$  ( $k_\tau$  and  $\alpha_\tau$ ). Since  $\alpha_\sigma$  increases sharply with a decrease in the round-off radius in the concentration point and  $k_\sigma$  also increases, but to a lesser degree, the value  $q = \frac{k_\sigma - 1}{\alpha_\sigma - 1}$  drops as the round-off radius at the top of the concentration point diminishes.

For structural steel, on an average,  $q=0.6-0.8$ , the larger values of  $q$  corresponding to steel with a higher ultimate strength.

The problem of the sensitivity of high-strength steel to stress concentration has been the subject of special study in recent years. It has been established that the sensitivity to the concentration point first grows as the steel hardness increases. The maximum sensitivity has been observed at a hardness of  $R_C=30-35$ . As the hardness continues to increase the sensitivity to the concentration point drops, especially noticeably at a hardness exceeding  $R_C=45$ ; thus, at  $R_C=60$  and more, the sensitivity to the concentration point is 2-2.5 times smaller than at  $R_C=30$ . These results show that steels possessing very high strength are less sensitive to concentration points at cyclic loading than less strong steels. The results of these investigations should be taken into consideration when designing components from high-strength steel with foci of sharp stress concentration.

For cast iron  $k_\sigma$  approximates unity.

The value of  $k_\sigma$  also depends on the absolute dimensions of the component cross-section: when the proportions of parts are increased while preserving their geometrical similarity the values of  $k_\sigma$  increase and approximate  $\alpha_\sigma$ .

With identical concentration points  $k_\tau$  is smaller at cyclic torsion than  $k_\sigma$  in bending or in tension-compression.

An approximate connection between them can be expressed by the formula

$$k_{\tau} = 1 + 0.6(k_{\sigma} - 1).$$

The problem of the effect stress concentration has on strength under alternating stresses with an asymmetric cycle has not been studied theoretically. On the basis of experimental data the effective stress concentration factor is assumed to be independent of the cycle asymmetry and its effect in the region of fatigue failure is relegated to the cycle amplitude.

It should also be noted that if two concentration points operate in the design cross-section (for example, a force-fitted part and a keyway) then the maximum stress is often determined by taking into account only the larger of the two values  $k_{\sigma}(k_{\tau})$ . In important cases the strength can be evaluated only after a special study of the problem.

The effect of the absolute dimensions of cross-section on the limit of endurance manifests itself also when smooth samples are tested: as the size of the cross-section increases the limits of endurance diminish. This phenomenon is accounted for in calculations by the factor of the effect of the *absolute dimensions of the cross-section* (scale factor)  $\epsilon$  equal to the ratio between the limit of endurance of a component with the diameter  $d$  and the limit of endurance of a similar sample with small proportions ( $d_0 = 7-10$  mm). Thus,

$$\epsilon_{\sigma} = \frac{(\sigma_{-1})_d}{(\sigma_{-1})_{d_0}} \quad \text{and} \quad \epsilon_{\tau} = \frac{(\tau_{-1})_d}{(\tau_{-1})_{d_0}} \quad (5,a)$$

and with stress concentration

$$\epsilon_{\sigma k} = \frac{(\sigma_{-1k})_d}{(\sigma_{-1k})_{d_0}} \quad \text{and} \quad \epsilon_{\tau k} = \frac{(\tau_{-1k})_d}{(\tau_{-1k})_{d_0}}. \quad (5,b)$$

When calculating for strength the factor accounting for the effect of absolute dimensions is relegated to the cycle amplitude.

Fig. 12 shows a diagram for determining the factor accounting for the effect of absolute dimensions of cross-section ( $\epsilon_{\sigma}$ ) for parts made from carbon (1) and alloy (2) steel.

The decrease in the limit of endurance when the absolute dimensions of the component cross-section are increased is due to several causes.

As the dimensions of the component cross-section increase there is a greater probability of the development of a fatigue fracture, because the mechanical properties and the stress in individual granules are not the same and because all sorts of inner defects (pits, microcracks, inclusions) are possible.

The methods of manufacture of samples and components have a considerable effect on their endurance, since machining changes the properties of the surface layer. For the reasons outlined below the strength of the surface layer as a rule exerts a decisive influence on the endurance of the component.

It is clear that when the processing methods produce a cold hardening effect, this influences parts of smaller diameter to a greater extent, because the cold hardened layer extends to a relatively greater depth.

The problem of the effect the length of the sample has on the limit of endurance has been inadequately studied. According to some data, an increase in the length of the tested part of the sample diminishes the limit of endurance of steel and, depending on the grade of steel and the nature of machining and heat treatment, this decrease can reach 15-16%.

In this way the total effect of stress concentration and the absolute dimensions of cross-sections can be evaluated by the relation of the limit of endurance of smooth laboratory samples of small diameter ( $d_0 = 6-10$  mm) to the limit of endurance of a component with the diameter  $d$ :

$$(k_\sigma)_D = \frac{(\sigma_{-1})_{d_0}}{(\sigma_{-1k})_d} \quad (6)$$

Since

$$k_\sigma = \frac{(\sigma_{-1})_d}{(\sigma_{-1k})_d} \quad \text{and} \quad \varepsilon_\sigma = \frac{(\sigma_{-1})_d}{(\sigma_{-1})_{d_0}}$$

then

$$\frac{k_\sigma}{\varepsilon_\sigma} = \frac{(\sigma_{-1})_{d_0}}{(\sigma_{-1k})_d}$$

and according to the equation (6)

$$(k_\sigma)_D = \frac{k_\sigma}{\varepsilon_\sigma} \quad (7)$$

Therefore, if we know the limit of endurance of the sample  $d_0$ , the effective stress concentration factors and the factors accounting

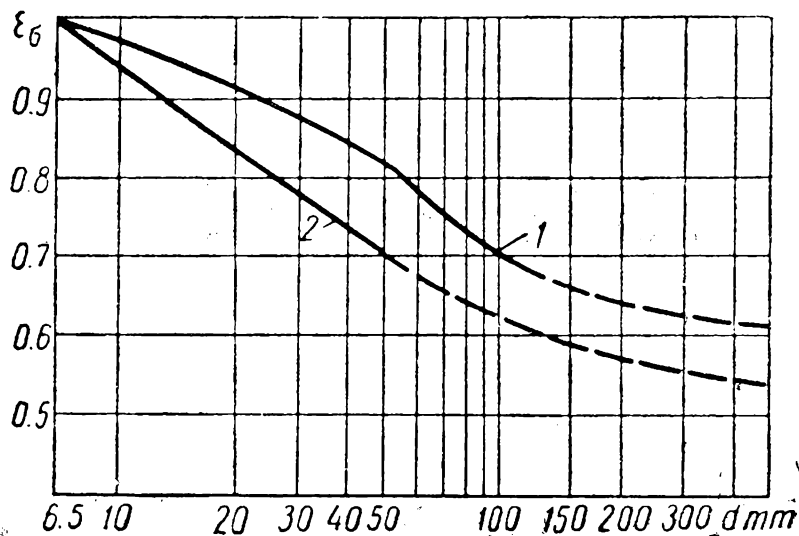


Fig. 12

for the absolute dimensions of cross-section can be used to determine the limit of endurance of a component with the diameter  $d$ :

$$(\sigma_{-1k})_d = \frac{(\sigma_{-1})_{d_0}}{(k_\sigma)_D} = \frac{(\sigma_{-1})_{d_0}}{k_\sigma} \varepsilon_\sigma. \quad (8)$$

For tangential stresses the formulae are derived from the previous formulae after substituting  $\tau$  for  $\sigma$ .

*The effect of the state of surface and the properties of the surface layer of machine elements on their endurance.* The surface layers are important in that, as a rule, primary fatigue fractures develop on the surface. This is due to: 1) the presence on the surface of stress concentration points, which are either provided by the design, or form during machining (for example, microirregularities), or else are due to operating and other causes; 2) the specific properties of the surface layer, which is a boundary layer containing broken and, therefore, weakened crystalline granules; 3) the effect of the external medium; 4) a state of higher stress on the surface layers under the main kinds of loading (flexure, torsion).

The cutting of metal, which imparts the required forms to machine elements, has a considerable influence on the state of the surface. This effect is primarily connected with the formation of microrelief on the surface, the appearance of plastic deformation—cold hardening on the surface layer—and heating of the surface layer.

The machining traces left on the surface act as stress concentration points and lessen the strength of the component.

The factors which are characteristic of the processes of plastic deformation in the surface layer (intensity and thickness of cold hardening, amount of residual stresses) and of its heating (degree of softening of the layer, degree of ageing, amount of residual stresses) affect the strength of machine elements in different ways. Cold hardening and residual compressive stresses in the surface layer increase the limit of endurance while, conversely, the appearance of residual tensile stresses decreases it.

Fig. 13 shows how the methods of machining the surface and corrosion affect the magnitude of the limit of endurance. If we assume the limit of endurance of a ground sample to be 100%, polishing further improves its strength; other kinds of machining decrease the limit of endurance to a greater extent, the higher the ultimate strength of the material  $\sigma_{ul}$  is.

Not only the machining methods, but also the mode of cutting has a considerable effect on endurance.

For example, the widely employed methods of high-speed metal-cutting not only prove advantageous in that they accelerate the

process of manufacture but also help to increase the endurance of machine elements.

It is important to emphasise at this juncture the need for a close cooperation between the designer and the production engineer. The designer must know which machining methods will be employed in the manufacture of the parts he has designed and on this basis establish the values of the maximum endurance. The production engineer must assign such methods and modes of processing as will accelerate the production process and ensure the optimal strength characteristics provided by the design.

To improve the physical state of the surface layers of components use is made in mechanical engineering of special methods of processing called "*strengthening techniques*".

Greater strength is achieved by:  
a) cold working of metal (shot peening, burnishing with rollers or balls, etc.); b) heat and thermochemical treatment (surface hardening, casehardening, nitriding, etc.).

In these cases strengthening is due to an increase in the strength of the surface layer and the appearance of residual compressive stresses in it.

*Shot peening* creates a cold hardened thin layer 0.2-0.8 mm thick which proves very effective in the presence of production and design stress concentration points; a lesser effect is obtained when this method is used to process smooth samples.

In principle, the same cold hardening effect is obtained when the surface is burnished with hardened rollers. As distinct from shot peening, which produces a pattern of dents on the surface, burnishing results in a clean and smooth surface and the cold hardening penetrates to a greater depth—up to 2 mm and more.

Experimental data show that the burnishing of samples with a cross drilling and with circular groove increases the limit of endurance by 60%; with a force-fitted part the strengthening reaches 38% and more.

The effect of the surface quality due to machining is completely eliminated by subsequent burnishing; ground and roughly turned samples have practically the same limit of endurance after burnishing.

A considerable strengthening is likewise obtained by roll-burnishing parts subjected to corrosion.

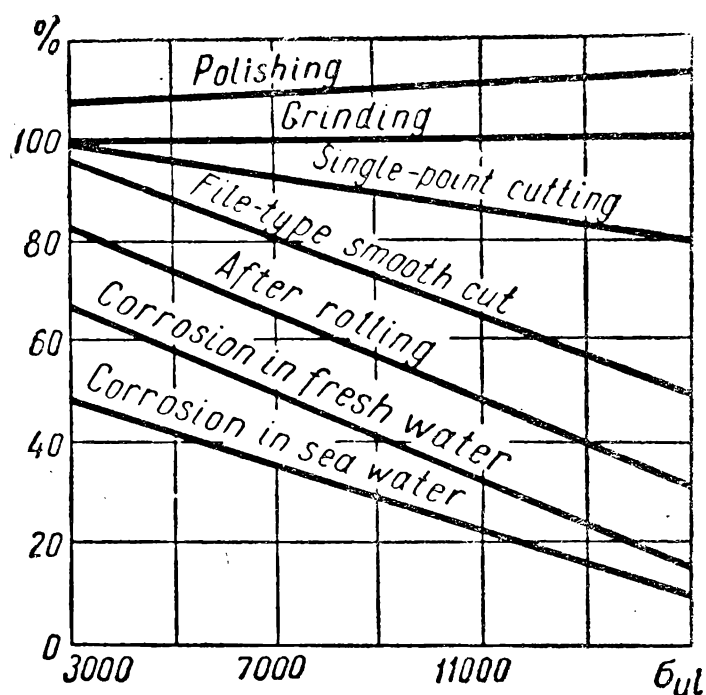


Fig. 13

It should be borne in mind that shot peening and burnishing are effective only when carried out correctly. Too intensive cold hardening decreases the limit of endurance, as it causes microcracks to develop in the surface layers because of high pressures.

*Surface hardening* by induction heating considerably reduces the sensitivity of the material to stress concentration. Depending on the grade of steel the limit of endurance of smooth samples increases by 40-100% compared to their initial state.

The employment of incorrect modes of hardening may cause microcracks which reduce strength. The entire working surface of a component should be strengthened, since the point of transition from the strengthened to the unstrengthened portion is weakened. If the site of transition is within the zone of action of a stress concentration point the limit of endurance may be considerably reduced.

*Casehardening* (saturation of the surface layer of steel with carbon) with subsequent hardening considerably improves the endurance of machine elements (1.5-2 times). Fatigue fractures in casehardened samples develop as a rule on the boundary line between the strengthened case and the core; when stress concentration has a sharply expressed character failure may begin on the surface.

*Nitriding* (the surface saturation of steel with nitrogen) produces a strengthening effect when testing smooth samples (up to 30%), with a stress concentration (up to 60%) and when machine elements have to operate in corrosive environments. The microgeometry determined by the preceding machining does not affect the endurance of nitrided items.

This method of strengthening is of especial interest, since nitriding is the final production operation and the properties of the case acquired as a result of the application of this method do not change.

*Cyaniding* (saturation of the surface layer with carbon and nitrogen) also improves the fatigue strength of machine elements, especially of gears, shafts, etc., which require shallow surface strengthening. When the strengthening case is increased, the limit of endurance first increases to a certain value and then becomes stable.

The increase in endurance as a result of the application of different kinds of strengthening (nitriding, casehardening, etc.) is accompanied by a change in other properties of the material, for example a reduction in its resilience. Therefore, when selecting a method of strengthening, all changes in the mechanical properties of the material caused by these methods should be taken into account.

The utilisation of complex methods of strengthening, which combine the advantage of heat and thermochemical treatment and subsequent cold hardening is very promising.

*The effect of the external medium on the endurance of machine elements.* The external medium in which machine elements are made



to operate has a considerable effect on their endurance. The effect of the medium at alternating stresses manifests itself in the phenomena of adsorption and corrosive fatigue of metals.

*Adsorption fatigue* is a reduction in the endurance of machine elements, occurring in superficially active media (which have no chemical effect on metal). The oils employed in machines as ordinary lubricants (nonactivated) which belong to this group of media decrease fatigue strength by 15-20%.

The effect of these media is connected with the phenomena taking place on the boundary line between two phases: metal and the surface active medium. The molecules of the surface active substance are adsorbed by the surface of the metal and weaken the interatomic link in the surface layer, thus favouring the development of submicroscopic cracks under the influence of external tensile stresses. The penetration of the molecule of the active surface substance into these cracks causes an adsorbing unwedging effect (so-called Rebinder effect) which facilitates the development of the processes of fatigue failure.

The fatigue curve in tests for adsorption fatigue is similar in character to an ordinary curve.

*Corrosive fatigue*, the reduction in the endurance of machine elements occurring in corrosive media (acting chemically on metals), is a far more dangerous process. Many important machine elements operate in such media. Premature failure of marine propeller shafts, turbine blades, diesel engine piston rods and other parts is due precisely to such corrosive fatigue.

The reduction of fatigue strength in these media is very considerable. For example, the limit of endurance of ordinary structural steel at the test base of  $10^7$  cycles is in fresh water twice and in sea water four times less than the limit of endurance obtained when the tests are conducted in air.

When testing for corrosive fatigue the fatigue curve has a distinctively shaped form: as the number of cycles increases it continuously descends; hence, only restricted limits of endurance can be determined for these processes.

There are two stages in the development of the corrosive fatigue process. The first is the adsorption stage and the second is the corrosive process proper inside the microcracks; simultaneously the products of corrosion accumulate in the microcracks and further reduce fatigue strength.

Experiments have shown that roll-burnishing, shot peening, surface hardening, nitriding and other methods of strengthening, which create compressive stresses in the surface layers, increase the endurance of machine elements operating in media favouring the formation of the processes examined.

*The effect of load conditions.* The loading of standard samples on the conventional testing machines for plotting fatigue curves is not

typical of the conditions under which machine elements actually operate. Each point on a curve obtained experimentally characterises the strength of the sample when it is continuously loaded with a constant load.

The sinusoidal nature of variations in the stresses arising in the sample cross-sections is due to its flexure in rotation at  $n = \text{const.}$  In reality both the acting load and the number of revolutions are as a rule varying magnitudes and the operation—intermittent. This kind of service is called *fluctuating*.

Parts of automobiles, hoisting and other machines, internal combustion engines, farm machines, metal-cutting machine tools, etc., operate under fluctuating load.

Loading conditions are characterised by: a) the presence of overloads and underloads, b) the frequency of stress variation, c) intermittent loading. Let us consider in general outline the present-day concepts of the effect of these factors.

An *overload* is understood to mean such loading of a component as would cause over a definite number of cycles alternating stresses which exceed the corresponding limit of endurance, and an *underload*—such loading as would cause alternating stresses below the limit of endurance.

Considerable overloads reduce the fatigue strength of the tested material, which can be explained by the appearance of microcracks and their intensive development at high stresses.

At small overloads—small overstresses operating within a limited number of cycles—the limit of endurance does not decrease; sometimes it even slightly increases.

Within certain limits underloads considerably increase the limit of endurance (up to 30%). This phenomenon—called “*training of the material*”—is made wide use of in engineering practice (for example, in the process of running-in machines) although it has not yet been estimated quantitatively in calculations.

The value of the limit of endurance of smooth samples or of components with an insignificant stress concentration does not practically depend on the velocity with which stresses change at the frequencies usual in present-day mechanical engineering. At frequencies exceeding 60,000 cycles per minute, their further increase somewhat improves the limits of endurance.

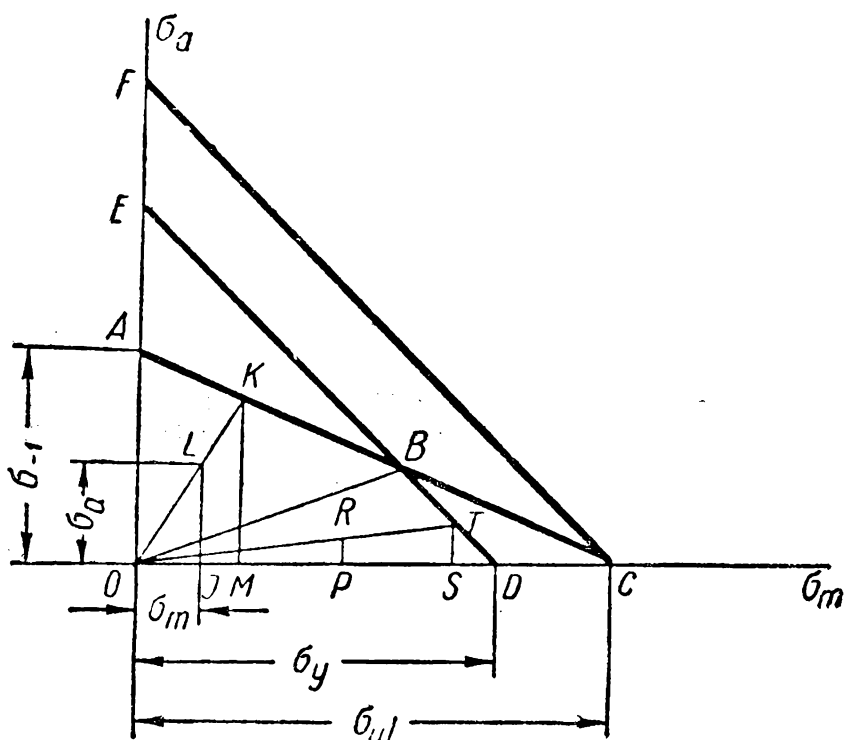
Experiments have shown that at overloads (overstress) a change in the frequency of stress variation materially affects the fatigue strength within the investigated interval of frequencies from 340 to 3,000 cycles per minute. The main effects of the frequency of stress variation are as follows: a) for smooth samples from carbon steel (normalised) the lower frequency increases the fatigue strength for the entire investigated region of overstress; b) for smooth samples from alloy

steel (tempered) in the region of lower overstress the lower frequency decreases the fatigue strength and in the region of high overstress increases it; c) the fatigue strength of samples with concentration points is reduced as the frequency of stress variation drops.

The effect of intermittent operation has not yet been adequately investigated and the results obtained do not always agree. There is ground to believe that rest somewhat increases the cyclic service life.

*Calculation for strength at stable conditions of alternating stresses. With a state*

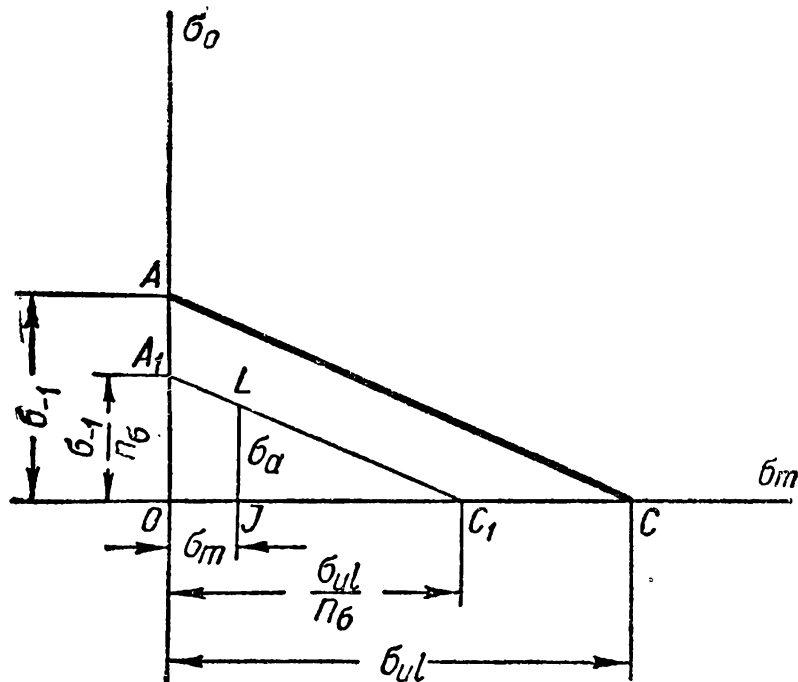
compression, pure flexure, beam flexure if the tangential stresses arising in cross-section are neglected) the margin of safety is calculated with the help of diagrams of limit stresses.



**Fig. 14**

If we assume that during the process of loading the mean stress of the cycle  $\sigma_m$  and the cycle amplitude  $\sigma_a$  change proportionally, i. e., so that  $\frac{\sigma_a}{\sigma_m} = \text{const}$  (such loading is called *simple*), the margin of safety for a cycle characterised by a point (for example,  $L$ ) within  $\triangle OAB$  (Fig. 14) is equal to

$$n_{\sigma} = \frac{\sigma_r}{\sigma_{\max}} = \frac{OM + MK}{OI + IL} = \frac{MK}{IL} = \frac{OM}{OI} = \frac{OK}{OL}.$$



**Fig. 15**

If the point characterising the cycle is within  $\triangle OBD$  the margin of safety should be calculated by the yield point since  $n_{\nu\sigma} < n_{\sigma}$ , i. e.,

$$n_{y\sigma} = \frac{\sigma_y}{\sigma_{\max}} = \frac{OS + ST}{OP + PR}.$$



Then the formulae (9) and (10) will take the form

$$n_{\sigma} = \frac{1}{\frac{k_{\sigma}}{\varepsilon_{\sigma}} \frac{\sigma_a}{\sigma_{-1}} + \frac{\sigma_m}{\sigma_{ul}}} = \frac{1}{(k_{\sigma})_D \frac{\sigma_a}{\sigma_{-1}} + \frac{\sigma_m}{\sigma_{ul}}} \quad (11)$$

and

$$n_{\sigma} = \frac{\sigma_{-1}}{\frac{k_{\sigma}}{\varepsilon_{\sigma}} \sigma_a + \psi_{\sigma} \sigma_m} = \frac{\sigma_{-1}}{(k_{\sigma})_D \sigma_a + \psi_{\sigma} \sigma_m} \quad (12)$$

The formula

$$n_{y\sigma} = \frac{\sigma_y}{\sigma_{\max}} = \frac{\sigma_y}{\sigma_m + \sigma_a} \quad (13)$$

is used to determine the margin of safety according to the resistance offered to plastic deformations (by the yield) at cycles when a fatigue failure may be preceded by a considerable remanent deformation.

At cyclic torsion the strength is calculated in a similar manner; the corresponding formulae are obtained from the above formulae after substituting  $\tau$  for  $\sigma$ .

The formulae obtained are written in a form suitable for revised calculations.

In some cases the proportions of components can be determined from design calculations when allowable stresses are known. The formulae for their calculation can be obtained with the help of the same diagrams.

Thus, for example, if we assume (to provide for a margin of safety) that the point  $B$  in Fig. 16 is on the straight line connecting the point  $A$  ( $0, \sigma_{-1}$ ) with the point  $C$  (the point  $C$  is not shown in the drawing; its coordinates are  $\sigma_{ul}, 0$ ) we can obtain a formula for  $[\sigma_0]$ :

$$[\sigma_0] = \frac{2\sigma_{-1}}{nk_{\sigma} \left( 1 + \frac{\sigma_{-1}}{k_{\sigma}\sigma_{ul}} \right)} \quad (14)$$

This formula is often used when assigning allowable stresses in the calculation of toothed gears.

At a *complex* nature of loading  $\sigma_m$  and  $\sigma_a$  can change irrespective of each other. For example, when  $\sigma_a$  changes at a constant mean stress  $\sigma_m$  the margin of safety is (Fig. 17):

$$n_{\sigma} = \frac{\sigma_{-1} \left( 1 - \frac{\sigma_m}{\sigma_{ul}} \right)}{\sigma_a}$$





minute  $n_1, n_2, n_3, \dots, n_i, \dots$  act during  $T_1, T_2, T_3, \dots, T_i, \dots$  hours respectively.

According to the so-called *cumulative hypothesis*, we assume that the damaging effect of each group of loads does not depend on the sequence of these loads and that the same cyclic relations (a cyclic relation is understood to mean the ratio between the actual number of stress repetitions and the damaging number of repetitions of the same stress, i.e., the cyclic service life) of overloads differing in magnitude cause the same degree of fatigue failure.

For this reason the actual condition of a varying load is replaced by a constant value equivalent to the actual condition in its fatigue action. In this case, depending on which (from the operating loads) load is selected as the constant load ( $Q$ ) of equivalent conditions, the number of cycles of action of this load will change (the equivalent number of cycles— $N_{eq}$ ).

The equation of the left-hand portion of the endurance curve (Fig. 7) has an exponential form

$$\sigma_i^m N_i = \text{const} \quad (21)$$

where  $\sigma_i$  is the limit stresses;

$N_i$ —the number of cycles of action of the corresponding stresses;

$m$ —an exponent characterising the slope of the left-hand portion of the endurance curve; in the logarithmic system of coordinates it equals the cotangent of the angle of inclination of the left-hand portion.

On the basis of this hypothesis and the equation (21) we can write

$$\sigma_1^m N_1 + \sigma_2^m N_2 + \dots + \sigma_n^m N_n = \sigma^m N_{eq} \quad (22)$$

whence the equivalent number of cycles  $N_{eq}$  of the load causing the stress  $\sigma$  will be

$$N_{eq} = \Sigma \left( \frac{\sigma_i}{\sigma} \right)^m N_i. \quad (23)$$

Using the equations (21) and (22) for the point of transition from the inclined portion of the endurance curve to the horizontal portion we can write

$$\sigma^m N_{eq} = \sigma_r^m N_{base}$$

and after substituting the value of  $N_{eq}$  in conformity with the equation (23)

$$\frac{\sigma}{\sigma_r} = \sqrt[m]{\frac{N}{N_{eq}}} = \sqrt[m]{\frac{N_{base}}{\Sigma \left( \frac{\sigma_i}{\sigma} \right)^m N_i}}$$



where  $\sigma_r$  is the continuous limit of endurance established for the base number of cycles  $N_{base}$ .

If we introduce

$$k_l = \sqrt[m]{\frac{N_{base}}{\sum \left( \frac{\sigma_i}{\sigma} \right)^m N_i}} \quad (24)$$

then

$$\sigma = \sigma_r \times k_l. \quad (25)$$

The factor  $k_l$  is called the *load factor*. As follows from the equations (23), (24) and (25), when the equivalent number of stress cycles  $N_{eq}$  is smaller than the base number of cycles  $N_{base}$  ( $k_l > 1$ ), the stress  $\sigma$  can exceed the magnitude of the limit of endurance  $\sigma_r$ .

Bearing in mind the connection between stresses and loads (depending on the nature of a stressed state) the formula (24) can be written thus

$$k_l = \sqrt[m']{\frac{N_{base}}{\sum \left( \frac{Q_i}{Q} \right)^{m'} N_i}}. \quad (24')$$

As applied to a circumferential bending  $m = m' = 6-9$ .

*General grounds for the selection of margins of safety and allowable stresses.* The design values of margins of safety or of stresses found from the above formulae should conform to the allowable values. Revised calculations consist in comparing design and allowable values of the margins of safety or stresses. The rational design of a component depends on the correct assignment of these values. Values, which have not been checked, if unduly large, can result in an uneconomical design, while values which are too low produce a weak design.

The *table* method is the oldest method of establishing allowable stresses. During the earliest stages of mechanical engineering allowable stresses were selected from tables which were the same for all branches of mechanical engineering. Since a limited range of materials was used for the manufacture of machines (cast iron, wrought iron, ingot iron and some of the nonferrous alloys) and the machines were operated under light conditions, the calculations were reduced to the mere evaluation of static strength by elementary formulae. At that time the use of these tables was justified, besides, this method required only very simple calculations.

As mechanical engineering was further developed the disadvantages of the table method became more and more pronounced. With the development of new branches of mechanical engineering, together with the appearance of more complex load conditions for machines and their elements, a continuous increase in the range of

the materials employed and the necessity to account in strength calculations for the effect of production, operating and other factors, the unified tables of allowable stresses could no longer satisfy the requirements of design practice. Various branches of mechanical engineering therefore worked out their own *specialised tables* of allowable stresses and the standards of the margins of safety.

Such tables and standards are still widely used today. In engineering practice the values of margins of safety and allowable stresses are sometimes strictly regulated and, what is also very important, the method of calculation for determining the design value of the margin of safety is specified. For example, in designing special components and mechanisms of hoisting machines (ropes, hooks, brakes, etc.) the margins of safety and the methods of calculation are now regulated in the Soviet Union by state technical inspection bodies.

However, in many instances the designer does not possess such legalised standards and must therefore himself establish the values of allowable margins of safety or stresses.

As a result of this, in the early thirties there was a move towards the rejection of the table methods and the substitution of *analytical* methods of selecting margins of safety.

The idea of the differentiated determination of the margin of safety was first advanced by A. I. Sidorov (1866-1931). This idea was developed in greater detail by I. A. Oding. His method was first published in 1932 and has been continuously improved since then.

According to this method the margin of safety  $n$  for calculating volume strength can be represented as the product

$$n = S_1 S_2 K_1 M_1 \quad (26)$$

where  $S_1$  is a factor representing the reliability of the material;  
 $S_2$ —a factor representing the degree of importance of the component (service conditions);

$K_1$ —a factor representing the accuracy of calculation;

$M_1$ —a factor representing the degree of correspondence between the mechanical properties of the tested samples and the mechanical properties of the component in the zone of maximum stresses.

The factors  $S_1$  and  $S_2$  are the safety margin factors in the true sense of the word. The factor of material reliability  $S_1$ , with a stable production process of manufacture of a component, beginning with the blank, should be evaluated only on the basis of the results of numerous tests. As tentative data and also for the manufacture of single and unique components we can assume that:

for parts machined from forgings and rolled stock  $S_1 = 1.05-1.40$ ;  
 for parts machined from castings  $S_1 = 0.15-1.2$ .

These recommendations are based on the assumption that only those faults can be detected in a forged material which reduce its strength by more than 5-10% while in cast metal faults reducing the strength by 15-20% usually remain undetected. The minimum values of the factor  $S_1$  apply to cases when the most efficient methods of fault detection are employed (for example, ultrasound inspection).

The value of the factor  $S_2$ , representing the degree of importance of the component during operation, can hardly be found by design calculations: the idea of the degree of importance is as a rule purely subjective and the values of  $S_2$  should therefore be regulated.

According to I. A. Oding, the values of  $S_2$  should vary between 1.0 and 1.3.

Usually machine elements are calculated according to schemes which do not fully reflect actual service conditions because sufficiently reliable data on the interaction of the component in the machine are not available. An incorrect design scheme naturally leads to an incorrect estimation of the acting stress, which may cause the failure of the component.

It is also extremely difficult to determine the acting efforts in machine elements in connection with the operating process. As a rule, the designer finds the acting efforts by means of the averaged indices of power, resistance forces, etc.

For this reason the factor  $K_1$  representing the degree of accuracy of calculations should be introduced in the formula to determine the margin of safety, although it can hardly be specified. Experimental methods of investigating loads acting in machines make it possible to specify more accurately the factors which affect the magnitude of  $K_1$ .

On an average we can take  $K_1=1.2-1.3$ .

The mechanical properties of a component are estimated from tests carried out on special samples made from the same bar or cut from the component blank. In rare cases whole units and assemblies are tested. But here too we cannot be sure of the complete identity of the mechanical properties of the whole consignment of parts, and when samples cut from blanks are tested we are not sure that the place from which the sample was taken corresponds to the zone of maximum stresses. For this reason the factor  $M_1$  should be introduced in the formula for the margin of safety; on the basis of experimental data we can tentatively assume that  $M_1=1.15$ .

If we take therefore the numerical values of factors as recommended by I. A. Oding the maximum value of the margin of safety for steel components will be

$$n = S_1 \times S_2 \times K_1 \times M_1 = 1.10 \times 1.30 \times 1.30 \times 1.15 \approx 2.2.$$

When operating conditions and the nature of external load must be more accurately evaluated and also when the mechanical character-

istics of the material and the acting stresses are trustworthy, the values of the margin of safety can be reduced to 1.2-1.5.

The idea of calculating the margin of safety by a differentiating method has gained a widespread recognition in recent years. Valuable results have been obtained by the further development of Oding's method in electrical engineering, ship-building, crane-building, etc.

**Surface Strength.** The operating capacity of many machine elements with adequate volume strength is restricted by the insufficient strength of their working surfaces.

*The strength of the working surfaces at cyclic contact loads.* The nature of the conjunction of some machine elements is distinguished by the fact that the loads they transmit over a limited (small) surface cause high so-called *surface* stresses in the area of contact. Among such components are gears, friction wheels, antifriction bearings, etc. Theoretically, before load is applied, the contact in races and balls of ball bearings is a point contact and in gears, roller bearings, etc.— a line contact. Under load the nature of contact changes: it occurs over limited surfaces. When the stresses arising in the area of contact exceed the allowable values plastic deformation or cracks may develop. At considerable overloads the component may fail (diagrams of failure of antifriction bearing races at high overloads are shown in Fig. 249).

The first solution to the problem of a stressed state in the area of contact between elastic bodies, the so-called contact problem, was provided in 1882 by H. Hertz (1857-1894). The development of this solution and its application to engineering practice is largely due to the work of A. N. Dinnik (1876-1950), N. M. Belyaev (1890-1944), I. Y. Staerman, M. M. Saverin and other researchers.

The solution of the contact problem is given in the 'theory of elasticity.

The following assumptions underlie the classical solution of the contact problem:

- 1) the materials of the contacting bodies are homogeneous and isotropic;
- 2) the area of contact is very small as compared with the surfaces of the contacting bodies;
- 3) the acting efforts are normally directed to the contact surface of both bodies;
- 4) the load applied to the bodies creates in the area of contact only elastic deformations which obey Hooke's law.

Not all these assumptions are observed in real designs. Thus, the third condition is not observed in gears, antifriction bearings, etc. Here, in addition to normal pressures in the area of contact, there are also tangential friction forces, due to which the resultant of these forces is deflected from the normal to the surface of contact. Despite this, experimental verification of the theory of contact deformation fully confirms its capability of being applied in practice as a rational design scheme. These solutions do not provide absolute values for stresses; they give only arbitrary values which should be compared with the data of revised calculations for components operating efficiently in these conditions in order to decide on the admissibility of these values.

By these assumptions the outline of the surface of contact is in a general case an ellipse. In particular cases the area of contact is transformed either into a circular area or a strip confined within two parallel straight lines.

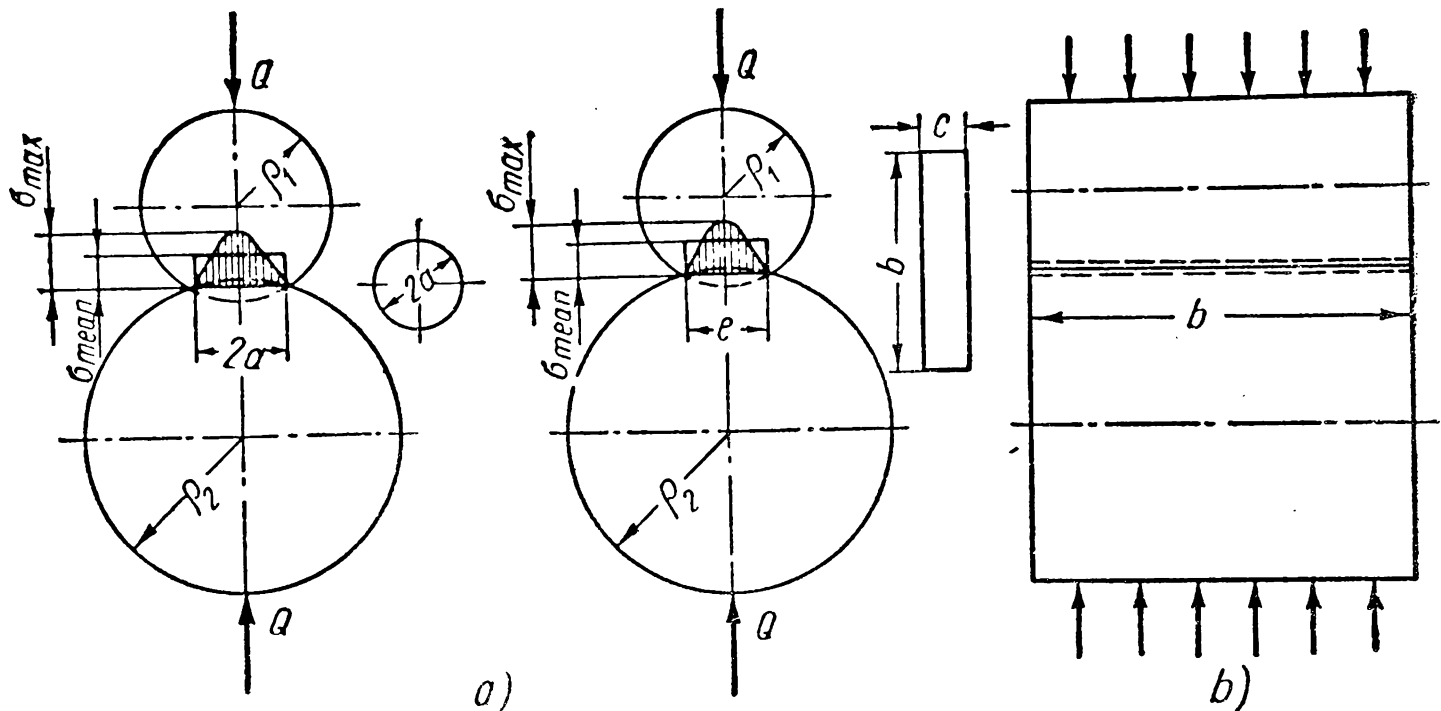


Fig. 19

When two balls with the radii  $\rho_1$  and  $\rho_2$  are compressed with the forces  $Q$  (Fig. 19,a) the local elastic deformations form an area of contact, circular in shape.

The radius of the area  $a$  at the Poisson ratio  $\mu=0.3$  is determined by the expression

$$a = 1.109 \sqrt[3]{\frac{Q\rho}{E}} \text{ cm} \quad (27)$$

where  $E = \frac{2E_1E_2}{E_1 + E_2}$  is the reduced modulus of elasticity of the compressed bodies in  $\text{kg/cm}^2$ ; and  $\rho = \frac{\rho_1\rho_2}{\rho_1 \pm \rho_2}$  is the reduced radius of curvature in the area of contact of the compressed bodies in cm; the minus sign is taken for a case of contact between a convex surface with radius  $\rho_1$  and a concave surface with radius  $\rho_2$ .

The pressures are not distributed uniformly over this area. The maximum pressure acting in the centre of the area of contact exceeds the average value by 1.5 times:

$$p_{\max} = \frac{3Q}{2\pi a^2} \quad (28)$$

It follows from the analysis of the stressed state at the characteristic points for a circular area of contact that the maximum compressive stress  $\sigma_3$  occurs in the centre of the area, in which case  $\sigma_3 = -p_{\max}$ .

Thus, from the equations (27) and (28)

$$\sigma_{\max} = 0.388 \sqrt[3]{\frac{QE^2}{\rho^2}} \text{ kg/cm}^2. \quad (29)$$

It follows from the formula (29) that, despite the fact that Hooke's law holds for the material of the components, the stress does not grow in direct proportion to the load  $Q$  but at a considerably slower rate.

For the case of contact of a ball with diameter  $d_1 = 2\rho_1$  and the plane  $\rho = \rho_1$

$$\sigma_{\max} = 0.388 \sqrt[3]{\frac{QE^2}{\rho^2}} = 0.62 \sqrt[3]{\frac{QE^2}{d_1^2}} \text{ kg/cm}^2.$$

When two cylinders with parallel axes are in compression (Fig. 19, *b*) the area of contact takes the form of a narrow strip confined within parallel lines; its width  $e$  is determined by the expression

$$e = 3.04 \sqrt{q \frac{\rho}{E}} \text{ cm}$$

where  $q = \frac{Q}{b}$  is the load per unit length of the cylinders in kg/cm on the assumption that it is distributed uniformly over the length  $b$ .

The maximum pressure occurs at the points of the centre line of the contact strip; it exceeds the mean pressure  $\frac{4}{\pi}$  times:  $p_{\max} =$

$$= \frac{4}{\pi} \times \frac{q}{e} = 0.418 \sqrt{\frac{qE}{\rho}} \text{ and hence}$$

$$\sigma_{\max} = 0.418 \sqrt{\frac{Q}{b} \frac{E}{\rho}} = 0.418 \sqrt{\frac{qE}{\rho}}. \quad (30)$$

The maximum value of tangential stress is observed under the surface of the area of contact; for steel at all kinds of contact  $\tau_{\max} \approx 0.3\sigma_{\max}$ . For a circular area of contact  $\tau_{\max}$  occurs at a depth of approximately  $0.5a$ ; for an area of contact shaped as a strip confined within parallel lines—at a depth of  $0.4e$ .

The conditions of loading of the contact working surfaces of the examined components during their relative shift (rolling) differ from those for which the formulae (28), (29) and (30) were obtained. Since the area of contact is in continuous motion the load is cyclic and, hence, the stresses which arise are alternating. This predetermines the nature of crack development, which depends on the number of load cycles, and allows us to classify this type of failure as a fatigue failure.

When the rolling of the contacting surfaces is accompanied by their relative sliding, fatigue fractures arising on these surfaces under the action of the friction forces (depending on their direction) develop

in different directions. Further development of these fractures is due to the presence of grease in the area of contact (a feature typical of closed-type toothed and worm gears and some of the friction drives, antifriction bearing, etc.) since the grease penetrates into the fractures. This process develops as follows.

For the case of relative motion of the working surfaces which is being examined, one surface is leading and the other following (Fig. 20). On the leading surface  $a$  the fracture is so located that the subsurface end of the fracture reaches the area of maximum contact

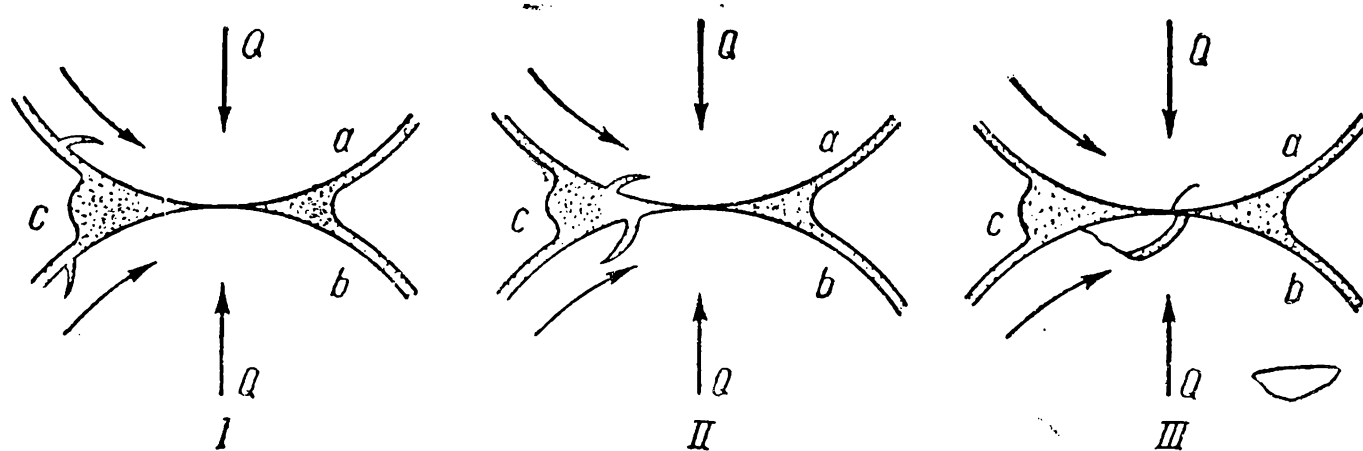


Fig. 20

pressures first, as a result of which oil is squeezed out from the fracture and the latter does not increase. The fracture on the following surface  $b$  is so located that its opened end on the surface approaches the area of maximum pressures first. Owing to this, oil is forced into the fracture. On meeting the conjugate surface the fracture edges close and the pressure in the oil layer inside it sharply increases, producing an unwedging effect favouring a gradual development of the fracture and its penetration to the surface (metal particles are broken out, Fig. 20, *III*).

This kind of failure of the working surfaces is called *pitting*.

Without oil the nature of failure of the surface layers changes—the fractures do not develop into pits, since the surface layer where initial fractures develop is worn before pits can form in it.

Pitting can be limited or progressive. In the first case it is observed only over restricted portions of the working surfaces. This type of failure can sometimes not be dangerous. The progressive pitting of the working surfaces is very dangerous since it increases dynamic loads and noise, and wears the parts at a faster rate.

The *limit of contact endurance* is the maximum stress at which a sufficiently large number of stress cycles does not cause pitting. The magnitude of the limit of contact endurance is established on the basis of endurance curves obtained experimentally and plotted in the coordinates of "the maximum unit pressure (or stress) in the area of contact and the number of stress cycles".

Curves of contact endurance resemble ordinary endurance curves. The relation between the stress and the number of cycles for the left-hand portion of the curve is the same as in ordinary fatigue tests

$$\sigma^m N = \text{const.} \quad (21')$$

A number of factors affect the magnitude of the limit of contact endurance, of which the most important are: the properties of the lubricant, the ratio between the hardness of the working surfaces in contact, the quality of machining, etc.

Operating experience and special research show that greater oil viscosity increases the limit of contact endurance. This phenomenon is evidently to be explained by the effect of relieving the area of contact with an oil film. Obviously, as the oil viscosity increases this effect will be seen to a greater degree. On the other hand, the ability of oil to penetrate into the fatigue fractures forming on the surface lessens at higher viscosities, and this is also bound to increase the limit of contact endurance.

Improved hardness and machining of the contact surfaces increase their resistance to pitting.

The surface strength cannot as yet be calculated taking into account all the factors affecting the processes of failure. But since the formation and development of a fracture depend on the magnitude of the maximum compressive stress in the area of contact, the process of surface pitting can be prevented by limiting this stress in conformity with data obtained from designs which are in satisfactory operation.

When the load condition is unstable, fluctuating service is replaced by an equivalent constant service on the basis of the hypothesis on the summation of fatigue processes examined earlier.

For example, when applied to calculations of components with line contact for surface strength, and remembering that  $\sigma_i$  from the formula (30) is proportional to the load raised to 0.5 degree, by analogy with the formulae (23) and (24')

$$N_{eq} = \sum \left( \frac{Q_i}{Q} \right)^{\frac{m}{2}} N_i$$

and since  $N_i = 60 n_i T_i$ , then

$$N_{eq} = \frac{60}{Q^{\frac{m}{2}}} \sum Q_i^{\frac{m}{2}} n_i T_i \quad (23')$$

and

$$k_l = \sqrt[m]{\frac{N_{base}}{N_{eq}}} = \sqrt[m]{\frac{N_{base}}{\sum \left( \frac{\sigma_i}{\sigma} \right)^m N_i}} = \sqrt[m]{\frac{N_{base}}{\sum \left( \frac{Q_i}{Q} \right)^{\frac{m}{2}} N_i}} \quad (24'')$$



It is far more difficult to determine the allowable stresses in surface strength calculations than in volume strength calculations, because the corresponding phenomena have not yet been sufficiently studied.

The data on the continuous limits of surface endurance of materials  $\sigma_{sur}$ , in relation to which allowable surface stresses are established are available only in limited quantities. Therefore, attempts are made to establish the values of  $[\sigma_{sur}]$  depending on static and fatigue characteristics of the strength of materials.

Work on experimental data makes it possible to establish a connection between  $\sigma_{sur}$  and the surface hardness—the characteristic which most actively affects the endurance of the working surfaces

$$\sigma_{sur} = C_B H_B \text{ or } \sigma_{sur} = C_R R_C \quad (31)$$

where  $C_B$  and  $C_R$  are factors depending on the material and heat-treatment and  $H_B$  and  $R_C$  are the values of Brinell and Rockwell hardness.

The effect of other factors on the allowable contact surface is accounted for by introducing correction factors  $k$  whose values are given in respective chapters of this textbook (for example, for gears, refer to p. 279). Thus,

$$[\sigma]_{sur} = \sigma_{sur} \times k$$

and taking into account the varying nature of load conditions

$$[\sigma]_{sur} = \sigma_{sur} \times k_l \times k. \quad (32)$$

*Wear resistance of machine elements.* The service life of many machine elements is reduced by the wear of their working surfaces. Wear changes the nature of conjunction of components in a unit; the operation of a gear becomes jerky and the nonuniform rotation of gears causes an additional dynamic load on the teeth. In this case their ability to transmit useful load diminishes; the lubrication of the thrust surfaces of the shaft and bearing deteriorates; the precision of the movement of parts (for example, machine-tool spindles, lathe carriages along the bedways, etc.) is disturbed; the airtightness of joints is destroyed, etc.

*Wear is the process of gradual change in the surface proportions of a component due to friction.*

Wearing friction can be produced either by a rubbing surface which itself also becomes worn or by hard particles (abrasives) that form part of the medium in which the components operate. In the latter case wear is called *abrasive wear*.

*Abrasive wear* accompanies the work of many elements in agricultural, construction and boring machines (plough mouldboards, parts of bulldozers, digger buckets, bore-bits, etc.).

The nature of mutual friction and wear of a pair of conjugate surfaces somewhat differs from abrasive friction and wear. In the first instance two causes

are present: the mechanical adhesion of microirregularities and the molecular cohesion of particles of the conjugate surfaces.

In case of abrasive wear molecular cohesion and wear can be represented as a result of the continuous scratching and shearing of metal by harder abrasive particles. If abrasives penetrate between the rubbing parts (for example, together with contaminated oil) the mutual wear of two conjugate surfaces is supplemented by abrasive wear.

The entire period of service from the moment the component is first put in operation to the moment it is rejected due to excessive wear can be divided into three stages (Fig. 21, *a*). The first stage is called the *running-in* period and the process of wearing occurring in

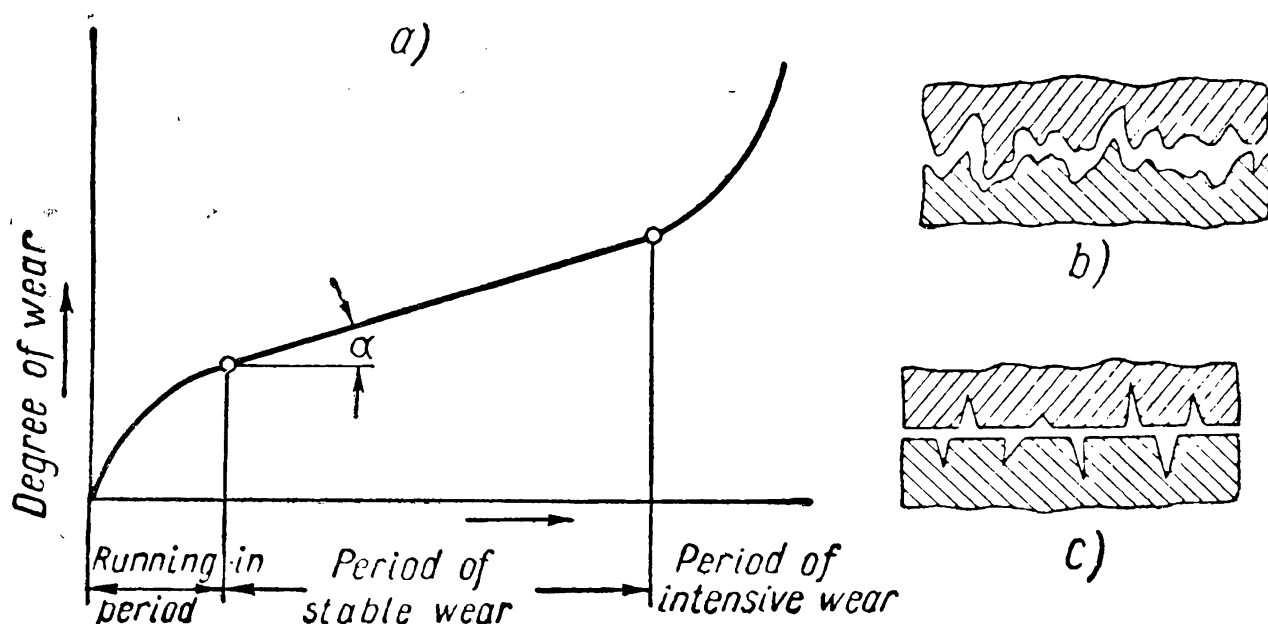


Fig. 21

this time is called *running-in*. Running-in is mainly due to the adhesion of large peaks (Fig. 21, *b*) left after machining; during this time the peaks are either shorn off or plastically deformed and decrease in height. Running-in continues until the area of contact becomes larger than the area of the valleys (Fig. 21, *c*).

Running-in is an extremely important period in the operation of machines, which should be assigned light service while it is proceeding. Otherwise, excessive heat formation in the friction zones will burn the oil film and melt together and break off particles of metal of the conjugate surfaces.

The running-in period is followed by the period of *normal operation* characterised by stable wear. The relation between the amount of wear and the time during which it has occurred—the so-called *rate of wear*—( $T = \tan \alpha$ , Fig. 21, *a*)—is the main index of this period. The slower the rate of wear the greater is the service life of the component.

The third period—*intensive wear*—is due to excessively large clearances between the mating surfaces. They deteriorate lubrication

conditions and increase the force of collision of the working surfaces. As a result, the latter become cold hardened and excessively brittle.

Micrometric measurements of the components or of clearances in the friction unit should give timely warning of the setting in of the period of intensive wear.

The rate of wear depends on many factors. The main among them are the magnitude and nature of load, the velocity of sliding, lubrication, cooling and the chemical and physical activity of the medium, etc.

Since friction is accompanied by very high pressures transmitted through separate points projecting on the surface and, hence, by high local temperatures, the surface layer is subjected to structural and chemical changes.

When the process of wear develops normally its products have the form of fine powder; at higher pressures and velocities of sliding impermissible for the given pair, with scanty lubrication or poor cooling the amount of heat produced increases to such an extent that large particles of metal melt together and are broken out. This most harmful type of wear is called scoring. It can lead finally to *seizure* which makes the normal operation of the unit impossible.

The large number of factors which influence wear makes it difficult to find well-substantiated methods of calculating machine elements for wear.

Wear resistance is usually evaluated approximately from the value of the unit pressure  $p$  or from the magnitude which is proportional to the work of the friction forces  $p v$ , where  $v$  is the velocity of sliding; the design values of  $p$  and  $p v$  are compared with allowable values of  $[p]$ , and  $[p v]$ , established from data obtained from reliably operating machines. Values of  $[p]$  and  $[p v]$  are given in the respective sections of this textbook.

Copious lubrication of the rubbing surfaces is the main means of decreasing the rate of wear.

When certain conditions are observed a state of fluid friction can be achieved at which there is practically no wear.

To prevent the failure of expensive components, the friction surfaces of cheaper components are made from a relatively soft material which effectively resists wear and does not allow the rapid wear of the mating surface of the more expensive component. Babbitts, bronze, some grades of cast iron and plastics are used as such *anti-friction* materials.

The wear resistance of friction surfaces is also improved by increasing their hardness by means of heat and thermochemical treatment (hardening of the surface layer, nitriding, etc.) and by applying various coatings (chrome-plating, weld surfacing with a hard alloy).

The wear in machines can also be decreased by design measures (the provision of conditions ensuring fluid friction; the correct choice of material for the conjugate pair, etc.), by production measures

(the mode of manufacture and strengthening, the coating, etc.) and by operating measures (ensuring proper lubricating conditions, the protection of friction surfaces from abrasive particles, etc.).

\* \* \*

*The principal methods of increasing the strength of machine elements.* The form of machine elements is of especial importance in increasing their strength. From this point of view it should satisfy the following two main requirements:

1. The form of a component should ensure such a direction of the force flux as to make the largest possible volume of the component take the load.

2. The form of the component in assembly with other elements of the unit should ensure the transmission of load over the entire designed surface of the contact, and over it alone.

Despite the fact that these two requirements are independent of each other (the first determines the volume strength of the component and the other—the surface strength and normal temperature conditions), a proper choice of form can very frequently satisfy both requirements.

From these two principal requirements we can formulate *certain general principles for the shaping of machine elements*.

1. When designing a component abrupt changes of form should be avoided wherever possible.

This is very important since abrupt changes of conjugated cross-sections cause a considerable stress concentration, which decreases the strength of the component when alternating stresses act in its cross-sections.

2. The component should be so designed as to ensure as far as possible equal strength in all its cross-sections.

The attempt to make all cross-sections equally strong is primarily due to economical considerations. However, it is frequently very difficult from a production point of view to produce such designs. For these reasons the components with forms of “equal resistance” are replaced by more production-sound designs. In this case the theoretical proportions for the majority of cross-sections are usually increased on the assumption that this will improve strength. In other words, the form of the component is such, that its theoretical outline (contour of equal resistance) can be inscribed within the assigned configuration. It should be remembered, however, that, if under static load larger dimensions really increase strength, under alternating stresses such increase in proportions may reduce the margin of safety in the given cross-section. This is confirmed by the effect of the absolute dimensions of a component on its strength—as the size of cross-section increases the limit of endurance diminishes. Besides, if the

component is designed in this manner abrupt changes in the size of adjacent cross-sections are possible.

The magnitude of the stress concentration factor depends not only on the form of the transition curve but also on the ratio between the dimensions of adjacent cross-sections of the component: abrupt changes in these dimensions increase local stresses.

3. To distribute the force flux evenly over the component volume it should be directed away from the zones of possible load concentration.

There are different methods for improving the distribution of the force flux over the component volume. Special mention should be made of so-called *relieving concentration points* which make it possible to increase the endurance of parts by 20-30%.

The action of relieving concentration points is based on the fact that if such a point is provided in the least stressed cross-section, the stress peaks diminish in the zone of the main concentration point operating in the same cross-section (see diagram in Fig. 22). Another modification of the method of relieving concentration points is the provision of *additional concentration points* which change the direction of the force flux and weaken its concentration near the main concentration point (place of stress concentration) created for design considerations (Fig. 23).

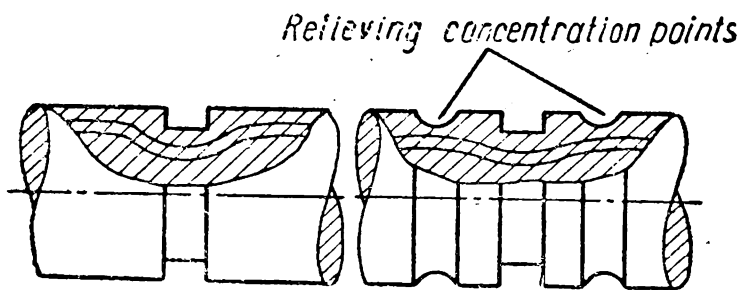


Fig. 23

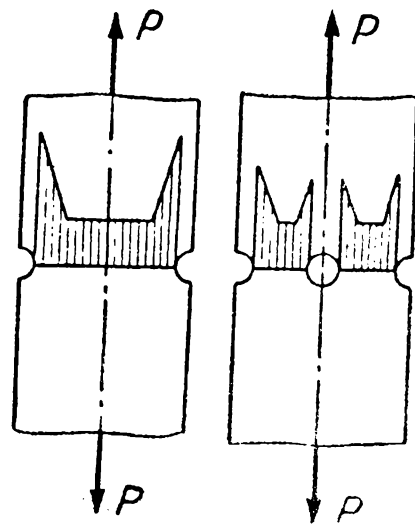


Fig. 22

4. The *removal of places* of probable load concentration favours the uniform load distribution over the entire designed area of contact.

It is often extremely difficult to provide for an adequate contact between the conjugate surfaces. Besides, even if such a contact is available the load may not be spread uniformly over the designed surface of contact.

For uniform load distribution the components are given forms without places of probable load concentration.

This method is employed as follows: when designing gears, barrel-like teeth (Fig. 154) are used to prevent load from concentrating on the portions of teeth adjacent to the end surfaces of the wheels; when designing shells for sliding bearings provision is made for an elliptic or hyperbolic boring (with a cylindrical journal), etc.

## RIGIDITY OF MACHINE ELEMENTS

The operating properties of machines are often determined by the *degree of rigidity of their individual units and parts; by rigidity is understood the limitation imposed on the magnitude of their deformation under the action of external load.*

For some designs determination of rigidity is the principal feature since they have to be calculated for displacements specified in advance. These are helical and leaf springs, elastic elements in various instruments, etc. In these cases the calculation for rigidity is usually intended to satisfy the requirements of strength.

When designing shafts, bearings, toothed, worm and other gears it is important to ensure adequate rigidity. Shaft deflections which exceed the allowable values, twisting and flexural deformations of a pair of meshing wheels in a gear cause uneven load distribution over the width of the wheel teeth and the load is concentrated nearer to the wheel end-faces. In especially unfavourable cases this may be the cause of the tooth failure.

When a shaft is deflected, its journals are misaligned in the bearings thereby causing the uneven wear of the shells, heating and seizure in the sliding bearings. With the deflection of an insufficiently rigid shaft the operating conditions of antifriction bearings sharply deteriorate if the bearings cannot self-align.

The requirements of rigidity also affect the choice of material for the component. For example, the strength characteristics of steel continuously increase, whereas the values of the moduli of elasticity remain practically the same.

When high-strength steel is used for the manufacture of shafts the shaft diameter (from the strength condition) can be very small but its deflections and angles of twist may exceed the allowable values. In this connection, for considerations of rigidity, the diameter of the shaft has frequently to be increased to a magnitude at which adequate strength can be also ensured when cheaper steel with lower mechanical properties is used.

Rigidity is particularly important for ensuring the adequate accuracy of items produced on machine tools. Inadmissible errors may be due to the deformation of the component itself (for example, when it is clamped) and the parts of the machine tool (spindle, arbor, bearings, etc.). Beside inaccuracy of manufacture, elastic depressions of the joints during machining cause vibration which considerably lowers productivity.

In certain cases machine elements should be able to give to a certain extent. Flexible bolts, teeth and the rims of toothed wheels, etc., have better endurance.

Calculation for rigidity is obligatory in designing statically inde-

terminable systems since the internal force factors (bending moments and torque, normal and shear forces) cannot be determined here only by the equilibrium conditions; an additional requirement is the equalisation of displacement. It is important to evaluate rigidity when calculating components loaded with compressive forces (lifting screws, lead screws, springs, etc.) for stability, when the components are designed for operation under dynamic loads.

Calculations for rigidity should sometimes take into account both the rigidity of the component itself (deformation of the basic volume of the component material) and its contact rigidity (deformation of the surface layers).

The rigidity of machine elements is found with the help of formulae from the theory of the strength of materials; sometimes it is evaluated from the *factors of rigidity*, which are the ratios between the force factor (force, torque) and the deformation they cause. For example, the factor of rigidity of a bar with constant cross-section  $F$  and length  $l$  loaded in tension by the force  $P$  is equal to

$$C = \frac{P}{\lambda} = \frac{EF}{l}; \quad (33)$$

the factor of rigidity of a portion of a shaft with diameter  $d$  and length  $l$  loaded in torsion by the torque  $M_t$  is

$$C = \frac{M_t}{\varphi} = \frac{G \times l_{work}}{l}. \quad (34)$$

The value opposite to the factor of rigidity is called the *factor of yielding*  $\left(\frac{l}{C}\right)$ .

Because it is difficult to account for the effect of the rigidity of housings, bedplates and bearings, an accurate calculation of rigidity even for such parts as shafts and axles is very complicated. Rigidity is evaluated by comparing design deformations (deflections, angles of turn, angles of twist, etc.) with their allowable values, established by the data of especially arranged experiments, or by the results of processing statistical data for similar units of tested machines.

As follows from the formulae (33) and (34) the degree of component rigidity can be actively influenced by a proper choice of materials ( $E$ ) and of design methods.

*The most important design methods for increasing the rigidity of machine elements are the following:*

- a) the reduction of the arms of bending and twisting forces;
- b) the incorporation of additional supports;
- c) the application of cross-sections which effectively resist bending (in which the cross-sectional area is removed as far as possible from the neutral axis) and torsion (closed tubular);



d) the decrease of the length of the parts in tension and the increase of their cross-sectional area.

It is obvious that increased yielding of machine elements is obtained by measures opposite in character.

When joining most components considerable contact deformations occur. For parts in which, after joining, the initial contact (before the load is applied) occurs at a point (for example, ball bearings), or along a line (roller bearings, gears, etc.) contact deformations are determined by the respective formulae of the Hertz-Belyaev theory of surface strength. Contact deformations also arise when joining components with a large *rated* area of contact (described by the external contour of the area of contact) since the *actual* area of contact, due to the roughness of the contact surfaces, is the sum of the actual small areas of contact.

*The most important design recommendations for improving contact rigidity are the following:*

a) improving the quality of machining the contact surfaces;

b) assembling the units under preload or pretension (for example, antifriction bearings are often assembled under such a preload that the applied external load is distributed over all balls or rollers);

c) reducing the number of joints;

d) introducing an oil layer between the contact surfaces. Greater oil viscosity increases contact rigidity.

## RESISTANCE TO VIBRATION OF MACHINE ELEMENTS

The higher working velocities of machines and their elements and the accompanying tendency to lighten them often cause vibrations, by which are understood periodic deformations whose amplitudes are very small as compared to the dimensions of the vibrating part. Vibrational loads are especially dangerous in that they may be the cause of fatigue failure.

When the natural frequency of a machine oscillations or the oscillations of its components coincides with the frequency of change in the external periodic forces which cause them, resonance sets in, which sharply increases oscillating amplitudes and sometimes leads to failure.

The vibration of spindles of metal-cutting machine tools deteriorates the quality of the machined surfaces and quickly blunts or even destroys the tool.

Oscillations of parts of gears (toothed wheels, shafts, housings of reduction gears, etc.) due to the elasticity of parts and their elements (wheel teeth, walls of housings, etc.), cyclic errors in the work-



ing surfaces of teeth and changes in the tooth deformations and friction forces generate noise.

Various methods are employed to damp oscillations dangerous for elastic systems.

The principal method is the elimination of those external forces which cause dangerous oscillations.

However, this principle can be employed only on a limited scale. The task can be often solved by changing the dynamic properties of the system—by changing the moments of inertia of the masses and the yielding of the joints.

When these methods are ineffective the system is provided with special devices—vibration dampers or antivibrators.

The fundamentals of calculating shafts for the critical velocity are given in the chapter «Shafts and Axles».

### HEATING OF MACHINE ELEMENTS

For the normal functioning of many machines it is important to ensure definite temperature conditions in which their components (units) will operate. Such requirements arise when, in the process of operation, friction causes considerable losses of power accompanied by profuse heat generation or when the temperature of the environment is likely to change.

Thermal calculations in general mechanical engineering are performed mainly to determine the temperature of heating (or cooling) of parts and to find methods of limiting its amount to allowable values. When these allowable limits (the standards are established on the basis of experimental data) are exceeded, heat deformations may develop which change the nature of interaction of components in a machine (unit); this may also cause additional (temperature) stresses, violation of normal conditions of lubrication (change in the clearances and oil viscosity favouring seizure of the contact surface) and other faults.

An account of these factors proves essential, for example, when calculating the components of threaded joints for strength—for a correct evaluation of the developing stresses when the temperature of the environment changes.

When designing certain drives (especially friction, worm and other drives) and certain clutches, thermal conditions often restrict their operation and dictate the design and size of the components and also the choice of materials for their manufacture, lubrication conditions, etc.

As a rule, these calculations are reduced to finding the conditions of thermal balance, which are then used to establish the relation between the amount of generated and dissipated heat during operation.

For example, if the power  $L$  h.p. lost in transmission is transformed into heat whose amount is

$$Q = \frac{75}{427} 3,600L = 632L \frac{\text{Cal}}{\text{hr}} \quad (35)$$

the cooling surface  $F_m$  m<sup>2</sup> needed to dissipate heat in a closed-type drive operating in oil at *stable* thermal conditions will be found from the condition of thermal balance

$$Q \leq F_m k (t_1 - t_2) \quad (36)$$

where  $k$  is the heat transfer factor in Cal/m<sup>2</sup> × hr × degrees;  $k$  is taken from 7.5 to 15 depending on the velocity of the air flowing over the housing of the drive;

$t_1$  — the temperature of oil in °C; usually  $t_1 = 75-85^\circ$ ;

$t_2$  — the ambient temperature.

To satisfy the condition (36) the cooling surface of the machine housing should sometimes be made larger (by ribbing it, for example), or its strongly heated surfaces should be cooled with a fan.

The designing of machine elements which are to operate at high temperature requires special calculations, since in these cases the behaviour of metals under stress differs from their behaviour at normal temperature. At higher temperature the phenomenon of metal creep and relaxation of stress are of especial importance.

*Creep* is the property of metal to deform slowly and continuously at a constant stress.

The quantitative characteristic of creep is the *creep limit*, which is the maximum continuously acting stress at which the velocity of creep finally becomes zero.

*Relaxation* is the spontaneously attenuated decrease in stress in a component at a given constant deformation. The phenomenon of relaxation is observed in tightened bolted joints of flanges (the drop in the magnitude of the tightening stress with constant deformation of the bolts), in interference joints of turbine discs and the shaft (spontaneous decrease in fitting stresses), etc.

## CHAPTER II

### SELECTION OF MATERIAL

The selection of materials is an important stage in the process of designing, and for it a good knowledge of their properties and behaviour during operation and manufacture is required.

The following materials are used in mechanical engineering: steel, cast iron, nonferrous metals and alloys, powder-metals and nonmetallic materials. In the Soviet Union the initial composition

and properties of almost all materials employed in mechanical engineering conform to state standards. The properties they acquire as a result of different kinds of heat, thermochemical treatment and machining are outlined in reference books.

The chemical composition, properties and methods of treatment of the main types of materials are outlined in courses of metallography, technology of metals, and technology of engineering industry.

The general requirements which materials must satisfy under operating conditions were given above. Special requirements will be considered further in connection with the theory and functioning of respective parts.

At all stages in its development mechanical engineering has stimulated the appearance of new materials with such properties as would ensure continued progress. For example, the development of aircraft construction brought into being high-strength light alloys, the development of jet engines created heat-resistant alloys, etc. Together with the creation of new materials the operating qualities of the existing materials have been continuously improved. For example, the ultimate strength in tension of structural steel, which before hardly reached 60 kg/mm<sup>2</sup>, has increased to 180 kg/mm<sup>2</sup>, i.e., threefold, due to the application of various alloy elements and heat treatment\*. The strength of cast iron has increased even more. Fifty years ago the ultimate strength in tension of cast iron, as a structural material, never rose above 10-15 kg/mm<sup>2</sup>; today effective methods of alloying and modifying have increased its ultimate strength to 80 kg/mm<sup>2</sup> and over, i.e., 5-8 times. The increase in the strength of modified cast iron and cast iron with globular graphite in the cast structure while still preserving the features inherent in the material—high cyclic resilience, high limit of endurance, indifference to stress concentration points, good castability and also low cost—makes cast iron an extremely valuable material. It is now even employed for the manufacture of crankshafts, which formerly were made exclusively of steel.

These examples show that the various recommendations on assigning definite grades of materials to definite components are of a *temporary nature*. Such recommendations should be regularly revised taking into account the appearance of new materials and new data on the properties of materials employed before\*\*. It is difficult to

---

\* There are experimental grades of steel with the ultimate strength in tension of  $\sigma_{ult} \approx 240$  kg/mm<sup>2</sup>.

\*\* In recent years titanium alloys have become more and more widely used; they have apparently an immense future: they are 2-3 times stronger than aluminium alloys, 5 times stronger than magnesium alloys and exceed in strength some alloy steels. Titanium is half the weight of steel and resists corrosion better than stainless steel.

find in the development of mechanical engineering during the last 15-20 years more rapid progress than that achieved in the sphere of the application of various materials.

When selecting materials for the component of a machine we proceed from the following main assumptions:

1. From an operational point of view the material should ensure the proper functioning of the element in the unit.

2. From a production point of view the material should require as little labour as possible for the manufacture of the component.

3. From an economical point of view the material should favourably affect the production cost of the component, which besides the cost of the material itself also includes all other production expenses.

A substantiated choice of material for a component with full consideration of these premises is a complicated technical and economic problem. Its solution is made difficult also by the fact that the form and size of a component made from various materials change in accordance with the mechanical properties and production possibilities of the corresponding material.

For example, a pulley 100 mm in diameter for  $n=5,000$  rpm can be made from cast iron or aluminium. Which material should be chosen? For such a velocity of rotation the pulley should be finished all over to balance it correctly. Since the speed of cutting aluminium is 8-10 times greater than that of cutting cast iron the reduction in the cost of machining and expenditures involved not only doubly compensates for the higher cost of the material but also reduces the cost of the aluminium pulley as compared with a cast-iron one by 25%. In this case therefore the pulley should be made from aluminium.

In a general case the material can be correctly chosen only by comparing several versions. This is actually done in important cases (for example, when selecting material for the housing of a toothed reduction gear; deciding whether it should be made from cast iron or steel) when the choice of a material for the component determines the design of a complex unit, its weight, size and cost.

In some cases the choice of material is facilitated by using a system of indices which characterise not one property of the material disregarding the others (for example, only strength, endurance or rigidity) but a combination of several properties. The structure of these indices changes in accordance with the requirements which the design must fulfil—for example, minimum cost or minimum weight of the component at a given strength, endurance, rigidity, etc. As a rule, use is made of the indices in which the initial value is the weight of the component, since for many machines weight is an independent important factor indicating the efficiency of the design; besides, weight, together with the cost of unit weight, gives an idea of the amount of metal in the designed unit and its cost; both factors are important in all cases.

Below we calculate these indices for some of the most important cases.

**Comparative Evaluation of Various Materials by Weight.** Let a bar  $L$  in length be subjected to tension by the force  $P$ ; the specific weight of the material is  $\gamma$ , the ultimate strength in tension— $\sigma_{ult}$ , the margin of safety— $n$ . The area of the cross-section of the bar  $F$ , its volume  $V$  and weight  $G$  are determined from the following expressions:

$$F = \frac{P}{[\sigma]_t} = \frac{nP}{\sigma_{ult}}; \quad V = FL; \quad G = V\gamma = nPL \frac{\gamma}{\sigma_{ult}}.$$

Obviously, when  $L$ ,  $P$  and  $n$  are the same, the relation between the weights of two bars from various materials ( $\gamma'$ ,  $\sigma'_{ult}$  and  $\gamma''$ ,  $\sigma''_{ult}$ ) will be

$$\frac{G'}{G''} = \frac{\sigma''_{ult}}{\gamma''} : \frac{\sigma'_{ult}}{\gamma'}. \quad (37)$$

Thus, the weights of bars of equal strength (in tension) are inversely proportional to the ratio  $\sigma_{ult}/\gamma$ . The greater this ratio is the more advantageous is this material in respect of weight. The ratio  $\sigma_{ult}/\gamma$  is called the *unit strength*. It is one of the main criteria of the quality of the material in designs where weight is the prime consideration.

If calculations are done by the limit of endurance,  $\sigma_{-1t}$  analogous reasoning may be used to show that the utility of the material is determined by the ratio  $\sigma_{-1t}/\gamma$ , which is called the *unit endurance* of the material.

For cases of bending and torsion of bars with geometrically similar cross-sections the relations are different

$$\frac{G'}{G''} = \frac{\sigma_{ulb}^{\frac{2}{3}}}{\gamma''} : \frac{\sigma_{ulb}^{\frac{2}{3}}}{\gamma'} \quad \text{and} \quad \frac{G'}{G''} = \frac{\tau_{ul}^{\frac{2}{3}}}{\gamma''} : \frac{\tau_{ul}^{\frac{2}{3}}}{\gamma'}. \quad (38)$$

The weight criteria for the quality of the material in bending and torsion are ratios  $\sigma_{ulb}^{\frac{2}{3}}/\gamma$  and  $\tau_{ul}^{\frac{2}{3}}/\gamma$  respectively. It can be seen from the comparison of the expressions (37) and (38) that in bending and torsion high strength influences the economy in weight to a less degree than in tension, since smaller cross-sections possess a much lower section modulus. It is also clear that the expression (38) holds only for the case when the cross-sections of the bars are geometrically similar.

As was shown above rigidity is very important for many components.

In the case of tension (or compression) the weights of bars of equal rigidity, i. e., with the same ratios of  $P/\lambda$  are related by the following expression

$$\frac{G'}{G''} = \frac{\gamma' F'}{\gamma'' F''} = \frac{E''}{\gamma''} : \frac{E'}{\gamma'} . \quad (39)$$

The ratio  $E/\gamma$  which characterises the quality of the material for components which should chiefly satisfy requirements of rigidity is called *unit rigidity*. Since the modulus of elasticity of steel varies within very narrow limits ( $2.0 \times 10^6$ - $2.2 \times 10^6$  kg/cm<sup>2</sup>) it is not rational to use, for example, alloy steel for components in which rigidity is of utmost importance. Of the materials employed in mechanical engineering the greatest modulus of elasticity is observed in hard alloys ( $5 \times 10^6$ - $6 \times 10^6$  kg/cm<sup>2</sup>).

The ability of the material to resist the action of impact load is characterised by the work spent on elastic deformation of the component. This work, referred to the unit of volume of the bar, is depicted tentatively on the tension diagram in the form of a right-angled triangle with height equal to the limit of proportionality  $\sigma_{pr}$  and with base equal to the unit deformation on attaining this limit ( $e = \sigma_{pr}/E$ ). The work of elastic deformation per unit of volume of the bar (area of the triangle) is equal to  $\Delta = \sigma_{pr}e/2 = \sigma_{pr}^2/2E$ . The sections  $F'$  and  $F''$  of two bars showing equal impact strength made from different materials with geometrically similar sections and with the same length are inversely proportional to the factor  $\sigma_{pr}^2/E$  and the weights of the bars are

$$\frac{G'}{G''} = \frac{\sigma_{pr}''^2}{E''\gamma''} : \frac{\sigma_{pr}'^2}{E'\gamma'} . \quad (40)$$

The factor  $\sigma_{pr}/E\gamma$  is the *unit impact strength* characterising the advantages in respect of weight of bars of equal impact strength made from different materials.

In addition to the indices calculated above this method can also be employed to obtain other indices characterising the material with respect to its volume, cost, sensitivity to temperature fluctuations, centrifugal effects, etc.

Table 5 shows by way of comparison the values of unit strength and rigidity of some materials.

**The Principle of "Local Quality" and Its Utilisation in the Selection of Materials.** Various surfaces and volumes of the same component have sometimes to satisfy different requirements: friction or antifriction properties, wear resistance, surface or volume strength, rigidity or flexibility, resistance to corrosion, thermal conductivity, shock-absorbing capacity, etc.

The different requirements are explained by the different conditions in which respective machine elements operate.

Table 5

Unit Strength and Rigidity of Some Materials

Material	Grade	Specific weight $\gamma \times 10^3$ in kg/cm <sup>3</sup>	Modulus of elasticity $E$ in kg/cm <sup>2</sup>	Ultimate strength in tension $\sigma_{ult}$ in kg/cm <sup>2</sup>	Unit strength		Unit rigidity in tension $E/\gamma$	Unit impact strength $\frac{\sigma_{pr}^2}{E \times \gamma}$
					in tension $\sigma_{ult}/\gamma$	in bending $\frac{\sigma_{ult}^2}{2E\gamma}$		
Steel:								
low-carbon . . . . .	20	7.8	$2.1 \times 10^6$	4,000	$5.1 \times 10^5$	$3.2 \times 10^4$	$2.7 \times 10^8$	410
medium-carbon . . . . .	45	7.8	$2.1 \times 10^6$	6,000	$7.6 \times 10^5$	$4.2 \times 10^4$	$2.7 \times 10^8$	1,070
alloy . . . . .	40X	7.8	$2.1 \times 10^6$	10,000	$12.7 \times 10^5$	$6.0 \times 10^4$	$2.7 \times 10^8$	3,900
	30XГCA	7.8	$2.1 \times 10^6$	16,000	$20.4 \times 10^5$	$8.1 \times 10^4$	$2.7 \times 10^8$	7,800
Cast irons:								
gray cast iron . . . . .	ЧЧ21-40	7.2	$1 \times 10^6$	2,100	$2.9 \times 10^5$	$3.5 \times 10^4$	$1.4 \times 10^8$	220
high-strength cast iron . .	ВЧ40-10	7.2	$1.5 \times 10^6$	4,000	$5.5 \times 10^5$	$5.1 \times 10^4$	$2.1 \times 10^8$	530
Duralumin . . . . .	Д6Т	2.8	$7.5 \times 10^5$	4,200	$14.7 \times 10^5$	$9.14 \times 10^4$	$2.6 \times 10^8$	3,300
Magnesium-base alloy . .	МЛ4	1.8	$4.3 \times 10^5$	2,400	$13.4 \times 10^5$	$9.8 \times 10^4$	$2.4 \times 10^8$	1,850
Pine-wood . . . . .	—	0.5	$1.1 \times 10^5$	830	$16 \times 10^5$	$14.4 \times 10^4$	$2.2 \times 10^8$	3,600
Fabric laminated plastics	ЛТ	1.3	$1 \times 10^5$	850	$6.5 \times 10^5$	$10 \times 10^4$	$0.8 \times 10^8$	1,600

In many cases it is completely impossible to select for the component a material which would simultaneously satisfy all these requirements. Even if such a material exists it is as a rule expensive.

Formerly, when the operating conditions of components were not so severe as at the present, compromise solutions could be employed to select the materials which only partly satisfied all the necessary requirements. Today such solutions are inadequate and in these cases the principle of *local quality* indicates the most rational and progressive solution. Its essence can best of all be illustrated by concrete examples.

1. The blades of hydraulic turbines should possess adequate strength and resistance to corrosion. To satisfy these requirements the blades of all large propeller-type turbines were until recently made from expensive stainless steel which is difficult to machine. However, other solutions are also possible. In actual fact only the surface of the blades is required to resist corrosion; therefore, the blades need not be made entirely from stainless steel; they can be made from carbon or less expensive alloy steel and then faced with thin coatings of stainless steel, as for example, are the experimental blades in one of the turbines of the Tsimlyanskaya hydroelectric station, which required half the usual time for manufacture and cost 30% less. This design of the blades has now also been accepted for the turbines of other hydroelectric power stations under construction. The saving achieved in this manner is illustrated by the following figures: in the turbines of the Kuibyshev hydroelectric station the weight of each blade is 18 tons and there are 6 blades in each turbine.

2. The material of the friction surfaces of friction clutches should satisfy various requirements (see p. 503). There is no homogeneous material which can satisfy them all. Powder-metal materials are most effective in this respect. The approximate composition of the charge of copper-base powder-metal friction materials is the following: copper 60-70%, iron 5-10%, lead 5-15%, tin 5-15%, carborundum, quartz and other abrasives 2.5-7%. The respective roles of these components are:

a) *copper* effectively removes heat and requires no high pressures for caking;

b) *iron* and abrasive materials serve to increase the coefficient of friction;

c) *lead* melts and forms a thin lubricating film which protects the working surfaces against scoring.

Powder-metal friction materials are highly brittle. Therefore, they are applied in a thin layer, 0.2 mm thick, onto a stiff steel or cast-iron base.



In this way, artificially combining various elements, we obtain a component each point of which possesses the required properties.

3. In recent years, despite the increased loads transmitted by gears, the high-alloy steels used in their manufacture have been replaced in many cases by carbon or low-alloy steel. This is quite natural: the gear disc, containing the main mass of metal, experiences only negligible stresses; the teeth are the elements which carry the heaviest load. They should be highly resistant, have a high strength of the working surfaces and a high limit of endurance in bending. The first is obtained by induction *hardening* of the active profile of the teeth and the second by *strengthening* the surface at the tooth root and creating at this point residual compressive stresses by means of cold hardening.

Thus, in this case also the effect is obtained by *changing locally* the properties and state of the component material in the required direction.

4. In piston aircraft and automobile engines the crankshaft bearing bushings are among those components which resist the severest loads, and whose qualities frequently limit the forcing of the engines. Let us examine in what way the design of the shells of these bearings was developed and improved.

a) To begin with the shells were made entirely from tin bronze—the best among the antifriction materials known at that time;

b) when special bearing alloys—babbitts possessing higher antifriction properties than bronze—came into use they began to be employed for lining the working surfaces of bronze bearing shells;

c) but since the role of bronze had been in this case relegated to the second place (it had to serve as a bed for babbitt) it could be replaced by sheet steel, which allowed the important transition to thin-walled shells to be made. In this case, for a better adhesion to babbitt, the steel was precoated with copper (by the galvanic method);

d) while an excellent antifriction material for small and medium loads, babbitts cannot withstand very high pressures and temperatures. This is due to their low yield point and low limit of endurance, which in addition rapidly decrease as the temperature increases. For this reason a change over was made to steel shells lined with lead bronze and not with babbitt;

e) antifriction properties of lead bronze are much inferior to those of babbitt, primarily because of its greater hardness and poorer affinity to oil. A further growth in unit pressures and sliding velocities resulted in the development of stratified bearings designed as follows. Steel is lined with an intermediate layer of lead bronze after which knurling is carried out, which leaves grooves on the surface of the bronze (Fig. 24). The corrugated surface obtained in

this manner is lined with a layer of lead babbitt and machined. As a result, recesses filled with babbitt are formed, whose area comprises from 25 to 60% of the total surface of the bearing; the babbitt lining is about 0.5 mm thick. When the bearing is to operate at high temperatures the heat resistance of the upper layer is improved by a coating of indium.

Thus, the development of the designs of bearing shells has progressed from a solid bronze shell about 5 mm thick to a thin-walled stratified metal shell only 2 mm thick. In this thin body each metal is assigned its own strictly limited role.

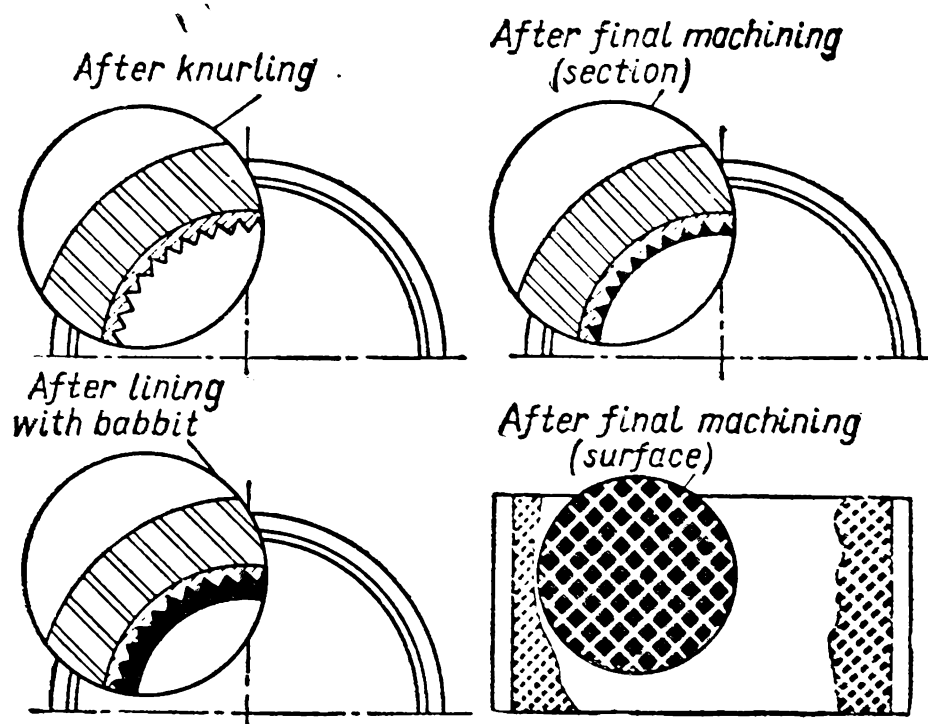


Fig. 24

Such examples could be continued. Cutters in which formerly the holder and the cutting tool were made integral now have brazed-on or mechanically fastened plates from high-speed steel, sintered ceramic powders or hard alloys; machine-tool guide-ways formerly made from cast iron and then as renewable steel designs are now manufactured from plastics or cast iron with a hardened surface. All this illustrates the same principle of local quality.

The various methods of working metal employed today, and in particular, various methods of coating, heat and thermochemical treatment, mechanical strengthening by means of creating artificially residual stresses, open up bright prospects for directed influence on design with a view to creating the required properties in each cross-section and at each point.

The majority of the above methods concern the processing of the surface. This is explained by the fact that almost all kinds of failure—from corrosion to fatigue fracture—develop on the surface of the component and then penetrate inside, spreading over the

entire cross-section. It is natural therefore that the efforts of designers have been directed towards the protection, strengthening and changing of the properties of the surface layers.

For the rational designing of machine elements the above production methods should be thoroughly mastered.

**Reduction in the Range of the Materials Employed.** When selecting materials for the components of the designed machine, alongside other considerations, it is necessary to take into account the difficulties of supply and production, due to the extremely wide range of materials used which should be decreased as much as possible. A reduction in the number of grades of steel and other materials employed for the manufacture of machine elements at one plant has a number of advantages.

They are the following:

a) a reduction in the number of grades and range of materials used by the plant considerably facilitates the supply of the plant with materials and reduces its cost, since the materials can be loaded onto freight cars directly at iron and steel works without subsequent reloadings;

b) the material of each grade should be stored and accounted for separately in the storage area and shop. A reduction in the number of grades simplifies storage and stock-taking and requires less storage space;

c) material of each grade requires special methods of machining and heat treatment. A reduction in the number of grades enables the workers to study and master the most rational modes of treatment better; the work of heat-treatment shops is especially simplified;

d) a reduction in the number of grades of the materials used decreases the amount of wastage, which otherwise may be due to the employment of inadequate material and inadequate heat treatment.

In practice the grades and types of the materials used are reduced by compiling special grade lists and prohibiting the use of the materials not included in these lists if not absolutely necessary.

### CHAPTER III

## STANDARDISATION OF MACHINE ELEMENTS

Standardisation establishes obligatory norms to which different types, parameters (for example, dimensions) and qualitative characteristics of items should conform. It limits the number of types, dimensions, etc., of the items produced and reduces them to a definite number of models. In this two stages should be distinguished: a) the creation of models, i.e., the establishment of properties

which a given item should possess and b) the reduction of the number of these items, processes and methods to a rational minimum.

*Normalisation* and *unification* are terms closely related to standardisation.

In the Soviet Union *normalisation* is standardisation carried out by a separate department or plant.

*Unification* is the elimination of a superfluous diversity of items by reducing their types to the minimum, the utilisation in new machines of components and units borrowed from previously designed and tested machines. In this case the unified items are not altered. Both standardised and nonstandardised items can be unified.

Standardisation is of prime importance in all branches of modern industry especially in mechanical engineering. No other branch of industry possesses such a variety of types and sizes of items which may be required in single quantities (heavy machine tools, presses) or in millions (sewing machines), such a wide range of materials used and such a diversity of production processes. It is only standardisation (and also normalisation and unification) that enables all the required machines to be manufactured comparatively quickly and economically despite this diversity.

The importance of standardisation lies in the following:

1. The reduction of a large number of various types and dimensions of identical components to a rational number makes it possible to organise the mass production of standardised components by the most progressive methods. In this case the consumption of labour, expenditure of materials and finally the cost of components are considerably decreased.

2. The standardisation of specifications and methods of testing machine elements improves quality and increases operating capacity and service life.

3. The application of standard elements and especially of units decreases the time and effort needed to master new machines, because it is no longer necessary to design, manufacture and finish these units and elements.

4. Standardisation facilitates the servicing of machines and simplifies maintenance, which can then be carried out at nonspecialised plants because the faulty standard parts (for example, screws, keys, antifriction bearings, belts, etc.) can be easily replaced by spare ones.

As regards machine elements Soviet standards extend to the proportions of all ordinary fasteners; elements of toothed and worm gears and screw drives; the diameters of shafts; the main parameters, specifications and testing methods of antifriction bearings, driving belts and chains and also the main dimensions of their pulleys and

chain sprockets; dimensions of certain types of couplings and many other parts.

In view of the great national importance of standardisation the designer, besides making extensive use of the available standards, should also strive to create favourable conditions for the standardisation of new components and units.

As a first step in this direction new designs of machine should utilise components and units designed for other machines, which have already been tested and put into operation. When developing a new design the designer should introduce only those new components and units which make for better productivity and more convenient servicing of the machine. All other components and units which do not in principle affect these two main indices should not be altered. Replacement of *all* or *most* of the components when changing from one design to another of the same type is usually the result of lack of skill and attention or carelessness on the part of the designer.

If for some reason or other an available unit having a similar purpose cannot be utilised in a new machine it is expedient to have at least the same connection dimensions of these units to facilitate their future normalisation.

Unification and subsequent normalisation is especially effective when a group of machines for the same or similar purposes but of different dimensions are designed simultaneously. In this case it is possible to use a small number of initial models to create a large group of various machines.

An analysis of the design of various machines shows that, despite their external differences and sometimes different purposes, they consist of units which perform essentially the same functions. By making such units as independent assemblies, a strictly limited number of such assemblies can be used to obtain machines of varying uses. Simultaneously, this considerably facilitates the designing of new machines and reduces the cycle of machine assembly.

Fig. 25, *a* shows an aircraft stripped down into separate units: fuselage, wings, tail, engine and landing gear. Fig. 25, *b* shows the separate units of a multi-spindle drilling machine. Identical units are marked by the same figures.

The use of preferred numbers is very important in standardisation and unification.

**Preferred Numbers.** These are specially selected values recommended for use in all branches of the national economy. They specify the proportions of items and structures, power, load-carrying capacity, speed and all other parameters used in production and expressed numerically. An international standard for preferred numbers has been recently approved. Its main part is Table 6 given below.

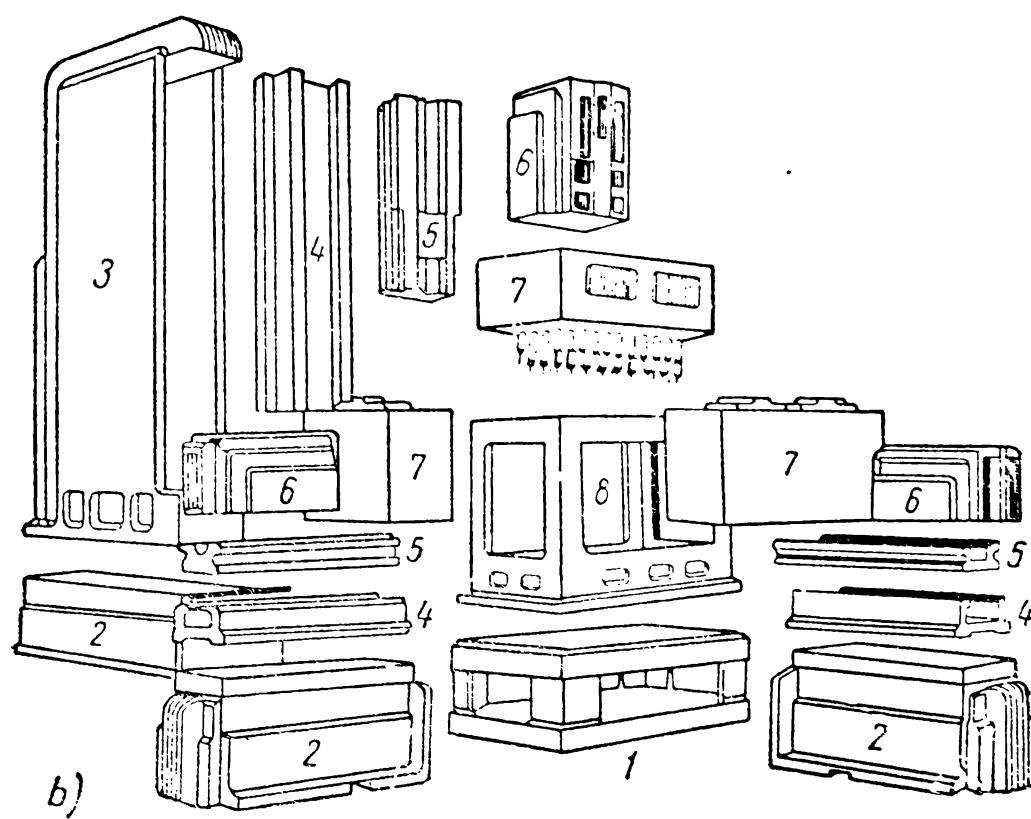
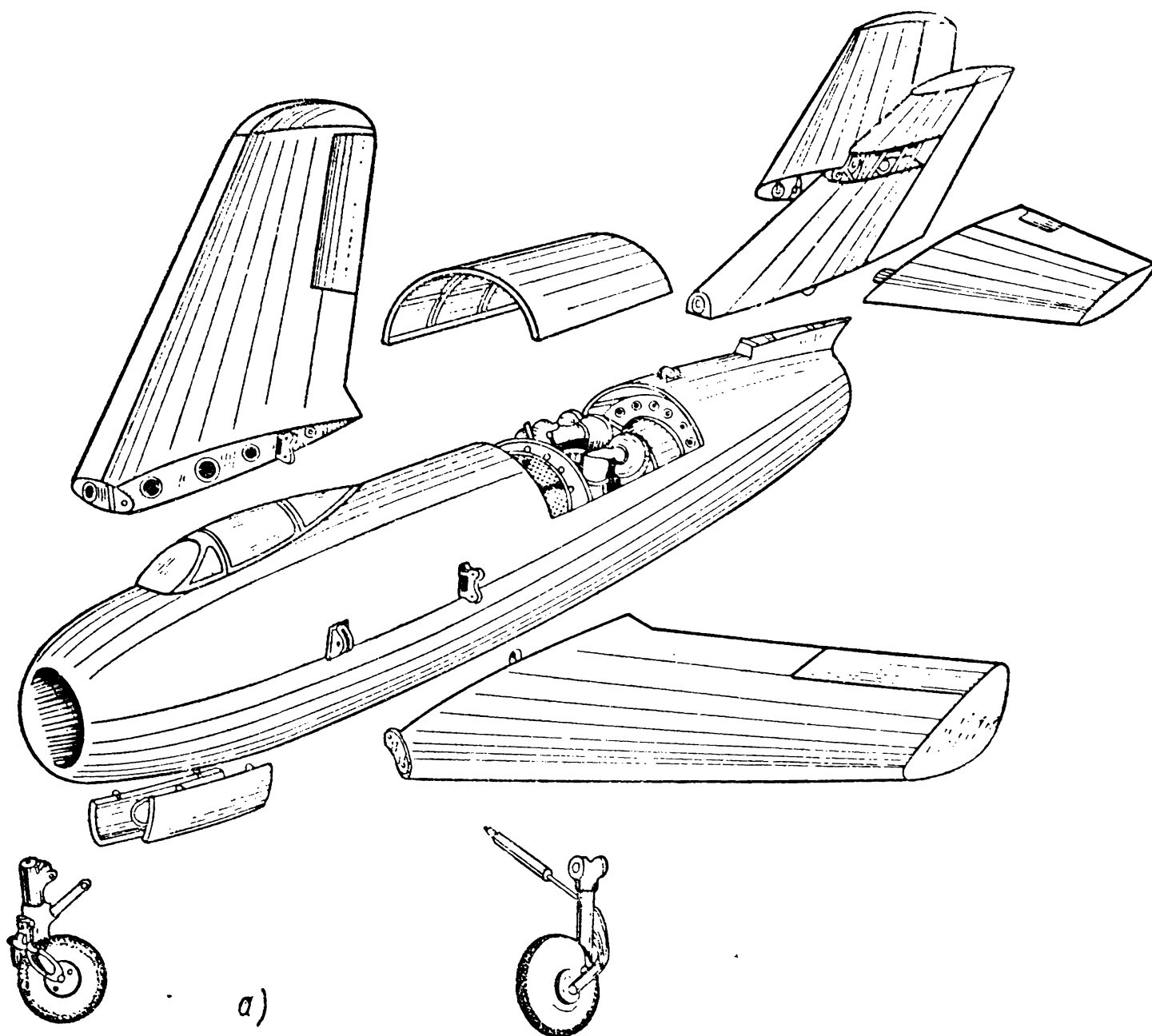


Fig. 25

Table 6

Ordinal numbers of the series	Series of preferred numbers			
	Series 5	Series 10	Series 20	Series 40
0	1.00	1.00	1.00	1.00
1	—	—	—	1.06
2	—	—	1.12	1.12
3	—	—	—	1.18
4	—	1.25	1.25	1.25
5	—	—	—	1.32
6	—	—	1.40	1.40
7	—	—	—	1.50
8	1.60	1.60	1.60	1.60
9	—	—	—	1.70
10	—	—	1.80	1.80
11	—	—	—	1.90
12	—	2.00	2.00	2.00
13	—	—	—	2.12
14	—	—	2.24	2.24
15	—	—	—	2.36
16	2.50	2.50	2.50	2.50
17	—	—	—	2.65
18	—	—	2.80	2.80
19	—	—	—	3.00
20	—	3.15	3.15	3.15
21	—	—	—	3.35
22	—	—	3.55	3.55
23	—	—	—	3.75
24	4.00	4.00	4.00	4.00
25	—	—	—	4.25
26	—	—	4.50	4.50
27	—	—	—	4.75
28	—	5.00	5.00	5.00
29	—	—	—	5.30
30	—	—	5.60	5.60
31	—	—	—	6.00
32	6.30	6.30	6.30	6.30
33	—	—	—	6.70
34	—	—	7.10	7.10
35	—	—	—	7.50
36	—	8.00	8.00	8.00
37	—	—	—	8.50
38	—	—	9.00	9.00
39	—	—	—	9.50
40	10.00	10.00	10.00	10.00

The figures indicated in the Table can be increased or decreased 10, 100, 1,000, 10,000 and 100,000 times.

Let us assume that we have to establish the power needed for tractors, which, when produced in five types, would fulfil all the tasks of agriculture. Using series 5 of the preferred numbers we take for their powers 10, 16, 25, 40 and 63 h. p., or using series 10—the powers 12.5, 20, 31.5, 50 and 80 h. p. According to the preferred numbers, the load-carrying capacity of automobiles should be 1.6, 2.5, 4.0, 6.3 and 10 tons, of dump lorries—4.0, 6.3, 10, 16, 25, 40 and 63 tons. The greater the quantity of production the greater can be the number of typical sizes. For limited quantities use is made of series 5 of the preferred numbers; as the scale of production is increased, change over is made to the series 10, 20 and 40.

Together with the preferred numbers, standards for normal diameters and lengths, materials, tolerances and fits, surface finish, etc., are also very important in mechanical engineering.

#### CHAPTER IV

### PRODUCTION SOUNDNESS OF MACHINE ELEMENTS

A *production-sound* design is one which ensures the assigned operating characteristics and which at the same time can be produced in the minimum time with the minimum labour and cost.

The use of the term «production sound» in this sense began shortly before the war and has only now been fully accepted by designing bureaus although machine designers always strove to create economical designs. This is explained by the fact that in the past there was a much simpler relation between the design of a machine and its economical manufacture. Production possibilities in mechanical engineering before the twenties and thirties were highly primitive, the range of materials and the methods of changing their properties very limited and, finally, machines were produced, with rare exceptions, in such small numbers that there was no noticeable difference between the designs for various scales of production. When only one method (process) existed for processing a component production soundness was quite naturally understood to mean the possibility of manufacturing the designed part in general, and also the possibility of assembling a unit or a machine. Today many methods differing in the principles of processing and equipment used may be employed to give a component the required form. Many elements with the same functions can be made from various materials—ranging from ferrous metals to plastics. Components made even from the same material can be given different properties by methods of chemical and heat treatment, or by means of mechanical strengthening or coating. The scale of machine production changes from limited quantity production (for example, of special-purpose and



experimental machines) to large-scale production when the number of the items produced runs into hundreds of thousands every year (for example, machines for domestic use). It is clear that under these new conditions it is much more difficult to make a design production sound than it was 20 or 30 years ago. To select the best version from among a large number of designs for given concrete conditions is a complex task. Its solution can be undertaken only by a designer well versed in the possibilities of modern techniques. At the same time the designer should constantly cooperate with production, foundry, forging and welding engineers and other specialists and receive their assistance. Below we briefly examine the main requirements which the designs of machine elements must fulfil with respect to their production soundness.

1. *Correspondence of the design to the scale and conditions of production.* It is clear from what has been said above that, generally speaking, the concept of production soundness is closely bound up with conditions of production. A design which is completely production sound under some conditions, particularly with one scale of production, should, as a rule, be revised and in some cases radically altered to suit another scale and, correspondingly, another organisation of production.

Suppose, for example, collinear bore holes for shafts and bearings have to be made in the walls of a housing. The question arises: which location of the bores will be most satisfactory?

Depending on the scale of production and the assigned method of machining the answer to this question will be different. It is natural to assume that in *limited quantity production* the bore holes will be machined according to the layout marks on a horizontal boring mill in a single operation by normal boring bars (replacing the cutters and reamers); in *batch production*—on a horizontal boring mill using a jig by a set of special bars with the tools set up to the size of the bore hole combining as far as possible the working of bore holes of various diameters; in *mass production*—on a special double-side multi-spindle boring machine with the use of compound tools. Obviously, a location of the holes, which is satisfactory with one method, may prove very unprofitable with another.

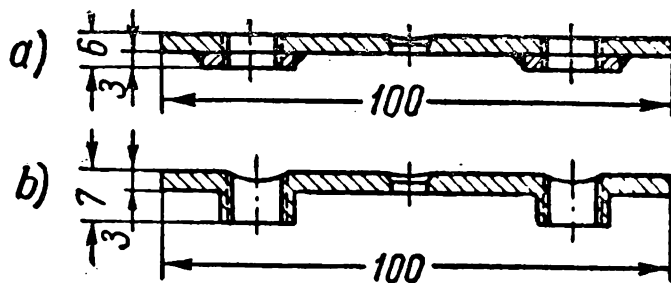


Fig. 26

Another example. In tyre-pneumatic clutches use is made for fastening purposes of strips cut from 3 mm sheet. Originally they were made with two welded threaded bosses (Fig. 26, a). When the demand for strips rose to nearly 10,000 a month the design had to be altered and resort was made to die-forming with the simultaneous drawing of bosses (Fig. 26, b). A cold-formed strip required 67 times less labour than the welded one.

Therefore, *there are no* production-sound designs generally, i. e., irrespective of the concrete conditions of production.

Similarly, the production soundness of a component cannot be evaluated in isolation from the production soundness of the machine as a whole. It may happen that easier machining of the component will make the assembly of the machine or its subsequent maintenance more complex and will reduce the advantages of the improved production processes to nil.

The requirements enumerated below hold for all cases and all production conditions.

2. *Simplicity and expediency of design.* A simple design has as its aim to create a machine from the minimum number of simple parts of minimum weight by the most convenient methods of manufacture and ease of assembly. When selecting design forms of components use should be preferably made of simple surfaces (cylindrical and flat) and their combinations. Simultaneously an attempt should be made to decrease the number and area of machined surfaces to a minimum.

3. *Accuracy of manufacture and surface finish.* When specifying the accuracy for a component it must not be forgotten that although mean accuracy has increased more than fourfold during the last 50 years and limit accuracy tenfold (from 0.02 to 0.002 mm) an increase in the degree of accuracy inevitably involves more labour and increases

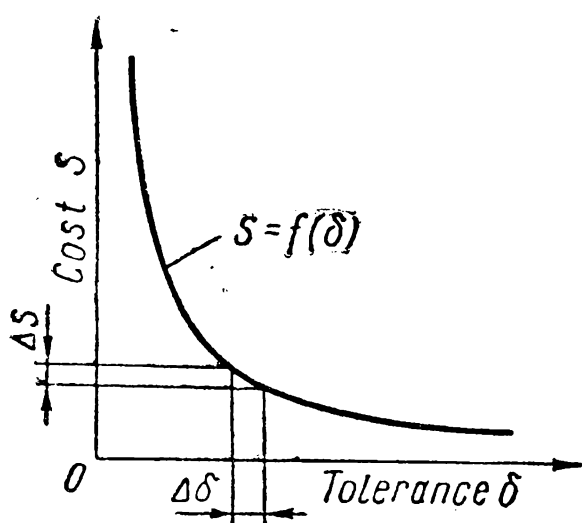


Fig. 27

the cost of manufacture. It has been established that for the majority of production processes the relation between the expenditure for production  $S$  and the required accuracy (manufacture tolerance  $\delta$ ) approximates a hyperbolic curve (Fig. 27): with a decrease in the tolerance, especially in the region of close tolerances, the costs rapidly increase.

Therefore, when high accuracy is not strictly necessary, it should not be stipulated; on the other hand, this factor should not be neglected when it is really important for effective operation.

In the same manner the degree of surface finish should be coordinated with the real operational conditions of the conjugate surfaces. Superfluous surface finish should be avoided since this involves costly finishing operations and requires special equipment.

For example, a connecting rod screw with the surface roughness of 0.4 mc costs 22% more than at 0.8 mc and 38% more than at 0.1 mc.

4. *Preparation of the blank.* The production soundness of a part

rial and the mode by which it is obtained. Machining costs much more than die-forging, metal-working or casting and entails the waste of the metal rejected in chips. The tendency is therefore to transfer the main amount of processing work from machine shops to preparation shops. The form and size of the blank should be as close as possible to the form and size of the finished part, so that machining need be employed only for surfaces demanding especial accuracy or finish.

The following main types of blank are used in mechanical engineering: normal or special rolled stock; open-die and closed die-forgings, metal-worked parts, castings (including permanent-mould, centrifugal and die-castings, etc.). Each of these types of blanks makes its own demands of production soundness on the design of components.

Table 76 gives the main rules for designing cast elements.

5. *Machining.* Machining accounts for a considerable share of the general amount of labour used to manufacture machine elements. Above some of the means of reducing the amount of labour spent on machining have been indicated (simple and rational form, correct specification of accuracy and surface finish, use of blanks requiring the minimum machining). In general those parts in which the amount of machining is reduced to the minimum are most satisfactory. In concrete cases the requirements of machining are extremely different.

They are determined by the character of the treatment and of the equipment used in the manufacture of the component.

Sometimes the form of the working surfaces of components is dictated by the possibility of employing highly productive machining methods. For example, involute surfaces are geometrically very complex and if simple forms are aimed at involute surfaces should be avoided. But highly accurate involute surfaces can be easily, automatically and very efficiently obtained by generation. Therefore, today involute form is used not only for the profiles of gear teeth but also with increasing frequency for the teeth of toothed clutches, Oldham couplings and splines. Square threads which are simple in form and have the advantage of less friction as compared with threads of other profiles, are not standardised and are hardly ever used since they cannot be obtained by the most productive method—milling—and, when cut on a screw-cutting lathe, involve higher costs than trapezoidal or vee threads.

The specific features of production requirements can be illustrated by shaft designing. These requirements can be formulated as follows:

1. *Minimum diameter of blank and minimum amount of chips removed in machining.* The difference between the diameter of a

main working portions of the shaft and its steps should be as small as possible; the diameters of the steps should equal the diameter of the blank (bar).

2. *A minimum number of steps.* Each step of the shaft, when turned or ground, means a new abrupt change and therefore requires a new measuring tool.

3. *The lengths of the shaft portions of various diameter should be as far as possible equal.* When this rule is observed the shafts can be most productively machined on multi-tool lathes.

4. *Provision should be made for a groove between the step to be ground and the face of the adjacent step.*

Grooves should be made only when they are permitted by the strength conditions when calculating the shaft for endurance.

5. *Maximum unification of the radii of curvature.* This reduces the number of round-nose cutting tools used and the number of tool resettings.

6. *Maximum unification of the width of keyways.* A change in the width of the keyway entails the replacement of the cutter and, consequently, the loss of time.

7. *Woodruff keys should be used instead of feather keys* when the strength conditions allow it. Feather keys should be handfitted while Woodruff keys should not.

8. *All keyways should be located along one generatrix of the shaft.* This allows the cutting of all keyways on key-milling machines without resetting the workpiece.

Standardisation, normalisation and unification are also among the main production requirements which machine elements should satisfy.

## PART TWO

# JOINTS OF MACHINE ELEMENTS

---

### CHAPTER V

## TYPES OF JOINTS AND THEIR PRINCIPAL FEATURES

**Types of Joints.** Every machine is made up of hundreds or often thousands of parts. To cite a few examples: the simplest coal-loader has more than three thousand parts, an automobile (together with the engine)—about 16 thousand, a vertical boring mill with the maximum turning diameter of up to 13 m—over 20 thousand, a V-2 missile—nearly 30 thousand, the hydraulic turbine of the Kuibyshev Hydroelectric Plant—over 50 thousand while a beam rolling mill requires 1.5 million components of 400,000 parts-list items.

In order to function in machines parts are joined together to form *sliding* and *fixed joints*. The first group includes joints which link, for example, a connecting rod and a crank pin, a shaft and shaft bearings or a toothed wheel and rack; the second group is illustrated by joints fastening the plates of a boiler together or with its dishes, a cover and bearing housing or a rod and piston.

While the presence of sliding joints is exclusively dictated by machine kinematics, fixed joints are employed to split the machine into units and sets and the units into parts and elements to facilitate or make possible the manufacture of the machine, its transportation and maintenance.

Engineering practice qualifies as *joints* proper only fixed joints. Depending on the reasons which make the dismountability of a work imperative, detachable or permanent joints are chosen. The general classification of the joints is given in Fig. 28.

*Permanent* joints do not allow a work to be disassembled without destroying the connecting components. As a rule, permanent joints are provided wherever the dismantling of a work is necessitated by production considerations—possibility, convenience or economy in manufacture. Such joints are made in locations where they usually either do not increase the weight of the work at all over the weight of an integral work or increase it negligibly.

Permanent joints can be made by mechanical methods—riveting, expanding, interference fits—and by physico-chemical adhesion—welding, brazing, soldering and adhesive bonding.

In modern engineering practice preference is given to the latter group—welded, brazed, soldered and, during the recent years, also adhesive-bonded joints. Adhesive bonds have been particularly developed in the aircraft industry—the appearance of honeycomb elements is entirely due to this method. In machine tools adhesives are employed to bond carriage guide-ways to beds, and in the automobile industry—to fasten friction linings to clutch discs and brake bands.

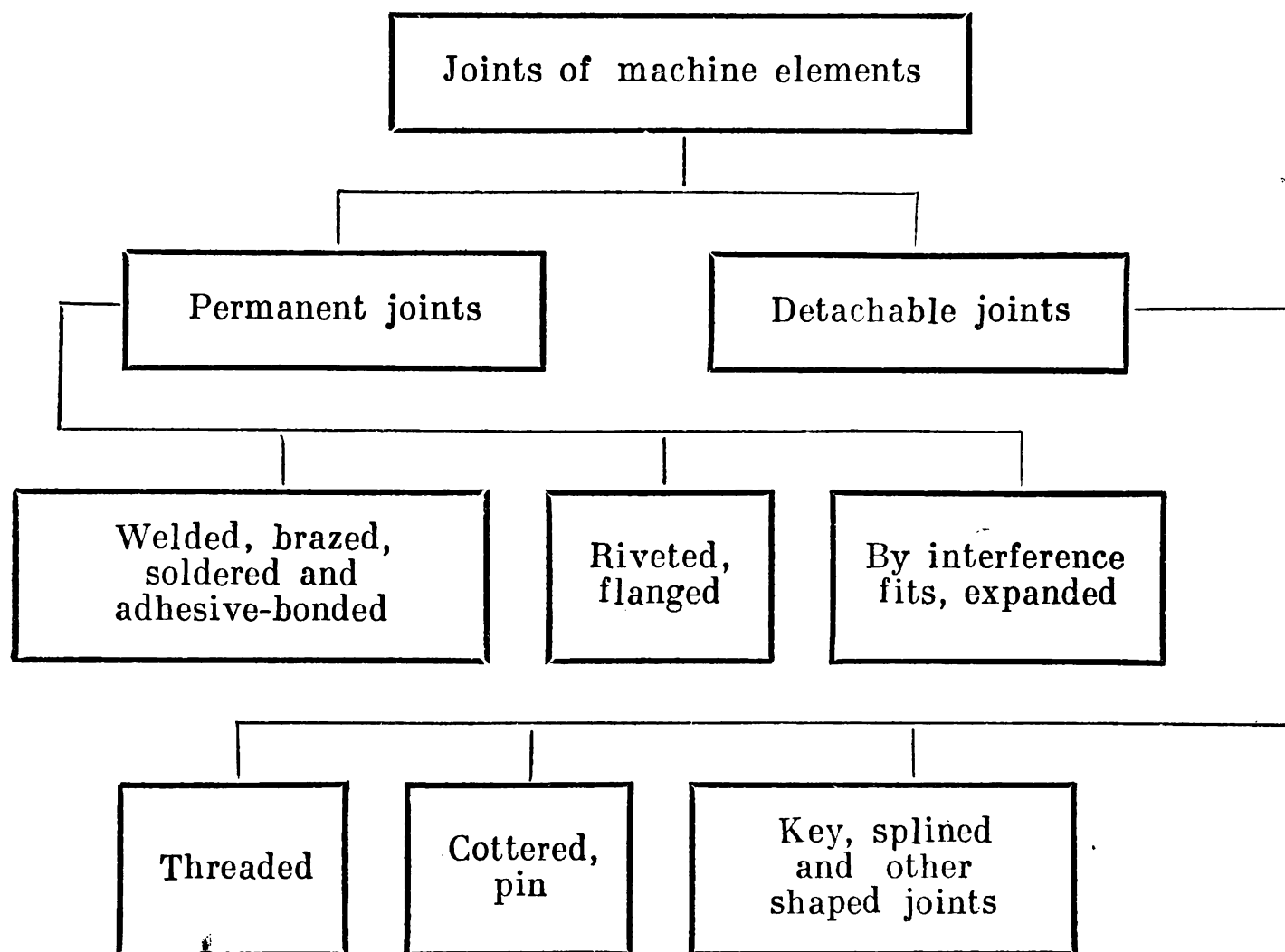


Fig. 28

The general course of machine elements examines joints made by welding, interference fits and riveting which are particularly widely used.

*Detachable* joints allow the disassembly of a unit without damaging the fastened elements and the connecting components. Here belong all types of threaded joints, pin and cotter joints as well as key, splined and others which can be called shaped joints.

Detachable joints can be subdivided into *design* joints, required by special features of the work (for instance, joints between elements made from different materials) and *operational* joints, required by considerations of ease of operation and sometimes of maintenance and transportation.

The designing of joints is an extremely responsible task since the majority of failures occur in a machine exactly at the joints.

As well as being economical, joints should satisfy, depending on their purpose, the requirements of strength, tightness and stiffness.

**Strength of Joints.** The strength of joints is evaluated from the magnitude of allowable limit load or from the factor of safety  $\varphi$ —the relation between this load and the limit load of the weakest of the fastened elements.

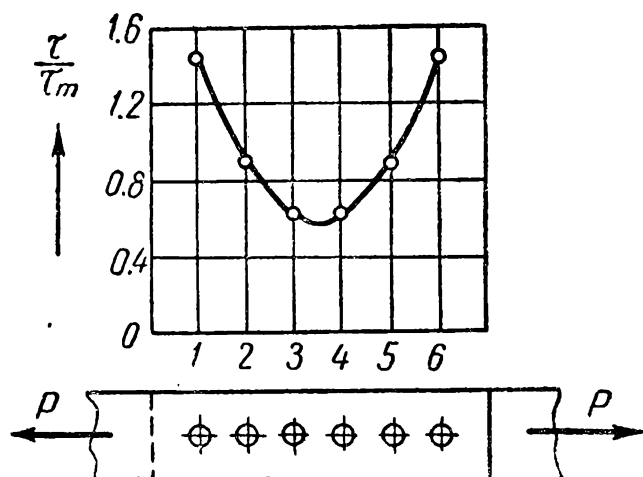


Fig. 29

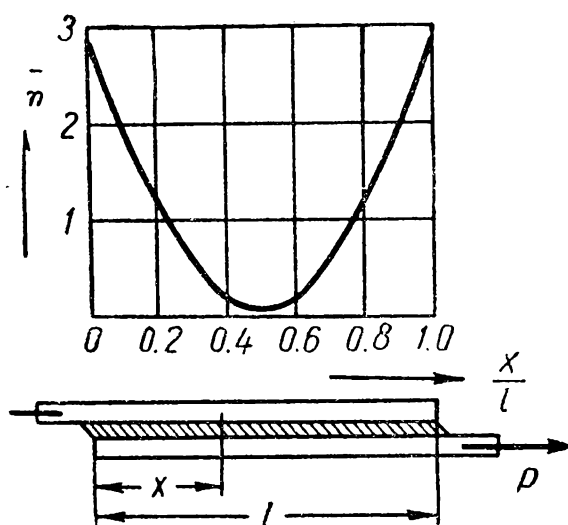


Fig. 30

The main task here is to bring the strength of the joint as near as possible to the strength of the elements to be joined. Thus, a joint with  $\varphi=0.9$  has a strength amounting to 90% of that of the weakest element.

In riveted joints  $\varphi$  is always below unity because the plates are weakened by rivet holes; in welded joints under similar conditions  $\varphi$  sometimes approximates unity. In special cases the presence of rivet holes or weld metal with poorer mechanical properties is compensated for by a corresponding increase in the cross-section of the elements in the region of the joint.

The degree of uneven distribution of stress along the section of the parts and the magnitude of stress concentration at individual points of the joint are extremely important in ensuring proper strength of joints subjected to varying load.

Numerous experimental and theoretical investigations have established that stress distribution between rivets (Fig. 29), along the length of a weld (Fig. 30), or through the thickness of a nut—between the threads of the bolt and nut (Fig. 31)—is not uniform. As a rule, stresses reach their maximum at the end points of joints where they can exceed several times the mean stress  $\tau_m$  determined by the magnitude of the load related to the joint area\*.

\* The problem of load distribution between the threads of a screw through the thickness of a nut was solved in 1902 by N. Y. Zhukovsky and that of force distribution between rivets—in 1878 by F. S. Yasinsky.

Despite the fact that riveted, welded and other joints as well as threaded joints differ in external appearance, the nature of non-uniformity in stress distribution is the same in all of them. As is shown below, this non-uniformity is due to two causes—the difference in deformation of the jointed elements and their flexure.

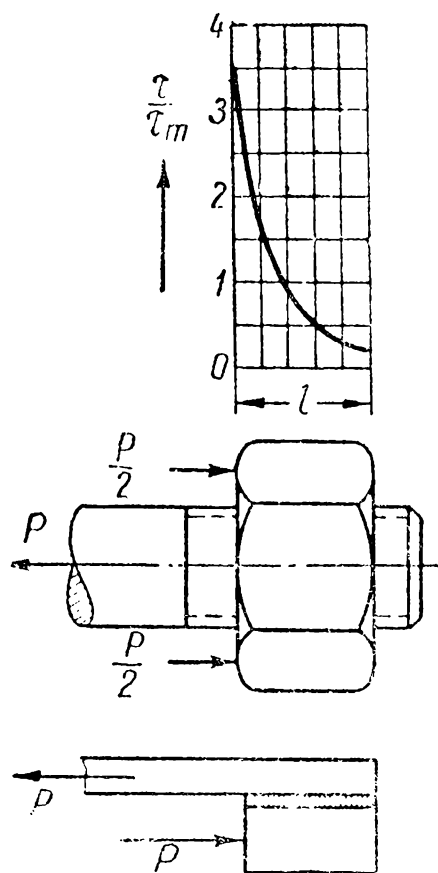


Fig. 31

*Difference in deformation.* Stresses arising as a result of different deformation of the jointed elements can be assessed from the comparison of the following joints: a) between very rigid unstrained elements and b) between expansible elements which do not flex. For the sake of clarity in Fig. 32 the thickness of the connecting layer in both cases is exaggerated (this layer is represented in a riveted joint by rivet shanks; in a welded, brazed, soldered or adhesive-bonded joint—by weld or brazed metal, solder and adhesive respectively; in a threaded joint—by the threads of bolt and nut). Unstrained elements shift as rigid beams while the connecting layer undergoes a shearing strain which is constant along the entire length of the joint (Fig. 32, b). However, directly at the overlap each of the connected elements is subjected to the action of the entire applied load  $P$  and gradually transmits it to the second element through the connecting layer. Thus the stress in

element  $I$  is at its maximum at point  $A$  and gradually diminishes until it reaches point  $B$  where it equals unity. Conversely, the stress in element  $II$  is highest at point  $B$  and decreases to zero at point  $A$ . This change in the stress is of secondary importance if elements  $I$  and  $II$  behave as absolutely hard bodies; if, however, they are expansible and their behaviour is governed by the laws of elasticity these elements develop deformations proportional to the acting stresses. This deformation is shown schematically in Fig. 32, c. The formerly vertically coincident (in Fig. 32, c) points  $B, B$  in the middle of the overlap and points  $C, C$  at the ends shift by unequal lengths  $e_1$  and  $e_2$ , the end displacements being considerably larger; therefore, maximum stresses in the connecting layer arise at both ends of the overlap. The longer the overlap (the joint in general), the greater the difference between the mean stresses—along the overlap length—and the maximum—at the ends. On this basis the length of joint is usually limited to some optimal value determined by the ratio between the pliability of the connecting and the connected elements. Thus, for example, the length of the

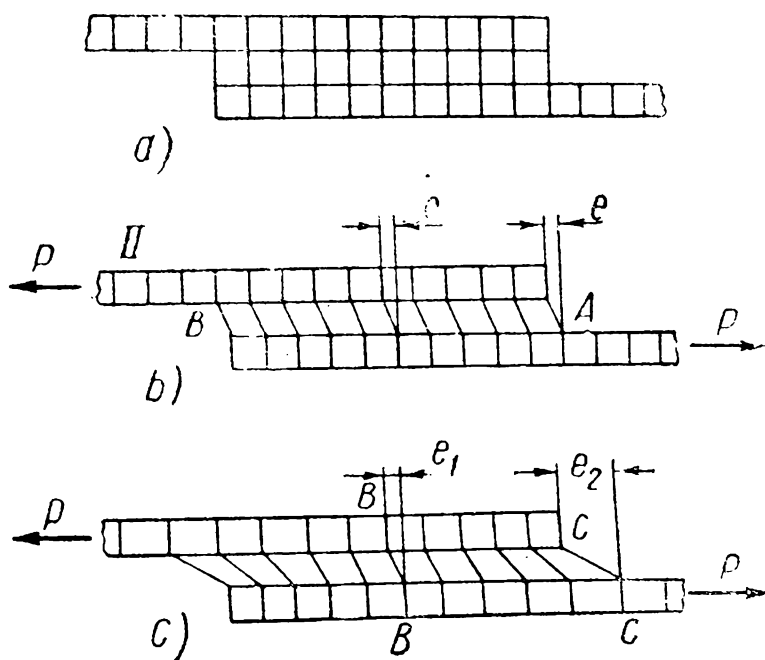


Fig. 32



overlap in a welded joint should not exceed 50 times the thickness of the weaker of the joined plates, the number of rivets along the tractional load should be

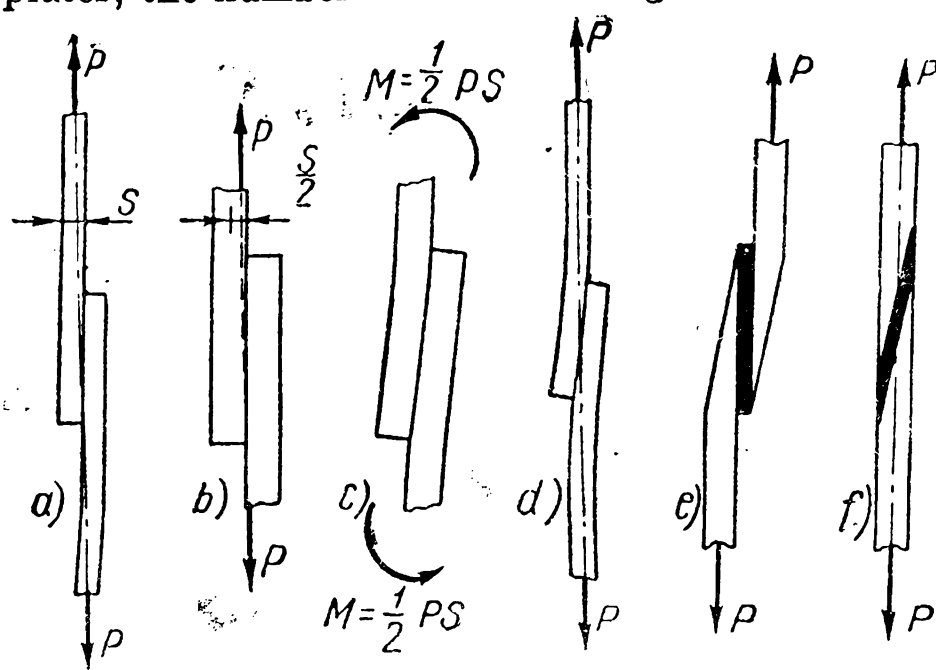


Fig. 33

confined to 5-6, and the thickness of a nut to 0.8 of the bolt diameter, etc. Increasing the length of joint beyond the optimal value (i. e., the length of overlap, the number of rivets, the thickness of nut, etc.), without adding to the strength of the joint, requires greater amount of labour and makes the joint heavier.

All that has been said regarding the uneven distribution of stresses along the joint length and the stress concentration at the ends characterises the functioning of joints in the region subject to elastic deformation and should be taken into consideration when designing joints liable to fatigue failure.

As the yield point is approached, the stress distribution along the length of the joint becomes more uniform. This circumstance is valid, however, only for a static load.

**Load eccentricity.** The elements of a lap joint are inevitably displaced relative to each other by at least the magnitude of their thickness  $s$  (Fig. 33, a and b).

The inclined line along which the tensile force acts connects the points where loads  $P$  are applied and passes through the middle point of the joint. The eccentricity of the applied load creates the bending moment  $M = \frac{1}{2} P s$  (Fig. 33, c)

under the action of which the connected members, if they are of sufficient length, bend and the joint is subjected to

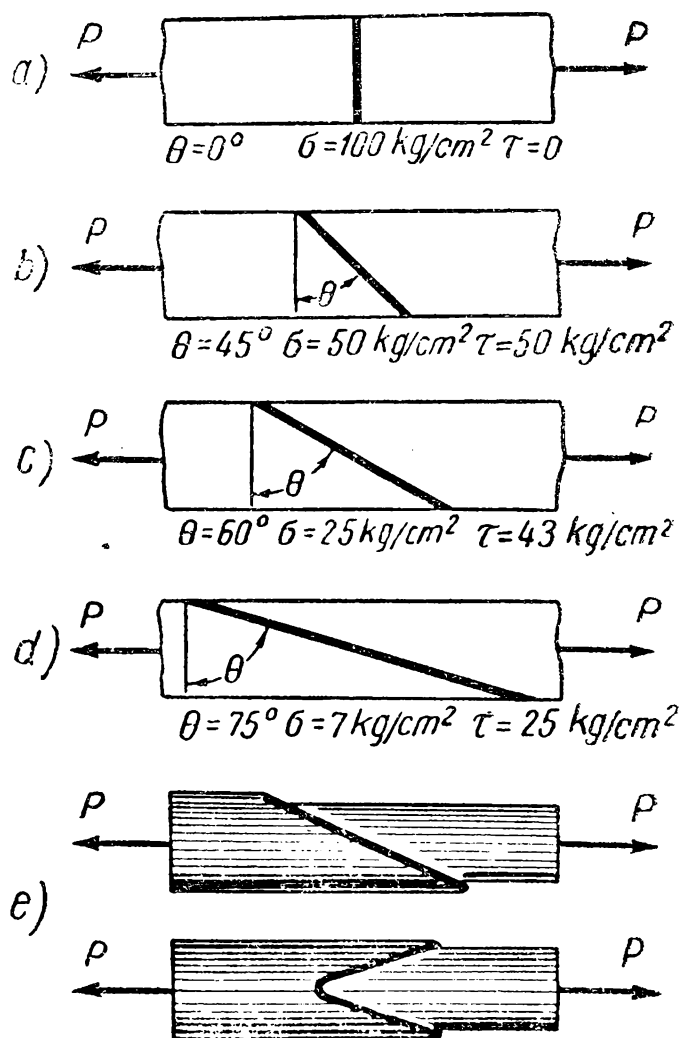


Fig. 34.

of the applied load is located nearer to the axes of both members and the magnitude of the bending moment is therefore smaller.

The stresses due to the action of the moment  $M$  which can be called separating stresses are tensile stresses and are directed normally to the surfaces. They are confined to those sections of the surface which adjoin the overlap ends and can markedly lessen the strength of the joint.

The desire for a more uniform stress distribution resulted in the development of joints having an overlap with bevelled edges (Fig. 33, *e*) and oblique joints (Fig. 33, *f*). The former type weakens the effect of deformation difference while the latter also excludes load eccentricity. Different angles of obliquity give different relations between the normal and tangential stresses in the joint (Fig. 34). In Fig. 34, *a* the maximum tensile stress is arbitrarily taken as  $100 \text{ kg/cm}^2$ . If the connecting layer (for instance, an adhesive or brazing material) is weaker than the material of the joined elements, the properties of the oblique joint can be used to obtain adequate strength. This is utilised in welded joints since the material of a welded seam or the heat-affected zone may prove weaker than the base material.

Fig. 34, *e* shows some typical joints of aircraft piping.

**Tightness of Joints.** Tightness is indispensable in joints connecting parts of machines, pipes and tubes, vessels and apparatus containing fluids and gases.

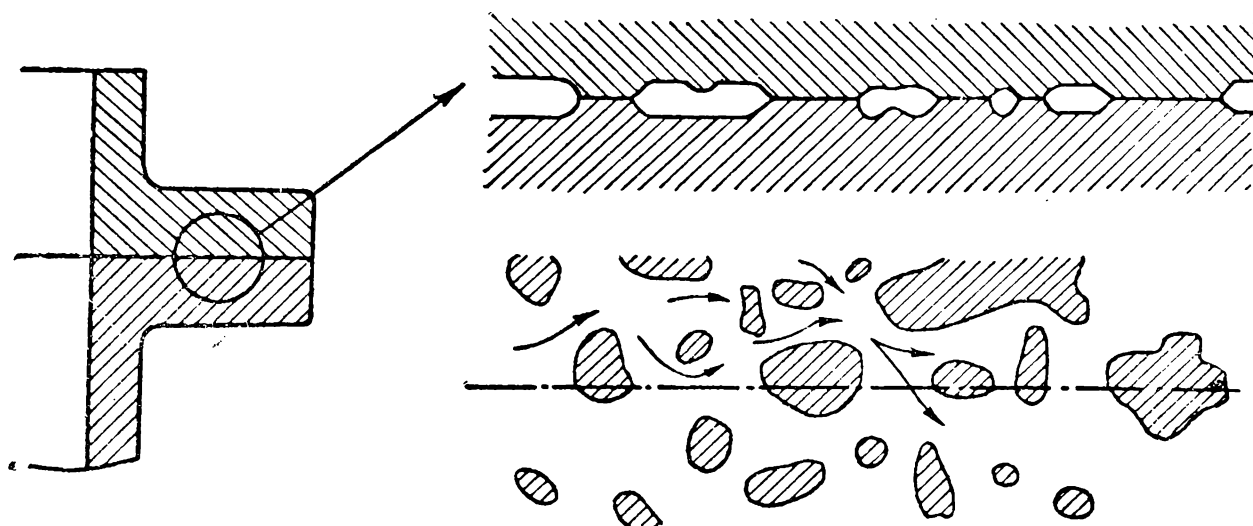


Fig. 35

Besides permitting losses due to leakage, poor sealing is dangerous if the vessels and apparatus contain fluids and gases harmful to the health.

The essence of the term *tightness* can be illustrated by a flanged joint of two pipes which pass fluid (or gas) under certain pressure (Fig. 35).

No matter how carefully the surfaces of these flanges are machined, they will touch each other not over their entire nominal geometrical area but only at separate points which under pressure form microirregularities shown in Fig. 35 as shaded patches. The hollows between them permit fluid (and, even more, gas) to leak out, its rate being dependent on the pressure of the fluid, its viscosity and the size of the hollows.

Proper sealing of a detachable joint to prevent the leakage of fluid (or gas) can be ensured: 1) by subjecting the finely finished mating surfaces to *strong pressure*, and 2) by *inserting gaskets* which will fill the hollows between the microirregularities with a comparatively soft readily deformed material.

Tight joints are calculated on the basis of the unit pressure which must be created between the contacting surfaces. For different methods of sealing and different gasket material the working unit pressure  $q$  lies within  $q=(1.5-4)p$  where  $p$  is the internal pressure of the fluid or gas in the pipe, tube, vessel, etc. The lesser value ( $1.5p$ ) refers to soft corrugated gaskets with asbestos cord, the greater value ( $4p$ )—to the direct contact of hand-scraped flanges.]

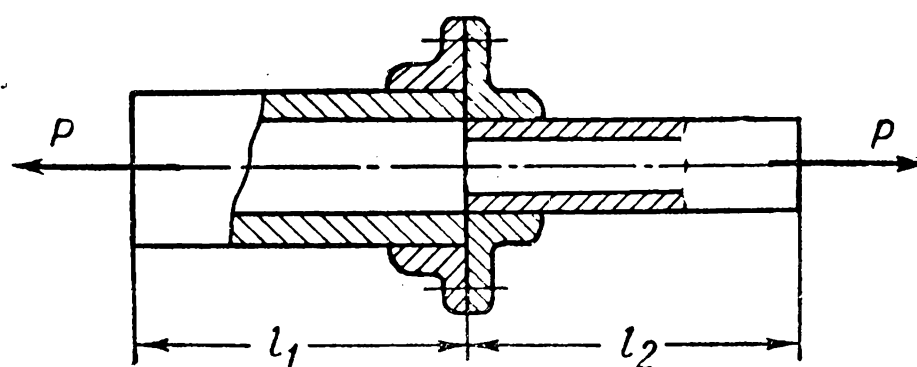


Fig. 36

**Stiffness of Joints.** The stiffness of a system is the ratio between the straining force  $P$  (in kg) and the magnitude of deformation  $\lambda$  (in mm). The stiffness  $c=P:\lambda$ , and in case of a nonlinear dependence  $\lambda=f(P)$ —the relation of the increments of these magnitudes within a given interval:  $c=\Delta P : \Delta \lambda$ . On the basis of this general definition we can easily arrive at the stiffness of a joint. Fig. 36 shows a flanged joint under the tension of forces  $P$ . Let the deformations of two parts of the system,  $l_1$  and  $l_2$  in length, be  $\lambda_1$  and  $\lambda_2$ , respectively. The total deformation of this system  $\lambda_0$  is greater than  $\lambda_1 + \lambda_2$  and the difference  $\lambda_0 - (\lambda_1 + \lambda_2)$  is the joint deformation. Hence the stiffness of the joint is

$$c_v = \frac{P}{\lambda_0 - (\lambda_1 + \lambda_2)} \text{ kg/mm.}$$

Experimental research has shown that the stiffness of the joint as a whole is several times less than the stiffness of the connected members.

The stiffness of the system ( $c_0$ ) found from the expression

$$\frac{1}{c_0} = \frac{1}{c_v} + \frac{1}{c_1} + \frac{1}{c_2}$$

is always less than the stiffness of the least stiff member; hence, it

is the joint (the less stiff member) that determines the stiffness of the system as a whole.

In machine-tool designing much attention has been given in recent years to the problems of the stiffness of joints, since the stiffness of the system—machine tool-workpiece-tool—determines the productivity of machine tools and the precision of the articles they turn out. The stiffness of fixed joints is improved by greater flatness and better finish of the connected surfaces and increased unit pressure brought to act upon them due to preload.

## CHAPTER VI

### RIVETED JOINTS

Until recently riveted joints were the main type of permanent joint extensively used in the construction of boilers, ships, bridges, etc. During the last decade, however, the rapid development of welding methods has considerably reduced the sphere of their application.

Today riveted joints are primarily employed in structural and machine work exposed to severe vibrational loads since the dependability of welded joints under these conditions has not been sufficiently studied.

Up to now riveted joints have retained their leadership as the main type of permanent fastening in the manufacture of metal structures from light alloys. To illustrate, in the production of modern all-metal aircraft the labour spent on riveting accounts for 30-35 per cent of all labour.

Rivets are also used to connect metal elements having poor weldability.

Fig. 37 shows how riveted joints are employed in some units: an aircraft fuselage strut (Fig. 37, *a*); the fastening of an end link and a crane brake strap (Fig. 37, *b*); a sprocket of a multi-bucket trench digger ЭТ-251 (Fig. 37, *c*).

The main element of a riveted joint is the rivet which originally consists of a shank 1 and set head 2 (Fig. 38, *a*).

The rivet is applied by passing its shank through a hole (drilled or punched in advance) in the members to be fastened, after which the protruding point of the shank is upset to form a second, closing, head 3.

The forming of the second head is called *riveting*.

Riveting is termed *hot* when before being clinched the rivet is heated to the required temperature, *cold* when the closing head is formed without heating and *mixed* when, in case of long rivets, only the end which is upset into the closing head is heated and not the whole shank.

Steel rivets up to 12 mm in diameter can be driven cold; rivets of larger diameters—hot or by the mixed method.

To facilitate the entrance of the rivet, the hole should be somewhat larger than the rated diameter of the shank. The diameters of the holes are designated on working drawings in accordance with industrial standards depending on the accuracy required of the joint.

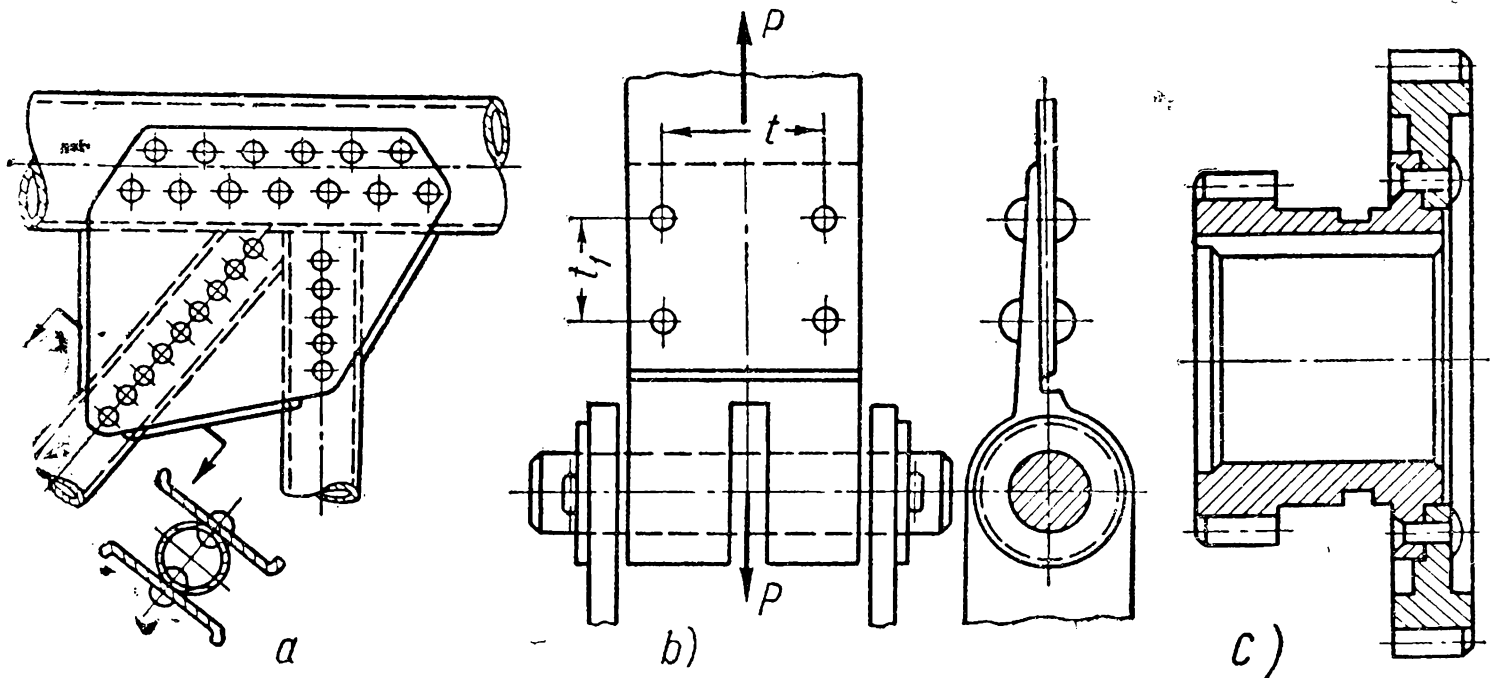


Fig. 37

The length of an undriven rivet (Fig. 38, *a*) is found from the formula

$$l = \Sigma S + (1.5-1.7) d.$$

Rivets are driven either manually if they are few or by impact or pressure machines if they are many.

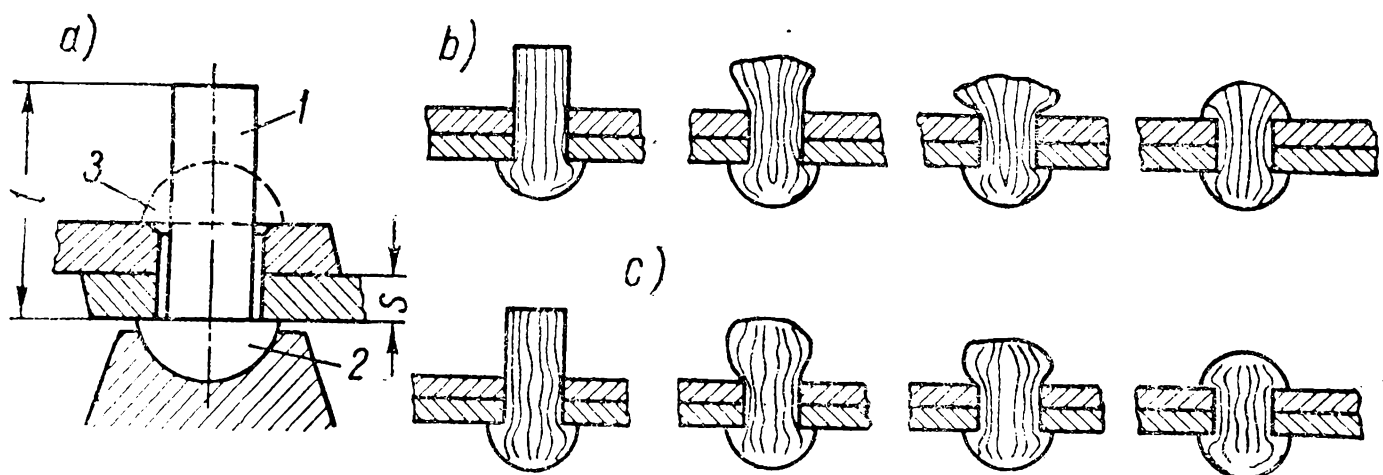


Fig. 38

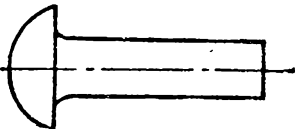
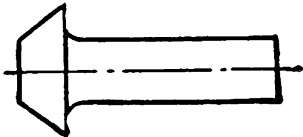
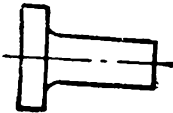
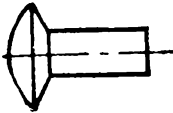
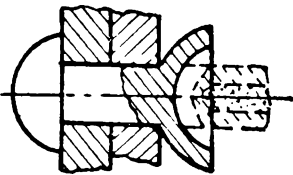
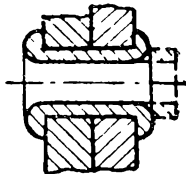
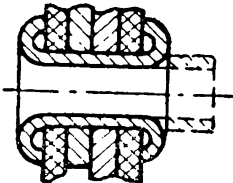
As the shank end is being clinched by a hammer it takes the form of a button (Fig. 38, *b*); when riveting machines are used it looks

like a barrel (Fig. 38, c). In the latter instance the hole is more efficiently filled, thus improving the reliability of the joint.

Rivets are made from ordinary soft steel and sometimes from alloy steel. Use is also made of copper, brass, aluminium and some other metals. The use of simple carbon steels of a higher ultimate strength hampers the effective formation of the closing head.

Table 7

Types of Rivets

Types of rivets	Diameter of shank in mm.	Sketch
Button-head rivets	From 1 to 37	
Pan-head rivets	From 2.6 to 6	
Flat-head rivets	From 2.3 to 6	
Half-countersunk rivets	From 2 to 7	
Explosive rivets	Up to 8	
Flanged tubular rivets	From 4 to 20	
Beaded tubular rivets	From 4 to 20	

The aircraft industry makes wide use of duralumin rivets, which are driven cold.

Before driving duralumin rivets have first to be tempered and driven within three hours of tempering since they quickly lose their plastic properties.

Rivets fall into two categories—*solid* and *tubular*.

Some of the rivets are shown in Table 7.

Steel button-head rivets are most widely used.

*Explosive* rivets are employed where the head cannot be formed by conventional methods. The shank end of such rivets is provided with a chamber filled with an explosive. The rivet is inserted cold and a hot holder is pressed to the set head, heating the rivet and causing an explosion which forms the other end into a distinctively shaped head. Explosive rivets are manufactured from duralumin and special carbon or chromium-molybdenum steel.

*Tubular* rivets are used in aircraft, precision machinery and machines produced by light industry. The walls of these rivets vary in thickness from 0.25 to 1.5 mm. The closing head of a tubular rivet is formed by tools of the tube-expander type. *Flanged* rivets are used to connect metal parts and *beaded* rivets—to join parts made from elastic materials, as for example leather, fabrics, etc.

Tubular rivets for unimportant joints are made from steel, copper and other metal tubes with or without a seam; in vital joints machined rivets are used.

Together with the parts they fasten rivets form *riveted seams* which, depending on their purpose, are classed as *strong* (machine units, columns, trusses, etc.) and *tight-strong* (steam boilers, gas receivers, pressure vessels, tanks, etc.).

The principal classification of riveted seams is given in Fig. 39.

By the method of fastening the parts together seams can be subdivided into *lap* and *butt-jointed*, and by the arrangement of rivets into *chain* (Fig. 39, *b*, *d*) and *staggered* (Fig. 39, *c*, *e*, *f*, *h*, *i*).

All lap and one-strap joints are said to be *in single shear* because only one crosssection of the rivet is exposed to shearing force (Fig. 39, *a-f*) while two-strap joints (Fig. 39, *g-i*) are *in double shear* and are therefore stronger than the former.

### THE FUNCTIONING OF RIVETS IN A SEAM

When a hot driven rivet cools, considerable longitudinal forces arise in its shank which draw the fastened members tightly together and cause strong friction forces to arise between them. While cooling, the diameter of the rivet shank decreases producing a clearance between the shank and the hole wall which essentially affects the strength and firmness of the joint.

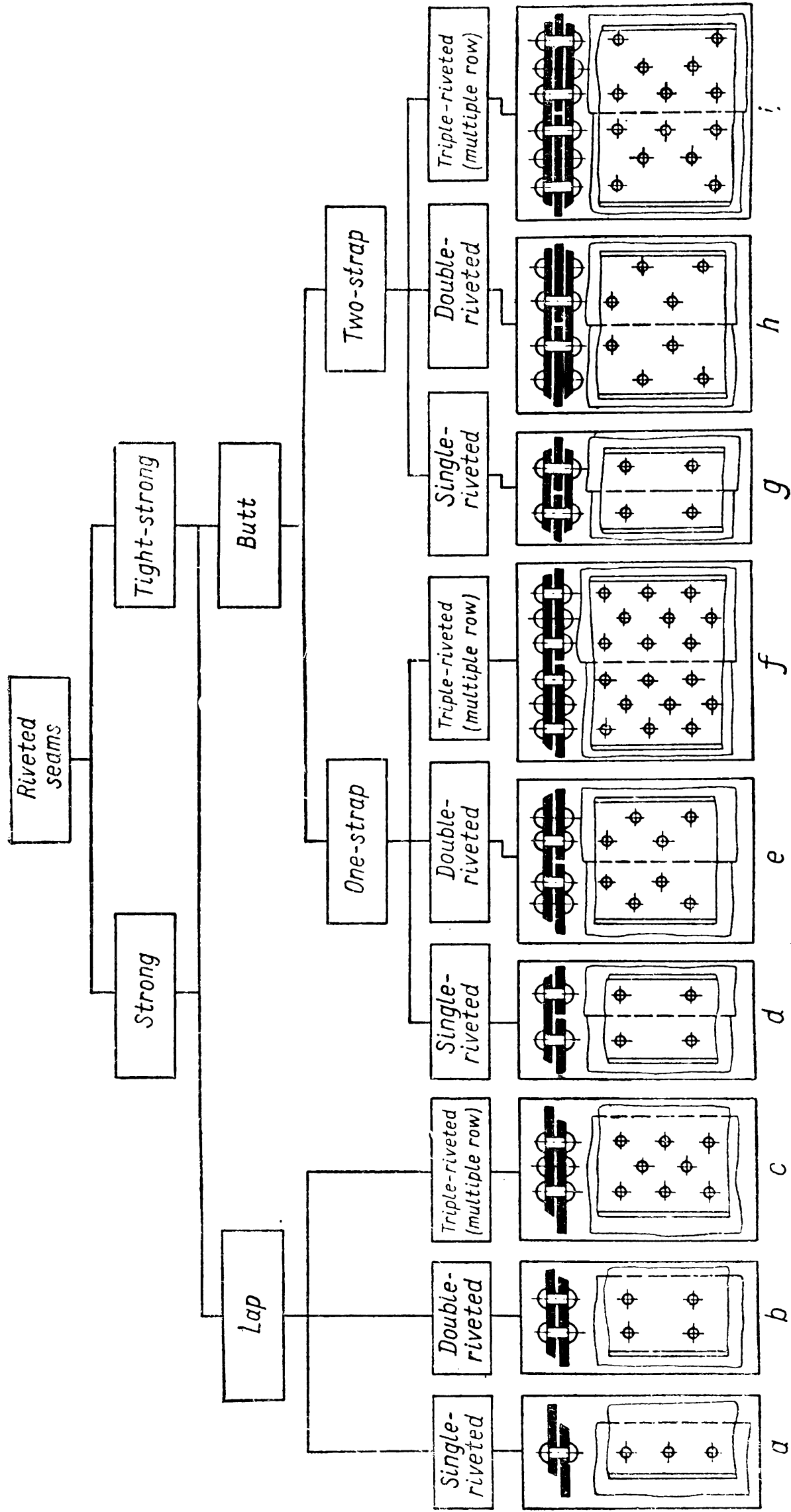


Fig. 39



The curves in Figs. 40, *a* and *b*, plotted in coordinates «load  $P$ -deformation  $\Delta$ » illustrate the service of a riveted joint. Curve  $A$  shows this relation for the friction forces and curve  $B$  for the rivet shank whose deformation in the seam has no sharply expressed region of yield.

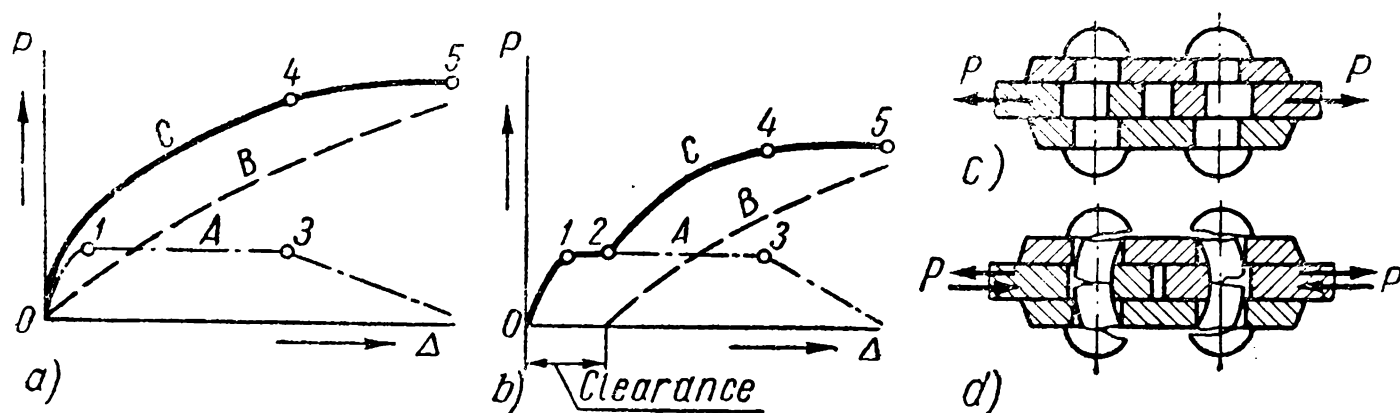


Fig. 40

Three sections can be marked on curve  $A$ . Up to point 1 we observe an elastoplastic shear when the friction forces reach their maximum with a small displacement of the fastened members. From this point and up to point 3 the friction forces are stabilised and, when their magnitude becomes constant, a slip occurs.

The third section—from point 3—depends on the behaviour of the rivet shank which is strongly deformed and sometimes even ruptured thus weakening the initial pinching together of the riveted members and reducing the friction forces.

If the rivet fits the hole without clearance as in the case of cold riveting, the load-carrying capacity of the joint determined by the mutual action of the friction forces and the shank is represented as curve  $C$  (Fig. 40, *a*) where the ordinates of each point on it are the sum of the ordinates of the respective points on curves  $A$  and  $B$ .

If there is clearance the load-carrying capacity of the joint is determined in the initial period of its functioning only by the magnitude of the friction forces (Fig. 40, *b*) due to which mutual displacement of the fastened members may occur within the clearance up to point 2. From point 4 the plastic deformations in the rivet sharply increase while the friction forces grow weaker.

Finally, at point 5, the joint fails.

For many designs even the slightest residual sliding is inadmissible. In a seam of a steam boiler, for example, this may cause loss of tightness and in a metal structural work—the redistribution of stresses in the shanks due to changes in their length. In order to increase the strength and rigidity of the joint, therefore, the clearance between the rivet shank and hole should be reduced to a minimum.

With this aim in view some members are preferably fastened together by cold rivets or by rivets heated only at the end, while the size of the hole is so selected that the rivet can be driven in by a hammer.

The presence of clearance between the shank and the hole predetermines the nature of the rivet failure.

Under static load, hot and cold driven rivets fail as a result of shank shear (Fig. 40, c).

Under vibrational load hot driven rivets fail from brittle fractures due to bending and elongation of the shank caused by fatigue (Fig. 40, d).

Cold driven rivets whose shank fits the hole tightly are ruptured in this case by shearing forces.

After the shank of a hot driven rivet has cooled through  $100^\circ$ , it develops longitudinal stresses whose magnitude, if we assume that the fastened members do not deform at all, will be

$$\sigma = \alpha \times \Delta t \times E = 11 \times 10^{-6} \times 100 \times 2 \times 10^6 = 2,200 \text{ kg/cm}^2.$$

Here  $\alpha = 11 \times 10^{-6}$  is the thermal coefficient of linear expansion of steel and  $E = 2 \times 10^6$  — the modulus of elasticity of steel in tension in  $\text{kg/cm}^2$ .

This high stress approximating to the elastic limit of the material of steel rivets is of no great consequence

since it acts statically and is not increased by the forces acting upon conventional rivets and directed perpendicular to their axes. This stress can be dangerous for rivets in tension when external loads are applied along the axis; in this case the stress may exceed the yield point and the permanent deformation of the shank will lessen the stiffness of the joint.

If the external load applied to the seam is  $P$  (Fig. 41) then the force  $Q$  required to prevent sliding can be found from the condition

$$Qf \geq P, \text{ i. e., } Q \geq \frac{P}{f},$$

where  $f$  is the coefficient of friction between the plates.

The force  $Q$  ruptures the shank, crushes the head from below and tends to shear it off. The corresponding equations for strength will be:

$$\text{in shank tension } Q \leq \frac{\pi d^2}{4} [\sigma]_t; \quad (41)$$

$$\text{in head compression } Q \leq \frac{\pi}{4} (D^2 - d^2) [\sigma]_c; \quad (42)$$

$$\text{in head shear } Q \leq \pi d h_0 [\tau]. \quad (43)$$

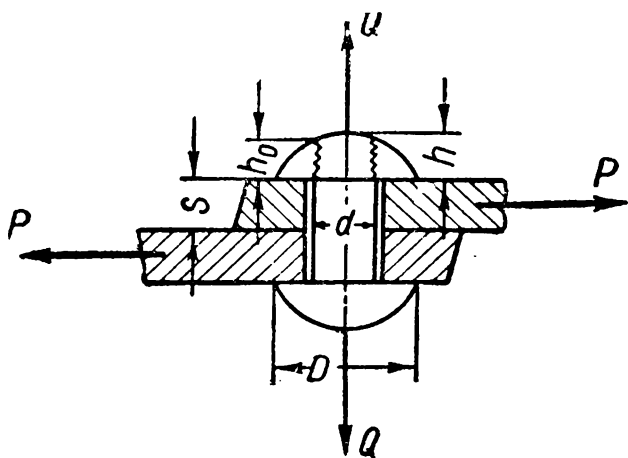


Fig. 41

Solving equation (41) together with (42), and (41) together with (43) we obtain:

$$D = \left( \sqrt{\frac{[\sigma]_t}{[\sigma]_c} + 1} \right) d \approx 1.4d;$$

$$h_0 = 0.25d \frac{[\sigma]_t}{[\tau]_s} \approx 0.3d$$

and

$$h \approx 0.35d.$$

To provide for a safety factor we take

$$D \approx 1.75d \text{ and } h \approx 0.65d.$$

The distance between the centres of two adjacent rivets is called the pitch. The rivets may run perpendicular to the applied force, pitch  $t$ , or parallel to it, pitch  $t_1$ , (Fig. 37, *b*).

If the force  $P$  is brought to act on a unit (Fig. 42, *a*) it is distributed between the rivets so that

$$P_1 + P_2 = P.$$

The load  $P_2$  applied to the element of part *II* between the rivets causes stress

$$\sigma_2 = \frac{\lambda E_2}{t_1}$$

to arise in it where  $\lambda$  is the absolute elongation of the given element;  $E_2$  is the elastic modulus of material *II*.

Hence,

$$P_2 = \sigma_2 bs = \lambda \frac{E_2 F_2}{t_1}.$$

The deformation of the part *II* depends on the stiffness  $\frac{E_1 F_1}{t_1}$  of the element of equal length of part *I*. If  $\frac{E_1 F_1}{t_1} = \infty$ , then  $\lambda = 0$  and  $P_2 = 0$ . In this extreme case the entire load would be taken by the first rivet. *It is therefore inexpedient to join parts of sharply differing stiffness by means of a multiple-row seam.*

The more rivets there are in the row, the less evenly the load is spread among them and the less uniform is their behaviour in the elastic region. The greatest load is carried by the end rivets because the middle rivets are underloaded.

With six rivets in a seam, as shown in Fig. 42, *b*, the end rivets are overloaded by 26 per cent relative to the mean load (see Fig. 42, *c*).

In the joints shown in Fig. 42, *d* the load distribution is equalised (Fig. 42, *e*). In a joint of this design, high stresses in the plate

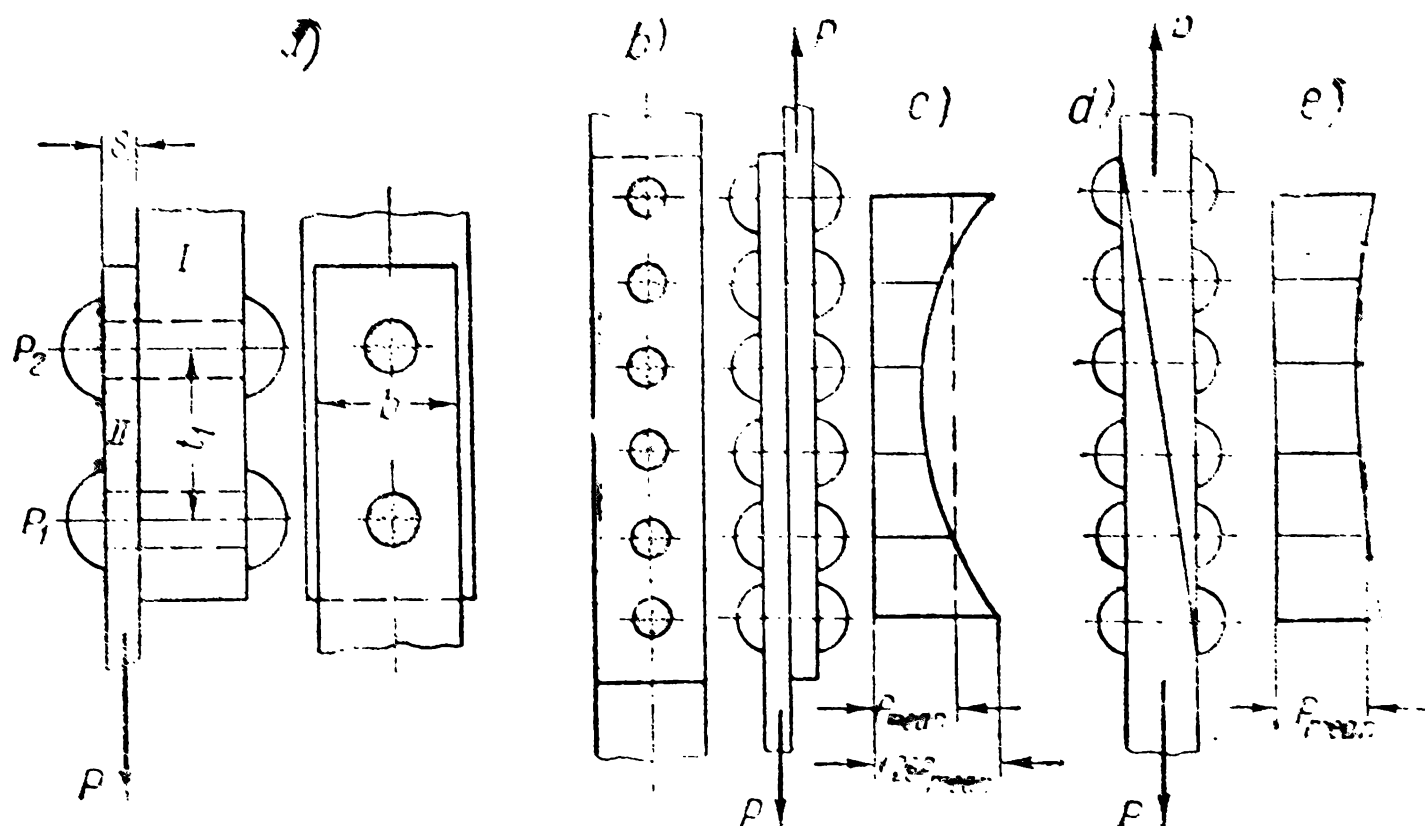


Fig. 42

sections near to the edge cause respectively larger deformations, as a result of which the neighbouring rivets resist higher loads.

### STRENGTH OF RIVETED JOINT ELEMENTS

The friction forces in a riveted joint are not easily determined, due to the presence of a large number of factors, difficult to assess, which affect the magnitude of these forces. Therefore, in calculating the strength of riveted seam elements friction forces are neglected. This gives a certain excess of strength.

A single-riveted joint in single shear (Fig. 43, a), for example, can fail if: a) the rivets are shorn off; b) the part tears along the line of the rivet holes; c) the rivets tear to the plate edge along the planes  $ab$  and  $cd$  or d) the surface of the joint between rivets and plate is crushed.

Let us assume that the force  $P$  acts on a seam with  $i$  rivets, then the load applied to the section of the seam which is  $t$  wide will be

$$P_0 = \frac{P}{i}. \quad (44)$$

Making use of the designations in Fig. 43, the following strength equations can be composed:  
for shearing the rivet

$$P_0 \leq \frac{\pi d^2}{4} [\tau]_s; \quad (45)$$

for tearing the plate between rivets

$$P_0 \leq (t-d)s[\sigma]_t; \quad (46)$$

for tearing to the plate edge assuming that this will occur along the length  $e - \frac{d}{2}$

$$P_0 \leq 2\left(e - \frac{d}{2}\right)s[\tau]'; \quad (47)$$

for crushing the surface of the joint between rivet and plate

$$P_0 \leq ds[\sigma]_c. \quad (48)$$

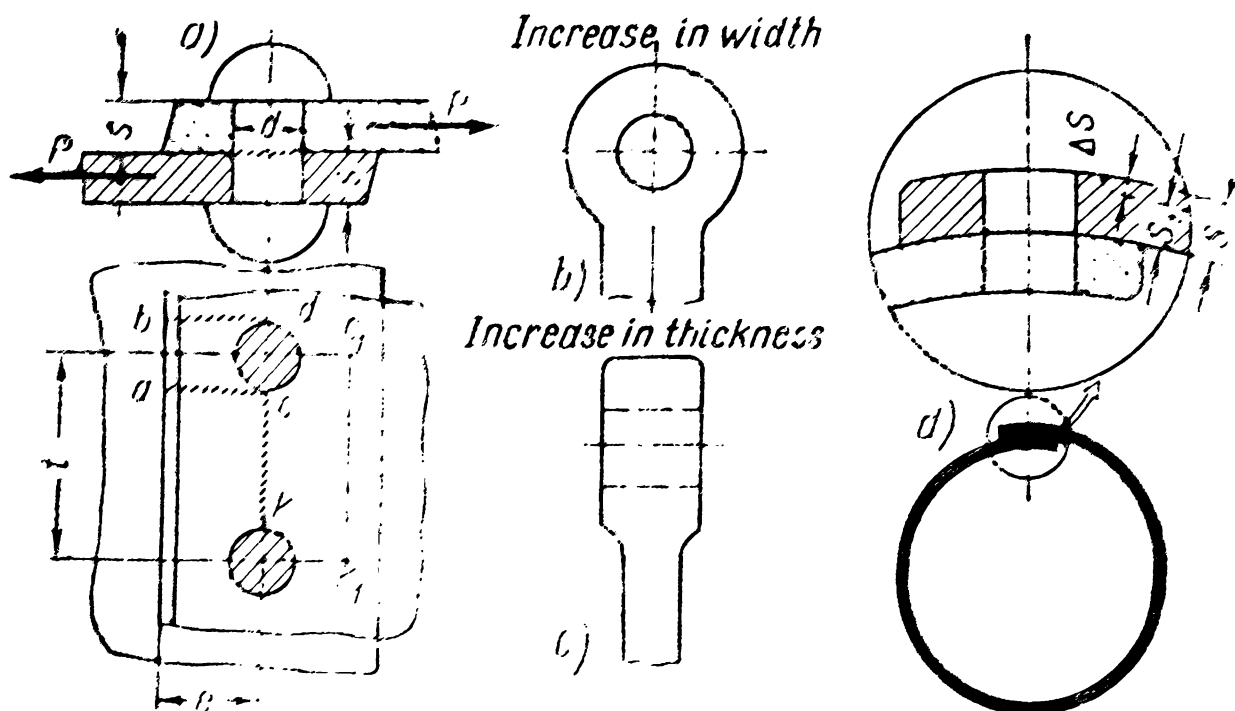


Fig. 43

The simultaneous solution of equations (45) and (48) at  $[\sigma]_c = 1.6[\tau]_s$  gives us

$$d = \frac{4}{\pi} \times \frac{[\sigma]_c}{[\tau]_s} s \approx 2s$$

and the simultaneous solution of equations (45) and (46) at  $[\tau]_s = [\sigma]_t$  and  $d = 2s$  gives

$$t = d \left( \frac{\pi}{2} \times \frac{[\tau]_s}{[\sigma]_t} + 1 \right) \approx 2.6d.$$

Finally, solving equations (45) and (47) and assuming  $[\tau]' = 0.8[\tau]_s$  and  $d = 2s$  we find that

$$e = 0.5d \left( \frac{\pi}{2} \times \frac{[\tau]_s}{[\tau]'} + 1 \right) = 1.47d.$$

In practice, for a single-riveted joint in single shear  $t = 3d$  and  $e = 1.5d$  (for drilled holes) are taken.

Similarly from the condition of the equal strength of the seam element it can be found that:

$$\left. \begin{array}{l} \text{for a single-riveted two-strap joint (Fig. 39, g) } t = 3.5d \\ \text{for a double-riveted lap joint (Fig. 39, b) } t = 4d \\ \text{for a double-riveted two-strap joint (Fig. 39, h) } t = 6d \end{array} \right\} . \quad (49)$$

If the stress in the section weakened by the hole (Fig. 43, a) is denoted as  $\sigma_1$  and in the unaffected section  $c_1 k_1$  as  $\sigma_2$  then, taking into account the stress concentration factor at the hole  $k_\sigma$ , we obtain

$$\sigma_{\max} = k_\sigma \sigma_1 = k_\sigma \frac{P_0}{(t-d)_s} \quad \text{and} \quad \sigma_2 = \frac{P_0}{ts} .$$

Hence the factor of safety of the riveted seam is

$$\varphi = \frac{\sigma_2}{\sigma_{\max}} = \frac{l-d}{k_\sigma t} . \quad (50)$$

With  $k_\sigma = 1$  for a single-riveted joint in single shear at  $t = 3d$  we obtain  $\varphi = 0.67$ .

With the corresponding values of pitch we find from the relation (49):

for a single-riveted two-strap joint  $\varphi = 0.71$ ;

for a double-riveted lap joint  $\varphi = 0.75$ ;

for a double-riveted two-strap joint  $\varphi = 0.83$ .

Thus, the strength of the fastened members decreases with a single-riveted joint in single shear by 33 per cent but with a double-riveted joint in double shear by only 17 per cent.

To obtain high values of  $\varphi$  attempts are made to increase the cross-sectional area of the region weakened by the hole provided for the rivet. In single-rivet joints this is achieved by the methods shown in Fig. 43, b and c.

In seams in sheet or plate material the weakening caused by the rivet holes brings about a considerable increase in the weight of the whole work. Indeed, if  $s_1$  is the calculated thickness of a plate for a group riveted joint, for instance, for a longitudinal seam of a steam boiler (Fig. 43, d) whose safety factor is  $\varphi$ , where the plate has been weakened by the rivet holes it will require a thickness of  $s = \frac{s_1}{\varphi}$ .

Great advantage could be derived from increasing the thickness of the metal only in the region to be riveted, as in the case of single riveting, but the production of plates with thickened edges is impracticable. Therefore, the entire plate has to be made  $\Delta s$  thicker.

## CALCULATION OF RIVETED SEAMS

**Strong Seams.** The complex phenomena taking place in a riveted seam makes the accurate design of its elements difficult. The existing methods of calculation are based on the assumptions that:

- a) the load is spread evenly between all elements;
- b) there is no friction force between the elements to be fastened.

When designing *strong riveted seams* the *diameter* of the rivets is first chosen and then, calculating from the total load, the number of rivets required in the seam is determined. Sometimes the *number* of rivets is chosen first and then, by calculation, the diameter of the rivet bearing the greatest load.

When the *load is applied symmetrically* the force taken by one rivet is found from the relation (44) and if the number of simultaneously shorn off sections is  $z$  the strength equation will be

$$P_0 = \frac{P}{i} \leq z \frac{\pi d^2}{4} [\tau]_s. \quad (51)$$

Hence, the number of rivets in the seam will be

$$i \geq \frac{4}{\pi} \times \frac{P}{zd^2 [\tau]_s}. \quad (52)$$

In computing the rivets for compressive forces the strength equation will be

$$P_0 = \frac{P}{i} \leq sd [\sigma]_c \quad (53)$$

and the required number of rivets in the seam will be

$$i \geq \frac{P}{sd [\sigma]_c}. \quad (54)$$

The greater of the two values of  $i$  which are found is taken as the basis for the seam design.

In the formulae (52) and (54):

$d$  is the rivet hole diameter in cm;

$s$ —the minimum thickness of the fastened parts in cm.

$[\tau]_s$  and  $[\sigma]_c$ —allowable shearing and compression stresses respectively in kg/cm<sup>2</sup>.

When applied to metal structural work, for rivets made from steel 2,  $[\tau]_s = 1,000-1,400$  kg/cm<sup>2</sup> in which case the higher value is taken for drilled and the lower for punched holes.

For fastened parts made from steel 2 and 3  $[\sigma]_c$  is 2,100 and 2,400 kg/cm<sup>2</sup>, respectively.

If the joint is subjected to a varying load, the allowable stress for a work made from low-carbon steel is decreased by multiply-

ing it by the correction factor  $\gamma$  found from the formula

$$\gamma = \frac{1}{1 - 0.3 \frac{P_{\min}}{P_{\max}}} \quad (55)$$

The forces  $P_{\min}$  and  $P_{\max}$  appear in the formula (55) each with its sign; hence  $\frac{P_{\min}}{P_{\max}} < 0$  and, therefore,  $\gamma < 1$ .

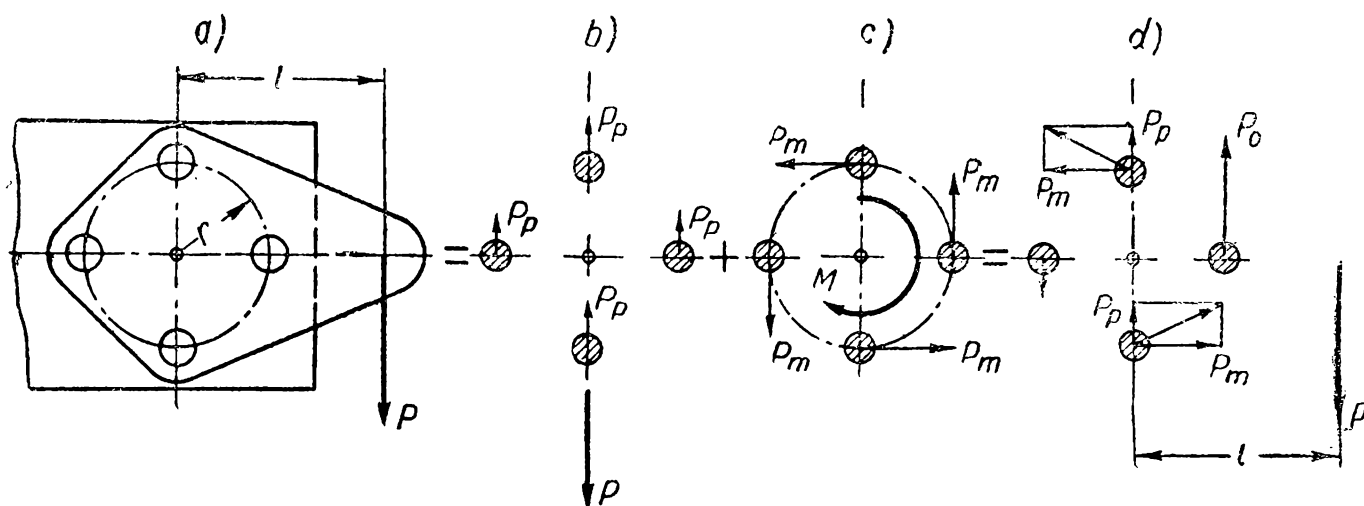


Fig. 44

When the load is applied eccentrically (Fig. 44, a) its action can be replaced by the action of a symmetrically applied force (Fig. 44, b) and a moment (Fig. 44, c). The severest load carried by the rivet in a given joint (Fig. 44, d) will be

$$P_0 = P_p + P_m = \frac{P}{i} + \frac{Pl}{ri} = \frac{P}{i} \left( 1 + \frac{l}{r} \right) \text{ kg}$$

In the same way, when applied to the unit shown in Fig. 45, a the force acting on each rivet as a result of the load  $P$  (Fig. 45, b) will be  $P_p = \frac{P}{i}$ . The greatest force  $P_{m1}$  from the moment  $Pl$  will fall on the end rivets farthest removed from the so-called centre of rigidity  $O$  of the riveted joint.

Since the deformations (in shear) of the rivets are in direct proportion to their distances  $r_1, r_2, \dots$  from the centre of rigidity, the forces  $P_{m1}, P_{m2}, \dots$  acting upon the rivets are also in direct proportion to  $r_1, r_2, \dots$ , i.e.,

$$\frac{P_{m1}}{P_{m2}} = \frac{r_1}{r_2}; \quad \frac{P_{m1}}{P_{m3}} = \frac{r_1}{r_3}; \quad \dots, \text{ etc.} \quad (55')$$

The external moment is equalised by the moments of the reactions of the rivets (Fig. 45, c). i.e.,



Substituting here  $P_{m2} = P_{m1} \frac{r_2}{r_1}$ ,  $P_{m3} = P_{m1} \frac{r_3}{r_1}$ , ... etc., we obtain

$$P_{m1} = \frac{Pl}{2 \left( r_1 + \frac{r_2^2}{r_1} + \frac{r_3^2}{r_1} + \dots \right)} = \frac{Plr_1}{2(r_1^2 + r_2^2 + r_3^2 + \dots)}.$$

Hence the force acting upon the most heavily loaded rivet is (Fig. 45, d)

$$P_0 = \sqrt{P_p^2 + P_{m1}^2}.$$

When the rivets in the seam are of the same size, their diameter is found with the help of  $P_0$  from the equations (45) and (48).

**Tight-Strong Seams.** Seams of this category should be not only strong but also tight: this is achieved by avoiding mutual displacement of the plates.

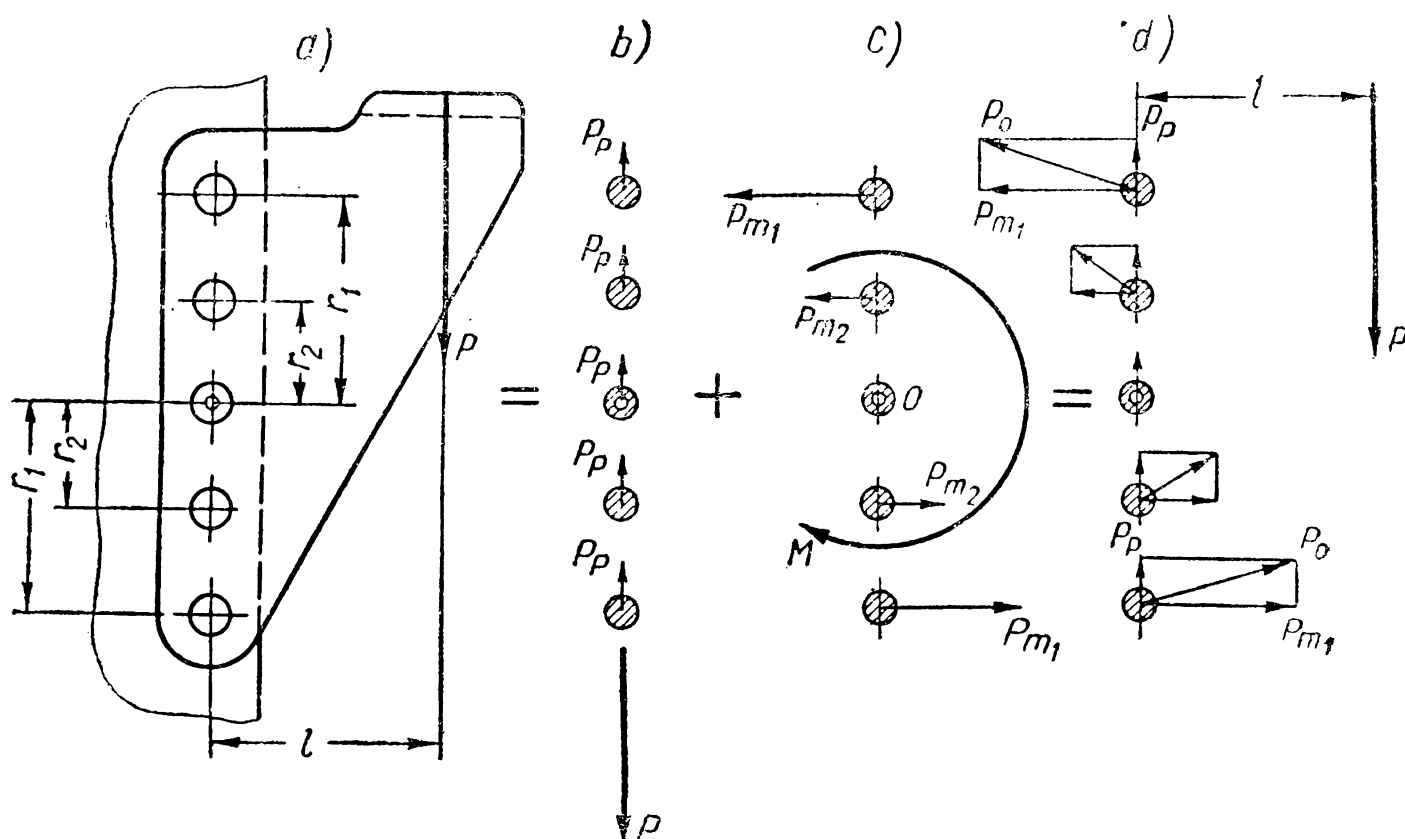


Fig. 45

The tightness cannot be theoretically determined. Therefore, the resistance to slip of the plates caused by friction forces created by the rivets is found experimentally as the *coefficient of sliding*.

The coefficient of sliding is taken as the *force resisting the slip of the plates arbitrarily referred to unit area of rivet cross-section, i.e.,*

$$\xi = \frac{P'_0}{k \frac{\pi d^2}{4}} \leq [\xi] \quad (56)$$

Table 8  
Principal Characteristics of Tight-Strong Seams

Type of seam	$c = \frac{Dp}{2}$ in kg/cm	Diameter of rivet $d$ in mm	Pitch $t$ in mm	$\varphi = \frac{t-d}{t}$	$[\xi]$ in kg/cm <sup>2</sup>
Single-riveted lap joint (Fig. 39, a) . . . . .	Up to 500	$s + 8$ mm	$2d + 8$ mm	0.56-0.60	600-700
Double-riveted lap joint (Fig. 39, b) . . . . .	350-950	$s + 8$ mm	$2.6d + 15$ mm	0.70	600-650
Triple-riveted lap joint (Fig. 39, c) . . . . .	450-1,350	$s + (6-8)$ mm	$3d + 22$ mm	0.75	550-600
Double-riveted two-strap butt joint (Fig. 39, h) . . . . .	450-1,350	$s + (5-6)$ mm	$3.5d + 15$ mm	0.75	2 (475-575)
Triple-riveted two-strap butt joint (Fig. 39, i) . . . . .	450-2,300	$s + 5$ mm	$6d + 20$ mm	0.85	2 (450-550)

where  $P'_0$ —is the force applied to the plate in the pitch area. For the longitudinal seam of a steam boiler  $P'_0 = \frac{Dpt}{2}$ ; for the girth seam  $P'_0 = \frac{Dpt}{4}$ . Here  $D$  is the internal diameter;  $p$ —pressure;  $k$ —the number of rivets per strip with width equal to pitch;  $[\xi]$ —allowable value of the coefficient of sliding dependent on the type of seam (Table 8).

With the given boiler diameter  $D$  and pressure  $p$  the seam safety factor  $\varphi$  is chosen from Table 8 depending on  $c = \frac{Dp}{2}$ .

The thickness of the boiler wall is found from the formula

$$s = \frac{Dp}{2\varphi [\sigma]_t} + \Delta \quad (57)$$

where  $[\sigma]_t$  is the allowable stress intensity in kg/cm<sup>2</sup> varying between 700–1,100 kg/cm<sup>2</sup> which is selected according to type of seam, mechanical properties of the material and temperature of the wall;  $\Delta = 0.1$ –0.3 cm. is the corrosion allowance.

The value  $s$  is used to find  $d$  and  $t$  from the empirical relations in Table 8. Calculated from the formula (56) the value  $\xi$  should not exceed  $[\xi]$  shown in the Table.

To improve the tightness of the seam when all rivets have been driven *calking* should be carried out—the edges of the outside and inside plates should be driven together by a hammer struck against a calking iron, a tool in the form of a blunt chisel.

## CHAPTER VII WELDED JOINTS

The obvious advantages of welding lead to its widespread use in all branches of mechanical engineering.

Depending on the source of heat, welding is divided into the following *types*: chemical (gas and oxygen welding), chemico-mechanical (forge or furnace and thermit welding), electro-chemical (atomic hydrogen welding), electro-mechanical (resistance welding) and electric (arc welding). In modern machine production preference is given to electro-mechanical and electric welding.

There are several types of *electro-mechanical or resistance welding*: butt welding, spot welding, seam welding and projection welding.

Fig. 46 shows by way of illustration various automotive parts butt-welded by the resistance method.

Spot welding is used to join sheet packs up to ~36 mm thick, and seam welding to join parts up to 4 mm thick.

A projection weld, when several spots are welded simultaneously (Fig. 46, f) (a modification of spot welding), is used to connect parts touching each other at several points.

In electric or arc welding the heat for the melting of the metal is provided by an electric arc the ionised stream of which at steady burning reaches a temperature of up to  $5,000^{\circ}\text{C}$ . Especially widespread is the metal arc welding process suggested in 1888 by the Russian engineer N. G. Slavyanov (1854-1897).

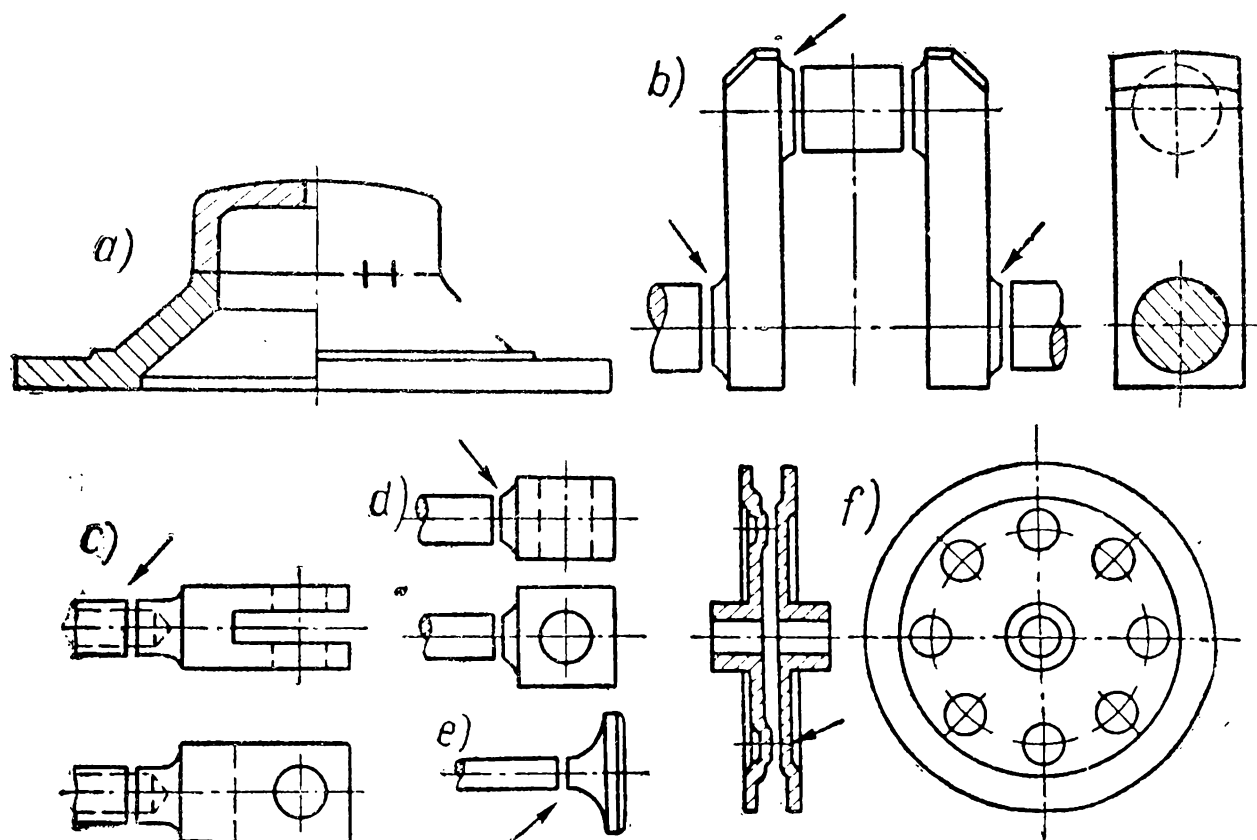


Fig. 46

A highly-productive *electric slag* welding method has been developed by the Paton Institute of Electric Welding of the Ukrainian Academy of Sciences.

Electric slag welding is based on the use of the heat given off by a current flowing through liquid current-conducting slag placed between the surfaces of the parts to be welded.

Since several electrode wires are brought simultaneously into the welding zone this method allows thick metal to be welded in one pass.

An *arc weld* can be effected automatically or manually. In automatic welding the arc burns between the base metal of the parts to be welded and the electrode wire, which is automatically fed into the arc zone by a special welding head. Manual welding is employed when automatic welding is difficult because of short seams or sharp turns.

Electric welding is successfully used to produce a great variety of machine parts. Fig. 47 shows (a) the welded thrust bearing of a jib crane pillar, (b) the frame of an eccentric press and (c) the rotor of an electric motor.

During welding the heat developed by the electric arc melts the surface of the joined parts with the result that a molten pool forms

between them to which the filler metal of the fused electrode (welding wire) is added. The parts to be fastened are melted to a depth of 2-5 mm (the depth of penetration).

When the quality of welding is poor the seam may develop various faults of which the main ones are (Fig. 48): (a) the *inclusion of slags and oxides* in the form of dots, chains or strips, (b) *undercut weld* and (c) *poor penetration* at the heel of the seam.

These faults reduce the strength of welded joints especially under varying loads when their role as stress concentration points is especially important.

Automatic submerged arc welding (under a layer of flux) developed by the Institute of Electric Welding of the Ukranian Academy of Sciences under the direction of Y. O. Paton (1870-1953) makes it possible to obtain seams which are stronger and more uniform than those obtained by hand welding.

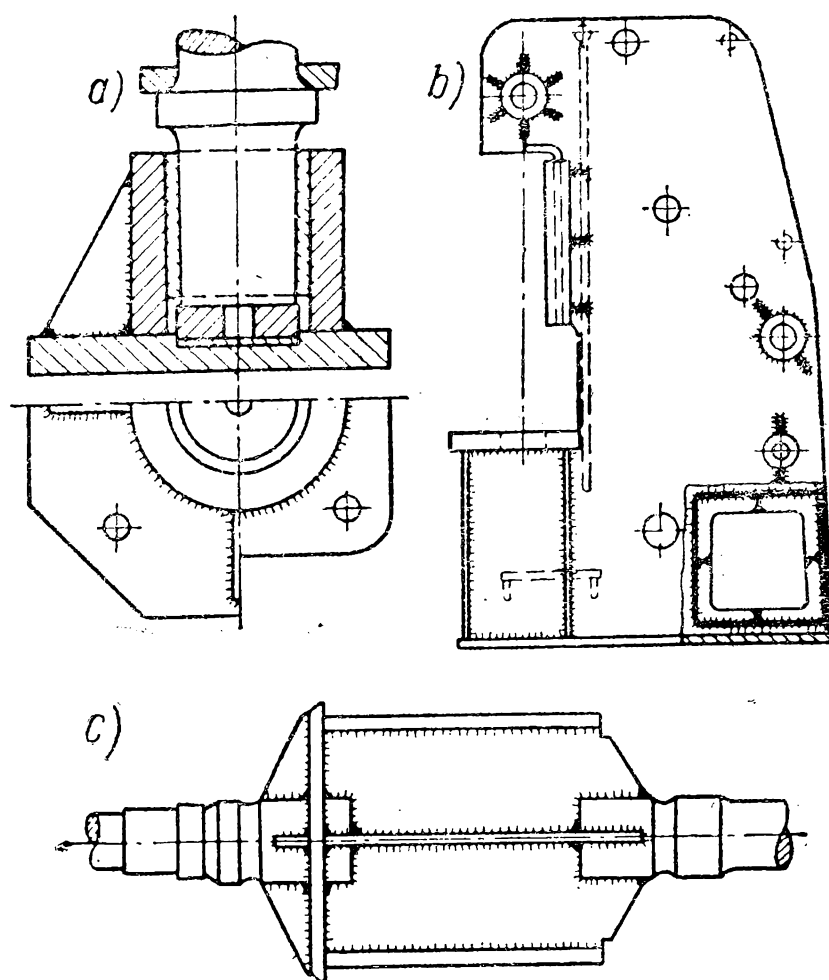


Fig. 47

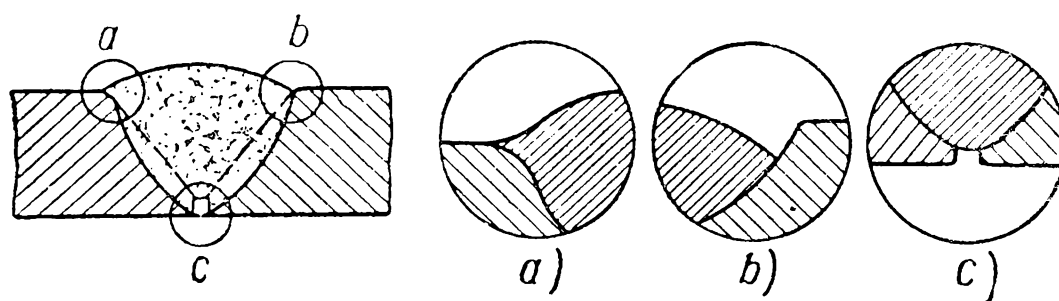


Fig. 48

Most metals and alloys utilised in modern engineering can be satisfactorily welded.

In our further exposition the problems of designing welded joints are dealt with on the assumption that the structures are made from ordinary carbon steel and joined by electric welding.

*Advantages of welded work over riveted and cast work. The application of welding instead of riveting to make permanent joints has*

a number of advantages, the chief being economy of material and labour.

Metal is saved due to:

a) the lighter weight of members joined by welding (the weight of welds comprises  $\sim 1$ -1.5 per cent of the work weight while the weight of rivets  $\sim 3.5$ -4 per cent);

b) the better utilisation of metal due to the absence of holes which weaken the effective sections;

c) the possibility of a wide use of butt-jointed seams requiring no additional elements such as straps.

The use of welding instead of riveting saves on an average 10 to 20 per cent in weight.

Less labour is required because it is no longer necessary to lay out, punch or drill the holes. Besides, riveting is a much more complicated and less productive job than welding which can be often largely automatised.

The *use of welding in place of casting* in the manufacture of machine parts reduces the volume of metal due to: a) lesser machining allowances and b) the possibility of utilising smaller sections since the wall thickness of cast parts, determined in many cases by the casting process, is as a rule 2-3 times greater, and sometimes even more, than that of welded parts.

As an illustration, the cast housing of a heavy crane reduction gear weighs 11,500 kg and a welded housing—7,840 kg; the weight of a cast toothed wheel is 7,700 kg and of a welded one—5,420 kg. The saving of metal in welded machine components as compared with cast ones may amount to 40 per cent.

Whether machine parts should be welded is decided in each particular case by design and economy considerations. Electric welding nearly always proves advantageous in limited quantity production where the cost of casting patterns is distributed among a limited number of articles produced.

Electro-mechanical welding is successfully used in mass production, especially in fabricated weldments when the formed blanks are welded by the resistance butt method into components with a great variety of shapes (see Fig. 46, *a* and *f*).

A *welded joint* is a combination of parts fastened together by means of a weld. *According to their purpose* welded joints are subdivided into *strong* and *tight-strong*. Their functions are the same as those of riveted joints: to transmit load from one member to the other in strong joints and to provide, besides, for fluid and gas impermeability in tight-strong joints.

Welded joints are divided into the following types: *butt*, *lap* and *strapped*, *Tee* and *corner* joints. The classification of the main types of welds used for various joints is illustrated in Fig. 49 where

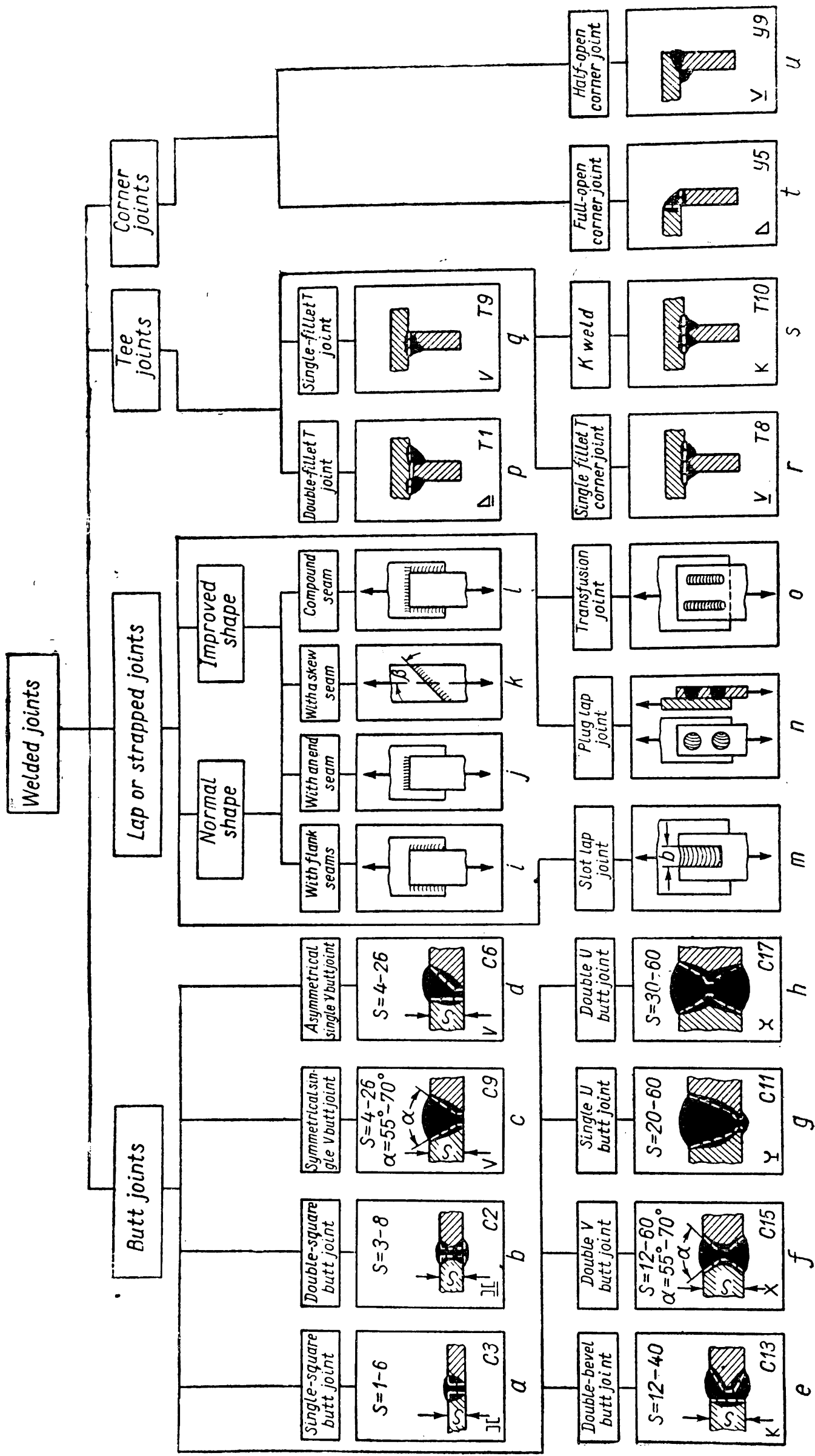


Fig. 49

the symbols for each weld are shown in the left-hand corner graphically and in the right-hand corner in letters and figures.

Seams used to join members located in one plane are called *butt-jointed*. The type of a butt-jointed seam is determined by the manner in which the edges of the elements to be joined are prepared (Fig. 49, a-h).

When comparing V and U joints it should be noted that U joints require less electric power and electrode material since the cross-

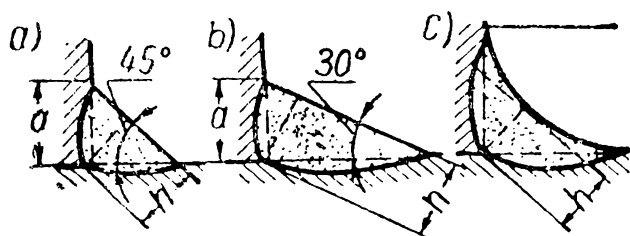


Fig. 50

section of a U joint for a given plate thickness is less than that of a V joint. Another advantage of U joints lies in the fact that due to the insignificant bevel of the edges the shrinkage of molten metal on cooling occurs almost uniformly over the entire section and the plates warp less than in case of V joints.

Double V and U joints are by no means inferior to single V joints when plates of 12 mm and over are welded because the cross-sectional area of double V and U joints is 30-40 per cent less than that of single V joints at the same bevel angle  $\alpha$ . The shortcomings of double V and U joints accrue from poor penetration liable to occur inside the butt and the greater cost of edge preparation especially in the case of U joints.

The types of butt-jointed seams described above formed by manual electric arc welding are widely used in the manufacture of welded machine components. In automatic arc welding the edges of the members to be joined differ slightly, having another bevel angle  $\alpha$ , which is here from 30 to 50°.

Welds intended to join elements located in different planes are called *corner welds*.

Depending on the form of the weld section there are *normal* welds in the shape of isosceles triangles (Fig. 50, a), *improved* welds in the shape of triangles with the base larger than the height (Fig. 50, b) and improved welds in the shape of curvilinear triangles (Fig. 50, c). The main type of a fillet weld is shown in Fig. 50, a.

The minimum length of the weld cathetus  $a_{\min} = 3$  mm when the thickness of the joined plates  $s \geq 3$  mm. The minimum length of a fillet weld  $l_{\min} = 30$  mm. In welds of smaller length the faults at the beginning and the end noticeably lessen the strength of the weld.

Strapped joints can be *single-strap* with or without butt-welding of the fastened elements or *double-strap* (Fig. 51, c). The thickness of a single strap is  $s_s = (0.7-1)s$  and of a double-strap— $s_s = (0.3-0.5)s$ .



## CALCULATION OF WELDS

**Welded Joints Designed for Static Load.** Welds are designed on the assumptions that:

- a) load is distributed evenly along the entire weld length;
- b) stress is spread evenly over its effective section.

*Butt-jointed* seams are calculated for tension or compression, the thickness  $s$  of the thinner of the jointed plates being taken as the design throat of the weld (Fig. 51, a).

Irrespective of type, the effective length of a butt-jointed seam in joints in tension (Fig. 51, a) is found from the formula

$$l = \frac{P}{s[\sigma']_t} \text{ cm} \quad (58)$$

where  $P$  is the load applied to the weld in kg,

$[\sigma']_t$  — the allowable stress for the weld in tension in kg/cm<sup>2</sup> chosen from Table 9 depending on the type of the electrode and allowable stress for the base metal.

With welds in compression  $[\sigma']_t$  in the formula (58) should be replaced by the allowable stress for compression  $[\sigma']_c$  for the given material of the electrode.

When the weld length is equal to the width of the welded parts, i.e., at  $l = b$ , the safety factor of the butt-jointed seam is

$$\varphi = \frac{ls'[\sigma']_t}{bs[\sigma]_t} = \frac{[\sigma']_t}{[\sigma]_t}.$$

In this way equal strength of joint and base metal ( $\varphi = 1$ ) can be obtained when  $[\sigma']_t = [\sigma]_t$ . In case  $[\sigma']_t < [\sigma]_t$  the strength of a straight joint is weaker than the strength of the integral element ( $\varphi < 1$ ).

A skew joint increases the strength of the joint. At  $\beta = 45^\circ$  (Fig. 49, k) the weld and the base metal in elements made from low-carbon steel have the same strength.

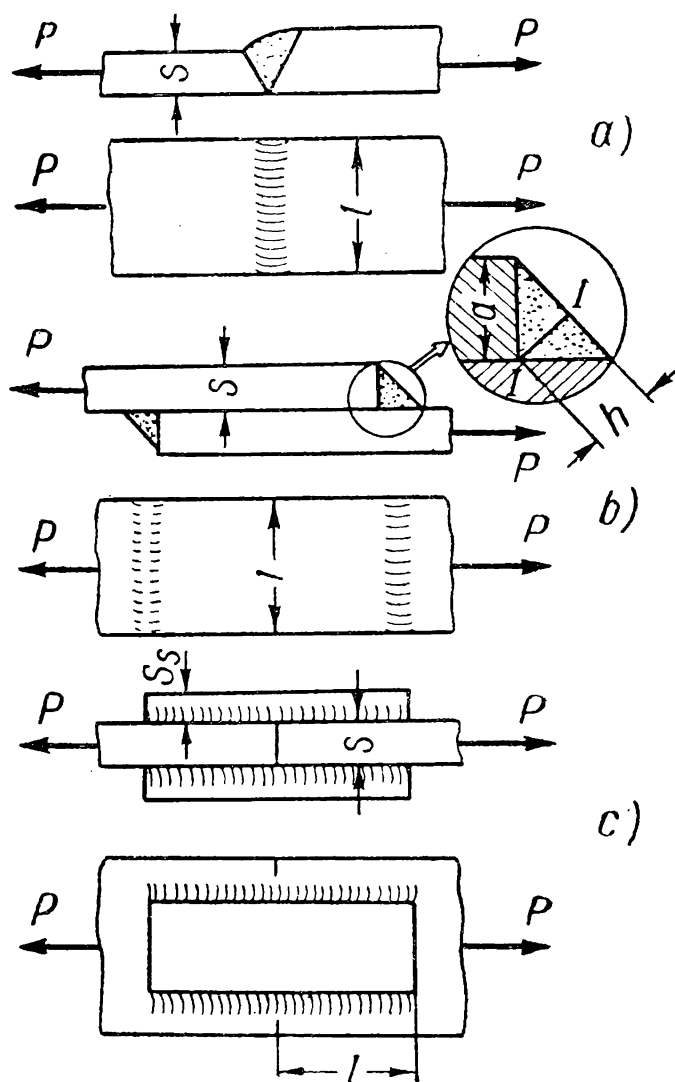


Fig. 51

For a *K weld* in a T joint subject to the action of a tensile force  $P$  (Fig. 52, *a*) the strength equation is

$$\sigma = \frac{P}{sl} \leq [\sigma']_t.$$

Hence, the minimum necessary length of the weld is

$$l = \frac{P}{s[\sigma']_t} \text{ cm.} \quad (59)$$

Here the effective throat of the weld is taken as equalling the thickness  $s$  of the welded element. If a moment  $M$  acts upon this joint simultaneously with a force  $P$  (Fig. 52, *b*) the strength equation will take the form

$$\sigma = \frac{P}{sl} + \frac{6M}{sl^2} \leq [\sigma']_t. \quad (60)$$

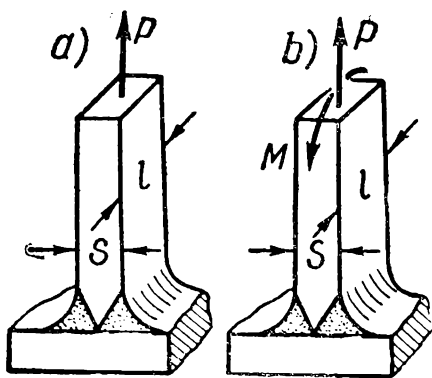


Fig. 52

Double fillet lap joints are calculated for shear. The section *I-I* in such a weld is the weakest (Fig. 51, *b*). The design throat of a weld in an isosceles triangle is  $h = a \sin 45^\circ \approx 0.7 a$  where  $a$  is the weld cathetus. The

throat  $h$  of various types of corner joints is shown in Fig. 50, *a-c*.

For a double fillet lap joint (Fig. 51, *b*) the equation for strength will be

$$P = 2hl[\tau'] = 2 \times 0.7a \times l[\tau']$$

whence the necessary length of the weld

$$l = \frac{P}{1.4a[\tau']}. \quad (61)$$

Here  $[\tau']$  is the allowable stress for the weld metal in shear in  $\text{kg/cm}^2$  chosen from Table 9 depending on the value  $[\sigma]_t$  for the base metal.

When the length of weld  $l$  is equal to the width  $b$  of the jointed elements and  $a = s$  the joint safety factor is

$$\varphi = \frac{2 \times 0.7al[\tau']}{sb[\sigma]_t} = 1.4 \frac{[\tau']}{[\sigma]_t}.$$

It can be seen that equal strength of weld and base metal is possible at  $[\tau'] = 0.7[\sigma]_t$ , i.e., when welding is done with an Э42А electrode (see Table 9).

*Longitudinal fillet welds* are also calculated for shear. The necessary length  $l$  of such a weld (Fig. 51, *c*) can be found from the formula (61).

Table 9

## Allowable Stresses in Welds under Static Load

Ratio of allowable stress to $[\sigma]_t$ for base metal	Method of welding				
	Hand welding with electrode			Automatic submerged-arc welding	Semi-automatic welding with inclined or lying electrodes
	Э34*	Э42**	Э42А		
in compression $\frac{[\sigma']_c}{[\sigma]_t}$	0.75	0.90	—	—	0.90
in tension $\frac{[\sigma']_t}{[\sigma]_t}$	0.60	0.80	0.90	0.90	0.80
in shear $\frac{[\tau']}{[\sigma]_t}$	0.50	0.65	0.70	0.70	0.60

\* Base metal—low-carbon steel.

\*\* Base metal—low-carbon steel, carbon low-alloy structural steel.

The calculation of *compound welds* is based on the principle of the independence of the force action. For a compound weld (shown, for example, in Fig. 49, *l*) the safe load it can carry is

$$P = P_{lon} + P_{tr} = h \Sigma l [\tau'] = 0.7a \Sigma l [\tau']$$

whence the necessary total length of all welds (longitudinal and transverse) at a given weld cathetus  $a$  will be

$$\Sigma l = \frac{P}{0.7a [\tau']}. \quad (62)$$

*Fillet welds in T joints* are calculated in the same manner as transverse or longitudinal welds when the load is applied in a direction perpendicular to the plane of the welds (Fig. 53, *a*) or parallel to their plane with a small eccentricity (Fig. 53, *b*). If the force acts parallel to the plane of the welds with a considerable eccentricity (Fig. 53, *c*) the welds are calculated for joint action of the bending moment and shearing force according to the formula of total stress.

The stress in a weld due to a shearing force  $P$

$$\tau_1 = \frac{P}{0.7F} \text{ where } F = 2al.$$

The stress in a weld due to a moment  $PH$

The coefficient 0.7 at  $W$  and  $F$  takes into account the possibility of rupture in the dangerous section—the plane of the weld bisectrix (see Fig. 51,  $b$ ).

The total stress is

$$\tau = \sqrt{\tau_1^2 + \tau_2^2} = \frac{P}{0.7F} \sqrt{1 + \left(\frac{6H}{l}\right)^2} \leq [\tau']. \quad (63)$$

If the joint under examination is acted upon by a bending moment  $M$  and a force  $P$  as shown in Fig. 53,  $d$  the strength equation will take the form

$$\tau = \frac{M}{0.7W} + \frac{P}{0.7F} \leq [\tau']. \quad (64)$$

Depending on the shape of an all-around weld corresponding values of  $W$  and  $F$  are substituted in the formulae (63) and (64).

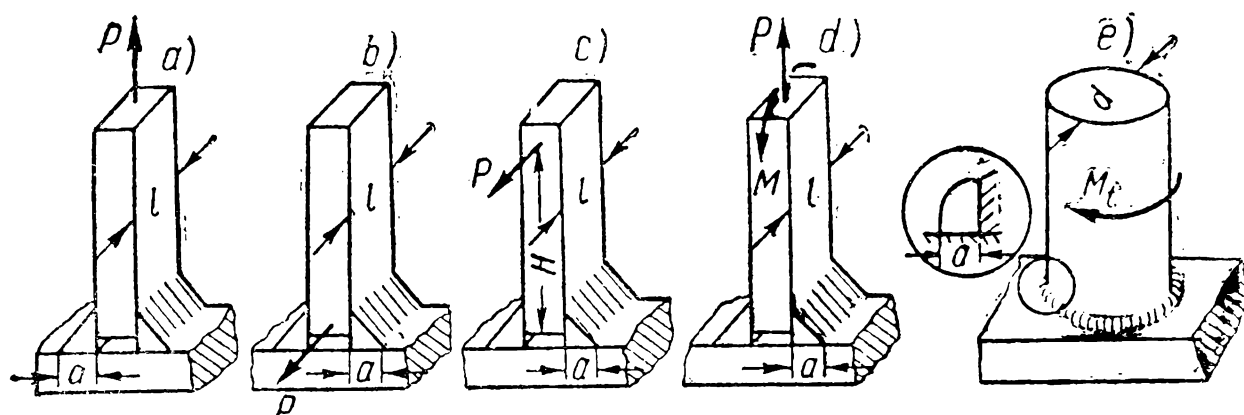


Fig. 53

If a rod,  $d$  in diameter, welded by a circumferential corner joint is subjected to the action of torque  $M_t$  (Fig. 53,  $e$ ) the necessary value of the weld cathetus can be found in the following way.

The torque which a weld of unit length can carry is

$$\Delta M_t = 1 \times 0.7a [\tau]' \frac{d}{2},$$

hence

$$M_t = \pi d \Delta M_t = \frac{0.7}{2} \pi d^2 a [\tau]'$$

and

$$a = \frac{2M_t}{0.7\pi d^2 [\tau]'} \quad (65)$$

*Slot* welds are calculated for shear. The slot is made parallel to the applied load. The recommended width of slot (Fig. 49,  $m$ )  $b = 2s$  where  $s$  is the thickness of the cut metal. The necessary length of slot is

$$l = \frac{P}{b [\tau]'} = \frac{P}{2s [\tau]'} \quad (66)$$

The slot length  $l$  should not exceed  $30s$ .

*Plug* welds (Fig. 49,  $n$ ) are used to increase the contact tightness of joint elements in combination with other loaded welds. The plug is usually  $2s$  in diameter.

A *transfusion* weld is a modification of a slot weld (Fig. 49,  $o$ ). The elements are joined in this case by welding through the upper plate which should not be more than 12 mm thick. Transfusion welds are made by the automatic submerged-arc method.

**Strength of Welds at Varying Load.** The strength of welded seams at varying loads depends to a considerable degree on the quality of the welding. Small faults in the form of local poor penetration, undercuts and fractures, being points of stress concentration, reduce the endurance limit of the welded joints as compared to that of the base metal.

Automatic welding gives a higher quality weld; therefore, at varying load, the strength of joints made by automatic welding is higher than of joints welded manually.

Joints formed by the resistance butt welding method also possess high strength at varying load.

The endurance of different types of joint varies: it is lower in work where the imaginary force flux has a larger inflection.

The direction of the force flux and the nature of stress distribution in dangerous weld sections and in sections of elements at the weld are shown in Fig. 54.

In butt joints the flux of the lines of force is almost rectilinear. Joints of this type are superior to joints with fillets.

Lap and strapped joints have low strength at varying loads due to very uneven stress distribution along the section of the weld and the base metal (Fig. 54,  $b$ ). Longitudinal fillet welds should be avoided as far as possible because they cause additional unevenness of stress along the weld length at varying load.

The T joints shown in Fig. 54,  $c$  are much better than the similar joints in Fig. 54,  $d$ .

The endurance limit of a T joint with a double-bevel weld (Fig. 54,  $e$ ) is considerably higher than that of a fillet T joint. The fatigue strength of joints with improved fillets (Fig. 50,  $b$  and  $c$ ) is very high.

Peening by shot blasting or roll burnishing of the weld areas in work made from mild steel tends to increase their strength at varying load.

*The strength of welded joints at varying load* is calculated according to the formulae of static load with reduced allowable stresses. For this purpose the values  $[\sigma']_t$  and  $[\tau']$  found from Table 9 are multiplied by the empirical factor  $\gamma$  whose value depends on the weld design and the ratio  $\frac{P_{\min}}{P_{\max}}$  where  $P_{\min}$  and  $P_{\max}$  are the lowest and highest loads in absolute value taken with their signs.

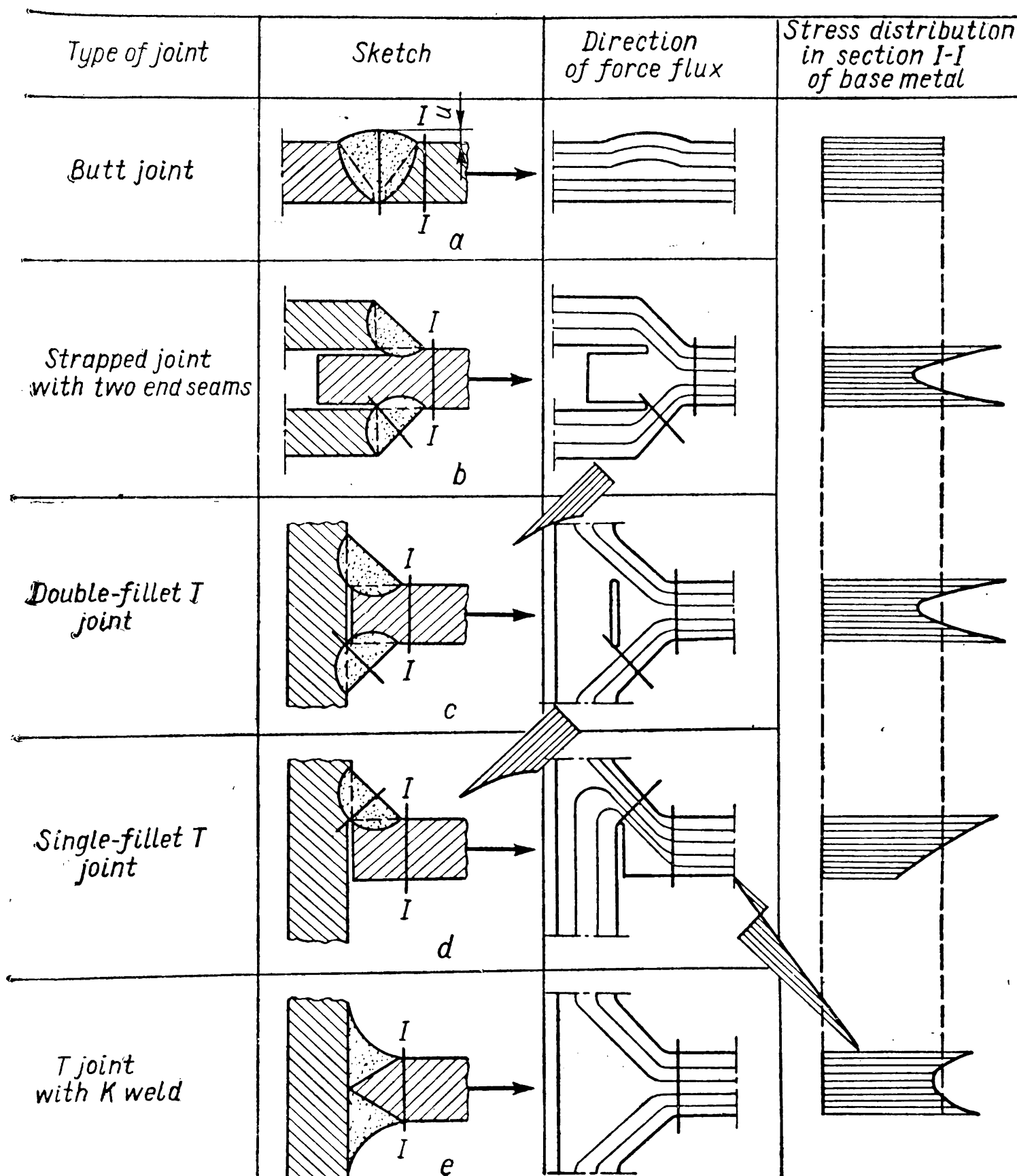


Fig. 54

The factor  $\gamma$  is found from the formula used for riveted joints [formula (55)] and is introduced in *calculating butt joints* only for cycling load.

For corner and slot welds  $\gamma = \frac{1}{1.3 - 0.3 \frac{P_{\min}}{P_{\max}}}$  is introduced into the calculation for any cycles of varying loads.

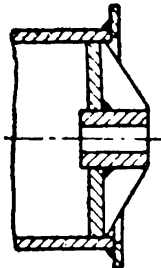
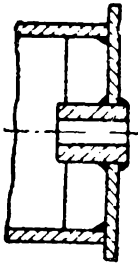
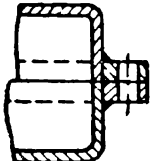
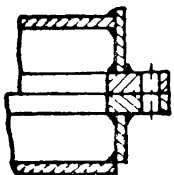
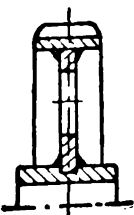
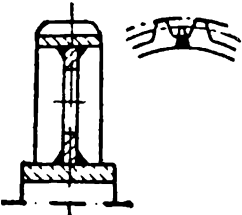
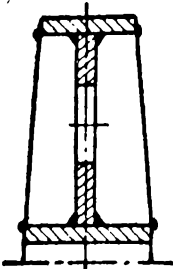
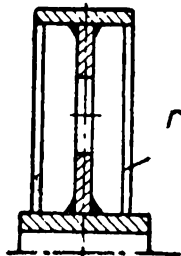
In tightness welded joints are much superior to riveted joints. Special calculations to ensure the tightness of welds are not required.

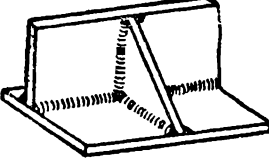
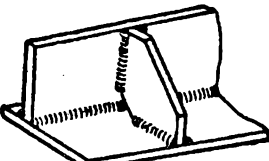



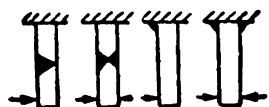
In welded cylindrical pressure vessels the longitudinal weld is the design throat.

*Welding of machine components.* The efficiency of welding in the manufacture of various machine components can be ensured through the observance of a number of production and design factors. The latter include the proper choice of the type of joint and the shapes of stiffening ribs, the rational location of welds, etc.

By way of illustration Table 10 shows satisfactory and poor designs of certain welded parts and joints.

Table 10

Poor	Satisfactory	General recommendations
<i>Rope drum</i> 		Reduce the number of welded members, welds and ribs. Apply double welds only for severest acting loads.
		
<i>Housing flanges</i> 		Never locate seams in the flange parting planes. Make inner welds only in heavy housings.
		
<i>Toothed wheel</i> 		Make the rim from flat steel and butt-weld so as to locate the weld in the tooth gash. Do not machine the hub and rim before welding.
		
<i>Brake wheel</i> 		Do not cut out the ribs but form them from flat steel. The rim should overhang the ribs.
		

Poor	Satisfactory	General recommendations
		Cut off the corner of the rib to eliminate the weld intersection.
		Locate the sealing welds inside.
		Do not locate the weld base in the zone of tension.

*Example.* Determine the stresses in the fillets of an I beam welded all-around (Fig. 55, a).

Given: Load  $P=10\text{ t}$ , beam height  $h=25.2\text{ cm}$ , beam length  $l=15\text{ cm}$  weld cathetus  $a=0.6\text{ cm}$ , flange width  $b=18\text{ cm}$ .

Short vertical welds are neglected.

Assuming the shearing force is taken only by the vertical welds whose area is  $F=27.4\text{ cm}^2$  we obtain the mean stress in them from  $P$ :

$$\tau_1 = \frac{P}{0.7F} = \frac{10,000}{0.7 \times 27.4} = 520\text{ kg/cm}^2.$$

The maximum stress from the moment  $Pl$  at the farthest edge of the vertical plate at the moment of inertia of the fillets (Fig. 55, c) being  $I=8,000\text{ cm}^4$ .

$$\tau_2 = \frac{Pl}{0.7I} \times y_a = \frac{10,000 \times 15}{0.7 \times 8,000} \times 12 = 322\text{ kg/cm}^2.$$

The total stress

$$\tau = \sqrt{\tau_1^2 + \tau_2^2} = \sqrt{520^2 + 322^2} = 612\text{ kg/cm}^2.$$

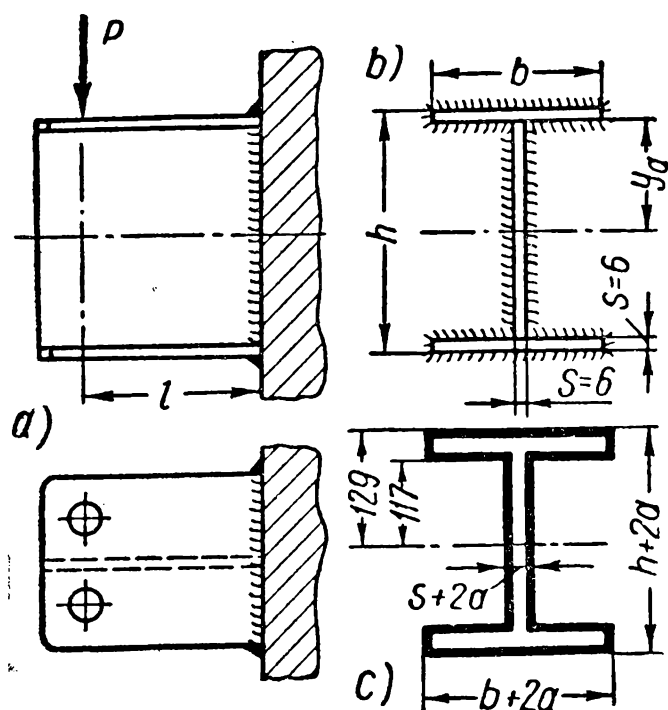


Fig. 55

This is below the allowed stress which is equal to  $0.5[\sigma]_t = 0.5 \times 1,400 = 700\text{ kg/cm}^2$ , and the weldment can be approved.



## CHAPTER VIII

## JOINTS FORMED BY INTERFERENCE FITS

Joints formed by interference fits are permanent-type joints which fall into two categories:

1) joints with interference between the fastened members, usually referred to as *press-fitted joints* (or press fits).

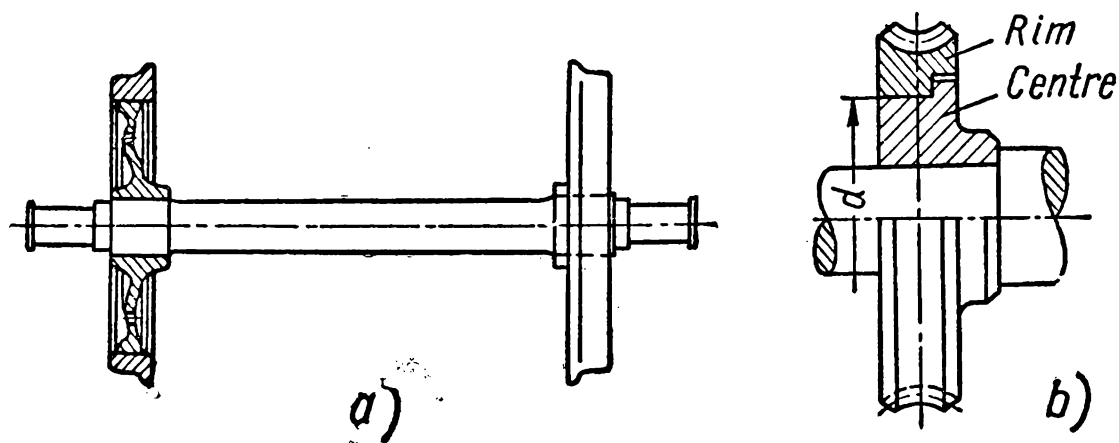


Fig. 56

These fits are used to fasten axles to the wheels of railway rolling-stock, and tyres to these wheels, worm gear rims to wheel centres and various bushings in machine housings, etc. (Fig. 56);

2) joints secured by *ancillary parts* (shrink collars and links) which are pressed onto the mating parts (Fig. 57).

Press-fitted joints are more extensively used. They are distinguished by simple design and reliability achieved by adequate machining of the contact surfaces (with regard to finish and geometrical accuracy) and proper assembly. Such joints can be repeatedly disassembled (pressed out) and assembled (pressed in) without undue reduction in the strength of the joint.

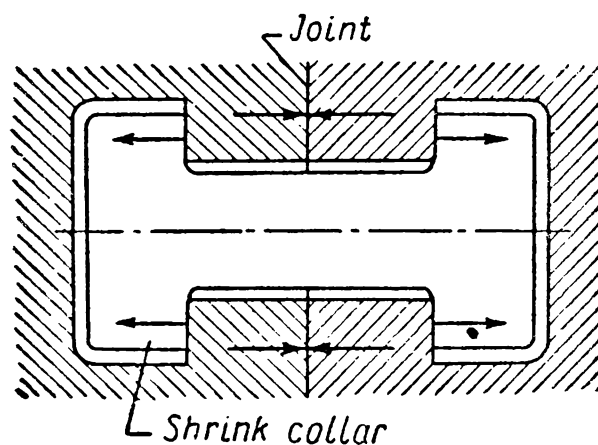


Fig. 57

The main disadvantage of these joints is the difficulty of controlling their dependability during assembly and the high accuracy required of the mating sizes. Such joints of a shaft-hub type lose some shaft (axle) strength due to stress concentration caused by fitting and also to frictional resistance between the contact surfaces which arises at cyclic load.

*Press-fitted joints.* The strength of a press-fitted joint may be defined as its ability to resist an axial thrust or torque, or the joint action of both forces, which tend to displace one part relative to the other.

The load-carrying capacity of a press-fitted joint depends primarily on the amount of interference  $\delta_i$ , i. e., the difference between the actual diameters of the shaft and hole measured before assembly.

Joints of this type may be assembled by force or shrink fits, heating the female or cooling the male part.

A force fit is carried out by applying an axial thrust to move one member by the required distance relative to the other. To prevent scores and reduce the pressing effort the mating surfaces are lubricated with rape or linseed oil. The member should be fitted at maxi-

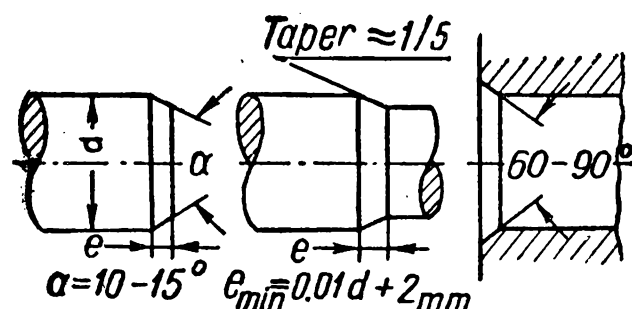


Fig. 58

mum  $\sim 5$  mm/sec since greater speeds lessen the strength of the joint. The form of the edges of the mating surfaces determines the pressing effort and the state of the surface. Recommended forms and dimensions are shown in Fig. 58. A chamfer on the end-face of the external member ensures better centering of fit in pressing.

Press-fitted joints can also be formed by heating the external member or cooling the internal member to a temperature at which it can be readily inserted.

The member is heated to the required temperature either in hot oil or in a gas or electric furnace.

To cool the internal member use is made of liquid air or dry ice (solid carbon dioxide). When using liquid air as a cooling medium never forget to degrease the cooled members and open and heat-insulate the vessel containing liquid air, etc.

Shrink fits form stronger (about 2.5 times) joints than force fits since during the forcing operation abrasion takes place and interference is reduced.

In a joint assembled by interference (Fig. 59) the elastic deformation of the mating members (the external member expands and compresses the internal member) causes unit pressure  $p$  to arise on the contact surfaces. If the size of the members and the mechanical properties of material from which they are made are known the value of  $p$  can be found from the formula

$$p = \frac{\delta \times 10^{-3}}{d \left( \frac{c_1}{E_1} + \frac{c_2}{E_2} \right)} \text{ kg/mm}^2 \quad (67)$$

where  $\delta$  is the design interference in mc;

$d$ —the rated diameter of the mating surfaces in mm;

$E_1$  and  $E_2$ —the moduli of elasticity of the internal and external members in kg/mm<sup>2</sup>;

$c_1$  and  $c_2$ —the coefficients estimated from Lamé's formula for thick-walled cylinders deformed symmetrically relative to their axes,

$$c_1 = \left( \frac{d_2^2 + d_1^2}{d_2^2 - d_1^2} - \mu_1 \right); \quad c_2 = \left( \frac{d_2^2 + d^2}{d_2^2 - d^2} + \mu_2 \right).$$

Here  $\mu_1$  and  $\mu_2$  are the values of Poisson's ratio; for steel  $\mu \approx 0.3$ , for cast iron  $\mu \approx 0.25$ ; the diameters  $d_1$  and  $d_2$  are shown in Fig. 59.

When the joint is subjected to an axial thrust  $P$  which tends to shift axially one part relative to the other, friction forces hindering this displacement arise on the contact surfaces. The tightness of the joint is preserved if the following condition is satisfied

$$P \leq \pi d l p f \quad (68)$$

where  $l$  is the length of the joint engagement in mm and  $f$  is the coefficient of friction.

The torque which can be applied to the joint is

$$M_t \leq \pi d l p f \frac{d}{2} = \frac{\pi}{2} d^2 l p f. \quad (69)$$

If the joint transmits the torque  $M_t$  and simultaneously resists the axial thrust  $P$  the relation will assume the form

$$\sqrt{\left( \frac{2M_t}{d} \right)^2 + P^2} \leq \pi d l p f. \quad (70)$$

The magnitude of the coefficient of friction in a press-fitted joint depends on many factors: the material of the mated couple, machining and finish of the contact surfaces, lubrication, direction of shift (axial, circumferential), the operation (pressing in or out) and the force of contact pressure.

In designing practice use is made in the formulae (68), (69) and (70) of the mean values of the coefficient of friction for steel and cast-iron parts which are characteristic of pressing out at stable shift:

$f \approx 0.08$  for a force fit;

$f \approx 0.14$  for a shrink fit.

On the basis of the formulae (67) and (68), (67) and (69), (67) and (70) and with a corresponding nature of loading we can find the amount of design interference  $\delta$ :

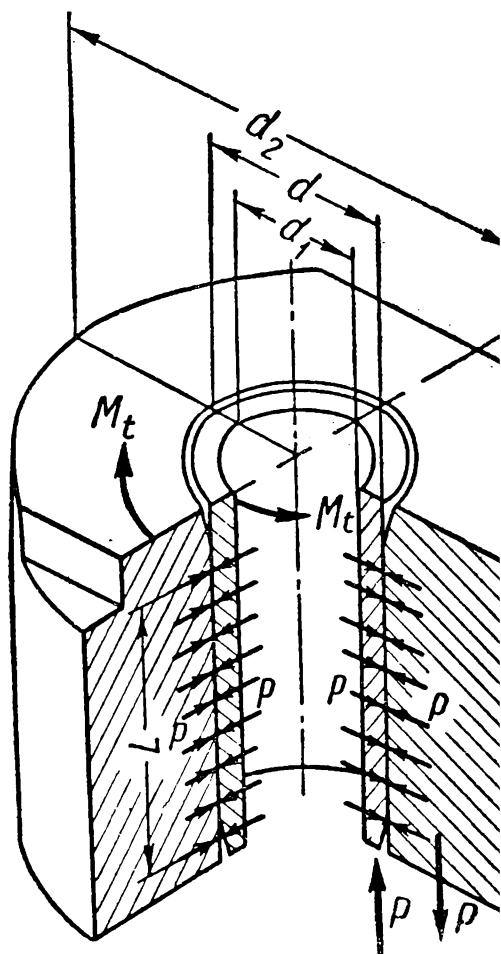


Fig. 59

under axial thrust

$$\delta = \frac{P}{\pi l f} \left( \frac{c_1}{E_1} + \frac{c_2}{E_2} \right) \times 10^3 \text{ mc}; \quad (71)$$

under torque

$$\delta = \frac{2M_t}{\pi d l f} \left( \frac{c_1}{E_1} + \frac{c_2}{E_2} \right) \times 10^3 \text{ mc}; \quad (72)$$

under joint action of torque and axial thrust

$$\delta = \frac{\sqrt{\left( \frac{2M_t}{d} \right)^2 + P^2}}{\pi l f} \left( \frac{c_1}{E_1} + \frac{c_2}{E_2} \right) \times 10^3 \text{ mc}. \quad (73)$$

Abrasion due to the forcing operation partially smooths the surfaces and the actual interference becomes less than the initial value measured before assembly. To compensate for this phenomenon, the interference  $\delta_i$  should exceed the design value

$$\delta_i = \delta + u \quad (74)$$

where  $u$  is the abrasion during the forcing operation assumed to be equal to

$$u \approx 1.2(h_1 + h_2).$$

Here  $h_1$  and  $h_2$  indicate the maximum height of microirregularities on the contact surfaces in mc. They depend on the machining methods. Thus, for example:

- at rough turning  $h_{\max} = 16-40 \text{ mc}$ ;
- at finish turning  $h_{\max} = 2.5-6 \text{ mc}$ ;
- at fine grinding  $h_{\max} = 2.5-6 \text{ mc}$ ;
- at extra fine grinding  $h_{\max} = 1-2.5 \text{ mc}$ .

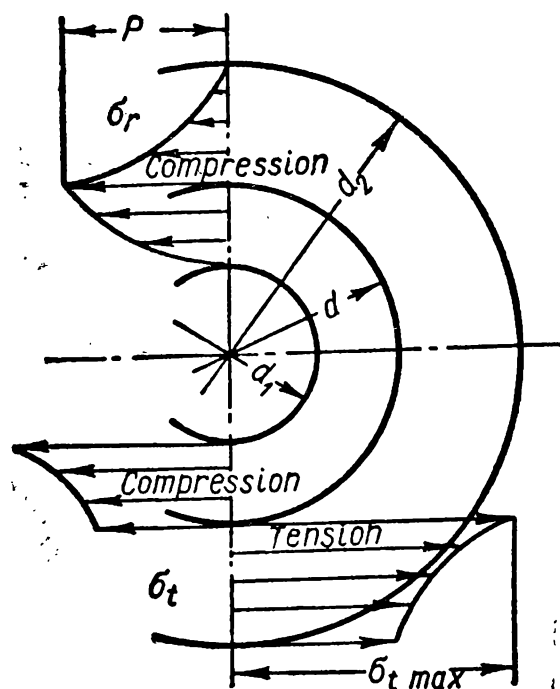


Fig. 60

The value  $\delta_i$  is used to select the standard press fit whose minimum interference equals  $\delta_i$  or is somewhat larger.

Research data show that surfaces with microirregularities give more dependable and homogeneous press-fitted joints.

Press fits develop considerable stresses in the joint members which at large interferences can cause failure.

The nature of change in the tangential  $\sigma_t$  and radial  $\sigma_r$  stresses for the external and internal members is shown in Fig. 60.

Maximum stresses occur on the contact surface of the external member, where

$$\sigma_{t \max} = p \frac{d_2^2 + d^2}{d_2^2 - d^2}; \quad \sigma_r = -p. \quad (75)$$

Plastic deformations on the contact surfaces are by no means always to be avoided: reliable joints can also be obtained with a circular plastic zone in the external member.

Fig. 61 shows the curves of change in the axial thrust from pressing in  $P_{in}$  and pressing out  $P_{out}$ . From the comparison of these curves it can be seen that an interference joint always possesses a safety reserve ( $P'_{out} > P_{out}$ ) because the coefficient of friction of rest is always larger than the coefficient of friction of motion.

To expand the external member the temperature to which it should be heated is approximately

$$t_2^\circ \approx \frac{\delta_{i\max} + \delta_0}{\alpha \times d \times 10^3} + t^\circ.$$

To shrink the internal member the temperature to which it should be cooled is

$$t_1^\circ \approx t^\circ - \frac{\delta_{i\max} + \delta_0}{\alpha \times d \times 10^3}.$$

Here  $\delta_{i\max}$  is the maximum interference in mc;

$\delta_0$  — the minimum clearance needed for assembly which depends on the devices used, weight and size of members in mc;

$\alpha$  — the coefficient of linear expansion (compression) of parts;

$t^\circ$  — the ambient temperature.

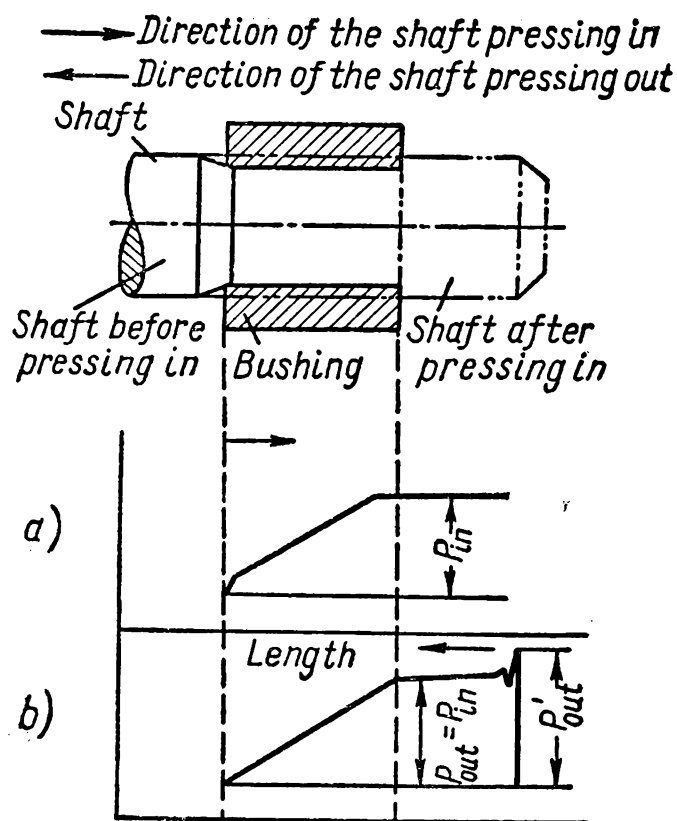


Fig. 61

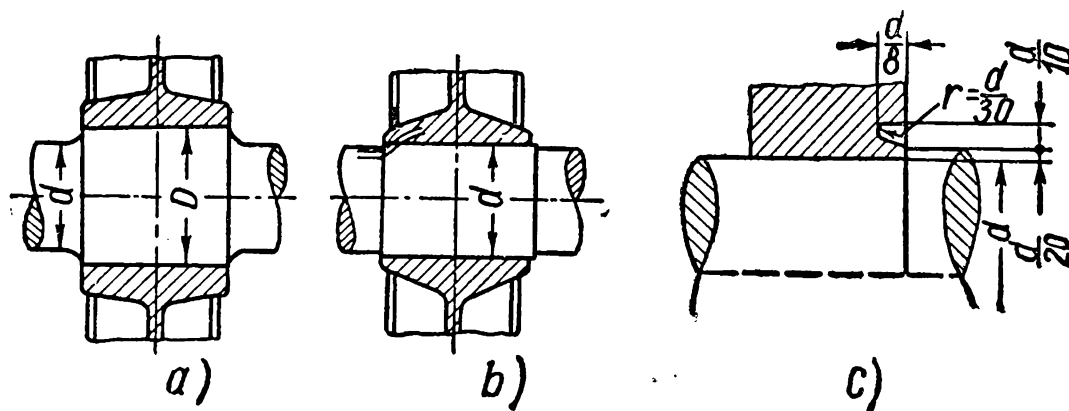


Fig. 62

The strength of press-fitted joints at repeated varying load has not yet been thoroughly studied.

Recent research into this field gives grounds to assert that at repeated varying load the joint loses nothing of its initial static strength.

Under such load conditions the strength of the members forming the joint largely depends on their design forms. Thus, the endurance

of the shafts (axles) is improved by increasing their diameter within the hub (Fig. 62, *a*), by rounding off the sharp edge of the hub bore, and giving the hub a conical form (Fig. 62, *b*) and by providing relieving grooves on the hub end-faces (Fig. 62, *c*), etc.

## CHAPTER IX

### THREADED JOINTS

A number of advantages offered by threaded joints favour their large-scale application in mechanical engineering. Threaded couples are highly reliable in operation, are convenient to assemble and disassemble, can be obtained in a wide range adapted to various operating conditions, and are relatively cheap to produce due to standardisation and the employment of highly efficient manufacturing processes.

The main disadvantages of threaded joints are the following:

a) the presence of numerous points of stress concentration on the threaded surfaces which makes them vulnerable under loads causing varying stresses and necessitates the employment of special methods to improve their endurance; b) the processing inadequacy of certain specific types of threaded parts which nevertheless have the highest strength.

Classification into *cylindrical and taper threads* depends on the basic surface on which thread is formed.

Thread can be cut into the surface or hole of a cylindrical bar or cone, the former being an *external* thread and the latter an *internal* thread.

When the threaded cylinder is turned clockwise to engage the second member the thread is said to be *right-hand* and when counterclockwise—*left-hand*.

The form of thread profile gives us *vee*, *trapezoidal* (and its modification *buttress*), *square* and *round* threads.\*

A screw made by cutting a single helical groove is called a *single* thread screw; when a greater lead per turn is required than can be had by a single thread—*double*, *triple*, etc., threads are used known as *multiple threads*. The number of threads can be easily counted by the fillet ends on the end-face of a threaded part.

For fastening purposes *metric* and *inch* single V threads\*\* are mainly used.

The main dimensions of thread are (Fig. 63): major diameter  $d_0$ , minor diameter  $d_1$ , pitch diameter  $d_p$ , thread pitch  $s$ , thread depth  $t_2$ , effective thread depth  $t'_2$ , thread angle  $\alpha$  and helix angle  $\psi$ .

\* In accordance with metric thread definitions.

\*\* Trapezoidal and square threads are intended to transmit motion; they are considered in Chapter XIX "Power screws".

The main dimensions of metric threads are given in Table 11.

Table 11

Metric Threads

Thread	Rated diameter in mm	Pitch in mm
Basic fastening . . . . .	0.3-0.9	0.075-0.225
Basic fastening . . . . .	1-5	0.25-0.8
Basic fastening . . . . .	6-68	1-6
Basic fastening . . . . .	72-600	6
First fine . . . . .	1-400	0.2-4
Second fine . . . . .	6-300	0.5-3
Third fine . . . . .	8-200	0.5-2
Fourth fine . . . . .	9-150	0.35-1.5

Basic metric threads are employed for principal fasteners. Fine metric threads are used in the manufacture of thin-walled parts, adjusters and also in joints exposed to the action of a dynamic load.

With the same rated diameters, fine thread differs from the basic type only in pitch and depth of thread. The ratio between the pitch of a basic thread and that of a fine thread of the same diameter is known as the *reduction ratio*; in the Soviet Union standards provide for four types of fine thread: 1st to 4th with the ratios of 1.5, 2, 3 and 4 respectively.

The imperfect thread section before the uncut portion is due to the form of the cutting tool. Sometimes, with a view to obtaining a perfect thread along the entire length, a neck is made instead for the withdrawal of the cutting tool.

The bisectrix of the thread angle of taper thread is perpendicular either to the axis of the taper (Fig. 64, a) or to the taper generatrix (Fig. 64, b).

Nowadays, preference is given to the former type because it allows the screwing of a taper thread from a cylindrical one and easier inspection of the taper thread. Taper threads are superior to cylindrical in that they:

- 1) ensure tightness of a joint without any sealing medium;
- 2) by means of an axial shift take up thread play caused by inaccuracies due to improper manufacture and wear of the thread working length;

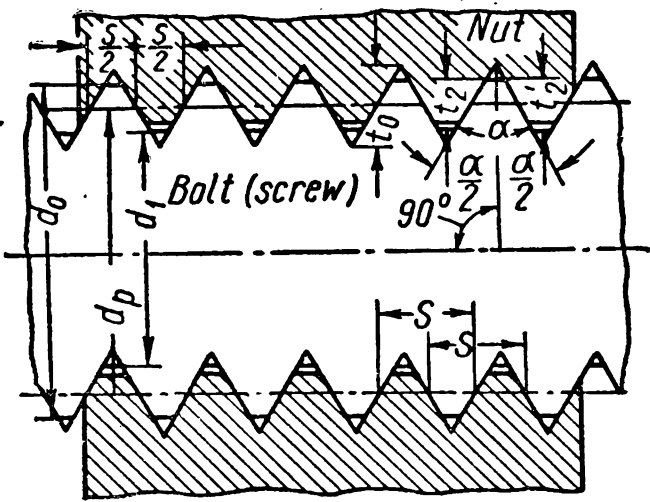


Fig. 63

- 3) spread the load more uniformly over the length of engagement;
- 4) save time in assembling and disassembling the joint.

Taper threaded joints are extensively used to connect pipes, especially for drilling operations in oil-fields where adequate tightness under high pressure and considerable load is the prime demand.

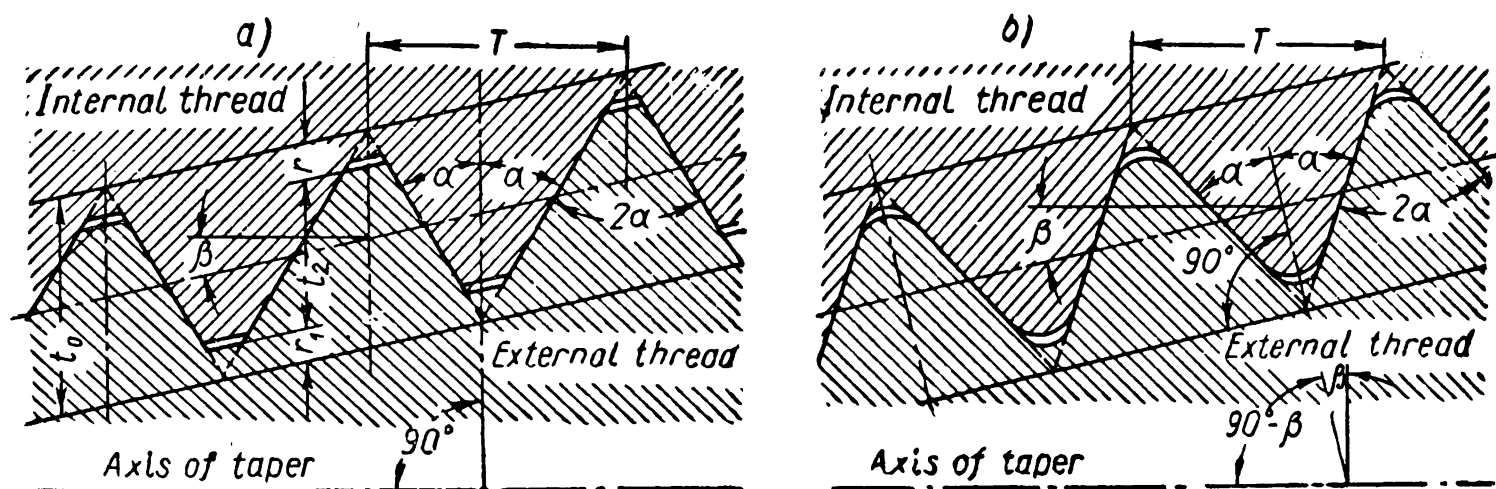


Fig. 64

The main standard threaded fasteners include bolts, studs, screws and nuts (Fig. 65). They are used in combination with washers and nut locks (retainers) of various design.

In general use a threaded joint can be formed without parts intended exclusively for fastening (see, for example, Fig. 66).

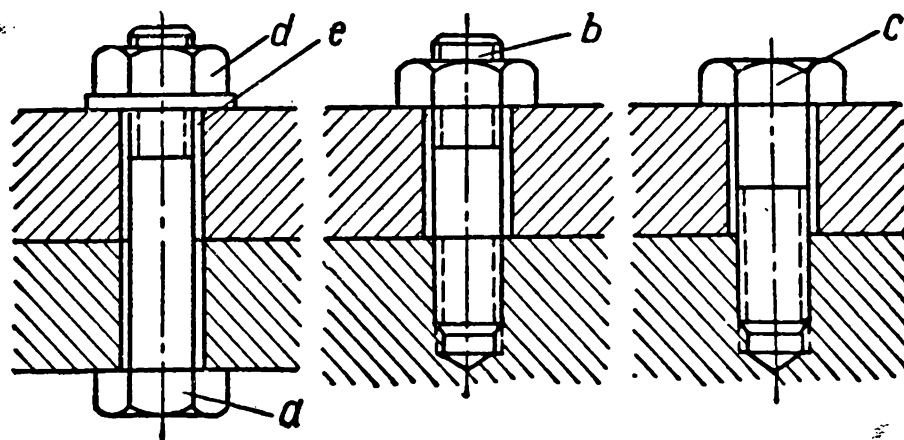


Fig. 65

A *bolt* (Fig. 65, a) is a bar with a thread for a nut at one end and a head at the other.

A *stud* (Fig. 65, b) is a bar threaded at both ends; the mating end of the stud is screwed into a tapped hole in one of the parts to be connected while the nut is screwed onto the other end.

A *screw* (Fig. 65, c) differs from a bolt in that its threaded portion is screwed into one of the fastened parts (without a nut).

A *nut* (Fig. 65, d) has a threaded hole to engage the threaded end of a bolt or stud and is the locking part of the system—bolt (stud)-fastened parts-nut.



A *washer* (Fig. 65, *e*) is placed under a nut or the head of a bolt (screw) to transmit and distribute evenly the force exerted on the connected parts or to lock them.

A *nut lock* is a device preventing a nut or bolt from loosening. Table 12 shows some designs of nut locks.

General-purpose bolts are made in three versions:

*Finished* bolts are turned from cold-drawn hexagonal bars.

*Semi-finished* bolts are produced by die-forging or heading with turned bearing face of the head and the shank end.

*Unfinished* bolts are made by cold or hot heading or forging without machining the shank and head. The thread of these bolts is machined or rolled.

General-purpose bolts are usually made from machine or alloy steel. In recent years, titanium alloys have also begun to be widely used.

In some machines use is made for special purposes of nonstandard designs. These include foundation bolts with asymmetric, Tee and intermediate heads, etc.

Studs are used when the design of a joint provides no space for the bolt head or when a blind hole has to be drilled. Under dynamic loads a standard stud proves stronger than a standard bolt of the same size.

As a rule, a stud is screwed in by means of two nuts—a nut and a locknut. Sometimes studs have two special parallel flats by which they can be gripped with a wrench.

The design of the imperfect thread portion subdivides studs into two types: without neck and with neck.

Depending on the length of thread engagement there are studs with  $l \approx 1.35d$  for soft and cast-iron material and with  $l = d$  for steel;  $d$  is the rated diameter of thread.

The design of the threaded portion distinguishes between studs for conventional nuts and studs for castellated nuts or conventional nuts with cotter pins.

In most cases the thread diameter on each end of the stud is the same.

Standard studs are manufactured from the same steel as bolts. For joints carrying heavy loads studs can be made from alloy steel.

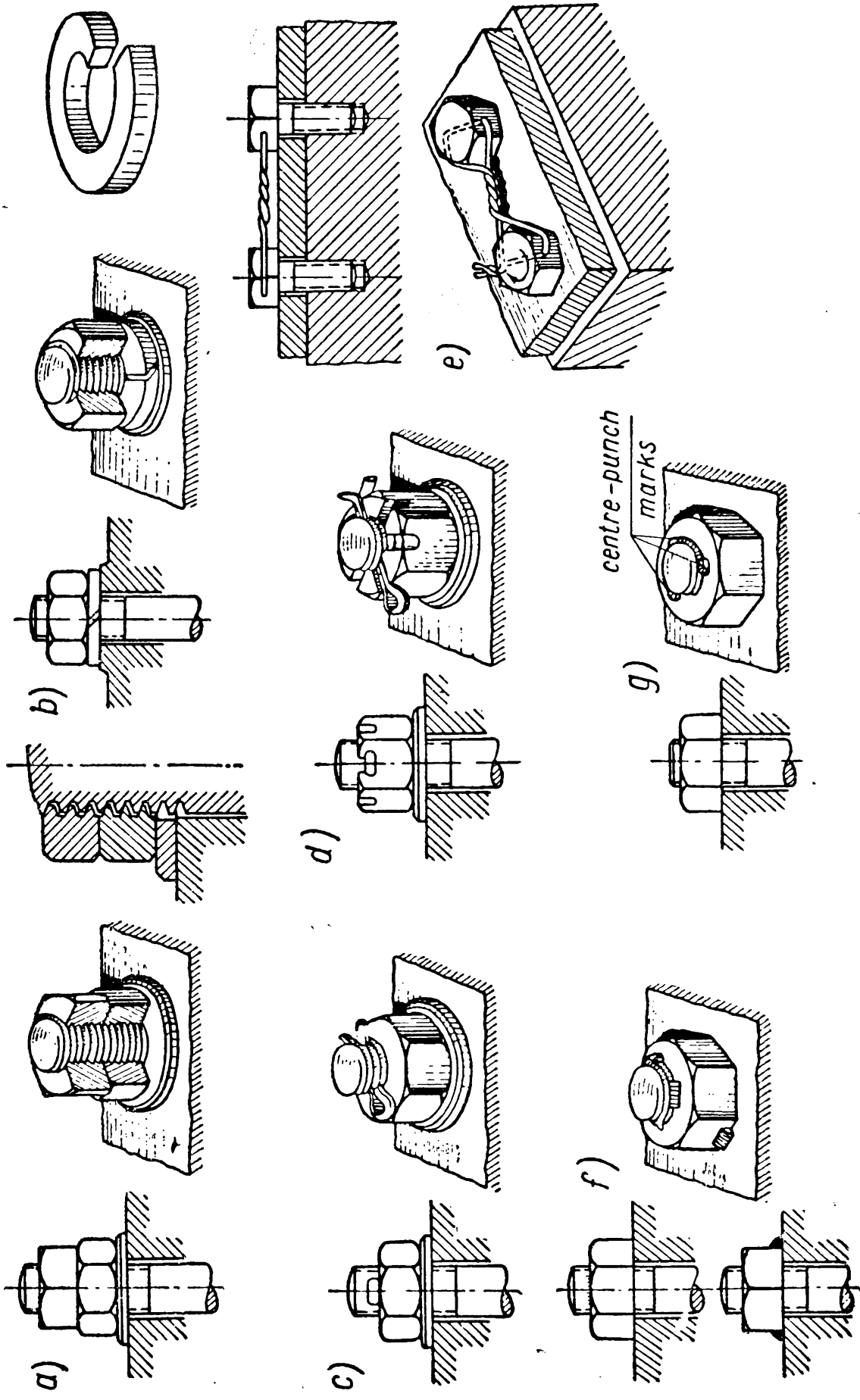
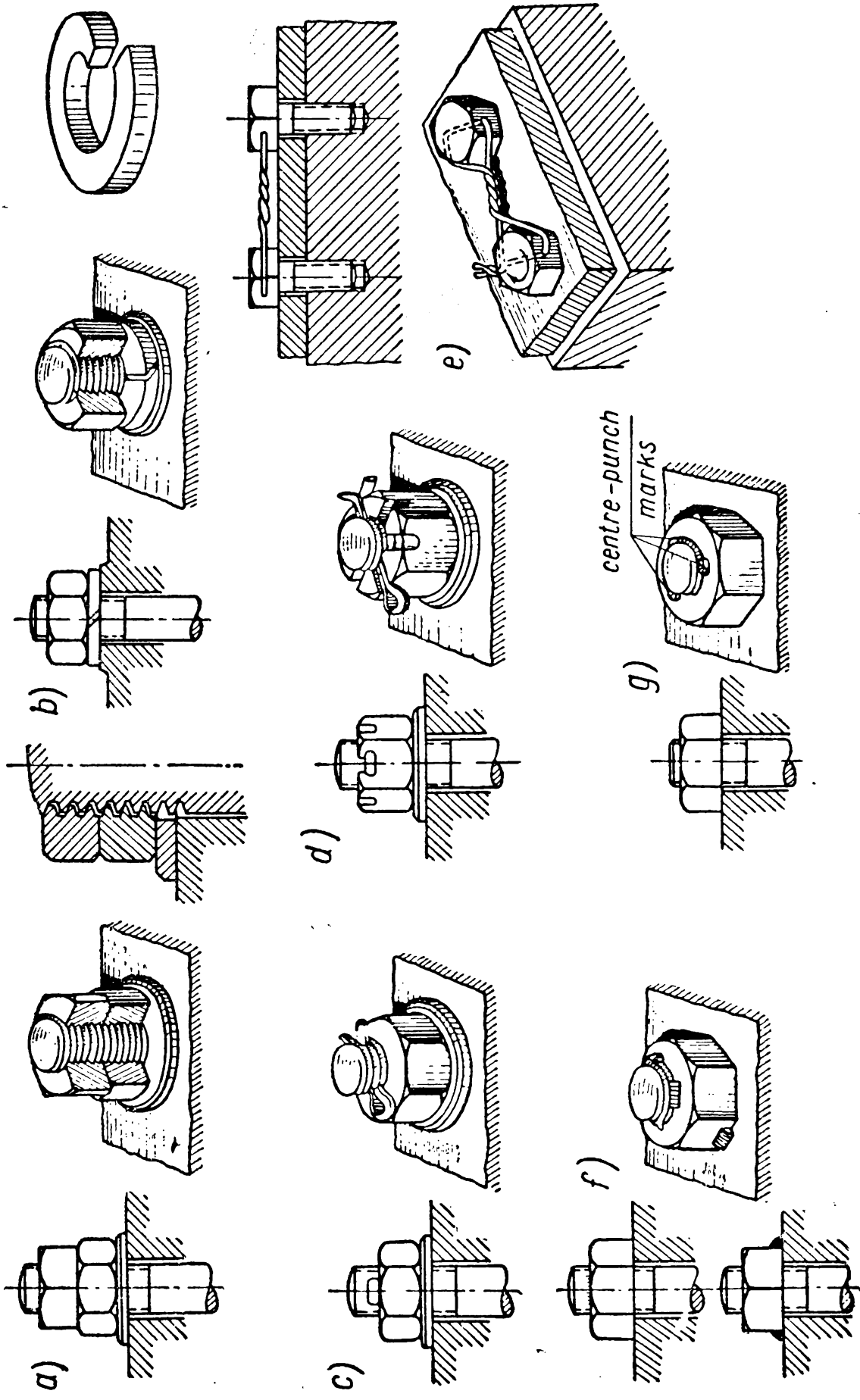
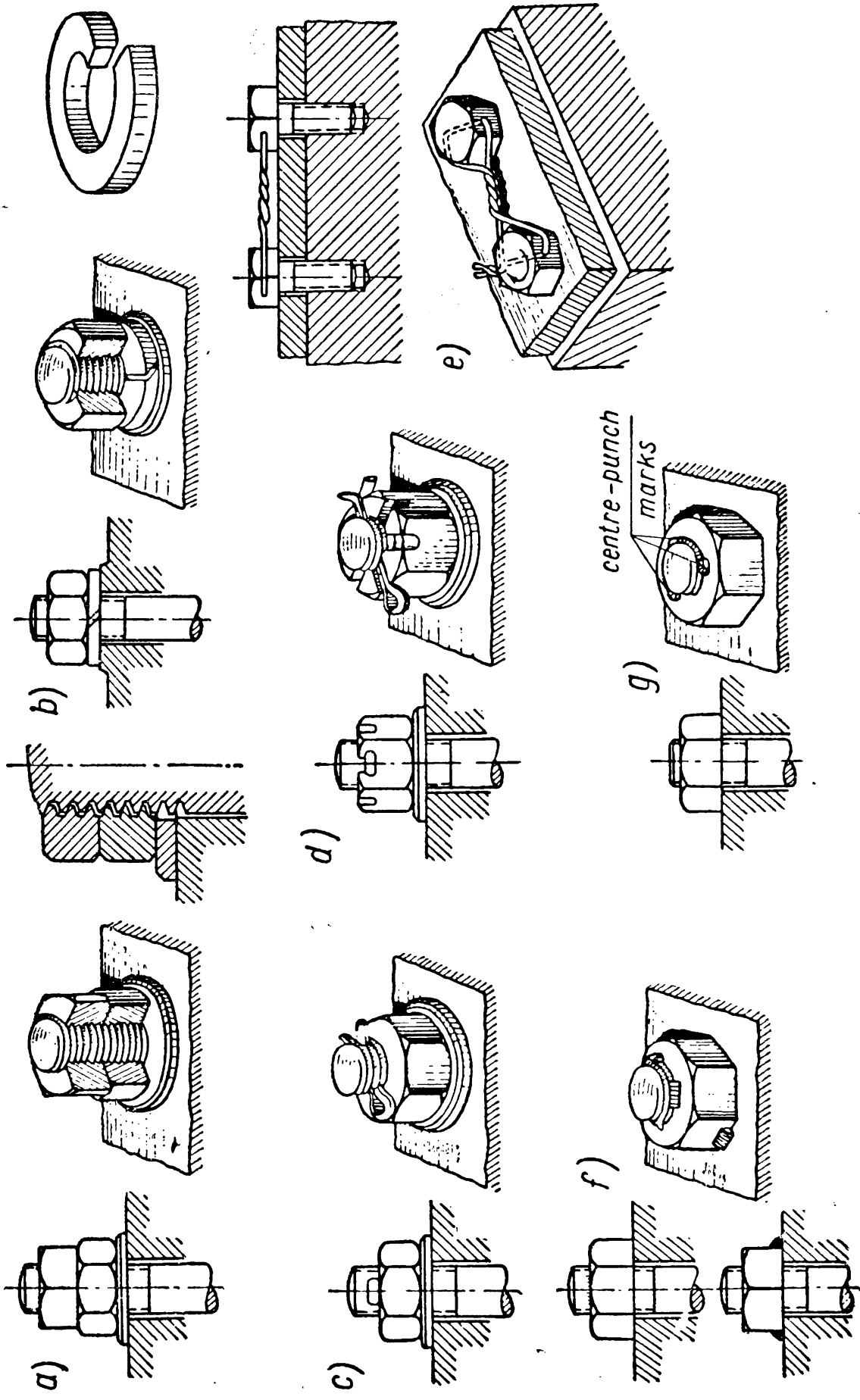
Screw heads can be slotted for a *screw driver* or a hexagonal or square head can be provided for a *wrench*.

One screw modification is an eyebolt (Fig. 183) which is screwed into the housing of a unit (a reduction gear, an electric motor, etc.) to suspend the machine (the component) on hoisting.

The material used for standard screws is the same as that used for bolts and studs.

Table 12

Standard Designs of Nut Locks

Principle of work	Designs	
Increased friction forces between the contact surfaces of the joint		
Employment of cheap stops which are easy to remove and which prevent a relative shift of the joint parts		
Permanent lock		

Standard nuts are manufactured in three versions: finished, semi-finished and unfinished.

In most machines hexagonal nuts are used. Square form is used only for unfinished nuts.

The normal thickness of a nut is  $H \approx 0.8d_0$ . In some cases nuts of a different thickness are employed: *thin* nuts in conditions of limited space, *thick* nuts ( $H=1.2d_0$ ) and *extra thick* nuts ( $H=1.6d_0$ ).

Castellated and slotted nuts are design varieties of semi-finished and finished nuts; they are used to simplify the locking of important joints (Table 12, *d*).

In addition to the above-mentioned types, nuts of special design are also employed: wing nuts, ring nuts and others and also nonstandard nuts (to ensure the tightness of the thread, to retain a part in place, etc.).

The material used for nuts is steel of grades 3, 5, 10, 45, 35, etc.

Black washers and finished washers are made from machine steel; black washers are blanked from strip or sheet steel with subsequent cleaning while finished washers are machined from cold-drawn round bars with drilled holes and chamfered edges.

Threaded joints are assembled with standard and special-purpose wrenches.

Nut locks have of necessity to be used for the majority of threaded joint designs. When the joint members carry static load these devices are not needed since all fastening threads are proof against loosening—their helix angle is smaller than the angle of friction. Under dynamic load, vibration, chatter, etc., a threaded joint may be relieved of load during some periods of its work. Bearing this in mind, as well as the instability of the coefficient of friction under these conditions, a threaded joint has to be locked to prevent its loosening.

The numerous designs of nut locks employed in machines are based on the following principles:

1) the increase of friction forces between the contact surfaces (in the thread, on the bearing face of the head or nut; Table 12, *a, b*);

2) the application of special cheap stops which can be easily replaced and which preclude mutual displacement of the joint parts (Table 12, *c, d, e*);

3) the use of permanent locks (Table 12, *f, g*) where the joint cannot be disassembled without destroying or plastically deforming the lock elements.

Table 12 shows some locking devices. Fastening by means of a locknut (Table 12, *a*) increases friction forces. When the locknut is tightened the bolt develops additional elastic deformation and causes redistribution of play in the engaged thread portion; this increases friction forces between the contact surfaces. The use of this method is declining at present because it fails to ensure adequate

dependability, especially during vibration, and requires greater threaded length of the bolt and twice the number of nuts.

The same principle of increased friction forces between the contact surfaces underlies the use of lock washers (Table 12, *b*), slit nuts, etc.

Locking by means of stops preventing unscrewing is widely used in modern machines due to its reliability, low cost, convenient assembly and disassembly of the units. For stops use is made of split cotter pins (Table 12, *c*, *d*), wire (*e*), etc.

Such methods of making *permanent locks* as local welding of nuts and bolt heads (screws, *f*) centre-punching (*g*) and others, though fairly dependable, cannot, however, be used in cases involving frequent assembly and disassembly.

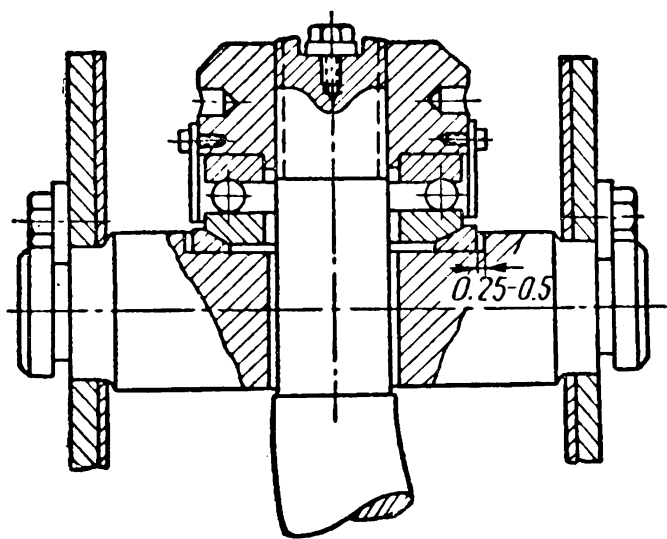


Fig. 66

Depending on the nature of loading and the method of assembly threaded joints are either *prestressed* or *used unstressed*.

Joints of the latter type are comparatively rare in practice. Examples of it are an eyebolt screwed into the housing of a reduction gear (Fig. 183); the joint shown in Fig. 69, *a*; the fastening of a hook to the traverse of a block tackle (Fig. 66).

In most cases threaded joints are prestressed, i. e., their threaded parts and, consequently, the connected members are tightened with a certain torque before external load is applied to prevent the separation of the joint and loss of tightness which will impair the joint operation of the joint parts after the application of external load.

Already during assembly prestressing causes more or less considerable tensions to arise in the threaded parts which cannot be disregarded; this makes the method of designing such joints radically different from that used for joints which are not prestressed.

Joints of this type can take both static and dynamic loads. Therefore, the fastenings of bearings, flanges, cylinder end covers in engines, connecting rod cups, etc., are invariably prestressed.

Depending on their purpose joints are *strong* or *tight-strong*. It follows from the remarks above that the nature of load predetermines the prestressing of strong joints. Tight-strong joints are effective only when adequately prestressed.

Depending on the number of bolts\* resisting the load joints are

---

\* Here and elsewhere the term «bolt» should be understood to mean also other similar parts (screws, studs, etc.).

divided into those with *one bolt* or a *group of bolts*. In the latter case the load is not necessarily uniformly spread between the bolts.

**Types and Causes of Thread Failure.** Under static load threaded parts seldom fail. Under heavy overloads the bolt shank may be shorn off in the solid or threaded section and the thread stripped, bent or crushed. Statistical analysis of thread failure shows that about 90% of all failures are due to fatigue.

This is primarily accounted for by the fact that under varying stresses the strength of a part is weakened by the thread and abrupt changes in cross-section (the imperfect thread portion, the transition of the bolt shank into the head) which are points of stress concentration.

Fig. 67 shows some typical cases of bolt failure due to fatigue. Most bolt failures occur in the first or second thread of engagement (counting from the nut thrust face, Fig. 67, *a*); rupture in the imperfect thread portion (Fig. 67, *b*) and near the bolt head (Fig. 67, *c*) is much rarer.

Sometimes bolts break because additional loads arising in service due to careless assembly, faults in accuracy, etc., were not taken into account. In such cases failures also due to fatigue may affect the smooth

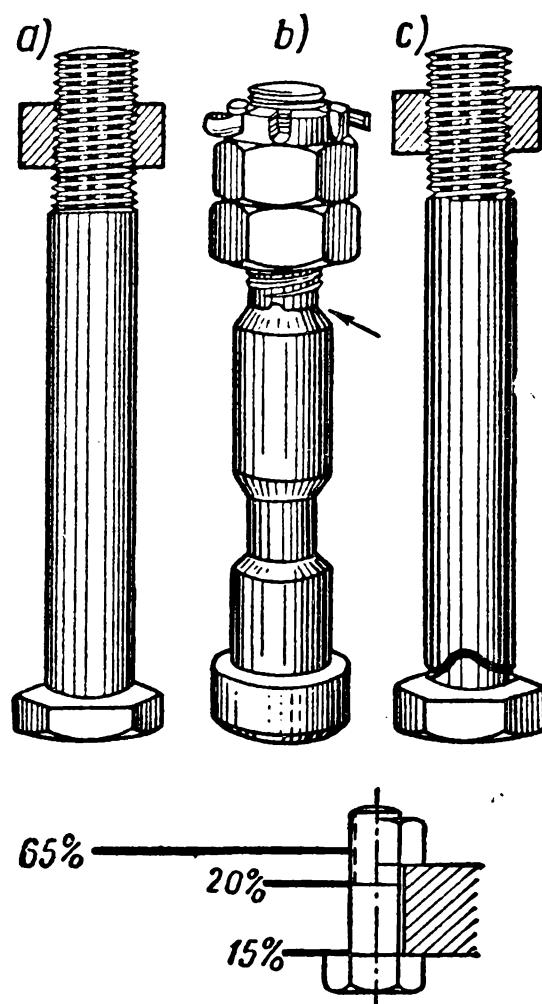


Fig. 67

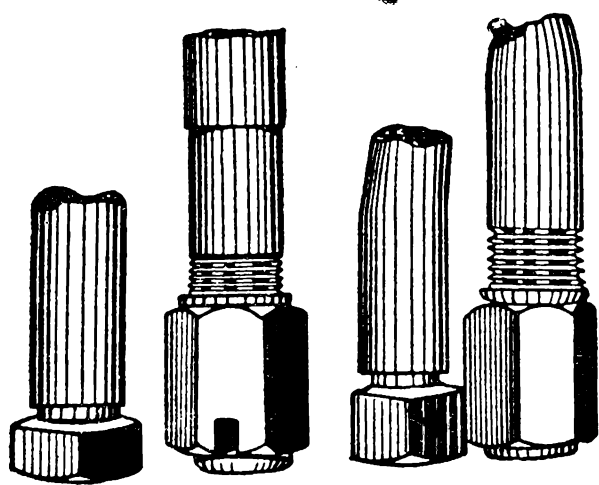


Fig. 68

portion of the bolt shank. An example which may be cited is the frequent failure, over the past years, of connecting rod bolts of tractor engines (Fig. 68). High additional stresses were produced by play in the parting plane—the relative shift of the joint parts due to inadequate tightening; in this case, the bolts were additionally loaded with transversal forces which caused a cyclic bending of high frequency resulting in failure.

There also occur cases of thread failures due to additional temperature stresses. These failures are sometimes of the nature of «spontaneous» breakdowns since they occur solely under the influence of changed temperature conditions before external loads are applied.

Failures of fastening parts entail after-effects of differing importance. Sometimes it is enough to replace the broken part but not infrequently such failures cause long interruptions in the normal operation of the machine; sometimes the after-effects are so serious that the entire machine is put out of commission.

Breakdowns can be avoided by proper calculation which takes into account the specific features of the behaviour of threaded parts under respective load conditions, by improving their design, by taking proper processing and operational measures and strictly observing assembly rules.

### STRENGTH UNDER STATIC LOAD

Threaded joints are used in a wide variety of ways calling for a great number of designs. Every design has its own specific features which should be taken into account. A survey of the principal designs for threaded joints is given in Table 13.

In designing it is important not only to assess correctly the size of parts in order to ensure proper strength in accordance with the accepted design, but also to choose such structural features as would preclude the appearance of additional loads during operation which are not provided for by the design.

**Joints Designed Without Initial Stress.** *Joints designed for axially loaded threaded parts.* Threaded parts carry mainly axial loads. The design under consideration is, therefore, the basic one. By selecting proper values for design loads many other cases can be reduced to it.

In the joint shown in Fig. 69, *a*, the bolt carries an axial load  $P$ . The case considered is one which rules out the subsequent tightening of the joint.

The following assumptions are made:

1) The joint operates symmetrically and the load taken by the bolt is considered to act along its axis.

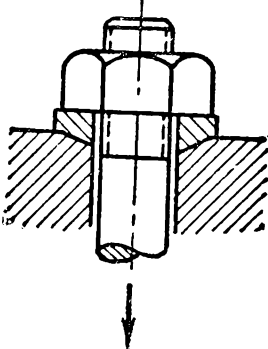
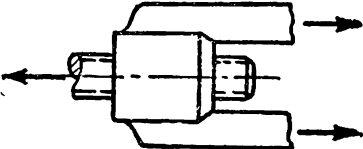
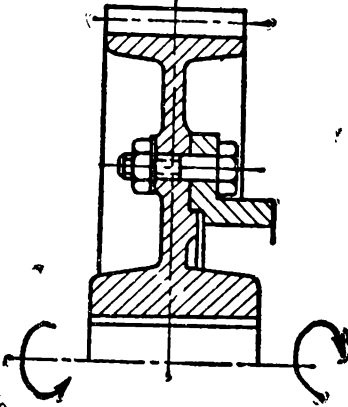
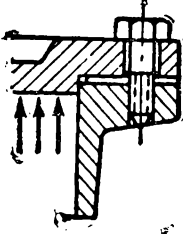
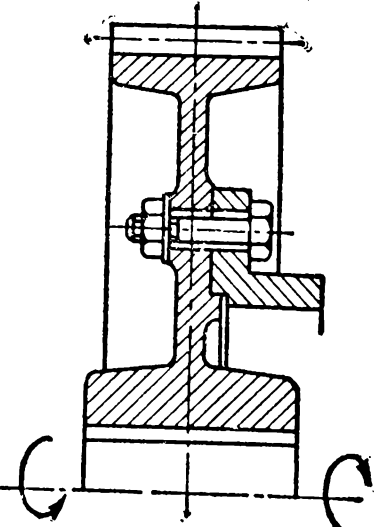
2) The design area of the bolt in its threaded portion is taken as the area of a circle,  $d_1$  in dia (the actual sectional area enclosing part of the fillet as well is somewhat larger than the design area).

3) Stresses in the sections are distributed uniformly. In actual fact, the thread and other abrupt changes in formation cause non-uniform stress distribution. When parts made from plastic material resist static load, the effect of stress concentration cold-hardens the material of the parts.

4) The load is distributed uniformly between the thrust fillets (through the nut thickness). This assumption contradicts data obtained from theoretical and experimental research (p. 82), which should be taken into account when allowable stress is selected.

Table 13

Principal Designs for Threaded Joints

Presence of initial stress	Load carried by threaded parts	Joint
Not prestressed	Parts carry axial load	
	Parts carry axial load; subsequent tightening of joint is possible	
	Parts carry transverse load	
Prestressed	Parts carry axial load; subsequent tightening of joint is possible	
	Parts carry transverse load	

The condition for strength precluding the tear of the dangerous section can now be written as follows:

$$P \leq \frac{\pi d^2}{4} [\sigma]_t$$

whence

$$d_1 \geq \sqrt{\frac{4}{\pi} \times \frac{P}{[\sigma]_t}}. \quad (76)$$

The allowable stress can be assumed to be:

$[\sigma]_t \leq 0.8\sigma_y$  for unhardened bolts, screws and studs;

$[\sigma]_t \leq 0.6\sigma_y$  for hardened and cyanided bolts.

Here  $\sigma_y$  is the yield point of the bolt material.

The thickness of the bolt head  $h$  can be found from its behaviour under shear, compression and bending forces. As analyses and the

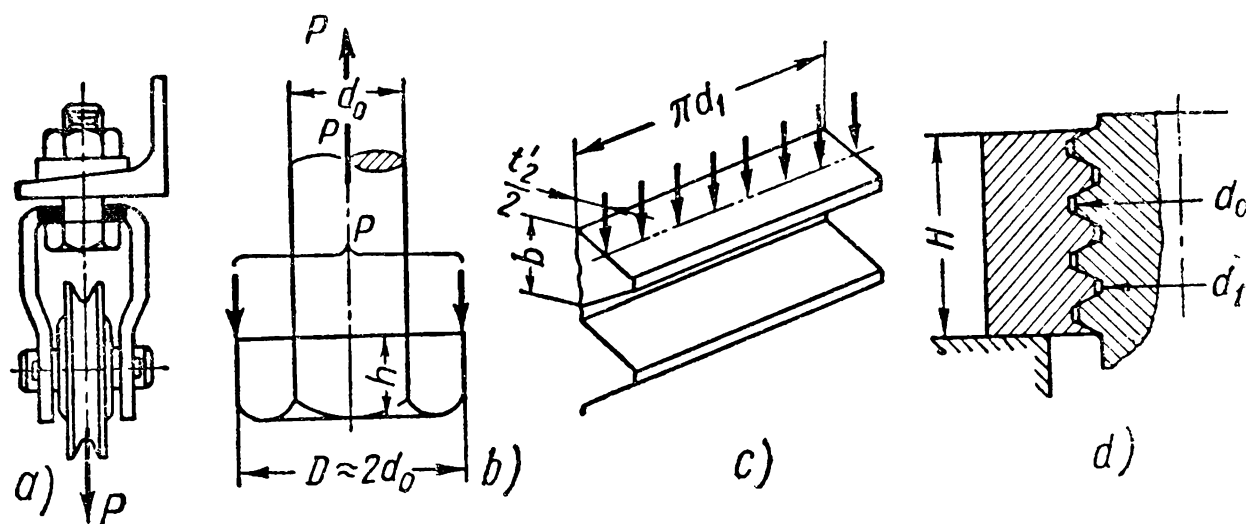


Fig. 69

experience in use of bolts show, the thickness  $h$  calculated for bending stress also satisfies the conditions for shear and compression.

The design diagram of the bolt head in bending is shown in Fig. 69, *b*. If the bolt head is developed by the diameter  $d_0$  on a plane and represented in the form of a cantilever beam resisting a force  $P$  at a distance of  $l \approx \frac{d_0}{2}$  from the restrained section (such a design diagram is, of course, highly arbitrary), then

$$M = P \frac{d_0}{2};$$

since

$$W = \frac{\pi d_0 h^2}{6}$$

the thickness of the bolt head  $h$  can be found from the equation

$$P \frac{d_0}{2} = \frac{\pi d_0 h^2}{6} [\sigma]_b. \quad (77)$$



The nut thickness can be found from the strength condition of thread in shear, bending and compression.

The shearing strength condition of the bolt thread engaged in the nut (Fig. 69, *d*) is

$$P \leq \pi d_1 \beta H [\tau]_s \quad (78)$$

where  $\beta$  is the depth engagement; for V thread  $\beta \approx 1$ .

Thread can be calculated for bending under the following additional assumptions: the fillet developed on plane is regarded as a cantilever beam having a restrained end (Fig. 69, *c*); the load spread over the fillet surface is replaced by the concentrated load  $\frac{P}{z}$  ( $z$  is the number of fillets in the nut) applied to the middle of the effective fillet depth  $\left(l = \frac{t'_2}{2}\right)$ . In this instance

$$\frac{P}{z} \times \frac{t'_2}{2} = \frac{\pi d_1 b^2}{6} [\sigma]_b. \quad (79)$$

Bearing in mind the standard relations between thread sizes we can use this condition to determine the size  $H = z \times s$ .

The thread is calculated for compression as follows

$$P \leq \frac{\pi}{4} (d_0^2 - d_1^2) z [\sigma]_c$$

and, hence,

$$H = z \times s = \frac{4Ps}{\pi (d_0^2 - d_1^2) [\sigma]_c}. \quad (80)$$

In the majority of cases threaded joints carrying static load are made from parts of standard form and dimension, which are fitted so as to provide, as far as possible, equal strength in different cross-sections. The employment of standard parts, therefore, considerably simplifies the design process—it is necessary only to calculate one characteristic size of the bolt to be able to choose all the others in standard values. For threaded parts this size is usually the minor diameter  $d_1$ .

Thus, if we substitute  $P$  from the formula (76) in the equation (77) and assume  $[\sigma]_t = [\sigma]_b$  and  $d_1 \approx 0.8d_0$  for V thread we shall obtain  $h \approx 0.9d_1$  or  $h \approx 0.7d_0$  which is in keeping with the standard ratios.

If we substitute  $P$  from the formula (76) in the condition (78) and assume  $d_1 \approx 0.8d_0$  then for steel parts at  $[\tau]_s = 0.75 [\sigma]_t$  the nut thickness will be  $H \approx 0.45d_1$  or  $H \approx 0.36d_0$ .

From the relations (76) and (79) with the standard relations for metric thread  $b = 0.85s$  and  $t'_2 \approx 0.65s$  we can obtain

$$H \approx 0.7 d_1 \text{ or } H \approx 0.55 d_0.$$

In a similar way the nut thickness can be calculated from the relations (76) and (80). In a particular case, for steel 3 at smaller values of  $[\sigma]_c = (250-350)$  kg/cm<sup>2</sup> and  $[\sigma]_t = 800$  kg/cm<sup>2</sup> we get:

$$H \approx 0.9 d_1 \text{ or } H \approx 0.73 d_0.$$

The standard provides for the relation  $H \approx 0.8 d_0$  which satisfies all the cases examined above.

Thus, the design of standard fasteners is reduced to determining the diameter  $d_1$  from the formula (76).  $d_1$  is then used to choose other sizes from the corresponding standards.

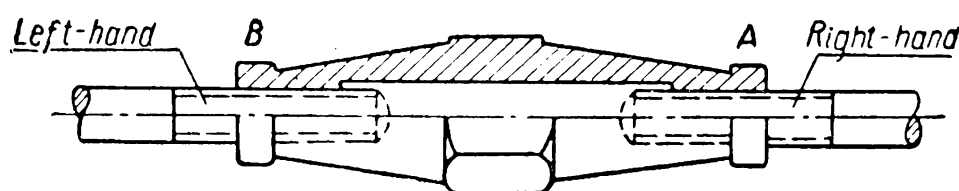


Fig. 70

*Joints designed for axially loaded threaded parts; subsequent tightening of joint is possible.* Such load conditions arise if, after the bolt has taken the force  $P$ , it is tightened (always in prestressed joints). An example is provided by a *turnbuckle* (Fig. 70). In this case, the bolt shank will carry in addition, between the head and the nut, the torque on the thread  $M_t$  whose value is determined by the ratio we know from the theory of mechanisms and machines.

$$M_t = P \frac{d_p}{2} \tan(\psi + \varrho) \text{ kg/cm} \quad (81)$$

where  $\varrho$  is the angle of friction,  $P$ —in kg,  $d_p$ —in cm.

The components of the resultant stress  $\sigma_{res}$  are equal to:

$$\sigma = \frac{4P}{\pi d_1^2} \text{ and } \tau = \frac{M_t}{W_{polar}} = \frac{P \times 0.5 d_p \tan(\psi + \varrho)}{0.2 d_1^3}$$

and

$$\sigma_{res} = \sqrt{\sigma^2 + 3\tau^2}. \quad (82)$$

For standard designs of bolts with metric thread we can assume  $d_p = 1.12 d_1$ . Recalling that in their case  $\tan \psi \approx 0.0194-0.0433$  and  $\tan \varrho \approx 0.2$  we obtain:  $\frac{\tau}{\sigma} \approx 0.5$  and  $\sigma_{res} \approx 1.3\sigma$ .

Thus, the case under consideration can be reduced, with an accuracy sufficient for engineering practice, to the main task if we take  $P_0 = 1.3P$  as the design load. Then the minor diameter of thread will be

$$d_1 \geq \sqrt{\frac{4 \times 1.3P}{\pi [\sigma]_t}}. \quad (83)$$

Data for the selection of  $[\sigma]_t$  vary with the material and diameter of the bolt—for smaller diameters lesser values of  $[\sigma]_t$  should be taken to avoid overstraining in tightening. Thus, for example, for bolts made from ordinary carbon steel  $[\sigma]_t = (0.25-0.4)\sigma_y$  at  $d_0 = (16-30)$  mm and at  $d_0 = (30-60)$  mm  $[\sigma]_t = (0.4-0.6)\sigma_y$ , etc.

**Joints Designed with Initial Stress.** *Joints designed for axially loaded threaded parts; subsequent tightening is possible.* This design is typical of the majority of group joints used in mechanical engineering to fasten covers, flanges, base plates, etc. In some cases these joints should also be tight: for example, the joint between the cover and cylinder of an internal combustion engine. In other cases the joint must not be allowed to yawn if this impairs the conjoint operation of the parts in the unit. Connecting-rod and foundation bolts, etc., must comply with these conditions.

They are achieved by prestressing the threaded joints sufficiently in order to prevent the joint yawn or leakage after the external load is applied. This means that after the external load  $P$  which tends to reduce the effect of the prestressing force  $V$  has been applied, the joint parts should be pinched together with the force  $V'$  termed residual stress.

The drop of the tightening force  $(V - V')$  is determined by the value of the external load  $P$  and the elastic properties of all parts in the joint (both threaded and held together).

Fig. 71 shows a cylinder cover fastening with  $z$  bolts. At an above atmospheric pressure in the cylinder of  $p$  kg/cm<sup>2</sup> the load imposed on the cover and bolts is  $Q = p \frac{\pi D^2}{4}$  kg (here  $D$  is in cm). Assuming that all bolts carry the same load and that the cover is sufficiently stiff it can be taken that each bolt resists the tensile axial force  $P = \frac{Q}{z} = p \frac{\pi D^2}{4z}$  kg. This is the external load. To ensure normal operating conditions the joint should be compressed with the force  $V'$  provided by the initial stress  $V$ .

If we neglect the deformation of the bolt head and of its end threaded section and assume the bolt working length to be equal to the sum of the thicknesses of the flanges, i. e.,  $l = l_1 + l_2$ , then the elastic deformation of the bolt due to the force  $V$  (Fig. 72, b)  $\lambda_1 = \frac{Vl}{F_b E_b} = \frac{V}{C_b}$  and the elastic deformation of the joint  $\lambda_2 = \frac{Vl}{F_\theta E_\theta} = \frac{V}{C_\theta}$  where  $C_b$  and  $C_\theta$  are the coefficients of stiffness of the bolt and joint respectively.

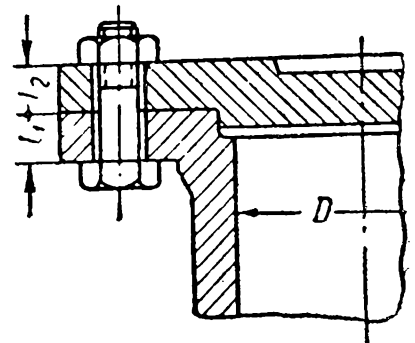


Fig. 71

After an external load has been imposed on the joint (Fig. 72, c) the bolt will carry an additional force which will stretch it further ( $\Delta\lambda_1$ ) and relieve the joint—the force holding the joint tightly compressed will drop to  $V'$  and, consequently, the joint will stretch the bolt with the same force  $V'$ . Thus, the force acting on the bolt equals the sum of the external load  $P$  and the residual stress  $V'$  in the joint after the external load has been applied, i. e.,

$$P_0 = P + V'. \quad (84)$$

Let the drop in the tightening force be equal to  $\Delta P$ , i. e.,

$$\Delta P = V - V'. \quad (85)$$

The increase in the bolt elongation after the external load is applied is due to the force  $(P - \Delta P)$  and will amount to  $\Delta\lambda_1 = \frac{P - \Delta P}{C_b}$ . The conjoint action of the parts will «smooth out» the joint by the same value  $\Delta\lambda_1$  under the action of the force  $\Delta P$  since the force formerly compressing the joint has dropped exactly by the same value:  $\Delta\lambda_2 = \Delta\lambda_1 = \frac{\Delta P}{C_\partial}$ .

Hence

$$\frac{P - \Delta P}{C_b} = \frac{\Delta P}{C_\partial}$$

and

$$\Delta P = P \frac{C_\partial}{C_b + C_\partial}. \quad (86)$$

We find from the equations (85) and (86):

$$V = V' + \Delta P = V' + P \frac{C_\partial}{C_b + C_\partial}. \quad (87)$$

The load taken by the bolt can be represented on the basis of the relations (84) and (87) in the following form:

$$P_0 = V + P \frac{C_b}{C_b + C_\partial} \quad (88)$$

or

$$P_0 = V + P_2,$$

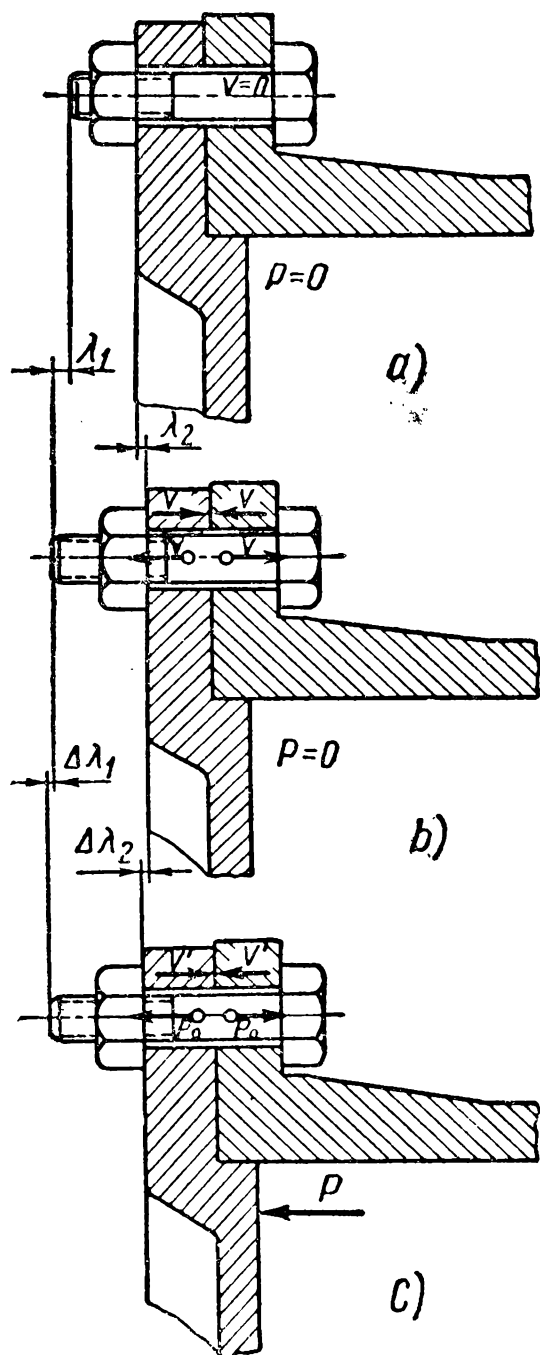


Fig. 72

i.e., in joints with the prestressing force  $V$  after the external load has been imposed the force acting on the bolt increases by

$$P_z = P \frac{C_b}{C_b + C_\partial} < P. \quad (89)$$

The residual stressing force  $V'$  is estimated on the basis of designing practice as a factor of the external load  $P$  according to the formula  $V' = \gamma P$  where  $\gamma$  is the experimental coefficient assumed in the calculations as 0.2-1.8 depending on operating conditions. Thus, to ensure proper sealing of pipe joints we take  $\gamma = 1.5-1.8$ .

We can thus write  $P_0 = P(1 + \gamma)$ . (90)

The relation (84) is also observed in extreme cases. When the bolt stiffness  $C_b$  is considerably less than the stiffness of the joint  $C_\partial$ , i. e., if unlike  $C_\partial$   $C_b$  can be disregarded, we obtain from the equation (88)  $P_0 = V$ . But in this case from the equation (87)  $V = V' + P$  and, consequently,  $P_0 = P + V'$ .

If the joint stiffness  $C_\partial$  is considerably less than the stiffness of the bolt  $C_b$  then, assuming  $C_\partial = 0$ , we obtain  $P_0 = P + V$ ; and since from the equation (87)  $V = V'$ , then  $P_0 = P + V'$ .

From the formulae (83) and (84) the bolt diameter in the threaded portion is equal to

$$d_1 = \sqrt{\frac{4 \times 1.3 P_0}{\pi [\sigma]_t}} \text{ cm.} \quad (91)$$

To determine the necessary prestressing force  $V$  which gives the required value of  $V'$  at the external load  $P$  we must find the values of the coefficients of stiffness  $C_b$  and  $C_\partial$ . As a rule, they are found from the arbitrary relations (92), (93) and (94); in important cases special experiments should be carried out to obtain their values with greater accuracy.

For a bolt of constant diameter

$$C_b = \frac{F_b E_b}{l}. \quad (92)$$

For a stepped bolt  $C_b$  is found from the condition

$$\frac{1}{C_b} = \frac{1}{E_b} \left( \frac{l_1}{F_{b_1}} + \frac{l_2}{F_{b_2}} + \dots + \frac{l_n}{F_{b_n}} \right). \quad (93)$$

In these formulae

$F_b, F_{b_1}, \dots, F_{b_n}$  — are the sectional areas of various bolt parts;

$l, l_1, \dots, l_n$  are the respective lengths of various bolt parts; in this case the design lengths of the end portions include half the thickness of the bolt head and half the nut thickness;

$E_b$  is the elastic modulus of the bolt material.

$C_\partial$  is found for a joint by following a suggestion put forward in 1911 by I. I. Bobarykov who investigated the relation between the

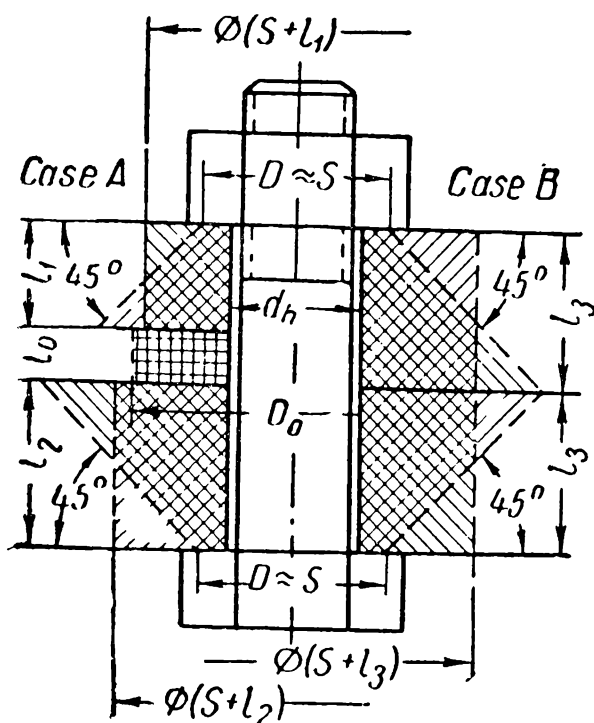


Fig. 73

efforts and the elastic properties of parts of the joints under consideration. It is presumed that the force is transmitted from the head and the nut to the joint parts along «cones of influence» (Fig. 73) whose generatrices are inclined to the plane of the joint at  $45^\circ$ , while the diameters of the smaller bases of the cones are equal to the width across the flats of the bolt head or nut. To simplify calculations these deformed «cones of influence» are replaced by cylinders whose axial sectional areas are equal to the areas of the cones within the same sections. Under these conditions

$$\frac{1}{C_\partial} = \left( \frac{l_1}{F_{\partial_1} E_{\partial_1}} + \frac{l_2}{F_{\partial_2} E_{\partial_2}} + \dots + \frac{l_n}{F_{\partial_n} E_{\partial_n}} \right). \quad (94)$$

where  $l_1, l_2, \dots, l_n$  are the thicknesses of the jointed parts;  
 $F_{\partial_1}, F_{\partial_2}, \dots, F_{\partial_n}$ —the sectional areas of respective cylinders characterising the deformed joint;  
 $E_{\partial_1}, E_{\partial_2}, \dots, E_{\partial_n}$ —the moduli of elasticity of the material of respective joint parts.

Areas  $F_\partial$  are calculated as follows:

Case B (Fig. 73):

$$F_{\partial_1} = F_{\partial_2} = \frac{\pi}{4} [(S + l_3)^2 - d_h^2];$$

Case A (Fig. 73):

$$F_{\partial_1} = \frac{\pi}{4} [(S + l_1)^2 - d_h^2];$$

$$F_{\partial_2} = \frac{\pi}{4} [(S + l_2)^2 - d_h^2];$$

for the gasket

$$F_{\partial_3} = \frac{\pi}{4} \left[ \left( S + \frac{l_1 + l_2}{2} \right)^2 - d_h^2 \right].$$

The force-deformation relation of the joint parts is shown graphically in Fig. 74.

If we lay off the forces along the Y-axis and the deformations along the X-axis then, within the range of elastic deformations, the stiffness is characterised by the tangent of the angle between the straight



less initial stress ( $V_1$ ); but at the same time  $P_z (P'_z > P_z)$  increases; under the same conditions greater joint stiffness requires greater initial stress.

The joints under examination are thus designed in the following order:

- 1) the number of bolts and external load  $P$  carried by one (generally that resisting the heaviest load) bolt is determined;
- 2) the required magnitude of residual stress  $V' = \gamma P$  is determined;

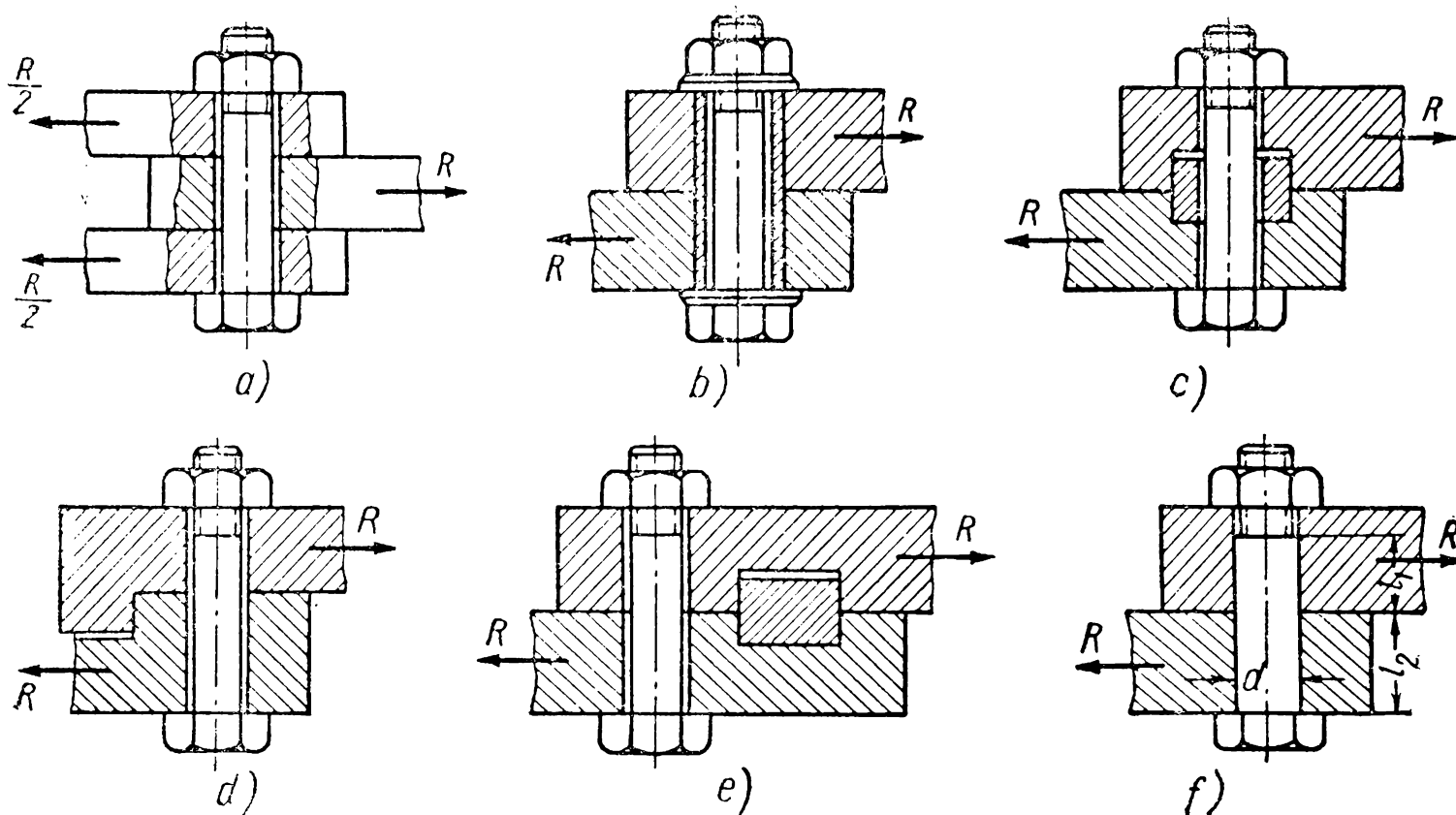


Fig. 76

- 3) the design axial load  $P_0 = P + V'$  is found;
- 4) the cross-section of the bolt from the formula (91) is found;
- 5) the design of the unit is worked out;
- 6) the values  $C_b$  and  $C_\theta$  are calculated;
- 7) the required prestressing force  $V$  to maintain the given conditions is found.

Control over tightening to maintain  $V$  and hence  $V'$  stable is of extreme importance for these joints (see p. 143).

*Joints designed for shear-loaded threaded parts.* When the bolt fits the hole with some play (Fig. 76, a-e) the joint should be tightened before the external load  $R$  is applied in order to prevent inadmissible relative displacement of the elements in the direction of the acting forces which would load the bolt additionally with a bending moment.

The value of  $V$  is determined by the required friction force  $F$  acting between the contact surfaces according to the condition:



$F = V \times f \times i \geq R$  where  $f$  is the coefficient of friction and  $i$ —the number of joints. Whence

$$V \geq \frac{R}{f \times i}. \quad (95)$$

For the designs shown in Fig. 76,  $a$  ( $i=2$ ) and taking  $f=0.2$  for dry steel and cast-iron surfaces we obtain  $V = \frac{R}{0.2 \times 2} = 2.5 R$ . If the number of joints  $i=1$ , the required stress  $V=5R$ .

The result obtained shows that such designs cannot be considered rational because of the large diameter of bolts required in such cases.

It is expedient to provide for special devices in the joints which relieve the bolt from shearing forces and ensure relative immobility of the fastened parts.

In the designs shown in Fig. 76,  $b$ , the shearing load is taken by a bush (sleeve) inserted into the hole with a small interference; the bolt is entirely free from shearing load. Fig. 76,  $c, d, e$  shows other possibilities (lock and key).

When the bolt is inserted into a *reamed hole with a small interference* (Fig. 76,  $f$ ) the shearing load is taken by the bolt shank. Such a joint is not necessarily prestressed.

In this case the design equation will have the form:

$$R = \frac{\pi d^2}{4} [\tau]_s. \quad (96)$$

The dimensions of the bolt shank in Fig. 76,  $f$  should be checked for compression. If  $l_1 < l_2$ , then of necessity  $R \leq d l_1 [\sigma]_c$ .

In these formulae:

$$[\tau]_s \leq (0.2-0.3) \sigma_y;$$

$$[\sigma]_c \leq (0.3-0.4) \sigma_y \text{—for steel;}$$

$$[\sigma]_c \leq (0.25-0.3) \sigma_{ult} \text{—for cast iron.}$$

*Bending stress in threaded joints.* In some threaded joint designs the bolts are also subjected to bending forces. Bending forces arise either due to specific structural features or to the misalignment of the contact surfaces of the bolt, nut and connected parts, or as a result of their elastic deformation.

Fig. 77,  $a$  shows parts fastened by a bolt with an *asymmetric head*. Such bolts are employed when a standard (symmetric) head cannot be used or when a hole cannot be drilled in one of the fastened parts. As follows from the load diagram the stress arising in the bolt sections is

$$\sigma_{res} = \sigma + \sigma_b$$

where  $\sigma$  is the stress due to axial load;

$\sigma_b$  — the maximum stress due to bending moment.

A similar case may occur with a bolt (stud) when threaded parts of standard design are used if the bearing surfaces do not contact normally (see the example in Fig. 77, b).

An eccentrically loaded nut will bend the stud. The bending stresses arising in the stud can be determined from the following assumptions.

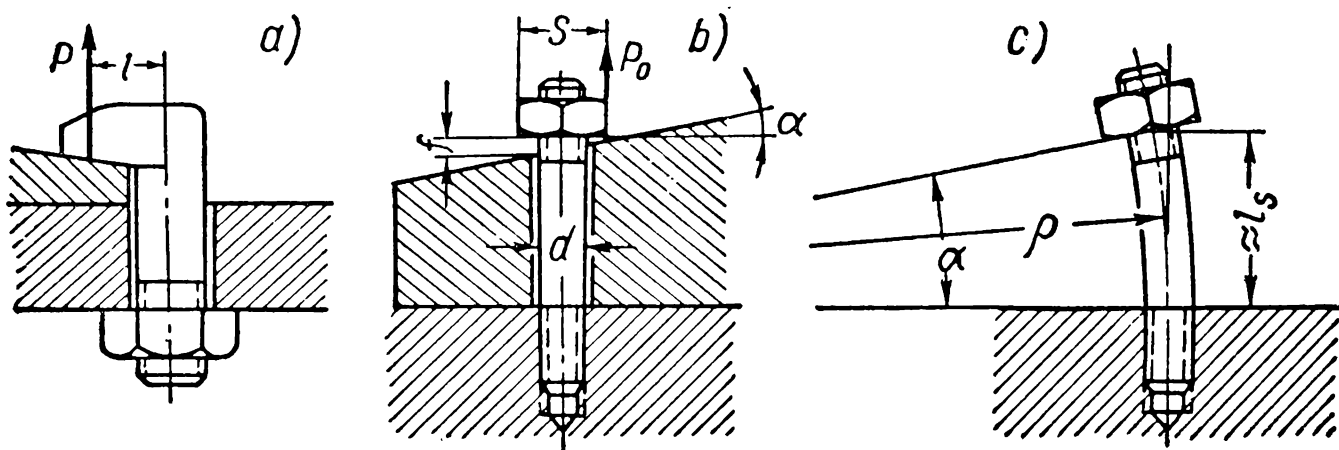


Fig. 77

The theory of the strength of materials gives us the equation for an elastic line  $M = \frac{E \times I}{\rho}$ ; but it follows from Fig. 77, c that  $\rho \approx \frac{l_s}{\tan \alpha}$ .

Since the angle  $\alpha$  is small, we can assume that  $\tan \alpha \approx \alpha$  where  $\alpha$  is in radians, i. e.,  $\rho = \frac{l_s}{\alpha}$ .

Since

$$I = \frac{\pi d^4}{64} \quad \text{and} \quad W = \frac{\pi d^3}{32}$$

we obtain

$$\sigma_b = \frac{M}{W} = \frac{1}{2} \alpha E \frac{d}{l_s}. \quad (97)$$

In the threaded portion of the stud the bending stresses will be

$$\sigma_b = \frac{M}{W_1} = \frac{M}{\frac{\pi d_1^3}{32}} = \frac{1}{2} \alpha E \left( \frac{d}{d_1} \right)^3 \frac{d}{l_s}. \quad (98)$$

Analysis of the formulae (97) and (98) shows that the smaller the diameter of the bolt (stud) shank and the longer the bolt, the less the bending stress will be (all other conditions being equal).

Experimental verification of the effect of bending stress due to misalignment has shown that at angles of misalignment  $\alpha \leq 2^\circ$  the static strength of bolts made from steels with  $\sigma_{ult} \leq 90-120 \text{ kg/mm}^2$  changes but little.

This effect is material at small angles of misalignment only for parts made from high-strength steel with  $\sigma_{ult}=130\text{--}180 \text{ kg/mm}^2$  especially under loads entailing varying stresses. Thus at an angle of misalignment  $\alpha \approx 35'$  the endurance of threaded joints with minimum crest clearance is 12% lower and at an angle of misalignment  $\alpha = 2^\circ 30' \text{--} 56\%$  lower. It follows from this that consideration should be given to proper working of contact surfaces and to the designing of special units which would eliminate the misalignment factor.

## STRENGTH AT VARYING LOADS (ENDURANCE OF BOLTED JOINTS)

**Calculation of Strength.** When threaded parts carry loads causing varying stresses, as a rule *prestressed* joints are employed. Fig. 78 shows that when the external load changes from 0 to  $P$  the bolt sections develop varying stresses with a maximum cycle stress

$$\sigma_{\max} = \sigma_m + \sigma_a$$

where  $\sigma_a = \frac{\sigma_{\max} - \sigma_{\min}}{2} = \frac{P_z}{2F_b}$  is the cycle amplitude ( $\sigma_{\min} = \sigma_t$ );

$$\sigma_m = \frac{\sigma_{\max} + \sigma_{\min}}{2} = \frac{V}{F_b} + \sigma_a = \sigma_t + \sigma_a \text{ — the mean cycle stress; } \sigma_t \text{ — the stress due to tightening.}$$

To calculate the bolt strength  $V$  and  $P_z$  should be first found from the formulae (87) and (89), and also design (stress concentration, scale factor), processing (mode of manufacture, cold hardening) and other factors, which influence strength at varying stresses, should be taken into account.

The dimensions of the joint components are found from the data provided by preliminary calculation from the condition of static strength at lower values of allowable stress. These data allow the joint design to be worked out after which it is possible to find the forces  $V$  and  $P_z$  and hence  $\sigma_a$  and  $\sigma_m$ .

If diagrams of limit stresses obtained from experimental investigation of bolted joints of corresponding design and material, etc., are available, the *strength can be evaluated* from the following condition:

$$\sigma_a = \frac{P_z}{2F_b} \leq \frac{\sigma_a \text{ lim}}{n} \quad (99)$$

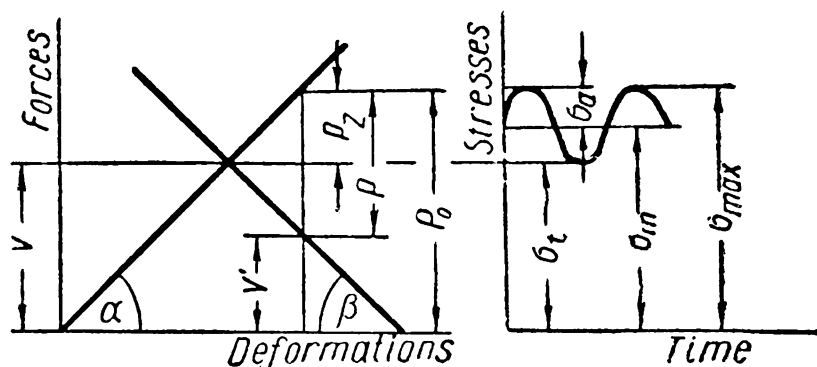


Fig. 78

where  $\sigma_{a \text{ lim}}$  is the limit cycle stress amplitude at the given  $\sigma_m$ ;  $n$  is the factor of safety assumed equal to 1.5-2.5.

In the absence of such diagrams the limit cycle stress amplitude  $\sigma_{a \text{ lim}}$  is found from the formula

$$\sigma_{a \text{ lim}} = \frac{(\sigma_{-1})_t}{k_\sigma} \quad (100)$$

where  $(\sigma_{-1})_t$  is the endurance limit of the bolt material in a symmetric tension-compression cycle, in which case for machine steels 3, 4 and 5 we take respectively  $(\sigma_{-1})_t = 1,300-1,500-1,700$  kg/cm<sup>2</sup>;  $k_\sigma$  is the effective stress concentration factor depending on the material, size, mode of manufacture and thread form, etc.

Thus, for example, for carbon steel parts with metric thread  $k_\sigma = 3.0-4.5$ ; larger values refer to threads with  $d_0 \geq 24$  mm; with a rolled thread  $k_\sigma$  should be reduced by 20-50%, etc.

For items made from alloy steel, the respective values of this factor are:  $k_\sigma = 5.5$  and  $k_\sigma = 6$ .

**Methods of Improving the Endurance of Threaded Joints.** It follows from what has been said previously that endurance can be

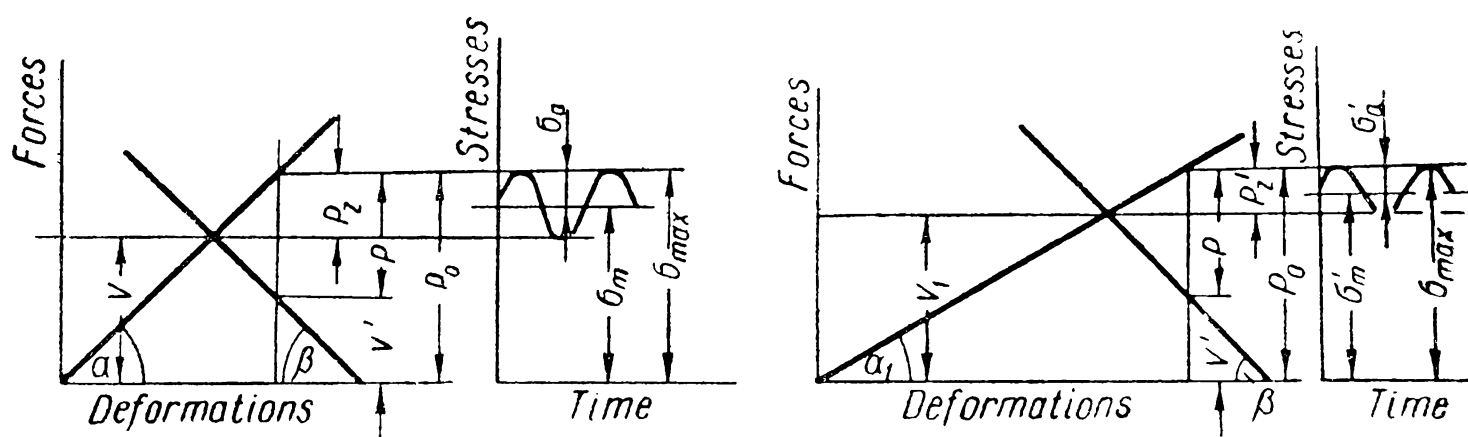


Fig. 79

improved: a) by decreasing  $\sigma_a$  at the given  $\sigma_{\max}$  to approximate the stress to that with  $\sigma = \text{const}$ ; b) by reducing stress concentrations; c) by improving load distribution among the active fillets. Below we examine the design methods used for this purpose.

A change in the structure of maximum cycle stress ( $\sigma_{\max} = \sigma_m + \sigma_a$ ), i. e., a change in the relation between  $\sigma_m$  and  $\sigma_a$  due to lesser  $\sigma_a$  is attained through the use of «elastic» bolts.

Fig. 79 shows design graphs plotted for joints with bolts of different stiffness under comparable conditions—similar values of an external load  $P$  varying from 0 to  $P$  and a residual stress  $V'$ . The different values of bolt stiffness are characterised by the angles of the corresponding straight lines ( $\alpha_1 < \alpha$ ). It is easy to see that a reduction in bolt stiffness (an increase in elasticity) will require greater

initial stress ( $V_1 > V$ ) to maintain  $V'$ ; in this case,  $\sigma'_a$  decreases ( $\sigma'_a < \sigma_a$ ) while  $\sigma_{\max}$  remains constant.

We know that the smaller  $\sigma_a$  is at the same  $\sigma_{\max}$  the greater are the number of load variations required to cause the joint to fail, i. e., such a joint has a longer service life. It follows from the relation  $C_b = \frac{F_b E_b}{l}$  that the stiffness of a bolt can be reduced by lengthening it; by decreasing the diameter of the shank unthreaded portion

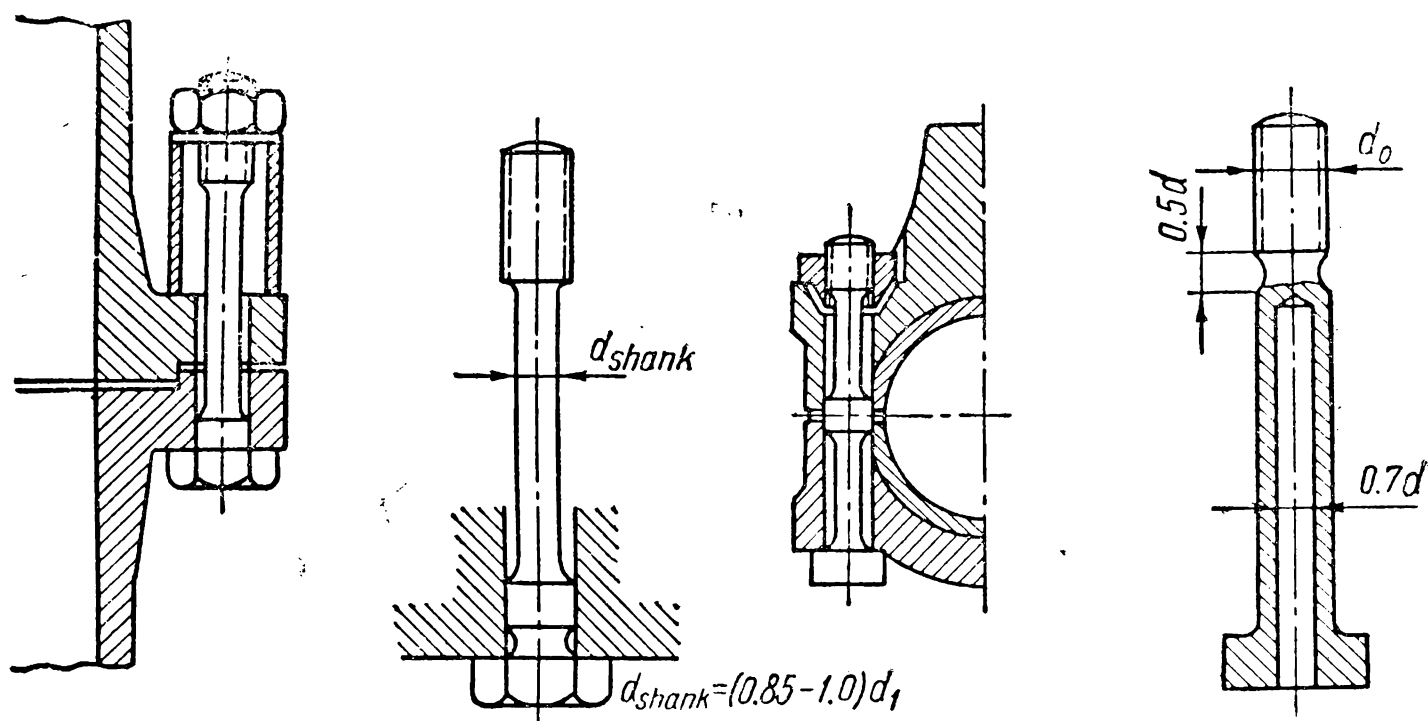


Fig. 80

to the size at which the static strength is equal in the threaded and unthreaded parts; by using hollow bolts; by incorporating special elastic elements in the bolt system. Examples of such designs are given in Fig. 80.

When deciding upon the number of bolts for a joint, the load should be spread among as many bolts as possible (with approximately equal cross-sectional areas); however, the bolts should be large enough to resist thread shear during assembly of the unit. In this case endurance is enhanced due to the scale effect. Thus, for example, the limits of endurance for metric thread M20, M45 and M72 relate to each other as 2.5 : 1.5 : 1.

The effect of initial stress on the structure of maximum stress, pointed out earlier, accounts for the practice of subjecting threaded joints to high prestress. Usually  $\sigma_t = \frac{V}{F_b} = (0.4-0.5)\sigma_y$ ; in certain cases  $\sigma_t = 0.8\sigma_y$ .

Adequate control over tightening during the assembly of the joint ensures the maintenance of the required stress value.

Today the most widespread methods of control are the measuring of: a) elongation, i. e., the difference in a datum length measured before and after tight-

ening (Fig. 81, *a*); *b*) the angle of the nut turn; *c*) torque when turning the nut with a torque wrench.

Fig. 81, *b* shows some designs of such wrenches.

Soviet standards provide for three types of wrenches with adjustable torque (within 20 and 200 kg/cm): side wrenches, box wrenches adjusted by one spring, box wrenches adjusted by two springs. For a more convenient handling of such wrenches use can be made of adapters and also changeable heads.

The first method is more dependable.

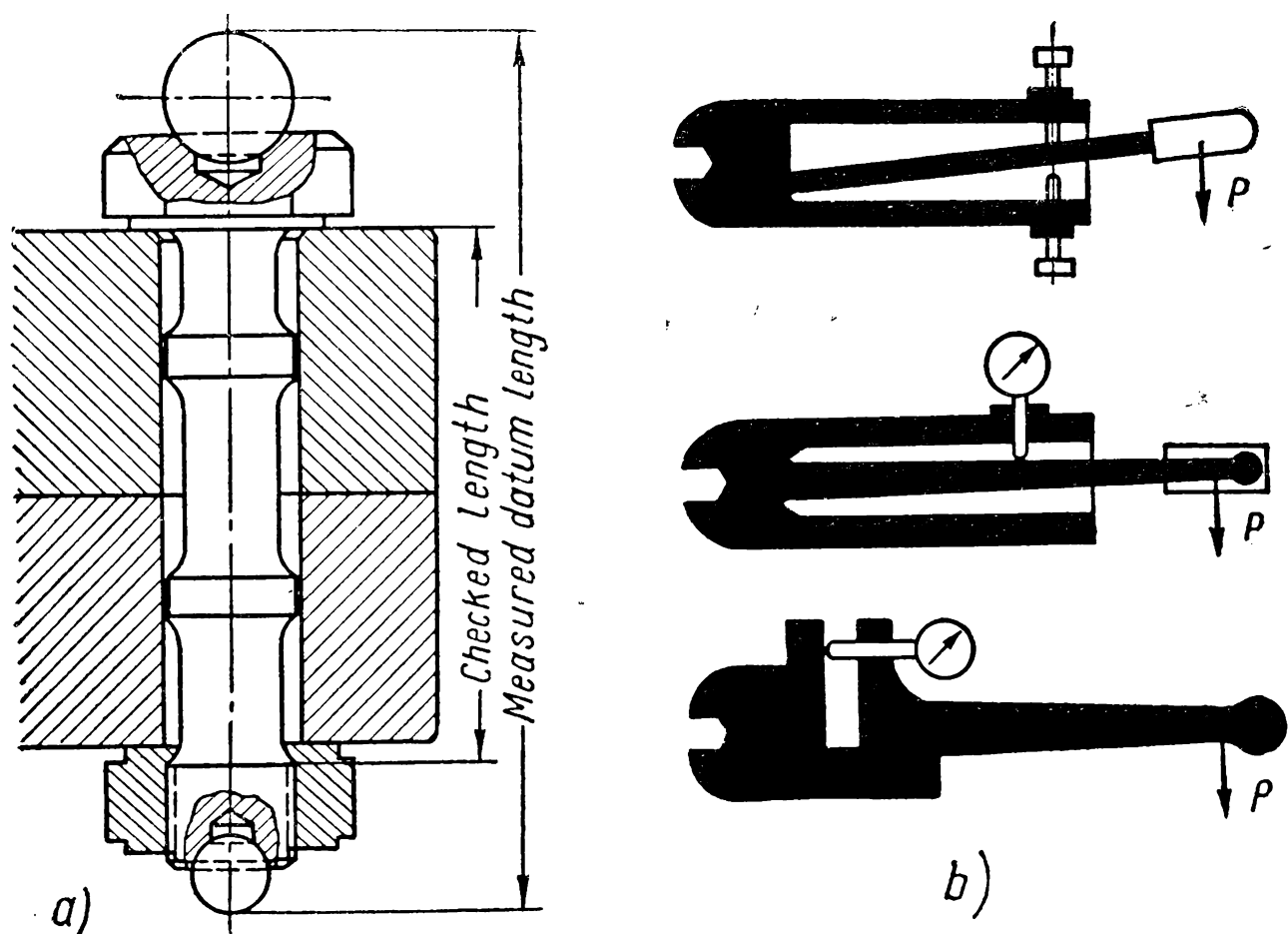


Fig. 81

The joint should be kept adequately tightened throughout the entire period of service. Nevertheless, practice shows that the continuous action of varying load impairs the strength of the joint. This is due to the presence of a large number of roughly machined contact points (joints with poor finish are crushed more easily), the stripping of threads, the unscrewing of nuts, and the loosening of screws and studs caused by vibration and other factors. Important designs should therefore preferably have as few joints as possible; loosening should be prevented by locking devices and the degree of tightness regularly checked.

Stress concentration can be decreased by the employment of improved thread profiles, new designs of the imperfect-thread region and of the transition zone between the shank and the head.

The stress concentration factor of the threaded portion depends, all other conditions being equal, on the radius  $r$  of the root rounding. Higher endurance is achieved when a root rounding, inscribed by a greater radius, is employed. Bearing in mind the effect of the scale factor and the sensitivity to stress con-

centration, the greater the bolt diameter and the higher the material ultimate strength, the larger should be the radius of root rounding.

Experimental data show that at  $r=0.2s$  the strength of heavily loaded threaded joints increases by 24-40%. Further increase in the radius of root rounding may lessen the efficiency of the joint since this reduces the area of contact of the bolt and nut threads and increases unit pressure.

The transition section from the unthreaded to the threaded part should have the form of a smoothly curved elongated neck (with length  $l=0.5d_0$  and diameter  $d_2=0.96d_1$ ); this relieves stress and equalises the force flux.

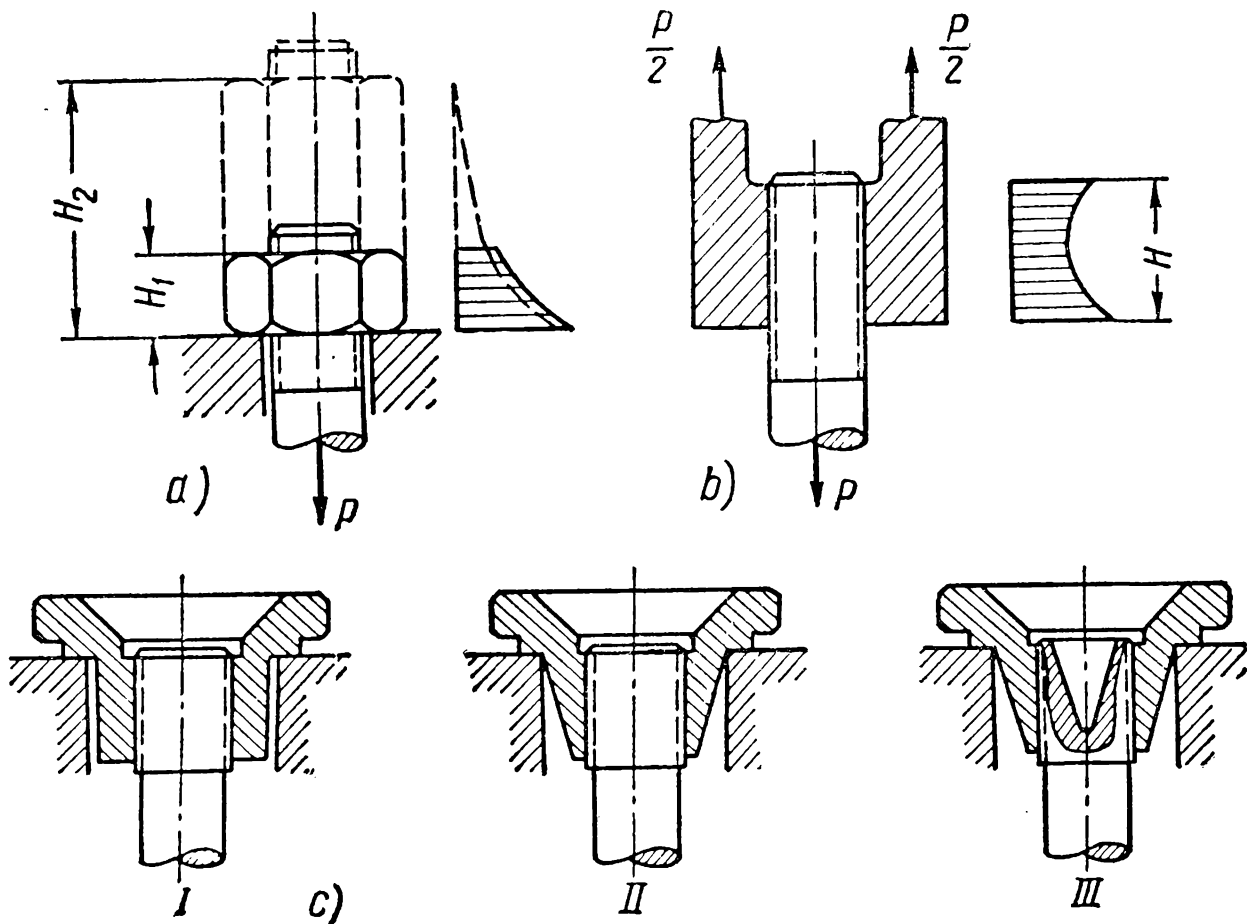


Fig. 82

However, because of high cost of such bolts they are employed only in important designs resisting heavy loads. In a general case, the radius of root rounding should be taken as  $R \geq 0.2d_0$ .

The solution of the problem of load distribution across the nut fillets put forward by N. E. Zhukovsky confirms the fact that in nuts in tension a more favourable distribution of the force flux is attained than in nuts in compression (i. e., ordinary nuts).

Fig. 82 gives an idea of load distribution across the thread for (a) an ordinary nut and for (b) a nut in tension. It is evident from the diagram (a) that in practice it is useless to increase the number of nut threads and hence its thickness.

Fig. 82, c shows the consecutive stages (I, II, III) of a design with a nut in tension aimed at equalising the load distribution over the active fillets.

The employment of nuts with a groove in the end-face and the first thread of engagement removed (that under the heaviest load), with the threads which resist the greatest load chamfered (Fig. 83) (more rarely of a bolt) also helps to equalise stress concentration. In the latter case (case *B*) due to thread chamfer the magnitude of the arm of force applied to individual threads of engagement on the bolt becomes variable.

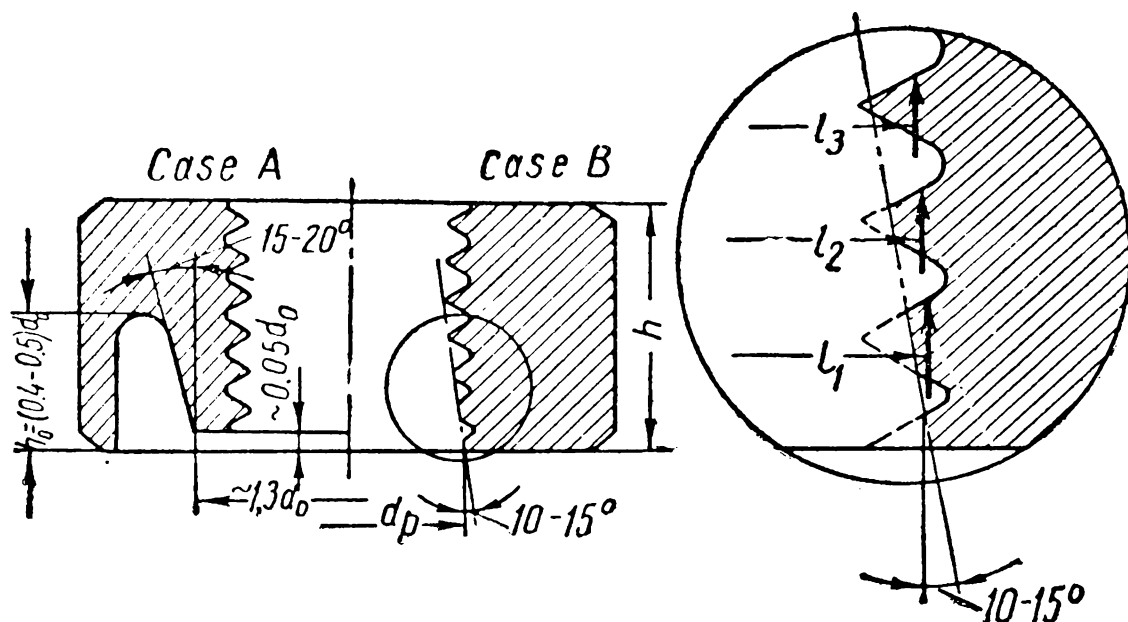


Fig. 83

A greater arm decreases the stiffness of the bolt thread and hence the elasticity of fillets across the nut becomes variable. Since the fillets, which in ordinary nuts carry the heaviest load, have in this case higher elasticity the load shifts to the upper (usually less loaded) fillets.

Such nuts improve the endurance of bolted joints up to  $\sim 30\%$ .

Provision for a permanent crest clearance is another effective means of increasing the elasticity of the thread. The earlier theory that threaded joints without crest clearance possess the greatest strength has been disproved by experiments which have shown that permanent crest clearance can increase the endurance strength of a threaded joint by 50%.

Better load distribution between the active fillets is obtained when nuts are made from a material whose modulus of elasticity  $E_n$  is lower than the modulus of elasticity of the bolt material  $E_b$ . Thus, at  $E_n = \frac{1}{3}E_b$ , the load carried by the first thread of engagement decreases by 30-40% when compared with a joint where  $E_n = E_b$ .

The effect of processing on the static strength of threaded parts is negligible. It proves material only at varying stress.

Among the most important factors which determine the effect of processing are: the surface finish of the thread, the physical proper-



ties of the threaded surface (the degree of cold hardening, the residual stresses depending on the processing methods and machining speeds and feeds employed).

Thus, for example, when the surface finish of cut or ground thread is raised from the 7th to the 10th class the cycle stress amplitude may increase 30-50%.

This naturally has the greatest effect on bolts made from high-strength steel.

Endurance is affected to a still greater degree by residual stresses that develop in the thread surface during manufacture and processing.

When the thread has been rolled in conformity with a correct production method, plastic deformations produce a profile with favourable grain flow (as distinct from a cut thread where the grains are always cut) and with residual stresses, due to compression, in the surface. This raises the endurance for rolled thread by  $\sim 40-95\%$  as compared with ground thread.

The method of roll-burnishing the bottoms of thread after preliminary grinding or cutting is highly effective; endurance can be almost doubled.

### TEMPERATURE STRESSES IN THREADED JOINTS

Let the joint shown in Fig. 71 be prestressed with force  $V$ .

In this case, the deformations of the joint elements will comprise  $\lambda_1$  and  $\lambda_2$  and therefore the total deformation of the joint will be represented in Fig. 84 as the segment  $(\lambda_1 + \lambda_2)$ .

Excluding the end portion of the bolt and taking its length (Fig. 71) to equal  $l_b = l_1 + l_2 = l_a = l$  then, due to the effect of temperature increment, the bolt in a free state will stretch by  $l\alpha_1 t_1$  and the parts by  $l\alpha_2 t_2$  where  $\alpha_1$  and  $\alpha_2$  are the coefficients of linear expansion of the material of the bolt and of the fastened parts;  $t_1$  and  $t_2$  are the temperature increments of the bolt and the fastened parts compared with the temperature of the unit assembly.

If, as is often the case, the joined components are made from a material having a higher coefficient of linear expansion than the bolt material, then if the temperature increments  $t_1$  and  $t_2$  differ but little  $l\alpha_2 t_2$  will obviously be larger than  $l\alpha_1 t_1$ .

Since the joined components deform together (when compressed) the elongation of the joint due to temperature will amount to  $\lambda_T = l(\alpha_2 t_2 - \alpha_1 t_1)$ . Simultaneously, the additional force  $V_{T_1}$  develops in the joint, which tends to stretch the bolt and compress the joint. This force may be determined by the usual method—by means of plotting, as shown in Fig. 84 by the dash line on the assumption

that the values  $C_b = \tan \alpha$  and  $C_\partial = \tan \beta$  are not affected by temperature.

In actual fact the additional force  $V_T$  which can be regarded as an increment of the magnitude of the initial stress is smaller than the obtained value  $V_{T_1}$  since an increase in temperature of the joint changes the moduli of elasticity of the material of the parts ( $E_{1T} < E_1$ ;  $E_{2T} < E_2$  and, consequently,  $\alpha_T < \alpha$  and  $\beta_T < \beta$ ).

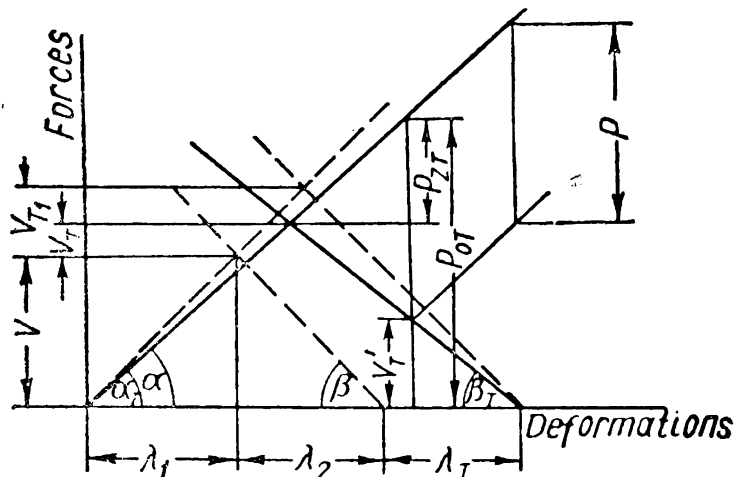


Fig. 84

load  $P$ ) are found graphically (Fig. 84), or analytically. In the latter case we can obtain formulae similar to (84)-(90).

The problem can be also solved from another angle: with the known  $C_{bT} = \tan \alpha_T$ ;  $C_{\partial T} = \tan \beta_T$ ;  $P$ ;  $V'_T$ ;  $t_1$ ;  $t_2$ , the force of initial stress can be found that would ensure the required magnitude of the residual stress  $V'_T$  at which the design load  $P_{OT}$  conforms to the conditions of bolt strength.

The design load for the bolt

$$P_{OT} = V'_T + P \quad (101)$$

and under continuous static load

$$d_1 = \sqrt{\frac{4 \times P_{OT} \times n}{\pi \sigma_t}} \quad (102)$$

where  $\sigma_t$  is the ultimate strength of the bolt in the thread at the given temperature equal approximately to 0.8 of the corresponding ultimate strength of the material;

$n$  is the safety factor assumed as 2-3.

Under varying load

$$d_1 = \sqrt{\frac{2 P_{zT} T^n}{\pi \sigma_{aT}}} \text{ cm} \quad (103)$$

where  $\frac{P_{zT}}{2}$  is the amplitude of varying load found from the graph;  $\sigma_{aT}$ —the limit stress amplitude at the given temperature in  $\text{kg/cm}^2$ .

The method outlined here for designing threaded joints is used when the joints have the following temperatures:  $t \geq 300^\circ\text{C}$  for steel parts and  $t \geq 100^\circ\text{C}$  for light-alloy parts. The method can be employed only after preparatory calculation and design work to show the magnitude necessary for the evaluation of  $P_{OT}$  and  $P_{zT}$ .

### LOAD DISTRIBUTION BETWEEN THREADED PARTS IN A GROUP JOINT (DETERMINATION OF DESIGN LOAD IN A GROUP JOINT)

In a joint fastened by several bolts the law of external load distribution depends on the design of the joint and the nature of load it carries.

In group joints the bolts most frequently have equal diameters although from the viewpoint of design this is far from being always justified; it holds good only if external load is spread uniformly over the threaded parts. Nevertheless, it is admissible if sharp variations in the load carried by individual bolts are excluded with a view to cut down the range of items required. This is very important in production. In this case the diameter of all bolts in a joint is taken as equal to the diameter of the bolt resisting the heaviest load.

In solving the problem of load distribution between the bolts in a group joint it is assumed that:

- 1) due to adequate stiffness of the fastened parts the flatness of the joint surfaces is not disturbed;
- 2) the tension caused by initial stress is the same in all bolts of the joint\*.

Some of the most typical designs of group joints are given below.

*1. A set of bolts carrying loads whose resultant is perpendicular to the contact surface and passes through its centre of gravity.*

This occurs in securing bearing caps (Fig. 188) and round and rectangular pressure vessel covers. For round covers (Fig. 71) when bolts of equal length are arranged symmetrically it can be assumed that all bolts carry the same load.

With prestress the design load on the bolt is found from the formulae (84) and (88) and the bolt diameter from the formula (91).

*2. A set of bolts resisting a shearing force acting in the plane of the joint along its axis of symmetry.*

This case corresponds to the problem examined on p. 137 with several bolts in the joint. We assume that the external load is distributed evenly while the design load depends on whether the bolts are fitted into the holes with an interference or clearance.

---

\* When tightening observe the sequence outlined in the manufacturer's instructions.

In the first case

$$R_1 = \frac{R}{z} \quad (104)$$

in the second case

$$V_1 = \frac{R}{zif} \quad (105)$$

In these formulae  $z$  is the number of bolts.

3. *A set of bolts carrying design torque  $M_t$  acting in the plane of the joint.*

This case is illustrated, for example, by the design of a joint between two discs of a flange coupling (Fig. 262). The load is assumed to be evenly distributed between the bolts of the joint. When the bolts are fitted with an interference the diameter of the bolt shank is found from the work in shear; the rated force acting on the bolt is

$$R_1 = \frac{2M_t}{D_b z} \quad (106)$$

When the bolts are inserted into the holes with a clearance the tightening force  $V$  necessary to transmit torque from one disc of the coupling to the other through friction alone is considered; the design force in this case is

$$V \approx \frac{4M_t}{(D_{out} + D_1) f z} \quad (107)$$

In these formulae

$M_t$  —torque in kg/cm.

$D_b$  —centre diameter of the bolts in cm;

$D_{out}$ —outside diameter of the coupling in cm;

$D_1$  —diameter of the coupling recess or inside diameter of the centering collar in cm.

4. *A set of bolts in a split hub (Fig. 85).*

The problem is to find the required tightening force that will ensure that:

1) when the joint takes torque  $M_t$  (Case I)—the contact friction forces will create the moment  $M_{fr}$  satisfying the condition  $M_{fr} \geq M_t$ ;

2) when the joint takes the axial force  $R$  (Case II) —the contact friction force  $F$  will satisfy the condition  $F \geq R$ .

In the first instance, since the law of distribution of unit pressures on the contact surface is unknown, two design diagrams are usually considered. In the first case it is assumed that at points  $m$  and  $n$  (Fig. 85) there arise friction forces  $fVz$  (where  $z$  is the number of bolts) which create the moment  $M_{fr} = Nfzd$  equalising the external torque  $M_t$ .

If we assume that both halves of the hub hinge-turn, when the bolts are tightened, about points located along the line of action of the friction forces and lying at a distance  $a_1 = a$  from the line of action of the forces  $Nz$ , then, designating the bolt tightening force as  $V$ , we obtain  $N = 2V$  and  $M_{fr} = 2Vzfd$ .

In the second case we assume that unit pressure is spread uniformly over the contact surface determined by the angle of contact  $\approx 2\pi$ , i. e.,

$$p = \frac{Nz}{ld} = \frac{2Vz}{ld} = \text{const.}$$

The pressure on an elementary area equals

$$p \frac{d}{2} l d\alpha = Vz d\alpha$$

and the elementary friction force is  $Vzf d\alpha$ .

Therefore, the moment of friction is

$$M_{fr} = \int_0^{2\pi} Vz f \frac{d}{2} d\alpha = \pi Vz f d.$$

In actual fact

$$2Vzf d < M_{fr} < \pi Vz f d \quad (108)$$

and at  $f = 0.2$  we take the mean value for the tightening force

$$V \approx \frac{2M_t}{zd}. \quad (109)$$

For the second case the values of the tightening force can be obtained from the condition obtained by analogous reasoning:

$$4Vzf < R < 2\pi Vz f \quad (110)$$

and at  $f = 0.2$

$$V \approx \frac{R}{z}. \quad (111)$$

*Example.* What will be the efficient dimensions of bolts fastening the cover of a vessel under a working pressure  $p = 0.5$  kg/cm<sup>2</sup>, where the inside diameter of the vessel  $D = 1,100$  mm, the modulus of elasticity of the joint steel parts  $E = 2.1 \times 10^6$  kg/cm<sup>2</sup>, the modulus of elasticity of the gasket material (in compression)  $E_g = 500$  kg/cm<sup>2</sup> and the number of bolts  $z = 20$ .

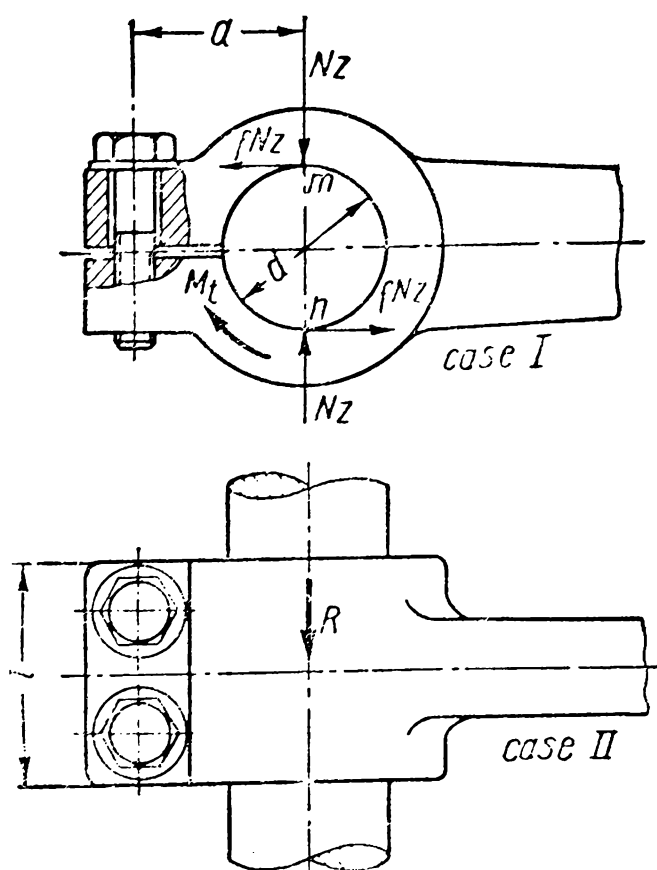


Fig. 85



The mean cycle stress is

$$\sigma_m = \frac{\sigma_{\max} + \sigma_{\min}}{2} = \frac{595 + 364}{2} = 480 \text{ kg/cm}^2$$

$$\left( \text{or, } \sigma_m = \sigma_t + \sigma_a = \frac{V}{F_b} + \sigma_a = 364 + 115 \approx 480 \text{ kg/cm}^2 \right).$$

The limit stress cycle amplitude  $\sigma_{a \text{ lim}}$  from the formula (100) is

$$\sigma_{a \text{ lim}} = \frac{(\sigma_{-1})_t}{k_\sigma} = \frac{1,800}{5} = 360 \text{ kg/cm}^2.$$

The safety factor from the formula (99) equals  $n = \frac{\sigma_{a \text{ lim}}}{\sigma_a} = \frac{360}{115} = 3.1$  which is permissible.

The safety factor can be calculated from the formula (15) (see p. 40) which is recommended for such computations:

$$n = \frac{(\sigma_{-1})_e \left( 1 - \frac{\sigma_m}{\sigma_{ult}} \right)}{\sigma_a} = \frac{\frac{(\sigma_{-1})_t}{k_\sigma} \left( 1 - \frac{\sigma_m}{\sigma_{ult}} \right)}{\sigma_a} = \frac{\frac{1,800}{5} \left( 1 - \frac{480}{5,000} \right)}{115} = 2.8.$$

When this method of calculation is used  $n$  should be within  $2.5 < n < 5$ .

## CHAPTER X

### COTTERED FASTENINGS

#### COTTERED JOINTS

In these designs members are fastened by cotter keys (Fig. 87). Cotter keys are made *single-tapered* (a), *double-tapered* (b) or with straight sides, the latter type being called *dowels* (Fig. 88).

For single-tapered cotter keys the taper is

$$i = \frac{h_2 - h_1}{l} = \tan \alpha$$

and for double-tapered cotter keys

$$i = \frac{h_2 - h_1}{l} = \tan \alpha_1 + \tan \alpha_2.$$

At small angles of taper

$$\tan \alpha_1 + \tan \alpha_2 \approx \tan (\alpha_1 + \alpha_2).$$

Consequently, if  $\alpha = \alpha_1 + \alpha_2$  single- and double-tapered cotter keys have equal force-transmitting features. Preference is given to single-tapered cotter keys which are more easily manufactured.

The taper lies within  $i = \frac{1}{5} - \frac{1}{100}$ . For joints which are frequently disassembled (*adjusting* cotters)  $i = \frac{1}{5} - \frac{1}{10}$  and for joints which are seldom disassembled (*fastening* cotters) —  $i = \frac{1}{20} - \frac{1}{100}$ .

In all cases, when  $i > \frac{1}{20}$  devices are required which prevent the cotter key from

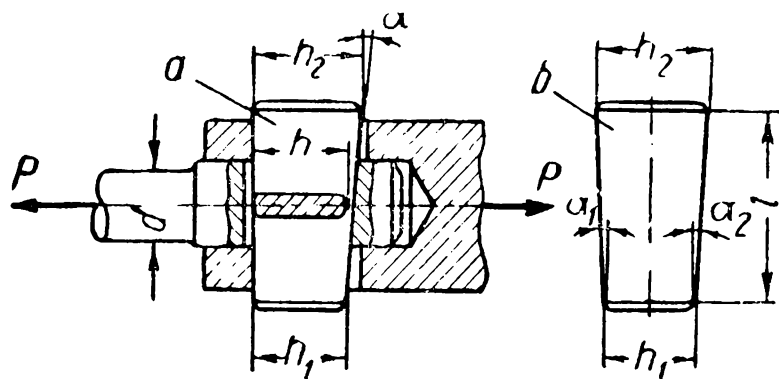


Fig. 87

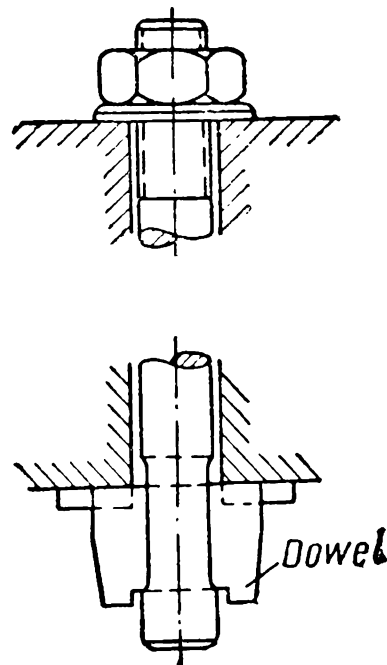


Fig. 88

being thrown out of position (Fig. 89, a); when  $i < \frac{1}{20}$  and at static loads such devices are not needed because the cotter key does not tend to back out being a self-locking joint.

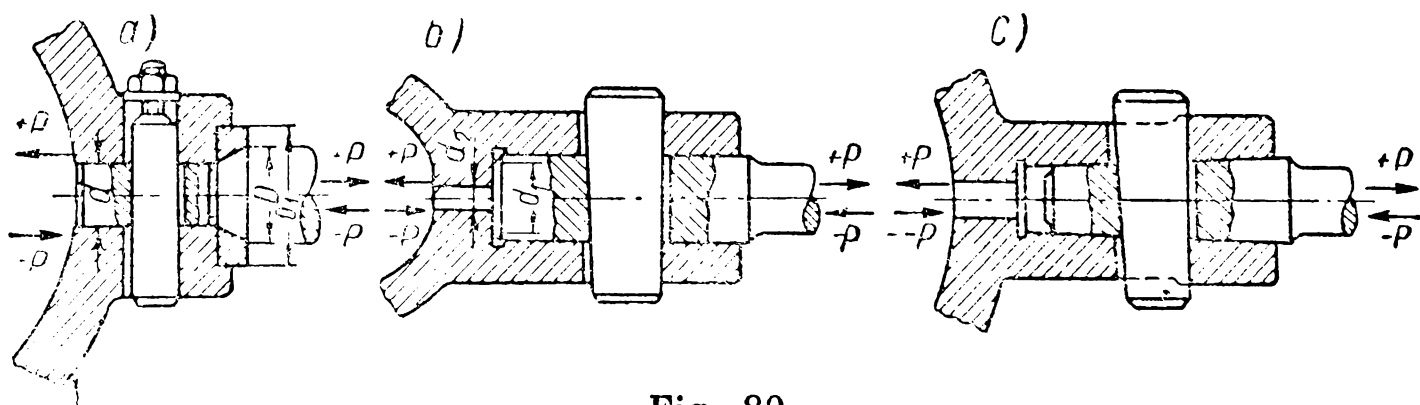


Fig. 89

Self-locking is considered adequate if the following condition is satisfied

$$\alpha_1 + \alpha_2 \leq 2\varphi$$

where  $\varphi$  is the angle of friction.

The bearing surfaces of the cotter key as well as the contact faces of the joint members are usually rounded which reduces stress concentration caused by the hole, increases the coefficient of friction on the bearing surfaces and simplifies the machining of the hole.

Cotter joints are advantageous in that they are simple in design and allow a convenient and rapid assembly and disassembly of the



unit; among their main shortcomings are production inadequacy of design, weakening of the main parts by the holes for cotter keys and the need for locking devices in important cases.

These shortcomings prevent cotter joints from being used on an extensive scale. However, they continue to be used where convenience and rapidity of assembly and disassembly are the prime considerations (for example, as fasteners for the joints of piston rods and crossheads in steam engines and internal combustion engines, in tool fixtures).

*Classification of cotter joints.* Depending on the method of assembly and the nature of the load carried there are *unstrained* (not prestressed) and *strained* (prestressed) cotter joints.

Unstrained joints are intended to resist loads constant in magnitude and sign (Fig. 87).

When the joint takes axial loads varying in magnitude and sign, use is made of strained joints. In these joints the pressing in of the cotter key causes initial stress to arise before external load is applied. Its magnitude should guarantee the work of the joined components at a varying external (axial) load. Such joints work dependably only if their parts retain residual stress after external load is applied.

In the design shown in Fig. 89, *a*, prestress is created by a collar. Fig. 89, *b* shows a strained joint with an end-face stop and Fig. 89, *c*—a joint with a tapered rod tail-end. In the last case the rod end-face should not bear against the socket bottom. Here the rod tail-end is enveloped by the socket which also ensures the stress of the joint relative to the forces acting perpendicular to the rod axis.

*Calculating a cotter joint parts for strength. Unstrained joints.* When calculating unstrained cotter joints the maximum external load applied to the joint is considered as the design load. If the joint is designed as shown in Fig. 87 the size of its parts is found in the following way.

*Calculation of the shank head* (Fig. 90, *a*). From the condition of the shank strength in tension

$$P \leq \left( \frac{\pi d_1^2}{4} - b d_1 \right) [\sigma]_t \quad (112)$$

we find the size  $d_1$ .

The width  $b$  of the hole is so chosen as to ensure equal strength of the shank in tension and compression under the cotter key. As a rule, this condition is satisfied when  $b = (0.25 - 0.35) d_1$ ; in this case compressive stress under the cotter key is

$$\sigma_c = \frac{P}{b d_1} \leq [\sigma]_c \quad (113)$$

The distance  $h_1$  from the hole to the rod end can be found from the condition of the shank shear in two planes

$$P \leq 2h_1d_1[\tau]_s.$$

As a rule, the size  $h_1$  found from the last formula is small. Therefore, it is taken as:  $h_1 = (0.7-1.0)h$  where  $h$  is the cotter key height in its middle section (see Fig. 87).

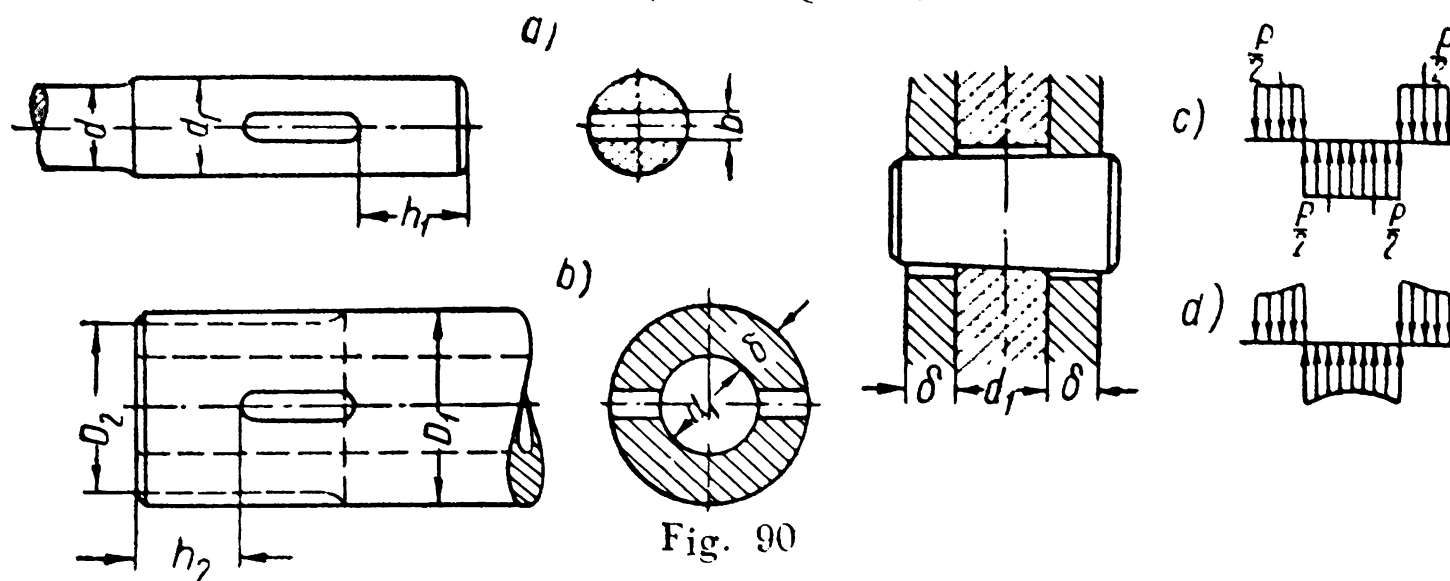


Fig. 90

Calculation of the socket (Fig. 90, b). To avoid crushing of the cotter key bearing surfaces in the socket we should have

$$P \leq 2b\delta[\sigma]_c;$$

whence

$$\delta = \frac{P}{2b[\sigma]_c}$$

and, therefore,

$$D_1 = 2\delta + d_1 = \frac{P}{b[\sigma]_c} + d_1. \quad (114)$$

If the shank and the socket are made from the same material the relations (113) and (114) give us:  $D_1 = 2d_1$ .

The socket strength in tension is checked from the relation

$$\sigma_t = \frac{P}{\left| \frac{\pi}{4} (D_1^2 - d_1^2) - 2b\delta \right|} \leq [\sigma]_t. \quad (115)$$

If, in this case, the stress  $\sigma_t$  appears materially below  $[\sigma]_t$  then to decrease the socket weight its diameter can be reduced to the size  $D_2$ , as shown in Fig. 90, b by the dash line, within the free section of the cotter key.

The size  $h_2$  can be found from the condition

$$P \leq 4\delta h_2[\tau]_s.$$

As a rule,

$$h_2 = h_1 = (0.7-1.0)h.$$

*Calculation of the cotter key.* The height of the cotter key  $h$  can be found from its work in bending and shear. The sizes of the cotter key obtained during calculation for shear do not safeguard it against bending; on the other hand, the sizes of the cotter key found from the calculation for bending ensure it against shear. Therefore, the size  $h$  is found from the cotter key strength in bending.

The cotter key is calculated as a simple beam taking into account only normal stresses.

It should be noted that the classical theory of flexure gives satisfactory results in these designs when  $\frac{h}{D_1} \leq 0.6$  where  $D_1$  is the cotter key bearing length (Fig. 90, *b*). If  $\frac{h}{D_1} > 0.6$  the stresses calculated by the usual method appear to be 10-20% smaller when compared with those found by a more accurate calculation in which the cotter key is regarded as a beam-wall.

The design diagram of the cotter key is given in Fig. 90, *c*. The accepted law of uniform pressure distribution over the bearing sections differs from the actual law. A tentative pressure distribution diagram is represented in Fig. 90, *d*. Experiments have shown that the deviation of the maximum and minimum unit pressures from the mean value taken in the design diagram does not exceed  $\pm 5\%$ . This error makes the accepted law applicable in calculations.

The bending strength condition is written as follows (Fig. 90, *c*):

$$\frac{P}{2} \left( \frac{d_1}{2} + \frac{\delta}{2} \right) - \frac{P}{2} \times \frac{d_1}{4} = \frac{P}{4} (0.5d_1 + \delta) \leq \frac{bh^2}{6} [\sigma]_b;$$

hence

$$h = \sqrt{\frac{3}{2} P \frac{0.5d_1 + \delta}{b [\sigma]_b}}. \quad (116)$$

In a particular case, if  $b = 0.25d_1$  and  $\delta = 0.5d_1$ , we obtain

$$h = \sqrt{\frac{6P}{[\sigma]_b}}.$$

Cotter keys are usually made from steel 5 or 6. The following stresses are recommended as allowable:

$$[\sigma]_c \leq 2,000 \text{ kg/cm}^2; \quad [\sigma]_b \leq 1,500 \text{ kg/cm}^2.$$

This design of shank head and socket is valid only for the end sections of respective parts fastened by means of a cotter key; material for them is chosen taking into account the design and load conditions.

*Strained joints.* In strained cotter joints the magnitude of the design load is determined from the external load and the required residual stress of the joint. The latter, in turn, is determined from

the magnitude of initial stress, obtaining in the joint, and depends on external load. The evaluation of the design load requires therefore a proper estimation of elastic deformations of the joint parts during their operation and is a rather complicated task. As a rule, the strength of the parts of a strained joint is found by the methods used for unstrained cotter joints. In this case the design load is assumed equal to

$$P_0 = 1.25P,$$

where  $P$  is the maximum external load.

PIN JOINTS

Pins are used as fixation elements for determining the mutual location of the jointed parts; they can also be employed as fasteners.

In some designs they are used to safeguard against overloads.

Fig. 91 shows some widespread pin designs:

*Taper pins* (Fig. 91, *a*);  
*cylindrical pins* (Fig. 91, *c*)  
and *taper bifurcated pins* (Fig. 91, *e*).

Cylindrical pins are held in the hole by frictional resistance which is due to an interference fit (Fig. 92, *a*), caused by the opening of the pin ends (Fig. 92, *b*) or other means.

Taper pins have a taper of 1 : 50. They are superior to cylindrical pins in that they can be inserted into the same hole several times.

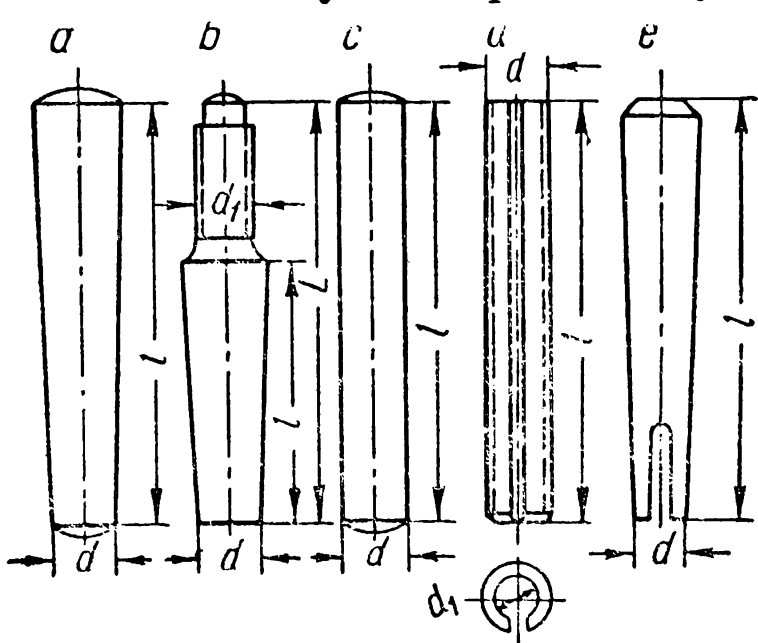


Fig. 91

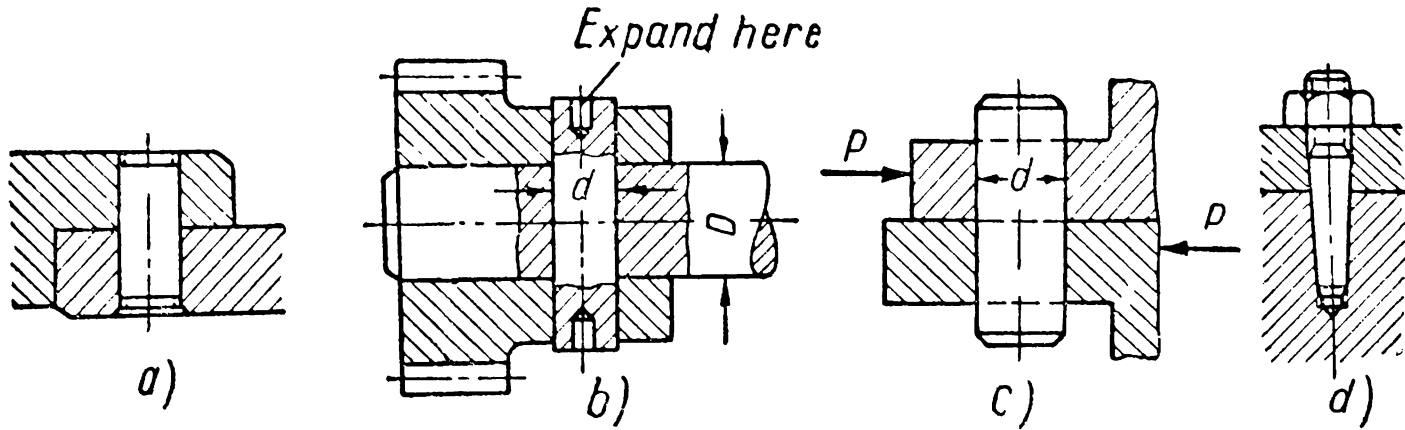


Fig. 92

The pin can be removed only from a through hole; another possible solution is shown in Fig. 92, *d*.

Taper bifurcated pins (Fig. 91, e) are prevented from backing out by bending their ends apart.

A recent development is the design of cylindrical and taper pins with grooves formed by coining or cutting along all or part of the

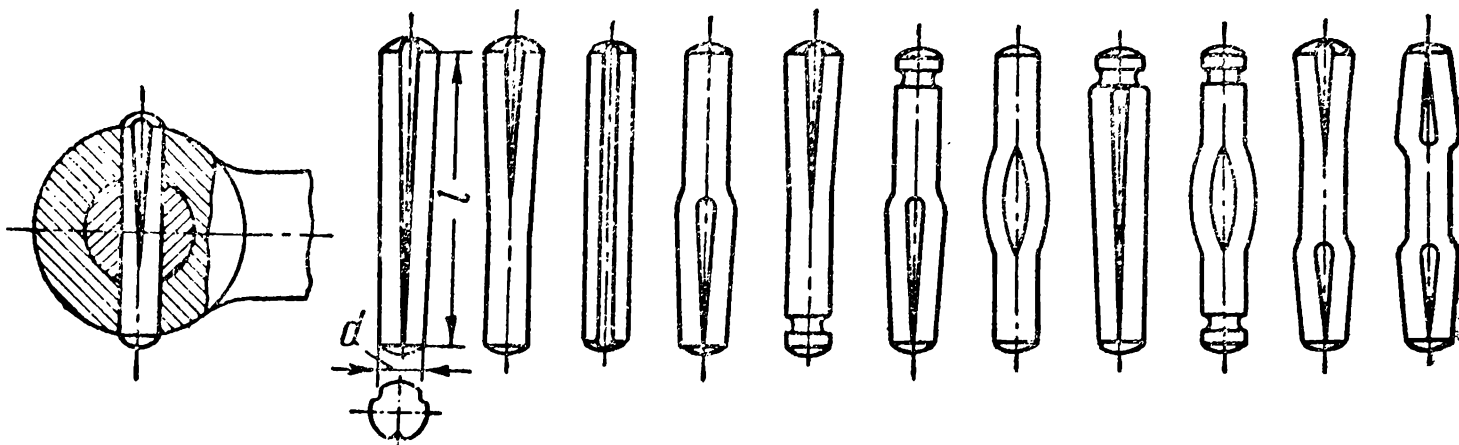


Fig. 93.

pin length; such pins are called *grooved* pins (Fig. 93). They are inserted into drilled unreamed holes. Such pins can be used repeatedly to fit the same hole.

The pin diameter is calculated for shear. When the joint carries the shearing force  $P$  (Fig. 92, c) the strength condition is

$$P \leq z \frac{\pi d^2}{4} [\tau]_s$$

where  $z$  is the number of pins in the joint. Whence

$$d = \sqrt{\frac{4}{\pi} \times \frac{P}{z [\tau]_s}}. \quad (117)$$

For the design shown in Fig. 92, b

$$\frac{2M_t}{D} = 2 \frac{\pi d^2}{4} [\tau]_s$$

whence

$$d = \sqrt{\frac{4}{\pi} \times \frac{M_t}{D [\tau]_s}}. \quad (118)$$

For taper pins,  $d$  is the mean diameter.

Cylindrical taper and bifurcated pins are made from machine steel or tool steel. For  $[\tau]_s$  the recommended value is  $[\tau]_s \leq 800 \text{ kg/cm}^2$ . On designing pins for protective purposes see p. 530.

## CHAPTER XI

KEY, SPLINED AND SERRATED\*, AND KEYLESS  
(SHAPED AND OTHER) JOINTS

These joints are employed as fasteners to transmit torque, usually in combinations of the shaft-hub type, to secure toothed wheels, pulleys, discs and other similar parts to shafts and axles.

An extensive use of *key joints* is largely due to their simple and dependable design, convenience of assembly and disassembly, low cost, etc.

The main disadvantage of this type of joint is the need for a keyway which not only makes the effective cross-section of the part smaller but also involves considerable stress concentration. Failures of shafts and axles are very often caused by high local stresses arising in the area of the keyway.

Another important shortcoming of key joints is that they cannot be fitted closely enough to ensure accurate concentricity of parts and that one key cannot transmit large torques.

Complicated load conditions and the greater accuracy required in the movement of parts stimulated the development of splines made integral with the shaft. These joints are superior to key joints because they ensure:

- 1) greater strength of the splined shafts at varying and impact load;
- 2) larger contact area of splines which can transmit greater loads;
- 3) better centering of the jointed parts and better guidance of the hub along the axle; this is achieved by the employment of more accurate machining methods in the manufacture of the members of this type of joint.

Splined joints have the following main disadvantages:

- 1) local stresses in the reentering corners of the grooves (especially with *straight-sided splines*) which are, however, lower than in the case of keyways;
- 2) inevitable uneven load distribution between the splines;
- 3) the need for special plant and cutting and measuring tools for the manufacture of splined shafts and hubs.

Further development of this group of joints has led to the appearance of *keyless* designs.

As compared to key and splined joints they have a greater endurance due to the absence of keyways, recesses and other similar points of stress concentration on the bearing surfaces, and ensure better centering.

---

\* For the sake of brevity in further exposition we shall use the more general term «splines».

## KEYS

The main designs of keys and key joints employed in mechanical engineering are shown in Table 14. There are three main groups of keys: *taper*, *feather* and *Woodruff* keys.

*Taper* keys which form strained joints include *sunk* and *tangential* as well as nonstandardised *flat* and *saddle* keys.

Sunk and flat keys have rectangular cross-section; the broad side of a saddle key section adjoining the shaft is confined within a cylindrical surface whose radius equals the radius of the shaft. This circumstance is the great advantage of saddle keys: they do not need a keyway or a flat on the shaft. Sunk, flat and saddle keys fit on their broad sides while at overload sunk keys fit also on their lateral narrow sides.

Taper keys have a *taper* of  $i=1 : 100$ . The bottom of the hub keyway has the same taper while the keyway in the shaft is not tapered.

A tangential key is so placed that its broad side is directed along the tangent and one of the narrow sides—along the radius of the shaft. The key comprises two single-tapered ( $i=1 : 100$ ) rectangular wedges. Their relative shift causes considerable normal pressures to arise on the bearing surfaces of the keyway and the key. The standards provide for *normal* and *reinforced* tangential keys which differ in size. The dimensions of keyways differ likewise.

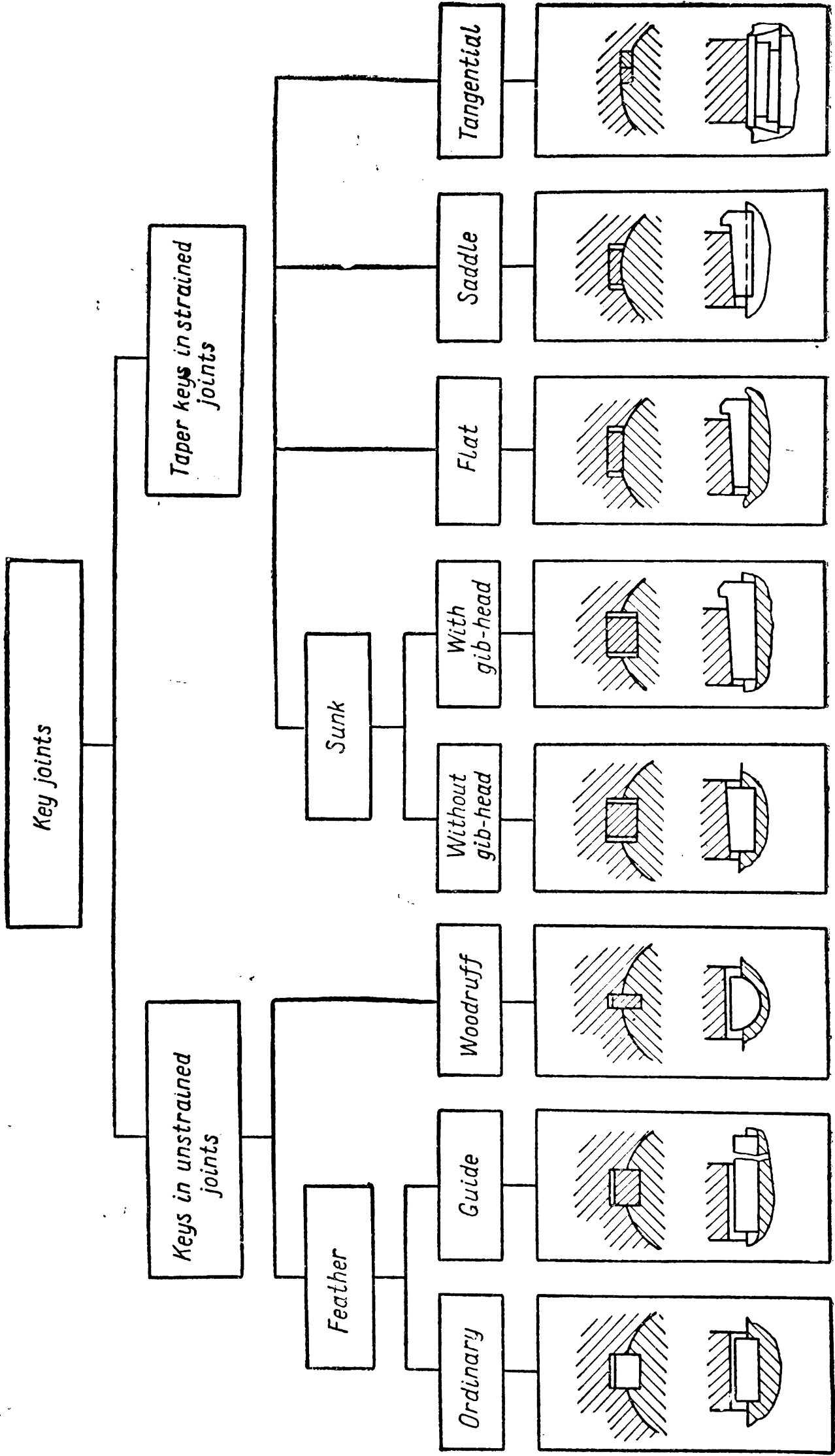
The direction of rotation is very important for a tangential key joint (see, for example, Fig. 94, *a*). A reversible unit requires two tangential keys usually located at an angle of  $120-135^\circ$  as shown in Fig. 94, *b*.

Sunk keys are the most widespread type of taper keys. Saddle and flat keys are capable of transmitting only comparatively small torques.

The magnitude of a torque transmitted by a joint formed by a taper key depends on the friction forces created on the bearing sides. To increase these forces considerable normal pressures should be created on the bearing surfaces; they arise as a result of fitting the key into the keyway and thus straining the joint before external load is applied. In this case the part fitted onto the shaft carries considerable radial-thrust forces which may shift its axis relative to that of the shaft by the amount of the fit clearance or may even deform the part. The fastening of parts with short hubs by means of taper keys may cause their misalignment.

These reasons reduce the sphere of application of taper keys: they are used only where accuracy is not the prime consideration. In such cases fitted parts should not necessarily be protected from an axial shift, for the friction forces arising on the bearing sides do not allow such displacement.

Table 14





Greater accuracy of fit is achieved through the use of feather and Woodruff keys forming unstrained joints.

Rectangular *feather* keys fit only on their lateral narrow sides. They are employed to form fixed joints (without relative axial shift of parts) and sliding joints (when axial shift is possible). In the latter instance they are secured by screws either to the shaft (*guide* keys) or move with the hub (*sliding* keys).

*Woodruff* keys fit on the sides alone. Since they are fitted into deep keyways which weaken the shaft they are employed only for comparatively small loads.

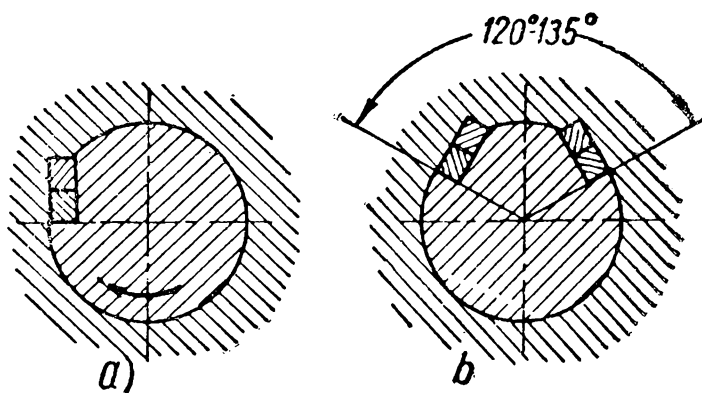


Fig. 94

The main elements (sections, keyways, length) of key joints conform to standards, where the sizes of keys ( $b \times h$ ), keyways, etc., of various design are fixed according to the shaft diameter  $d$ . The design of a joint can therefore be reduced to checking the stresses which arise on the bearing surfaces or dangerous sections or, when admissible stresses have been fixed, to determining the design length of the key.

**Calculation of Unstrained Joints.** It follows from the load conditions for a feather key (Fig. 95) that its failure may be caused by the crushing of the sides of the bearing sections and by shear.

To avoid crushing the following condition should be satisfied

$$P \leq \frac{h}{2} l [\sigma]_c$$

where  $l$  is the design length of the key.

If we take  $y = \frac{d}{2}$  then the torque transmitted by the joint equals

$$M_t = P \frac{d}{2} = 0.25 h l d [\sigma]_c. \quad (119)$$

The condition of the key strength in shear

$$P = b l [\tau]_s$$

gives us the relation

$$M_t = P \frac{d}{2} = 0.5 d b l [\tau]_s. \quad (120)$$

With the given value of the moment  $M_t$ , the formulae are used to find the design length of the key; of the two values obtained the larger should be selected. If, in doing this,  $l$  turns out to be greater

than the hub length the length of the latter, if possible, or the number of keys (which seldom exceeds two) should be increased.

Joints formed by means of Woodruff keys are designed on the basis of the same considerations. Denoting (Fig. 96)  $c = t + h - d$ , the

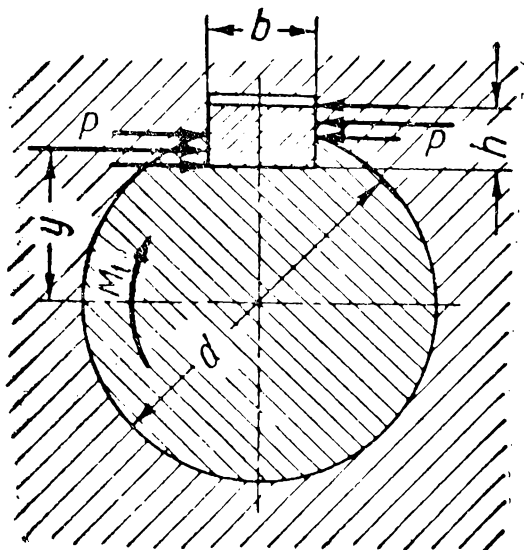


Fig. 95

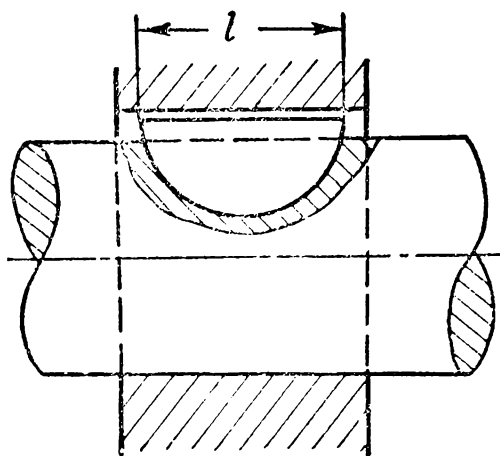


Fig. 96

compressive strength of the projecting part of the key can be written thus

$$M_t = 0.5 dcl [\sigma]_c \quad (121)$$

and the strength in shear

$$M_t = 0.5 dbl [\tau]_s. \quad (122)$$

When two keys must be fitted, then, with a view to reducing the stresses, they should be placed either at  $180^\circ$  or, if the hubs are long, one behind the other.

**Calculation of Strained Joints.** Fig. 97 shows a joint formed by means of a taper sunk key.

The broad top of the fitted key bears on the bottom of the hub keyway, and the key bottom on the bottom of the keyway of the shaft, which is pressed against the opposite part of the hub (Fig. 97, a). Because of the hub radial-thrust created in this manner it can be assumed that the shaft contacts the hub only within the arc *atc*.

The key is so fitted to the bearing surfaces of the keyways of hub and shaft as to ensure a uniform distribution of the spots of contact; this gives us ground to suppose that before external moment is applied the pressure on these surfaces is spread evenly (Fig. 97, b).

The magnitude of normal pressure created on the key bearing surfaces is closely related to the force *S* applied to the key gib-head (or end) during pressing in and is determined by the relation known

from the theory of mechanisms and machines

$$N = \frac{S}{\tan \varrho + \tan (\alpha + \varrho)} \quad (123)$$

where  $\alpha$  is the key taper angle and  $\varrho$ —the angle of friction. Since for conventional materials the coefficients of friction  $f_1$  and  $f_2$  for the friction surfaces key-shaft and key-socket differ but little we assume in this formula that  $\varrho_1 = \varrho_2 = \varrho$ .

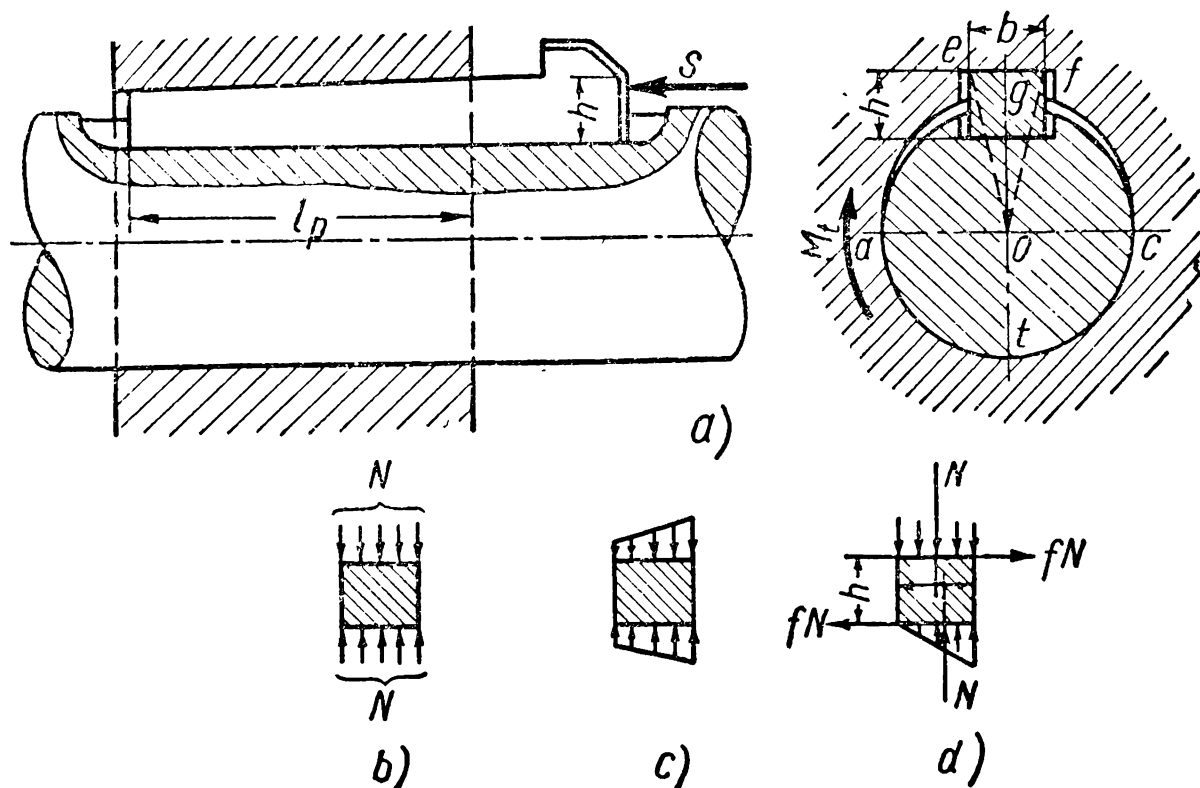


Fig. 97

In turn the magnitude of the force  $S$  is limited by the condition

$$S \leq bh [\sigma]_c'. \quad (124)$$

The allowable stress  $[\sigma]_c'$  can in this case be taken as sufficiently large; bearing in mind that the fitting effort is applied only once  $[\sigma]_c'$  is recommended to equal  $(0.8-0.9)\sigma_y$ .

When the torque  $M_t$ , having overcome the moment applied to the shaft, begins to act upon the hub, there occurs a redistribution of pressures on the bearing surfaces of the joint.

To elucidate the nature of this redistribution let us assume that the reactive torque applied to the shaft is so great that it cannot be overcome by the torque applied to the hub. If, in this case, the angular displacement of the hub relative to the shaft is  $\alpha$  the points  $e$  and  $f$  will shift by the same angle along the circumference of the radius  $oe=of$  (Fig. 97, a). Since the angle  $\alpha$  is small the new position of the line of contact can be assumed to be that given by the turn of the segment  $ef$  around the point  $g$  by the same angle  $\alpha$  as shown by the dash line. Hence, within the section  $eg$  on the key surface the pressures will tend to diminish from  $g$  towards  $e$  and within the section  $gf$  to grow from  $g$  towards  $f$ . Pressure distribution will change on the lower face of the key in the same manner.

Essentially the same picture of pressure redistribution will be observed with any transmitted torque.

Fig. 97, *c* shows a possible case of such redistribution with an assumed direction of rotation and neglecting the effect of the friction forces. But since the joint bearing surfaces develop the friction forces  $F=fN$  forming a couple whose moment equals  $M=fNh$  (Fig. 97, *d*), the pressure distribution becomes more uniform on the top surface of the key and less uniform on the bottom surface.

An actual picture of pressure distribution depends on many factors and, first of all, on the effort applied to fit the key, on the nature and magnitude of load, on the accuracy of fitting, on the stiffness of the joint parts, etc. This problem has so far no definite solution and the load diagram for the key shown in Fig. 97, *d* is therefore arbitrary.

To simplify our problem let us assume that the original law of pressure distribution remains unchanged on the top of the key while on the bottom pressure is distributed in conformity with the law of a triangle.

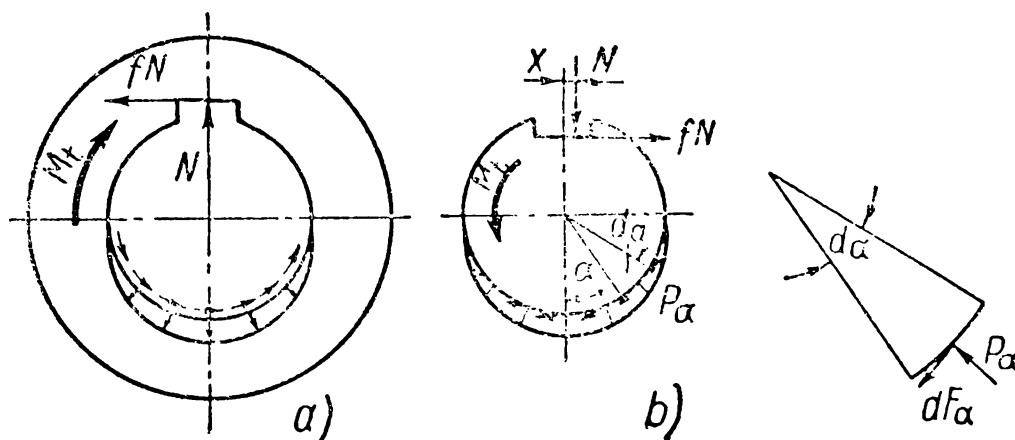


Fig. 98

It follows from the equilibrium condition of the key  $Nx=fNh$  that  $x=fh$ .

Fig. 98 gives a schematic picture of the load carried by hub (*a*) and shaft (*b*) when the torque  $M_t$  is transmitted from the hub. The main design relations can be obtained from the equilibrium condition of the hub or the shaft.

Let us assume that the external torque does not affect the law of pressure distribution within the arc *atc* equal to  $180^\circ$  (Fig. 97, *a*) which is taken to be cosinusoidal ( $p_\alpha=p \cos \alpha$ ). In this case, the pressure falling on the element of the shaft surface (assumed to be absolutely stiff) enclosed by the angle  $d\alpha$  comprises at the design length of the key  $l$

$$P_\alpha \times \frac{d}{2} \times d\alpha \times l.$$

The equilibrium condition of forces acting upon the shaft

$$N = 2 \int_0^{\frac{\pi}{2}} p_\alpha \frac{d}{2} l \times \cos \alpha \times d\alpha = 2 \int_0^{\frac{\pi}{2}} p \frac{d}{2} l \times \cos^2 \alpha \times d\alpha = \frac{\pi}{4} pld$$

and therefore

$$p = \frac{4}{\pi} \times \frac{N}{ld}. \quad (125)$$

Since the elementary friction force on the contact surface of the shaft and hub is  $dF_a = p_a \times \frac{d}{2} \times d\alpha \times l \times f$ , where  $f$  is the coefficient of friction and  $dM_{fr} = dF_a \frac{d}{2}$  — the elementary moment of this force, the moment of friction within the arc  $atc$  is equal to

$$M_{fr} = 2 \int_0^{\frac{\pi}{2}} p_a \frac{d^2}{4} \times l \times f \times d\alpha = \frac{4}{\pi} N f \frac{d}{2}. \quad (126)$$

Recalling that  $x = fh$  we obtain from the condition  $\Sigma M = 0$

$$M_t = M_{fr} + fN \left( \frac{d}{2} - \frac{h}{2} \right) + Nx = 1.14 Nfd + 0.5 fNh$$

or

$$M_t = fN(1.14d + 0.5h). \quad (127)$$

To "safeguard" the bottom side which resists the heaviest load against crushing the following condition should be satisfied:

$$N \leq \frac{bl[\sigma]_c}{2}.$$

After substituting this magnitude  $N$  in the equation (127) at the mean value of  $f = 0.15$  we get

$$M_t = f \frac{bl[\sigma]_c}{2} \left( 1.14d + \frac{h}{2} \right) \approx 0.04bl[\sigma]_c (2.28d + h). \quad (128)$$

The relation (128) gives us the interrelation between the transmitted torque and the main sizes of key joint. For the calculated diameter  $d$  of the shaft and the sizes  $b$  and  $h$  chosen from the standards, the formula (128) is used to find the design length of the key after having specified the value  $[\sigma]_c$ .

Joints with a taper key on-flat are designed in exactly the same manner since the same phenomena are dealt with.

A joint with a saddle key can be designed as shown in Fig. 99. From the condition  $\Sigma M = 0$  and on the basis of the relation (126)

$$M_t = M_{fr} + fN \frac{d}{2} = \frac{4}{\pi} N f \frac{d}{2} + N f \frac{d}{2} = 1.14 Nfd. \quad (129)$$

From the relation (123) and the condition (124) we obtain

$$M_t = 1.14 \frac{bh[\sigma]_c'}{\tan \varphi + \tan(\alpha + \varphi)} fd.$$

Since  $\tan \alpha = i = 1 : 100$  and the coefficient of friction can be taken on the average as  $f = 0.15$ , then

$$[\tan \varrho + \tan (\alpha + \varrho)] \approx 0.3.$$

Hence,

$$M_t \approx 0.55 b h d [\sigma]_c'. \tag{130}$$

The stresses on the key bearing surfaces should satisfy the condition

$$\sigma_c = \frac{N}{bl} \leq [\sigma]_c.$$

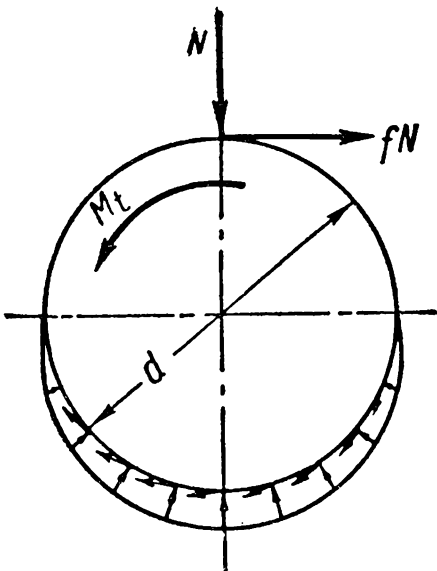


Fig. 99

**Key materials. Allowable stresses.** Keys are usually made from cold-drawn steel. The values of  $[\sigma]_c$  are usually differentiated according to the type of joint (fixed, sliding) and the nature of load. If the joint parts—shaft, hub, key—are made from different materials  $[\sigma]_c$  is chosen for the material with the lowest mechanical characteristics. Table 15 shows, as an example, the values of  $[\sigma]_c$  recommended for cranes.

The allowable shearing stress  $[\tau]_s$  is chosen for the key materials with the load classification shown in Table 15;  $[\tau]_s = 1,200\text{--}870\text{--}540 \text{ kg/cm}^2$ .

Table 15

Allowable Stresses  $[\sigma]_c$

Type of joint	Material	Nature of load		
		Steady	Intermittent	Impact
		in kg/cm <sup>2</sup>		
Fixed	Steel	1,500	1,000	500
	Cast iron	800	530	270
Sliding	Steel	500	400	300

*Example.* Find the values of torque which can be transmitted by various designs of key joints when:

$$d = 100 \text{ mm}; \quad l = 1.2d = 120 \text{ mm};$$

$$[\sigma]_c = 1,500 \text{ kg/cm}^2; \quad [\sigma]_c' = 2,500 \text{ kg/cm}^2.$$

*Solution.* When fitting a feather key we find for  $d = 100 \text{ mm}$  the standard section  $b \times h = 28 \times 16 \text{ mm}^2$ . From the formula (119)

$$M_t = 0.25 h l d [\sigma]_c = 0.25 \times 1.6 \times 12 \times 10 \times 1,500 = 72,000 \text{ kg/cm}.$$

When fitting a taper sunk key we find  $b \times h = 28 \times 16 \text{ mm}^2$  and from the formula (128)

$$M_t = 0.04bl [\sigma]_c \times (2.28d + h) = 0.04 \times 2.8 \times 12 \times 1,500 \times (2.28 \times 10 + 1.6) = 49,000 \text{ kg/cm.}$$

For a saddle key the section  $b \times h = 28 \times 8 \text{ mm}^2$ ; from the formula (130)  $M_t = 0.55 bhd [\sigma]_c' = 0.55 \times 2.8 \times 0.8 \times 10 \times 2,500 = 31,000 \text{ kg/cm.}$

### MULTIPLE SPLINES

These joints are divided into *sliding* multiple splines, when the part fitted onto a shaft is allowed to move axially (for example, toothed wheels of lathe and automobile transmissions, etc.) and *fixed* multiple splines, when the part is permanently secured to the shaft.

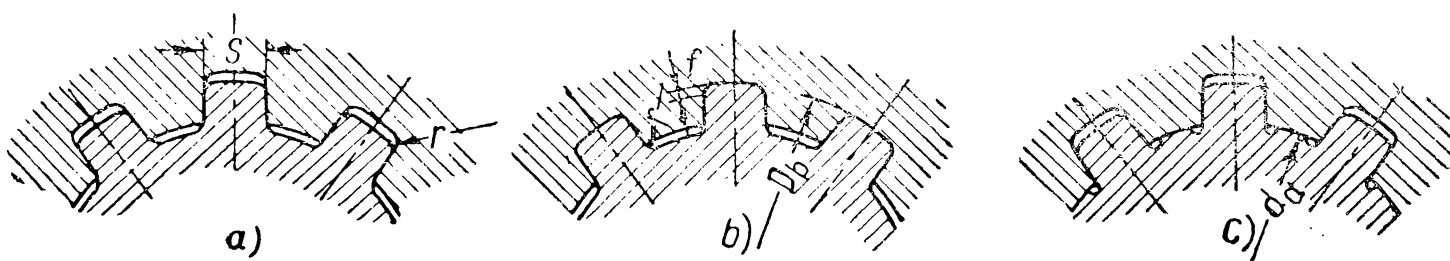


Fig. 100

In sliding joints the splined section of the shaft has a cylindrical form; in fixed joints the splines can also be cut on a tapered surface. Conical splines ensure a tighter fit of the hub on the shaft; this obviates the hazard of the joint loosening under varying load.

Multiple splines are chiefly employed in automobiles, tractors, etc. In our further exposition we shall deal only with cylindrical splines.

According to profile form splines are termed *straight-side* (Fig. 100) and *involute* (Fig. 101) splines and *serrations* (Fig. 102).

The main sizes of joints with straight-side splines are standardised.

Multiple splines are centered as follows: by the major diameter (Fig. 100, b), the minor diameter (Fig. 100, c) and by the spline faces (Fig. 100, a). The method of centering depends, first of all, on the required accuracy with which the hub is to be fitted onto the shaft and on the load condition. At considerable loads when the accuracy factor is of secondary importance, resort is had to side centering of the hub as this permits a better load distribution between the splines.

When accuracy is the prime consideration, centering is done by the major or minor diameter, the first method being applied when the surface of the socket hole is not heat-treated or when its hardness permits finishing to size by a broaching operation. Otherwise, centering is done by the minor diameter.

Involute splines are markedly (Fig. 101) superior to straight-side splines, since:

a) they possess greater endurance due to the gradual thickening of the spline and the absence of abrupt change at the root. This considerably decreases stress concentration and the load-carrying capacity of involute splines is thus higher than that of straight-side splines;

b) the elements of this type of joint are manufactured by improved production methods ensuring an accuracy almost as high as that of toothed wheels which prolongs the service life of the joint;

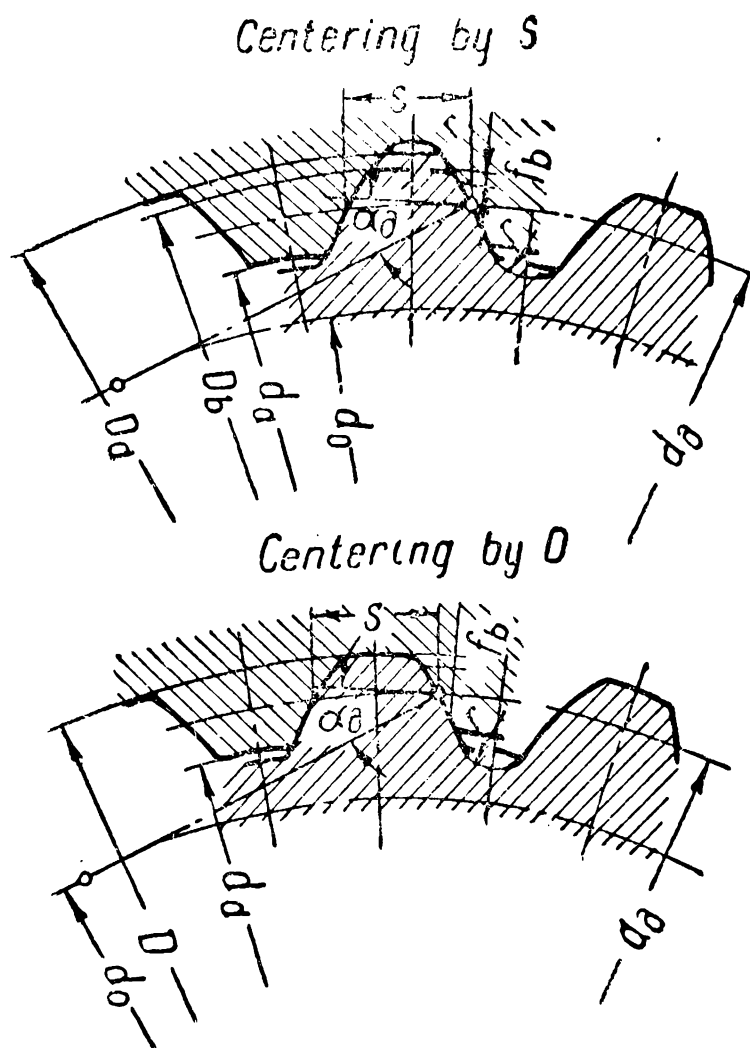


Fig. 101

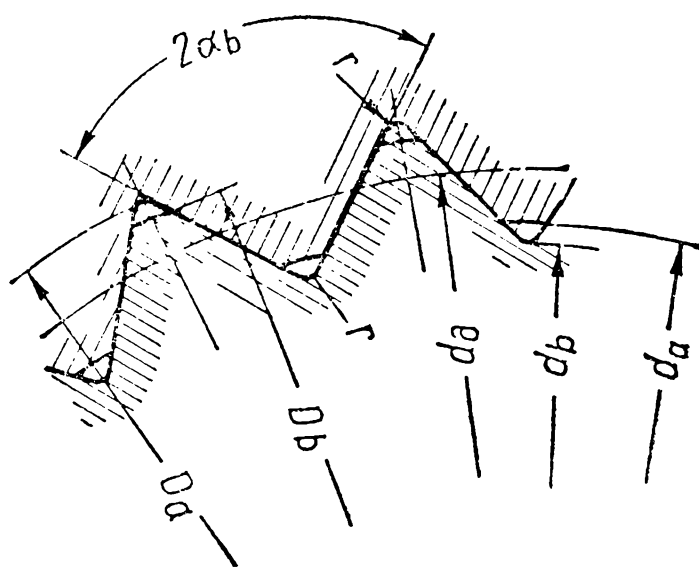


Fig. 102

c) a better centering of parts is obtained; a hub with involute splines self-aligns under load;

d) the cost of production can be cut down through the use of simpler cutting tools (hob cutters with rectilinear cutting edges), the employment of fewer types of cutter (a cutter of each module can be used to generate splined parts of different diameter and number of splines), etc.

The main sizes of involute splines are standardised in the Soviet Union as follows: the number of splines—from 11 to 50, the series of modules—1, 1.5, 2, 2.5, 3.5, 5, 7, 10 mm and the pressure angle of basic rack— $30^\circ$ . Centering is done by the spline faces or by the major diameter.

Serrations (Fig. 102) are frequently employed instead of press-fitted joints to transmit small torques.

**Design of Multiple Splines.** On examining the load conditions of splines it is seen that they correspond to the operating conditions



of a feather key. An analysis of the failures observed during machine operation confirms the extreme importance of calculating the bearing faces of splines for crushing.

Let us introduce the following denominations:

$z$ —number of splines;

$l$ —effective length of spline which is taken as equal to the length of the hub fitted onto the splines, in cm;

$\psi$ —a coefficient taking into account the nonuniform load distribution on the bearing surface of the splines, usually taken as  $\psi=0.75$ ;

$F$ —design bearing surface of the spline in  $\text{cm}^2$  found as a projection of the bearing surface of a spline on its mean diametral plane, i.e.,

$$F=l \left[ \frac{D_b-d_a}{2} - (f+r) \right] \text{ cm}^2 \text{ for straight-side splines (Fig. 100);}$$

$$F=0.8 \times m \times l = 0.8 \frac{d_\partial}{z} l \text{ cm}^2 \text{ for involute splines (Fig. 101);}$$

$$F=l \frac{D_b-d_a}{2} \text{ cm}^2 \text{ for serrations (Fig. 102);}$$

$R_m$  is the spline mean radius equal to:

$$R_m = \frac{D_b+d_a}{4} \text{ for straight-side splines,}$$

$$R_m = \frac{d_\partial}{2} \text{ for involute splines and serrations.}$$

To prevent the crushing of the splines the following condition should be satisfied:

$$\sigma_c = \frac{M_t}{R_m F z \psi} \leq [\sigma]_c \quad (131)$$

where  $M_t$  is the transmitted torque.

Since the above-mentioned standards give the main sizes of the joints as a factor of shaft diameter, the design of the joint can be usually reduced to determining either the spline design length  $l$  or the stress  $\sigma_c$  on the bearing surfaces; the latter is then compared with the recommended values of  $[\sigma]_c$ .

The values  $[\sigma]_c$  found experimentally are specified in the respective reference books. They are differentiated depending on their purpose, operating conditions and heat treatment of the spline bearing surfaces. Thus, for example, for fixed joints and under favourable operating conditions  $[\sigma]_c=800-1,200 \text{ kg/cm}^2$ , without heat treatment, and  $[\sigma]_c=1,200-2,000 \text{ kg/cm}^2$  if special heat treatment is carried out.

For sliding joints, with the view of protecting the splines from excessive wear and sometimes from seizure, the values  $[\sigma]_c$  are drastically reduced: for loaded joints and under favourable operating conditions  $[\sigma]_c=100-200 \text{ kg/cm}^2$  and under arduous conditions  $[\sigma]_c=30-100 \text{ kg/cm}^2$  for splines with heat-treated bearing surfaces.

## KEYLESS JOINTS

A keyless joint of a hub and shaft can be formed as a) a joint with permanent interference (p. 115), b) a shaped joint, c) a joint held by friction clamping collars, etc.

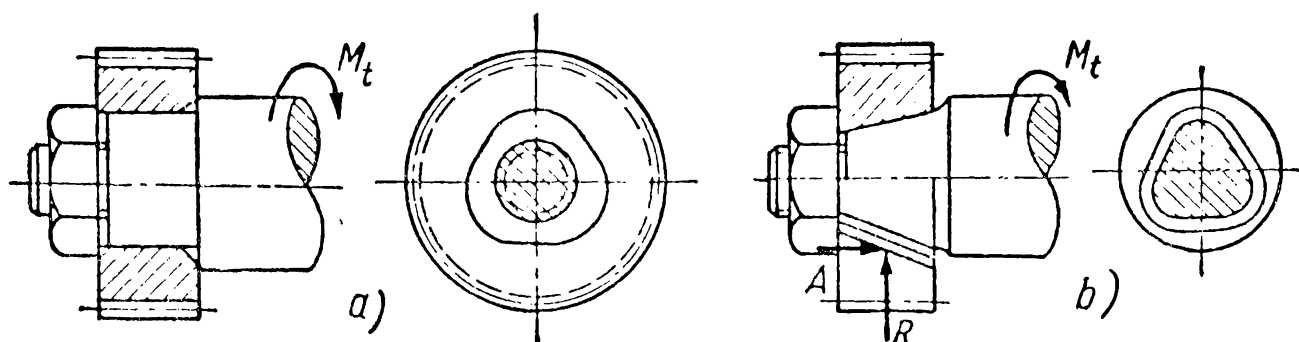


Fig. 103

In shaped joints (Fig. 103) the mating parts touch over a smooth noncircular cylindrical (a) or conical (b) surface. In addition to torque, these conical joints can also transmit an axial load. They are

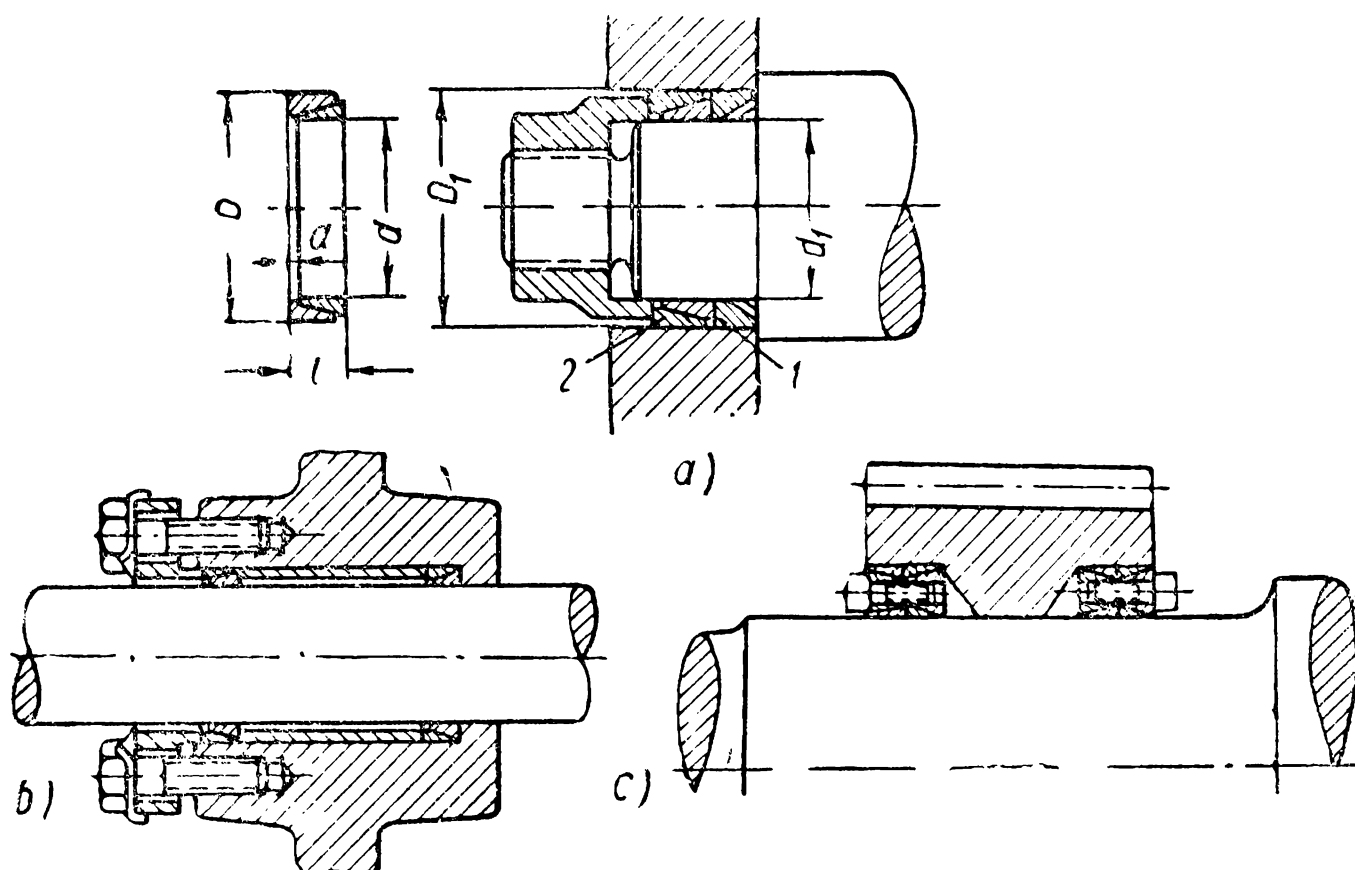


Fig. 104

remarkable for their high degree of reliability. However, because of certain machining difficulties they are used on a limited scale. The problems of geometry, calculation for strength and manufacture of shaped joints are dealt with in specialised literature.

A recent development is the use of joints fastened by means of friction clamping (unsplit) collars (Fig. 104). When the collars are

clamped axially (Fig. 104, *a*) inner collar 1 contracts while the diameter of outer collar 2 increases. The high radial pressure created by the elastic collars causes considerable friction forces to arise on the contact surfaces: shaft-inner collar and hub-outer collar—which transmit the torque.

Collars are made from special steel in automatic lathes or are blanked from steel plates and then heat-treated.

Fig. 104, *b*, *c* shows examples of fastening the hub to the shaft by means of friction clamping collars.

# PART THREE

## POWER TRANSMISSION

---

### CHAPTER XII

#### POWER TRANSMISSION SYSTEMS AND THEIR PRINCIPAL FEATURES

*A mechanical drive is a mechanism intended to transmit power from the prime mover to the machine, usually involving a change in velocities, forces and torques and sometimes in the character and law of motion.*

The presence of a transmission linking the prime mover and the machine is due to a number of reasons:

a) the required velocities of the machine operating members very often fail to coincide with the optimal velocities of prime movers (they are usually much lower) or are altogether different from the velocities of standard motors;

b) the machine velocity has to be frequently changed (regulated) whereas the prime mover cannot be used to the full advantage for this purpose;

c) certain periods of the machine operation may require torques far in excess of those obtaining on the motor shaft;

d) sometimes one motor has to be used to actuate several mechanisms with different velocities;

e) as a rule, standard motors are designed for uniform rotary motion whereas the machine operating members have sometimes to move rectilinearly with varying velocity or periodic halts;

f) sometimes considerations of safety, convenience of maintenance or the dimensions of the machine do not allow its direct coupling with the prime mover shaft.

Until recently mechanical drives were practically the only devices used in machines for the above purposes. A prominent feature in present-day mechanical engineering is the extensive employment for the same tasks, together with mechanical drives, of electric, hydraulic and pneumatic (or vacuum) transmissions. Frequently both mechanical drives and these transmissions are simultaneously used to actuate various mechanisms.

The comparative advantages offered by these transmissions and drives are outlined in Table 16 which gives only a general picture.

The *proper choice* of a drive for each concrete case can be made only through comparing the technical and economical features of several designs.

Table 16

Advantages of Transmissions and Drives

Properties and advantages	Transmissions			Mechanical drives	
	electric	hydraulic	pneumat- ic	By fric- tion	By mesh
	1	2	3	4	5
Centralised power supply	+		+		
Simplicity of power trans- mission over large dis- tances . . . . .	+				
Easy accumulation of power . . . . .			+		
Step-by-step velocity change over a wide range . . .	+			+	+
Stepless change over a wide range . . . . .	+	+		+	
Maintaining accurate veloc- ity ratio . . . . .					+
High velocities of rotation	+		+		
Simplicity of the machine designed for rectilinear motion . . . . .		+	+	+	+
No effect of ambient tem- perature . . . . .	+		+		+
Comparatively high prac- tically obtainable pres- sures acting upon the machine . . . . .		+			+
Easy control, both auto- matic and remote . . .	+				

The general course of «Machine Elements» examines mechanical drives designed for uniform rotary motion. Mechanical drives of other types as well as pneumatic, electric and hydraulic transmissions are the subjects of special courses for designing those machines in which they are widely used.

TYPES OF DRIVES

By the mode they transmit motion from the prime mover mechanical drives fall into the following types:

- 1. *Transmission by friction*: with direct contact (*friction drives*) or a flexible connection (*belt drives*);

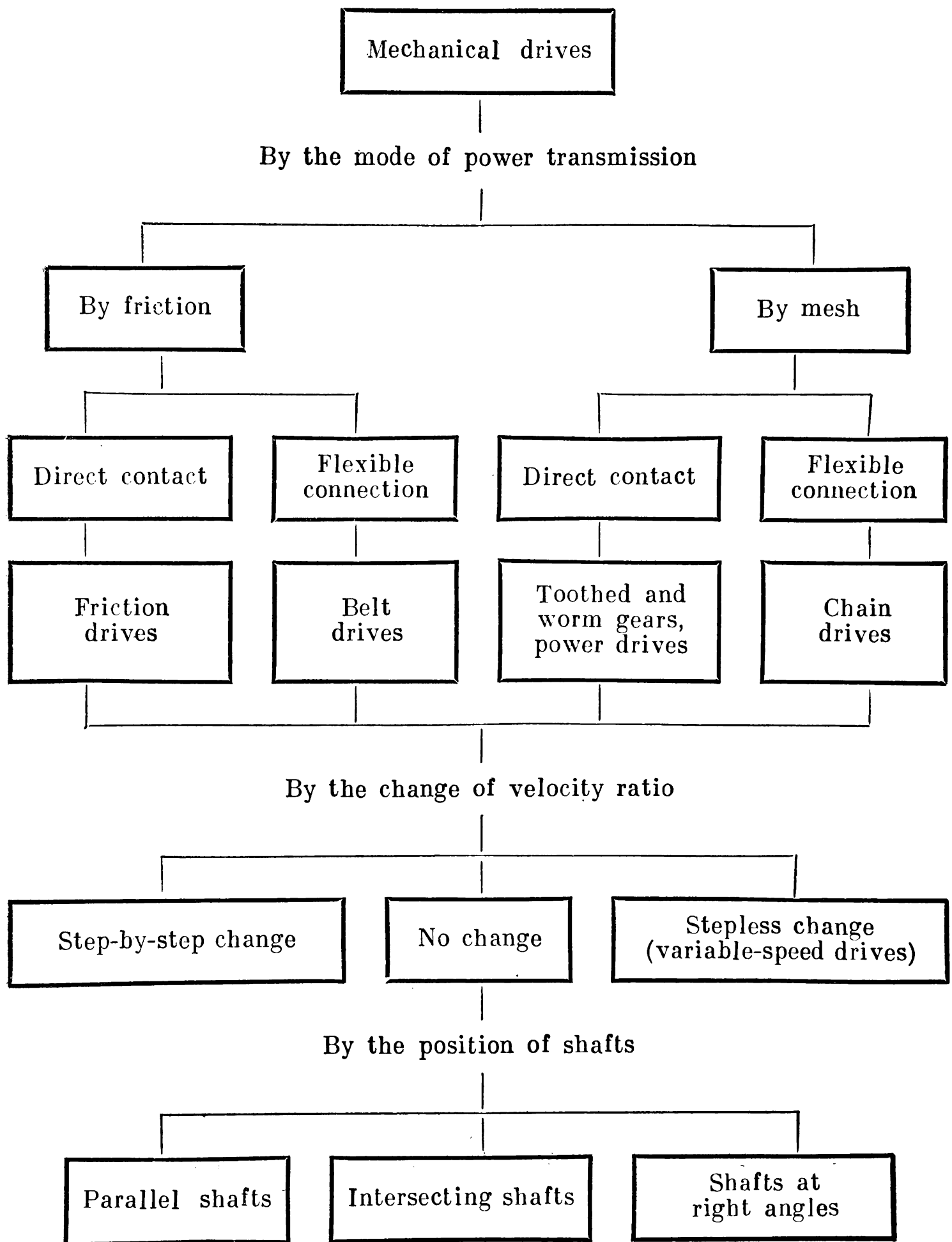


Fig. 105

2. *transmission by mesh*: with direct contact (*toothed and worm gears*) or with a flexible connection (*chain drives*)\*.

Transmissions by friction and mesh are differentiated by the mutual location of shafts and the constancy of the velocity ratio. The general classification of mechanical drives is tabulated in Fig. 105.

Whether power is transmitted by friction or mesh predetermines the form of the bearing surfaces and, simultaneously, the characteristic properties of the drive.

In friction transmissions the cross-sections of the bearing surfaces normal to the axis of rotation are circles. The manufacture of such surfaces, even when great accuracy is required, is rather easy. In transmissions by mesh the parts provided with teeth transmit torque from the driving to the driven wheel. As the drive operates some teeth disengage and others are meshed together. Even slight inaccuracies in tooth profile and deformations of the elements cause accelerations manifested in *noise* and *rapid tooth wear*. This is the principal disadvantage of toothed gearing. Though the higher accuracy of gear wheels and teeth of special form can reduce this shortcoming, it cannot be entirely eliminated. Therefore, for example, in lathes intended for fine finishing of working surfaces the spindle as a rule is brought into motion not by gears but by belting.

In friction drives the transition from the periphery of contact of one diameter to the periphery of the other can be made as smooth as is desired. The change in velocity ratio can likewise be effected gradually.

In toothed gearing this can be done only through the employment of complex artificial devices\*\*.

### DRIVES WITH A CONSTANT VELOCITY RATIO

The design of a drive with a constant velocity ratio should, as a rule, include at least the following data: transmitted horse power ( $N$ ) or torque ( $M_t$ ) on the driven shaft; velocity of rotation (rpm) of the driven ( $n_2$ ) and the driving shaft ( $n_1$ ); mutual location of the shafts and the distance between them; overall dimensions; the drive operating conditions  $M_t=f(t)$  and  $n=F(t)$ .

In general this design has several solutions, i. e., the given conditions can be used to develop drives of various types. All possible designs should be compared as to efficiency, weight, size, original and operational cost with a view to selecting the most advantageous

---

\* An interesting modification of a chain drive is the recently developed power-grip belt drive: a plastic belt is provided with evenly pitched teeth on its inner side which mesh with the corresponding grooves on the pulleys.

\*\* In practice, only the chain drive has a stepless velocity change (see p. 365).

design. Some general considerations, mainly the available experience of designing, manufacture and operation of various drives, enable us to outline generally the limits of *priority* application of these drives. However, these limits are of a *temporary* nature; as new materials are produced, manufacturing methods are improved and our knowledge of the processes taking place in transmissions becomes deeper and designs are being perfected to suit broader fields of application.

**Velocity Ratio.** The assigned velocity ratio  $i = n_1 : n_2$  can be obtained through one stage of a drive of any type ( $i = i_1$ ) or several stages of drives of the same or different types ( $i = i_1, i_2, \dots, i_p$ ).

High velocity ratios in one stage are possible in toothed wheel gearing. Worm gears are distinguished by the highest values of  $i_1$  (usually  $i_1 \leq 40$ ); then follow toothed gears ( $i_1$  from 4 to 20) and chain drives (roller chain drives  $i_1 \leq$  from 6 to 10; silent chain drives up to 15). In toothed wheel gearing the obtainable values of  $i_1$  are generally speaking limited only by the size of the drive.

In belt drives the admissible  $i_1$  are confined to the minimum allowable arc of contact on the smaller pulley (see p. 237). Here, the greatest values of the velocity ratio are to be had from a V belt drive ( $i_1 \leq$  from 8 to 15), then from a flat-belt drive with an idler pulley ( $i_1 \leq 10$ ) and finally from an open flat-belt drive ( $i_1 \leq 5$ ). Friction drives usually have  $i_1 \leq$  from 5 to 10. In practice the lesser (first) values of  $i_1$  indicated above are the most usual. When greater velocity ratios are to be obtained it is more advantageous to employ several stages; this considerably reduces the size and weight of the drive as compared to a one-stage drive.

The above referred to *underdrives* ( $n_1 > n_2$ ). An *overdrive* ( $n_1 < n_2$ ) usually works less efficiently than an underdrive. This is especially true of toothed wheel gearing: here the maximum is  $i_1 = 1 : 1.5$  to  $1 : 2$ . For friction and belt overdrives designers are usually content with  $i_1 \approx 1 : 3$  to  $1 : 5$ . The poor performance of overdrives—vibration and noise—is due to the fact that, with a similar error in the manufacture of the two meshing wheels, the driving wheel of greater diameter (in an overdrive) causes larger angular accelerations on the smaller driven wheel while the reverse is true in an underdrive.

**Peripheral Velocity.** At a given transmitted horse power  $N$  the peripheral effort  $P = N : v$  where  $v$  is the peripheral velocity. In turn, the peripheral effort can be expressed as a product of the width  $b$  of the element transmitting power (width of belt, roller, wheel, etc.) and the unit load  $p$  per unit of width:  $P = p \times b$ . All other conditions being equal, to reduce the size of the drive ( $b$ ) it is advantageous to transmit power at the maximum allowable velocity  $v = v_{\max}$ . The value of  $v_{\max}$  is limited by various factors.



For all belt and chain drives the centrifugal forces adding load to the belt and lessening its useful tension are an important factor. For *drives with usual flat belts*  $v_{\max} \leq 25$  m/sec; for special belts made from artificial fibre  $v_{\max} \approx 50$  m/sec. In *V belt drives* heating due to elastic hysteresis is another vital factor. Its effect at a high number of belt inflections per second sharply grows in intensity. Standard V belts allow  $v_{\max} \approx 25$  and 30 m/sec; special quality V belts with a steel wire core—40 m/sec. In a *steel-band drives* velocities up to 80 m/sec can be attained.

Because meshing links are subject to knocking the velocity of *chain drives* should not exceed  $v_{\max} = 25\text{--}30$  m/sec.

In *toothed gears* an increase in velocity requires considerably higher accuracy in the manufacture of the gear wheels for, otherwise, added loads caused by faults in the teeth will reach inadmissible magnitudes. Spur gears at  $v > 10$  m/sec and bevel gears at  $v > 15$  m/sec should be of high precision (6th degree of accuracy). At the present-day level of gear manufacture the greatest velocities employed are 120–150 m/sec.

In *worm gears* the peripheral velocity on the worm  $v_{\max} \leq 20$  m/sec. It is limited here by the wear resistance of the materials from which the worm-wheel couple is made.

The velocity of *friction drives* usually does not exceed 20–25 m/sec.

**Transmitted Horse Power.** *Toothed gears* can transmit the greatest power. Gear reducers for marine turbines are known to reach 50,000 h. p. and more. In fact the horse power transmitted by toothed gears is restricted only by the difficulty of transporting precision parts of large size.

In worm gears the horse power is limited by the great amount of heat given off and the consequent increase in temperature. The horse power transmitted by existing *worm gears* never exceeds  $\sim 750$  h. p. However, it could probably be increased several times by altering the form of the teeth (in particular, through the use of hourglass worms) and thus reducing the amount of heat given off, and by improving dissipation of heat.

In *chain* and *V belt drives* greater horse power is transmitted by increasing their cross-section and the number of parallel chains or belts. However, when many driving elements are used the probability of uniform load distribution between them diminishes and further increase in the number of belts or chains becomes ineffective. Thus, for example, a V belt of the maximum standard size (type E) at  $v = 25$  m/sec and under most favourable operating conditions can transmit 45 h. p. Twenty-two belts would therefore be needed to provide 1,000 h. p. if load is spread uniformly between all belts. For *V belts* 1,000–1,500 h. p. is the maximum. *Drives with flat leather belts* can handle 2,500 h. p. and *chain drives*—5,000 h. p.

The working capacity of friction drives and toothed gears is restricted mainly by contact pressure. But while in a toothed gear the normal pressure approximates the peripheral effort, in a friction drive it exceeds the latter almost tenfold (it equals the peripheral effort divided by the coefficient of friction). It is true that in friction wheels the radius of curvature of contact surfaces with the same design diameters is several times larger than in gear wheels but even this fails to compensate for the difference in normal pressures.

The effective width of the friction wheels is likewise limited since due to inaccuracies and deformations only a small part of the nominal contact surface actually participates in transmitting the peripheral effort.

It is now clear why the maximum power of *friction drives* never exceeds 200-300 h. p.

**Loss of Horse Power and Efficiency.** These indices occupy a special place among transmission characteristics. Firstly, they show unproductive power expenditure; since drives are employed on a wide scale this is of itself very important. Secondly, they indicate the amount of heat given off in transmission and indirectly characterise the wear of the drive, because the power lost in transmission is transformed into heat and goes in part to destroy the active surfaces. A detailed study of power and efficiency losses belongs to the theory of mechanisms. Here we concentrate on the power loss only insofar as it is necessary to design a drive, substantiate the choice of material and stimulate the development of new, more rational designs.

Losses in any drive can be represented in the following general form:

$$L = L_0^m + L_v^n \quad (132)$$

where  $L$  is the loss of horse power (in kw or h. p.);

$L_0^m$  is the constant part of losses which on the whole does not depend on load;

$L_v^n$  is the variable part of losses which is on the whole proportional to load;

$m$  and  $n$  are exponents in a functional relation to useful horse power:

$$m = f_1(N) \text{ and } n = f_2(N).$$

At  $m=1$  and  $n=1$  (conditions to simplify calculations which frequently satisfy the requirements of design accuracy)

$$L = L_0 + L_v. \quad (133)$$

The loss  $L_0$  approximates the horse power of idle run, i. e., the horse power needed to rotate the drive at  $N=0$ . It depends on the

weight of the drive parts, the velocity of rotation and the friction in the bearings and teeth. The loss  $L_v$  approximates  $k_L \times N = (1/\eta - 1)N$  where  $\eta$  is the efficiency accounting only for a part of losses in transmission ( $L_v$ ) proportional to the load  $N$ . Thus, the total efficiency of the drive considering all losses is equal to

$$\eta_{total} = \frac{N}{L + N} = \frac{N}{L_0 + \frac{1-\eta}{\eta} N + N} = \frac{N}{L_0 + \frac{N}{\eta}} = \frac{1}{\frac{L_0}{N} + \frac{1}{\eta}}. \quad (134)$$

It follows from the above expression that the total efficiency of the drive is related to load ( $N$ ): as load decreases efficiency markedly deteriorates; only when  $L_0/N \ll 1/\eta$  can it be assumed that  $\eta_{total} \approx \eta$ . But investigations show that in high-speed drives the loss  $L_0$  is not only commensurable with  $N$  but even exceeds it in many cases. In particular this is the case with certain types of drive in high-speed lathes. In our further exposition we shall consider only the factor  $\eta$ , i.e., that part of the total efficiency ( $\eta_{total} < \eta$ ) which takes account of the losses proportional to the useful load.

Let us take some efficiency values characterising one-stage drives. Since the magnitudes  $\eta$  are close to unity it is not the efficiency ( $\eta$ ) but the *loss factors*  $k_L = 1/\eta - 1 \approx 1 - \eta$  expressed as percentages which are more convenient for comparison.

The losses in toothed gears are minimal—1% (correspondingly  $\eta=0.99$ ), in a chain drive—2%, in a flat-belt drive—2.5%, in a friction drive—4%, in a V belt drive—4% and in a worm gear—10-25%. Hence, although the efficiency of a worm gear is comparatively high ( $\eta=0.9$ ) its losses are ten times (!) greater than in a toothed gear.

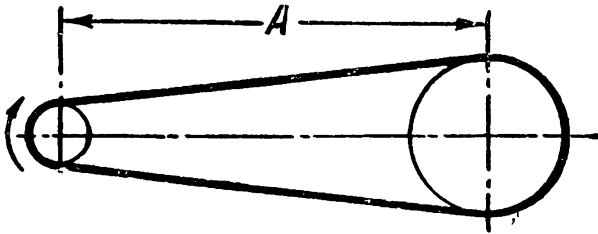
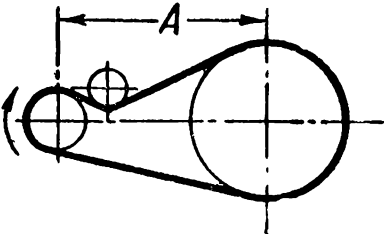
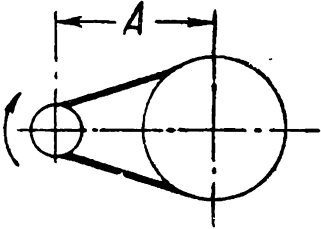
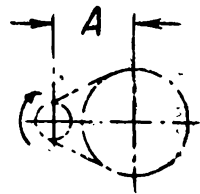

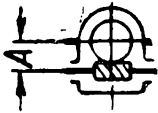
It should be pointed out that the cited values are only of a comparative nature. The actual efficiency and power loss values are due to structural parameters of the drive as will be shown in detail in respective sections.

**Weight, Size and Cost of Drives.** Let us illustrate this point by a concrete example: we take a 100 h. p. drive with a velocity ratio in one stage  $i_1 = n_1 : n_2 = 1,000 : 250 = 4$ . The sketches of drives conforming with these figures and the main indices are given in Table 17.

An idea of the size of drives is given by the centre distances  $A$ , the width of pulleys or wheels and also by a direct comparison of the diagrams drawn in the Table to one scale.

The cost of drives is given as a percentage of the cost of a V belt drive. The weight of the drives includes the weight of their shafts and bearings. The peripheral velocities are assumed: for belt drives—23.6 m/sec, for chain drives—7 m/sec, for toothed and worm gears—5.85 m/sec.

Table 17

Drives (all sketches are drawn to one scale)		Centre distance, in mm	Width of gear wheel of respec- tive pulley, in mm	Approximate weight, in kg	Cost in %
Flat belt		5,000	350	500	106
Flat belt and idler pulley		2,300	250	550	125
V-belt		1,800	130	500	100
Chain		830	360	500	140
Toothed		280	160	600	165
Worm		280	60	450	125

It can be seen from Table 17 that the toothed and worm gears have a more compact layout and can be easily fitted into machines. If we take into account the approximate nature of the cited figures, the difference in weight is by no means great. The weight of all types of drives conforming to our condition lies within 450-600 kg. The lesser value refers to a worm gear and the larger—to a toothed gear.

### DRIVES WITH A VARIABLE VELOCITY RATIO

As a rule, operating machines need drives with variable velocity ratios which can be adjusted manually or automatically. For instance, in automotive vehicles the velocity ratio is changed between the driving wheels and the engine in order to obtain adequate speed and torque to suit road and traffic conditions; in lathes the spindle speed is changed to maintain the most advantageous cutting speed when turning items of various size made from various materials with different tools.

Similar requirements for adjustment are met with in many other machines.

*Drives with step-by-step ratio change.* In designing drives with *changeable velocity ratio*\* we proceed from the given series of velocities at which the driven shaft rotates  $n_{\min}=n_1, n_2, \dots, n_{j-1}, n_j, \dots, n_{\max}=n_z$ , revolutions per minute of the driving shaft  $n_0$  (usually constant) and the torque on the driven shaft  $M_t=f(n)$ .

In the absence of any special considerations the series of velocities (rpm) should as a rule amount to a *geometrical progression*\*\*.

The relation  $n_{\max} : n_{\min} = R$  is called the *velocity control range*; the ratio of two neighbouring numbers of revolutions  $n_j : n_{j-1} = \varphi$ —*velocity control factor* or the *common ratio of the series*.

If the given velocity series amounts to a geometrical progression as is frequently the case the following relations hold:

$$R = \frac{n_{\max}}{n_{\min}} = \frac{n_z}{n_1} = \varphi^{z-1}; \quad \varphi = \sqrt[z-1]{\frac{n_z}{n_1}} = \sqrt[z-1]{R}; \quad z = 1 + \frac{\log R}{\log \varphi} \quad (135)$$

where  $z$  is the total number of stages.

The values of the velocity control factor (common ratio of the series)  $\varphi$  are standardised in the Soviet machine-tool industry; most frequently values of  $\varphi$  equalling 1.26, 1.41 and 1.58 are used.

---

\* In automotive vehicles these are called gearboxes, in lathes—speed gearboxes and feed gearboxes depending on where they are installed—in the main drive or the feed drive.

\*\* For metal-cutting lathes this was proved in 1876 by Academician A. V. Gadolin (1828-1892).

With two shafts in toothed wheel gearing the simplest method of obtaining the given series of velocities of the driven shaft at a constant velocity of the driving shaft is to change the velocity ratios *by changing gear wheels* (gearbox with replaceable wheels). For a faster and easier change from one speed to another the usual practice is to place in advance on the geared shafts a definite number ( $z$ ) of different pairs of gear wheels corresponding to the number of stages required and connect the proper wheel with the driven shaft with a clutch or key. The possible velocity control range is limited in this case usually by the maximum velocity ratio. Thus, for example, at  $n_0 : n_{\min} = 4$  and  $n_0 : n_{\max} = 1 : 1.5$  the velocity control range equals  $R = n_{\max} : n_{\min} = 4 \times 1.5 = 6$ . A larger velocity control range and, hence, larger number of speeds, can be obtained in a multi-shaft gearbox. Thus, in modern lathes the velocity control range of the spindle speed reaches  $R = 100$  and more and the number of speeds  $z \approx 24$ .

Step-by-step control in belt drives is easily obtained with the help of so-called cone pulleys with several steps and a belt shifted from one step to another.

In a flat-belt drive the velocity control range reaches 2-6, the number of stages—2-4; for V belts (or ropes) it is respectively 8 and 7.

The problems pertaining to the design of transmissions with step-by-step change are outlined in detail in textbooks on designing metal-cutting machine-tools where such drives are most frequent.

*Variable-speed drives.* The step-by-step change drives examined above permit only a partial establishment of optimal operating conditions in machines. If instead of the required optimal velocity  $n_x$  the nearest smaller number of revolutions  $n_{j-1}$  is established, and  $n_{j-1} < n_x < n_j$ , then the resulting relative loss of speed (sometimes of capacity) of the machine is equal to  $\Delta v = \frac{n_x - n_{j-1}}{n_x}$ . Since all values of  $n_x$  within the interval  $n_{j-1} - n_j$  are equally probable then to characterise the losses within the interval  $n_{j-1} - n_j$  we can take their mean value proceeding from  $n_x = \frac{n_{j-1} + n_j}{2}$ .

Then

$$\Delta v_m = \frac{n_j - n_{j-1}}{n_j + n_{j-1}} = \frac{\varphi - 1}{\varphi + 1} \quad (136)$$

In this way, for example, step-by-step change at  $\varphi = 1.58$  is dependent on the relative loss of speed

$$\Delta v_m = \frac{\varphi - 1}{\varphi + 1} 100 = \frac{1.58 - 1}{1.58 + 1} 100 \approx 22\%.$$

The actual loss in machine *capacity* is in general less than  $\Delta v$  since the very value of the optimal velocity, i. e., the optimal number of revolutions per minute  $n_x$ , is known only approximately; besides, sometimes instead of the nearest smaller velocity  $n_{j-1} < n_x$  we can also choose the larger  $n_j > n_x$ . Nevertheless, a certain loss in the capacity at step-by-step change is inevitable and can be completely avoided only in variable-speed drives. In addition to ensuring higher capacity as was mentioned above, variable-speed drives cost less and their control mechanisms are much simpler in design.

It has been noted above that stepless speed change is simplest in friction and belt drives. Diagrams of the most widespread types called *variable-speed drives, friction and belt*, respectively, are shown in Fig. 106. The elements of such transmissions will be examined together with belt and friction drives and we shall therefore confine ourselves here to a few general remarks.

The velocity control range of simple variable-speed drives without an intermediate link is usually 3-4. With an intermediary link the velocity control range is usually arranged symmetrically towards acceleration and slowing down and equals the square of the velocity control range of a simple variable-speed drive of the same type. The maximum values of  $R_V$  never exceed 8-12.

By combining a variable-speed drive with a velocity control range  $R_V$  and a gearbox with a step-by-step change with  $\phi = R_V$  we can obtain stepless change within any required range  $R = n_{\max} : n_{\min}$ . The number of stages in the gearbox needed for this is  $q \geq \frac{\log R}{\log R_V}$ .

## CHAPTER XIII

### FRICTION DRIVES

The simplest drives of this type are composed of two wheels (rollers)—driving and driven—which press against each other with such force as to make the frictional resistance between them equal to the transmitted peripheral effort.

The required pressure can be *permanent* or *variable*, changing automatically as a factor of the transmitted torque. In the first instance it can be produced by the weight of the machine itself and levers, manually or against the action of springs; in the latter instance it is created by special devices.

The *advantage* of friction drives is that they are very simple in design and operate noiselessly; among the *disadvantages* are considerable pressure brought to bear upon the shafts and bearings and also variability of the velocity ratio which persists even when the

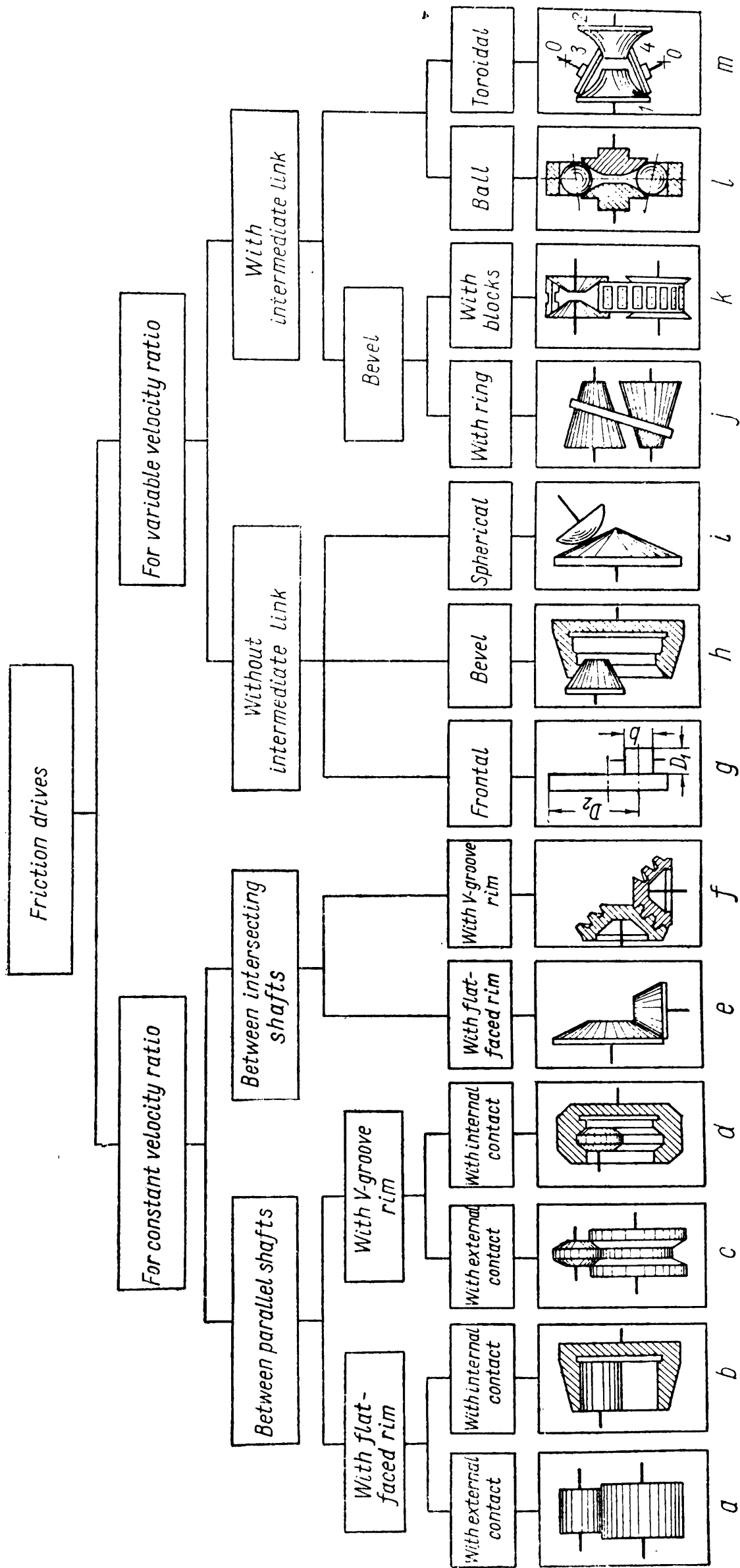


Fig. 106



drive elements have been carefully machined and set up. Friction drives are therefore employed only when an accurate velocity ratio is not essential.

The principal classification of friction drives is given in Fig. 106.

Accurately made friction drives can operate at velocities reaching 25 m/sec and velocity ratios  $i$  up to 10. The horse power they transmit varies from negligible values (in instruments, for example) to 300 h.p. in power transmissions.

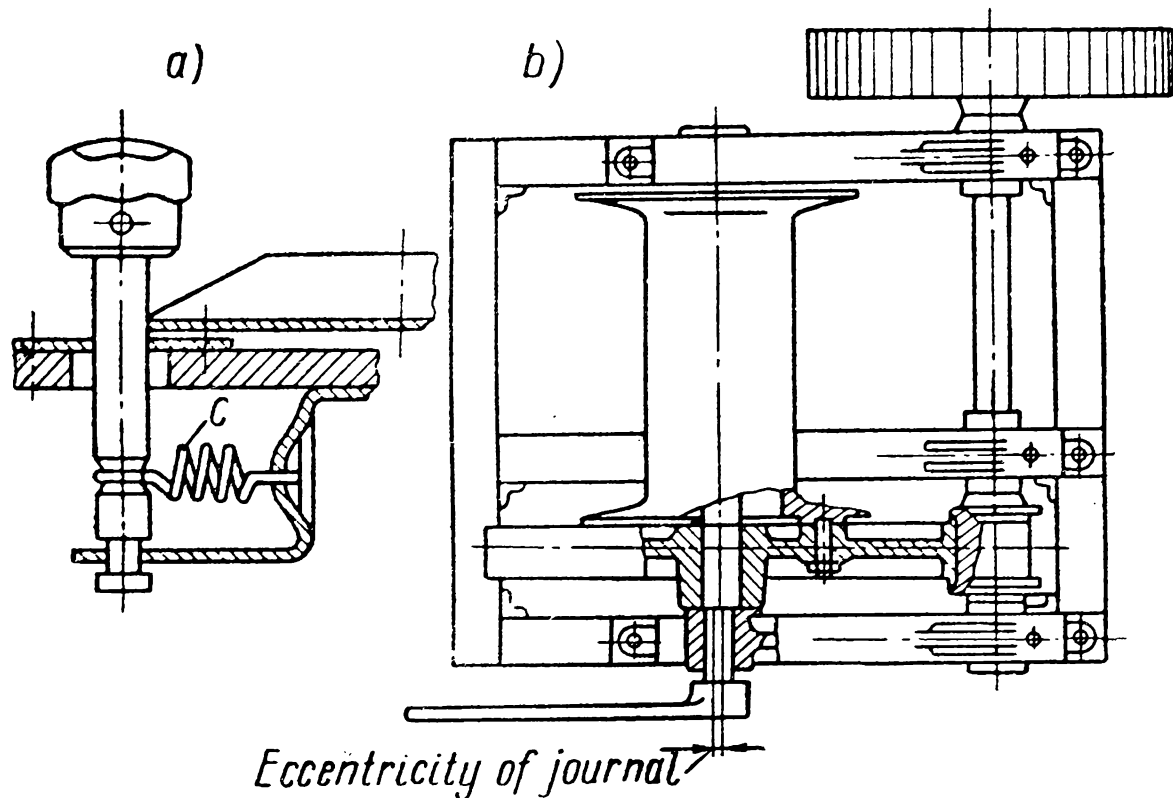


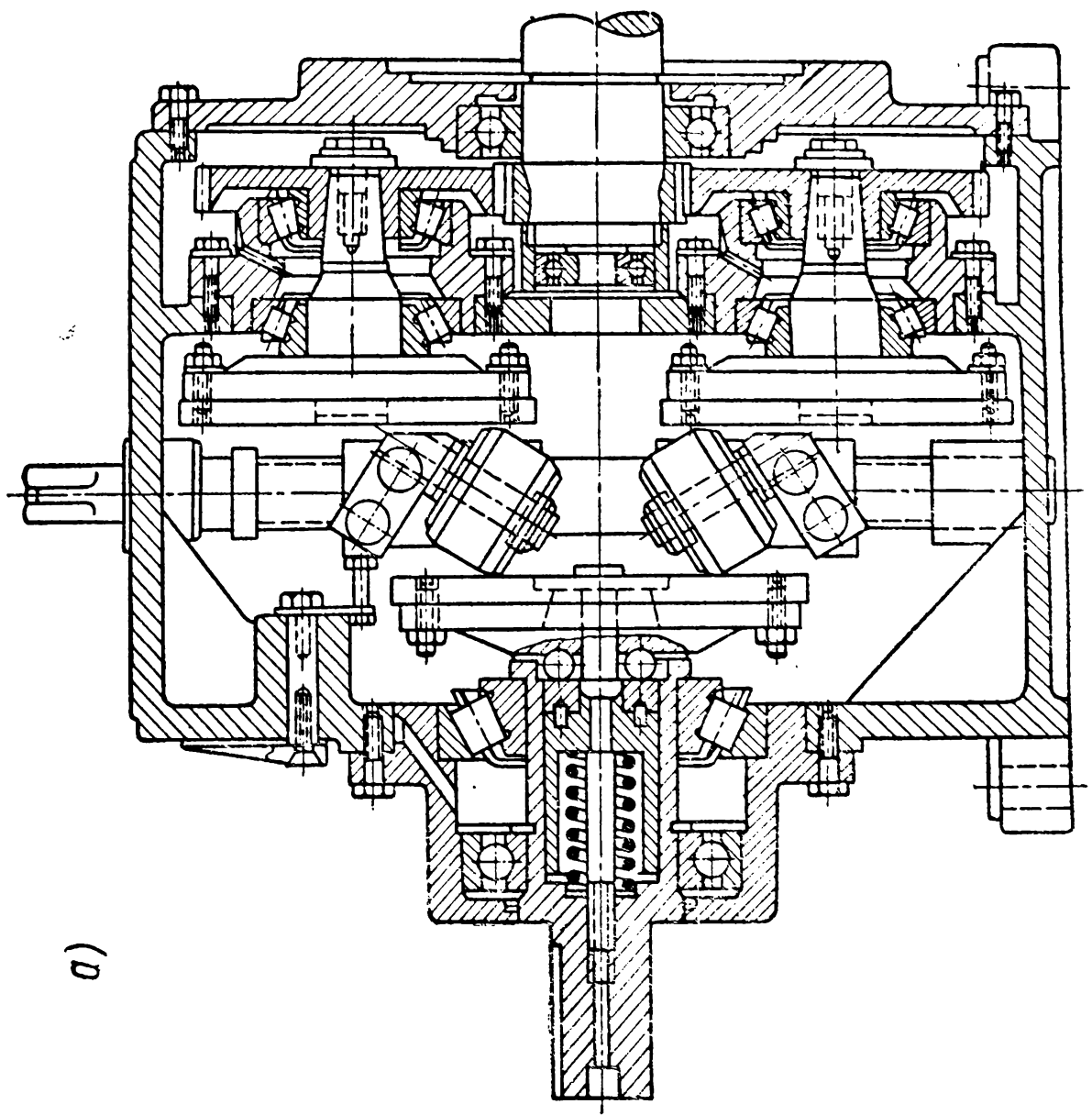
Fig. 107

By way of illustration Fig. 107, *a* shows a friction drive with pressure provided by a spring and Fig. 107, *b*—a winch whose friction wheels are brought into contact by turning a lever on the drum axle which is fitted with eccentric journals.

A frontal friction drive with bevel rollers is shown in Fig. 108, *a*.

Fig. 108, *b* shows the assembly drawing of a toroidal variable-speed drive designed by the Central Research Institute of Heavy Machine-Building. In this drive the friction wheels are made in the form of cups 1 and 2 and rollers 3 and 4 running over them (Fig. 106, *m*). The latter can turn on the axes  $O$  to change the velocity ratio. The friction members are pressed against each other with a force changed automatically by means of wedge mechanisms comprising balls and collars with inclined grooves (see p. 193). Transmissions of this type can handle up to 12 h. p.

Depending on the material of the wheels friction drives can operate dry or in oil.



b)

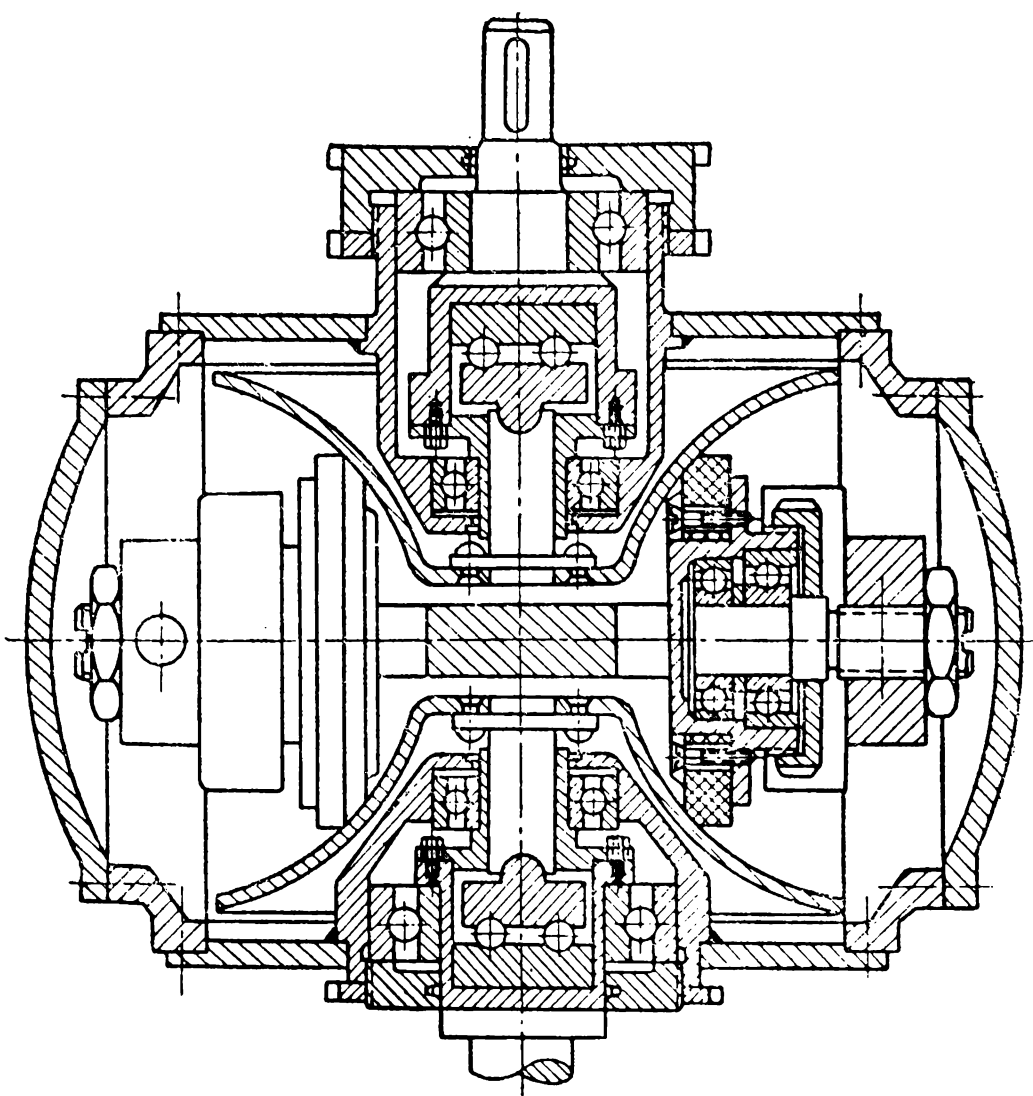


Fig. 108

## FUNDAMENTALS OF THE THEORY AND OPERATION OF FRICTION DRIVES

**Slip and Creep in Friction Drives.** Slip and creep arising in friction drives cause loss of speed of the driven wheel and also heating and wear of the contact surfaces.

Therefore the form and material of the wheels should be chosen so as to lessen the effect of this phenomenon.

*Slip* develops over the length of the contact area along the generatrices of the wheels and depends on their form. In V-groove wheels, for example, pure rolling occurs only at one point on the line of contact while at other points slip takes place, which is the greater the longer the line of contact.

A similar phenomenon is also observed in frontal drives. Without load the velocities of the driving and driven wheels at the point corresponding to  $\frac{b}{2}$  (Fig. 106, g), i. e., the middle of the width of the smaller wheel, are the same and amount to

$$v = \frac{\pi D_1 n_1}{60} = \frac{\pi D_2 n_2}{60} \text{ m/sec}$$

where  $D_1$  and  $D_2$  are in m, and  $n_1$  and  $n_2$  in rpm.

The velocities on the driven wheel depend on the distance from the axis of rotation and in places corresponding to the edges of the driving wheel will be

$$v'_2 = \frac{\pi (D_2 + b) n_2}{60} = v + \frac{\pi b n_2}{60}$$

and

$$v''_2 = \frac{\pi (D_2 - b) n_2}{60} = v - \frac{\pi b n_2}{60}.$$

The greater width  $b$  of the driving wheel is, i. e., the longer the line of contact, the larger is the difference in the velocities  $v'_2 - v''_2 = \frac{\pi b n_2}{30}$ .

The position of the point where no slip takes place changes as the magnitude of the transmitted load alters. Therefore, in drives operating with slip the velocity ratio is not constant.

To eliminate slip in drives with parallel shafts the line of contact should run parallel to the shafts and in drives with intersecting shafts it should be directed towards the point of intersection.

In Fig. 106 all drives, except  $a$ ,  $b$  and  $e$ , operate with some sort of slip.

*Creep* is always present in friction drives with wheels of any form. As the friction couple transmits torque the elements of the surface

of the driving ( $dg$ ) wheel approach point 1 of the contact compressed (Fig. 109,  $a$ ) and leave point 3 stretched. Conversely, the elements of the surface of the driven ( $dn$ ) wheel approach point 1 of the contact stretched and leave point 3 compressed.

The stresses in the surface elements of the contacting wheels do not change immediately the wheels meet but only at point 2 when the friction force on the remaining area corresponding to the angle of creep  $\alpha_{cr}$  becomes smaller than the applied peripheral effort.

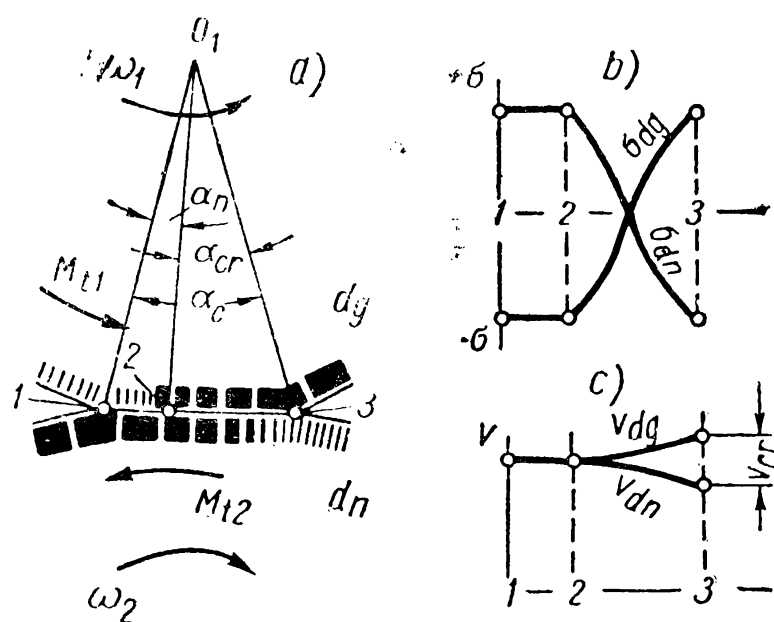


Fig. 109

Fig. 109,  $b$  shows the nature of the stress change on the contacting elements of the driving and driven wheels.

Stretching of the surface elements on one wheel and their compression on the other gives rise to *elastic creep* which likewise begins at point 2 (Fig. 109,  $c$ ) growing in intensity to point 3 where it reaches the maximum. Elastic creep causes the driven wheel to lag behind the driving wheel, the lag being the greater the larger the angles of

contact  $\alpha_c$  and of creep  $\alpha_{cr}$ . The magnitude of the latter depends on the elastic properties of the wheel material and the transmitted peripheral effort.

The velocity of elastic creep comprising 0.5-1 % of the peripheral velocity increases as the moduli of elasticity of the wheel material diminish, with the rolling losses increasing simultaneously.

An increase in the transmitted peripheral effort lengthens the area within which elastic creep takes place and at  $\alpha_{cr} = \alpha_c$ , i. e., at  $\alpha_n = 0$  slippage occurs which cannot be tolerated in friction drives.

With account taken of relative slip  $s$  the velocity ratio can be found from the formula

$$i = \frac{n_1}{n_2} = \frac{D_2}{D_1(1-s)}.$$

**Pressure.** The pressure necessary to generate friction force in a friction drive depends on the peripheral effort  $P$  to be transmitted and the coefficient of friction  $f$  of the wheel material. The magnitude of  $f$  depends on the state of the surfaces of the drive and its kind of service. To ensure against slippage the force of pressure is calculated from  $\beta P$  where the contact factor  $\beta = 1.5-2$ .

Below are given the main relations for simplest drives.

*Drives with parallel shafts.* The pressure  $S$  is determined from the horse power  $N_2$  on the driven shaft. In this case it is necessary to know the losses in the driving shaft bearings and for the wheel rotation. Since these losses depend on proportions of the drive parts which are not known in design calculations then with negligible

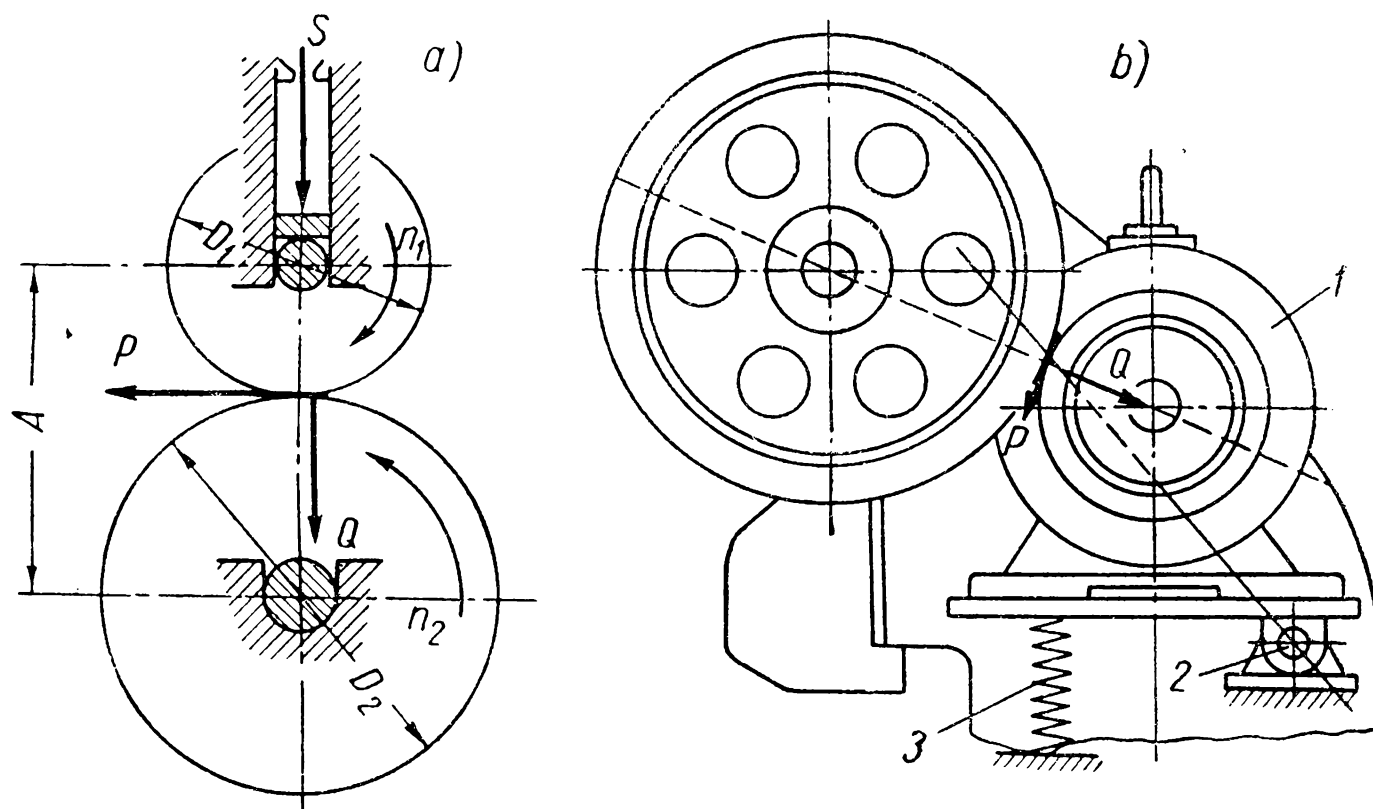


Fig. 110

error (bearing in mind that this adds to reliability) the pressure can be determined from the full horse power  $N_1$  on the driving shaft. Then for wheels with a flat-faced cylindrical rim (Fig. 110, a) the force of pressure equal to the pressure normal to the contact surface will be

$$S_1 = Q = \frac{\beta P}{f} = \frac{\beta 75 N_1}{f v} = \frac{\beta 75 N_1 60 \times 100}{f \pi D_2 n_2} \text{ kg.}$$

Here  $f$  is the coefficient of friction;  $D_2$ —the diameter in cm and  $n_2$ —rpm of the driven wheel;  $N_1$  is in h. p.

Since the centre distance is

$$A = \frac{D_2}{2} \pm \frac{D_1}{2} = (i \pm 1) \frac{D_1}{2} = \frac{(i \pm 1) D_2}{2i} \quad (137)$$

then substituting from this expression  $D_2 = \frac{2Ai}{i \pm 1}$  in the formula for  $S_1$  we obtain

$$S_1 = Q = 71,620 \frac{\beta}{f} \times \frac{N_1}{n_2} \times \frac{i \pm 1}{Ai} \text{ kg.} \quad (138)$$

In the latter formulae the plus sign represents external, and the minus sign internal contact of the wheels.

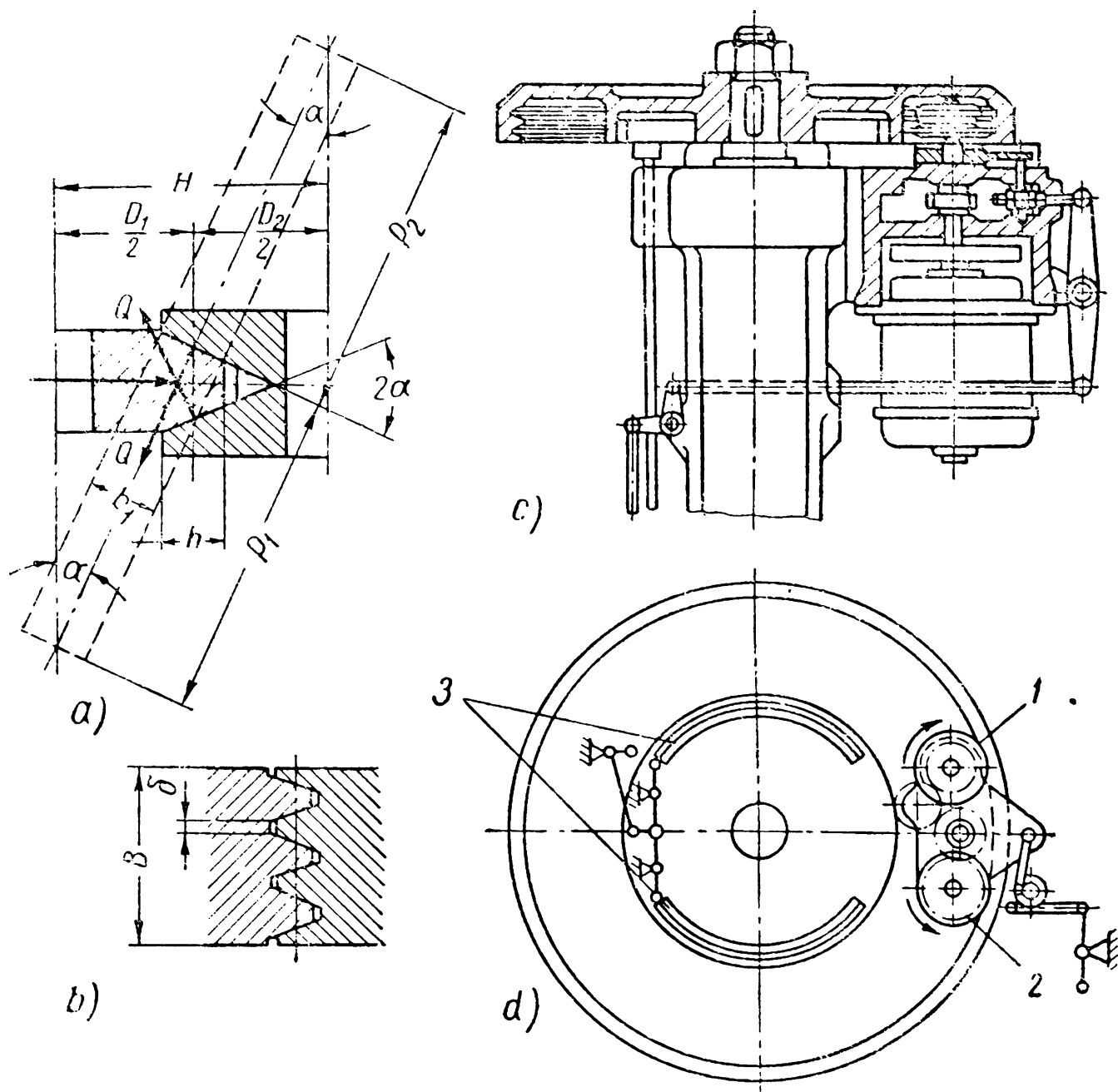


Fig. 111

In wheels with V-groove rims the force of pressure  $S$  creates the normal pressure  $Q$  (Fig. 111, *a*) whose value in a general case with  $z$  crests will be

$$Q = \frac{\beta P}{2zf}.$$

In a similar fashion and with the same designations in this case we obtain

$$Q = 35,810 \frac{\beta}{zf} \times \frac{N_1}{n_2} \times \frac{i \pm 1}{Ai} \text{ kg.} \quad (139)$$

In V-groove drives with one crest ( $z=1$ ) and from the equilibrium condition for the upper wheel  $S = 2Q \sin \alpha$ , the required pressure will be

$$S = 71,620 \frac{\beta}{f} \times \frac{N_1}{n_2} \times \frac{i \pm 1}{Ai} \sin \alpha \text{ kg.} \quad (140)$$

Here  $\alpha$  is half the angle of the wheel V-groove in diametral section. It follows from the equations (138) and (140) that  $S = S_1 \sin \alpha$ , i. e., the required pressure in V-groove drives, all other conditions being equal, is less than in drives with flat-faced rims.

The pressure  $S$  diminishes with a decrease in  $\alpha$ ; however, to obviate the hazard of pinching the crests in grooves we assume  $\alpha \geq 15^\circ$ . At  $\alpha = 15^\circ$  the required pressure is  $S = 0.26 S_1$ .

The transmission by means of V-groove wheels in a 200-ton screw press is represented in Fig. 111, c. The ram is brought into reciprocating motion by a special device (Fig. 111, d) controlled manually or automatically. As wheel 1 is engaged the ram makes a downward stroke, when wheel 2 is engaged—an upward stroke.

The inner smooth flange of the flywheel with blocks 3 acts as a brake.

The constant pressure of friction wheels effected manually, by springs, weight or other means is permissible only in systems transmitting a constant peripheral force. In transmissions operating under varying load the pressure should be changed automatically in accordance with the transmitted peripheral force. Such transmissions have a longer service life and higher efficiency, since in this case there are no unnecessary high normal pressures causing rapid wear when small peripheral forces are transmitted.

Fig. 110, b shows an eccentric press friction drive with automatically adjustable pressure. The electric motor 1, on whose shaft a driving friction wheel is fitted, fulcrums around axle 2 under the action of its own weight, thereby causing normal pressure  $Q$  to arise between the elements of the friction drive. The spring 3 serves to adjust the amount of initial pressure necessary to generate the friction forces which automatically bring the parts into contact.

*Drives with intersecting shafts.* For bevel wheels (Fig. 112, a) which ordinarily have  $\alpha_1 + \alpha_2 = 90^\circ$  the amount of normal pressure needed to transmit the peripheral force is

$$Q = \frac{\beta P}{f} = \frac{\beta 75}{f \pi} \times \frac{N_1}{n_2} \times \frac{60 \times 100}{D_2}. \quad (141)$$

It follows from Fig. 112, a that

$$L - \frac{b}{2} = \frac{1}{2} \sqrt{D_1^2 + D_2^2} = \frac{D_2}{2} \frac{\sqrt{i^2 + 1}}{i};$$

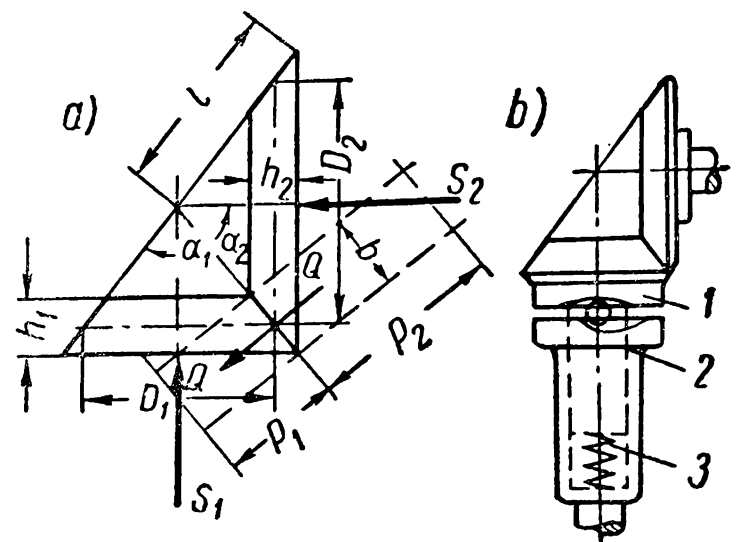


Fig. 112

hence

$$D_2 = \frac{(2L-b)i}{\sqrt{i^2+1}}.$$

Substituting this expression for  $D_2$  in the equation (141) we obtain

$$Q = 2 \times 71,620 \frac{\beta}{f} \times \frac{N_1}{n_2} \times \frac{\sqrt{i^2+1}}{(2L-b)i} \text{ kg.} \quad (142)$$

From the equilibrium condition of the wheels: for the driving wheel

$$S_1 = Q \sin \alpha_1 \quad (143)$$

and for the driven wheel

$$S_2 = Q \sin \alpha_2. \quad (144)$$

When  $\alpha_1 < \alpha_2$ ,  $S_1 < S_2$ , i. e., the required pressure is less when it occurs on the side of the smaller wheel.

After substituting the value  $Q$  from the equation (142) in the equation (143) we obtain for the pressure value in a bevel drive

$$S = 2 \times 71,620 \frac{\beta}{f} \times \frac{N_1}{n_2} \times \frac{\sqrt{i^2+1}}{(2L-b)i} \sin \alpha_1 \text{ kg.} \quad (145)$$

Here  $L$  is the cone distance in cm,  $b$ —the length of the wheel cone generatrix in cm.

A diagram of a device for bringing bevel wheels into contact automatically is shown in Fig. 112, *b*. Two or three balls are located in the inclined grooves of collars 1 of the wheel and 2 of the shaft. As the shaft rotates the balls are pressed out moving the wheel and creating the required pressure. A preliminary pressure is created by spring 3 arranged in the shaft bore.

For frontal wheels (Fig. 106, *g*) the pressure equals the normal pressure

$$Q = \frac{\beta P}{f} = \frac{\beta}{f} \times \frac{75N_1}{v} = \frac{\beta}{f} \times \frac{75N_1}{\pi} \times \frac{60 \times 100}{D_2 n_2} \text{ kg}$$

and since  $D_2 = iD_1$ , then

$$Q = 2 \times 71,620 \frac{\beta}{f} \times \frac{N_1}{n_2} \times \frac{1}{D_1 \times i} \text{ kg.} \quad (146)$$

### PARTS OF FRICTION DRIVES

The main elements of friction drives are friction wheels whose design is determined mainly by the material of the contact surfaces.

The *materials* of friction wheels should possess the following qualities:



a) high modulus of elasticity—to lessen elastic creep and rolling losses;

b) high coefficient of friction—to decrease the required pressure;

c) high surface strength and wear resistance—to ensure adequate service life.

Friction wheels are ordinarily made from combinations of the following materials:

*Hardened steel on hardened steel* usually grade IX15 with subsequent heat treatment of the surface to  $R_C = 60$ .

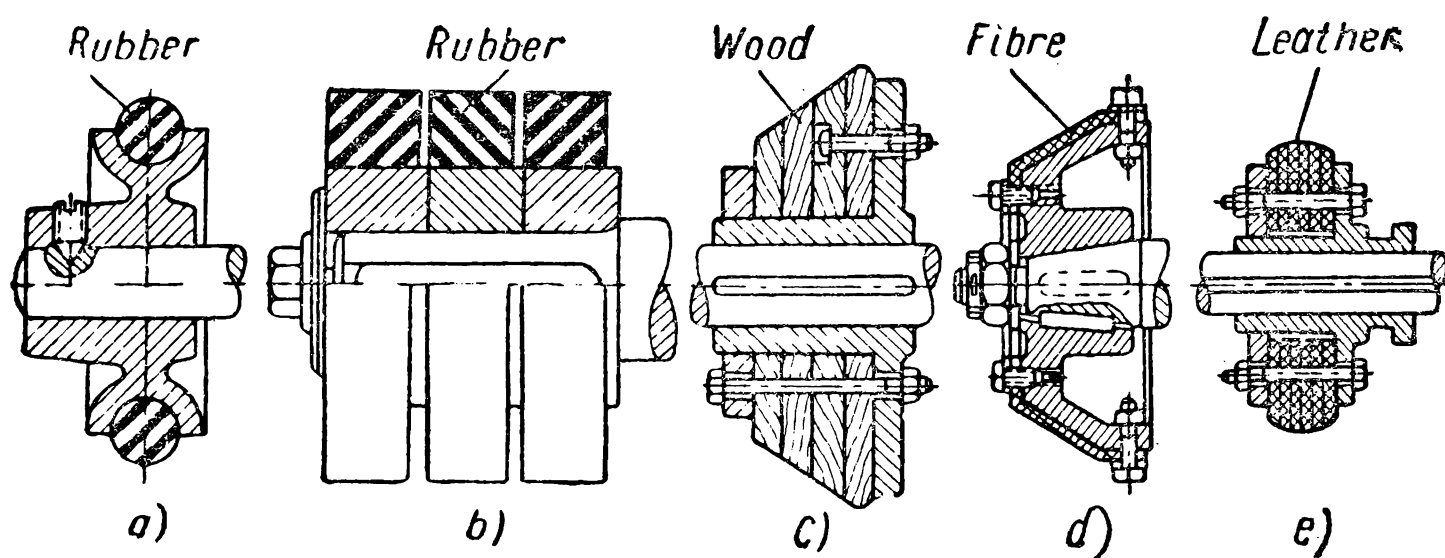


Fig. 113

*Cast iron on cast iron or steel*, in which case the bearing surfaces are given the greatest possible hardness (chilled cast iron, bleached or surface-hardened).

Drives made from these materials can work in oil or dry. In the first instance, the efficiency is less but the service life of the drive is longer due to reduced wear.

*Textolite or fibre on steel*. Drives made from these materials require less pressure due to their high coefficients of friction.

*Leather, wood, or rubber on steel or cast iron* give high coefficient of friction values, but since their surface strength is low they are rarely used in modern power friction drives.

Nonmetallic wheels are run dry; as a rule, the driving wheel is made from a softer material to avoid cold hardening on the surface of the driven wheel due to slippage.

The design values of the coefficients of friction for various materials are given in Table 18.

Some designs of friction wheels with nonmetallic elements are shown in Fig. 113, a-e. Pressure devices in friction drives have been examined above.

Table 18

Design Values of Coefficients of Friction  $f$  for Various Materials

Wheel material	Operating conditions	$f$
Steel on steel or cast iron	in oil	0.05
Steel on steel or cast iron	dry	0.1-0.15
Textolite on steel or cast iron	dry	0.2-0.25
Fibre on steel or cast iron	dry	0.15-0.20
Leather on cast iron	dry	0.25-0.35
Wood on cast iron	dry	0.40-0.50
Special rubber on cast iron	dry	0.50-0.75

### CALCULATION OF FRICTION DRIVES

**Design for Strength.** The design for strength of the wheels of power friction drives can be reduced to determining their proportions from the standpoint of limiting the magnitude of surface compressive stresses.

*Drives with parallel shafts.* For cylindrical wheels with flat-faced rims the reduced radius of curvature is

$$q = \frac{q_1 q_2}{q_2 \pm q_1} = \frac{D_1 D_2}{2(D_2 \pm D_1)} = \frac{D_2}{2(i \pm 1)}.$$

Taking the value  $D_2$  from the relation (137) we obtain

$$q = \frac{Ai}{(i \pm 1)^2}. \quad (147)$$

If we now substitute in the formula (30) the value  $Q$  from the formula (138) and  $q$  from the formula (147) after replacing  $\sigma_{\max}$  by  $[\sigma]_{sur}$  and denoting  $\frac{b}{A} = \psi$ , the expression for the centre distance will take the form

$$A = (i \pm 1) \sqrt[3]{E \frac{\beta}{\psi f} \times \frac{N_1}{n_2} \left( \frac{112}{i [\sigma]_{sur}} \right)^2} \text{ cm.} \quad (148)$$

Here  $E = \frac{2E_1 E_2}{E_1 + E_2}$  is the reduced modulus of elasticity in kg/cm<sup>2</sup>;

$E_1$  and  $E_2$ —the moduli of elasticity of the materials of the driving and driven wheels,  $N_1$ —the transmitted horse power;

$[\sigma]_{sur}$ —the allowable surface compressive stress in kg/cm<sup>2</sup> (Table 19);

$\psi$ —the wheel width factor usually taken as  $\psi = 0.2-0.4$ .

The larger  $\psi$  is, the smaller the proportions of the drive but the larger the peripheral force and pressure on the bearings will be. The smaller the drive efficiency. Besides, the larger the

rigidity and accuracy of manufacture of the drive parts must be greater.

For V-grooved wheels (Fig. 111, a)

$$Q = \frac{Q_1 Q_2}{Q_2 \pm Q_1} = \frac{R_1 R_2}{(R_2 \pm R_1) \sin \alpha} = \frac{D_2}{2(i \pm 1) \sin \alpha}$$

and since from the equation (137)  $D_2 = \frac{2Ai}{i \pm 1}$ , then

$$Q = \frac{Ai}{(i \pm 1)^2 \sin \alpha} \quad (149)$$

To lessen the wasteful slip the depth of the V-groove is made small. Usually (see Fig. 111, a)

$$h = 0.04D_1 = 0.04 \frac{D_2}{i} = \frac{0.08A}{i \pm 1}.$$

The length of the line of contact taking normal pressure is

$$b = \frac{h}{\cos \alpha} = \frac{0.08A}{(i \pm 1) \cos \alpha} \quad (150)$$

Substituting in the formula (30) the values  $Q$  from the formula (139),  $Q$  from the formula (149) and  $b$  from the formula (150) and assuming  $\sin \alpha \times \cos \alpha = \frac{1}{2} \sin 2\alpha = 0.25$  at  $\alpha = 15^\circ$ , we obtain for the centre distance

$$A = (i \pm 1) \sqrt[3]{E \frac{\beta}{zf} \times \frac{N_1}{n_2} \left( \frac{140}{i [\sigma]_{sur}} \right)^2 (i \pm 1)} \text{ cm.} \quad (151)$$

As the number of grooves  $z$  is increased the centre distance diminishes. As a rule,  $z \leq 5$  because it is impossible to ensure a uniform load distribution between all crests when there are many of them.

The width of V-groove wheels (Fig. 111, b)  $B = 2z(h \tan \alpha + \delta)$ .

For cast-iron wheels  $\delta = 0.5$  cm, for steel wheels  $\delta = 0.3$  cm.

*Drives with intersecting shafts.* For bevel wheels (Fig. 112, a) if the drive is orthogonal ( $\alpha_1 + \alpha_2 = 90^\circ$ ),  $\frac{D_1}{D_2} = \tan \alpha_1 = \frac{1}{i}$  and the radii of curvature for the driving and driven wheels will be respectively

$$Q_1 = \left( L - \frac{b}{2} \right) \tan \alpha_1 = \left( L - \frac{b}{2} \right) \frac{1}{i};$$

$$Q_2 = \left( L - \frac{b}{2} \right) \tan \alpha_2 = \left( L - \frac{b}{2} \right) i.$$

The reduced radius of curvature

$$Q = \frac{Q_1 Q_2}{Q_1 + Q_2} = \frac{\left( L - \frac{b}{2} \right) i}{i^2 + 1} \quad (152)$$

Substituting in the formula (30) the values  $Q$  from the formula (142),  $q$  from the formula (152) and assuming  $b = \psi_b L$ , we obtain for the cone distance the formula

$$L = \sqrt{i^2 + 1} \sqrt[3]{E \frac{\beta}{\psi_b f} \times \frac{N_1}{n_2} \left[ \frac{112}{i [\sigma]_{sur} (1 - 0.5\psi_b)} \right]^2} \text{ cm.} \quad (153)$$

Usually  $\psi_b = 0.2-0.25$  is taken.

For frontal wheels the reduced curvature is

$$\frac{1}{q} = \frac{1}{q_1} \pm \frac{1}{q_2} = \frac{1}{q_1} = \frac{2}{D_1} \quad (154)$$

since in this case the wheel contacts a plane, the curvature of which is  $\frac{1}{q_2} = 0$ .

Substituting in the formula (30) the values  $Q$  from the formula (146),  $q$  from the formula (154) and assuming  $b = \psi_f D_1$  we obtain

$$D_1 = \sqrt[3]{E \frac{\beta}{\psi_f f} \times \frac{N_1}{n_2 i} \left( \frac{224}{[\sigma]_{sur}} \right)^2} \text{ cm.} \quad (155)$$

We usually take  $\psi = 0.2-1$ .

The above formulae are used to calculate friction drives for maximum transmitted horse power.

The effect of varying operating conditions and service life can be accounted for when calculating metal wheels operating in oil with the help of the service life factor [see formula (24'')]. In this case in the formulae (149), (151), (153) and (155) we shall have the relation

$$\frac{N_1}{n_2} = \left( \frac{N_1}{n_2} \right)_{rated} k,$$

where the rated ratio  $\left( \frac{N_1}{n_2} \right)_{rated}$  is determined from the maximum horse power.

Table 19

Allowable Surface Stresses for Some Materials

Wheel material	Operating conditions	$[\sigma]_{sur}$ in kg/cm <sup>2</sup>
Steel on steel	in oil	(25-30) $H_B$
Cast iron on cast iron	in oil	1.5 $\sigma_{ulb}$
Steel on steel	dry	(12-15) $H_B$
Textolite on steel or cast iron	dry	500

Note:  $H_B$ —Brinell hardness;  $\sigma_{ulb}$ —ultimate strength of cast iron in bending.

**Shaft Loads.** The forces acting in drives with flat-faced or V-groove friction wheels with parallel shafts are shown in Fig. 114, *a*.

Radial load on the shafts of the driving and driven wheels is

$$R_1 = R_2 = R = \sqrt{P^2 + S^2}. \quad (156)$$

For wheels with *flat-faced rims* the pressure equals normal pressure, i. e.,  $S = Q \frac{\beta P}{f}$ , hence

$$R = \sqrt{P^2 + S^2} = P \sqrt{1 + \left(\frac{\beta}{f}\right)^2}. \quad (157)$$

For *V-groove* wheels  $S = \frac{\beta P}{f} \sin \alpha$  and

$$R = P \sqrt{1 + \left(\frac{\beta}{f} \sin \alpha\right)^2}. \quad (158)$$

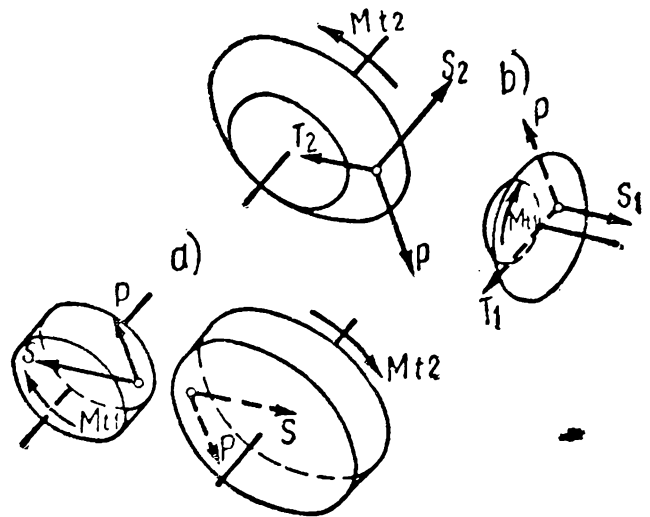


Fig. 114

In bevel friction wheels (Fig. 114, *b*) the shaft of the driving wheel resists an axial pressure, equal to the pressure  $S_1$ , and also pressures in a plane perpendicular to the axes  $P$  and  $T_1 = Q \cos \alpha_1$ . Together  $P$  and  $T_1$  give the radial load

$$R_1 = \sqrt{P^2 + T_1^2} = \sqrt{P^2 + (Q \cos \alpha_1)^2}.$$

Since  $Q = \frac{\beta P}{f}$ , after substitution we obtain

$$R_1 = P \sqrt{1 + \left(\frac{\beta}{f} \cos \alpha_1\right)^2}. \quad (159)$$

The shaft of the driven bevel wheel resists the axial pressure  $S_2$  and the total radial load

$$R_2 = P \sqrt{1 + \left(\frac{\beta}{f} \cos \alpha_2\right)^2}. \quad (160)$$

It follows from the formulae (156), (158) and (159) that the radial pressures exerted on the shafts of the driving and driven wheels are the same only in drives with parallel shafts. In drives with intersecting shafts  $R_1 \neq R_2$ .

**Losses and Efficiency of Drives.** In drives operating without slip the total horse power loss is

$$L = L_h + L_{cr} + L_b. \quad (161)$$

Here  $L_h$  is the loss due to hysteresis during wheel rolling (from the theory of mechanisms and machines).

$$L_h = \frac{Qk}{75 \times 100} \times \frac{\pi}{30} (n_1 + n_2),$$

or, on substituting here the value  $Q$  from the equation (138)

$$L_h = 2 \frac{\beta k}{f} \times \frac{N_1}{D_2} \times \frac{i+1}{i} \text{ h.p.} \quad (162)$$

$L_{cr}$  are losses due to elastic creep

$$L_{cr} = \frac{P_{sv}}{75} \text{ h.p.,}$$

where  $s = \frac{v_{cr}}{v}$  is the relative value of elastic creep, or through the horse power on the driving shaft

$$L_{cr} = sN_1 \text{ h.p.} \quad (163)$$

$L_b$  are losses in the bearings (see p. 475).

In the formulae (162) and (163)  $k$  is the coefficient of rolling friction in cm;  $N_1$  is the horse power on the driving shaft;  $D_2$  is the diameter of the driven wheel in cm.

In drives with wheels made from materials with high moduli of elasticity the total hysteresis loss in rolling and elastic creep can be less than the loss in the bearings.

If a friction drive operates with slip we should introduce in the right-hand side of the equation (161) the losses due to it  $L_{g.cr}$ , determined depending on the form of the wheel contact surface.

In drives with a variable velocity ratio slip is inevitable.

The efficiency of the drive will be found from the formula

$$\eta = \frac{N_1 - L}{N_1} = 1 - \frac{L}{N_1}. \quad (164)$$

The efficiency of friction drives varies within 0.70-0.95.

Their efficiency increases with the growth of the coefficient of friction and moduli of elasticity of the wheel materials.

To reduce losses and improve efficiency it is rational to increase the wheel diameters and maintain the ratio  $\frac{P}{Q}$  constant during operation.

This is attained by employing mechanisms which automatically adjust the pressure depending on the transmitted peripheral force.

**Design for Heating.** The horse power lost in transmission is converted into heat whose amount can be found from the formula (35).

In closed-type drives operating in oil the cooling surface from the formula (36) necessary to dissipate heat in stable thermal conditions is

$$F_m = \frac{Q}{k_m(t_1 - t_2)} = \frac{632L}{k_m(t_1 - t_2)} \text{ m}^2$$

where  $L$  is the horse power lost in transmission in h.p.;

$k_m$ —the heat transfer factor in  $\text{Cal/m}^2 \times \text{hr} \times \text{degrees } ^\circ\text{C}$ ;

$k_m$  lies within 7.5-15 depending on the velocity of the air circulation;

$t_1$  is the oil temperature in  $^\circ\text{C}$ ; usually,  $t_1 = 75-85^\circ$ ;

$t_2$  is the ambient temperature.

If the surface  $F$  of the designed smooth housing is smaller than the surface  $F_m$  found from this formula the cooling surface should be increased by employing a ribbed housing.

The thermal design of nonmetallic drives consists in determining the proportions of the crown rim section of textolite, fibre or any other material depending on the permissible maximum temperature. However, the absence of sufficiently reliable experimental data makes such calculation difficult.

*Example.* Calculate a friction drive with cylindrical wheels for a conveyor drive if the transmitted horse power  $N_1 = 5$  h.p.;  $n_1 = 1,000$  rpm;  $n_2 = 350$  rpm; the drive is open-type (i. e., not enclosed in a housing).

First select the material for wheels: textolite-steel.

Using the tables we select  $f = 0.22$ ;  $[\sigma]_{sur} = 500 \text{ kg/cm}^2$ . We assume  $\beta = 1.5$ ;  $\psi = \frac{b}{A} = 0.3$ .

At  $E_1 = 9 \times 10^4 \text{ kg/cm}^2$  for textolite and  $E_2 = 2.15 \times 10^6 \text{ kg/cm}^2$  for steel the reduced modulus of elasticity is

$$E = \frac{2E_1E_2}{E_1 + E_2} = 1.73 \times 10^5 \text{ kg/cm}^2.$$

The velocity ratio  $i = \frac{n_1}{n_2} = \frac{1,000}{350} = 2.85$ .

The centre distance, from the formula (148), is

$$\begin{aligned} A &= (i+1) \sqrt[3]{E \frac{\beta}{\psi f} \times \frac{N_1}{n_2} \left( \frac{112}{i [\sigma]_{sur}} \right)^2} = \\ &= (2.85+1) \sqrt[3]{\frac{1.73 \times 10^5 \times 1.5 \times 5}{0.3 \times 0.22 \times 350} \left( \frac{112}{2.85 \times 500} \right)^2} = 27 \text{ cm} = 270 \text{ mm}. \end{aligned}$$

Wheel width

$$b = A \times \psi = 27 \times 0.3 \approx 80 \text{ mm}.$$

Wheel diameter

$$D_1 = \frac{2A}{i+1} = \frac{2 \times 27}{2.85+1} = 14 \text{ cm} = 140 \text{ mm}.$$

For wheels from the selected material  $s=0.5\%=0.005$ ; in this case

$$D_2=D_1i(1-s)=14\times 2.85(1-0.005)=39.8\text{ cm}=398\text{ mm}.$$

Finally  $A=\frac{D_1+D_2}{2}=\frac{140+398}{2}=269\text{ mm}.$

The required pressure is found from the formula (138):

$$S=71,620\frac{\beta}{f}\times\frac{N_1}{n_2}\times\frac{i+1}{Ai}=71,620\frac{1.5\times 5\times 3.85}{0.22\times 350\times 26.9\times 2.85}=350\text{ kg}.$$

CHAPTER XIV

BELTING

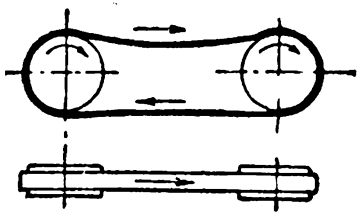
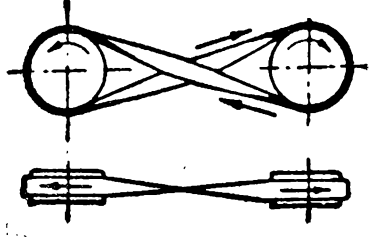
In its simplest form a drive of this type consists of an endless belt fitted tightly over two pulleys—driving and driven—transmitting motion from the driving to the receiving pulley by frictional resistance between belt and pulleys.

The flexibility of the belt makes it possible to arrange the shafts of the driving and driven pulleys in any manner and to use as many pulleys as necessary. The main types of belt drives are shown in Table 20.

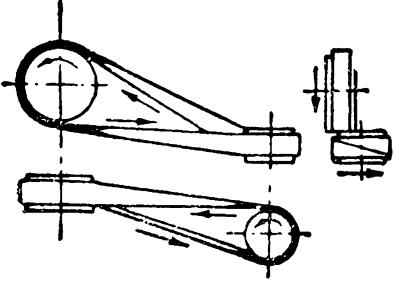
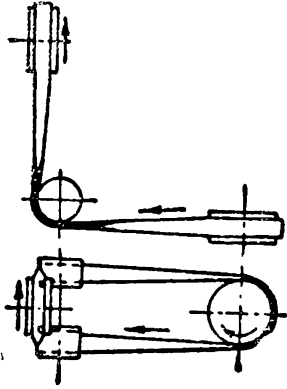
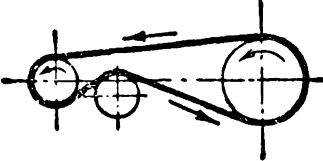
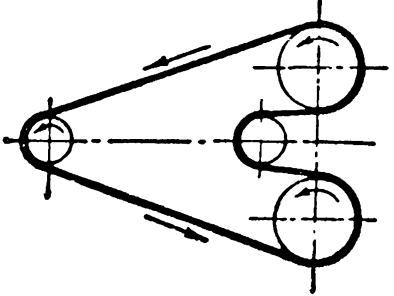
Belt drives are also classified by the type of belt, the way tension is produced and other characteristics (see below).

Table 20

Main Types of Belt Drives

Type	Application
<div>1. Open-belt drive</div> <div></div>	<div>Used with shafts arranged in parallel and rotating in the same direction. When the shafts are far apart the tight side of the belt should be the lower one.</div>
<div>2. Twist-belt drive</div> <div></div>	<div>Used with shafts arranged in parallel and rotating in opposite directions. At the point where the belt crosses it rubs against itself and wears. To avoid excessive wear the shafts should be placed at a maximum distance from each other (<math>A_{min}\geq 20b</math>, where <math>b</math> is the belt width) and operated at low velocity (<math>v\leq 15\text{ m/sec}</math>).</div>



Type	Application
<p>3. Quarter-twist belt drive</p> 	<p>Used with shafts at right angles rotating in one definite direction. In order to prevent the belt from leaving the pulleys the latter should be sufficiently wide (<math>B \geq 1.4b</math>) and fixed and secured finally only after a trial run.</p>
<p>4. Quarter-twist belt drive with guide pulleys</p> 	<p>Used with shafts at right angles when the pulleys cannot be arranged as shown in diagram 3 or when reversible action is required.</p>
<p>5. Belt drive with an idler pulley</p> 	<p>Used when an open-belt drive (diagram 1) cannot be employed because of the small arc of contact over the smaller pulley (high velocity ratio with small distance between the shafts) or when the required tension of the belt cannot be obtained by other means.</p>
<p>6. Belt drive with many pulleys and guide pulleys</p> 	<p>Used to transmit motion from one shaft to several shafts arranged in parallel.</p>

## FUNDAMENTALS OF THE THEORY AND OPERATION OF BELT DRIVES

**Tension in a Flexible Cord Embracing a Cylinder.** The design of belt drives is based on the analytical relation between the tensions of a flexible cord winding on a cylinder established by L. Euler in 1775 (Fig. 115)

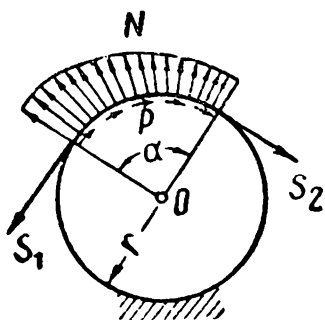


Fig. 115

$$\frac{S_1}{S_2} = e^{f\alpha} = m; \quad (165)$$

here  $S_1$  and  $S_2$  are forces applied to the cord ends;

$P = S_1 - S_2$ —friction force between the cord and the cylinder surface;

$f$ —coefficient of friction between the cord and the cylinder surface;

$\alpha$ —arc of contact between the cord and the cylinder; the designation  $e^{f\alpha} = m$  is used to make the expression shorter.

Euler's formula (165) is derived for a flexible unstretchable and weightless cord gliding over an immobile cylinder.

The belt in a drive differs from such a cord in many ways. The difference lies, first of all, in the elasticity of the belt. Further, the belt does not glide over an immobile pulley but tends to bring it into motion. Finally, the belt has a mass, and, as it moves over a curvilinear path generates inertial forces which cannot be disregarded.

During the 180 years that have elapsed since Euler's formula was first published many attempts have been made to supplement it and make it more specific as regards its application to the real conditions of operation of a belt drive. However, even today we have not yet obtained a formula that would take account of all the peculiarities of a belt used as a tractive element. Therefore, Euler's classical formula continues to remain the basis of the theory of belt-ing.

The specific features accruing from the fact that the belt, as distinct from the cord in Euler's formula, possesses elasticity and mass will be considered below.

**Elastic Creep.** The masses of a belt passing in unit time over given points on the tight and slack sides of an endless belt obviously remain constant. For stable motion we can therefore write the ratio

$$qv = \text{const}$$

where  $q$  is the weight of the belt unit length, and  $v$ —belt velocity at a given point.

As the belt tension changes, its length and hence the unit weight of this length also change. The magnitude  $q$  can be expressed by means of the weight  $q_0$  of unit length of an unstretched belt and relative elongation  $\varepsilon$ :

$$q = \frac{q_0}{1 + \varepsilon};$$

hence,

$$\frac{v}{1 + \varepsilon} = \text{const.} \quad (166)$$

This formula shows that the *belt velocity is higher at the points of maximum elongation and the belt must therefore creep on the surface of the pulleys.*

Indeed, since the belt moves onto the power pulley with tension  $S_1$  (elongation  $\varepsilon_1$ ) and leaves it with the tension  $S_2 \neq S_1$  ( $\varepsilon_2 \neq \varepsilon_1$ ) the respective velocities of the belt, in conformity with the expression (166), will likewise be different ( $v_1 \neq v_2$ ). But since the velocity of the pulley is constant, the particles of the belt creep back on the pulley as the belt approaches the delivery side. This phenomenon caused by belt elasticity ( $\varepsilon \neq 0$ ) and unequal tension ( $S_1 \neq S_2$ ) is called *elastic creep*.

Elastic creep is very important in the work of a belt drive. The most valuable data concerning elastic creep have been obtained experimentally. This is accounted for by the complexity of the phenomenon and the difficulty of describing it in the language of analytical formulae.

The first to investigate elastic creep was N. Y. Zhukovsky, who in 1893 built an ingenious device for the purpose. In the years that followed, as new methods of measuring creep were developed and new types of belt designed, these investigations were continued on available drives operating under various conditions.

Experimental research has shown that in a normally operating drive elastic creep does not occur over the entire area of contact between the belt and the pulley. On each pulley the full arc of contact  $\alpha$  is divided into two portions (Fig. 116)—the arc of creep  $\alpha_c$  and the arc of rest  $\alpha_r$ , where there is no creep.

On both pulleys the arc of rest is located on the receiving side and the arc of creep on the delivery side.

As load ( $P$ ) is increased the arc of creep increases due to a smaller arc of rest. At overloads creep is spread over the entire arc of contact  $\alpha$ ; in this case elastic creep becomes *slipping* which is harmful creep.

To return to Euler's formula (165) derived for a cord gliding over the entire arc of contact it should be noted that for a belt drive

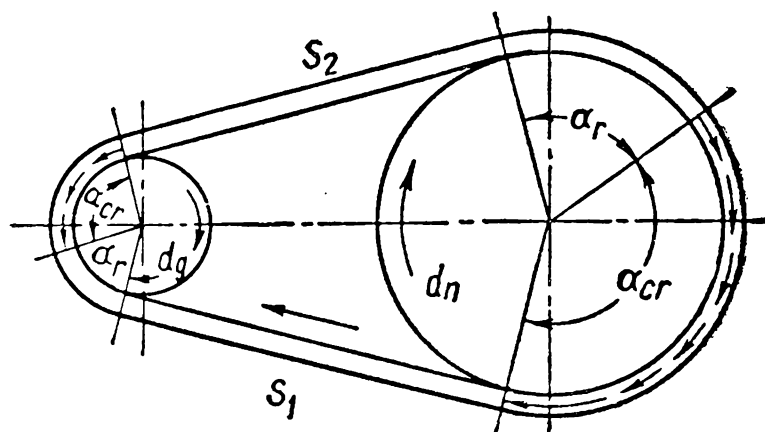


Fig. 116

it gives only an approximate but very simple relation between the tensions obtaining on the belt sides. The degree of this approximation depends on the truth of the value of the coefficient  $f$ , which stands for the reduced coefficient of friction over the entire arc of contact  $\alpha$ .

Experiments have shown that the magnitude  $f$  depends on temperature, unit pressure and velocity of creep. The mean values of the coefficients of friction are given in Table 21.

Table 21

Mean Values of Coefficients of Friction  $f$  between Belt and Pulley

Type of belt	Pulley material			
	Compressed paper	Wood	Steel	Cast iron
Leather:				
tanned with vegetable compound	0.35	0.30	0.25	0.25
tanned with mineral compound	0.50	0.45	0.40	0.40
Cotton:				
solid-woven . . . . .	0.28	0.25	0.22	0.22
stitched . . . . .	0.25	0.23	0.20	0.20
Woollen . . . . .	0.45	0.40	0.35	0.35
Rubber . . . . .	0.35	0.32	0.30	0.30

**Velocity Ratio.** Having taken elastic creep into account the principal kinematic relations in a belt drive are found in the following manner.

The relation between the velocities of the belt on the driving and driven pulleys is found from the condition (166)

$$\frac{v_1}{1 + \varepsilon_1} = \frac{v_2}{1 + \varepsilon_2}$$

whence

$$v_1 \approx v_2 [1 + (\varepsilon_1 - \varepsilon_2)] = v_2 (1 + s) \quad (167)$$

where  $s = \varepsilon_1 - \varepsilon_2$  is the coefficient of the belt creep.

On the other hand, these velocities can be expressed in curvature radii ( $\rho_1, \rho_2$ ) of the belt neutral section and revolutions per minute ( $n_1, n_2$ ) of the driving and driven pulleys:

$$\text{and } \left. \begin{aligned} v_1 &= \frac{2\pi\rho_1 n_1}{60 \times 100} \approx \frac{\pi(D_1 + h)n_1}{60 \times 100} \text{ m/sec} \\ v_2 &= \frac{2\pi\rho_2 n_2}{60 \times 100} \approx \frac{\pi(D_2 + h)n_2}{60 \times 100} \text{ m/sec} \end{aligned} \right\} \quad (168)$$

where  $h$  is the belt thickness in cm and  $D_1, D_2$ —diameters of the pulleys in cm.

Solving simultaneously the equations (167) and (168) we obtain an expression for velocity ratio:

$$i = \frac{n_1}{n_2} = (1 + s) \frac{D_2 + h}{D_1 + h} \approx (1 + s) \frac{D_2}{D_1} \quad (169)$$

provided  $h \ll D$ .

The maximum practical values of  $i$  for various types of drives are given on p. 178.

**Pull Factor.** In a belt on pulleys which in practice retains the same length, the stretching of one side causes a corresponding shortening of the other. In other words, an increase in tension of one side causes a corresponding decrease in tension of the other while the sum of the tensions remains the same. This is expressed in Poncelet's formula

$$S_1 + S_2 = 2S_0 \quad (170)$$

where  $S_0$  is the initial tension which is the same on both sides of the belt.

This relation is not fully confirmed by experiments; *the sum of operating tensions always proves somewhat larger than the double initial tension* and is not a constant magnitude; as belt speed increases this sum becomes larger.

Besides, the tensions of the sides  $S_1$  and  $S_2$  are also connected with the transmitted horse power  $P$  (see p. 204)

$$S_1 - S_2 = P. \quad (171)$$

Solving simultaneously the equations (170) and (171) we obtain

$$S_1 = S_0 + \frac{P}{2}; \quad S_2 = S_0 - \frac{P}{2}. \quad (172)$$

Thus in a drive standing idle or in a drive which is operating under no load the belt tension determining the pressure between it and the pulleys is the same in both sides and equals the initial tension  $S_0$ . When the drive is loaded with the peripheral force  $P$  the tensions are redistributed: in the tight side the tension increases by  $\frac{P}{2}$  and in the slack side it diminishes by the same magnitude.

The relation between the peripheral effort transmitted by the belt, i. e., the belt useful load, and the sum of tensions of its sides is called the *pull factor*

$$\varphi = \frac{P}{2S_0} = \frac{S_1 - S_2}{S_1 + S_2} = \frac{m - 1}{m + 1}. \quad (173)$$

The latter expression is formulated on the basis of the relation (165).

In the experimental investigation of a belt drive, laying off the pull factor  $\varphi$  on one coordinate axis and the coefficient of the belt creep  $s$  on the other we obtain the *belt pull curve* (Fig. 117).

The point  $O$  of the curve denotes idle run. As greater load is added to the drive and with a definite initial tension  $S_0$  the pull

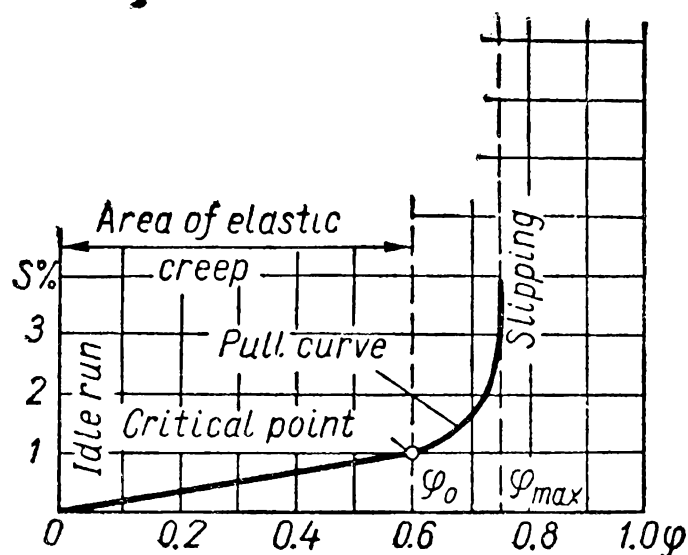


Fig. 117

and creep factors increase simultaneously. As load is further increased elastic creep gradually passes over into slipping.

The pull curve is divided into two portions. One is rectilinear where  $s$  grows in direct proportion together with  $\varphi$ . This is the operating portion of the curve. The second portion is curvilinear. Here the belt operation is unstable: a slight occasional increase in load causes the belt to slip. This is the nonoperating portion of the curve.

The point of transition from the rectilinear to the curvilinear portion is the *critical point* of the pull curve.

The value  $\varphi_0$  of this point corresponds to the maximum value of load when the belt is operated rationally. At  $\varphi < \varphi_0$  the pulling capacity of the belt is not used to the full advantage. At  $\varphi > \varphi_0$  the belt operates unstably and wears at a fast rate.

Numerous investigations give us the following mean values of the pull factor: for flat belts  $\varphi_0 = 0.5-0.6$ , for V-belts  $\varphi_0 = 0.7-0.9$ .

**Tension Due to Centrifugal Forces.** In a moving belt in addition to the initial tension ( $S_0$ ) and the tension caused by the transmitted peripheral effort ( $P$ ) there also occurs tension due to the action of centrifugal forces. They arise in all elements of the moving belt (Fig. 118, a).

To determine these tensions, let us take a belt element with the length  $dl = q d\alpha$  (Fig. 118, b). The mass  $dm$  of this element takes the centrifugal force  $dU$  which is equalised by the tensions  $V$ .

The equilibrium condition:

$$-dU + 2V \sin \frac{d\alpha}{2} = 0.$$

The centrifugal inertial force can be expressed by the formula

$$dU = \frac{v^2 dm}{g} = \frac{v^2}{g} \times q \times \frac{q d\alpha}{g} = q \frac{v^2}{g} d\alpha$$

where  $q$  is the weight of the belt unit length.

Assuming further that  $\sin \frac{d\alpha}{2} \approx \frac{d\alpha}{2}$  we obtain

$$V = q \frac{v^2}{g}. \quad (174)$$

As can be seen, the tension  $V$  caused by the centrifugal forces does not depend upon the curvature radius of the considered element of the belt—it is the same for all portions of the belt. The direction of the tension  $V$  is always bound to coincide with the direction of the belt elastic curve and hence cannot change the shape of the belt because the required lateral forces are absent.

Tension due to centrifugal forces does not directly affect the pressure between the belt and the pulley which is determined by the above factors ( $S_0$  and  $P$ ). Centrifugal inertial forces manifest themselves in a belt only in tensile stresses arising across the belt sections and, naturally, in the stretching of the belt brought about by these stresses.

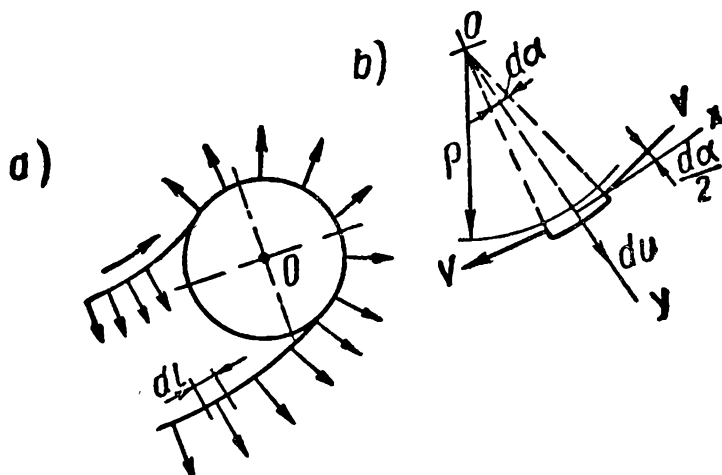


Fig. 118

**Stresses in Belts.** Various portions of a belt are subject to various stresses. For a general case the components of these stresses are: tensile stresses due to initial tension, transmitted horse power and centrifugal forces; bending stresses in a belt travelling over pulleys and rollers.

For a flat belt with a sectional area  $F=bh$  ( $b$ —width,  $h$ —belt thickness) these stresses are determined in the following way:

Stress due to initial tension

$$\sigma_0 = \frac{S_0}{F} = \frac{S_0}{bh}; \quad (175)$$

stress due to peripheral effort transmitted by the belt

$$k = \frac{P}{F} = \frac{P}{bh}; \quad (176)$$

stress due to centrifugal forces

$$\sigma_v = \frac{V}{F} = \frac{q}{F} \times \frac{v^2}{g} = \frac{\gamma v^2}{10g} \quad (177)$$

where  $\gamma$  is the belt specific weight (in  $\text{kg}/\text{dm}^3$  or  $\text{gm}/\text{cm}^3$ ).

Stress due to bending

$$\sigma_b = E_b \frac{h}{D} \quad (178)$$

where  $E_b$  is the reduced modulus of elasticity of the belt in bending and  $D$ —the diameter of the enveloped pulley or roller.

Using these stress components it is easy to calculate stresses in the various portions of an operating belt. A tentative picture of stress distribution in a drive without an idler pulley is shown in Fig. 119. The maximum stresses  $\sigma_{\max}$  obtain in the tight side on the smaller pulley and comprise

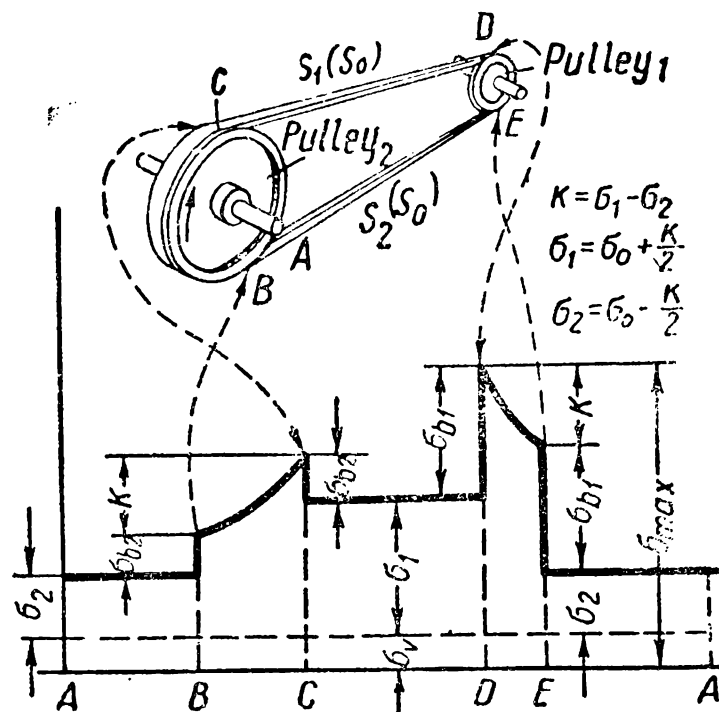


Fig. 119

$$\sigma_{\max} = \sigma_0 + \frac{k}{2} + \sigma_v + \sigma_{b \max} =$$

$$= \frac{S_0}{F} + \frac{P}{2F} + \frac{\gamma v^2}{10g} + E_b \frac{h}{D_{\min}}. \quad (179)$$

**Losses in Transmission.** In belt drives losses not only involve the unproductive expenditure of energy but are also very harmful in that, whatever their origin, they cause the development of heat which pri-

marily affects the belt. As distinct from the materials of the majority of machine parts, the materials used for belts—natural or artificial fibre, rubber and various impregnating compounds—are highly sensitive to heat. An increase in temperature sharply reduces the strength and service life of belts. Since, with all other conditions equal, the belt temperature is proportional to the losses, the magnitude of the latter can serve as one of the indications of the efficiency and rationality of the drive design.

In a belt drive losses may be due to:

- 1) creep of the belt on the pulleys;
- 2) elastic hysteresis (inner friction between the belt particles at varying bending, tension and compression);
- 3) air resistance to the movement of the belt, pulleys and idler pulleys;
- 4) friction in the bearings of pulleys and idler pulleys carrying the tension of the belts.

The first two kinds of losses, which comprise the majority of all losses in a belt drive, are of special interest here, for the belt is heated directly by energy expended in creep and by elastic hysteresis.

Losses due to air resistance are taken into account only in special cases—with spoked pulleys of large diameter; in conventional, even in high-speed drives, these losses are negligible. The bearings of pulleys and idler pulleys in a belt drive resist the tension



under which the belt is placed on the pulleys. The method of accounting for these losses is outlined in the section dealing with bearings.

The total losses due to creep and hysteresis amount to

$$L_e = L_c + L_h$$

The subscript  $e$  shows that these losses are connected with the belt elasticity\*.

The magnitude of losses in unit time ( $L_e$ ) can be written as follows

$$L_e = F \times v \times k_p \quad (180)$$

where  $F$  is the belt cross-sectional area;

$v$ —the belt velocity;

$k_p$ —the proportionality factor depending on the drive design, internal structure and properties of the belt.

The physical meaning of the factor  $k_p$  is the magnitude of losses per unit of belt volume.

### COMPONENTS OF BELT DRIVES

**Belts.** In a belt drive the pulling member—a belt—is the most important element determining the operating capacity of the entire drive. The service life of the belt is many times shorter than that of the other elements of a belt drive. Therefore, belts should be always correctly selected and their designs constantly improved.

The most important factors of a belt are as follows:

- 1) high *pulling* capacity;
- 2) adequate service life and fatigue strength;
- 3) low cost.

The formulae (179) for stresses and (180) for losses indicate concrete methods for the rational design of belts which satisfy the above requirements. Obviously, to reduce losses, the cross-sectional area of a belt  $F$  should be reduced mainly at the expense of its thickness  $h$  in order to decrease stresses due to bending  $\sigma_b$ . But smaller  $F$  involves greater tensile stresses  $\sigma_0$  and  $k$  and to preserve the belt strength it should be therefore reinforced with cords of high tensile strength. Further, bending stresses can be reduced by decreasing the modulus of elasticity in bending  $E_b$ , while retaining the modulus of elasticity  $E$  in tension at a high level in order to lessen losses caused by elastic creep. Simultaneously, an attempt should be made to obtain the minimum specific weight  $\gamma$ , taking into account stresses due to centrifugal forces  $\sigma_v$ , and the minimum loss factor  $k_l$  with due regard to the heating of the belt. Present-day techniques, and

---

\* To be more precise, the loss  $L_h$  is connected with imperfect elasticity of the belt.

especially the production of synthetic materials, has opened up wide possibilities in this field.

Belts are classified according to their cross-section, design, material and methods of processing.

Belt cross-section is the most important factor determining the design of pulleys and the entire drive. It divides them into rope, flat and V-belts.

Hemp and steel *ropes* were once extensively used to transmit high horse power over large distances. The main disadvantage of ropes is the high unit pressure developed on the pulley and the resultant comparatively rapid wear of the outermost wires and grooves.

This shortcoming is eliminated in V-belts which have almost completely ousted ropes. Today, leather and cotton ropes are used only in low-powered drives—for example, in sewing machines.

*Flat belts* are most widely used in drives of various machinery. They are furnished in various widths (from 15 to 500 mm) and designs and are made from various materials. In the USSR four types of flat belts have been standardised and put into centralised production: a) leather, b) rubber, c) woven cotton and d) woven woollen. Data on these belts are given in Table 22.

a) *Leather belts* are made from shabrack tanned with vegetable, chrome-vegetable and chrome compounds. Of all types of flat belts leather belts possess the best pulling capacity. However, because of the high cost of leather, these belts are used comparatively rarely and only in especially important cases.

b) *Rubber belts* are made from several layers of strong fabric cemented together by rubber and vulcanised. For better flexibility rubber linings are placed between the layers of fabric.

Rubber belts can operate in drives under varying load if a belt fork is available.

c) *Woven cotton belts* are made from fabric woven from warp and weft thread. They are impregnated with an ozocerite and bitumen compound which protects them from atmospheric effects, increases their strength and reduces shrinkage in a free state.

d) *Woven woollen belts* are made from three kinds of thread—warp of ground (woollen) weave, connecting warp and cotton picks of weft.

They are impregnated with a compound made from drying oil, crushed chalk and red ochre.

In addition to the above four standard types of flat belt, inter-stitched, rubber, semi-linen and silk belts are produced for special purposes (high-speed transmissions, internal grinding machines, etc).

*V-belts* began to be used extensively in industry a comparatively short time ago—in the 1920-1930s. Their rapid spread was due

Table 22

Flat Belts

	Leather	Rubber canvas	Solid-woven cotton	Woven woollen	Interstitched rubber	Woven semi-linen
Width <i>b</i> in mm	20-300	20-500	30-250	50-500	20-135	15-55
Thickness <i>h</i> in mm	Single 3-5.5, double 7.5-10	2.5-13.5	4.5-6.5- 8.5	6-9-11	1.75-2.5- 3.3	1.75
Ultimate tensile strength in kg/cm <sup>2</sup>	200	440 (without layers), 370 (with layers)	350-405	300	300	500
Maximum elongation	10% at 100 kg/cm <sup>2</sup>	18% at rupture	20-25% at rupture	60% at rupture	16% at rupture	10% at rupture
Ratio $\frac{D_{min}}{h}$ recommended	35	40	30-40	30	40	30
allowable	25	30	25-35	25	30	25
Recommended maximum velocity $v_{max}$ in m/sec	40	20-30	25	30	50	50
Specific weight $\gamma$ in kg/dm <sup>3</sup>	0.98	1.25-1.50	0.75-1.05	0.90-1.24	≈1.2	≈1.0
Constants <i>a</i>	29	25	21	18	23	21
in formula (191) <i>w</i>	300	100	150	150	200	150
Modulus of elasticity <i>E<sub>t</sub></i> in kg/cm <sup>2</sup>	1,000-1,500	800-1,200	300-600	—	1,000-1,200	—

to the introduction of individual motor drives which made new demands on belt drives: small distance between the pulley axles and high velocity ratios. At the same time automobile engines required other types of reliable belting to transmit motion from the crankshaft to the fan, water pump and dynamo, as flat belts with their inadequate pulling capacity failed to stand the test.

A V-belt has a better pulling capacity than a flat belt because of a higher coefficient of friction.

All the formulae derived above for flat belts are also valid for V-belts if we replace in Euler's formula in the exponent the coefficient of friction  $f$  by the reduced coefficient of friction  $f' = f / \sin \frac{\varphi}{2}$  where  $\varphi$  is the angle of groove of a V-belt, i. e., for a V-belt

$$\frac{S_1}{S_2} = e^{f'a} = e^{\frac{fa}{\sin \frac{\varphi}{2}}} = m'. \quad (181)$$

To prevent the pinching of the belt in the groove, the angle  $\varphi$  should be larger than the double angle of friction  $2 \tan^{-1} f$ . Hence with the coefficient of friction between rubber fabric and cast iron  $f=0.30$ ,  $\varphi > 2 \tan^{-1} 0.3 \approx 34^\circ$ .

For pulleys of different diameters the angle of groove lies within  $\varphi=34-40^\circ$ . Within these limits the mean value of the coefficient of friction is

$$f' = \frac{f}{\sin 18.5^\circ} \approx \frac{f}{0.32} \approx 3f.$$

Thus, all other conditions being equal, an element of arc of a V-belt is capable of transmitting a peripheral effort nearly three times greater than in a flat-belt drive.

This constitutes the main advantage of a V-belt over a flat belt. However, this feature cannot be used to full advantage because unit pressure between a V-belt and its groove is much higher than between a flat belt and pulley rim and, as we know, higher unit pressure increases wear of the belt and reduces the coefficient of friction\*.

There are three main types of V-belts.

Cord fabric belts (Fig. 120, *I*) comprise several layers of cord fabric  $a$  in the high tension section, rubber  $b$  in the high compression section and an outer cover  $c$  made from rubber fabric.

Cord wire belts (Fig. 120, *II*) consist of several very strong cord wires  $a$  located in the neutral section and therefore not affecting the belt flexibility, a rubber filler  $b$  which is very elastic in the high

---

\* Comparative calculations show that for the standardised profiles of V-belts the relation of unit pressure to the tensile stress (arbitrarily referred, to the entire sectional area of the belt) is 4.5-5 times more than a similar relation for flat belts.

tension section and more stiff in the high compression section, and an outer cover *c*.

Cord wire toothed belts (Fig. 120, *III*) differ from simple cord wire belts in that they have evenly pitched teeth in the high compression section (and sometimes in the high tension section too) to obtain greater flexibility which is especially essential at high speeds and with pulleys of small diameter.

The development of V-belt designs has the object of increasing the strength of the cord wires (for this purpose use is also made of capron and other synthetic threads and also of thin steel cords)

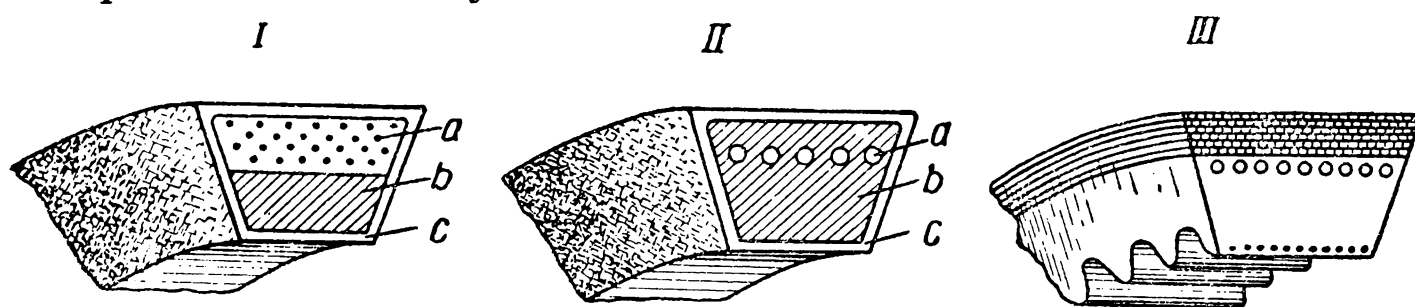


Fig. 120

and reducing the total belt cross-sectional area. A recent development is the use of narrow V-belts allowing high speeds and transmitting the same loads although their cross-sectional area is almost four times less than that of conventional belts.

The Soviet standards provide for seven cross-sections (Fig. 121) of V-belts made from cord fabric or wire and, in addition, for five cross-sections (Fig. 122) of cord wire belts for the fans of automobiles, tractors and harvesters. All these endless belts are from 0.5 to 14 m long, different lengths being used for different cross-sections. V-belt standards specify their inner length  $L_{in}$  and design length  $L_d$  by the neutral section. The relation between them is  $L_d - L_{in} = 2\pi(h - h_0)$  where  $h$  is the height of the belt cross-section and  $h_0$ —the distance between the neutral section and its larger base ( $h_0 \approx \frac{1}{3}h$ ). The main data for standard V-belts are given in Table 23.

The perspectives for the development of belts are determined by the following circumstances.

The operating capacity and service life of all types of belt depend on the properties of the cord thread, rubber fillers and impregnation and the structure of fabric. The most important is cord thread which carries the main load. Cotton cord thread which was until recently used for belts is unsuitable for high-speed drives since flexing of high frequency heats the belt to 100-120 °C, a temperature causing fatigue in cotton thread—it dries up, becomes hard and brittle and rapidly disintegrates. Today industry employs thread made from synthetic materials which is much superior in its qualities to cotton thread.

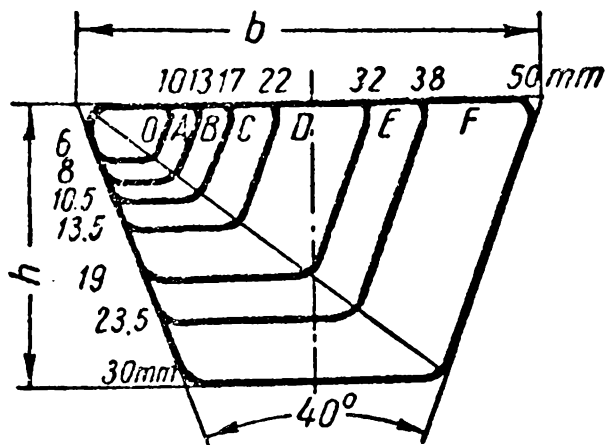
Table 23

V-Belts

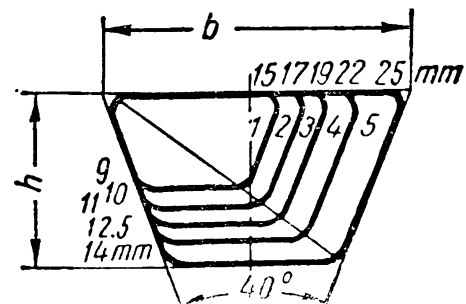
Cross-sections of V-belts	(sizes in Fig. 121)										(sizes in Fig. 122)				
	O	A	B	C	D	E	F	1	2	3	4	5			
Cross-section area $F$ in $\text{cm}^2$	0.5	0.8	1.4	2.3	4.8	7.0	11.7	1.1	1.2	1.6	2.2	2.7			
In conformity with the min standard, design or inner* length of belt in mm	500*	500*	630*	1,800	3,150	4,500	6,300	560*	560*	900*	950*	950*			
	2,500	4,000	6,300	9,000	11,000	14,000	14,000	1,120*	1,400*	1,400*	1,400*	1,400*			
Difference between design and inner length of belt in mm	25	33	40	55	76	95	120	38	42	46	52	59			
Minimum allowable design diameters of pulleys in mm	63	90	125	200	315	500	800	80	90	105	125	140			
Constants in formula	$a$	23	25	28	30	32	32								
(191)	$w$	100	120	180	215	280	350								
Maximum recommended velocity $v_{\text{max}}$ in m/sec	25	25	25	25	30	30	30	30	30	30	30	30			
Design width of belt $a_d$ in mm	8.5	11	14	19	27	32	42								
Rated sizes of pulley grooves (Fig. 125)*	$e$	10	12.5	16	21	28.5	34								
	$c$	2.5	3.5	5	6	8.5	10								
	$t$	12	16	20	26	37.5	44.5								
	$s$	8	10	12.5	17	24	29								
	$\varphi^\circ$	34-40					36-40								

Note. The angle of groove ( $\varphi$ ) is selected depending on the pulley diameter; a lesser angle corresponds to a lesser diameter.

It is obvious that the utilisation of such thread in the manufacture of belts will make it possible to reduce the size of pulleys and of the entire drive, improve the pull and increase the service life of belts and ensure dependable operation of belts at high velocities.



**Fig. 121**



**Fig. 122**

*Belt joints.* V-belts and some special types of flat belts are made endless. Other belts, i. e., almost all flat belts, should be jointed. A joint of any type is as a rule the most vulnerable part of the belt: the tensile strength of the joint rarely exceeds 30-85% of the strength of the other portions of the belt. The joint is usually more rigid and sometimes heavier than other portions of the belt; it strikes against the pulleys and causes variations in the velocity of motion. It is therefore clear that the presence of joints in a belt is altogether undesirable and in certain cases, for example, when transmitting power to the spindles of precision lathes they must not be used at all.

However, the production of endless belts is more complicated and expensive. Provision should be made for spare belts of every type, cross-section and length to replace faulty belts damaged during operation. When designing drives with endless belts, the pulley shafts should be arranged in conformity with the standardised lengths of belts. Endless belts require for easier replacement special belt tension adjusters, an overhung position of the pulleys and readily removable bearings. Therefore, despite certain advantages offered by endless belts wide use is also made of home-laced or hinged belts. The most widespread types of belt joint are shown in Table 24. They are formed by cementing, stitching and fastening. Only leather and rubber belts can be cemented.


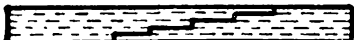

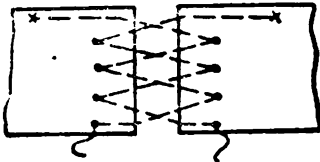
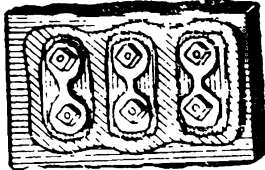
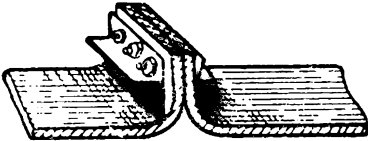
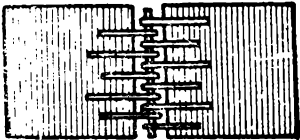
**Pulleys.** A belt pulley comprises a rim, spokes or a solid piece and a hub. Pulleys are classified according to the form of the rim face and the material and structural features of the elements.

The form the rim face is determined by the type of belt and the operating conditions of the drive.

For *flat belts* preference is given to flat-faced finely polished

Table 24

Belt Joints

	Type of joint		Joint strength relative to the strength of integral belt in %
Cemented joints	Cemented leather		80-85
	Cemented rubber		80-85
Laced joints	Rawhide strips		30
			50
Laced joints	Twines		50
Hinged joints	Bolts with plates (butt joint)		30
	Bolts with plates (crest joint)		25
	Wire hooks or spirals with a pin		50-80



cylindrical pulleys. The wear of the belt due to the inevitable elastic creep is here reduced to the minimum.

The main dimensions of pulleys—diameter  $D$ , width  $B$  (depending on the belt width  $b$ ) and the crown  $y$  (see below)—conform to standards.

For quarter-twist and twist belt drives and for drives with a sharply varying load, the width of pulleys  $B=(1.5-2.0)b$ .

If pulleys are not strictly aligned the thickness of the rim is increased at the centre to give it a crown since a belt tends to run off unparallel flat-faced pulleys.

If, on the other hand, one or both pulleys are made convex at the centre any lateral displacement of the belt will tend to return it to the middle. This feature of a crowned pulley is illustrated by Fig. 123, *a*, which shows a number of consecutive positions of a point  $c$  of the belt side moving onto the convex face of the pulley.

The crown may have different forms: a cone rounded at the top (Fig. 123, *b*), a circular arc (Fig. 123, *c*) or any other curve.

The height of the crown  $y$  depends on the belt width and the anticipated misalignment of the pulley axes. The following ratios are recommended:

Width of pulley in mm	40-60,	70-100,	125-150,	175-250	300-400,	450-600
Crown height $y$ in mm	1	1.5	2	2.5	3	4

In certain cases (for example, in agricultural machinery) the height of the crown is larger.

The presence of a crown somewhat reduces the belt life. The middle of the belt passing over a convex pulley tends to cover a greater path than the belt edges. But since all elements of a belt cross-section cover the same path in unit time it is clear that the crown causes additional creep and wear of the belt. Therefore, the rim is made convex only on the driven pulley in open-belt drives; both pulleys are crowned only if the drive operates at high velocity ( $v > 20-30$  m/sec).

Run-off of the belt and its complete pulling away from the pulley is always inevitable on slipping.

This is explained by definite characteristics of friction: when a body slides at a high velocity in one direction (slipping of the belt over the pulley) a small effort is enough to shift it in a perpendicular direction (i. e., sideways off the pulley). In a belt drive these

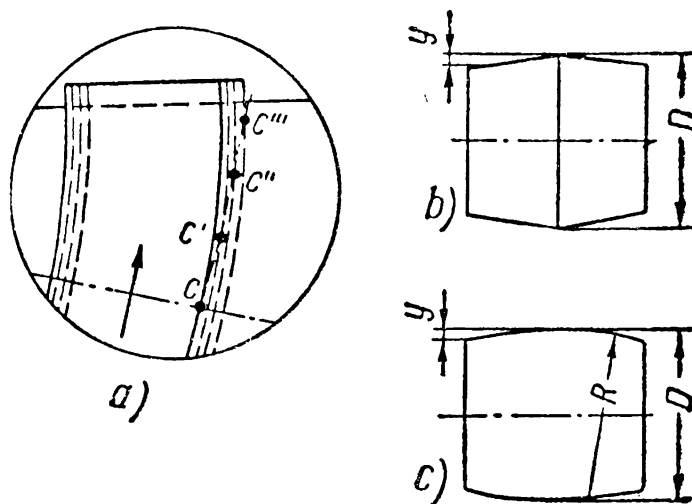


Fig. 123

small forces are always present, usually because of a slight misalignment of the pulleys.

Therefore, if the nature of load involves slipping and the belt cannot be permitted to run off the pulley (because of the danger of damaging the belt or for other reasons) such pulleys should be provided with one or two flanges (Fig. 124, c). To keep the belt strictly in line these flanges should be undercut and have sufficient height—some 40-70 mm. Low filleted flanges will tend to rupture the belt.

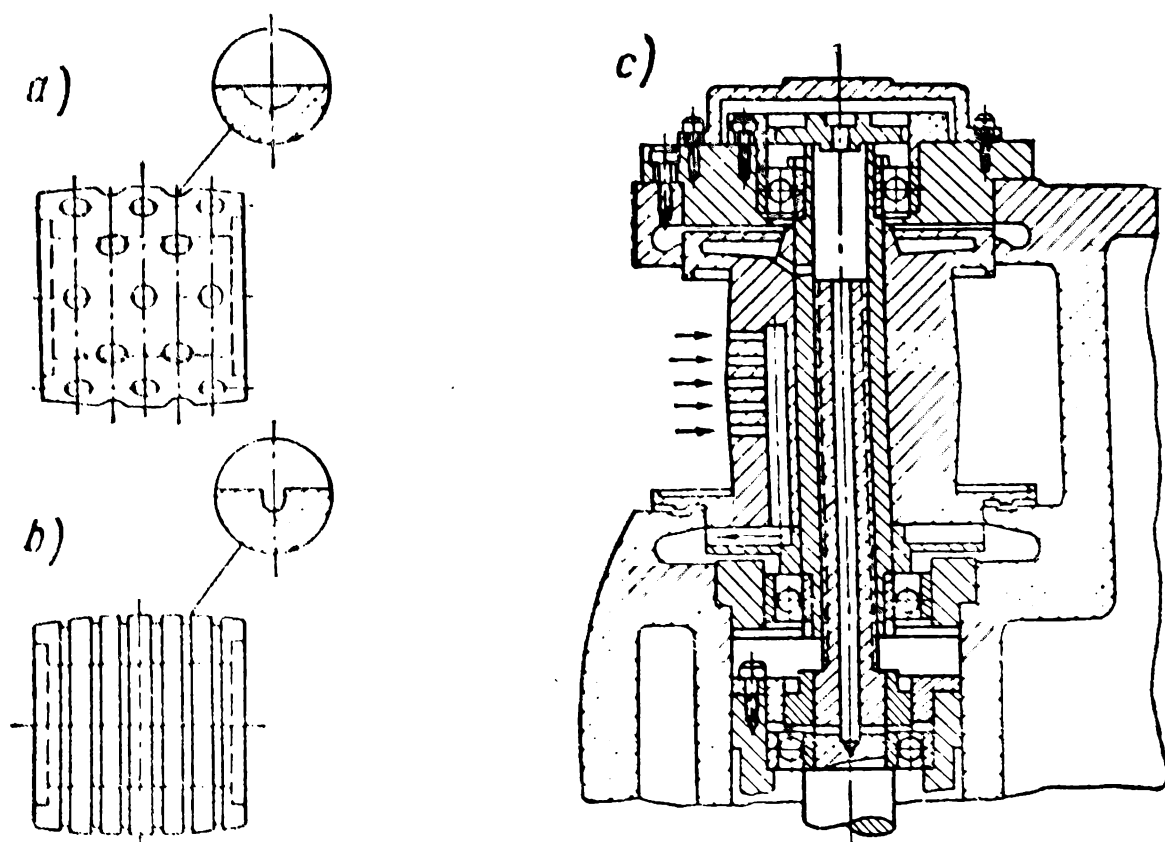


Fig. 124

It should be noted that the flanges prevent the belt from leaving the pulley only on slipping. In normal operation the belt is held in place due to the accurate adjustment of both pulleys and also partly by the crown. Constant friction of the belt against the flange reduces its service life.

In high-speed drives account should be taken of air suction into the wedge-shaped slit between the oncoming side of the belt and the pulley. This decreases the angle of contact and lessens the pressure between the belt and the pulley.

The attempt to obviate this has led to the development of some special designs.

In the design shown in Fig. 124, b the pulley periphery is provided with shallow *circular grooves* to remove the air sucked under the belt. Fig. 124, a shows a pulley with *spherical recesses* over the face; here use is made of the phenomenon of vacuum suction when the air is quickly expelled from the cavity. Finally, in the design in Fig. 124, c, an intensive vacuum is created between the belt and the

pulley by a *special impeller* built into the pulley. The air is sucked from underneath the belt along ducts which have their outlet on the pulley face and expelled by the impeller. Such pulleys are known to operate at some 40,000 rpm.

For a *V-belt* the bearing surfaces are the sides of a V-groove in the pulley rim. The size and number of such grooves are determined by the selected profile of the belt and the calculated number of belts. These sizes are so assigned as to prevent the belt touching the groove bottom or protruding outside. The belt profile is distorted in bending; its angle changes relative to the initial angle ( $\varphi_0 = 40^\circ$ ). Therefore, the angle of the pulley groove depends on the pulley diameter.

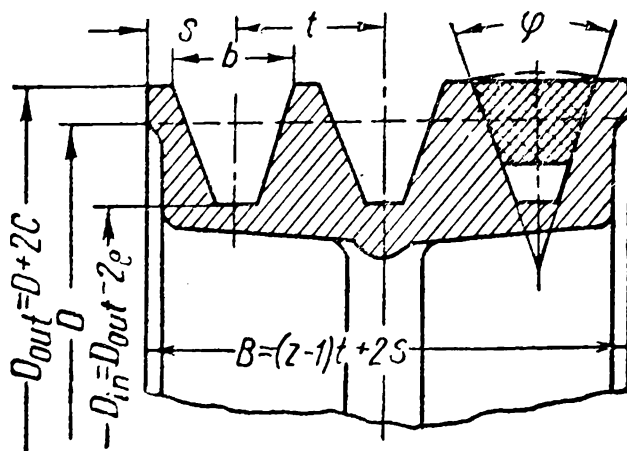


Fig. 125

Since the distortion of the profile angle as well as the position of the neutral section in the belt depend on its inner structure and properties, the size of the grooves in the pulleys and belt profiles are decided upon by the manufacturer. For standard V-belts these sizes are shown in Fig. 125 and Table 23. In multi-belt drives the uniform work of all belts is ensured above all by equal design diameters of all grooves and the lengths of belts. As investigations have shown the equality of the diameters of grooves is of paramount importance. Therefore, in working drawings of pulleys the sizes of grooves should be limited by tolerances.

Belt pulleys are *cast* from cast iron or aluminium alloys or *welded* together from steel. Wooden pulleys are now a rare feature.

The design and material of the pulley are closely interrelated.

The choice of material depends primarily on the required number of pulleys, their diameters and peripheral velocity.

Pulleys for special-purpose machines delivered in limited numbers are usually welded. This saves money spent on casting patterns and reduces the production time. Besides, welded pulleys of 500 mm and more in diameter are lighter than cast-iron pulleys. Cast-iron pulleys are limited to a peripheral velocity of 30-35 m/sec (see below). High-speed drives with frequent starting and stopping and velocity changes employ pulleys made from aluminium alloys. Compared to cast-iron pulleys they involve lesser loss of power during acceleration and braking in proportion to the ratio of specific weights  $\gamma_{\text{cast-iron}} : \gamma_{\text{al}} = 2.5-2.7$  or at the same amount of loss make it possible to increase the transmission rate in proportion to the square root of this ratio, i. e., in proportion to 1.6-1.65.

For heavy duty (impact loads, frequent reversing, etc.) pulleys made from light alloys are provided with cast-iron hubs. The hub has a fit hole, keyway and threaded holes for lock screws. Large bimetallic pulleys save 60% in weight as compared to pulleys made entirely from cast iron.

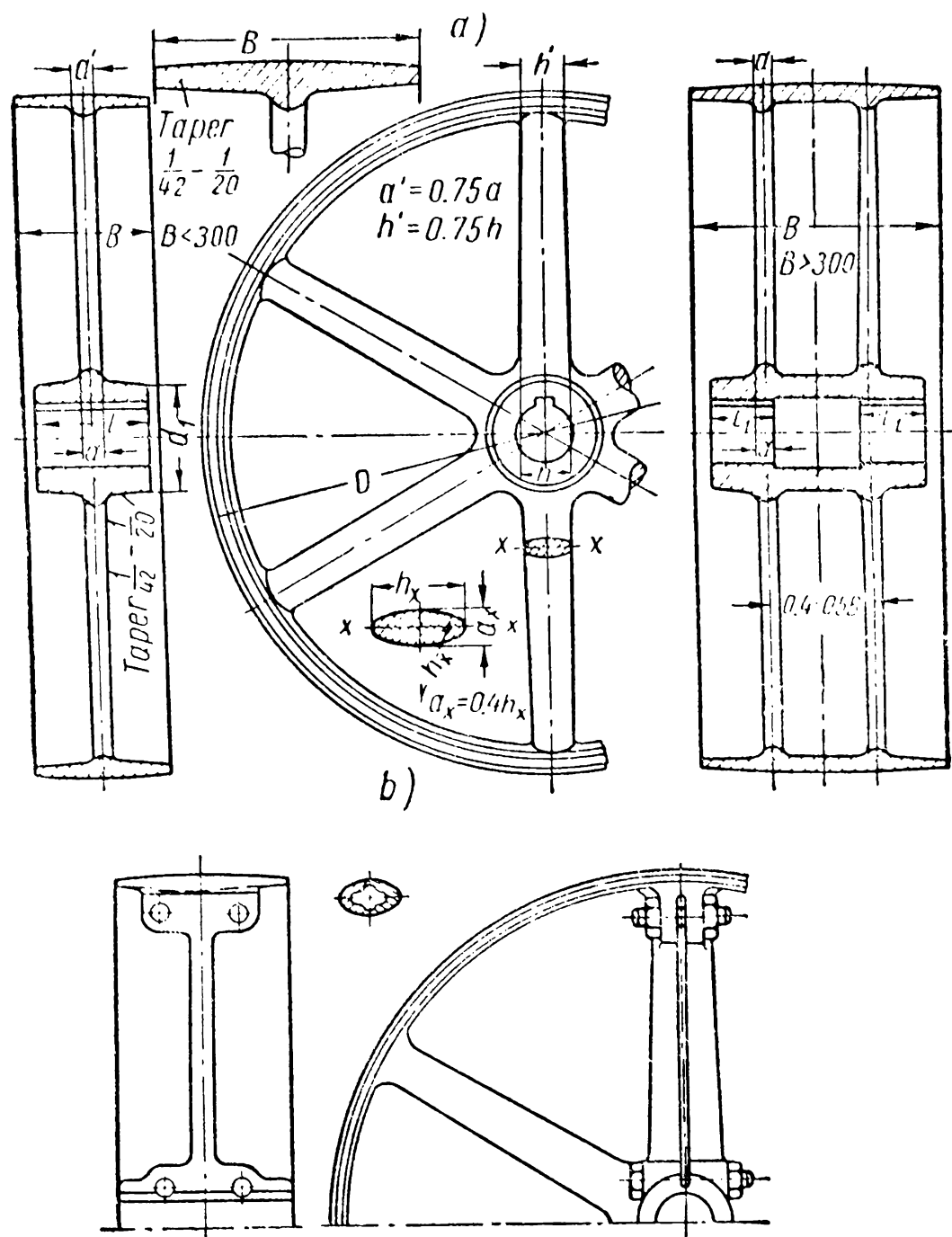


Fig. 126

*Cast-iron* pulleys are the most frequent, pulleys of small diameter being made as a solid cylinder, those of medium diameter with the hub connected to the rim by a solid web and those of large diameter with the hub and rim connected by spokes.

The dimensions in Fig. 126, *a* are established for members of cast-iron pulleys.

The design of a cast-iron pulley for strength is usually confined to determining stresses in the rim due to centrifugal forces and the sectional sizes of the spokes as regards their bending strength.

The stresses in a thin circular rim caused by centrifugal forces are determined as for belts [see equation (177)]

$$\sigma = \frac{\gamma \times v^2}{10 \times g} \leq [\sigma]_t.$$

Hence the maximum peripheral velocity permissible for a rim made from the given material

$$v_{\max} \approx 10 \sqrt{\frac{[\sigma]_t}{\gamma}} \text{ m/sec.} \quad (182)$$

Consequently,  $v_{\max}$  does not depend on the rim size but is found only from the specific weight of the rim material  $\gamma$  kg/dm<sup>3</sup> and the stress due to tension  $[\sigma]_t$  kg/cm<sup>2</sup> allowable for the rim.

Pulleys with a peripheral velocity of up to 25 m/sec are made from cast iron CЧ 12-28. Speeds of 25-30 m/sec require cast iron CЧ 15-32 and speeds of 30-35 m/sec cast iron CЧ 21-40.

When the pulley diameter does not exceed 300 mm three spokes are used, 600 mm—four, after which for every 600-1,000 mm increase in diameter two more spokes are added.

The rim width of  $B \leq 300$  mm requires spokes arranged in one row; greater width requires two rows of spokes.

The cross-section of the spokes at the hub is calculated for bending on the basis of the arbitrary moment  $\frac{PD}{2}$  spread over one-third of the total number  $A$  of the spokes in the pulley.

The strength equation of a spoke is

$$\frac{1}{3} AW_{sp} [\sigma]_b = \frac{PD}{2} \quad (183)$$

where  $W_{sp}$  is the section modulus of the spoke. For an elliptic cross-section (see Fig. 126, a)

$$W_{sp} = 0.1 \times a \times h^2 = 0.04 \times h^3. \quad (184)$$

At  $[\sigma]_b = 300$  kg/cm<sup>2</sup> we find from the relations (183) and (184) the major axis of the ellipse

$$h = \sqrt{\frac{PD}{8A}}. \quad (185)$$

The arbitrary nature of such computation is obvious because: 1) the deformations of the rim and spokes are accounted for separately whereas actually they are interrelated; 2) the peripheral effort is assumed to be spread over one-third of the total number of spokes whereas actually this distribution depends on the relation between the rigidities of the spokes and the rim. Therefore, to design pulleys of large size carrying severe loads use is made of more accurate methods which are free from the arbitrary nature of this elementary design.

*Split* cast-iron pulleys are intended to be fitted onto shafts between the bearings and couplings without disassembling them. The split should be made along the spokes for which purpose their number should be even. The major axis of ellipse of split spokes (see Fig. 126, *b*) is increased by 30-40% while the minor axis is the same in all spokes. Fastening bolts or, more often, studs are located

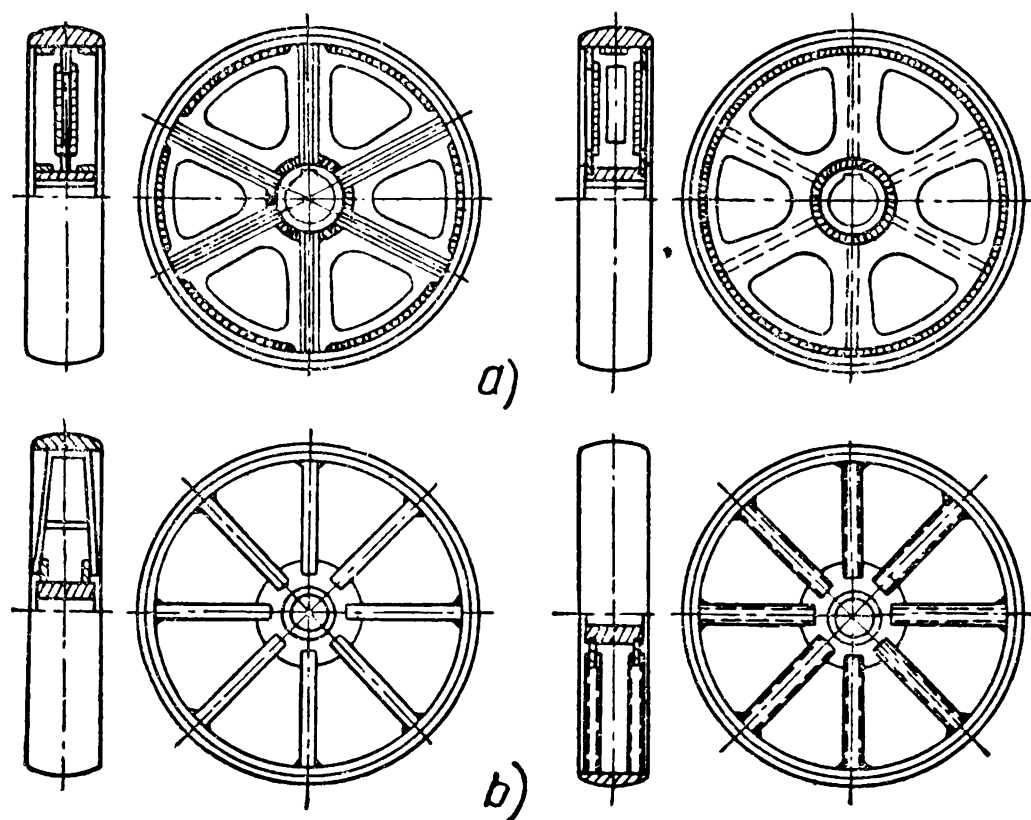


Fig. 127

as close to the shaft and the rim centre of gravity as possible to eliminate bending stresses in the joints. Solid pulleys are much more preferable than heavier and more complicated split pulleys, the latter being employed only when other designs prove inadequate.

In *welded belt pulleys* the rim is roll-bent from flat steel while the hub is made from round rolled stock or a forging.

The hub is usually fastened to the rim by means of solid webs: one web being used with rims up to 350 mm wide and two webs when the rim width is larger. To reduce weight round or pyriform holes are cut in the solid webs and stiffeners are welded to increase rigidity (Fig. 127, *a*). Sometimes instead of solid webs spokes made from flat steel or pipes are used (Fig. 127, *b*). Spoked pulleys are lighter than solid-web pulleys but since they are composed of many elements they are more difficult to manufacture.

Hubs are made from steel 5 and webs and rims from steel 3.

Calculations in welded pulleys are made for the rim, solid webs or spokes and the seams connecting these elements and fastening them to the hub.

Mass produced *pulleys for V-belts* are sometimes welded from press-worked blanks (Fig. 128).

Axial flexibility ranks among the advantages offered by these pulleys. This favours a more uniform load distribution over the belts than in pulleys with rigid cast rims.

**Belt Tension Adjusters.** In drives without special adjusters tension is provided by elastic deformation of the belt tightly fitted onto the pulleys. However, in course of time the belts stretch and must be shortened to maintain tension at the required level. Frequent

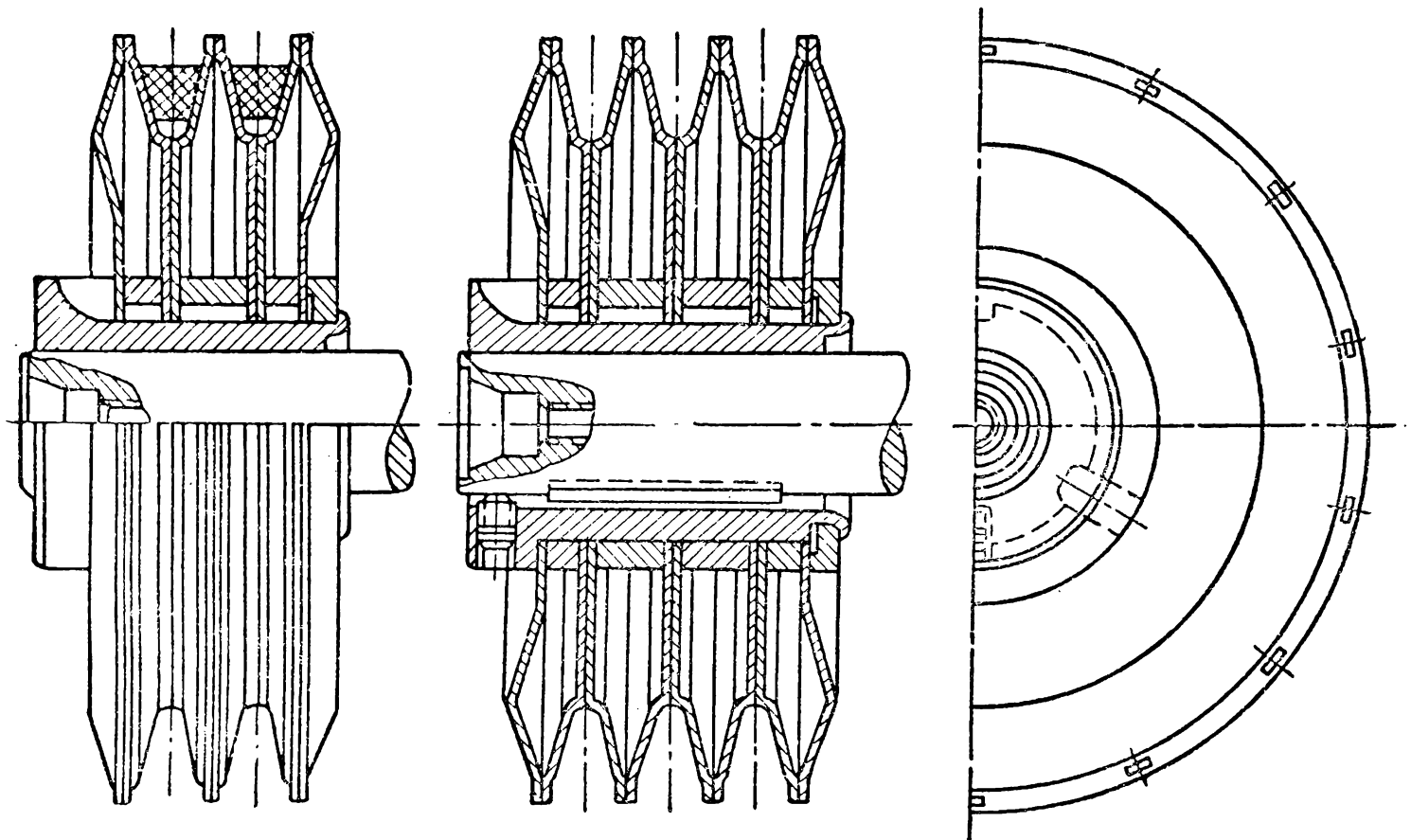


Fig. 128

restitching of the belts is most undesirable while endless belts cannot be restitched at all. Therefore, in modern drives provision is usually made for belt tension adjusters.

The travel of a tension adjuster accounting for possible stretching of the belts is assumed to be 5-10% of the centre distance. In V-belt drives for easy assembly a shift of twice the belt thickness in a reverse direction is required.

According to their design and principle of operation belt tension adjusters fall into three groups: 1) *take-up slides and tilting plates*, 2) *idler pulleys*, 3) *automatic tighteners*. Let us briefly examine each of them.

1. In ordinary tension adjusters the electric motor with the power pulley shifts on slides (Fig. 129, a) or is pivoted on an axle (Fig. 129, b). Constant initial tension is attained by fixing the electric motor on pivoted slides (Fig. 129, c).

The necessary arm  $c$  is found from the equilibrium equation (Fig. 129, c).  $G \times c = S_2 c_2 + S_1 c_1$ .

When necessary the free end of the slides is made to act against the action of a spring or a counterweight.

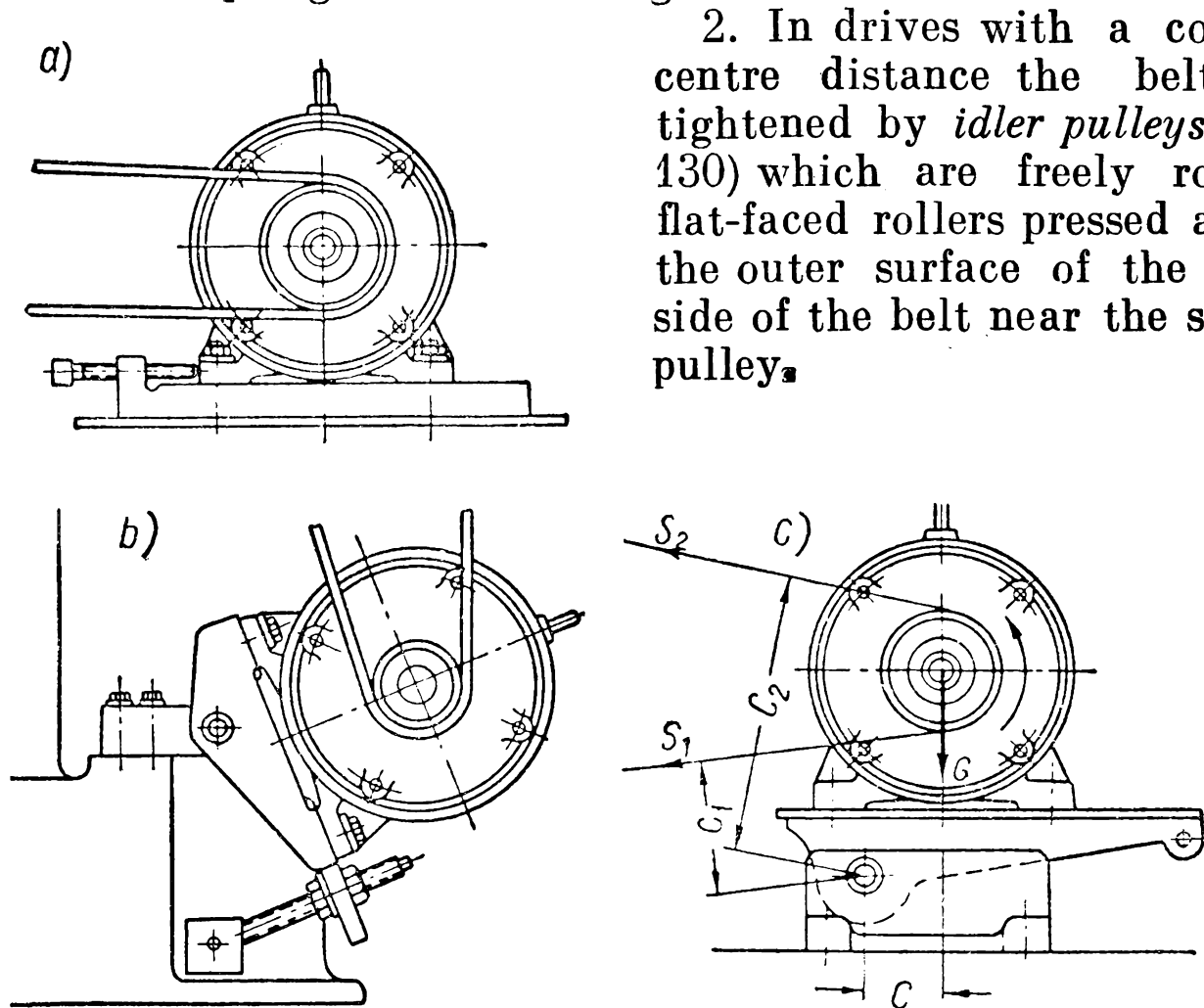


Fig. 129

Before V-belts appeared idler pulleys were the only devices in flat-belt drives which permitted high velocity ratios with small distances between the shafts. In drives with idler pulleys this was achieved due to a larger arc of contact. However, the employment of idler pulleys has its negative aspect: they cause an additional reverse flexing of the belt which wears it at a faster rate. V-belts, therefore, which give the same efficiency without idler pulleys, made them to a large extent unnecessary.

Since the harmful effect of bending is greater the smaller the bending radius and the less time between two consecutive flexures, the diameter of the idler pulley  $D_p$  should never be below the diameter  $D_{\min}$  of the smaller pulley; the distance  $A_p$  between the axes of the idler pulley and the nearest (usually smaller) pulley should not be excessively small;  $A_p \geq D_{\min} + D_p$  is recommended.

The fulcrum axle of the idler pulley is so fixed as to increase the arc of contact on the pulleys and maintain belt tension as the belt stretches. The required pressure exerted by the idler pulley on the



belt is created by a counterweight (Fig. 130, *a*) or a spring (Fig. 130, *b*). The idler pulley axle should be as strictly aligned as the axles of the pulleys. Therefore, an idler pulley should be sufficiently rigid in design. The idler pulley should freely rotate on antifriction bearings on which it is usually secured.

The size of the counterweight  $G$  (or the spring load) is found from the equilibrium condition (Fig. 130, *a*)

$$Gl_3 - G_p l_2 - Q_p l_1 = 0$$

where  $G_p$  is the idler pulley weight,  $l_1$ ,  $l_2$ ,  $l_3$ —arms determined from a sketch of the drive drawn to scale,

$Q_p = \bar{S}_1 + \bar{S}_2 = 2S_2 \sin \frac{\alpha_p}{2}$ —the load brought to act on the idler pulley by belt tension,  $\alpha_p$ —the arc of contact between the idler pulley and the belt.

Idler pulleys in drives with a sharply varying load are provided with dashpots to damp the system vibrations.

In V-belt drives it is usually unnecessary to increase the arc of contact. Idler pulleys are used here only to tighten the belts. This makes it possible to avoid reverse flexure of the belt by installing deflecting pulleys with V-shaped grooves (Fig. 130, *c*). Only in extreme cases have the usual flat-faced idler pulleys to be mounted.

3. The devices we have examined above (take-up slides, tilting plates, idler pulleys) make it possible only to create a definite ten-

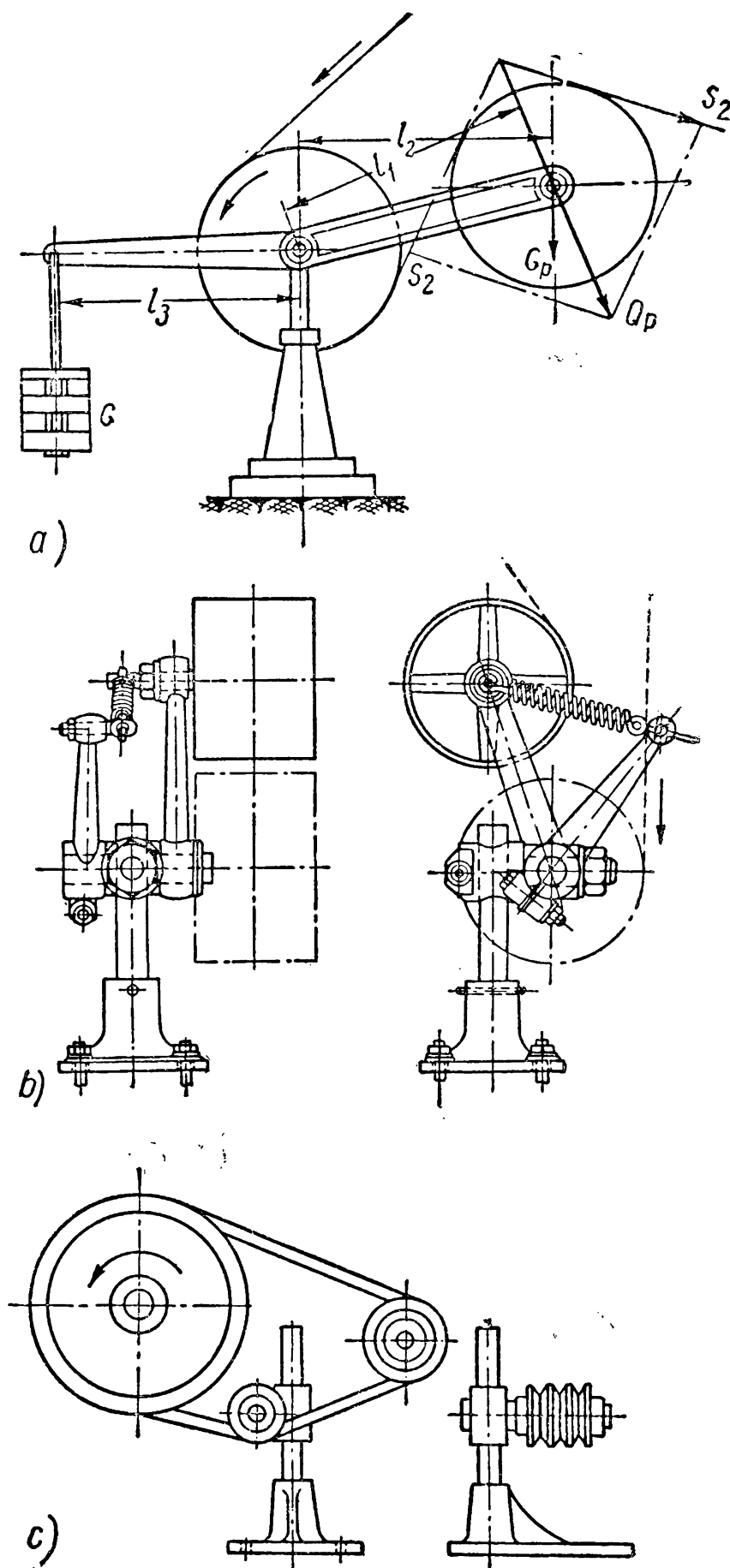
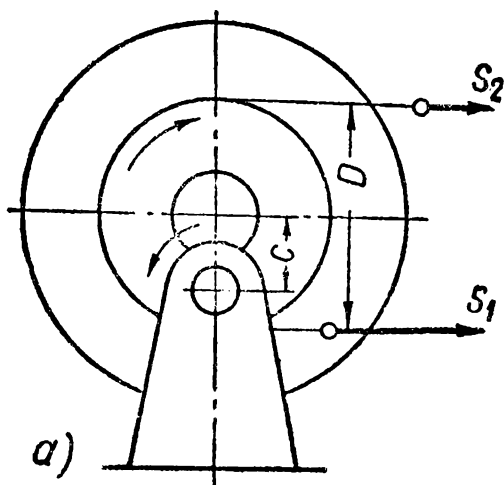


Fig. 130

sion of the belts and maintain it at a constant level\*. However, the development of friction drive designs proceeds along the lines of making belt adjustment automatic in accordance with the actual load carried by the drive. In recent years more and more of such devices have been used in belt drives.



The general principle of their operation is illustrated by the diagram in Fig. 131, *a*. It is based on the utilisation of reactive torque in an electric motor stator or gear wheel.

Thus, as the rotor of an electric motor turns clockwise, together with the pulley (Fig. 131, *a*), its stator pivoted on an axle displaced by the distance  $c$  relative to the shaft axis,

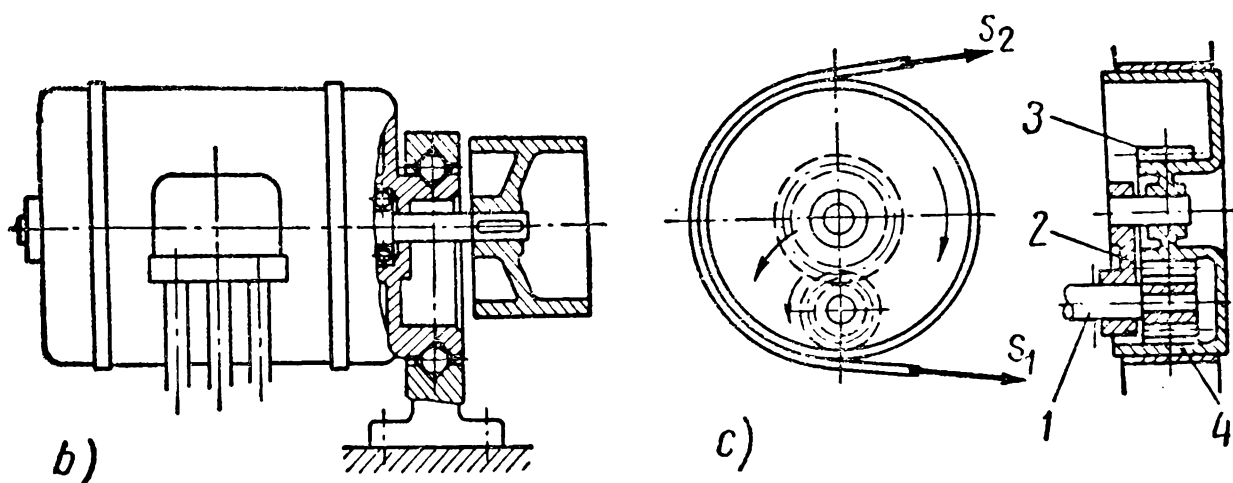


Fig. 131

tends to turn counterclockwise under the action of the reactive torque. Simultaneously, the axis of the rotor with the pulley shifts to the left, the distance between the centres increases and the belt tightens.

It can be seen from the system equilibrium equation (Fig. 131, *a*)

$$S_1 \left( \frac{D}{2} - c \right) = S_2 \left( \frac{D}{2} + c \right)$$

that we can always find such value of  $c$  (the distance between the rotor and stator axes) at which the ratio of tensions  $S_1/S_2$  ensures the work of the drive without slippage. In this case a change in load—rest, starting, operation, idle run—will correspondingly alter the tension of the belt sides.

The above-described general principle shows that belt tension adjusters can be designed in a number of ways.

\* The constant initial tension  $S_0$  is obtained with the help of take-up slides and plates; the constant tension of the driven side  $S_2$  is created by idler pulleys.

In the design in Fig. 131, *b* the end-shield of an electric motor stator carries an eccentric disc with a ball raceway. The disc is arranged to fit into the post with a similar inner raceway and a number of balls are inserted between them. The belt is tightened by the reactive torque acting upon the electric motor stator.

Another design is shown in Fig. 131, *c*. Here shaft 1 of an electric motor carries a keyed driving pinion 4 and a freely swinging link 2, on whose axle rotate the driven gear 3 and the belt pulley rigidly secured to it.

When the rotor of the electric motor turns counterclockwise and the pulley clockwise, the link is acted upon by the moment from the peripheral effort on pinion 4 directed counterclockwise and creating in the belt a tension proportional to the transmitted load.

**V-Belt Variable-Speed Drives.** Thanks to its shape and comparatively large pulling capacity a V-belt facilitates the development of various designs of drives with a stepless speed change.

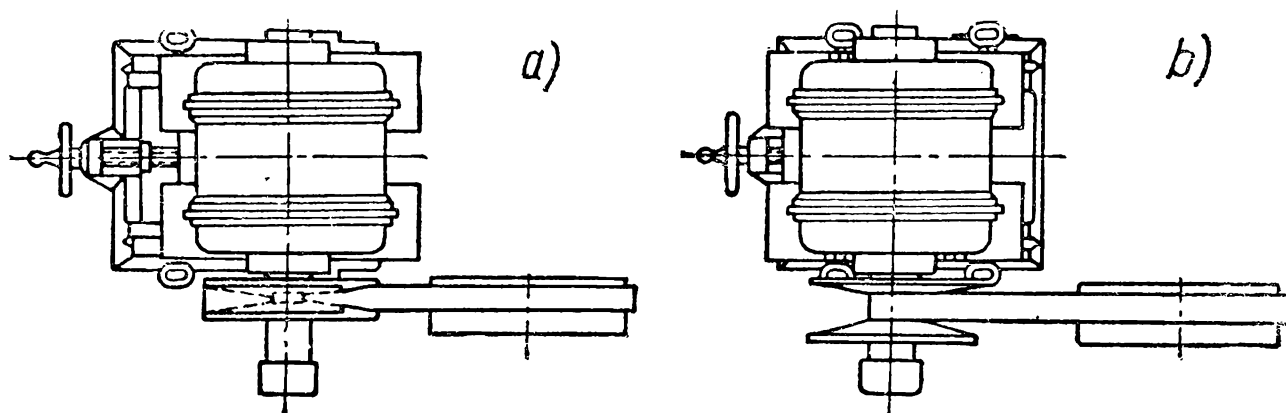


Fig. 132

The simplest design is shown in Fig. 132. A special broad V-belt travels over a flat-faced and a V-grooved pulley. Both sides of the pulley forming a V-groove are held together by a spring. A shift of the electric motor along the slides changes the position of the belt in the groove and at the same time the velocity of the belt and the driven pulley. Fig. 132, *a* shows a position for maximum and Fig. 132, *b* for minimum velocity of the driven pulley.

Other numerous designs of V-belt variable-speed drives are divided according to the following main characteristics: size of belt—with standard and special-purpose broad belts; number of adjusted pulleys—with 1, 2 or 4 pulleys. Besides, variable-speed drives differ in the way their belts are tightened and in other less important features.

The velocity control range is naturally the most important factor. The development of new types of variable-speed drives is entirely due to the work being done to broaden this range.

Let us find the velocity control range  $R$  of a V-belt variable-speed drive.

With one pulley adjusted and the other fixed the velocity control range is  $R_1 = r_{\max}/r_{\min}$  where  $r_{\max}$  and  $r_{\min}$  are the maximum and minimum radii of the circumference of the belt position on the adjusted pulley. The relation between  $r_{\max}$  and  $r_{\min}$  can be expressed by the size of the belt profile ( $b, h$ ) and the pulley groove ( $e, \varphi$ ) as follows (Fig. 133):

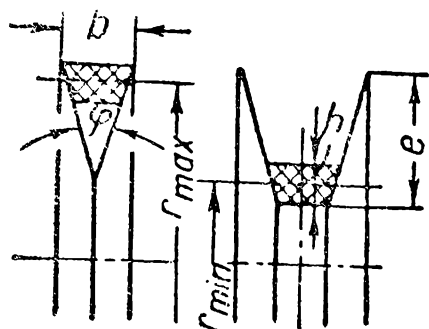


Fig. 133

and

$$r_{\max} = r_{\min} + e - h = r_{\min} + \frac{b}{2} \cot \frac{\varphi}{2} - h$$

$$R_1 = \frac{r_{\max}}{r_{\min}} = 1 + \frac{e}{r_{\min}} - \frac{h}{r_{\min}} = 1 + \frac{b}{2r_{\min}} \cot \frac{\varphi}{2} - \frac{h}{r_{\min}}. \quad (186)$$

If the second pulley is also adjusted and  $R_2 = R_1$  the total velocity control range of the variable-speed drive is  $R_{1,2} = R_1 R_2 = R_1^2$ .

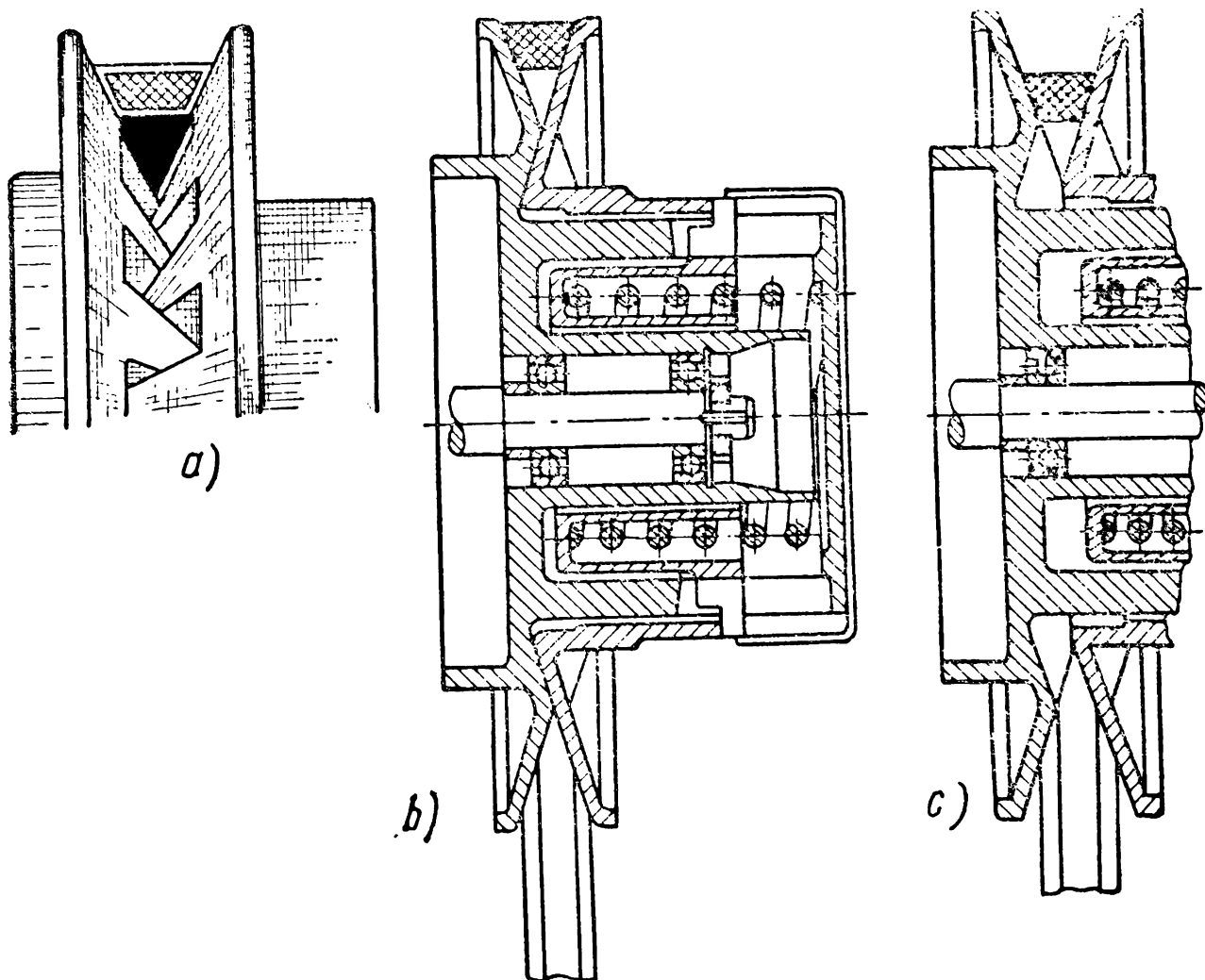


Fig. 134

To estimate the velocity control range obtainable in such drives using standard belts let us take as their optimal relations:  $\varphi = 34^\circ$ ,  $b = 1.8h$ ,  $r_{\min} = 5h$ . In this case we obtain for the two drives examined above  $R_1 \approx 1.4$  and  $R_{1,2} = R_1^2 \approx 1.96$ .

As we see the velocity control range is rather small. The formula (186) shows that it can be widened by using pulleys of a more complex design (with slots—Fig. 134) with the effective groove height

$e > \frac{b}{2} \cot \frac{\varphi}{2}$ , and also belts of a special cross-section—wide belts

with a higher (as compared with the standard  $b \approx 1.8h$ ) width/height ratio  $b \approx (2-3)h$ . Finally, a double drive with four adjustable pulleys (Fig. 135) can be employed in which the velocity control range is  $R_{1-4} = R_{1,2}^2 = R_1^4$ .

In designing V-belt variable-speed drives of all types it is important to maintain the required belt tension throughout the entire velocity control range.

The specific features of this task become clear from the following.

At definite centre distances  $A$  and pulley diameters  $D_1$  and  $D_2$  the necessary length of the belt (Table 25) is

$$L = 2A + \frac{\pi}{2}(D_2 + D_1) + \frac{(D_2 - D_1)^2}{4A}.$$

Obviously, in a variable-speed drive at constant  $A$  the length of belt  $L$  should be variable depending on the values of  $D_1$  and  $D_2$ . The minimum length of belt should be at  $D_1 = D_2 = D_m$ :  $L_{\min} = 2A + \pi D_m$ . The maximum length of belt is obtained for the maximum and minimum diameters:  $L_{\max} = 2A + \pi/2 \times (D_{\max} + D_{\min}) + (D_{\max} - D_{\min})^2/4A$ . Thus, for  $D_{\max} = 250$  mm,  $D_{\min} = 120$  mm,  $D_m = 185$  mm,  $A = 300$  mm,  $L_{\max} - L_{\min} = 1,194 - 1,180 = 14$  mm.

But since the length of belt of a variable-speed drive remains constant it should be chosen from  $L_{\min}$  or  $L_{\max}$ . Hence, to maintain the belt tension at the required level the adjuster should ensure nonuniform travel of the cones as the speed changes. Other possible methods are to change the centre distance during adjustment, employ idler pulleys, etc.

It is seen from the formulae for  $L$ ,  $L_{\max}$  and  $L_{\min}$  that the relative value  $(L_{\max} - L_{\min})$  diminishes with an increase in  $A$  and decrease in  $(D_{\max} - D_{\min})$ . Therefore, in some variable-speed drives (with large distances between the pulley axes, standard belts, small velocity control range) the difference  $(L_{\max} - L_{\min})$  is small and can be compensated for by additional stretching of the belts shifted over from the mean to the extreme position.

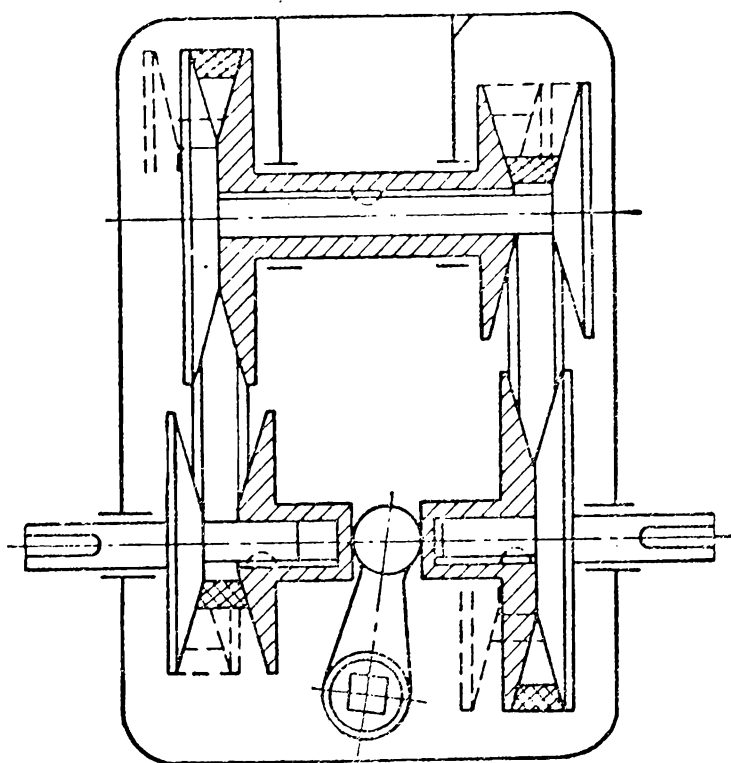


Fig. 135

Sketches of Most

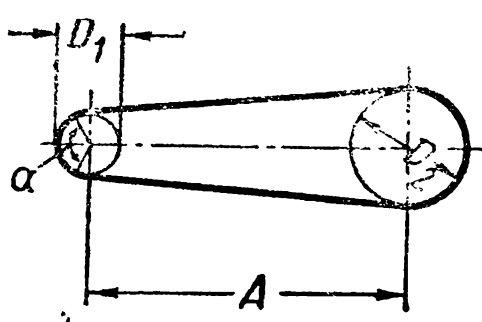
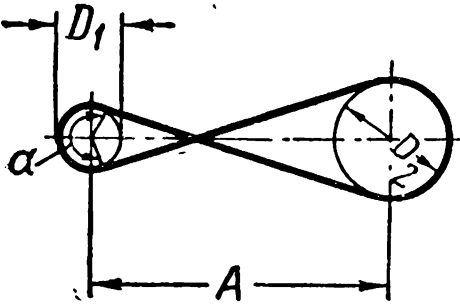
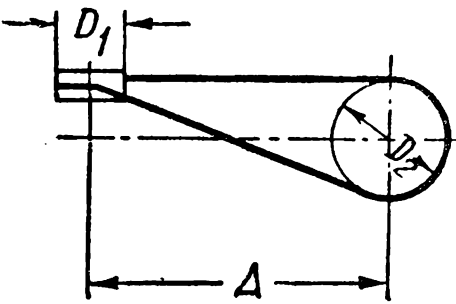
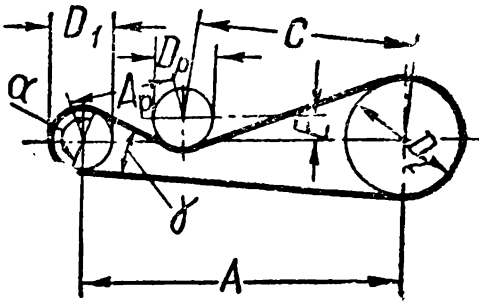
Sketch	
Arc of contact between the belt and the smaller pulley	$\alpha \approx 180^\circ - \frac{D_2 - D_1}{A} 60^\circ$
Geometrical length of belt (disregarding tension and sag)	$L = 2A + \frac{\pi}{2} (D_2 + D_1) + \frac{(D_2 - D_1)^2}{4A}$

Table 25

Widespread Belt Drives

		
$\alpha \approx 180^\circ + \frac{D_2 + D_1}{A} 60^\circ$	$\alpha \approx 180^\circ + \frac{D_1}{A} 60^\circ$	$\alpha \approx 180^\circ - \frac{D_2 - D_1}{2A} 60^\circ + \frac{(D_1 + D_p - 2E)}{2A_p}$
$L = 2A + \frac{\pi}{2} (D_1 + D_2) + \frac{(D_1 + D_2)^2}{4A}$	$L = 2A + \frac{\pi}{2} (D_1 + D_2) + \frac{D_1^2 + D_2^2}{2A}$	$L = (A + A_p + C) + \frac{\pi}{2} (D_1 + D_2) + \frac{(D_2 - D_1)^2}{8A} + \frac{(D_2 + D_p)^2}{8A} + \frac{(D_1 + D_p)^2}{8C} - \frac{E}{A_p} \left( \frac{D_1 + D_p}{2} \right) - \frac{E}{C} \left( \frac{D_2 + D_p}{2} \right)$

It should be noted in conclusion that for horse powers up to  $\approx 10$  kw and the velocity control ranges  $\approx 10$ -12, V-belt variable-speed drives, especially with broad belts, are today the simplest and most dependable stepless devices. In grain harvesters and other agricultural machinery they have completely ousted other types of drives.

### CALCULATION OF BELT DRIVES

In a narrow sense belt drive design can be reduced to determining the size of the pulling belt (or belts) on the basis of the assigned service. Simultaneously, this design gives us loads and basic dimensions of the drive members—pulleys, belt tension adjusters, shafts and bearings.

Different types of belts are mass produced by various branches of industry. Naturally, any belt design should be based on standard data while other changeable characteristics are neglected.

However, the available catalogues do not contain all data necessary for adequate belt design which makes it in some degree arbitrary. In this respect the following should be pointed out:

1. Some manufacturers specify the external sizes of the belt cross-sections without determining their structure. Therefore, in calculations the stresses due to tension are arbitrarily referred to the entire sectional area of the belt. But, in cord-wire V-belts, for example, only cords whose area comprises only 10-15% of the entire belt sectional area are in tension. It is impossible to evaluate the actual stress distribution from the data provided by the respective standard alone.

2. Calculation of service life is based on the mean values of the endurance limit obtained from the tests of belts of various design. The difference in these results is very great.

3. Losses in the belt and its heating depend to a large degree on the internal structure of the belt. Since we have so far no data for determining the type of this relation and the specific values of these losses, these calculations are likewise arbitrary.

However, for all their arbitrariness these calculations, without providing absolute values of stress, loss, temperature and service life of the belt, make it possible to compare and evaluate various designs and also to get some insight into the processes occurring in an operating belt.

**Geometry of Belt Drives.** The arc of contact between the belt and the smaller pulley  $\alpha$  and the belt length  $L$  are some of the initial values necessary for the belt design. These values are related to the distance between the axes of the pulleys  $A$  and their diameters  $D_1$  and  $D_2$  by simple geometrical relations. The expressions for  $\alpha$  and  $L$  for the most widespread drives are given in Table 25.



For more complex drives, in particular for drives with two or more driven pulleys, the values of  $L$  and  $\alpha$  are more easily and accurately found graphically from a sketch of the drive drawn to scale.

The diameters of belt drive pulleys are determined by the dimensions of the drive, required velocity ratio and minimum diameter of the smaller pulley found, on the one hand, from the ratio  $h/D_{\min}$  and, on the other, from  $v_{\max}$  for the given type of belt.

The diameters of pulleys are calculated as follows:

a) The type of belt and its thickness  $h$  are used to find the minimum recommended diameter of the pulley (see Tables 22, 23), for instance, of the power pulley  $D_1$ .

b) Find the diameter of the second pulley using the relation (169)

$$D_2 = \frac{D_1 \times i}{1+s} = \frac{n_1}{n_2} \times \frac{D_1}{1+s}.$$

Elastic creep seldom exceeds 1-2%, i.e., here  $s=0.01-0.02$ .

c) Using  $D_1$  and  $D_2$  and the centre distance  $A$  given by the machine design, draw a sketch of the drive to scale and, with account taken of the position of the belt tension adjuster, compare the obtained size with the given size.

d) If the given size allows it, the pull and service life of the belt can be increased by employing pulleys of larger diameters making sure that the maximum recommended velocity for the given type of belt is not exceeded (See Tables 22, 23).

e) When selecting the pulley diameters refer to respective standards for belt pulleys, approximating the values found from calculations as follows:  $D_1$ —usually to the nearest larger value and  $D_2$ —to the nearest smaller value.

**Calculating Belt Pull.** The initial tension  $S_0$  or the stress  $\sigma_0$  is the most important factor determining the pulling capacity of the drive.

It can be seen from the relations (173), (175) and (176)

$$P = 2\varphi S_0 \quad \text{and} \quad k = 2\varphi \sigma_0 \quad (187)$$

that  $k$  grows in proportion to  $\sigma_0$  and from this point of view it is more advantageous to choose the maximum possible values of  $\sigma_0$ . However, experience shows that there exists a certain optimal value of  $\sigma_0$ . If the belt tension exceeds  $\sigma_0$  several hours of operation will cause the belt to stretch and will reduce the tension approximately to this magnitude. Repeated stretching can only speed up the destruction of the belt. Having regard to this property of belts (due to their fibrous structure) it is irrational to increase the initial tension above the value  $\sigma_0=18 \text{ kg/cm}^2$  for all flat belts and  $\sigma_0=12 \text{ kg/cm}^2$  for V-belts.

These values of  $\sigma_0$  have been obtained experimentally under the following conditions: an open-belt drive with cast-iron pulleys, constant load, belt velocity  $v=10$  m/sec, arc of contact  $\alpha=\pi$ , the pull factor  $\varphi=\varphi_0$ .

Recalculation of the values  $\sigma_0$  for other kinds of service is based on the assumption that the maximum allowable tensions are constant in the belt.

In an operating belt the maximum tensions arise on the tight side. Their respective stresses are:

$$\sigma = \sigma_0 + \frac{k}{2} + \sigma_v.$$

Let us limit these stresses to a constant value  $[\sigma]$ .

Further, from the relations (173) and (187) we replace

$$\sigma_0 + \frac{k}{2} = k \frac{m}{m-1}.$$

After substitution we obtain  $[\sigma] = k \frac{m}{m-1} + \sigma_v$ ,

whence

$$k = ([\sigma] - \sigma_v) \frac{m-1}{m}. \quad (188)$$

The same formula for experimental conditions is

$$k_0 = ([\sigma] - \sigma_{v0}) \frac{m_0-1}{m_0}. \quad (189)$$

From the equations (188) and (189) we obtain *useful stress for any kind of service*

$$k = k_0 \frac{[\sigma] - \sigma_v}{[\sigma] - \sigma_{v0}} \times \frac{(m-1)m_0}{(m_0-1)m} = k_0 \times c_v \times c_\alpha \quad (190)$$

where  $c_v = \frac{[\sigma] - \sigma_v}{[\sigma] - \sigma_{v0}}$  is the velocity factor and  $c_\alpha = \frac{(m-1)m_0}{(m_0-1)m}$  is the factor of the arc of contact.

The factor  $c_v$  shows by what amount the velocity of the designed drive deviates from  $v=10$  m/sec and  $c_\alpha$  shows the deviation of the arc of contact from  $\alpha=\pi$ . The ordinarily recommended values of the factors  $c_v$  and  $c_\alpha$  are given in Tables 26 and 27.

Table 26

Velocity Factor  $c_v$

Belt velocity $v$ in m/sec		1	5	10	15	20	25	30
$c_v$	for flat belts	1.04	1.03	1.0	0.95	0.88	0.79	0.68
	for V-belts	1.05	1.04	1.0	0.94	0.85	0.74	0.60

Table 27

Factor of the Arc of Contact  $c_\alpha$ 

Arc of contact $\alpha^\circ$		80	120	140	160	180	220
$c_\alpha$	for flat belts	—	0.82	0.88	0.94	1.0	1.12
	for V-belts	0.62	0.83	0.90	0.96	1.0	1.08

The belt pull also depends on bending stresses in the belt and unit pressure between the belt and the rim. The former affect the belt stretch and the latter the contact between belt and pulley. These effects are accounted for by the expression

$$k_0 = a - w \frac{h}{D} \quad (191)$$

where  $a$  and  $w$  are constants found experimentally; their values for various types of belts are given in Tables 22 and 23 (pp. 213 and 216).

After finding the value  $k_0$  from the formula (191) and then  $k$  from the formula (190) we determine the width of a flat belt

$$b = \frac{P}{kh} \quad (192)$$

The value  $b$  is approximated to the nearest standard value.

With V-belts the usual practice is first to decide on the belt profile and then find  $k_0$ ,  $k$  and finally the number of belts in conformity with the constants  $a$  and  $w$

$$z = \frac{P}{kF} \quad (193)$$

To reduce the amount of intervening calculations reference books contain tables specifying the values  $P_1$  for one V-belt or per cm of the width of flat belts calculated from the above formulae.

The pull of the belt is limited, as a rule, by its adhesion to the smaller pulley. This pulley has a lesser arc of contact and less favourable ratio  $h/D$ . Therefore, the larger pulley always has extra adhesion which increases, the greater the difference between the diameters of the power and receiving pulleys.

Attempts to utilise this phenomenon have resulted in the development of a *flat V-belt drive*: a V-belt on the smaller pulley rides as usual in a V-shaped groove developing maximum pull, while on the larger pulley it operates as a flat belt riding on a flat-faced rim with its lower side (Fig. 136). This drive is employed for ratios 1 : 4 and higher when the design considerably reduces the cost of manufacture of the larger pulley.

V-belts of *O* profile (see p. 215) operate unsteadily on their lower side—they often tip up and are therefore not employed in the drives under consideration. The same is true of all belts which due to specific features of their manufacture are somewhat twisted. Belts for flat V-belt drives should be specially selected.

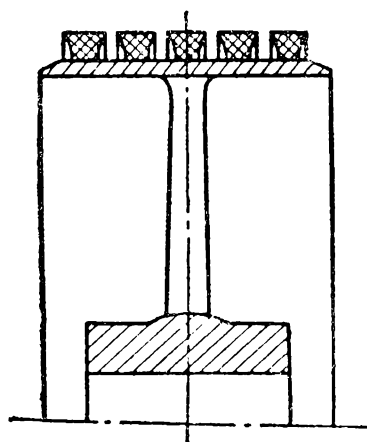


Fig. 136

**Calculating Belt Service Life.** Like the pull, service life is a very important characteristic of belts. Under normal operating conditions the belt is put out of commission as a result of the wear of separate fibres sustaining varying stresses, intensified by the heating of these fibres due to belt losses. The problem of ensuring adequate service life of belts has grown more urgent in recent years because newly developed

types of belt are frequently made to operate under heavy service (high speeds, small drive dimensions). A theoretically substantiated design method taking account of all the main factors which affect belt life has not yet been evolved. The data of recent research allow us only to come nearer to a separate appraisal of the effect cyclic stresses and heating have on the belt life.

The maximum changes in stress in a belt take place in its passage round the pulley (Fig. 119). We can say therefore that during one complete cycle (one turn of the belt) the stresses in the belt change as many times as there are pulleys and idler pulleys in the drive. Each of these individual cycles affects the belt service life and should not be neglected. However, up till now it has not yet been ascertained how and in accordance with what law a belt passing over pulleys of different diameters accumulates faults due to fatigue which finally cause its failure. All known investigations of belt life have been conducted on pulleys of the same diameter. Since a method of fault summation has not yet been worked out the calculations must be based on the stresses  $\sigma_{\max}$  which arise on the smaller pulley, i. e., in the severest part of the cycle.

Tests of belts have not revealed any stable endurance limit. After a sufficiently large number of cycles the belt disintegrates under any load\*.

The general *equation of belt service life* can be written thus

$$\sigma_{\max}^m \times 3,600 \times u \times x \times H = \sigma_{fat}^m \times N_{base}$$

whence

$$H = \frac{N_{base}}{3,600u \times x} \left( \frac{\sigma_{fat}}{\sigma_{\max}} \right)^m \text{ hrs.} \quad (194)$$

---

\* Only endless belts can be effectively tested for service life since in sewed belts the weak spot is as a rule in the joint.

Here  $N_{base}$  is the base of fatigue tests assumed equal to  $10^7$  cycles;  
 $\sigma_{fat}$ —endurance limit corresponding to the number of loadings  $N_{base}$ , determined from the mean fatigue curve;  
 $\sigma_{max}$ —maximum stress in the belt found from the equation (179);

$u$ —number of turns of the belt per second (equals the relation of the belt velocity in m/sec to its length in m,  $u=v/L$ );

$x$ —number of pulleys in the drive;

$H$ —service life of the belt in hours.

The investigation of previously published data combined with research into the fatigue failure of belts has enabled the Experimental Research Institute of Metal-Cutting Machine Tools to recommend the following mean values of  $m$  and  $\sigma_{fat}$ :

for flat (rubber and cotton) belts  $m=5$ ; for V-belts  $m=8$ ; limits of endurance at cycles  $N_{base}=10^7$  approximated: for flat rubber belts  $\sigma_{fat}=60$  kg/cm<sup>2</sup>; for flat cotton belts  $\sigma_{fat}=30$  kg/cm<sup>2</sup>; for V-belts  $\sigma_{fat}=90$  kg/cm<sup>2</sup>.

The effect of heat on belt service life can be taken into account in the following manner.

At the stable belt temperature which sets in after a certain period of operation all heat created will be dissipated into ambient air.

From the formulae (180) and (36) the heat balance equation for this case is

$$L_{\bullet} = S_{cool} \omega \tau = F \times v \times k_p.$$

Hence the temperature drop in the belt and ambient air

$$\tau = \frac{F \times v}{S_{cool} \omega} k_p. \quad (195)$$

The relation of the sectional area  $F$  to the outer surface of the belt  $S_{cool}$  equals

for flat belts

$$\frac{F}{S_{cool}} = \frac{bh}{2(b+h)L} \approx \frac{bh}{2bL} = \frac{h}{2L}$$

since  $h \ll b$ ;

for V-belts ( $\varphi_0=40^\circ$ ,  $b=1.6h$ )

$$\frac{F}{S_{cool}} = \frac{0.8bh}{2.9bL} \approx \frac{h}{3.6L}.$$

In a general form

$$\frac{F}{S_{cool}} = \frac{h}{jL},$$

where  $j=2$  for flat belts and  $j=3.6$  for V-belts.



As a rule, the arc of contact  $\alpha$  does not drop below  $120^\circ$ . Therefore, in the formulae (197)-(199) for preliminary calculations the term  $\sin \alpha/2$  can be omitted (i. e., replaced by unity). In this case the error in the sense of increasing the load will not exceed 15%.

**Transmitted Horse Power and Efficiency of Belt Drives.** A belt travelling at  $v$  m/sec and carrying a load  $P$  kg transmits the horse power

$$N = \frac{Pv}{75} \text{ h. p.} \quad \text{or} \quad N = \frac{Pv}{102} \text{ kw.} \quad (201)$$

The losses in a belt drive  $L_e$  are spread over the entire route from the power shaft to the driven shaft. Since the relative magnitude of these losses is small their detailed separation for the calculation of pull is of no practical value. Therefore, a belt drive can be designed on the basis of maximum useful peripheral effort on the driven pulley and respective useful horse power  $N$ , relegating all losses to the driving shaft.

In this case the efficiency of a belt drive (disregarding air resistance and friction in the bearings) will be

$$\eta = \frac{Pv}{Pv + L_e} \quad (202)$$

Mean values of efficiency for ordinary drives:

open flat belt drive— $\eta=0.98$ ;

ditto with an idler pulley— $\eta=0.95$ ;

V-belt drive— $\eta=0.96$ .

**Rational Design and Computation of a Belt Drive.** A belt drive is designed in the following sequence: a design sketch of the drive—design calculations and choice of belt—rational design of parts—revised calculation of the drive.

Design calculations include: a) choice of the type of drive, b) determining the diameters of pulleys, c) determining cross-section and number of belts, d) choice of belt in conformity with manufacturer's standards, e) specifying the centre distance. The revised calculation includes: a) calculating stresses in the belt, b) checking the belt for service life, c) determining loads carried by the shafts, d) design of belt tension adjusters, pulleys and other parts.

Calculations are repeated until the most advantageous design is developed.

*Example.* Design a belt drive from an electric motor to the flywheel of a forging press from the following data: motor horse power— $N=80$  kw; during operation the motor is overloaded, the overload factor being  $\beta=1.5$ ; rated speed of the motor  $n_1=730$  rpm, of the press flywheel  $n_2=300$  rpm; the flywheel with diameter  $D_2=1,500$  mm is preferably used as the driven pulley; distance between the axles of the flywheel and the motor pulley can be about  $A \approx 1,650$  mm.

Of the two types of belts (flat or V-shaped) for the given conditions—

comparatively small distance between the axles and varying load—a V-belt will be most effective.

The design diameter of the driving pulley is found from the equation (169):

$$D_1 = \frac{n_2}{n_1} D_2 (1 + s) = \frac{300}{730} 1,500 (1 + 0.02) = 630 \text{ mm.}$$

The belt velocity is

$$v = \frac{\pi D_1 \times n_1}{1,000 \times 60} = \frac{\pi \times 630 \times 730}{1,000 \times 60} = 24.1 \text{ m/sec.}$$

The rated peripheral effort from the formula (201) is

$$P_{rated} = \frac{102 \times N}{v} = \frac{102 \times 80}{24.1} \approx 340 \text{ kg.}$$

The design effort transmitted by the belts accounting for overload

$$P = \beta \times P_{rated} = 1.5 \times 340 \approx 500 \text{ kg.}$$

The belt cross-section is chosen in advance on the basis of stress due to initial tension (p. 235)  $\sigma_0 = 12 \text{ kg/cm}^2$  and of the pull factor (p. 207)  $\varphi = \varphi_0 = 0.7$ . In this case the stress in the belt caused by useful load will amount to [formula (187)]:

$$k = 2\varphi\sigma_0 = 2 \times 0.7 \times 12 = 16.8 \text{ kg/cm}^2.$$

The required total area of the belt cross-section

$$z \times F = \frac{P}{k} = \frac{500}{16.8} = 29.8 \text{ cm}^2.$$

Using Table 23 we find the number of belts of various cross-sections:

Belt cross-section . . . . .	C	D	E
Sectional area of one belt $F \text{ cm}^2$ . . . . .	2.3	4.8	7.0
Number of belts $z$ . . . . .	13	6.3	4.3

We choose cross-section D. Very few belts of this cross-section are required. The relation between belt height and the diameter of the smaller pulley is more favourable with this cross-section than in a belt with cross-section E; the service life of the belt will be correspondingly longer.

The design length of the belt (see Table 25) is

$$L = 2A + \frac{\pi}{2} (D_2 + D_1) + \frac{(D_2 - D_1)^2}{4A} = 2 \times 1,650 + \\ + \frac{\pi}{2} (1,500 + 630) + \frac{(1,500 - 630)^2}{4 \times 1,650} = 6,760 \text{ mm.}$$

The nearest standard length of belt D is  $L = 7,100 \text{ mm}$ .

Substituting the value  $L$  in the latter equation and solving it relative to  $A$  we find the distance between the axles corresponding to the chosen length of belt.

$$A = 1,850 \text{ mm.}$$

The minimum centre distance  $A$  needed to fit the belt is

$$A_{min} = A - 2h = 1,850 - 2 \times 19 = 1,812 \text{ mm.}$$



The maximum centre distance  $A$  needed to compensate for stretch is

$$A_{\max} \approx (1.05-1.10) \times A = 1.05 \times 1,850 \approx 1,950 \text{ mm}.$$

We now finally calculate the required number of belts. From the formula (191) and using Table 23 we find

$$k_0 = a - w \frac{h}{D_{\min}} = 32 - 280 \frac{19}{630} \approx 23.5 \text{ kg/cm}^2.$$

[The arc of contact on the smaller pulley (see Table 25) is

$$\alpha^\circ \approx 180^\circ - \frac{D_2 - D_1}{A} 60^\circ = 180^\circ - \frac{1,500 - 630}{1,850} 60^\circ = 152^\circ.$$

The factor of the arc of contact (Table 27)  $c_\alpha = 0.93$ , the velocity factor (Table 26) at  $v \approx 24.1$  m/sec is found by interpolation:  $c_v = 0.76$ .

With these magnitudes from the equation (190)

$$k = k_0 c_v c_\alpha = 23.5 \times 0.76 \times 0.93 = 16.6 \text{ kg/cm}^2.$$

The required number of belts (193) is

$$z = \frac{P}{kF} = \frac{500}{16.6 \times 4.8} = 6.3.$$

We take  $z$  to equal 6 belts.

Let us determine the service life of the belts (see p. 238).

For this purpose we first find the maximum stress in the belt (179)

$$\begin{aligned} \sigma_{\max} &= \sigma_0 + \frac{P}{2zF} + \frac{\gamma v^2}{10 \times g} + E_b \frac{h}{D_{\min}} = 12 + \frac{500}{2 \times 6 \times 4.8} + \frac{1.5 \times 24.1^2}{10 \times 9.81} + \\ &+ 1,000 \frac{19}{630} = 12 + 8.7 + 9 + 30 \approx 60 \text{ kg/cm}^2. \end{aligned}$$

The number of travels per second (see p. 239.)

$$u \frac{v}{L} = \frac{24.1}{7.1} = 3.4.$$

The belt service life from the formula (194) is

$$H = \frac{N_{\text{base}}}{3,600 \times u \times x} \left( \frac{\sigma_{\text{fat}}}{\sigma_{\max}} \right)^m = \frac{10^7}{3,600 \times 3.4 \times 2} \left( \frac{90}{60} \right)^8 \approx 10,500 \text{ hrs.}$$

With a two-shift working day and 300 working days per year this is approximately two years.

The size of the drive pulleys (according to Table 23 and Fig. 125) in mm:  $c=8.5$ ,  $e=28.5$ ,  $t=37.5$ ,  $s=24$ .

The outside diameters of the pulleys are:

$$D_{\text{out}1} = D_1 + 2c = 630 + 2 \times 8.5 = 647 \text{ mm};$$

$$D_{\text{out}2} = D_2 + 2c = 1,500 + 2 \times 8.5 = 1,517 \text{ mm}.$$

The inside diameters of the pulleys are:

$$D_{in1} = D_{out1} - 2e = 647 - 2 \times 28.5 = 590 \text{ mm};$$

$$D_{in2} = D_{out2} - 2e = 1,517 - 2 \times 28.5 = 1,460 \text{ mm}.$$

The angle of grooves on the pulleys  $\varphi_1 = 38^\circ$ ,  $\varphi_2 = 40^\circ$ .

The width of pulleys

$$B_1 = B_2 = (z - 1)t + 2s = (6 - 1)37.5 + 2 \times 24 \approx 240 \text{ mm}.$$

From the relations (197), (193) and (187) the pressure exerted on the shaft is:

$$R = 2\sigma_0 z F \sin \frac{\alpha}{2} = 2 \times 12 \times 6 \times 4.8 \sin \frac{152^\circ}{2} = 670 \text{ kg}.$$

## CHAPTER XV

### GEARING

Toothed gears have found wide application in various branches of mechanical engineering. In many machines, such as metal-cutting machine tools, automobiles, tractors, hoisting and transporting machinery, rolling mills, marine engines, etc., toothed gears form vital elements of main and ancillary mechanisms.

Toothed gears are distinguished by high efficiency, compact layout, reliable service and simple operation.

On the other hand: 1) their manufacture requires special equipment and tools and 2) errors in teeth machining may cause vibration and noise during operation.

For various kinds of service there are a number of mathematical curves which may be used for developing gear tooth outlines.

Toothed gears and wheels can be classified according to a number of features: the mutual position of shafts—giving spur\* (with parallel shafts) and bevel (with shafts inclined at an angle) gears (and respectively spur and bevel wheels, Fig. 138, *a*, *d*); the number of steps—giving one-, two-, three- and multi-step gears; the relative motion of shafts—giving row, planetary and differential gears; gears (and wheels) with external and internal toothing; the housing design—giving open and closed types; the peripheral velocity—giving low-velocity ( $v < 3$  m/sec), medium-velocity ( $v = 3-15$  m/sec) and high-velocity ( $v > 15$  m/sec); the accuracy of manufacture—with 12 degrees of accuracy; the position of the teeth on the wheel rim—giving gears with straight, helical, herringbone and curved teeth (Fig. 138, *a*, *b*, *c*, *f*).

In addition to gears composed of wheels wide use is made of rack and pinion drives to transform rotary into translatory motion or vice versa.

\* With straight or helical teeth.

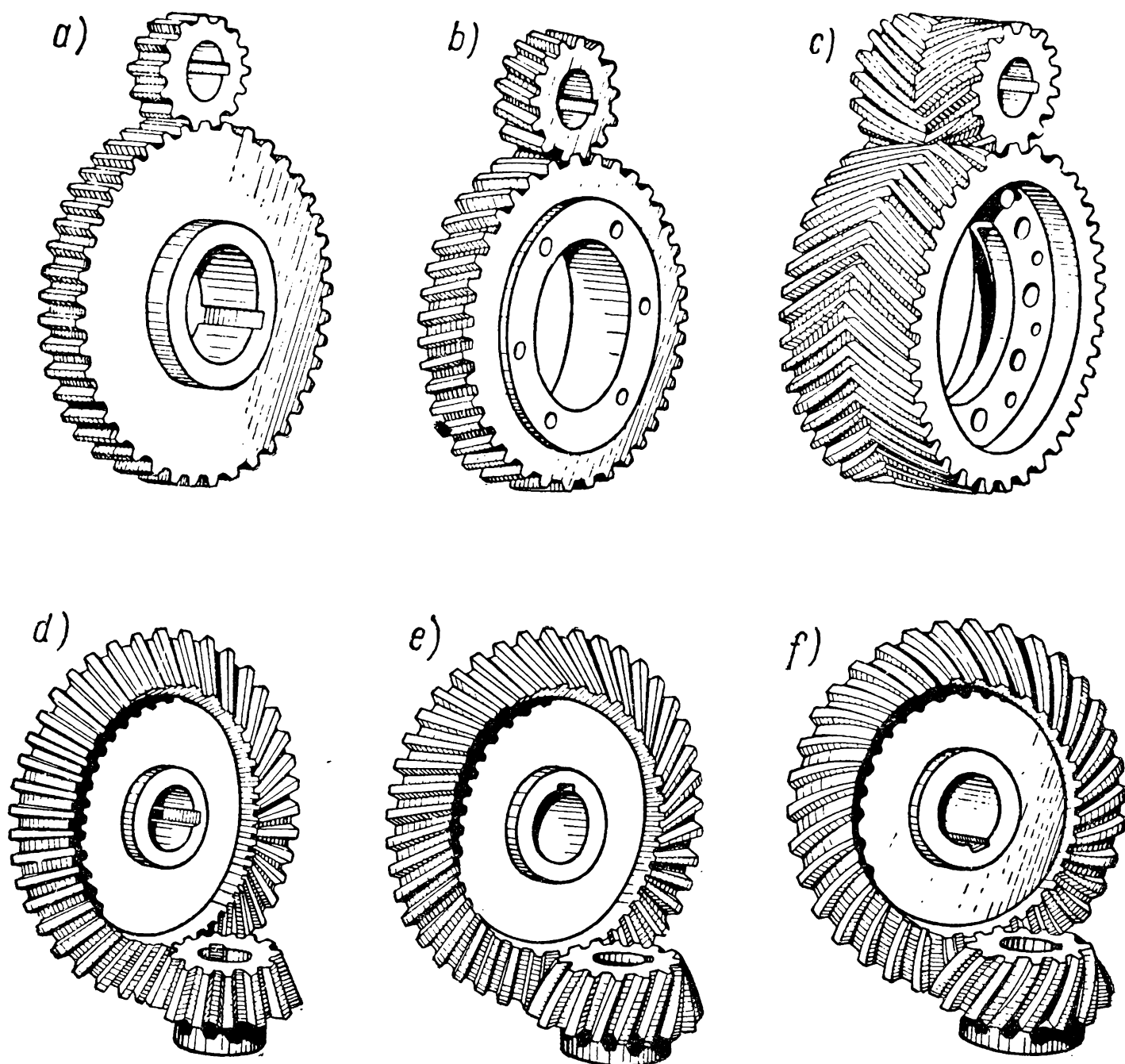


Fig. 138

The form of the tooth profile gives us *involute*, the most commonly employed, and *noninvolute* teeth, the latter type including rounded teeth used in the gear train designed by M. L. Novikov (Fig. 139). Preliminary tests of Novikov's gears have revealed their higher load-carrying capacity and efficiency as compared to involute gears and their lesser sensitivity to shaft deflections.

**Basic Rack.** We know from the theory of mechanisms and machines that to compose toothed pairs from different wheels they should be identical with the form of the basic rack. The parameters of the standard basic rack tooth profile

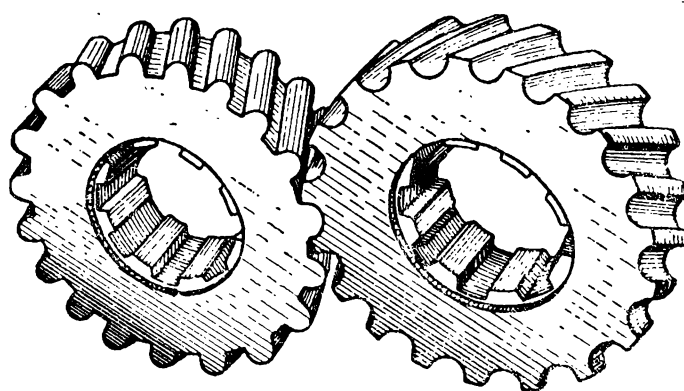


Fig. 139

for involute wheels are standardised (Fig. 140). The line  $a-a$  which is a datum line for constructing a contour where the tooth thickness equals the space width is called the *pitch line*. The sides of the rack forming the tooth outline are straight lines; hence, the pitch  $t$  along the pitch line and the pitch along any other straight line parallel to it are equal.

The pitch is found from the relation

$$t = \pi m \text{ mm} \quad (203)$$

where  $m$  is the module in mm.

The Soviet standards provide for the following modules\*: 0.3, 0.4, 0.5, 0.6, 0.7, 0.8, 1, 1.25, 1.5, 1.75, 2, 2.25, 2.5, (2.75), 3, (3.25), 3.5, (3.75), 4, (4.25), 4.5, 5, 5.5, 6, 6.5, 7, 8, 9, 10, 11, 12, 13, 14, 15, 16, 18, 20, 22, 24, 26, 28, 30, 33, 36, 39, 42, 45, 50 mm and further every 5 mm.

The proportions of the standard basic rack tooth profile are

usually given in fractions of a module (see Fig. 140): addendum  $h' = f_0 m$ ; dedendum  $h'' = (f_0 + c_0) m$ ; tooth thickness  $s = \frac{\pi}{2} m$ ; radius of fillet  $r_i = 0.4 m$ ; addendum factor is  $f_0 = 1$ , and clearance factor is  $c_0 = 0.25$ .

Half the angle between the sides of a basic rack tooth is called the *profile angle* and is designated by  $\alpha_0$ .

For external spur wheels with peripheral velocity exceeding certain limits the Soviet standards provide for a basic rack tooth profile with a tip relief whose size  $a_r m$  (Fig. 140, b) depends on the accuracy used in producing the gear and on the module. The tip relief is made to ensure a uniform motion of the teeth as they engage and to reduce shock at high peripheral velocities.

A rack whose teeth are proportioned according to a standard tooth form is called a *basic rack*. It determines the form and proportions of the teeth of wheels as a result of rolling the gear blank relative to the cutter.

Wheels cut with a shift of the basic rack are said to be corrected. This method is employed when different portions of the involute

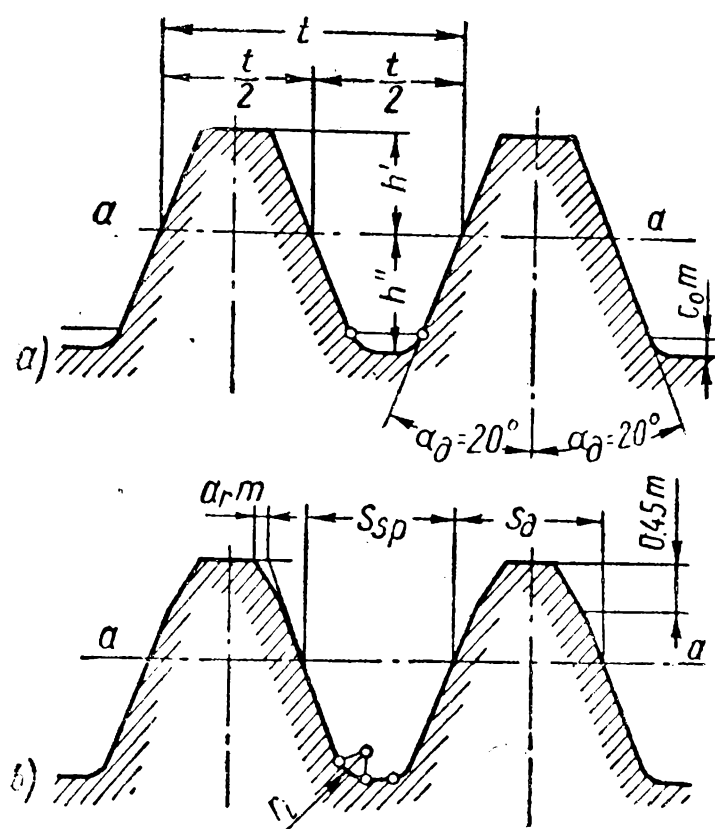


Fig. 140

\* The values in brackets are not recommended.

of the given base circle are to be used as active profiles to suit the changed nature of contact between the teeth. The degree of correction is characterised by *shift factors*:  $\xi_p$  for a pinion and  $\xi_v$  for a wheel. A change in these factors necessitates a change in the relative proportions of the teeth.

A proper choice of the amount of the tool shift enables us to change the form and proportions of the teeth as required thereby changing the properties of the gear as a whole. If the pitch line of the rack

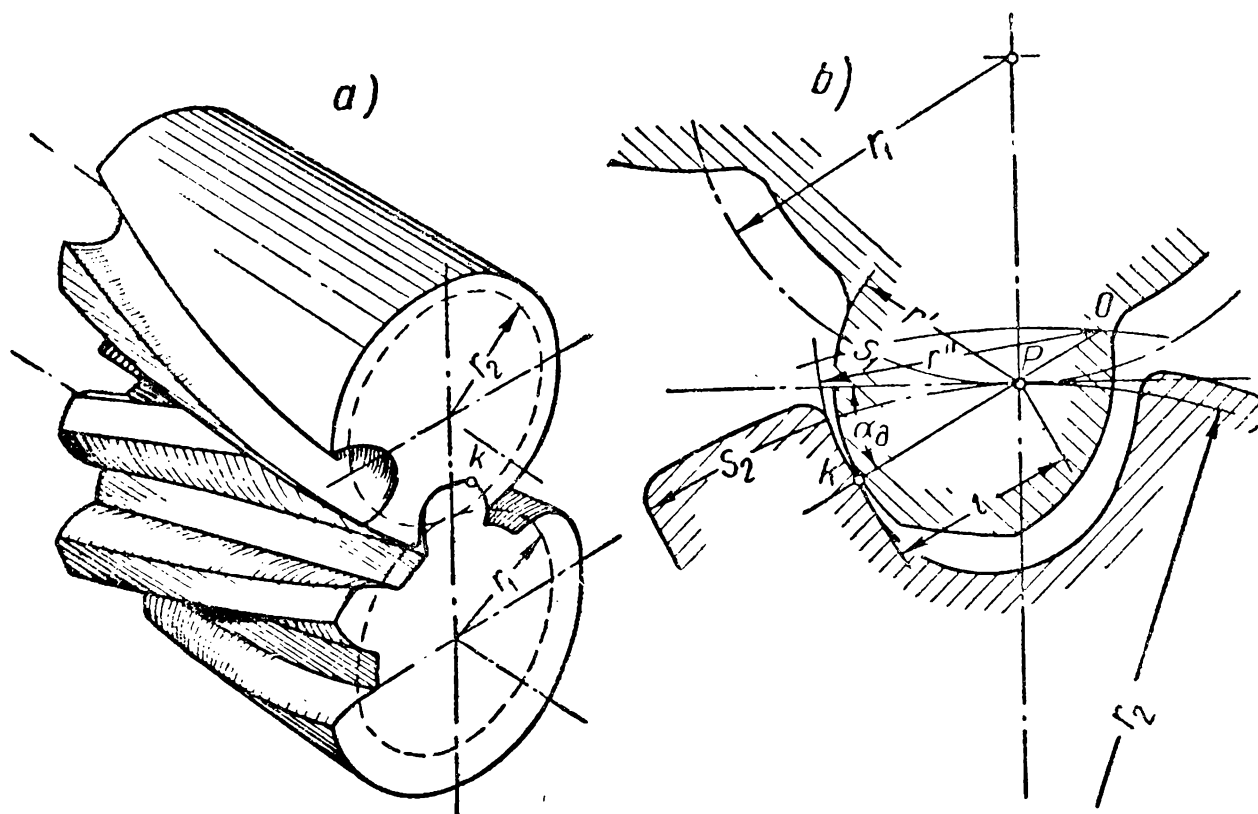


Fig. 141

is displaced from the centre of the wheel by a distance greater than the radius of the pitch circle the shift factor  $\xi$  is considered positive; otherwise, it is negative.

A standard for the basic rack tooth form of the gearing developed by M. L. Novikov does not yet exist. Below we give some information on this system.

The surfaces of rounded teeth are formed by motion along a spiral line on the pitch cylinder of a circle whose plane remains parallel to that of the wheel transverse section. The spiral surfaces obtained in this manner describe convex profiles of the teeth on the smaller wheel and concave profiles on the larger wheel (Fig. 141, a). For a gear with parallel shafts the line of action is parallel to them and is removed from the line of action (passing through the point P) by the distance  $l$  called displacement. The surfaces enter contact at the point K. As the wheels rotate one tooth rolls over the next, while the contact area shifts along the tooth length from one end to the other each time occupying the same position relative to the tooth height.

The following geometrical contact parameters are recommended (Fig. 141, b): displacement  $l = (0.05-0.20)r_1$ ;

radius of a convex tooth profile in the circumferential cross-section  $r' = l$ ;

radius of a concave tooth profile in the circumferential cross-section  $r'' = (1.01-1.05)r'$ ;

pitch-circle tooth thickness ratio  $\frac{s_1}{s_2} = 1.4-1.5$ ;

helix angle on the pitch cylinder  $\beta = 15^\circ \pm 10^\circ$ ;

pressure angle  $\alpha_\phi = 20-30^\circ$ ; overlap factor equal to the relation of the wheel width to the axial pitch on the pitch cylinder  $\varepsilon = 1.1-1.2$ .

**Accuracy of Gears.** To ensure normal operation of a gear the elements of its wheels and housing should be manufactured with sufficient accuracy.

The degree of accuracy is specified depending on the kind of service of the gear and the demands it has to meet. Adequate tolerances, which should be observed during cutting and finishing the teeth, gear housing, shafts and bearings, are specified for separate mating elements and for the gear as a whole in accordance with the degree of accuracy required and proportions of the gear.

In the Soviet Union, toothed gears with parallel shafts and cut metal spur wheels conform to standards which include wheels with external and internal straight, helical and herringbone teeth with a pitch circle up to 5,000 mm and modules over 1 to 50 mm.

The standards provide for twelve degrees of accuracy: from 1 to 12, 1 being the highest. The standards do not provide for tolerances and limits in the degrees of accuracy 1, 2 and 12. The degrees of accuracies 6 to 10 are those most commonly used.

Three types of norm have been established for each degree of accuracy: a) the kinematic accuracy of the wheel; b) its smooth operation; c) contact between the teeth.

Irrespective of the degree of accuracy of the wheels and the gear provision is made for a norm of backlash determined mainly by the thickness of teeth and centre distance.

This norm is intended to compensate for the decrease in backlash due to the gear heating when the temperatures of the toothed gear and the housing differ by  $25^\circ\text{C}$  and the coefficients of linear expansion are the same.

The nature of admissible errors in a toothed gear depends on its purpose. Thus, for example, in a high-speed gear the main requirement is smoothness, in a heavily loaded low-speed gear the most important factor is length of contact along the teeth and for reversible gears the main consideration is the magnitude of the backlash and the variations of this magnitude.

In the Soviet Union toothed gears with shafts inclined at an angle and cut metal bevel wheels conform to standards which include wheels with straight and curved teeth and pitch diameters up to 2,000 mm and modules over 1 to 30 mm.

The standards which specify the accuracy of bevel gears compared to those for spur gears are distinguished by the fact that provision is made for tolerances and limits only for degrees 5-11 (with the total number of degrees 12). The most frequently used degrees are 7, 8, 9, 10 and 11.

The degree of accuracy of wheels ensured by the tolerances given in the above standards by no means determines the operating properties of a gear as they depend on operating conditions, maintenance, anticipated service life, stresses in teeth, etc. Therefore, in designing toothed gears the degree of accuracy must be correctly selected.

For the selection of the correct degree of accuracy for gears employed in various machines the following tentative figures can be recommended: reduction gears in turbines and turbomachines—degrees 3-6; metal-cutting machine tools—3-8; automobiles—5-8; trucks—7-9; tractors—8-10; general-purpose reduction gears—6-9; gear wheels of rolling mills—6-10; mine winders—8-10; crane mechanisms—7-10; farm machinery—8-11.

Some data characterising specific features of the use of toothed gears for the degrees 6, 7, 8 and 9 are given in Table 28.

### COMPONENTS OF TOOTHED GEARS

**Materials.** The material for the manufacture of a designed toothed wheel should be so selected as to make it possible to cut and finish the teeth with the required accuracy and to ensure sufficient beam strength under the action of varying and impact load, adequate strength of the tooth surfaces and high resistance to abrasion.

Toothed wheels are ordinarily made from steel and cast iron, which can be used to produce wheels of any proportions. These materials are easily cast, especially cast iron, while steel has a good forgeability.

The tendency towards a reduction in size, the transmission of large loads in one assembly and at higher speed has stimulated the wide use of steel toothed wheels. A great variety of grades of steel and the possibility of obtaining various properties by means of heat treatment allow of the most favourable combination of required properties.

Carbon steel with 0.35 to 0.50% carbon content has proved highly efficient for medium loads. It possesses sufficient strength and hardness and good machinability (steel grades 35, 40, 45, 50 and 50Г).

As a rule, steel is used in a normalised or tempered state. The size of the wheel cross-section materially affects the mechanical properties obtained after heat treatment. This is explained by the fact that, as the size of the cross-section increases, the cooling rate diminishes, and, if it drops below some critical point, there will be no full hardening.

The size of cross-section is much less decisive in wheels made from alloy steel, which makes it possible to obtain better mechanical

Table 28

Use of Toothed Gears According to Degree of Accuracy

Element of classification	Degree of accuracy			
	6th degree (highly accurate)	7th degree (accurate)	8th degree (medium accuracy)	9th degree (lower accuracy)
Cutting method	Tooth generation on precision machines	Tooth generation on precision machines	Tooth generation or forming with a tool shaped to conform to the actual number of teeth	Any method
Tooth contact surface finishing	Thorough grinding or shaving	With precision tools. Finishing (grinding, shaving, lapping) is recommended for soft wheels and obligatory for hardened wheels	Teeth are not ground, when necessary run-in or lapped in pairs	No finishing operations required.
Operating conditions	Gear wheels intended for accurately timed transmissions or for operation at increased velocities and under severe load smoothly and noiselessly. Wheels of indexing and dividing gears or high-speed reduction gears, important wheels in aircraft, automobiles and machine tools	Gear wheels operating at increased velocities and under moderate load or vice versa; feed wheels in machine tools where timed movement is required; wheels of standard reduction gears, wheels in aircraft and automobiles	Gear wheels of general mechanical engineering requiring no special accuracy; wheels of machine tools not incorporated in dividing chains; unimportant pinions for aircraft, automobiles, and tractors; wheels of hoisting mechanisms; important pinions in farm machines	Gear wheels intended for rough work requiring no medium accuracy; moderately loaded transmissions built to a larger size than specified by the design
Peripheral velocities spur wheels bevel wheels Efficiency	up to 15 m/sec up to 30 m/sec minimum 0.99 (with bearings 0.98)	up to 10 m/sec up to 15 m/sec minimum 0.98 (with bearings 0.97)	up to 6 m/sec up to 10 m/sec minimum 0.96 (with bearings 0.95)	up to 2 m/sec up to 4 m/sec minimum 0.94 (with bearings 0.92)



properties for large wheels. Of all alloy steels used for the manufacture of toothed wheels preference is given to grades 40X and 40XH.

Finish cutting of such toothed wheels is done after final heat treatment; the hardness of the wheel bearing surfaces is therefore  $H_B < 350$  and more frequently  $H_B < 320$ .

In order to increase the load-carrying capacity of toothed wheels and reduce the overall dimensions of the gear, use is made of toothed wheels whose surface hardness is above  $H_B = 350$ , achieved by through or surface hardening, casehardening, cyaniding and nitriding.

In a through hardening of carbon and alloy steel with 0.35-0.5% carbon content the hardness obtained depends on the carbon content of the steel and can reach  $R_C = 50-65$ .

For important gears, when overloads and hammering effect are anticipated, steel grades 40XH and 40XHMA are used, and, more frequently, 40X. The maximum core hardness for carbon steel should never exceed  $R_C = 45$ , and for alloy nickel and molybdenum steel— $R_C = 50$ , since otherwise impact strength drops sharply.

The disadvantage of through hardening consists in the considerable warping of the wheels and a reduction in the toughness of the tooth core which reduces tooth resistance to bending under impact load. This shortcoming can be avoided by surface hardening which ensures adequate strength of the surface and retains the toughness of unhardened metal. This method of heat treatment can be used to advantage in large wheels and is especially effective in wheels with large cross-sections, since with a conventional method of hardening it allows the use of carbon steel instead of alloy steel. The surface hardness obtained amounts to  $R_C = 51-57$ .

Casehardening is another means of increasing the surface hardness of the teeth while retaining proper core toughness. For casehardening use is made of steel with 0.1 to 0.2% carbon content, 0.15% being the most suitable. Casehardened alloy steels possess high abrasion resistance. The hardness of the casehardened surface reaches  $R_C = 56-63$ .

Carbon steel of grades 15 and 20 subjected to casehardening is comparatively rarely used for making toothed wheels: the metal under the hard case resists poorly both surface and beam bending stresses, uneven hardening causes unequal surface hardness while at higher loads the hard case separates.

Alloy chromium steel, of grades 15X and 20X, ensures better quality of the wheels, reduced warping and greater core strength.

When overloads or impact loads are anticipated (gear wheels of automotive vehicles, aircraft reduction gears, etc.), and when the impact resilience and plastic properties of the core are of special importance, use is made of grade 12XH3A chrome-nickel

steel, grade 15XΦ chrome-vanadium steel, grade 18XIT chrome-manganese-titanium steel and other alloy steels.

Nitrided and cyanided wheels are extremely effective as they warp little, making subsequent grinding unnecessary. Wheels with internal toothing are very often nitrided. For such wheels steel grade 38XMIOA is employed.

The hard nitrided case is rather thin (0.1-0.3 mm); therefore wheels with nitrided teeth are employed for steady loads in well-lubricated reduction gears to preclude or reduce abrasive wear.

Toothed wheels for large gears are cast from steel. For adequate wear resistance the carbon steel casting should contain 0.35-0.55% of carbon. Steel castings of wheels are annealed or normalised. Such wheels are made from steel grades 35Л to 55Л.

Toothed wheels of cast iron are employed in low-speed open-type, and more rarely closed-type, gears carrying small load.

Cast iron has a reasonably high resistance to contact stress. However, cast-iron teeth do not resist bending and impact load as effectively as steel teeth, and this reduces the sphere of their application.

In the Soviet Union toothed wheels are made from gray cast iron, grades CЧ 28-48, CЧ 32-52 and CЧ 35-56 and malleable cast iron. For less important gears grades CЧ 15-32, CЧ 18-36 and CЧ 24-44 can be used.

Sometimes toothed wheels are made from fabric laminated and veneer laminated phenolic plastics, artificial leather and fibre.

Phenolic laminated toothed wheels cannot stand up to considerable loads because of their comparatively low resistance to wear and to contact effects. Phenolic laminated plastics are usually used to make one wheel of a pair, the other being manufactured from cast iron or steel with the hardness  $H_B \geq 250$ . Since the transmitted load is determined by the plastic wheel this combination proves effective only in individual cases, for example, when a gear operating at high peripheral velocity must be made noiseless without increasing the accuracy of its manufacture.

A phenolic laminated pinion should have a smaller width than its metal counterpart. Otherwise, the edges of the metal wheel teeth will damage the surface of the phenolic laminated teeth.

**Design of Pinions and Wheels.** If the diameter of the pinion dedendum circle is large enough for the pinion to be secured directly to the shaft by any method, the pinion is made *separate from the shaft* (Fig. 142, a). This is often the case with medium and high power transmissions at a low velocity ratio.

If the diameter of the pinion dedendum circle differs but little from the shaft diameter the pinion is made *integral with the shaft* (Fig. 142, b).

This design is more advantageous because it reduces the amount of machining, does away with key or other joints, increases rigidity and accuracy of contact.

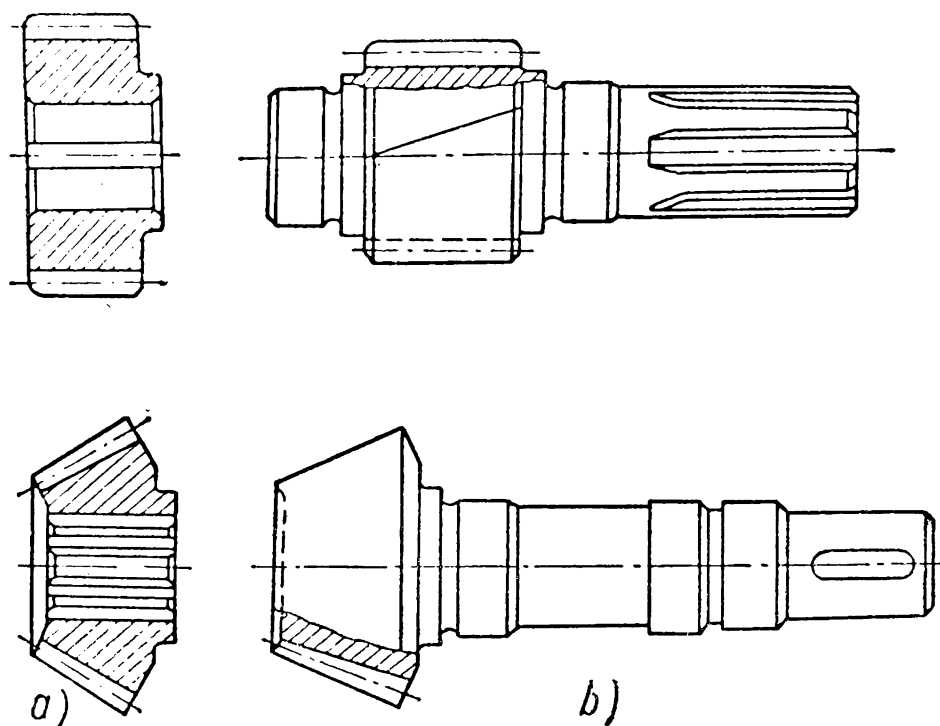


Fig. 142

A design of a pinion made from phenolic laminated plastics is shown in Fig. 143—plastic segments are arranged on a steel bushing which is fitted onto the shaft.

Wheels of diameter less than 500 mm are made from *open-die* or *closed-die forgings* (depending on the scale of production). Wheels of large diameter are either entirely *cast* or are *split* versions. In rare cases forged wheels are met with at diameters over 500 mm.

Forged wheels are made *solid* or cored *with round holes* (Fig. 144, *a*). The cored type is lighter but requires more machining. The type without holes is simpler to machine

but very heavy if of large width and does not allow homogeneous mechanical properties to be obtained in the teeth after heat treatment.

For a more convenient clamping of the wheels on the machine tool the web of the disc should be drilled between the rim and the hub. Sometimes large diameter holes are drilled to reduce weight.

Cast wheels *with crossed spokes* are used when the wheels are  $D_e \leq 1,000$

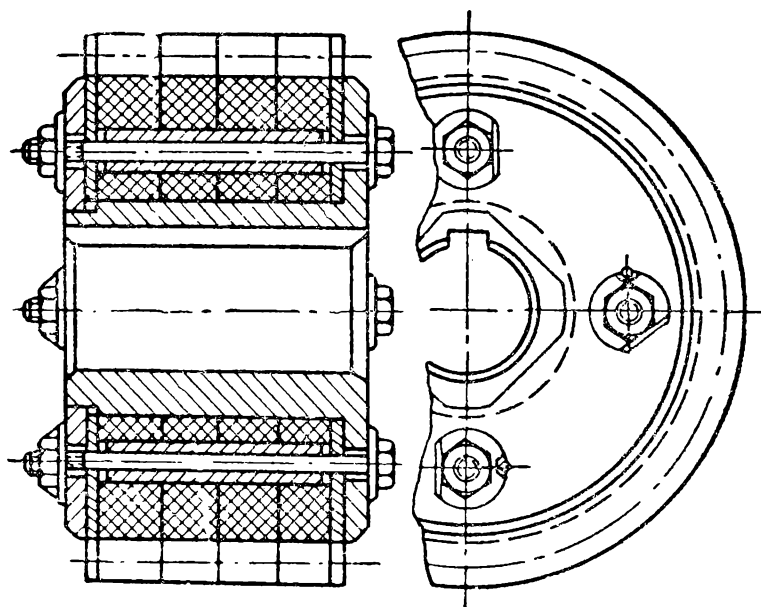


Fig. 143

mm in diameter and  $B < 200$  mm wide (Fig. 144, *b*). When  $D_e > 1,000$  mm and  $B > 200$  mm wheels are cast with I-shaped spokes.

Large-size wheels ( $D_e > 2,000$  mm and  $B > 600$  mm) are made *with split hubs* to prevent the rupture of spokes on cooling (due to excessive accumulation of material in the hub).

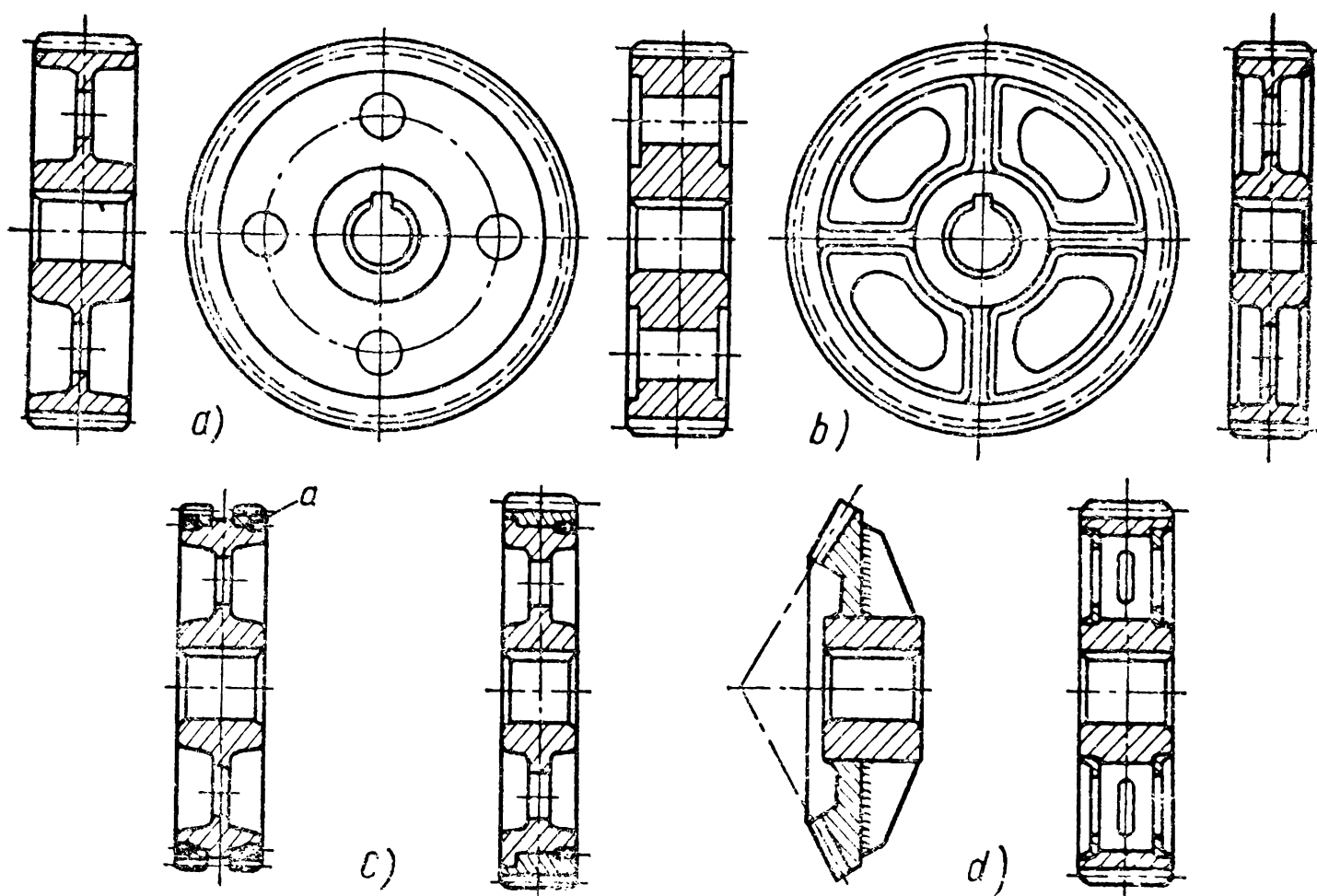


Fig. 144

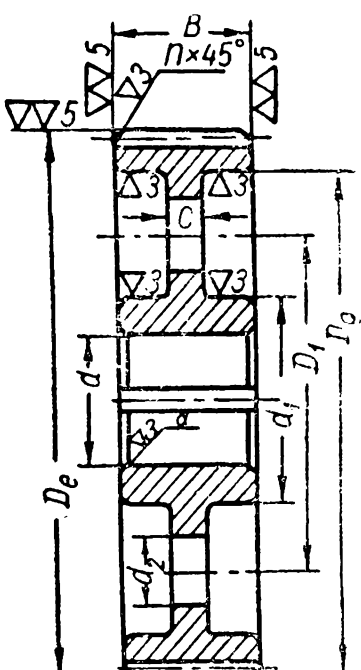
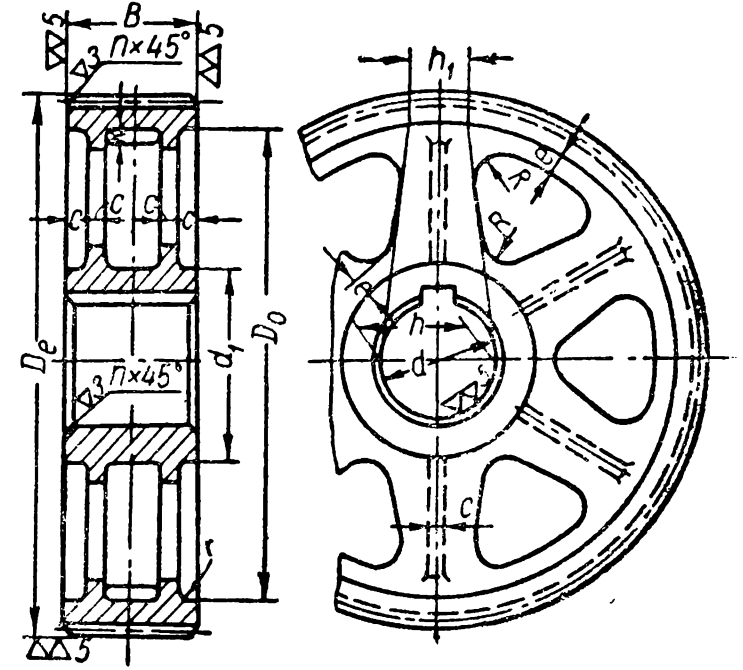
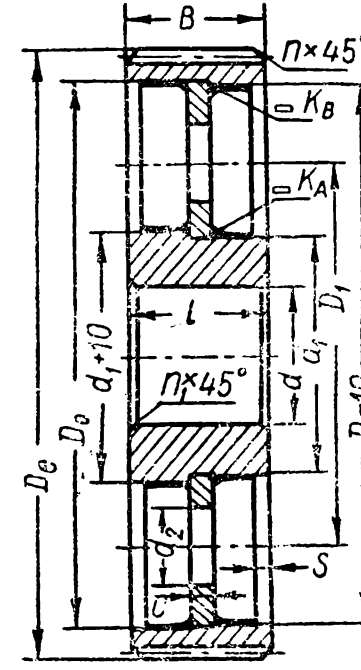
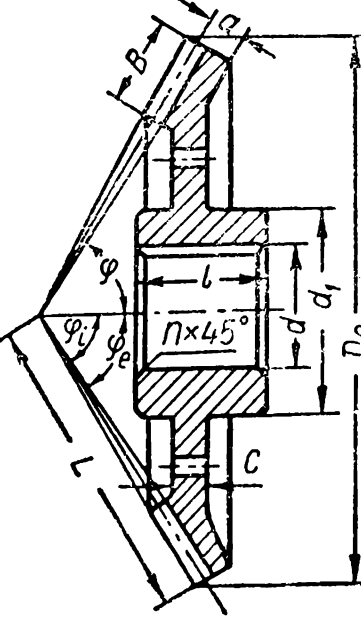
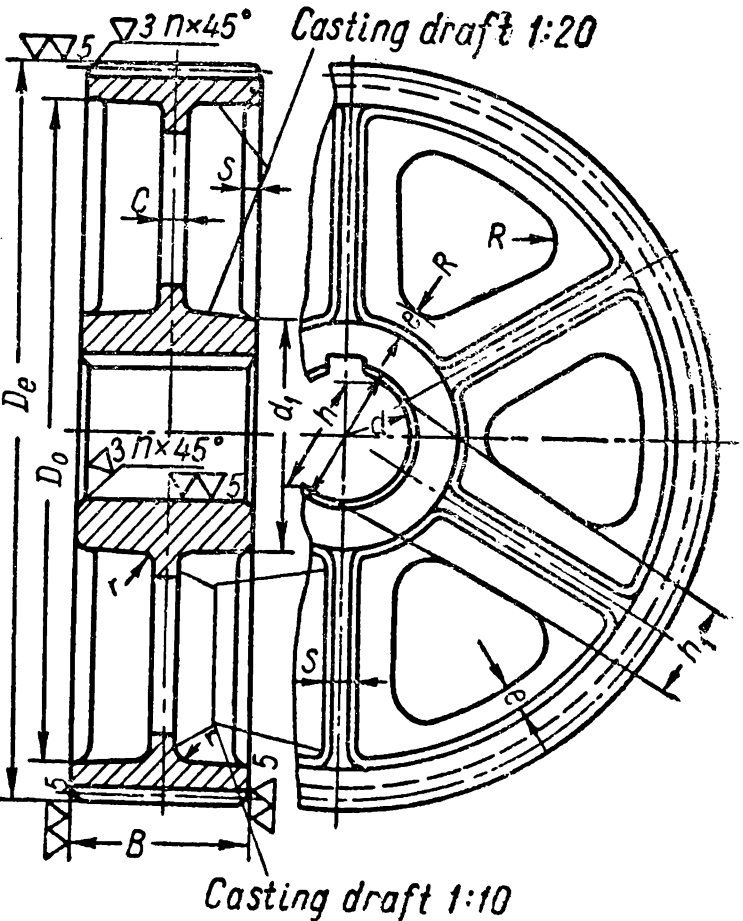
To save alloy steel large wheels are made *with fretting rings*. In this case the wheel centre is cast from cast iron (for example, CЧ 15-32), more rarely from steel; the ring *a* (Fig. 144, *c*) is forged or roll expanded from steel of the respective grade specified by the tooth design.

When the wheel width exceeds 500 mm two fretting rings are provided which are hot-fitted on the wheel centre. Slip of the rings is prevented by stop screws arranged round the circumference. When the wheels are produced in limited quantities and also to reduce weight *welding* is employed (Fig. 144, *d*). In this case care should be taken to ensure adequate rigidity.

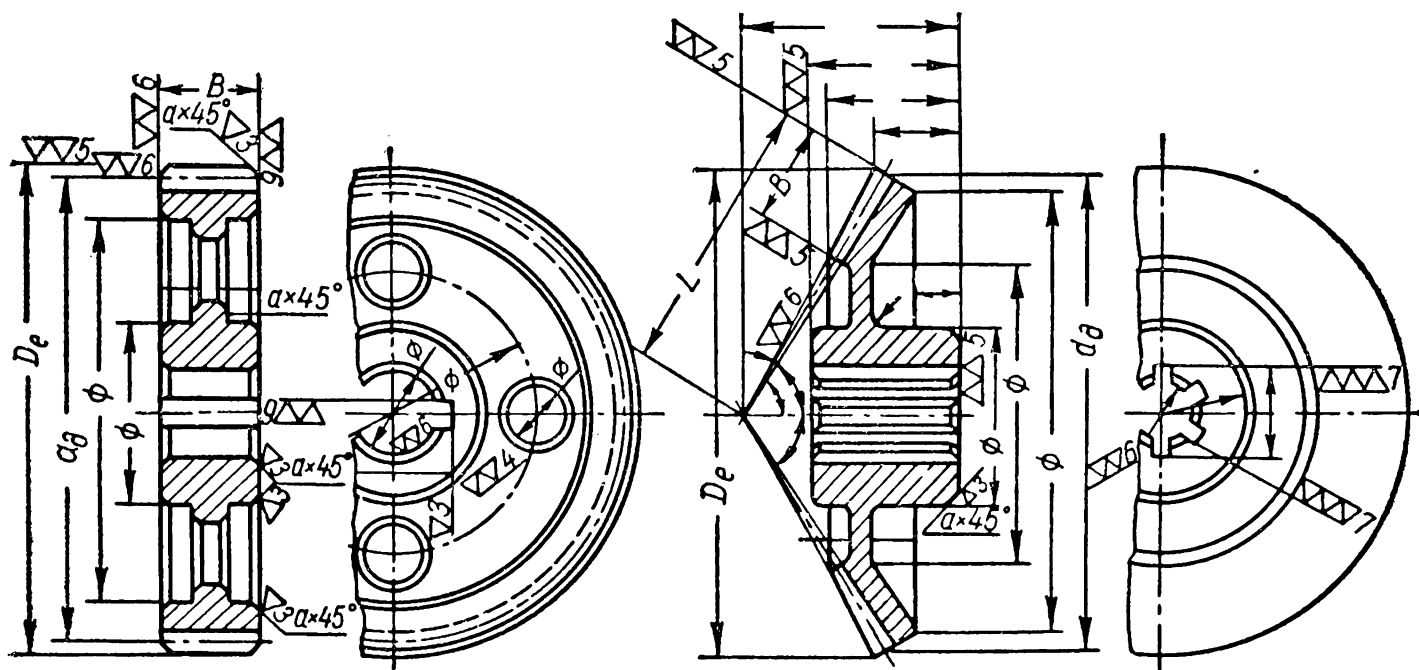
Table 29 shows some empirical relations for determining the main proportions of the wheel elements.

Toothed wheels, fixed on the shaft, are fitted by interference—for example, press or light-press fit. The former fit is employed at impact load or velocities above 2,000 rpm. If the wheel is to be removed from the shaft (to replace the bearings or the wheel itself) medium fits—extra-light drive or drive fit—are used.

Table 29  
Empirical Formulae for Determining Proportions of Wheel Elements

Forged and welded		Cast
	$\begin{aligned}d_1 &= 1.6d \\D_0 &\approx D_e - 10m \\c &\approx 0.3B \\n &= 0.5m \\D_1 &= \frac{D_0 + d_1}{2} \\d_2 &\approx \frac{D_0 - d_1}{5} \\d &\approx 0.3A\end{aligned}$	
	$\begin{aligned}d_1 &= 1.6d \\D_0 &\approx D_e - 10m \\c &= 0.4\sqrt{d} \text{ where } d \text{ is in mm} \\n &= 0.5m \\D_1 &= \frac{D_0 + d_1}{2} \\d_2 &= \frac{D_0 - d_1}{5} \\s &= 0.8c\end{aligned}$	$\begin{aligned}d_1 &= 1.6d; \quad D_0 = D_e - 10m \\d &= 0.3A; \quad h = 0.8d; \quad h_1 = 0.8h \\c &= 0.2h \text{ (but } \nless 10 \text{ mm)}; \quad n = 0.5m \\s &= 0.8c; \quad e = 0.2d; \quad k = 0.8e \\r &= 10 \text{ mm}\end{aligned}$
	$\begin{aligned}d &\approx 0.5L \\d_1 &\approx 1.6d \\l &\approx 1.1d \\c &\approx 0.3d \\a &\approx 0.2L\end{aligned}$	

The fit is selected depending on the degree of accuracy of the toothed gear: for gears of degree of accuracy 6 and 7, class 2 fit is used, for gears of degree of accuracy 8 and 9—class 2 or 3.



8	Meshes with wheel	Part No.	
7	Degree of accuracy	—	
6	Shift factor	$\xi$	
5	Helix angle	$\beta_d$	
4	Direction of thread	—	
3	Profile angle of tool	$\alpha_d$	
2	Number of teeth	$z$	
1	Module	$m$	
Item No.	Name	Symbol	Magnitude

Fig. 145

For a more convenient fitting of the wheels the shafts should be provided with a tapered portion extending to the unrounded parts of the keyway.

In addition to the main sizes  $d_d$ ,  $D_e$  and  $B$  characterising the toothed wheel and marked directly on the drawing (Fig. 145) the table should also contain data necessary for cutting and meshing control:  $z$ ,  $m$ ,  $\beta_d$ ,  $\xi$ ,  $\alpha_d$ ,  $f_0$  and the degree of tooth accuracy.

TYPES OF FAILURE IN GEAR TEETH

Before proceeding to describe the methods of toothed gear design let us consider causes and types of failure in teeth and also the effect of the principal factors on the load-carrying capacity of gears.

A correctly designed and manufactured gear should never over-heat or give out much noise in normal operation.

Lubrication is vital for faultless operation of gears. It is intended to reduce friction losses, dissipate heat generated in the mating gears, prevent abrasion and corrosion of teeth. In closed-type gears the lubricant is fed continuously, in open-type—periodically.

Excessive heating and noise testify to an inadequately designed gear, poor machining and improper lubricant.

Abnormally high temperature of a toothed gear is caused primarily by inadequate heat dissipation or excessive internal losses.

The temperature may also rise due to a poor quality of lubricant (causing an increase in friction), its excessive viscosity (when greater power is expended on churning) or an excessive amount (causing extra losses in churning). However, a correctly designed gear with natural cooling and properly selected lubricant should not fail in operation until temperature reaches a certain admissible limit.

Noise is mainly caused by cyclic errors, uneven load on the teeth and also static and dynamic unbalance of the revolving parts.

Uneven load carried by the teeth and change in their deformation in engagement cause toothed wheels to vibrate. Even the slightest vibration of the wheels transmitted through shafts and bearings to the housing may cause its vibration accompanied by excessive noise.

Higher accuracy in cutting the teeth considerably reduces noise. Therefore, the wheels of important gears transmitting much power at high peripheral velocities have helical or herringbone teeth of higher accuracy.

Teeth usually fail due to considerable inadequacies in design, inaccurate calculation or deviations from the normal service. Among typical failures are breaking-off, pitting, surface abrasion and seizure.

*Teeth mainly break off* due to fatigue. Each time the tooth engages and takes a varying load alternating bending stresses are developed at the root. A crack is therefore liable to develop in the area of maximum stress concentration at a definite load rate. If the contact is made each time on one side of the tooth, the crack usually occurs in the tension zone (zone A, Fig 146, *a*).

Stress distribution at the tooth root is illustrated in Fig. 146, *b* which shows a stressed transparent model of a tooth in polarised light.

In the case of long straight and more frequently of helical and herringbone teeth the crack develops first along the tooth root and then extends upwards along the section where the stress is at the maximum.



Considerable overloads may break the tooth off. Under occasional overloads failure of this type is observed in toothed wheels made from brittle material (cast iron, hardened steel). Load concentrated

along the tooth edges due to incomplete contact along the length of inaccurately cut teeth, to misalignment and deformation of the gear parts (especially of the shaft and pinion) can likewise cause rupture under heavy load.

Lesser overloads involving stresses above the yield point can cause residual bending deformation.

The resistance of a tooth to bending can be improved by increasing the beam strength of the dedendum portion and decreasing stress concentration at the root. This can be achieved by increasing the radius of fillet (for instance, by means of positive correction), improving the gear rigidity, the accuracy of machining and the mechanical properties of the wheel material.

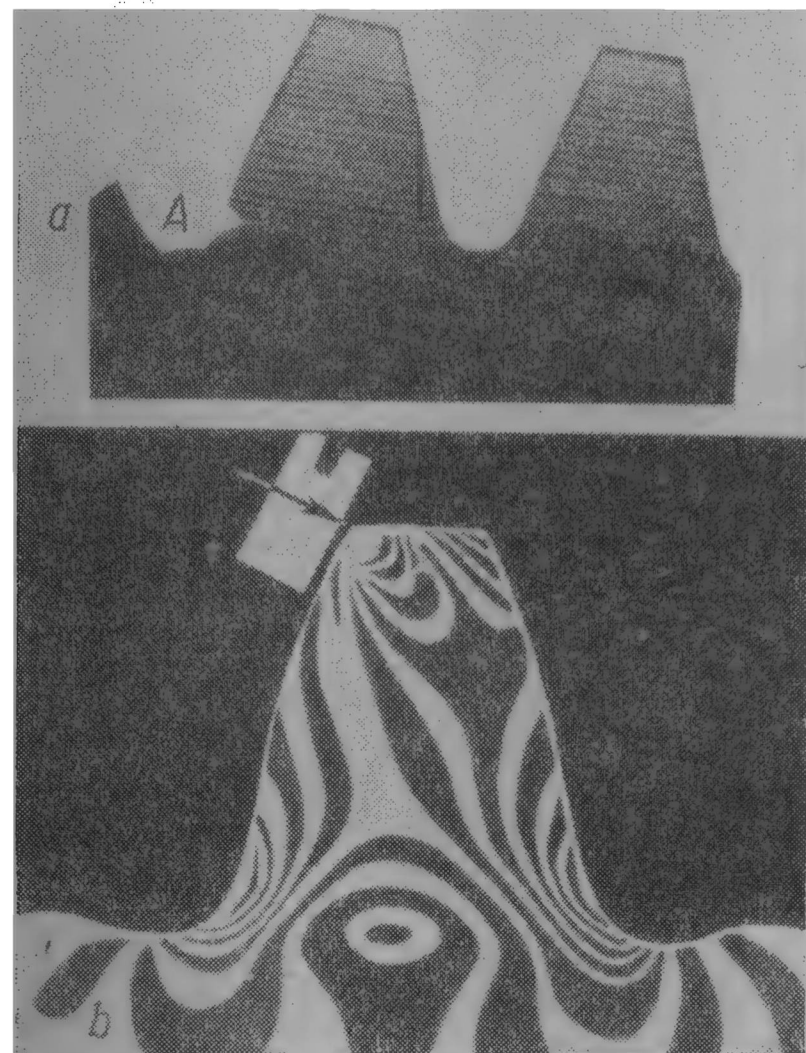


Fig. 146

*Pitting* of the tooth active surfaces is the most frequent cause of failure of wheels in closed-type copiously lubricated toothed gears.

Pitting of the steel teeth of wheels operating in grease occurs in the dedendum portion near the line of action (Fig. 147, *a*). The first pits appear across the width of the toothed wheel in the area of load concentration or on the rough surface left after finishing. During operation these pits grow in number and sometimes in size. This distorts the tooth profile, gutters the surface and increases dynamic load. The process of pitting is intensified and the entire working surface of the tooth below the line of action disintegrates. Vibration and noise become much stronger.

Pitting may be restricted or progressive. The former fault arises within a small portion of the wheel width due to temporary overloading of this portion. If the hardness of the tooth surfaces is  $H_B < 350$



then such pitting ceases after running-in. Under sufficiently high stress brought to act upon the tooth surfaces the process of pit formation spreads over the entire width of the toothed wheels. Then progressive pitting sets in. In this case, the size of the pits increases, sometimes reaching 2-5 mm in diameter.

When the hardness of the tooth surface is  $H_B > 350$  restricted pitting always develops into progressive. In this case the edges of the pits are not smoothed out as on a soft surface but simply break off, while the cracks spread out from the initial pit and gradually affect the entire working zone of the dedendum portion.

The specific feature of pitting is that the tooth surfaces are usually affected in the zone of the line of action and below it (on the dedendum portion of the tooth). This is explained by the fact that in the zone near the line of action the coefficient of friction and, hence, the friction force and stress on the surface will be greatest because the velocity of sliding is low. Therefore, cracks due to fatigue develop first of all in the zone of the line of action.

However, since the friction forces act in opposite directions the cracks on the dedendum and addendum portions of the tooth face opposite directions (Fig. 147, b). In the process of engagement the surface ends of the crack on the dedendum portions are the first to enter the area of contact; this locks the oil within the crack; acted upon by external pressure the oil splits the crack open. Repeated actions of this kind split off particles of metal. At the same time the cracks on the addendum portion of the surface have their inner ends compressed which squeezes the oil out of the crack. The cracks are not subject to hydrodynamic pressure of oil and do not develop into pits.

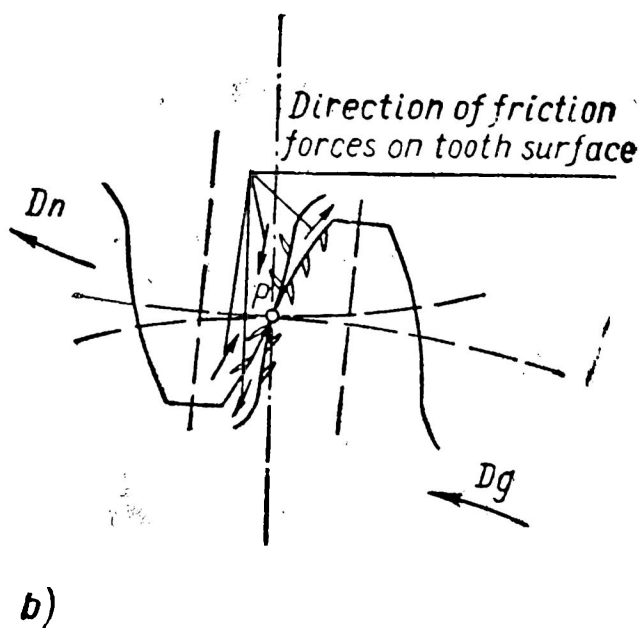
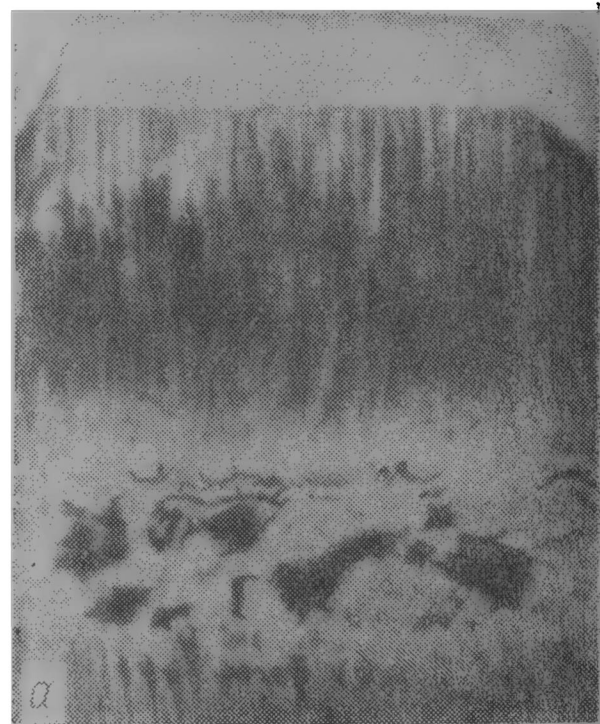


Fig. 147

Operating experience and experimental research have proved that the greater the oil viscosity the greater is the surface endurance limit of the teeth. A more viscous oil more effectively damps dynamic loads on the teeth thereby increasing the service life of toothed wheels.

In open-type gears where there is no oil or its amount is negligible, pitting is an extremely rare phenomenon since the surface

layer which develops initial cracks is worn off before all processes of fatigue failure have taken place in it.

The harder and smoother the working surfaces of the teeth are, the greater is the load they can withstand without the danger of pitting.

The resistance of the tooth surfaces to pitting can be improved by increasing their strength and employing correct lubricants.

Under the action of excessive loads the surface of steel teeth at  $H_B < 350$  may develop *plastic deformations* while at  $H_B > 350$  the surfaces of cast-iron teeth may be subjected to *brittle failure*.

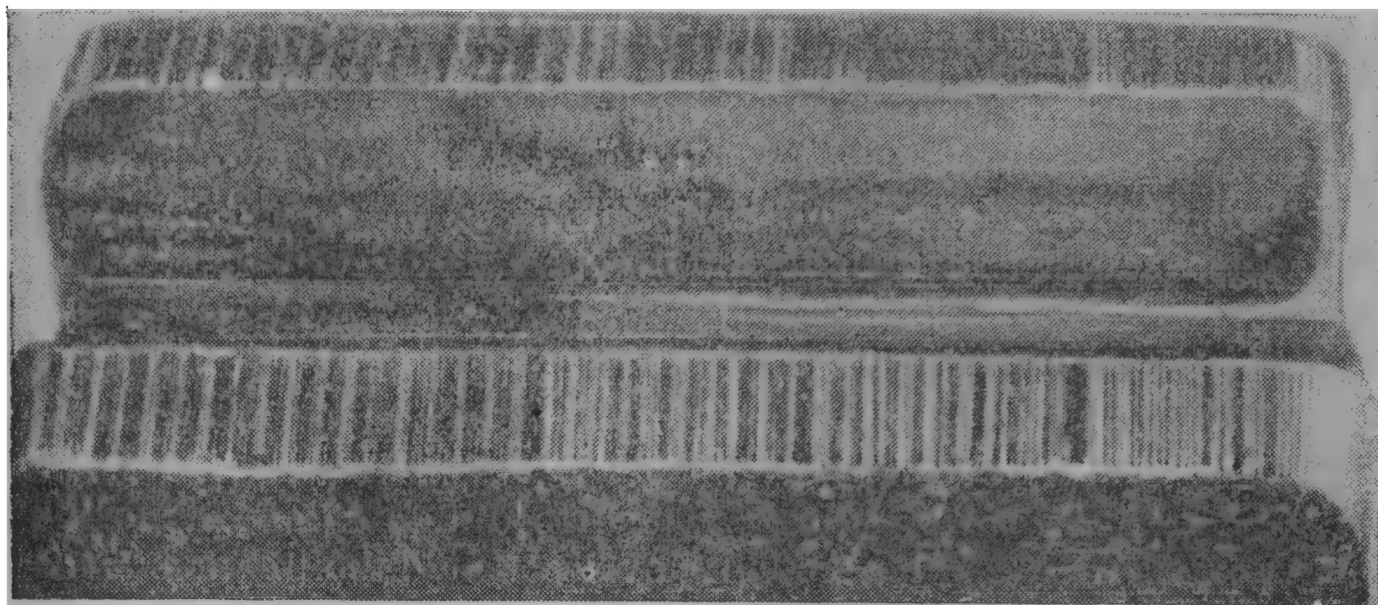


Fig. 148

*Surface abrasion* manifests itself in the wear of the working surfaces (Fig. 148). Wear in closed-type gears is, as a rule, considerably less than in open-type gears.

The flanks of the teeth will be affected by attrition in proportion to the unit sliding of the teeth and the contact compressive stress on these surfaces. Since the greatest unit sliding occurs at the initial and final points of contact the tooth point and root are subjected to greatest wear. At the pitch point there is no sliding and wear will be at a minimum.

The wear of teeth distorts their involute profile, increases dynamic load and weakens the dedendum portion, a phenomenon leading to increased stresses at the root.

If the surfaces of the mating teeth are rough the initial period of operation of the gear will noticeably wear the teeth until their surfaces become sufficiently smooth. After the microirregularities on the tooth surfaces are smoothed and their height becomes less than the thickness of the oil film between the teeth the rate of wear will drop. This is called initial wear.

An oil film of insufficient thickness which does not ensure fluid friction speeds up abrasion.

The thickness of the oil film depends on the oil viscosity, the speed of the wheels, the mode of feeding oil to the mating teeth, the amount of oil, etc. However, even if the oil film is adequately thick when all required conditions have been observed and the gear operates steadily, under overloads and especially during starting and stopping, the thickness of the oil film may prove insufficient. Contamination of the lubricant with abrasive particles materially intensifies wear.

Tooth wear can be slowed down by reducing unit sliding and compressive stresses, increasing the wear resistance of the tooth surfaces and using correct lubricants.

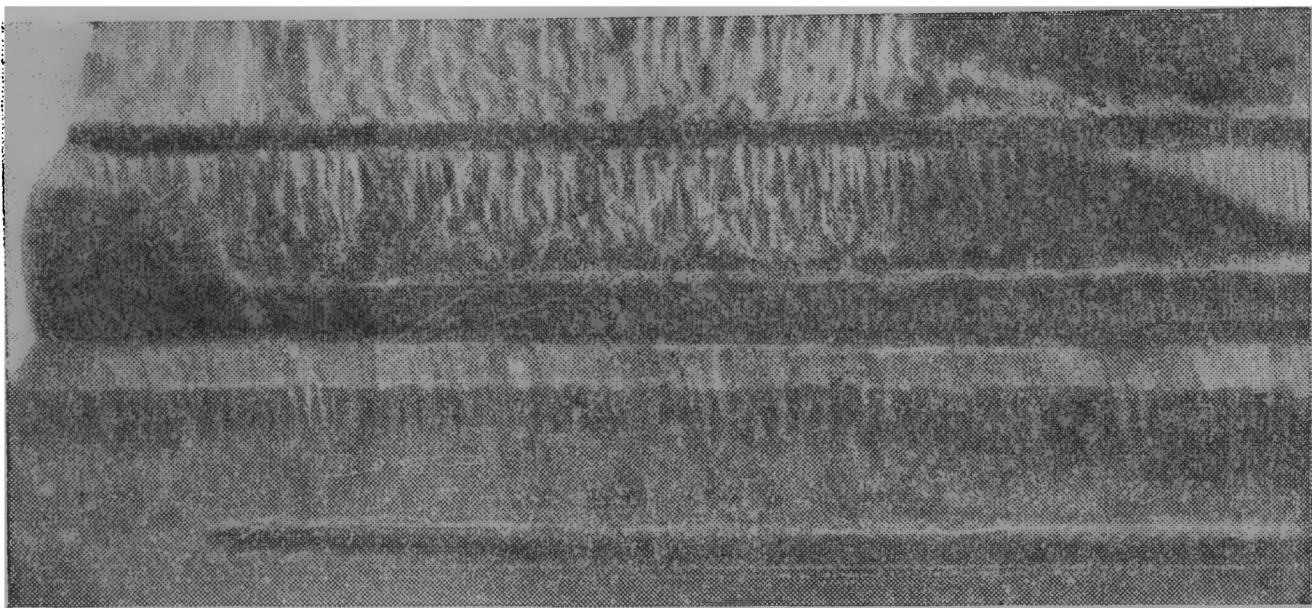


Fig. 149

To adjust unit sliding and compressive stresses to normal the toothed wheels should be corrected.

*Seizure* is caused when, under high pressures developing in the zone of the crushed oil film, the surfaces of the teeth mesh so tightly together that their subsequent relative motion causes particles of the softer metal to break away from the tooth surface and groove it (Fig. 149).

Seizure occurs both on soft and hard surfaces of the teeth.

The oil film can disintegrate or not form at all if the pressures are high and the speeds with which the oil is sucked into the contact area are insufficient; this occurs in low-speed gears carrying heavy loads. In high-speed gears the oil film disintegrates due to the lubricant becoming too hot and losing its viscosity because of higher temperatures in the zone of severe loads and high velocities of sliding.

As the load becomes greater, the velocity of sliding drops and the viscosity and softness of the metal increase, larger particles are broken off.

In low-speed gears seizure is eliminated by the use of extremely viscous lubricants and in high-speed gears by antiscuff lubricants.

Friction forces cause plastic flow of the material of steel teeth under severe load. Metal particles of the tooth surface on the driving wheel shift away from the pitch point and on the driven wheel towards the pitch point producing along the line of action a groove on the driving and a ridge on the driven teeth.

Such plastic deformations are more intensive on poorly lubricated steel teeth with low hardness in low-speed gears.

Lubricants of greater viscosity lessen the hazard of plastic deformations.

The strength calculation is employed to determine the minimum gear proportions which will not endanger the wheels. The most rational solution of such a problem is possible only if the strength and geometry of teeth are considered in interconnection since an effective change in the geometry (the number of teeth, correction factors, helix angles, etc.) can considerably increase the load-carrying capacity of the gear.

It follows from this that closed-type gears should be so designed as to preclude all the faults mentioned above while open-type gear designs should provide for the prevention of breaking-off, wear and plastic deformations of the teeth.

Since toothed gears are used extensively in various branches of mechanical engineering they are designed in a number of ways.

With the advent of greater transmitted powers and the peripheral velocities of toothed wheels the teeth of closed-type gears had to be computed for surface strength. The works of A. I. Petrusevich, V. N. Kudryavtsev, Y. G. Kistyan, M. S. Polotsky and other Soviet researchers and of foreign scientists—Buckingham (U.S.A), Merritt (England), Niemann (Germany)—have all contributed to improving the designs of toothed gears and allow calculations to be made to prevent breaking-off, pitting and plastic deformations. So far calculations for wear and seizure have not yet been elaborated to a point which would make them effective in all cases.

Below we describe the fundamental methods employed in calculating the beam strength of teeth and the strength of their active profiles.

### DESIGN OF STRAIGHT-TOOTH SPUR GEARS

The complete design of a gear comprises the calculation of its geometry, force and strength. The strength design is intended to find the diameters of pitch circles (or the centre distance), width of wheels, number of teeth and the module of the gear. Geometric calculations determine the diameters of wheels, proportions of the mating elements and also characteristics of meshing—overlap

factor, unit sliding, etc. Computation of the force concerns the finding of the forces acting upon the shafts and of the reactions in the bearings necessary for subsequent calculation of shafts and bearings.

**Main Geometrical Proportions.** The proportions of a toothed gear in a circumferential cross-section depend on the number of teeth  $z$ , module  $m$  and the shift of the basic rack  $\xi m$  and are found from the known formulae (Fig. 150):

pitch diameter

$$d_\theta = zm \text{ mm}; \quad (204)$$

diameter of base circle

$$d_0 = d_\theta \cos \alpha_\theta \text{ mm}; \quad (205)$$

diameter of the dedendum circle

$$D_i = d_\theta - 2(f_0 + c_0 - \xi) m \text{ mm}; \quad (206)$$

diameter of the addendum circle\*

$$D_e = D_i \pm 2h \text{ mm} \quad (207)$$

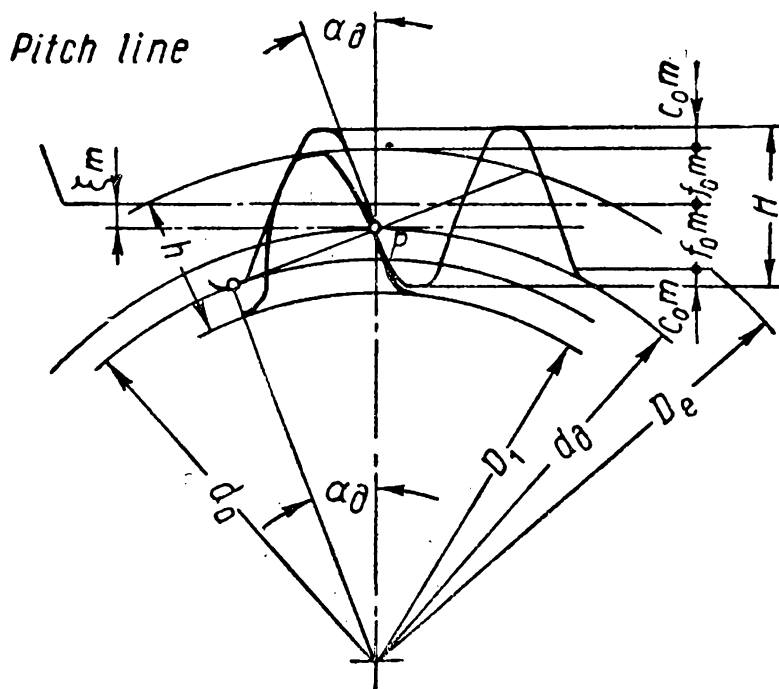


Fig. 150

where  $h$  is the height of teeth which at

$$\xi_p = \xi_w = 0 \text{ or } \xi_p = -\xi_w \text{ is equal to} \quad h = (2f_0 + c_0) m \text{ mm} \quad (208)$$

and at  $\xi_p \neq \xi_w$

$$h = \frac{2f_0 + c_0}{2(f_0 + c_0)} \left( \pm A - \frac{D_{ip} \pm D_{iw}}{2} \right) \text{ mm}. \quad (209)$$

The centre distance in an uncorrected gear or in a gear with height correction ( $\xi_p = -\xi_w$ ) will be

$$A_\theta = \frac{z_w \pm z_p}{2} m \text{ mm}, \quad (210)$$

for a gear with angular correction

$$A = A_\theta \frac{\cos \alpha_\theta}{\cos \alpha} \text{ mm} \quad (211)$$

where  $\alpha$  is the pressure angle.

\* Here and elsewhere the upper sign is for external toothing and the lower sign for internal toothing.

To simplify calculations we use the formula

$$A = A_d (\lambda_0 + 1) \text{ mm}$$

where  $\lambda_0$ , the axis shift factor, equal to  $\lambda_0 = \frac{\cos \alpha_d}{\cos \alpha} - 1$ , is given as a function of the magnitude

$$\xi_0 = \frac{2(\xi_w \pm \xi_p)}{z_w \pm z_p}.$$

When the wheels are cut with a shaping cutter with the addendum diameter  $D_{ec}$  and the number of teeth  $z_c$  the diameter of the dedendum circle will be

$$D_i = 2A_m \mp D_{ec} \text{ mm.}$$

The centre distance on the machine tool is

$$A_m = \frac{z \pm z_c}{2} m (\lambda_{oc} + 1) \text{ mm}$$

where  $\lambda_{oc}$  is taken as a function of

$$\xi_{oc} = \frac{2(\xi \pm \xi_c)}{z \pm z_c}$$

The shift factor for the shaping cutter is calculated from the formula

$$\xi_c = \frac{D_{ec}}{2m} - \left( \frac{z_c}{2} + f_c \right)$$

where  $f_c$  is the shaping cutter addendum factor indicated in the tool certificate.

**Forces Acting in a Gear.** Let us examine the forces acting between two mated straight-tooth wheels. We assume that the driven wheel takes the torque  $M_t$ .

The full pressure on the tooth  $P_n$  acts in the contact plane normal to the tooth surfaces (friction is neglected because it only slightly affects these forces). Let us resolve this normal force into two components (Fig. 151, a):

$$\text{peripheral force} \quad P = \frac{2M_t}{d_w} \text{ kg} \quad (212)$$

and radial force

$$P_r = P \tan \alpha \text{ kg.} \quad (213)$$

The peripheral force  $P$  acts in an opposite direction to the peripheral velocity on the driving wheel and coincides with it on the driven wheel.

The radial force is directed from the point of contact towards the centre of the wheel with external teeth and away from the centre of the wheel with internal teeth.

Fig. 151, b shows the reactions in the bearings of the driving and driven shafts of a one-step spur straight-tooth gear. It is usual



practice to take the points of application of the forces  $P$  and  $P_r$  as situated in the middle of the width of the wheels, and the points of application of the reactions—in the middle of the length of the bearing assemblies. Only in special cases when the wheels are very wide and the bearings are mounted close to the wheels are the loads  $P$  and  $P_r$  assumed to be spread over the width of the wheels.

The reactions in the bearings are determined on the basis of the known formulae from the theory of the strength of materials.

The normal force carried by the teeth will be (Fig. 151, a)

$$P_n = \frac{2M_t}{d_w \cos \alpha}$$

We know that

$$d_p = \frac{2A}{i \pm 1} \quad \text{and} \quad d_w = \frac{2Ai}{i \pm 1}$$

$$\left( \text{at } i = \frac{z_w}{z_p} \gg 1 \right)$$

and hence

$$P_n = \frac{M_t (i \pm 1)}{Ai \cos \alpha} \text{ kg.} \quad (214)$$

This force is utilised when calculating the strength of teeth.

**Design Load.** We know from the theory of mechanisms and machines that in the initial period of contact of any pair of teeth (in the section  $ab$  of the line of action, Fig. 152) the previous pair is mated.

In this way the load  $P_n$  is transmitted for some time (within the zone of two-pair engagement along the line of action in the

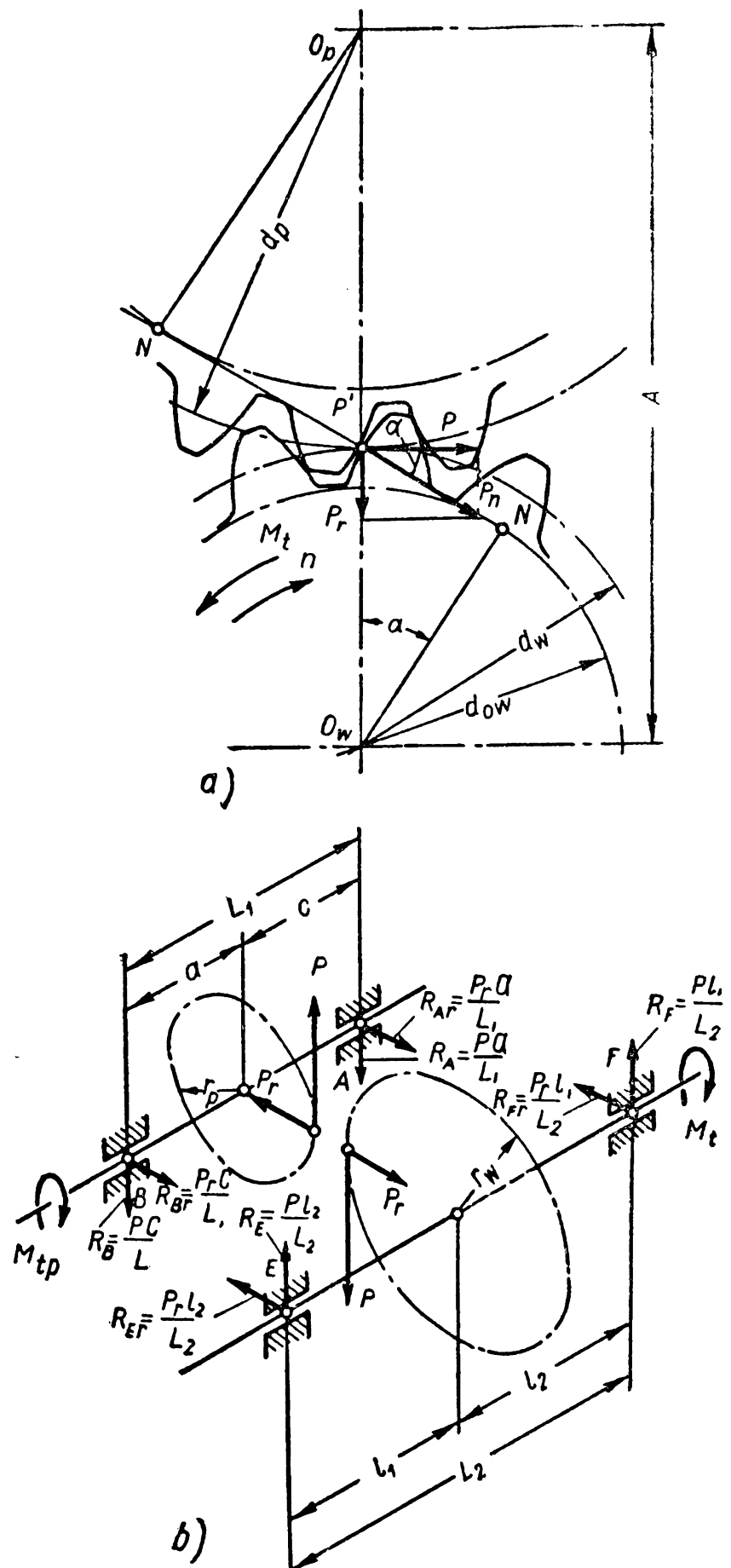


Fig. 151

portions  $ab$  and  $cd$ , Fig. 152) by two pairs of teeth along two lines of contact which are parallel to the wheel generating line. If we assume that the mating elements have been absolutely accurately machined then the full normal load  $P_n$  will be distributed between the simultaneously meshing pairs of teeth in direct proportion to their rigidity in the direction of the line of action.

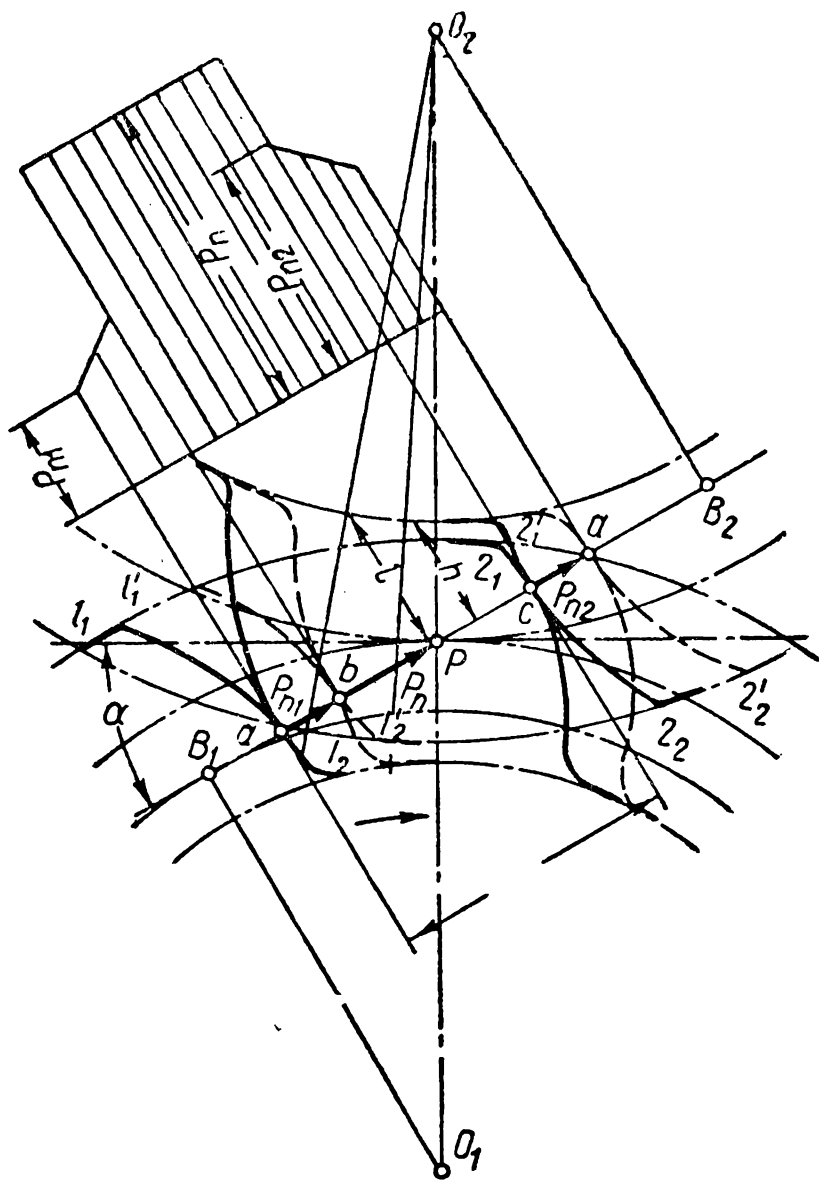


Fig. 152

Under the action of loads acting upon each pair of teeth the latter will experience deformations of contact compression, shear and bending. The total rigidity of the pair of teeth will be in inverse proportion to these deformations whose value depends on the position of the point of contact on the tooth profile, the form of the tooth, material of the wheel, etc. The point of application of the force and its direction relative to the tooth depend on the position of the point of contact on the line of action; the form of tooth depends on the geometry of mating, i. e., on the number of teeth, the type of cutting tool and its displacement when cutting a toothed wheel, etc.

If the rigidity of one pair of teeth at a given moment of contact is  $C_1$  kg/cm\* and of a second pair, meshing simultaneously with the first— $C_2$ , then the forces acting upon each pair of teeth can be determined from the condition of equal displacements of both pairs of teeth along the line of action

$$\frac{P_{n1}}{C_1} = \frac{P_{n2}}{C_2}$$

and the condition

$$P_{n1} + P_{n2} = P_n$$

\* For  $z_p=20$  and  $z_w=40$  at  $\xi_p=\xi_w=0$  the approximate values of rigidity at the moment of contact of the pinion tooth tip is  $C_1=112,500$  kg/cm<sup>2</sup>, at the moment of transition to a one-pair engagement  $C_2=145,000$  kg/cm<sup>2</sup>.



where  $P_{n1}$ ,  $P_{n2}$  are the loads taken by the first and second pairs of the teeth in contact.

In the process of mating and because the rigidities  $C_1$  and  $C_2$  continuously change, the loads  $P_{n1}$  and  $P_{n2}$  also change: as the tooth  $I_2$  enters contact at the top (Fig. 152) the load  $P_{n1}$  will be small due to the very low rigidity of the tooth in bending. As the line of contact shifts nearer to the tooth root its rigidity will quickly increase so that, despite a certain drop in the rigidity of the other tooth, the total rigidity will be greater than at the initial moment and the load  $P_{n1}$  will increase.

When the teeth leave the zone of two-pair contact (the section  $bc$  on the line of action, Fig. 152) the pair of teeth  $2_1-2_2$  disengages and the load  $P$  will be transmitted only by one pair of teeth along a line of contact equal in length to the wheel width  $B$ .

Depending on what fault the tooth design is intended to prevent, a load involving the most dangerous stress should be considered.

In a surface strength design the full load  $P_n$  acting in the zone of one-pair engagement should be taken, since surface pitting under the action of incompletely reversed contact compressive stresses occurs precisely in this zone.

In computing the tooth beam strength we should take the load which, when acting on the respective arm, will cause the maximum stresses in the dangerous section of the tooth: a) the load  $P_{n1}$  at the top acting on the longer arm  $l$  or b) the greater load  $P_n$  acting on the shorter arm  $h$ .

As has been noted before, two pairs of teeth can be expected to operate simultaneously only when the wheels have been accurately machined, particularly if the distances between the teeth of the pinion and the wheel along the line of action (i. e., the base pitches  $t_{01}$  and  $t_{02}$ ) are equal. Since inaccuracies in manufacture are inevitable, two pairs of teeth can actually operate simultaneously only if the total deformation of the pair of teeth under load exceeds the difference  $\Delta$  between the base pitches of the wheel and the pinion. This will be the case at small values of  $\Delta = t_{01} - t_{02}$ , i. e., in high-precision gears—7-6th and higher degrees of accuracy.

Since gears of the 8-12th degrees of accuracy display considerable errors in the base pitch the tooth will take almost the whole load  $P_n$  when its top is in contact. Therefore, when calculating the teeth of such gears for bending we take the entire load  $P_n$  applied at the top and acting along one line of contact whose length equals the wheel width  $B$ .

In this way, the rated load per unit of length of the line of contact—the *unit load*—is

$$q = \frac{P_n}{B} = \frac{M_t (i \pm 1)}{ABi \cos \alpha} \text{ kg/cm.} \quad (215)$$

However, in actual fact, the load is not distributed uniformly over the line of contact because during the gear operation its parts are deformed and change their mutual position. This is also due to inaccuracies in the machining of wheels, shafts and housing and to assembly errors.

Fig. 153 shows a one-step gear with straight-tooth wheels arranged asymmetrically relative to the bearings. When carrying no load the teeth of an accurately machined and assembled gear will contact uniformly along the entire width of the wheels  $B$ .

As the gear operates, the torque applied to the coupling of the pinion shaft (Fig. 153) gradually decreases from end  $a$  to end  $c$ . Conversely, on the wheel shaft the torque increases from end  $a$  to end  $c$ . Because of the pinion twisting strain and the shaft and pinion deflection, the generatrices of the teeth, originally rectilinear, are distorted as shown in Fig. 153,  $b$ . The same occurs on the driven shaft but to a lesser degree since it is more rigid.

If the teeth were absolutely rigid, they would contact and the entire load  $P_n$  would be transmitted at only one point. In actual fact, the deformation of the teeth causes contact to spread over a definite area whose length may be equal to or less than that of the theoretical line of contact. At the same time the load will not be spread uniformly over the length of the contact area; the greater the rigidity of the teeth, the less uniform load distribution will be.

The increase in unit load due to its uneven distribution along the length of the lines of contact is called *load concentration*, and the relation of the maximum unit load  $q_{\max}$  (Fig. 153,  $d$ ) to its mean value  $q$  assuming a uniform load distribution—the *load concentration factor*

$$k_c = \frac{q_{\max}}{q}. \quad (216)$$

The value of  $q_{\max}$  depends on many factors whose effect cannot be accurately established. The most important are as follows:

1) the location of the wheels on the shafts relative to the bearings—when narrow wheels are fitted near the shaft middle the bending strain affects load concentration negligibly;

2) the relative length of the gear shafts—the greater the ratio between shaft length and diameter  $\frac{l}{d_{sh}}$ , the more the shafts deflect and asymmetrically fitted wheels are misaligned;

3) the relative width of the pinion  $\psi_p = \frac{B}{d_p}$ —the larger this relation, the greater the relative shift of the tooth sections along the width of the misaligned wheels and the greater  $q_{\max}$  will be;

4) the total rigidity of the teeth on the wheels—the higher the rigidity of the mating teeth, the greater load concentration will be;

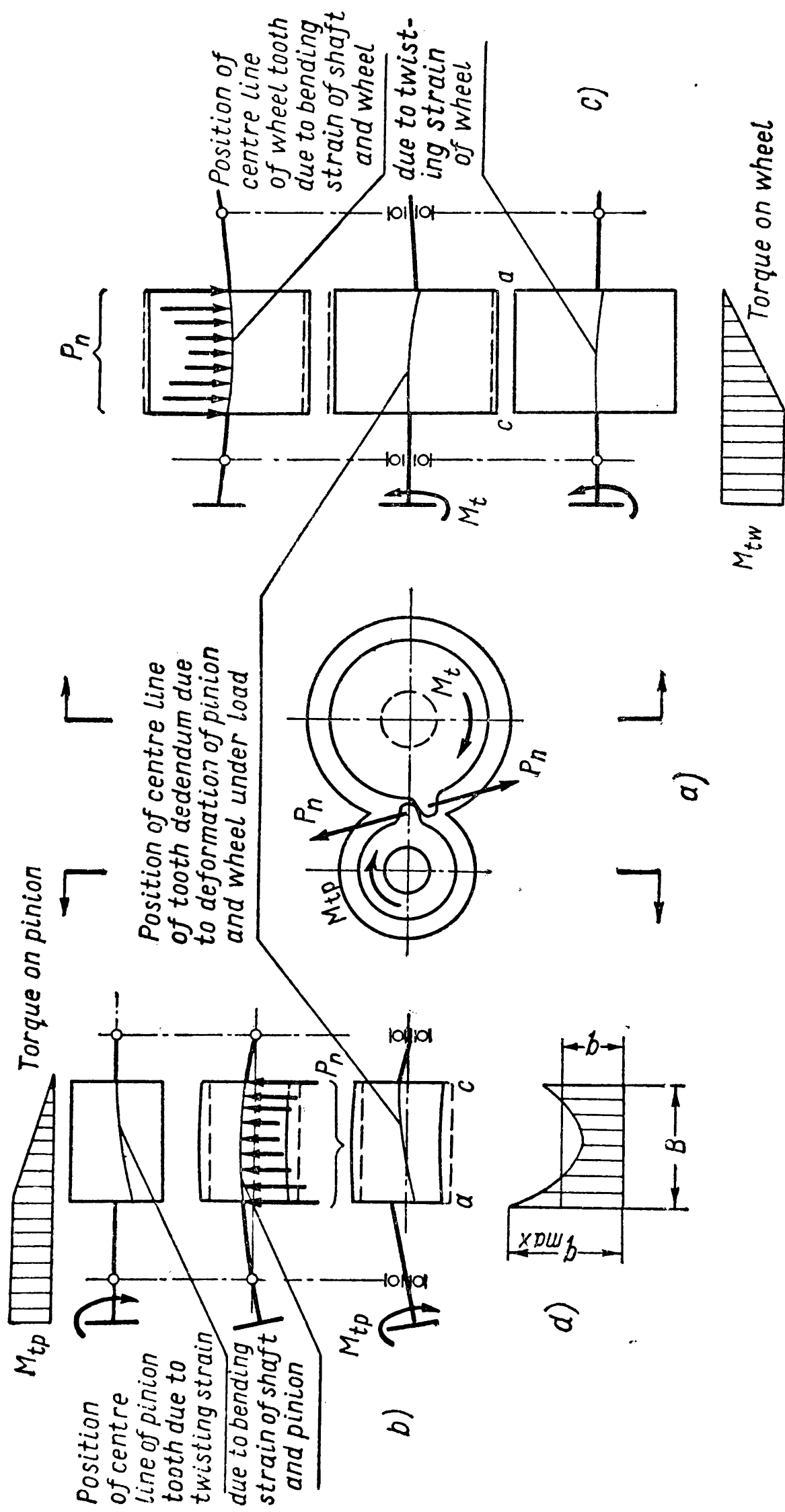


Fig. 153

5) the design of the pinion and the wheel—the rigidity of the wheel elements (rim, solid piece, spokes) determined by their proportions and design materially affects the magnitude of the twisting and bending strain of the pinion and wheel.

The design of a gear should be so arranged and the proportions of its parts so chosen as to reduce load concentration to a minimum. The bearings of the shafts should be preferably located near the wheels and symmetrically relative to them. When the wheels have to be arranged asymmetrically their shafts should be more rigid. Pinions and wheels fixed at an angle should be narrower and set as close to the bearings as possible.

It is extremely difficult to give an exact value of  $k_c$ .

For gears of the 8th degree of accuracy with steel wheels and with surface hardness  $H_B \geq 350$  the tentative values tabulated below may be used.

Table 30

Concentration Factors  $k_c$

$\psi_p = \frac{B}{d_p} = \psi \frac{(i \pm 1)}{2}$ $\left( \psi = \frac{B}{A} \right)$	Bearings arranged symmetrically near toothed wheels	Pinion arranged asymmetrically relative to bearings		Cantilever pinion
		very rigid shaft	less rigid shaft	
0.2	1	1	1.05	1.15
0.4	1	1.04	1.10	1.22
0.6	1.03	1.08	1.16	1.32
0.8	1.06	1.13	1.22	1.45
1.0	1.10	1.18	1.29	—
1.2	1.14	1.23	1.36	—
1.4	1.19	1.29	1.45	—
1.6	1.25	1.35	1.55	—

An example of a very rigid shaft is the connection shaft of a two-step gear when  $\frac{l}{d_{sh}} < 2.5-3$ . Less rigid shafts include high-speed shafts of multi-step gears in which  $\frac{l}{d_{sh}} > 3$ .

For gears of higher accuracy (7th degree and above) the tabulated values  $k_c > 1.05$  can be reduced and for less accurate gears (9th and below) the factor  $k_c$  should be increased by 5-10%.

If the gear incorporates even one cast-iron wheel the tabulated values  $k_c > 1.05$  should be decreased by 5% because of the low elastic modulus and hence lesser rigidity of the teeth.

For gears with a phenolic laminated pinion having a very low elastic modulus the load concentration factor should be unity.

When the hardness of the tooth surface of one wheel of the pair is  $H_B < 350$ , the teeth will be run in during operation due to more

rapid wear of portions carrying greater load. In case of a varying load the running-in will be partial and the load concentration factor can be assumed to equal approximately

$$k_c = \frac{k_{c \text{ table}} + 1}{2}.$$

(217)

Under constant load (at  $H_B < 350$ ) the teeth will be quickly run in and therefore  $k_c=1$ .

Table 30 shows the considerable effect the pinion width has on the magnitude of load concentration. Therefore, the width of the wheels should never be excessively increased if the danger of considerable deformations of the gear parts exists.

The width of wheels  $B$  may be selected from the following tentative figures in Table 31.

Table 31

Limit Values of Relation  $\psi_p = \frac{B}{d_p}$

Arrangement of bearings	Position of toothed wheels relative to bearings	Straight-tooth gears	
		Sufficiently constant load	Varying load
Bearings in a common rigid housing	Not cantilever	1.6	1.3
	At least one cantilever wheel	0.8	0.7
Bearings without a common rigid housing	Not cantilever	$\frac{12}{z_p}$	
	At least one cantilever wheel	$\frac{10}{z_p}$	

To decrease load concentration along the width of wheels use is made of barrel-shaped teeth (Fig. 154). Their ends are somewhat narrowed (by 0.01-0.025 mm), as a result of which before load is applied the teeth contact only in the middle portion of the width. Under load, since the teeth tend to be distorted in a direction opposite to the convexity of the side surface, contact spreads over the entire wheel width. In this case the unevenness of load distribution will be negligible.

Inaccuracies in contact due to inaccuracies of tools and tooth-cutting machines cause the jerky operation of a toothed gear. Although the velocity ratio  $i$  during one complete turn will equal  $i = \frac{z_w}{z_p} = \text{const}$ ,

the instantaneous velocity ratios will differ from this value. As a result, even at a constant velocity of the driving wheel the driven wheel will not rotate uniformly. The resulting angular accelerations will cause a hammering effect during engagement. This causes additional *dynamic loads*  $P_d$  to act upon the teeth. Dynamic loads during contact generate noise and vibration of the gear and weaken the capacity of the wheels to transmit useful load.

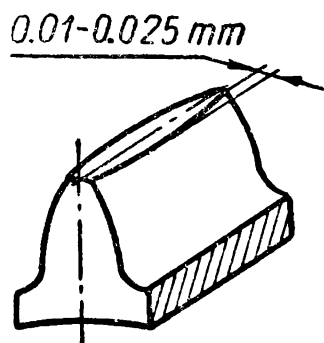


Fig. 154

Shocks occur on the tip edge and the face.

The first kind of shock occurs when the top of the driven wheel comes prematurely in contact with the dedendum portion of the driving wheel (Fig. 155, *a*). In this case, since the contact does not begin on the line of action, the correct ratio between the angular velocities is disturbed—the velocity of wheel 2 increases, an additional dynamic load arises and accelerates the motion of wheel 2.

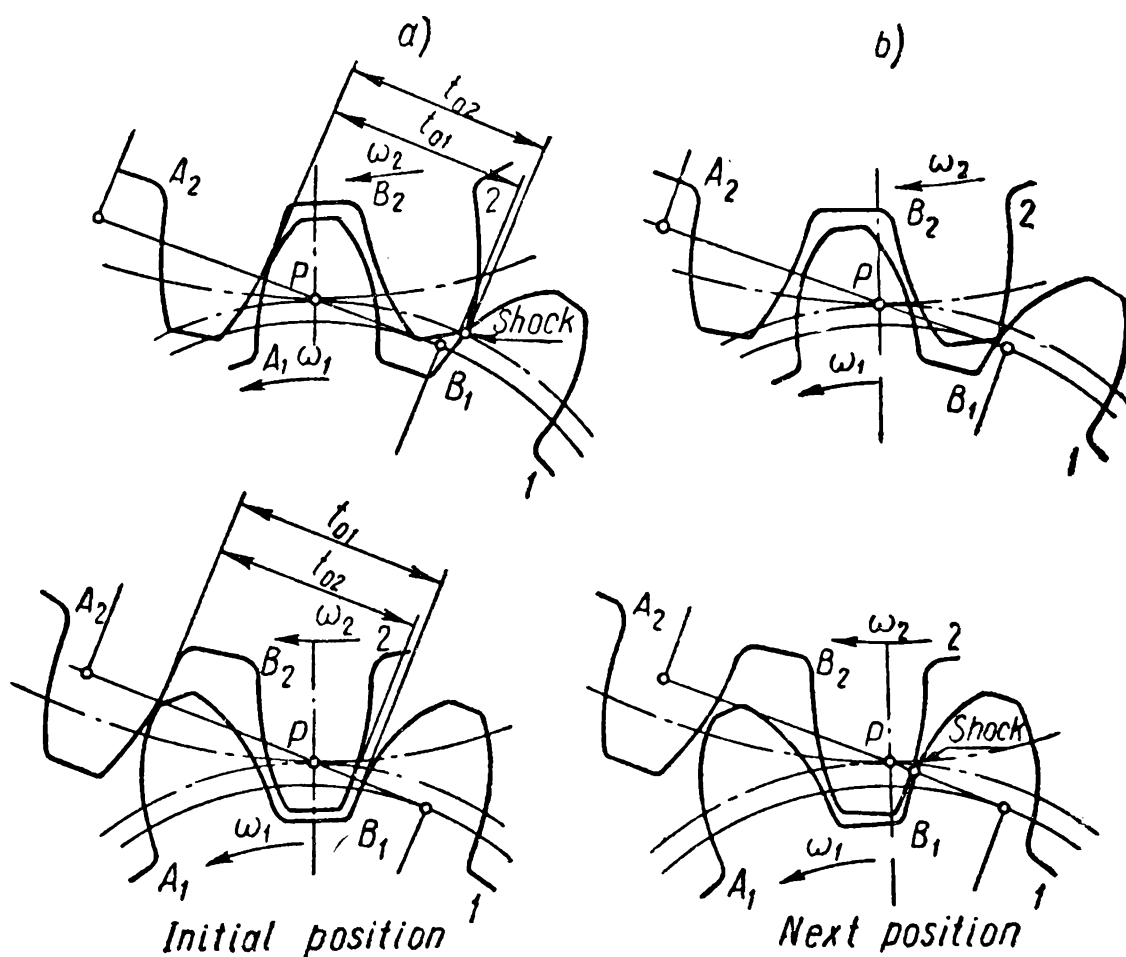


Fig. 155

A shock is also possible in accurately machined wheels because the teeth deform under load and the actual base pitches of a pair of wheels become different: on one wheel the pitch increases and on the other decreases.

As one pair of teeth leaves contact at  $t_{02} < t_{01}$  a shock against the face occurs (Fig. 155, *b*). In this case, due to backlash  $\Delta = t_{02} - t_{01}$  driven wheel 2 will be brought in motion by the tooth of the driving wheel owing to contact with tooth  $A_1$  beyond the line of action. In this period the velocity of wheel 2 will diminish until backlash  $\Delta$  equals zero and the teeth  $B_1$  and  $B_2$  enter contact.

As the teeth enter contact a shock will be caused by a difference in the velocities ( $v_2 < v_1$ ).

Errors in tooth profile can likewise entail dynamic loads.

The less the accuracy of wheel machining and the greater the velocity and masses connected with the gear shafts, the larger are dynamic loads. When choosing the degrees of accuracy for a gear, proceed as recommended in Table 28.

The higher the peripheral velocity of the wheels, the greater accuracy is required.

The relation between the full load ( $P_n + P_d$ ) and normal load  $P_n$  is called the *dynamic load factor*

$$k_d = 1 + \frac{P_d}{P_n} \quad (218)$$

A proper magnitude of  $k_d$  can be determined approximately from Table 32.

Table 32

Dynamic Load Factor  $k_d$  for Straight-Tooth Wheels

Degree of accuracy	Surface hardness of wheel teeth	Peripheral velocity $v$ in m/sec			
		$< 1$	1-3	3-8	8-12
6	$\leq 350$	—	—	1.2	1.3
	$> 350$	—	—	1.2	1.3
7	$\leq 350$	—	1.25	1.45	1.55
	$> 350$	—	1.2	1.3	1.4
8	$\leq 350$	1	1.35	1.55	—
	$> 350$	1	1.3	1.4	—
9	$\leq 350$	1.1	1.45	—	—
	$> 350$	1.1	1.4	—	—

Table 32 gives values of the factor  $k_d$  as a function of tooth surface hardness to account for the fact that an increase in the tooth strength makes it possible to increase the load  $P_n$  when the factor  $k_d$  will decrease [formula (218)].

As was pointed out earlier, to lessen the force of shock, use is made of tip relieves (Fig. 156). The tip relief changes the tooth

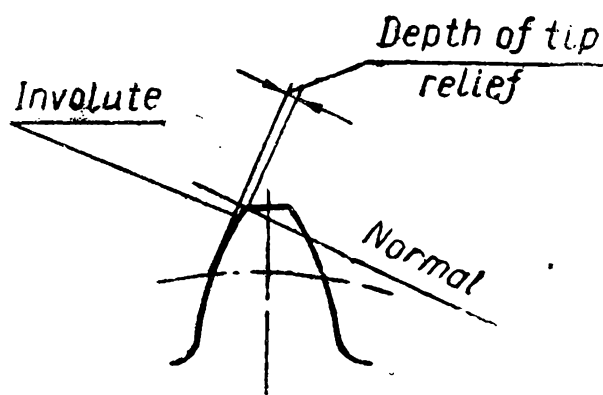


Fig. 156

profile to such an extent as to compensate for the change in the base pitch due to the tooth deformation under load. This makes for a smoother mating of the teeth and decreases the magnitude of dynamic load. For gears with tip relieved straight-tooth wheels tentative values of the dynamic load factors can be chosen from Table 39.

If a more accurate computation of dynamic load is required refer to special recommendations.

To ensure the required strength of teeth, calculations are done on the basis of maximum load acting in contact.

Consequently, the *design unit load*  $q_d$  can be written thus

$$q_d = q k_c k_d = \frac{M_t k_c k_d (i \pm 1)}{A B i \cos \alpha} . \quad (219)$$

**Calculation of Teeth for Surface Strength.** The strength of the surfaces in contact is evaluated on the basis of limiting the maximum surface compressive stress as found from the formulae (30) which deal with a classic contact problem. In actual fact the strength of the tooth working surfaces depends not only on the reduced radius of curvature and the modulus of elasticity of the material, but also on the quality of the tooth surface, on heat treatment, lubrication, etc. Hence, the formula (30) does not reflect the actual picture of the state of stress in the area of contact. However, in the absence of other theoretical data and also owing to the simplicity of this relation, it is still used in designing toothed wheels, while the difference between the theoretical presumptions of the formula (30) and the actual conditions of load on the tooth surfaces is compensated for by using allowable compressive stresses found experimentally; in this case the experimental results are also processed on the basis of the formula (30).

Let us transform the formula (30) to apply it to the teeth of mating wheels after replacing its values by the parameters of a toothed gear.

Since pitting begins in the area of the line of action (pitch circle) we must substitute in the formula (30) the magnitudes of the design unit pressure  $q_d$  and the reduced radius  $q$  for the mating moment in the pitch point.

It follows from Fig. 157, that

$$q_p = \frac{d_p}{2} \sin \alpha$$



and

$$Q_w = \frac{d_w}{2} \sin \alpha$$

and since  $d_p = \frac{2A}{i \pm 1}$  and  $d_w = \frac{2Ai}{i \pm 1}$  then

$$Q = \frac{Q_p \times Q_w}{Q_w \pm Q_p} = \frac{Ai}{(i \pm 1)^2} \sin \alpha. \quad (220)$$

Substituting in the equation (30) the design unit load from the formula (219) and the reduced radius of curvature from the formula (220) we find the surface compressive stress in the pitch point.

$$\begin{aligned} \sigma_{sur} &= 0.418 \sqrt{\frac{q_d E}{Q}} = \\ &= 0.418 \sqrt{\frac{M_t (i \pm 1)^3 E k_c k_d}{A^2 i^2 B \cos \alpha \sin \alpha}} \text{ kg/cm}^2. \end{aligned}$$

Replacing  $\cos \alpha \times \sin \alpha = \frac{1}{2} \sin 2\alpha$  we obtain

$$\begin{aligned} \sigma_{sur} &= 0.59 \frac{i \pm 1}{Ai} \sqrt{\frac{1}{\sin 2\alpha}} \times \\ &\times \sqrt{\frac{i \pm 1}{B} E M_t k_c k_d} \leq [\sigma]_{sur} \text{ kg/cm}^2 \end{aligned} \quad (221)$$

where  $[\sigma]_{sur}$  is the allowable surface stress.

In design calculations the centre distance  $A$  and the wheel width  $B$  should be found. Let us square the medium and right sides of the formula (221) and denote  $B = \psi A$ . Solving the equation obtained relative to  $A$  we get

$$\begin{aligned} A &= (i \pm 1) \times \\ &\times \sqrt[3]{\left( \frac{0.59}{i [\sigma]_{sur}} \right)^2 \frac{E}{\sin 2\alpha} \frac{M_t k_c k_d}{\psi}} \text{ cm.} \end{aligned} \quad (222)$$

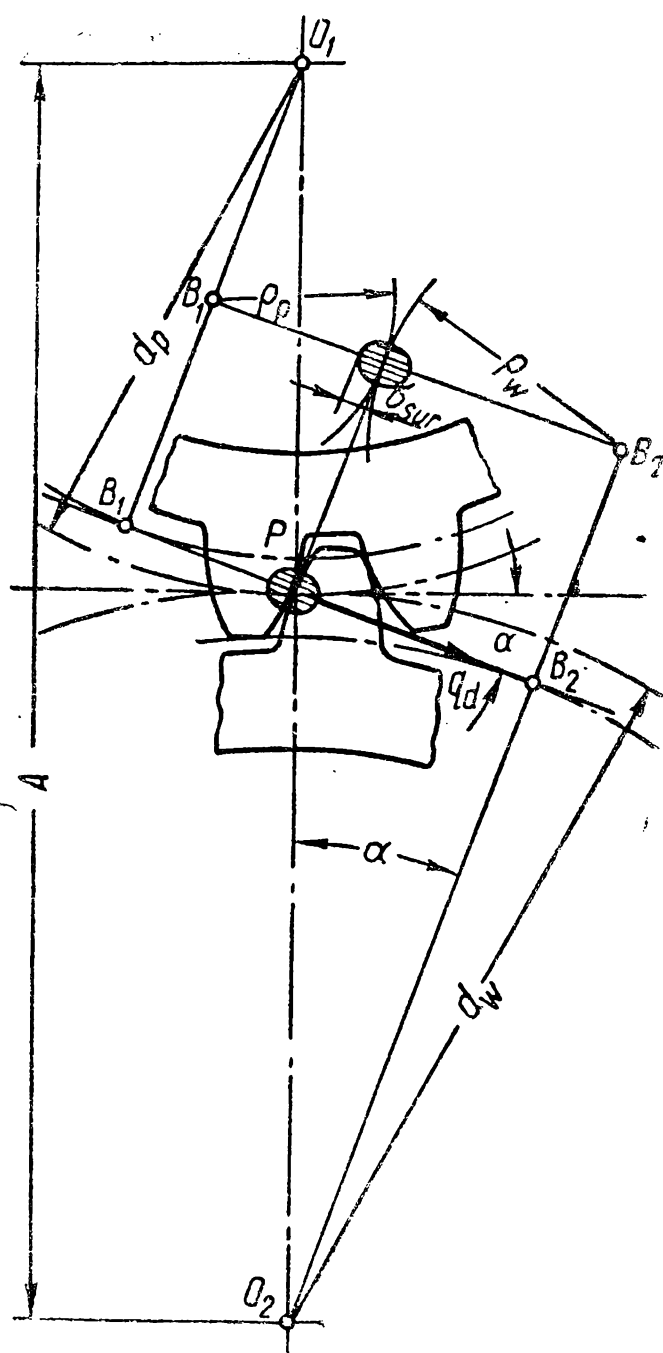


Fig. 157

Analysing the formula (222) we notice that the larger the pressure angle  $\alpha$ , the greater the load-carrying capacity of the gear will be. Thus, for example, for a gear with an angular cor-

rection at  $\alpha = 26^\circ$  the transmitted torque  $M_t$  will be larger than for an uncorrected gear ( $\alpha = 20^\circ$ ) by 22%.

When analysing the influence of the material on the gear proportions it is necessary to allow for the mutual change in allowable stress and modulus of elasticity, i. e., the ratio  $\frac{([\sigma]_{sur})^2}{E}$ .

For a gear with two uncorrected steel wheels we shall have  $E = 2.15 \times 10^6$  kg/cm<sup>2</sup> and  $\sin 2\alpha = 0.643$ , hence

$$A = (i \pm 1) \sqrt[3]{\left(\frac{1,070}{i [\sigma]_{sur}}\right)^2 \frac{M_t k_c k_d}{\psi}}. \quad (222')$$

If the gear wheel (with a steel pinion) is made from grade CЧ 28-48 cast iron then, instead of 1,070 in the formula (222'), we should substitute 915; with a phenolic laminated pinion the figure is 270.

Using the initial formula (221) we can obtain a formula for determining the stresses arising between a mating toothed wheel and a rack (for a steel pair) if we remember that  $q = q_p$

$$\sigma_{sur} = \frac{2,140}{d_{\partial p}} \sqrt{\frac{M_t k_c k_d}{B}} \text{ kg/cm}^2 \quad (223)$$

whence

$$d_{\partial p} = 165 \sqrt[3]{\frac{M_t k_c k_d}{([\sigma]_{sur})^2}} \times \frac{1}{\psi_p} \text{ cm} \quad (224)$$

where  $\psi_p = \frac{B}{d_p}$ .

The values  $\psi$  and  $\psi_p$  are specified on the basis of the following considerations.

In the gears under consideration the relative width of the wheels (the relation between the width and the centre distance  $\psi = \frac{B}{A}$ ) varies within a wide range:  $\psi = 0.1-1.2$ .

In gearboxes with shifting toothed wheels or trains of wheels where it is important to decrease their size along the axles, the relative width should be chosen within  $\psi = 0.1-0.2$ .

For closed-type medium-speed gears of medium power  $\psi$  is taken to equal 0.4-0.6.

In open-type gears where the accuracy of assembly and rigidity of the bearings is not high  $\psi$  should be  $\leq 0.3$ .

The greater the transmitted power, the more rigid the reduction gear housing and the more accurately the gear is designed, the larger the value  $\psi$  should be.

For a more convenient assembly of the gear, after the width of wheels has been found on the basis of the chosen  $\psi$  and the computed centre distance  $A$ , the pinion width is sometimes increased by

5-10 mm. If the pinion is made from plastics its width should be less than the width of the wheel.

The magnitude  $\psi_p = \frac{B}{d_p}$  should never exceed the values given in Table 31.

*Admissible surface compressive stresses.* The initial data for determining the values of the surface endurance limit are obtained from experiments on toothed wheels.

On the basis of loads acting upon the toothed wheels recorded during experiments we can calculate compressive stresses on the tooth surfaces and plot endurance curves. As was pointed out before the relation between continuous endurance limit and surface hardness is found from the formula (31):

$$\sigma_{sur} = C_B \times H_B; \quad \sigma_{sur} = C_R R_C.$$

Since the tooth surfaces can be adequately hardened by various types of heat treatment which heightens resistance to surface loads, the magnitudes of the factors  $C_B$  and  $C_R$  depend on the material and heat treatment employed (Table 33).

Table 33

Factors  $C_B$  and  $C_K$  in Formula (31) at  $N_{base} = 10^7$

Material of wheels	Heat treatment	Surface hardness of teeth	Factor $C_B$ or $C_R$
Various carbon and alloy steels	Annealing, normalising, tempering	$H_B \leq 350$	$C_B = 25$
High-alloy, chrome-nickel steel, grades 12XH3A, 20XH3A, 12XH4A, 18XГT and similar grades	Casehardening	$R_C = 55-63$	$C_R = 310$
Alloy steel, grades 20XH, 12XH2, 20X, 15X, 15XM, 20XΦ			$C_R = 280$
Carbon steel, grades 15, 20, 15Г, 20Г			$C_R = 220$
Carbon or alloy steel, grades 40, 45, 35X, 40X, 40XH	Through or surface hardening	$R_C = 40-55$	$C_R = 240$
Gray cast iron from CЧ 24-44 to CЧ 35-56		$H_B = 170-270$	$C_B = 15$

The magnitude of allowable stress depends, as follows from the analysis of the pitting process, on load conditions, surface finish, oil viscosity and other factors. The effect of each of these factors is taken into account by introducing correction factors: for load conditions— $k_l$ , surface finish— $k_s$  and oil viscosity— $k_o$ , which are found experimentally. From the formula (32) we obtain

$$[\sigma]_{sur} = \sigma_{sur} k_l k_s k_o. \quad (225)$$

Load conditions affect the allowable stress to the greatest degree. At a low number of load cycles  $N$  acting on teeth during the entire service life of the gear, the magnitude of allowable stress can be increased by making use of the curvilinear portion of the endurance diagram.

The load factor can be found from the condition (24'') if we take as mean values on the basis of experiments  $m=6$  and the base number of cycles  $N_{base}=10^7$ .

Under constant load we must substitute in the formula (24'') the number of load cycles  $N$  for  $N_{eq}$  which gives

$$k_l = \sqrt[6]{\frac{10^7}{N}}. \quad (226)$$

When a gear carries a varying load with stages  $M_i$  (including  $M_t$ ) for  $T_i$  hours and the number of the wheel revolutions is  $n_i$  the load factor  $k_l$  is calculated from the formula

$$k_l = \sqrt[6]{\frac{10^7}{N_{eq}}}. \quad (226')$$

The stress  $\sigma_{sur}$  is proportional to  $P_{ni}^{1/2}$ , and hence  $M_i^{1/2}$ . The equivalent number of load cycles will equal (see p. 50)

$$N_{eq} = \frac{1}{M_t^3} \sum M_i^3 N_i \quad (227)$$

where  $M_t$  is the maximum continuously acting torque substituted in the formula (221).

The number of load cycles is found from the formula

$$N_i = 60 \times n_i T_i. \quad (228)$$

Table 33 gives the factors  $C_B$  and  $C_R$  which determine according to the formula (31) the surface endurance limit with the base number of cycles  $N_{base}=10^7$ ; therefore, for steels with surface hardness  $H_B \leq 350$  the magnitude  $k_l$  cannot drop below unity even if  $N_{eq}$  proves above  $10^7$  cycles since for these steels this is the continuous endurance limit. Hence, when  $k_l < 1$  we must take  $k_l = 1$ . For steel

with surface hardness  $H_B > 350$  the continuous endurance limit is assumed at the number of cycles  $N_{base} = 25 \times 10^7$ ; therefore, the minimum value  $k_l$  will be at  $N_{eq} = N_{base} = 25 \times 10^7$ .

After substituting in the formula (226')  $N_{eq} = 25 \times 10^7$  we find  $k_{l\min} = 0.585$ . The same holds for cast-iron wheels.

The magnitudes of the factors  $k_s$  and  $k_o$  are given in specialised literature. Thus, for example, the surface finish factor for teeth with surface finish  $\nabla\nabla 5$  equals  $k_s = 0.95$ ; for gear teeth of degrees of accuracy 7 and 8 (surface finish  $\nabla\nabla 6$ ,  $\nabla\nabla\nabla 7$ )  $k_s = 1$ ; for wheels run in under load (surface finish  $\nabla\nabla\nabla 7$  and 8)  $k_s = 1.1-1.15$ .

For oils with viscosity  $E_t^0 = 10-40$  (temperature at which it is drawn into contact)  $k_o = 1$ .

In approximate calculations we can assume that  $k_s = k_o = 1$ .

As was noted above the surface of the teeth can fail even under transitory (instantaneous) action of heavy load. Such load does not affect the surface endurance but can cause plastic deformation if the surface hardness is  $H_B \leq 350$  or brittle fracture at  $H_B > 350$ . To safeguard against this failure the compressive stress found from the formula (221) with incorporated  $M_{t\max}$  should not exceed the limit value of allowable surface compressive stress (at static load)

$$\sigma_{sur.\max} \leq [\sigma]_{sur.\lim}. \quad (229)$$

We can tentatively assume for steel toothed wheels at  $H_B \leq 350$   $[\sigma]_{sur.\lim} \approx 3.1 \sigma_y$  and at a hardness  $H_B > 350$   $[\sigma]_{sur.\lim} \approx 420 R_C$ .

In closed-type gears surface endurance is computed separately for pinions and wheels. Calculations for the prevention of plastic deformation (or brittle fracture) are made for the teeth of the weaker wheel.

As was mentioned above, pitting is not observed in open-type gears. Therefore, surface stresses are computed in open-type gears only to prevent plastic deformation or brittle fracture of the tooth surface. The revised calculation requires the introduction of maximum load for  $\sigma_{sur}$  into the design formulae. The stress obtained should be below the extreme, allowable surface compressive stress.

In design calculations of a closed-type gear the dynamic load factor  $k_d$  should be specified in advance. For closed-type gears  $k'_d = 1.1-1.35$  can be recommended depending on the expected peripheral velocity. After determining the centre distance  $A'$  we must find the peripheral velocity and then, on the basis of the specified value  $k_d$ , compute the centre distance  $A$  again:

$$A = A' \sqrt[3]{\frac{k_d}{k'_d}}. \quad (230)$$

**Calculation of Teeth for Beam Strength.** Let us consider a tooth of a straight-tooth wheel, with width  $b = 1$  cm, and module  $m$  cm

(Fig. 158). It follows from the above that, as far as beam strength is concerned, the moment of application of load to the tooth top will be the most dangerous. Let us find the bending stresses in the

tooth root to a first approximation by conventional methods of the strength of materials.

Let us find the dangerous section of the tooth root under the load  $q_d$  applied at the tooth top. The direction of the force  $q_d$  relative to the tooth is determined by the form of the tooth (angles  $\alpha_e$  and  $\gamma_e$ ) and the angle of friction  $\varrho$ . Under the action of friction forces the full effort  $q_d/\cos \varrho$  is deflected from the normal by the angle of friction  $\varrho$ . We know from the theory of mechanisms and machines that on the faces of driving teeth the friction forces are directed towards the top and on the faces of driven teeth from the top towards the line of action. The angle of friction depends on the material, the surface finish of the teeth and lubrication. We tentatively assume for gears of the degree of accuracy 6-9  $\varrho = 5-8^\circ$ .

Thus, the angle of load action relative to the centre line of the tooth (Fig. 158) will be  $\delta = \alpha_e - \gamma_e \pm \varrho$ .

The plus sign is taken for driven wheels and the minus sign for driving wheels. Let us transfer the force  $q_d/\cos \varrho$  along its line of action to the point A. The component  $q_d \cos \delta / \cos \varrho$  of this force tends to bend the tooth while the component  $q_d \sin \delta / \cos \varrho$  tends to compress it. In determining the dangerous section we shall take into account only the tooth bending stresses since compressive stress and concentration at the root do not produce any material effect on its position.

We know from the theory of the strength of materials that a cantilever beam shaped as a quadratic parabola is a beam with equal

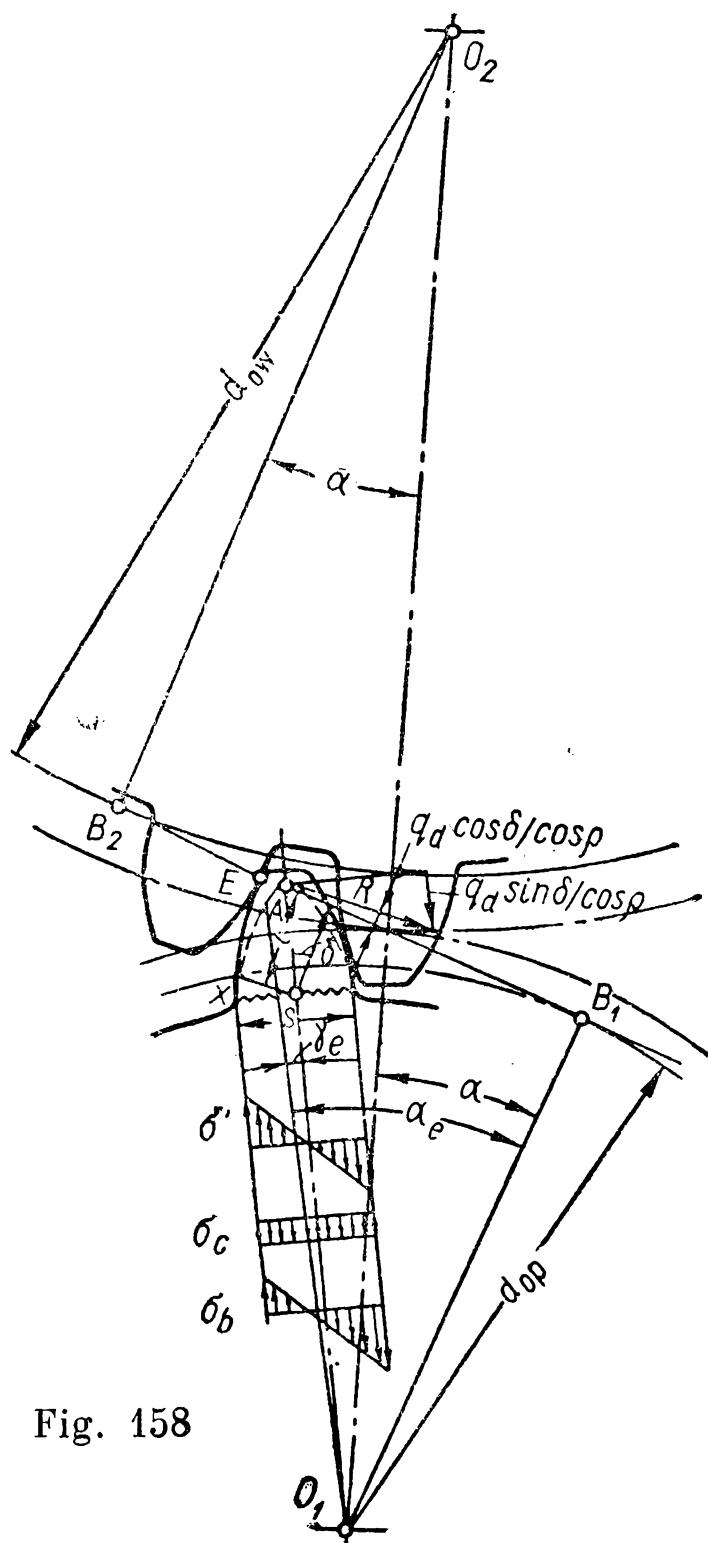


Fig. 158

maximum stresses. Hence, if we inscribe within the tooth contour a quadratic parabola so that its apex coincides with the point of application of force, then the point of contact of its legs with the tooth contour will give us the dangerous section of the tooth  $x-x$  in which the nominal bending stresses will be greatest.

On the working side where the tensile stresses determining the tooth resistance at varying stress operate we obtain

$$\sigma_b = \sigma' - \sigma_c.$$

Stress in bending

$$\sigma' = \frac{M_b}{W} = \frac{6q_d l}{s^2 \cos \varrho}.$$

Stress in compression

$$\sigma_c = \frac{q_c}{F} = \frac{q_d \sin \delta}{s \times \cos \varrho};$$

hence

$$\sigma_b = \frac{6q_d l}{s^2 \cos \varrho} - \frac{q_d \sin \delta}{s \times \cos \varrho}. \quad (231)$$

Let us divide and multiply the right side by  $m$ :

$$\sigma_b = \frac{q_d}{m} \left( \frac{6 \frac{l}{m}}{\frac{s^2}{m^2} \cos \varrho} - \frac{\sin \delta}{\frac{s}{m} \cos \varrho} \right);$$

denoting

$$\frac{6 \frac{l}{m}}{\frac{s^2}{m^2} \cos \varrho} - \frac{\sin \delta}{\frac{s}{m} \cos \varrho} = \frac{1}{y} \quad (232)$$

we obtain

$$\sigma_b = \frac{q_d}{m y} \quad (233)$$

where  $y$  is the tooth form factor whose value depends on the tooth outline.

Since with a given form of the tooth  $l$  and  $s$  are proportional to the module, the expression (232) does not depend on the magnitude of the module. The form of the teeth changes depending on their number  $z$  and the factor  $\xi$  and, therefore, the values of the form factor found graphically are given in the tables of diagrams as a function of the number of teeth  $z$  and the factor  $\xi$ .

For driven wheels the angle  $\delta$  (Fig. 158) is larger than for driving wheels and therefore the form factor of the driven teeth is greater. Figs. 159 and 160 show diagrams for determining the form factors of driving and driven wheels.

For wheels with internal toothing the form factor for the driving wheels can be found at  $z_w \geq 30$  from the formula

$$y = 0.46 \left( 1 + \frac{20}{z_w} \right); \quad (234)$$

and for the driven wheels

$$y = 0.52 \left( 1 + \frac{20}{z_w} \right). \quad (234')$$

Substituting in the formula (233) the design unit load from the formula (219) we get

$$\sigma_b = \frac{M_t k_c k_d (i \pm 1)}{ABim y \cos \alpha} \leq [\sigma]_b \text{ kg/cm}^2 \quad (235)$$

where  $[\sigma]_b$  is the allowable bending stress at the root.

In the formula (235)  $M_t$  is the torque on the wheel irrespective of whether stresses are determined in the teeth of a pinion or a wheel. The tooth form factor  $y$  corresponds to the number of teeth of the calculated wheel. After the bending stresses in the teeth of the pinion  $\sigma_{bp}$  have been found it is easy to arrive at the bending stresses in the teeth of the wheel  $\sigma_{bw}$  from the formula

$$\sigma_{bw} = \sigma_{bp} \frac{y_p}{y_w} \quad (236)$$

since the nominal bending stresses depend solely on the form factor of the tooth.

From the formula (235) it is easy to find the module of the toothed wheels in a gear. After replacing in the equation (235)  $\frac{i \pm 1}{A}$  by  $\frac{2}{d_p} = \frac{2}{z_p m}$  and denoting  $B/m = \psi_m$  we obtain

$$\sigma_b = \frac{2M_t k_c k_d}{z_p m^3 i \psi_m y_p \cos \alpha} \leq [\sigma]_b \text{ kg/cm}^2. \quad (237)$$

Whence we find the module  $m$  assuming  $\cos \alpha = 0.94$

$$m = 1.28 \sqrt[3]{\frac{M_t k_c k_d}{z_p i \psi_m y_p [\sigma]_b}} \text{ cm.} \quad (238)$$

The formula (238) is used to compute the gear module: we first specify the number of the pinion teeth  $z_p$  and the relation  $\psi_m$  and then, substituting in the formula (238) the value  $y_p$  taken from the diagram in Fig. 159, we find the module and approximate it to the nearest standard value.

For pinions of open-type gears, with a view to reducing gear overall dimensions to a minimum, the number of teeth should be small.



The minimum number of teeth without undercutting of uncorrected straight-tooth wheels at  $\alpha_d = 20^\circ$  is  $z_{\min} = 17$ . When smoothness of rotation is not essential (in low-speed or hand-operated gears) and the resultant slight undercutting of the teeth only negligibly reduces the strength of the teeth in bending,  $z$  may be less than 17.

The relation  $\psi_m$  is taken from 8 to 15.

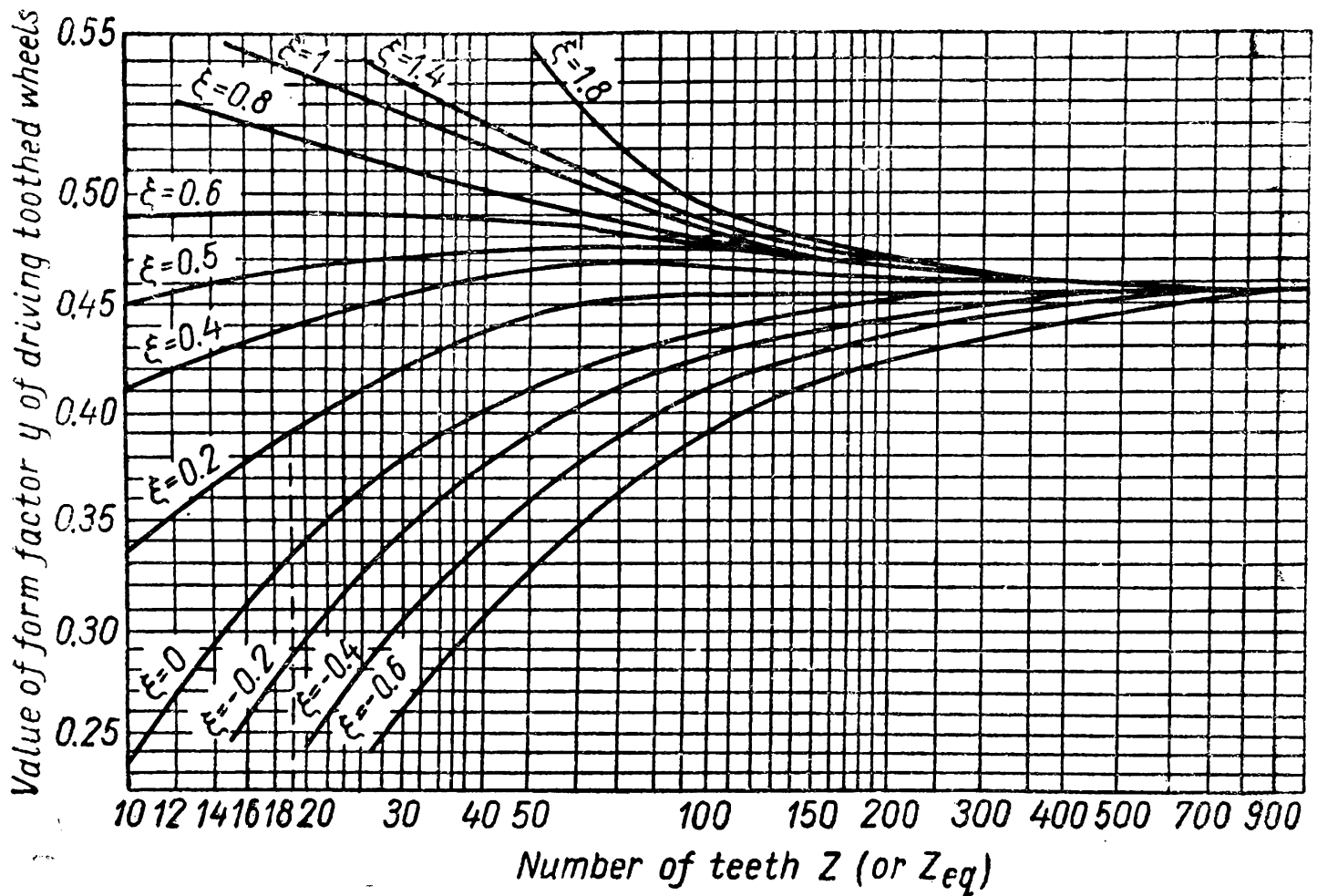


Fig. 159

In closed-type gears the number of teeth should be as large as possible (with the same diameter of the wheels found from the strength design of the teeth surfaces).

An increase in the number of teeth not only reduces costs involved in the manufacture of the gear but, since a smaller amount of metal has to be removed, increases the strength of the tooth-cutting tool, lessens deformation and stress in the wheels and improves the accuracy of contact.

In addition, a larger number of teeth also improves the operating characteristics of the gear: losses due to friction are reduced (since they are inversely proportional to the number of teeth) and the overlap factor increases.

When the teeth active profiles are very hard ( $H_B > 350$ ) and the diameters of the wheels found from calculations for surface endurance of the teeth are small, their number may have to be decreased to increase their module and thereby ensure the required beam strength.

If in this case a tendency towards undercutting arises the teeth should be corrected.

As we know from the theory of mechanisms and machines correction can be used to safeguard the teeth against undercutting (at  $z < 17$ ), to eliminate certain faults in the teeth contact (interference) and decrease unit sliding and pressure; if a given centre distance and number of teeth in a gear do not satisfy the formula (210), correction can be employed to obtain proper mating.

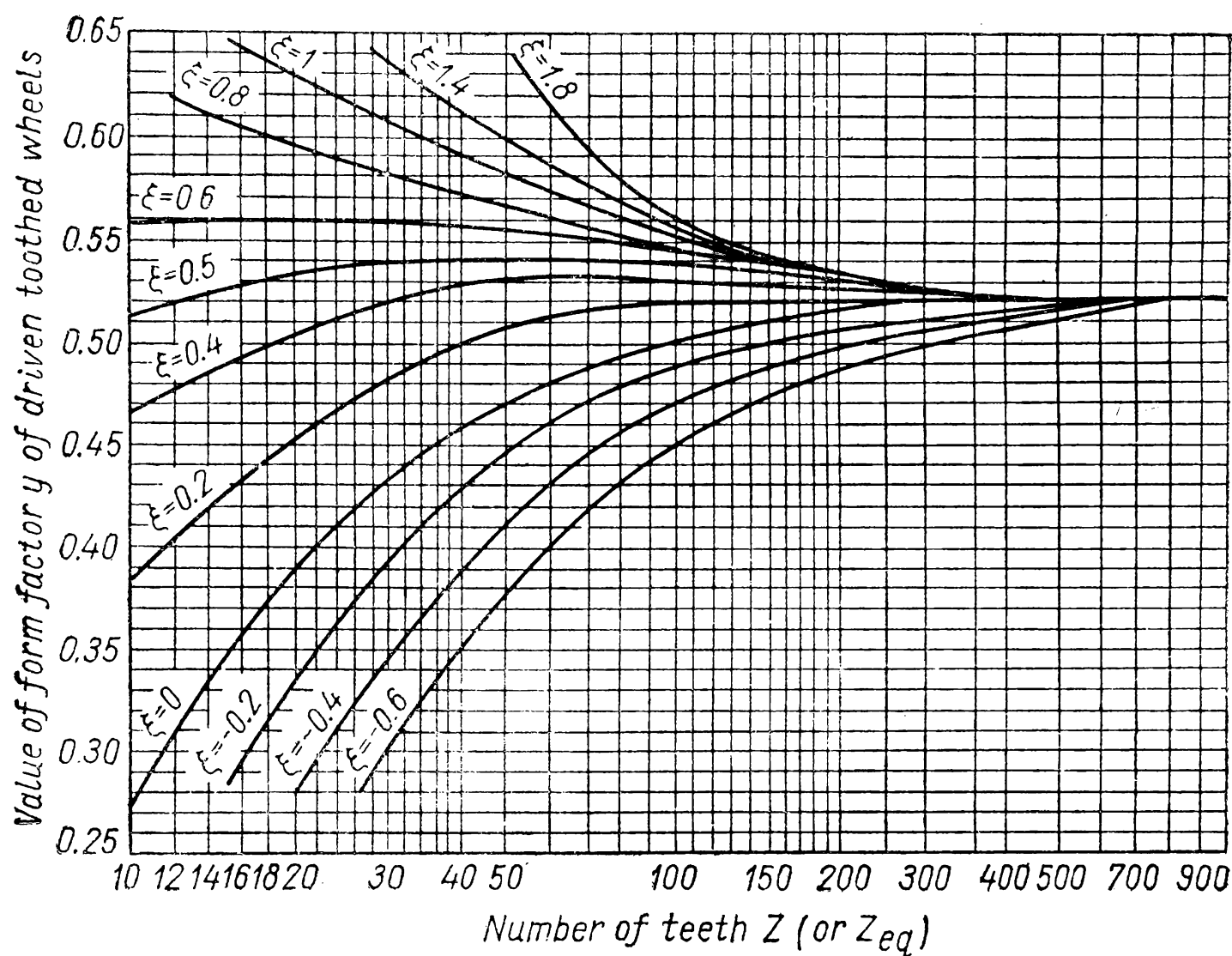


Fig. 160

It was pointed out before that the use of angular correction improves the surface strength of teeth.

Correction can also influence the bending strength of teeth. A positive shift of the tool increases tooth thickness at the root (Fig. 161) and improves the beam strength of the tooth.

The degree of change in tooth strength through correction is illustrated by the values  $y$  in the diagrams in Figs. 159 and 160.

The minimum values of shift factors are related to the undercutting of the teeth.

A larger shift factor does away with undercutting but can likewise thin the tooth at the top; therefore the maximum values of  $\xi$  are limited to certain conditions of thinness.

Usually the maximum tooth thickness at the top is assumed to equal  $s_e = 0.4 m$ .

Table 34 gives corresponding values of the shift factors of the tool:  $\xi_{\text{undercut}}$  for prevention of undercutting,  $\xi_{0.4}$  for  $s_e = 0.4 m$ .

Table 34

Shift Factor  $\xi_{\text{undercut}}$  and  $\xi_{0.4}$ 

$z$	$\xi_{\text{undercut}}$	$\xi_{0.4}$	$z$	$\xi_{\text{undercut}}$	$\xi_{0.4}$
13	0.24	0.39	17	0.01	0.53
14	0.18	0.43	18	-0.05	0.56
15	0.12	0.46	19	-0.11	0.59
16	0.06	0.50	20	-0.17	0.62

Calculation of the teeth for bending and prevention of plastic deformation or brittle fracture is done separately for the pinion and the wheel both for closed- and open-type gears.

Usually, when the surface hardness is  $H_B < 350$ , the proportions of a closed-type gear—centre distance and width of toothed wheels—are found from the calculations of the surface endurance of the teeth.

The calculation of bending is used to find the minimum module permitted by the beam strength. This is a revised calculation.

When the hardness of the working surfaces is  $H_B \geq 350$  a situation may arise when the load-carrying capacity of the gear will be limited not by the surface endurance (because of high allowable stresses  $[\sigma]_{\text{sur}}$ ) but by the beam strength of the teeth.

In this case the proportions of the gear found from the bending calculations of the teeth may prove larger than those found from the calculations of surface endurance. In this case to preserve the minimum proportions of the gear calculations should be repeated on the basis of corrected gear wheels.

The overall dimensions of an open-type gear are found from the calculations of the teeth for beam strength. The high rate of wear

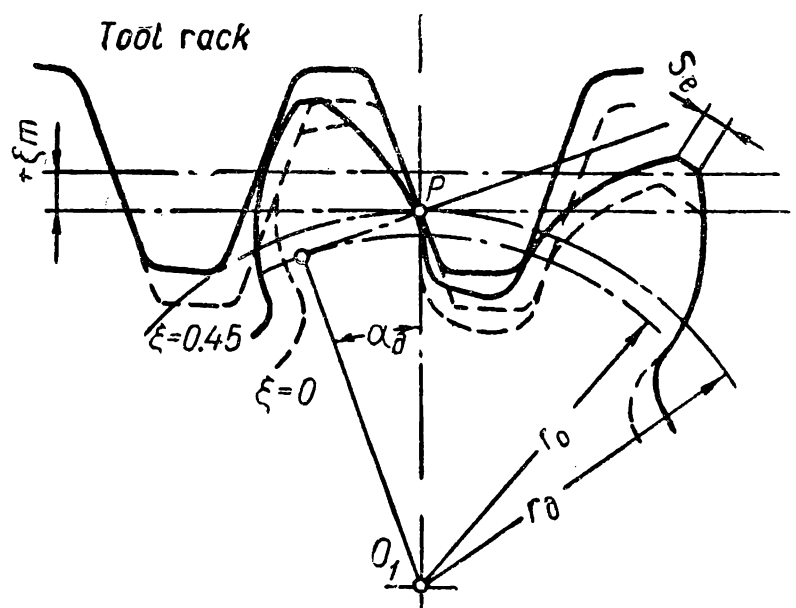


Fig. 161

in open-type gears was pointed out above. Since we have not as yet a reliable method for calculating a gear for wear, the possible wear of teeth in open-type gears is accounted for in the beam strength calculations.

Weakening of teeth due to a reduction in thickness in possible wear is compensated for by a certain increase in the module. For this purpose, a correction factor for wear  $k_w$  equal to 1.25-1.5 is introduced in the design formulae determining bending stresses. This factor has been taken as such on the assumption of the admissibility of tooth wear by 10-20% of its initial thickness.

The design formulae (237) and (238) for straight-tooth gears will take the following form (at  $\cos \alpha = 0.94$ ) for the stresses

$$\sigma_b = \frac{2.12 M_t k_c k_d k_w}{z_p m^3 i \psi_m y_p} \text{ kg/cm}^2; \quad (237')$$

for the module

$$m = 1.28 \sqrt[3]{\frac{M_t k_c k_d k_w}{z_p i \psi_m y_p [\sigma]_b}} \text{ cm.} \quad (238')$$

Due to the presence of stress concentration the actual stresses will be higher than those found from the formula (235)  $k_\sigma$  times ( $k_\sigma$  is the stress concentration factor). Stress concentration is more conveniently accounted for when specifying allowable stresses.

*Allowable bending stresses.* The magnitude of allowable stress depends on the material and its heat treatment, the nature of load carried by the tooth (on one or on both sides), kind of service of the gear, the form of the clearance line and the surface finish in a given spot. When the tooth is loaded one way (with incompletely reversed stress) the magnitude of the allowable stress can be found from the formula

$$[\sigma]_b = \frac{\sigma_0}{n' k_\sigma} k_l$$

where  $\sigma_0$  is the endurance limit of the teeth,  $n'$ —the factor of safety;

$k_\sigma$ —stress concentration factor at the root;

$k_l$ —load factor.

The endurance limit  $\sigma_0$  can be found from the formula (14) after replacing the denominator by a certain constant value.

For heat-treated steel  $\sigma_{ult} = 50-160 \text{ kg/mm}^2$  and  $\sigma_{-1} = 24-80 \text{ kg/mm}^2$ , i. e.,  $\frac{\sigma_{-1}}{\sigma_{ult}} \approx 0.5$ ; at  $k_\sigma = 1.1-1.7$  the denominator in the formula (14) will equal (1.45-1.28)  $n k_\sigma$ .

With the maximum denominator in the formula (14)  $\sigma_0 = 1.4 \sigma_{-1}$ .

For cast iron, assuming on the average  $\frac{\sigma_{-1}}{\sigma_{ult}} = 0.25$  and  $k_\sigma = 1.2$ , we obtain the same relation  $\sigma_0 \approx 1.4 \sigma_{-1}$ .

Hence

$$[\sigma]_b = \frac{1.4\sigma_{-1}}{n'k_\sigma} k_l.$$

(239)

As far as the value of the load factor is concerned, then, in a similar way to that in which the effect of service conditions on the magnitude of allowable surface stress was calculated, the magnitude  $k_l$  can be found from the formula  $k_l = \sqrt[9]{\frac{5 \times 10^6}{N}}$ , if we assume the magnitude  $m$  in the formula (24) for volume strength to equal 9. Under a stepped load instead of  $N$  we use  $N_{eq}$  from the formula (227) with the exponent 9 and not 3 since the bending stresses are proportional to the bending moment.

Hence,

$$N_{eq} = \frac{1}{M_t^9} \sum M_i^9 N_i.$$

(240)

When the teeth are similarly loaded in both ways the allowable stress will be

$$[\sigma]_b = \frac{\sigma_{-1}}{n'k_\sigma} k_l.$$

(241)

The stress concentration factor at the tooth root depends on the number of teeth; the parameters of the basic rack tooth form and the tool shift factor  $\xi$ , since all these factors affect the form of the clearance line, and also on the tooth material and the finish of the crest surface.

A larger tool displacement increases stress concentration.  
Some data on stress concentration factors are tabulated below.

Table 35

Stress Concentration Factors  $k_\sigma$

Toothed wheels	$\xi$	Number of teeth				
		$\leq 20$	30	40	60	$\geq 100$
Steel normalised, hardened ( $r_i$ of basic rack contour $\approx 0.4$ m)	$\xi=0$	1.24	1.34	1.37	1.41	1.45
	$\xi \neq 0$	$k_{\sigma\xi} = k_{\sigma} + \xi \frac{1.54 - k_{\sigma}}{0.6}$				
Ditto at $r_i < 0.4$ m		1.8			2	
Steel—casehardened, nitrided, cyanided; cast-iron		1.2				

To ensure a high quality of the surface at the crest surface the stress concentration factor must be somewhat below those given in the Table.

The factor of safety  $n'$  depends on the kind of blank and subsequent heat treatment. The less homogeneous the structure of the material after manufacture and the more brittle the core after heat treatment, the larger  $n'$  should be.

The numerical values of this factor are given in Table 36.

Table 36

Values of the Factor of Safety  $n'$

Material of wheel	Kind of blank	Heat treatment	Safety factor $n'$
Steel and cast iron	Casting	None	2
		Annealing, normalising or tempering	1.8
Steel	Casting or forging	Surface hardening, casehardening	2.5
	Forging	Through hardening ( $H_B > 350$ )	2
		Normalising or tempering	1.6

To prevent sudden failure or plastic deformation due to bending under excessive load the following condition should be satisfied

$$\sigma_{b \max} \leq [\sigma]_{b \lim}. \tag{242}$$

The maximum stresses due to bending are found from the formula (237) after substituting  $M_{t \max}$ .

The maximum allowable stresses at the tooth root when load is applied statically are determined by the condition of the material. For brittle materials (with core hardness of  $H_B > 350$ ), to prevent possible failure, the stress should not exceed

$$[\sigma]_{b \lim} = \frac{\sigma_{ul}}{n' k_{\sigma}}.$$

The safety factor can be assumed to equal  $n'=2.5-3$ .

To prevent plastic deformation in the bending of steel teeth with the core hardness  $H_B < 350$  the maximum stress should not be over

$$[\sigma]_{b \lim} = \frac{\sigma_y}{n'}.$$

In this case the stress concentration factor is disregarded since stress concentration at static load does not reduce strength.

The safety factor can be assumed equal to  $n' = 1.4-2$ .

**Lubrication and Efficiency.** The lubricant is selected depending on peripheral velocity and unit load. Since the higher the mechanical properties of the wheel material, the larger is the load taken by the teeth, Table 37 gives the recommended values of arbitrary viscosity of oil in Engler's degrees  $E_{50}^{\circ}$ , the values of oil viscosity at  $100^{\circ}\text{C}$  being given in brackets.

The grade of oil is chosen according to the viscosity required.

For toothed wheels without casehardening made from chrome-nickel steel at  $\sigma_{ult} > 80 \text{ kg/mm}^2$  the viscosity of lubricant should be one degree higher than indicated in Table 37.

Table 37

Recommended Values of Oil Viscosity in Engler Degrees  $E_{50}^{\circ}$ 

Material	$v$ in m/sec				
	$<0.5$	$0.5-1$	$1-2.5$	$2.5-5$	$5-12.5$
Plastics, cast iron, bronze	24 (3)	16 (2)	11	8	6
Steel $\sigma_{ult} = 47-100 \text{ kg/mm}^2$	36 (4.5)	24 (3)	16 (2)	11	8
Steel $\sigma_{ult} = 100-125 \text{ kg/mm}^2$	36 (4.5)	36 (4.5)	24 (3)	16 (2)	11
Steel $\sigma_{ult} = 125-150 \text{ kg/mm}^2$ and also all casehardened or surface-hardened steels	60 (7)	36 (4.5)	36 (4.5)	24 (3)	16 (2)

*Losses in mesh* are caused by sliding and rolling friction. Their amount depends on the form of the teeth, their number in the mating wheels and the coefficient of friction in contact. The main losses are due to sliding friction.

These losses depend on the surface finish of the teeth, the properties and amount of the lubricant, the velocity of wheels and the transmitted load since all these factors affect the coefficient of friction  $f$ . Experiments have shown that the coefficient of friction  $f$  decreases as the oil viscosity, velocity of sliding and peripheral velocities grow. The coefficient of friction reaches its maximum at very low velocities of sliding (in the area of the line of action).

At low peripheral velocities the coefficient of friction is markedly affected by the surface finish of the teeth.

Depending on the surface finish, peripheral velocity and oil viscosity, the coefficient  $f$  can change from 0.05 to 0.10. In the case of open-type gears operating dry, the coefficient of friction sharply increases and can reach 0.7-0.8.

The mean value of losses at the transmitted power  $N$  h. p. can be approximately determined from the following formula

$$L_m = \frac{\pi \epsilon f}{(2.5)} \left( \frac{1}{z_p} \pm \frac{1}{z_w} \right) N \text{ h. p.} \quad (243)$$

For straight-tooth wheels the numerical coefficient in the denominator of the right side is taken as 2.

Taking for straight-tooth wheels an average overlap factor of  $\epsilon = 1.45$  we obtain

$$L_m = 2.3f \left( \frac{1}{z_p} \pm \frac{1}{z_w} \right) N \text{ h. p.} \quad (243')$$

Losses in churning the oil cannot be determined analytically. They become higher the greater the values of the peripheral velocity  $v$  m/sec, the width of wheel  $B$  cm, the depth of wheel immersion and the oil viscosity  $E^0$  are, and the smaller the total number of teeth on the wheels  $z_t = z_p + z_w$ ; they can be approximately found from the formula

$$L_{ch} = 0.001vB \sqrt{E^0 \frac{200}{z_t}} \text{ h. p.} \quad (244)$$

The full loss of power is calculated from the formula

$$L = L_m + L_{ch} + L_b \quad (245)$$

where  $L_b$  are the losses in the bearings (p. 475).

The efficiency of the gear can be found from the formula

$$\eta = \frac{N}{N + L} \quad (246)$$

To increase efficiency the gears should have the maximum possible number of teeth (with the minimum module), a sufficiently smooth surface of teeth and be lubricated with oil or grease of optimal viscosity. During operation the gear should be loaded with the maximum allowable load since smaller loads decrease its efficiency.

## DESIGN OF HELICAL AND HERRINGBONE SPUR GEARS

The principal methods employed in designing straight-tooth gears are also valid for helical gears. Below we shall examine the specific features of design which are due only to the geometry of helical and herringbone wheels.

**Main Geometrical Proportions.** The proportions of helical (and herringbone) wheels are found from the formulae used for straight-tooth wheels if we assume that their magnitudes  $m$ ,  $f_0$ ,  $c_0$  and  $\xi$  refer to the circumferential cross-section.



Since the standard parameters of the mating elements of helical wheels occur in normal cross-section then, taking into account their relation in the circumferential and normal cross-sections (with indices  $n$ ), namely  $m = \frac{m_n}{\cos \beta_\partial}$ ;  $f_0 = f_{0n} \cos \beta_\partial$ ;  $c_0 = c_{0n} \cos \beta_\partial$ ;  $\xi = \xi_n \cos \beta_\partial$  we obtain

$$d_\partial = z \frac{m_n}{\cos \beta_\partial} \text{ mm}, \quad (247)$$

$$D_i = d_\partial \mp 2(f_{0n} \pm c_{0n} \mp \xi_n) m_n \text{ mm}, \quad (248)$$

$$D_e = D_i \pm 2h. \quad (207')$$

For uncorrected gears ( $\xi_{np} = \xi_{nw} = 0$ ) or with height correction ( $[\xi_{np}] = [\xi_{nw}]$ )

$$A_\partial = \frac{z_w \pm z_p}{2} \times \frac{m_n}{\cos \beta_\partial} \text{ mm}, \quad (249)$$

the pressure angle of the gear in circumferential cross-section  $\alpha_s$

$$\tan \alpha_s = \tan \alpha_{\partial s} = \frac{\tan \alpha_\partial}{\cos \beta_\partial}; \quad (250)$$

$$h = (2f_{0n} + c_{0n}) m_n \text{ mm}. \quad (251)$$

For gears with angular correction

$$A = \frac{z_w \pm z_p}{2} \times \frac{m_n}{\cos \beta_\partial} \times \frac{\cos \alpha_{\partial s}}{\cos \alpha_s}; \quad (252)$$

$$\text{inv } \alpha_s = \frac{2(\xi_{sw} \pm \xi_{sp})}{z_w \pm z_p} \tan \alpha_{\partial s} + \text{inv } \alpha_{\partial s}; \quad (253)$$

$$h = \frac{2f_{0n} + c_{0n}}{2(f_{0n} + c_{0n})} \left( \pm A - \frac{D_{ip} \pm D_{iw}}{2} \right) \quad (254)$$

where  $\alpha_{\partial s}$  is the pressure angle of the rack in the circumferential cross-section;

$\beta_\partial$ —the helix angle on the pitch cylinder.

We take  $f_{0n} = 1$ ;  $c_{0n} = 0.25$ ;  $m_n$  according to the standard;  $\xi_n$  from Table 34.

**Forces Acting in a Gear.** Let a torque  $M_t$  be acting upon the wheel. The full pressure on a tooth  $P_n$  acts in the plane of action normal to the teeth surfaces. Since in the plane of action the teeth are inclined at an angle  $\beta_0$  then the vector  $P_n$  is likewise inclined, relative to the transversal plane, at an angle  $\beta_0$  (the effect of friction is neglected). This normal force (Fig. 162, *a*) can be resolved into three components: peripheral effort  $P$ , radial effort  $P_r$  and axial effort  $P_a$ .

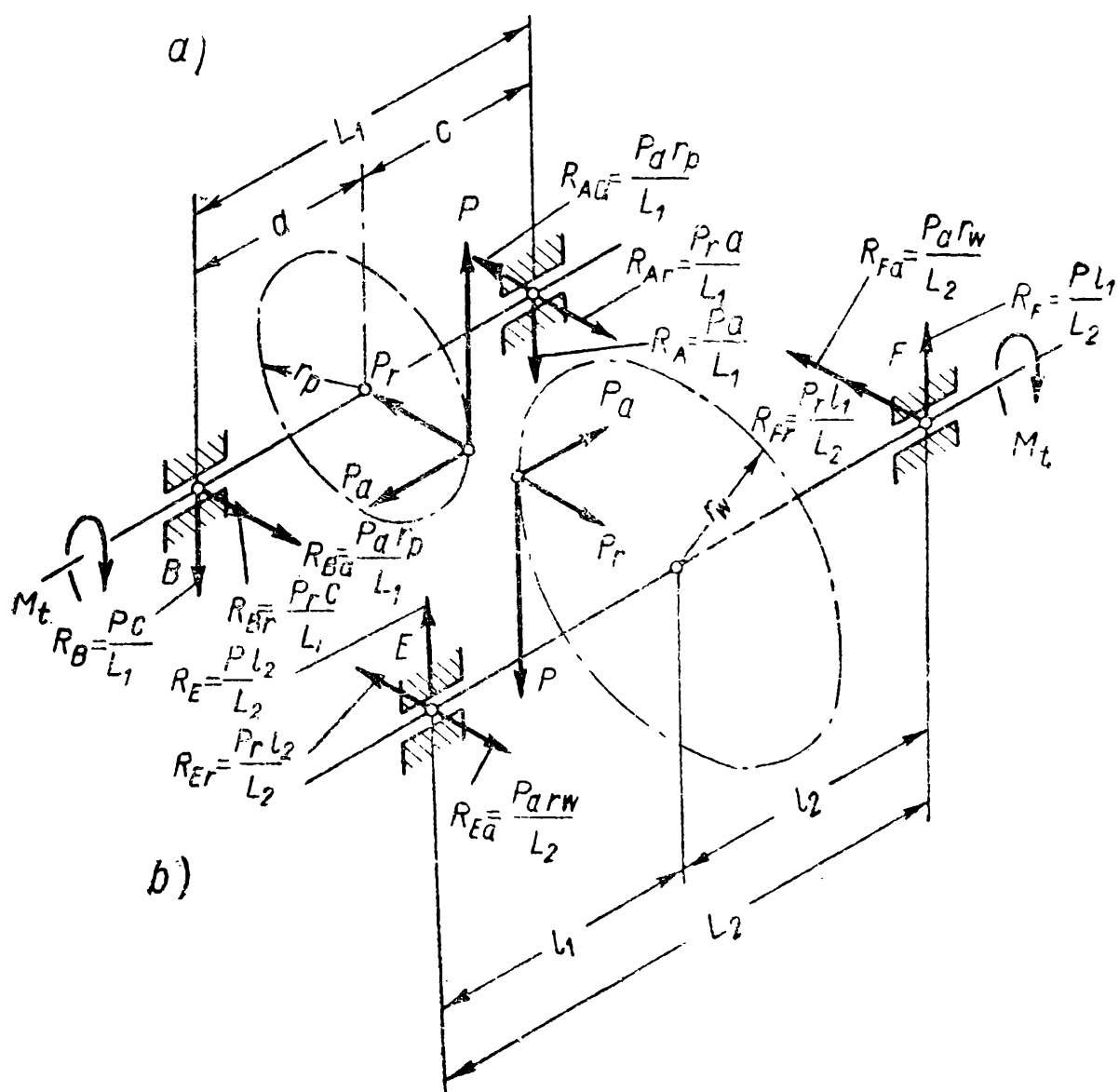
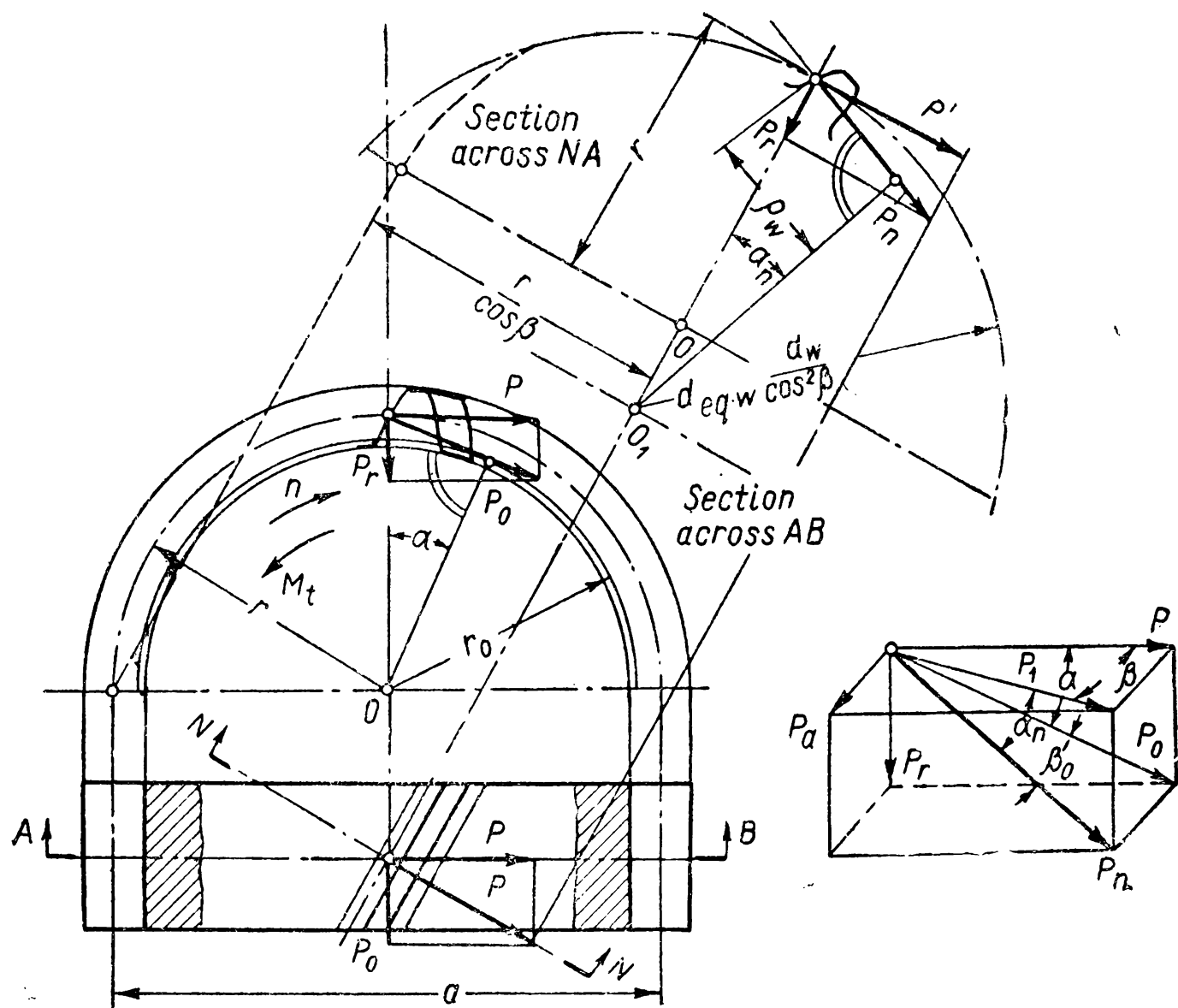


Fig. 162

The magnitude and direction of the peripheral and radial efforts are determined in the same way as in the case of a straight-tooth gear.

The axial force will be

$$P_a = P \tan \beta \quad (255)$$

where  $\beta$  is the helix angle on the pitch cylinder.

The direction of the axial force depends on the direction of rotation and the inclination of the teeth. Fig. 162 shows the forces with teeth inclined to the right on a driven wheel rotating clockwise.

When the direction of the teeth inclination or that of rotation is changed, the direction of the axial force is reversed.

Reactions in the bearings (Fig. 162, *b*) are found by conventional methods. In a helical gear, even if the wheels between the bearings are arranged symmetrically, the loads carried by the bearings will be different: reaction  $R_a$  from the moment  $P_a r_w$  on the left-hand bearing is added to the reaction  $R_r$ , while on the right-hand side it is subtracted. The bearings should be so designed that the axial force  $P_a$  is taken by the bearing carrying the smaller radial load.

The magnitude of the normal force can be found from the relations in Fig. 162.

$$P_0 = P_n \cos \beta_0$$

and

$$P_0 = \frac{2M_t}{d_{ow}} = \frac{2M_t}{d_w \times \cos \alpha},$$

whence, remembering that  $d_w = \frac{2Ai}{i \pm 1}$

$$P_n = \frac{2M_t}{d_w \times \cos \alpha \times \cos \beta_0} = \frac{M_t (i \pm 1)}{Ai \cos \alpha \times \cos \beta_0}. \quad (256)$$

This force is taken as a basis for calculating the strength of helical and herringbone wheels.

**Design Load.** As distinct from straight-tooth gears (p. 267) a helical gear should be designed so that at least two pairs of teeth mesh simultaneously. This is ensured by choosing proper inclination of the teeth and width of the wheels.

We know from the theory of mechanisms and machines that for the above condition to be satisfied the width of the wheels  $B$  should be larger than the axial pitch  $t_a$ . As in an operating gear, due to inevitable inaccuracies, the actual contact of the teeth will be spread over part of the theoretical length of the line of contact (for gears of the 7th degree of accuracy over 80% of the length) the following condition should be obviously satisfied

$$B \geq \frac{t_a}{0.8}. \quad (257)$$

If this condition is not satisfied the gear will operate as a straight-tooth gear.

When the width of the wheels and the helix angle are large, ten or more pairs of teeth can mesh simultaneously.

The teeth of helical gears enter contact gradually: contact begins at one point, as the wheels turn the line of contact lengthens, remains for some time constant and then gradually diminishes to zero. On the teeth sides the lines of contact are inclined.

Thus, the load is transmitted from the driving to the driven wheel over a much greater number of lines of contact than in a straight-

tooth gear. The total length of the lines of contact when the width of wheels is not a multiple of the axial pitch does not remain constant but varies from  $L_{\min}$  to  $L_{\max}$  as the wheels turn by the amount of the circumferential pitch.

To reduce vacillation in the total length of the lines of contact the width of wheels should be a multiple of the axial pitch.

In a herringbone gear load is transmitted in the same way as in a helical gear. Since the contact on the left and right sides of the herringbone gear occurs simultaneously, the condition (257) is satisfied if we substitute in this formula  $B/2$  instead of  $B$ .

Load is spread over the lines of contact in a helical gear as in a straight-tooth gear, i. e., unevenly. However, this is caused not

only by the deformation of shafts and wheels and other parts of the gear, but also because the lines of contact are inclined on the teeth. As can be seen from Fig. 163, when a pair of helical teeth enter contact the area of the maximum total rigidity of the pair of teeth is located near the line of action. At the ends of the line of contact the rigidity is less: at  $C$  because the addendum portion of tooth 1 is deformed to a much greater degree and at  $B$  because the addendum portion of tooth 2 displays greater resilience.

As a result, load concentration along the lines of contact in a helical gear will be variable.

Load concentration will be especially great along the lines of contact near the line of action where the teeth enter contact near the end planes of the wheels.

To simplify the determination of the maximum unit load near the line of action the normal load  $P_n$  is assumed to be uniformly spread over the minimum length  $L_{\min}$  of the lines of con-

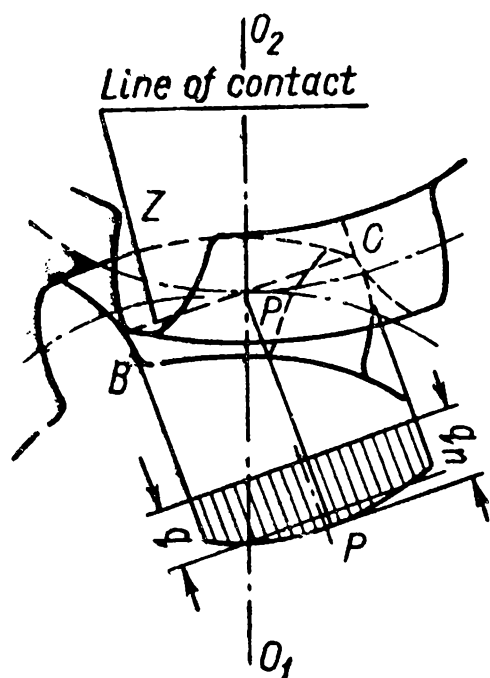


Fig. 163

tact and concentration is accounted for by multiplying the obtained value  $q$  by a load concentration factor.

Utilising the formula (256) we obtain

$$q = \frac{P_n}{L_{\min}} = \frac{M_t (i \pm 1)}{A i \cos \alpha \times \cos \beta_0 L_{\min}} \text{ kg/cm} \quad (258)$$

and

$$q' = q \times k.$$

Here  $k$  is the maximum load concentration factor along the line of contact which, to simplify further calculation, is represented as a product of two magnitudes:  $k_c$  whose nature has been elucidated in examining straight-tooth gears and the load concentration factor in the pitch point  $k_n = \frac{q_n}{q}$ :

$$k = k_c \times k_n. \quad (259)$$

We know from the theory of mechanisms and machines that

$$L_{\min} = \frac{B \varepsilon \lambda}{\cos \beta_0} \text{ cm}$$

where  $\varepsilon$  is the overlap factor in the circumferential cross-section;

$\lambda$ —the factor of variation in the total length of the lines of contact; then the design load with account taken of the dynamic load factor  $k_d$  will be

$$q_d = q' k_d = \frac{M_t (i \pm 1) k_c k_d k_n}{A i \cos \alpha B \varepsilon \lambda} \text{ kg/cm.} \quad (260)$$

To calculate the teeth for bending we must take the load acting at tooth addendum, i. e., according to the formula (260), without the factor  $k_n$ .

In selecting a rational wheel width  $B$  the tentative data in Table 38 can be used.

Table 38

Limit Values of Ratio  $\frac{B}{d_p}$  for Helical and Herringbone Gears

Arrangement of bearings	Arrangement of toothed wheels relative to bearings	Sufficiently constant load	Varying load
Bearings in one rigid housing	not cantilever	2	1.6
	at least one cantilever wheel	0.9	0.8

As was pointed out before, helical and herringbone gears operate more smoothly and noiselessly than straight-tooth gears because

the teeth do not mate at once along the entire width, as is the case with straight-tooth gears, but gradually, the contact beginning first at one point. Besides, during operation of a helical or herringbone gear a minimum of two pairs of teeth are always engaged simultaneously and the teeth are more readily run in. Therefore, dynamic loads in helical and herringbone gears are less than in straight-tooth gears.

Tentative values of the dynamic load factor  $k_d$  for helical and herringbone wheels are given in Table 39.

Table 39

Dynamic Load Factor  $k_d$  for Helical Wheels

Degree of accuracy	Surface hardness of teeth $H_B$	Peripheral velocity $v$ in m/sec				
		<3	3-8	8-12	12-18	18-25
6	$\leq 350$	—	1	1.1	1.2	1.4
	$> 350$		1	1	1.1	1.2
7	$\leq 350$	1	1	1.2	1.3	1.5
	$> 350$	1	1	1.1	1.2	1.3
8	$\leq 350$	1.1	1.3	1.4	—	—
	$> 350$	1.1	1.2	1.3		
9	$\leq 350$	1.2	1.4	—	—	—
	$> 350$	1.2	1.3			

**Calculation of Teeth for Surface Strength.** For a gear with helical or herringbone wheels we must substitute in the formula (30) the reduced radius of curvature of profiles in normal cross-section.

In the cross-section of a helical wheel normal to the direction of the teeth  $NN$  we obtain an ellipse (Fig. 162). The tooth profile in this cross-section sufficiently coincides with the profile of a straight tooth with a module equal to the normal module  $m_n$  on a spur wheel of radius  $\frac{d_{eq}}{2}$  which equals the radius of the ellipse curvature at this point.

The radius of curvature of an ellipse with axes  $a = \frac{r}{\cos \beta}$  and  $b = r$  in the direction of the minor semi-axis  $b$  will equal (Fig. 162)  $\frac{d_{eq}}{2} = \frac{a^2}{b}$ , and hence

$$d_{eq.p} = \frac{d_p}{\cos^2 \beta}$$

and

$$d_{eq.w} = \frac{d_w}{\cos^2 \beta} .$$

In this way

$$Q_p = \frac{d_{eq.p}}{2} \sin \alpha_n = \frac{d_p}{2 \cos^2 \beta} \sin \alpha_n$$

and

$$Q_w = \frac{d_w}{2 \cos^2 \beta} \sin \alpha_n.$$

Remembering that  $d_p = \frac{2A}{i \pm 1}$ ,  $d_w = \frac{2Ai}{i \pm 1}$ ,  $\sin \alpha_n = \sin \alpha \times \cos \beta_0$  and  $\beta_0 \approx \beta$  we obtain

$$Q = \frac{Q_p \times Q_w}{Q_w \pm Q_p} = \frac{Ai}{(i \pm 1)^2} \frac{\sin \alpha}{\cos \beta}. \quad (261)$$

After substituting, in the equation (30),  $Q$  from the equation (261) and the design unit load from the equation (260) we shall have

$$\sigma = 0.418 \sqrt{\frac{(i \pm 1)^3 EM_t k_c k_n k_d \cos \beta}{A^2 i^2 B \epsilon \lambda \cos \alpha \sin \alpha}} \text{ kg/cm}^2.$$

Assuming  $\cos \alpha \times \sin \alpha = \frac{1}{2} \sin 2\alpha$  we get

$$\sigma = 0.59 \frac{i \pm 1}{Ai} \sqrt{\frac{i \pm 1}{B} EM_t k_c k_d} \times \sqrt{\frac{\cos \beta k_n}{\epsilon \lambda \sin 2\alpha}} \leq [\sigma]_{sur}. \quad (262)$$

For design calculations after transforming the formula (262) as was done for the straight-tooth gear we find

$$A = (i \pm 1) \sqrt[3]{\left(\frac{0.59}{i [\sigma]_{sur}}\right)^2 \frac{EM_t k_c k_d}{\psi} \times \frac{\cos \beta k_n}{\epsilon \lambda \sin 2\alpha}} \text{ cm.} \quad (263)$$

For uncorrected gears or gears with height correction at  $k_{n \max} = 1.3$  we can assume  $\frac{\cos \beta \times k_n}{\epsilon \lambda \times \sin 2\alpha} = 1.35$ . Then for steel wheels we obtain

$$A = (i \pm 1) \sqrt[3]{\left(\frac{1,000}{i [\sigma]_{sur}}\right)^2 \frac{M_t k_c k_d}{\psi}} \text{ cm.} \quad (263')$$

When selecting the magnitude  $\psi$  refer to the recommendations for straight-tooth wheels. It should be remembered that the relation  $B/d_p = \frac{\psi}{2} (i \pm 1)$  should not exceed the values in Table 38.

Allowable stresses should be in conformity with the recommendations for straight-tooth gears.

**Calculation of Teeth for Beam Strength.** It is far from easy to determine analytically maximum bending stresses in helical teeth because of their curvilinear form and the inclined positions of the lines of contact.

The bending stresses will be especially dangerous when the teeth will enter contact along their edges. In this case the lines of contact may be situated as shown in Fig. 164. If the teeth are sufficiently long the possible dangerous section will not pass across the root but will assume an inclined position  $x-x$  due to the supporting effect of the unloaded part of the tooth and also to the marked change in bending moment along the tooth length. The more the line of

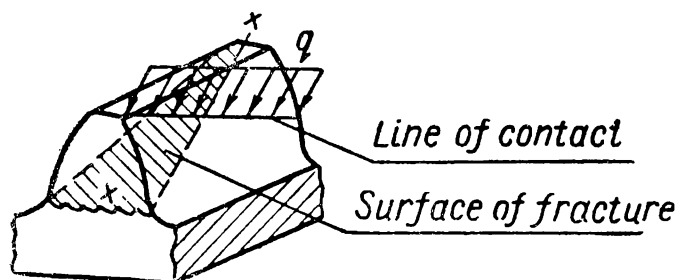


Fig. 164

contact is inclined the greater will be the inclination of the section  $x-x$ . This is corroborated by experiments.

Nominal bending stresses can be determined in the same way as in the case of straight-tooth wheels, by examining the normal section of helical teeth.

In this case we must substitute in the formula (233), instead of  $m$ , the module in the normal cross-section  $m_n$  and take the tooth form factor  $y$  from the diagrams in Fig. 159 and 160 for  $z_{eq}$  number of teeth of an equivalent straight-tooth wheel in normal section, i. e.,

$$\sigma_b = \frac{q_d \times x}{m_n \times y^3} \quad (264)$$

where  $x$  is a factor accounting for a decrease in bending stresses due to teeth inclination.

The equivalent number of teeth is calculated from the formula borrowed from the theory of mechanisms and machines.

$$z_{eq} = \frac{z}{\cos^3 \beta} \quad (265)$$

Preliminary research into the stressed state of a tooth allows us to presume that bending stresses in the dangerous section of helical teeth found from the formula (264) are proportional to the factor  $x = \cos^2 \beta$ .

Thus, for helical and herringbone teeth after substituting the value  $q_d$  in the formula (260) we obtain

$$\sigma_b = \frac{M_t k_c k_d (i \pm 1) \cos^2 \beta}{A i B m_n \varepsilon \lambda \cos \alpha y} \leq [\sigma]_b \text{ kg/cm}^2. \quad (266)$$

For preliminary approximate calculations we can assume

$$\frac{\cos^2 \beta}{\varepsilon \lambda \cos \alpha} = C,$$

then

$$\sigma_b = C \frac{M_t k_c k_d (i \pm 1)}{A i B m_n y} \leq [\sigma]_b \text{ kg/cm}^2. \quad (266')$$



where  $C$  is a factor depending on the helix angle assumed to equal  $C=0.75-0.5$  for helix angles  $\beta=8-45^\circ$ .

In a manner similar to formula (238) we obtain for helical and herringbone teeth (approximately)

$$m_n = 1.15 \times \cos \beta_\theta \sqrt[3]{\frac{M_t k_c k_d}{z_p i \psi_{my} [\sigma]_b}} \text{ cm.} \quad (267)$$

When specifying the helix angle  $\beta_\theta$  it should be borne in mind that helical wheels cost somewhat more than straight-tooth wheels of the same accuracy. Therefore, it is pointless to take an excessively small inclination since greater production and control costs will not be compensated for by the advantages of their application—at a small  $\beta_\theta$  the smoothness of contact does not noticeably increase.

On the other hand, an excessive helix angle will cause a high axial force and will require larger proportions of the gear, larger bearings or additional thrust bearings.

In practice, therefore, the helix angle of helical teeth is taken from  $8$  to  $15^\circ$ . Ordinarily  $\beta_\theta$  varies within  $8-10^\circ$ .

Herringbone wheels have helix angles  $30^\circ$  and more. In this case the axial forces on both sides of the herringbone wheel are mutually equalised (if the gear has been erected correctly).

When selecting allowable stresses refer to the recommendation on pp. 286-289.

The efficiency of helical and herringbone gears is found from the formula (246), the factor 3 being substituted in the denominator of the formula (243) for high-speed gears.

## DESIGN OF BEVEL GEARS

The basic methods for designing spur gears can be also applied to bevel gears. In our further exposition we shall consider only the ways of drawing up design formulae and their specific features due to the geometry of bevel wheels.

**Main Geometrical Proportions.** Most frequently use is made of shafts arranged at right angles. In this case

$$\tan \varphi_p = \frac{1}{i}; \quad (268)$$

$$\varphi_w = 90^\circ - \varphi_p$$

where  $\varphi_p$  and  $\varphi_w$  are half angles of the pitch cones and  $i = \frac{z_w}{z_p}$  is the velocity ratio of the gear.

The cone distance  $L$  is found from Fig. 165:

$$L = 0.5 \sqrt{d_{\partial p}^2 + d_{\partial w}^2}. \quad (269)$$

When the cone distance relates to the wheel width as  $\psi_w = \frac{L}{B}$  the mean diameter of the bevel wheel will be

$$d_m = \left(1 - \frac{0.5}{\psi_w}\right) d_{\partial} \quad (270)$$

and the mean module

$$m_m = \left(1 - \frac{0.5}{\psi_w}\right) m \quad (271)$$

where  $d_{\partial}$  and  $m$  are the diameter of the pitch circle and the module on the larger diameter of the wheel ( $d_{\partial} = mz$ ).

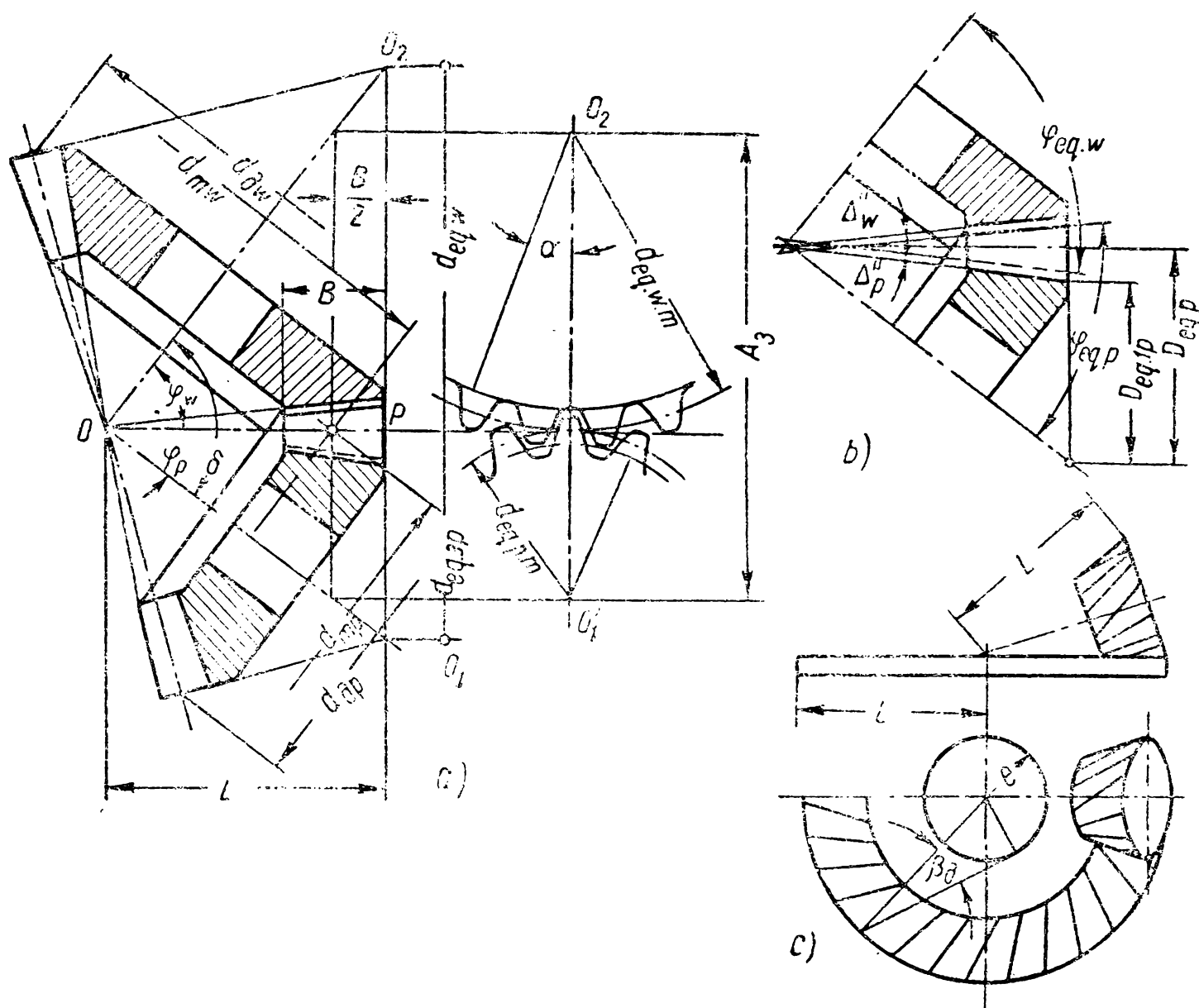


Fig. 165

To simplify calculations for determining the proportions of bevel wheels the latter are replaced by equivalent spur wheels (index  $eq$ ) and use is made of the formulae given above on p. 263.

It follows from Fig. 165 that \*

$$d_{eq.\delta} = \frac{d_\delta}{\cos \varphi}; \quad d_{eq} = \frac{d}{\cos \varphi}; \quad D_{eq.i} = \frac{D_i}{\cos \varphi}; \quad D_{eq.e} = \frac{D_e}{\cos \varphi}; \quad (272)$$

$$i_{eq} = i^2; \quad (273)$$

$$A_{eq} = (L - 0.5B) \frac{i^2 + 1}{i}. \quad (274)$$

The addendum cone is so designed as to match its apex with the apex of the pitch cone; or, to increase the strength of the teeth during correction, the generatrix of the addendum cone is made parallel to the generatrix of the dedendum cone of the other wheel.

In the first instance (Fig. 165, a)

$$\varphi_e = \varphi + \Delta'';$$

$$\tan \Delta = \frac{D_{eq.e} - d_{eq}}{2L}.$$

In the second instance (Fig. 165, b)

$$\varphi_{ep} = \varphi_p + \Delta''; \quad \varphi_{ew} = \varphi_w + \Delta'';$$

$$\tan \Delta = \frac{d_{eq} - D_{ei}}{2L}.$$

For a straight-tooth bevel wheel with  $z$  teeth an equivalent straight-tooth spur wheel will have  $z_{eq}$  teeth equal to

$$z_{eq} = \frac{z}{\cos \varphi_\delta}; \quad (275)$$

for a spiral bevel wheel

$$z_{eq} = \frac{z}{\cos \varphi_\delta \times \cos^3 \beta_m}; \quad (275')$$

here  $\beta_m$  is the angle of tooth inclination in the middle of the width of the toothed rim equal to

$$\beta_m = \beta_\delta \left( 1 + \frac{0.5}{\psi_w} \right). \quad (276)$$

The angle of tooth inclination  $\beta_\delta$  (Fig. 166, c) is found from the formula

$$\tan \beta_\delta \geq \frac{\pi m}{B} \left( 1 - \frac{1}{\psi_w} \right).$$

**Forces Acting in a Gear.** Let us determine the components of full pressure between the teeth of a bevel straight-tooth gear.

---

\* For a pinion an additional index  $p$  is required and for a wheel— $w$ .

After replacing a bevel gear by an equivalent spur gear we shall employ the formulae (212) and (213) for a spur gear with the centre distance  $O_1O_2 = A_{eq}$  (Fig. 166, *a*).

The peripheral force on the mean diameter of a bevel wheel is found from the relation (212) after substituting in it  $d_{mw}$  from the equation (270) for  $d_w$

$$P = \frac{2M_t}{d_{mw}} = \frac{2M_t}{d_w \left(1 - \frac{0.5}{\psi_w}\right)} = \frac{2M_t}{d_{eq.w} \cos \varphi \left(1 - \frac{0.5}{\psi}\right)}. \quad (277)$$

The radial force on the mean diameter will be

$$P_r = P \tan \alpha.$$

Let us resolve this force in two directions parallel to the wheel axes. It follows from Fig. 166, *a* that the radial force on the driving shaft will comprise

$$P_{rp} = P \tan \alpha \cos \varphi_p. \quad (278)$$

The axial force on the driving shaft will be

$$P_{ap} = P \tan \alpha \sin \varphi_p. \quad (279)$$

The magnitude of the radial force on the driven shaft equals the axial force on the driving shaft, while the directions of these forces are opposite:

$$P_{rw} = -P_{ap}. \quad (280)$$

Similarly

$$P_{aw} = -P_{rp}.$$

We use the forces  $P$ ,  $P_r$  and  $P_a$  to calculate the bearing pressures and then to determine the proportions of the gear shafts and bearings (Fig. 166, *c*). To lessen bending moments the pinion should be fixed as close to the bearings as possible.

The forces in a spiral bevel gear can be computed on the basis of the formulae (213) and (255) for an equivalent spur gear.

After finding  $P$  from the relation (277) we determine the radial force  $P_r$  from the formula (213) and the axial force  $P_a$  from the formula (255) replacing  $\beta$  by  $\beta_m$ . Let us transfer these forces to the pitch point on the mean diameter of bevel wheels and resolve them into two directions perpendicular to their axes (Fig. 166, *b*). Summation of the components of these forces gives us radial and axial forces acting upon the shafts of the pinion and wheel.

The radial force on the driving shaft of the bevel gear (see Fig. 166, *b*)

$$P_{rp} = P \tan \alpha \cos \varphi_p + P \tan \beta_m \times \sin \varphi_p. \quad (278')$$

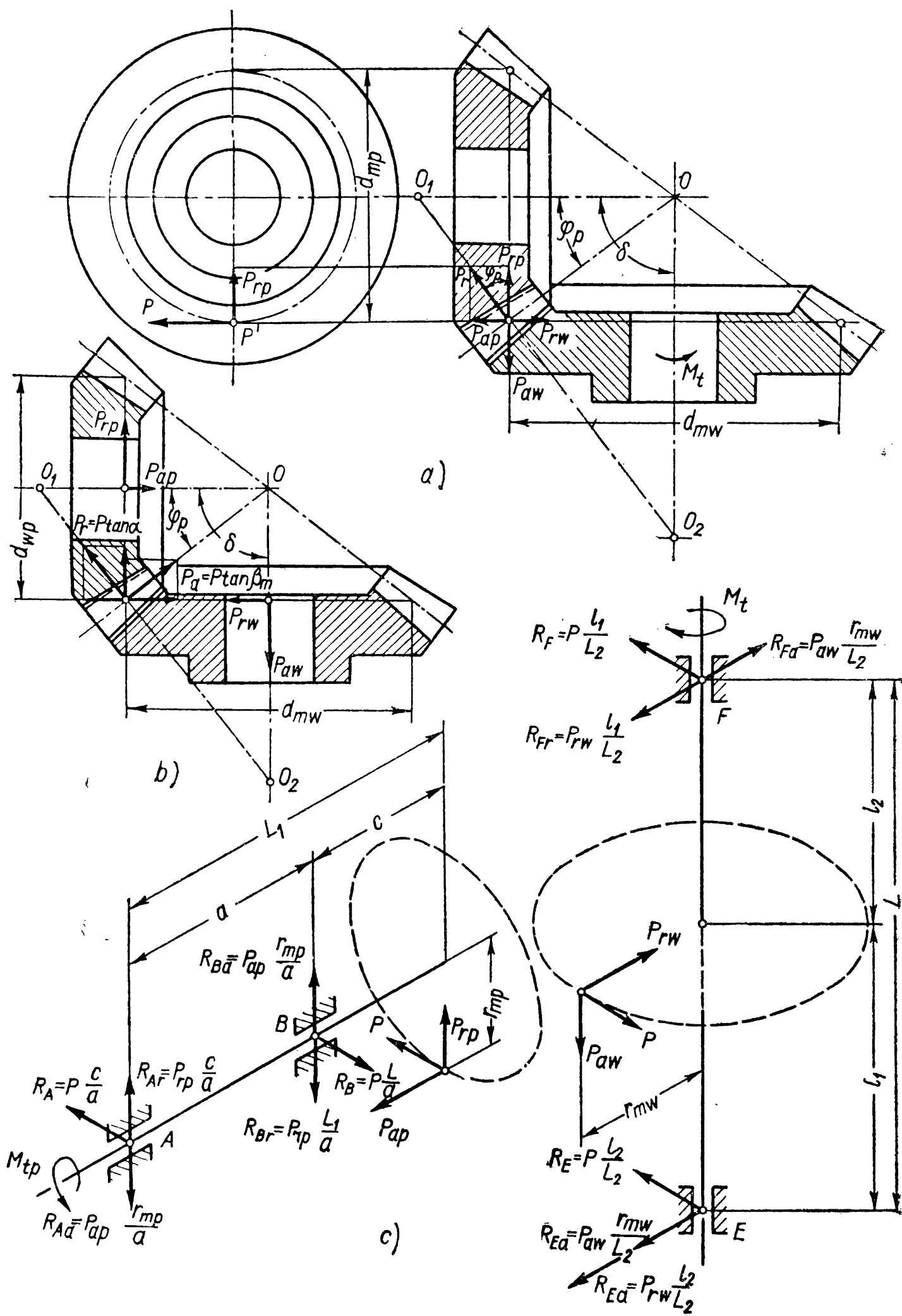


Fig. 166

The axial force on the driving shaft of the bevel gear

$$P_{ap} = P \tan \alpha \times \sin \varphi_p - P \tan \beta_m \times \cos \varphi_p. \quad (279')$$

If, in the two latter equations, we take  $P \times \sin \varphi_p$  out of the brackets, account for the relation (268) and recall that a change in the direction of teeth inclination also changes the direction of the axial force in an equivalent spur gear we shall get for a general case:

$$P_{rp} = -P \sin \varphi_p (i \tan \alpha \pm \tan \beta_m); \quad (278'')$$

$$P_{ap} = -P \sin \varphi_p (-\tan \alpha \pm i \tan \beta_m). \quad (279'')$$

The plus sign before the second member in the brackets is taken when the direction of teeth inclination and the rotation of the driving wheel from the side of the major diameter coincide (for example, if the tooth is inclined to the right and rotation is clockwise); the minus sign is used when these directions are opposed (for example, if the tooth is inclined to the right and rotation is counterclockwise).

If the radial force  $P_r$  on the driving wheel, according to the formula (278'), has a plus sign it is directed from the point of contact towards the shaft axis, with a minus sign—in the opposite direction.

If the axial force  $P_a$  on the driving wheel, according to the equation (279'), has a plus sign it is directed towards the apex of the cone, with a minus sign—in the opposite direction.

The formulae (280) also hold for spiral bevel wheels.

**Calculation of Teeth for Surface Strength.** The design of a bevel gear is based on the assumption that its load-carrying capacity equals that of an equivalent spur gear when the width of its wheels is the same as that of the bevel wheels. We use, therefore, the formulae for spur wheels after replacing  $A$ ,  $i$  and  $M_t$  by  $A_{eq}$ ,  $i_{eq}$  and  $M_{t.eq}$ , respectively.

Because of the approximate nature of such design one formula can be taken for both straight-tooth and helical gears. In the formula (221) we can take  $\sqrt{\frac{1}{\sin 2\alpha}} \approx 1.25$ , in the formula (262)

$\sqrt{\frac{\cos \beta k_n}{\epsilon \lambda \sin 2\alpha}} \approx 1.16$ ; an average is 1.20 and then

$$\sigma_{sur} = 0.71 \frac{i_{eq} + 1}{A_{eq} i_{eq}} \sqrt{\frac{i_{eq} + 1}{B} M_{t.eq} k_c k_d E} \leq [\sigma]_{sur} \text{ kg/cm}^2. \quad (281)$$

The magnitudes incorporated in the formula (281) are found for equivalent wheels in the middle section of the rim of bevel wheels (Fig. 166).

Since the pressure between the teeth of an equivalent spur gear should equal the pressure between the teeth of the designed bevel

gear, then using the equation (277) we find

$$\frac{M_t}{d_w} = \frac{M_t}{d_{eq.w} \cos \varphi} = \frac{M_{t.eq}}{d_{eq.w}}$$

whence

$$M_{t.eq} = M_t \frac{1}{\cos \varphi_w} = M_t \sqrt{\tan^2 \varphi_w + 1} = M_t \sqrt{i^2 + 1} \text{ kg/cm.} \quad (282)$$

After substituting in the formula (281) corresponding values from the formulae (272), (273) and (282) we get

$$\sigma_{sur} = \frac{0.71}{(L - 0.5B) i} \sqrt{\frac{V(i^2 + 1)^3}{B}} M_t E k_c k_d \leq [\sigma]_{sur} \text{ kg/cm}^2. \quad (283)$$

For steel wheels

$$\sigma_{sur} = \frac{1,050}{(L - 0.5B) i} \sqrt{\frac{V(i^2 + 1)^3}{B}} M_t k_c k_d \leq [\sigma]_{sur} \text{ kg/cm}^2. \quad (283')$$

By simple transformation, similar to that done for spur gears, we obtain from the formula (283') for steel wheels a formula for design calculations

$$L = \psi_w \sqrt{i^2 + 1} \sqrt[3]{\left[ \frac{1,050}{(\psi_w - 0.5) i [\sigma]_{sur}} \right]^2 M_t k_c k_d}. \quad (284)$$

The relation  $\psi_w = \frac{L}{B}$  is assumed to be from 2.8 at  $i = 1$  to 5 at  $i = 6$ .

The load concentration factor  $k_c$  is taken from Table 30; the dynamic load factor  $k_d$ —from Tables 32 or 39. When determining peripheral velocity, calculations are based on the mean diameter of bevel wheels. Allowable stresses should conform to the recommendations on p. 277.

**Calculation of Teeth for Beam Strength.** It is usual practice to proceed from the assumption adopted earlier in designing bevel wheels for surface strength that a bevel wheel gear is identical to a spur gear with equivalent wheels in the middle section of the toothed rim. In this case the stress at the root of bevel wheel teeth is equal to the bending stress of teeth of equivalent spur wheels whose width is equal to that of the toothed rim of bevel wheels. It follows from this that in the formula (235)

$M_t$  should be replaced by  $M_{t.eq} = M_t \sqrt{i^2 + 1} \text{ kg/cm}$ ;

$A$  " "  $A_{e1} = (L - 0.5B) \frac{i^2 + 1}{i} \text{ cm}$ ;

$i$  " "  $i_{eq} = i^2$ ;

$m$  " "  $m_m = m \frac{L - 0.5B}{L} \text{ cm}$

and as a result we obtain for straight-tooth wheels

$$\sigma_b = \frac{L \sqrt{i^2 + 1} M_t k_c k_d}{B m i y (L - 0.5B)^2 \cos \alpha} \leq [\sigma]_b \text{ kg/cm}^2. \quad (285)$$

Making a similar substitution in the formula (266') we get for helical wheels

$$\sigma_b = C \frac{L \sqrt{i^2 + 1} M_t k_c k_d}{B m_n i y (L - 0.5B)^2} \leq [\sigma]_b \text{ kg/cm}^2. \quad (286)$$

In the formulae (285) and (286) the tooth form factor  $y$  is taken from the diagrams in Figs. 159 and 160 for the number of teeth of equivalent spur wheels found for straight-tooth bevel wheels from the formula (275) and for helical wheels from the formula (275').

We can use the formula (285) to determine the cone distance  $L$ . After substituting  $\frac{L}{B} = \psi_w$  and  $B = \frac{L}{\psi_w}$  we obtain

$$\sigma_b = \frac{\psi_w^2 \sqrt{i^2 + 1} M_t k_c k_d}{m i y (\psi_w - 0.5)^2 L^2 \cos \alpha} \leq [\sigma]_b \text{ kg/cm}^2.$$

Hence, for straight-tooth gears

$$L = \frac{\psi_w}{\psi_w - 0.5} \sqrt{\frac{\psi_w \sqrt{i^2 + 1} M_t k_c k_d}{m i y [\sigma]_b \cos \alpha}} \text{ cm.} \quad (287)$$

Similarly for spiral bevel gears we obtain from the formula (286)

$$L = \frac{\psi_w}{\psi_w - 0.5} \sqrt{\frac{C \psi_w \sqrt{i^2 + 1} M_t k_c k_d}{m i y [\sigma]_b}} \text{ cm.} \quad (288)$$

The factor  $C$  is assumed to be the same as for spur gears.

The velocity ratio of a bevel gear should not exceed  $i = 6$ .

The overall dimensions of an open-type gear are found from the calculation of teeth for bending. Similar to the formula (238') we get for the module on the mean diameter of the pinion

$$m_m = 1.28 \sqrt[3]{\frac{M_t k_c k_l k_w}{z_p i \psi_m y_p [\sigma]_b}} \text{ cm.} \quad (289)$$

The number of teeth should be specified in advance. Remembering that the number of teeth of an equivalent spur wheel  $z_{eq}$  is always larger than the number of teeth of a bevel pinion  $z_p$  the latter can be less than 17. The relation  $\psi_m = \frac{B}{m_m}$  is assumed equal up to 10.

Allowable stresses are taken in conformity with the recommendations outlined in the calculations for straight-tooth gears.



## CHAPTER XVI

## SCREW, HYPOID, WORM AND GLOBOIDAL GEARS

Screw, hypoid, parallel worm and globoidal worm gears are employed to transmit torque between shafts arranged at an angle to each other.

Since all these gears are modifications of toothed gears the basic considerations regarding the formation of contact and its properties can be also applied to them.

The shafts of these gears can be fixed at any angle but the usual practice is to place them at right angles ( $\delta=90^\circ$ ).

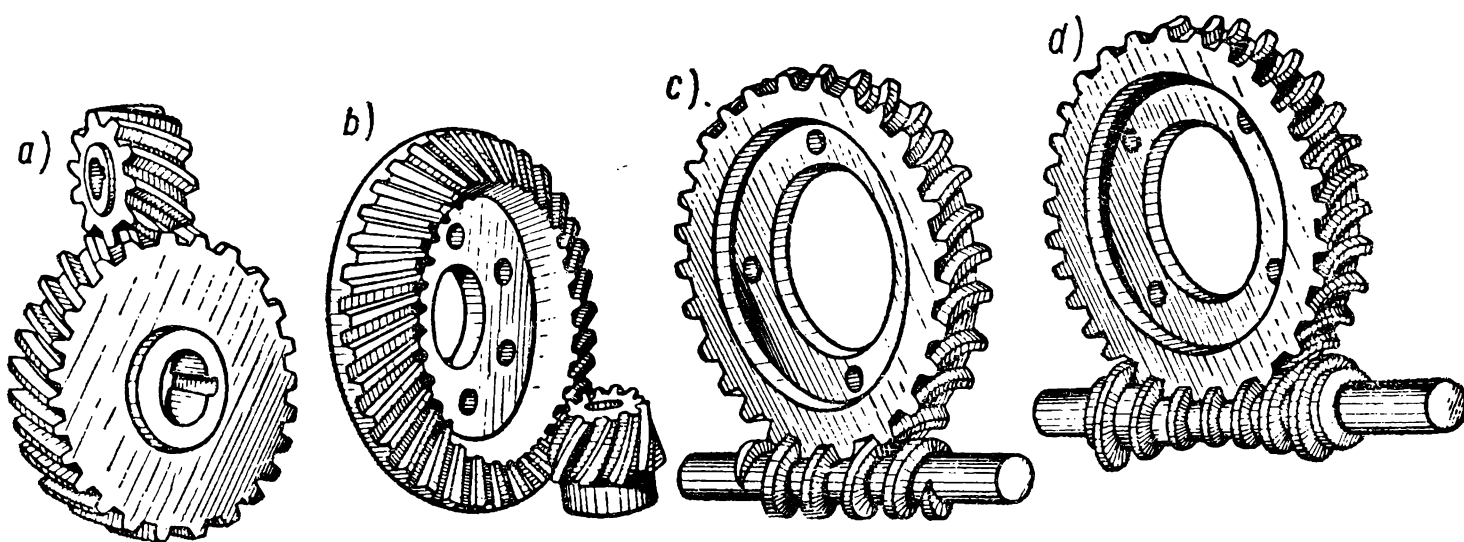


Fig. 167

Sliding along the teeth is a shortcoming common to all these gears; their efficiency is therefore lower than that of toothed gears and the horse powers they handle are confined to a narrower range.

The advantage of these gears lies in their noiseless operation which is more easily obtainable than in toothed spur and bevel gears.

A *screw* gear (Fig. 167, *a*) comprising two helical gear wheels is the simplest combination for transmitting torque between shafts at right angles. Since in such a gear a point contact takes place the transmitted horse power is not high and is limited to several kilowatts. Therefore, these gears are not employed on a large scale: as a rule, they are used as «kinematic» gears with the velocity ratio  $i \leq 5$ .

*Hypoid* gears (Fig. 167, *b*) have a wider field of application. They are employed to handle horse powers of the order of several dozen kilowatts. Since the wheel shafts may be arranged to continue past each other, which makes the gear more rigid, the load-carrying capacity of hypoid gears is higher than that of bevel gears (with intersecting shafts). Hypoid gears are employed in the rear axles of automobiles (the arrangement of the pinion axle below the wheel axle lowers the centre of gravity of the automobile) and in some types

of textile machines, for example, to transmit power from one shaft to several dozen spindles.

When the velocity ratio is not high a hypoid gear can be used instead of a worm gear which costs more and requires nonferrous metals for manufacture.

To transmit considerable horse powers of the order of hundreds of kilowatts at a high velocity ratio, use is made of *worm* (Fig. 167, c) and *globoidal* (Fig. 167, d) gears.

Worm gears offer the following advantages: a) compact layout; b) dependable operation and simple maintenance; c) high velocity ratios. These gears are usually intended for velocity ratios  $i > 8$ . Velocity ratios between 25 and 200 are considered normal for power worm gears.

There are worm gears with very high velocity ratios—500-1,000—but in this case they are employed to transmit low powers.

The disadvantages of worm gears are as follows: large power losses; b) the need for high-quality grades of bronze; c) the use of costly cutting tools. The manufacture of an accurate worm wheel requires hob cutters which conform to the parameters of the worm which is to run with the wheel being cut.

Worm gears are used in drives transmitting horse power from electric motors to the driving axle-shafts of trolley-buses, in tooth-cutting and other machine tools, in auxiliary equipment of rolling mills, etc.

Globoidal gears are employed in the drives of passenger and freight elevators, in trolley-buses, etc. They are used for the same ranges of transmitted horse power and velocity ratios as worm gears while being of smaller outside proportions.

The disadvantages of globoidal gears are: a) the need for artificial cooling because of the relatively small cooled surface of the body; b) high sensitivity to inaccuracies in the gear assembly.

We know from the theory of mechanisms and machines that, in effecting transmission between two shafts at right angles, the axoids of relative motion are hyperboloids of revolution  $a$  and  $b$  (Fig. 168, a). If on these hyperboloids teeth with the same normal pitch and pressure angles are cut we shall obtain a gear with a constant velocity ratio.

In practice, only the narrow portion of pitch hyperboloids is used which, moreover, gives place, in the utilised portion, to a bevel or cylindrical surface. As a result, instead of a line contact we have a point contact of the mating teeth.

If we use for a gear the middle (throat) section of the hyperboloids we shall get a screw gear (Fig. 168, b). In this case the toothed wheels forming the screw gear will be helical wheels with the helix angles  $\beta_p$  and  $\beta_w$  on the respective pitch cylinders.

When we use for toothed wheels portions removed from the middle of the hyperboloids (Fig. 168, *c*) we obtain a hypoid gear (the angle between the wheel axles is  $90^\circ$ ).

A worm gear is a modification of a screw toothed gear differing from the latter in that the number of teeth—starts—on the driving member, the worm, is small and the contact between the teeth occurs not at separate points but along lines of contact. This is due

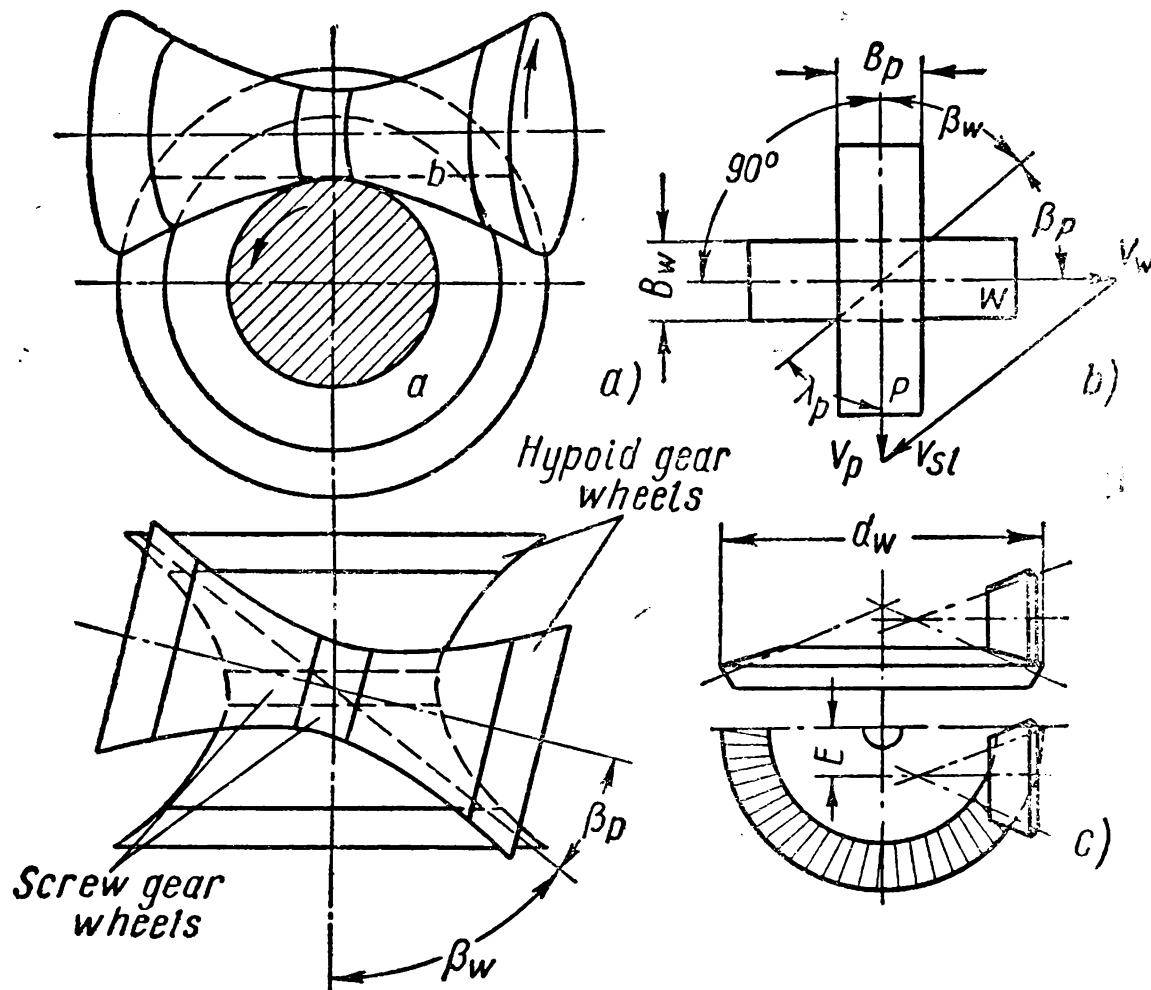


Fig. 168

to the fact that the teeth on the worm wheel are cut by the generating method with a hob cutter of the same form as the worm which is to run with the wheel.

After cutting the wheel the centre distance should equal the centre distance of the worm gear. To increase the length of the lines of contact the external surface of a worm wheel is concave.

The fact that the teeth of the wheel are generated with a tool which corresponds to the worm conjugate with this wheel makes it possible to employ not only involute worms but also worms having other forms, for example, worms with straight-sided threads in axial section (Archimedean worms) or with straight-sided tooth gashes in normal section (convolute worms).

A globoidal gear differs from a worm gear in the form of the cut portion of the worm which is the surface of a globoid (Fig. 167, *d*) contacting the wheel along an arc.

## SCREW GEARS

Since screw gears are formed from helical spur gear wheels the proportions of the screw wheels can be found from the formulae determining the proportions of helical spur wheels.

The distance between shafts which gives us the proportions of the gear with corrected wheels will approximately equal

$$A = \frac{m_n}{2} \left[ \left( \frac{z_p}{\cos \beta_p} + \frac{z_w}{\cos \beta_w} \right) + 2(\xi_{np} + \xi_{nw}) \right] \quad (290)$$

and the width of the wheels is assumed to be

$$B_{p, w} = 3\pi m_n \sin \beta_{p, w}$$

where  $z_p, z_w$  is the number of teeth of the mating pinion and wheel;  
 $m_n$ —the normal module;

$\xi_{np}, \xi_{nw}$ —the shift factors in normal sections of the wheels.

The materials used for the wheels of a screw gear should possess sufficiently high antifriction properties. This requirement is satisfied best of all by combinations of heterogeneous materials: textolite-cast iron, textolite-hardened steel or cast iron-bronze. If a comparatively high load is to be transmitted both wheels can be made from hardened steel and lubricated with antiscuff grease.

To find the forces acting in a screw gear the formulae (212), (213), (255) for helical wheels should be used. At an angle  $\delta = 90^\circ$  the radial forces for both wheels will be the same; but in general the axial force on the pinion equals the peripheral force on the wheel while the peripheral force on the pinion equals the axial force on the wheel.

The load-carrying capacity of a screw gear is limited because of point contact and sliding along the teeth.

With shafts at right angles the velocity of sliding will be (Fig. 168, b)

$$v_{sl} = \frac{v_p}{\cos \lambda_p} = \frac{\pi d_p n_p}{60 \times 1,000 \times \cos \lambda_p} \text{ m/sec.} \quad (291)$$

The most dangerous fault of teeth in a screw gear is *seizure*. To prevent it the gear should be lubricated with viscous oils. Anti-scuff lubricants are very effective.

Mild antiscuff lubricant containing mineral oil and 3-15% of lead soap of oleinic or naphthenic acid dissolved in it is in most common use. The tractor «nigrol» employed in low-speed gears carrying severe loads is one of the most effective antiscuff greases.

Screw gears are calculated in conformity with an empirical formula which determines the maximum effort in a direction normal to the teeth for the prevention of seizure

$$P_n = d_{dp}^2 k_{sc} Q_i \varphi \quad (292)$$

where  $Q_i = \frac{2i}{i + \frac{\cos\beta_w}{\cos\beta_p}}$  is the velocity ratio factor;  
 $\varphi = \frac{1 + 0.5v_{sl}}{1 + v_{sl}}$  —the velocity factor;  
 $k_{sc}$  — the empirical stress selected from Table 40.

Table 40

Values of Factor  $k_{sc}$

Wheel materials	$k_{sc}$ in kg/cm <sup>2</sup>	
	With short-time lapping in pair	With thorough lapping in pair
Steel ( $R_C \geq 50$ )-bronze . . . . .	0.35	0.84
Steel ( $R_C \geq 50$ )-steel ( $R_C \geq 50$ ) . . . . .	0.40	1.05
Cast iron-cast iron or bronze . . . . .	0.55	1.40
Textolite-cast iron or steel ( $R_C \geq 50$ ) . . . . .	0.70	1.75

In design calculations it is necessary to find  $d_{ap}$  from the formula (292) after specifying the velocity factor  $\varphi \approx 0.7-0.5$  and the helix angles  $\beta_p$  and  $\beta_w$ .  
To increase the smoothness of the wheel operation the number of teeth in the pinion should be over 20.  
The beam strength of the teeth can be found from the formulae used for helical wheels.

HYPOID GEARS

Hypoid gears can be designed both with point and line contact of the meshing teeth. The angles at which the teeth are inclined on the wheel  $\beta_w$  and the pinion  $\beta_p$  are different:  $\beta_p > \beta_w$ . For a normal engagement of a pair of wheels their teeth should have the same normal pitch. This condition should be also satisfied in the case of hypoid gears. Here, since the teeth on the pinion are inclined at a greater angle than on the wheel, the circumferential module on the pinion will likewise be larger than on the wheel. Therefore, with the same wheel diameter and the same velocity ratios in bevel and hypoid gears the pinion of the latter will have a larger diameter than that of the bevel gear. Due to the different helix angles of teeth on the wheel and the pinion the pressure angle also changes as the direction of rotation is reversed. The length  $E$ —the offset of shafts (Fig. 168, c)—is limited to prevent seizure. Usually the offset is from  $0.33d_w$  at  $i=1$  to  $0.20d_w$  at  $i>2.5$  ( $d_w$  is the wheel diameter).

The wheels of hypoid gears intended to transmit high loads are made from steel with high surface hardness of the teeth. The failure of hypoid gears is usually occasioned by seizure which is prevented by making the surface of the teeth smoother and harder and by applying antiscuff greases.

The forces acting in the engagement of a hypoid gear can be found by using the formulae adapted for spiral bevel gears, when instead of the angle  $\beta$  we introduce the angles  $\beta_p$  for the pinion and  $\beta_w$  for the wheel and instead of the peripheral effort  $P$  we substitute the peripheral effort  $P_p$  for the pinion and  $P_w$  for the wheel since they differ in magnitude (because  $\beta_p \neq \beta_w$ ).

In the absence of adequate methods of calculation of hypoid gears for seizure we resort to arbitrary calculations for surface strength of the active profiles and for beam strength using the formulae intended for bevel gears. The allowable stresses are assumed to be the same as for toothed gears.

The helix angles of teeth on hypoid wheels should be assumed to equal:  $\beta_w = 30-35^\circ$ , and on the pinions at  $z_p \leq 13$   $\beta_p = 50^\circ$ , at  $z_p = 14-15$   $\beta_p = 45^\circ$  and at  $z_p \geq 16$   $\beta_p = 40^\circ$ .

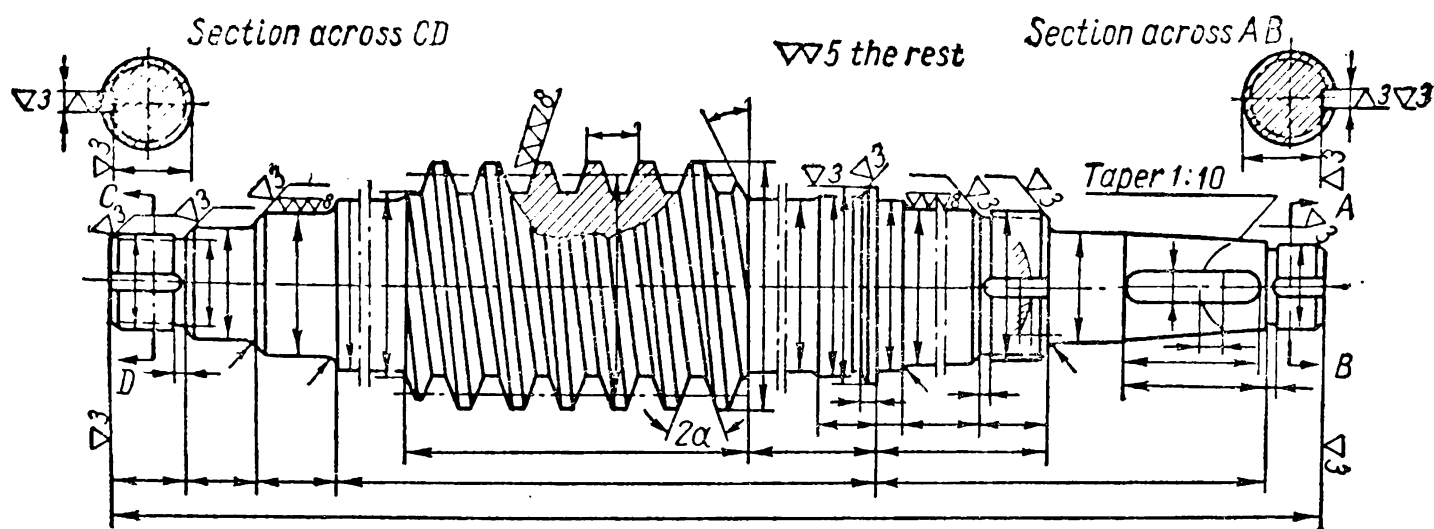
## WORM GEARS

**Materials.** Besides the properties pointed out in the chapter «Gearing» the materials of a worm-gear combination should have a low coefficient of friction. This is ensured by combining heterogeneous materials with a high-quality finish of the contact surfaces. If these conditions are neglected, high velocities of sliding and poor conditions for the formation of an oil wedge will impair the load-carrying capacity of the gear because of the danger of seizure.

High-tin bronze ОФ 10-1 and ОНФ have the best antifriction properties as compared to other grades of bronze. Wheels made from this grade of bronze are used in vital gears at velocities of sliding of  $v_{sl} > 3$  m/sec. Tin-free bronze АЖ 9-4 and АЖН 10-4-4 resist seizure less effectively and should not therefore be used when  $v_{sl} > 4$  m/sec. To improve the mechanical properties of bronze wheels they are cast by the centrifugal method.

At low velocities of sliding ( $v_{sl} < 2$  m/sec) the wheels are made from gray cast iron of grades СЧ 15-32 to СЧ 21-40.

Worms are ordinarily made from carbon or alloy steel and, less frequently, for unimportant low-speed gears, from cast iron of grade СЧ 18-36. Worms made from steel 15X, 15XA, 10X, 20XФ are casehardened to thread surface hardness of  $R_C = 56-62$ . Worms from steel 6 or 40, 45, 40X and 40XH are hardened to  $R_C = 45-50$ . Soft worms with surface hardness  $H_B < 270$  are used mainly in hand-operated gears.



8	Degree of accuracy		
7	Direction of thread		
6	Type of worm		
5	Lead angle of worm	$\lambda$	
4	Pressure angle in axial cross-section	$\alpha$	
3	Relative thickness of worm	$q$	
2	Number of starts on worm	$z_{wo}$	
1	Axial module	$m$	
Item No.	Name	Symbol	Magnitude

Fig. 169

**Design of Worms and Wheels.** As a rule, worms are made integral with the shaft; less frequently they are fitted on. A design of a worm is shown in Fig. 169. The Table specifies the worm characteristics.

Worm wheels are made solid (Fig. 170, a) or composite (Fig. 170, b, c) with a bronze rim.

The rim of a worm wheel is fitted onto the wheel centre with interference (Fig. 170, c). To obtain dependable transmission of the torque and prevent axial shift of the rim, keys or dowels and bolts are arranged on both sides of the wheel in a staggered pattern. The holes for dowels and screws are machined after assembly. After the screws are fitted, their heads are cut off. The screw diameter is taken at  $(1.2-1.5)m$ , and the length at  $(0.3-0.4)B$ . The length of dowels of the same diameter does not exceed half of the rim width.

Another method of fastening the rim of a worm wheel to its centre by means of flanges is employed if the wheel is large in diameter (Fig. 170, d). Coupling bolts are inserted into holes reamed simul-

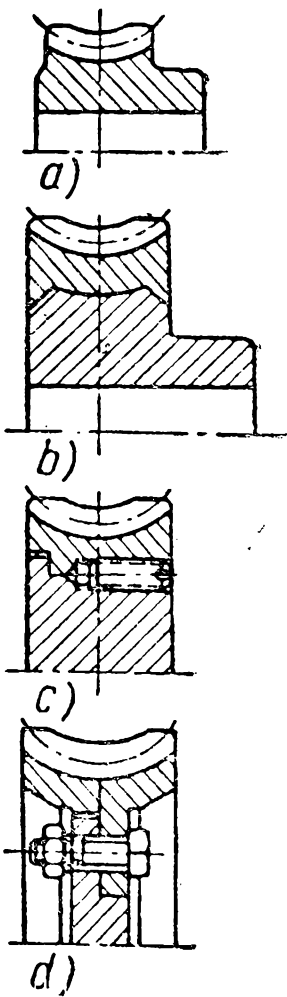
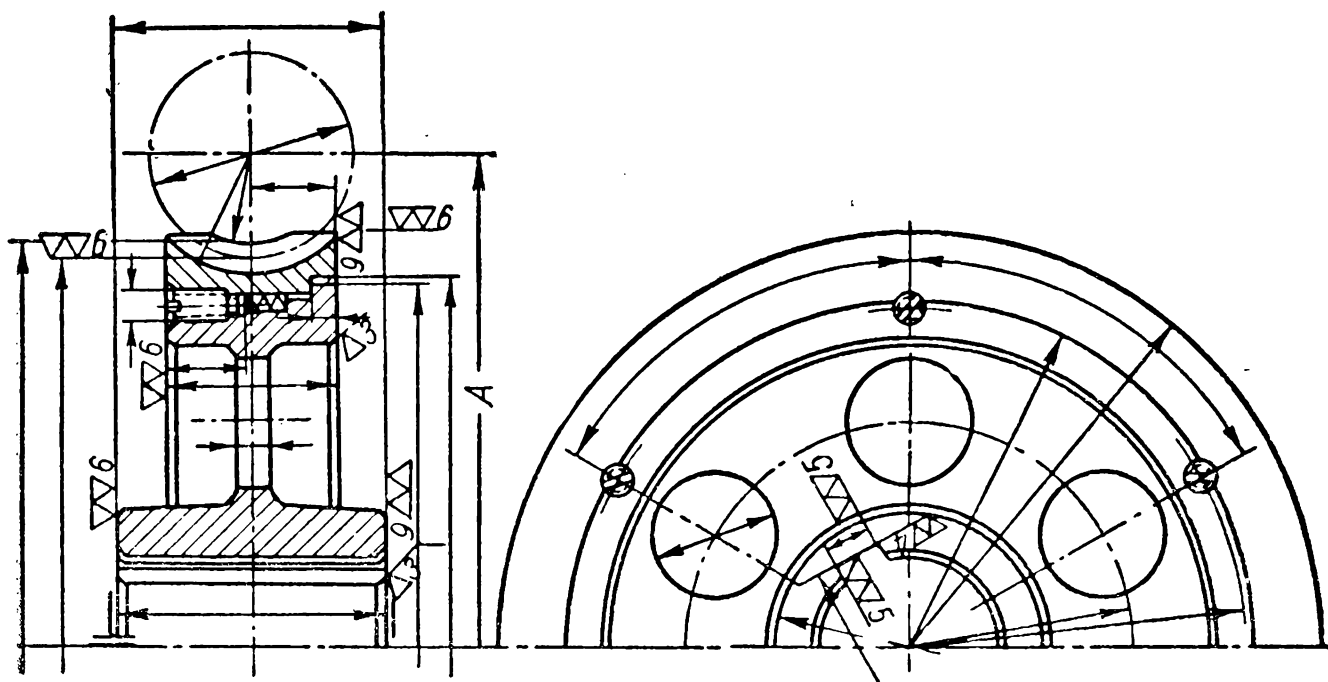


Fig. 170

taneously in the rim and the hub flange. The bolts are calculated for shear and the joints are checked for compression. To prevent radial and axial run-out, the worm wheel is fitted onto the shaft with interference. When wheels are mounted on splined shafts or



9	Degree of accuracy		
8	Direction of thread		
7	Type of worm		
6	Lead angle of worm	$\lambda$	
5	Pressure angle in axial cross-section	$\alpha$	
4	Relative thickness of worm	$q$	
3	Number of teeth on wheel	$z_w$	
2	Number of starts on worm	$z_{w0}$	
1	Module	$m$	
Item No.	Name	Symbol	Magnitude

Fig. 171

when the hub has to be periodically removed from a smooth shaft small interference fits are used. A drawing of a worm rim is shown in Fig. 171.

**Accuracy of Gears.** As distinct from toothed gears correct engagement in a worm gear is possible only when the centre distance of the gear is equal to that of the machine tool during generation of the teeth. The accurate machining of a worm gear affects its operation to a larger degree than in a toothed gear since the mating elements are more rigid. To reduce manufacturing inaccuracies standards provide for tolerances in worm gears. Altogether there are 12 degrees of accuracy: from 1 to 12. For power gears Soviet



Table 41

Classification of Worm Gears According to Degrees of Accuracy

Elements of classification	6th degree (highly accurate)	7th degree (accurate)	8th degree (medium accuracy)	9th degree (lower accuracy)
Method of cutting and processing.	<p>Casehardened or hardened worms. Side surfaces of the worm threads are always ground and polished.</p> <p>Worm wheels are generated by hobs. Worm wheels are finished by hob shavers with a profile identical to that of the worm. Running-in under load is recommended.</p>	<p>Case hardening or hardening of worms is recommended. Tooth profiles of hardened worms are always ground and then polished.</p> <p>Worm wheels are generated by ground hob cutters. Finishing of worm wheels with hob shavers is recommended. Without finishing operations the wheels should be run-in under load.</p>	<p>Finishing of worms on lathes or milling machines.</p> <p>The wheels are generated with a ground hob or a fly-cutter. Running-in under load is recommended.</p>	<p>Finishing of worms on lathes or milling machines.</p> <p>Worm wheels are generated by any method.</p>
Operating conditions.	<p>End dividing gears of semi-precision machine tools, drives in engine regulators, highly accurate drives from artillery systems to reading-off devices.</p>	<p>Locomotive and industrial power worm drives of medium velocity, drives in hoisting and turning devices, artillery systems absorbing the recoil.</p>	<p>Unimportant drives with low peripheral velocities with an intermittent daily operation.</p>	<p>Unimportant drives with low velocity or hand-operated drives.</p>
Peripheral velocities (on worm wheel).	Over 5 m/sec.	Up to 7.5 m/sec.	Up to 3 m/sec.	Up to 1.5 m/sec.

standards provide for degrees of accuracy, from 5 to 9. The peripheral velocity of the worm wheel and the purpose of the gear are the factors determining the required degree of accuracy and the method of cutting and finishing the teeth.

The standards are extended to power gears with modules above 1-30 mm with pitch diameters of worm wheels up to  $d_{\partial w}=2,000$  mm and diameters of pitch cylinders of worms up to  $d_{\partial wo}=400$  mm.

When selecting the proper degree of accuracy for a worm gear the recommendations in Table 41 should be consulted.

**Failures of Worm Wheel Teeth.** The operational defects and failures of toothed gears examined above also occur in worm gears.

However, the relative sliding of the profiles of the mating members increases the probability of seizure and wear.

Seizure, which is a rather rare phenomenon in toothed gears, is as frequent in worm gears as surface pitting. In certain cases the possibility of seizure is more dangerous than surface pitting and this limits the load-carrying capacity of the gear. In worm gears particles of the surfaces of the wheel teeth being of softer material may stick to the particles on the surface of the worm threads so firmly that they scratch the active profiles of the wheel teeth as they contact the worm threads.

The hazard of seizure is greatest in the zone where the conditions for the formation of an oil wedge are least favourable.

The carrying ability of an oil wedge between two bodies moving relative to one another depends on the magnitude of the velocity of sliding, and its direction relative to the line of contact of these two bodies and the form of the conjugate surfaces. The larger the angle between the line of contact and the direction of the relative velocity of two bodies and the smaller their curvature at the point of contact, the more favourable conditions there are for the formation of an oil wedge and the higher its carrying ability.

Fig. 172 shows several lines of contact in a worm gear and the direction of velocity of some points of the worm lying on the line of contact. As can be seen from Fig. 172 the angle between the lines of contact and the direction of the velocity of motion of the points under examination is not constant: it is smallest (near zero) in the area  $a$  at the main plane and largest (near  $90^\circ$ ) on the tooth edge on the side where the worm threads leave contact. Therefore, in the area  $a$  it is quite possible, provided certain additional conditions

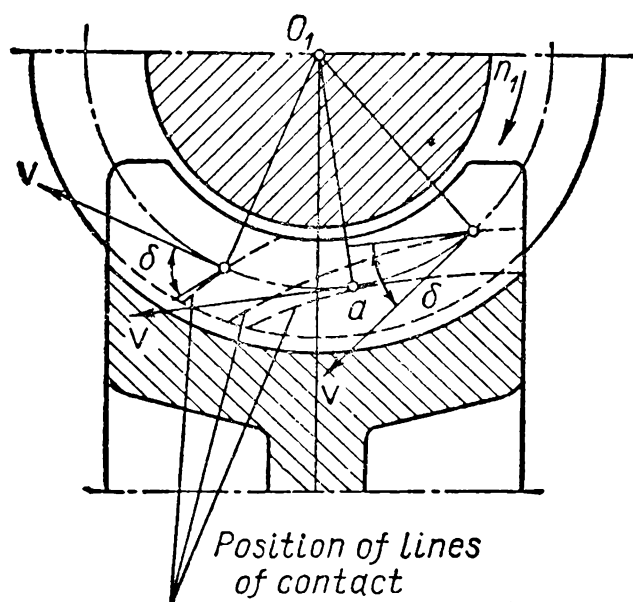


Fig. 172

exist, that the oil film will be destroyed thereby reducing the load-carrying capacity of the gear.

The resistance of gears to seizure can be improved by selecting materials for the wheel-worm combination which possess high anti-friction properties, better finish of the active profiles (especially of the worms) and by applying antiscuff greases.

Pitting appears in the same manner as on toothed gears, but in worm gears only the wheel teeth are affected. As a rule, the teeth of worm wheels are subject to a greater wear than those of toothed gears. This is due to the sliding of teeth. Intensive wear occurs during the initial period of gear operation when the existing microirregularities on the tooth surfaces exceed the thickness of the oil film. Running-in smooths the rough surfaces and diminishes wear. If the surface hardness of one element considerably exceeds that of the other the wear continues. For this reason the worms should be thoroughly finished. In gears which are frequently started and stopped under load wear continues throughout the entire period of operation since during this time lubrication is inadequate. In open-type and also in closed-type gears, if the oil is dirty, the wear is more intensive. To safeguard closed-type drives against such intensive wear the oil should be drained after the initial wear-in period, the body washed and filled with fresh oil. The wear resistance of the gear is increased by thorough finishing of the teeth surfaces and worm threads and by selecting a lubricant of the proper viscosity.

Despite the importance attached to the calculation of these gears for seizure and wear, adequate methods for this have not yet been found. Therefore, worm gears are calculated in the same way as toothed gears—for surface and beam strength of teeth while the allowable stresses are corrected against wear and seizure on the basis of experimental data and observations made during operation.

The proportions of closed-type gears are calculated with the aim of preventing damage to the active profiles of the teeth; the calculation of teeth for beam strength is done for checking. The proportions of open-type gears are found from the calculation of the teeth for beam strength (on the basis of the gear module).

Since in a worm gear the worm threads slide along the wheel teeth causing very high losses the gear is calculated for heating.

**Main Geometrical Proportions.** Since a worm gear can be regarded as a modification of a spiral gear with the shafts at right angles, the geometrical proportions of a worm gear can be found from the formulae used for toothed wheels. The plane passing through the axis of the worm and perpendicular to the axis of the wheel is called the *main plane* (Fig. 173). The section of this plane with an Archimedean worm gives us contact between an involute wheel and a straight-sided rack. The mating elements in the axial section of

an Archimedean worm are identical to a rack of rectilinear contour with an angle of  $2\alpha=40^\circ$ .

In the sections parallel to the main plane we likewise obtain racks and flat wheels but the teeth on the rack and the wheel will be curvilinear (Fig. 177).

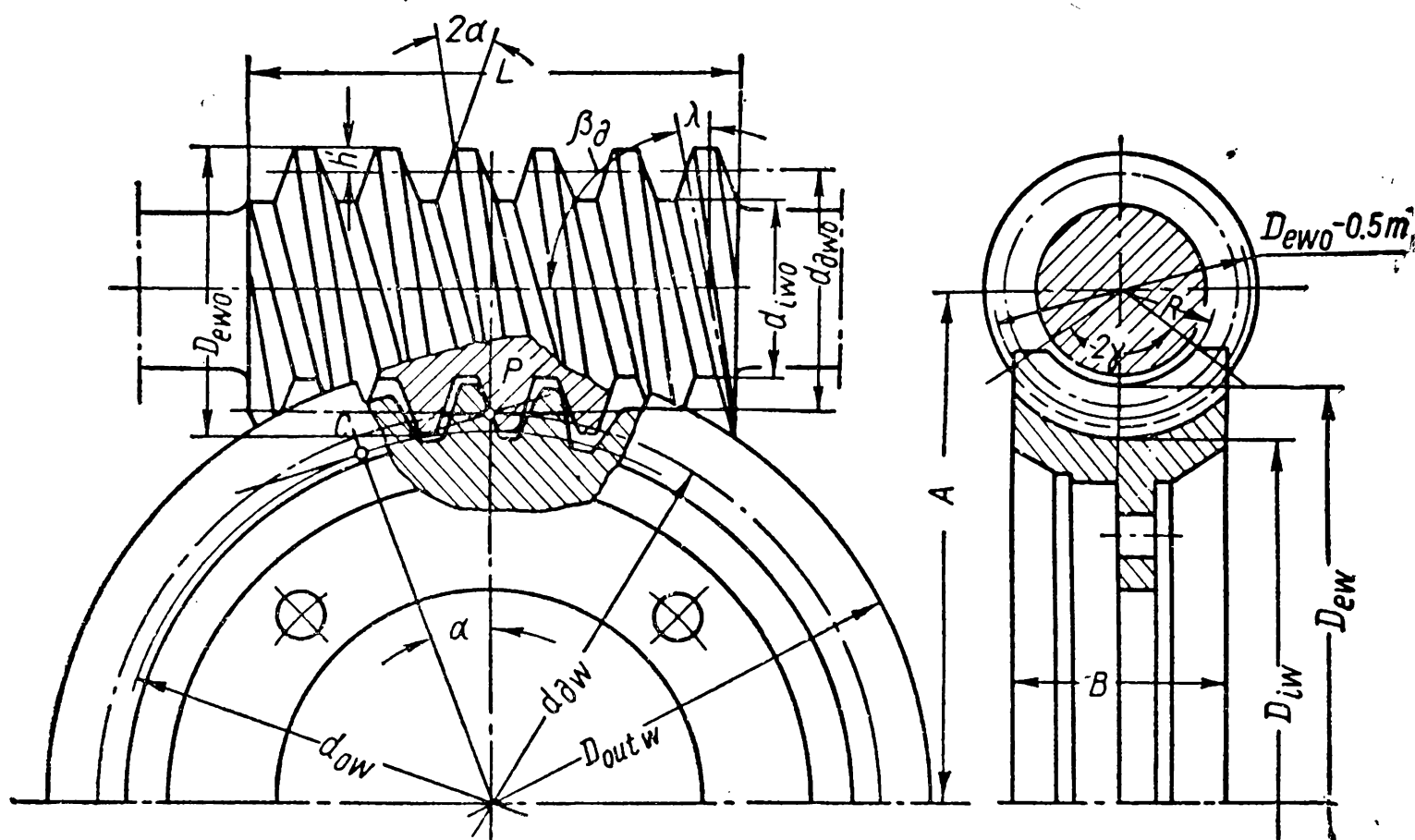


Fig. 173

For an involute worm a straight-sided profile of the tooth will be obtained when section is done by planes tangential to the pitch cylinder of the worm.

For the module of a worm gear  $m$  we take the worm axial module equal to the circumferential module of the wheel.

If the number of the worm starts is  $z_{wo}$ , its pitch diameter is

$$d_{ewo} = m_s z_{wo} \quad (293)$$

where  $m_s$  is the circumferential module of the worm.

We know that

$$m_s = m \tan \beta_\delta \quad \text{and} \quad \tan \beta_\delta = \frac{1}{\tan \lambda}.$$

After substituting these values in the formula (293) we obtain

$$d_{ewo} = \frac{m z_{wo}}{\tan \lambda}.$$

Denoting for convenience  $\frac{z_r}{\tan \lambda} = q_{wo}$  we find

$$d_{ewo} = m q_{wo} \quad (293')$$

where  $q_{wo}$  is the number of modules in the pitch diameter of the worm. On the basis of formulae for toothed gearing Table 42 gives similar formulae for determining the main geometrical proportions of a worm gear with an Archimedean worm (Fig. 173).

Table 42

Formulae for Determining Geometrical Proportions of Worm and Worm Wheel

	Worm	Worm wheel
Diameter of worm pitch cylinder and wheel pitch circle	$d_{\partial wo} = q_{wo} m$	$d_{\partial w} = z_w m$
Diameter of base circle	$d_{wo} = m (q_{wo} + 2\xi)$	$d_w = d_{\partial w}$
Correction factor		$\xi = \frac{A}{m} - 0.5 (q_{wo} + z_w)$
Centre distance	$A = \frac{m}{2} (q_{wo} + z_w + 2\xi)$	
Diameter of addendum circle	$D_{ewo} = q_{\partial wo} + 2f_o m$	$D_{ew} = d_{\partial w} + 2m (f_o + \xi)$
Diameter of dedendum circle	$D_{iwo} = d_{\partial wo} - 2m (f_o + c_o)^*$	$D_{iw} = d_{\partial w} - 2m (f_o + c_o - \xi)$
Module	$m = \frac{2A}{q_{wo} + z_w + 2\xi}$	
Number of modules in the pitch diameter of worm	$q_{wo} = \frac{d_{\partial wo}}{m}$	
Lead angle on pitch cylinder	$\tan \lambda = \frac{z_{wo}}{q_{wo}}$	

\* The clearance factor is  $c_o = 0.2$ .

Worm gears are corrected in the same way as toothed gears—by feeding the generating tool. However, in a worm gear only the wheel is corrected while the size of the worm remains the same (Fig. 174). The correction of the gear changes only the diameter of the worm pitch cylinder while the diameter of the wheel pitch cylinder does not change.

According to standards the correction of worm gears is effected by changing the number of wheel teeth as shown in Fig. 174 in order to decrease the number of standard tools required for cutting the wheels and to retain the same proportions of the gear with a slightly changed velocity ratio.

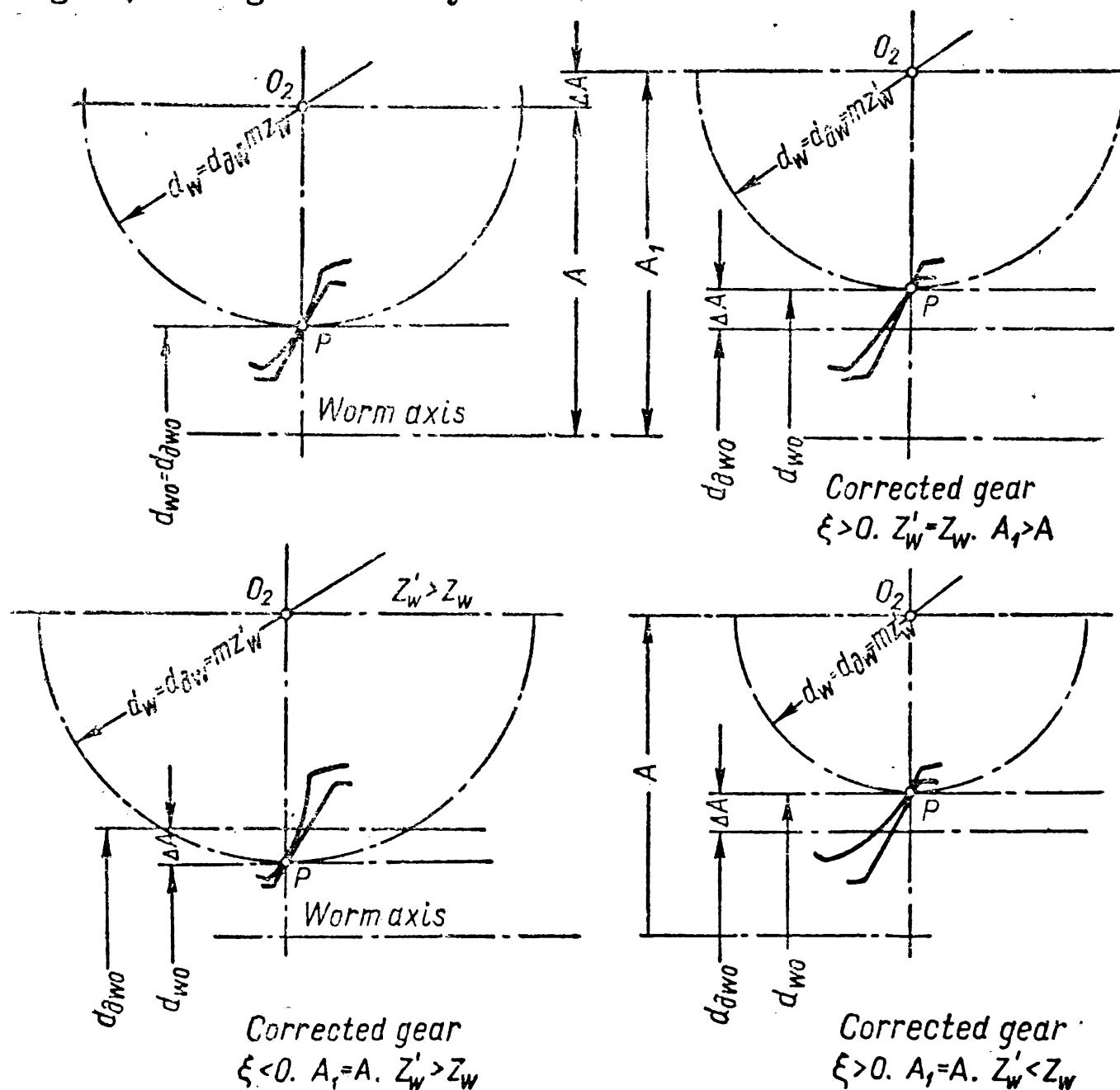


Fig. 174

It can be seen from the formula determining the correction factor that for the given worm ( $q_{wo}$  is constant) and at a constant  $A$  the shift factor can assume only definite values since the number of teeth  $z_{wo}$  can only be an integer. Soviet standards specify  $\xi$  as equal to  $-1$ ,  $-0.5$ ,  $0$ ,  $+0.5$  and  $1$ .

The length of the cut portion of the worm  $L$ , the wheel width  $B$  and the outside diameter of the wheel  $D_{out w}$  (for a gear with an Archimedean worm) are found from the relations in Table 43.

The arbitrary angle of contact between the worm and wheel  $2\gamma$  is that formed by lines drawn from the worm centre through the

points where the circle with diameter  $D_{ewo} - 0.5m$  intersects the lines of the wheel faces (Fig. 173):

$$\sin \gamma = \frac{B}{D_{ewo} - 0.5m}.$$

Table 43

Formulae for Determining the Length of Cut Portion of Worm  $L$  mm, Wheel Width  $B$  mm and Outside Diameter of Wheel  $D_{out\ w}$  mm

Number of worm starts $z_{wo}$	$L$	$B$	$D_{out\ w}$
1	$L \geq (11 + 0.06z_w)m$	$B \leq 0.75D_{ewo}$	$D_{out\ w} < D_{ew} + 2m$
2			
3	$L \geq (12.5 + 0.09z_w)m$	$B \leq 0.67D_{ewo}$	$D_{out\ w} < D_{ew} + 1.5m$
4			$D_{out\ w} \leq D_{ew} + m$

**Forces Acting in a Gear.** To determine the forces acting in a worm gear let us assume that the force of normal pressure  $P_n$  is concentrated at the point  $P$  (Fig. 175, *a*).

Using formulae (212), (213) and (255) and recalling that the lead angle on the worm wheel  $\beta_w$  equals the lead angle on the worm  $\lambda$  we obtain: the peripheral effort on the wheel equal to the axial effort on the worm with torque on the wheel  $M_t$  is

$$P_w = \frac{2M_t}{d_w} = P_{awo}; \tag{294}$$

the radial effort on the wheel and worm

$$P_r = P_w \tan \alpha. \tag{295}$$

The axial effort on the wheel equals the peripheral effort on the worm; allowing for the fact that the sliding along the teeth develops friction forces it will equal

$$P_{aw} = P_w \tan (\lambda + \varrho) = P_{wo} = \frac{2M_{wo}}{d_{wo}} \tag{296}$$

where  $\varrho$  is the angle of friction.

The direction of the forces is found in the same way as in a toothed gear.

Fig. 175, *b* shows a schematic diagram of forces acting upon the shafts of a worm gear. These forces are used to find the pressures in the bearings and calculate the shafts for strength.

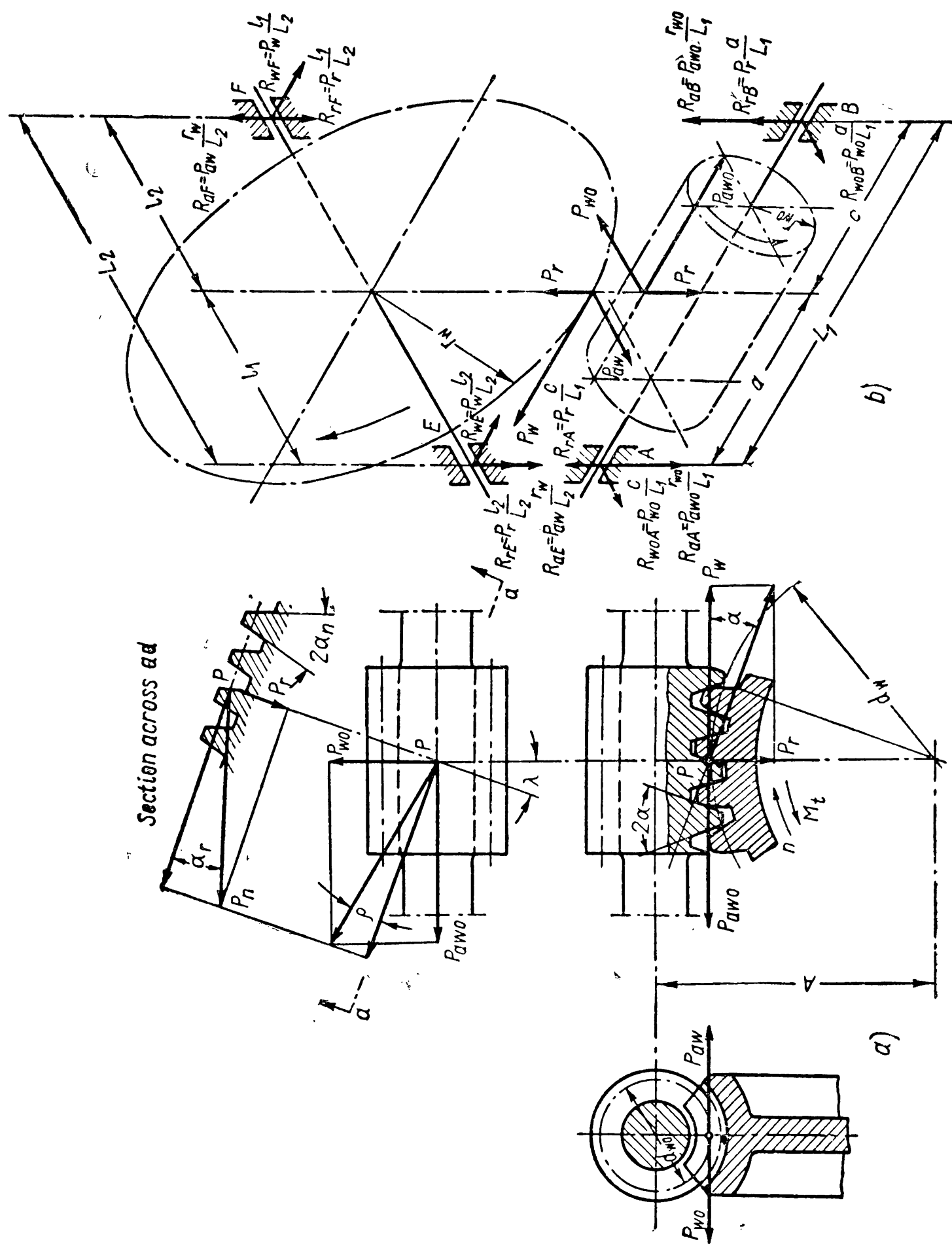


Fig. 175



The normal pressure at  $\cos \alpha_n \approx \cos \alpha$  and  $\cos (\lambda + \varrho) \approx \cos \lambda$  will be

$$P_n = \frac{P_{awo}}{\cos (\lambda + \varrho) \cos \alpha_n} \approx \frac{P_w}{\cos \lambda \cos \alpha} = \frac{2M_t}{d_w \cos \lambda \cos \alpha} . \quad (297)$$

The normal pressure is used in calculating the strength of the gear.

**Design Load.** The rotation of a worm wheel can be regarded not as a result of rotation of the worm but as a result of the wheel mating with a combination of progressively moving racks. In both cases the elements of the worm gear in these sections engage as in a rack. Each section has its own lines of action (one of all lines—in the main section of an Archimedean worm—is straight) the combination of which forms the contact surface. The lines of intersection of the contact surface with the wheel teeth and the worm threads are the lines of contact; the combination of lines of contact on the contact surface is called the *contact area*. The contact area of a worm gear is curvilinear and the lengths of separate lines of contact differ essentially.

These lines of contact transmit load from the worm threads to the wheel teeth. The maximum unit load can be approximately found by dividing the normal load  $P_n$  by the minimum total length of the lines of contact  $L_{\min}$ .

The length of one line of contact will be in direct proportion to the pitch diameter of the worm  $d_{\partial wo}$  and the angle of contact  $2\gamma^\circ$ . If we remember that an increase in the lead angle  $\lambda$  causes the length of the line of contact to increase in inverse proportion to  $\cos \lambda$  then, if the overlap factor is  $\varepsilon$  and the factor of variations in the total length of the lines of contact is  $\lambda'$ , we get

$$L_{\min} = \frac{\pi d_{\partial wo} \varepsilon \lambda' 2\gamma^\circ}{\cos \lambda 360^\circ} \text{ cm.}$$

We can assume approximately  $2\gamma^\circ = 100^\circ$ ;  $\varepsilon \approx 1.8$ ;  $\lambda' = 0.75$  (because of considerably greater range of variation in the total length of the lines of contact than in a helical gear); then

$$q = \frac{P_n}{L_{\min}} = \frac{2M_t \cos \lambda 360^\circ}{d_w \cos \alpha \cos \lambda \pi d_{\partial wo} \varepsilon \lambda' 100^\circ} = \frac{1.8M_t}{d_w d_{\partial wo}} \text{ kg/cm.} \quad (298)$$

Due to the deformation of the worm, wheel shaft, bearings and gear housing and inaccuracies of manufacture and assembly the load along the lines of contact does not spread uniformly.

As in toothed gears an increase in the design load  $q_d$  compared with the mean load  $q$  is taken account of by introducing correction factors

$$q_d = q k_c k_d = \frac{1.8M_t}{d_w d_{\partial wo}} k_c k_d \text{ kg/cm} \quad (299)$$

where  $k_c$  is the load concentration factor;

$k_d$  is the dynamic load factor.

The degree of nonuniformity is primarily affected by the deformation of the worm which is a less rigid element than the worm wheel. Under the action of the forces  $P_{wo}$ ,  $P_a$  and  $P_r$  (Fig. 176) the worm undergoes a flexural deformation in two mutually perpendicular

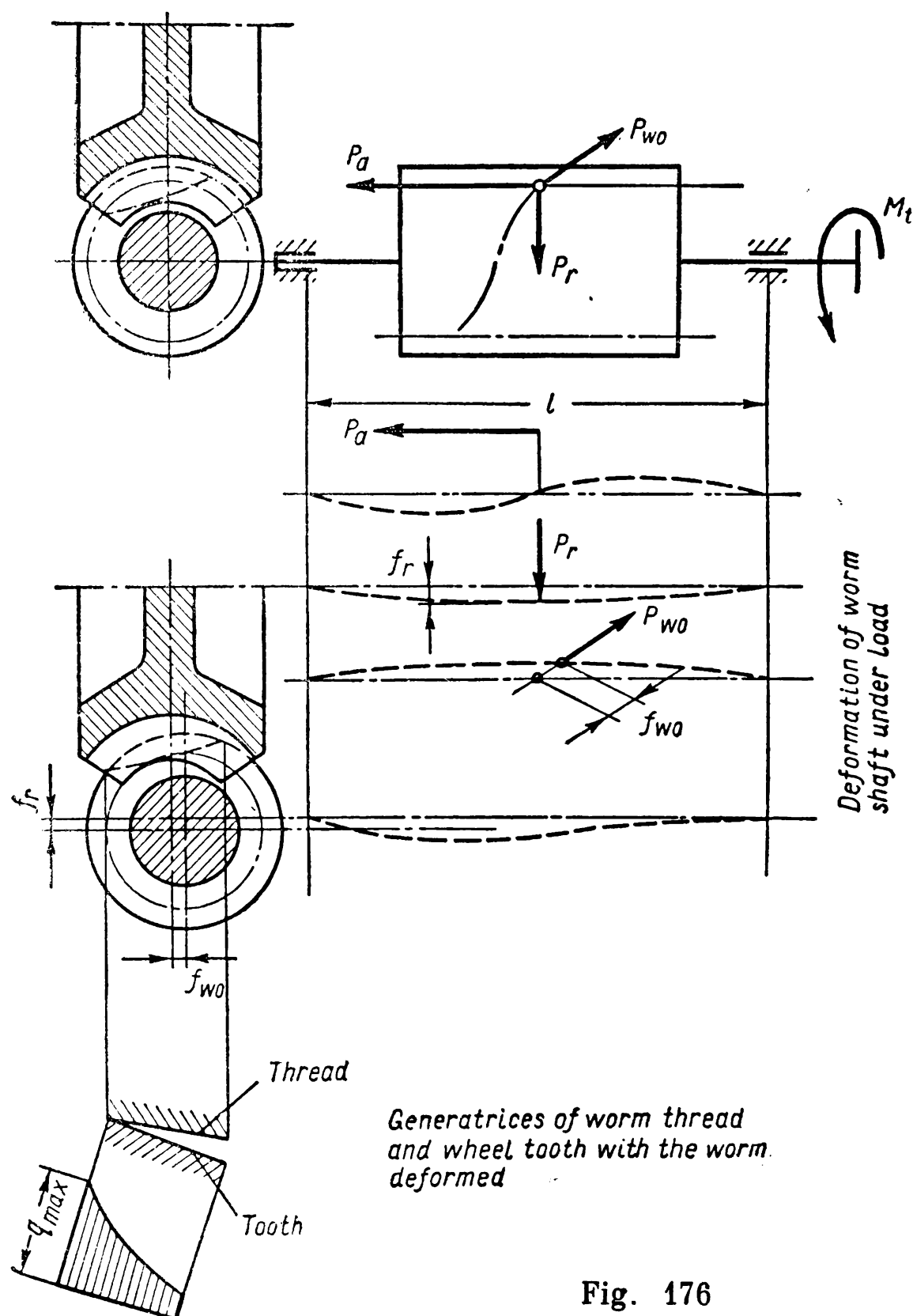


Fig. 176

planes: due to the forces  $P_a$  and  $P_r$  in a vertical plane and to the force  $P_{wo}$  in a horizontal plane. Because of worm deflection relative to the wheel correct contact between the worm threads and the wheel teeth is disturbed: the closeness of contact at one end of the tooth increases and at the other diminishes. The diagram of unit load

(Fig. 176) will be limited by an inclined line and the maximum pressure will be found from the formula

$$q_{\max} = qk_c \quad (300)$$

whence it follows that

$$k_c = \frac{q_{\max}}{q} = \frac{q + \Delta q}{q} = 1 + \frac{\Delta q}{q}.$$

The magnitude  $\Delta q$  will be proportional to the flexural deformation of the worm. The latter can be approximately found as for a beam on two supports with the force  $\overline{P}_{res} = \overline{P}_r + \overline{P}_{wo}$  acting in the middle of the length  $l$ . Taking approximately  $l = 0.9D_{aw} = 0.9 m z_w$  and the worm moment of inertia  $I_{wo} = 0.05 d_{wo}^4 \mu$  ( $\mu$  is a factor accounting for the effect of the worm threads on its deflection) we find the deflection  $f$ :

$$f = \frac{P_{res} l^3}{48 E I_{wo}} = P_{res} \frac{0.9^3 m^3 z_w^3}{48 E I_{wo}} = P_{res} \left( \frac{z_w}{\theta'} \right)^3.$$

It follows from this expression that the flexural deformation is proportional to the magnitude  $\left( \frac{z_w}{\theta'} \right)^3$  where  $\theta'$  is a factor depending on the worm proportions.

As the gear operates under constant load the softer surfaces of the worm wheel teeth are run in, causing a more uniform load distribution. Then  $k_c = 1$ . If the gear carries varying load the alternating deformation of the worm will prevent it from being completely equalised. It can be assumed, however, that under the action of a torque of average time the load will spread uniformly. The action of a load different from this mean torque will cause greater non-uniformity the greater the difference between the torques is.

Therefore, the load concentration factor can be found from the formula

$$k_c = 1 + \left( \frac{z_w}{\theta} \right)^3 (1 - m_d) \quad (301)$$

where  $\theta$  is the worm deformation factor taken from Table 44 depending on  $q_{wo}$  and  $z_{wo}$ , and  $m_d$  is the relation of the average torque to the maximum torque

$$m_d = \frac{\sum M_i T_i}{M_t \sum T_i};$$

here  $M_i$ —are the torques acting upon the wheel (including the torque  $M_t$  assumed as the design torque);

$T_i$ —the continuity of action of the torque  $M_i$  in hours during the entire service life of the gear.

Due to specific features of operation of a worm-wheel combination («screwing in» of the worm) the gear runs more smoothly than a

toothed gear. Therefore, considerably lesser values can be taken for the dynamic load factor  $k_d$  than in case of toothed gears: at  $v_w \leq 3$  m/sec  $k_d = 1-1.1$ ; at  $v_w > 3$  m/sec  $k_d = 1.1-1.2$ .

Table 44

Worm Deformation Factors  $\Theta$ 

$q_{wo}$ $z_{wo}$	6	7	8	9	10	11	12	13
1	40	55	72	89	108	127	147	178
2	32	44	57	71	86	102	117	134
3	29	39	51	61	76	89	103	118
4	27	36	47	58	70	82	94	108

**Design for Surface Strength.** We take the formula (30) as the initial relation for calculating the active profiles in the same way as with toothed gears.

As with toothed gears we substitute in the formula (30) the value of the reduced curvature radius in normal section for the moment of contact in the pitch point  $P$  (Fig. 173) on the assumption that the area of minimum surface strength lies in the region of the pitch point.

In its main section the worm wheel and worm can be likened to a helical wheel and a rack. Since the radius of the worm thread curvature  $q_{wo} \approx \infty$  then  $q = q_w$  and, consequently,

$$q = \frac{d_{\partial w} \sin \alpha}{2 \cos \lambda}$$

(the angle at which the teeth are inclined on the wheel  $\beta_w$  equals the lead angle of the worm thread  $\lambda$ ).

After substituting the values  $q$  from the latter equation and  $k_d$  from the formula (298) in the equation (30) we get

$$\sigma_{sur} = \frac{1.35}{d_w} \sqrt{\frac{M_t E}{d_{wo}}} k_c k_d \leq [\sigma]_{sur} \text{ kg/cm}^2 \quad (302)$$

or,

$$\sigma_{sur} = \frac{1.35}{d_w/d_{wo}} \sqrt{\frac{M_t E}{d_{wo}^3}} k_c k_d.$$

Substituting here

$$\frac{d_w}{d_{wo}} = \frac{z_w}{q_{wo}}; \quad d_{wo}^3 = m^3 q_{wo}^3; \quad m = \frac{2A}{q_{wo} + z_w} \quad (\text{from Table 42 at } \xi = 0)$$

we obtain

$$\sigma_{sur} = \frac{0.5}{z_w/q_{wo}} \sqrt{\left(\frac{z_w/q_{wo} + 1}{A}\right)^3 E M_t k_c k_d} \leq [\sigma]_{sur} \text{ kg/cm}^2. \quad (303)$$

For a steel worm ( $E_{wo} = 2.15 \times 10^6$  kg/cm<sup>2</sup>) and a bronze rim of the worm wheel ( $E_w = 0.9 \times 10^6$  kg/cm<sup>2</sup>) the reduced modulus of elasticity  $E = 1.27 \times 10^6$  kg/cm<sup>2</sup>; in this case too the relations (302) and (303) will assume the form

$$\sigma_{sur} = \frac{1,500}{d_w} \sqrt{\frac{M_t}{d_{wo}} k_c k_d} \leq [\sigma]_{sur} \text{ kg/cm}^2 \quad (304)$$

and

$$\sigma_{sur} = \frac{540}{z_w/q} \sqrt{\left(\frac{z_w/q_{wo} + 1}{A}\right)^3 M_t k_c k_d} \leq [\sigma]_{sur} \text{ kg/cm}^2. \quad (305)$$

From the formula (305) we find the centre distance  $A$  (for design calculations of a closed-type gear)

$$A = \left(\frac{z_w}{q_{wo}} + 1\right) \sqrt[3]{\left(\frac{540}{z_w/q_{wo} [\sigma]_{sur}}\right)^2 M_t k_c k_d} \text{ cm.} \quad (306)$$

The magnitude of the centre distance  $A$  found from the formula (306) should be approximated to the values given by the standards. If the gear is not an independent unit,  $A$  may deviate from the recommended values.

In design calculations the magnitudes  $q_{wo}$  and  $z_w$  should be specified in advance.

The choice of the value  $q_{wo}$ —the number of modules in the pitch diameter of the worm—is limited to the range of  $q_{wo} = 6-13$ . Larger values of  $q_{wo}$  are taken in case of fitted-on worms and when their rigidity has to be increased. The number of starts of the worm  $z_{wo}$  and the value  $q_{wo}$  determine the lead angle  $\lambda$ . The larger  $\lambda$  is, the higher is gear efficiency but the smaller is worm diameter; at high velocity ratios the distance between the bearings of the worm is increased. This drastically reduces the worm rigidity.

The number of the worm starts  $z_{wo}$  is related to the velocity ratio  $i$  and the number of teeth on the wheel  $z_w$ . When the values of  $i$  are very small  $z_{wo}$  should be as large as possible so that the number of teeth  $z_w$  is not below 22-26; otherwise the contact surface is significantly diminished. Hence, for example at  $i=15$ ,  $z_{wo}$  should be 2. Another very important condition is the necessity to reduce the number of sizes of cutting tools. Therefore the worm elements should be taken from the series specified by the standards for worm-gear speed reduction gears— $z_{wo} = 1-4$ . These values may be disregarded only when the wheels are cut by a fly-cutter and also when the worm gear has to be assembled into a mechanism with a strictly defined design and dimensions.

The maximum number of teeth may vary, but in power gears  $z_w$  should not exceed 80, since, otherwise, the wheel diameter and the distances between the worm bearings will be increased and

worm deformation will be more pronounced. At a greater  $z_w$  (with the same diameter) the beam strength of teeth may become a factor limiting transmitted power. In gear trains of dividing mechanisms  $z_w$  reaches 600-1,000.

Allowable surface stresses  $[\sigma]_{sur}$  are assigned for the material of the wheel rim depending on the material of the worm running with it.

When the wheels are made from cast iron or bronze with ultimate strength  $\sigma_{ult} > 30 \text{ kg/mm}^2$  faults in the gear will in all probability be due to seizure. Therefore, allowable stresses are assigned depending on the combination of contacting materials and the velocity of sliding, neglecting the number of load cycles since the magnitude of allowable stresses is considerably below the surface endurance limit. Table 45 gives experimental values of  $[\sigma]_{sur}$  for thoroughly run-in and liberally lubricated gears. In other gears the tabulated values should be decreased approximately by 30%.

Table 45

Values of  $[\sigma]_{sur}$  in  $\text{kg/cm}^2$

Material		$v_{sl}$ in m/sec						
Worm	Wheel	<0.25	0.25	0.5	1	2	3	4
Casehard- ened steel 20 (at $R_C > 45$ )	Cast iron Ч 15-32	1,870	1,580	1,300	1,150	860	—	—
	Cast iron Ч 18-36	—	1,900	1,830	1,760	1,680	1,590	1,490
	Bronze АЖ 9-4							
Steel 6	Cast iron Ч 12-28 Cast iron Ч 15-32	1,720	1,440	1,150	1,000	720	—	—

If the wheels are made of bronze with ultimate strength  $\sigma_{ult} < 30 \text{ kg/mm}^2$  the load-carrying capacity of the gear is limited by contact fatigue and the allowable stress should be taken from the following formula

$$[\sigma]_{sur} = [\sigma]_{sur}' k_l. \tag{307}$$

The load factor  $k_l$  is taken from the formula analogous to (226) with  $m = 8$  found experimentally

$$k_l = \sqrt[8]{\frac{10^7}{N}}. \tag{308}$$

The number of cycles  $N$  is calculated by the formula (228) and at a varying (stepped) load  $N_{eq}$  is found from the formula similar to (227), at  $m = 8$ .

$$N_{eq} = \frac{60}{(M_t)^4} \sum (M_i)^4 T_i n_i. \quad (309)$$

If  $N_{eq} > 25 \times 10^7$  we assume  $N = 25 \times 10^7$  and, therefore, the minimum value of  $k_l$  will equal 0.67.

The values of  $[\sigma]_{sur}'$  kg/cm<sup>2</sup> for some materials of wheels running with steel worms are given in Table 46.

Table 46  
Values of  $[\sigma]_{sur}'$  in kg/cm<sup>2</sup> for Differently  
Cast Rims

Material and method of casting	Surface hardness of worm threads	
	$H_B \leq 340$	$R_C \geq 45$
Bronze OΦ 10-1, sand-mould casting . . . . .	1,300	1,550
Bronze OΦ 10-1, metal-mould casting . . . . .	1,900	2,260
Bronze OHΦ, centrifugal cast- ing . . . . .	2,100	2,500

**Design of Teeth for Bending.** Since the worm threads possess very high strength only the wheel teeth are calculated for bending. The assumptions made for the teeth of spur wheels are also true for the teeth of worm wheels. The intricate form of the tooth due to varying cross-section along its length and curved restrained section makes determination of actual stresses extremely difficult and calculation arbitrary.

Since the restrained section of the tooth is curved and the lines of contact are inclined relative to the tooth root the strength of the teeth of worm wheels is higher than that of helical teeth on spur wheels.

To simplify computation we take as the initial relation the formula for determining the stresses in the dangerous section of helical teeth and introduce in the design formula corrections whose approximate magnitude can be found from the following reasoning.

The tooth root is longer than the arbitrary line of contact which is assumed equal to the arc on the worm pitch cylinder within the angle of contact  $2\gamma^\circ$ . The increase in the tooth strength can be assumed to be proportional to the increase in the length of its root as

compared to the length of the line of contact along which load is applied to the tooth. This circumstance can be tentatively assessed from the relationship of these lengths (see Fig. 177) and by assuming the length of the tooth root  $l_0$  to be equal to the arc

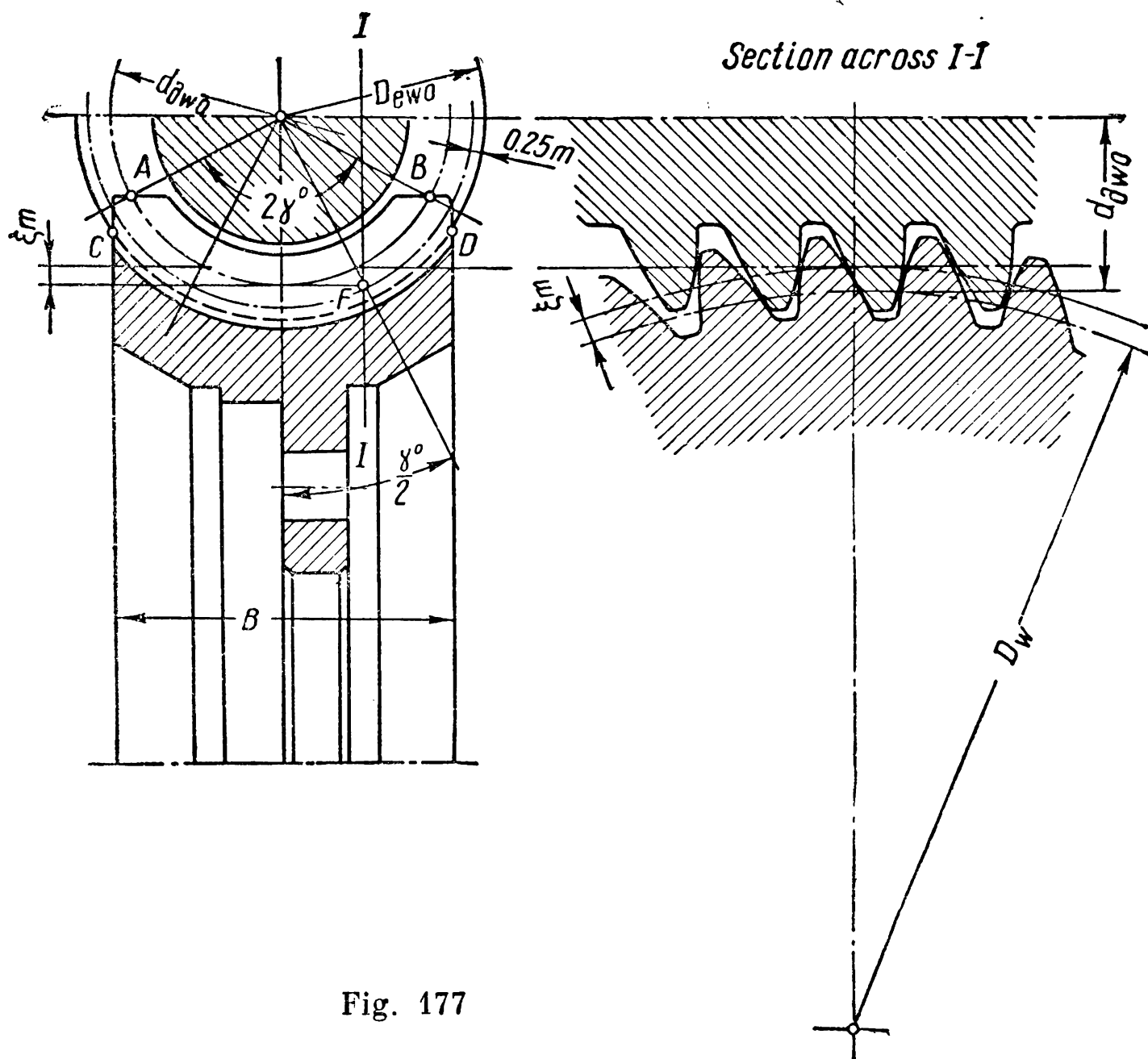


Fig. 177

on the worm addendum cylinder and the length of the line of contact  $l_c$  equal to the arc on the pitch cylinder within the angle of contact  $2\gamma^\circ$ .

$$\frac{\text{arc } CD}{\text{arc } AB} = \frac{l_0}{l_c} \approx \frac{D_{ewo}}{d_{wo}} \approx \frac{q_{wo}m + 2m}{q_{wo}m} = \frac{q_{wo} + 2}{q_{wo}}.$$

Besides, as can be seen from Fig. 177, the strength of the tooth is greater in sections parallel to the main plane than in the plane of main section. For example, in the section  $I-I$  a tooth of a worm wheel has the form of a tooth corrected by a positive shift  $\xi m$ .

The mean magnitude of the shift factor can be found for a section passing through point  $F$  which is determined by the intersection



of a horizontal line tangential to the worm pitch circle with a line drawn from the worm centre at an angle of  $2\gamma^\circ/4$ . It follows from Fig. 177 that

$$\xi = \frac{q_{wo}}{2} \left( 1 - \cos \frac{2\gamma^\circ}{4} \right) \approx 0.05 q_{wo}.$$

Taking on an average  $q_{wo} = 10$  we find

$$\frac{l_o}{l_c} = \frac{10+2}{10} = 1.2$$

and

$$\xi = 0.5.$$

With such a shift the increase in the tooth form factor at  $z_w = 30-80$  equals 1.24-1.1. Taking on an average 1.17 we find a relative increase in tooth strength:  $1.2 \times 1.17 = 1.4$ , i. e., approximately 40%. Substituting the value  $q_d$  from the formula (299) in the formula (264) and replacing the angle  $\beta$  by  $\lambda$ , and  $m_n$  by  $m \cos \lambda$  and accounting for the factor 1.4 and also introducing the factor 1.5 to compensate for the possible wear of teeth we obtain

$$\sigma_b = \frac{q_d \cos^2 \lambda}{m y \cos \lambda} \times \frac{1.5}{1.4} \approx \frac{1.9 \cos \lambda}{m d_w d_{wo} y} M_t k_c k_d \leq [\sigma]_b \text{ kg/cm}^2. \quad (310)$$

For design calculations of open-type gears we find from the latter formula (neglecting the effect of the angle  $\lambda$ )

$$m = 1.24 \sqrt[3]{\frac{M_t k_c k_d}{z_w q_{wo} y [\sigma]_b}} \text{ cm}. \quad (311)$$

The tooth form factor  $y$  is taken from the diagram in Fig. 160 (for driven wheels) according to the equivalent number of teeth  $z_{eq}$  [formula (265)].

The allowable bending stresses in the dangerous section of a worm wheel tooth are found from the formulae (239) and (241).

For some materials the allowable stresses are given in Table 47 at  $N = 10^6$ . At  $N > 10^6$  the tabulated values should be multiplied by the load factor  $k_l = \sqrt[9]{\frac{10^6}{N}}$ . At  $N > 250 \times 10^6$  we should take  $N = 250 \times 10^6$ . Under varying load  $N_{eq}$  is computed from the formula (240).

**Lubrication and Efficiency.** Losses in the gear are mainly due to the sliding of the worm threads along the teeth. The loss factor  $\varphi$  which accounts for the sliding contact can be approximately found as for a power screw from the formula

$$\varphi = 1 - \frac{\tan \lambda}{\tan (\lambda + \rho)} \quad (312)$$

where  $\varrho$  is the angle of friction depending on the material of the conjugate pair, the surface finish, lubrication and velocity of sliding.

Table 47  
Values of  $[\sigma]_b$  for Different Materials of Wheels

Material and casting methods	One-side tooth loading	Both-side tooth loading
Bronze OΦ 10-1, sand-mould casting . . . . .	400	290
Bronze OΦ 10-1, metal-mould casting . . . . .	580	420
Bronze OHΦ, centrifugal casting . . . . .	650	460
Bronze AЖ 9-4, sand-mould casting . . . . .	780	640
Cast iron CЧ 12-28 . . . . .	340	210
Cast iron CЧ 15-32 . . . . .	380	240
Cast iron CЧ 18-36 . . . . .	430	270
Cast iron CЧ 21-40 . . . . .	480	300

The velocity of sliding in a worm gear is determined from the formula (291) after substituting in it

$$d_p = d_{\partial wo} = m q_{wo}$$

and (Fig. 175)

$$\cos \lambda_p = \cos \lambda = \frac{\pi m q_{wo}}{\sqrt{(\pi d_{\partial wo})^2 + (\pi z_{wo} m)^2}}$$

which gives

$$v_{sl} = \frac{mn_{wo}}{19,100} \sqrt{z_{wo}^2 + q_{wo}^2} \text{ m/sec} \tag{313}$$

where  $m$  is the module in mm;

$n_{wo}$ —the number of the worm revolutions per minute.

It can be seen from the formula (312) that the amount of losses in gearing depends on the magnitude of the angle of friction  $\varrho$ .

The materials of the wheel and worm have a noticeable effect on the magnitude  $\varrho$ . Minimum losses occur with a steel, casehardened, finely polished worm and a wheel with a rim made from tin-phosphor bronze. Minimum losses will be likewise observed in a gear lubricated with castor oils (since they help diminish the coefficient of friction); mineral oils tend to increase losses. A higher velocity of sliding favours formation of an oil wedge, lubrication conditions

improve, friction in the gearing decreases and the value  $\rho$  drops. For gears with cast-iron wheels and steel worm  $\rho$  can be taken within  $3^{\circ}30'-6^{\circ}$ . Smaller values should be chosen when the velocity of sliding exceeds 1-2 m/sec. For gears with bronze worm rims and steel worms the data for  $\rho$  (depending on the velocity of sliding) are found from experiments on worm gears operating with antifriction bearings (Table 48). The experimental results have been processed according to a formula taking into account the losses in the gearing and bearings; the magnitude  $\rho$  is therefore arbitrary since it takes into account all losses in the gearing and antifriction bearings.

Table 48

Values of Angles of Friction  $\rho$

$v_{sl}$ in m/sec	$\rho$	$v_{sl}$ in m/sec	$\rho$
0.01	$6^{\circ}20'-6^{\circ}50'$	2.5	$1^{\circ}40'-2^{\circ}20'$
0.1	$4^{\circ}30'-5^{\circ}10'$	3	$1^{\circ}30'-2^{\circ}00'$
0.5	$3^{\circ}10'-3^{\circ}40'$	4	$1^{\circ}20'-1^{\circ}40'$
1.0	$2^{\circ}30'-3^{\circ}10'$	7	$1^{\circ}00'-1^{\circ}30'$
1.5	$2^{\circ}20'-2^{\circ}50'$	10	$0^{\circ}55'-1^{\circ}20'$
2	$2^{\circ}00'-2^{\circ}30'$		

Smaller values of  $\rho$  can be taken for casehardened ground and polished worms liberally lubricated with viscous oil.

An analysis of the formula (312) shows that the losses in the gearing depend on the lead angle  $\lambda$ : as  $\lambda$  increases the losses diminish.

The minimum losses will be at  $\lambda=45^{\circ}-\frac{\rho^{\circ}}{2}$ . However, gears with such a large lead angle are rare since it is difficult to manufacture worms with  $\lambda>25^{\circ}$ , the accuracy of gearing falls while the effect obtained is negligible: as  $\lambda$  grows from 30 to 40° the losses drop by 1% but the proportions of the gear become excessive.

Losses for oil churning (with a wheel in an oil bath) can be found from the formula

$$L_{ch}=0.001v_wB\sqrt{E_t^{\circ}}\text{ h.p.} \tag{314}$$

where  $v_w$  is the peripheral velocity of the wheel in m/sec;

$B$ —the wheel width in cm;

$E_t^{\circ}$ —arbitrary oil viscosity in Engler's degrees at the temperature of oil in the gear casing  $t$ .

If a worm is immersed in oil then, instead of  $B$ , we should substitute the length of the worm threaded portion  $L$  cm and instead of  $v_w$ —the peripheral velocity of the worm  $v_{w0}$  m/sec.

The efficiency of the gear can therefore be represented as

$$\eta = \frac{\tan \lambda}{\tan (\lambda + \varrho)} \left( 1 - \frac{L_{ch}}{N} \right) \tag{315}$$

where  $N$  is the horse power on the wheel in h. p.

For approximate calculations the full efficiency of worm gears can be assumed equal to

$$\begin{array}{lll} \text{at } z_{wo} = 1 & \text{at } z_{wo} = 2 & \text{at } z_{wo} = 3-4 \\ \eta = 0.7-0.75 & \eta = 0.75-0.82 & \eta = 0.82-0.92. \end{array}$$

The proper choice of oil and method of lubrication is extremely important for normal operation of a worm gear.

When the temperature of the ambient air is  $t_{air}=20^\circ$  and the mean temperature of the oil bath  $t_{bath}=70^\circ$  the oil viscosity and method of lubrication should be taken from Table 49.

Table 49

Recommended Values of Oil Viscosity for Worm Gears

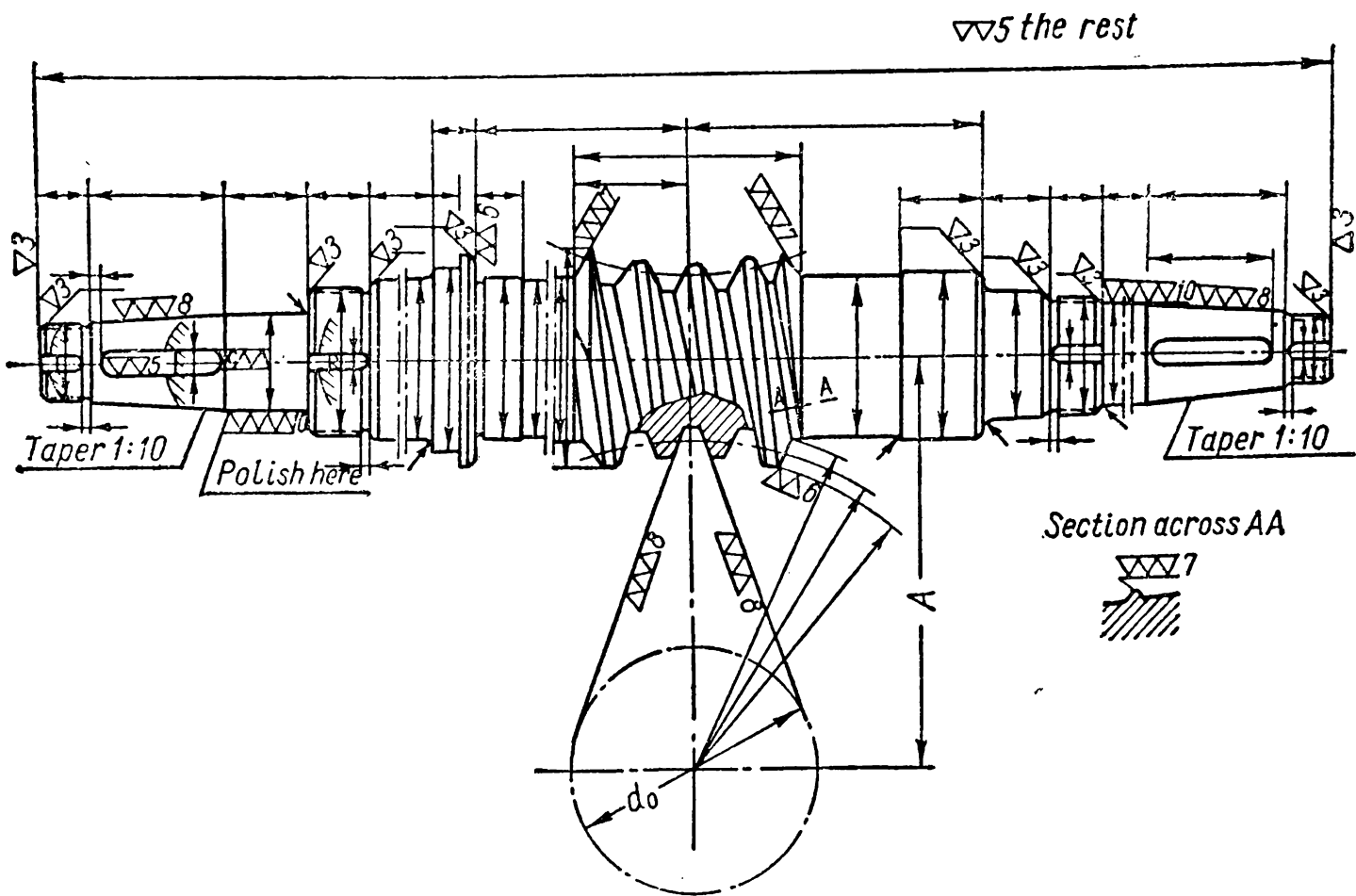
Velocity of sliding $v_{sl}$ in m/sec	<2.5	<5	5-10	10-15
Service	Severe	Medium	.	
Arbitrary oil viscosity $E_{50}^\circ$ (in Engler's de- grees)	36	24	16	11
Method of lubrication	Immersion		Stream or immersion	Pressure

At  $t_{air}<20^\circ$  or during limited intermittent operation of the gear the oil viscosity should be less than that given in Table 49. To improve antiscuff properties 3-10% of vegetable or animal fats should be added to mineral oil. Strong antiscuff lubricants should never be used for worm gears with bronze wheels since in this case the bronze is strongly corroded.

GLOBOIDAL GEARS

**Materials.** When selecting material for the wheel and worm of a globoidal gear it should be borne in mind that a normal operation of the gear can be ensured only when there is good contact between the worm threads and the wheel teeth obtained by running them in simultaneously. At the same time, the surface hardness of the worm threads should not be excessively low because of the hazard

of seizure and faster rates of wear. Gears with improved worms hardened to  $R_C=32-35$  have proved highly efficient. Globoidal worms are not ground, as worms of this hardness can be finished with a cutting tool. For important gears steel of grades 35XMA, 38XГH or 40XH are used; more often it is 40X.



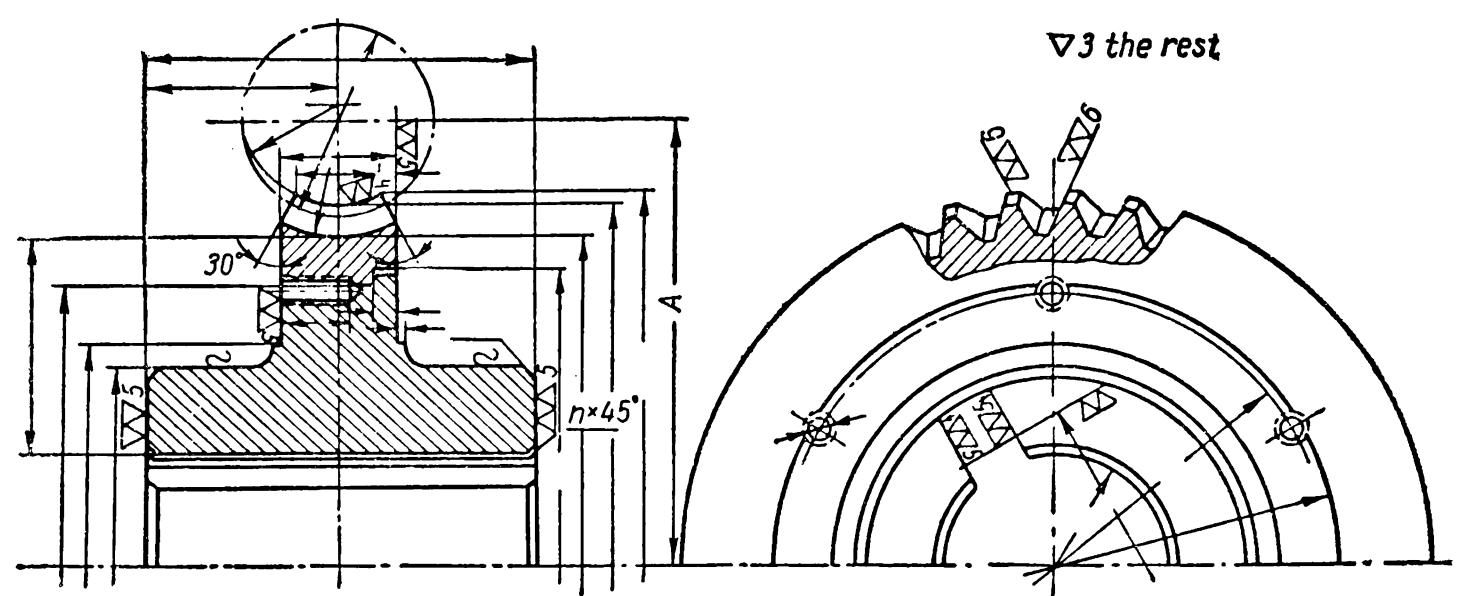
11	Direction of thread		
10	Type of worm		
9	Diameter of wheel pitch circle	$d_{\theta w}$	
8	Theoretical angle of contact of worm	$2\alpha_0$	
7	Lead angle of worm in the throat of <i>pitch globoid</i>	$\lambda_0$	
6	Diameter of base circle	$d_0$	
5	Centre distance of gear	$A$	
4	Velocity ratio of gear	$i$	
3	Number of teeth on wheel	$Z_w$	
2	Number of starts on worm	$Z_{w0}$	
1	Module	$m$	
Item No.	Name	Symbol	Magnitude

Fig. 178

The combination of the materials of the worm and wheel should have a minimum coefficient of friction and effectively resist seizure. These requirements are satisfied best of all by tin-nickel bronze OHΦ and to a somewhat lesser degree by tin-phosphor bronze OΦ 10-1.

The low-tin bronzes ОЦС 5-5-5, ОЦС 6-6-3 and others are very effective. When the velocity of sliding is  $v_{sl} \leq 2 \text{ m/sec}$  use can be made of bronze АЖ 9-4. However, in this case, the allowable load will be smaller than in wheels made from tin bronze. Satisfactory results are obtained from brass of grades ЛМЦС 58-2-2, ЛМЦОС 58-2-2-2.

**Design of Worms and Wheels.** When designing worms and wheels for globoidal gears the recommendations suggested for plain worm gears can be consulted.



11	Direction of thread		
10	Type of worm		
9	Diameter of wheel pitch circle	$d_{dw}$	
8	Theoretical angle of contact of worm	$2\alpha_0$	
7	Lead angle of worm in the throat of <i>pitch globola</i>	$\lambda_0$	
6	Diameter of base circle	$d_0$	
5	Centre distance of gear	$A$	
4	Velocity ratio of gear	$i$	
3	Number of teeth on wheel	$z_w$	
2	Number of starts on worm	$z_{w0}$	
1	Module	$m$	
Item No.	Name	Symbol	Magnitude

Fig. 179

Figs. 178 and 179 show sketches of a globoidal worm and wheel. Accuracy of manufacture and assembly noticeably affects the operating ability of globoidal gears.

In assembling the gear it is essential to maintain within definite limits the centre distance, the position of the worm on its axis and the mean plane of the worm wheel relative to the worm axis.

**Calculation.** A globoidal gear offers more favourable conditions for the formation of an oil wedge than an ordinary worm gear. A globoidal worm forms contact with all wheel teeth within the angle  $2\alpha_0$  along constant lines of contact in the main plane, which are located at right angles relative to the direction of velocity of sliding (Fig. 180). Besides, in the area of the first half of the gear (along the worm length), on the side of the worm rotating drive there are additional shifting lines of contact located at an angle of approximately  $90^\circ$  relative to the direction of the speed  $v$  (Fig. 180). Another favourable factor is that the curvature of the surfaces of the teeth contacting along the additional lines of contact is extremely small. This helps the formation of a stable oil wedge and reduces the contact compressive stress. As a result the load-carrying capacity of a globoidal gear exceeds that of a worm gear of the same size.

The load-carrying capacity of a globoidal gear does not depend upon the module because nearly  $1/9$  of all teeth are engaged simultaneously whereas in a worm gear the load is at times taken only by one tooth.

Wear resistance of teeth and thermal capacity are the main criteria for the evaluation of the operating ability of a worm gear. Therefore, such proportions of the gear (centre distance  $A$ ) must be found by calculation which will safeguard the teeth from noticeable wear after the running-in period and operation under load and prevent the temperature of the oil bath from rising above the allowable limits.

A universal method for calculating globoidal gears does not yet exist; therefore, resort is had to an approximate method. According to this method, the horse power that can be handled by a globoidal gear is found from calculations for wear after which the thermal capacity of the gear is checked.

The forces acting in engagement can be approximately found from the respective formulae for worm gears.

**Main Geometrical Proportions.** The proportions of a globoidal gear related to the main plane in the worm throat section can be found from the formulae used for worm gears at  $\xi=0$  (Table 42). Other proportions characteristic only of globoidal gears are easily

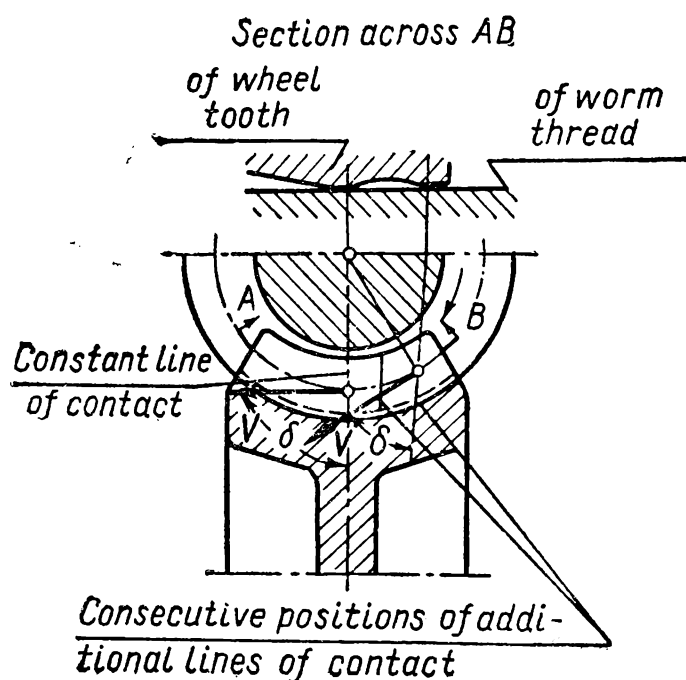


Fig. 180

found from the diagram showing a section of the gear in the main plane (Fig 181). The theoretical angle of contact of the worm  $2\alpha_0$  determining the worm thread angle should be within  $2\alpha_0=36-46^\circ$ .

The length of the wheel pitch circle within this arc can

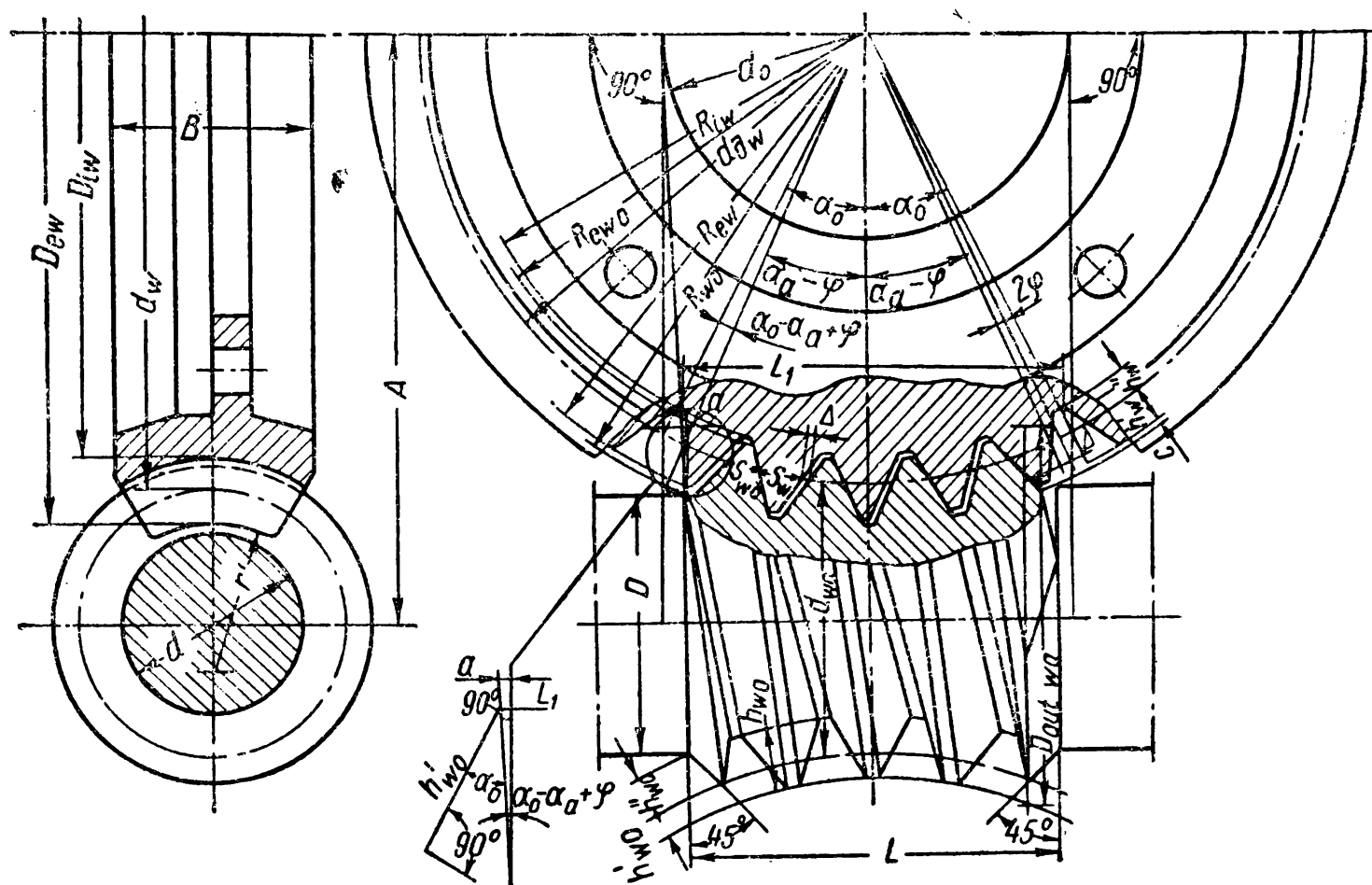


Fig. 181

accommodate  $z_0$  pitches. The arc of contact of the worm and the wheel should be decreased so that the number of active pitches  $z_a$  along this arc is  $z_a \approx 0.9z_0$  and the number of the wheel teeth  $x$  distributed on this arc is an integer.

The latter condition is written thus

$$(x - 0.5)t = z_a t$$

whence it follows that the length of this arc should accommodate the number of pitches  $z_a$  from the series 1.5, 2.5, 3.5, 4.5, etc.

Assuming in advance  $2\alpha^\circ = 40^\circ$  we find

$$z'_0 = \frac{\alpha_0}{180^\circ} z_w = \frac{z_w}{9}$$

and

$$z'_a = 0.9 \frac{z_w}{9} = 0.1z_w \quad (316)$$

In geometrical calculations, the formula (316) is first used to find  $z'_a$ , then to approximate the obtained value to  $z_a$  from the



above series (1.5, 2.5, 3.5, etc.) and then find  $z_0 = z_a/0.9$ ; further

$$\alpha_0 = z_0 \frac{180^\circ}{z_w} \quad (317)$$

and finally the diameter of the base circle

$$d_0 = d_{\partial w} \sin \alpha_0. \quad (318)$$

The addendum factor is assumed to equal  $f_0 = 0.8$ . The clearance factor is  $c_0 = 0.2$ .

The thickness of the wheel tooth along the arc of pitch circle equals half the pitch

$$s_w = 0.5\pi m \text{ mm.} \quad (319)$$

The wheel width is selected within  $B = (0.6-0.8) d_{w0}$ ; larger values are taken for gears with low velocity ratios.

The external surface of the wheel is described over the arc whose radius is larger than the maximum radius of the worm dedendum surface to make radial assembly possible. Usually,

$$r' = 0.53D$$

where  $D$  is the diameter of the worm due to design considerations.

The maximum addendum diameter of the wheel  $D_{out w}$  is found graphically.

The backlash in the main plane section is assumed to equal  $\Delta = 0.002A$  but should not be below  $\Delta = 0.2 \text{ mm}$ .

The thickness of the worm thread along the arc of pitch circle is

$$s_{w0} = s_w - \Delta. \quad (320)$$

The length of the worm threaded portion is found from the following relations (Fig. 181):

$$L = L_1 - 2a \approx d_{\partial w} \sin(\alpha_a - \varphi) - 2 \frac{h_{w0}''}{\cos \alpha_0} \sin(\alpha_0 - \alpha_a + \varphi) \quad (321)$$

where  $\alpha_a = z_a \times 180^\circ / z_w$ ;  $\varphi = 3,440 \Delta / d_{\partial w}$ .

The maximum addendum diameter of the worm  $D_{out w0}$  is found by trial drafting.

**Calculation of the Gear for Wear.** These calculations are carried out by the try-and-check method according to the empirical formula which determines the allowable horse power on the worm

$$N_{w0} = \frac{H}{i} \times \frac{k_{mat} k_{ac} k_{serv}}{I} \quad (322)$$

where  $H$  is the power factor in h. p. depending on the centre distance of the gear  $A$  and rpm of the worm; it is taken from the graph in Fig. 182

$i$  is the gear velocity ratio;  $i = \frac{n_{wo}}{n_w}$ ;

$k_{mat}$ —the factor of the material depending on the material used for the wheel rim taken from Table 50;

Table 50

Factor of Material $k_{mat}$	
Material of wheel rim	$k_{mat}$
Tin bronzes (OHΦ, OΦ 10-1, etc.) . .	1
Bronze AЖ 9-9, etc. . . . .	0.8

$k_{ac}$ —the factor of the gear manufacturing accuracy taken from Table 51.

Table 51

Factor of Accuracy $k_{ac}$	
Degree of accuracy	$k_{ac}$
7	1
8	0.8

$k_{serv}$  —the service factor allowing for the nature of load (Table 52).

Table 52

Service Factor $k_{serv}$	
Service	$k_{serv}$
Continuous smooth round-the-clock . . . . .	1.0
Continuous with impact load for 8-10 hours per day . . . .	0.85
Continuous round-the-clock with impact load . . . . .	0.75
Intermittent with long intervals (15 min of operation, 2 hours or more of standing idle) . . . . .	1.4

$I$  is the velocity ratio factor taken from the graph in Fig. 182; at  $i > 25$   $I$  should be unity.

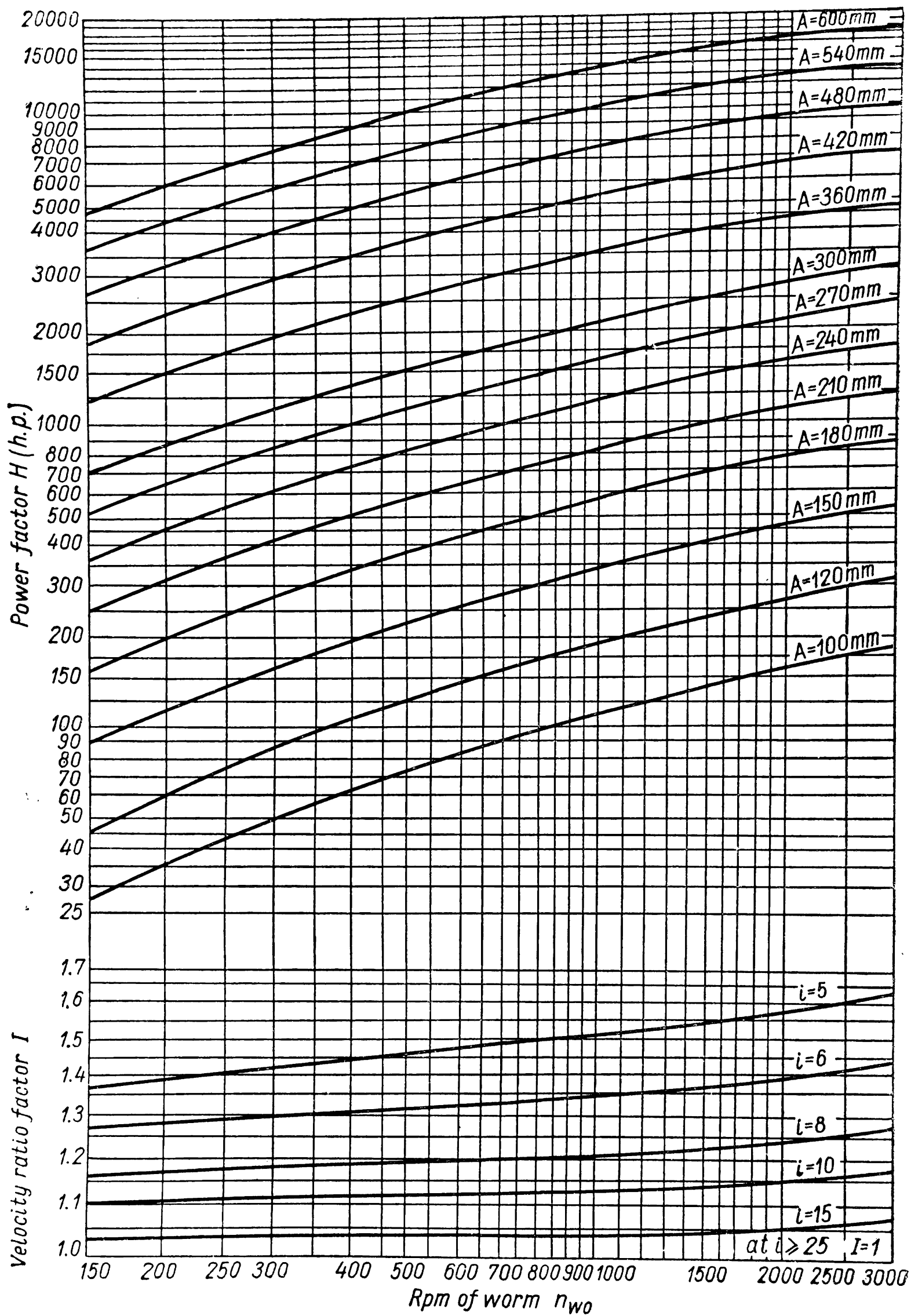


Fig. 182

The centre distance should be specified in advance. Its value is selected from the series provided by standards for worm gears. The horse power on the worm  $N_{wo}$  found from the formula (322) should be compared with the assigned value.

Under varying load, calculations should be done according to the mean load registered during the entire period of operation, because even considerable short-time overloads do not essentially affect the wear of the gear.

After it has been proved with the help of the formula (322) that the assumed centre distance  $A$  really corresponds to the design load the value  $q_{wo}$  is selected and the gear module determined by the formula (Table 42).

$$m = \frac{2A}{z_w + q_{wo}} \text{ mm.}$$

The module for globoidal gears is not specified by Soviet standards and can be a fractional number.

To ensure adequate rigidity of the worm the magnitude  $q_{wo}$  should be such that the worm deflection under load does not exceed  $f = 0.2\Delta A$  ( $\Delta A$  is the limit deflection of the centre distance of the gear). As a rule, this condition is satisfied when  $q_{wo} = 8-9$  for  $z_w < 30$ ;  $q_{wo} = 9-10$  for  $z_w = 30-40$ ;  $q_{wo} = 10-11$  for  $z_w = 41-60$ ;  $q_{wo} = 11-12$  for  $z_w = 61-100$ .

When selecting the number of teeth  $z_w$ , values should be taken which are not multiples of the number of the worm starts in order to increase the meshing accuracy.

**Lubrication and Efficiency.** Losses in a globoidal gear are found in the same way as in a worm gear, from the formula

$$\eta = \frac{\tan \lambda_0}{\tan (\lambda_0 + \varrho)} \left( 1 - \frac{L_{ch}}{N_{wo}} \right) \left( 1 - \frac{L_b}{N_{wo}} \right) \quad (323)$$

where  $\lambda_0$  is the lead angle in the globoid throat;

$\varrho$ —the angle of friction; low values are taken from Table 48 depending on the velocity of sliding;

$L_{ch}$ —losses for churning the oil in h. p. found from the empirical formula  $L_{ch} = 1.45 \times 10^{-9} \times n_{wo} \times A^2 \sqrt{E_t^0}$ ;

$L_b$ —losses due to friction in the bearings in h. p. (see p.475). In the formula (323) the first multiplier accounts only for the losses in engagement.

The thermal capacity of a continuously operating gear is found from the formulae (36) and (326). The temperature of the oil bath can rise to  $t_{bath} = 80^\circ-90^\circ\text{C}$  because a globoidal gear is smaller in size than a worm gear of the same power. Therefore, globoidal gears should be lubricated with more viscous oils than those used in worm gears.

## CHAPTER XVII

## TOOTHED AND WORM REDUCTION GEARS

## MAIN TYPES OF REDUCTION GEARS

When toothed gears are used as independent units to *reduce* the velocity of driven shafts they are encased in rigid housings which keep off oil and dust and support the shaft bearings. These gears are called *reduction gears*.

Similar mechanisms intended to *increase* the velocity of driven shafts are called *multiplying gears*.

The main parameters of spur toothed reduction gears are standardised.

Soviet standards specify a number of centre distances for single-, double-, and triple-reduction gears, tooth wheel width factors, modules, velocity ratios and the maximum angles at which the teeth are inclined.

Schematic diagrams of the most widespread types of reduction gears are shown in Table 53 (the letters *H*, *L* and *I* stand for high-speed,—low-speed and intermediate gears).

The simplest reduction gear with a pair of spur wheels (Fig. 183) is reliable in operation and is employed for a wide range of powers (up to 50,000 h. p.) but for small velocity ratios ( $i_{\max}=8-10$ ). For a higher velocity ratio ( $i=10-60$ ) use is made of the reduction gears shown in the Table as *II, a* and *IV, a*.

The disadvantage of these reduction gears is the asymmetric arrangement of the wheels relative to the bearings. As the reduction gear shafts sag under load the wheels incline on the shafts. This causes mutual misalignment of the mating wheels and hence overloading of the points of the mating teeth, which may lead to the premature failure of the reduction gear.

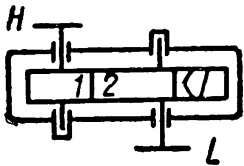
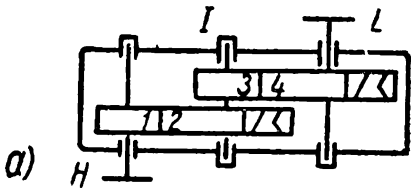
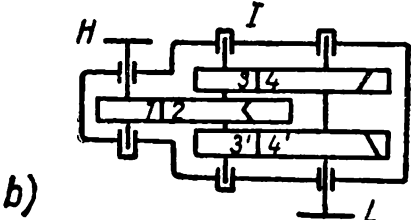
Reduction gears with «bifurcation» of power (diagrams *II, b* and *IV, b*) partly compensate for these shortcomings since the wheels of the high-speed gear mounted on the thinnest shafts are arranged in the middle of the span and are not misaligned when the shaft deflects.

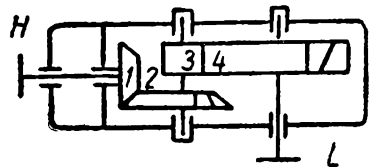
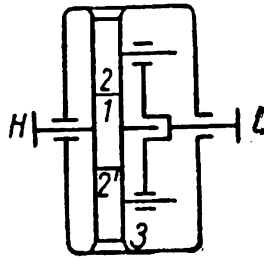
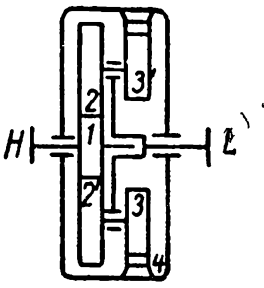
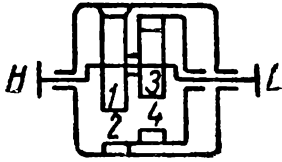
Coaxial reduction gears (diagram *III*) are superior to other types when the shafts of the connected mechanisms are to be arranged in a line.

The disadvantages of this type of reduction gear are their larger dimensions along the axles, since the bearings of the high- and low-speed shafts have to be arranged in one geometrical axis, the considerable misalignment of the wheels on the connecting shaft which sags considerably owing to its length and the difficulty in making effective use of the load-carrying capacity of the high-speed

Table 53

Most Widespread Types of Reduction Gears

Item No.	Reduction gear	Sketch
1	Single-reduction spur gear	<div><div>I</div></div>
2	Double-reduction spur gear	<div><div>II</div><div><div>a)</div></div><div><div>b)</div></div></div>

Item No.	Reduction gear	Sketch
6	Double-reduction bevel-spur gear	<div><div>VI</div></div>
7	Single-reduction planetary gear	<div><div>VII</div></div>
8	Double-reduction planetary gear	<div><div>VIII</div><div><div>a)</div></div><div><div>b)</div></div></div>

gear wheels because the centre distances of the high- and low-speed gears are the same while the torques on them noticeably differ.

Planetary reduction gears (diagrams VII, VIII, a and VIII, b) are considerably smaller in size than simple toothed reduction gears and are employed for high velocity ratios. To ensure the reliable operation and high efficiency of these reduction gears, high precision in manufacture is required.

To transmit horse power between shafts inclined at an angle to one another use is made of bevel (Fig. 185) or combined bevel-spur reduction gears (diagram VI, Table 53).

The main dimensions of worm reduction gears ( $A$ ,  $m$ ,  $q_{w0}$ ,  $z_{w0}$ ,  $z_w$ , etc.) are standardised in the Soviet Union.

Usually single-reduction gears (Table 54) with shafts placed horizontally, vertically or sideways are used, and less frequently—double-reduction gears. Sometimes worm-spur reduction gears are employed (diagram 5, Table 54 and also Fig. 190).

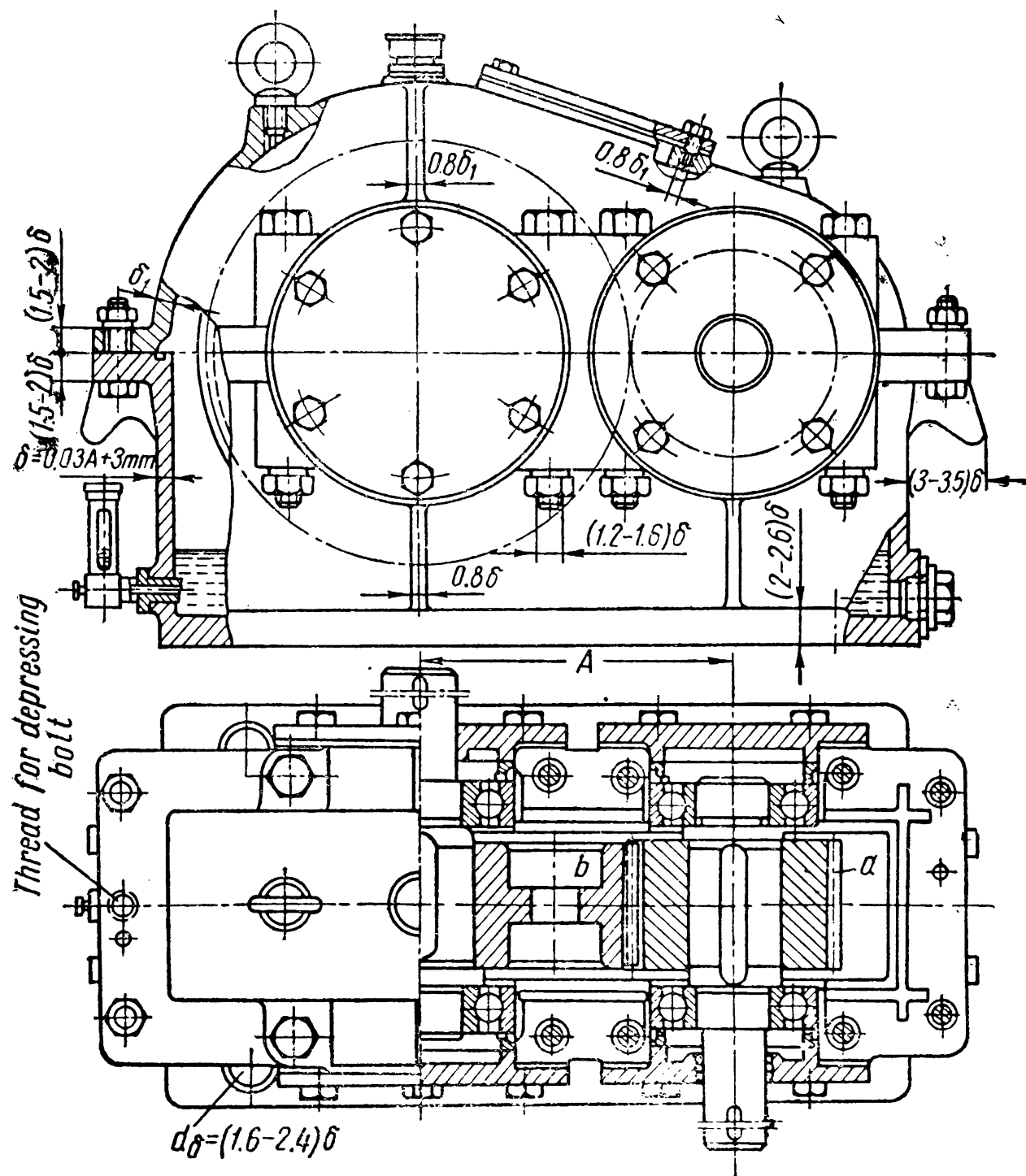


Fig. 183

Reduction gear wheels are designed on the basis of the data cited in the preceding chapters. When calculating a planetary reduction gear it should be remembered that the dynamic load factor  $k_d$  and also the load factor  $k_l$  are determined taking into account relative velocities.

When selecting a type of reduction gear close attention should be paid to its efficiency, dimensions, weight, cost of manufacture and operation, etc.



Table 54 •

Common Types of Worm Reduction Gears

Item No.	Reduction gear	Sketch
1	Single-reduction worm gear with worm underneath	
2	Single-reduction worm gear with worm arranged vertically	
3	Single-reduction worm gear with worm arranged sideways	
4	Double-reduction worm gear	
5	Combined worm-spur reduction gear	

As was noted above the efficiency of a toothed gear is markedly higher than that of worm and globoidal gears (the losses in the latter are almost five times greater than those in a double-reduction toothed gear). When reduction gears are operated continuously for a long period the cost of the electric power necessary to overcome the losses in a worm gear may prove considerably higher than the

cost of a toothed reduction gear. Therefore, worm and globoidal reduction gears are preferably employed to ensure noiseless operation, the required layout of a machine and for intermittent service.

Special attention should be paid to efficiency in selecting the design of a planetary reduction gear. High efficiency is characteristic of the reduction gears shown in diagrams VII and VIII, *a*, Table 53. The reduction gears shown in VIII, *b* possess lower efficiencies but can be used for higher velocity ratios since with an insignificant difference in the number of teeth of wheels 4 and 3 (internal toothing) the losses in engagement are negligible.

Comparing the proportions of various types of reduction gears we notice that at low velocity ratios worm reduction gears are the largest in size and planetary reduction gears with very hard tooth

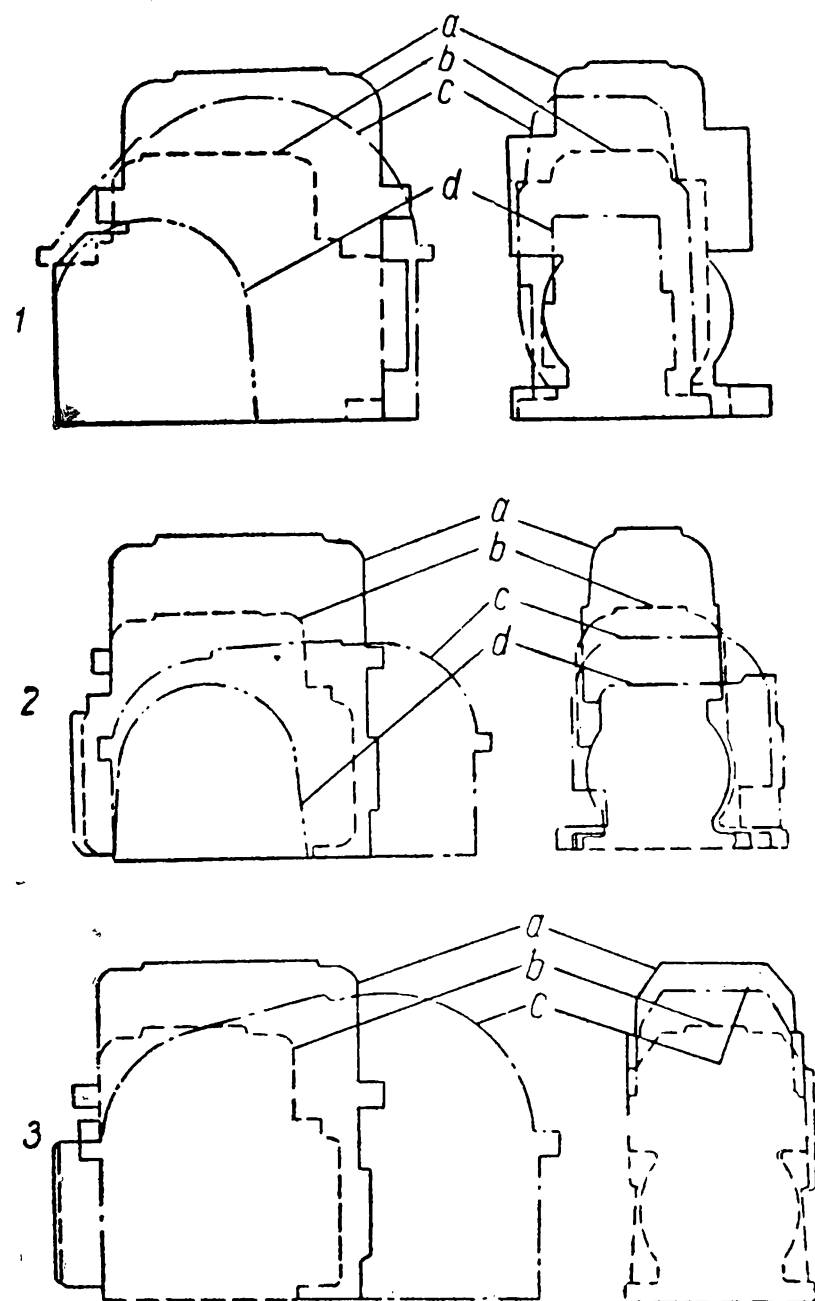


Fig. 184

surfaces—the smallest. Fig. 184 compares the proportions of gears: 1) for  $N_w = 50$  h. p. and  $i = 7$ ; 2) for  $N_w = 25$  h. p. and  $i = 21$ ; 3) for  $N_w = 12$  h. p. and  $i = 50$ ; *a* is a worm reduction gear with the wheel made from tin bronze; *b* is a globoidal reduction gear; *c* is a reduction gear with spur wheels; and *d*—a planetary reduction gear. With an increase in the velocity ratio the relative dimensions of worm and globoidal reduction gears diminish.

All this gives us grounds to presume that, for general cases, toothed reduction gears offer the greatest advantages.

Single-reduction gears with spur wheels have a velocity ratio of  $i=25$ ; however, under ordinary conditions, the velocity ratio should never exceed 8 for a single-reduction gear. Higher values of velocity ratio are permitted for helical and herringbone wheels, and smaller—for straight-tooth wheels.

When the velocity ratio is high a multiple-reduction gear should be used.

If the velocity ratio ranges between 10 and 50 the gear should be designed as a double-reduction gear. At  $i>40$  a triple-reduction gear can be employed.

Gears with external toothings are most common in use. All other conditions being equal, internal gears have smaller dimensions; the contact stresses on the bearing surfaces will be less because the convex surfaces of the pinion teeth run over the concave surfaces of the wheel teeth.

However, internal gears cannot be used for large loads since the gear wheels are overhung and under high loading the load concentration across the width of a cantilever wheel will be extremely large.

Wheels with internal toothings are extensively used in planetary reduction gears where proper layout helps to decrease the load concentration across the wheel width.

A straight-tooth gear employed for small peripheral velocities is the simplest in design. When axial forces or axial play of the wheels are inadmissible resort is also had to straight-tooth wheels.

At peripheral velocities  $v>5$  m/sec helical wheels are recommended. Under severe loads gears with helical wheels require special thrust bearings—therefore herringbone wheels are to be preferred.

Since it is extremely difficult to manufacture bevel wheels of large size accurately, bevel gears are employed as the first stages in multiple-reduction gears. Straight-tooth bevel wheels can operate satisfactorily only when  $v\leq 2$  m/sec. For this reason for higher speeds use is made of bevel wheels with spiral teeth.

In combined reduction gears worm gears act as high-speed gears since they are more efficient at high speeds.

## DESIGNS OF REDUCTION GEARS

The housings of reduction gears are usually made from cast iron CЧ 15-32 and CЧ 18-36; sometimes they are steel castings of grade 15Л, 20Л or 25Л. The parts can also be made in form of weldments (Fig. 186).

The reduction gear parts should be as simple as possible in form with a minimum number of projections, ribs, beads, etc., to ensure stiffness. The proportions of the housing and cover elements are specified by design (Figs. 183, 185).

The locations of bearing units are provided with bosses. To increase the rigidity of reduction gears where bearings transmit power to the body the walls should be ribbed or their form changed. The outer diameter of bosses for the bearings is determined by the diameters of the bolts fastening the end covers and the outer diameters of these covers. Bolts securing the cover to the body are preferably arranged as close to the bearings as possible, the nuts being provided with bosses.

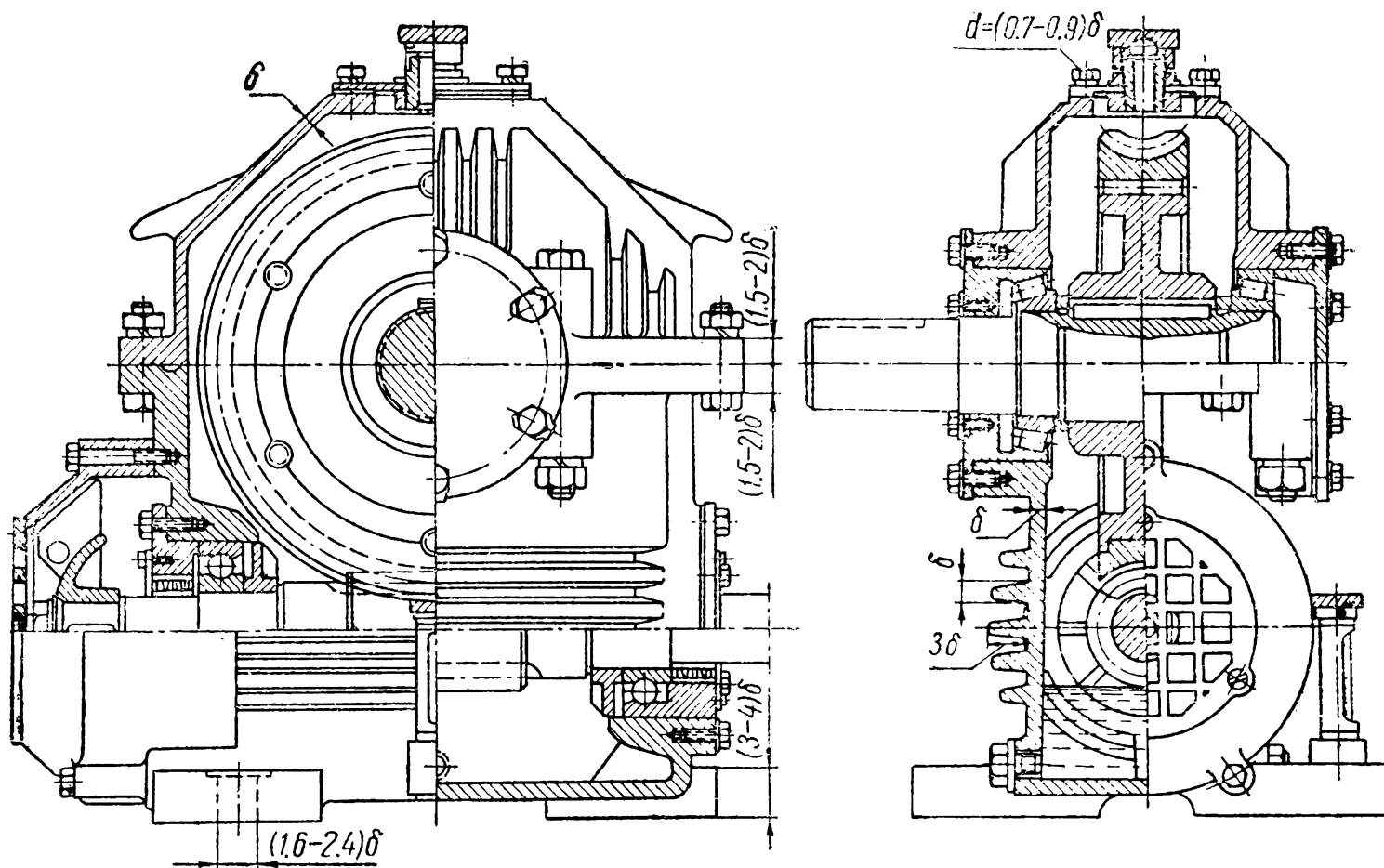


Fig. 185

The borings for bearings or sleeves are made to correspond to the 2nd degree of accuracy; the surface finish should be not below  $\nabla\nabla 6$ .

For the easier removal of the cover, the body is sometimes provided with threaded holes for *depressing bolts*. For the purposes of inspection, oil insertion and draining and the mounting of an oil-level indicator or thermometer the cover and body are provided with drilled holes of the required form and size shut with lids, plugs, nipples, etc. The cover and body should be provided with lifting *eye-bolts* and *hooks* for hoisting and handling these parts and the entire reduction gear.

To prevent oil leakage from the body the joint on the horizontal surface of the body has *grooves* communicating (via inclined holes) with the interior (Fig. 187).

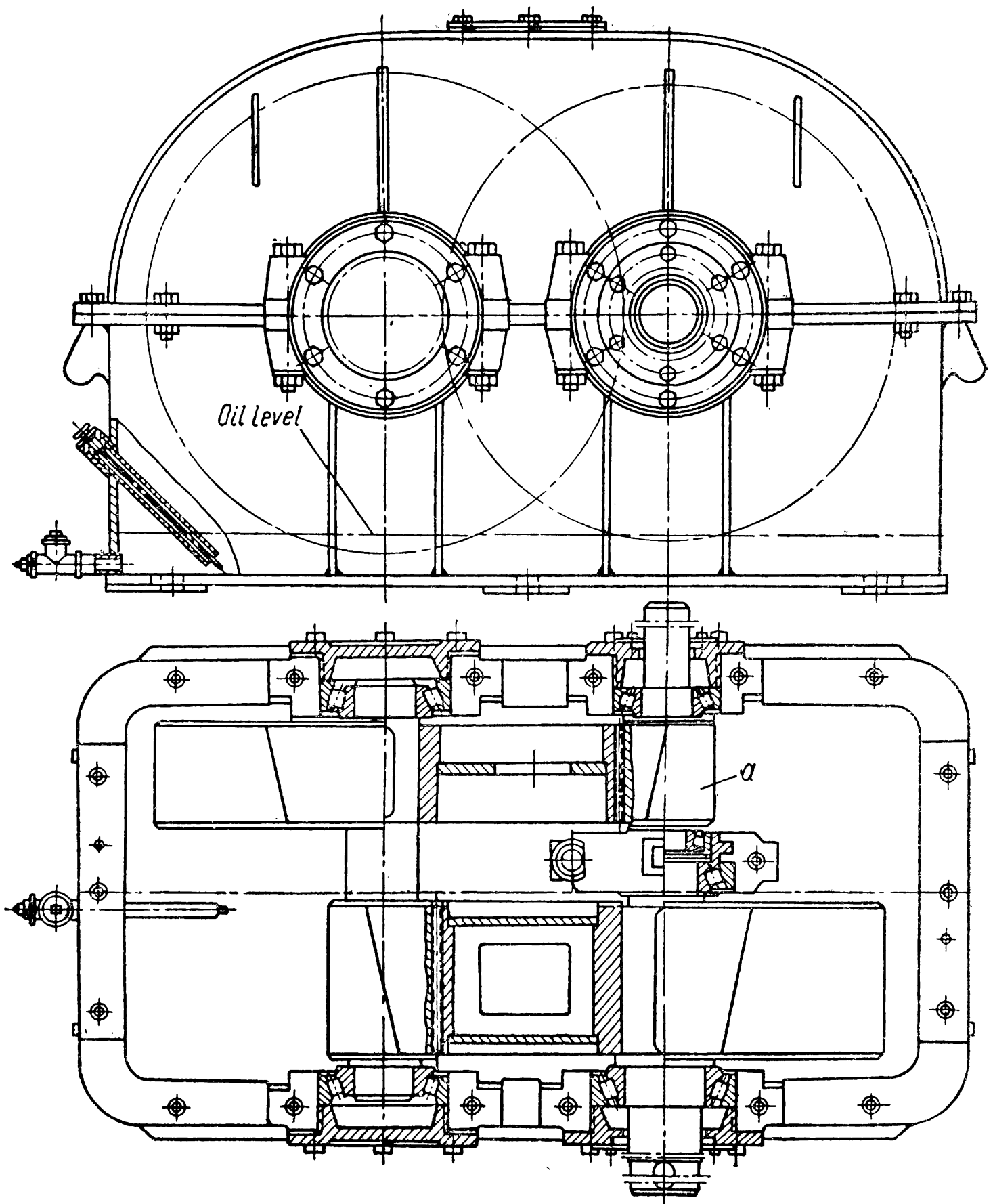


Fig. 186

The cover is fixed relative to the body during the reduction gear assembly by two *taper pins* removed as far as possible from each other (Fig. 183).

In reduction gears handling small and medium powers the shafts rest on antifriction bearings while high-power and high-speed reduction gears employ sliding bearings.

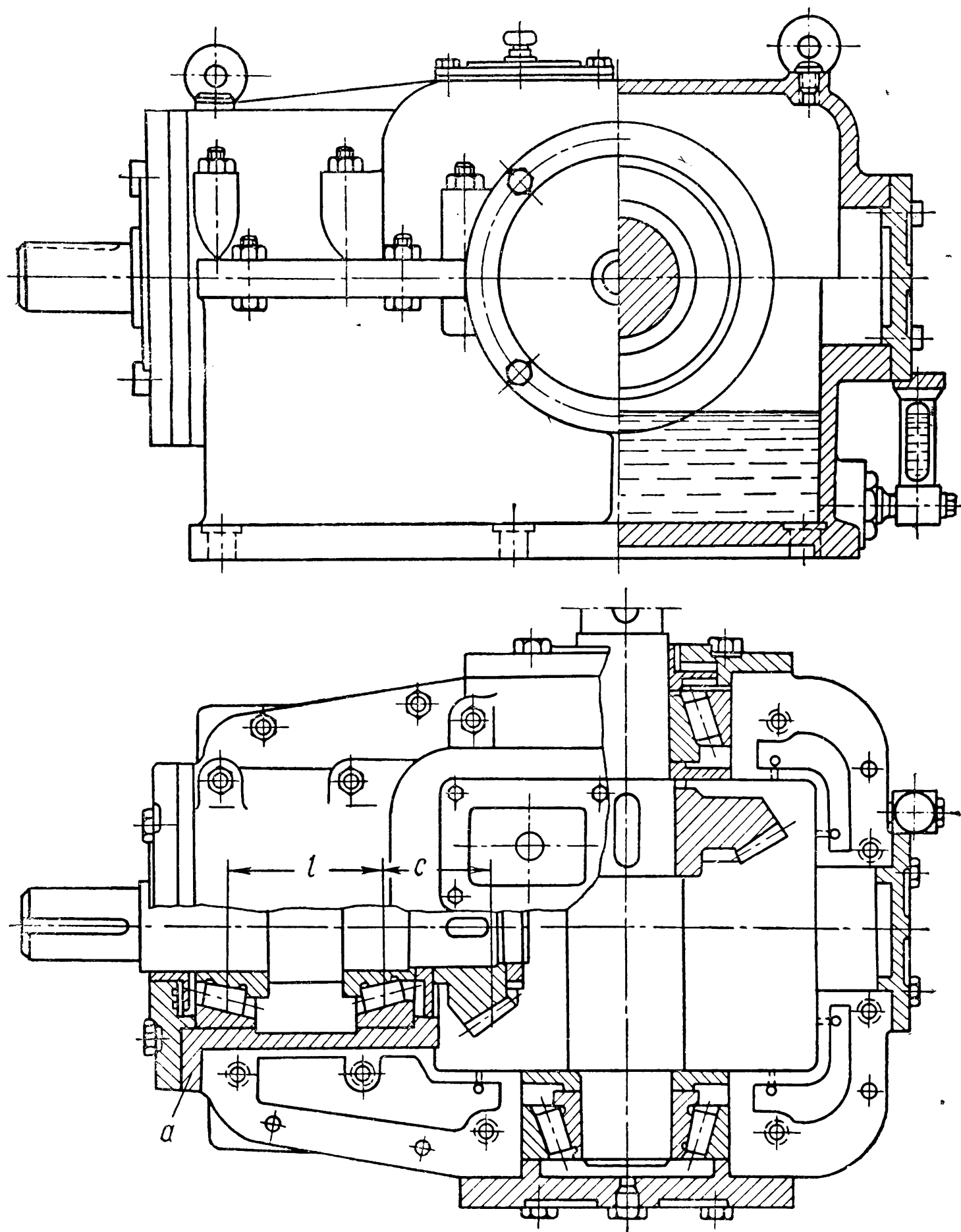


Fig. 187

The type of bearing should be selected depending on the kind of contact. For straight-tooth wheels any type of bearing can be used. Shafts with helical wheels should be mounted on single-row radial and radial-thrust bearings or on conical bearings.

In reduction gears with herringbone wheels or bifurcation of power *one of the shafts* (preferably the pinion shaft as the lighter element) should be secured on roller bearings. Bearings of this type permit axial play; as a result, during the gear operation the pinion can self-align relative to the wheel (under the action of axial forces on each side of the herringbone) and the load will be uniformly spread between the sides of the herringbone.

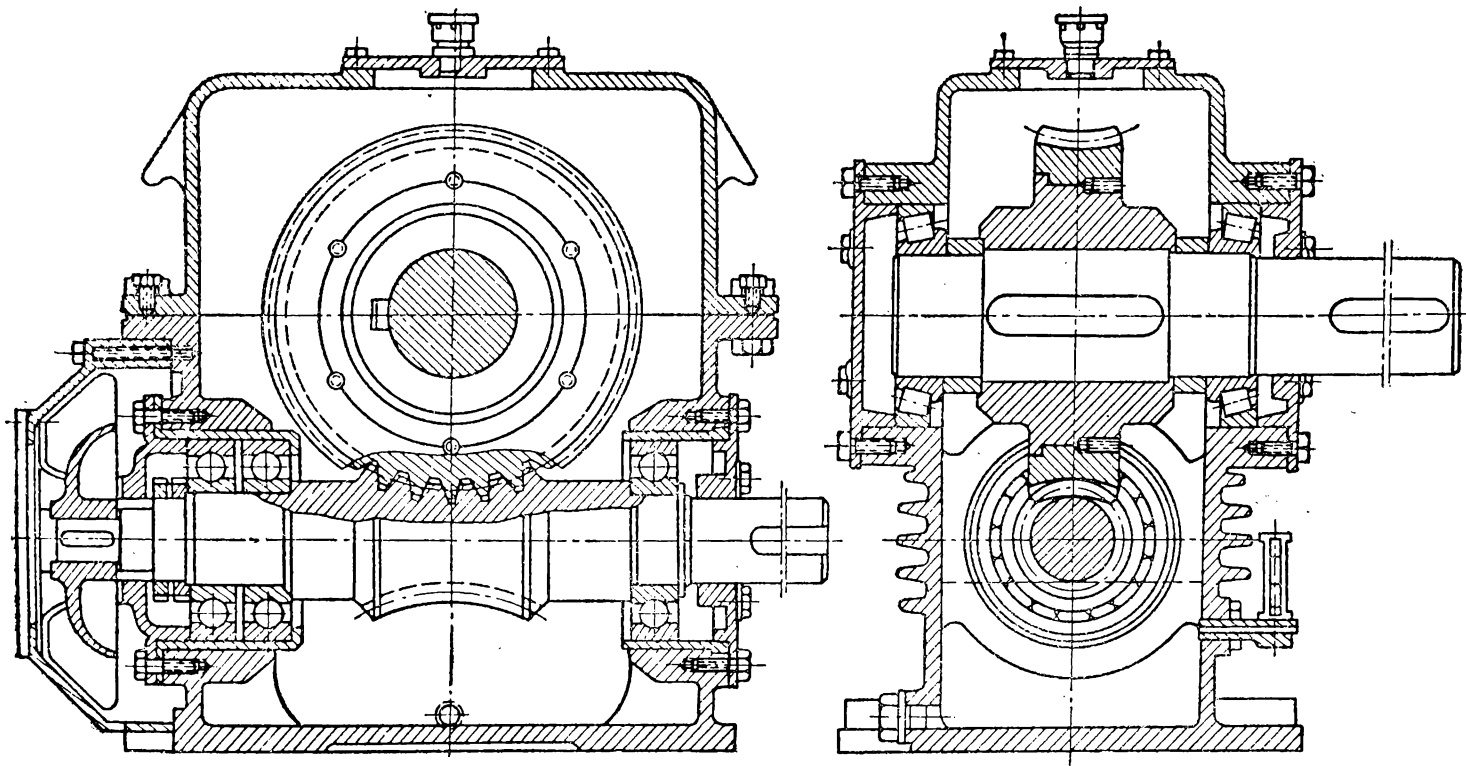


Fig. 188

For a bevel gear to operate satisfactorily the distance  $l$  between the bearings of a cantilever shaft should equal  $(2.5-3.0)$  of the distance  $c$  from the middle of the pinion to the middle of the first bearing. A very effective method is to assemble the shaft with the pinion into a special sleeve which is then installed into the reduction gear housing (part *a* in Fig. 187).

In order to fix the wheels in bevel reduction gears correctly and to align the apexes of the pitch cones all covers of the bearing units rest on mounting shims.

By selecting proper shims for the bearing units the mating wheels can be shifted together with the shafts along their axes in the required direction to obtain correct contact.

Because of considerable axial forces in worm and globoidal reduction gears use is mainly made of radial-thrust bearings for supporting the shafts of worms and wheels. Such bearings are superior to radial ball bearings in that they possess greater stiffness ensuring a stabler relative arrangement of the elements of this type of gear. Most compact units are obtained when antifriction bearings are set at  $\beta=26-30^\circ$ .

When radial-thrust bearings are assembled in both bores of the worm-gear housing (Fig. 185) the rollers or balls may be pinched because the heating of the worm increases. To obviate this danger (when the distance between the supports is over 350 mm) both radial-thrust bearings are arranged on one side, and an auxiliary radial ball or roller bearing—on the other side of the worm to take only radial load (Fig. 188). For convenient assembly and to simplify the machining of the housing the bearings are assembled in sleeves fitted snugly into the body.

### LUBRICATION AND CALCULATION FOR HEATING

The mating surfaces in reduction gears are lubricated with liquid oil either simply by immersing the teeth in an oil bath (*immersion lubrication*) or by feeding oil to the area of contact through specially provided nozzles (*stream lubrication*).

*Immersion lubrication* is limited to a peripheral velocity of  $v \approx 12 \text{ m/sec}$ . At higher velocities the oil is thrown off by centrifugal force and the teeth receive an inadequate oil supply. Simultaneously, resistance to the wheel rotation and the temperature of the oil increase. Therefore, as the peripheral velocity of the gear rises, the depth of immersion is decreased. The oil bath lubricates the larger wheel. The recommended depth of immersion for high-speed wheels is about 0.7 of the tooth height but not less than 10 mm. Low-speed wheels should not be immersed by more than 100 mm. In bevel gears the teeth should be immersed in oil along the entire length.

If all contact points of a multiple-reduction gear cannot be lubricated by immersing the larger wheels, some wheels (not immersed in oil) can be oiled by special devices or by pinions, rings, etc. (Fig. 189, *a*). The capacity of the oil bath should be such as to provide 0.35-0.7 litres of oil per kw of transmitted power.

*Stream lubrication* is used for peripheral velocities of  $v \geq 12-15 \text{ m/sec}$ . It is effected by means of special nozzles into which the oil is fed via a pipe by a pump (Fig. 189, *b, c*). This forced lubrication requires special pipe conduits and devices for filtering, cooling the oil and regulating its delivery.

At high peripheral velocities ( $v > 20 \text{ m/sec}$ ) oil is fed to the teeth of each wheel separately for otherwise the operating conditions of the gears deteriorate. At very high wheel velocities the oil is fed into the area of contact from the side opposite to the direction in which the teeth move in the area of contact.

In multiple reduction gears the oil viscosity should be between the values required for lubricating the extreme stages of the gear. When the toothed wheels and bearings have to be lubricated with the same oil the grade used for tooth wheels is preferred.



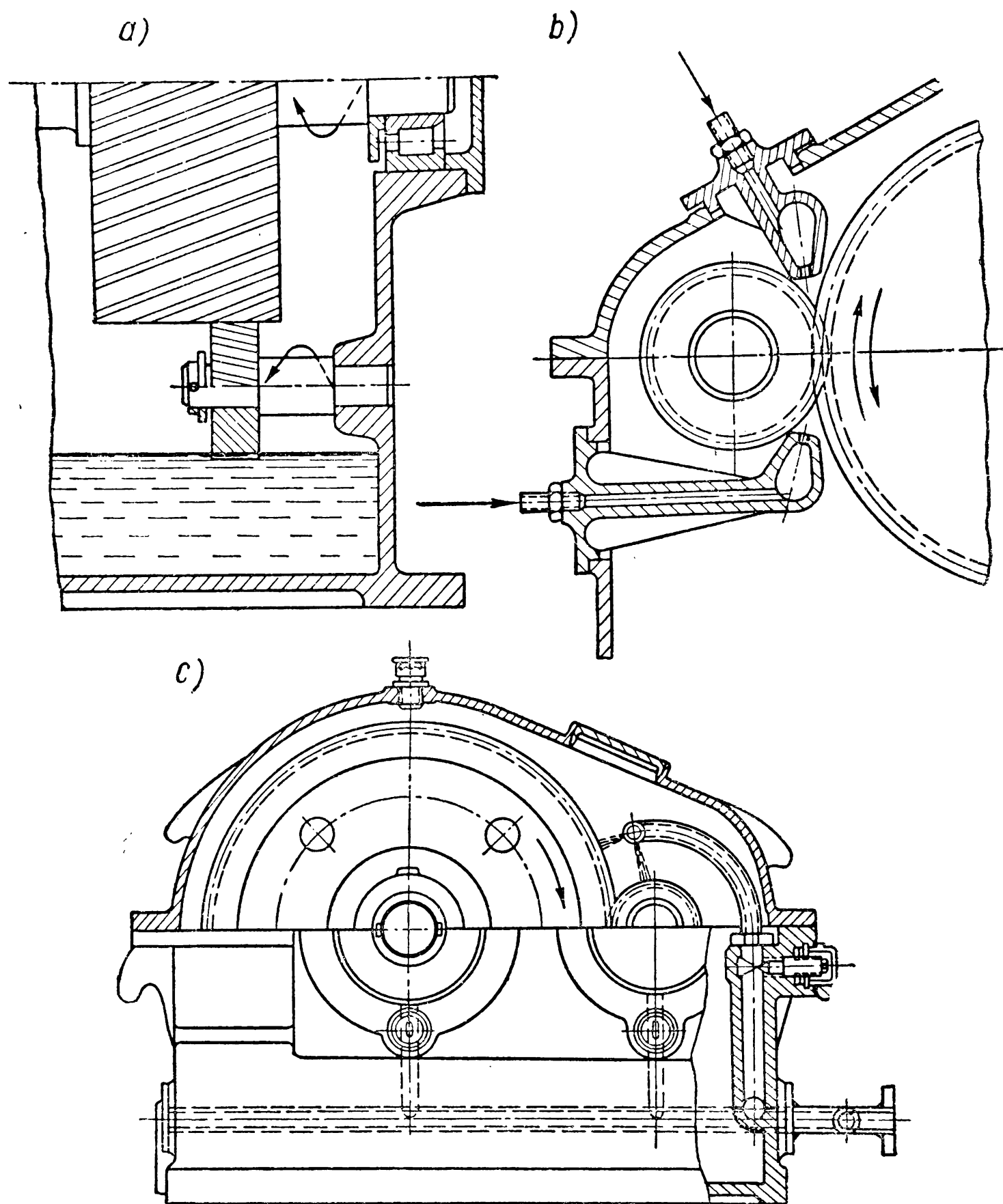


Fig. 189

Immersion lubrication in worm reduction gears is employed at peripheral velocities of the worm up to  $\sim 10$  m/sec. The wheel (when the worm is above the wheel) or the worm should not be immersed in oil deeper than the height of their teeth or threads. However, when the worm is mounted under the wheel the oil level should not rise above the centre of the lower roller or ball of the worm shaft bear-

ings in order to reduce losses in the bearings and simplify the design of sealing. If, nevertheless, the worm is not immersed in oil it should be provided with rings with blades (Fig. 185) which, as the worm rotates, throw the oil on to the wheel. This method of lubrication may prove unsatisfactory for gears which are frequently stopped since the amount of oil in the area of contact, when the gear is started or stopped, will not be sufficient.

When the velocity of worm is  $v_{wo} < 4$  m/sec the wheel should be mounted on top; at  $v_{wo} \geq 4$  m/sec the worm should be on top; at  $v_{wo} > 10$  m/sec the teeth should be lubricated through a nozzle from the side where the worm threads make contact with the wheel teeth.

Power losses increase the temperature of the gear, which should not be allowed to rise above the permitted value so as not to endanger the gear. To satisfy this condition the amount of heat given off in the reduction gear [equation (35)] should be less than the amount of heat dissipated from the body surface into the ambient air, i. e., the condition (36) should be satisfied.

If the condition (36) is not satisfied, an auxiliary cooling device may be required. This is usually achieved by ribbing the body and, in addition, by applying impellers fitted on to the worm which produce a continuous flow of air over the ribbed body of the gear (Fig. 188).

If the body is ribbed, then, in calculating the magnitude  $F_0$  in the formula (36), half of the ribbed surface should be taken into account. With a fan, the heat transfer factor is taken depending on the mean velocity of the air  $v$  m/sec according to the formula

$$k_0 = 12 \sqrt{v} \text{ Cal/hr} \times \text{m}^2 \times \text{degrees.} \quad (324)$$

The velocity of the air can be approximately found depending on the impeller speed from the empirical relation

$$v \approx \frac{n_{w_2}}{200} \text{ m/sec.} \quad (325)$$

Then the thermal condition will be

$$Q \leq (k_n F_n + k_0 F_0) (t_{bath} - t_{air}) \text{ Cal/hr} \quad (326)$$

where  $F_n$ ,  $F_0$  are noncooled and cooled surfaces of the gear housing in  $\text{m}^2$ , respectively;

$k_n$ ,  $k_0$ —respective heat-transfer factors in  $\text{Cal/hr} \times \text{m}^2 \times \text{degrees}$ .

*Example.* In calculating toothed and worm gears two main problems may arise:

1. On the basis of the given type of gear service we must choose its design, determine its dimensions and assign materials for the wheels.

2. With the known dimensions of the gear we must find the design stresses in the teeth or the load-carrying capacity of the gear.

The first problem — that of design calculations — is more complicated and is solved in three stages: a) preliminary determination of main dimensions; b) calculation of tooth geometry; c) revised calculation of the gear to finally assign the material and specify the method of heat-treatment.

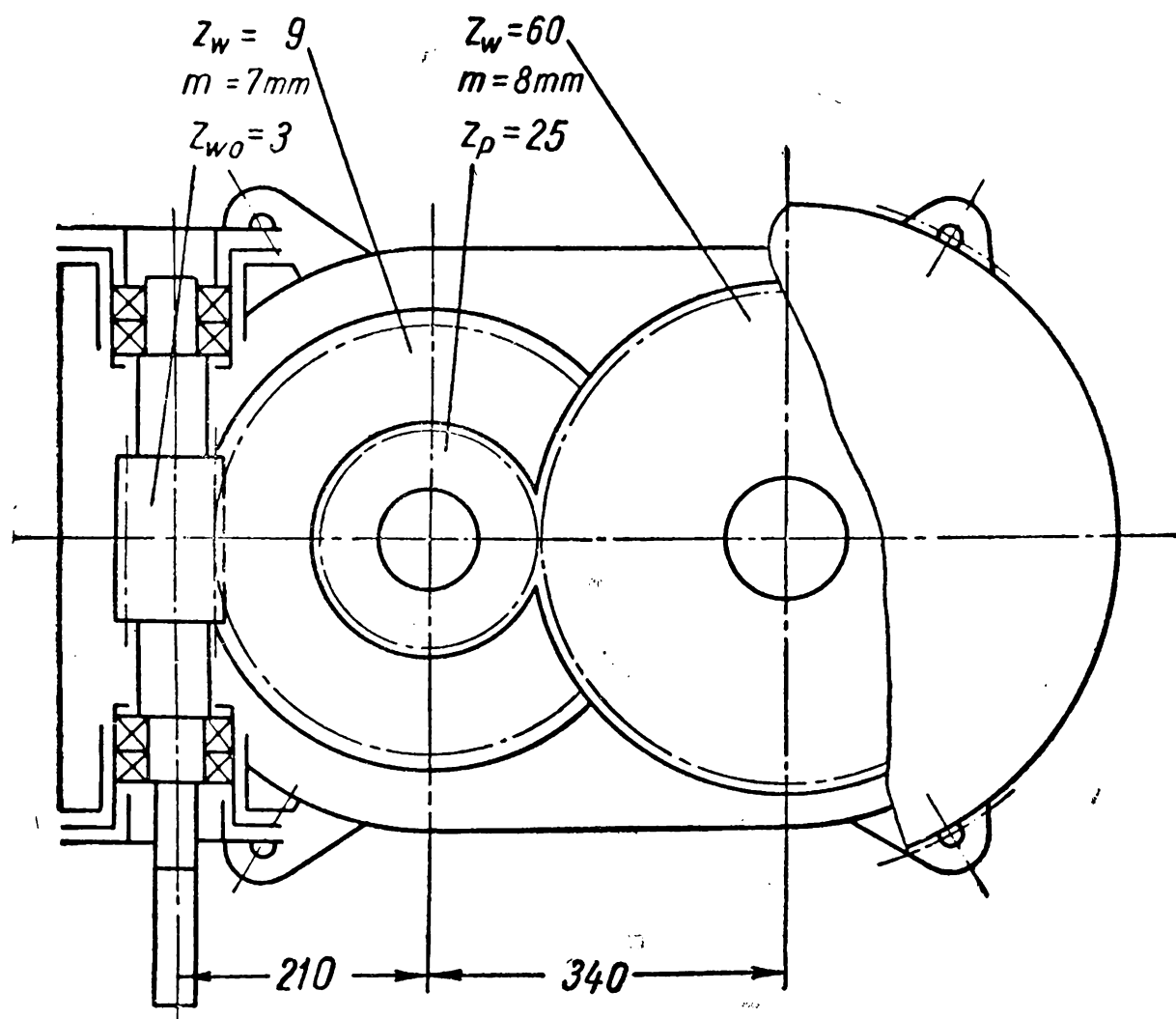


Fig. 190

For carrying out design calculations the following data should be available:

1. Purpose of the gear, transmitted load and the nature of its variations in time.
2. Velocity of the driving and driven shafts and the law of velocity variations in time.
3. The total continuity of the gear operation.

The sequence of calculation is illustrated by the following example.

Calculate a worm-spur reduction gear for a mixer drive (Fig. 190).

The power of the electric motor  $N=7$  kw, velocity  $n_{eq}=980$  rpm, number of revolutions of the driven shaft of the reduction gear  $n_w=25$  rpm, design service life  $T=20,000$  hours, load — steady and constant. The gear is nonreversible, degree of accuracy — 8th, lubrication — by immersion.

Torque on the worm

$$M_{t_{wo}} = 97,500 \frac{N_{wo}}{n_{wo}} = 97,500 \frac{7}{980} \approx 695 \text{ kg/cm.}$$

According to the conditions of the machine layout we choose a design with a worm fixed at the side and vertically mounted wheel shafts. To obtain minimum dimensions of the reduction gear and higher efficiency, its

total velocity ratio  $i = \frac{980}{25} = 39.2$  is divided as follows  $i = i_{wo} \times i_{tooth} = 16.3 \times 2.4$ .

A comparatively low velocity ratio of the worm gear allows the use of a multi-start worm. We take a worm with  $z_{w0}=3$ .

Then

$$z_w = z_{w0} \times i = 3 \times 16.3 \approx 49.$$

Assuming that the velocity of sliding will be above  $v_{sl}=3-4$  m/sec we shall use bronze of grade OHΦ for the rim of the worm wheel and steel of grade 45 for the worm.

The number of load cycles of the wheel teeth for the estimated service life is according to the formula (228)

$$N = 60 \times n_w \times T = 60 \times 980 \frac{3}{49} 20,000 = 7.2 \times 10^7.$$

When the surface hardness of the worm threads is  $H_B \leq 340$  the allowable surface compressive stress will be [Table 46 and formula (308)]

$$[\sigma]_{su_r} = 2,100 \sqrt[8]{\frac{10^7}{7.2 \times 10^7}} = 1,640 \text{ kg/cm}^2.$$

The number of modules in the pitch diameter of the worm is assumed to be  $q_{w0}=11$ ; then

$$\tan \lambda = \frac{z_{w0}}{q_{w0}} = \frac{3}{11} = \tan 15^\circ 15' 18''.$$

Taking from Table 48 the angle of friction  $\rho = 1^\circ 40'$  (at  $v_{sl}=4$  m/sec and with the worm finished on a lathe) the efficiency will approximately equal

$$\eta = \frac{\tan \lambda}{\tan (\lambda + \rho)} = \frac{\tan 15^\circ 15'}{\tan (15^\circ 15' + 1^\circ 40')} \approx 0.87.$$

The load concentration factor at constant operating conditions is

$$k_c = 1.$$

The dynamic load factor, assuming that  $v_w < 3$  m/sec, is

$$k_d = 1.1.$$

The torque on the wheel will be

$$M_t = M_{tw0} \times i \times \eta = 695 \frac{49}{3} \times 0.87 \approx 9,750 \text{ kg/cm}.$$

The centre distance from the formula (306) is

$$\begin{aligned} &= \left( \frac{z_w}{q_{w0}} + 1 \right) \sqrt[3]{\left( \frac{540}{\frac{z_w}{q_{w0}} [\sigma]_{su_r}} \right)^2 M_t \times k_c \times k_d} = \\ &= \left( \frac{49}{11} + 1 \right) \sqrt[3]{\left( \frac{540}{\frac{49}{11} \times 1,640} \right)^2 9,750 \times 1 \times 1.1} = 20.6 \text{ cm}. \end{aligned}$$

We select  $A' = 210$  mm,  $m = 7$  mm,  $z_{wo} = 3$ ,  $q_{wo} = 11$ ,  $z_w = 49$ ,  $\xi = 0$ ,  $\lambda = 15^\circ 15' 18''$ .

Since the centre distance is increased above the design value the actual surface stress will be

$$\sigma_{sur} = [\sigma]_{sur} \sqrt{\left(\frac{A}{A'}\right)^3} = 1,640 \sqrt{\left(\frac{206}{210}\right)^3} \approx 1,600 \text{ kg/cm}^2.$$

We check the peripheral velocity of the wheel:

$$v_w = \frac{\pi z_w m n_w}{60 \times 1,000} = \frac{\pi \times 49 \times 7 \times 60}{60 \times 1,000} = 1.08 \text{ m/sec}$$

and the worm velocity of sliding using the formula (313)

$$v_{sl} = \frac{m n_{wo}}{19,100} \sqrt{z_{wo}^2 + q_{wo}^2} = \frac{7 \times 980}{19,100} \sqrt{3^2 + 11^2} = 4.1 \text{ m/sec}$$

which is very close to the assumed value  $v_{sl}$ .

The wheel teeth are calculated for beam strength [according to the formula (310) replacing  $d_w = z_w m$ ;  $d_{wo} = q_{wo} m$

$$\sigma_b = \frac{1.9 M_t k_c k_d \cos \lambda}{m^3 q_{wo} z_w y}.$$

The tooth form factor from Fig. 160 at  $z_w = 49$  will be

$$y = 0.47,$$

hence

$$\sigma_b = \frac{1.9 \times 9,750 \times 1 \times 1.1 \times 0.965}{0.7^3 \times 11 \times 49 \times 0.47} \approx 230 \text{ kg/cm}^2.$$

The allowable bending stress in the tooth dangerous section (see Table 47) is

$$[\sigma]_0 = [\sigma]_b k_l = 650 \sqrt[9]{\frac{10^6}{72 \times 10^6}} \approx 400 \text{ kg/cm}^2,$$

$$\sigma_b = 230 \text{ kg/cm}^2 < [\sigma]_0 = 400 \text{ kg/cm}^2.$$

Let us now determine the main geometrical proportions of the gear (Tables 42, 43).

#### *Proportions of worm:*

Diameter of pitch cylinder

$$d_{dwo} = d_{wo} = q_{wo} m = 11 \times 7 = 77 \text{ mm.}$$

Diameter of addendum cylinder

$$D_{ewo} = d_{dwo} + 2f_o m = 77 + 2 \times 1 \times 7 = 91 \text{ mm.}$$

Diameter of dedendum cylinder

$$D_{iwo} = d_{dwo} - 2m(f_o + c_o) = 77 - 2 \times 7(1 + 0.2) = 60.2 \text{ mm.}$$

Length of threaded portion

$$L \geq (12.5 + 0.09 z_{wo}) m = (12.5 + 0.09 \times 49) \times 7 \approx 118 \text{ mm.}$$

To prevent dynamic unbalance of the worm the length  $L$  should accommodate an even number of pitches. Since

$$\frac{L}{\pi m} = \frac{118}{\pi \times 7} \approx 5.4 \text{ we assume finally } L = 6\pi m = 6 \times \pi \times 7 = 132 \text{ mm.}$$

The lead of thread

$$S = tz_{wo} = \pi m z_{wo} = \pi \times 7 \times 3 = 65.973 \text{ mm.}$$

*Proportions of worm wheel:*

Diameter of pitch circle

$$d_{\partial w} = d_w = m z_w = 7 \times 49 = 343 \text{ mm.}$$

Diameter of addendum circle

$$D_{ew} = d_{\partial w} + 2f_0 m = 343 + 2 \times 1 \times 7 = 357 \text{ mm.}$$

Diameter of dedendum circle

$$D_{iw} = d_{\partial w} - 2m(f_0 + c_0) = 343 - 2 \times 7(1 + 0.2) = 326.2 \text{ mm.}$$

Outside diameter of wheel

$$D_{out} = D_{ew} + 1.5m = 357 + 1.5 \times 7 = 367.5 \text{ mm.}$$

Width of wheel

$$B = 0.75 \times D_{ewo} = 0.75 \times 91 \approx 68 \text{ mm.}$$

The lubricant is selected from Table 49; at  $v_{sl} < 5$  m/sec, under average operating conditions and for immersion lubrication the required arbitrary oil viscosity is  $E_{50}^\circ = 24$ .

We select the grade of oil—oil tar.

Let us now specify the efficiency of the gear with greater precision.

The velocity of the worm is

$$v_{wo} = \frac{\pi d_{\partial wo} n_{wo}}{60 \times 100} = \frac{\pi \times 7.7 \times 980}{60 \times 100} = 3.95 \text{ m/sec.}$$

Horse power on the wheel

$$N_w = N_{wo} \eta = 7 \times 1.36 \times 0.87 \approx 8.3 \text{ h. p.}$$

Losses for oil churning amount to

$$L_{ch} = 0.001 \times v_{wo} \times L_{wo} \times \sqrt{E_t^\circ} = 0.01 \times 3.95 \times 13.2 \times \sqrt{10} = 0.17 \text{ h. p.}$$

(at the working temperature  $t_{bath} = 70^\circ$  the viscosity of oil tar amounts to  $E_{70}^\circ = 10$ ).

Final efficiency from the formula (315) will be

$$\eta = 0.87 \left( 1 - \frac{0.17}{8.3} \right) = 0.85.$$

The amount of heat given off by the reduction gear, from the formula (35):

$$Q = 632 N_{wo} (1 - \eta) = 632 \times 7 \times 1.36 (1 - 0.85) = 900 \text{ Cal/hr.}$$

The required cooled surface is found from the formula (36) at  $k = 14$  Cal/m<sup>2</sup> × hr × degrees and  $t_{air} = 20^\circ$ :

$$F_m = \frac{Q}{k(t_{bath} - t_{air})} = \frac{900}{14(70 - 20)} \approx 1.3 \text{ m}^2.$$

We now determine the forces in engagement.

The peripheral force acting upon the wheel (294) is

$$P_w = P_{awo} = \frac{2M_t}{d_w} = \frac{2 \times 9,750}{34.3} = 570 \text{ kg.}$$

The peripheral force acting upon the worm, from the formula (296), is

$$P_{wo} = P_{aw} = P_w \tan(\lambda + \rho) \approx 570 \times \tan 16^\circ 55' \approx 175 \text{ kg.}$$

The radial force, from the formula (295), is

$$P_r = P_w \tan \alpha = 570 \times \tan 20^\circ \approx 208 \text{ kg.}$$

These forces are used to calculate the worm and the wheel shaft for strength and also to select the bearings.

Let us now calculate the second stage of the reduction gear—the toothed gear.

The torque on the pinion (equal to the torque on the worm wheel) will be

$$M_{tp} = M_{t wo} i_{wo} \eta_{wo} = 695 \times \frac{49}{3} \times 0.85 \approx 9,650 \text{ kg/cm.}$$

As material for the wheels we select cast iron of grade CЧ 32-56; the teeth are cut on a gear-milling machine.

The surface endurance limit of the wheel material (Table 33) with the surface hardness of teeth  $H_B = 250$  is

$$\sigma_{sur} = C_B \times H_B = 15 \times 250 = 3,750 \text{ kg/cm}^2.$$

The working number of stress cycles for the pinion is

$$N_p = 60 \times n_p \times T = 60 \times 25 \times 2.4 \times 20,000 = 7.2 \times 10^7$$

and for the wheel

$$N_w = 60 \times n_w \times T = 60 \times 25 \times 20,000 = 3 \times 10^7.$$

The load factor, from the equation (226), will be:  
for the pinion

$$k_{lp} = \sqrt[6]{\frac{10^7}{N_p}} = \sqrt[6]{\frac{10^7}{7.2 \times 10^7}} \approx 0.72;$$

for the wheel

$$k_{lw} = \sqrt[6]{\frac{10^7}{3 \times 10^7}} \approx 0.83.$$

The allowable surface compressive stress, from the formula (225):  
for the pinion

$$[\sigma]_{sur} = \sigma_{sur} k_{lp} = 3,750 \times 0.72 = 2,700 \text{ kg/cm}^2;$$

for the wheel

$$[\sigma]_{sur} = \sigma_{sur} k_{lw} = 3,750 \times 0.83 = 3,100 \text{ kg/cm}^2.$$

To increase the surface strength of the pinion teeth and thereby reduce the proportions of the gear the surface hardness of the pinion teeth should be increased to  $H_B = 270$ .

Then

$$[\sigma]_{sur} = C_B H_B k_{lp} = 15 \times 270 \times 0.72 \approx 2,920 \text{ kg/cm}^2.$$

Under constant load  $k_c = 1$ .

Assuming that the peripheral velocity of the wheels will be below  $v = 1$  m/sec we find for straight-sided teeth from Table 32 that  $k_d = 1$ .

The torque on the wheel is

$$M_t = M_{tp} \times i = 9,650 \times 2.4 = 23,200 \text{ kg/cm.}$$

For the width factor we take

$$\psi = \frac{B}{A} = 0.3.$$

The reduced modulus of elasticity is

$$E = 1.25 \times 10^6 \text{ kg/cm}^2.$$

The centre distance, from the formula (222), is

$$\begin{aligned} A &= (i+1) \sqrt[3]{\left(\frac{0.59}{i[\sigma]_{sur}}\right)^2 \frac{E}{\sin 2\alpha} \frac{M_t k_c k_d}{\psi}} = \\ &= (2.4+1) \sqrt[3]{\left(\frac{0.59}{2.4 \times 2,920}\right)^2 \frac{1.25 \times 10^6 \times 23,200 \times 1 \times 1}{0.643 \times 0.3}} = 34.6 \text{ cm.} \end{aligned}$$

The wheel diameter will equal

$$d_w = \frac{2Ai}{i+1} = \frac{2 \times 346 \times 2.4}{2.4+1} \approx 490 \text{ mm.}$$

The wheel peripheral velocity is

$$v_w = \frac{\pi d_w n_w}{60 \times 1,000} = \frac{\pi \times 490 \times 2.4}{60 \times 1,000} \approx 0.62 \text{ m/sec.}$$

consequently, the assumed value  $k_d=1$  is correct.

The number of the pinion teeth is assumed at  $z_p=25$ ; then

$$z_w = z_p \times i = 25 \times 2.4 = 60.$$

The module of the gear

$$m = \frac{2A}{z_w + z_p} = \frac{2 \times 346}{25 + 60} = 8.15 \text{ mm.}$$

We approximate this magnitude to the nearest standard value:  $m=8$  mm; then the centre distance will be

$$A = \frac{m}{2} (z_p + z_w) = \frac{8}{2} (25 + 60) = 340 \text{ mm.}$$

The increase in the stress due to surface compression is

$$\left( \sqrt{\frac{346^3}{340^3}} - 1 \right) 100\% < 3\%.$$

The width of wheels  $B = \psi A = 0.3 \times 340 \approx 100$  mm.

The bending stress in the tooth dangerous section is found from the formula (235)

$$\sigma_\sigma = \frac{M_t k_c k_d (i+1)}{AB i m y \cos \alpha} \leq [\sigma]_\sigma.$$

The tooth form factor for the pinion (Fig. 159) is

$$y_p = 0.365$$

and for the wheel (Fig. 160)

$$y_w = 0.485$$



Then

$$\sigma_{bp} = \frac{23,200 \times 1 \times 1 \times (2.4 + 1)}{34.0 \times 2.4 \times 10 \times 0.8 \times 0.366 \times 0.94} \approx 360 \text{ kg/cm}^2$$

and

$$\sigma_{bw} = \sigma_{bp} \frac{y_p}{y_w} = 360 \frac{0.365}{0.485} \approx 275 \text{ kg/cm}^2.$$

The allowable stress due to bending, from the equation (239), is

$$[\sigma]_s = \frac{1.4\sigma_{-1}}{n'k_\sigma} k_l.$$

The limit of endurance for cast iron

$$\sigma_{-1} = 0.45\sigma_{ul} = 0.45 \times 3,200 = 1,440 \text{ kg/cm}^2.$$

The safety factor (Table 36):

$$n' = 2.$$

The stress concentration factor (Table 35):

$$k_\sigma = 1.2.$$

The load factor in calculation of bending

$$k_l = \sqrt[9]{\frac{10^7}{7.2 \times 10^7}} = 0.805.$$

After substituting in the equation (239) we obtain

$$[\sigma]_s = \frac{1.4 \times 1,440}{2 \times 1.2} \times 0.805 = 675 \text{ kg/cm}^2.$$

Hence,

$$\sigma_{bp} = 360 \text{ kg/cm}^2 < [\sigma]_s = 675 \text{ kg/cm}^2.$$

Let us now find the main geometrical proportions of the gear.

The basic rack of toothed wheels is selected according to standards.

The pitch diameter, from the relation (204), is:

for the pinion

$$d_{dp} = z_p m = 25 \times 8 = 200 \text{ mm};$$

for the wheel

$$d_{dw} = z_w m = 60 \times 8 = 480 \text{ mm}.$$

The diameter of addendum circle:  
of the pinion

$$D_{ep} = d_{dp} + 2mf_0 = 200 + 2 \times 8 \times 1 = 216 \text{ mm};$$

of the wheel

$$D_{ew} = d_{dw} + 2mf_0 = 480 + 2 \times 8 \times 1 = 496 \text{ mm}.$$

The diameter of dedendum circle, from the formula (206), is:  
of the pinion

$$D_{ip} = d_{dp} - 2m(f_0 + c_0) = 200 - 2 \times 8(1 + 0.25) = 180 \text{ mm};$$

of the wheel

$$D_{iw} = d_{dw} - 2m(f_0 + c_0) = 480 - 2 \times 8(1 + 0.25) = 460 \text{ mm}.$$

## CHAPTER XVIII

## CHAIN DRIVES

In its most simple form a chain drive consists of a chain and two sprockets — driver and driven. Drives operating under severe load and at high velocity are encased in a housing and provided with a lubrication system (Fig. 191).

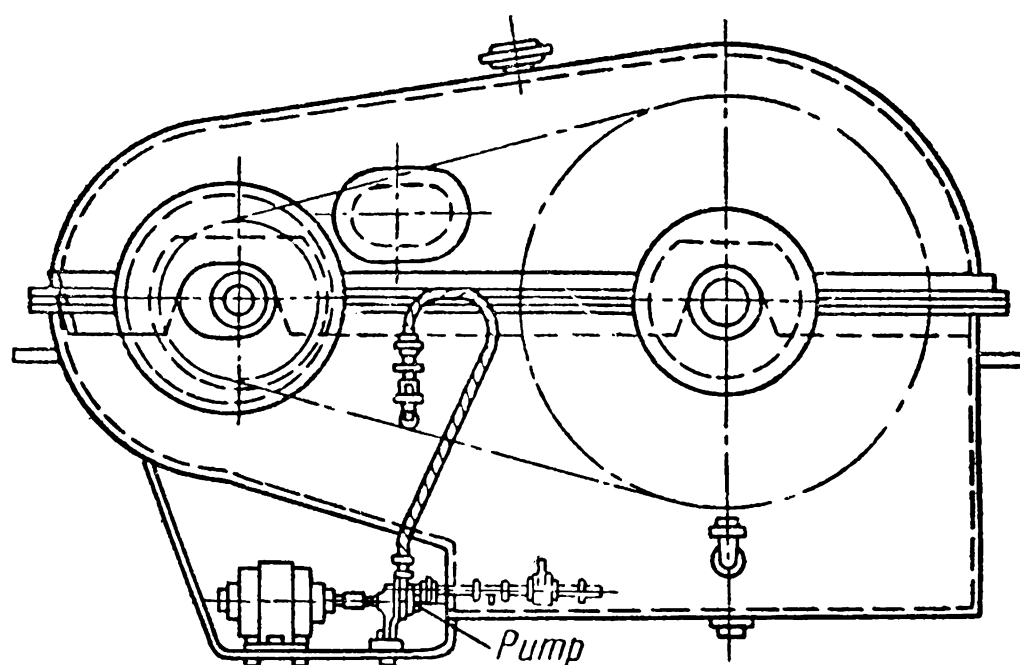


Fig. 191

The principal advantages of chain drives are as follows:

- a) the effective transmission of power when the distance between the shaft centres is large ( $A_{\max}=8$  m);
- b) high efficiency reaching  $\eta=0.98$ ;
- c) less load on the shafts compared to a belt drive;
- d) the ability of one chain to transmit motion to several shafts.

Chain drives are predominantly employed to handle up to 150 h. p. at peripheral velocities up to  $v=15$  m/sec and velocity ratios  $i \leq 8$ .

Chain drives are used in agricultural machinery, bicycles, motorcycles, the transmissions of auxiliary mechanisms in rolling mills, lathes, conveyors, coal-cutters, etc.

Among the disadvantages of chain drives are: relatively high production costs, velocity fluctuations, especially when the chain is unduly stretched, the need for accurate mounting and careful maintenance and the impossibility of using them for periodic reversals without intervals.

The chain consisting of hinge-jointed links is the main element of the drive, which determines its reliability and service life. Of the three groups of chains used in mechanical engineering—driving, crane and tractive—chain drives employ only the more accurate and carefully machined driving chains.

Crane chains serve for suspending and lifting loads and operate at a maximum of 0.25 m/sec, while tractive chains are used for moving loads in elevators, conveyors, etc., at speeds up to 2 m/sec.

Driving chains are subdivided into the following main types: bush, bush-roller, silent and link-belt. The last type is employed to handle small horse powers at maximum peripheral velocities of 3-4 m/sec.

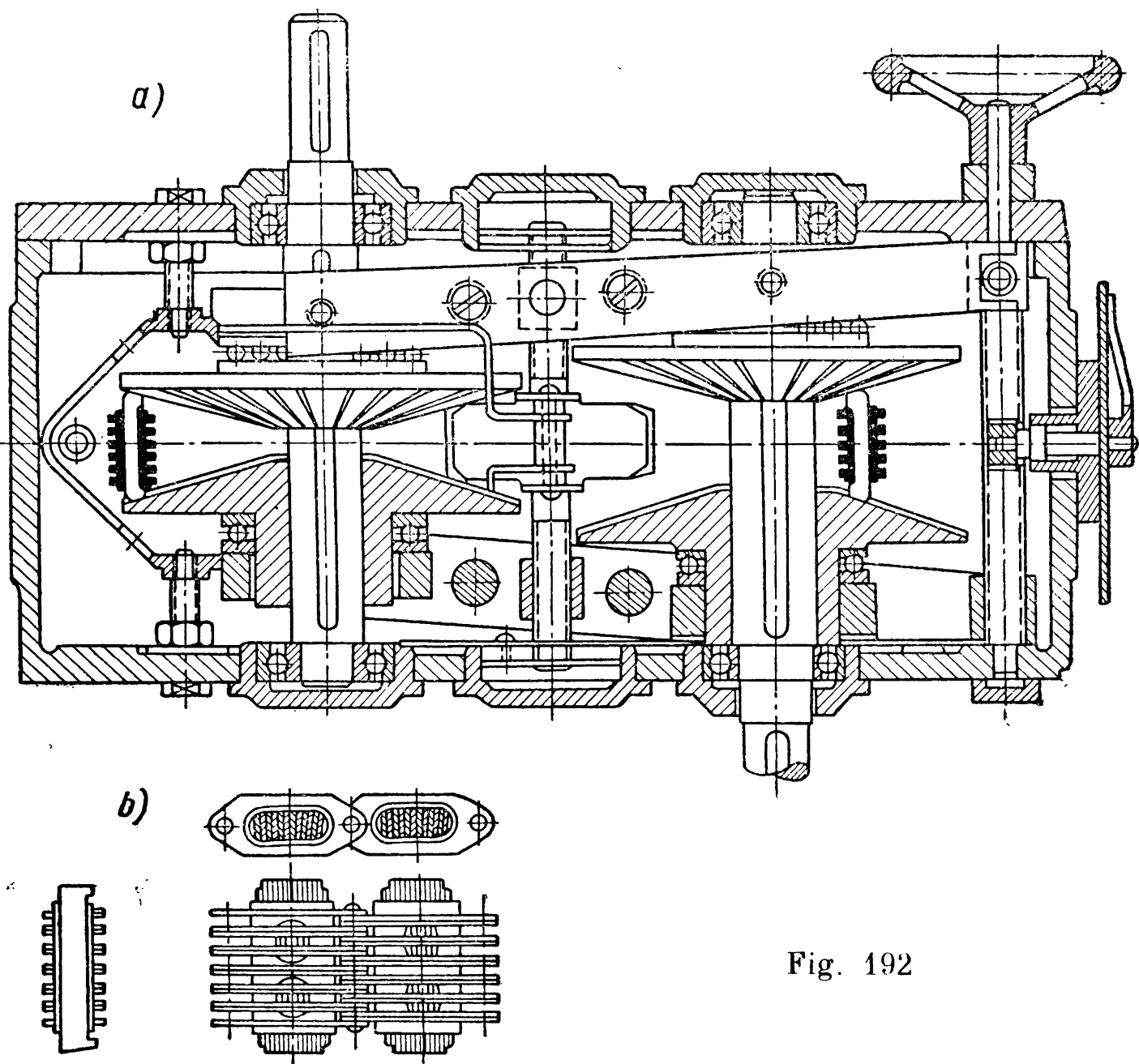


Fig. 192

The strength of a chain is determined by its ultimate strength  $Q$ . Its value is found experimentally and given by the manufacturer.

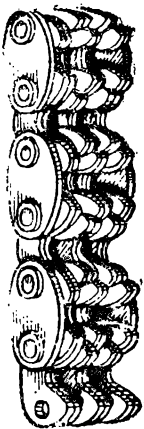
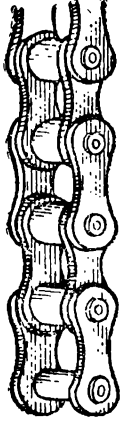
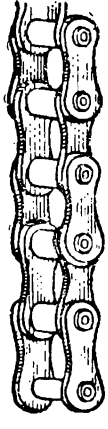
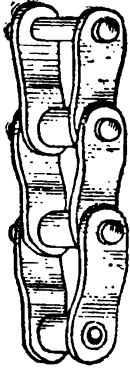
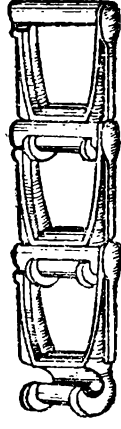
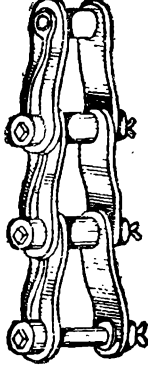
The pitch  $t$  and width  $b$  are the main geometrical characteristics of chains. They are used to select the proper type of chain.

Table 55 gives some data on the main types of driving chains.

Chain drives are usually employed at a constant velocity ratio. However, in special chains with movable plates the stepless change of velocity ratio is possible. This may be illustrated by a chain variable-speed drive with toothed bevels (Fig. 192, transmission *PIV*). The chain plates (Fig. 192, *b*) mesh with the teeth on the bevel surfaces with the chain in different positions relative to the cone shaft due

Table 55

Driving Chains

Item No.	Type of chain	Pitch <i>t</i>	Ultimate strength <i>Q</i> kg	Application	Sketches
1	Silent chain	1/2-1 1/4 in. 12.7-31.75 mm	1,900-69,500	Main drives in various machines	
2	Bush-roller chain	12.7-15.875 mm 15.87-41.3 mm 8-50 mm	750-2,000 1,750-5,000 200-16,000	Drives in motor-cycles and bicycles Agricultural machinery General mechanical engineering Oil-field machinery	
3	Bush chain	20-65 mm 15-100 mm 8-9.525 mm	3,800-43,000 1,250-50,000 500-1,200	General mechanical engineering Drives in motor-cycles	
4	Bush-roller chain with bent plates	40-100 mm	8,000-50,000	Drives operating at heavy duty	
5	Hooked link-belt chain	30-38 mm	600-900	Agricultural machinery	
6	Stud link-belt chain	42 mm	2,500	Drives operating under impact load	

to the displacement of the teeth by half a pitch and gashes on two bevels of one shaft (Fig. 192, *a*). The maximum velocity control range is 7, transmitted horse power—up to 3 kw, chain velocity—5-9 m/sec; under full load the efficiency depends on the velocity ratio and amounts to  $\eta=0.85-0.95$ .

**Velocity Ratio.** Since the chain links are located round the sprocket on the sides of a polygon the actual velocity of the chain is not constant and varies as links enter contact. As the sprocket rotating uniformly with an angular velocity  $\omega_1$  turns through the angle

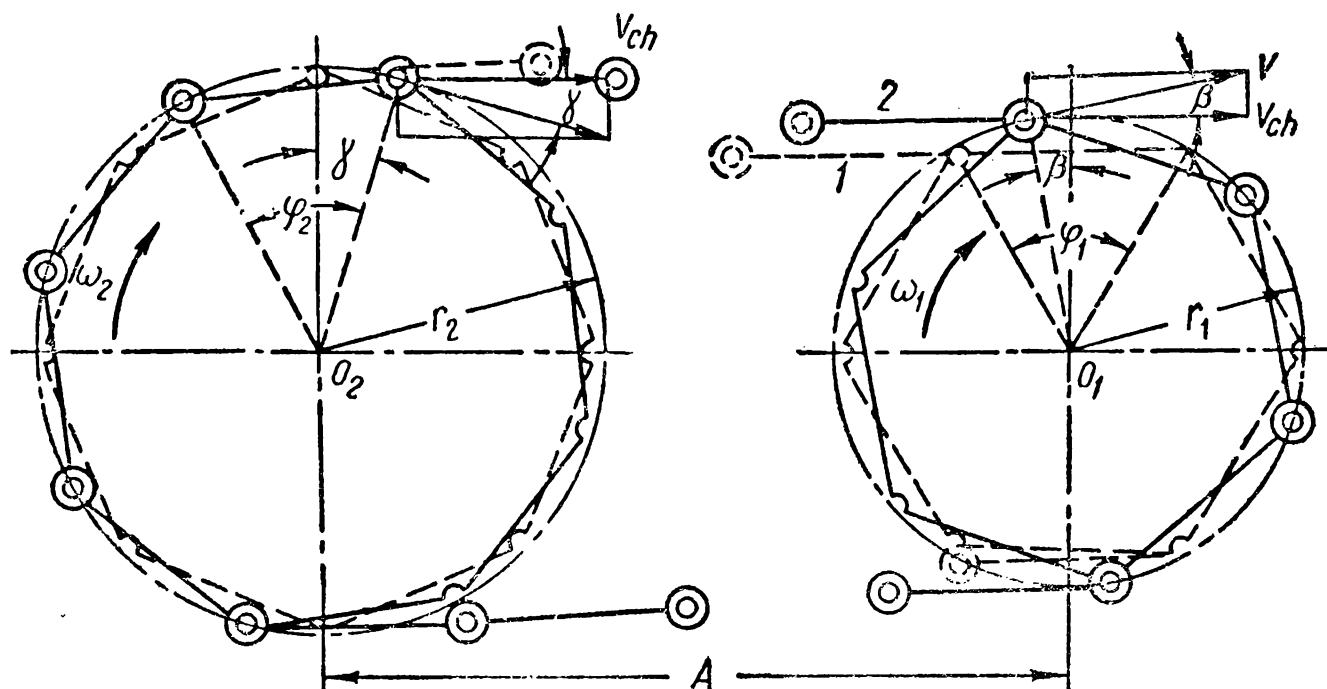


Fig. 193

$\frac{\varphi_1}{2} - \beta$  (Fig. 193), the link, which in the initial moment of meshing occupied position 1, will assume position 2. We can say therefore that in practice the link moves progressively with a velocity equal to the peripheral velocity  $v$  of the sprocket. Resolving the velocity  $v$  in two mutually perpendicular directions we can find the velocity with which the chain climbs onto the sprocket:

$$v_{ch} = v \cos \beta = \omega_1 r_1 \cos \beta.$$

The maximum value of the chain climbing velocity corresponding to  $\beta=0$  is  $v_{ch \max} = \omega_1 r_1$ .

As the sprocket continues to rotate the chain velocity will drop, reaching its minimum at  $\beta = \beta_{\max} = \frac{\varphi_1}{2}$ .

During the sprocket's turn through the angle  $\varphi_1$  the link will be shifted radially with a varying velocity, decelerating at the angle  $-\frac{\varphi_1}{2}$  and accelerating at the angle  $+\frac{\varphi_1}{2}$ . This periodic shift of the links causes regular oscillations of the chain.

The angular velocity of the driven sprocket is

$$\omega_2 = \frac{v_{ch}}{r_2 \cos \gamma} = \frac{\omega_1 r_1 \cos \beta}{r_2 \cos \gamma}.$$

Hence, the instantaneous velocity ratio

$$i = \frac{\omega_1}{\omega_2} = \frac{r_2 \cos \gamma}{r_1 \cos \beta}. \quad (327)$$

The angle  $\beta$  changes from  $\frac{\varphi_1}{2} = \frac{180^\circ}{z_1}$  to zero, the angle  $\gamma$  from  $\frac{180^\circ}{z_2}$  to zero where  $z_1$  and  $z_2$  are the numbers of teeth on the sprocket.

In this case the relationship between the angles  $\beta$  and  $\gamma$  depends in turn on the distance between the sprocket shafts and the number of teeth in the sprockets. Consequently, at  $\omega_1 = \text{const}$   $\omega_2 \neq \text{const}$ .

The more teeth there are on the smaller sprocket the less the velocity of the driven sprocket will vary. Complete uniformity is attainable, as can be seen from the formula (327), only when the length of the driving side is a multiple of the chain pitch at  $i=1$ .

The uneven rotation of the driven sprocket lessens the operating capacity of the drive, for the load arising in the chain due to accelerations causes additional stresses in the chain elements.

As a chain joint enters the gash between the sprocket teeth there occurs a shock whose force depends on its speed.

In bush-roller chains the speed of shock will be the less, the smaller the chain pitch  $t$  and the more teeth  $z$  there are on the sprocket. The speed with which a silent chain strikes the sprocket teeth does not depend on the number of teeth and is nearly half that of roller chains. This largely accounts for the smaller noise produced by silent chains compared to bush-roller chains.

**Chain Tension.** As distinct from a belt drive, the tension in the sides of a chain drive at standstill is entirely due to its sag against its own weight (Fig. 194).

The magnitude of this tension  $S_2$  with the unit weight  $q$  per metre of chain and chain sag  $f$  can be approximately found from the chain equilibrium condition from the formula

$$S_2 f = q \frac{A}{2} \times \frac{A}{4}$$

whence

$$S_2 = \frac{q A^2}{8f}. \quad (328)$$

In transmitting useful load the tension of the driving side increases by the amount of peripheral effort  $P$  on the sprocket. Hence

$$S_1 = S_2 + P. \quad (329)$$

As a rule, the tension of the driven side, equal to the tension due to sag  $S_2$ , amounts to less than 10% of the peripheral effort  $P$  and can be neglected in calculations.

As the chain links move together with the sprocket they undergo the action of centrifugal forces causing additional tensions  $S_v$  in the chain sides.

The chain tension due to the action of centrifugal forces can be found from the formula (174) employed for belt drives because, since the pitch  $t$  is small as compared to the sprocket diameter, the chain can be regarded as a flexible band. Errors in such calculations very insignificantly increase the tension force  $S_v$  as compared to the actual value: at  $z \geq 15$  it is less than 3%.

The action of these forces causes stresses due to tension to arise in the chain plates and compressive stresses on the surfaces of the joint parts.

The magnitude of unit pressure  $p$  in the joint depends on the area of contact  $F$  of the joint parts.

The maximum allowable unit pressure is determined by the quality of the chain joints and is constant for a given chain. As the drive operates the total pressures in the joint due to the force  $P$  and the force  $S_v$  should never exceed the maximum pressure allowed for a given chain. A larger chain velocity increases the unit pressure in the joint caused by the force  $S_v$ . The magnitude of design allowable unit pressure found from the formula  $p = \frac{P}{F}$ , which takes into account only the peripheral effort, diminishes as chain pitch and velocity increase.

The allowable magnitudes of unit pressures  $[p]$  kg/mm<sup>2</sup>—depending on the chain pitch and the velocity of the smaller sprocket—are from  $[p]=3.5$  kg/mm<sup>2</sup> at  $n \leq 50$  rpm to  $[p]=1.37$  kg/mm<sup>2</sup> at  $n=2,800$  rpm for bush-roller chains and, respectively, from 2 to 0.78 kg/mm<sup>2</sup> for silent chains.

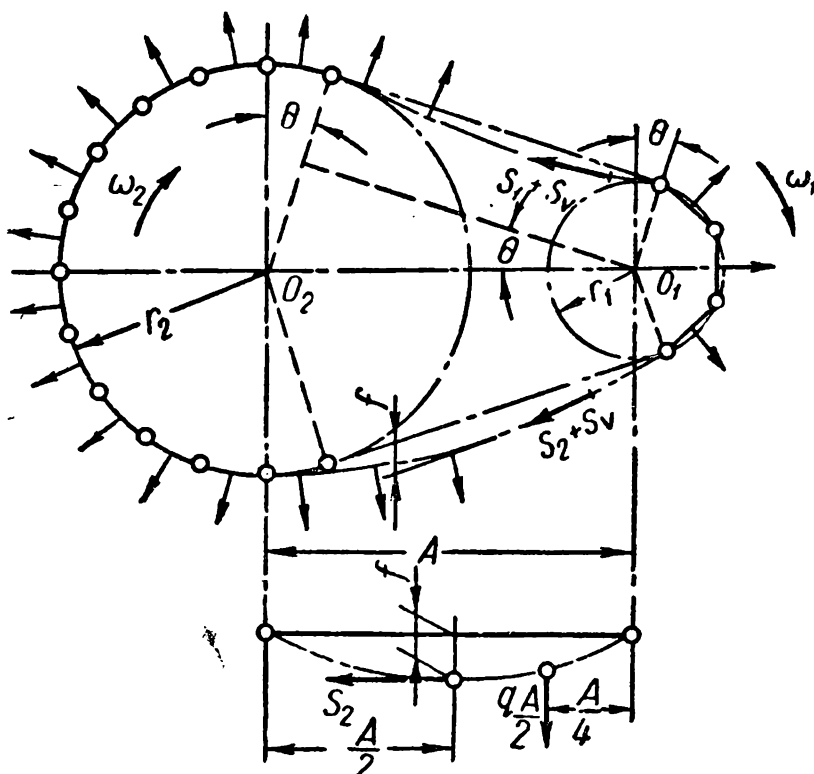


Fig. 194

## COMPONENTS OF CHAIN DRIVES

**Chains.** A bush-roller chain (Fig. 195, *a*) consists of alternating inner 1 and outer 2 links hinge-jointed together. Each joint consists of pin 3 pressed into the outer plates and bush 4 secured in the

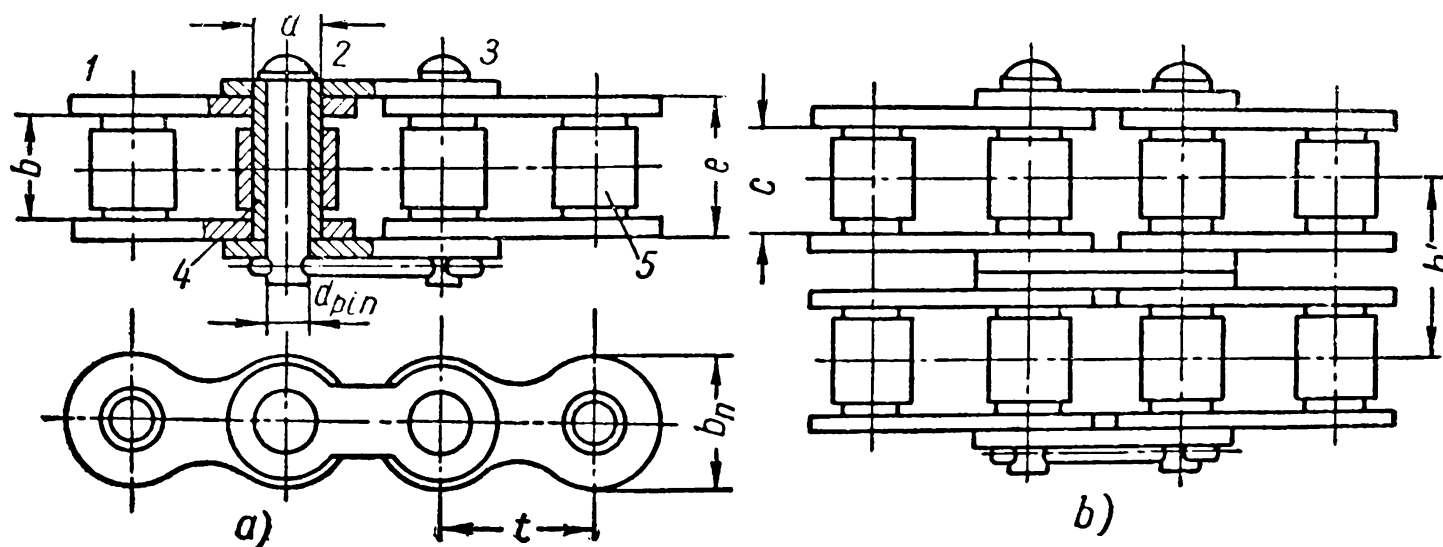


Fig. 195

holes of the inner plates. Roller 5 fitted onto bush 4 serves to safeguard the sprocket teeth against wear. The diametral area of the contact surface for such a joint is  $F=ab$ .

The chain ends are jointed together by means of detachable connecting links—with an even number of links as in Fig. 196, *a* and with an odd number as in Fig. 196, *b*. Since connecting links of the latter type are weaker than the normal ones chains with an even number of links are preferable.

Bush chains differ from bush-roller chains in that they have no rollers. Such chains are lighter and, in this respect, superior to bush-roller chains. However, the absence of rollers intensifies wear of the sprocket teeth due to sliding friction between the teeth and bushes instead of rolling friction.

When large loads are to be transmitted chains should have a long pitch; then the sprockets are likewise increased in diameter. In order to diminish the sprocket diameters and employ chains with a short pitch use is made of multi-row bush-roller chains (Fig. 195, *b*) which consist of components of ordinary single chains except for the pins whose length equals the total width of the chain.

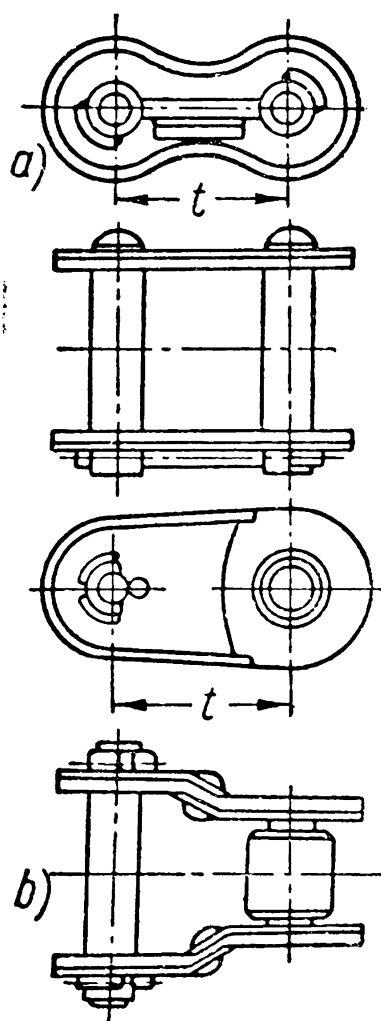


Fig. 196



The ultimate strength of multi-row chains  $Q_m$  is proportional to the number of rows in the chain  $c$ :

$$Q_m = cQ. \quad (330)$$

Duplex and triplex chains are in most frequent use.

When the drive operates under impact load (reversals, overloads, shocks) preference should be given to bush-roller chains with bent plates comprising links similar to the connecting link in Fig. 196, *b*. The flexure in the plates imparts a higher elasticity to the chain.

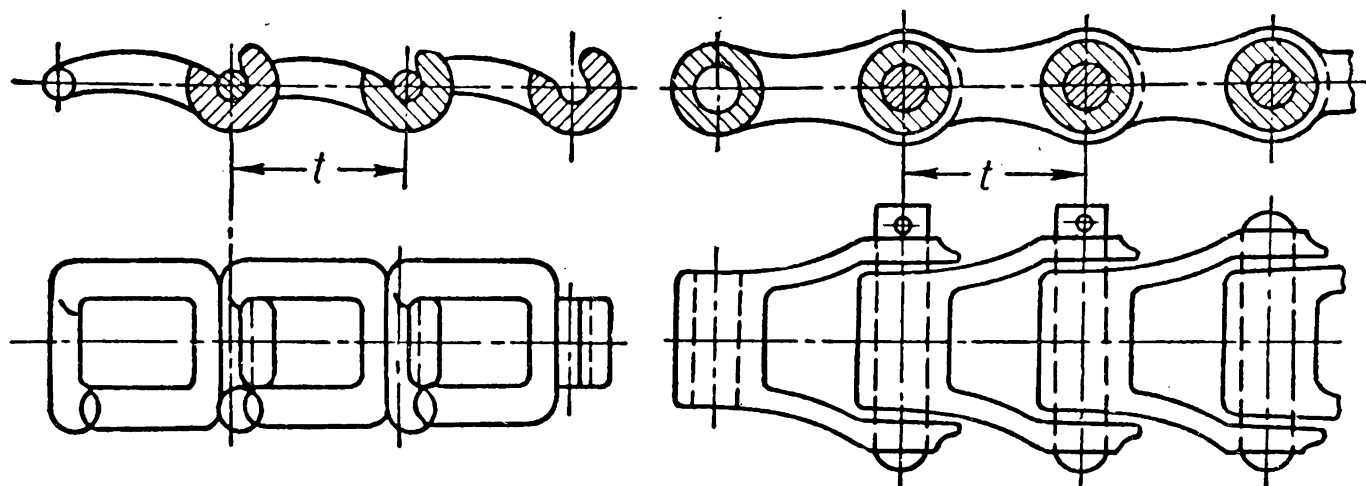


Fig. 197

The deformation of the plates helps to damp shocks on one of the shafts and thereby protect the second shaft of the drive from them. To ensure adequate operating ability of the drive the material of its elements should possess high wear resistance and strength. This is achieved by using carbon or alloy steel heat-treated to obtain hardness within  $R_C=35-60$ .

At low horse powers and velocities ( $v < 3-4$  m/sec) hooked or stud link-belt chains composed of cast unmachined links are used. In the Soviet Union such chains are produced in two versions: hook-link and bush-stud chains (Fig. 197). The shape of the links in hooked chains makes it possible to dispense with auxiliary fastening parts. The links are assembled by sliding them sideways together, with one at an angle of  $60^\circ$  to the other.

Bush-stud chains are built up of links with the help of steel studs secured by cotter pins. The links of these chains are made from malleable iron and the studs from steel 3. These chains are widely employed in agricultural machinery.

Silent chains (Fig. 198) consist of a series of toothed steel plates pinned together in rows across the width of the chain. The advantage of silent chains is their smooth and noiseless operation at high velocities. In design silent chains are more complex than bush-roller types, more expensive and require more careful maintenance. The active faces of the toothed links resisting pressure from the sprocket

teeth are the side outer surfaces of the tooth-shaped projections in the plates; therefore, to ensure adequate wear resistance of the active faces they are hardened to  $R_C=40-50$ .

To keep the chain from running off the sprocket wheel in motion it is provided with plate retainers. At low velocities it is recommended

to use chains with two side retainers and at higher velocities chains with middle plate retainers.

In these cases grooves should be cut in the sprocket teeth for the plate retainers (see Fig. 199, e).

The operating efficiency of the chain depends essentially on the joint design. Ordinary and bush joints are in common use. The first type is formed by a pin passing through the round holes in the connected plates. The disadvantage of such a joint is the small area of the bearing surface  $F=0.5db$ . Chains with ordinary joints fail to handle high loads since they are subject to rapid wear.

Large horse powers are transmitted by chains with bush joints composed of two segment bushes 1

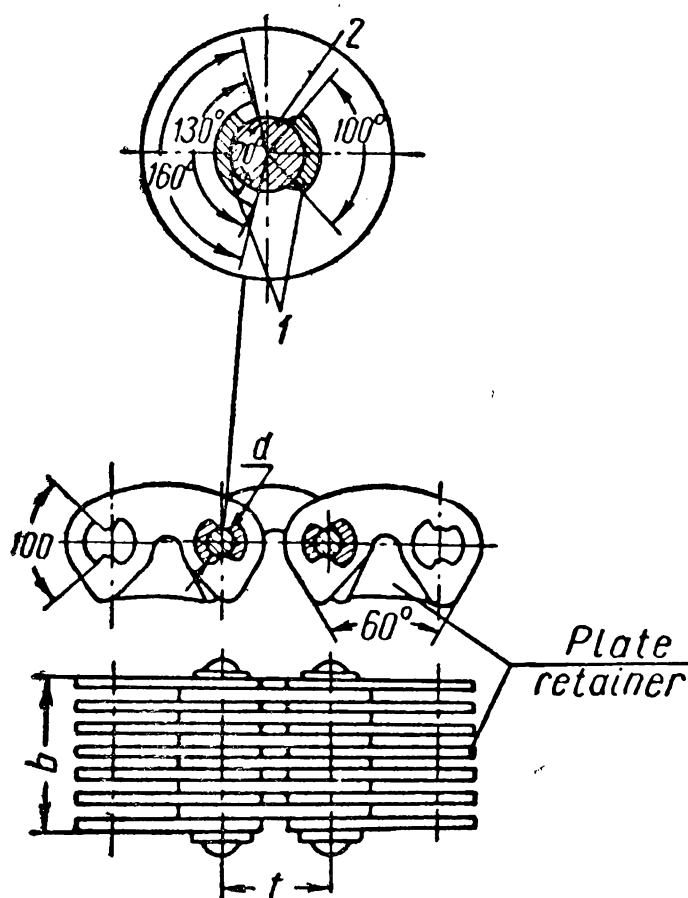


Fig. 198

bush with length equal to the chain width is fixed only to one half of the links. The other half of the links can freely turn within a certain angle (about  $25^\circ$ ) due to a greater hole relative to the given bush. By means of such bushes the pressure from one section of the links to another is transmitted over the entire length of the pin. The diametral area of the bush (see Fig. 198) is:

$$F = 2 \frac{d}{2} \sin \frac{100^\circ}{2} b = 0.76db.$$

This allows a chain with bush joints to carry greater load compared to chains with ordinary joints.

**Sprockets.** The operating ability of a chain drive depends in large measure on the quality of the sprockets. Precision in the manufacture of the sprocket elements, surface finish of the teeth, material and heat treatment are of special importance.

The sprockets (Fig. 199, a) are made from cast iron of a grade not below CЧ 15-32 and carburised (15, 15X) or hardened (40, 40X, etc.) steel.

The sprocket teeth are shaped depending on the type of chain so that during the operation of the drive they may easily disengage from the chain links.

For silent chains the tooth profile is limited to straight lines (Fig. 199, *b*) with a constant link face angle  $\alpha=60^\circ$  (on the chain).

Bush-roller chains employ sprockets with convex, concave, rectilinear and combined (rectilinear-convex) profile of teeth (Fig. 199, *c*).

Experiments have shown that concave profiles have greater wear resistance due to the increased length of the working section of the tooth profile. For high peripheral velocities such sprockets are therefore strongly recommended.

For link-belt and bush chains sprockets with cast unmachined teeth (Fig. 199, *d*) from gray cast iron hardened to  $H_B=280-420$  are used.

**Chain Housings and Slack Adjusters.** The housing protects the drive from dust, preserves grease and damps the noise of the drive. The housing should be as small as possible but should nevertheless provide for a minimum clearance of  $t+30$  mm between the inner walls of the housing and the chain in the sprocket plane and of 30 mm along the shaft axes.

The housing has a bottom and a cover cast or welded from sheet steel. Provision should also be made for lidded inspection eyelets. The housing should not interfere with the adjustment of the distance between shafts when the chain becomes stretched.

Chain sag is regulated and the required tension ensured by means of movable bearings or slack adjusters. Usually slack adjusters are used to compensate for the elongation of the chain by the length

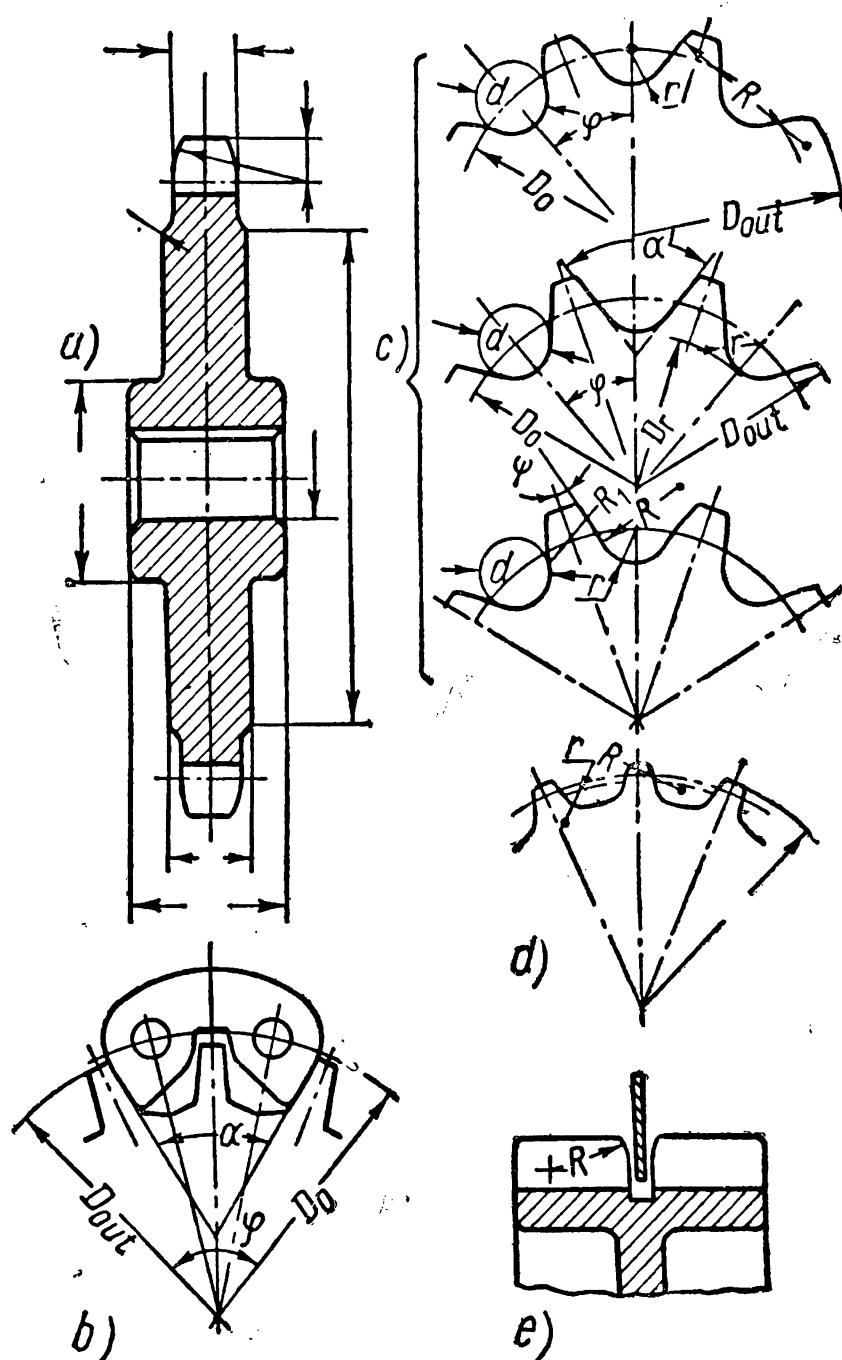


Fig. 199

of two links after which two links are removed from the chain and the slack adjuster fixed in the initial position.

The moving bearings are in the form of slides in which the sprocket shaft is installed. If the drive is actuated by an electric motor the

latter is mounted on a tilting plate or on slides.

When the centre distance is constant slack adjusters must be used (Fig. 200).

According to the way in which they act on the chain, slack adjusters can be automatic (the jockey wheel is pressed against the chain by the elastic pressure of a spring or counterweight) or periodically regulated (when the position of the jockey wheel is changed when necessary by shifting its shaft). Jockey wheels engage with the slack side of the chain where its sag is greatest. Their diameter

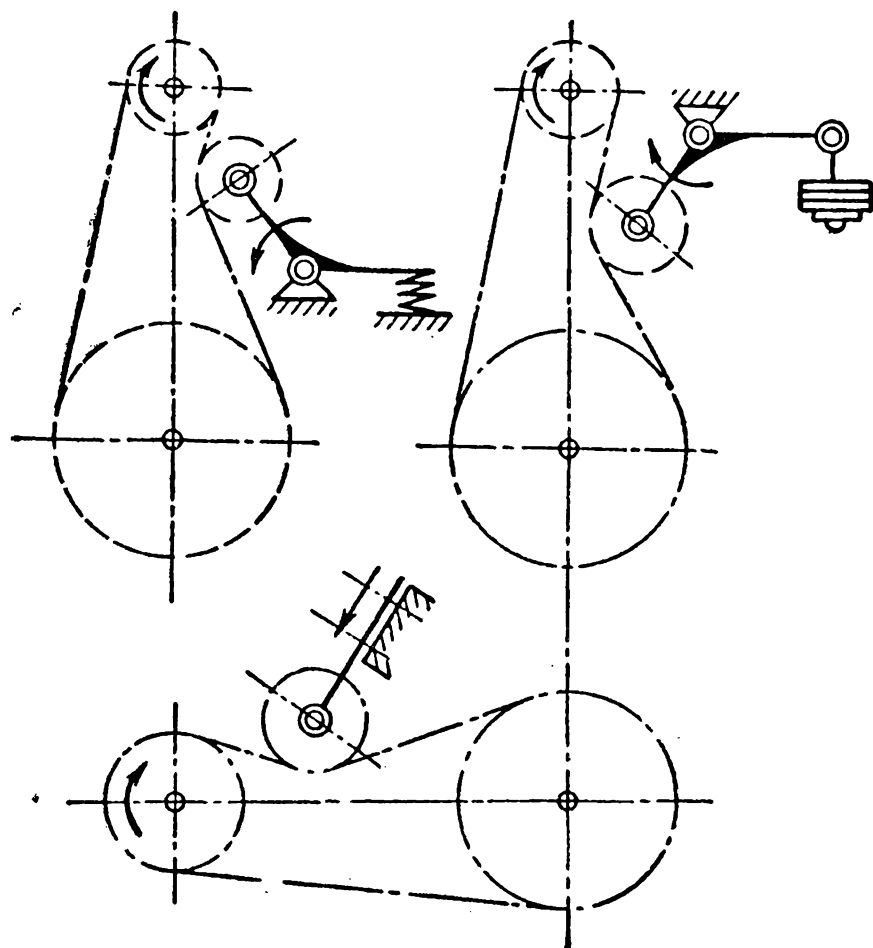


Fig. 200

ter should be not below that of the smaller sprocket of the drive. The wheel should engage at least three links simultaneously.

Smooth rollers instead of sprockets are used in drives inclined at an angle over  $60^\circ$  with the horizontal when the velocity ratio is minimum  $i=3$ .

## DESIGN OF DRIVES

**Kinds of Failure in Chain Drives.** Chain drives are usually put out of commission due to chain elongation, failure of the joints and plates and wear of the sprocket teeth.

Elongation is produced by increased pitch caused by joint wear under the action of tension and dynamic forces during operation.

With time the chain pitch grows so large that it fails to match the sprocket teeth and the chain may run off the sprockets. Experience shows that the maximum chain elongation should not exceed 3% while at  $v > 6$  m/sec it should be still less.

Under the action of repeated shocks, as the chain enters contact with the sprocket teeth, pitting occurs on the surfaces of the

rollers and bushes; strong knocks may even split the rollers and bushes.

Wear of the sprocket teeth occurs due to the relative motion of the rollers or bushes along the teeth under impact load. The teeth of the driving sprocket are worn at a faster rate because of greater impacts of the joints climbing onto the sprocket teeth. The amount of sprocket wear is also influenced by the form of the teeth.

Chain failure may be also caused by manufacturing defects. If the pins and bushes are pressed poorly into the plates, they are subject to slip thereby intensifying the wear of the conjugate parts. This considerably increases the pitch of some links. A chain with even one link faulty in this way is not satisfactory in operation. Damage is also caused by the wear of the plate side surfaces due to their friction against the side surface of the sprocket. This fault is caused by improper erection (misalignment and displacement of the sprockets on the shafts) and the curvilinear nature of the chain centre line.

The main criterion of operating ability of a drive is the wear resistance of the chain joints.

Calculations are carried out to determine those optimal proportions of the chain and sprockets at which the drive will be able to operate under the assigned duty without risk of damage.

The design recommendations and formulae are based on the analysis of the effect different factors produce on the operating ability of the drive and on experimental data which characterise this effect quantitatively—the factors ensuring adequate wear resistance of the chain.

**Determining Chain and Sprocket Proportions.** A very small number of teeth in the sprocket unfavourably affects chain service life and intensifies noise.

The number of teeth of the smaller sprocket should be selected depending on the magnitude of the velocity ratio according to the data in Table 56.

*Table 56*

Number of Teeth in a Smaller Sprocket						
Type of chain	Number of sprocket teeth at velocity ratio $i$					
	1	2	3	4	5	6
Bush-roller chain . . . . .	31	27	25	23	21	17
Silent chain . . . . .	40	35	31	27	23	19

When the number of teeth has to be decreased we take for bush-roller chains  $z_{\min} \geq 9$  and for silent chains  $z_{\min} \geq 13$ .

The maximum number of teeth is limited by the value of the allowable chain stretch. If the chain pitch is increased by  $\Delta t$ , the links of a stretched chain will be displaced by (Fig. 201)

$$\Delta D = \frac{\Delta t}{\sin \frac{180^\circ}{z}} \quad (331)$$

from the centre as compared to the position occupied by the new chain. An excessive displacement of the chain deteriorates operating conditions and may cause the chain to run off the sprocket. The maximum allowable relation  $\frac{\Delta D}{t} = B$  is found experimentally.

Hence, the following condition should be satisfied:

$$\frac{\Delta t}{t} \frac{1}{\sin \frac{180^\circ}{z}} \leq B. \quad (332)$$

With the allowable relative wear rate up to 1.25%  $\left(\frac{\Delta t}{t} = 0.0125\right)$  the maximum number of teeth for bush-roller chains should not exceed 120; for silent chains  $z_{\max} \leq 140$ .

Theoretical analysis and the operating experience of

chain drives shows that the smaller the chain pitch the more favourable conditions for the drive operation are since, all other conditions being equal, the force of shock, centrifugal force and friction become weaker in intensity.

The maximum allowable velocity, depending on the type of chain, number of teeth of the smaller sprocket and the chain pitch are shown in Table 57.

After selecting the type of chain and number of teeth of the smaller sprocket and knowing its rpm we find the chain pitch from Table 57.

The mean peripheral velocity of the sprocket should not exceed 12 m/sec for bush-roller and 16 m/sec for silent chains.

If the drive has been made to adequate standards of precision the chain velocity in conditions of careful maintenance may be up to 25-30 m/sec at the pitch  $t \leq 12.7$  mm and the number of teeth of the smaller sprocket  $z_1 > 35$ .

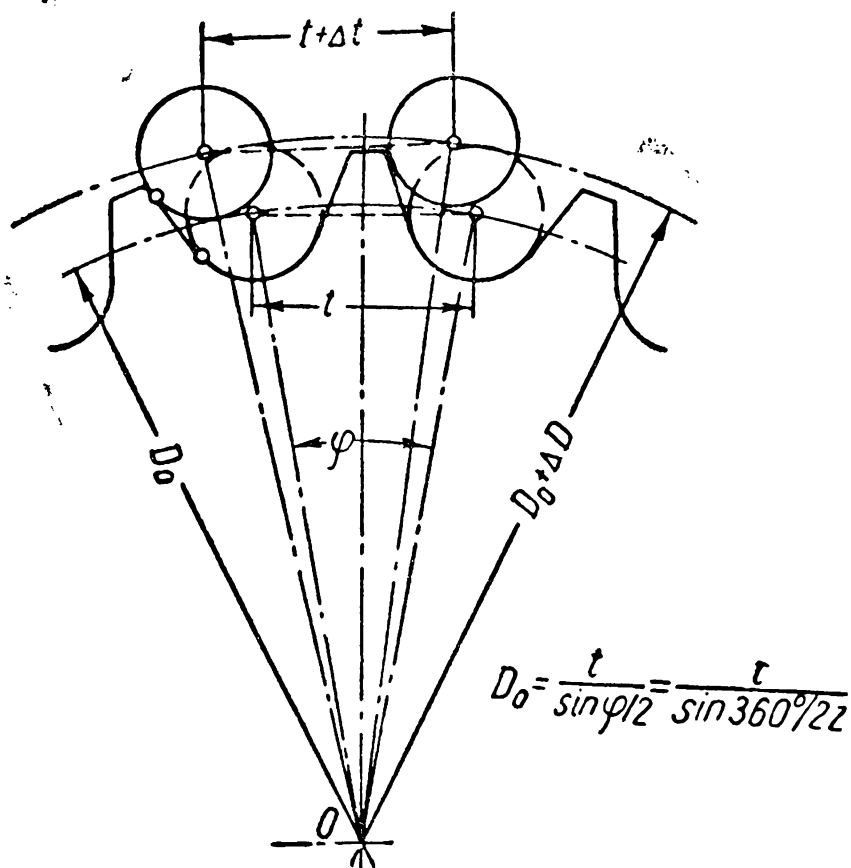


Fig. 201

Table 57

Maximum Velocity for Various Types of Chains, rpm

Type of chain	Number of sprocket teeth $z_1$	Chain pitch $t$ in mm				
		12	15	20	25	30
Bush-roller chains	15	2,300	1,900	1,350	1,150	1,000
	19	2,400	2,000	1,450	1,200	1,050
	23	2,500	2,100	1,500	1,250	1,100
	27	2,550	2,150	1,550	1,300	1,100
	30	2,600	2,200	1,550	1,300	1,100
		12.7	15.87	19.05	25.4	31.75
Silent chains	17-35	3,300	2,650	2,200	1,650	1,300

The choice of chain according to the obtained pitch is done from the condition that the useful force  $P$  does not exceed the following maximum values:

for a bush-roller chain

$$P_{\max} = \frac{Q}{n_s k} ; \tag{333}$$

for a silent chain

$$P_{\max} = \frac{Qb}{10n_s k} . \tag{334}$$

Here  $Q$  is the chain ultimate strength in kg (for silent chain with the width of 10 mm),  $n_s$ —safety factor,  $k$ —drive operating factor,  $b$  in cm.

Depending on rpm the value of  $n_s$  for the smaller sprocket at  $z_1=17-35$  is chosen from Table 58.

Table 58

Factor s of Safety  $n_s$

Chains	Rpm of the smaller sprocket								
	50	200	400	600	800	1,000	1,200	1,600	2,000
Bush-roller chains									
$t=12-15$ mm . .	7.0	7.8	8.55	9.35	10.2	11.0	11.7	13.2	14.8
$t=20-25$ mm . .	7.0	8.2	9.35	10.3	11.7	12.9	14.0	16.3	—
$t=30-35$ mm . .	7.0	8.55	10.2	13.2	14.8	16.3	19.5	—	—
Silent chains									
$t=12.7-15.87$ mm	20	22.2	24.4	28.7	29.0	31.0	33.4	37.8	42.0
$t=19.05-25.4$ mm	20	23.4	26.7	30.0	33.4	36.8	40.0	46.5	53.5

The factor  $k$  is the product of three factors  $k = k_s k_l k_p$  which account for the effect of separate phenomena on the chain operating ability. The service factor  $k_s = 1$  at constant load, intermittent operation;  $k_s = 1.3$  at impact load, continuous operation;  $k_s = 1.5$  at very jerky load, continuous operation; the lubricating factor  $k_l = 1$  at continuous lubrication;  $k_l = 1.3$  at periodic lubrication; the factor accounting for the position of the chain  $k_p = 1$  with the centre line of the sprockets horizontal or inclined at an angle up to  $45^\circ$  with the horizontal,  $k_p = 1.3$  with this line inclined at an angle above  $45^\circ$  with the horizontal.

These factors correct the magnitude of useful force taking into account the effect the operating conditions of the drive have on its wear resistance.

The minimum centre distance is selected depending on the velocity ratio so that the arc of contact on the smaller sprocket is not below  $120^\circ$ .

Approximately we can assume:

at  $i < 4$

$$A_{\min} = \frac{D_1 + D_2}{2} + (30-50) \text{ mm} \quad (335)$$

where  $D_1$  and  $D_2$  are the diameters of addendum circles of the sprockets.

The normal operating conditions of the drive correspond to  $A = (30-50)t$ . When the centre distance is greater the chain length becomes excessive—it rapidly stretches and causes jerky operation of the drive. Usually  $A < 80t$  is recommended for the centre distance.

After having selected centre distance the value  $A$  should be accurately specified.

The number of links in the chain is found from the condition (see Fig. 194)

$$y = \frac{z_1}{2} - z_1 \frac{\theta}{\pi} + \frac{z_2}{2} + z_2 \frac{\theta}{\pi} + 2 \frac{A}{t} \cos \theta. \quad (336)$$

Since the angle  $\theta$  is small

$$\theta \approx \sin \theta = \frac{D_2 - D_1}{2A} \approx \frac{z_2 - z_1}{2\pi A} t,$$

$$\cos \theta = (1 - \sin^2 \theta)^{1/2} \approx 1 - \frac{1}{2} \sin^2 \theta = 1 - \frac{1}{2} \left( \frac{z_2 - z_1}{2\pi} \right)^2 \frac{t^2}{A^2}$$

after substituting in the formula (336) we obtain

$$y = \frac{z_1 + z_2}{2} + \frac{2A}{t} + \left( \frac{z_2 - z_1}{2\pi} \right)^2 \frac{t}{\pi}. \quad (337)$$



The number of links found from this formula is approximated to the nearest even number. After this the accurately specified centre distance will be

$$A = \frac{t}{4} \left[ y - \frac{z_1 + z_2}{2} + \sqrt{\left( y - \frac{z_1 + z_2}{2} \right)^2 - 8 \left( \frac{z_2 - z_1}{2\pi} \right)^2} \right]. \quad (338)$$

The obtained value  $A$  should be decreased by 2-5 mm to ensure adequate slack in the chain.

The profiles of the teeth and the sprocket are then drawn according to standardised values.

The forces acting on the drive shafts are found approximately, depending on the drive position, from the formula

$$P_{sh} = P + 2kqA \quad (339)$$

where  $k$  is the factor accounting for the position of the centre line.

For a vertical position  $k=1$ , for the centre line inclined at an angle up to  $45^\circ$ ,  $k=2$  and for a horizontal position  $k=4$ .

Loads on the supports are determined in conformity with the location of the sprockets and other components which take the forces acting on the shafts.

The housing and slack adjuster are designed after calculating the shafts and bearings.

**Lubrication and Efficiency.** The drive operates normally only if the chain links and sprocket teeth are adequately lubricated.

The lubricant can be fed periodically and continuously. Periodic lubrication with an oil cup or brush is not so effective and can be resorted to if the velocity is below 4 m/sec.

When the chain operates at  $v=4-6$  m/sec it should be removed at definite intervals and immersed in slightly heated oil. Lubrication is most effective when oil is fed continuously to the driven side into the gaps between the plates of a bush-roller chain or along the entire length of a silent chain.

If the drive operates at  $v=6-8$  m/sec it should be provided with a housing filled with oil. The bottom side of the chain should not be immersed in oil by more than the height of its plate.

If  $v > 8$  m/sec oil should be supplied continuously by means of a pump or special splash rings and splash plates to the bottom side where it enters contact.

The grade of oil is selected depending on the magnitude of unit pressure in the joint, chain velocity and mode of lubrication (Table 59).

The horse power losses in a chain drive include losses in overcoming the chain stiffness (friction in the joints and between the plates of adjacent links), friction between the chain and the sprocket teeth,

Table 59  
Viscosity of Oil for Lubricating Chain Drives (in degrees  $E_{50}^{\circ}$ )

Unit pressure in chain joint in kg/mm <sup>2</sup>	Manual or drip feed oiling systems			Oil bath lubrication	
	Chain velocity in m/sec				
	<1	1-5	>5	<5	≥5
<1	3	4-5	5-7	3	4-5
1-2	4-5	5-7	7-9	4-5	5-7
2 to 3	5-7	7-9	10-11	5-7	7-9

in the shaft bearings and resistance to the motion of the chain in the oil bath.

The greatest losses are due to chain stiffness. They not only determine the total efficiency but also limit the load-carrying capacity of the drive.

The nature of these losses will be clear from the following.

As the chain climbs onto the sprocket a relative turn of the links occurs. Relative motion causes friction to arise in the loaded joints of the chain.

The work performed by the friction  $A_x$  in the chain joint as the chain climbs onto the sprocket (or leaves it) is

$$A_x = M_{fr} \alpha = P_x \mu \frac{d}{2} \times \frac{2\pi}{z} \tag{340}$$

where  $M_{fr} = P_x \mu \frac{d}{2}$  is the moment of friction in the joint with the force  $P_x$  acting in the joint;

$\alpha = \frac{2\pi}{z}$  — the angle of the relative turn of the chain links;

$\mu$  — the coefficient of friction in the joint.

The force  $P_x$  changes from  $S_2 + S_v$  to  $S_1 + S_v$  depending on whether the losses due to friction are considered for a chain climbing onto or leaving the sprocket. Thus, we should distinguish between the work done by friction when the joint climbs onto the driving and driven sprockets and the work when it leaves them, found from the formula (340) after substituting a respective  $P_x$ .

The work done by friction in the joints is affected by the centre distance  $A$  and the slack of the driven side  $f$ . The greater the distance between shafts and the smaller the slack, the greater will be the tension of the slack side  $S_2$  and the greater the losses due to friction.

The total work done by friction of all  $y$  joints of the chain will be

$$A_{fr} = y \sum A_x. \tag{341}$$

The horse power loss due to friction in the joints can be found from the formula

$$L = \frac{A_{fr}}{75T} \text{ h. p.} \quad (342)$$

where  $T = \frac{yt}{100v}$  sec is the time of the chain travel;  $t$ —the pitch in cm; the velocity  $v$  is in m/sec.

The drive efficiency can be approximately found (with the transmitted horse power  $N$  h. p.) from the formula

$$\eta = \frac{N}{N+L} \quad (343)$$

Other kinds of loss are of lesser importance. Thus, for example, the losses in overcoming the oil resistance amount to about 4-5% of the total. The losses due to friction between the plates largely depend on adequate precision of manufacture and erection of the chain.

Mean efficiency values of adequately designed drives vary within 0.96-0.98.

*Example.* Calculate a chain drive to actuate a compressor from a 10-kw electric motor at  $n_1=970$  rpm, the compressor rpm  $n_2$  being 330. The compressor operates in two shifts. The centre distance should be minimum 550 mm. The chain tension can be adjusted by shifting the motor on slides.

Since the velocity of the driving sprocket is low we assume that chain velocity will not exceed  $v=12$  m/sec; we therefore select a bush-roller chain as a simpler and cheaper type.

The drive velocity ratio is  $i = \frac{970}{330} \approx 2.94$ . From Table 56 we find at  $i=3$  for a bush-roller chain the value  $z_1=25$ . Then  $z_2=25 \frac{970}{330} \approx 74$ . This may be permitted if we limit elongation to  $\frac{\Delta t}{t} = 1.25\%$  ( $z_{\max}=120$  is possible). At  $z_1=23$  and  $n_1=970$  rpm the chain may have any pitch indicated in Table 57. We take  $t=15$  mm.

The mean peripheral velocity of the chain will be

$$v = \frac{z_1 t n_1}{60 \times 1,000} = \frac{25 \times 15 \times 970}{60 \times 1,000} = 6.05 \text{ m/sec,}$$

i. e., below 12 m/sec.

The factor  $k$  accounting for service conditions is selected from the data on p.378.

The load is constant,  $k_s=1$ ; the centre line is inclined at an angle less than  $45^\circ$  with the horizontal,  $k_p=1$ ; lubrication is continuous,  $k_l=1$ . Hence,  $k=k_s k_p k_l=1 \times 1 \times 1=1$ .

The safety factor is taken from Table 58.

$$n_s=11.$$

The peripheral force is

$$P \approx \frac{100 N}{v} = \frac{100 \times 10}{6.05} = 165 \text{ kg.}$$

The ultimate strength from the formula (333)

$$Q \geq Pkn_s = 165 \times 1 \times 11 \approx 1,820 \text{ kg.}$$

According to force  $Q=1,820$  kg and the pitch  $t=15$  mm we select a duplex chain for which the ultimate strength is 2,500 kg.

We arbitrarily assume the distance between shafts to be

$$A = 40 \times t = 40 \times 15 = 600 \text{ mm.}$$

The number of links is found from the formula (337)

$$y = \frac{z_1 + z_2}{2} + \frac{2A}{t} + \left( \frac{z_2 - z_1}{2\pi} \right)^2 \frac{t}{A} =$$

$$= \frac{25 + 74}{2} + \frac{2 \times 600}{15} + \left( \frac{74 - 25}{2\pi} \right)^2 \frac{15}{600} = 49.5 + 80 + 60.8 \times \frac{1}{40} \approx 130.$$

To ensure proper slack of the chain the centre distance should be diminished by 2-5 mm.

The total length of chain is

$$L = y \times t = 130 \times 15 = 1,950 \text{ mm.}$$

The loads acting on the shafts, from the formula (339),

$$P_{sh} = 165 + 2 \times 2 \times 2.2 \times 0.6 \approx 170 \text{ kg.}$$

Here  $q=2.2$  kg/m is the weight of one linear metre of the chain.

Using the data provided by standards we find the parameters of the sprocket elements (see Fig. 199, c):

$$D_{01} = \frac{1}{\sin \frac{180^\circ}{z_1}} = \frac{15}{\sin \frac{180^\circ}{25}} = 119.96 \text{ mm}; D_{02} = 353.29 \text{ mm};$$

$$D_{out 1} = D_{01} + 0.9d = 119.96 + 0.9 \times 10 \approx 129.0 \text{ mm}; D_{out 2} \approx 362.3 \text{ mm};$$

$$r = 0.505d = 0.505 \times 10 = 5.05 \text{ mm};$$

$$D_{r1} = D_{01} - 2r = 119.96 - 2 \times 5.05 \approx 109.9 \text{ mm}; D_{r2} = 343.2 \text{ mm};$$

$$l = 0.90C - 0.15 = 0.90 \times 10 - 0.15 \approx 8.8 \text{ mm};$$

$$n'' = n' + 0.03C = 18 + 0.03 \times 10 = 18.3 \text{ mm};$$

$$D_{C1} = t \cot \frac{180^\circ}{z_1} - 1.3b_p = 15 \times \cot \frac{180^\circ}{25} - 1.3 \times 14 \approx 100 \text{ mm}; D_{C2} = 334 \text{ mm};$$

$$\alpha' = 58^\circ \text{ at } \frac{t}{d} = 1.5 < 1.6.$$

Here  $b_p$  is the width of the plate.

## CHAPTER XIX

### POWER SCREWS

A *power screw* is employed to convert rotary motion into rectilinear motion. The advantages of this drive are simple design, high velocity ratio, self-locking and the possibility of producing it with a high pitch accuracy. Among the disadvantages are comparatively

high friction in the thread with resulting rapid wear and low efficiency. All these qualities determine the field of application of power screws. In jack screws, screw presses and pressing screws of rolling mills these drives are used as load drives to transmit large forces at comparatively low speeds. In machine tools, measuring instruments and machines power screws are widely used for setting-up, working and idle travel which may require high precision. A power screw should possess high resistance to wear and retain its precision for a long time.

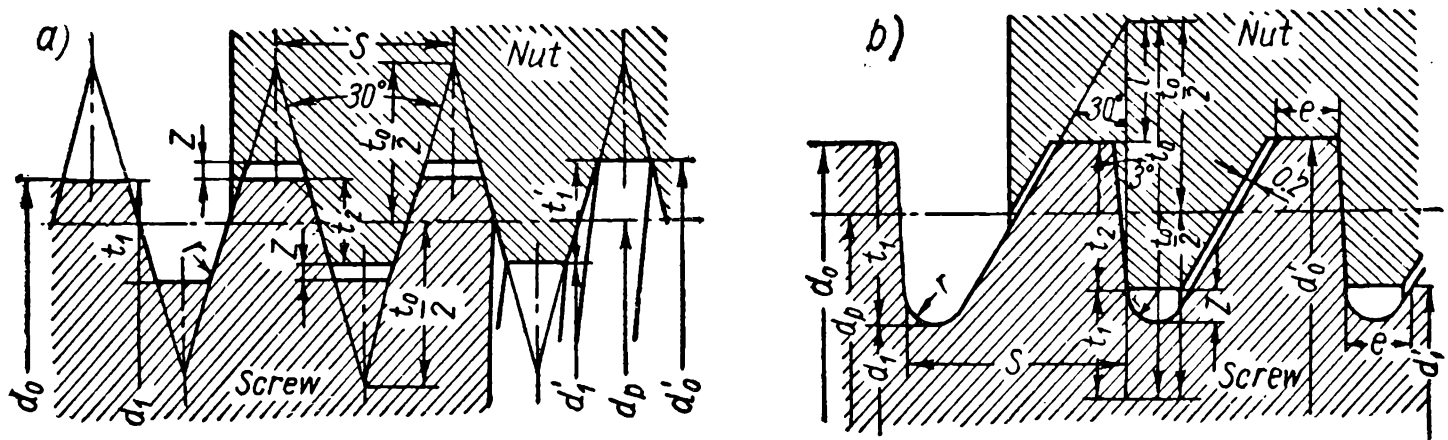


Fig. 202

Power screws ordinarily have a *trapezoidal thread* or at very high unilateral loads—a *buttress thread*. The profiles of these threads are shown in Fig. 202, *a* and *b*.

Although square thread is somewhat superior as regards the work done by friction to trapezoidal thread it is not standardised and is used rarely. This is due to several reasons: a) trapezoidal thread can be easily cut by all existing methods while the cutting of a square thread is more involved; besides, it cannot be milled; b) trapezoidal thread is stronger than square thread since, with the same pitch, the thickness of thread at the root in a trapezoidal type is greater than in a square type; c) axial clearance in trapezoidal thread can be adjusted by tightening a split nut while this cannot be done with square thread.

A buttress thread (Fig. 202, *b*), according to Soviet standards, has an asymmetric trapeziform profile with an angle at the crest of  $3^\circ$ ; the roundings at the root increase the strength under dynamic load.

#### MATERIALS AND DESIGN OF SCREWS AND NUTS

The *screw material*, as well as possessing sufficient strength, should have high wear resistance and good machinability. Screws which are not treated to obtain adequate hardness are made from steel 45 or 50. For finally heat-treated screws in order to obtain

a high degree of hardness use is made of tool and alloy steel grades Y10, XГ, XБГ, 65Г or 40X.

The *nut material* is tin bronze—ОФ 10-1 and ОЛС 6-6-3 and also antifriction cast iron. To reduce the amount of bronze, bimetallic

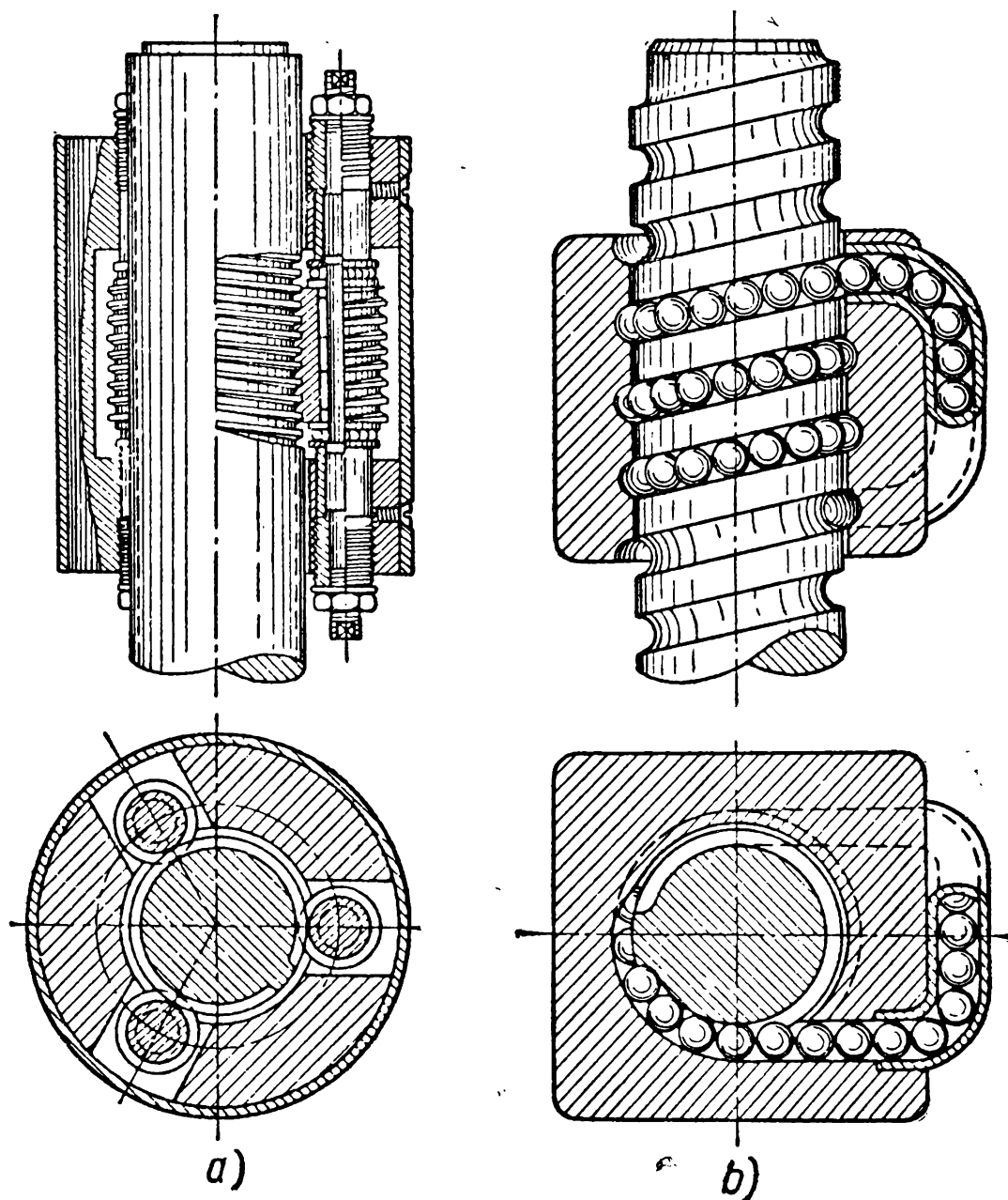


Fig. 203

nuts are used in the form of a steel or cast-iron shell lined with bronze (by the centrifugal method). Nuts for rapid motion are sometimes lined with babbitt.

*Screws* are extremely simple *in design*. The tendency is to avoid shoulders of large diameter on the screws (and on all shafts) because they make machining more difficult and increase the volume of metal to be removed. To facilitate processing long screws are composed of two or more parts.

*Design of nuts.* In its simplest form the nut is a bush or body with a threaded hole and with external thrust surfaces which prevent its displacement and rotation in the component to which it is rigidly connected. In the design of power screws for metal-cutting machine tools it is usual practice to provide for periodic or continuous (auto-

matic) compensation for the wear of thread and taking up backlash (axial play). All different solutions for this problem basically involve the use of, instead of one integral nut, two nuts separated by a wedge, a spring or any other device.

Nuts on the screws of screw-cutting lathes are split so that the nut can be separated from the driving screw when plain turning or boring is carried out.

The effort to reduce friction in a power screw, which is of especial importance in hand-operated drives, has resulted in the development of designs in which sliding friction is replaced by rolling friction. In one design of this type the nut (Fig. 203, *a*) consists of three hardened rollers arranged symmetrically around the screw in one common housing. Each roller is a round rack and has a profile to match the screw thread. The axial forces of the rollers are taken by thrust ball bearings and the radial forces by needle bearings. The nut shown in Fig. 203, *b* employs balls which are brought into continuous motion by the rotating screw since the beginning and end of the thread in the nut are connected by a by-pass tube. The thread in the screw and nut is shaped in this case as bearing races of radial ball bearings.

### CALCULATION OF POWER SCREWS

Experience shows that the unsatisfactory operation of power screws is primarily due to increased thread wear. Wear can be reduced by selecting proper materials for the screw and nut, by liberal lubrication and by decreasing unit pressure. Calculation for wear is obligatory for all types of power screws. Load drives and lead screws and nuts of lathes are also calculated for strength and, in case of relatively long screws, also for stability. In special cases (machine-tool fine-feed drives with graduated limbs) calculations are made for stiffness and precision. We shall not deal here with the methods of these special calculations.

*Calculation for wear* for the majority of power screws is the main method of determining the screw diameter and the nut thickness. It is done by checking the mean unit pressure  $p$  in the thread according to the formula

$$p = \frac{P}{\pi d_p t_2 \frac{H_z}{s}} \leq [p] \quad (344)$$

where  $P$  is the force acting along the screw;

$d_p$ —thread pitch diameter;

$s$ —thread pitch;

$t_2$ —depth of thread engagement;

$H$ —nut thickness;

$z$ —number of threads.

Introducing  $\psi = \frac{H}{d_p}$  we obtain

$$p = \frac{Ps}{\pi \psi d_p^2 t_2 \times z} \leq [p]; \quad (345)$$

and hence

$$d_p \geq \sqrt{\frac{Ps}{\pi \psi t_2 z [p]}}. \quad (346)$$

For trapezoidal threads which are most common in power screws  $t_2 = 0.5 \frac{s}{z}$ . After substituting this value in the latter formula we obtain

$$d_p = \sqrt{\frac{2p}{\pi \psi [p]}}. \quad (347)$$

The values  $s$  and  $z$  are usually found through kinematic calculations; the relation  $\psi = H : d_p$  is selected from 1.2 to 2.5 for unsplit nuts and from 2.5 to 3.5 for split nuts. From operating experience the mean unit pressure  $[p]$  can be assumed to equal: steel screw, bronze nut— $[p] = 120 \text{ kg/cm}^2$  (in pressing screws of rolling mills  $[p] = 150\text{--}200 \text{ kg/cm}^2$ ); steel screw, cast-iron nut— $[p] = 80 \text{ kg/cm}^2$ .

After determining  $d_p$  we select the nearest standard diameter of the screw.

*Calculation for strength* is done only for heavily loaded screws. Since the screw simultaneously operates under compression (or tension) and torsion, the combined stress in the screw material is

$$\sigma_{com} = \sqrt{\sigma^2 + 4\tau^2} \quad (348)$$

where  $\sigma = \frac{P}{F_1} = \frac{P}{\frac{\pi}{4} d_1^2} \approx \frac{P}{0.8 d_1^2}$  is the stress due to tension (com-

pression) caused by the axial force  $P$  and  $\tau = \frac{M_t}{W_1} = \frac{M_t}{0.2 d_1^3}$  is the shearing stress due to the action of the torque  $M_t$ .

The torque transmitted by the screw is \*

$$M_t = P \frac{d_p}{2} \tan(\beta + \rho') + M_{fr}. \quad (349)$$

---

\* The formula (349) is used when the nut and thrust bearing are located on one side of the place where torque is applied. If the nut and thrust bearing are located on both sides of the torque the design section resists the action of a part of torque  $M_t$ . In this case we introduce in the formula (349) either only the moment of friction in the thread accounted for in the expression  $P \frac{d_p}{2} \tan(\beta + \rho')$  or only  $M_{fr}$  depending on which of these moments is the larger



Here  $\beta = \tan^{-1} \frac{s}{\pi d_p}$  is the helix angle;

$\rho'$ —the reduced angle of friction in the thread;

$M_{fr}$ —the moment of friction forces on the pivot or any other support taking the reaction from the force  $P$ . For trapezoidal threads  $\rho' \approx \rho = \tan^{-1} f = 6-8^\circ$  where  $f$  is the coefficient of friction.

The moment of friction on the pivot can be expressed through the force  $P$ :  $M_{fr} = P \frac{d_{red}}{2}$  where  $d_{red}$  is the reduced diameter of the friction forces on the pivot. In this case

$$M_t = P \left[ \frac{d_p}{2} \tan(\beta + \rho') + \frac{d_{red}}{2} f \right]. \quad (350)$$

The screw strength is

$$\sigma_{com} \leq \frac{\sigma_y}{5-3} \quad (351)$$

where  $\sigma_y$  is the yield point of the screw material.

Nuts made from bronze and cast iron sometimes experience thread shear. Therefore, the calculations of a power screw for strength should also include the checking of the nut thickness for thread shear. The strength equation for this case is

$$\tau = \frac{P}{\pi d'_0 \frac{H_z}{s} h} \leq [\tau], \quad (352)$$

where besides the above named designations,  $d'_0$  is the major diameter of thread in the nut;  $h$ —the thickness of thread base. In nuts made from phosphor bronze  $[\tau]_s$  may be 250-350 kg/cm<sup>2</sup>.

*Calculation for stability* as regards buckling due to axial compression should be performed for screws whose length considerably exceeds their diameter—at  $\nu l \geq (7.5-10)d_1$ , where  $\nu l$  is the reduced length of screw (see below) and  $d_1$  is the minor diameter of thread. Since it is difficult to give an exact evaluation of the screw restraint in the supports, the calculations are confined to finding the stability of the screw acting as a bar subjected only to compression from the axial force  $P$ . In this case the critical value of the force ( $P_{Eul}$ ) can be expressed through the well-known formula

$$P_{Eul} = \frac{\pi^2 E I_{min}}{(\nu l)^2}. \quad (353)$$

Here  $E$  is the modulus of longitudinal elasticity;

$I_{min}$ —the minimum moment of inertia of the screw transverse section;

$\nu l$ —the reduced length of screw.

The index  $Eul$  (Euler's force) shows that the critical force corresponds to the static loading of the bar.

The reduced length is obtained by multiplying the length  $l$  between the screw supports (the nut can be one of them) by the length factor  $v$ . The magnitude of this factor depends on the mode of securing the bar ends and also on the nature of distribution of inner forces along the screw. Screw supports with the ratio  $l_{sup} : d_{sup} \approx 1.5-2$  should be classed among pivoted supports; for them  $v=1$ . For horizontally placed screws account should be taken of sag under their own weight. For  $v=1$  this effect is approximately accounted for in the formula

$$P_{Eul} = \frac{\pi^2 EI_{\min}}{l^2} - 0.5ql \quad (354)$$

where  $q$  is the intensity of screw load due to own weight. For the stability factor  $n_{st} = \frac{P_{Eul}}{P}$  we take  $n_{st} \geq 2.5-4$ .

In the strength and stability formulae above, the screw was considered as a bar with diameter  $d_1$  equal to the minor diameter of thread. But the presence of thread increases the strength and stiffness of the screw as compared to a smooth bar of diameter  $d_1$ . As shown by experimental research this increase is not very large and depends mainly on the ratio of the major diameter of thread ( $d_0$ ) to the minor diameter ( $d_1$ ). For a standard trapezoidal thread with a thread angle  $\alpha=30^\circ$

$$I_s = I_1 \left( 0.40 + 0.60 \frac{d_0}{d_1} \right)$$

where  $I_s$  is the moment of inertia of screw and  $I_1$  is the moment of inertia of shaft,  $d_1$  in diameter.

In ordinary calculations this correction is neglected.

*Example.* Select and calculate a power screw for the travel of the arm of a radial drilling machine. The maximum force acting on the screw,  $P=3,640$  kg, arises as the arm is lifted; it is composed of the arm weight and frictional resistance when the arm travels along the column. Kinematic calculations of the arm lift mechanism gave us the thread pitch  $s=8$  mm and the number of starts  $z=1$ . During the handling of the machine with a sling strapped round the arm, the arm lifting screw is loaded—for compression—with the force  $P_c=3,000$  kg by the weight of the column and foundation plate. The maximum length of screw from the thrust bearing to the nut  $l=1,500$  mm.

The work of the arm lifting screw is characterised by frequent starting and comparatively short travel. Under these conditions it is difficult to provide satisfactory lubrication. Therefore, we select for the power screw materials which are sufficiently wear resistant even if poorly lubricated; the screw is made from grade 45 improved steel and the nut from OLC 6-6-3 bronze. To save bronze the nut is bimetallic.

We find the screw pitch diameter first from the formula (347) for a trapezoidal thread assuming the relative length of the nut to be  $\psi=1.5$  and unit pressure  $[p]=100 \text{ kg/cm}^2$ .

$$d_p = \sqrt{\frac{2P}{\pi\psi[p]}} = \sqrt{\frac{2 \times 3,640}{\pi \times 1.5 \times 100}} = 3.93 \text{ cm.}$$

According to standards, the nearest to the required thread ( $d_p=39.3 \text{ mm}$ ,  $s=8 \text{ mm}$ ,  $z=1$ ) is normal thread with a rated diameter of 44 mm. Its main proportions are as follows: pitch diameter of thread  $d_p=40 \text{ mm}$ ; minor diameter of screw thread  $d_1=35 \text{ mm}$ ; major diameter of thread in nut  $d'_0=45 \text{ mm}$ ; thickness of thread base  $h=5.2 \text{ mm}$  and the basic area of bar section  $F_1=9.62 \text{ cm}^2$ .

The helix angle is

$$\beta = \tan^{-1} \frac{s}{\pi d_p} = \tan^{-1} \frac{8}{\pi \times 40} = \tan^{-1} 0.064 \approx 3^\circ 40'.$$

The angle  $\beta$  is considerably smaller than the angle of friction ( $\rho'=6-8^\circ$ ), and hence, the self-locking of the screw even neglecting friction in the bearing is ensured.

*Calculating the screw for strength.* The stress due to tension in the screw is

$$\sigma = \frac{P}{F_1} = \frac{3,640}{9.62} = 378 \text{ kg/cm}^2.$$

The torque transmitted by the screw—from the formula (349)—is

$$M_t = P \frac{d_p}{2} \tan(\beta + \rho') + M_{fr} = 3,640 \frac{4.0}{2} \tan(3^\circ 40' + 7^\circ) = 1,370 \text{ kg/cm}.$$

The shearing stress is

$$\tau = \frac{M_t}{0.2d_1^3} = \frac{1,370}{0.2 \times 3.5^3} = 160 \text{ kg/cm}^2.$$

The combined stress in the screw material [formula (348)]

$$\sigma_{com} = \sqrt{\sigma^2 + 4\tau^2} = \sqrt{378^2 + 4 \times 160^2} = 495 \text{ kg/cm}^2.$$

The yield point of steel 45 high-tempered and hardened to  $H_B=241-285$  is  $\sigma_y \geq 55 \text{ kg/mm}^2$ . In this case the safety factor for strength is

$$n = \frac{\sigma_y}{\sigma_{com}} = \frac{5.500}{495} \approx 11.$$

This considerably exceeds the required value ( $n=3-5$ ).

We check the thickness of the nut  $H = \psi \times d_p = 1.5 \times 40 = 60 \text{ mm}$  for shear of thread according to the formula (352):

$$\tau = \frac{P}{\pi d'_0 \frac{Hz}{s} h} = \frac{3,640}{\pi \times 4.5 \times \frac{60 \times 1}{8} \times 0.52} \approx 66 \text{ kg/cm}^2$$

which also is considerably below the allowable value (for bronze  $[\tau]_s \leq 250-350 \text{ kg/cm}^2$ ).

The critical value of the compressive force from the equation (353):

$$P_{Eul} = \frac{\pi^2 EI_{\min}}{(\nu l)^2} = \frac{\pi^2 2.1 \times 10^6 \times 7.4}{(1 \times 150)^2} \approx 6,800 \text{ kg};$$

here

$$I_{\min} = \frac{\pi d_1^4}{64} = \frac{\pi 3.5^4}{64} = 7.4 \text{ cm}^4.$$

The stability factor is

$$n_{st} = \frac{P_{Eul}}{P_c} = \frac{6,800}{3,000} \approx 2.25.$$

The stability factor  $n_{st}$  obtained is somewhat below the permitted value ( $n_{st} \geq 2.5-4$ ). However, it is irrational to increase the dimensions of the screw only for considerations of stability during the shipment of the machine. It will be more correct to employ another method of shipping, for example—strapping the sling directly to the foundation plate.

# PART FOUR

## SHAFTS AND AXLES, BEARINGS AND COUPLINGS AND CLUTCHES

---

### CHAPTER XX

#### SHAFTS AND AXLES

An *axle* or a *shaft* supports the revolving parts of a machine and is the geometrical axis of their rotation.

Axles are intended only for supporting revolving parts and may either be fixed relative to their supports or rotate together with the parts fitted on them (an axle made integral with the parts). In each case the load carried by revolving parts is taken by the axle as a bending load.

As distinct from an axle, a shaft is designed not only to support revolving parts but also transmit torque; as a result, a shaft resists not only bending forces but also torque, either along its entire length or on separate sections.

According to the form of the geometrical axis we distinguish between *straight shafts* and *crankshafts*; the specific design of the latter makes them the subject of special courses and is beyond the scope of this book.

*Flexible wire shafts* with curvilinear or changing forms of the geometrical axis belong to a special group.

The portion of the shaft or axle within the bearing is called the *journal*.

Journals which take radial bearing pressures are called *pins* if they are fixed at the shaft ends (in Fig. 204 they are designated by the letter *P*) and *necks* (*N*, Fig. 204, diagram *III*) if they are arranged between the shaft ends.

Journals taking axial bearing pressures are called *thrust bearings*.

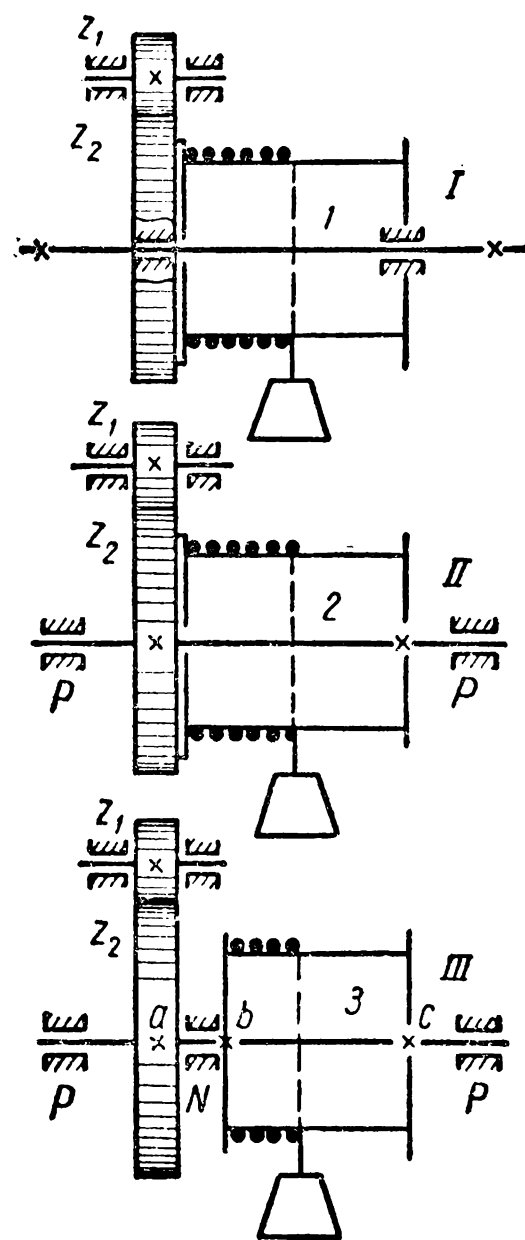


Fig. 204

## STRAIGHT SHAFTS AND AXLES

**Design.** In certain cases the same design problem can be solved by employing either an axle or a shaft. For example, the drum drive of a crane hoist can be designed in accordance with any diagram shown in Fig. 204.

In diagram *I* the drum is fitted onto an immobile axle 1 and is driven by a pair of toothed wheels  $z_1$  and  $z_2$  with the second wheel ( $z_2$ ) secured on the drum and rotating together with it. The load is transmitted to the axle where the drum is held in place.

In diagram *II* the same system is designed with a revolving axle: the drum is secured on axle 2 resting in bearings.

The difference in the load carried by axles 1 and 2 consists in the fact that with the same—in magnitude and direction—working load created by the weight of a suspended load, drum, load-gripping device, etc., axle 1 is subjected to a unilateral bending and axle 2—to a symmetric bending. The stresses arising in the sections of axle 2 change in magnitude and sign while in the sections of axle 1 they change in magnitude alone (as the rope is wound the magnitudes of bearing pressures change and, hence, the magnitudes of bending moments).

With the same external load the diameter of a revolving axle will be greater than that of a fixed axle; from this point of view design *I* is preferable for it reduces the system weight to a minimum. However, design *II* offers certain operating advantages. For example, in design *I* access to the bearings is difficult.

In diagram *III* the same design problem is solved by fitting the drum on a shaft 3 and not on an axle. The torque transmitted to the shaft through the toothed wheel  $z_2$  is taken by it in full on the section *ab* and is then transmitted to the drum via its hubs fastened on the shaft with keys.

The nature of distribution of the force flux between the drum hubs depends on the drum design, manufacturing and assembly precision; these factors also determine the torque on the section *bc*.

In this way the nature of the shaft loading essentially differs from and is more complex than the nature of the axle loading.

An advantage of design *III* is that it offers free access to the friction units and simplifies the design and manufacture of the drum because the toothed wheel is fitted on the shaft. Consequently, the adoption of one or other design is decided after carefully considering all factors (weight included) and depending upon which requirements are considered most important.

In the problem we took as an example any design of drum drive is acceptable in principle. Sometimes only one design is possible.

Axles and shafts are usually designed and made in the form of stepped cylindrical bars (with various diameters along their length), and less frequently—with a constant diameter.

Shafts with a constant diameter are the easiest to produce. However, such a cross-section does not correspond to the nature of stress which varies along the length; such shafts and axles are also unacceptable because of considerations of setting-up and maintenance, since they complicate the process of assembly and disassembly and also make more difficult the fastening of parts fitted to them and especially the bearings on shafts. For these reasons axles and shafts made in the form of smooth cylindrical bars are seldom used in mechanical engineering practice.

The length of each carrying section of a stepped shaft depends on the length of the hub of the fitted-on part; if possible, the length of the hub should somewhat exceed that of the respective carrying section on the shaft (see, for example, Fig. 188) to relieve the surfaces of the shaft from excessive surface pressures.

When the shaft has many abrupt changes of cross-section the use of normal standard diameters only may lead to difficulties. In such cases sections carrying no parts may have diameters deviating from the standard values.

When determining the form of a stepped shaft the diameter of each cross-section should be such as to allow each part fitted onto the shaft to reach its seat easily.

The basic hole system which is predominantly used in mechanical engineering allows various fits to be made by corresponding machining—by grinding separate sections of the shaft with a constant nominal diameter along the entire length or along considerable portions.

Fig. 205 shows designs of the unit and shaft (*I*) of the revolving mechanism of a 10-ton gantry crane; the form of the shaft is determined taking into account the acting stresses and the duties of the fitted parts, the nature of the fits, etc.

Abrupt changes of cross-section can cause stress concentrations which are most unwelcome with the nature of load typical for shafts and many designs of axle, the load producing varying stress.

The rounded-off place where two cross-sections of different diameter meet on an axle or shaft is called a *fillet*.

To decrease local stresses due to abrupt changes of cross-section fillets should have arcs of as large a radius as possible ( $\rho > 0.1d$ , Fig. 208, *b*) or be given a special form.

The best designs which ensure the stress concentration factor of  $k_\sigma \approx 1$  provide for so-called relieving transitions (unstressed fillets, Fig. 206, *a*).





Their application is limited because of the comparatively long transition section—about  $1.6d$  within which parts cannot be mounted. Fillets profiled as an elliptic curve (Fig. 206, *b*) can increase the endurance limit by 10%. According to some data, optimal

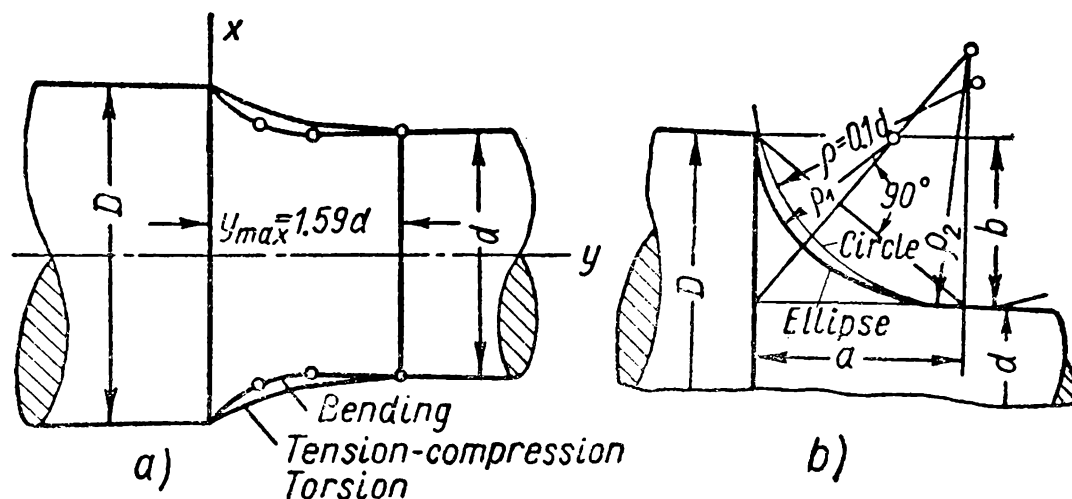


Fig. 206

results are obtained by recessed fillets (Fig. 207, *b*) of constant radius or by double- or triple-radius fillets (i. e., on different sections of the fillet described by various radii) which preserve the full length of the fitted portion of the shaft (axle) and greatly reduce stress concentration.

On the basis of assembly requirements the fillet radius is taken somewhat smaller than the radius describing the corresponding section of the part to be fitted ( $\rho < R$ , Fig. 207, *a*). If the radius of fillet is small, and this may tend to increase  $k_\sigma$ , the designs shown in Fig. 207, *b*, *c* are recommended, which allow an increase in the radius  $\rho$  to obtain the required strength.

The forms of the journals are determined by the magnitude and direction of bearing pressures and by the requirements of shaft fixing, clearance adjustment, etc., and also by considerations of manufacture.

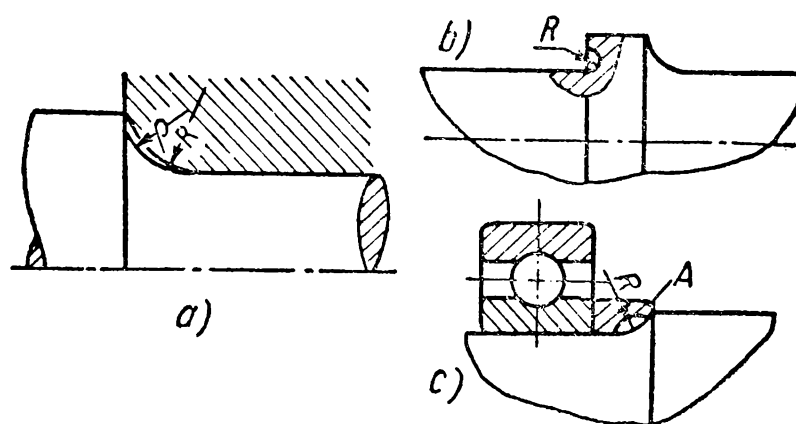


Fig. 207

The designs of a journal and bearing should conform to one another.

Some of the most common designs of journals are shown in Fig. 208.

The cylindrical journal at the end of a shaft or axle is turned to shape. The shoulder formed by this is used for fixing in an axial direction—it prevents the shaft or axle from shifting unilaterally

relative to the fixed bearing. Another such projection on the other end of the shaft or axle limits the axial shift of the part in the opposite direction. In some cases this method of axial fixing cannot be used since it hampers the free elongation of a shaft or axle under sharp temperature fluctuations. In such cases only one end of shaft is fixed (Fig. 208, *b*). This method of assembling the shaft (axle) has yet another advantage—namely, the distance between the bearings need not be so accurate.

Sometimes axial shift is reduced by special welded collars or adjusting rings. In such cases any section of a smooth shaft can act as a journal.

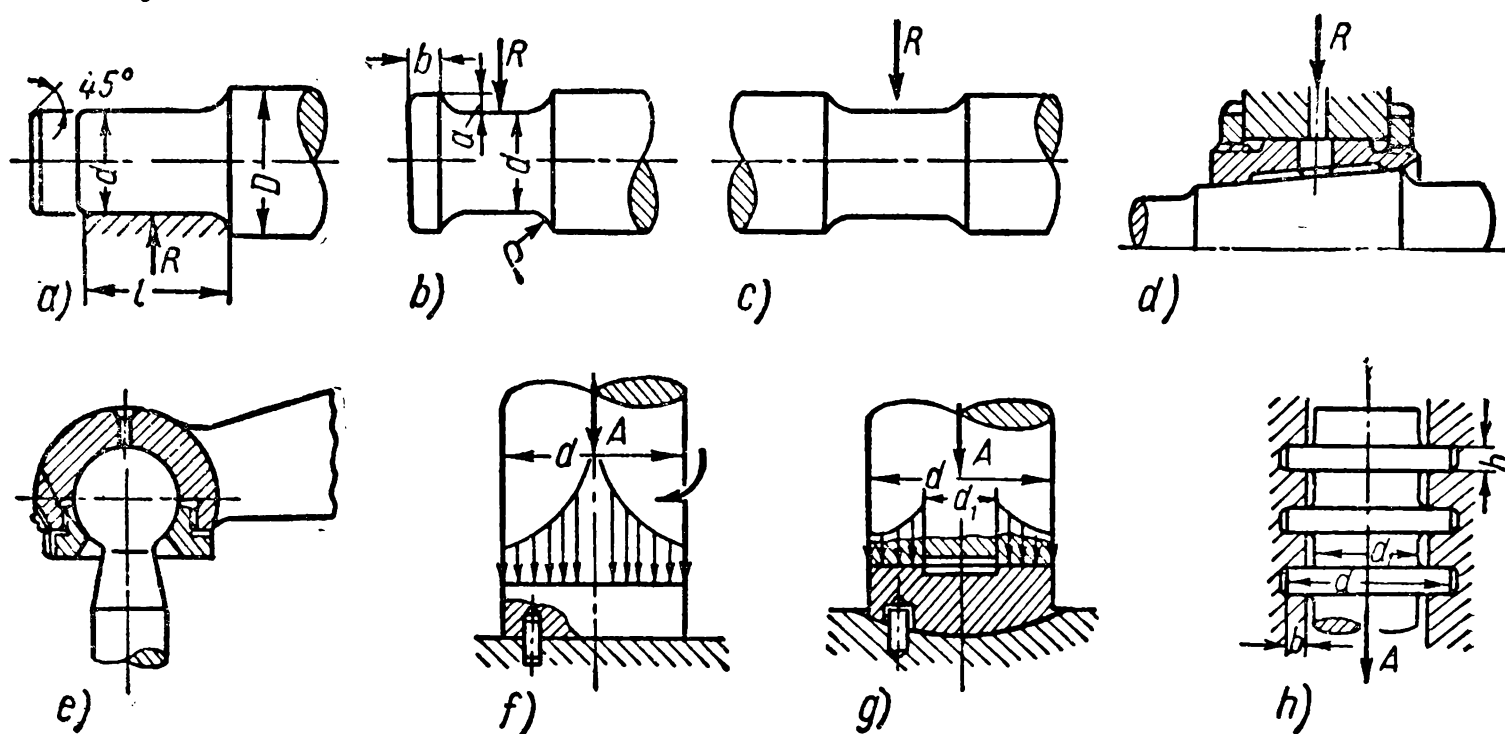


Fig. 208

Taper journals (Fig. 208, *d*) are used when the radial clearance has to be adjusted during operation. The adjustment is done by shifting the shaft or bearing in an axial direction.

Ball journals (Fig. 208, *e*) are employed to provide for an angular displacement of journals. Since it is difficult to machine the surfaces of the journal and bore such bearings with adequate precision their application is extremely limited.

The working surface of a solid thrust bearing (Fig. 208, *f*) is the flat end-face of a shaft or axle. Analysis shows that unit pressures on such end-faces are not spread uniformly. A ring thrust bearing (Fig. 208, *g*) allows a more uniform pressure distribution.

When the designed unit pressure on the surface of a ring thrust bearing exceeds the allowable magnitude use is sometimes made of multi-collar thrust bearing (Fig. 208, *h*). As structural modifications of ring thrust bearing they allow the load to be distributed (although not uniformly) between several parallel ring thrust bear-

ings. The main disadvantages of such a design are the following: relatively high losses due to friction and the difficulty of production and assembly arising from the tendency to make all collars take the load.

The length of the shaft or axle depends on the number of fitted-on parts and their width, the location of the bearings and their design, etc. To reduce the weight and cost of these parts the length of the shaft should be reduced as much as possible; this in turn tends to decrease the diameter of the designed part.

For various reasons long shafts are built up of several sections.

Hollow shafts and axles considerably reduce weight without noticeably affecting the section modulus  $W$ . Fig. 209 shows how the relation  $\beta = \frac{d_1}{d_2}$  affects the section modulus and the weight of an axle.

It can be seen from the diagram that at certain values of  $\beta$  (for instance,  $\beta=0.4-0.5$ ) hollow shafts and axles while markedly lighter in weight have a negligible effect on the magnitude of  $W$ . This phenomenon is utilised where minimum weight is a prime concern.

In complex designs of machines of reduced size other elements (shafts, tie-rods, etc.) are sometimes assembled in or passed through the bores of shafts and axles to simplify the design.

**Kinds and Causes of Failure in Shafts and Axles and Defects in Operation.** Shafts and axles usually fail due to fatigue.

The causes of such failure are as follows:

1) the presence of cyclic overloads due to the incorrect estimation by the designers of the magnitude and nature of load acting during operation;

2) stress concentration due to production or operation causes (undercuts, machining traces, notches and other points of stress concentration);

3) violation of technical norms (wrong adjustment of the bearings, insufficient clearances, etc).

More often than not failure due to fatigue begins to develop in points of maximum stress concentration. These include: fillets 1 (Fig. 210), keyways 2, drilled holes 3, portions with pressed-on parts 4, etc.

The calculation of shafts and axles for volume strength is therefore an extremely important stage of their design.

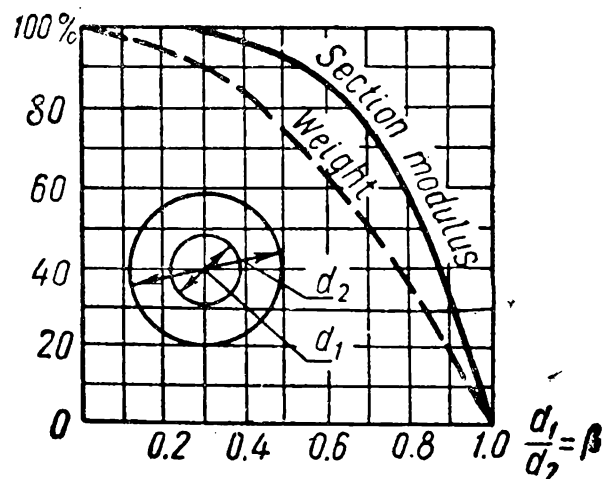


Fig. 209

When shafts and revolving axles are assembled in sliding contact bearings the lubrication conditions may be violated. As a rule, this leads to a faster rate of wear of the bearing shell and sometimes of the journal, a phenomenon accompanied by an intensive generation of heat. In this case seizure, scoring and melting out of the backing may make further operation impossible. Every design should be proof against such defects.

An adequate bending stiffness of shafts and axles is very important for the normal operation of every unit and of the entire machine. Excessive flexure of these components can lead to unfavorable operating conditions of bearings (a shift of the journal in the bearing alters the clearance space and hence the thickness of the oil film, sometimes causing it to break) and hinder the proper interaction

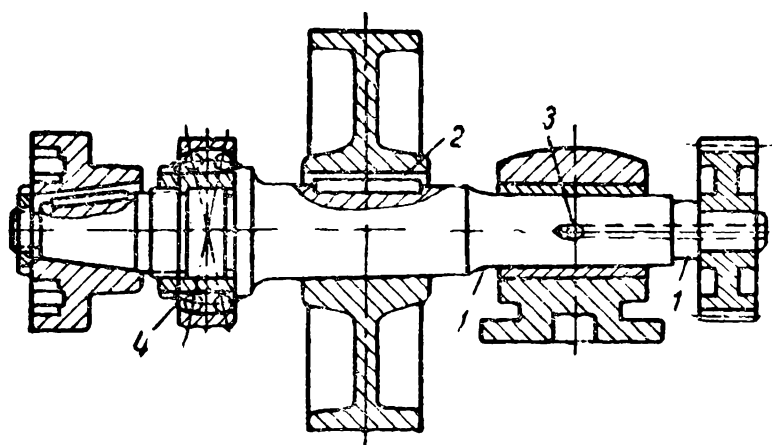


Fig. 210

of the conjugate parts mounted on the shafts. Insufficient rigidity of spindles in metal-cutting machine tools is directly responsible for the inadequate precision and surface finish of the components machined.

In some designs it is extremely important to limit the torsional deflection of shafts.

For example, in transmission shafts of travel mechanisms of overhead cranes this protects the bridges of cranes from misalignment.

At high angles of twist of a splined shaft, the splines assume the form of spirals which tend to displace axially the movable toothed wheels mounted on the shaft. This unfavourably affects their meshing.

Shafts sometimes fail as a result of transverse or torsional vibrations.

Shafts should therefore always be checked for vibrational stability while measures should be taken to preclude dangerous transverse or torsional vibrations. The design of shafts for torsional vibrations is beyond the scope of this book; it forms the subject of special courses and textbooks.

**Materials for Shafts and Axles.** In accordance with the operating conditions of axles and shafts which we have considered, the materials employed for their manufacture should possess: sufficiently high strength characteristics, a low sensitivity to stress concentration, the ability to withstand heat and case-hardening treatment to lessen the effect of stress concentration and increase the wear resistance of journals, and good machinability.

To meet these requirements shafts and axles are made from carbon steel of grades 25, 30, 40, and 45 and normalised and tempered steels 3, 4 and 5. Steel 45, which possesses good machinability, is in most frequent use. Adequate heat treatment can impart to it high mechanical properties: up to  $\sigma_{ult} \geq 80 \text{ kg/mm}^2$  and  $\sigma_y \geq 55 \text{ kg/mm}^2$ . The greater local hardness required to increase the wear resistance of the journals is obtained by hardening and tempering this steel to  $R_C = 40-50$ .

In order to obtain minimum diameters and increased wear resistance of heavily loaded shafts they are made from alloy steels of various grades treated by heat and case-hardening methods. However, high cost of these steels and also their increased sensitivity to stress concentration reduce the sphere of their application. Besides, the high mechanical properties of alloy steel can not always be utilised to the best advantage since the small shaft diameter obtained in design often fails to guarantee the required rigidity.

With the development of methods of heat and case-hardening treatment carbon structural steels are ousting alloy steels from many branches of industry where they were used on a large scale until recently.

Recent years have witnessed a tendency towards the manufacture of axles and shafts from inoculated cast iron, which is distinguished by high strength, low sensitivity to the action of design and other stress concentration points and, compared with steel, superior ability to damp vibrations.

**Calculation for Strength.** A shaft or axle is designed for strength on the basis of a scheme set out in advance. In doing this shafts and axles of ordinary design are regarded as beams resting in fulcrum supports.

Such a scheme corresponds to the case of these parts being mounted in antifriction bearings—one in each bearing or two in each bearing, if it is a self-aligning type. If this condition is neglected the shaft should be calculated as resting in two bearings (one in each bearing, the external bearings being ignored).

If the shaft or axle is assembled in short sliding contact bearings the bearing pressures are regarded as being applied in the middle of the bearing length; with long sliding bearings which do not self-align the bearing pressures should be regarded as being applied at a distance of  $1/3-1/4$  of the bearing length from the edge on the side of the span.

Line shafts are usually calculated for each span with subsequent checking (obligatory in important cases) of the deflection of the intermediate bearings.

In many cases the effect of the weight of the shaft or axle and that of the fitted-on parts may be neglected. We may also neglect (without

excessive error) the magnitude of moment of friction forces in the bearings.

Since the nature of load distribution over the surfaces is frequently not known, the design load is assumed either to be uniformly spread or, more frequently, concentrated.

The scheme drawn up makes it possible to determine the required dimensions of the component with the aid of formulae from the theory of the strength of materials, the values of allowable stresses being specified for each given material.

These are *preliminary* calculations.

The proportions found at this stage allow the shaft or axle to be given the required form taking into account production, assembly and other factors. After this it is possible to find the design margins of safety in the dangerous cross-sections by means of revised calculations and by the comparison of these with the admissible values. If necessary the design is altered after which the values of the safety margins are calculated again.

By consecutive approximation we can establish the required proportion between the design and allowable values of the safety margins.

*Preliminary calculations of shafts and axles.* The most frequent case is that where the shaft is loaded simultaneously with the torque  $M_t$  and the bending moment  $M$ .

Sometimes separate sections of shafts may be additionally loaded in tension or compression.

If the shaft takes loads lying in different planes they should be resolved into components in two mutually perpendicular planes common to all loads, after which the known rules are used to find the bearing pressures.

The diagrams of bending moments are plotted for each plane of load resolution which in turn are used to construct the total (resultant) diagram by geometrical summation of the bending moments:

$$M = \sqrt{M_h^2 + M_v^2}.$$

With a diagram of operating torques at hand we can now find for corresponding sections the values of reduced moments. From the strength condition we find the shaft diameters in the design cross-sections.

Torque ordinarily either changes in magnitude alone (not in sign) or remains constant; tangential stresses change accordingly.

The sequence of preliminary calculations of a shaft can be illustrated by an example. Let us take the shaft of a worm gear. Fig. 211 shows the design diagram and the forces acting upon the shaft of the worm (see "Worm Gears", p. 324).<sup>1</sup>

The peripheral effort on the worm wheel  $P_w$  acting along the worm ( $P_a = P_w$ ) bends the shaft (diagram of the bending moments is plotted in Fig. 211, *a*) and at the same time compresses or extends it depending on how and where the shaft is fastened to prevent axial shift. In the diagram the worm shaft in the section *cd* is in compression.

The radial force  $P_r$  bends the worm shaft in the same plane (Fig. 211, *b*).

The peripheral force on the worm  $P_{w0}$  bends the shaft in a plane perpendicular to that in which the forces  $P_a$  and  $P_r$  are acting (Fig. 211, *c*).

Finally, if we neglect the weight of the parts fitted on the shaft end we can assume that in the section *ac* the shaft is loaded only in torque (Fig. 211, *d*).

$$M_t = 71,620 \frac{N}{n} \text{ kg/cm}$$

where  $N$  is the design power in h. p. and  $n$  is the shaft rpm.

On the basis of diagrams of bending moments acting in different planes we find the summation diagram of bending moments.

For an arbitrary section  $x$

$$M_x = \sqrt{(M_{dx} + M_{rx})^2 + (M_{wox})^2}.$$

The reduced moments  $M_{red}$  for design sections (in the given case in the section *bc*) are usually found from the 3rd theory of strength in accordance with which

$$M_{red} = \sqrt{M^2 + M_t^2}$$

if we disregard the difference in the stress change conditions due to bending and torsion. If it is taken into account, then

$$M_{red} = \sqrt{M^2 + (\alpha M_t)^2} \quad (355)$$

where  $\alpha$  is a correction factor whose value is determined when specifying allowable stresses.

The diameters of the shaft in the design sections are found from the strength condition

$$M_{red} = W [\sigma]_b.$$

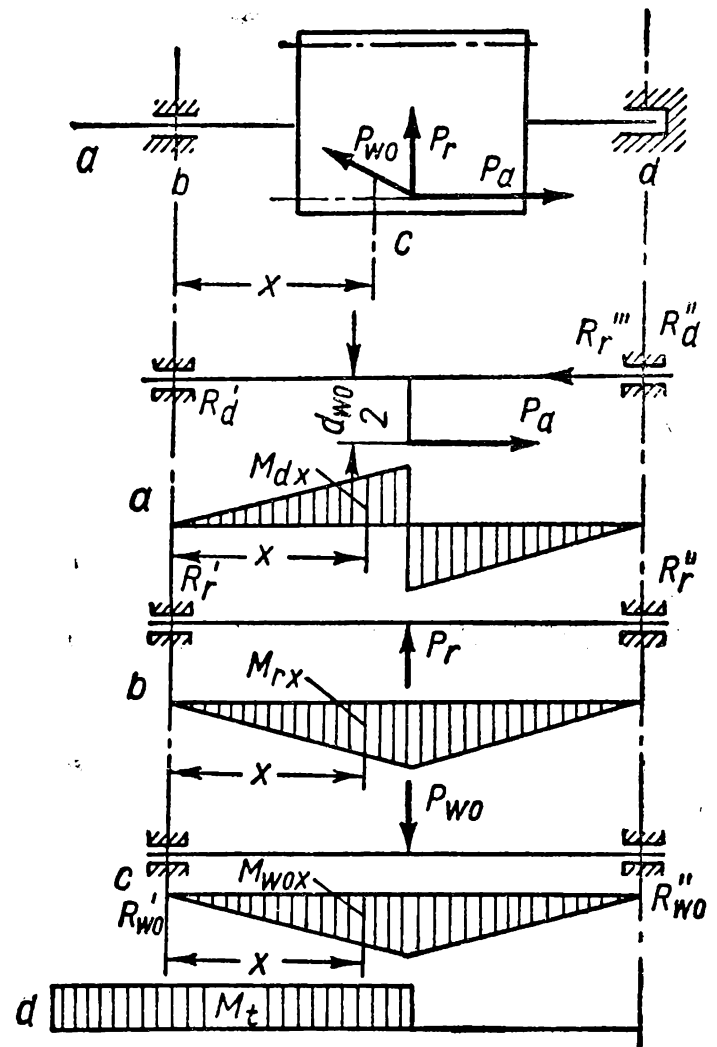


Fig. 211

The section modulus in bending is equal to  $W=0.1 d^3$  for a round solid shaft and  $W=0.1 (1-\beta^4)d^3$  for a hollow shaft; here  $\beta$  is the ratio between the shaft inside diameter and its outside diameter.

The values of allowable stresses  $[\sigma]_b$  for preliminary calculations of shafts and axles are different for different materials and depend on the operating conditions.

Here we differentiate:

service I, when the stresses caused by load remain constant in magnitude and sign;

service II, when the stresses change in a pulsating cycle;

service III, when the nature of change in stress is a symmetric cycle.

The values of allowable stresses for carbon and alloy steels according to conditions of operation correspond roughly to the following ratios:

$$[\sigma]_{bI} : [\sigma]_{bII} : [\sigma]_{bIII} = 3.8 : 1.7 : 1;$$

in this case

$$[\sigma]_{bI} \approx 0.33\sigma_{ul}.$$

For a preliminary calculation of the shaft diameter  $[\sigma]_b$  is selected according to service III.

When the tangential stresses change in a pulsating cycle the values of  $M_t$  are decreased by introducing the reduction factor  $\alpha = \frac{[\sigma]_{bIII}}{[\sigma]_{bII}} < 1$

in order to assess correctly the role of these stresses. If the tangential stresses change in accordance with a symmetric cycle, then  $\alpha=1$ .

Thus we find the diameter of a solid shaft from the strength condition in the following way:

$$d = \sqrt[3]{\frac{\sqrt{M^2 + (\alpha M_t)^2}}{0.1 [\sigma]_{bIII}}} \text{ cm.} \quad (356)$$

We can use the formula (356) to determine the shaft diameters at various points of the section  $bc$  (Fig. 211).

Bearing in mind the fact that the shaft should be given a form which will satisfy the requirements of production, convenience of assembly, etc., it is enough to calculate the diameters for several characteristic cross-sections and determine the form of the shaft in separate cross-sections and along the entire length.

The shaft diameters in the section  $cd$  (Fig. 211) can be calculated taking into account the fact that it is here relieved from the action of torque (the moment of friction forces in the bearings can be neglected) and that additional stresses due to the compressive force  $P_a$  act in these cross-sections. These stresses are, as a rule, insignificant as compared to the bending stresses. Besides, when adding them



to the bending stresses the nature of change of these stresses should be allowed for and, hence, the total normal stress is

$$\sigma = \sigma_b + \alpha \sigma_c$$

where  $\alpha$  is the reduction factor (p. 401).

It has also to be borne in mind that the appearance of compressive stresses of such force and at such nature of loading may even have a positive effect: the stresses in the elongated zone of the shaft in bending decrease thereby promoting its endurance.

For this reason those designs are preferred which cause the axial load to develop compressive, and not tensile, stresses in the shaft cross-sections (provided the shaft is sufficiently stable).

The worm shaft in the section  $cd$ , which is not so heavily loaded, can therefore be designed on the basis of the design data obtained for the section  $bc$ .

Preliminary calculations of some shaft designs can be carried out taking into account only the magnitude of the transmitted torque if the acting bending moments cause low stresses in the cross-sections. This is sometimes possible in designs of high-speed drives of comparatively low power.

In such cases the strength is calculated on the basis of reduced magnitudes of allowable torsional stresses to compensate for the bending stresses which are ignored. Here the strength condition is

$$M_t = W_t [\tau]_t.$$

The section modulus in torsion is:

$W_t = 0.2d^3$  for a solid round shaft and  $W_t = 0.2(1 - \beta^4)d^3$  for a hollow shaft where  $\beta$  has the former value. Since

$$M_t = 71,620 \frac{N}{n} \text{ kg/cm},$$

then, for a solid shaft,

$$d = \sqrt[3]{\frac{71,620 \times N}{n \times 0.2 \times [\tau]_t}} = A \sqrt[3]{\frac{N}{n}} \text{ cm} \quad (357)$$

where  $A$  is a factor depending on the allowable stress in torsion  $[\tau]_t$ . Its magnitude varies from 9 to 14.4, which corresponds to the allowable stresses in torsion for steel 4:  $[\tau]_t = (490-120) \text{ kg/cm}^2$ .

Preliminary calculations of solid axles can be carried out by the formula (356) assuming  $M_t = 0$ .

In this case the diameters of the axle in the design cross-sections are equal to:

$$d = \sqrt[3]{\frac{M}{0.1 [\sigma]_b}} \text{ cm.} \quad (358)$$

When calculating revolving axles  $[\sigma]_b$  is selected according to service III —  $[\sigma]_{bIII}$ ; when calculating fixed axles, depending on the nature of stress variation created by external load, we should introduce in the formula  $[\sigma]_{bII}$  or  $[\sigma]_{bI}$ .

For hollow shafts and axles the formulae (356), (357) and (358) are written thus:

$$d = \sqrt[3]{\frac{\sqrt{M^2 + (\alpha M_t)^2}}{0.1 (1 - \beta^4) [\sigma]_{bIII}}} \text{ cm}; \quad (356')$$

$$d = \sqrt[3]{\frac{71,620 \times N}{n \times 0.2 (1 - \beta^4) [\tau]_t}} = A \sqrt[3]{\frac{N}{(1 - \beta^4) n}} \text{ cm}; \quad (357')$$

$$d = \sqrt[3]{\frac{M}{0.1 (1 - \beta^4) [\sigma]_b}} \text{ cm}. \quad (358')$$

The cross-sections of a shaft (axle) intended to support parts secured by keys or interference fits should be increased in diameter (by 8-10%) to compensate for the weakening of the shaft.

The diameters at the ends of a shaft (axle) determine the diameters of journals since the latter are calculated for volume strength in the same way as the respective sections of the shaft.

The length of the carrying sections, determined by the relation  $\varphi = \frac{l}{d}$  where  $l$  and  $d$  are the length and diameter of the support, depends on the design of the bearing and can be finally evaluated only after proper calculation of the bearing.

For sliding contact bearings  $\varphi = 0.4-1.5$  and sometimes reaches  $\varphi = 3$ . A natural tendency is to decrease the length of such bearings and consequently the length of the journals.

In high-speed designs dimensions of the journals found from the strength condition do not always ensure adequate size. In such designs the proportions of antifriction or sliding contact bearings found from the condition of their operating ability determine the size  $l$  and  $d$  of the journals. Revised calculations of such designs for strength show the stresses frequently to be below the allowable values.

*Revised calculation of shafts and axles.* The proportions of a shaft (axle) found after preliminary calculations and structural designing are subjected to revised calculations to determine the design margins of safety in the dangerous cross-sections. For this purpose use is made of the formulae given before (p. 40):

$$n = \frac{1}{\sqrt{\left(\frac{1}{n_\sigma}\right)^2 + \left(\frac{1}{n_\tau}\right)^2}} \quad (359)$$

where

$$n_{\sigma} = \frac{\sigma_{-1}}{\frac{k_{\sigma}}{\varepsilon_{\sigma}} \sigma_a + \psi_{\sigma} \sigma_m} \text{---margin of safety accounting only for bending;}$$

$$n_{\tau} = \frac{\tau_{-1}}{\frac{k_{\tau}}{\varepsilon_{\tau}} \tau_a + \psi_{\tau} \tau_m} \text{---margin of safety accounting only for torsion.}$$

Since for axles  $\tau = 0$ , then for them  $n = n_{\sigma}$ .

With a symmetric cycle of loading typical of revolving axles  $\sigma_m = 0$  and, hence,

$$n = \frac{\varepsilon_{\sigma} \sigma_{-1}}{k_{\sigma} \sigma_a}. \quad (360)$$

For fixed axles when the law of stress variation corresponds to a pulsating cycle the formula can be written thus

$$n = \frac{2\sigma_{-1}}{\sigma_{max} \left( \frac{k_{\sigma}}{\varepsilon_{\sigma}} + \psi_{\sigma} \right)}. \quad (361)$$

The values  $\sigma_a$  and  $\sigma_m$  are found as follows: when the stresses change according to a symmetric law

$$\sigma_m = 0; \quad \sigma_a = \sigma_{max} = \frac{M}{W_{net}}$$

and

$$\tau_m = 0; \quad \tau_a = \tau_{max} = \frac{M_t}{W_{t\ net}}.$$

When the stresses change according to a pulsating cycle

$$\sigma_m = \sigma_a = \frac{\sigma_{max}}{2} \text{ and } \tau_m = \tau_a = \frac{\tau_{max}}{2}$$

where

$$\sigma_{max} = \frac{M}{W_{net}} \text{ and } \tau_{max} = \frac{M_t}{W_{t\ net}}.$$

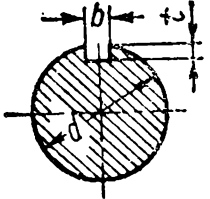
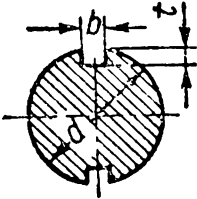
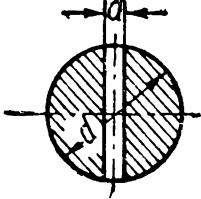
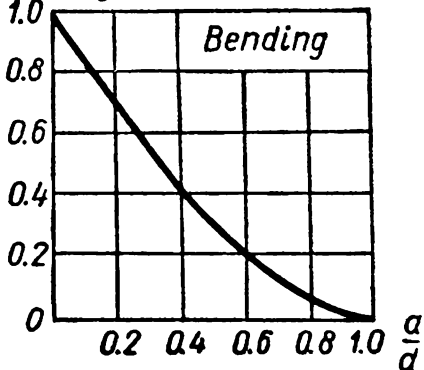
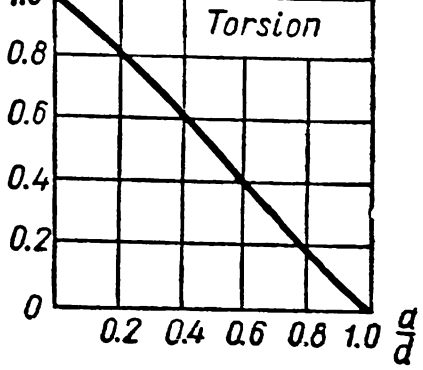
The approximate formulae for the calculation of  $W_{net}$  and  $W_{t\ net}$  for some cross-sections are given in Table 60.

The approximate values of the factors  $\psi_{\sigma}$  and  $\psi_{\tau}$  taking into account the diameter of the blank and its hardness are as follows: for steel 5 with a blank of any diameter and  $H_B \geq 190$ :  $\psi_{\sigma} = 0$ ;  $\psi_{\tau} = 0$ ; for steel 45 at  $d \leq 120$  mm and  $H_B \geq 240$ :  $\psi_{\sigma} = 0.1$ ;  $\psi_{\tau} = 0$ ; for the same steel at  $d \leq 80$  mm and  $H_B \geq 270$ :  $\psi_{\sigma} = 0.1$ ;  $\psi_{\tau} = 0.05$ , etc.

For a minimum allowable margin of safety we may take  $n_{min} = 1.3-1.5$  if the loads and stresses have been determined accurately. Otherwise,  $n = 1.5-2.5$  and over depending on the degree of importance of the design, the accuracy of the design data, etc.

Table 60

Formulae for Calculating  $W_{net}$  and  $W_{t\ net}$  for Some Cross-Sections

Cross-section	Bending	Torsion
	$W_{net} \approx \frac{\pi d^3}{32} - \frac{bt(d-t)^2}{2d}$	$W_{t\ net} \approx \frac{\pi d^3}{16} - \frac{bt(d-t)^2}{2d}$
	$W_{net} \approx \frac{\pi d^3}{32} - \frac{bt(d-t)^2}{d}$	$W_{t\ net} \approx \frac{\pi d^3}{16} - \frac{bt(d-t)^2}{d}$
	$W_{net} = \xi W_{gross} = \xi \frac{\pi d^3}{32}$ <div><math display="block">\xi = \frac{W_{net}}{W_{gross}}</math></div>	$W_{t\ net} = \xi W_{t\ gross} = \xi \frac{\pi d^3}{16}$ <div><math display="block">\xi = \frac{W_{t\ net}}{W_{t\ gross}}</math></div>

**Calculation for Stiffness.** *Flexural strain of axles and shafts.* Stiffness is calculated for the purpose of determining deflections and the angles of inclination of the elastic curve of the axle in definite cross-sections. The calculations are done by the methods outlined in the theory of strength of materials.

As a rule, it is extremely difficult to find these magnitudes accurately, due to the effect of the rigidity of the bearing housings of a shaft or axle, clearances, local forms of the shaft, etc. For this reason, design for rigidity is usually arbitrary. The degree of rigidity can be assessed only after comparing the design values with the allowable values of deflection and the angles of inclination of the elastic curve obtained from observations of systems operating satisfactorily. The latter circumstance has led to the employment by

various branches of mechanical engineering of their own standards which are established in accordance with that factor which is definitive for a given design. For example, some machine-tool building plants take the magnitude of the maximum deflection of shaft to equal 0.01 of the minimum module of toothed wheels fitted onto the shaft, in order to ensure satisfactory operation of the toothed gear. For an electric motor the maximum deflection of shaft should be coordinated with the mean size of the air gap  $\delta$ ; for an asynchronous motor the standard is  $y_{\max} \leq 0.1\delta$ , etc.

The following standards are widely used in Soviet mechanical engineering: the maximum deflection of shaft (axle) should not exceed 0.0002 of the span between the bearings; the maximum angle of inclination in a sliding contact bearing is 0.001 radian (3', 5); for a radial ball bearing the angle of misalignment of the races should not exceed 0.008 radian, for a self-aligning bearing—0.05 radian, etc.

In general the deflection depends on the magnitude of applied load and its location on the span. The deflection can be decreased by the following methods:

1) parts mounted on axles and shafts should be arranged as close to the bearings as possible;

2) pulleys, toothed wheels and other parts fitted onto axles and shafts should be of the light-weight type;

3) parts should be balanced; the shafts of high-speed systems should be balanced together with the parts secured on them.

*Torsional deflection of shafts.* In calculating shafts for torsional deflection their stiffness should be evaluated by the angle of twist  $\varphi$ .

For a smooth shaft of constant diameter (or for a cylindrical section of a shaft)

$$\varphi = \frac{M_t l}{G \times I_p} \quad (362)$$

where  $I_p$  is the polar moment of inertia of the cross-section in  $\text{cm}^4$ ;

$G$ —the torsional modulus of elasticity in  $\text{kg/cm}^2$ ;

$M_t$ —the torque operating within the calculated section of the shaft of length  $l$ , in  $\text{kg/cm}$ .

The formula (362) can also be used when the calculated section of the shaft has short tapered portions, transverse holes of small diameter, short individual keyways,\* etc., which in this case are neglected.

---

\* According to data provided by P. F. Papkovich, one keyway of a rectangular section decreases shaft rigidity by approximately 5%, two keyways for tangential keys—by 18%, while four splined slots decrease it by about 24%.

Remembering that  $M_t = 71,620 \frac{N}{n}$  kg/cm and  $I_p = \frac{\pi d^4}{32}$  cm<sup>4</sup> the formula (362) can be written thus

$$d = A_1 \sqrt{\frac{N}{n}} \text{ cm.} \quad (363)$$

The factor  $A_1$  for the given material depends on the accepted value of  $\varphi$  which is the maximum allowable angle of twist per linear metre. When  $\varphi = (0.25-2.5)^\circ$  and  $G = 8 \times 10^5$  kg/cm<sup>2</sup> for steel shafts the factor  $A_1 = 12-6.8$ .

The standards for the allowable angles of twist in shafts are differentiated for some designs of machines.

For the spindles of drilling machines the standard is: the angle of twist at maximum torque should not exceed  $1^\circ$  over the length  $L = (20-25)D$  where  $D$  is the outside diameter of the spindle.

For some designs these standards should be very strict: when designing the travel mechanism for gantry cranes the limitation of the torsional deflection of the transmission shaft is the principle design factor and the allowable angle of twist for different designs varies within  $\varphi \approx (0.25-0.35)^\circ$  per linear metre.

In calculating high-speed shafts loaded with small torsional and bending moments the determination of their diameters by formula (357), although ensuring the required strength, fails to make the shafts sufficiently rigid. Therefore, the formula (363) can be recommended for the preliminary determination of the proportions of such shafts.

**Methods of Increasing the Endurance of Shafts and Axles.** Methods of increasing the strength of axles and shafts have as their aim either the complete elimination of the causes of stress concentration or the quest for such designs as will reduce the magnitude of the effective concentration factor to the minimum.

This emphasises the importance of never letting any stress concentration points be formed on the component surface unless they are inevitable.

A bead is frequently provided on the shaft to prevent a part fitted to it from moving axially. At the same time the stress concentration factor is determined not only by the magnitude  $q$  but also by the ratio  $\frac{D}{d}$  (Fig. 208, *a*).

For this reason, the diameter of shaft should never be increased by beads for «design considerations» unless absolutely necessary.

The effective stress concentration factor can be reduced by means of relieving grooves (Fig. 212, *b*).

A part can sometimes be reliably secured by means of spacers or other methods in order to dispense with beads.

Close attention should be given to the formation of keyways; usually they are undercut at the corners and have abrupt changes of cross-section liable to cause serious damage. Investigations have proved the importance of the form of the longitudinal section of the keyway: as a rule, failure occurs at the keyway end, in the section *I-I* (Fig. 213). The effective stress concentration factor for parts grooved with a double-side milling cutter (with a smooth end, diagram *b*) is approximately 30% less than for those with the end obtained when the groove is made by an ordinary keyway cutter (diagram *a*).

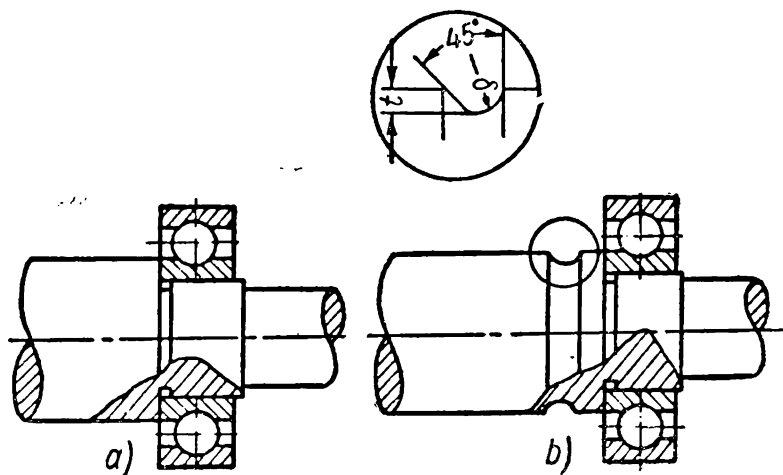


Fig. 212

The fillet radius  $q$  of the inner angles has a marked effect on the shaft endurance. As the ratio  $\frac{q}{b}$  increases the effective stress concentration factor diminishes considerably.

When designing splined shafts the advantages inherent in an involute profile should never be forgotten. The stress concentration factors in torsion amount for straight-sided splines to  $k_\tau \approx 2$  and for involute splines to  $k_\tau \approx 1.2-1.3$ .

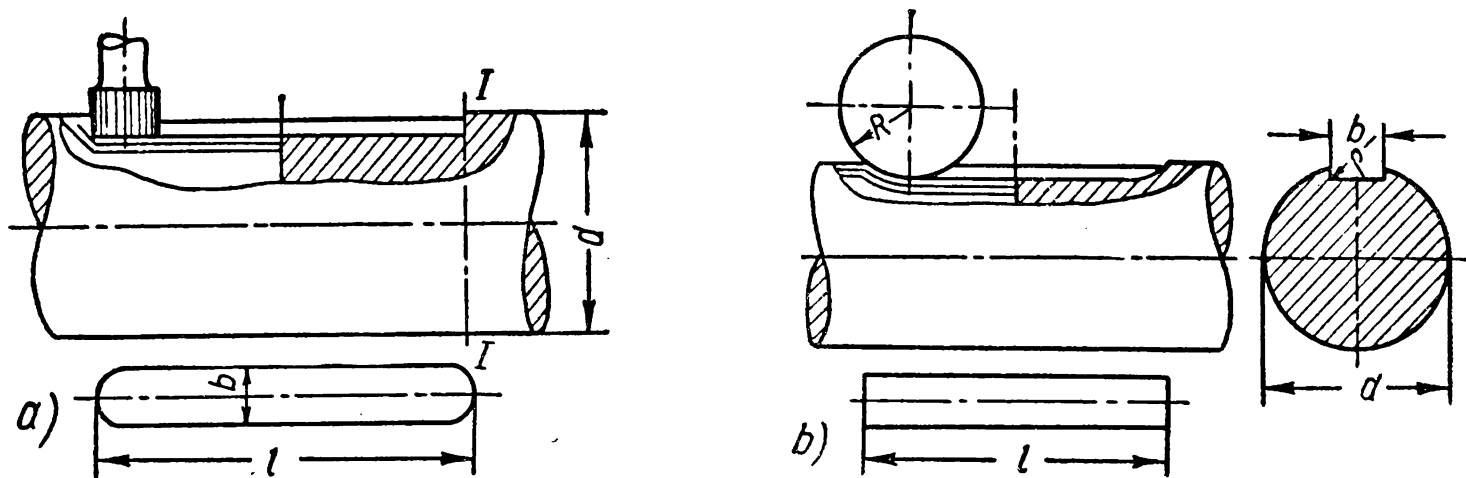


Fig. 213

To increase the endurance of splined shafts preference should be given to involute splines.

Transverse holes, both through and blind, somewhat lessen the endurance of shafts and axles. Since cracks due to fatigue develop as a rule at the hole edges these are countersunk or chamfered to weaken the effect of these concentration points.

The diagram of pressure distribution in a flexed shaft or axle with a pressed-on hub of ordinary design (Fig. 214) shows that the surface pressure of the hub end sections on the surface layers sharply increases causing stress concentration to arise in the respective cross-sections of shafts and axles. An increase in the yielding of the hub in its end cross-sections brought about by relieving recesses and a smooth transition from the maximum diameter of the hub to the axle (Fig. 62) will obviously tend to diminish the concentration of these stresses. According to some data a proper choice of the form of a shaft and hub can increase its endurance 1.5-2 times.

Approximately the same design problems occur in dealing with inner races of antifriction bearings, because their arrangement on the shaft decreases the strength of the latter in about the same way as the pressing-on of parts with hubs without relieving recesses.

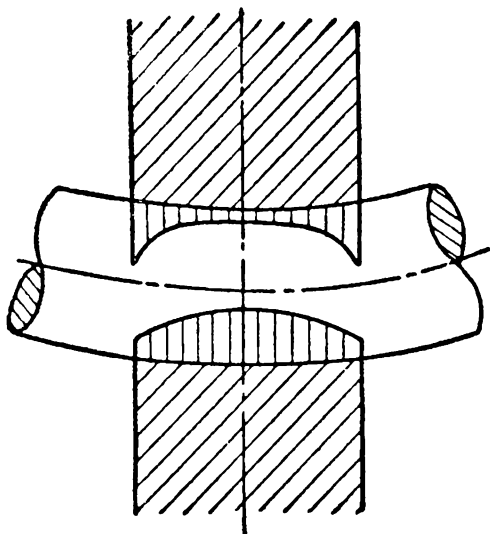


Fig. 214

On the basis of the fact that for structural steel the fatigue strength in compression is greater than that in tension Academician E. A. Chudakov suggested that for a better use of metal the section of a part in repeated bending should be given such forms as would load the compressed zones to a greater extent than the extended zones; this is possible with asymmetric cross-sections. The value of this suggestion has been confirmed both by specially arranged experiments and by operating evidence. Thus,

automobile axles which take fluctuating load in the most dangerous cross-section are usually made asymmetric with the maximum stresses in the zone of compression.

Obviously, such recommendations are applicable in all cases of the design of stationary axles.

The wear resistance of the carrying sections of axles and shafts can be increased by different methods of heat and case-hardening treatment.

The best method of increasing the wear resistance is that of nitriding which ensures a high and homogeneous hardness of the surface.

**Transverse Vibrations of Shafts. Critical Shaft Velocity.** The calculations of the shaft for transverse vibrations are done to safeguard it against resonance when the vibration amplitude sharply increases and can reach values which will cause failure of the shaft. Resonance sets in when the shaft velocity reaches a *critical* point at which the frequency of variation of the external forces coincides with the frequency of vibration of the system comprising the shaft and parts fitted to it. Resonance can also occur when the frequency of variation



of the external forces is a multiple of the frequency of the system vibrations.

Let a disc of weight  $G$  whose centre of gravity is displaced relative to the axis of rotation by the magnitude  $e$  be mounted on a shaft (Fig. 215). As the shaft and the disc rotate uniformly the centrifugal force  $C$  will cause the shaft to deflect.

The centrifugal force  $C = m\omega^2(y + e)$ . Neglecting the effect of the weight of the system the amount of deflection  $y$  for the accepted design (analogous to a simple beam) is equal to

$$y = \frac{CL^3}{48EI}$$

whence

$$C = \frac{48EI}{L^3} y = ky,$$

where  $k$  is the force causing the shaft deflection equal to unity, for example 1 cm.

In this manner,  $m(y + e)\omega^2 = ky$  and

$$y = \frac{e}{\frac{k}{m\omega^2} - 1}. \quad (364)$$

An increase in the angular velocity  $\omega$  causes the value of the deflection  $y$  to grow and at  $\omega = \sqrt{\frac{k}{m}}$ ,  $y \rightarrow \infty$ ; this means that at such angular velocity the shaft must fail.

The angular velocity in approaching to which the deflection grows infinitely is called *critical velocity*.

Hence,

$$\omega_{cr} = \sqrt{\frac{k}{m}}.$$

Since  $\omega_{cr} = \frac{\pi n_{cr}}{30} \text{ sec}^{-1}$ , then the critical velocity of the shaft per minute is

$$n_{cr} = \frac{30}{\pi} \sqrt{\frac{k}{m}} = \frac{30}{\pi} \sqrt{\frac{k \times g}{G}} \approx 300 \sqrt{\frac{k}{G}} \quad (365)$$

where  $g = 981 \text{ cm/sec}^2$  is the gravity acceleration.

The conclusions just arrived at also hold for the case where account is taken of the shaft deflection due to the weight of the system, since the system rotates relative to a shaft flexed under its own weight.

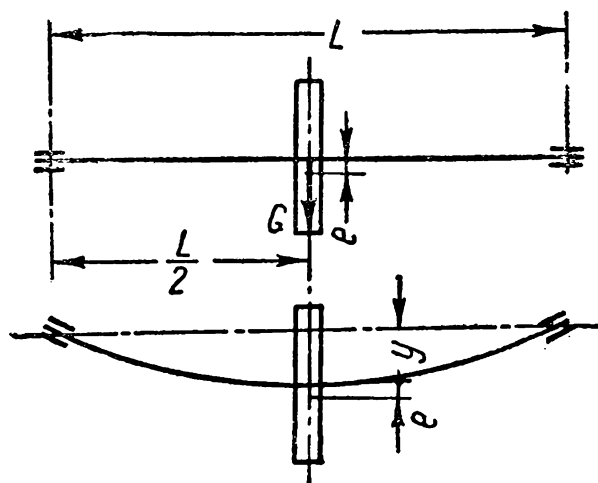


Fig. 215

Since  $f = \frac{G}{k}$  cm is the static deflection of the shaft from the weight ( $G$ ) of the part fitted onto the shaft, then

$$n_{cr} \approx 300 \sqrt{\frac{1}{f}}. \quad (366)$$

In this way the critical velocity of shaft can be easily obtained from the static deflection  $f$ .

Excessive vibration of the shaft indicates that its velocity is close to the critical point. If the shaft continues to operate in these conditions it will inevitably fail.

Because of different magnitudes of resistance arising during vibration (internal friction, friction in the bearings, effect of environment) the shaft does not fail suddenly. Since at  $\omega > \omega_{cr}$  the shaft deflection has the limit value, then if the shaft passes quickly through the zone of critical velocities its rotation becomes stable. Therefore, shafts can also operate at  $n > n_{cr}$ . Such shafts are called *flexible* shafts.

At  $\omega \rightarrow \infty$ ,  $y \rightarrow e$ , i. e., the shaft self-centres. The transition through the zone of critical velocities should be effected as quickly as possible. Incorporation of vibration dampers into the system is also very useful.

Thus, resonance can be eliminated by employing rigid shafts with a high natural frequency which effectively resist bending strain or thin little-vibrating flexible shafts with a low natural frequency which bend freely under the action of centrifugal forces and take a new form of elastic equilibrium.

At high velocities, for example, in centrifuges with  $n = 20,000$ – $40,000$  rpm, flexible shafts make not only simple and cheap designs but are the only possible solution.

It follows from the above that for high-speed shafts the careful balancing of the shaft together with all parts fitted on it is of extreme importance.

### FLEXIBLE WIRE SHAFTS

Flexible wire shafts (Fig. 216) transmit motion between parts whose axes of rotation are so arranged that it is impossible to effect a rigid coupling between them, or when in the process of operation the mutual position of the axes changes. Sometimes they are used to transmit rotation between coaxial shafts.

Flexible shafts are employed in the drives of concrete vibrators, devices for cleaning the hulls of ships, in mechanical picks, remote control instruments, etc. Especially widespread is the use of flexible shafts as the driving elements of various types of portable electrical tools which allow the mechanisation of many labour-consuming jobs.

There are three types of drive: power drives, control drives and

instrument drives. In all cases the drive comprises the following main elements: flexible shaft, shaft end-fittings and protection.

Fig. 217 shows a flexible power drive design. A typical drive of a control device (speedometer, tachometer, etc.) is shown in Fig. 218.

A flexible shaft (Fig. 216) is composed of consecutively wound layers of carbon steel or bronze wire. The first layer from the centre is wound around the central wire—the core—which can then either be removed from the shaft or left inside.

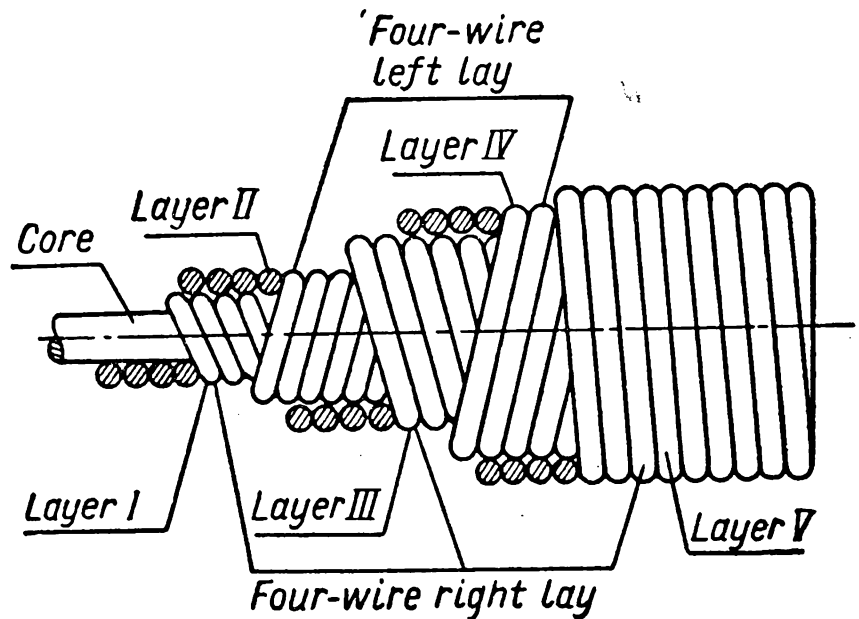


Fig. 216

In design a flexible shaft resembles a multi-wire helical spring with closely wound coils and layers. Adjoining layers are wound in opposite directions. The direction of shaft rotation should be

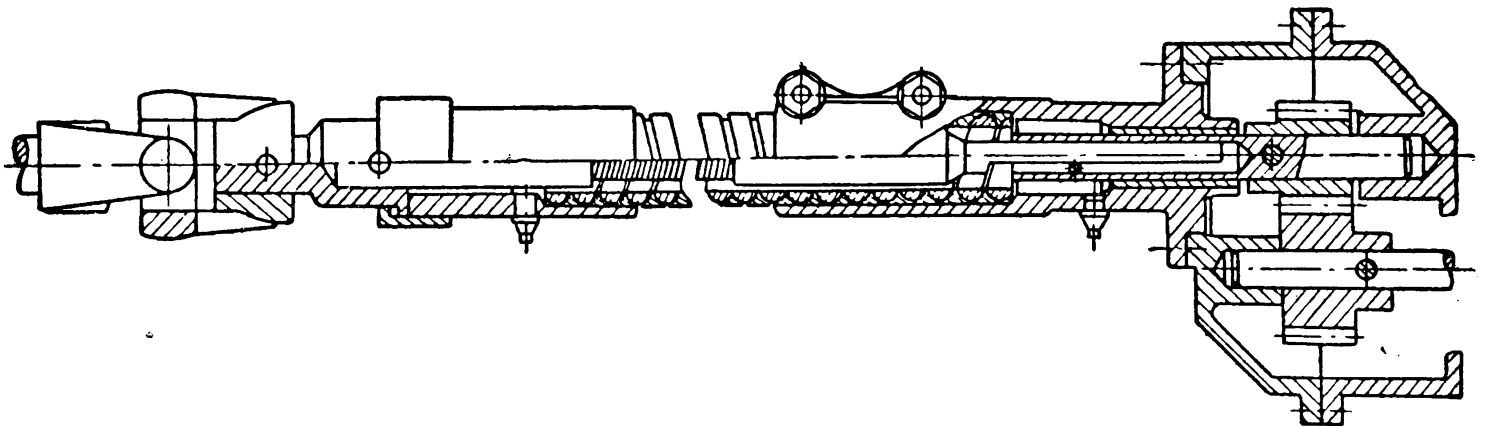


Fig. 217

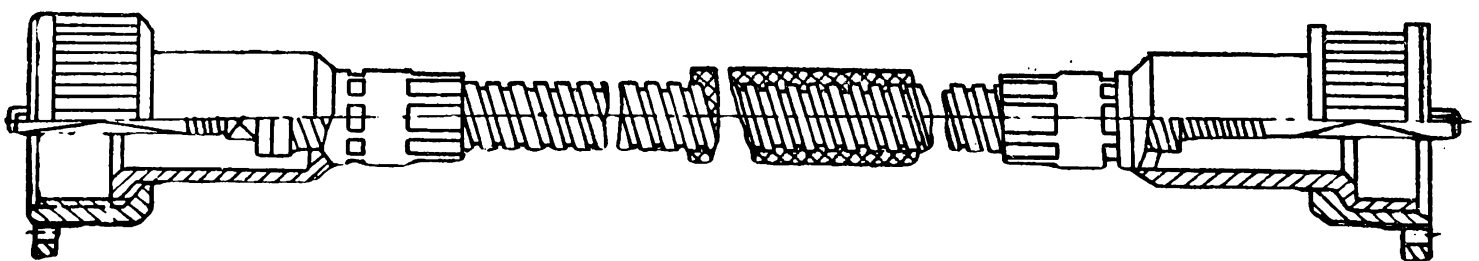


Fig. 218

such that in transmitting torque the spring forming the outer layer twists.

The wires usually increase in thickness from the centre to the outer layer and in items produced in quantity they vary from 0.3 to 3 mm; the number of wires in a layer is from 4 to 12 and the maximum number of layers is 8.

The Soviet industry produces two types of shafts: B1 with diameter 10 to 40 mm and B2 with diameter 4 to 8 mm. Shafts of type B1 ordinarily have a small number of wire layers (only when the shaft diameters exceed 12 mm does the number of layers exceed 4); B2 type shafts consist of many layers of thin wire always provided with a core.

Wear resistance and flexibility are the most important factors of flexible power shafts. For control drive shafts, besides flexibility, the essential feature is the torsional rigidity of the shaft. Shafts

composed of many layers of thin wire possess better flexibility.

The *casing* is a distinctive flexible bearing which takes the forces transmitted to the shaft. In addition it retains the grease on the shaft surface, protects the shaft from dirt, safeguards personnel and prevents shaft failure and the formation of loops in operation.

The *end-fittings* of flexible shafts are intended to couple the latter to the motor shaft and the shaft of the service machine.

The *end of the casing* is intended to connect the casing

to the motor and the service machine. At the same time it frequently acts as a bearing for the end-fittings.

At the moment the theory of flexible wire shafts does not yet allow their design calculation. Usually the task is reduced to selecting a shaft from the range produced by the industry in quantity according to the given load and depending on the kind of service.

*Example.* Calculate a shaft I of the reduction gear shown in Fig. 219. The torque on the shaft  $M_t = 51,500$  kg/cm. Standard  $20^\circ$  tooth form.

*Solution.* For material we take steel 45 with the following mechanical properties:  $\sigma_{ult} = 70$  kg/mm<sup>2</sup>;  $\sigma_y = 32$  kg/mm<sup>2</sup>;  $\sigma_{-1} = 30$  kg/mm<sup>2</sup>;  $\tau_{-1} = 18$  kg/mm<sup>2</sup>.

The peripheral effort on the toothed wheel 1 is

$$P_1 = \frac{2M_t}{m_1 z_1} = \frac{2 \times 51,500}{1.6 \times 16} = 4,000 \text{ kg.}$$

The normal pressure acting on the tooth of wheel 1 is

$$Q_1 = \frac{4,000}{\cos 20^\circ} = \frac{4,000}{0.94} = 4,250 \text{ kg.}$$

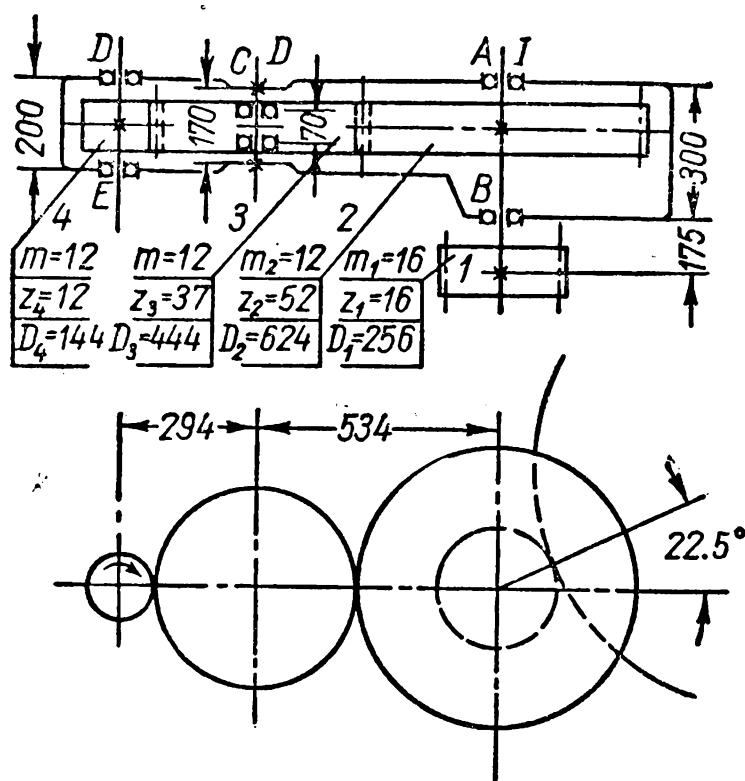


Fig. 219

The components of the normal pressure in horizontal and vertical planes:  
 $Q_{1h} = Q_1 \cos [(90^\circ - 22^\circ 30') - 20^\circ] = Q_1 \cos 47^\circ.5 = 4,250 \times 0.676 = 2,860 \text{ kg};$

$$Q_{1v} = Q_1 \sin 47^\circ.5 = 4,250 \times 0.737 = 3,100 \text{ kg}.$$

The peripheral effort on toothed wheel 2 (component in a vertical plane of normal pressure  $Q_2$  acting upon the tooth of wheel 2)

$$P_2 = \frac{2M_t}{m_2 z_2} = \frac{2 \times 51,500}{1.2 \times 52} = 1,650 \text{ kg}.$$

The thrust force (component in a horizontal plane of normal pressure  $Q_2$ ):

$$P_{r2} = 1,650 \times \tan 20^\circ = 1,650 \times 0.364 = 600 \text{ kg}.$$

Fig. 220, *a*, *b*, *c* shows the forces acting on the shaft in a horizontal and vertical planes and the diagrams of bending moments.

In the dangerous cross-section passing through the middle of the bearing *B* the total bending moment is:

$$M_B = \sqrt{50,000^2 + 54,000^2} = 74,000 \text{ kg/cm}.$$

The reduced moment in the same cross-section is

$$M_{red} = \sqrt{M^2 + (\alpha M_t)^2}$$

where  $\alpha = \frac{[\sigma]_{bIII}}{[\sigma]_{bII}}$ . For the selected material:

$$[\sigma]_{bIII} = 650 \text{ kg/cm}^2$$

$$\text{and } [\sigma]_{bII} = 1,100 \text{ kg/cm}^2.$$

Hence,

$$M_{red} = \sqrt{74,000^2 + \left( \frac{650}{1,100} \times 51,500 \right)^2} = 80,000 \text{ kg/cm}.$$

The required section modulus is

$$W = 0.1d^3 = \frac{M_{red}}{[\sigma]_{bIII}} = \frac{80,000}{650} = 123 \text{ cm}^3.$$

The shaft diameter in the calculated cross-section is

$$d = \sqrt[3]{1,230} \approx 10.7 \text{ cm}.$$

We take:  $d = 110 \text{ mm}$ .

In the section where the toothed wheel is fitted the total bending moment is

$$M = 21,400 \text{ kg/cm}$$

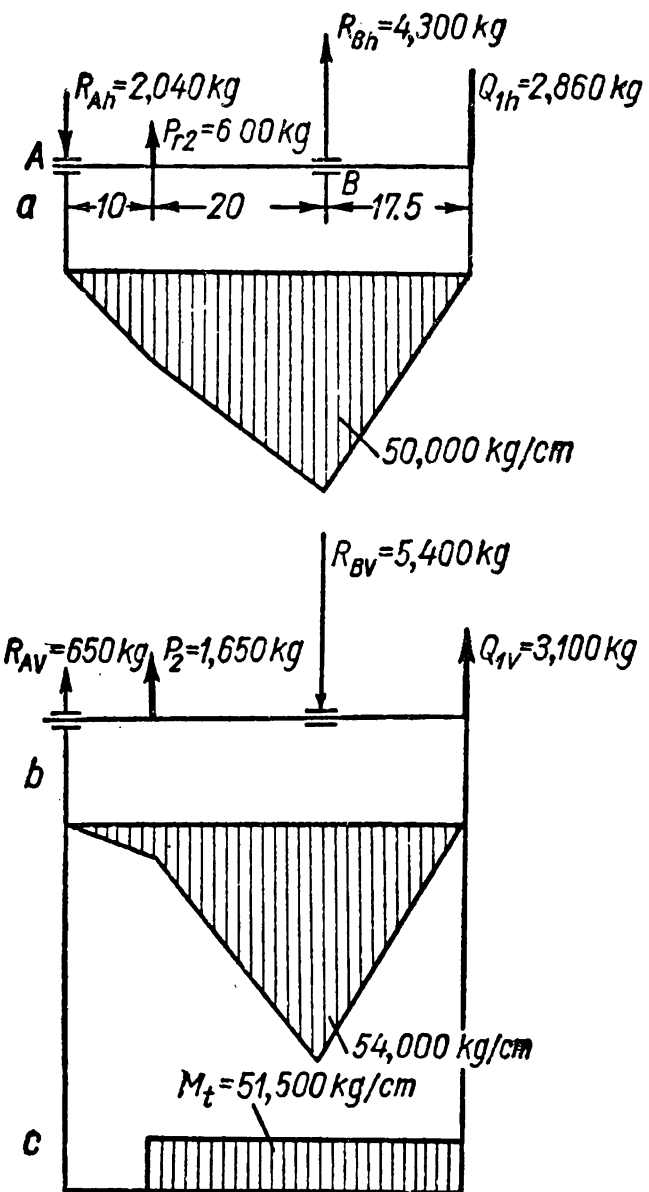


Fig. 220

and the reduced moment

$$M_{red} = 37,000 \text{ kg/cm.}$$

At the same  $[\sigma]_{bIII} = 650 \text{ kg/cm}^2$  we obtain

$$d_2 = \sqrt[3]{\frac{37,000}{0.1 \times 650}} = 8.3 \text{ cm.}$$

Since the shaft section in this place is splined the obtained value  $d_2$  is approximated to the nearest standard value.

The design of the shaft is shown in Fig. 221.

Margins of safety are checked for the dangerous sections.

*Cross-section in the middle of the bearing B.*

We find

$$\sigma_{\max} = \frac{M_B}{0.1d^3} = \frac{74,000}{0.1 \times 11^3} \approx 560 \text{ kg/cm}^2;$$

$$\tau_{\max} = \frac{M_t}{0.2d^3} = \frac{51,500}{0.2 \times 11^3} \approx 195 \text{ kg/cm}^2.$$

For normal stresses which change according to a symmetric cycle:

$$\sigma_m = 0; \sigma_a = \sigma_{\max} = 560 \text{ kg/cm}^2.$$

For tangential stresses if the torque changes from 0 to  $M_t$ :

$$\tau_m = \tau_a = \frac{\tau_{\max}}{2} \approx 98 \text{ kg/cm}^2.$$

With the unit pressure due to fit of  $p \geq 3 \text{ kg/mm}^2$  the ratio  $\frac{k_\sigma}{\varepsilon_\sigma}$  for  $d = 110 \text{ mm}$  is  $\left(\frac{k_\sigma}{\varepsilon_\sigma}\right)_{p=3} = 3.7$ .

In actual fact the unit pressure due to the pressed-on antifriction bearing is below  $3 \text{ kg/mm}^2$  and is approximately  $0.75 \text{ kg/mm}^2$ .

Therefore,

$$\left(\frac{k_\sigma}{\varepsilon_\sigma}\right)_{p=0.75} = \left(\frac{k_\sigma}{\varepsilon_\sigma}\right)_{p=3} \times 0.78 = 3.7 \times 0.78 \approx 2.9.$$

According to some data

$$\frac{k_\tau}{\varepsilon_\tau} = 1 + 0.6 \left( \frac{k_\sigma}{\varepsilon_\sigma} - 1 \right);$$

$$\text{hence } \frac{k_\tau}{\varepsilon_\tau} = 1 + 0.6 (2.9 - 1) = 2.14.$$

The margin of safety taking only normal stresses into account is

$$n_\sigma = \frac{\sigma_{-1}}{\frac{k_\sigma}{\varepsilon_\sigma} \times \sigma_b} = \frac{3,000}{2.9 \times 560} = 1.85.$$

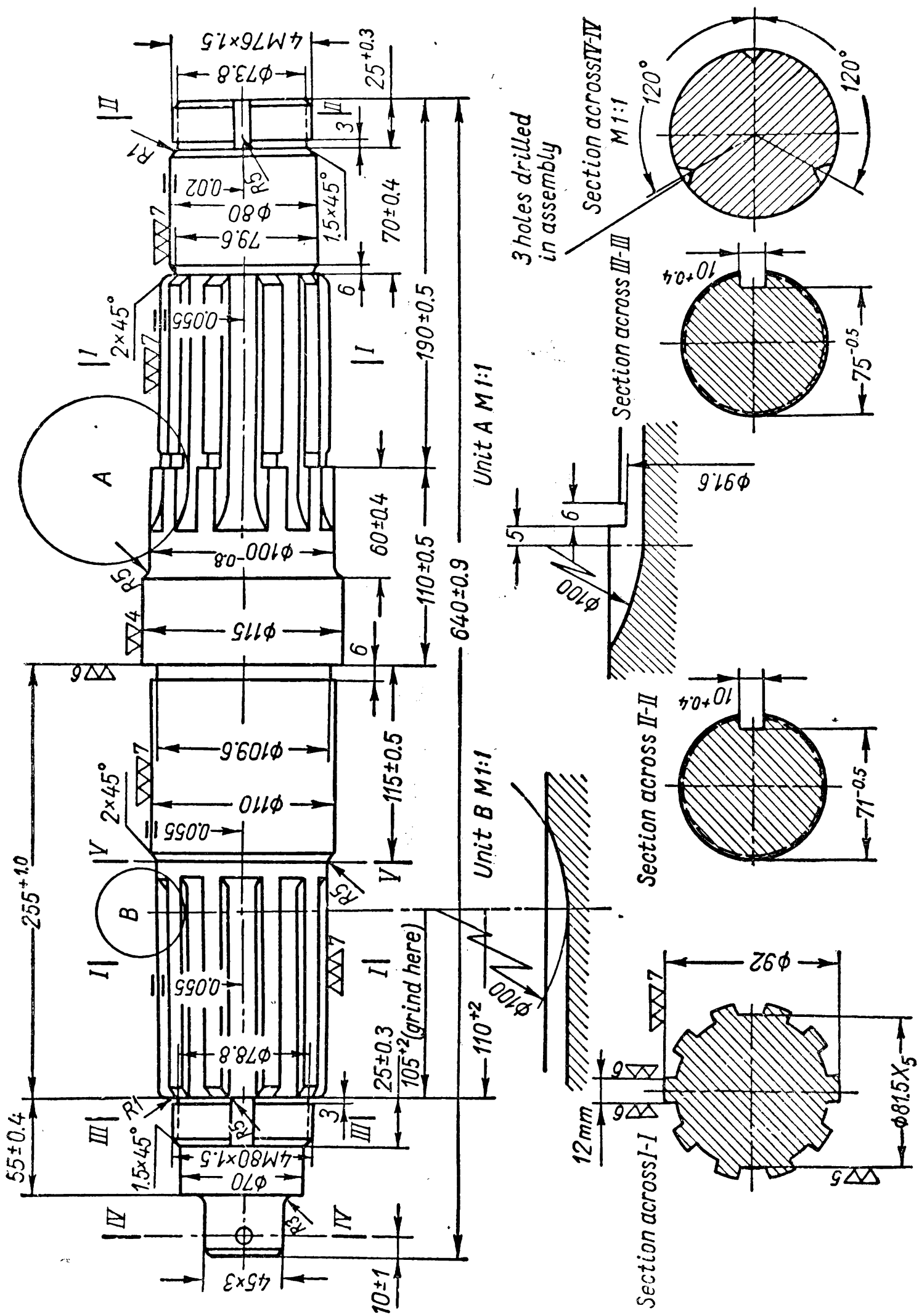


Fig. 221

The margin of safety taking only tangential stresses into account is

$$n_{\tau} = \frac{\tau_{-1}}{\frac{k_{\tau}}{\epsilon_{\tau}} \times \tau_a + \psi_{\tau} \times \tau_m} = \frac{1,800}{2.14 \times 98} \approx 8.6.$$

The total margin of safety in the cross-section is

$$n = \frac{1}{\sqrt{\left(\frac{1}{n_{\sigma}}\right)^2 + \left(\frac{1}{n_{\tau}}\right)^2}} = \frac{1}{\sqrt{\left(\frac{1}{1.85}\right)^2 + \left(\frac{1}{8.6}\right)^2}} \approx 1.80$$

which is admissible.

In the section V-V, located at a distance of 80 mm from the centre of the bearing stress concentration is due to a fillet. The bending moment in the cross-section  $M=40,000$  kg/cm and the torque  $M_t=51,500$  kg/cm.

The stresses in the cross-section

$$\sigma_{\max} = \frac{40,000}{0.1 \times 9.23} = 515 \text{ kg/cm}^2; \quad \tau_{\max} = \frac{51,500}{0.2 \times 9.23} = 330 \text{ kg/cm}^2.$$

Hence,

$$\sigma_a = \sigma_{\max} = 515 \text{ kg/cm}^2; \quad \sigma_m = 0; \quad \tau_a = \tau_m = \frac{\tau_{\max}}{2} = 165 \text{ kg/cm}^2.$$

We take the values of factor of absolute dimensions at:  $\epsilon_{\sigma}=0.7$  and  $\epsilon_{\tau}=0.6$ . We also find  $k_{\sigma}$  and  $k'_{\tau}$  determined for  $\frac{D}{d}=1.25-2.0$  depending on the ratio  $\frac{Q}{d}$ .

In this case  $\frac{Q}{d} = \frac{5}{92} \approx 0.055$  and, hence,  $k'_{\sigma}=1.9$  and  $k'_{\tau}=1.4$ .

Since in the examined cross-section  $\frac{D}{d} = \frac{110}{92} \approx 1.2 < 1.25$  the design values of the effective stress concentration factors are found as follows:

$$k_{\sigma} = \left(2.28 \frac{D}{d} - 1.9\right)(k'_{\sigma} - 1) + 1 = (2.28 \times 1.2 - 1.9)(1.9 - 1) + 1 \approx 1.75;$$

$$k_{\tau} = \left(2.88 \frac{D}{d} - 2.72\right)(k'_{\tau} - 1) + 1 = (2.88 \times 1.2 - 2.72)(1.4 - 1) + 1 \approx 1.3.$$

The margin of safety accounting only for normal stresses is

$$n_{\sigma} = \frac{3,000}{\frac{1.75}{0.7} \times 515} = 2.33.$$

The margin of safety accounting only for tangential stresses is

$$n_{\tau} = \frac{1,800}{\frac{1.3}{0.6} \times 165 + 0.1 \times 165} = 4.8.$$



The total margin of safety is

$$n = \frac{1}{\sqrt{\left(\frac{1}{2.33}\right)^2 + \left(\frac{1}{4.8}\right)^2}} \approx 2.1$$

which is permissible.

Margins of safety in other dangerous cross-sections are found similarly.

## CHAPTER XXI

### SLIDING CONTACT BEARINGS

Bearings are intended to direct the motion of shafts and axles and take forces acting on them.

Depending on the type of friction caused by relative movement of the bearing surfaces we distinguish between *sliding contact bearings* and *rolling contact (antifriction) bearings*.

Bearings loaded with transverse forces through a journal are called *radial bearings* and bearings loaded with axial forces through a shaft end-face—*thrust bearings*.

The choice of a sliding or antifriction bearing depends on many operational and production factors and also on the layout and design of the system. In many cases bearings of either type are equally effective.

With adequate design and lubrication the losses due to friction under stable operating conditions of a machine with a sliding bearing do not exceed those obtaining with antifriction radial bearing (or thrust bearing) in similar conditions.

Fluid friction in a sliding bearing has one extremely valuable feature: the higher the shaft rotation velocity, the greater the load-carrying capacity (or service life at a given load) of the bearing.

An increase in the velocity of a shaft mounted in rolling contact bearings at a given load tends to reduce their life sharply.

Since the races of antifriction bearings are integral (unsplit) pieces they are sometimes unsuitable for mounting; for example, they cannot be fitted on crankshaft journals.

Because rolling contact bearings have negligible contact surfaces they are more rigid. This is one of the causes of noise or sometimes vibration of the system which frequently accompany the work of antifriction bearings especially at high velocities.

If fluid friction cannot be ensured in a sliding bearing, the losses due to friction sharply increase (as compared to losses in fluid friction) which materially impairs the operating value of the bearing. Besides, as a result of direct contact of separate sections of the shaft and bearing, especially on starting, the wear of these surfaces is inevitable.

The losses due to friction in antifriction bearings remain negligible even at starting while the wear of the shaft journal or end-face is entirely excluded.

Antifriction radial or thrust bearings may be lubricated at less frequent intervals; such bearings do not therefore require the complicated lubricating devices which have to be used with sliding bearings.

The main factor determining the magnitude of the force resisting shaft rotation at a given load on the bearing—the magnitude of the friction force—is the coefficient of sliding friction  $f$ . This coefficient depends on a number of factors related to the nature of the conjugate surfaces and the properties of the intervening layer.

*Facet of adhesion*

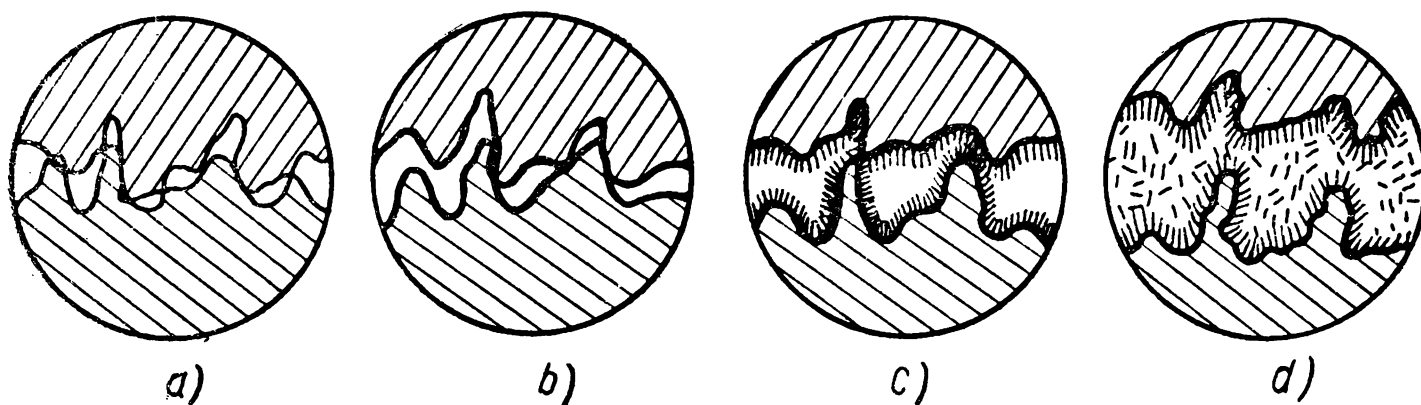


Fig. 222

There are four types of sliding friction: dry, semi-dry, boundary and fluid.

*Dry and semi-dry friction.* *Dry friction* (Fig. 222, *a*) occurs between two ideally clean surfaces without any substance between them.

Dry friction is caused by two mutually related phenomena: the force of molecular adhesion and mutual cohesion of irregularities which cannot be removed even by the most thorough machining.

The irregularities result in the load being distributed unevenly between the carrying surfaces; it is spread over projections and therefore the actual area of contact is hundreds and thousands of times less than the design (rated) area.

The enormous local pressures and the heat generated in sliding tend to soften the irregularities and increase the cohesive action of the contacting surfaces.

For this reason, carelessly machined surfaces increase the intensity of mechanical cohesion of the irregularities and the force of molecular adhesion.

The process of breaking and shearing off of the irregularities causes new roughness to develop; this phenomenon is aggravated by the fact that the hardness of metal at various points on the surface and hence its deformation under load are different at different points.

The coefficient of dry friction is higher than the coefficients of other kinds of sliding friction and can be considerably in excess of unity.

Dry friction is obtainable only in laboratory conditions. In practice even thoroughly cleaned surfaces always carry thin films of gas, moisture and grease adsorbed from the environment.

The friction which obtains in the presence of intermediate films adsorbed from outside is called *semi-dry* friction (Fig. 222, *b*).

Although such films are extremely thin, in the order of several angströms ( $1 \text{ \AA} = 10^{-8} \text{ cm}$ ), the film reduces the possibility of molecular adhesion and cohesion of the irregularities. The coefficient of semi-dry friction is noticeably smaller than that of dry friction, its magnitude being limited to a few tenths.

*Boundary friction* (Fig. 222, *c*) takes place when a layer of lubricant, for example oil 0.1-0.5 mc thick, is artificially introduced. One of the principal properties of a lubricant—its so-called oiliness—is manifested within this layer.

The ability of a lubricant to form intermediate layers which are stable in respect to the action of external forces is brought about by two independent properties—oiliness and viscosity.

The various oils used in mechanical engineering are primarily mixtures of various hydrocarbons.

Oil molecules are elongated in form. On interaction with a hard surface they take up a position perpendicular to it. Subsequent layers of molecules lose this orientation to a greater degree the thicker the *boundary* film is. The ability of oil to form thick and strong boundary films on a hard surface is called *oiliness*.

Oiliness depends not only on the quality of oil but also on the ability of the given metal to interact with the given grade of oil. For instance, oiliness on the surface of different grades of cast iron depends on the number and form of graphite inclusions in cast iron.

Boundary friction does not exclude the mutual cohesion of irregularities and therefore wear, but the latter extends only to most prominent projections.

The coefficient of boundary friction is of the order of several hundredths.

*Fluid friction.* An increase in the thickness of the oil layer lessens the effect of a hard surface on the molecules of oil and the layers located at a distance approximately of more than 0.5 mc can shift freely relative to one another. This lubricating layer, unaffected by the surfaces, possesses a property common to fluid and gaseous substances—*viscosity*—by which is meant the force resisting a mutual shear of the adjoining layers of the substance.

Friction in the presence of an integral viscous layer is called *fluid* friction (Fig. 222, *d*).

Fluid friction is most desirable for the operation of the bearings of a machine since it completely eliminates direct contact of the bearing surfaces.

There are two ways of retaining a viscous layer in the clearance between the loaded surfaces: 1) by feeding oil into the clearance between the conjugate surfaces under a pressure capable of equalising the external load; 2) by creating appropriate conditions under which this ability will arise in the layer itself.

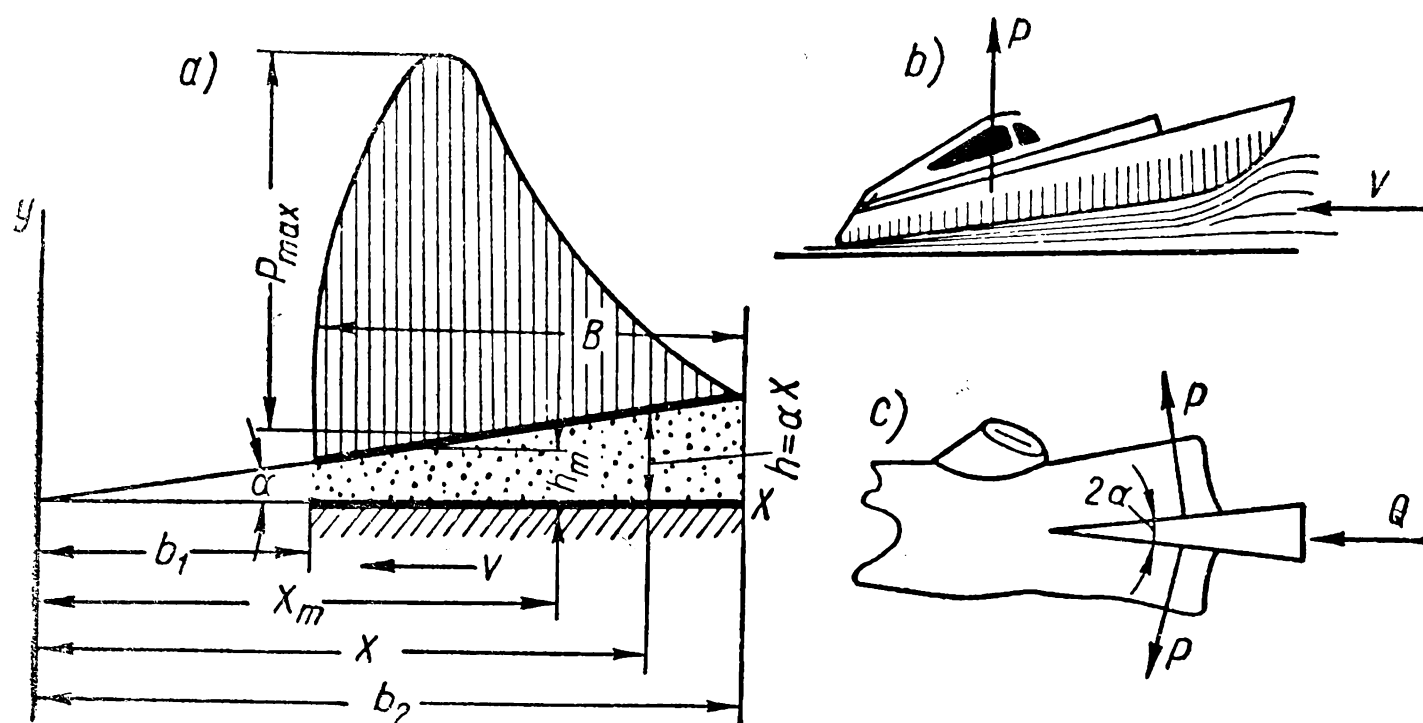


Fig. 223

The oil can be fed into the clearance of a bearing at required pressure only by sufficiently powerful pressure devices through a network of conduits which is unprofitable and practically not always possible.

The second way is more acceptable.

Fig. 223, *a* shows two planes representing the surfaces of a bearing. Let us assume that the planes stretch in the direction perpendicular to the drawing to an infinite distance. Let us further assume that the lower plane moves with a velocity  $v$  and that the upper, inclined at a slight angle to the first, is stationary. The minimum section of a tapered clearance between both planes will be considered sufficiently large to accommodate a layer of viscous fluid, for example oil.

With the direction of motion of the lower plane as shown in Fig. 223, *a* the flow of oil enters the broad section of the tapered clearance and emerges through its narrow section.

Since the compressibility of fluid is extremely small the condition of the flow integrity (for this purpose the rate of flow of fluid through the broad and narrow sections of the clearance should be the same) shows that in such a clearance the internal, hydrodynamic, pressure should arise tending to force the surfaces apart as a result of which

one of them is raised in the same manner as a hydroplane begins to plane (Fig. 223, *b*).

The force  $P$  separating the surfaces arises in this case just as with a solid wedge (Fig. 233, *c*) where the wedging factor is the force  $Q$  and not the velocity  $v$ .

The outstanding Russian scientist and engineer N. P. Petrov (1836-1920) who developed the hydrodynamic theory of lubrication was the founder of the theory of fluid friction in the machine bearings.

The hydrodynamic pressure in the clearance changes from  $p=0$  at the flow input to  $p=0$  at the output after passing through the values  $p=p_{\max}$  (Fig. 223, *a*).

The change in pressure along the length of the tapered clearance at a two-dimensional flow (the delivery of oil through the ends is excluded because we have assumed the clearance to be of infinite width) is expressed by the formula

$$\frac{dp}{dx} = 6\eta v \frac{h-h_m}{h^3} \quad (367)$$

where  $\eta$  is the dynamic factor of oil viscosity;

$v$  — the velocity of relative shear of the surfaces;

$h_m$  — the height of clearance in the section where  $p=p_{\max}$ ;

$h$  — the height of clearance in a section at a distance  $x$  from the coordinate origin.

If the conjugate surfaces are parallel the flow of fluid in the clearance cannot resist the outside load and therefore fluid friction is impossible.

### MATERIALS FOR SLIDING RADIAL AND THRUST BEARINGS

Economical operation of a bearing is assessed according to friction losses and maintenance costs.

The antifriction properties of a material change depending on operating conditions. For example, when copiously lubricated some grades of cast iron possess high antifriction properties at low velocities of relative sliding. Failure to observe these conditions sharply increases losses due to friction and causes rapid wear of the contacting surfaces and sometimes their seizure.

**Metals.** Metals possessing antifriction properties include alloys, powder-metal compounds as well as thin electrolytic coatings of pure chrome. Bronzes and babbitts rank among the most widespread types of antifriction alloys.

*Babbitts* are white antifriction alloys mainly with tin, lead and antimony bases. The number of different grades of babbitts is extremely great (tin, lead, calcium and other alkali-earth babbitts).

The high antifriction properties of babbits arise from their high plasticity, which facilitates the bearing initial wear-in, good thermal conductivity and ability to retain thick oil films.

The soft products of babbit wear preclude one of the most dangerous causes of scoring.

The best grade is high-tin babbit of grade B 83 containing  $11 \pm 1\%$  of antimony,  $6 \pm 0.5\%$  of copper and not over  $0.55\%$  of admixtures; the rest is tin (81-84%). Tin babbits effectively resist impact loads.

Among the disadvantages of babbits is their low melting point which makes it impossible to use these alloys in heavily loaded bearings. In selecting grades of babbit due regard should be given to the saving of nonferrous metals, especially tin.

*Bronzes* are alloys of copper and various metals—mainly tin (tin bronzes), lead (lead bronzes) and aluminium (aluminium bronzes), zinc-free or with a negligible percentage. Since bronzes are harder than babbits they are more difficult to wear in while the presence of hard products of wear in the area of contact of the rubbing surfaces constitutes a certain danger.

Bronze bearings require a more dependable lubricant than babbit bearings. The melting point of bronzes—of the order of  $1,000^{\circ}\text{C}$ —considerably exceeds that of babbits.

Inexpensive aluminium-base alloys of copper and iron (for instance, alcu-zines) are in extensive use today. At low velocities of relative sliding they can be used not only instead of bronze but also instead of babbit.

Certain grades of brasses, zinc-base alloys of copper and aluminium, etc., likewise exhibit good antifriction properties.

At very low velocities of relative sliding—up to 1-2 m/sec and with copious lubrication use is made of antifriction cast iron.

The reliable service of this material in bearings is explained by a special form of graphite inclusions which act as an additional lubricant. The brittleness of cast iron limits its use in bearings subjected to shocks.

Powder-metal bushings of bearings are made either by sintering bronze chips and graphite under pressure or by sintering clean shavings of mild steel.

The porous structure of powder-metal bushings helps to retain a certain amount of oil which appears on the surface of the bushing as it heats up during operation.

Powder-metal bushings can therefore operate for a long time with little lubrication but only under steady load without shocks.

Sometimes steel parts are coated with electrolytic porous chromium. This very hard and smooth antifriction coating offers effective resistance to wear while a network of microscopic channels on its surface ensures a constant flow of oil to the area of contact.

**Nonmetallic Materials.** Nonmetallic antifriction materials include hard wood, rubber and some plastics.

The antifriction properties of these materials are due to the fact that they are easily worn-in, yield soft products of wear and are dissimilar to the conjugate metal surface. The latter property precludes the phenomenon of molecular adhesion and seizure.

Wooden bearing members are made from oak, alder, box and guaiacum.

Since wood has a poor thermal conductivity sliding bearings made from it should be water-lubricated, the water simultaneously cooling the bearing.

Water-lubrication is also obligatory in rubber bearings.

Because of the corrosive action of water on steel shafts they should be made from stainless steel or protected with coatings.

As a rule, two types of plastics are used for sliding bearings: veneer or fabric laminated plastics. A recent development are bearings in the form of nylon bushings.

In the process of manufacture veneer laminated plastics are pressed and impregnated with resins to make them sufficiently tight and hard.

Fabric laminated plastics are formed from pressed cotton fabric impregnated with phenolic resins.

The poor thermal conductivity of fabric laminated plastics limits their application since at a temperature slightly above 100°C they decompose.

**Lubricants.** The most widespread grades are liquid oils and semi-solid lubricants (greases).

Oiliness depends both on the nature of oil and the nature of the friction surfaces; therefore it has been impossible up till now to establish a criterion of oiliness to suit all cases.

Viscosity can be evaluated in absolute and relative (arbitrary) units.

The criterion of absolute or dynamic viscosity is based on Newton's hypothesis expressed by the relation

$$T = \eta S \frac{v}{h}$$

where  $T$  is the force resisting the mutual shear of two adjacent layers of fluid;

$S$ —the area of contact between the layers;

$h$ —the distance between them;

$v$ —the velocity of relative shear of the layers;

$\eta$ —the proportionality factor (dynamic factor of viscosity).

If we take  $T=1$  kg,  $S=1$  m<sup>2</sup>,  $h=1$  m,  $v=1$  m/sec the absolute unit of viscosity according to the metric system will be expressed in kg sec/m<sup>2</sup>.

The unit of absolute viscosity is the force in kg necessary to move a layer of fluid 1 m<sup>2</sup> in area at a rate of 1 m/sec relative to an immobile layer of the same size located at a distance of 1 m from the first layer.

In the physical system (cgs system) the unit of dynamic viscosity is the *poise* and is expressed in dyne  $\times$  sec/cm<sup>2</sup>.

1 poise = 100 centipoises = 0.0102 kg sec/m<sup>2</sup>.

1 kg sec/m<sup>2</sup> = 9,810 centipoises.

In practice use is made of more convenient arbitrary units expressed in viscosity degrees.

The arbitrary viscosity in Engler degrees is understood to mean the quotient received by dividing the time during which 200 cm<sup>3</sup> of the tested fluid flows through a platinum tube with an inside diameter of 2.8 mm by the time during which 200 cm<sup>3</sup> of water with a temperature of 20°C passes through the same tube.

The degree of viscosity is denoted by  $E_t^\circ$  where the subscript  $t$  shows the temperature of the tested fluid.

To convert units of arbitrary viscosity into absolute units the following relation can be used

$$\eta = 10^{-6} \gamma_t \left( 0.737 E_t^\circ - \frac{0.635}{E_t^\circ} \right) \text{ kg sec/m}^2 \quad (368)$$

where  $\gamma_t$  is the specific weight of the fluid in kg/m<sup>3</sup> at a temperature of  $t^\circ\text{C}$ .

The change in the viscosity  $\eta$  depending on temperature is expressed by the formula

$$\eta = \frac{i}{(0.1t^\circ)^3} \text{ kg sec/m}^2. \quad (369)$$

Here  $i$  is a characteristic number of the given grade of oil ( $i \approx 1.4-2.8$ ).

Fig. 224 shows a diagram illustrating the change in viscosity of some oils with an increase in temperature.

The relationship between viscosity and pressure has the following form

$$\eta_p = \eta_0 a^p$$

where  $\eta_p$  is the dynamic factor of oil viscosity at above-atmospheric pressure  $p$ ;

$\eta_0$ —the dynamic factor of viscosity at atmospheric pressure (i.e., when  $p=0$ );

$p$  —the pressure in kg/cm<sup>2</sup>;

$a$  —the factor constant for the given grade of oil.

Since  $a$  varies within 1.001-1.004, with pressures  $p$  up to 400 kg/cm<sup>2</sup> changes in oil viscosity due to change in pressure can be neglected.



Bearings are lubricated with *mineral, vegetable and animal* oils. Mineral oils are obtained by distilling petroleum and its residues. The viscosity of these oils measured at 50°C amounts to (2.5°-25°)  $E_{50}$ .

Mineral oils include industrial, automobile, tractor, diesel engine, turbine, cylinder and other oils.

Vegetable oils include linseed, castor and other oils. Castor oil is especially widespread in mechanical engineering. Besides high oiliness it possesses considerable viscosity (up to 15°  $E_{50}$ ).

Among animal oils are bone, sperm and other oils. Animal oils are the most expensive and possess the highest oiliness. Their viscosity is very low.

Compound oils are mixtures of cheap and viscous mineral oils with animal or vegetable oils having high oiliness.

To improve the operation of a system during the initial wear-in period use is sometimes made of small oil additives. Some of them increase the physical activity of the oil so that the irregularities detach from the surface more easily while the others fill the valleys between the irregularities and make the surface smoother.

For additives of the first type use is made of the so-called fatty organic acids (stearic, palmitic and other acids) while the second type of additive is colloidal graphite.

When the design does not permit the easy feeding of oil from the lubricating device to the rubbing surfaces of an operating bearing (valve control mechanisms, universal joints, etc.) the bearing is filled with grease.

Greases are mixtures of mineral oils and small additions of animal and vegetable oils, solidified by lime-base (constalines) or soda-base (solid oils) soaps. The main characteristic of greases is penetration—i.e., the number of hundredths of a centimeter that a standard needle penetrates the grease vertically in 5 sec at a standard temperature.

In addition to liquid oils and greases resort can be had to lubrication by water (for example, in the bearings of marine propeller shafts and water pumps) and air which at high velocities of rotation forms an intervening layer in which under certain conditions internal pressure is created in accordance with the formula (367).

Finally, at high and superhigh unit pressures bearings are lubricated by chemically active greases which employ sulphur and chlorine compounds (sulphur flowers, carbon tetrachloride, etc.) as additives.

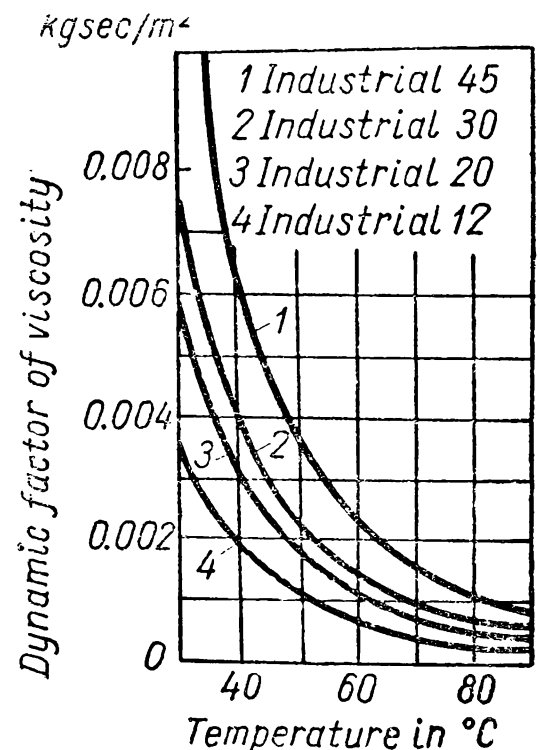


Fig. 224

As they chemically combine with metal surfaces these substances form thin separating films which ensure a low coefficient of friction and remain in the clearance even at very high pressures.

### RADIAL BEARINGS

**Design.** In its simple form a bearing is a supporting surface obtained by drilling or boring a part—frame, housing, connecting rod, etc.

A *solid bearing* is a specially machined part forming a sliding surface. Such a bearing can be designed with a baseplate (Fig. 225, *a*) or a flange (Fig. 225, *b*) by which it is fastened to a corresponding component.

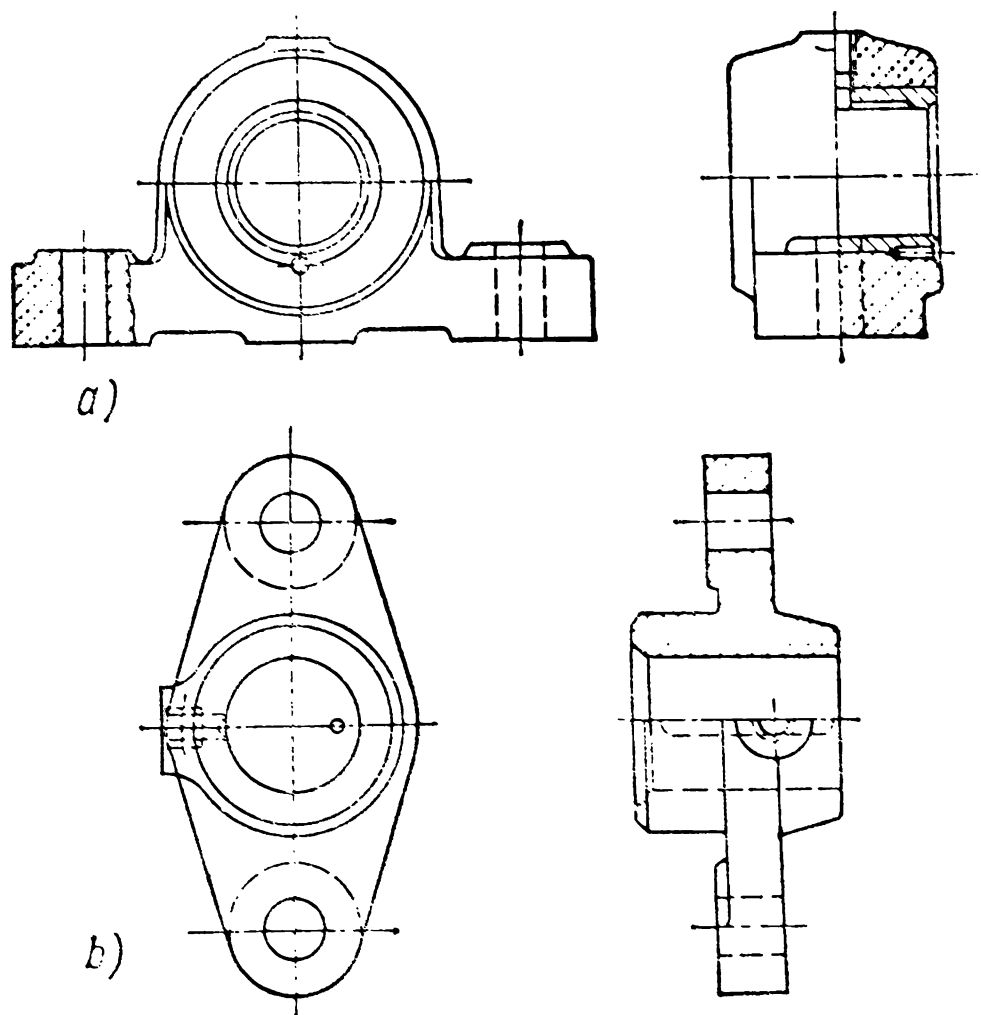


Fig. 225

Solid bearings are provided with bushings made from antifriction materials (cast iron, bronze, etc.) which are pressed into the bearing or are retained in place by stop screws (Fig. 225, *a*).

Sometimes the bearing itself serves as a rubbing surface (Fig. 225, *b*). The bushing or entire bearing should be replaced if affected by considerable wear.

Solid bearings of this type are employed for slowly revolving shafts and small unit pressures.

To increase the service life of solid bearings use is made of springy bushings with tapered outer surfaces (Fig. 226, *a*). Such bushings

are grooved along three generatrices and cut through along the fourth (Fig. 226, *b*). The bushing is shifted along its axis by means of nuts to decrease its diameter and take up the clearance caused by wear.

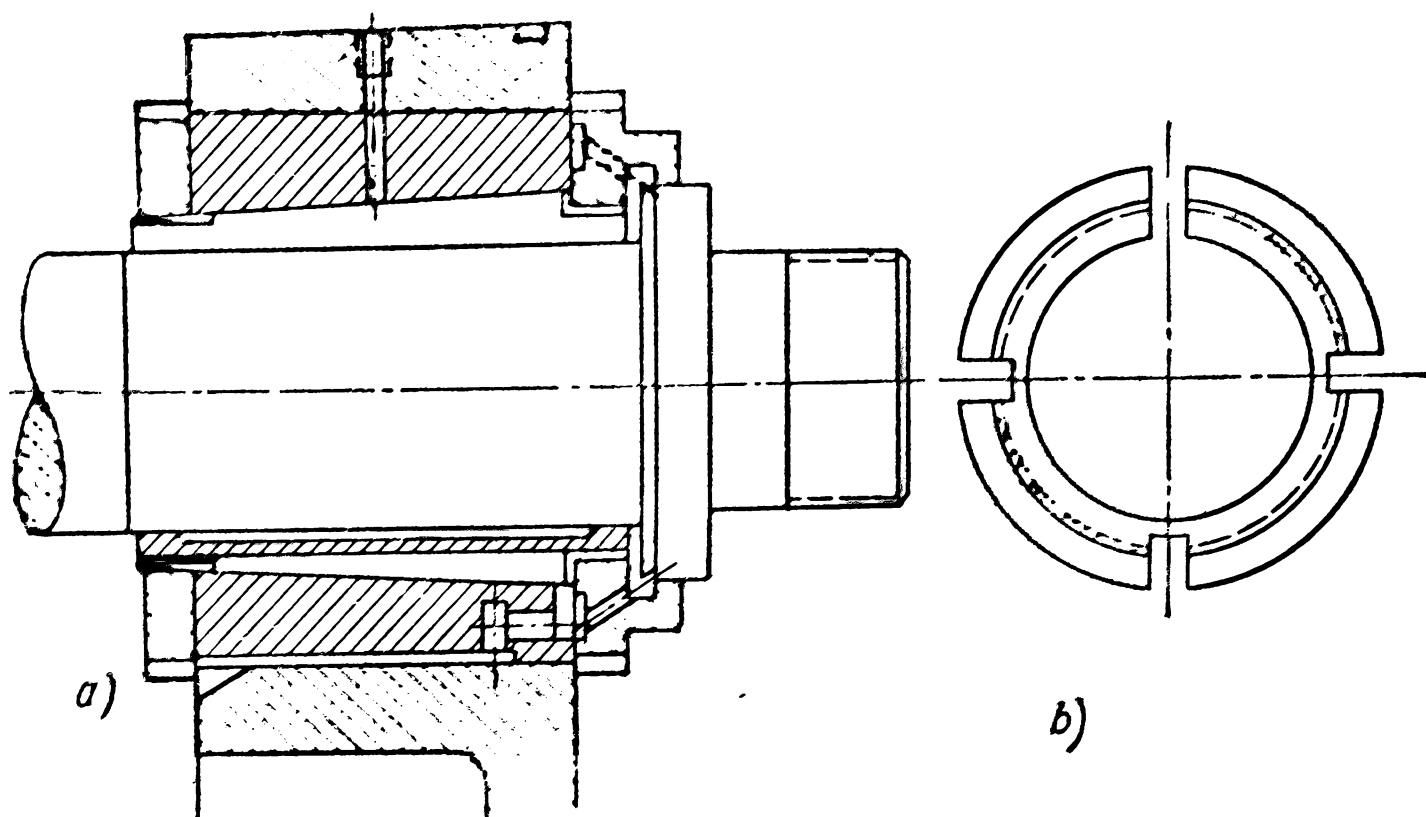


Fig. 226

Bearings of such design are widely used in turning and turret lathes, milling and other machine tools.

Parts mounted in solid bearings can be assembled into them only axially and this affects the design of the shaft and the conjugate parts.

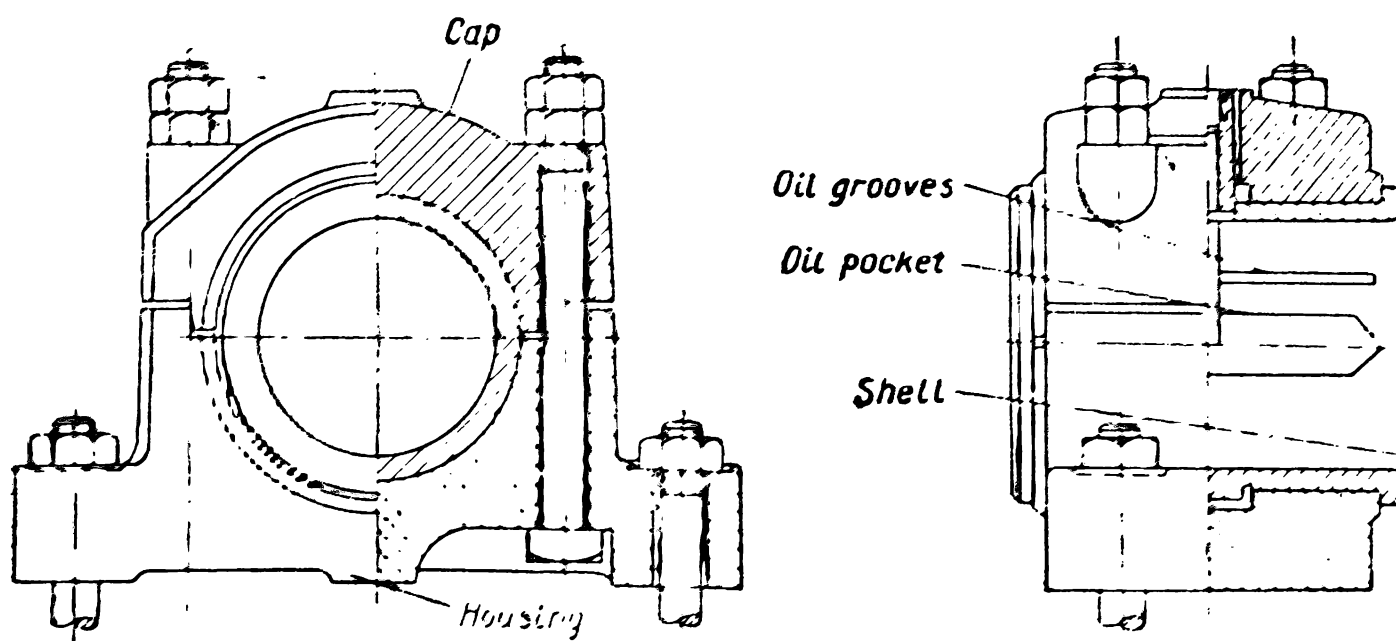


Fig. 227

A *split* bearing (Fig. 227) allows a shaft to be inserted perpendicular to the axis and the clearance to be adjusted as the bushing wears down. The bushing is locked axially by shoulders.

To relieve the bolts from possible transverse forces the joint between the bearing cap and housing is stepped.

A welded split bearing is shown in Fig. 228.

The shells whose internal surface should be lined with antifriction metal (bronze, babbitt, etc.) are made from steel or cast iron.

The thickness of the antifriction lining varies within a wide range—from 0.3 to 6 mm. To retain the lining on the shells during operation and cooling, the lined surface is usually provided with dovetail slots (Fig. 242, *b*) located longitudinally or transversely.

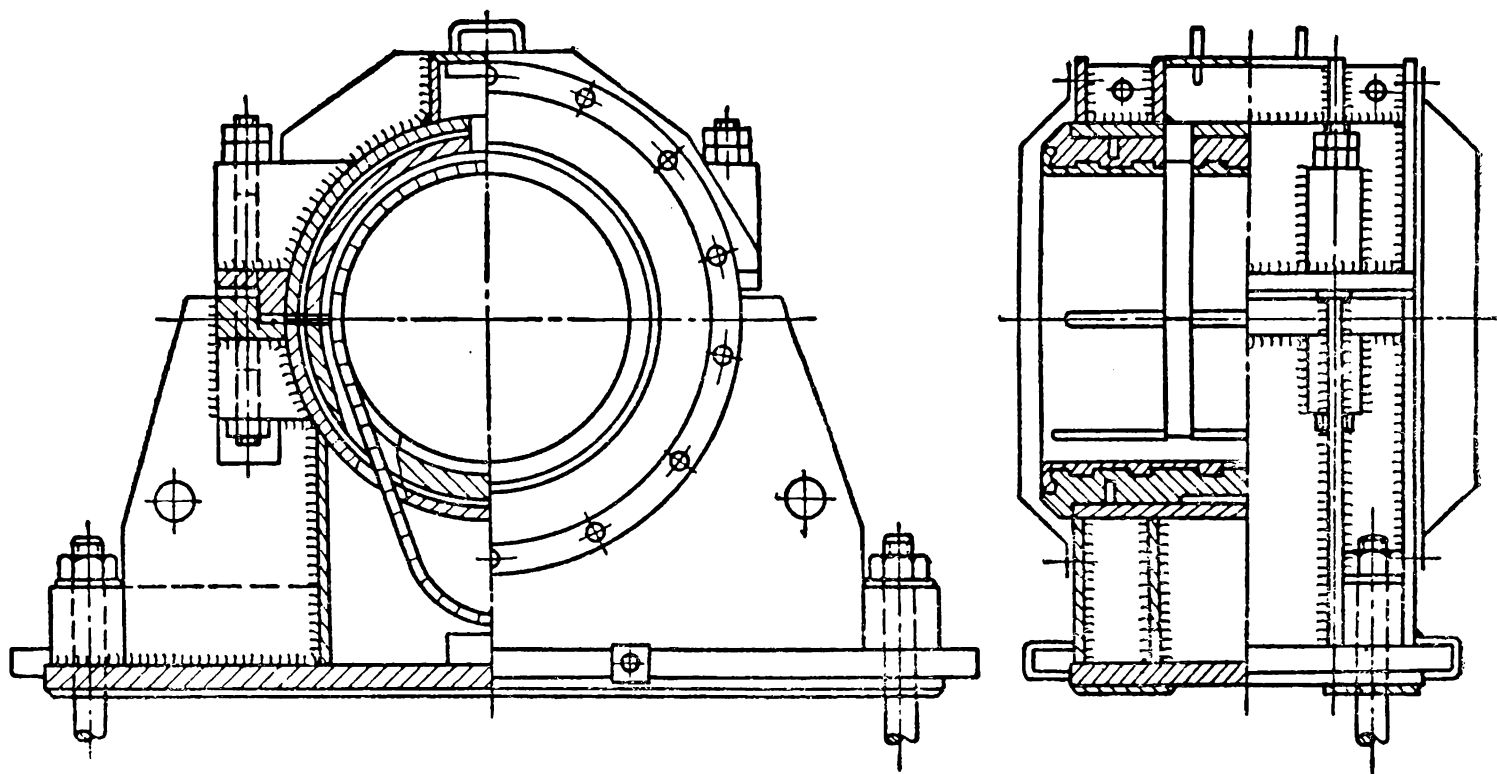


Fig. 228

The length of the bearing surface of the shell  $l$  is selected according to its ratio to the diameter  $d$  of the journal which varies within 0.8-1.5. An increase in length above this magnitude—(to 3-3.5) $d$ —increases the sensitivity of the entire bearing unit to shaft misalignment and can rupture the oil films at the ends and cause seizure. A shorter length increases pressures in the bearing.

If the bearings are of a considerable length use is made of *self-aligning* spherical shells (Fig. 229).

Sometimes partial shells in the form of a segment with an arc of contact of  $\leq 180^\circ$  are employed. Such designs are extensively used in axle boxes of railway cars where they are arranged at the top since the bearings take an upward load.

There are also multiple bearings with three (Fig. 242, *a*) or four (Fig. 242, *b*) shells tightened by means of screws and wedges. Such designs are employed where the loads change sharply in direction, for instance in the crank bearings of horizontal piston machines.

With a load applied in a constant direction the unit is ordinarily lubricated through the bearing. For this purpose the housing and shell are provided with ducts (boreholes) and the internal surface of the shell with additional longitudinal and circular grooves which facilitate oil distribution (Figs. 227 and 235).

An *oil feed duct* is provided in the unloaded section of the bearing to avoid clogging.

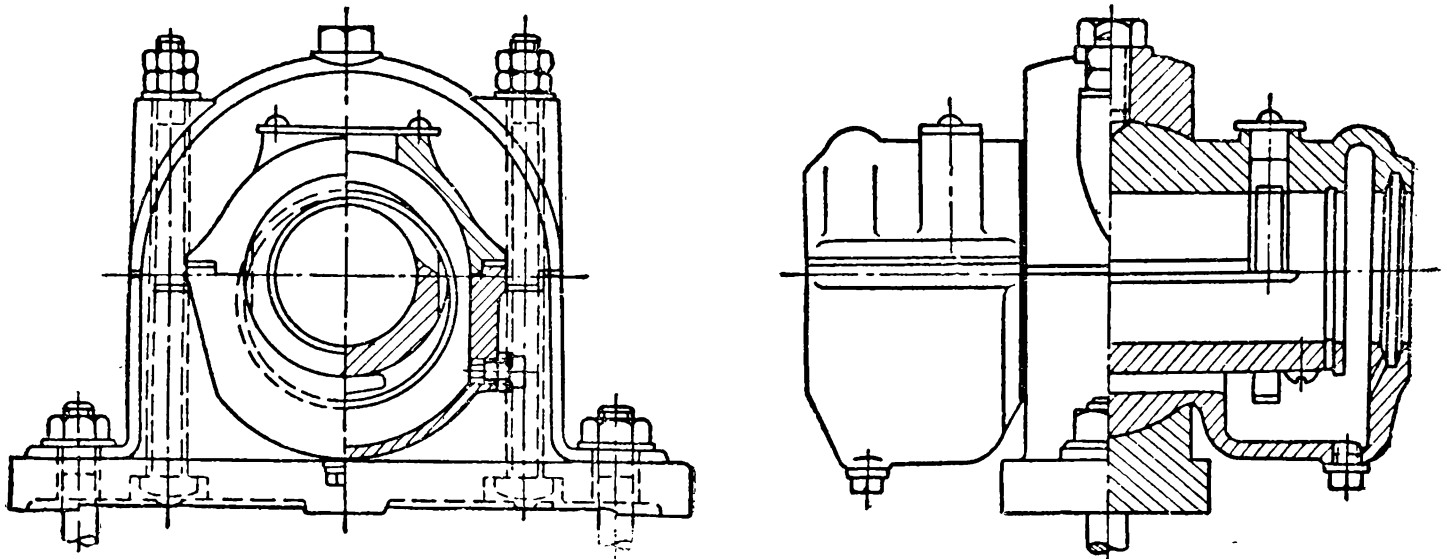


Fig. 229

If the bearing is designed to operate in conditions of boundary friction, then the *distributing grooves* should be arranged near the region of maximum pressure.

To ensure a more effective supply of oil to the operating zone the internal surfaces of the shells are provided with bevelled grooves — *oil pockets* (Fig. 227)—used as auxiliary reservoirs.

In bearings operating in conditions of fluid friction the oil grooves should be located outside the zone of hydrodynamic pressures to avoid the rupture of the oil wedge (Fig. 235).

If the bearing revolves round a fixed axis (as in the bearings of driven wheels in trolleys, the bearings of idle pulleys, pinions, etc.) the oil should be fed through the axle (Fig. 230). In this case oil grooves are made on the surface of the axle or shaft for the same reasons as in the case of bearings with revolving shafts.

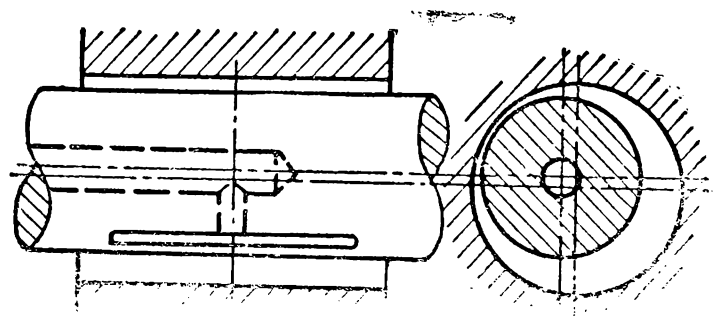


Fig. 230

The need for an intensive supply of cooling fluid which can simultaneously act as a lubricant determines the design of shells made from nonmetallic materials.

Fig. 231 shows some designs of bearings with shells composed of veneer laminated plastic bars and some common types of rubber bear-

ings. Such bearings are mainly produced in two modifications: *smooth* (Fig. 231, *a*, *c*) and *grooved* (Fig. 231, *b*, *d*, *e*, *f*).

Grooved bearings allow more cooling water to pass and are affected by dirt and alien substances in the water to a lesser extent.

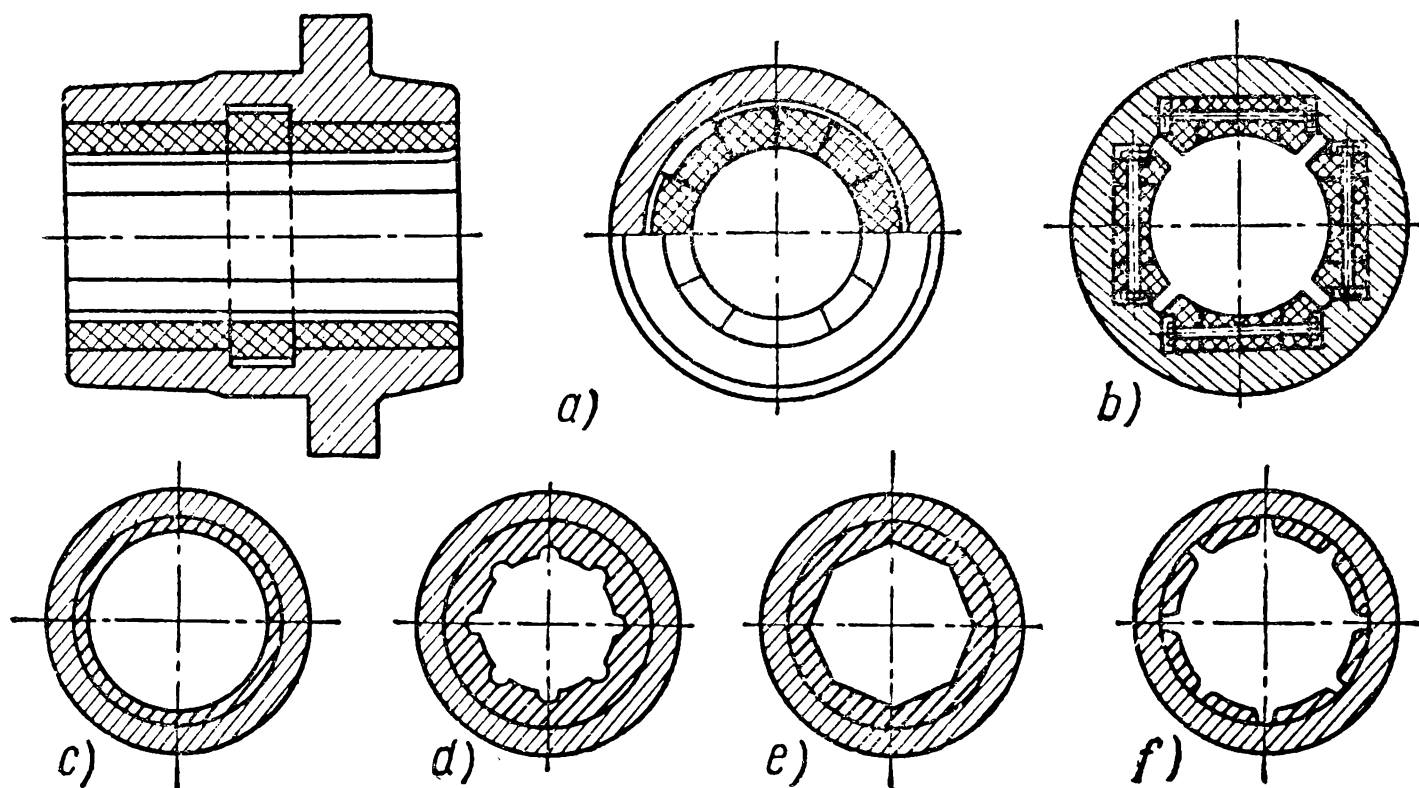


Fig. 231

**Calculation of Sliding Bearings.** Sliding bearings are calculated depending on the anticipated service conditions.

When the bearing unit is to operate in conditions of boundary friction the calculations are done either for strength by the surface compressive stress  $\sigma_{sur}$  or for the absence of seizure by the arbitrary criterion  $kv$  (p. 433).

If the unit is designed for operation in conditions of fluid friction the calculations are reduced to determining some one parameter, most frequently the diametral clearance between the journal and the bearing which will ensure, together with the other given values, service with fluid friction.

However, in this case too checking by the criterion  $kv$  should not be excluded since during starting and stopping the bearing operates in conditions of boundary friction when the hazard of seizure of the conjugate surfaces still exists.

*Calculations for limiting surface stress* are done for the bearing units where the peripheral velocity of the journal does not exceed 0.3 m/sec.

Since the diameters of the journal and shell differ but little the Herz formula for the contact of an external and an internal cylinder gives in this case only an approximate value which increases the

margin of safety of the bearing. In calculating important sliding bearings the contact pressures should be found by more precise methods.

*Calculation for the avoidance of seizure* is carried out for bearings operating in conditions of boundary friction at a peripheral velocity of  $v > 0.3$  m/sec.

In this case the design value is the product  $kv$ , where  $k = \frac{R}{ld}$  kg/cm<sup>2</sup> is the arbitrary unit load on the bearing and  $v = \frac{\pi dn}{60 \times 100}$  m/sec the peripheral velocity of the journal.

Here  $R$  is the full pressure on the bearing in kg,  $l$  and  $d$  the length and diameter respectively of the bearing in cm and  $n$  is the journal rpm.

The product  $kv$  cannot be regarded as a reliable indication of the ability of a material to carry load; it only allows a tentative choice of material to be made.

[Multiplying the two latter equations we obtain the condition of the bearing operating capacity

$$\frac{Rn}{1,910 \times l} \leq [kv]. \quad (370)$$

The allowable values of  $kv$  for various bearing materials are given in reference books.

*Calculation for fluid friction.* It was pointed out earlier that under certain conditions a layer of fluid flowing in a wedge-shaped clearance develops internal (hydrodynamic) forces.

In a cylindrical bearing a wedge oil layer is obtained very simply—by creating in the bearing a *clearance* which allows the journal to be arranged eccentrically (Fig. 232, *a*).

[As the journal rotates it carries with it concentric layers of oil: the first layer which moistens it through its *oiliness* and the next layers through their *viscosity*. In this way the oil circulates permanently around the journal.

The journal acts as a pump feeding oil into the clearance which narrows gradually in the direction of rotation and causes considerable pressures to arise.

An increase in the pressure of the oil layer, on the one hand, raises the journal and increases the passage cross-sections and, on the other, increases the velocity of oil flow. As a result of this joint action a state of equilibrium sets in, when the pressure distribution in the oil layer is such, that the volume of oil flowing in all directions in one unit of time is equal to the amount carried into the narrowing clearance space by the shaft.

The hydrodynamic forces  $p_\phi$  acting on the journal (Fig. 232, *a*) coincide in direction with the normal to the shaft surface, i. e., with





its radius. If we resolve these forces into vertical and horizontal components, then only the vertical components  $p_{\varphi v}$  will be the forces capable of resisting the external load  $R$ .

The horizontal forces  $p_{\varphi h}$  will cause the shaft to shift in the bearing so that the line drawn through the centres of the shaft and bearing (centre line) will be turned by the angle  $\varphi_a$  relative to the vertical diameter.

As distinct from the distribution of the hydrodynamic forces between two flat surfaces (Fig. 223, *a*) the force distribution between the surfaces of the shaft and shell must reflect the cylindrical form of these parts.

The formula for the load-carrying capacity of a bearing at fluid friction is drawn up on the basis of the following main assumptions of the hydrodynamic theory of lubrication.

1. In the region where hydrodynamic forces arise the flow of oil is laminar.

2. The oil so adheres to the surfaces of the shaft and shell that the velocity of particles of the extreme layers of oil relative to the corresponding surface equals zero.

3. The effect of the force of gravity of the oil layer, the forces of inertia of its particles and capillary forces arising in the clearance can be ignored.

4. The oil is not compressed by external load.

On the basis of Fig. 232, *a* we introduce the following designations:

$\delta = \frac{\Delta}{2} = \frac{D}{2} - \frac{d}{2} = \frac{D}{2} - r$ —the radial clearance ( $\Delta$  is the diametral clearance);  $\psi = \frac{\Delta}{D} = \frac{2\delta}{D}$ —the relative clearance,  $h_{\min}$ —the height of the clearance cross-section where the shaft is nearest to the shell;  $e = \delta - h_{\min} = \frac{\Delta}{2} - h_{\min}$ —the absolute eccentricity;  $\chi = \frac{e}{\delta} = \frac{2e}{\Delta}$ —the relative eccentricity.

After simple transformations the value of the relative eccentricity can be expressed by the formula

$$\chi = 1 - \frac{2h_{\min}}{D\psi}. \quad (371)$$

Let us find the force  $p_{\varphi}$  arising in the cross-section of the oil layer lying at an angle  $\varphi$  from the centre line.

Since the eccentricity  $e$  is extremely small we assume that the angle  $\varphi$  at the shaft centre  $O$  equals a corresponding angle at the shell centre  $O'$ .

It then follows from Fig. 232, *a* that

$$\frac{D}{2} = O'b + Oa + h = e \cos \varphi + r + h.$$

After necessary substitution we get

$$h = \psi \frac{D}{2} (1 - \chi \cos \varphi) \approx \psi r (1 - \chi \cos \varphi)$$

where  $r$  is the shaft radius.

The height of the cross-section where the hydrodynamic force  $p_\varphi = p_{\max}$  will be at  $h = h_m$  and  $\varphi = \varphi_m$

$$h_m = \psi r (1 - \chi \cos \varphi_m).$$

Substituting the values  $h$  and  $h_m$  in the formula (367) and remembering that  $dx = r d\varphi$  we get

$$dp_\varphi = 6\eta \frac{v}{\psi^2} \times \frac{(1 - \chi \cos \varphi) - (1 - \chi \cos \varphi_m)}{(1 - \chi \cos \varphi)^3} d\varphi. \quad (372)$$

The region of the clearance in which hydrodynamic forces operate ends in a cross-section located at the angle  $\varphi_2$  from the reference line. Beyond this cross-section the oil passes into the broader part of the clearance and begins to flow in separate jets.

Integrating the equation (372) from  $\varphi_2$  to  $\varphi$  at  $\eta = \text{const}$  and  $v = \text{const}$  we shall get a formula for the forces at any point on the journal

$$p_\varphi = \frac{6\eta v}{\psi^2} \int_{\varphi_2}^{\varphi} \frac{(1 - \chi \cos \varphi) - (1 - \chi \cos \varphi_m)}{(1 - \chi \cos \varphi)^3} d\varphi. \quad (373)$$

The vertical component is

$$p_{\varphi v} = p_\varphi \cos(\varphi - \varphi_a). \quad (374)$$

Summation of all vertical components within the boundaries where hydrodynamic forces operate from  $\varphi_2$  to  $\varphi_1$  will give the force  $p_v$  in the middle cross-section of the oil wedge

$$\begin{aligned} p_v &= \int_{\varphi_2}^{\varphi_1} p_{\varphi v} d\varphi = \int_{\varphi_2}^{\varphi_1} p_\varphi \cos(\varphi - \varphi_a) d\varphi = \\ &= \frac{6\eta v}{\psi^2} \int_{\varphi_2}^{\varphi_1} \int_{\varphi_2}^{\varphi} \frac{(1 - \chi \cos \varphi) - (1 - \chi \cos \varphi_m)}{(1 - \chi \cos \varphi)^3} d\varphi [\cos(\varphi - \varphi_a)] d\varphi. \end{aligned} \quad (375)$$

To obtain the total force that raises the journal we should have multiplied  $p_v$  by the length  $l$  of the bearing. Then the force distribution would have the form shown in Fig. 232, *b* as  $I$ .

In a real bearing the oil can flow out at the ends; this means that at these places the hydrodynamic forces equal zero. The forces are distributed as shown in  $I$  only when the journals are of infinite length and are ideally sealed at the end-faces.

Experiments have shown that the forces in the hydrodynamic layer along the length of a real bearing are distributed in accordance with the law of parabola  $II$  (Fig. 232,  $b$ ) whose equation is

$$p'_v = p_v C \left[ 1 - \left( \frac{2z}{l} \right)^2 \right] \quad (376)$$

where  $z$  is the coordinate by the length of the shell;

$l$ —the length of the shell;

$C$ —the factor showing how the force  $p_v$ , calculated for bearings of infinite length, changes when real bearings are taken. The theoretical determination of  $C$  leads to the formula

$$C = \frac{5}{4} \frac{1}{\left[ 1 + a \left( \frac{D}{l} \right)^2 \right]} \quad (377)$$

where  $a$  is a variable magnitude depending on the relative eccentricity  $\chi$ .

The final load-carrying capacity of the oil wedge taking into account the shell length is

$$P = \int_{-\frac{l}{2}}^{+\frac{l}{2}} p'_v dz. \quad (378)$$

Substituting in the equation (376)  $p_v$  from the equation (375) and then  $p'_v$  in the equation (378) from the equation (376) we obtain after integration

$$P = \frac{\eta v l}{\psi^2} \Phi \quad (379)$$

where

$$\begin{aligned} \Phi = 6 \int_{-\frac{l}{2}}^{+\frac{l}{2}} \int_{\varphi_2}^{\varphi_1} \int_{\varphi}^{\varphi} \frac{(1 - \chi \cos \varphi) - (1 - \chi \cos \varphi_m)}{(1 - \chi \cos \varphi)^3} d\varphi [\cos(\varphi - \varphi_a)] d\varphi C \times \\ \times \left[ 1 - \left( \frac{2z}{l} \right)^2 \right] dz. \end{aligned}$$

From the equation (379) we get

$$\Phi = \frac{\psi^2 P}{\eta v l} = 19.11 \frac{k \psi^2}{\eta n}. \quad (380)$$

Here  $k$  is the pressure per unit of the diametral projection of the journal;

$n$ —the velocity of the shaft in rpm.

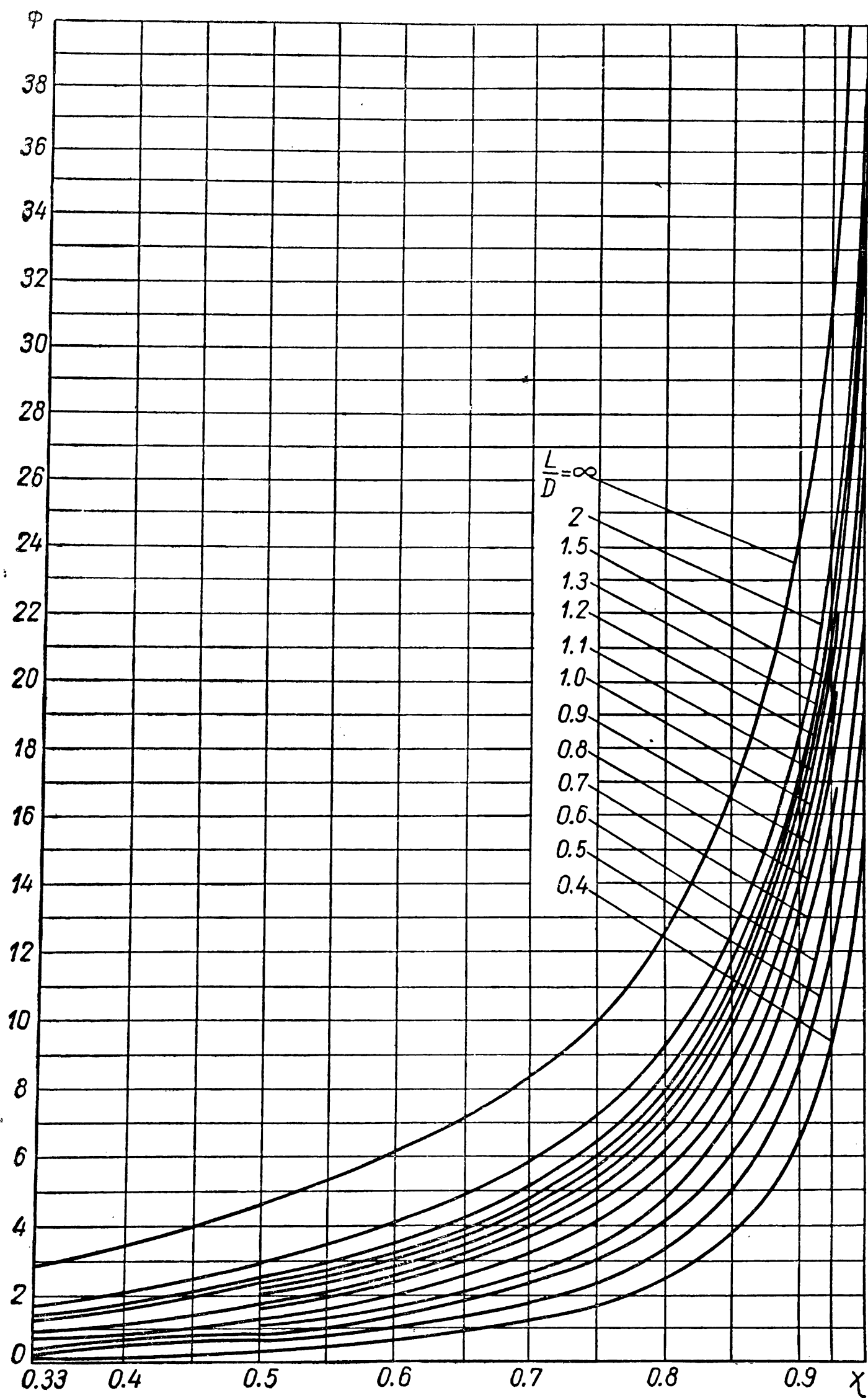


Fig. 233

It is extremely difficult to calculate the integral  $\Phi$  in a general form.

If we introduce an additional condition to the effect that the hydrodynamic forces arise within an arc of  $180^\circ$  of the common clearance between the shaft and shell it is possible to get the equation  $\Phi = f(\chi)$  for each ratio  $\frac{l}{D}$ .

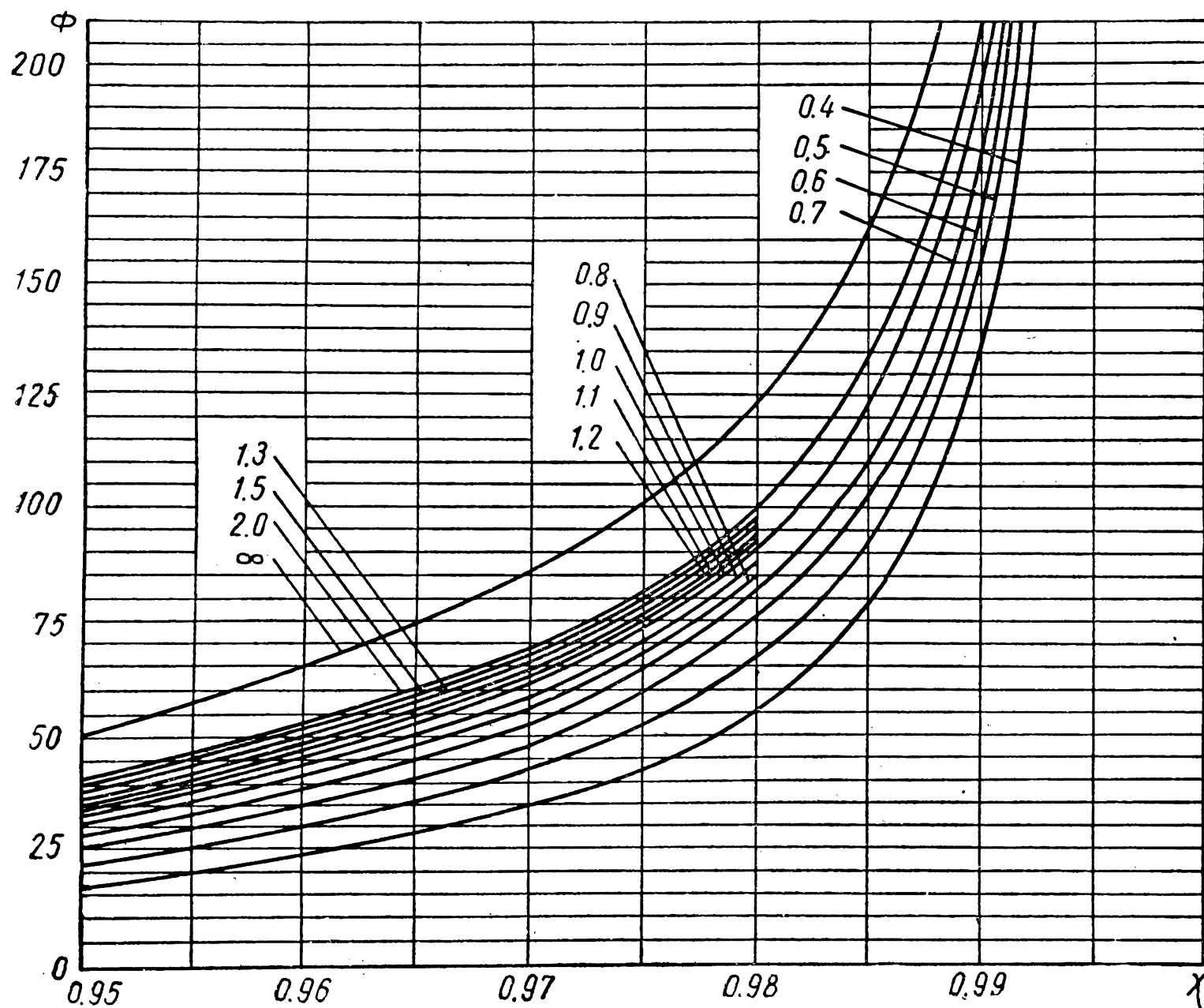


Fig. 234

Figs. 233 and 234 show corresponding graphs of  $\Phi = f(\chi)$  which are used to calculate the bearings for fluid friction.

These graphs can be illustrated for the most frequent values of  $\chi$  (from 0.333 to 0.995) with a sufficient degree of accuracy by the formula

$$\Phi = \frac{P\psi^2}{\eta v l} = 19.11 \frac{k\psi^2}{\eta n} = \frac{1.02}{\frac{h_{\min}}{D\psi} \left[ 1 + \left( \frac{D}{l} \right)^2 \left( 0.12 + 4.62 \frac{h_{\min}}{D\psi} \right) \right]} \quad (381)$$

where  $P$  is the total force arising in the layer of oil (the load-carrying capacity of the bearing) in kg;

$\psi$ —the relative clearance;

$\eta$ —the oil viscosity in kg sec/m<sup>2</sup>;

$v$ —the shaft velocity in m/sec;

$k$ —the load per unit of diametral projection of the bearing in kg/m<sup>2</sup>;

$h_{\min}$  —the minimum thickness of the oil layer in the clearance in m.

It follows from the equation (381) that the smaller  $h_{\min}$  the greater is the force  $P$  arising in the oil layer. The magnitude of  $h_{\min}$  should be such that the irregularities left after machining on the surfaces of the shaft and shell do not rupture the oil film. In order to account for possible inaccuracies in the shape of the part and insufficient rigidity of the unit,  $h_{\min}$  should be taken with an allowance.

For automobile and tractor engines when the surfaces of the shaft and shell are machined to the 8-9th degrees of accuracy  $h_{\min} = 5-6$  mc.

In the bearings of rolling mills the surface finish is to the 10-12th degrees of accuracy and  $h_{\min} = 10-30$  mc.

The relative clearance  $\psi$  is from 0.0005 to 0.002. Usually, the rated diameter of the journal (shell)  $D$ , its length  $l$ , the velocity of rotation  $v$  (or  $n$ ) and load on the support  $R$  are specified in advance. The calculation of a sliding bearing is reduced to finding the maximum allowable clearance  $\Delta$  or choosing a grade of oil of required viscosity so as to obtain fluid friction in the bearing, i. e., so as  $P \geq R$ .

The oil viscosity  $\eta$  should be taken for the mean temperature of the lubricating layer of an operating bearing.

For the bearings of automobile and tractor engines and metal-cutting machine tools  $t_{op} = 70-90^\circ\text{C}$  and for separately arranged toothed reduction gears and rolling mills  $t_{op} = 50-60^\circ\text{C}$ .

*Example.* Calculate a diametral clearance  $\Delta$  which will ensure fluid friction.

*Given:*

The bearing diameter  $D = 50$  mm, its length  $l = 75$  mm, shaft rpm  $n = 1,000$ , load on the bearing  $R = 3,000$  kg, thickness of the oil layer at smallest clearance  $h_{\min} = 8$  mc, lubricant—industrial oil 45 (machine oil “C”). The mean temperature of the lubricant layer  $50^\circ\text{C}$ .

*Calculation.* We take tentatively  $\psi = 0.0008$ .

The relative eccentricity [formula (371)] is

$$\chi = 1 - \frac{2h_{\min}}{D\psi} = 1 - \frac{2 \times 0.008}{50 \times 0.0008} = 0.6.$$

In accordance with the graph (Fig. 233) at  $\chi = 0.6$  and  $\frac{l}{d} = \frac{75}{50} = 1.5$ ,  $\Phi$  will equal 3.

The mean pressure from the equation (380)

$$k = \frac{P}{ld} = \frac{\Phi \eta n}{19.11 \psi^2} = \frac{3 \times 0.0038 \times 1,000}{19.11 \times 0.0008^2} = 935,000 \text{ kg/m}^2 = 93.5 \text{ kg/cm}^2.$$

The value of viscosity  $\eta = 0.0038$  is chosen from the graph in Fig. 224 for the respective grade of oil at  $t = 50^\circ\text{C}$ .

Then  $P = kld = 93.5 \times 7.5 \times 5 = 3,500 \text{ kg}$ .

The condition  $P \geq R$  is satisfied.

The diametral clearance  $\Delta = \psi D = 0.0008 \times 50 = 0.04 \text{ mm}$ .

The material for the manufacture of the shell should satisfy the condition (370)

$$\frac{Rn}{1,910 \times l} = \frac{3,000 \times 1,000}{1,910 \times 7.5} = 210 \frac{\text{kgm}}{\text{cm}^2 \times \text{sec}} \leq [kv].$$

In this case

$$v = \frac{\pi dn}{60 \times 100} = \frac{\pi \times 5 \times 1,000}{60 \times 100} \approx 2.6 \text{ m/sec}.$$

Consequently, the material should satisfy the condition

$$[k] \geq \frac{210}{2.6} \approx 81 \text{ kg/cm}^2.$$

We choose lead bronze of grade C30 for which  $[k] < 250 \text{ kg/cm}^2$  and  $[v] \leq 10\text{--}12 \text{ m/sec}$ .

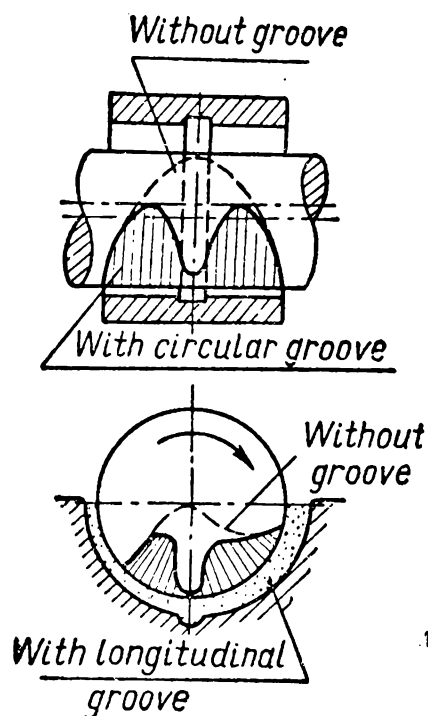


Fig. 235

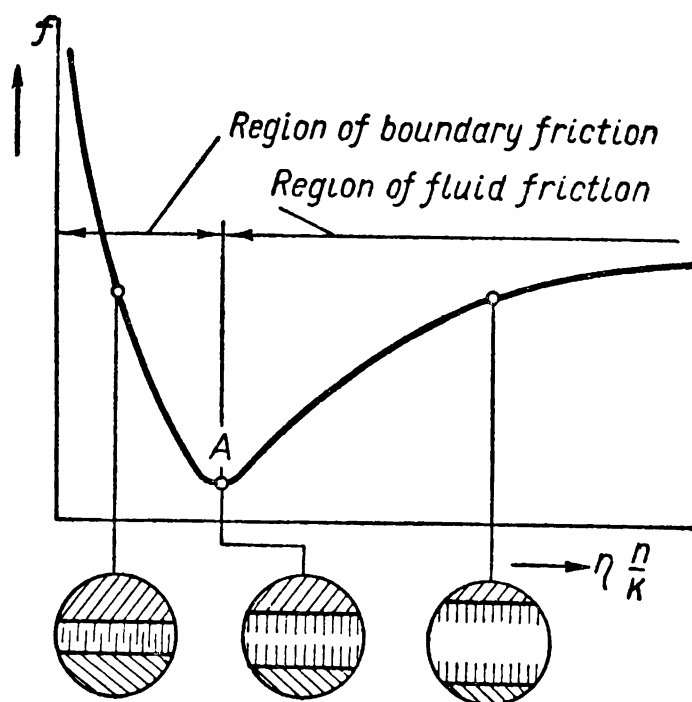


Fig. 236

Fig. 235 shows schematically the effect of oil grooves situated in the region of hydrodynamic pressures on the distribution of these pressures. The diagram shows that oil grooves should be located outside the loaded zone.

The coefficient of fluid friction in a designed bearing is computed with allowances which make the result very approximate. In the

general form the coefficient of fluid friction is

$$f = F \left( \frac{\eta n}{k} ; \Delta ; d ; l \right) .$$

The graph showing the dependence of the coefficient of friction  $f$  on the argument  $\frac{\eta n}{k}$  with the other given parameters is shown in Fig. 236.

At a point  $A$ , called the critical point, the friction passes, depending on service factors, from boundary to fluid friction or vice versa. This graph shows that the coefficient of fluid friction may have the same order of magnitude as the coefficient of boundary friction.

### THRUST BEARINGS

**Design.** Since a thrust bearing operates without a clearance between the conjugate parts an adequate supply of oil to the rubbing surfaces is extremely important.

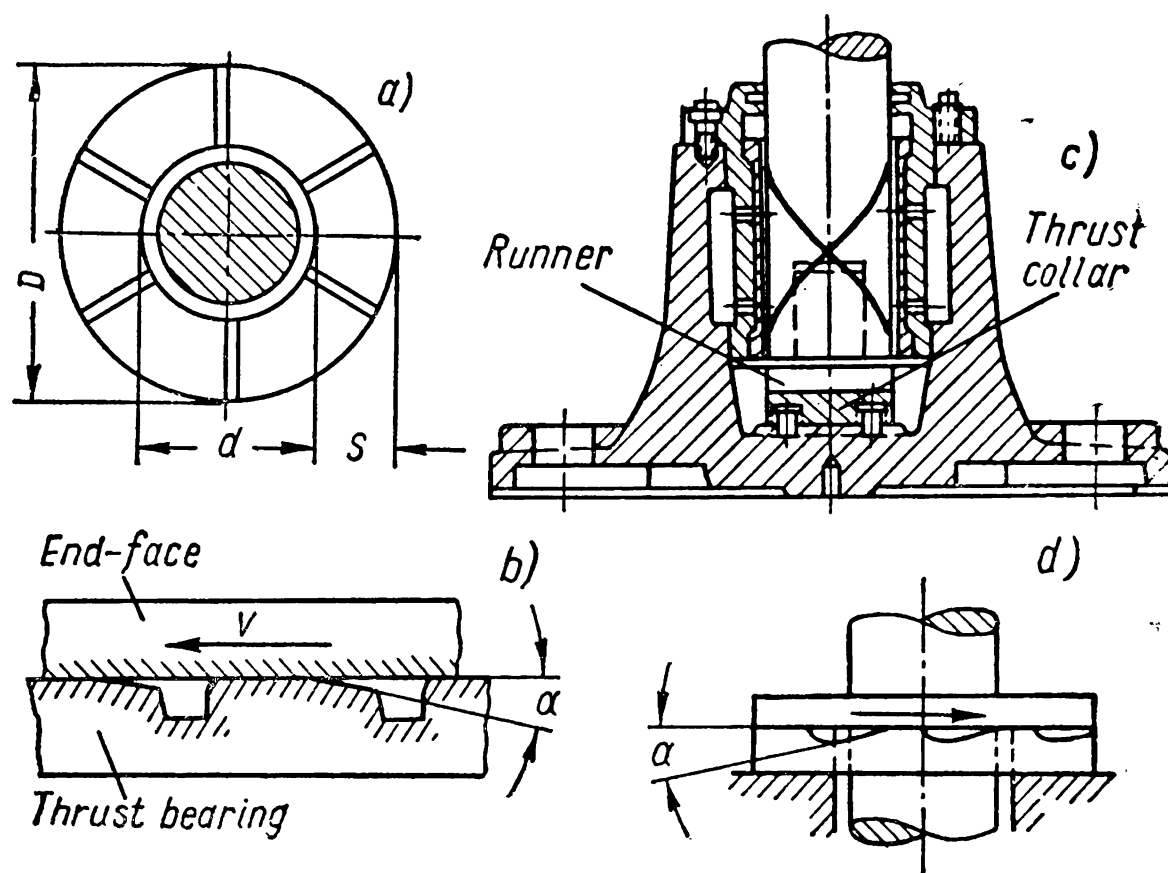


Fig. 237

Ordinarily the carrying section of a thrust bearing is designed as a grooved ring (Fig. 237, a). The oil flows along the grooves and the bevels on the ring segments (Fig. 237, b) facilitate the penetration of the oil into the area of contact.

If the thrust bearing is intended to operate in conditions of reversible rotation of the shaft, bevels are provided on both sides of the segments.



To eliminate local overloads on the bearing due to possible shaft misalignment, the thrust collar of the thrust bearing is made spherical in shape and mounted on fixing pins (Fig. 237, *c*).

In a runner the upper surface is of improved hardness and is easily replaced during maintenance.

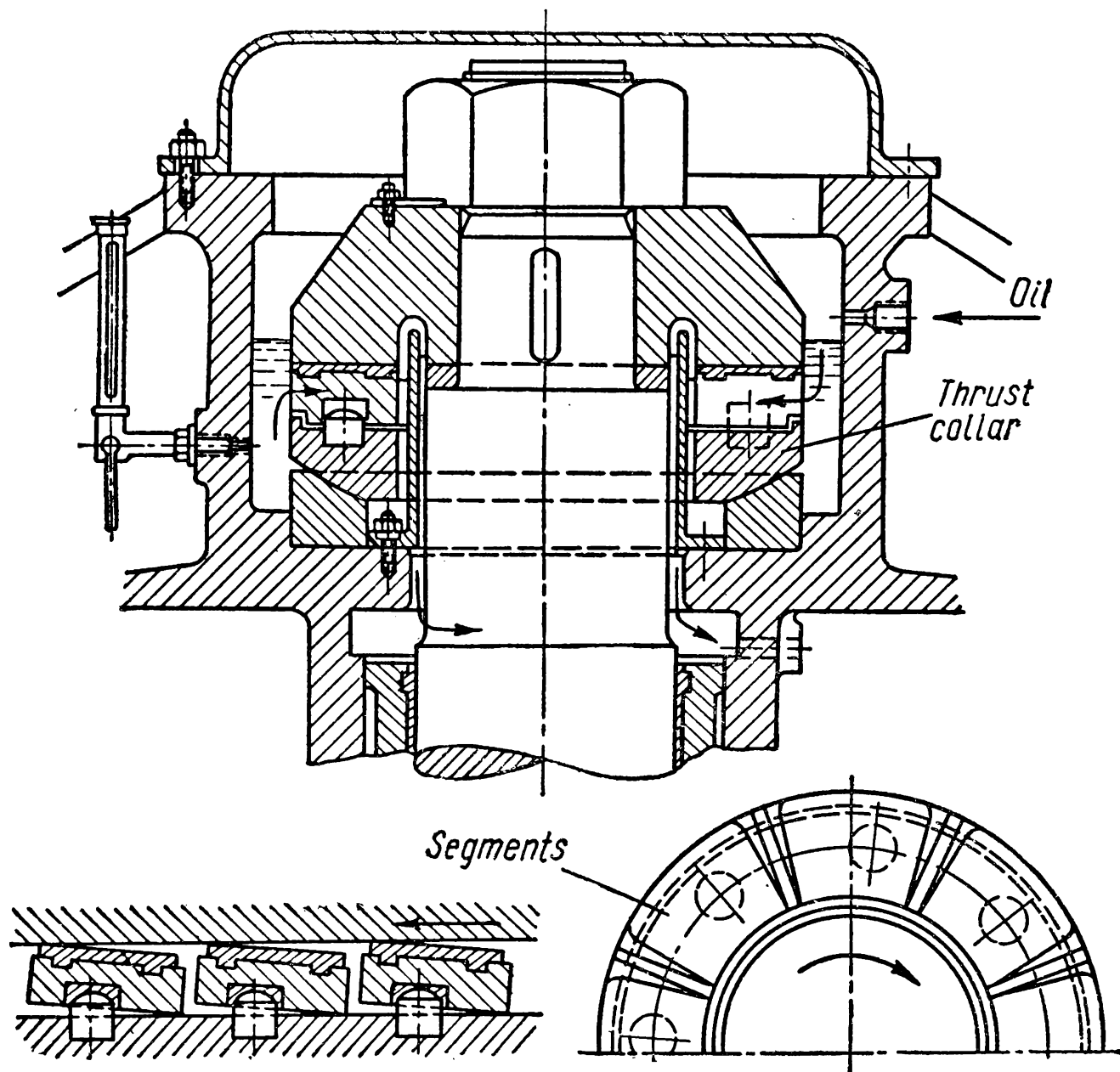


Fig. 238

When conditions exist for fluid friction the segments are beveled on one side (Fig. 237, *b* and *d*) to conform to the angle  $\alpha$  of the oil wedge calculated in advance.

However, fluid friction can be more reliably ensured by a design of a thrust bearing with self-aligning segments in which oil wedges are formed automatically during operation (Fig. 238).

The number of segments is from 4 to 16.

The load between separate segments is redistributed in case of shaft misalignment by means of an additional thrust collar with a spherical bottom (Fig. 238). The upper flat surface of this collar supports the segments.

The segments are made either from cast iron or bronze or from steel with a babbit lining.

**Calculation of Thrust Bearings.** When a thrust bearing operates in conditions of boundary friction the calculations are limited to checking for the absence of seizure by the arbitrary criterion  $kv$ .

If the thrust bearing is intended to operate in conditions of fluid friction, checking by  $kv$ , as in a similar case for a sliding bearing, is done only to choose an appropriate antifriction material and methods for machining its parts.

The main calculations for fluid friction conditions are reduced to finding one of the parameters; usually it is the number of the segments  $z$ .

*Calculations for the avoidance of seizure.* Unit pressure on the carrying surface of a thrust bearing is found from the formula

$$k = \frac{4A}{\pi(D^2 - d^2)\psi}$$

where  $A$  is the full load on the bearing;

$D$  and  $d$ —the outside and inside diameters of the thrust bearing carrying surface (Fig. 237,  $a$ );

$\psi$ —a factor accounting for incomplete utilisation of the carrying surface (oil grooves). Usually  $\psi \approx 0.9$ .

We denote (see Fig. 237,  $a$ ):

$$D_{mean} = \frac{D+d}{2} \text{ and } d = D - 2s.$$

Then, recalling that  $v = \frac{\pi D_{mean} n}{60 \times 100}$  m/sec, and after simple transformations, the absence of seizure can be expected when the following condition is satisfied:

$$\frac{An}{5,400 \times s} \leq kv_{mean} \quad (382)$$

where  $A$  is in kg,  $n$ —rpm, the segment width  $s$  in cm,  $k$  in kg/cm<sup>2</sup>, velocity by the mean diameter  $D_{mean}$  of the thrust bearing  $v_{mean}$  in m/sec.

The values of  $kv$  for various materials are taken from reference tables.

*Calculation for fluid friction.* Fig. 233,  $a$  can serve as a schematic representation of the end-face and segment of a thrust bearing. Since the angle of wedge  $\alpha$  is very small,  $\tan \alpha \approx \alpha$  and we can, therefore, write

$$h_m = \alpha x_m \text{ and } h = \alpha x.$$

Here  $x_m$  is the abscissa of cross-section of the fluid layer in which the hydrodynamic pressure is  $p = p_{max}$ .

After substituting in the equation (367) we obtain

$$\frac{dp}{dx} = \frac{6\eta v}{\alpha^2} \times \frac{x - x_m}{x^3}.$$

We designate the corresponding abscissae of the clearance ends as  $b_1$  and  $b_2$  (see Fig. 223, *a*). Then the pressure in the clearance cross-section expressed by the coordinate  $x$  is

$$\begin{aligned} p &= -\frac{6\eta v}{\alpha^2} \left[ \int_{b_1}^x \frac{dx}{x^2} - x_m \int_{b_1}^x \frac{dx}{x^3} \right] = \\ &= \frac{6\eta v}{\alpha^2} \left[ \left( \frac{1}{x} - \frac{1}{b_1} \right) - \frac{x_m}{2} \left( \frac{1}{x^2} - \frac{1}{b_1^2} \right) \right]. \end{aligned} \quad (383)$$

At  $x = b_2$  we have  $p = 0$  and from the latter equation we get

$$x_m = \frac{2b_1b_2}{b_1 + b_2}.$$

Substitution of this value in equation (383) gives

$$p = \frac{6\eta v}{\alpha^2} \left[ \left( \frac{1}{x} - \frac{1}{b_1} \right) - \frac{b_1b_2}{b_1 + b_2} \left( \frac{1}{x^2} - \frac{1}{b_1^2} \right) \right]. \quad (384)$$

The maximum hydrodynamic pressure  $p_{\max}$  is found from the latter expression when  $x = x_m$ :

$$p_{\max} = \frac{3}{2} \times \frac{\eta v}{\alpha^2} \times \frac{(b_2 - b_1)^2}{b_2b_1(b_2 + b_1)}. \quad (385)$$

The total force arising within one segment,  $s$  in width, in a radial direction is

$$P_1 = s \int_{b_1}^{b_2} p dx = \frac{6\eta vs}{\alpha^2} \left( \ln \frac{b_2}{b_1} - \frac{2B}{b_1 + b_2} \right). \quad (386)$$

Here  $B = b_2 - b_1$  is the length of the oil wedge.

We replace  $b_1 = \frac{h_{\min}}{\alpha} = \frac{h_{\min}}{\alpha B} B = mB$  where  $m = \frac{h_{\min}}{\alpha B}$ ,

$$b_2 = b_1 + B = (m + 1)B.$$

Then the equation (385) will take the form

$$p_{\max} = \frac{6\eta v}{\alpha^2 B} \times \frac{1}{4m(1+m)(1+2m)}. \quad (387)$$

Substituting in the right-hand side of the latter equation

$$\frac{6\eta v}{\alpha^2 B} = \frac{6\eta v B}{(\alpha B)^2} = \frac{6\eta v B}{h_{\min}^2} \times m^2$$

we can write this equation in the form

$$p_{\max} = \frac{6\eta v B}{h_{\min}^2} \times \frac{m^2}{4m(1+m)(1+2m)} = \frac{6\eta v B}{4h_{\min}^2} \times \frac{m}{2m^2+3m+1}. \quad (388)$$

The greatest of all possible values of  $p_{\max}$  will be determined by finding the maximum of the right-hand side of the equation (387) by differentiating by the argument  $m$ .

The value of  $p_{\max}$  is greatest when

$$m = \frac{h_{\min}}{aB} = \frac{\sqrt{2}}{2} \approx 0.7. \quad (389)$$

Utilising this value  $m$  for  $b_1$  and  $b_2$  we obtain after substituting in the equation (386)

$$P_1 = 0.182 \frac{\eta v B^2 s}{h_{\min}^2} \text{ kg}. \quad (390)$$

The flow of oil from the ends in the case of flat surfaces is accounted for by the correction

$$\beta = \frac{5}{3} \frac{1}{\left[1 + \left(\frac{B}{s}\right)^2\right]}.$$

For  $z$  segments taking into account the correction  $\beta$  the load-carrying capacity of the thrust bearing is

$$P = P_1 \beta z.$$

For fluid friction it is necessary that  $P \geq A$ , where  $A$  is the external axial load in kg.

After all substitutions and simple transformations the required number of segments ensuring fluid friction will be

$$z = 12.6 \frac{P h_{\min}^2 \left[1 + \left(\frac{B}{s}\right)^2\right]}{\eta D_{\text{mean}} n B^2 s} \quad (391)$$

where  $h_{\min}$  is the minimum thickness of the clearance cross-section in m;

$B$ —the length of the segment along the chord of mean diameter in m;

$\eta$ —the oil viscosity in kg sec/m<sup>2</sup>;

$D_{\text{mean}}$ —the mean diameter of the thrust surface in m;

$n$ —the shaft rpm.

For stationary segments we must in addition find from the relation (389) the angle  $\alpha$  at which the segment surfaces are inclined.

The values of  $h_{\min}$  and  $\eta_t$  are selected on the basis of the same considerations as those used in calculating radial bearings.

In practice the ratio  $\frac{B}{s}$  is taken from 0.5 to 1.

The number of segments  $z$  obtained from calculations [by the formula (391)] should satisfy the following obvious condition

$$z < \frac{\pi (D_{mean} - s)}{B}.$$

Otherwise, the segments will not be located on the perimeter of the thrust collar.

### LUBRICATING DEVICES FOR BEARINGS

Lubricating devices can supply either liquid oil or grease.

Depending on the mode of lubrication there are devices for lubricating each rubbing pair separately—*individual* devices—and

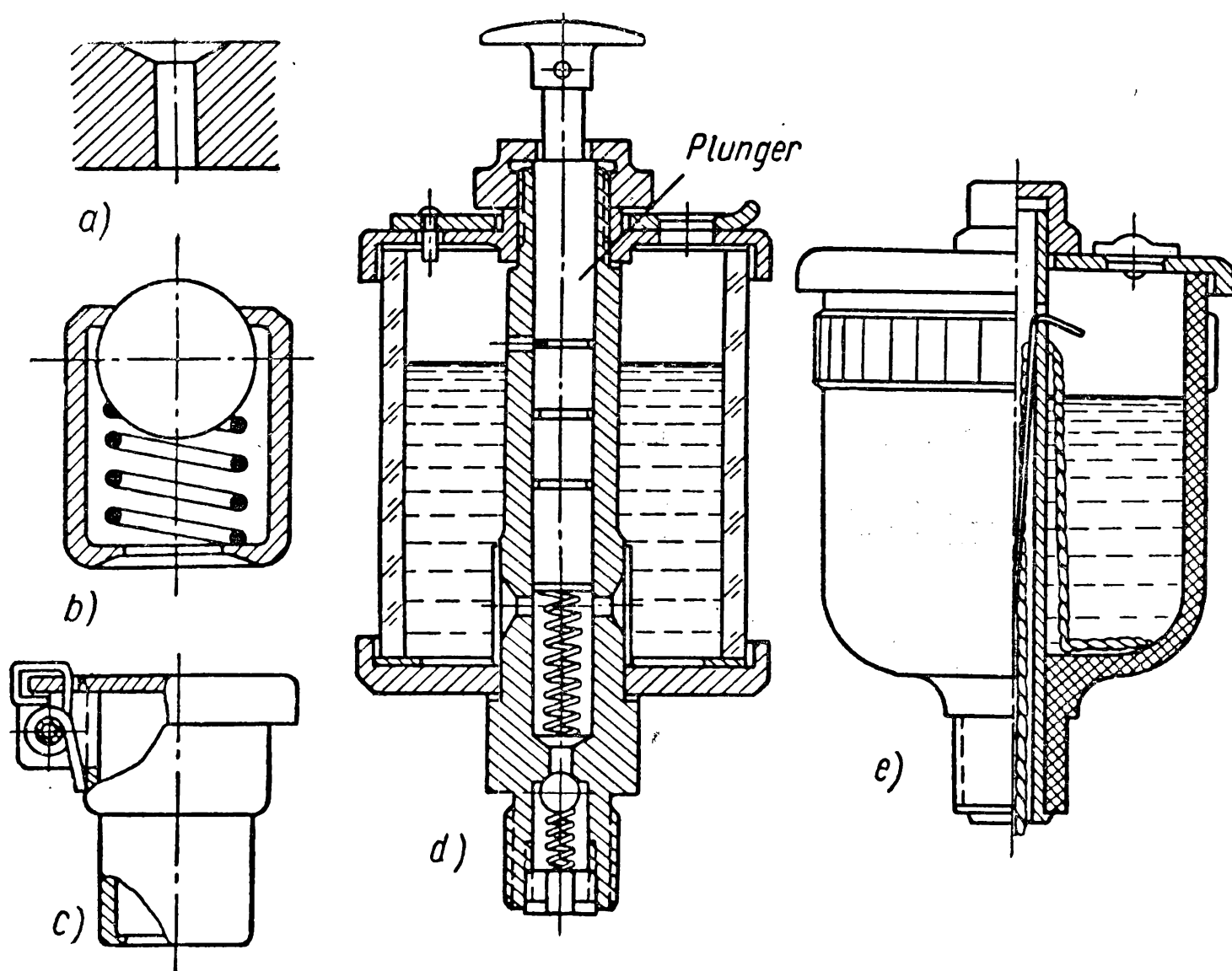


Fig. 239

*centralised* devices. The latter type feeds the lubricant from one oiling unit to several rubbing pairs simultaneously.

A simple device for individual lubrication is a countersunk hole (Fig. 239, *a*) into which oil is fed with the help of hand oilers.

To protect the unit from dirt use is made of oil holes with a ball (Fig. 239, *b*) or with a cover (Fig. 239, *c*). An oil hole with a cover can retain a certain reserve of oil.

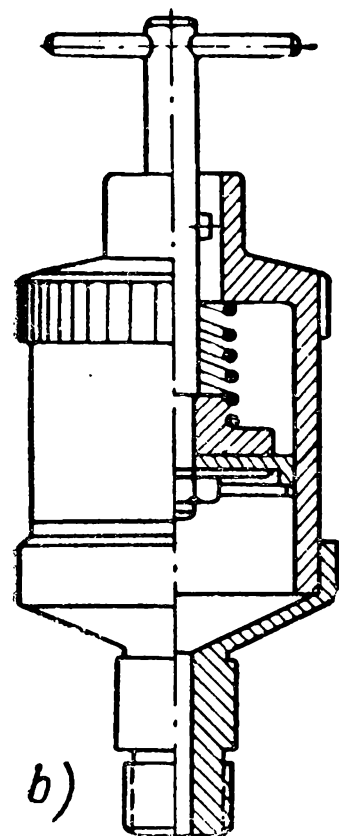
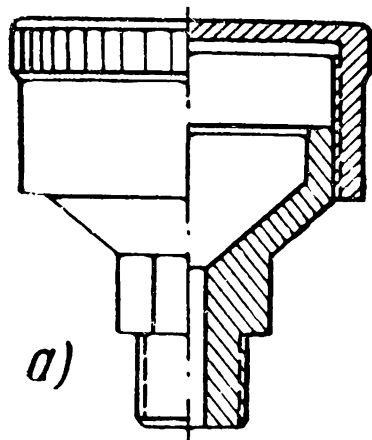


Fig. 240

Feeding the grease by a grease cup with a piston which presses the grease out continuously (Fig. 240, *b*) is a more reliable method.

Centralised grease lubrication can be effected only under pressure by means of a plunger or piston pump.

#### METHODS OF INCREASING THE OPERATING CAPACITY OF SLIDING BEARINGS

It is practically impossible to prevent the wear of a sliding bearing even if it operates in conditions of fluid friction.

As can be seen from the formulae (380) and (391) the load-carrying capacity of a bearing increases, all other conditions being equal, as

The lubricator shown in Fig. 239, *d* where oil is fed by pressing the plunger is a more convenient device ensuring a reserve of oil. A glass tube allows the level of oil in the lubricator to be seen.

All these devices are intended only for periodic lubrication.

A continuous supply of oil is ensured by means of wicks or oil rings.

Wick lubrication is based on the principle of a siphon through capillary channels in the wick fibres (Fig. 239, *e*).

Oil-ring lubrication is also very effective.

A metal ring with a diameter larger than that of the shaft is freely suspended from the journal (Fig. 229). The rotating shaft carries with it the ring which passes through an oil bath. From the ring the oil reaches the journal and spreads over it.

Centralised lubrication can be effected either by gravity from a reservoir mounted sufficiently high or by means of a pump.

Centralised lubrication is mainly employed for closed-type drives which allow oil circulation in the lubricating system.

A grease cup (Fig. 240, *a*) gives excellent service as an individual grease lubricator. The grease is pressed into the cup reservoir and is fed when necessary by turning the cover.

the velocity of shaft rotation increases. At low shaft velocities (when starting and stopping) the hydrodynamic pressure in the bearing drops so that friction is outside the fluid region, i. e., it is boundary or even semi-dry friction and it is then that the conjugate surfaces are subject to wear.

Wear in a bearing unit affects the work of the entire supporting member due to the changed geometry of the rubbing surfaces and increased clearance.

All antifriction materials can be tentatively subdivided into plastic (babbits, plastics) and brittle (bronzes, cast irons, powder-metals). The nature of the material affects in a definite way the nature of change in the form of the shell during wear.

Wear of babbitt is accompanied by denting because of a high plasticity of this material. Although in this case the form of the bore changes somewhat from a circle to an oval the total length of the oil wedge remains practically the same (Fig. 241, a).

Wear of a shell made from brittle material does not involve the crushing of the worn boundaries. In this case the section  $h_{min}$  where the region of hydrodynamic pressures ends noticeably shifts to the right and the length of the oil wedge and the clearance change (Fig. 241, b).

Thus, if we take the rate of wear of shells made from cast iron or lined with babbitt to be the same the former will lose the ability to carry external load much earlier than babbitt shells.

The service life of sliding bearings can be increased by design, production and operating measures.

When designing a bearing an attempt should be made to ensure the most favourable service conditions—fluid friction. Simultaneously, the factors neglected in design formulae but most essential for the effective operation of bearings with any mode of sliding friction should be taken into account. These factors include the correct location and adequate proportions of oil grooves, the rational choice of a lubricating device ensuring the supply of the necessary amount of oil to the working surfaces, effective heat dissipation and high rigidity of the entire bearing.

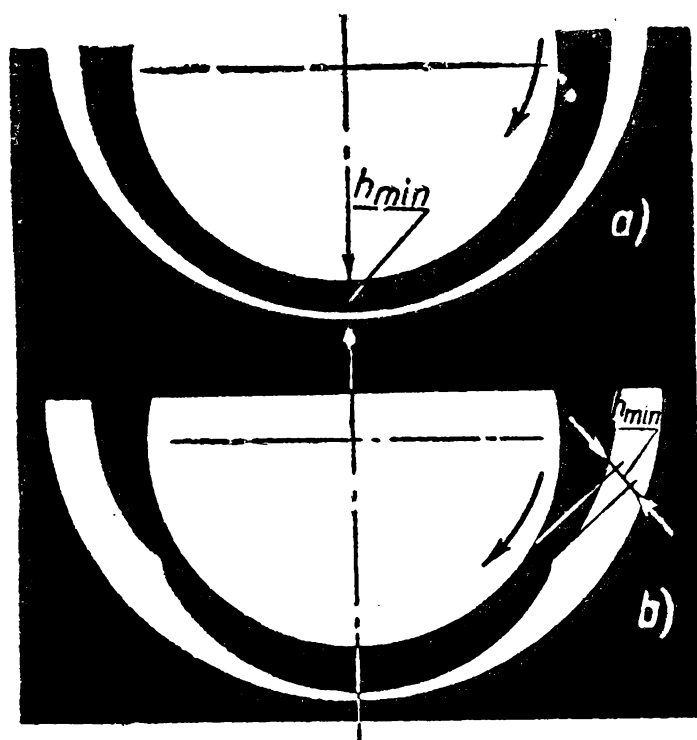


Fig. 241

The latter factor is especially important. Inadequate rigidity of the bearing unit will cause the excessive and constantly changing distortion of the forms and proportions of parts which will deteriorate lubricating conditions, increase local loads and finally put the entire unit out of order.

Special measures intended to increase service life should be looked for in each concrete case.

For example, in the bearings shown in Fig. 242 the clearance can be adjusted by means of a screw (Fig. 242, *a*) or wedges (Fig. 242, *b*) as the shell becomes worn.

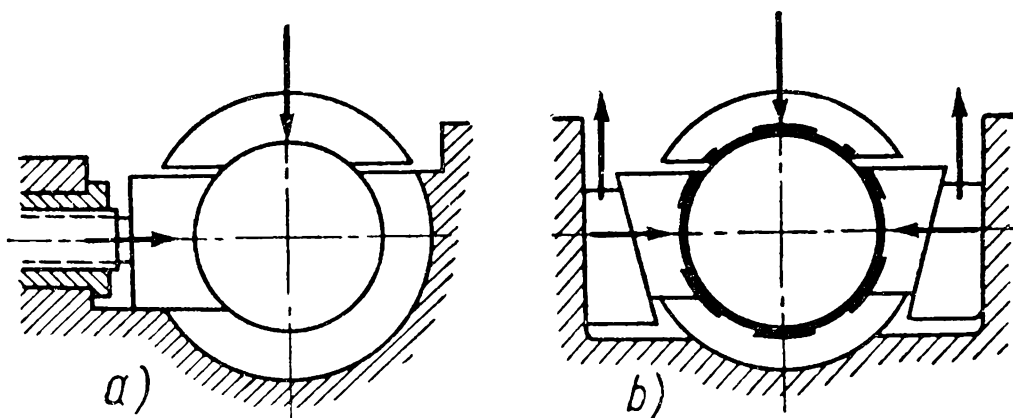


Fig. 242

The use of dissimilar materials for shell and journal is very effective in prolonging service life. When the materials of the shell and journal are interchanged the clearance increases negligibly because the antifriction bushing fitted to a steel shaft wears uniformly. The fact that the form of the region of hydrodynamic pressures is maintained for a long time is another material factor in the increased life of the bearing.

Production measures which can increase the bearings life consist mainly in exact adherence to the design forms and proportions of parts specified in the drawings, adequate preparation of antifriction surfaces, good finish and accurate assembly.

Precision in machining the shaft and bore is extremely important.

Operating conditions are most vital for the service life of a bearing unit. Much attention should be given to correct initial wear-in of the bearing, reliable and timely lubrication and careful oil filtering.

Oil with alien particles of dust, grit, wear products, etc., may damage the rubbing surfaces; besides, such oil cannot flow through the clearance in a continuous stream and ensure adequate conditions of fluid friction.



## CHAPTER XXII

## ROLLING CONTACT BEARINGS

*Types and designs of antifriction bearings.* The main elements of a rolling contact bearing are an antifriction bearing and housing which may have any form depending on the structural features of the machine.

Fig. 243 shows the pillow block of a line shaft with an antifriction bearing, Fig. 244—the mounting of a revolving housing on a fixed axle and Fig. 245—the compound mounting of a vertical engine shaft.

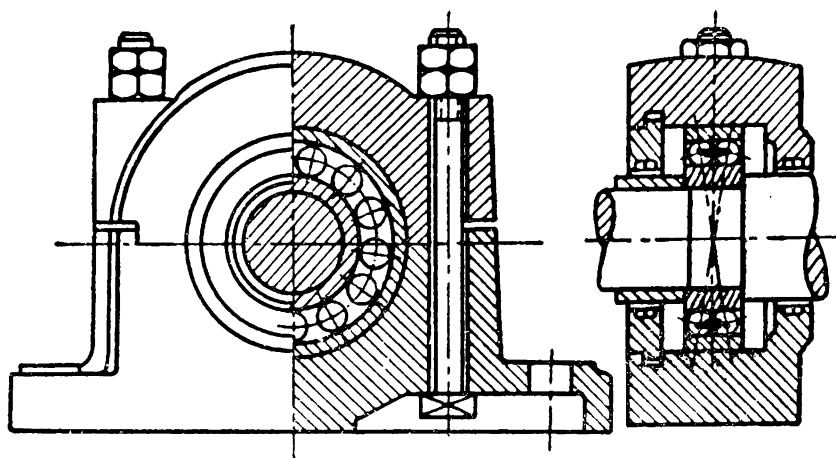


Fig. 243

The invention of the bicycle gave an impetus to the quantity production of antifriction bearings. A further development in the production and employment of these bearings was the result of the progress made in the automobile industry. Today there is hardly a branch of industry which does not employ antifriction bearings.

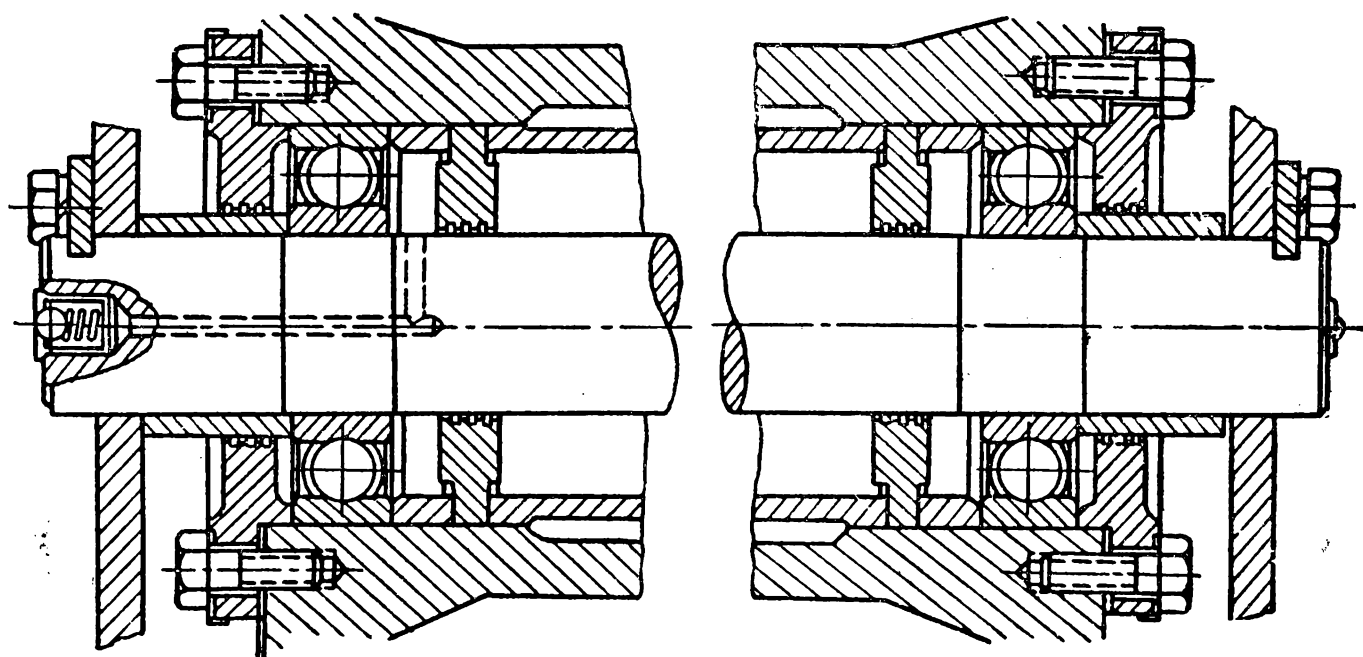


Fig. 244

The Soviet industry manufactures bearings in sizes from 1.5 mm to 2.6 m in outside diameter and weighing from 0.5 gm to 3.5 tons.

An antifriction bearing is composed of inner race 1 (Fig. 246), outer race 2, antifriction elements (balls or rollers) 3 and cage 4 which separates the balls or rollers.

In the Soviet Union bearing races, balls and rollers are made from chromium steel of grades IIIX6, IIIX9, IIIX15, IIIX15ГC and chrome-

nickel steel 12XH3A, 12X2H4A, etc. The bearing components made from these materials are heat-treated to the hardness  $R_C=62-65$ , ground and thoroughly polished. Cages are made from sheet steel (press-formed cages), bronze of grade АЖМц 10-3-1.5, aluminium (cast cages) and fabric laminated plastics.

The bearing can be installed in a unit so as to make the inner race rotate together with the shaft while the outer race is stationary (Fig. 243) or vice versa (Fig. 244).

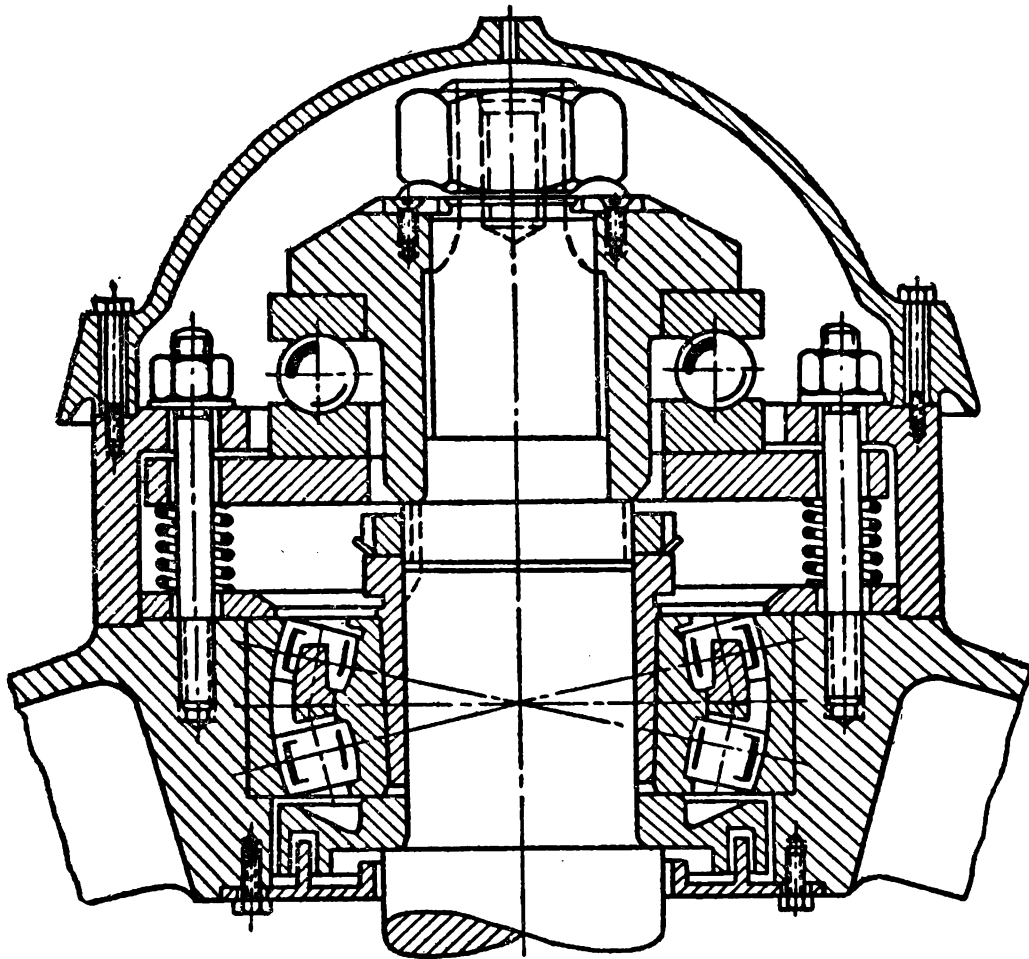


Fig. 245

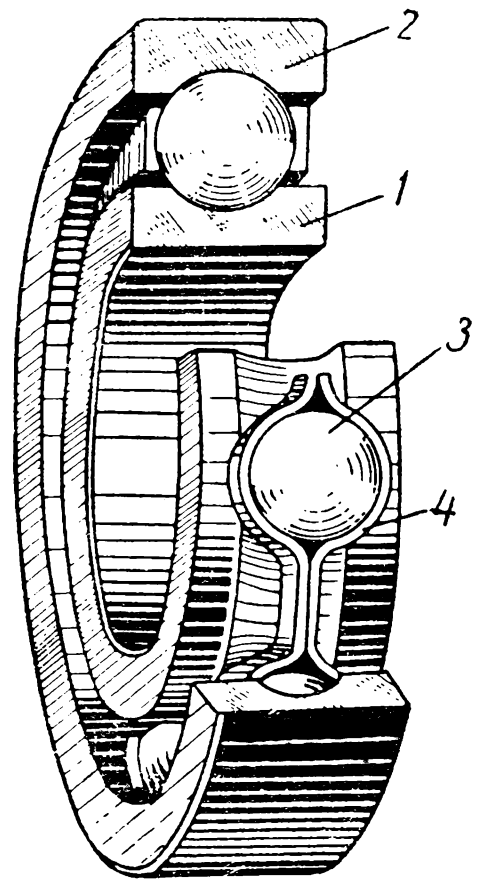


Fig. 246

Depending on the form of antifriction elements we have *ball* and *roller* bearings. A *needle* bearing is a modification of a roller bearing.

According to the way in which they take the load, bearings are subdivided into *radial* which carry mainly radial load, directed perpendicular to the geometrical axis of the shaft, *thrust* bearings carrying load along the axis of rotation of the bearing, and *radial-thrust* bearings resisting simultaneously both radial and axial forces.

*Single-row*, *double-row* and *four-row* bearings are distinguished, according to the number of rows of balls or rollers.

Fig. 247 gives a principal classification of the main types of anti-friction bearings.

Depending on overall dimensions, outside diameter, inside diameter and width, bearings fall into the following series: very light, light, medium, heavy, light wide and medium wide.

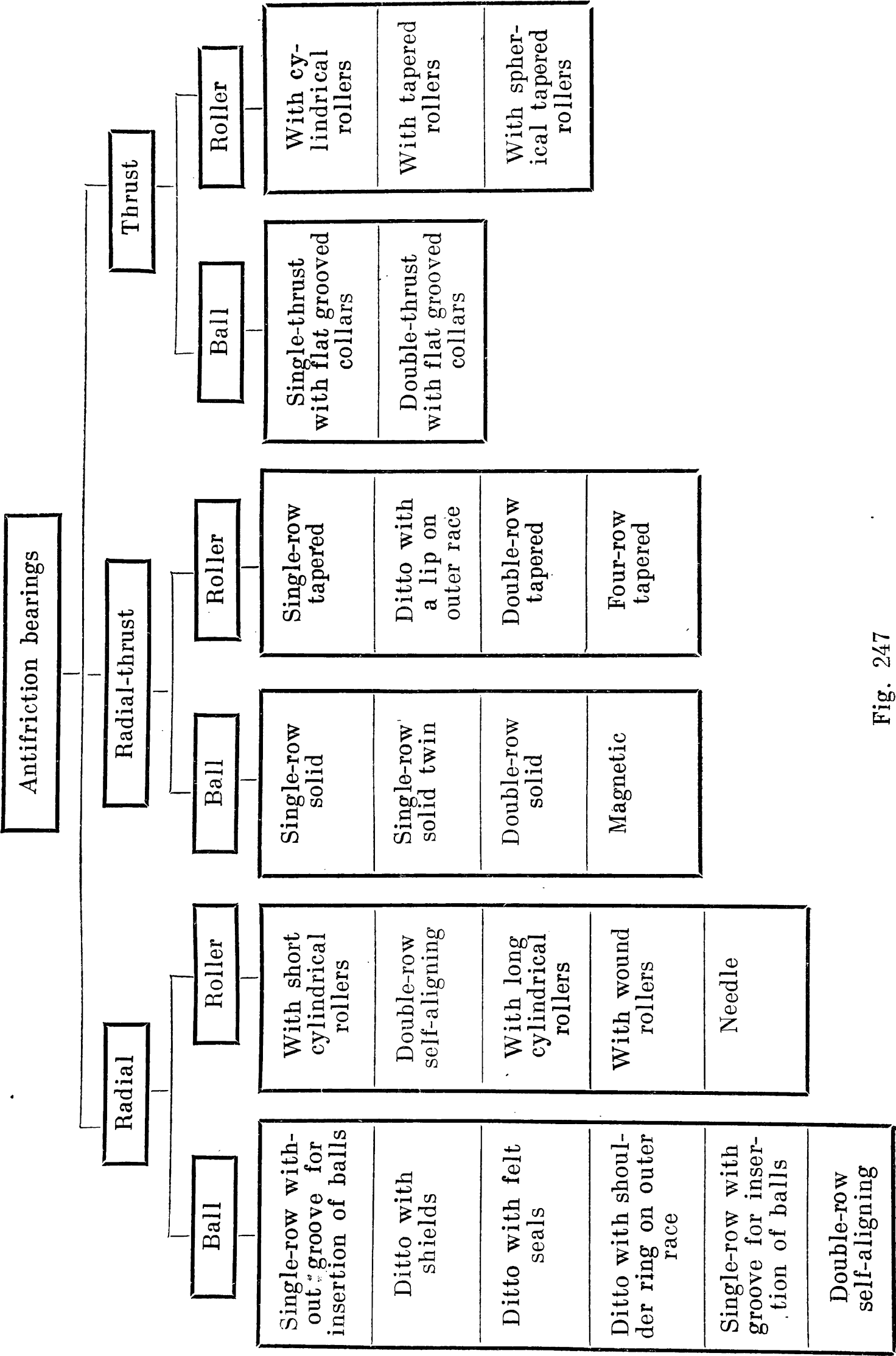


Fig. 247

The dimensions of bearings of different series with a constant  $d$  are shown in Fig. 248.

Some types of ball and roller bearings with their approximate load-carrying capacities are shown in Tables 61 and 62.

The load-carrying capacities of the main types of radial and radial-thrust bearings is compared in each series in the following way:

a) The load-carrying capacity of a single-row radial ball bearing (type 0000) is arbitrarily taken as unity.

b) The allowable axial load is shown in fractions of unity of the allowable unutilised purely radial load-carrying capacity of the given type of bearing.

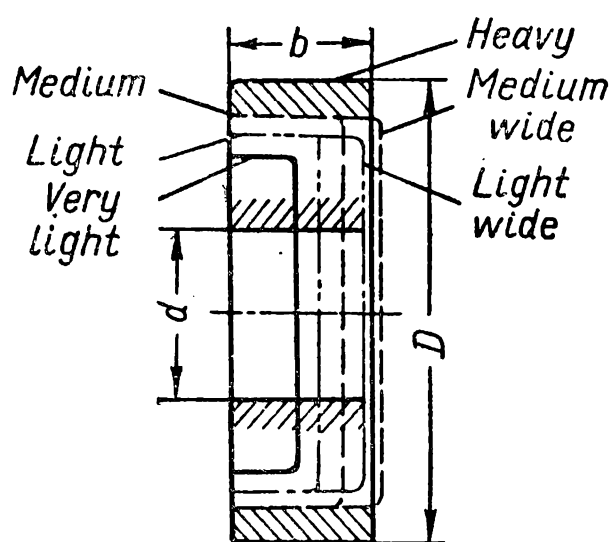


Fig. 248

If the purely radial load-carrying capacity of a bearing is  $Q$  then the allowable axial load  $A$  on the same bearing acting simultaneously with the radial load  $R$  amounts to  $k(Q-R)$ , where  $k$  is the factor indicated in the last column of Tables 61 and 62.

The bearings  $b$  (Table 61) and  $d$  (Table 62) are *self-aligning bearings*; all the other types *do not self-align*.

It follows from the data in Tables 61 and 62 that the bearings of type 56000 and 3000 possess the greatest radial load-carrying capacity. A large radial load-carrying capacity is also found in single-row roller bearings of all types.

The angle of taper  $\beta$  of the outer races (Fig.  $f$  in Table 62) of tapered bearings is usually  $9^\circ$ - $18^\circ$ . Bearings intended to carry mainly axial load have an angle  $\beta=25^\circ$ - $30^\circ$ .

To decrease the size and weight of antifriction bearings use is made of thin rollers—needles—1.6-5 mm in diameter. The length of needles is 5-10 times greater than their diameter. Such roller bearings, called *needle bearings*, are designed to take considerable radial loads without axial load.

In cageless needle bearings the total peripheral clearance (between the first and last needle) is 1-2 mm while the radial clearance between the needles and raceways is considerably larger than in ball and roller bearings and approximately equals the radial clearance of sliding bearings of the same diameter.

These clearances have an effect on the operating conditions of the needles which noticeably differ from the operating conditions of rollers in other types of roller bearings.

In the Soviet Union the markings and symbols of ball and roller bearings on drawings are expressed in figures. Each figure denotes some feature of the bearing in accordance with the following scheme.

The first and second figures from the right denote the rated inside diameter

Table 61

Some Types of Ball Bearings

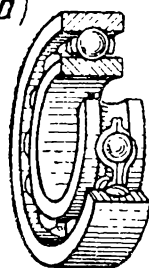
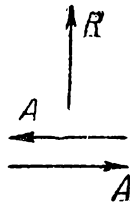
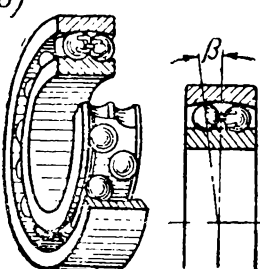
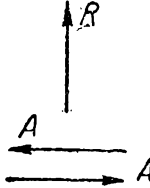
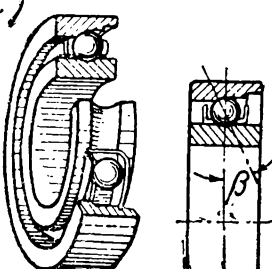

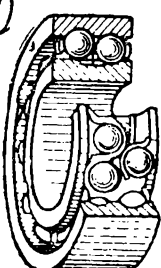

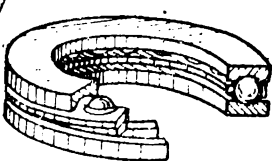

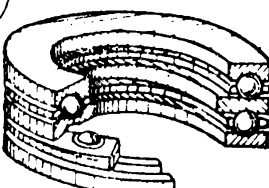

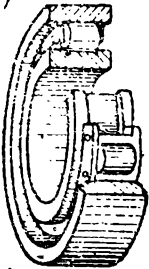

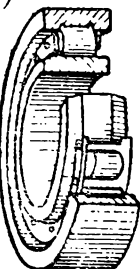

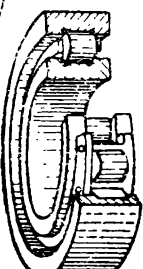
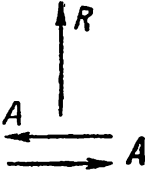
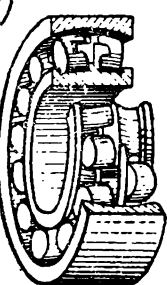
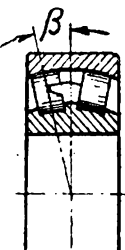

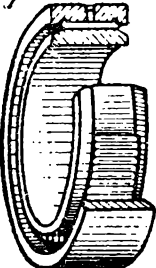

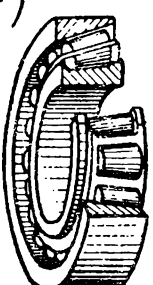
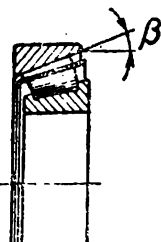
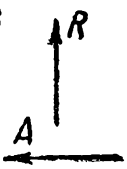
Sketch	Direction of applied load	Type	Sym- bol	Load-carrying capacity	
				Allowable load	
				purely radial	axial
Radial					
a) 		Single-row . . .	0000	1	up to 0.7
b) 		Double-row self-aligning . . .	1000	1	up to 0.2
Radial-thrust					
c) 		Single-row . . .	36000	1.4	up to 0.7
d) 		Double-row . . .	56000	2.3	up to 0.7
Thrust					
e) 		Single-thrust . .	8000	no	1
f) 		Double-thrust . .	38000	no	1

Table 62

Some Types of Roller Bearings

Sketch	Direction of applied load	Type	Sym- bol	Load-carrying capacity	
				Allowable load	
				purely radial	axial
a) 		Radial Without lips on outer race . . .	2000	1.7	no
b) 		Without lips on inner race . . .	32000	1.7	no
c) 		With one lip on inner race and with collar . .	92000	1.7	very low
d)  		Double-row self-aligning . . .	3000	2.0	up to 0.2
e) 		Needle with two lips on outer race . . . . .	74000	specified specially	no
f)  		Radial-thrust Single-row tapered	7000	1.9	up to 0.7

of the bearing (the rated diameter of the shaft at the point where the bearing is fitted) in mm; in this case:

a) for all bearings, except for magnetic bearings, with a hole diameter of 20 mm and over these two figures are the quotient of the division of the diameter in mm by 5;

b) for all bearings, except for magnetic bearings, the inside diameters from 10 to 17 mm are denoted as follows:

inside diameter of the bearing in mm	10	12	15	17
designation	00	01	02	03

c) for small bearings with an inside diameter up to 9 mm the first two figures from the right denote the actual size of the inside diameter in mm.

If the third figure from the right is 0, this indicates that in this case the first two figures refer to actual and not arbitrary diameter.

The third and seventh figures from the right denote the series of the bearing according to its diameter (3rd figure from the right) and width (7th figure). The series designations are as follows:

3rd figure	1	2	3	4	5	6
series	very light	light	medium	heavy	light wide	medium wide

The fourth figure from the right shows the type of bearing. The types are designated as follows:

Single-row radial ball bearing	0
Double-row self-aligning radial ball bearing	1
Radial bearing with short cylindrical rollers	2
Double-row self-aligning radial roller bearing	3
Needle or roller bearing with long cylindrical rollers	4
Roller bearing with wound rollers	5
Radial-thrust ball bearing	6
Tapered roller bearing	7
Thrust ball bearing	8
Thrust roller bearing	9

Tables 61 and 62 give the arbitrary designations of the main types of some bearings.

The fifth and sixth figures from the right indicate structural features of the bearing.

In the Soviet Union the degree of accuracy of an antifriction bearing is denoted by one or two Russian letters placed before the bearing number:

Normal degree of accuracy	H (not marked)
Increased degree of accuracy	II
Extra-increased degree of accuracy	BII
High degree of accuracy	B
Extra-high degree of accuracy	AB
Precision degree of accuracy	A
Extra-precision degree of accuracy	CA
Super-precision degree of accuracy	C

Examples. 1. Single-row thrust ball bearing (8), heavy series (4), for the shaft 55 mm (11) is designated 8411. 2. Radial-thrust ball bearing (6), light series (2), with an angle  $\beta=12^\circ$  (3) for the shaft 35 mm is designated 36207.

*Types and causes of failure in bearing components.* Antifriction bearings fail due to breakdown or to damaged working surfaces of the balls or rollers.

*Breakdown of bearing components.* When standard bearings are correctly mounted and operated the proportions of their elements ensure adequate strength.

In an antifriction bearing overloads usually cause the breakage of the outer race. A fracture in a ball bearing race usually occurs along the raceway, the plane of fracture being perpendicular to the bearing axis. The plane of fracture in the race of a roller bearing lies

in the same plane as the axis of rotation.

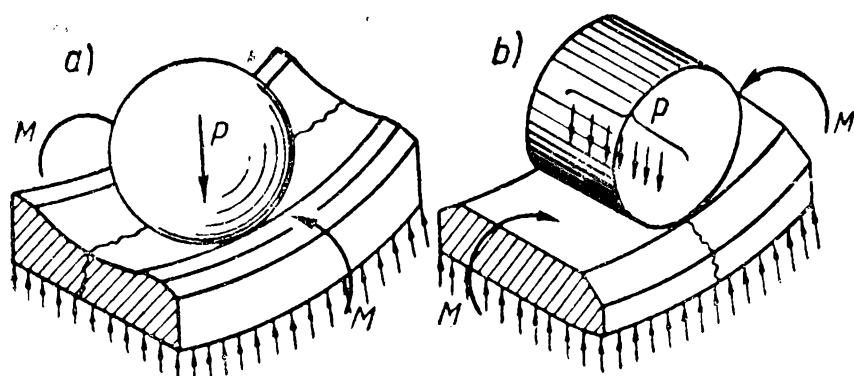


Fig. 249

The element of the outer race in the bearing can be regarded as a plate lying on an elastic base and loaded on one side with the pressure applied by the ball or roller and on the other with a combination of forces and moments applied along the

edges of this element. Fig. 249 shows diagrams of volume failure of the outer races of a ball (a) and roller (b) bearings.

When the bearings are misaligned the load acting on some balls or rollers sharply increases and may even crush them.

The cage is the element liable to fail first. In thin-walled press-formed cages the failure usually occurs where they are weakened by holes provided for rivets. In massive cages the webs between the balls or rollers are usually damaged.

The failure of cages is caused primarily by the high pressure exerted on them by the balls or rollers as a result of centrifugal forces which increase with a rise in the peripheral velocity. Therefore, the cages for high-speed bearings are made from materials with a high strength and small specific weight (fabric laminated plastics, aluminium alloys, etc.)

As a rule, the failure of antifriction bearings is occasioned by damage done to the working surfaces of their parts. The main types of surface failure of bearings are the following:

*Abrasive wear*, which occurs when a poorly protected bearing is made to operate in a medium contaminated with abrasive dust.

If the bearings operate for a long time in conditions of abrasive wear they develop large clearances between the races and balls or rollers.

*Seizure*, which takes place due to friction at high pressure exerted by the balls or rollers on the soft metal of the cage when there is no lubrication.



*Pitting due to fatigue* of the working surfaces occurring as a result of cyclic contact load is the main cause of the failure of antifriction bearings.

### FUNDAMENTALS OF THE THEORY OF ANTIFRICTION BEARINGS

**Load Distribution between Balls or Rollers.** *Radial ball bearings.* The load in radial bearings is not spread uniformly between the balls.

Let the load  $R$  be acting on a bearing (Fig. 250). Denoting the forces compressing the balls by  $P_0, P_1, \dots, P_n$  and utilising the equilibrium condition of the inner race acted upon by these forces we obtain

$$R = P_0 + 2P_1 \cos \gamma + 2P_2 \cos 2\gamma + \dots + 2P_n \cos n\gamma. \quad (392)$$

Here  $\gamma, 2\gamma, \dots, n\gamma$  are the angles between the direction of action of the force  $R$  and the radial plane of each respective ball.

If we assume that the bearing races retain their circular form (do not bend under load) the displacement of the inner race relative to the outer will be due to the contact deformations  $\delta_0, \delta_1, \delta_2, \dots, \delta_n$  where the balls touch the raceways and then

$$\delta_1 = \delta_0 \cos \gamma; \delta_2 = \delta_0 \cos 2\gamma; \dots; \delta_n = \delta_0 \cos n\gamma. \quad (393)$$

From the theory of contact deformations the relation between the deformation of the ball  $\delta$  and the force  $P$  that causes it in the bearing can be represented as  $\delta = c_b P^{\frac{2}{3}}$ , i. e.,

$$\delta_0 = c_b P_0^{\frac{2}{3}}; \delta_1 = c_b P_1^{\frac{2}{3}} \dots; \delta_n = c_b P_n^{\frac{2}{3}}$$

where  $c_b$  is the proportionality factor.

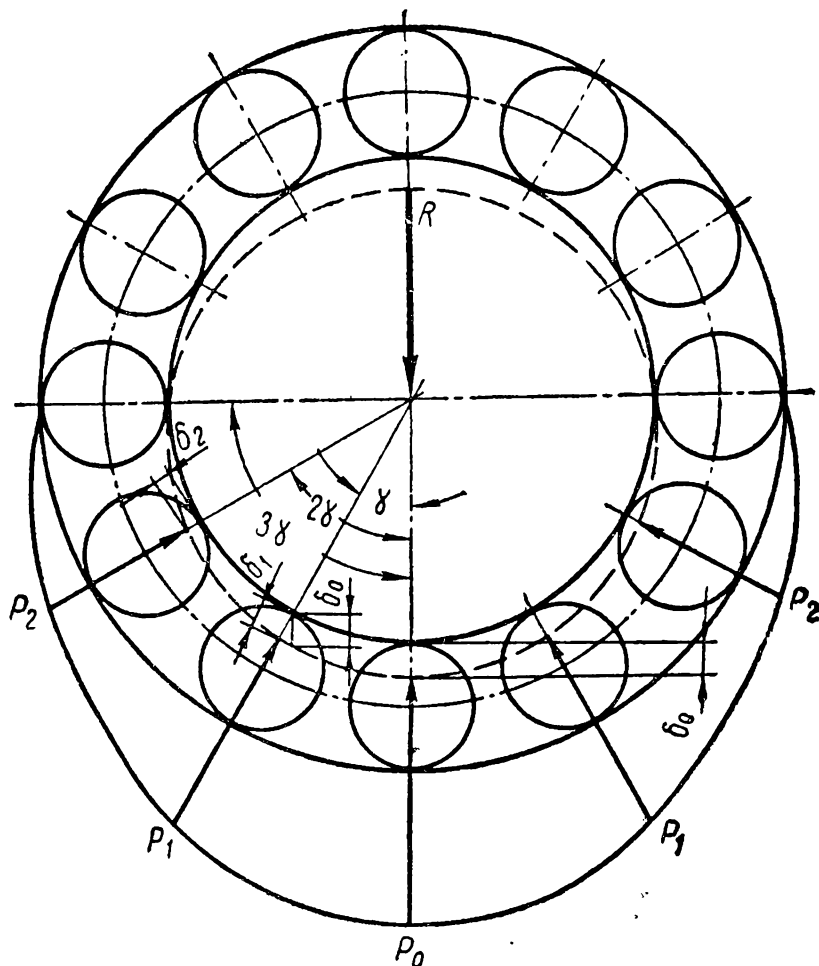


Fig. 250

It follows from these equations that

$$\frac{\delta_1}{\delta_0} = \left( \frac{P_1}{P_0} \right)^{\frac{2}{3}}; \quad \frac{\delta_2}{\delta_0} = \left( \frac{P_2}{P_0} \right)^{\frac{2}{3}}; \quad \dots; \quad \frac{\delta_n}{\delta_0} = \left( \frac{P_n}{P_0} \right)^{\frac{2}{3}}. \quad (394)$$

From the equations (393) and (394) we have

$$P_1 = P_0 \cos^{\frac{3}{2}} \gamma; \quad P_2 = P_0 \cos^{\frac{3}{2}} 2\gamma; \quad \dots; \quad P_n = P_0 \cos^{\frac{3}{2}} n\gamma.$$

Substituting these values in the equation (392) we get

$$R = P_0 \left( 1 + 2 \sum_{i=1}^n \cos^{\frac{5}{2}} i\gamma \right). \quad (395)$$

Multiplying and dividing the right-hand side of this equation by  $z$  and introducing

$$k_b = \frac{z}{1 + 2 \sum_{i=1}^n \cos^{\frac{5}{2}} i\gamma} \quad (396)$$

where  $z$  is the number of balls we get for the maximum load on a ball the following expression

$$P_0 = \frac{k_b R}{z}. \quad (397)$$

At  $z = 10, 15, 20$  the angle  $\gamma = 36^\circ, 24^\circ, 18^\circ$  and, respectively,  $k_b = 4.38, 4.37, 4.36$ .

Taking the mean value we have

$$P_0 = \frac{4.37R}{z}.$$

This formula has been obtained on the assumption that in a bearing under load there is no radial clearance between balls and races.

*Thrust ball bearings.* With the load  $A$  acting along the axis of a thrust bearing and assuming that only 80% of all balls take the load, the force acting on each ball will be  $P_0 = \frac{A}{0.8z}$ .

*Radial roller bearings.* In these bearings, as in radial ball bearings, the load is not spread uniformly between the rollers.

The relation between the force  $P$  compressing the roller and its deformation  $\delta$  has the form

$$\delta = c_r \times P,$$

then

$$\delta_0 = c_r P_0; \quad \delta_1 = c_r P_1; \quad \dots; \quad \delta_n = c_r P_n. \quad (398)$$

Here  $c_r$  is the proportionality factor.  
It follows from these equations that

$$\frac{\delta_1}{\delta_0} = \frac{P_1}{P_0}; \quad \frac{\delta_2}{\delta_0} = \frac{P_2}{P_0}; \quad \dots; \quad \frac{\delta_n}{\delta_0} = \frac{P_n}{P_0}. \quad (399)$$

The formulae (392) and (393) also hold for roller bearings.  
Solving simultaneously the equations (393) and (399) we obtain

$$P_1 = P_0 \cos \gamma; \quad P_2 = P_0 \cos 2\gamma; \quad \dots; \quad P_n = P_0 \cos n\gamma.$$

Substituting these values in the equation (392) we get the formula

$$R = P_0 \left( 1 + 2 \sum_{i=1}^n \cos^2 i\gamma \right).$$

Denoting

$$k_r = \frac{z}{1 + 2 \sum_{i=1}^n \cos^2 i\gamma} \quad (400)$$

we shall get, with the number of rollers  $z = 10-20$ , the mean value  $k_r = 4$  and for the most heavily loaded roller  $P_0 = \frac{4R}{z}$ .

The magnitude of radial clearance has a material effect on the nature of load distribution between the balls and rollers and on the value  $P_0$ . If the clearance increases, even within the norm, the maximum load on the ball or roller grows by 15-20%. Therefore, in the formulae for  $P_0$  of ball and roller bearings we take  $k_b = 5$  and  $k_r = 4.6$  and these formulae for the maximum load take the form

$$P_0 = \frac{5R}{z} \quad (401)$$

and

$$P_0 = \frac{4.6R}{z}. \quad (402)$$

The correct geometry of the bearing components has the greatest effect on the magnitude  $P_0$ . If the outer race bends under load and loses its original circular form the loads between balls or rollers will be redistributed.

**Stresses at Points of Contact of Bearing Components.** The load  $P_0$  is used to find the maximum stress at the point of contact between balls or rollers and the bearing races.

When applied to a single-row radial ball bearing the formula (29) for determining the maximum stress at the point of contact between the most heavily loaded ball and the raceway will

take the form

$$\sigma_{\max} = \frac{4,100}{m_1 m_2} \sqrt[3]{P_0 \left( \frac{4}{d_b} \pm \frac{1}{r_{in(out)}} - \frac{1}{r_\theta} \right)^2} \text{ kg/cm}^2. \quad (403)$$

Here  $m_1$  and  $m_2$  are the numerical factors taking into account the curvature of the contact surfaces;

$d_b$ —the diameter of the ball in cm;

$r_{in}$  and  $r_{out}$ —the radii of the circumference along which the ball rolls in the raceway, for the inner and outer races of the bearing respectively in cm (Fig. 251, a);

$r_\theta$ —the radius of curvature of the raceway in cm.

The plus sign in the formula (403) is taken for the inner race and the minus sign for the outer race.

It follows from this formula that, all other conditions being equal, the smaller the radius  $r_\theta$  is, i. e., the closer the contact

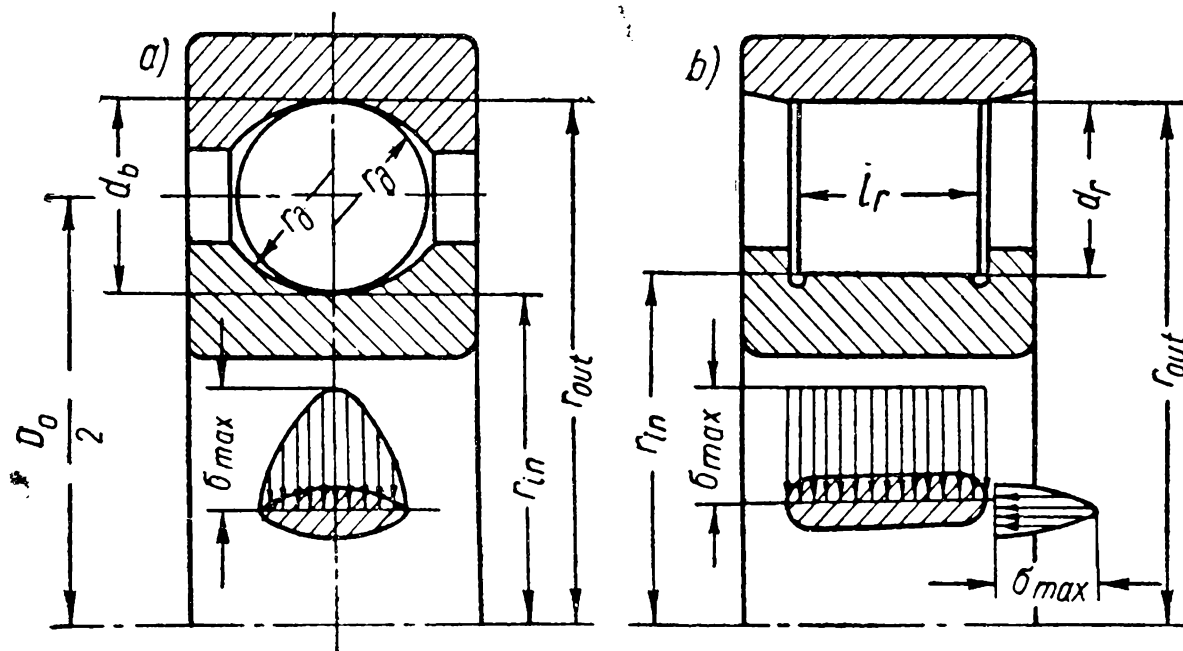


Fig. 251

between the ball and the bearing surface, the smaller  $\sigma_{\max}$  will be and, consequently, the more favourable the conditions for transmitting the effort.

A load which causes the same stress in the area of contact of two balls is 5.4 times less than in the case of a ball contacting a sphere with  $r_\theta = 3.5d$ . As the radius  $r_\theta$  of the raceway approaches the radius of the ball the allowable load increases and at  $r_\theta = 0.515d_b$  becomes 70 times greater than in the case of contact between two balls (Fig. 252).

A larger contact area, while favourably affecting the stress magnitude, simultaneously increases the sliding friction between the ball and the raceway.

The arc of contact is always larger on the raceway of the outer race, which is concave relative to the ball (see Fig. 251, *a*), than on the convex raceway of the inner race. For this reason, the stress  $\sigma_{\max}$  is larger on the inner race [see formula (403)] and, in

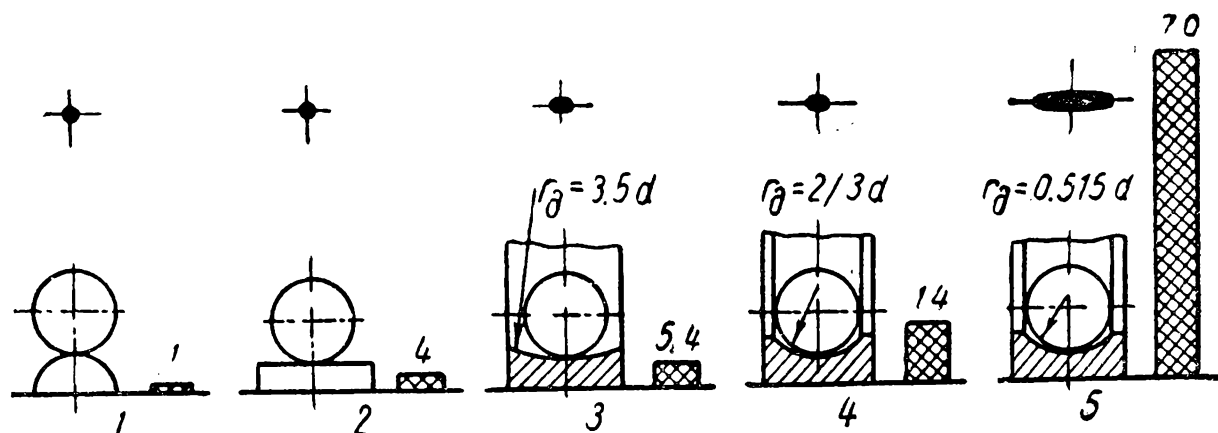


Fig. 252

order to equalise to some extent the stresses when the radius of the raceway on the inner race is  $r_d = 0.515d_b$ , we sometimes take  $r_d = 0.533d_b$  on the outer race.

If in the equation (403) we denote  $r_{in(out)} = \alpha d_b$  and  $r_d = \beta d_b$  where  $\alpha$  and  $\beta$  are constants we shall get

$$\sigma_{\max} = \frac{4,100}{m_1 m_2} \sqrt[3]{\left(4 + \frac{1}{\alpha} - \frac{1}{\beta}\right)^2} \sqrt[3]{\frac{P_0}{d_b^2}} = \lambda_b \sqrt[3]{\frac{P_0}{d_b^2}}. \quad (404)$$

Here  $\lambda_b = \frac{4,100}{m_1 m_2} \sqrt[3]{\left(4 + \frac{1}{\alpha} - \frac{1}{\beta}\right)^2}$ ; this magnitude depends only

on the design of the bearing. For standard ball bearings  $\lambda_b = 5,100-5,400$ .

The formula (30) for determining the maximum surface stresses between the roller and races has the form\*

$$\sigma_{\max} = 610 \sqrt{\frac{P_0}{l_r} \left( \frac{2}{d_r} \pm \frac{1}{r_{in(out)}} \right)} \text{ kg/cm}^2 \quad (405)$$

where  $l_r$  and  $d_r$  are the length and diameter of the roller in cm;  $r_{in}$  and  $r_{out}$ —the radii of the circumference of the raceway along which the roller moves, for the inner and outer races (Fig. 251, *b*).

The plus sign is taken for the inner race and the minus sign—for the outer race.

\* According to research carried out by Academician P. L. Kapitsa, the actual stresses during rotation of a lubricated bearing are considerably less than the stresses found from the formulae (403) and (405) because the oil film increases the area of contact of the conjugate bearing elements.

Denoting  $r_{in} = \alpha' d_r$  where  $\alpha'$  is a constant value, the equation (405) may be written thus

$$\sigma_{\max} = 610 \sqrt{2 + \frac{1}{\alpha'}} \sqrt{\frac{P_0}{l_r d_r}} = \lambda_r \sqrt{\frac{P_0}{l_r d_r}} \tag{406}$$

Here  $\lambda_r = 610 \sqrt{2 + \frac{1}{\alpha'}}$ .

For standard radial bearings with short cylindrical rollers  $\lambda_r = 955$ .

*Frequency of load repetition on the bearing elements.* As a radial bearing rotates each ball or roller first passes through the loaded zone where it is subjected to compressive stresses and then through the unloaded region where it is relieved of load.

In this way the balls and rollers are under cyclic loading. All other conditions being equal, the periodicity of loading depends on whether the inner or outer race revolves.

Table 63 gives formulae for determining the number of revolutions of the elements of a radial bearing and, to aid their understanding, the results calculated by these formulae for the bearing 210.

Table 63

Kinematic Ratios for Elements of a Radial Bearing

Race in rotation	Rpm		Rpm for bearing 210 ( $D_0 = 70$ and $d_b = 12.7$ mm)			
	of cage	of ball around its axis	of inner race $n_{in}$	of outer race $n_{out}$	of cage $n_o$	of ball $n_b$
inner race $n_{out} = 0$	$n_o = \frac{n_{in}}{2} \times \frac{D_0 - d_b}{D_0}$	$n_b = n_{in} \frac{D_0^2 - d_b^2}{2D_0 d_b}$	1,000	0	442	2,652
outer race $n_{in} = 0$	$n_o = \frac{n_{out}}{2} \times \frac{D_0 + d_b}{D_0}$	$n_b = n_{out} \frac{D_0^2 - d_b^2}{2D_0 d_b}$	0	1,000	592	2,652

Here  $D_0$  and  $d_b$  are the mean diameter of the cage and the diameter of the ball respectively.

It follows from the data cited in Table 63 that the velocity of the cage is less when the inner race rotates.

The velocity of the ball does not depend on what race is in rotation.

Since the balls are enclosed in cages the frequency of load repetitions experienced by any point on the raceway also depends on what race is in motion.

The frequency of load repetitions can be calculated from the formulae in Table 64.

It follows from the comparison of the expressions given in Table 64 that the number of load repetitions taken by the inner race is larger than that taken by the outer.

In addition, the formulae (403) and (405) show that the compressive stresses, all other conditions being equal, are greater on the raceway of the inner race. Therefore, when the outer race is rotated failure due to metal fatigue sets in earlier than with the inner race in rotation.

As a result, preference is given to designs with a rotating inner race.

Table 64

Formulae for Determining the Number of Load Repetitions

Race in rotation	Number of load repetitions experienced per minute by any point on the raceway with a constant direction of loading	
	on inner race	on outer race
Inner race	$u_1 = \frac{z}{2} \times \frac{D_0 + d_b}{2D_0}$	$u_4 = z \frac{D_0 - d_b}{2D_0}$
Outer race	$u_2 = z \frac{D_0 + d_b}{2D_0}$	$u_3 = \frac{z}{2} \times \frac{D_0 - d_b}{2D_0}$

**Operating Capacity of Antifriction Bearings.** *The service life  $N$  of a bearing is understood to mean the time expressed in a total number of revolutions during which not less than 90% of a batch of bearings of the given type would operate without failure in similar operating conditions.*

Within a batch of identical bearings under the same operating conditions the service life (the total number of revolutions before failure sets in) varies within a wide range, approximately 1 : 40. Such a range of service life is accounted for by different materials, heat treatment, surface finish and accuracy of the bearing elements.

Fig. 253 shows a typical curve for the range of service life, the mean service life  $N_{mean}$  being taken as unity. The graph shows that only 40% of the bearings have a service life which equals the arithmetical mean for the given batch and that 90% of the bearings have a service life equal to 20% of this mean value.

If one batch of radial bearings of a definite type operates under constant load  $R_1$  and another, in similar conditions, under the load

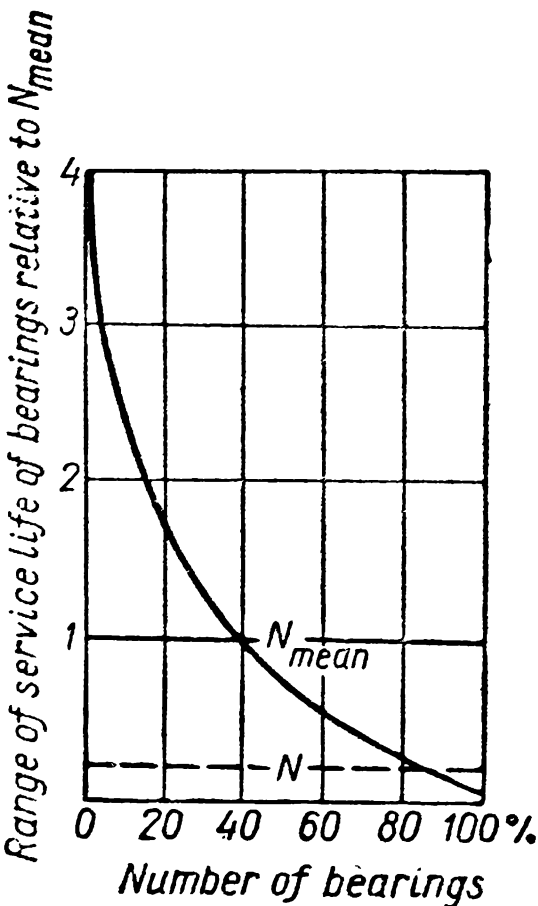


Fig. 253

$R_2$  then the magnitudes  $R_1, N_1$  and  $R_2, N_2$  are connected by the following relation found experimentally:

$$\frac{R_1}{R_2} = \left( \frac{N_2}{N_1} \right)^{0.3};$$

whence

$$R_1 N_1^{0.3} = R_2 N_2^{0.3} = \text{const} \quad (407)$$

where  $N_1$  and  $N_2$  are the service lives of a bearing of the respective batch.

If the axial load  $A$  acts upon a bearing simultaneously with the radial load  $R$ , both these loads can be replaced by some combined radial load  $Q = f(R, A)$ , which is equivalent in its effect on the service life of the bearing to the joint action of the forces  $R$  and  $A$ . Then, on the basis of the relation (407), the relation between  $Q$  and the design service life  $N$  with the inner race of the bearing in motion will be

$$QN^{0.3} = C_1. \quad (408)$$

If we calculate the service life  $N$  in millions of revolutions then the value  $N=1$  (i. e., one million revolutions) corresponds to the value  $Q$  which is numerically equal to  $C_1$  [see relation (408)]; hence,  $C_1$  is the load-carrying capacity of the bearing in kg which corresponds to its service life of one million revolutions. The magnitude  $C_1$  depends on the size, design and material of the bearing.

Since  $N = 60 \times 10^{-6} nh$ , where  $h$  is the service life in hours and  $n$ —rpm at a constant velocity of rotation we obtain after substituting this value in the formula (408)

$$Q(nh)^{0.3} = \frac{C_1}{(60 \times 10^{-6})^{0.3}}$$

or, if we denote

$$\frac{C_1}{(60 \times 10^{-6})^{0.3}} = C$$

then

$$Q(nh)^{0.3} = C. \quad (409)$$

Here  $C$  is the *operating capacity factor* which depends on the same factors as  $C_1$ .

The *limit velocity* of a bearing is the maximum allowable rpm which, if exceeded, will not ensure its design service life.

The maximum allowable number of revolutions for any bearing of a light series is

$$n_{\max} = \frac{L}{d} \quad (410)$$



Here  $d$  is the diameter of the shaft in mm.

The values of  $L$  found experimentally for bearings of the main types of high degrees of accuracy (from B to C inclusive) are shown in Table 65.

Table 65

Limit Values of  $L$  at  $d > 10$  mm

Type of bearing	$L = dn \text{ mm} \times \text{rpm}$
Single-row radial and double-row self-aligning ball bearings with press-formed cages . . . . .	300,000
Single-row radial and radial-thrust ball bearings with massive cages made from nonferrous metal or fibre laminated plastics . . . . .	1,000,000
Thrust ball bearings . . . . .	100,000
Self-aligning roller bearings . . . . .	150,000

For the medium series  $n_{\max}$  is 20% less and for the heavy series 50% less than for the light series.

CALCULATION OF ANTIFRICTION BEARINGS

**Calculation of Statically Loaded Bearings.** If antifriction bearings experience considerable overloads and do not turn (or rotate at  $n < 1$  rpm) as, for example, in the hook casings of cranes, or the blades of variable pitch aircraft propellers, etc., the formula for service life (409) cannot be used in calculations because the relation (408) at  $N=0$  gives  $Q \rightarrow \infty$ .

The limit load of such statically loaded bearings is determined not by the service life of the bearing parts but by the magnitude of the remanent deformations of the contact surfaces.

With the compressive stresses allowed for antifriction bearings the remanent deformations are so small that they do not damage the surfaces of the raceways.

From the equations (401) and (404) we get the following expression for calculating the allowable static load on a radial ball bearing

$$R_{st} = \frac{\sigma_{\max}^3}{5\lambda_b^3} z d_b^2 = \varepsilon_b' z d_b^2.$$

(411)

For all ball bearings—radial and thrust—the formula (411) is the same in structure and can be represented in this form

$$Q_{st} = \varepsilon_b z d_b^2 \text{ kg}$$

(412)

where  $z$  is the number of balls in one row;  
 $d_b$ —the diameter of the ball in cm.

The values of  $\epsilon_b$  for ball bearings of different types at  $\sigma_{\max}=\sigma_{\text{sur}}=50,000 \text{ kg/cm}^2$  are given in Table 66.

Solving simultaneously the equations (402) and (406) we get for the calculation of the allowable static load on a radial roller bearing

$$R_{st} = \frac{\sigma_{\max}^2}{4.6\lambda_r^3} z l_r d_r = \epsilon'_r z l_r d_r. \tag{413}$$

For all roller bearings—radial and thrust—the formula (413) has the form

$$Q_{st} = \epsilon_r z l_r d_r \text{ kg.} \tag{414}$$

Here  $z$  is the number of rollers in one row;  
 $l_r$  and  $d_r$ —are the length and diameter of the roller in cm.

The values of  $\epsilon_r$  for roller bearings of various types at  $\sigma_{\max}=\sigma_{\text{sur}}=35,000 \text{ kg/cm}^2$  are given in Table 66.

Table 66

Values of Factors  $\epsilon_b$  and  $\epsilon_r$

Ball bearings		Roller bearings	
Type of bearing	$\epsilon_b$	Type of bearing	$\epsilon_r$
Single-row radial bearing	85	Radial bearing with short cylindrical rollers . . . . .	160
Double-row self-aligning radial bearing . . . . .	72	Double-row self-aligning radial bearing . . . . .	300
Single-row radial-thrust bearing . . . . .	$85 \cos \beta$	Single-row radial-thrust (tapered) bearing . . . . .	$160 \cos \beta$
Thrust bearing . . . . .	330	Thrust bearing with cylindrical rollers . . . . .	600

*Note.* In a ball bearing  $\beta$  is the angle between the pressure line and the mean plane of the bearing (Fig. c in Table 61).  
In a roller bearing  $\beta$  is the angle of taper (Fig. f in Table 62).

The value of allowable static load is indicated for each standard antifriction bearing in the catalogues for these parts.

**Calculation of Dynamically Loaded Bearings.** A bearing rotating under load is calculated according to the operating capacity factor.

The rotating element is usually the inner race. If the outer race is in rotation then, all other conditions being equal, the load on the bearing should be decreased because the frequency of loading on the inner race has been increased. For the same reason if the outer race of the bearing rotates we introduce the factor  $k_r>1$  in the left-hand side of the equation (409) before the value  $R$  of the radial load (see p. 466).

Since the service life of a bearing is unfavourably affected by shocks during operation we introduce in the left-hand side of the equation (409) the factor  $k_l > 1$  which also depends on the nature of loading if the load fluctuates. The effect of the working temperature of a bearing on its service life is accounted for by the correction factor  $k_t > 1$ .

The radial load  $R$  and axial load  $A$  can be replaced by a combined radial load  $Q$  which affects the service life of the calculated bearing in the same way as both the actual loads  $R$  and  $A$ . In a general form

$$Q = k_r R + mA \quad (415)$$

where  $m$  is the factor of reducing axial load to radial load and accounting for the different effect these loads have on the bearing service life. Thus, the formula for calculating radial bearings has the form

$$(k_r R + mA) \times k_l k_t (nh)^{0.3} = C. \quad (416)$$

Here  $R$  is the actual radial load in kg;

$A$ —the actual axial load in kg;

$m$ —0.5-4.5—the factor of reducing the load chosen depending on the type and size of the bearing;

$k_r$ —the factor introduced when the outer race of the bearing is in rotation; it is assumed to be equal to 1.1 for self-aligning ball bearings and 1.35 for bearings of all other types;

$k_l$ —the factor of the nature of loading which is between 1 and 3.

$k_t$ —the temperature factor; at

$$t = 125 \quad 150 \quad 175 \quad 200 \quad 225 \quad 250^\circ \text{C};$$

$$k_t = 1.05 \quad 1.10 \quad 1.15 \quad 1.25 \quad 1.35 \quad 1.40;$$

$n$ —the number of revolutions of the bearing in min;

$h$ —the desired service life in hours.

For thrust bearings which take only axial load both races assume the same position relative to the balls and therefore in the equation (415)  $Q=A$ ,  $k_r=1$  and the general formula takes the form

$$Ak_l k_t (nh)^{0.3} = C. \quad (417)$$

For needle bearings which take only radial load  $Q=R$  and the design formula is

$$Rk_r k_l k_t (nh)^{0.3} = C. \quad (418)$$

When calculating radial-thrust bearings, in addition to external load, axial load due to the action of radial load should also be considered.

The axial component  $A_1 = 1.2R \tan \beta$ .

In this case the formula (416) will take the form

$$(k_r R + m \sum A) k_i k_t (nh)^{0.3} = C. \quad (419)$$

When determining the algebraic sum of all axial loads we consider the forces which decrease the internal clearance in the bearing as positive; if  $\sum A < 0$  calculations are done only by radial load.

The operating capacity factor  $C$  cannot be found by a purely theoretical method. Its values for standard bearings are found by experiment.

When calculating nonstandard bearings the value of  $C$  can be found approximately from empirical formulae.

If the bearing operates under varying load and varying angular velocity it is calculated according to the equivalent load  $Q_{eq}$  and the equivalent number  $n_{eq}$  of revolutions.

Let us assume that out of the total number of hours  $h$  of the bearing operation before its replacement it has operated under a load  $Q_i$  at a speed  $n_i$ ; in this case the time of operation at  $Q_i, n_i$  is  $\alpha_i$  fractions of the total service life of the bearing, i. e.,  $\alpha_i = \frac{h_i}{h}$  where  $h_i$  is the number of hours of operation at  $Q_i, n_i$ . The formulae (416) and (417) show that the service life of a bearing, all other conditions being equal, is inversely proportional to the product  $Q_i^{\frac{10}{3}} \times n_i$ . Therefore, the equivalent load for an antifriction bearing of any type can be found from the formula

$$Q_{eq} = \left( \sum_{i=1}^k \alpha_i \beta_i Q_i^{\frac{10}{3}} \right)^{0.3}; \quad (420)$$

$$\alpha_i = \frac{h_i}{h} \quad \text{and} \quad \beta_i = \frac{n_i}{n_{eq}}. \quad (421)$$

Here  $n_{eq}$  is an arbitrary number of revolutions usually chosen from the predominant kind of service.

*Spheres of application of ball and roller bearings.* Mechanical engineering employs for the most part ball bearings. Radial ball bearings are very effective for high velocities especially when used with cages made from nonferrous metals or fibre laminated plastics (see Table 65).

In thrust bearings at  $dn > 1 \times 10^5 \text{ mm} \times \text{rpm}$  the balls tend under the action of centrifugal force to leave the raceways causing additional friction and intensive wear on the external edges of the raceways. For this reason radial-thrust ball bearings should be used to take axial load at high velocities.

The limit velocity of bearings with short cylindrical rollers is the same as that of ball bearings of the same size.

Roller bearings of the same size as ball bearings possess load-carrying capacity 70% greater (see Table 62) and resist impact loads especially well.

Tapered roller bearings are employed in units where radial and axial loads act simultaneously. These bearings resist impact loads effectively and are therefore frequently used in the wheel hubs of automotive vehicles.

Needle bearings differ advantageously from other bearings in that they have small diametral proportions. Bearings of this type are used in heavily loaded units at  $dn < 1.6 \times 10^4 \text{ mm} \times \text{rpm}$ .

### MOUNTING, LUBRICATION AND SEALING OF ANTIFRICTION BEARINGS

In designing bearing units close attention should be given to the problems of assembly since an incorrectly mounted bearing may quickly fail.

If the shaft is mounted in several ball bearings then all the bearings except that which is a locking bearing should be mounted with an axial clearance between the outer races and housing to ensure self-alignment of the shaft in an axial direction. If this has been ignored temperature fluctuations and the resultant variations in shaft length may cause considerable axial pressures on the ball bearings and reduce their service life.

For the same reason of all the ball bearings mounted on the same shaft only one should be a thrust bearing.

If the shaft supports have only radial bearings the thrust bearing should be the one which carries the smallest radial load.

Self-aligning ball and roller bearings mounted on smooth shafts without shoulders can be fitted on slotted adapter sleeves (Fig. 254, *a*). The nut is screwed in a direction opposite to that of the shaft rotation.

In long line shafts the bearing of one of the central sections is usually secured (Fig. 254, *a*). In short transmissions one of the most heavily loaded bearings is fixed.

The type of fit of an antifriction bearing on the shaft and in the housing depends on many factors—the nature of loading, type of load on the races (local or peripheral), the precision and quality of the places where the fit is made, type of bearing, etc.

Ball and roller bearings are fitted on the shaft in conformity with the basic hole system and into the housing in conformity with the basic shaft system.

When assembling a bearing in a split housing it should be seen that the housing cap does not deform the outer race when the nuts are tightened in order to prevent the pinching of balls or rollers. Fig. 254, *b* shows an incorrect and Fig. 254, *c*—a correct design.

In many cases provision should be made in antifriction bearings for reducing radial and axial (end) run-outs which have an adverse effect on the machine operation. Run-out is caused by inaccuracies in form, by elastic deformations of the bearing parts and also by radial and axial clearances in the bearings.

Inaccuracies in form can be remedied only to the extent dictated by consideration of economy, while it is impossible to safeguard bearing components completely against elastic deformation. The

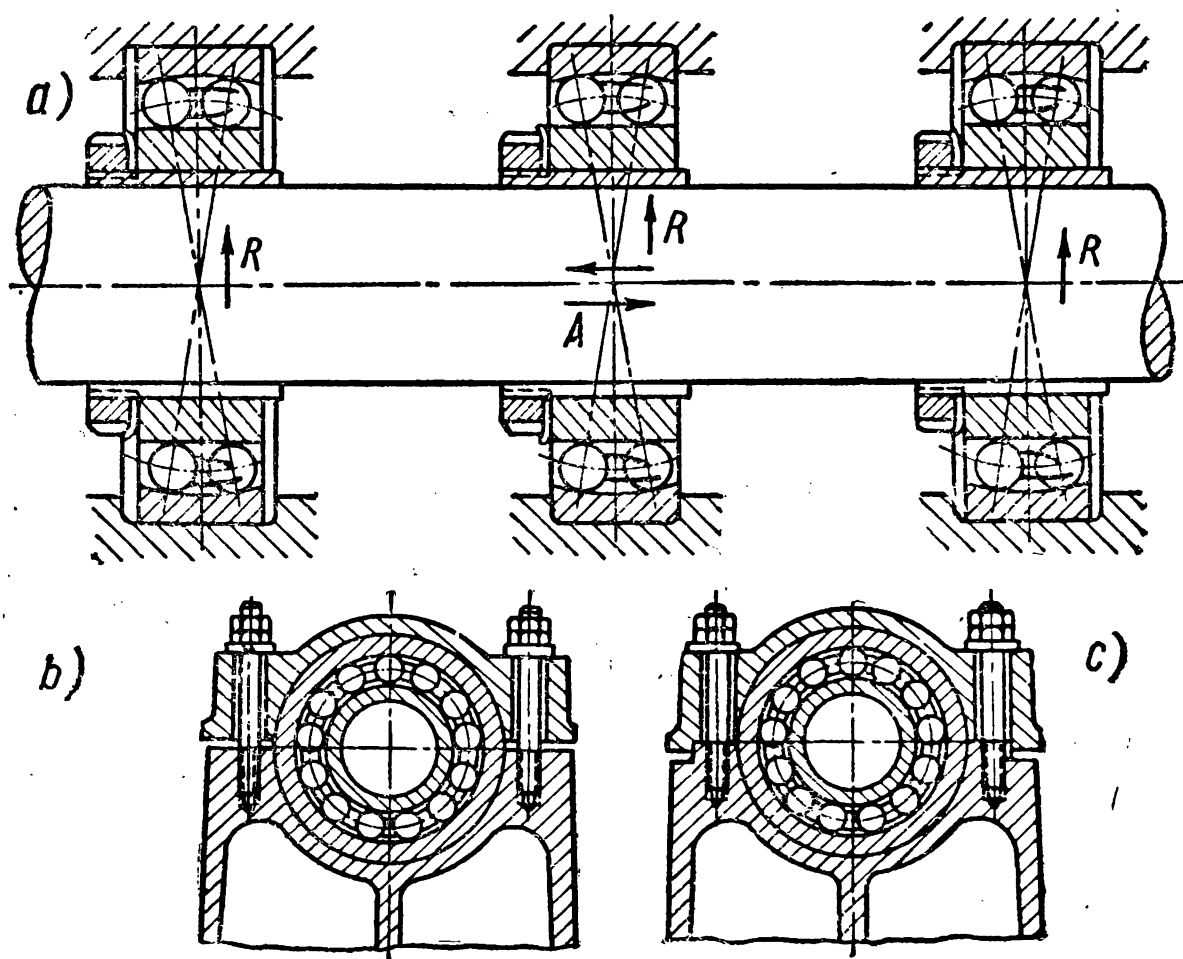


Fig. 254

reduction of internal clearances is therefore the main method of decreasing run-out. This is achieved in ball bearings by *prestressing*, obtained by displacing the races axially by some small distance  $\Delta$  as a result of which the balls assume on the raceways positions shown in Fig. 255, a,

Initial stress can also be caused by placing distance sleeves of various lengths between the outer and inner races of the bearings (Fig. 255, b). Sometimes prestressing is created by means of springs acting on one of the bearing races.

Fig. 255, c shows a bearing of a precision spindle whose radial-thrust bearings are prestressed with the help of springs.

*Antifriction bearings are lubricated by oils and greases.*

For bearings operating at  $dn < 3 \times 10^5 \text{ mm} \times \text{rpm}$  (on the shaft) it is frequently enough to press a small amount of grease into bearing

from time to time or apply splash lubrication. At  $dn > 3 \times 10^5 \text{ mm} \times \text{rpm}$  a circulating oil system should be used.

Antifriction bearings should be moderately lubricated. The oil level in a bearing should be sufficiently low to avoid additional losses due to friction because of oil movement, especially at high velocities. When antifriction bearings are lubricated in an oil bath the oil level should not rise above the centre of the lower ball or roller (Fig. 256).

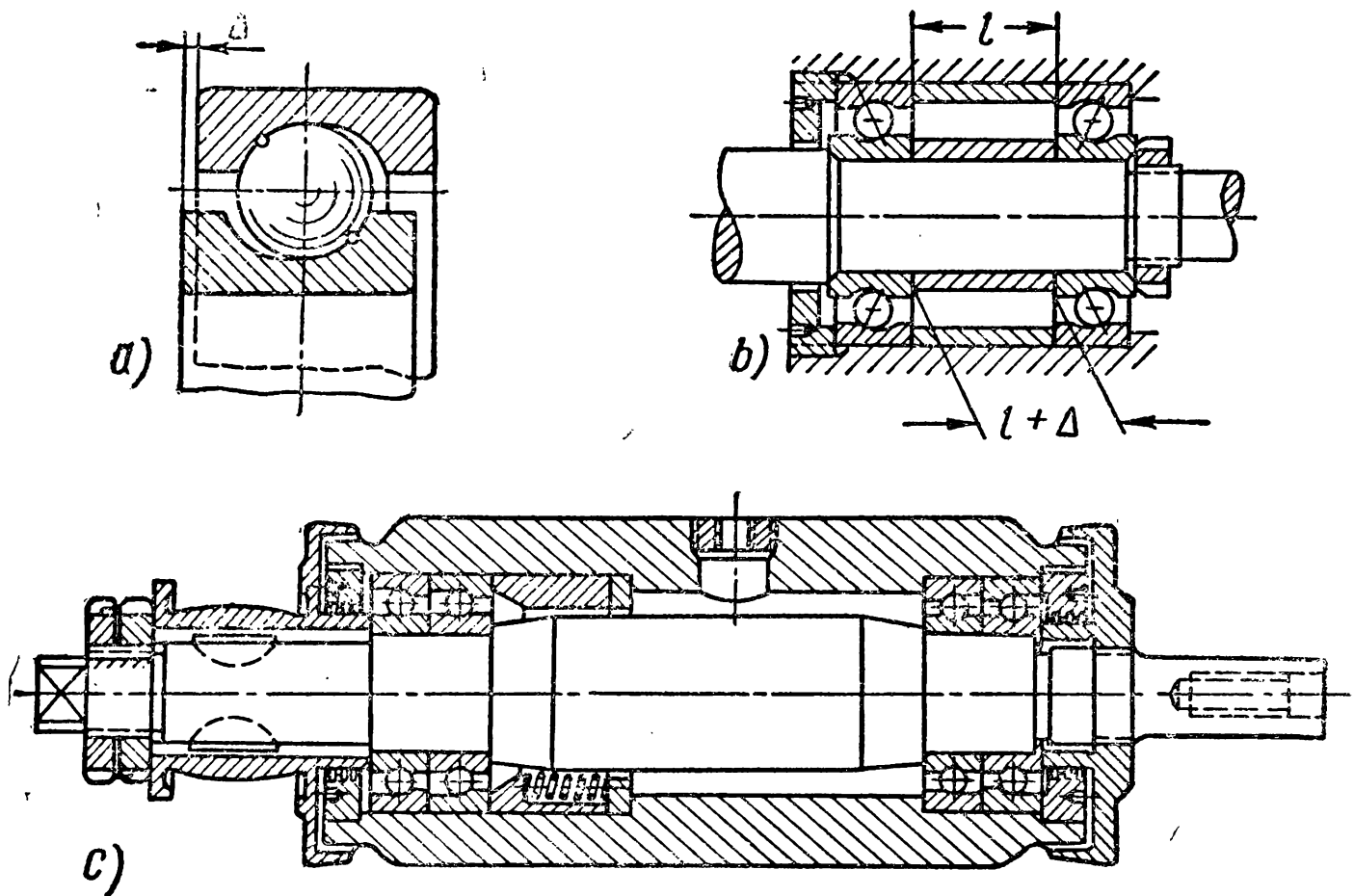


Fig. 255

In addition to decreasing friction and dissipating heat the grease in the clearances between the bearing parts lessens the jerky nature of load fluctuation and prevents corrosion on the rolling surfaces.

Greases used for antifriction bearings should be neutral and chemically and physically stable.

Seals prevent the leakage of oil from the lubricated areas and protect the bearings against dust and dirt.

All seals can be divided into: 1) those which make the joint tight by close contact between the parts in relative motion and the sealing elements—so-called *contact seals*; 2) those in which the tightness of joint between the parts in relative motion is ensured by the ability of narrow slits or gaps to exert a considerable hydraulic resistance to the oil flowing through them—so-called *slit or labyrinth seals*.

The most common seals of the first group are shown in Fig. 257, a (a felt seal for retaining grease) and in Fig. 257, b (a cup leather seal for high oil pressures).

Fig. 257, c shows a synthetic rubber seal. Seals of this group are employed at  $d\omega \leq 1.2 \times 10^4$  mm  $\times$  rpm.

The principal disadvantage of contact seals made from felt, cork and leather is the fact that these materials can retain abrasive particles on the sealing surface, as a result of which in time the sealing elements begin to operate as abrasive tools causing rapid wear on the conjugate surfaces.

Seals of the second group are free from this shortcoming. Some designs of these seals are shown in Fig. 257, d—a slit seal, Fig. 257, e—

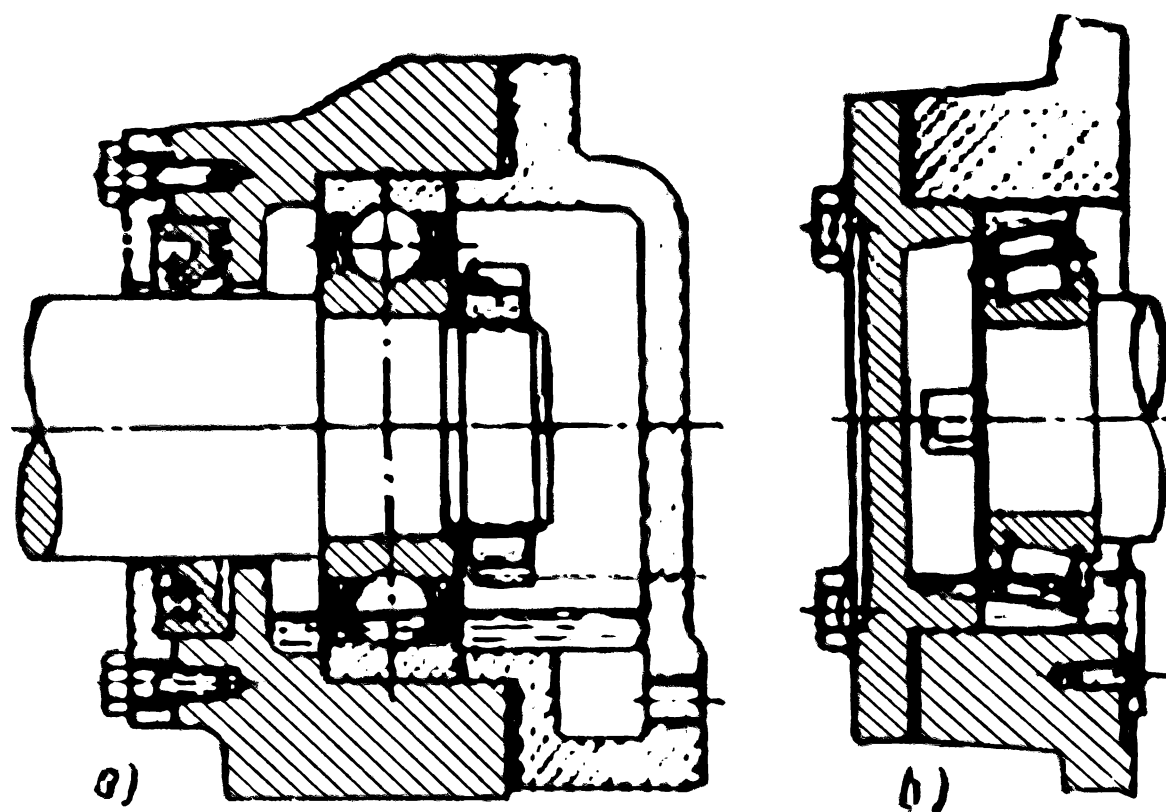


Fig. 256

a labyrinth seal with a centrifugal slinger and Fig. 257, f—a labyrinth seal. Seals of this group are employed at  $d\omega > 1.2 \times 10^4$  mm  $\times$  rpm.

The amount of oil flowing in unit time through a smooth circular slit can be found from the formula

$$V \approx 2,600 \frac{\delta^3 d_\omega}{\eta l} (p_1 - p_2) \text{ cm}^3, \text{ sec.} \quad (422)$$

The values of  $d_\omega$ ,  $\delta$  and  $l$  (all dimensions are in cm) are shown in Fig. 257, d;  $\eta$  is the dynamic factor of oil viscosity in kg sec./m<sup>2</sup>;  $p_1$  and  $p_2$ —the pressures at the beginning and end of the clearance in kg/cm<sup>2</sup>. It follows from this equation that the effective operation of a slit seal depends in large measure on the value  $\delta$  of the radial clearance and to a lesser degree on its length  $l$ .

Usually we assume

$$\delta = 0.1-0.3 \text{ mm.}$$



Losses due to friction in antifriction bearings are found from the formulae:

moment of friction

$$M_{fr} = \frac{Qd}{2} \text{ kg/cm;}$$

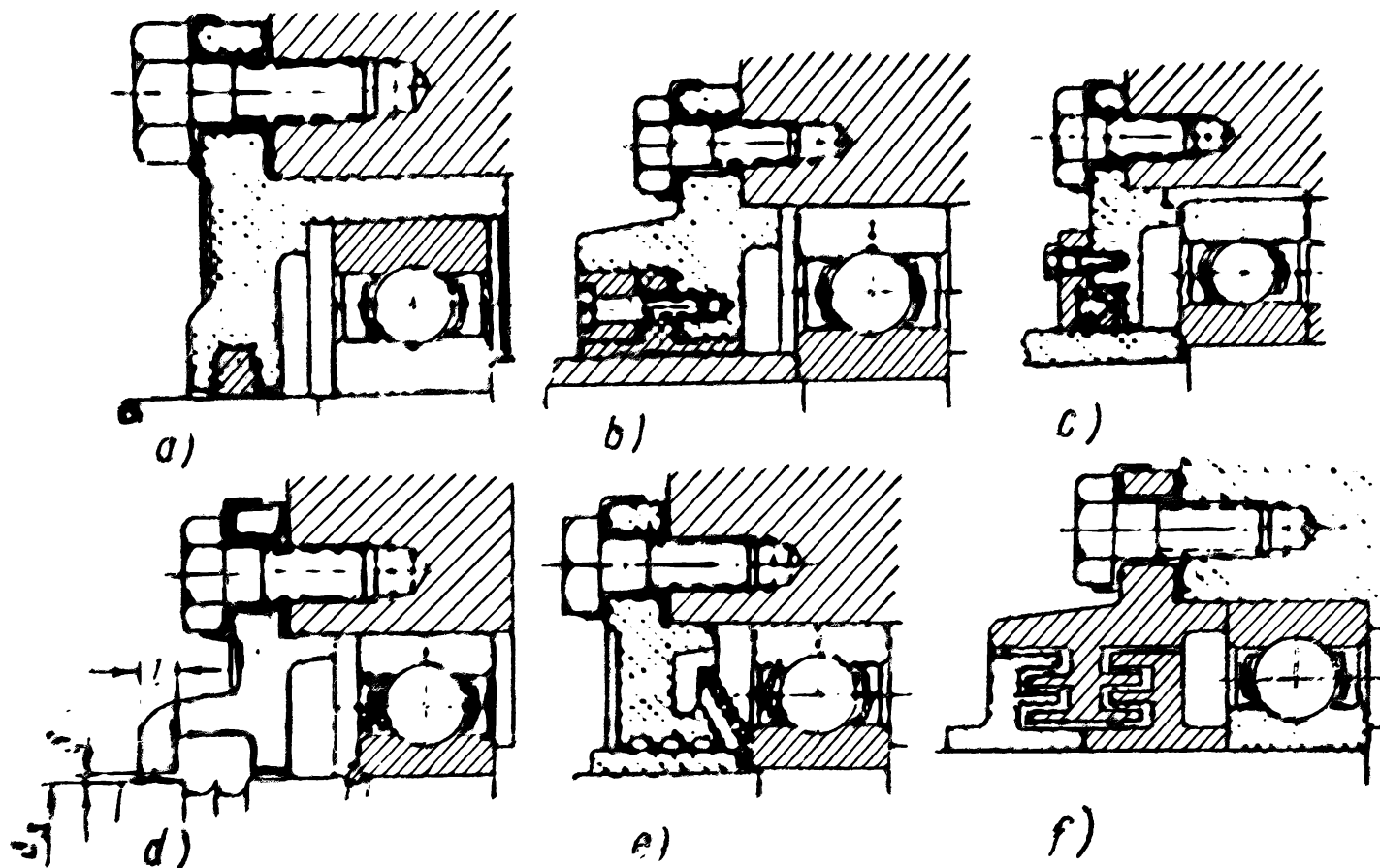


Fig. 257

loss of power on friction

$$L_n = \frac{Qf\pi dn}{1,000 \cdot 60 \cdot 75} = 7 \times 10^{-7} Qf\pi dn \text{ h. p.} \quad (423)$$

Here  $Q$  is the load acting on the bearing in kg;

$f$ —the coefficient of friction reduced to the shaft. For approximate calculations we can take for bearings of all types  $f=0.005-0.01$ ;

$d$ —the shaft diameter in mm;

$n$ —the number of shaft revolutions per minute.

#### METHODS OF INCREASING THE OPERATING CAPACITY OF ANTIFRICTION BEARINGS

The service life of antifriction bearings can be increased by different production, operation and design measures.

The main production factors which affect the service life of antifriction bearings include precision in the form and proportion of all elements of a bearing, which influences the nature of load distribution

between balls or rollers, and the magnitude and homogeneity of the hardness of the contact surfaces. When the hardness of the contact surfaces of an antifriction bearing components is  $R_C < 62$  its service life decreases.

The manufacturer is responsible for increasing the service life of the bearings by taking proper production measures.

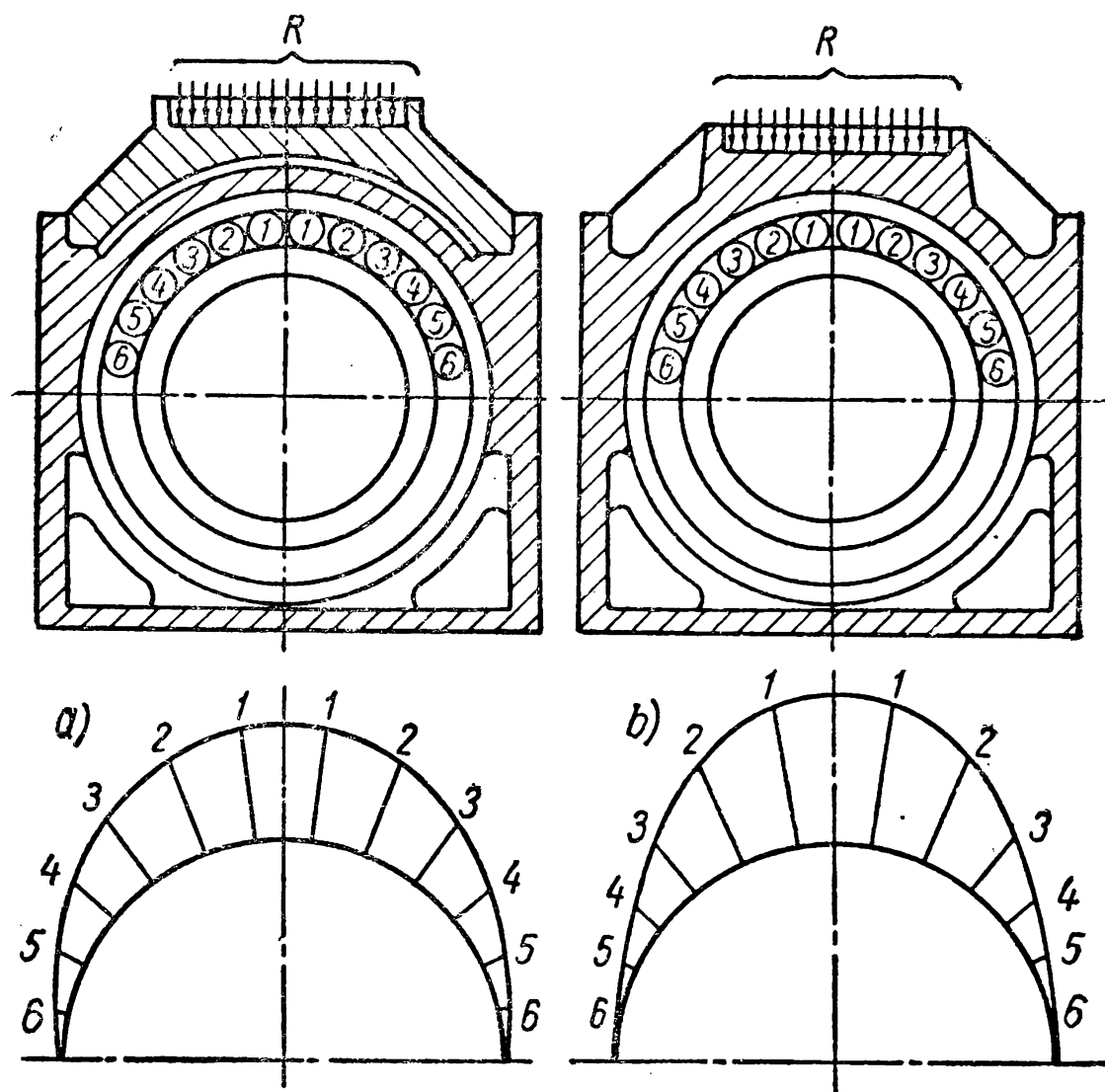


Fig. 258

Among the operation measures that increase the service life of bearings are: their reliable protection from dirt, dust, moisture, acids, alkalis, etc., and timely and adequate lubrication.

In some cases the service life of bearings can be increased by design measures—by giving the bearing the most rational layout for the given operating conditions.

If the most important requirement of a bearing is the length of its service life and not precision in rotation, it is expedient to provide for the elasticity of the housing in the loaded part of the bearing. As a result, the load on the ball or roller carrying the greatest load is diminished.

Fig. 258 shows the axle boxes of a railway car, *a* — elastic and *b*—rigid, and the corresponding load distributions between the rollers of a roller bearing.

For the given roller bearing, we can obtain on the basis of the equations (406) and (408)

$$Q = C_2 \sigma_{\max}^2 \text{ and } N = \left( \frac{C_1}{Q} \right)^{\frac{10}{3}} \quad (424)$$

where  $C_1$  and  $C_2$  are constants depending on the size and design of the bearing.

Solving simultaneously these equations we get

$$N = \left( \frac{C_1}{C_2 \sigma_{\max}^2} \right)^{\frac{10}{3}} = \frac{C_3}{\sigma_{\max}^{6.66}} \quad (425)$$

Here  $C_3$  depends on the same factors as  $C_1$  and  $C_2$ .

This equation shows that even a negligible reduction in stress on the thrust surface of the roller, due to decreased load, considerably increases the service life of the bearing. A decrease of  $\sigma_{\max}$  by 10% increases the service life  $N$  by  $1.1^{6.66} \approx 2$  times.

## CHAPTER XXIII

### COUPLINGS AND CLUTCHES

Couplings and clutches are intended to connect shafts or other revolving parts and in modern mechanical engineering they form integral components of almost all machines. Couplings and clutches link together the shafts of turbines and generators, prime movers and driving mechanisms, as well as the shafts of separate units and assemblies; effect smooth or instantaneous starting, stopping, reversing and gear change of machines; protect against overloads and racing and prevent reverse rotation. Hence the great diversity of types of couplings and clutches and the continuous development of new designs.

There are two general types of couplings—*permanent couplings* and *clutches*.

Couplings are used to make permanent connections between shafts, while clutches are used to connect and disconnect them.

These main two groups are subdivided according to various characteristics which will be given below in sections dealing with couplings and clutches of each group.

*Standardisation.* The wide application of couplings and clutches makes their standardisation imperative.

Soviet standards specify proportions and other parameters of the following types of couplings: *flexible box-pin*, *gear* and *universal-joint* couplings. A large number of types of coupling also conform to industry branch standards.

The main standardising parameter is usually the shaft diameter, the torque transmitted by the coupling or the value  $N/n$  proportional to this torque where  $N$  is the transmitted power in h. p. and  $n$  in rpm.

For a series of couplings with gradually increasing power, i. e., couplings of identical design, whose main sizes conform to the principle of geometrical similarity, the relation  $M_t = l^3$  holds, i. e., *the torque transmitted by the coupling increases in proportion to the cube of linear dimensions of the coupling*. Indeed, when the coupling components resist the same unit loads the transmitted peripheral effort is proportional to the area, i. e., the square, and the transmitted torque to the cube of the coupling linear dimensions. Since the weight of such couplings is also proportional to the cube of their linear dimensions, the *specific weight*, that is the ratio between the weight of the coupling  $G$  and the transmitted torque  $M_t$ ,

$$k_{sp} = \frac{G}{M_t} \text{ kg/kgm} \quad (426)$$

is constant for a given type of coupling. This relation is rather approximate since, as a rule, geometrical similarity is not strictly adhered to.

The specific weight ( $k_{sp}$ ) is important as an index of the consumption of metal in couplings of different design.

*Design torques.* A coupling of required size is chosen from the tables of respective standards or catalogues on the basis of the design torque  $M_{td}$ , which takes into account the severest possible loading conditions during operation. It is frequently impossible to find the value of  $M_{td}$  directly due to the inadequacy of initial data. In these cases, the experience of operating couplings under similar conditions should be used to find the *design torque* from the relation

$$M_{td} = M_{rated} \nu = 71,620 \frac{N}{n} \nu \text{ kg/cm} \quad (427)$$

where  $M_{rated}$  is the rated torque of the working load in kg/cm;

$\nu$ —overload factor;

$N$ —power in h. p.;

$n$ —rpm.

The value of the factor  $\nu$  varies within a wide range from 1 to 6 and depends mainly on the type of prime mover and driving mechanism.

The physical nature of the factor  $\nu$  and its calculation for a simple case will be clear from the following.

Let the prime mover and driving mechanism be connected by a rigid coupling\*. We denote the moment of inertia of the moving masses of the prime mover, reduced to the coupling axis, by  $I_1$ , and of the driving mechanism by  $I_2$ .

---

\* The case of an elastic coupling will be considered on p. 492.

The characteristics of the mover  $M_t = f(t)$  are such that the torque developed on its shaft is variable with the maximum value of  $M_{\max}$ .

Let us first examine the starting period of the driving mechanism. If during starting the useful load and static resistance in general are absent then the torque of the mover is expended only to bring the assembly into motion. In this case the maximum acceleration will be  $j = \frac{M_{\max}}{I_1 + I_2}$  and the maximum torque transmitted by the coupling

$$M_{td} = I_2 \times j = M_{\max} \frac{I_2}{I_1 + I_2}$$

or, if we introduce the rated torque  $M_{rated}$ ,

$$M_{td} = M_{rated} \frac{M_{\max}}{M_{rated}} \times \frac{I_2}{I_1 + I_2} = M_{rated} \nu$$

where the overload factor is

$$\nu = \frac{M_{\max}}{M_{rated}} \times \frac{I_2}{I_1 + I_2}. \quad (428)$$

When the machine reaches the rated velocity and is loaded with the torque  $M_{rated}$  then the surplus torque ( $M_{\max} - M_{rated}$ ) also creates acceleration. In this case the maximum torque transmitted by the coupling will be

$$\begin{aligned} M_{td} &= M_{rated} + (M_{\max} - M_{rated}) \frac{I_2}{I_1 + I_2} = \\ &= M_{rated} \left[ 1 + \left( \frac{M_{\max}}{M_{rated}} - 1 \right) \frac{I_2}{I_1 + I_2} \right] = M_{rated} \nu \end{aligned}$$

where the overload factor is

$$\nu = 1 + \left( \frac{M_{\max}}{M_{rated}} - 1 \right) \frac{I_2}{I_1 + I_2}. \quad (429)$$

As can be seen from the equations (428) and (429) the overload factor  $\nu$  depends on the magnitude of the maximum torque of the prime mover  $M_{\max}$ , the rated torque of the driving mechanism  $M_{rated}$  and the ratio between the moments of inertia  $\frac{I_2}{I_1 + I_2}$ . The greater  $I_2$  as compared to  $I_1$ , the greater is the load taken by the coupling. The magnitude  $\nu$  reaches its maximum when the driving mechanism is started.

The experimental values of  $\nu$  for various types of prime movers and driving mechanisms are given in reference books.

## COUPLINGS

These couplings are used to make permanent connections between shafts. According to the relative position of the connected shafts and the constancy with which they maintain this position they are subdivided into *rigid couplings* connecting collinear shafts with a constant relative position and *flexible couplings* connecting non-collinear shafts with a varying relative position.

The general classification of couplings is shown in Fig. 259.

**Rigid Couplings.** Rigid couplings are intended for the permanent connection of shafts whose axes are strictly aligned and which are not offset relative to each other. As distinct from other types of couplings, they transmit from one shaft to the other not only torques but also bending moments and axial forces arising in the assembly.

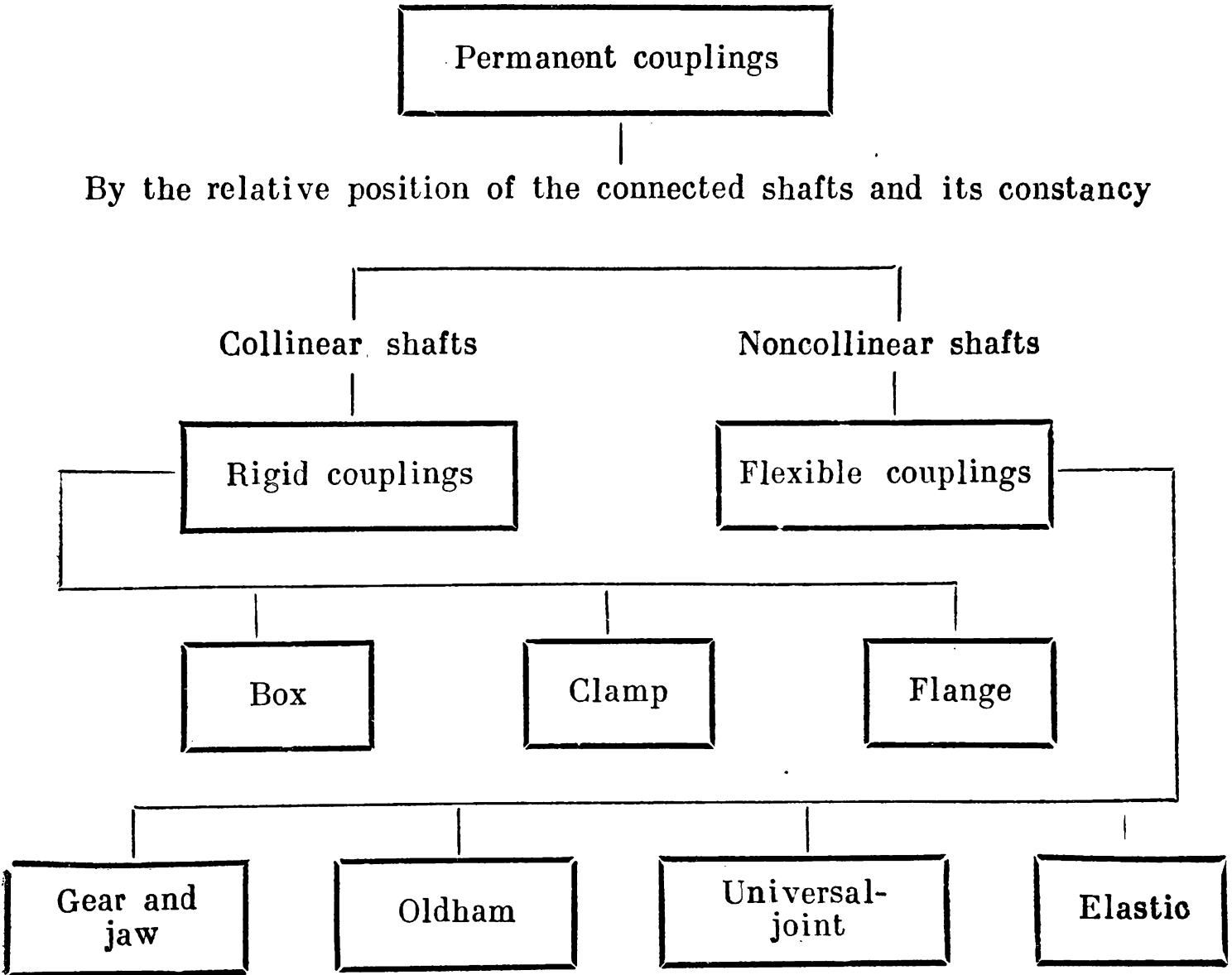


Fig. 259

In an attempt to relieve couplings from these additional forces (except for torques) they are often arranged near the shaft bearings.

Rigid couplings include box, clamp and flange couplings.

A *box coupling*—the simplest type of rigid coupling—comprises a steel or cast-iron sleeve fitted on to the ends of the shafts and secured to them by means of taper pins (Fig. 260) or, less frequently, by keys.

The relationships between the proportions of box couplings which satisfy the condition of equal strength of the elements are:

$$i \approx 3d_{sh}, e \approx \frac{3}{4}d_{sh}, D_{out} \approx 1.5d_{sh}, d_{pin} = (0.3-0.25)d_s;$$

in the last relation 0.3 is taken for small couplings and 0.25 for large.

Soviet machine-tool standards recommend the manufacture of box couplings from steel 35 or 45 and those to operate with shafts of  $d_{sh} > 80$  mm also from cast iron CY 21-40.

In important cases couplings chosen in accordance with these recommendations are checked for shear of the pins and crushing of the sleeve and shaft by the pin. As a rule, the tangential stresses in the pin material prove to be nearest to the shearing stress, therefore, in considerably overloaded box couplings the pin is the first to shear.

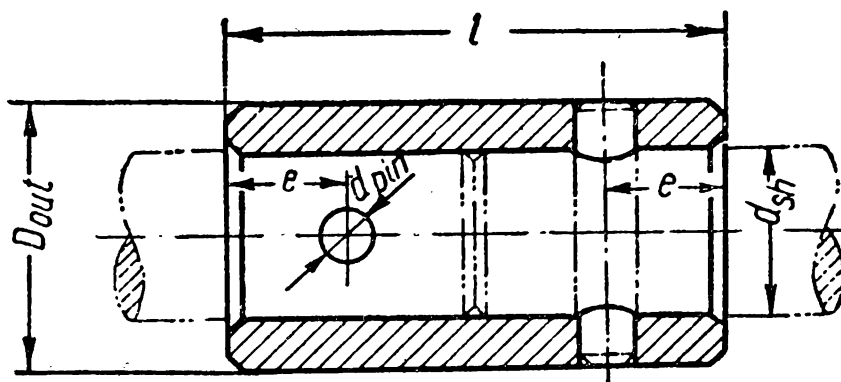


Fig. 260

A *clamp coupling* (Fig. 261) comprises two halves between which the ends of the connected shafts are clamped by bolts. To decrease the length of such a coupling adjacent bolts are inserted from opposite sides as shown in Fig. 261.

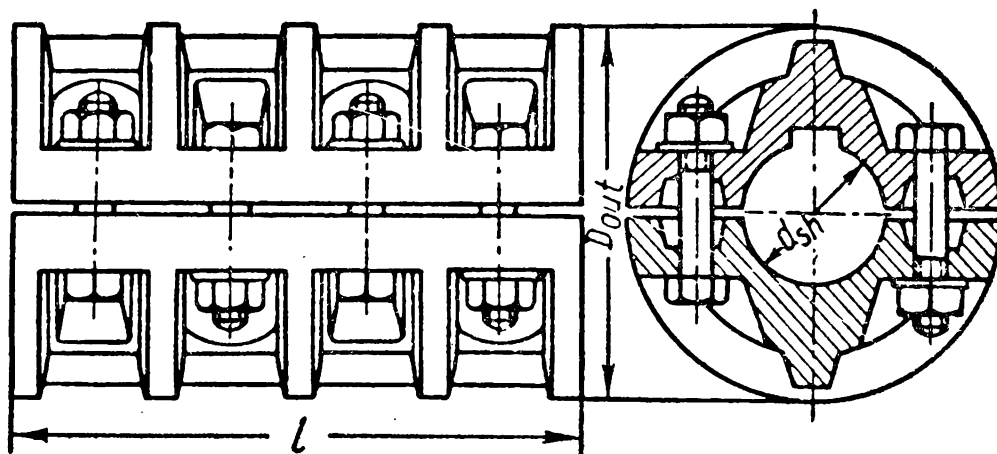


Fig. 261

The length of these couplings depends on the required number of bolts; usually  $l \approx (5-3.5)d_{sh}$ . The outside diameter of couplings  $D_{out} \approx (4-2)d_{sh}$ . In these relations the greater values (5 and 4) refer to couplings of small size, for shafts with  $d_{sh} \approx 25$  mm, while the smaller values (3.5 and 2) refer to large couplings, for shafts with  $d_{sh} \approx 300$  mm.

Small and medium-size couplings transmit torque through friction between the shafts and the coupling alone. In larger couplings a key incorporated between the shafts and coupling transmits the main torque.

Calculation of clamp couplings is reduced to finding the proportions and the number of bolts. It is done in the same way as for split hubs (see p. 150) on the assumption that even with a key the torque is transmitted only through friction between the shafts and coupling halves.

The box and clamp couplings we have examined are connected to the shafts after the latter have been assembled into bearings.

A *flange coupling* (Fig. 262), as distinct from the previous types, is fitted on to the shaft ends in a hot state or under pressure before the shafts are mounted into the bearings. For a more accurate connection, the ends of flange couplings and the centering surfaces are machined after assembly on to the shaft. To facilitate disassembly

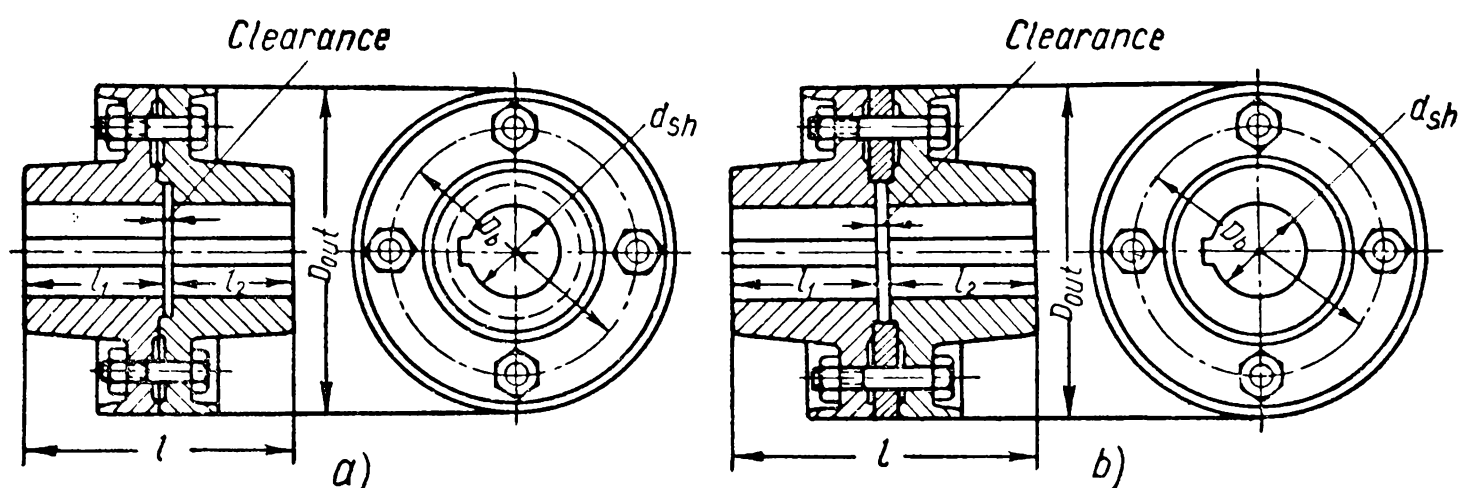


Fig. 262

of long line shafts the coupling halves can be centred by two half-rings (Fig. 262, b); with a coupling of this design the shaft need not be shifted axially for removal.

When large torques and forces are to be transmitted the flanges are made integral with the shafts. Fig. 263 shows the flanged connection of a shaft of a hydraulic turbine.

The presence of flanges on the shaft ends requires all parts fitted on to the shaft—toothed wheels, pulleys, flywheels, bearings, etc.—to be of a split type. Despite this disadvantage, flange couplings ensure the most accurate, rigid and strong connection of shafts. For this reason, in important cases the shafts of steam turbogenerators in three bearings, the shafts of vertical hydroturbines, marine propeller shafts, etc., are usually connected by flange couplings.

Flange couplings transmit torque either through friction between the ends of the halves clamped by bolts or through bolts in shear fitted tightly into the holes of the coupling halves (for calculations of bolts refer to p. 150).

In order to draw up a preliminary sketch the total length of a coupling can be assumed to equal  $l \approx (5-2.5)d_{sh}$ , the outside diameter  $D_{out} \approx (5.8-3)d_{sh}$  and the diameter of the bolt centre  $D_b \approx 2.6d_{sh}$ .



The diameter of the bolts and their number depend, on the one hand, on their total cross-section found from calculations and, on the other, on the necessity of arranging the bolts over the circumference of the coupling in such a manner as to allow the use of a wrench.

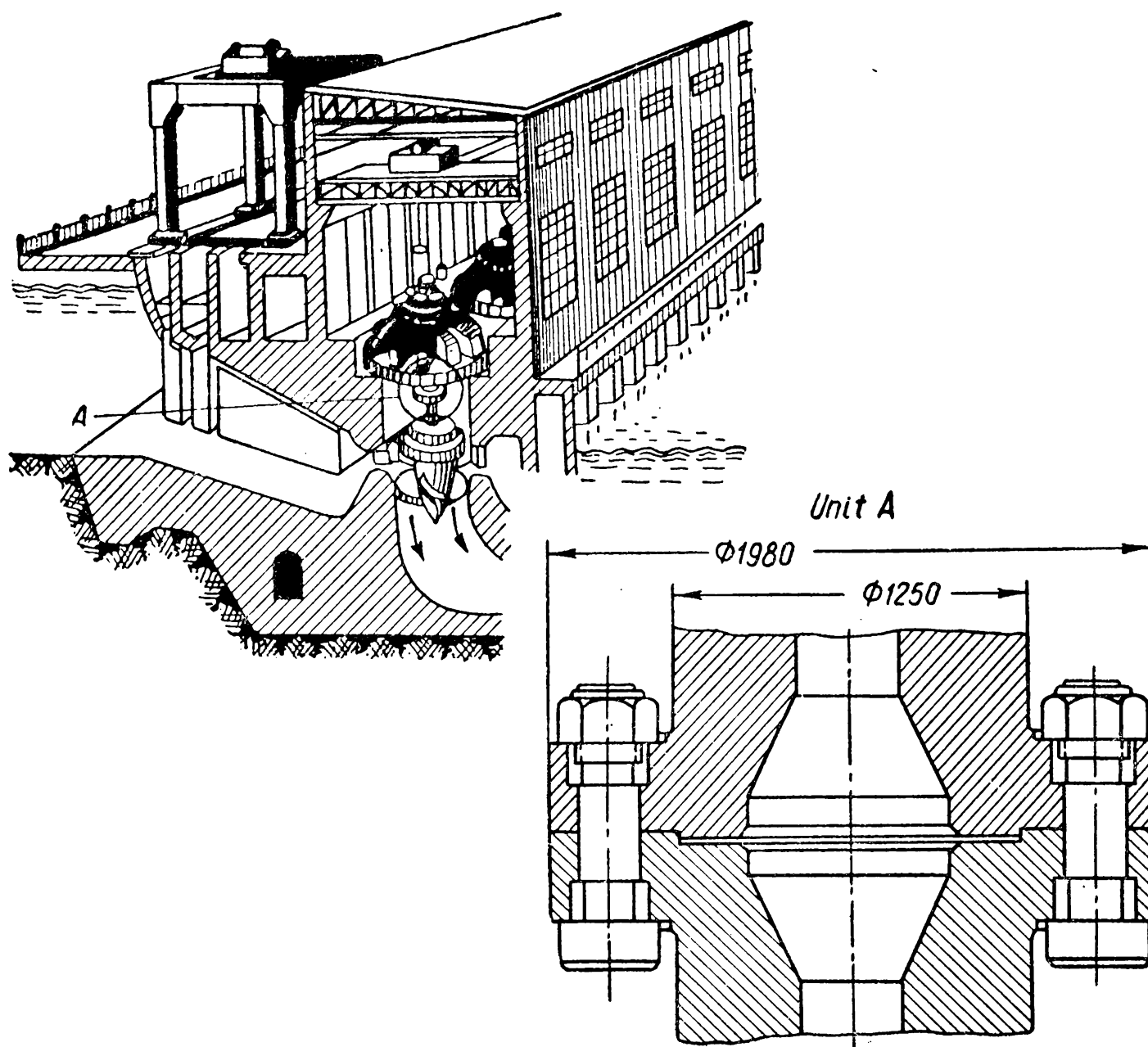


Fig. 263

As in other similar cases, the optimal solution is found after several attempts to determine the diameter  $d$  of the bolts— $d_1, d_2, \dots$  and their number  $z$ — $z_1, z_2, \dots$ —compared in a table for greater clarity\*.

It should be emphasised that the formulae (106) and (107) take into account only the transmission of torque. However, flange couplings frequently have to carry bending moments and tensile forces.

\* For a preliminary calculation of flange couplings the relation of the total cross-sectional area of the bolts to the cross-sectional area of the shaft can be assumed to equal 1/10-1/20.

For example, in a turbogenerator with a shaft in three bearings the coupling resists a bending moment due to the rotor weight and the forces of electromagnetic attraction; in a hydraulic turbine (Fig. 263) the coupling carries a tensile force due to the weight of the operating wheel and hydraulic pressure. In particular cases it is not difficult to determine these additional loads. However, they cannot be expressed sufficiently simply in a general form. In all such cases the calculations consist in finding that initial tight-

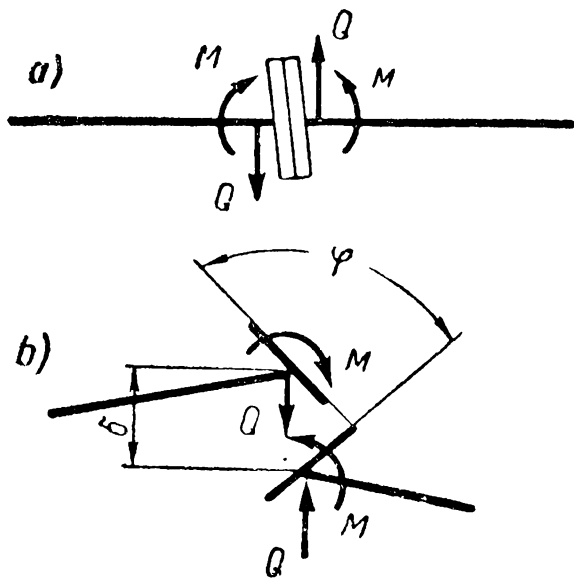


Fig. 264

ening of the bolts and those proportions which will preclude the yawning of joint between the coupling halves. The methods of such calculations are outlined in the section dealing with bolted-on connections (p. 150).

*Effect of inaccuracies of shafts connected by rigid couplings on the service of a line shaft.* Rigid couplings of all types are intended to connect shafts with axes in one line. However, in practice, because of inaccuracies in shafts, coupling halves and bearings, the shafts can be only approximately collinear. To make clear the effect of these inaccuracies on the work of a line shaft, let us assume that two shafts connected by flanges have various errors of manu-

facture and assembly due to which the centres of the flanges, before being connected, are offset by  $\delta$  and the angle between their working surfaces is  $\psi$  (Fig. 264)\*.

Obviously, in order to connect such flanges, a certain force  $Q$  and a certain moment  $M$  must be applied to each of them. The force  $Q$  and the moment  $M$  will cause in the shaft bearings additional reactions which, in the same way as the forces  $Q$  and  $M$ , will change their direction as the shaft rotates. The magnitudes of the additional reactions in the shaft bearings will naturally enough depend on the magnitude of displacements  $\delta$  and  $\psi$  as well as on the rigidity of the shaft and the location of the bearings along the shaft.

Proceeding from the magnitude of the additional load on shafts and bearings permitted in these conditions, and bearing in mind the higher cost of the production and assembly of highly accurate components, tolerances are established for inaccuracies of connected shafts. For example, the standards for the misalignment of marine propeller shafts permit a centre displacement of  $\delta = 0.05$  mm and a bend of 0.05 mm per 1 m, i. e.,  $\psi = 0.05/1,000 = 5 \times 10^{-5}$  radian.

**Flexible Couplings.** Sometimes accurate and constant alignment of shafts—an indispensable condition for the use of rigid couplings—cannot be even approximately ensured. The relative position of the connected shafts, inaccurate at the outset due to inevitable errors

\* We consider this phenomenon in one plane, for example in the plane of the drawing; in other planes the values  $\delta$  and  $\psi$  will be different.

of manufacture, is in the course of time aggravated by deformations caused by the working load, temperature fluctuations, the uneven sinking of the foundation, etc. In such cases ineffective rigid couplings are replaced by flexible couplings.

Possible displacements of the connected shafts are shown in Fig. 265. Generally, these displacements are characterised by a longitudinal shift  $\lambda$ , peripheral shift  $\varphi$ , offset of centres  $\delta$  and angular misalignment  $\psi$ .

In joints fastened by flexible couplings these shifts are compensated for by the relative mobility of the coupling elements. This is achieved by one of the following methods.

1. A large clearance between the conjugate parts of the coupling; such couplings are used only at low velocities for small loads;

2. The *sliding* of some parts relative to others; such couplings should be lubricated; they can be employed for any velocities and loads and cause comparatively small additional load on shafts and bearings;

3. The *elasticity* of the parts; these couplings require no lubrication but bring to bear on the shafts and bearings an additional load, which increases the more rigid the coupling is and the greater the relative shift of the connected shafts.

Couplings utilising the first two methods of compensation (large clearance and sliding) can be called *rigid slip* couplings to distinguish them from those utilising the third method of compensation (elasticity) which are called *flexible slip* couplings.

Rigid slip couplings are subdivided into gear, Oldham and universal-joint couplings.

All slip couplings perform their service only in part: they do not entirely eliminate the radial load on shafts and bearings caused by the misalignment of the connected shafts but only decrease it somewhat. On the other hand, these couplings are an additional source of radial load due to inaccuracies in their separate components\*.

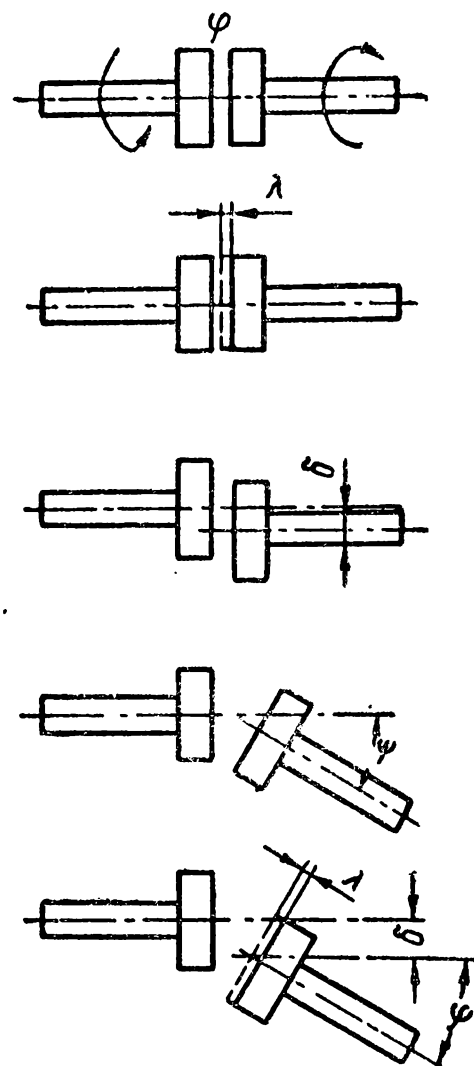


Fig. 265

\* This explains the tendency to replace flexible slip couplings in modern heavy and important machines (for example, in turbine units) by simpler and more reliable rigid couplings which, although requiring more accurate assembly of the connected shafts, are more dependable in operation.

In the most unfavourable case the flexible coupling, like a crank, transmits the torque  $M_t$  only at one point (for example, by one tooth in a gear coupling or by one pin in an elastic box-pin coupling, etc.) removed from the axis of rotation by  $D/2$ . In this case the radial load on the shafts  $R$  equals the full peripheral force  $R=P=2M_t/D$ .

In a general case the additional radial load will be within  $0 < R < P$

Experiments show that for common designs of slip couplings with the usual amount of noncollinearity and accuracy of manufacture the radial load amounts to  $R=(0.2-0.4)P$ .

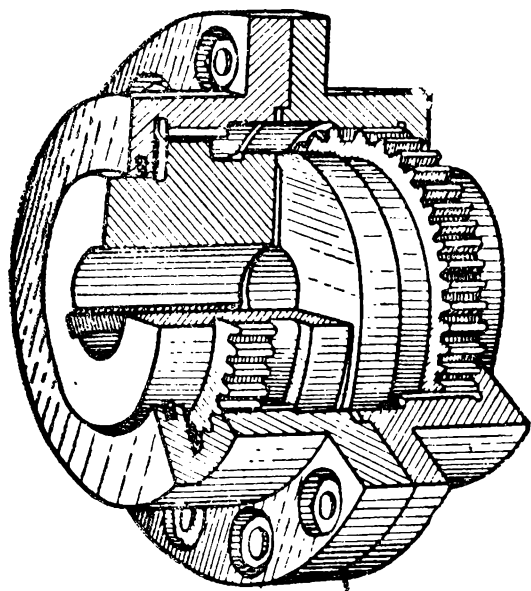


Fig. 266

Obviously, alongside other factors, the quality of a slip coupling should be also evaluated by the magnitude  $R$ . The coupling performs its task of compensating for noncollinearity the more efficiently, the less the additional load on shafts and bearings.

A *gear coupling* (Fig. 266) consists of two toothed sleeves and two casings with internal teeth. The sleeves are fitted on the ends of the connected shafts. The casings, which contain oil, are made in one block and mesh with the toothed sleeves round the entire circumference.

As the coupling rotates the oil is thrown towards the periphery and penetrates the points of contact. Oil is essential for the operation of a gear coupling: it reduces friction between the teeth and decreases resistance to the relative displacement of the coupling halves and the additional radial load on shafts and bearings.

The coupling teeth have an involute profile, usually with a pressure angle of  $20^\circ$ . To equalise the strength of the teeth on the sleeves and the halves their profiles are corrected. The top of teeth on the sleeves is rounded by a radius equal to the addendum radius of the sleeve teeth, i. e., it is spherical. The clearance between the teeth of the sleeves and halves allows a certain shift of the shafts.

The amount of this shift depends on the clearance and other parameters of the coupling in the following way:

The angle  $\psi$  of the allowable angular misalignment between the shaft axes is found from the equation (Fig. 267, a):

$$\sin \frac{\psi}{2} = \frac{\Delta}{b} \quad (430)$$

where  $\Delta$  is the backlash between the teeth and  $b$ —the active width of the teeth. The amount of the allowable offset of centres is found

from the similarity of triangles  $ABC$  and  $ADE$  (Fig. 267,  $b$ ):

$$\delta = DE = AE \frac{BC}{AC} \text{ or } \delta = \frac{l}{b} \Delta \quad (431)$$

where  $l$  is the distance between the tooth centres on both sleeves.

When  $\frac{1}{b} \approx 7$ ,  $\frac{\Delta}{b} \approx 0.13$  and  $\Delta \approx 0.1-1.5$  mm (depending on the size of the coupling) the limits for the allowable shift amount to  $\delta \leq 0.7-10.5$  mm,  $\psi \leq 1^\circ 30'$ .

To increase the allowable offset of the centres  $\delta$  use is made of a design with a connecting shaft. Further increase in the allowable shift  $\psi$  and  $\delta$  is provided by *barrel* teeth which have shown excellent service in toothed gears (Fig. 268,  $b$ ). Such tooth form should also be employed with the ordinary values of  $\psi$  and  $\delta$ . The more complicated machining of these teeth, which require a

special device for a gear-milling machine, is made good for by a considerable improvement in the coupling service, reduction of surface stresses and increased life of the joint as compared to ordinary teeth (Fig. 268,  $a$ ).

Like other slip couplings, gear couplings also cause an additional radial load on the shafts (see p. 485). Here it is due to the resistance to the relative displacement of the tooth surfaces and uneven load distribution between the teeth. Therefore the compensating ability of gear couplings can be improved by reducing friction between the teeth (for this purpose use is made of lubrication, greater hardness of the active profiles of teeth, lapping of teeth) and a more uniform load distribution between the teeth (achieved, for example, by employing elongated teeth, instead of ordinary teeth; the greater elasticity of elongated teeth makes for a more uniform load distribution between them).

Gear couplings, which appeared comparatively recently—in the thirties—have been used widely, especially in heavy machine-building.

Soviet standards cover connected shafts of diameters from 40 to 560 mm and with maximum transmitted torques from 71 to

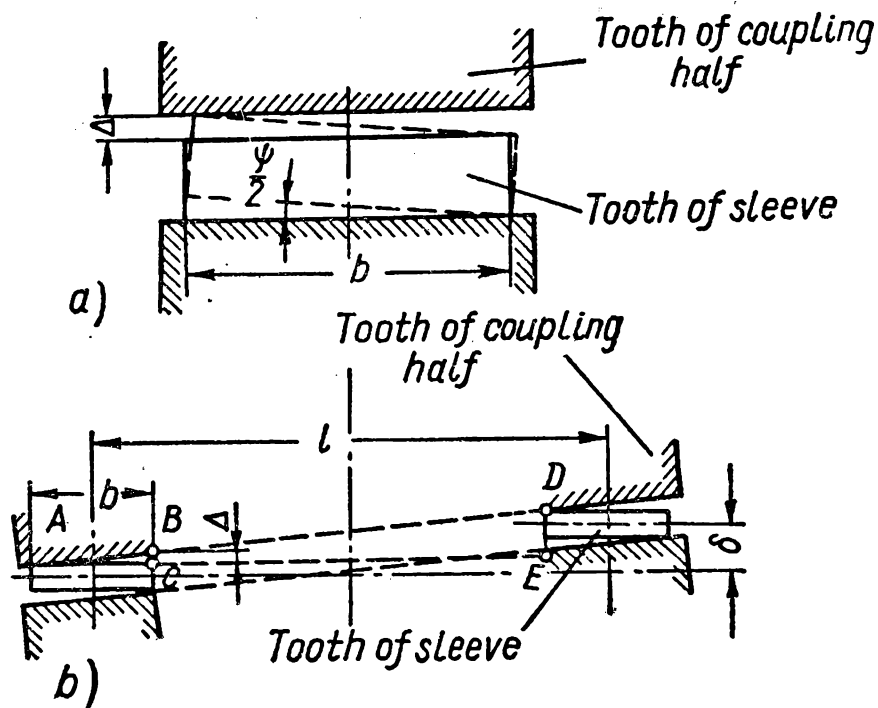


Fig. 267

100,000 kgm. The maximum velocity of couplings specified by Soviet standards corresponds to the peripheral velocity of 25 m/sec on the gear pitch circle.

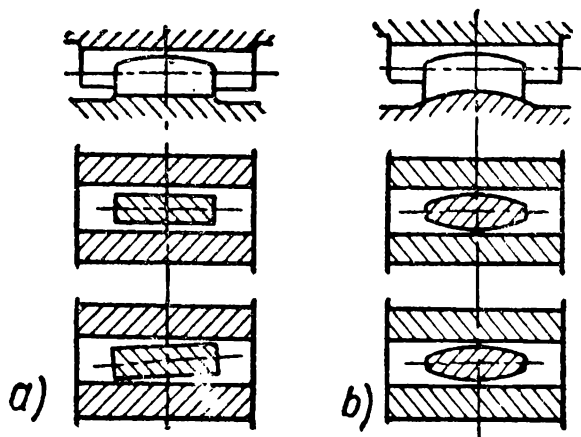


Fig. 268

Sleeves and casings of gear couplings are made from steel 40 when forged and steel 45ЛII when cast. The teeth of sleeves and casings are heat-treated to hardness: for sleeves not below 40  $R_C$ , for casings not below 35  $R_C$ . For couplings under less load operating at lower velocities (up to 5 m/sec) lower hardness of  $\geq 280 H_B$  of the tooth surfaces is permitted but the difference in the hardness of the teeth of sleeves and casings should be of the order of 30 units  $H_B$ .

Standard couplings allow a misalignment of the axle of each sleeve relative to the axle of the casing of maximum  $0^\circ 30'$  (i. e.,  $\psi/2 \leq 0^\circ 30'$ , Fig. 267), which may be due to the misalignment of the connected shafts during operation.

It is extremely difficult to calculate gear couplings for strength and service life because the nature of load distribution between their teeth is very complicated due to the shaft displacement. Standard couplings are selected according to the values of the maximum torque specified by the standard.

An *Oldham coupling* consists of two end pieces with rectilinear grooves and a centre piece with tongues positioned at right angles to each other (Fig. 269, a). It serves to connect the shafts whose axes are parallel or form a very small angle,  $\psi \approx 1^\circ$ , with an offset of the shaft axes of not more than  $\delta \approx 0.05d_{sh}$ .

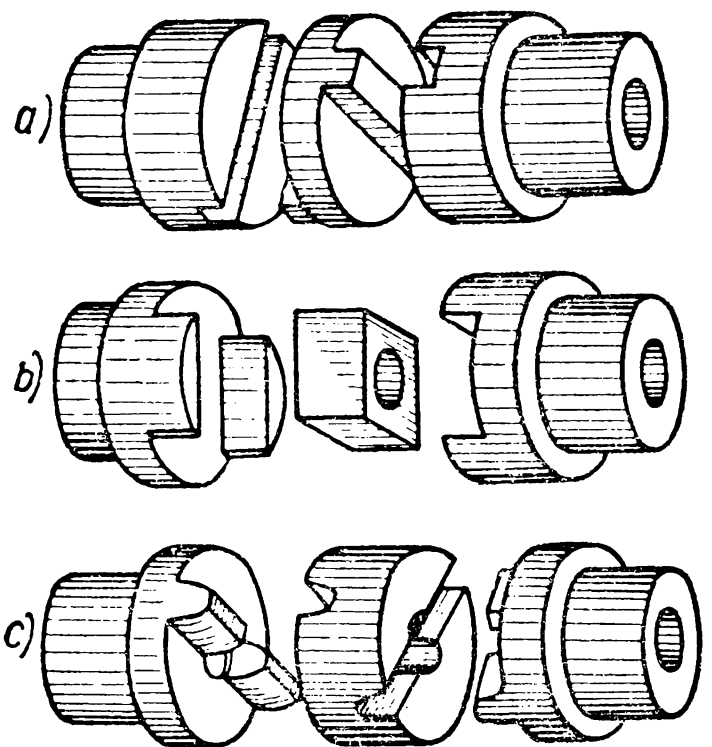


Fig. 269

The allowable misalignment of the shafts and, in general, the operating capacity of Oldham couplings are determined by the resistances which arise when the coupling parts move relative to one another. When the resistance is great the coupling is pinched and the load on the shafts increases considerably.

A modification of this coupling with the centre piece in the form of a square block (Fig. 269, *b*) has larger active surfaces, retains oil better and can permit  $\delta \approx 0.1 d_{sh}$  and  $\psi \leq 3^\circ$ .

Another modification with an involute tooth tongue and a wedge groove (Fig. 269, *c*) allows of a bigger misalignment of the order of  $\psi \leq 4^\circ$ .

As the shafts rotate the centre piece of Oldham coupling performs a planetary movement; with each turn of the shaft its centre makes two revolutions describing a circle of diameter  $\delta$  where  $\delta$  is the offset of the parallel axes of the shafts.

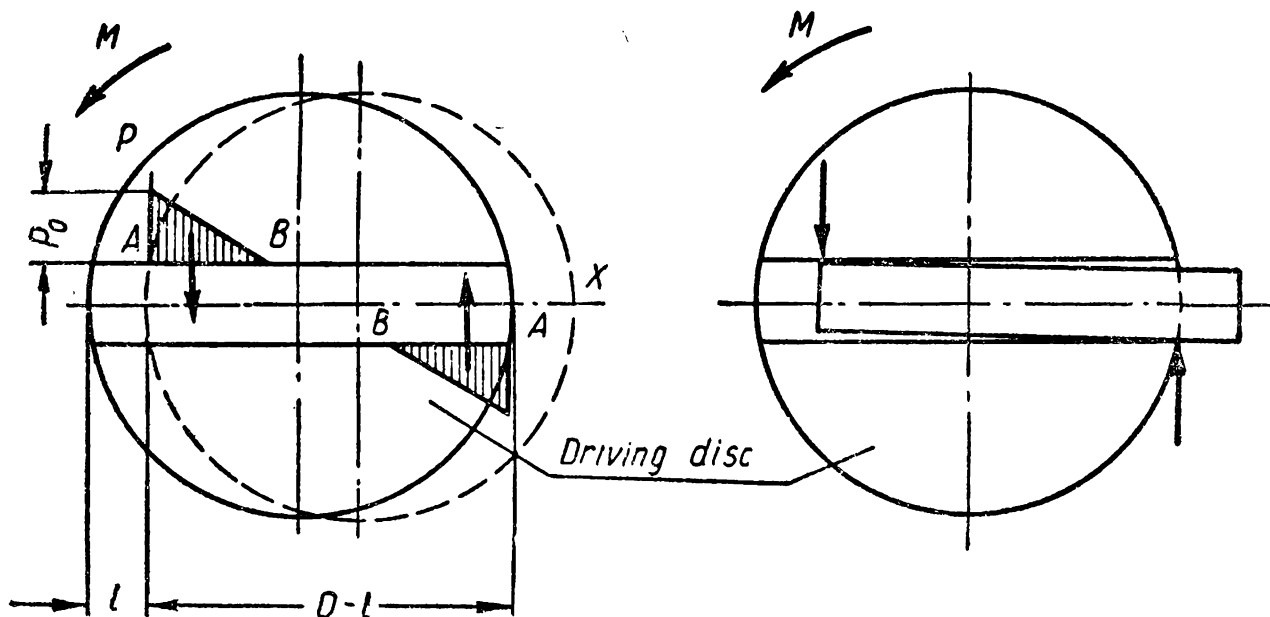


Fig. 270

The torque transmitted by the coupling causes pressure to arise on the working edges of the tongue, which is, generally speaking, not uniform over the length of the edge. If we assume the load to be distributed in accordance with the law of triangles (Fig. 270) over the edge section  $AB = kD$ , where the value of  $k$  depends on the clearance between the edges and the degree of their wear-in we shall obtain an expression for the torque transmitted by the coupling:

$$M_{td} = \frac{p_0 k D h}{2} \left[ (D - l) - \frac{2}{3} k D \right] = \frac{p_0 k D h}{2} \left[ D \left( 1 - \frac{2}{3} k \right) - l \right]$$

where  $h$  is the working height of the friction edges and  $l$  the tongue travel in the groove corresponding to an arbitrary moment of time.

Hence

$$p_0 = \frac{2M_{td}}{h \times D \times k \left[ D \left( 1 - \frac{2}{3} k \right) - l \right]}.$$

The magnitude  $p_0$  reaches its maximum at  $l = l_{\max} = \delta$

$$p_{\max} = \frac{2M_{td}}{h \times D \times k \left[ D \left( 1 - \frac{2}{3} k \right) - \delta \right]} = \frac{2M_{td}}{h \times D^2 \times k \left[ \left( 1 - \frac{2}{3} k \right) - u \right]}$$

where  $u = \frac{\delta}{D}$  is the relative offset of the shafts.

The probable value of  $k$  after the initial wear-in period is  $0.3 \leq k \leq 0.8$ . With these values of  $k$  the expression  $k \left( 1 - \frac{2}{3} k \right)$  in the denominator is 0.24-0.37. Taking the smaller of these values (0.24) which corresponds to  $k = 0.3$  we get from the last equation

$$p_{\max} \approx \frac{8M_{td}}{h \times D^2 (1 - 1.2u)}.$$

With a small offset  $\delta \ll D$ ,  $u \ll 1$ , and this expression with an approximation sufficient for practice can be written thus

$$p_{\max} \approx \frac{8M_{td}}{h \times D^2}. \quad (432)$$

For surfaces of casehardened steels 15X and 20X at  $R_C = 55-60$  we can assume  $p_{\max} = 2 \text{ kg/mm}^2$ .

*Universal joints\** connect shafts whose axes are located at an angle or slightly offset relative to each other.

Such couplings are used, for example, in automobiles to connect the shafts of the gearbox and the rear axle, in rolling mills to transmit torque to the rolls, in machine tools to transmit rotation to the spindles of multi-spindle heads, etc.

For shafts with diameter  $d_{sh} = 10-40 \text{ mm}$  the proportions of universal joints are standardised in the Soviet Union. One such coupling is shown in Fig. 271.

The centre cross and yokes of the coupling are made from steel 40X hardened to  $R_C = 48-53$ , or the centre cross is made from steel IX15 and the yokes from chromium steel hardened to  $R_C = 60-65$ . Universal joints should be lubricated and protected from dust and dirt.

The disadvantage of universal joints of ordinary design is the *nonuniform rotation* of the driven shaft at a constant velocity of the driving shaft\*\* if these shafts are noncollinear. Angular accelerations of the driven shaft caused by this phenomenon develop inertial forces which increase the load on the coupling components. Un-

\* Also called Cardan or Hooke's joints.

\*\* There are also special designs of universal joints with a constant angular velocity.



der certain conditions two universal joints can be employed to synchronise the rotation of the driving and driven shafts. In this case the connecting shaft too does not rotate uniformly\*.

If  $M_{t1}$  is the torque on shaft 1 and  $M_{t2}$ —on shaft 2 then it follows from the condition of equality of the instantaneous power  $M_{t2} \times \omega_2 = M_{t1} \times \omega_1$ , neglecting the losses in the coupling, that

$$\frac{M_{t1}}{M_{t2}} = \frac{\omega_2}{\omega_1}.$$

We know from the kinematics of a universal joint that its velocity ratio ( $\omega_2/\omega_1$ ) varies from  $1/\cos \psi$  to  $\cos \psi$ . Hence, knowing the maximum values of the torque  $M_{t2}$  on the driven shaft we can

determine the required torque on the driving shaft— $M_{t1(\max)} = M_{t2}/\cos \psi$ . On the basis of this torque and the distance between the journals  $2r$ , we can find the forces  $P_{\max}$  acting on the journals and yokes of the coupling,

$$P_{\max} = \frac{M_{t \max}}{2r} \times \frac{1}{\cos \psi} \quad (433)$$

and check them for bending and unit pressure on the friction planes. For universal joints made from the materials mentioned above the allowable unit pressures on the pins amount to  $p_{\max} \approx 4 \text{ kg/mm}^2$ . At high angular velocities and when large masses are connected with the driven shaft the stresses in the parts due to the forces of inertia should be checked.

Soviet standards specify the values of allowable torques as follows: from 2.5 kgm for  $d_{sh} = 10 \text{ mm}$  to 128 kgm for  $d_{sh} = 40 \text{ mm}$ .

*Elastic couplings.* Among the different types of joint couplings *elastic couplings* occupy a place of their own. In addition to compensating for the noncollinearity of the connected shafts they materially

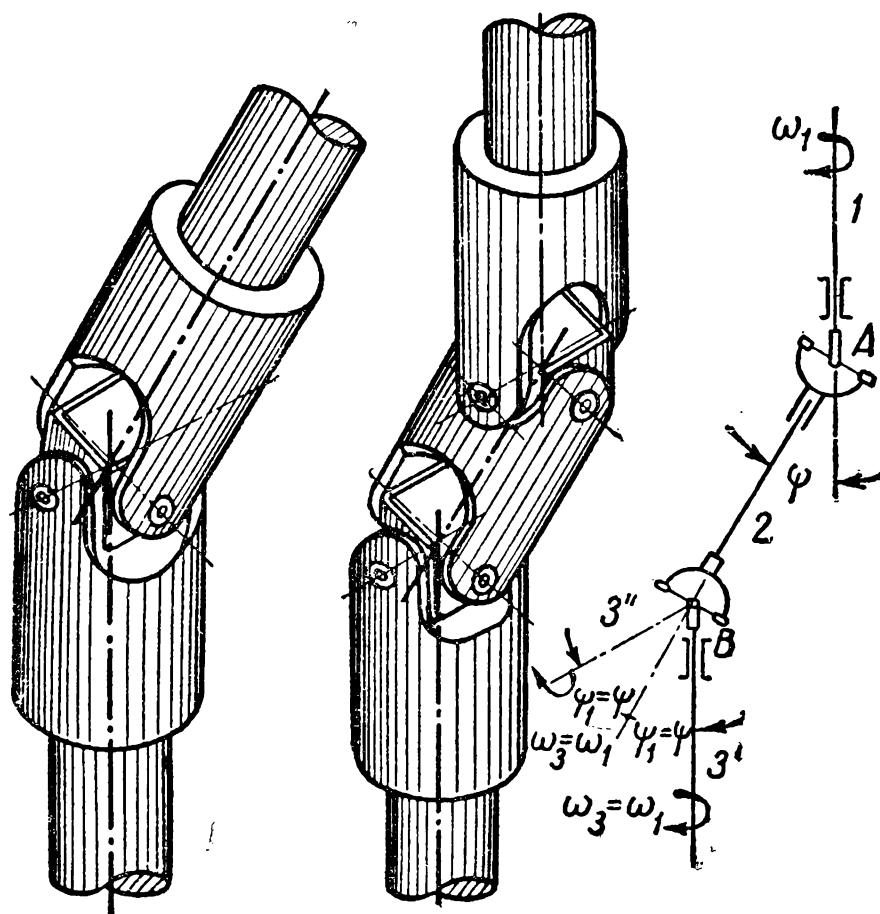


Fig. 271

\* Therefore the moment of inertia of the connecting shaft should be as small as possible to lessen its effect on the machine operation.

affect the dynamic characteristics of the system, changing it as desired.

*The fundamentals of the theory of elastic couplings.* The motor and driving mechanism or the two parts of a transmission connected by an elastic coupling form an *oscillating system* which for dynamic investigations can be represented by the sketch shown in Fig. 272.

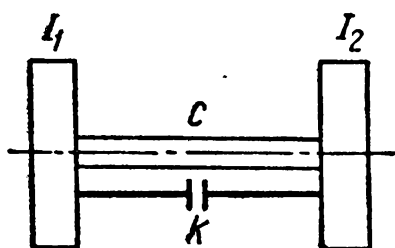


Fig. 272

Two discs with moments of inertia  $I_1$  and  $I_2$  are connected by a weightless rod with the torsional rigidity  $c$ . Since the torsional elasticity of an elastic coupling is considerably less than that of the connected shafts we can assume that  $c$  denotes simultaneously the rigidity of the system and the rigidity of the coupling.

We know from the theory of dynamics that if such a system is subjected to the action of the disturbing torque  $M = M_0 \sin \omega t$  then the *amplitude of the torque* on the coupling (the rod in the sketch) will be expressed by the formula

$$M_{td} = \pm M_0 \frac{I_2}{I_1 + I_2} \sqrt{\frac{1 + \left(\frac{k\omega}{c}\right)^2}{\left(1 - \frac{\omega^2}{p^2}\right)^2 + \left(\frac{k\omega}{c}\right)^2}} \quad (434)$$

where, in addition to the previous symbols, the following are denoted:  $M_0$  and  $\omega$ —the amplitude and frequency of the disturbing torque;  $p$ —the frequency of the system oscillations without damping  $\left(p = \sqrt{\frac{c}{I_1} + \frac{c}{I_2}}\right)$ ;  $c$ —the coupling rigidity (constant);  $k$ —the damping (extinction) factor (constant).

Introducing in the formula (434) the rated torque  $M_{rated}$  we obtain

$$M_{td} = \pm M_{rated} \frac{M_0}{M_{rated}} \times \frac{I_2}{I_1 + I_2} \mu = \pm M_{rated} \times v \times \mu \quad (435)$$

where

$$\mu = \sqrt{\frac{1 + \left(\frac{k\omega}{c}\right)^2}{\left(1 - \frac{\omega^2}{p^2}\right)^2 + \left(\frac{k\omega}{c}\right)^2}}; \quad v = \frac{M_0}{M_{rated}} \times \frac{I_2}{I_1 + I_2}. \quad (436)$$

It is clear from the comparison of the expressions (435) and (428) that the torque loading the coupling is composed of two parts: one accounted for by the factor  $v$  (as in a rigid coupling, see p. 479) and the other accounted for by the factor  $\mu$  typical of an elastic coupling.

The factor  $\mu$  depends mainly on the ratio of frequencies  $\frac{\omega}{p}$ .

At resonance ( $\omega = p$ ) it reaches the maximum:

$$\mu = \sqrt{\left(\frac{c}{k\omega}\right)^2 + 1} \approx \frac{c}{k\omega} \quad (437)$$

since usually  $\frac{c}{k\omega} \gg 1$ .

It can be seen from the expression for  $\mu$  that an elastic coupling, compared to a rigid coupling, gives a smaller value of torque ( $\mu < 1$ ) only when  $\omega > \sqrt{2p}$ , i. e., when the frequency of constrained oscillations ( $\omega$ ) is  $\sqrt{2}$  times larger than the frequency ( $p$ ) of the system. This is achieved by selecting the proper rigidity for the coupling  $c$ . The relations (437) and (434) also show that damping ( $k$ ) affects the value  $\mu$  particularly in the zone bordering on resonance.

Above, for the sake of simplicity, the coupling rigidity was assumed to be constant ( $c = \text{const}$ ) and, therefore, the elastic characteristic of the coupling in torsion ( $M_{el} = c\varphi$ ) is linear. In practice, use is generally made of couplings with a nonlinear elastic characteristic ( $c \neq \text{const}$ ). In this case the coupling changes, as it were, the frequency of the system ( $p$ ) and does not permit oscillations to increase to the point they would reach with a coupling of a constant rigidity. The formula (434) can therefore be also applied to this case, if we take the value  $c$  at the point of the elastic characteristic which corresponds to the amplitude ( $\varphi_0$ ) of the coupling twist angle. The most widespread form of a nonlinear characteristic has the shape of a curve with a gradually increasing slope from an almost horizontal (in the coordinate origin) to a vertical line. Fig. 276 shows a less frequent but more effective (for damping oscillations) characteristic. As distinct from the previous curve, it shows the presence of a prestress in the elastic joint.

Both in linear and nonlinear couplings the characteristic terminates, as a rule, in vertical sections, which indicate that the coupling halves have reached the stops necessary to protect the elastic elements against overstrain under occasional overloads.

*Design and calculation of elastic couplings.* The elastic element is the main part of an elastic coupling and determines its properties and design.

In modern couplings the elastic elements are usually made from steel and rubber. During the last decade preference has been given to rubber elastic elements which utilise a very important property of rubber—its ability to withstand large deformations with the dispersion of a considerable amount of energy per unit of volume. The unit energy of elastic deformation of rubber amounts to about 4,500 kgm/kg whereas for spring steel it is below 3 kgm/kg. The wide use of rubber elastic elements became possible after a method of reliably fastening rubber to metal had been developed. The strength of such a connection reaches 70 kg/cm<sup>2</sup> and is little affected by temperatures up to 80°C.

Existing designs of coupling use almost all known kinds of rubber-metallic elements as well as steel springs (compressive, flexural and torsional). The principal design features of these elements will be considered below in Chapter XXIV (p. 543).

The elastic characteristic of springs, usually linear at small deformations, is curved in the required manner by means of stops, clearances, prestresses and other similar methods. Fig. 273 shows in the force-path coordinates the characteristics of flat springs obtained in this manner.

Some typical designs of elastic couplings and their elastic characteristics are shown in Fig. 274.

A *box-pin coupling* (Fig. 274, *a*) consists of two flanged halves. In one half steel pins with tapered shanks are secured and rubber sleeves composed of trapezoidal rings are placed on them. The disc of the other half is provided with round holes for the pins and their sleeves. The range of standardised couplings consists of two series with 9 numbers in each, from 1 to 9, corresponding to the diameters of the connected shafts which increase from 28 to 150 mm and the transmitted torque which ranges from 12.8 to 1,538 kgm for the normal series of couplings (MH1 to MH9) and from 6.7 to 716 kgm for the light series of couplings (MO1 to MO9).

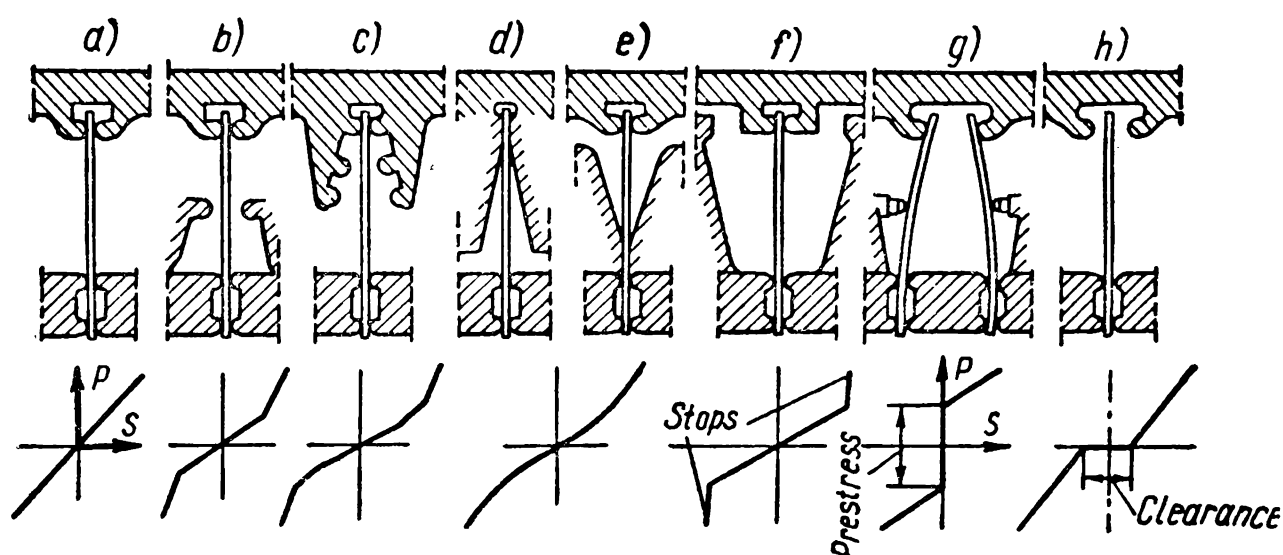


Fig. 273

Light couplings have the same bore diameters as normal couplings but are intended to transmit smaller torques and weigh less.

The number of pins in the couplings is from 4 to 12; the number of rings on the pin—3-4. The coupling halves are made from grade CЧ 21-40 cast iron, steel forgings of grade 30 or steel castings of grade 35 Л II; pins are made from normalised steel 45. The quality of rubber rings is specified by a number of indices corresponding to long-term operation in compression under a load of 20 kg/cm<sup>2</sup> (instantaneous overloads—40 kg/cm<sup>2</sup>).

The peripheral velocity on the outside diameter of these couplings is limited to 30 m/sec because at a higher frequency of load repetition the rubber sleeves become heated and disintegrate.

These couplings do not compensate for the noncollinearity of connected shafts; they are designed to compensate only for shaft axial shift, a feature common to the rotors of electrical machines (self-adjustment in a magnetic field), and to cushion the shocks in transmitting rotation. When these couplings are used to fasten together

noncollinear shafts their elastic sleeves are worn at a faster rate and additional radial loads are brought to act on the shafts and their bearings (see p. 485). The couplings are selected according to the available dimensions and tabulated values of torques.

The calculation of nonstandard box-pin couplings is usually limited to checking the pins for bending and the sleeves for compression. As operating experience shows these parts are subject to failure first.

The calculation is done on the basis of the peripheral effort  $P_1$  transmitted by one pin if the load ( $M_{td}$ ) is spread uniformly between all ( $z$ ) pins.  $P_1$ , the maximum bending stresses in the pin  $\sigma_b$  and the unit pressure  $p$  between the pin and the elastic sleeve are determined from the following formulae which require no further analysis:

$$P_1 = \frac{2M_{td}}{D_{pin}z},$$

$$\sigma_b = \frac{P_1 x}{0.1 d_{pin}^3} \leq [\sigma]_b,$$

$$p = \frac{P_1}{b \times d_{pin}} \leq [p] \quad (438)$$

where  $M_{td}$  is the design torque transmitted by the coupling;

$D_{pin}$ —diameter of the pin centre circle;

$z$ —number of pins in the coupling;

$d_{pin}$ —pin diameter;

$x$ —moment arm ( $x \approx b$ );

$b$ —length of the rubber sleeve (Fig. 275).

The actual load distribution between the pins depends on the accuracy with which the coupling halves are centred and generally is not uniform; this is allowed for by selecting reduced magnitudes of

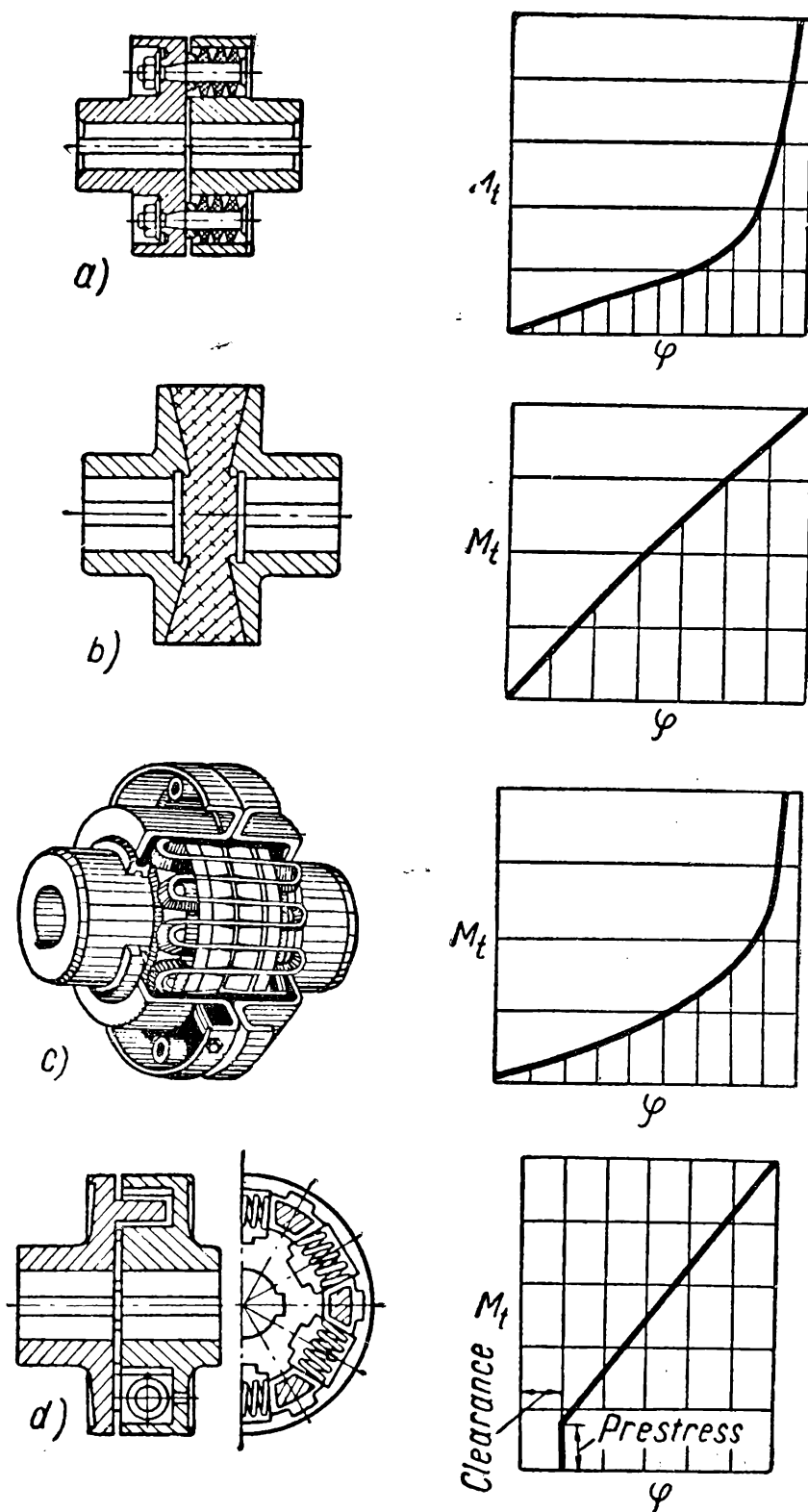


Fig. 274

allowable stress. The Soviet data on designing cranes recommend 2-2.5 as the margin of safety relative to the yield point, depending on the kind of service, i. e., for pins  $[\sigma]_b \leq (0.4-0.5) \sigma_y$ , the unit pressure between the pins and rubber should not exceed  $[p] \leq 30 \text{ kg/cm}^2$ .\*

*Rubber-metallic couplings* (Fig. 274, b). The chief characteristic of all couplings of this type is the strong adhesion of rubber to metal parts. In this case the load is uniformly distributed over the entire contact surface between the metal and rubber, thereby making it possible to utilise the elastic properties of rubber to the best advantage. In small couplings, for torques up to 650 kg/cm, the rubber is bonded directly to the coupling halves. In large couplings, up to 1,600 kgm, the rubber is bonded to intermediary flanges fastened to the coupling halves by bolts.

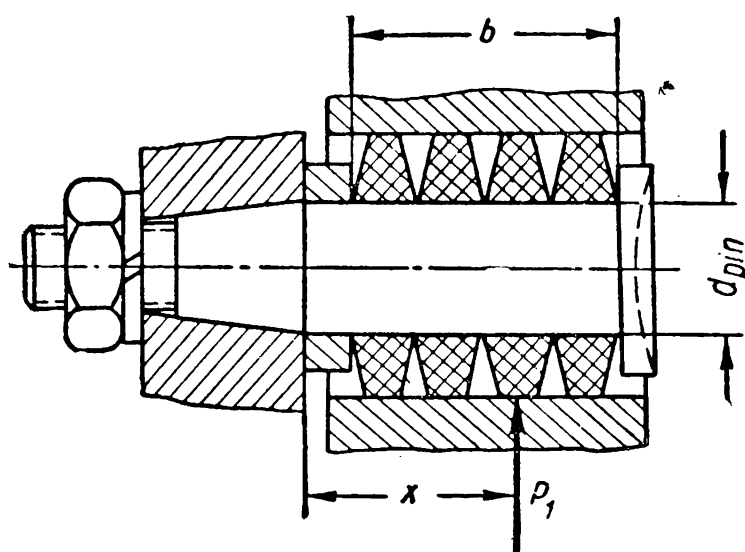


Fig. 275

These couplings operate noiselessly even during reversing. Rubber-metallic couplings are apparently the best type of joint for high-speed drives with low torques.

*Zigzag spring couplings* (Fig. 274, c) are the most efficient of all types of coupling with steel elastic elements. They comprise two toothed halves fitted on to the shaft ends, a zigzag spring fitted into the tooth gashes and a housing enclosing the copiously greased spring and teeth.

In large couplings to decrease the spring cross-section the coils are laid in two or three rows. Depending on the tooth contour these couplings may have a linear or nonlinear characteristic.

*Couplings with coil springs* (Fig. 274, d). Coil springs are fitted into one half of the coupling, usually with some initial deflection. The end of the other half is provided with cams which loosely fit the slots between the springs in the first half. In this way torque is transmitted from one coupling half to the other through the coil springs. The required elastic characteristic may be obtained by selecting proper initial deflection, clearance and stops. These couplings are employed when the assigned elastic characteristic must be strictly adhered to. In this case the main factors which determine this characteristic (the stiffness of the coil springs, the clearances and the

\* Soviet standards establish the transmitted torques on the basis of  $[p] = 20 \text{ kg/cm}^2$  and permit a momentary double overload.

distance between the stops) are rather easily found by calculation and duplicated in manufacture.

The main task in calculating spring-loaded couplings is reduced to finding the proportions of the springs and their conjugate parts for the given elastic characteristic of the coupling which, in turn, depends on the conditions of operation of the coupling in a machine.

For example, let the elastic characteristic of a coupling be represented by the curve shown in Fig. 276. This curve is distinctly nonlinear. In a coupling with coil springs it can be obtained by prestressing the springs and applying stops which lessen their deformation (Fig. 277).

The prestress torque  $M_{pre}$  is usually larger than the rated torque  $M_{rated}$  transmitted by the coupling. If  $M_{rated}$  together with the amplitude  $M_0$  of the torque arising in the coupling during oscillation is below  $M_{l\ pre}$ , i.e.,  $M_{rated} + M_0 < M_{l\ pre}$  the coupling acts as a rigid joint (its yield is zero). When this sum increases beyond  $M_{l\ pre}$  the coupling will

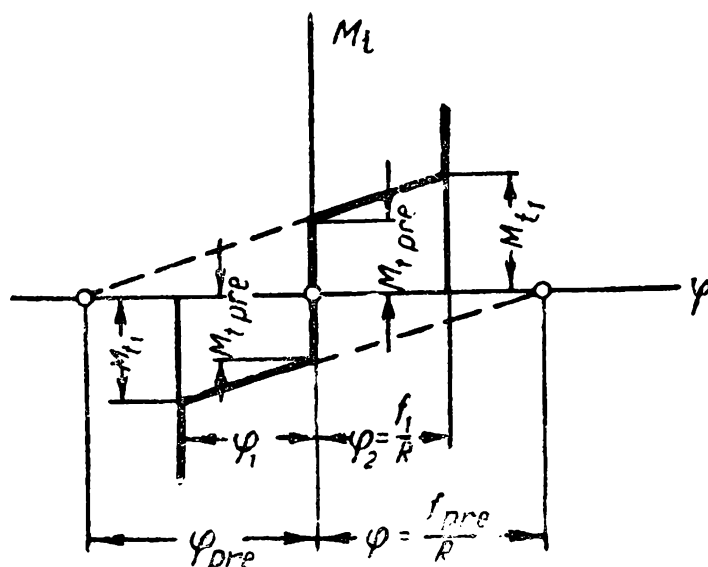


Fig. 276

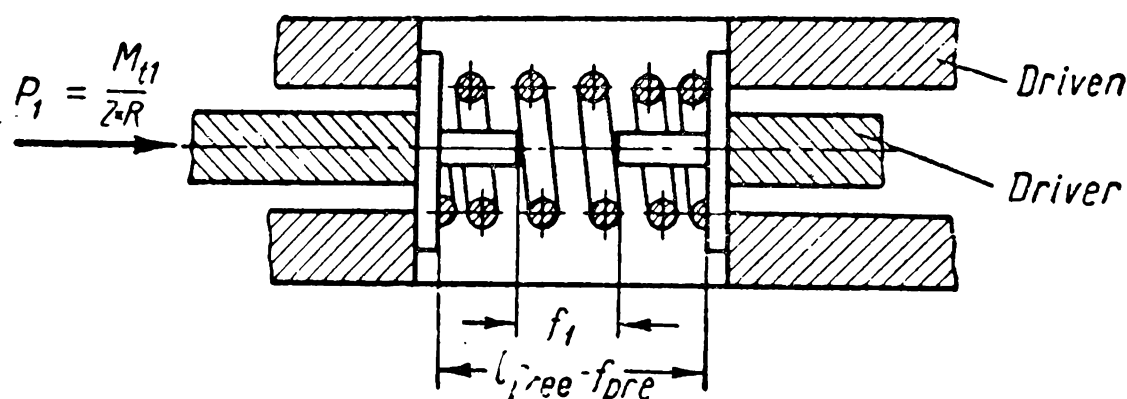


Fig. 277

display elastic properties: the springs in the coupling will begin to deform. When this sum exceeds the value of the torque  $M_{l1}$ , i. e., when  $M_{rated} + M_0 > M_{l1}$  and the condition  $M_{rated} - M_0 > M_{l1}$  is simultaneously satisfied, the coupling will again exhibit the properties of a rigid joint.

After selecting (on the basis of the intended proportions of the coupling) the number of springs  $z$  and the radius of their location  $R$ , and using the values  $M_l$  and  $\varphi$  taken from the coupling elastic characteristic (Fig. 276) we determine in succession:

the linear rigidity of the spring

$$c_1 = \frac{M_{t1} - M_{t\ pre}}{z\varphi_1 R^2} \text{ kg/cm};$$

the initial deflection of the spring

$$f_{pre} = \frac{M_{t\ pre}}{zc_1 R} = R\varphi_{pre} \text{ cm};$$

the distance between the stops (Fig. 277)

$$f_1 = R\varphi_1 \text{ cm};$$

the total deflection of the spring

$$f = f_{pre} + f_1 \text{ cm};$$

the maximum load on the spring

$$P_1 = \frac{M_{t1}}{zR} = c_1 f \text{ kg}.$$

The values obtained from these equations and the proportions of seats which are to accommodate the springs are used to find the size of the springs (see p. 543 for more detailed data on calculating the springs).

## CLUTCHES

Clutches are employed to connect and disconnect shafts during their relative motion (under load) or at standstill.

*According to the way in which they engage* clutches may be divided into four groups: *friction, jaw (toothed), electromagnetic fluid and electromagnetic powder, and hydraulic clutches.*

*Depending on the manner in which clutches are operated* they are subdivided into those *controlled by an operator* directly or by means of auxiliary force, and *power-controlled clutches.*

Shafts and other parts linked by clutches should satisfy one very important requirement—they should be strictly collinear. Defects in alignment markedly deteriorate the performance of all types of clutches and lead to their rapid failure.

A general classification of clutches is shown in Fig. 278. In our further exposition we shall consider: first, friction clutches as the largest and most developed group, then toothed and jaw clutches and finally fluid and powder clutches which have appeared only recently but which are now quickly developing. In the classification in Fig. 278 we use the term “electromagnetic” twice. However, we should differentiate between: 1) simply “electromagnetic clutches”, more precisely “friction clutches which are actuated electromag-



netically", i. e., in which the friction plates of ordinary (solid) material are drawn together by the force of electromagnetic attraction and b) "electromagnetic fluid and powder" clutches in which the

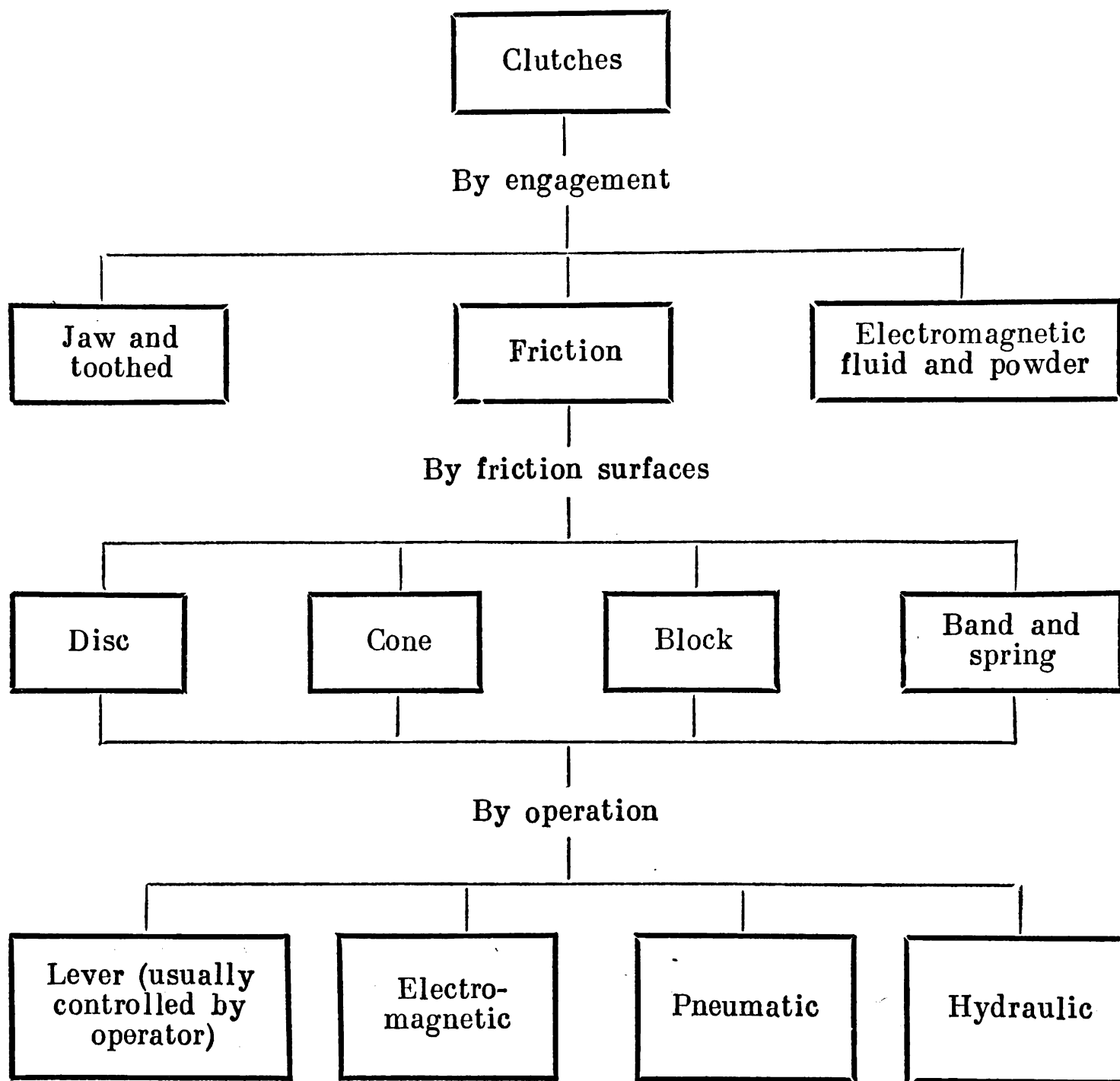


Fig. 278

magnetic flux changes the mechanical properties of a medium in the form of a fluid or powder with ferromagnetic particles.

**Friction Clutches.** Friction clutches are intended to engage smoothly two shafts in motion and release them quickly or slowly at will. In automobiles, tractors, power shovels, winches and some machine tools, friction clutches are the main mechanisms on which unfailing operation of the machine depends.

Of all various types of clutch, friction clutches are most widely used.

*Fundamentals of the theory of friction clutches.* There are four stages in the work of a friction clutch.

1st stage—engagement: the working surfaces of the clutch are drawn together and compressed, the driven shaft is accelerated to the velocity of the driving shaft;

2nd stage—the clutch is engaged: the driven and driving shafts rotate with the same velocity;

3rd stage—disengagement: the working surfaces of the clutch are pulled apart, the driven shaft slows down and then stops;

4th stage — the clutch is disengaged: the working surfaces are separated by a clearance, the driven shaft is immobile while the driving shaft continues to rotate or is likewise immobile.

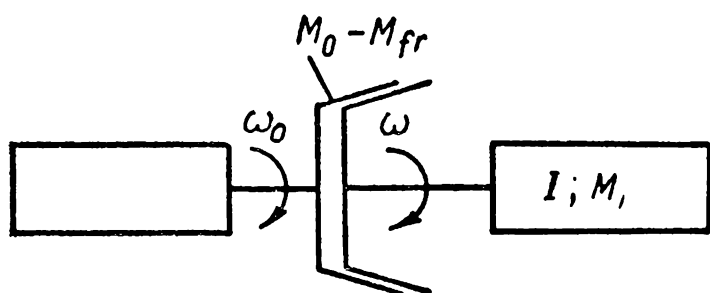


Fig. 279

Let us consider each of these stages.

*Clutch engagement.* The clutch (Fig. 279) divides a kinematic transmission into two parts: the driving (motor) and the driven (driving mechanism).

At the moment preceding engagement, the driving shaft rotates with a constant angular velocity  $\omega_0$  and the driven shaft is at stand-still ( $\omega=0$ ).

The work  $A$  expended by the clutch during engagement is composed of three parts:  $A_1$ —the work of friction during the time  $t_1$ , when  $\omega=0$  and the moment of friction in the clutch increases from  $M=0$  to  $M=M_r$ , which is the moment of external resistance on the driven shaft;  $A_2$ —the work expended on increasing the kinetic energy of the mass connected with the driven shaft including the losses during the time  $(t_2-t_1)$ , when  $\omega$  increases from 0 to  $\omega_0$ ;  $A_3$ —the work done to overcome the external resistance on the driven shaft, including the losses during the time  $(t_2-t_1)$ .

The values  $A_1$ ,  $A_2$  and  $A_3$  are determined from the known equations of mechanics

$$A_1 = \int_0^{t_1} M \times \omega_0 dt; \quad A_2 = \int_{t_1}^{t_2} (M - M_r) \omega_0 dt; \quad A_3 = \int_{t_1}^{t_2} M_r \omega_0 dt. \quad (439)$$

The driven shaft takes only that part  $A'$  of the work  $A$  which goes to increase the kinetic energy of the moving masses  $A'_2$  and the work of the external resistance  $A'_3$ ; in this case

$$A'_2 = I \frac{\omega_0^2}{2} \text{ and } A'_3 = \int_{t_1}^{t_2} M_r \omega dt \quad (440)$$

where  $I$  is the moment of inertia of the moving masses connected with the driven shaft reduced to the axis of this shaft. The losses in the clutch due to friction are therefore

$$A_{fr} = A - A' = A_1 + A_2 + A_3 - A'_2 - A'_3. \quad (441)$$

It is difficult (simple in a general case) to determine  $A_{fr}$  when the equations (439) and (440) are integrated, since the laws according to which the integrands change in time are often not known.

To determine  $A_{fr}$  approximately we make simple assumptions which are frequently used in designing practice: the moment of friction in the clutch increases so quickly that we can take  $t_1 \approx 0$  and  $M = \text{const} = M_{fr}$ ; the moment of external resistance does not change during engagement ( $M_r = \text{const}$ ).

The nature of motion of the driven shaft during the time  $(t_2 - t_1)$  is determined by the equation of momentum

$$I d\omega = (M_{fr} - M_r) dt.$$

In our case the acceleration is constant

$$\frac{d\omega}{dt} = \frac{M_{fr} - M_r}{I}$$

and the time  $t_2 = \frac{I\omega_0}{M_{fr} - M_r}$ .

Therefore

$$\left. \begin{aligned} A_1 &= 0; \quad A_2 = (M_{fr} - M_r) \omega_0 t_2 = I \omega_0^2 \\ A_3 &= M_r \omega_0 t_2 = I \omega_0 \frac{M_r}{M_{fr} - M_r} \\ A'_2 &= I \frac{\omega_0^2}{2}; \quad A'_3 = I \frac{\omega_0^2}{2} \frac{M_{fr}}{M_{fr} - M_r} \end{aligned} \right\} \quad (442)$$

Substituting these values  $A_1, A_2, A_3, A'_2, A'_3$  in the equation (441) we get this simple expression (443) for the work lost in friction during the clutch engagement

$$A_{fr} = I \frac{\omega_0^2}{2} \times \frac{M_{fr}}{M_{fr} - M_r}. \quad (443)$$

From the last expression conclusions can be drawn which are very important for the design of friction clutches. To decrease friction losses at the given velocity  $\omega_0$ ,  $I$  should be decreased as far as possible and the difference  $(M_{fr} - M_r)$  increased during starting (for example, at engagement with no load,  $M_r \approx 0$ ). However, an increase in the difference  $(M_{fr} - M_r)$  causes a proportionally greater increase of acceleration and the forces of inertia. The maximum value of  $(M_{fr} - M_r)$  gives the limit values of these forces.

*Operation of an engaged clutch.* An engaged clutch should transmit to the driven shaft torque from the driving shaft without slip under normal load\*. Let us find the maximum torque which can be transmitted by the clutch, i. e., the limit torque, after attaining which the clutch begins to slip.

When the force  $P$  compresses two surfaces in the form of flat annular plates with radii  $r_{in}$  and  $r_{out}$  it causes friction to arise between them, whose moment can be expressed by the formula

$$M_{fr} = fPr_{red} \quad (444)$$

where  $f$  is the coefficient of friction between the friction planes and  $r_{red}$  the reduced radius of the friction forces acting between the compressed surfaces, which can be assumed as equal to the mean radius

$$r_{red} = r_{mean} = 0.5(r_{out} + r_{in})^{**}.$$

Introducing in the equation (444) the area of one pair of friction surfaces  $S_{fr} = 2\pi r_{mean} \times b$  and the mean unit pressure  $p = \frac{P}{S_{fr}}$  we obtain

$$M_{fr} = fPr_{mean} = fpS_{fr}r_{mean}. \quad (445)$$

When  $z$  pairs of friction surfaces with different values of  $f$ ,  $P$  and  $r_{mean}$  are used, the torque they transmit will amount to

$$M_{fr} = \sum_{i=1}^z f_i P_i r_{mean\ i} = \sum_{i=1}^z f_i p_i S_{fr\ i} r_{mean\ i}. \quad (446)$$

The expression (446) is the main one used in calculating friction clutches.

*Clutch disengagement.* During clutch disengagement the losses that occur can be determined in the same way as during engagement. These are very small and as they have no practical importance are usually ignored.

*Operation of a disengaged clutch.* The chief function of a disengaged clutch is to ensure the absence of friction between the components in relative rotation. In this respect especial difficulties are met with in the case of multiple-disc clutches.

Friction between the discs of a disengaged clutch may be due to the following: a) deformation of the discs causing contact between them even after release; b) sticking of the discs together because of grease between their surfaces.

---

\* The operation of a friction clutch as a slipping clutch protecting against overloads is considered separately on p. 531.

\*\* In general the value of  $r_{red}$  depends on the law of distribution of elementary friction forces over the friction surfaces. Various hypotheses of this law give similar results which make it possible to assume  $r_{red} = r_{mean}$  for the calculation of clutches.

The first cause can be eliminated by a thorough machining of the discs, the removal of warping during operation and provision of sufficient clearances between them in the disengaged position and the second cause—by pulling the discs apart when the clutch is disengaged.

It is good practice to force oil between the discs of a disengaged clutch. Besides reducing friction between the discs this also provides intensive cooling for the friction surfaces.

*Designs of friction clutches.* In view of their purpose—to transmit torque by means of friction forces between tightly compressed surfaces—it is convenient to classify friction clutches according to the following characteristics: the material, form and the number of friction surfaces and the method of drawing them together (the clutch operating device).

*The materials of the friction surfaces.* The specific features of the operation of friction clutches we have considered above and the expressions (443) and (446) make it possible to formulate a number of requirements which must be met by the materials of the friction surfaces:

a) a high coefficient of friction, retaining a permanent value over a sufficiently wide range of surface velocities, temperatures and loads;

b) adequate mechanical and thermal strength;

c) little wear and no scoring;

d) high heat conductivity making for the rapid dispersal of heat from the friction surfaces.

Table 67 gives some of the most widely used friction materials.

Table 67

## Friction Materials in Wide Use

Material of friction surfaces		Operating conditions	Coefficient of friction $f$	Unit pressure $[p]$ in kg/cm <sup>2</sup>	Maximum operating temperature in °C
Hardened steel	Hardened steel	In oil	0.08	6-8	250
Cast iron	Cast iron or steel	In oil	0.06	6-8	250-300
Cast iron	Ditto	Dry	0.15	2.5-4	250-300
Bronze	Ditto	In oil	0.05	4	150
Pressed asbestos	Ditto	Dry	0.3	2-3	150-250
Powder-metal	Ditto	Dry	0.4	3	550
Powder-metal	Ditto	In oil	0.1	8	550

As a rule, clutches in which both friction surfaces are metallic (cast iron on cast iron, steel on steel, bronze on steel) require copious lubrication for intensive work (especially steel-steel and bronze-

steel combinations); when operated dry their wear is impermissibly high. Since the coefficient of friction of such pairs is comparatively low they should be made in large sizes or have many friction surfaces. In practice this can be attained only in multiple-disc clutches where metallic friction pairs are successfully employed.

Attempts to eliminate the shortcomings inherent in metal friction materials has led to the development of asbestos-base materials as well as powder-metal materials. These reduce the size of clutches, possess better resistance to wear and can be operated dry or in oil.

Results obtained seem to show that in the future powder-metal friction materials will be most extensively employed. They are made in the form of straps 0.25-6 mm thick (depending on the diameter) pressed on to steel discs on one or both sides. At a velocity of 50 m/sec and at temperatures between 350 and 500°C these straps allow a coefficient of friction of not less than 0.4-0.5 with sufficiently high mechanical and antiscuffing properties. They also allow unit pressures up to 10 kg/cm<sup>2</sup> when run dry and up to 30 kg/cm<sup>2</sup> in an oil bath. Possessing a low hardness (50-60  $H_B$ ) these facings operate effectively in combination with cast iron and carbon steel. Among other advantages powder-metal straps offer are high heat conductivity, wear resistance and the possibility of grooving them for the removal of oil in order to dissipate heat.

According to the arrangement and the form of the friction surfaces, friction clutches are subdivided into: a) *radial*, in which the friction surfaces are cylindrical and b) *axial*, with flat or tapered friction surfaces. These clutches are also classified depending on their structural features and the number of friction surfaces. Sketches of the main types of friction clutches are shown in Fig. 280.

*Clutch operating devices.* A clutch operating device should:

1) engage smoothly, increasing the velocity of a machine in conformity with a predetermined regularity (for example, in buses where passengers stand in the gangway the acceleration should not exceed  $\sim 4$  m/sec<sup>2</sup>);

2) uniformly distribute pressure over the entire area of the friction surfaces;

3) ensure that the effort and stroke required for control should not exceed (depending on the type of machine): on the gear shift lever 6-15 kg and 200-250 mm and on the clutch pedal 8-30 kg and 100-200 mm respectively;

4) provide for adjustment, so that wear of the friction surfaces does not lead to the deterioration of the operating capacity of the clutch and the ease of control;

5) ensure reliable operation within the complete range of assigned conditions (at different seasons, temperatures, etc.).

The most important characteristics determining the classification of clutch operating devices are: 1) the kind of power used for control and 2) the mode of transmitting effort to the friction surfaces.

Friction clutches

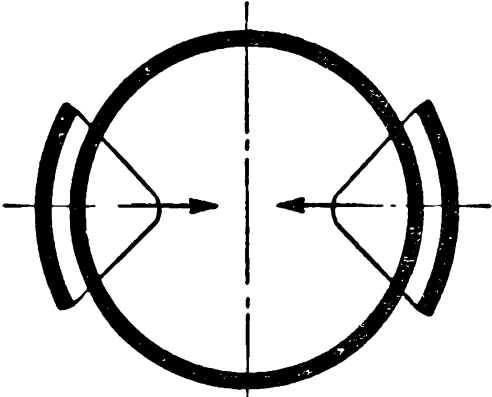
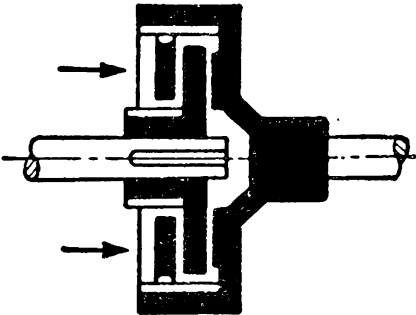
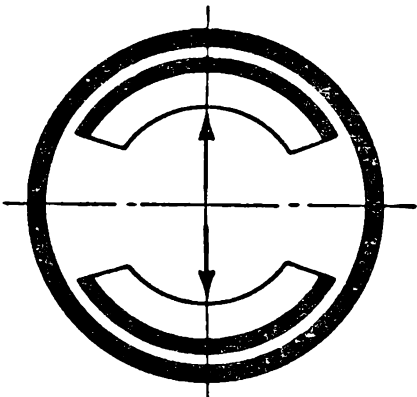
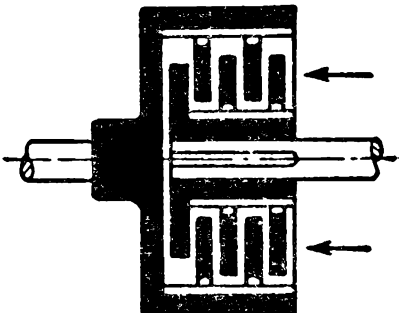
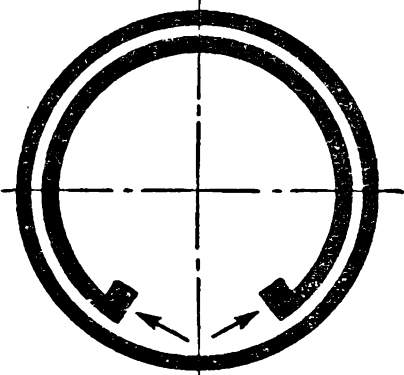
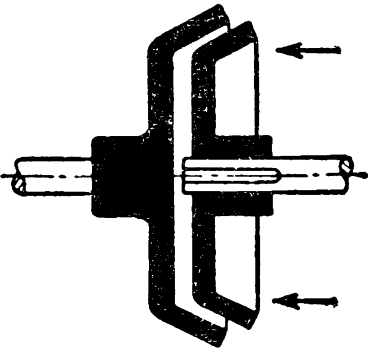
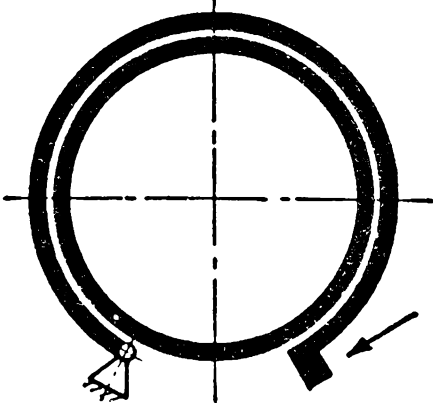
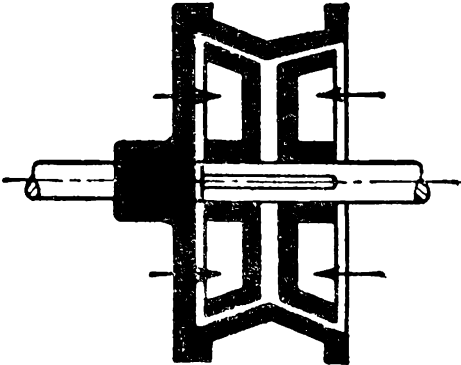
		Radial	Axial
Block	Disc	 <p>With outer shoes</p>	 <p>Single-disc</p>
		 <p>With inner shoes</p>	 <p>Multiple-disc</p>
Band and spring	Cone	 <p>With expanding ring</p>	 <p>Single-cone</p>
		 <p>With band</p>	 <p>Double-cone</p>

Fig. 280

Depending on the *power* used clutch operating devices fall into: a) those operated by muscular energy and b) those utilising the power of the prime mover or of any other source. In the past all clutches were operated by the hand or foot. Nowadays such control is employed only when little effort is required for engagement. In other cases the control is facilitated and simplified (automated) by auxiliary power delivered to the device.

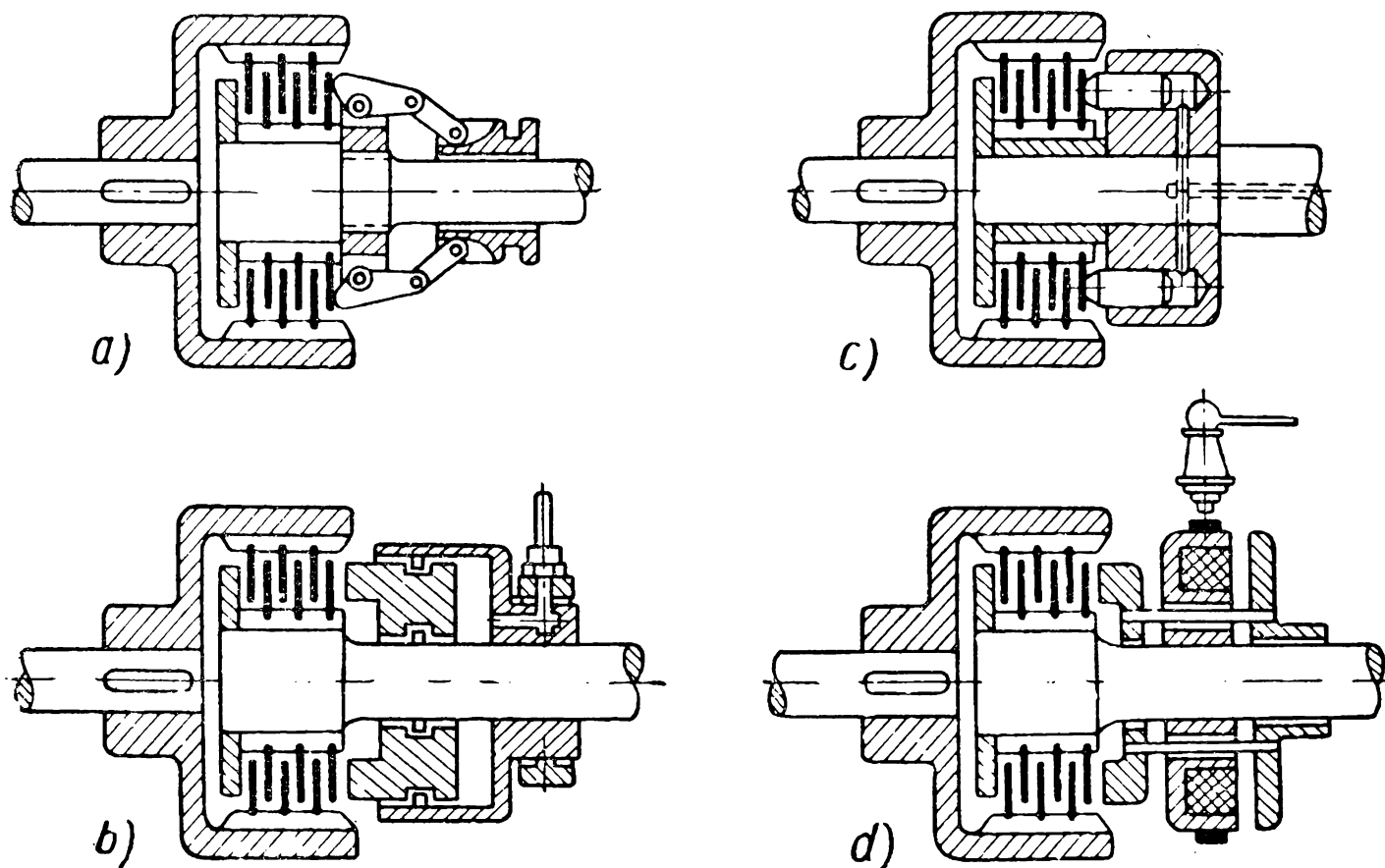


Fig. 281

According to the way in which effort is transmitted to the friction surfaces clutch operating devices are divided into the following groups: a) lever (also ball and jaw), b) hydraulic, c) pneumatic, d) electromagnetic.

Fig. 281 shows by way of example a multiple-disc friction clutch in four versions using each of these methods of compressing the friction surfaces.

Lever clutches used to be predominantly employed with hand and foot control. Their field of application was subsequently reduced and today lever control is very seldom used for large clutches.

*Typical designs of friction clutches.* From a great variety of designs of friction clutches we shall consider only a few designs which have gained widespread recognition because of their superiority over other types.

*Disc clutches.* Solid or strapped discs are easier to manufacture than friction elements of other forms. By varying the number



of discs of identical size, we can compose clutches for transmitting various torques, and this facilitates the standardisation and centralisation of their production. Disc clutches require less space than other types and their worn parts can more conveniently be replaced.

All these advantages allow disc clutches to be extensively employed in automobiles, tractors, machine tools, etc.

All modern cars employ single-disc clutches.

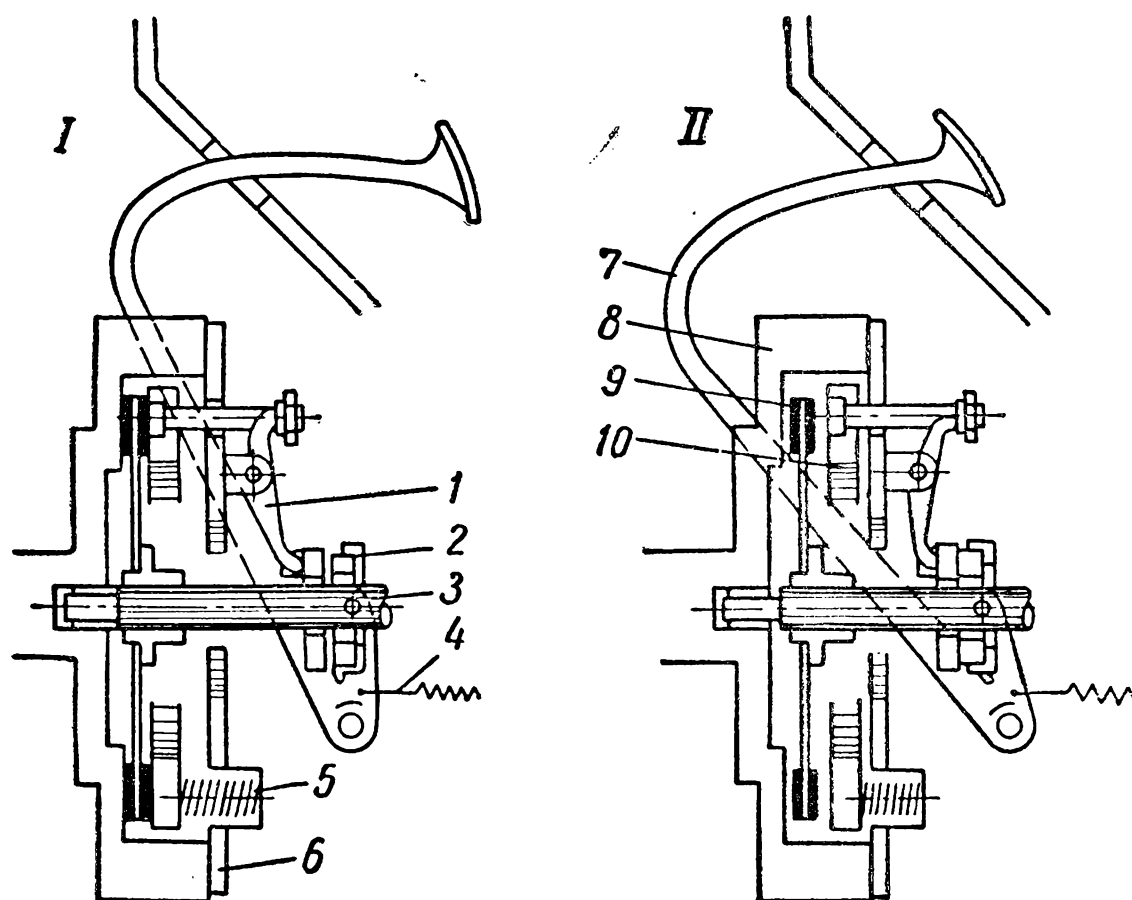


Fig. 282

Fig. 282 shows such a clutch schematically. In position *I* the clutch is engaged: the driven disc 9 is pressed by springs 5 between flywheel 8 and pressure ring 10. Simultaneously, torque is transmitted from flywheel 8 to driven shaft 3. In position *II* the clutch is disengaged: lever 7 by means of collar 2 and arms 1 pushes ring 10 away overcoming the tension of springs 5. Simultaneously, the friction surfaces are brought apart. After the pedal is released lever 7 is returned by spring 4 to the initial position and the clutch is engaged again. Cover 6 screwed to the flywheel serves to fasten springs 5, the axles of arms 1 and also protects the friction surfaces against dirt.

Fig. 283 shows a multiple-disc clutch employed in machine tools. In position *I* the clutch is engaged: discs 2 of external half 1 and discs 3 of internal half 7 are compressed by arms 5 and bushing 6. In position *II* the clutch is disengaged: bushing 6 is shifted to the right, arms 5 turn and release the discs. A specific feature of this design

is the special crimped section of the internal discs, due to which the discs on disengagement are forcibly separated, thereby reducing friction losses. The clutch is adjusted by sleeve 4 provided on half 7. The sleeve is retained in the required position by a spring stop.

Discs which develop friction forces on their side surfaces are the main components of disc clutches. Fig. 284 shows the most widespread designs of discs. Holes, slots and cuts in the discs make for better

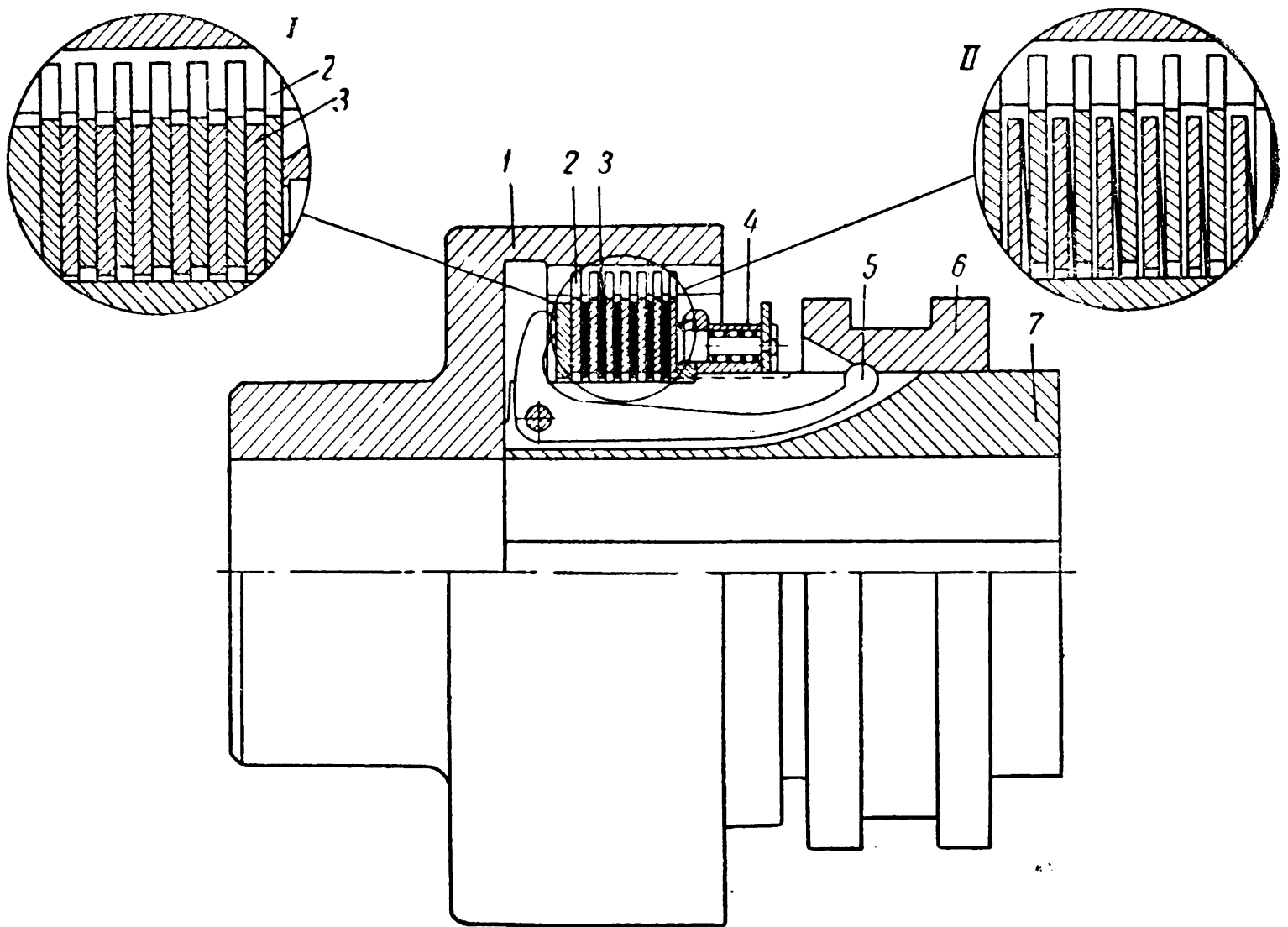


Fig. 283

lubrication and cooling, reduce warping of heated discs and allow a smoother engagement. For a clutch which is not frequently engaged and operates under light conditions the discs are made from steel and are flat in form (1). Clutches with frequent and continuous slipping employ discs with powder-metal facings and radial cuts (2).

The spiral groove on the discs is intended to ensure their rapid cooling in a disengaged clutch and to facilitate the expulsion of grease on engagement (3, 4 and 5). To reduce warping, the discs are provided with radial cuts (3). The discs transmit torque by splines provided on the external (1, 2 and 4) or internal (5) circumference. These splines enter spaces on the external or internal clutch halves.

Since the discs are thin these joints resist very heavy loads.

*Electromagnetic clutches.* The term “electromagnetic” is usually applied to those friction clutches in which the friction surfaces are compressed by the force of attraction of an electromagnet (solenoid) forming an integral part of the clutch.

Although in principle magnetic clutches with friction surfaces of any form are possible (and actually exist), only disc electromagnetic clutches have been widely used.

Some typical designs of electromagnetic clutches are shown in Fig. 285.

The main components of these clutches are an electromagnetic system comprising the electromagnet frame, winding and armature and a set of friction surfaces—friction discs. Direct current is fed to the winding, which is located in a circular groove on the frame, by two rings with brushes sliding over them. As the current flows across the winding the armature is attracted to the frame and the friction surfaces are drawn together. The maximum moment of friction of the clutch can be readily adjusted by varying

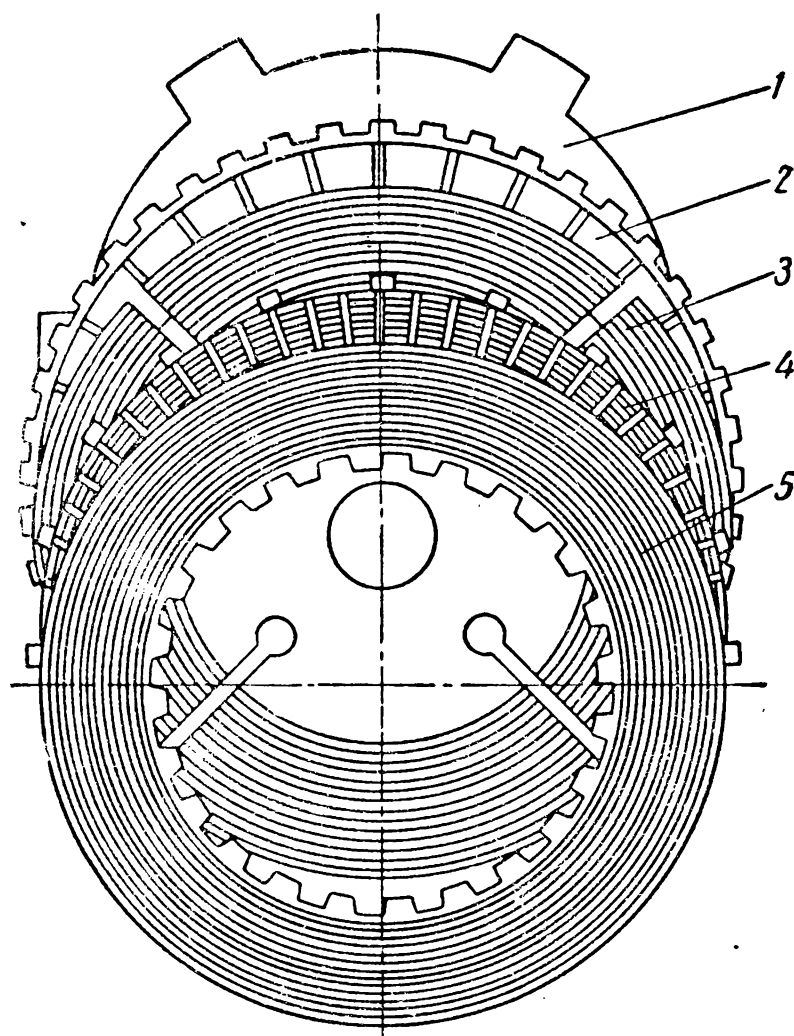


Fig. 284

the field current. When the current is switched off the armature is drawn away by compression springs and the friction discs are released.

In the clutch shown in Fig. 285, *a*, the armature and one of the friction surfaces move in an axial direction and slide on an immobile hub. Since the axial shift of the armature required is not large, it can be obtained by utilising the elasticity of the disc connecting armature and hub. In this case the clutch will be considerably shorter and lighter, as can be seen from the comparison of Figs. 285, *a* and 285, *b*. When a clutch of a smaller diameter is required the multiple-disc clutch shown in Fig. 285, *c* is used.

*Tyre-pneumatic clutches*, an interesting modification of pneumatic clutches, in recent years have been widely used in heavy machine-building. They are provided with a tyre (tube) used in place of the cylinders and pistons employed in former designs of pneumatic clutch.

A radial tube-pneumatic clutch with shoes (Fig. 286) consists of rim 1, connected to the driving shaft, and tyre 2, with shoes on the side facing rim 3, which is connected to the driven shaft. The tyre is oval in cross-section. The inner part of the tyre is an elastic tube intended to retain compressed air in the clutch. The tube is enveloped by numerous rubber-impregnated cord plies and plies of the external tread. The tread is bonded to rim 1. Torque is

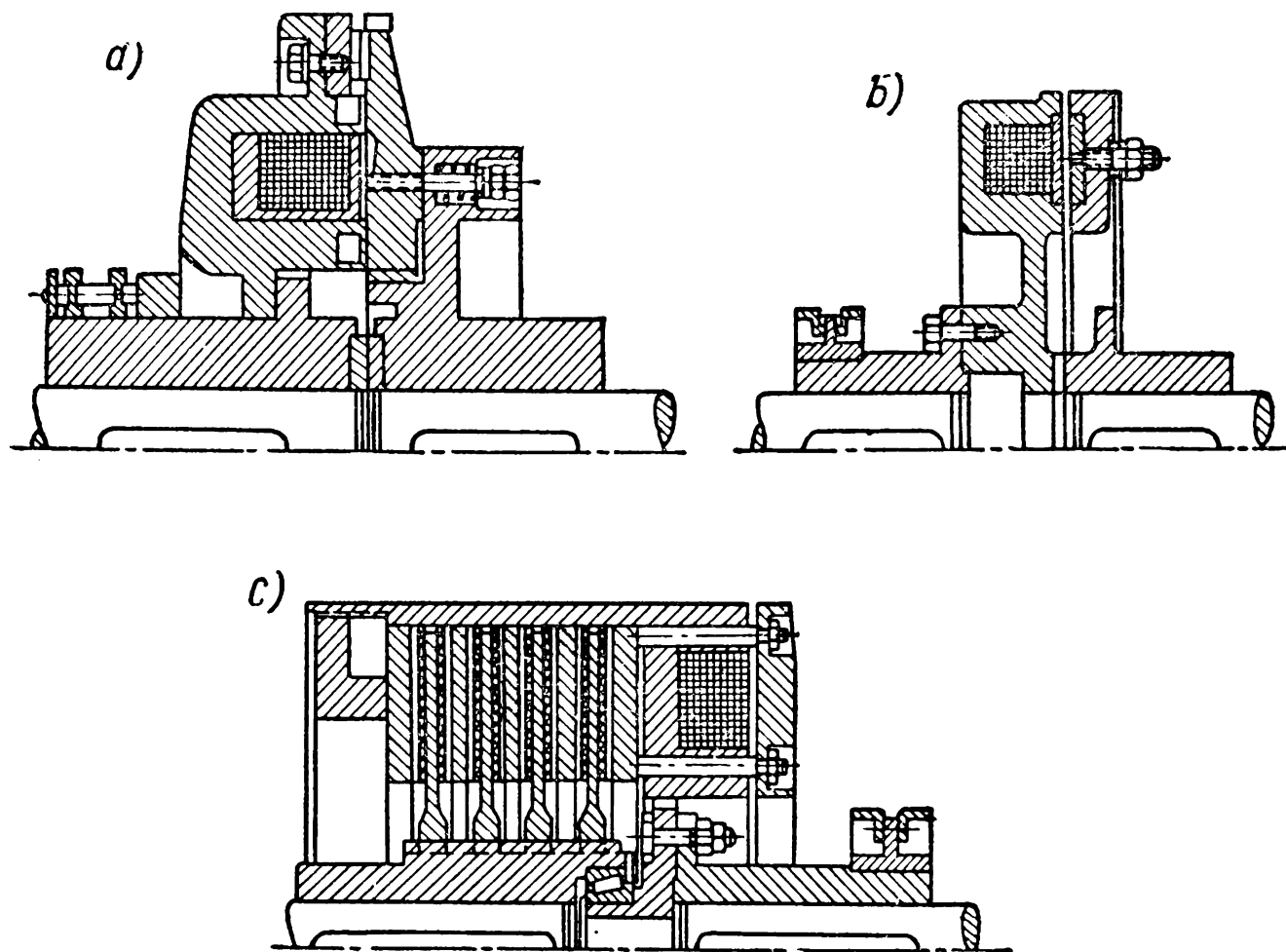


Fig. 285

transmitted by the strongest part of the tyre made from rubber-impregnated cord. The shoes are attached to the tyre by means of smooth pins. A friction strap is fastened to the shoe side which faces the driven shaft.

When compressed air is fed into the tyre through an elbow and nipple the tyre expands and presses the shoes to the rim (position *II* in Fig. 286). Friction between shoes and rim causes the driving shaft to engage with the driven shaft. When the clutch is released a clearance appears between the shoes and the rim (position *I* in Fig. 286).

The advantage of a tyre-pneumatic clutch of such design is not only its smooth engagement regulated by the supply of air to the tube. The elastic element provided in the clutch makes it possible, within certain limits, to compensate for the noncollinearity of the connected shafts. On the other hand, this clutch, as all other radi-

al-type clutches, requires the centrifugal effects on the shoes to be allowed for. In the clutch under consideration the shoes are forced outwards by centrifugal force which decreases the effort pressing them against the rim; but the same effect allows a more rapid separation of the friction surfaces on release. The tyre can be also arranged in a position in which it does not compress the driven rim but, conversely, expands within it.

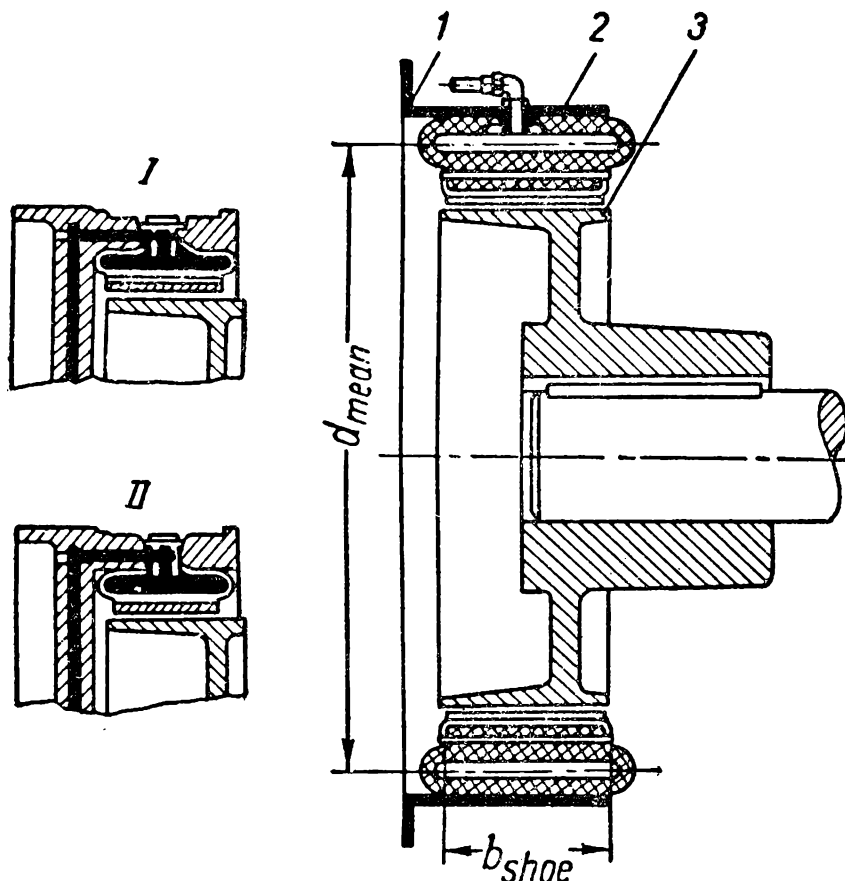


Fig. 286

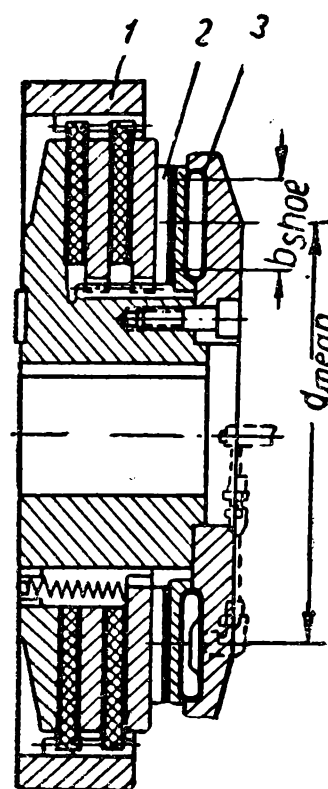


Fig. 287

In an axial tube-pneumatic tyre (Fig. 287) the tube of a corresponding form serves only to press the discs together\*.

*Calculation of friction clutches.* Friction clutches may be calculated in different ways. For clutches operating mainly under static conditions, calculation is limited to determining the proportions of the friction surfaces and the clutch operating device; if the clutch operates predominantly in dynamic conditions and is besides frequently engaged, it should also be checked for heating; for machines the time of whose working cycle is accurately regulated, the relation  $M_t = F(t)$  should be plotted which characterises the entire cycle of the clutch operation.

These calculations are beyond the scope of this book and form the subject of specialised courses on automation.

In our further exposition we shall deal with the calculations of

\* In Fig. 287: 1—external drum connected to the driven shaft, 2—pressure disc connected to the driving shaft, 3—tyre pressing the discs together.

friction surfaces and clutch operating devices which will be outlined separately. Such a method of presentation is justified by the fact that in principle any type of clutch operating device can be employed for one-type friction surface (as is shown in Fig. 281) and vice versa.

*Design load. Engagement factor.* The design torque ( $M_{td}$ ) which is used to select or calculate the clutch is found on the basis of the maximum torque of the motor ( $M_{mot \max}$ ) or the moment of static ( $M_{st}$ ) or dynamic ( $M_{dyn}$ ) resistance of the driven part of the transmission, i. e.,

$$\left. \begin{aligned} M_{td} &\geq M_{mot \max} \\ M_{td} &\geq M_{st} + M_{dyn} \end{aligned} \right\}.$$

The maximum moment of friction developed by the clutch is determined by the expression (445). The design torque  $M_{td}$  is connected with  $M_{fr}$  by the engagement factor

$$M_{fr} = \beta M_{td}. \quad (447)$$

The engagement factor  $\beta$  should guarantee the operation of the clutch without slipping under occasional circumstances not calculated for in design—at intermittent overloads or when the coefficient of friction ( $f$ ) or the radius of friction ( $r_{mean}$ ) are decreased from the design values due to a changed nature of contact between the friction surfaces.

The magnitude  $\beta$  is usually taken equal to:

for metal-cutting machine tools	$\beta = 1.25-1.5$
for automobiles	$\beta = 1.2-1.5$
for tractors	$\beta = 2-2.5$
for crane mechanisms	$\beta > 1.15$

Excessive values of  $\beta$  should be avoided since they cause increased dynamic loads on starting.

*Calculating the proportions of friction surfaces.* In connection with the relation (447) the main design formula (446) takes the form

$$M_{td} = \frac{1}{\beta} \sum_{i=1}^z f_i P_i r_{mean \ i} = \frac{1}{\beta} \sum_{i=1}^z f_i p_i S_{fr \ i} r_{mean \ i} \quad (448)$$

which shows that in determining the proportions and number of friction surfaces ( $S_{fr}, r_{mean}, z$ ) we should first select the values of  $f$ ,  $p$  and  $\beta$ . The values of  $f$  and  $p$  for various pairs of friction surfaces are given in Table 67. The usual values of  $\beta$  are given above. These values can be varied within a wide range.

Since  $f$ ,  $p$  and  $\beta$  are experimental values, their most reliable magnitudes can be obtained only from data concerning the work of

clutches of similar design and operated under conditions approximating those assigned for the designed clutch. If such data are available we can use the values  $M_{td}$ ,  $S_{fr}$  and  $r_{mean}$  for the existing and effectively operating clutch to find the value  $f \times p/\beta$  and then by the formula (448) calculate  $S_{fr}$ ,  $r_{mean}$  and  $z$  for a new clutch with the given value of  $M_{td}$ . In this case it is no longer necessary to determine separately the values  $f$ ,  $p$  and  $\beta$  which, as a rule, requires special research\*.

*Axial clutches. Disc clutches.* After selecting the values of  $f$ ,  $p$  and  $\beta$  as shown above we find the required value by the formula (448) assuming  $z=1$ :

$$S_{fr}r_{mean} = 2\pi b r_{mean}^2 = \frac{\beta M_{td}}{f \times p} \quad (449)$$

where  $b=r_{out}-r_{in}$  is the disc width.

The usual ratios between the proportions of friction discs are:  $\frac{r_{in}}{r_{out}} = 0.6-0.8$  and respectively

$$\frac{b}{r_{mean}} = \frac{r_{out}-r_{in}}{0.5(r_{out}+r_{in})} \approx 0.5-0.2.$$

A larger relative width ( $b > 0.5 r_{mean}$ ) should be avoided because of nonuniform wear and the heating and warping of wide discs.

In a multiple-disc clutch with  $z$  pairs of friction surfaces and an equal pressure  $p$  on them all the formula (448) takes the form

$$M_{td} = \frac{f}{\beta} z P r_{mean} = \frac{f p}{\beta} z S_{fr} r_{mean} = 2\pi \frac{f p}{\beta} z b r_{mean}^2. \quad (450)$$

The condition of constancy of pressure  $p$ , assumed to simplify the formula (450), for clutches engaged under load does not reflect the actual facts, for it disregards the friction of the discs in the splines of the housing and shaft during engagement.

If the pressure on the first pair of friction surfaces nearest to the clutch operating device is  $P_1=P$  then on the second pair it will amount to  $P_2=P(1-2f \times f_1)$  and on the last pair  $P_z=P(1-2f \times f_1)^{z-1}$  where  $f_1$  is the coefficient of friction of the discs in the splines.

After summing up the pressure on all surfaces we shall obtain, instead of  $zP$  used in the equation (450), another expression

$$\left[ \frac{1-(1-2f \times f_1)^z}{2f \times f_1} \right] P < zP.$$

When the product of  $f$  and  $f_1$  and the number of discs  $z$  are small the value in the brackets approximates  $z$ . At large values of  $z$  the correction for friction of the discs in the spline spaces grows more noticeable. Consequently, when there are many discs the torque transmitted by the clutch does not grow in proportion to their number but more slowly.

---

\*For clutches of machine tools with steel discs in oil baths  $fp/\beta \approx 0.3-0.35$ ; for clutches with the friction combination of asbestos and steel without lubrication  $fp/\beta \approx 0.5$ .

Partly for this reason and also because the middle discs are poorly cooled when there are many of them, clutches engaged in motion seldom employ more than 10-13 discs\*.

*Cone clutches.* The relations between the friction surfaces of cone clutches can be assumed to be the same as for disc clutches. The formula (450) also holds for cone clutches if the pressure  $P$  is normal to the cone generatrix. It is connected with the axial force  $P_{ax}$  by the following relation

$$P_{ax} = P \times \sin \alpha. \quad (451)$$

When analysing the operation of a cone clutch more profoundly, we must take into consideration the fact that we deal here not with a plane but with a spatial wedge. As the clutch is engaged in motion the internal cone screws, as it were, into the external cone and is pressed against its surface with greater force than after engagement at rest. The required effort of engagement is accordingly greater in the first case than in the second. Besides, in both cases, the clutch is more easily engaged in motion than at rest. To prevent the internal cone from being excessively screwed into the external one during engagement the angle  $\alpha$  should not be below  $\sim 10^\circ$ : usually  $\alpha = 10-15^\circ$  to avoid a wedging action.

*Radial clutches.* For radial clutches with a constant unit pressure  $p$  over the entire surface the formula (450) takes the form

$$M_{td} = \frac{fp}{\beta} S_{fr} r_0 = 2\pi \frac{fp}{\beta} b r_0^2 \quad (452)$$

where  $r_0$  is the radius of the rim (friction surface);

$S_{fr} = 2\pi r_0 b$ —the area of the friction surface.

The width of rim  $b$  in these clutches is limited only by the stiffness of the drum.

*Heating of friction clutches.* The work spent on friction during engagement and disengagement is accompanied by wear and heating of the friction surfaces. As a first approximation we can assume that all work spent on friction is transformed into heat.

A complete picture of clutch heating determining the temperature at separate points can be obtained only through experimental research. This is due to the complex form of the clutch parts and an instantaneous nature of the heating process.

The following calculation can be used for a comparative evaluation of heating by some mean temperatures.

Since the clutch is engaged very quickly we can neglect the heat loss to the surrounding air during this time and assume that the heat of friction is expended during engagement only to heat the clutch. In this case the heat balance towards the end of the first engagement of the clutch will have the form:

$$\frac{A}{427} = c \times G (\vartheta_1 - \vartheta_{air}) \text{ Cal}$$

---

\* Slipping clutches compressed when the discs are immobile may have more friction surfaces.



where  $A$  is the work expended on friction during engagement in kgm;  
 $c$ —the specific heat capacity of the material of the clutch parts being heated in Cal/kg  $\times$  degrees (for steel and cast iron  $c \approx 0.12$ );  
 $G$ —the weight of these parts in kg;  
 $\vartheta_1$ —the temperature of the clutch by the end of the first engagement in  $^{\circ}\text{C}$ ;  
 $\vartheta_{air}$ —the temperature of the surrounding air in  $^{\circ}\text{C}$ .  
 It follows from the last equation that the temperature at the end of the first engagement is

$$\vartheta_1 = \vartheta_{air} + \frac{A}{427 \times c \times G} = \vartheta_{air} + \frac{A}{427 \times 0.12 \times G} = \vartheta_{air} + 0.02 \frac{A}{G}.$$

During operation the clutch cools, because it gives up heat to the surrounding air; during the time  $dt$  the heat loss is

$$dQ = \alpha S_0 (\vartheta_1 - \vartheta_{air}) dt \text{ Cal}$$

where  $\alpha$  is the heat loss factor in Cal/m<sup>2</sup>  $\times$  hr  $\times$  degrees assumed to be constant:  $\alpha = 10$ -20 depending on the velocity of clutch rotation;

$S_0$ —the cooled surface in m<sup>2</sup>.

Continuing this reasoning we arrive at the conclusion that after a sufficiently large number ( $n \rightarrow \infty$ ) of engagements the temperature of the clutch will reach the value

$$\vartheta_{\infty} = \vartheta_{air} + 0.02 \frac{A}{8\alpha S_0 t} \quad (453)$$

where, in addition to the above symbols,  $t$  is the time between two consecutive engagements of the clutch.

When comparing clutches of similar design operating in similar conditions, only the values  $A$  and  $S_0$  turn out to be variable in the latter formula.

Therefore, if the relations  $A/S_0 = k_0$  are the same in the existing clutch and the clutch being designed, we can assume that the temperatures to which these clutches will be heated will be also the same. Assuming further the cooled surface  $S_0$  to be proportional to the area of the friction surfaces  $\Sigma S_{fr}$ , we obtain the empirical factor which is frequently used in calculating practice

$$k'_0 = \frac{A}{\Sigma S_{fr}}. \quad (454)$$

To allow for the intensity of the clutch operation we introduce the product of  $A$  and  $n_1$ , where  $n_1$  is the average number of the clutch engagements per hour, into the numerator of the expression for  $k'_0$ , instead of  $A$ , which is the work expended on friction at a single engagement of the clutch.

Then

$$k''_0 = \frac{An_1}{\Sigma S_{fr}} \text{ kgm/hr} \times \text{cm}^2 \quad \text{or} \quad k''_0 = \frac{An_1}{427 \times \Sigma S_{fr}} \text{ Cal/hr} \times \text{cm}^2.$$

The following values of  $k''_0$  are permissible for disc clutches:

Lubricated steel discs:  $k''_0 = 0.2$ -0.5 Cal/hr  $\times$  cm<sup>2</sup>, depending on the amount of oil; when the disc surfaces are cooled by forcing the oil through:  $k''_0 = 1.0$ -2.0 Cal/hr  $\times$  cm<sup>2</sup> depending on the disc design; when the discs operate dry:  $k''_0 = 0.2$ -0.3 Cal/hr  $\times$  cm<sup>2</sup>.

*Calculation of clutch operating devices.* The initial values for calculating clutch operating devices are, on the one hand, the required

unit pressure  $p$  or the total pressure  $P = p \times S_{fr}$  on the friction surfaces and, on the other, the available effort  $Q$  on the lever, pedal and electromagnet armature or the pressure  $q$  in the air or hydraulic system. Besides these efforts, the initial values also include the required and available travel.

Other important parameters for the comparative evaluation and adjustment of clutch operating devices are the velocity ratios:

$$\text{power } i_p = \frac{P}{Q} \text{ and kinematic } i_k = \frac{\lambda_q}{\lambda_p} \quad (455)$$

where  $\lambda_q$  is the travel of the clutch lever or pedal;

$\lambda_p$ —the travel of the last link of the device taking the pressure  $P$ .

Methods of calculation depend on the type of the operating device. For lever electromagnetic and pneumatic operating devices they are considered below.

*Lever clutch operating device.* The clutch is engaged by shifting a bushing (Fig. 288). Pressure on the discs (or on friction surfaces of another form) is transmitted through angle levers. In the extreme engaged position the ends of the long arms of these levers shift from the conical surface of the bushing onto the cylindrical surface. In this case the efforts compressing the discs are confined directly in the device and the controls connected to the bushing are relieved. In devices employing such locking the operating efforts are determined by the rigidity of the elements. This is a very important feature.

The total travel  $\lambda_{b0}$  of the engaging bushing is made up of the travel (1-2 mm) necessary to take up clearance in the joints, the travel  $\lambda_{b1}$  to take up clearance between the discs, the travel  $\lambda_{b2}$  to compress the discs due to the deformation of all parts subjected to the action of the pressure force and the locking travel (3-4 mm) during which the levers pass from the conical surface of the bushing onto the cylindrical surface. Thus,

$$\lambda_{b0} = \lambda_{b1} + \lambda_{b2} + (4-6) \text{ mm.} \quad (456)$$

The values of  $\lambda_{b1}$  and  $\lambda_{b2}$  are found from the formulae

$$\lambda_{b1} = z\Delta \frac{b}{h} \cot \theta = z\Delta i_k, \quad \lambda_{b2} = \frac{P}{c} i_k \quad (457)$$

where  $z$  is the number of pairs of the friction surfaces;

$i_k = b/n \cot \theta$ —the kinematic ratio—the ratio between the travel of the bushing and the operating device ( $b$ ,  $h$ ,  $\theta$  are shown in Fig. 288);

$c$ —the rigidity factor of the clutch operating device.

The relative position of the parts at which the required pressure force  $P$  is obtained at the end of the travel  $\lambda_{b3}$  is attained by adjusting

the clutch operating device. This adjustment is also necessary to regain the required position as the friction discs get worn. The higher the rigidity  $c$  the more frequently the adjustment must be carried out.

The value of the factor  $c$  depends on the design of the clutch operating device and the proportions of its parts and is found experimentally. Thus, for example, for the clutches employed in Soviet ЧТЗ and КД-35 tractors the mean value of  $c$  is about 4,700 kg/mm.

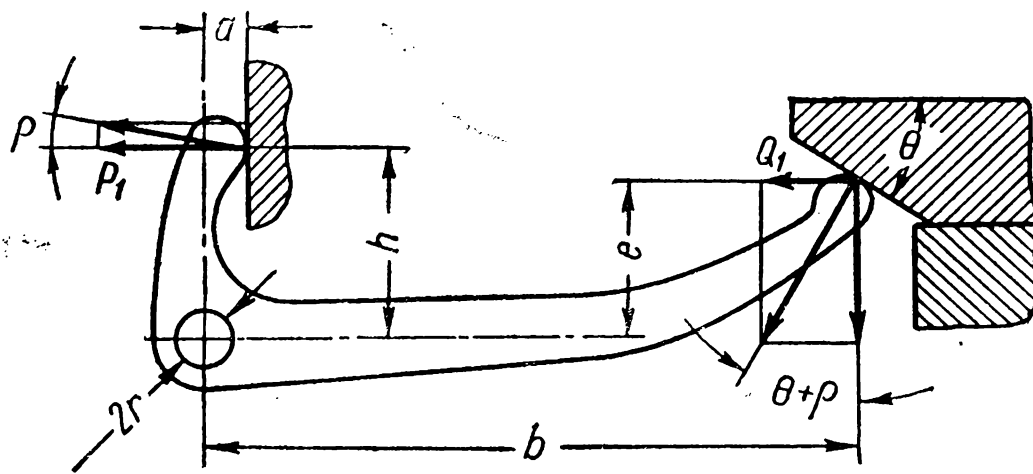


Fig. 288

For a preliminary calculation of the value  $c$  it is sufficient to take one part, the least rigid, ignoring the elasticity of the others. Thus, in the mechanism shown in Fig. 288 we can confine ourselves to the flexural rigidity of the lever arm  $b$ .

The efforts  $Q_1$  and  $P_1$ , acting from the side of the bushing and discs on one lever, if their number is  $n$  and the load is distributed evenly among them, will obviously be  $n$  times weaker than the corresponding total efforts  $Q = nQ_1$  and  $P = nP_1$ .

The ratio between  $Q_1$  and  $P_1$  is determined by the equation of equilibrium of momenta of all forces relative to the lever axis (Fig. 288).

$$Q_1 b \cot(\theta + \rho) - Q_1 e - Q_1 r f - P_1 h - P_1 a \tan \rho - P_1 r f = 0.*$$

From this at  $f = \tan \rho$  (coefficient of friction)

$$\frac{P_1}{Q_1} = \frac{b \cot(\theta + \rho) - e - r f}{h + (a + r) f} = \frac{P}{Q} = i_p \quad (458)$$

where  $i_p$  is the power velocity ratio of the clutch operating device.

\* This expression is true for uniform load distribution between the levers when the vertical components of the forces acting on the bushing are mutually equalised.

If this condition accepted in the design diagram is violated (for example, as a result of poor manufacture or careless adjustment) the force  $Q$  necessary to shift the bushing considerably increases due to additional friction between the bushing and the shaft.

The value of  $i_p$  changes in the process of engagement since the arms  $a, b, h, e$  and the pressure angle  $\theta$  change also. The design value is usually the extreme position which precedes the shift from the conical surface of the bushing to the cylindrical surface. These surfaces are connected by a smooth round-off.

*Electromagnetic clutch operating devices.* Electromagnetic clutches usually employ horseshoe electromagnets. The force of attraction  $Q$  of such an electromagnet is expressed by the well-known formula

$$Q = \left( \frac{B}{5,000} \right)^2 S_p \text{ kg} \quad (459)$$

where  $B$  is the magnetic induction in Gausses and  $S_p$  the area of the poles in  $\text{cm}^2$ .

When  $B$  equals 10,000 Gausses as is usual for soft annealed steel the unit force of attraction (the force per  $1 \text{ cm}^2$  of the area of the poles) is equal to

$$q = \frac{Q}{S_p} = \left( \frac{10,000}{5,000} \right)^2 = 4 \text{ kg/cm}^2. \quad (460)$$

From the formulae (459) or (460) we can find, using the known  $Q$ , the area of the poles  $S_p$  and specify the proportions of the electromagnet frame providing for a circular groove for the winding.

Subsequent calculations are reduced to determining the number of ampereturns to create the required magnetic flux, and then to determining the wire diameter and the number of the winding coils and to checking the winding for heating. The details of such calculations are outlined in special courses dealing with electrical engineering. Here we shall confine ourselves only to one remark.

The force of the electromagnetic attraction largely depends on the air gap  $\delta$  between the armature and the poles of the electromagnet. All other conditions being equal,  $Q=1/\delta^2$ , i. e., the force of the electromagnetic attraction changes in inverse proportion to the square of the magnitude of the air gap.

As the clutch is engaged, the armature approaches the poles, the gap decreases from  $\delta'_{\max}$  to  $\delta'_{\min}$  and the force of attraction grows from  $Q_{\min}$  to  $Q_{\max}$ . Since the force  $Q$  is variable, it should be checked in at least two positions: at the initial moment the force  $Q_{\min}$  should be larger than the sum of all resistance offered to the travel of the armature; in an engaged position the force  $Q_{\max}$  should be sufficient to deform the pressure springs and create the necessary moment of friction.

*Tyre-pneumatic clutch operating devices.* The total force developed by the tyre is determined by the pressure of the compressed air and the size of the tube

$$Q = (q - \Delta q) S_t \text{ kg} \quad (46)$$

where  $S_t$  is the active area of the tube in  $\text{cm}^2$ ;

$q$ —the pressure of the compressed air in the tube in  $\text{kg}/\text{cm}^2$ ;

$\Delta q$ —the pressure expended on the deformation of the tyre sides in  $\text{kg}/\text{cm}^2$ .

Usually  $q=6-8 \text{ kg}/\text{cm}^2$ . The magnitude of  $\Delta q$  is determined experimentally. The Soviet Urals Plant of Heavy Machine-Building specifies  $\Delta q$  to be about  $0.5 \text{ kg}/\text{cm}^2$ .

The active area of the tube in the tyre-pneumatic clutches shown in Figs 286 and 287 can be found from the formula

$$S_t = \pi d_t b_t \text{ cm}^2$$

where  $d_t$  and  $b_t$  are the mean diameter and width of the tube in cm.

In radial clutches during the transfer from the efforts developed by the tyre to the pressure force of the friction surfaces, the effect of centrifugal force on the shoes and the tyre should always be taken into account. Depending on the clutch design the centrifugal force  $P_c$  increases or decreases the pressure on the friction surfaces. For the clutch shown in Fig. 286  $Q \geq P + P_c$ .

**Jaw and Toothed Clutches.** A jaw clutch consists of two halves, moving and fixed, with jaws on their ends. The fixed half is rigidly fixed on one shaft while the other (which moves in an axial direction) is fitted on keys or splines of the second shaft. The shafts are connected by engaging the jaws of both halves together. The clutch is operated by hand, tractive electromagnet or pneumatic or hydraulic means acting through levers, fork and sprags on the moving half. To engage or disengage a jaw clutch under load (see below) high velocity over a short distance is required. In some cases use is made for this purpose of the tension of a preloaded spring, which is released at the required moment.

A tooth clutch comprises two pinions, one with external and the other with internal teeth. Both pinions have the same number of teeth. Externally, toothed clutches differ from jaw clutches by the location of the meshing elements (on the cylindrical surface and not on the ends of the halves) and by their form (involute teeth instead of jaws of any form). In our further exposition we shall call both types jaw clutches for brevity.

Jaw clutches are superior to friction clutches in that they ensure exact (without slipping) equality in the angular velocities of the connected shafts, have small proportions, are simpler in design and cost less. A material disadvantage of jaw clutches is that they can be engaged and disengaged only at low peripheral velocities and, as far as possible, under small loads. The essence of this limitation will be clear from the analysis of the processes of engagement and disengagement.

**Clutch engagement.** To engage a jaw clutch the lugs of one half should be opposite the sockets of the other. The probability of the halves being located on stopped shafts precisely in this position is equal to the relation of the clearance between the jaws  $\delta$  to their pitch  $t$  (see Fig. 289)  $B_{eng} = \delta/t$ .

Depending on the form and size of the jaws the value  $B_{eng}$  changes within  $0 < B_{eng} < 1$ . If the sockets and lugs fail to match they are brought into alignment by repeatedly starting the driving shaft. Within the arc  $\delta$  complete matching is obtained by turning the shafts relative to each other by the engagement force applied to the moving half.

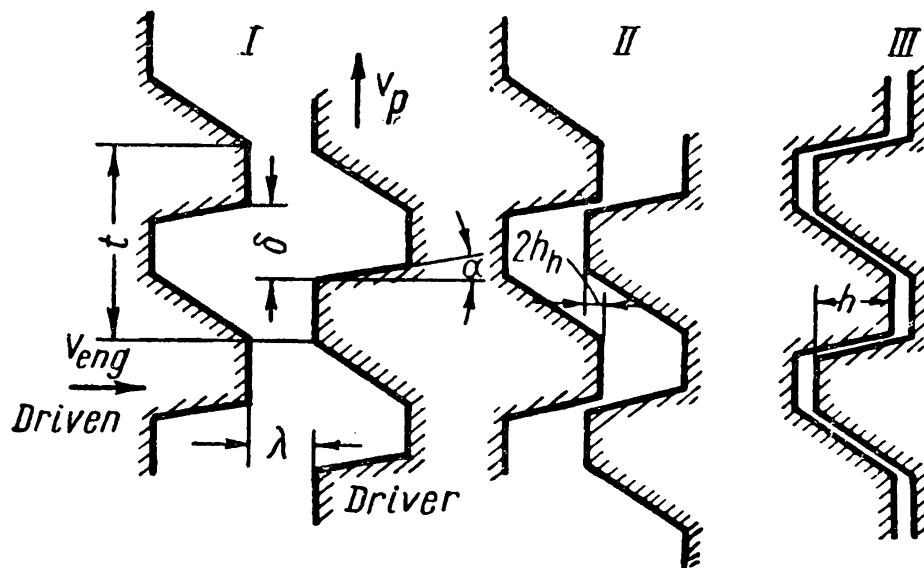


Fig. 289

When the clutch is engaged in motion the possibility of the jaws being engaged is determined not only by the magnitude of  $B_{eng}$  but also by the ratio of the relative velocities of the clutch halves—the peripheral  $v_p$  and the axial  $v_{eng}$ . The limit ratio between these velocities at which the clutch can still be engaged is determined from the condition

$$\frac{\delta}{v_p} = \frac{2h_h}{v_{eng}}. \quad (462)$$

Here, in addition to the symbols given above,  $h_h$  is the height of the jaw head (smaller than its total height  $h_h < h$ ) sufficient for a reliable fastening of the shaft at the beginning of engagement.

The expression (462) means that during the time  $\delta/v_p$  when the halves turn relative to each other by  $\delta$  the moving half should travel the length  $2h_h$ . We use the equality (462) to find the minimum value of the velocity  $v_{eng}$  at which the clutch can still be engaged in motion

$$v_{eng} = v_p \frac{2h_h}{\delta}. \quad (463)$$

When a half moves with constant acceleration over the length  $\lambda + 2h_h$  (Fig. 289) and its velocity at the end of the engagement period is  $v_{eng}$  we find the acceleration

$$j_{eng} = \frac{v_{eng}^2}{2(\lambda + 2h_h)} = v_p^2 \left( \frac{h_h}{\delta} \right)^2 \frac{2}{\lambda + 2h_h}. \quad (464)$$

The initial force of engagement is

$$Q_{j\,eng} = m j_{eng} = m v_p^2 \left( \frac{h_h}{\delta} \right)^2 \frac{2}{\lambda + 2h_h}. \quad (465)$$

Here  $m$  is the mass of the moving half and the parts of the clutch operating device connected with it reduced to the shaft axis.

To continue engagement (up to the full height of the jaw) it is necessary to overcome the friction between the jaws of the halves and the moving half on the splines or keys of the shaft

$$Q_{j\text{eng}} = f' \frac{2M_{\text{eng}}}{d_{sh}} + \frac{2M_{\text{eng}}}{d_{\text{mean}}} \tan(\alpha + \varrho) \quad (466)$$

where  $M_{\text{eng}}$  is the torque at the moment the clutch in motion is engaged;

$f'$ —the coefficient of friction of the half on the shaft;

$d_{sh}$ —the shaft diameter;

$d_{\text{mean}}$ —the mean diameter of the clutch on the jaws;

$\alpha$ —the angle of inclination of the jaw working face;

$\varrho$ —angle of friction on the jaws.

Taking the values  $m = 1 \text{ kg} \times \text{sec}^2/\text{m}$ ,  $\frac{\delta}{h_h} \approx 8$ ,  $\lambda + 2h_h \approx 8 \times 10^{-3} \text{ m}$  usual for jaw clutches of machine tools and assuming  $Q_{j\text{eng}} = 4 \text{ kg}$  we can get from the formula (465)

$$v_p = \frac{\delta}{h_h} \sqrt{\frac{Q_{j\text{eng}}(\lambda + 2h_h)}{2 \times m}} = 8 \sqrt{\frac{4 \times 8 \times 10^{-3}}{2 \times 1}} \approx 1 \text{ m/sec.}$$

The peripheral velocity  $v_p = 1 \text{ m/sec}$  is usually recommended as the maximum velocity when jaw clutches of machine tools are engaged manually.

*Clutch disengagement.* A jaw clutch should be disengaged in such a manner that the jaws are separated at a point sufficiently removed from their tops and that, once disengaged, there are no repeated collisions of the jaws. These may be caused by the relative rotation of shafts with the clutch halves at velocities equal to the sum of the peripheral velocity of rotation  $v$ , and also the velocities  $v_1$  and  $v_2$  of the torsional oscillations of the shafts which, after disengagement, turn towards each other.

The condition for the absence of repeated shocks is

$$v_{dis} \tan \alpha \geq v_1 + v_2 + v. \quad (467)$$

In the most unfavourable case

$$\left. \begin{aligned} v &= v_{\text{max}} = v_p \\ v_1 &= v_{1\text{max}} = r_{\text{mean}} \times \varphi_1 \times \omega_1 \\ v_2 &= v_{2\text{max}} = r_{\text{mean}} \times \varphi_2 \times \omega_2 \end{aligned} \right\} \quad (468)$$

where  $\omega_1, \omega_2$  are the rotational frequencies of the system oscillations connected respectively with the driver and driven halves;

$\varphi_1, \varphi_2$ —the angles through which the halves are turned by the transmitted torque before disengagement;

$r_{\text{mean}}$ —the mean radius of the clutch on the jaws;

$v_p$ —the peripheral velocity of rotation of the driver half over the radius  $r_{\text{mean}}$ .

Substituting in (467) the values of  $v, v_1$  and  $v_2$  from the relation (468) we get

$$v_{dis} \geq \frac{1}{\tan \alpha} [(\varphi_1 \omega_1 + \varphi_2 \omega_2) r_{\text{mean}} + v_p]. \quad (469)$$

The velocity  $v_{dis}$  should be imparted to the moving half at a point removed by  $h - 2h_h$  from the jaw base.

In this case the required acceleration is

$$i_{dis} = \frac{v_{dis}^2}{2(h - 2h_h)} \quad (470)$$

The effort needed for disengagement is

$$Q_{dis} = Q_{j\ dis} + Q_{f\ dis} \quad (471)$$

where

$$Q_{j\ dis} = m \times i_{dis} \quad (472)$$

is the effort necessary to impart the required acceleration to the moving half and

$$Q_{f\ dis} = f' \frac{2M_{dis}}{d_{sh}} - \frac{2M_{dis}}{d_{mean}} \tan(\alpha - \varrho) \quad (473)$$

is the effort necessary to overcome the friction of the moving half on the keys or splines of the shaft and the friction between the jaws of the clutch halves.

It can be seen from the last equation that the clutch will disengage by itself if  $Q_{f\ dis} < 0$ , i.e., when

$$f' \frac{d_{mean}}{d_{sh}} < \tan(\alpha - \varrho) \quad \text{or} \quad \tan \alpha > f' \left( 1 + \frac{d_{mean}}{d_{sh}} \right). \quad (474)$$

It is necessary to note at this juncture that jaw clutches, even when the angle of the front edge is  $\alpha = 0$ , still tend towards self-disengagement. This is explained by the fact that, as a result of elastic deformations of the jaws, shafts and bearings and also of the displacement of the halves due to manufacturing inaccuracies and wear of the conjugate surfaces, there arises a certain axial component tending to disengage the jaws and the teeth. Self-disengagement is completely eliminated in jaws where  $\alpha < 0$  (Fig. 290, *b*).

*Design of jaw clutches.* The analysis of the processes of engagement and disengagement of jaw clutches shows how the form and size of the meshing elements affect the clutch operation. The formulae we have obtained make it possible to select in each concrete case the most rational profile of the jaws and teeth to conform to the assigned conditions of operation.

Usually the profiles shown in Fig. 290 are used.

A recent development is that of clutches with involute teeth, which in the transmissions of automobiles and tractors have completely ousted jaw clutches. This is due to the fact that in manufacture they require much simpler production methods and tools.

To facilitate the engagement of toothed clutches it is common practice, in addition to rounding (pointing) the tooth tops, to shorten every other tooth on one half and remove it altogether on the other (Fig. 290, *d*). Without increasing backlash in the clutch this method makes the process of engagement much easier: the probability of engagement ( $B_{eng}$ ) increases and the efforts required to engage a clutch in motion ( $Q_{eng}$ ) are decreased.

In jaws with the profile shown in Fig. 290, *b* as a result of the choice of the angle  $\alpha < 0$  a force is created preventing self-disengagement of



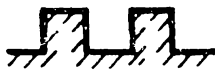
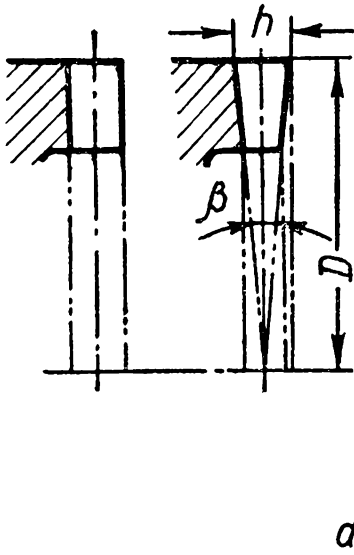



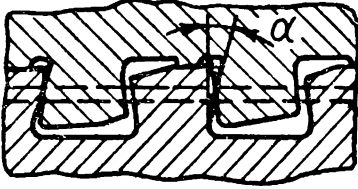
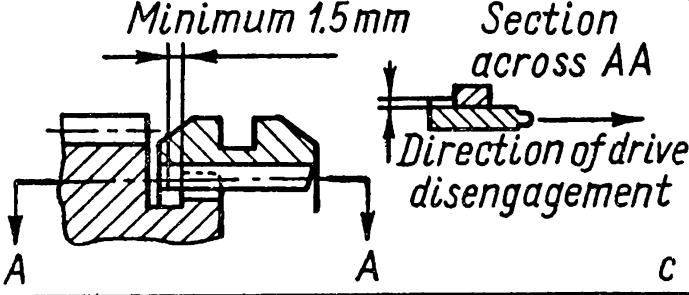
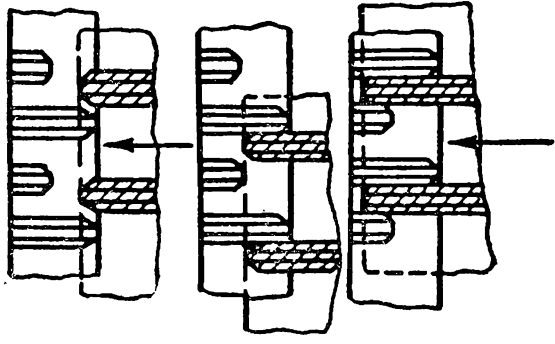
Jaw			Profile
			Square
			Trapezoidal symmetrical
			Tapered
		a	Trapezoidal asymmetrical
		b	Trapezoidal self-locking (against self-disengagement)
Toothed		c	Self-locking (against self-disengagement)
		d	Clutch engaged by small effort

Fig. 290

the clutch. In toothed clutches the same result is obtained by a lock—a step which forms as a result of compression and wear of the tooth active profiles. For this purpose a groove is cut in one of the halves so that the tooth of this half will contact the tooth of the other at a distance of 1.5-2 mm from its edge, ignoring the zone of the tooth rounding (Fig. 290, c). It stands to reason that such self-locking profiles can be employed only in clutches which are disengaged unloaded.

For a satisfactory operation of jaw clutches their halves should be thoroughly machined and assembled to ensure contact between all conjugate jaws. For a correct engagement of the jaws the moving half should be mounted correctly on the shaft. This is ensured by providing for an adequate length of the hub ( $l \geq 1.5 d_{sh}$ ) fitted onto the splined section of the shaft or on two diametrically opposite keys.

The working surfaces of the jaws and teeth and also of the hub of the moving half should have high hardness. For this reason, clutches engaged under load are made from steel 20X casehardened to  $R_C = 56-62$  and engaged at small velocities—from steel 40X induction hardened to  $R_C = 48-54$  or from steel 45 induction hardened to  $R_C = 35-54$ .

*The jaws are calculated for strength* on the basis of the force  $P_1$  transmitted by one jaw if the load  $M_{td}$  is spread uniformly between all  $z$  jaws.\*  $P_1$ , compressive stress  $p$  and bending stress  $\sigma_b$  are determined from the following formulae

$$P_1 = \frac{2M_{td}}{zd_{mean}}, \quad P = \frac{P_1}{F_1} \leq [\sigma]_c, \quad \sigma_b = \frac{P_1 h}{2W_1} \leq [\sigma]_b. \quad (475)$$

Here  $z$  is the number of jaws;

$F_1$ —the working area of one jaw in compression;

$h$ —the height of the jaw;

$W_1$ —the section modulus in bending of the jaw base.

Because of inevitable errors in machining and deformations under load, not all jaws of the clutch halves fit tightly and uniformly against each other; when there are many jaws some of them take no part at all in transmitting torque. For this reason reduced values of  $[\sigma]_c$  and  $[\sigma]_b$  have to be taken. For arbitrary compressive stress the following values are recommended:

- for clutches engaged at rest  $[\sigma]_c = 1,000-1,500$  kg/cm<sup>2</sup>;
- for clutches engaged in motion  $[\sigma]_c = 300-400$  kg/cm<sup>2</sup>.

These values refer to clutches in which the working edges of the jaws are casehardened.

The allowable stresses  $[\sigma]_b$  are assigned in conformity with the material of the clutches. When calculating according to dynamic torque during engagement and for clutches engaged at rest the values of  $[\sigma]_b$  are taken depending on the yield point with the safety margin of  $n \geq 1.5$ .

**Synchronising Devices for the Noiseless Engagement of Toothed Clutches.** Two shafts can be coupled by a toothed clutch easily

---

\* When the clutch halves are misaligned the load is taken only by two teeth in the plane of the maximum misalignment of the axes. Therefore, if it is not certain that the clutch has been thoroughly machined and assembled,  $z=2$  should be taken in calculations irrespective of the actual number of teeth. In the Soviet Union the rules for designing cranes even recommend  $z=1$ .

without shocks and noise only when their angular velocities are equal. Therefore, the process of the noiseless connection of shafts with different velocities can be imagined as consisting of two stages: during the first stage the velocities of the connected shafts are equalised and during the second stage the shafts are rigidly connected.

Devices for equalising (synchronising) the angular velocities of the connected shafts are called *synchronising devices*.

The existing designs of synchronising devices were developed for automobile transmissions where easy and noiseless engagement is especially important. This explains why synchronising devices are used predominantly in combination with toothed clutches, although, in principle, they can be adapted to operate also with jaw clutches.

Friction surfaces connected with toothed halves are the elements common to all types of synchronising devices. When the moving half shifts these friction surfaces are the first to come into contact. The friction between them quickly equalises the velocities of the connected shafts, after which a further axial movement of the half rigidly connects the shafts as in an ordinary toothed clutch. Widely used designs of synchronising devices differ mainly in the mode in which they coordinate the movements of the friction surfaces and the toothed halves so that the halves begin to engage only after the shaft velocities are equal.

As can be seen, a toothed clutch with a synchronising device combines the advantages of an ordinary friction clutch (the smooth equalisation of the velocities of the connected shafts) and a toothed clutch (rigid connection of the shafts, small clutch size). However, the application of these devices is limited. They can be used only to connect unloaded shafts with small flywheel masses, corresponding to the small proportions of the friction surfaces of the synchronising devices.

Fig. 291 shows by way of example a sketch of a simple "constant-pressure" synchronising device. Shaft 1 (driving) rotates with a certain velocity  $\omega_1$ . It is rigidly connected by a toothed clutch to the pinions 2 or 5. Let us examine the process of engagement of shaft 1 with pinion 5. At the moment preceding engagement, pinion 5 is immobile or rotates by inertia with the velocity  $\omega_5 \neq \omega_1$ . Hub 3 can move on the splines of shaft 1; half 4 with internal teeth can likewise shift both ways along the external teeth on hub 3. In the mean position half 4 is fixed relative to hub 3 by spring ball stops.

As half 4 shifts from its mean position to the right, it will carry with it, due to the presence of the stops, hub 3, until the conical friction surface of the latter comes to rest against the corresponding surface on the end of the toothed half integral with pinion 5 (diagram II in Fig. 291). At the same time, due to friction between the conical surfaces, forming a sort of a conical mesh, the velocities of shaft 1 and pinion 5 are equalised. Under further pressure hub 3 cannot move more to the right and half 4, after overcoming the resistance of the stops, will move further and engage with the toothed rim of half 5 (diagram III in Fig. 291).

Constant-pressure synchronising devices do not guarantee a completely smooth connection of shafts. When half 4 moves too fast engagement can occur before the velocities have been equalised and in this case will be accompanied by shocks of the teeth. Shock is completely eliminated in the so-called inertial

synchronising devices in which the movement of the clutch half actuates an inertial stop, which prevents the shafts from being connected until their velocities have been completely synchronised.

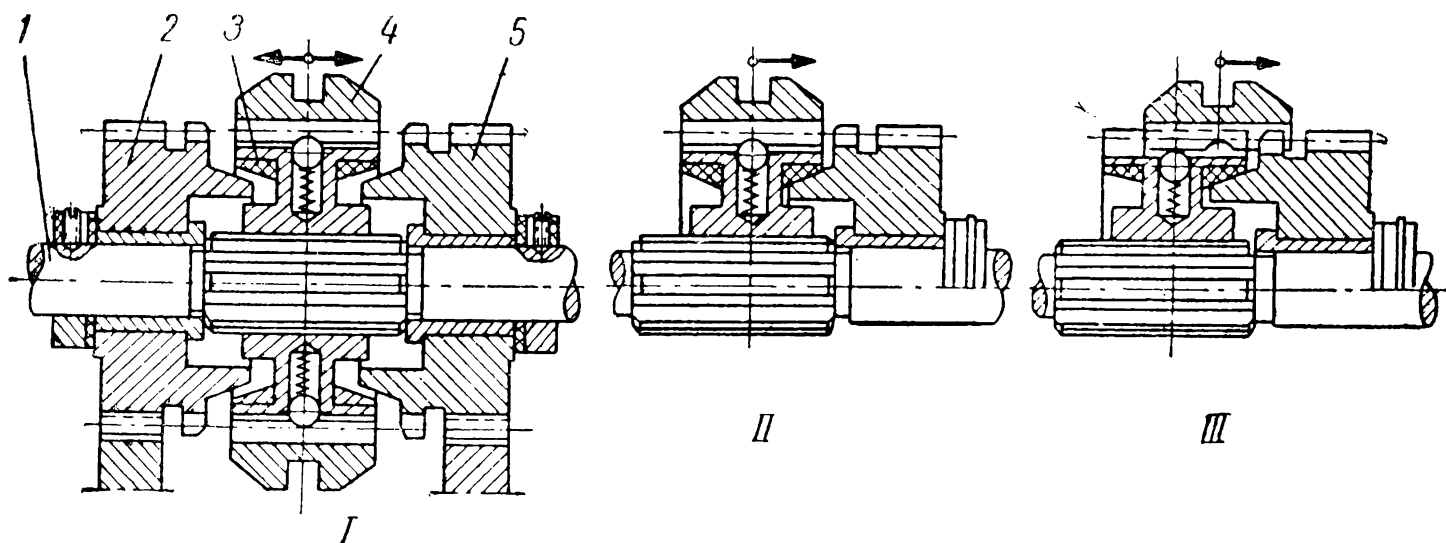


Fig. 291

**Electromagnetic Fluid and Powder Clutches.** The principle of operation of these clutches (also called magnetoemulsion clutches with a ferromagnetic filler), which began to be used in industry only in 1947-1948, is based on the ability of fluid and powder mixtures with moving ferromagnetic particles to change their structure in a magnetic field.

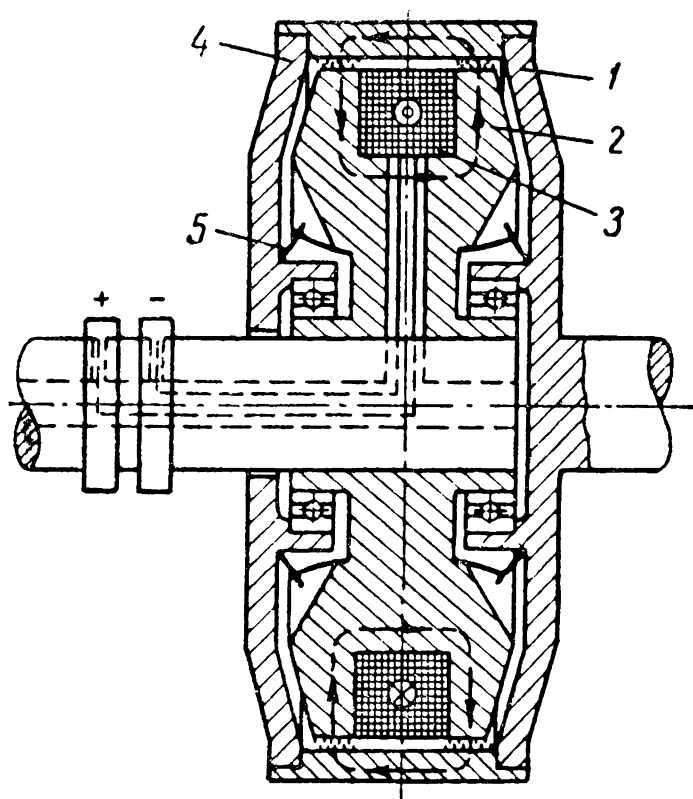


Fig. 292

The main components of such clutches are (Fig. 292): iron core 2 connected to the driving shaft; ring winding 3, with output leads connected to contact rings, placed in the core groove; housing 1, connected to the driven shaft, with a cylindrical rim surrounding the core with a small clearance (0.5-2 mm); mixture of iron powder (grain diameter 5-10 mc) with oil in fluid or with graphite in powder clutches, which fills the space between the core and rim 4; and seals

5. The iron-to-oil weight ratio is usually 5 : 1. With this ratio the magnetic permeability of the mixture is about eight times greater than that of air. Current fed across the clutch winding excites a magnetic field (the direction of flux is shown in Fig. 292 by arrows) under whose action the mixture turns into a jellylike substance with particles pressed against the surface of the poles (core) and rim with unit pressure  $q = (B/5,000)^2 \text{ kg/cm}^2$  [see formula (459)].

The torque transmitted by the clutch is

$$M_t = f q S r \text{ kg/cm} \quad (476)$$

where  $S$  is the working surface of the cylinder or disc taking part in transmitting the torque in  $\text{cm}^2$ ;

$r$ —the radius of the cylinder or the reduced radius of the clutch disc in cm;

$f$ —the cohesion factor.

For the above conditions experiments recommend  $f \approx 0.1-0.3$ .

In a deenergised clutch friction is due to the viscosity of the mixture.

A valuable feature of these clutches is the smooth velocity adjustment obtainable by varying the field current. In ordinary friction clutches continuous sliding causes rapid failure of the friction surfaces and should therefore be avoided. In this case, however, the specific conditions of engagement allow continuous sliding which is limited only by the maximum heating values. With the difference in the angular velocities of the driving and driven shafts ( $\omega_0 - \omega$ ) the power  $M(\omega_0 - \omega)$  determines the heat losses in the clutch. The allowable temperature of the clutch heating is determined by the heat endurance of the materials used and the heat expansion of the mixture.

The designs of fluid and powder clutches have not yet taken a final shape. Today many Soviet plants and institutions are seeking ways and means to perfect them. Some of the main difficulties in designing such clutches are outlined below.

In electromagnetic fluid clutches the fluid mixture sometimes tends to compress under the action of centrifugal forces in an operating clutch or due to sedimentation of the iron powder in a clutch which has been idle for a long time. Investigations show that radial accelerations below 60  $G$  ( $G$  is the gravity acceleration) affect the clutch operation negligibly; accelerations of the order of 120  $G$  compress the iron powder so much that the clutch cannot be controlled, for contact remains even in a deenergised clutch. Compression of the mixture is a fault primarily affecting disc clutches. In this respect cylindrical contact surfaces are much preferable because they almost completely eliminate the hazard of seizure. Sedimentation of the particles in an idle clutch can be reduced by selecting such mixtures in which the particles can remain in suspension for a long time.

Another complex problem is the provision of adequate sealing preventing the leakage of fluid mixture and keeping iron particles away from the bearings. This task has been solved by the use of rubber rings and magnetic traps in the form of horseshoe permanent magnets arranged between the rubber rings and the bearings.

In the course of operation the clutch "breathes". On heating some of the air in the clutch is forced out and on cooling, conversely, air with fresh oxygen and moisture is sucked in from outside. This intensifies the corrosion of the internal components of the clutch and the iron particles and oxydation and ageing of the heated oil. Several methods can be employed to slow down the ageing and one is the provision of adequate hermetic sealing.

Mainly fluid clutches were referred to above. Powder clutches (a mixture of iron and graphite powders) work less smoothly than fluid clutches but they allow much simpler sealing of the bearings.

POWER-CONTROLLED CLUTCHES

Power-controlled clutches include those which are engaged and disengaged automatically depending on a change in one of the following factors: torque (*slipping clutches*), direction of rotation (*overrunning or freewheeling clutches*) and velocity of rotation (*centrifugal clutches*). A general classification of power-controlled clutches is shown in Fig. 293.

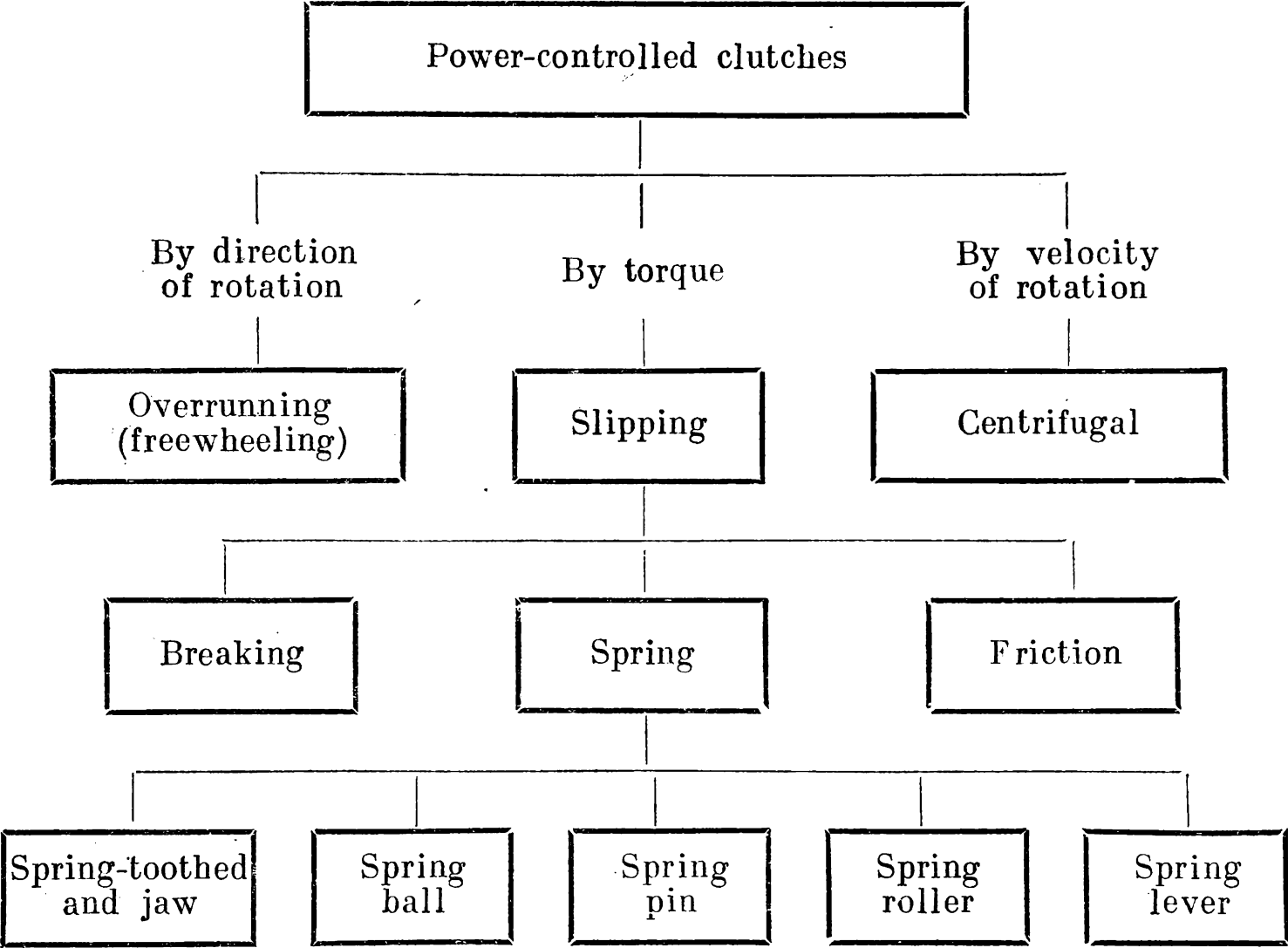


Fig. 293

It should be noted that the above classification is highly arbitrary. It originated historically when clutch control including automatic control was effected only by simple and purely mechanical means. Today, when electromagnetic, pneumatic and hydraulic devices are widely used in clutches, the possibilities of making clutch-control automatic by any of the parameters are practically limitless.

**Slipping Clutches.** Slipping clutches protect machines against overload. When the torque transmitted by such a clutch reaches

a definite predetermined value it operates, thereby preventing its further increase.

Slipping clutches combine the functions of two units: a) a *measuring unit* (dynamometer) subjected to the action of torque which compares it with the assigned maximum value and b) a *servo unit* which, at the moment of time determined by the measuring unit, prevents a further increase in load.

The designs of slipping clutches can be classified according to the main characteristics of each unit as follows:

1) depending on the kind of force utilised as a standard in the measuring unit: a) slipping clutches with a breaking element (use is made of the strength of a component); b) friction slipping clutches (use is made of the force of friction); c) spring slipping clutches (use is made of the elasticity of springs);

2) depending on the structural features of the main elements—slipping clutches: a) with a shear pin; b) with a tear bolts, etc.; friction slipping clutches: a) disc; b) cone, etc; spring slipping clutches: a) spring-toothed; b) jaw; c) pin; d) ball; e) roller; f) lever, etc;

3) depending on the mode of protection: a) slipping clutches breaking engagement; b) slipping clutches retaining engagement;

4) depending on the mode of reengagement: a) slipping clutches with automatic reengagement; b) slipping clutches with manual return; c) slipping clutches requiring replacement of the broken parts.

Slipping clutches should be reliable in operation. A faulty safety clutch is a useless, and sometimes a harmful, appendage to a machine. Lulling the attention of the operator it leads to the development of overloads. The accuracy of operation is directly related to the safety margin of the mechanisms protected by the clutch: the greater the accuracy of the clutch operation, the smaller the safety margin can be. When selecting a slipping clutch from among existing designs or creating new designs of such clutches we should first of all make sure that they satisfy these principal requirements.

Below we examine only some types of slipping clutches which are in especially widespread use.

*Slipping clutches with a shearing element* are the most simple devices for protection against overloads. When the load reaches its limit value of resistance to the pins shear or the bolts tear, etc., they break thus disengaging the clutch.

Typical slipping clutches with a shear pin and a tear bolt are shown in Figs 294\* and 295\*\*.

\* In a clutch with a shear pin (Fig. 294): 1—driving hub, 2—driven pinion, 3—standard parts of the shear pin, 4 and 5—bushings, 6—shear pin, 7—plug which is unscrewed to remove the fragments and replace the pin.

\*\* In a clutch with a tear bolt (Fig. 295): 1—pins secured in the driven half 5, 2—levers pressed to hub 4 of the driving shaft by tear bolt 3.



The design of these clutches should satisfy the following requirements: the failure of the pin (or bolt) should not damage other parts (for this purpose in the clutch shown in Fig. 294 shear pin 6 is placed in hardened bushings 4 and 5), for burrs there remains a circular clearance  $a$ ; the failing elements should be easily accessible for replacement and during operation their fragments should never

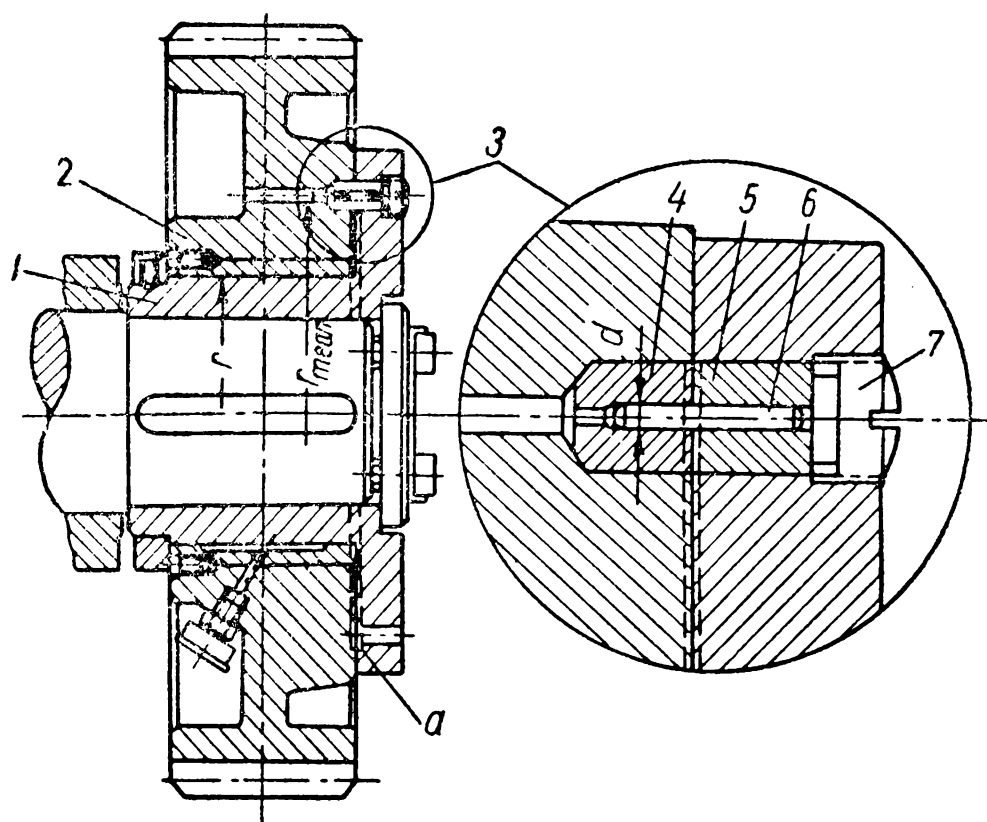


Fig. 294

fall out. To obtain greater uniformity of operation in slipping clutches the friction force should be reduced and the shearing elements designed with the same thoroughness as samples for testing materials (in principle, they are such materials).

Breaking pins and bolts are usually made from steel with  $\sigma_{ul}=60 \text{ kg/cm}^2$ . Bolts and pins are provided with grooves. The property of the material and the form of the groove serve one purpose—to make the rupture as brittle as possible with minimum remanent deformation. Besides, the groove in shear pins decreases burrs, which interfere with the removal of the fragments, and diminishes the effect of the clearance on the uniformity of operation of slipping clutches.

In a slipping clutch with one shear pin the equilibrium condition is

$$M_t - T \times r \times f' - T \times r_{mean} = 0$$

where  $r_{mean}$  is the mean radius of the pin shorn-off section in the clutch;

$r$ —the radius of the carrying surface to which the reaction from the force  $T$  is applied;

$f'$ —the reduced coefficient of friction on this surface.



Taking the usual values  $f' = f \times 4/\pi$ ,  $f = 0.2$ ,  $r/r_{mean} = 0.6$  and  $T = 0.75d^2\tau_{ul}$  (the load destroying the pin) we shall obtain the expression

$$M_t = 1.15 \times T r_{mean} = 0.86d^2 r_{mean} \tau_{ul} \quad (477)$$

which is used to find in the design calculations the proportions of the pin ( $d$ ) and the clutch ( $r_{mean}$ ) and in the revised calculations—the torque of the clutch operation  $M_t$ .

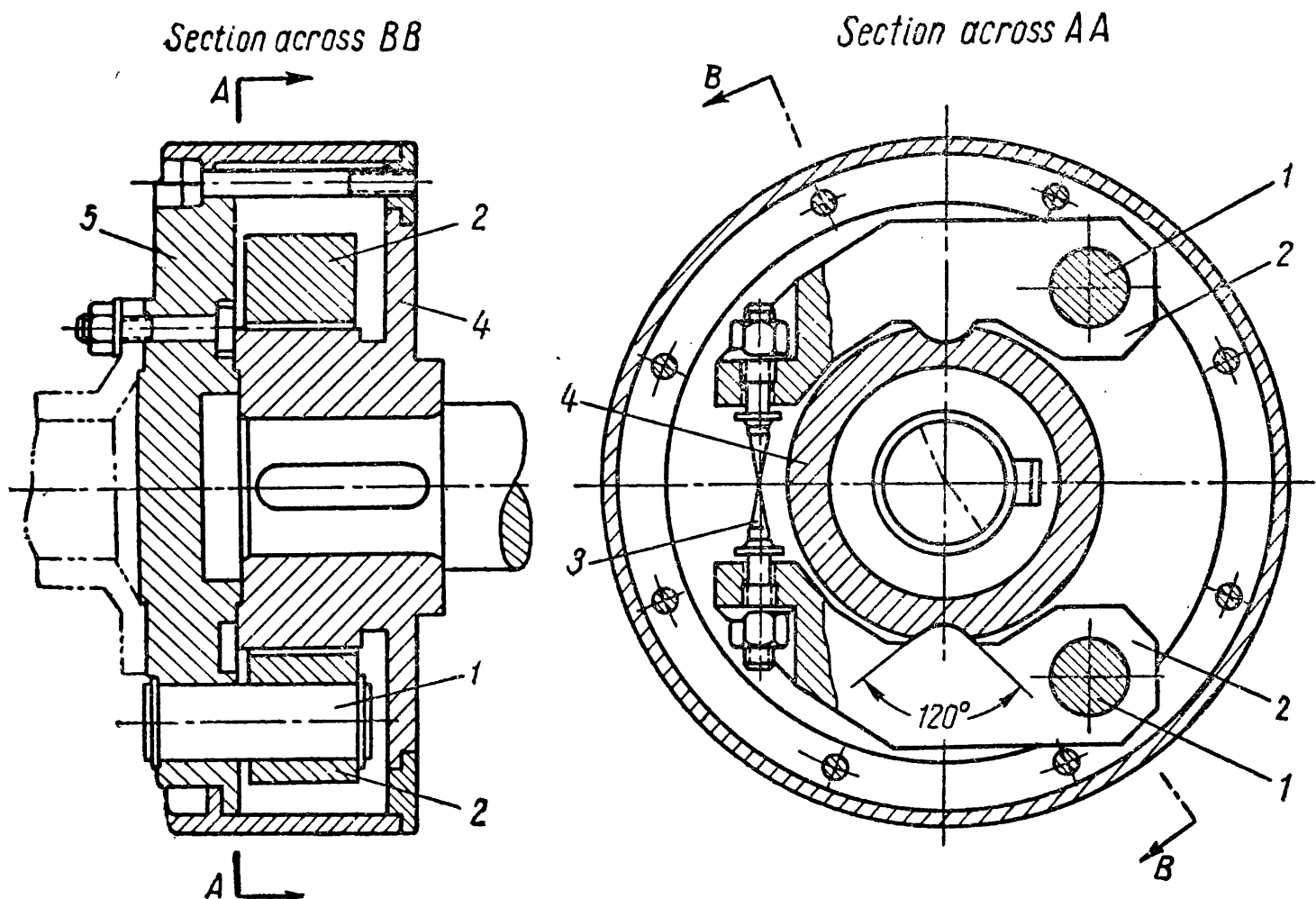


Fig. 295

*Friction slipping clutches*, the compressed surfaces of which slip after the external load has reached the limit value of the friction forces, are frequently used to protect various units against overload due to their simple design and dependability in operation.

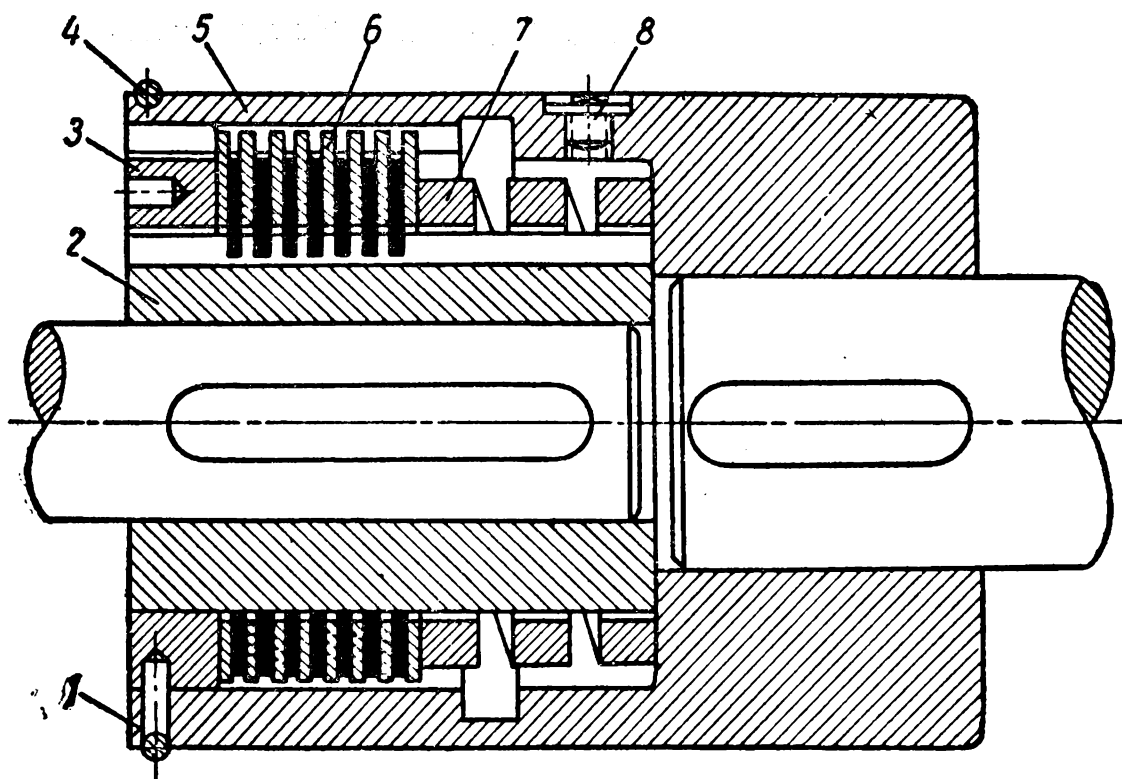
Fig. 296\* shows a multiple-disc clutch and Fig. 297\*\*—a cone friction clutch.

All that was said above on p. 500 concerning the design and calculation of the friction surfaces of friction clutches is also true for slipping clutches. As distinct from friction clutches, here more attention

\* In the clutch in Fig. 296: 1 and 2 are external and internal halves, 3—nut compressing the discs, 4—spring ring holding the nut in place, 5 and 6—discs, 7—spring, 8—lubrication plug.

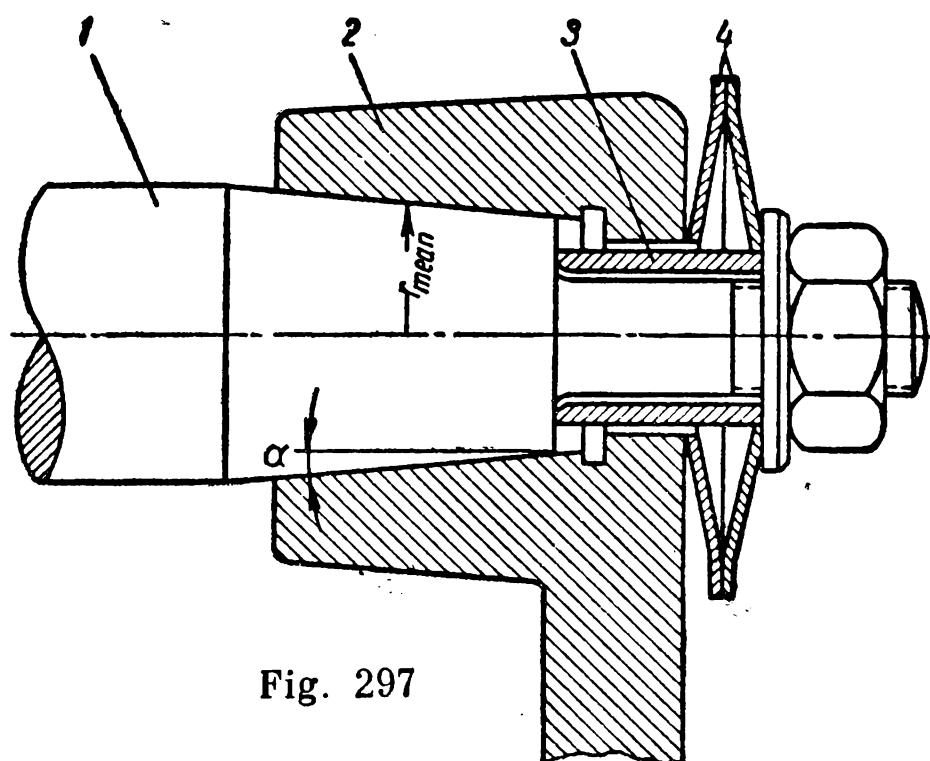
\*\* In the clutch in Fig. 297: 1—driven shaft, 2—lever hub, 3—sleeve of a definite length which determines the maximum allowable deflection of spring 4.

is given to the constancy of the torque transmitted by the clutch. which predetermines the accuracy of a slipping clutch.



**Fig. 296**

**Fig. 297 shows how the components of a slipping clutch can be combined with other components of a machine which perform other functions.**



**Fig. 297**

In this case the driver half is joined to the lever hub and the driven half to the shaft.

This example illustrates that such a combination is rational and is therefore often used also in clutches of other types: clutches are

fitted into pulleys which act as their housings; elastic elements are introduced into the rim of a toothed wheel which thus also performs the functions of an elastic clutch, etc. Similarly, there are combination clutches which unite elements and, consequently, functions of elastic and slipping clutches and couplings.

The formula (448) shows that the torque, at which a friction slipping clutch with a definite set of friction surfaces operates, depends on the compression force ( $P$ ) and the state of the friction surfaces which determines the coefficient of friction ( $f$ ).

To bring and maintain the friction surfaces in a state of definite compression ( $P$ ) during operation the clutch operating device is designed to support an elastic link in the form of a spring or a rubber ring, or compression may be effected by the pressure of air and the forces of electromagnetic attraction, which in different manners ensure a constancy of the compressive force.

To maintain the coefficient of friction ( $f$ ) at a constant level the friction surfaces are either completely lubricant-free or, conversely, operate with a permanent lubricating film after adjusting the clutch so that the discs periodically slip somewhat at starting.

*Spring-loaded slipping clutches* comprise the most numerous group of slipping clutches, due to the great diversity of their design modifications\*.

Figs. 298-301 show some of the most typical designs of spring-loaded clutches. They are identical in that all of them have one or several springs fitted with a certain preload. When the load brought to act on these springs by external forces exceeds the value of the initial tension the spring at first deflects and then, under considerable overloads, breaks the engagement. The various designs of spring-loaded clutches differ mainly in the mode in which the springs receive external load and break the engagement.

In spring protectors disengagement is usually made by a relative shift of parts in the form of teeth, jaws, balls, etc. After the load reaches a definite value, depending on the angle of contact of these components and the initial tension of the springs, the surfaces begin to shift relative to each other causing skipping accompanied by considerable wear of the contact surfaces. Attempts are made to reduce this by giving the contact surfaces a rational form, incorporating an accelerator, acting additionally on the parts being disengaged, by limiting operation to only one skipping after which the clutch components are retained in a disengaged position.

---

\* In principle, spring slipping clutches should also include elastic couplings (see p. 491). They reduce the amplitude of the varying torques acting in the system thereby protecting it against overloads.

*Spring toothed clutches* with a disc of cast iron or steel are extensively used in agricultural machinery. Their advantages are simple design and the presence of an overload warning system. The latter, however, is attained at too high a cost due to the wear of the discs on skipping. It would be more correct to separate the functions—as the clutch

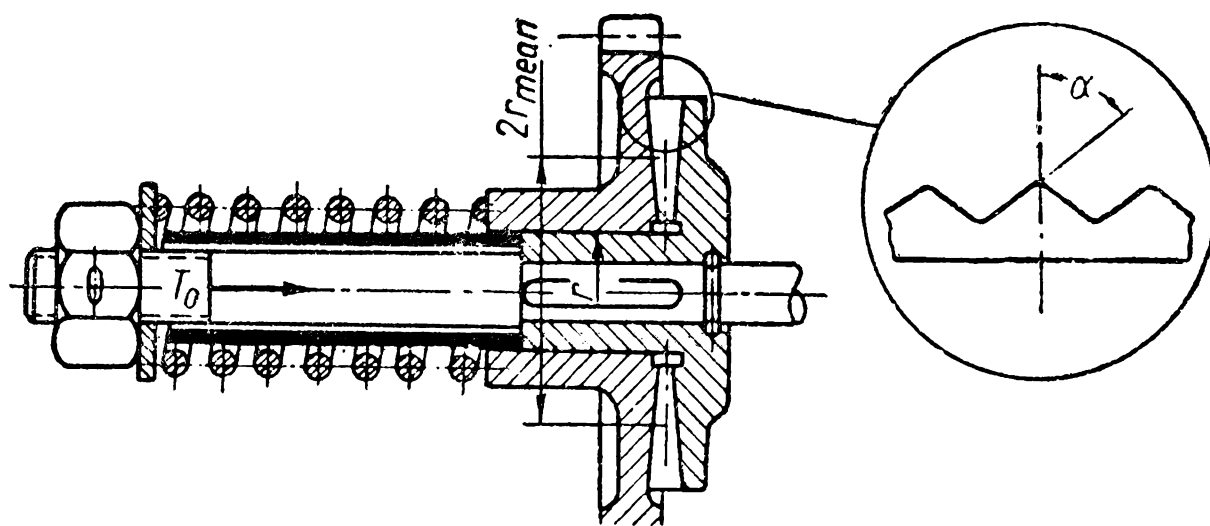


Fig. 298

operates breaking engagement a signal is sent separately by an ordinary ratchet. The design of such a clutch and a typical tooth profile are shown in Fig. 298.

The design formulae for toothed clutches are easily obtained from the equilibrium condition.

The maximum torque at which the clutch operates is

$$M_t = \frac{T \times r_{mean}}{\tan(\alpha - \varphi) - \frac{r_{mean}}{r} f'}; \quad T = T_0 + c\tau \quad (478)$$

where  $\alpha$  is the angle of inclination of the tooth working face (in the existing designs  $\alpha = 30-40^\circ$ );

$T_0$ —the force of the initial compression of the spring;

$c$ —the spring stiffness;

$\tau$ —the additional deflection of the spring at the moment of disengagement;

$\varphi$ —the angle of friction between the tooth surfaces;

$f'$ —the coefficient of friction reduced to the surface of the radius  $r$ ;

$r_{mean}$ —the mean radius of the clutch teeth.

*Spring jaw clutches* are essentially the same in design as toothed clutches. The jaws of these clutches have a special form which distinguishes them from teeth, are fewer in number and are usually arranged on a circumference of smaller diameter. One of the best designs of this type is the clutch employed in the tapping chucks shown

in Fig. 299. The design formulae for jaw clutches are the same as for toothed clutches.

Jaw clutches give excellent service only when their jaws are accurately machined and ensure reliable contact of the working surfaces with the discs in any position. Self-aligning discs considerably im-

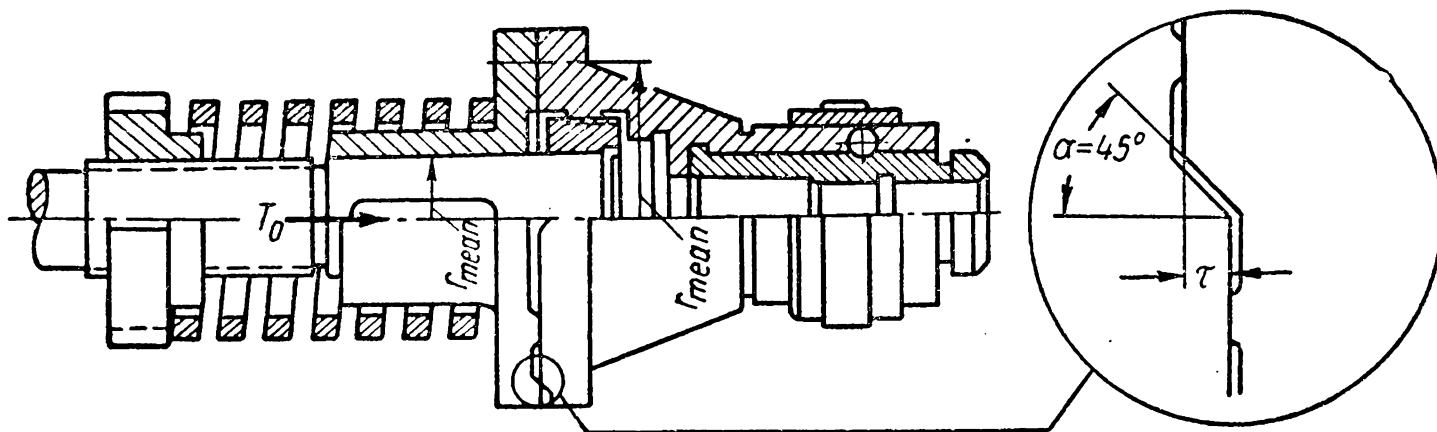


Fig. 299

prove the performance of the clutch. For this purpose the hub of the moving disc is short and fits freely on the shaft.

*Spring ball clutches* (Fig. 300) are modifications of jaw clutches. In them the sliding friction of the jaws is partly replaced by rolling friction. For these clutches the formula (478) remains true if  $r = r_{mean}$  and  $T = T_0 + z \times c \times \tau$ , where  $z$  is the number of balls.

A point contact of the balls causes considerable contact stress and rapid failure if the clutch operates frequently. Ball clutches are recommended only for relatively small loads, low velocities and with rare overloads.

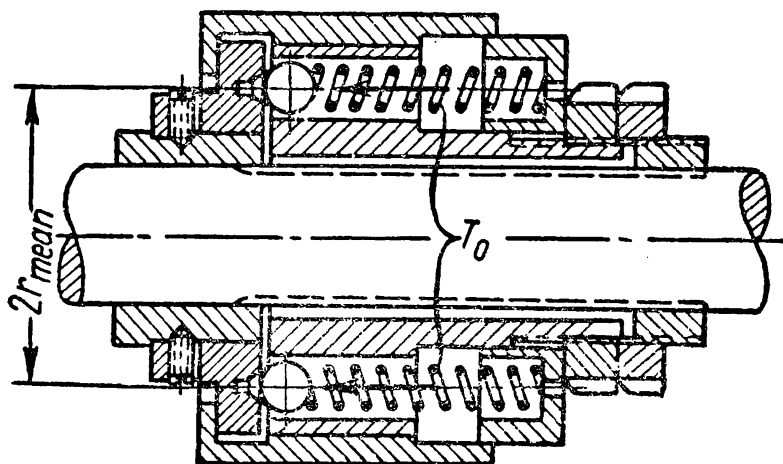


Fig. 300

*Spring lever clutches* (Fig. 301) make it possible to reduce to a minimum the effect of friction on the uniformity of operation. For them the design formulae are

$$M_t = \frac{T \times b \times r_{mean}}{\tan(\alpha - \varphi) a}; \quad T = T_0 + 2c\tau. \quad (479)$$

The symbols in these formulae are clear from Fig. 301 and from what has been said above in connection with the formula (478). These clutches are rather large but where size is not a limiting factor or when the transmitted loads are small and simultaneously high accuracy

and reliability of operation are required, these clutches are considered the best\*.

The formulae given in the section dealing with slipping clutches ignore forces of inertia which arise in operation. They hold for low rates of load increase and should be corrected for higher rates.

The problems of the dynamics of slipping clutches have not yet been elaborated to an extent as would make them the subject of study.

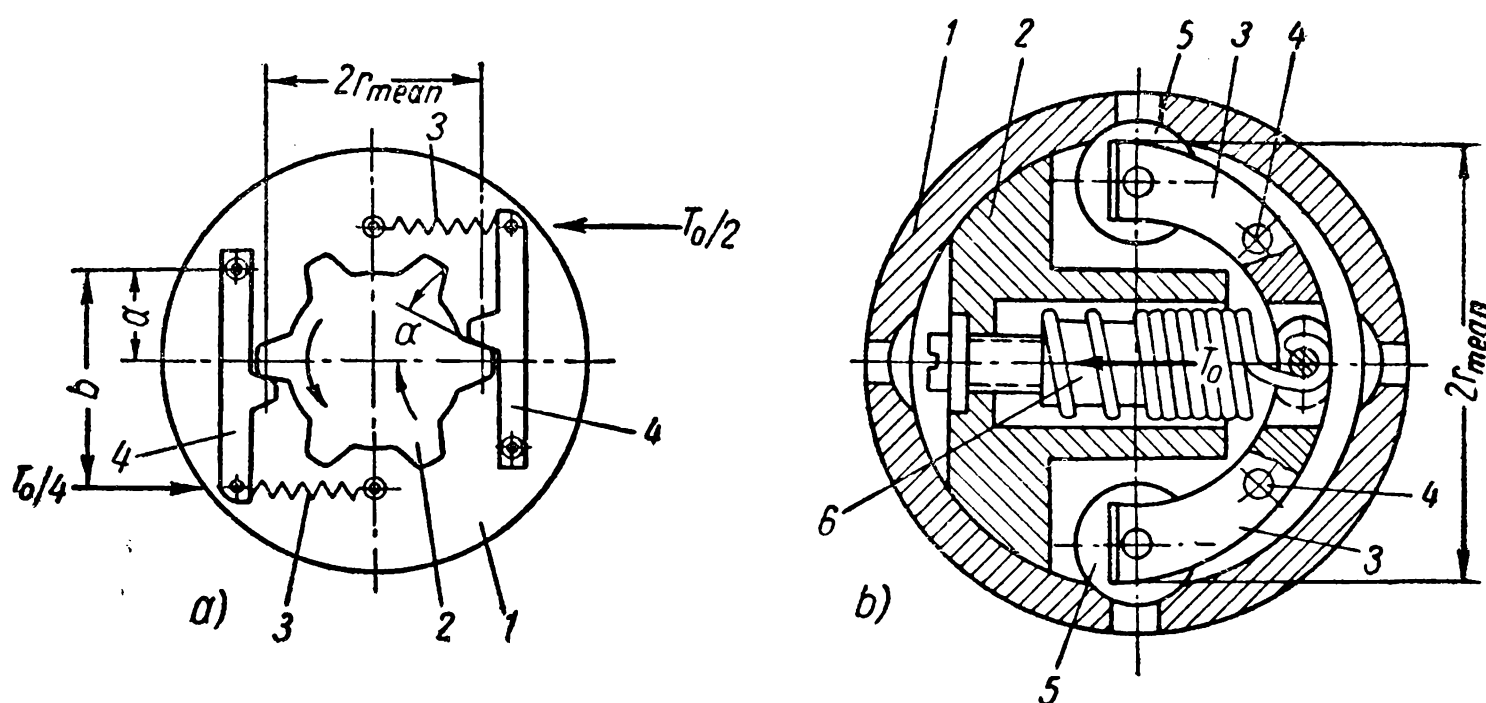


Fig. 301

**Overrunning Clutches.** Overrunning clutches, also called freewheeling clutches, automatically connect and disconnect shafts depending on the ratio of their angular velocities. When the velocity of the driving shaft exceeds that of the driven shaft the overrunning clutch connects the shafts. When the ratio of velocities is reversed the clutch is released without hampering the driven shaft to overtake the driving shaft.

Overrunning clutches are widely used in various starting devices, bicycles, motor-cycles, metal-cutting machine tools, and automobile transmissions.

Depending on the mode of engagement overrunning clutches are subdivided into *ratchet* and *friction* clutches. The latter category can be divided into *clutches with an axial or radial locking* and also according to the design of the elements between which the friction forces arise into *wedge*, *spring*, *band*, etc. Wedge clutches are of two types—

\* In the clutch in Fig. 301, *a*: 1 and 2—driven and driving halves of the clutch, 4—levers pressed against the jaws of the driving half by springs 3. In the clutch in Fig. 301, *b*: 1 and 2—driven and driving halves of the clutch, 3—levers, 4—axes of lever rotation, 5—rollers secured in the levers, 6—spring pressing rollers 5 to the clutch driven half.

*wedge proper* and *roller*—the latter, being simpler in design, are especially widespread.

*Overrunning roller clutches* (Fig. 302) consist of cage 1 and rotor 2 fitted on the connected shafts, and rollers 3 inserted between these components. To a certain degree such a clutch resembles a roller bearing, the essential difference being that, instead of smooth cylindrical surfaces on both races and on the bearing roller, one of these surfaces in an overrunning clutch has a special form of the rotor.

When the rotor rotates counterclockwise, relative to the cage, the rollers, without hindering this, rotate on their axles or slip. When the rotor begins to rotate clockwise the rollers are wedged between it and the cage thereby connecting the shafts. The tangents to the roller circumference at the point of contact with the rotor and the cage form the small angle  $\alpha$  (Fig. 302). The magnitude of this angle, called the angle of wedge,

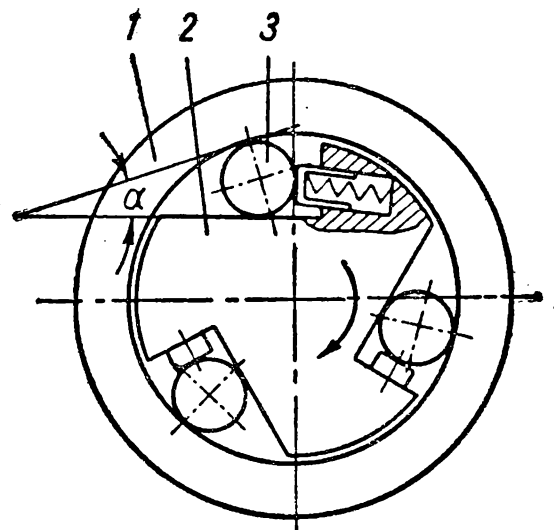


Fig. 302

is very important for the proper operation of the clutch. In existing designs the angle of wedge is  $\alpha=3-6^\circ$ . Lesser values of this angle should be avoided since in this case the release of the rollers from the wedge is rendered more difficult. Larger angles are not used because the clutch may tend to slip, especially after some wear and deformation of the contact surfaces.

Of the two possible versions of overrunning roller clutches—with the wedge surface on the rotor or cage—the former design is most frequently used. This is explained by the fact that a complex profile can be more easily obtained on the external surface than on the internal one. Overrunning clutch designs with rollers of a special form (Fig. 303) are a comparatively recent development. They have a large number of simultaneously operating rollers and therefore a better operating capacity.

In our further exposition we shall deal mainly with the design of the clutch shown in Fig. 302, which nowadays is employed more frequently than the other types.

Proceeding from the principle of operation of overrunning roller clutches, their designs should satisfy the following requirements: the angles of wedge of all rollers should be the same in all positions; all the rollers should participate equally in the work and carry the same load.

In order to satisfy all these requirements provision should be made for the reliable centering of the rotor and cage since, otherwise, when they are offset the angles of wedge and the loads on the rollers

will be different. Further, to obtain the same angles of  $\alpha$  for rollers of different (within the tolerance margin) diameter at various points of contact during the process of wedging, the groove on the rotor should have the form of a logarithmic spiral.

The number of rollers should be as large as possible ( $z \geq 3$ ) to decrease the load on each roller. To attain simultaneous and more uniform wedging of all rollers use is made of spring pushers. With these the rollers are continuously pressed against the cage and rotor causing friction and wear in overrunning. Some of the pushers often constitute the cause of trouble, because of seizure in their seats. At

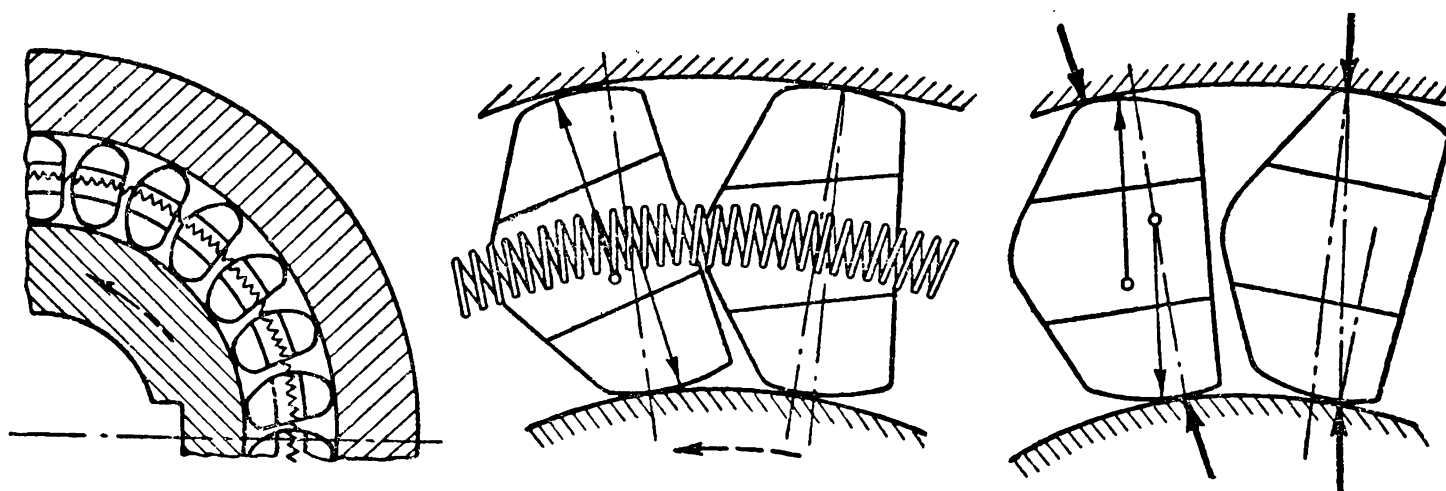


Fig. 303

high velocities, therefore, and with a large number of rollers these pushers are replaced by separators with a spring placed outside. Under all conditions the pressure exerted on the rollers (by the pushers or separator) should be low—only enough to retain them in contact with the operating surfaces. The rollers should be fixed in an axial direction as reliably as in roller bearings—by shoulders provided on the cage or rotor. To safeguard the rollers against skewing their length should not be below 1.25-1.5 of the diameter.

The cage carries concentrated forces due to the wedging action. It should be extremely rigid since deformations at the points of contact materially affect the magnitude of the angle  $\alpha$ .

In nature of loading and magnitude of contact pressures the operation of the cage or rotor and rollers of overrunning clutches is similar to that of the elements of rolling bearings. Therefore, for large loads the cage and rotor, and rollers are made from steel IX15, which has given good service in antifriction bearings. For small loads and in conformity with the allowable surface stresses steels of grades 20X and 40X are used.

*Calculation for strength* of roller clutches is reduced mainly to checking the compressive stresses at the points of contact. Here large normal and tangential forces act simultaneously and dynamically.



Elementary calculations take into account only the normal forces and are therefore of a comparative nature.

The diagram (Fig. 304) shows that the normal force acting on a wedged roller is

$$N_1 = \frac{M_{td}}{z \times r} \cot \frac{\alpha}{2} = \frac{T_1}{\tan \frac{\alpha}{2}} \quad (480)$$

where  $M_{td}$  is the design torque transmitted by the clutch;

$z$ —the number of rollers in the clutch;

$r$ —the radius of the working surface of the cage;

$N_1$  and  $T_1$ —the normal and tangential forces loading the roller in the area of contact between it and the cage;

$\alpha$  — the angle of wedge (usually  $\alpha = 3-6^\circ$ ).

From the Hertz formula (30) and using the given symbols the maximum pressure in the area of contact between the roller and the cage at  $E = E_1$  ( $2 \times 10^6$  kg/cm<sup>2</sup>) and  $r \gg d_2$  will equal

$$p_{\max} = 0.418 \sqrt{\frac{2N_1 E}{ld}} \text{ kg/cm}^2 \quad (481)$$

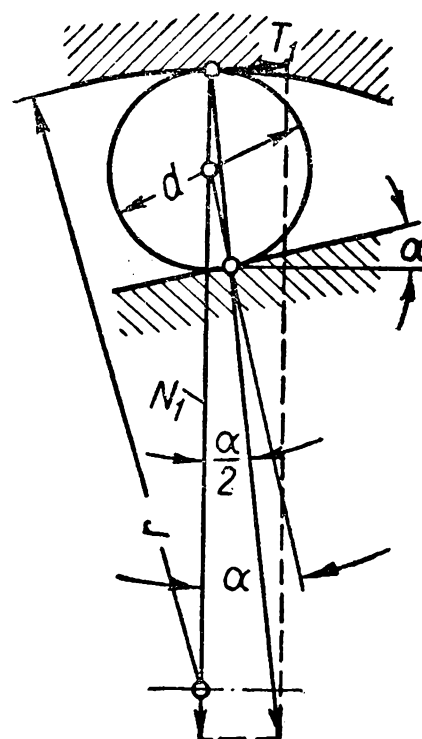


Fig. 304

where  $l$  and  $d$  are the length and diameter of the roller in cm.

The value  $p_{\max}$  in roller clutches calculated by this formula is 9,000-12,000 kg/cm<sup>2</sup>.

Substituting the value of  $N_1$  from (480) into (481) and solving this equation relative to  $M_{td}$  we shall obtain a formula for revised calculations

$$M_{td} = \frac{z p_{\max}^2 l d r \tan \frac{\alpha}{2}}{0.35 E} \text{ kg/cm.} \quad (482)$$

In the design diagram in Fig. 304, the spring pressure and the forces of inertia are neglected for the sake of simplicity. Since this has no effect on the general picture of affairs, it is usually considered as a reserve, i. e., the resultant of the ignored forces helps wedging.

**Centrifugal Clutches.** Centrifugal clutches are used to connect (or, less frequently, disconnect) two parts of a transmission after the driving part has attained a definite velocity of rotation. These clutches are predominantly employed to actuate machines which have considerable flywheel torques from squirrel-cage induction motors, as for instance the drives in centrifuges, drums of washing machines, belt conveyors, etc. This is due to the fact that ordinary

squirrel-cage induction motors possess a comparatively low starting torque, smaller than the maximum torque developed during rotation; while, on the other hand, considerable starting torque is necessary to bring machines with large masses into motion. A centrifugal clutch allows the motor (first without load) to pick up speed and then, after a definite velocity has been attained, to start the machine. As a re-

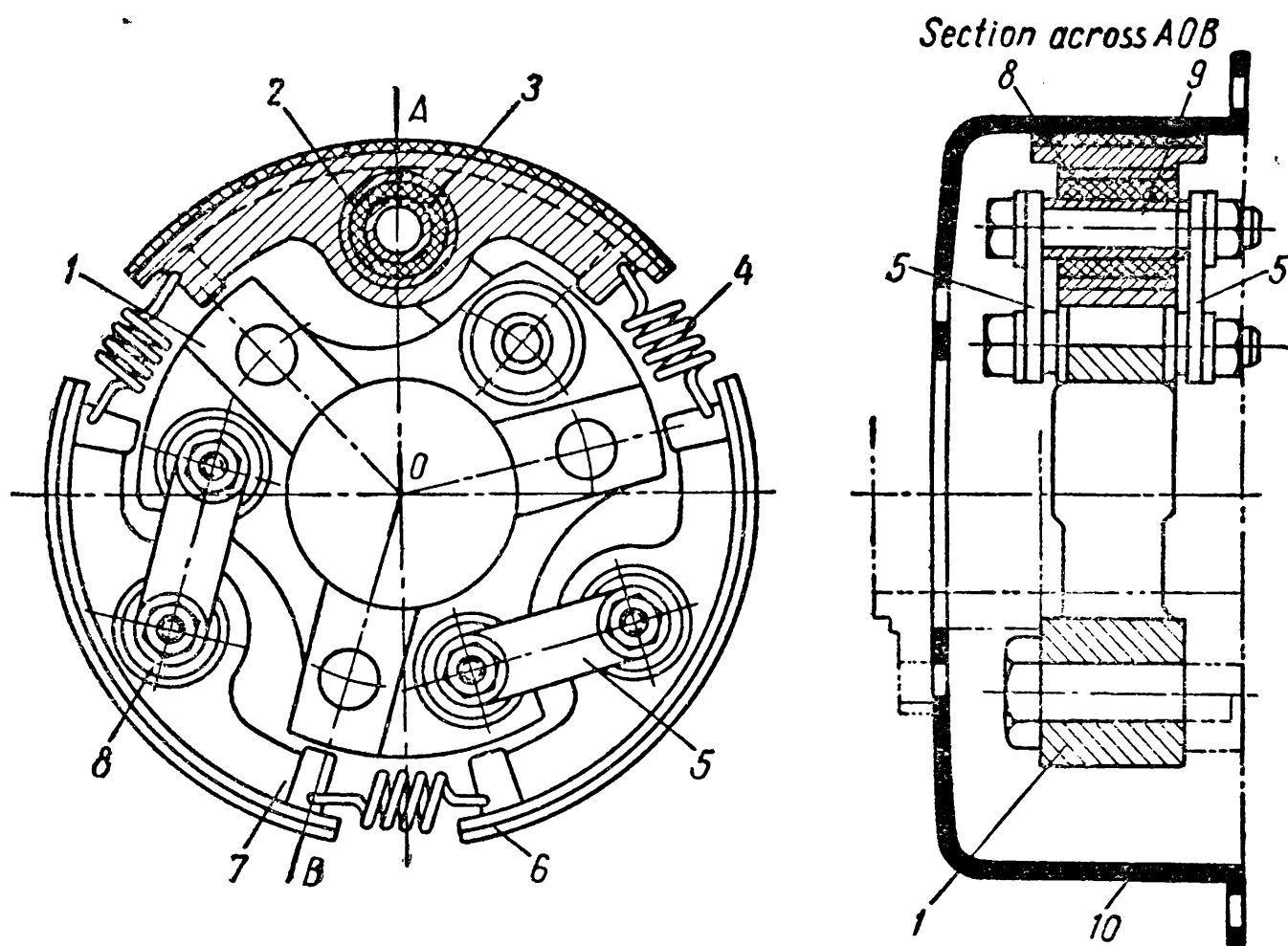


Fig. 305

sult, the starting proceeds smoothly without overloading the motor and driving mechanism.

Centrifugal clutches differ from ordinary friction clutches only in the design of the mechanism compressing the friction surfaces. In principle designs of centrifugal clutches are possible in which the friction surfaces of any type examined above (see p. 505) are compressed by the centrifugal forces of inertia. The most widely used are centrifugal clutches with radial friction surfaces (block, band, etc.) in which the centrifugal force compresses the friction surfaces directly. Axial clutches (disc, cone) require for this purpose also a lever mechanism which transforms radially-directed centrifugal forces into axial forces to compress the discs.

Let us consider the design of a centrifugal clutch with three shoes (Fig. 305), which presents some interesting features.

Three shoes 7 with friction facings 6 are connected to hub 1 of the driver half by means of plates 5. Pins 9 connecting the shoes and the

hub rest on rubber-metallic hinges comprising metal sleeves 2 and 3 and rubber spacers 8 between them.

Such a rubber-metallic hinge requires no lubrication, operates noiselessly and damps vibration at starting and under load variations.

The shoes are interconnected by springs 4 which provide an interval between the moment of starting and the time when the shoes begin to couple with the rim.

As the hub rotates, the shoes are pressed against drum 10 under the action of centrifugal force, which overcomes gravity and the forces of springs and hinges. As the velocity of rotation continues to grow the pressure on the friction surfaces increases, and when the moment of the friction forces becomes sufficient to overcome the resistance of the machine the driven half of the clutch begins to move.

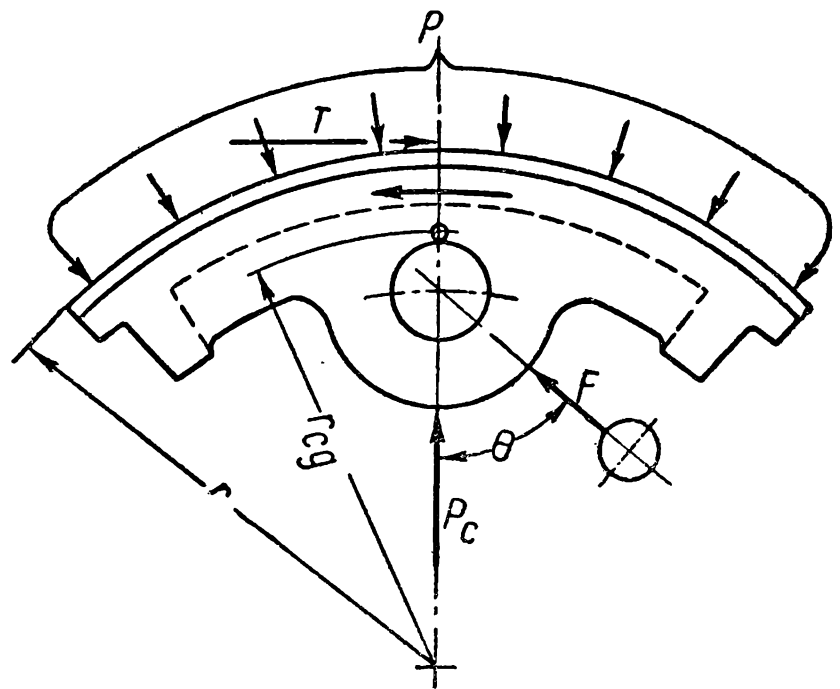


Fig. 306

In the process of operation the shoe (Fig. 306) undergoes the action of the following forces: centrifugal  $P_c$ , pull  $F$ , reaction from the pressure on the drum  $P$ , friction  $T$  and also the forces of gravity, of the springs and the elastic resistance of the hinges.

The effect of gravity (when the clutch axis is horizontal) on one shoe is compensated for by a reverse effect on the other two shoes. Therefore, as in the final analysis the total pressure that all shoes exert on the drum is important, the effect of gravity can be ignored. The forces of the springs and hinges (small in this case) can likewise be neglected.

From the equilibrium equations of the shoe

$$P - P_c - F \cos \theta = 0 \quad \text{and} \quad T - F \sin \theta = 0,$$

and also from the ratio between the normal force ( $P$ ) and the force of friction ( $T = fP$ ) we find the relation between the force of friction and the centrifugal force

$$\frac{T}{P_c} = \frac{f}{1 - f \cot \theta}$$

where  $P_c = m\omega^2 r_{cg}$  is the centrifugal force;

- $m$ —the mass of one shoe;  
 $\omega$ —the angular velocity of the shoe;  
 $r_{cg}$ —the distance from the shoe centre of gravity to the axis of the clutch rotation.

The torque transmitted by the clutch of this design is

$$M_{td} = \frac{1}{\beta} M_{fr} = \frac{1}{\beta} 3Tr = \frac{1}{\beta} 3P_c r \frac{f}{1 - f \cot \theta} . * \quad (483)$$

This formula shows that the magnitude of the centrifugal force ( $P_c$ ) required to transmit a definite torque ( $M_{td}$ ) in the clutch as shown in Fig. 305, all other conditions being equal ( $r, \beta$ ), depends not only on the coefficient of friction ( $f$ ) as in an ordinary radial clutch but also on the angle  $\theta$ . At the same time, since  $1 - f \cot \theta < 1$ , this reduces the required value of  $P_c$ . It is true that when the clutch rotates in the reverse direction (clockwise in Fig. 305) the sign in the denominator changes and the maximum torque transmitted by the clutch decreases several times, as a result of which this design is unsuitable for reversible drives.

---

\* For preliminary design calculations the formula (483) should be transformed. Substituting  $P_c = m\omega^2 r_{cg}$ ,  $\omega = \pi n/30$ ,  $m = G/g$  and  $r_{cg} = \psi r$  we obtain

$$M_{td} = \frac{1}{\beta} 3 \frac{G \times n^2}{900} \psi r^2 \frac{f}{1 - f \cot \theta} \text{ kgm.}$$

Here, in addition to the symbols we used before,  $G$  is the weight of one shoe in kg,  $n$ —rpm of the shoe,  $\psi$ —the ratio between the radii  $r_{cg}/r$ . For shoes in the form of a circular segment we can assume in advance  $\psi \approx 0.8$ .

PART FIVE

## SPRINGS, MACHINE FRAMES

---

CHAPTER XXIV

### SPRINGS

Springs are employed in machines as elastic elements. They take the work of the external forces and transform it into the work of elastic deformation of the material from which they are made.

After a spring is relieved from load, its deflection disappears and the work expended previously is almost completely restored.

The forms of springs allow them to take external forces over considerable distances, i. e., to be greatly deflected without losing any of their elasticity. Thus, for example, a helical spring made of steel wire can be expanded to twice its length without losing its elasticity. On the other hand, a bolt made from the steel of the same grade becomes permanently deformed if the load applied to it acts over the distance slightly in excess of 0.004 of its original length.

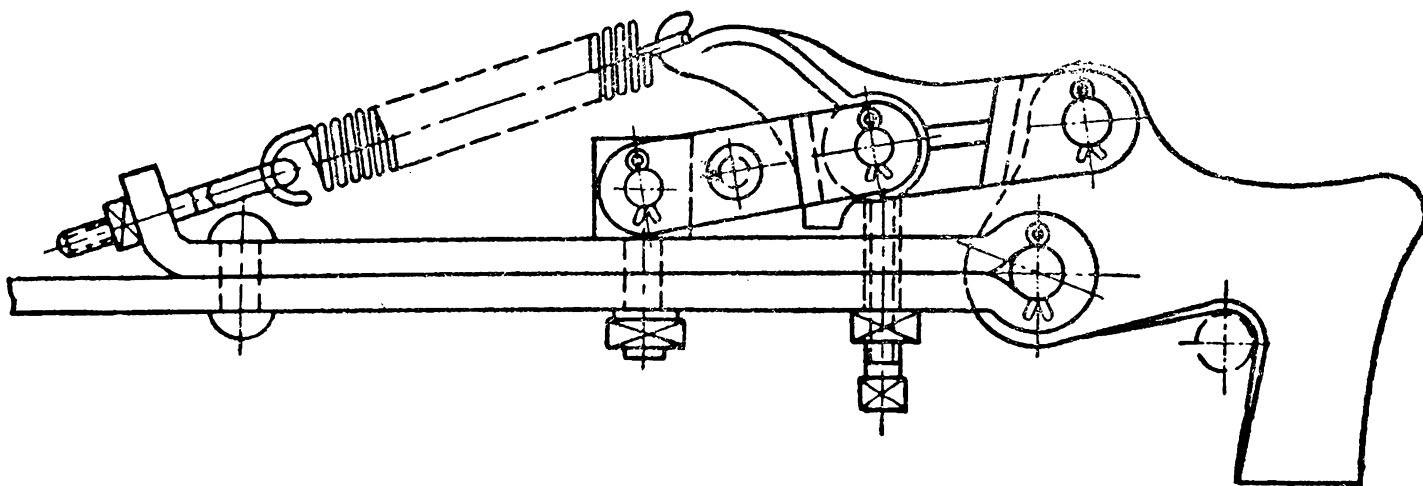


Fig. 307

Springs are employed in machines and devices as:

1. *Power elements* ensuring an effort over an assigned distance. This can be illustrated by springs used in the overload devices of tractor ploughs (Fig. 307).

2. *Shock absorbers*. Taking the instantaneous energy of a shock such a spring returns it in the form of elastic oscillations.

The spring used as a shock absorber in the front suspension of the Soviet "Pobeda" car is shown in Fig. 308.

3. *Drivers* (sources of motion) of a mechanism. For example, the springs employed in watches and clocks and in different devices, firearms, etc. (see, for example, Fig. 316).

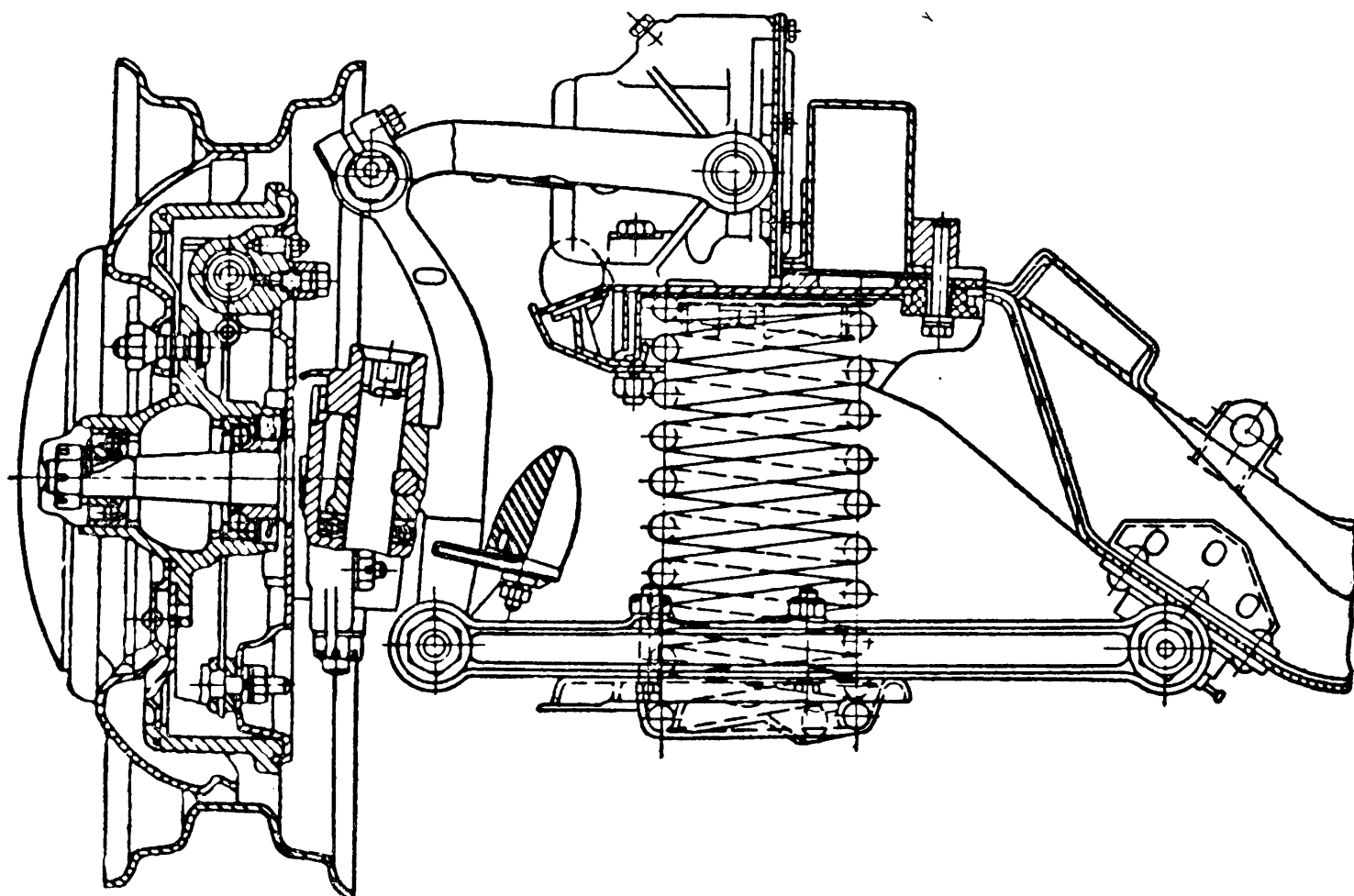


Fig. 308

Depending on the stresses arising in loaded springs they are subdivided into:

- 1) *torsional stressed* springs;
- 2) *flexural stressed* springs; and
- 3) *tension-compression stressed* springs.

A classification of the main types of springs is given in Fig. 309.

### TORSIONAL STRESSED SPRINGS

Helical *extension* and *compression* springs of this group are shown in Fig. 309, a-e.

They are usually made from high-carbon steel of grades 65, 70 and 75, manganese steel of grades 65Г, 55ГC or silicon steel of grades 55C2 and 60C2. For heavily loaded valve springs in internal combustion engines use is made of chromium and vanadium alloy steel.

Springs operating in humid or chemically active media (for example, in machines and apparatus of the chemical, food and other industries) are sometimes made from bronze or brass.

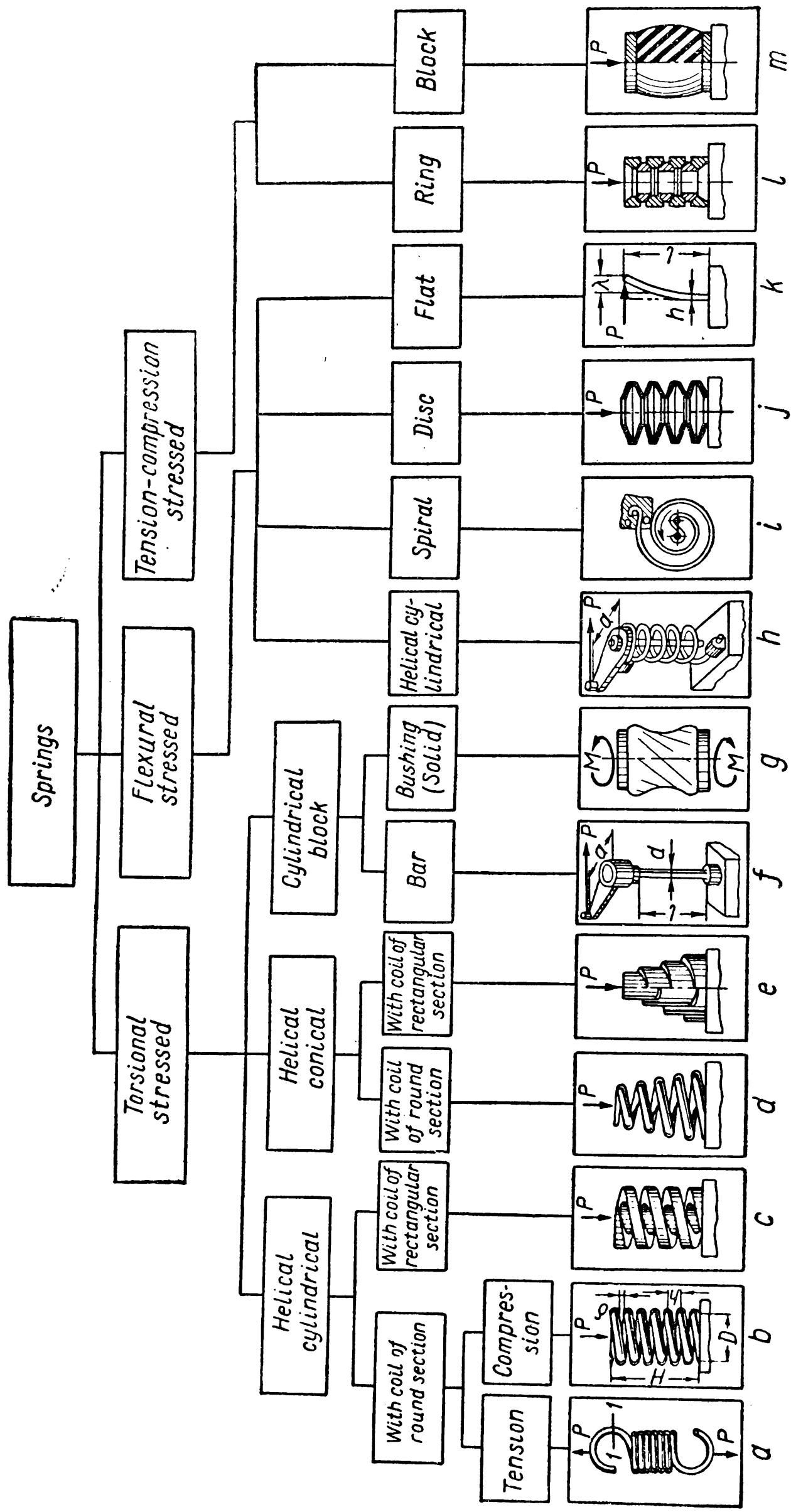


Fig. 309

A recent development is the method of producing high-quality helical springs from plastics.

Certain types of springs are made from rubber (Fig. 309, *g* and *m*).

The wire (or bar) intended for the manufacture of helical springs is subjected to heat treatment before being wound. When the wire diameter exceeds 12 mm it should be wound hot. In this case heat treatment of the wire is not rational.

To manufacture highly accurate springs for instruments and important mechanisms use is made of piano or patented wire made of high-carbon steel.

In the process of drawing this wire is patented, i. e., passed through a heating furnace after which it is submerged in a lead bath. This enlarges the grains on the surface of the wire so that during subsequent drawing its entire outer layer is considerably cold-hardened. This also improves the elastic properties of the material.

Helical springs are produced in quantity on special automatic spring winding machines. In other cases the spring is wound around a mandrel on a lathe.

For proper coiling the index  $c$  of the manufactured spring is of extreme importance.

In springs with coils of a round cross-section the index  $c = \frac{D}{d}$  where  $D$  is the mean diameter of the spring coils and  $d$  the diameter of the wire from which the spring is wound. The smaller the index the more difficult it is to wind the spring. Usually  $c = 4-12$ .

Compression springs are wound so as to allow a *certain clearance* between the coils. Extension springs have *closely wound* coils.

To obtain closed coils the wire is stretched during the process of winding to subject it to tensile elastic strain. When the wound spring is removed from the mandrel there occurs an elastic spring-back of the material, the spring expands in diameter and the coils are so tightly pressed against each other that the spring is given an *initial tension* increasing its carrying capacity.

Important springs are subjected to *presetting* to increase their carrying capacity.

For this purpose the spring is compressed until all adjacent coils touch and kept in this state for a more or less lengthy period (6-48 hours). During this process the layers of section resisting the maximum load are subjected to plastic deformation whereas the other layers are deformed elastically.

After the load is removed the deformed layers interact with each other and the spring is given a prestress.

If the load acting upon the spring is constant or changes smoothly in time, and the total number of load repetitions does not exceed



$10^5$  (as in firearms, safety and other springs) the calculations are made for static load.

**Extension Springs.** The calculation of springs of this type is reduced to determining the diameter of the wire  $d$ , the diameter of the spring coils  $D$ , the number of active coils  $i$  and also to plotting a *characteristic curve* showing the relation between the load and deflection.

We know from the theory of the strength of materials that under the action of the force  $P$  directed along the axis of a helical spring (either extension or compression) the maximum tangential stresses arising on the internal surface of the coil are found from the formula

$$\tau = \tau_s + \tau_t = \left( \frac{P}{S} + \frac{PD}{2W_0} \right) \cos \alpha. \quad (484)$$

Here  $\tau_s$  and  $\tau_t$  are the stresses due to the shearing force and the torsional moment  $P \frac{D}{2}$ , respectively;  $S$ —the area of the coil cross-section;  $W_0$ —the polar section modulus;  $\alpha$ —the helix angle of the coil, which in extension-compression springs usually amounts to  $6-15^\circ$ .

When applied to a spring of circular cross-section with  $\cos \alpha \approx 1$  the formula (484) will assume the form

$$\tau = \tau_s + \tau_t = \frac{4P}{\pi d^2} (1 + 2c).$$

With the usual values of  $c$ ,  $2c = 8-24$ . This means that tangential shearing stresses  $\tau_s$  are smaller by the same amount than tangential torsional stresses  $\tau_t$ .

To simplify calculations the insignificant effect of the shearing stress  $\tau_s$ , the helix angle  $\alpha$  and the effect of curvature is accounted for by the factor  $k > 1$ , which is found from an empirical formula depending on the spring index:

$$k \approx \frac{4c + 2}{4c - 3}. \quad (485)$$

Taking into account the factor  $k$  we obtain from the equation (484)

$$\tau = \frac{PDk}{2W_0} \leq [\tau]. \quad (486)$$

For a coil of round section

$$\tau = \frac{8PDk}{\pi d^3} \leq [\tau]. \quad (487)$$

Hence the required diameter of the wire

$$d = 1.6 \sqrt[3]{\frac{Pck}{[\tau]}} \text{ cm.} \quad (488)$$

Here  $[\tau] = 2 \times 10^3 - 1 \times 10^4$  kg/cm<sup>2</sup> is the allowable stress for the material of the spring in torsion. Its values for different materials are indicated in respective reference books.

The spring deformation caused by the shearing force  $P$  and the torsional moment  $P \frac{D}{2}$  is

$$\lambda = \left( \frac{P}{S} + \frac{PD^2}{4I_0} \right) \frac{l \cos^2 \alpha}{G}. \quad (489)$$

Here, additionally,  $l$  is the working length of the unwound wire or bar;

$G$ —the modulus of elasticity in shear;

$I_0$ —the polar moment of inertia of the cross-section.

If spring deflections occur from  $\lambda = \lambda_1$  to  $\lambda = \lambda_2$  under the action of the force changing from  $P = P_1$  to  $P = P_2$  the work expended here will be

$$U = (P_2 - P_1) \frac{\lambda_2 - \lambda_1}{2}. \quad (490)$$

For springs with coils of round section the formula (489) will take the form

$$\lambda = \frac{4P}{\pi d^2} (1 + 2c^2) \frac{l \cos^2 \alpha}{G}. \quad (491)$$

The second member of the expression in the parentheses is many times larger than the first since  $c \gg 4$ ; therefore the deflection of the spring caused by the shearing force can be neglected. If we also take into consideration the fact that  $\cos \alpha$  approximates unity and that the unwound length of the wire or bar is  $l = \pi D i$  where  $i$  is the number of active coils, we shall obtain from the equation (491) for a steel spring with  $G = 8 \times 10^5$  kg/cm<sup>2</sup>

$$i = 10^5 \frac{\lambda}{P} \times \frac{d}{c^3}. \quad (492)$$

Here  $\lambda$  is the spring deflection in cm;

$P$ —the effort in the spring in kg;

$d$ —the diameter of the wire (bar) in cm.

Accounting for the reservations made above, the formula (489) for springs with an *arbitrary cross-section of coil* made from any material will take the form

$$i = \frac{4}{\pi} \times \frac{\lambda}{P} \times \frac{GI_0}{D^3}. \quad (493)$$

The expression

$$\frac{4GI_0}{\pi D^3} = Z \text{ kg/cm} \quad (494)$$

is called the *spring stiffness*.

Finally, solving simultaneously the equations (487) and (493) for a spring made from round steel wire with the given dimensions  $D$  and  $d$  and the given deflection  $\lambda$ , we shall get

$$i = 2.54 \times 10^5 \frac{d}{D^2} \times \frac{\lambda k}{[\tau]}. \quad (495)$$

The effort of the initial tension  $P_0$  in a closely coiled spring is usually estimated in fractions of the limit effort  $P_{lim}$ .

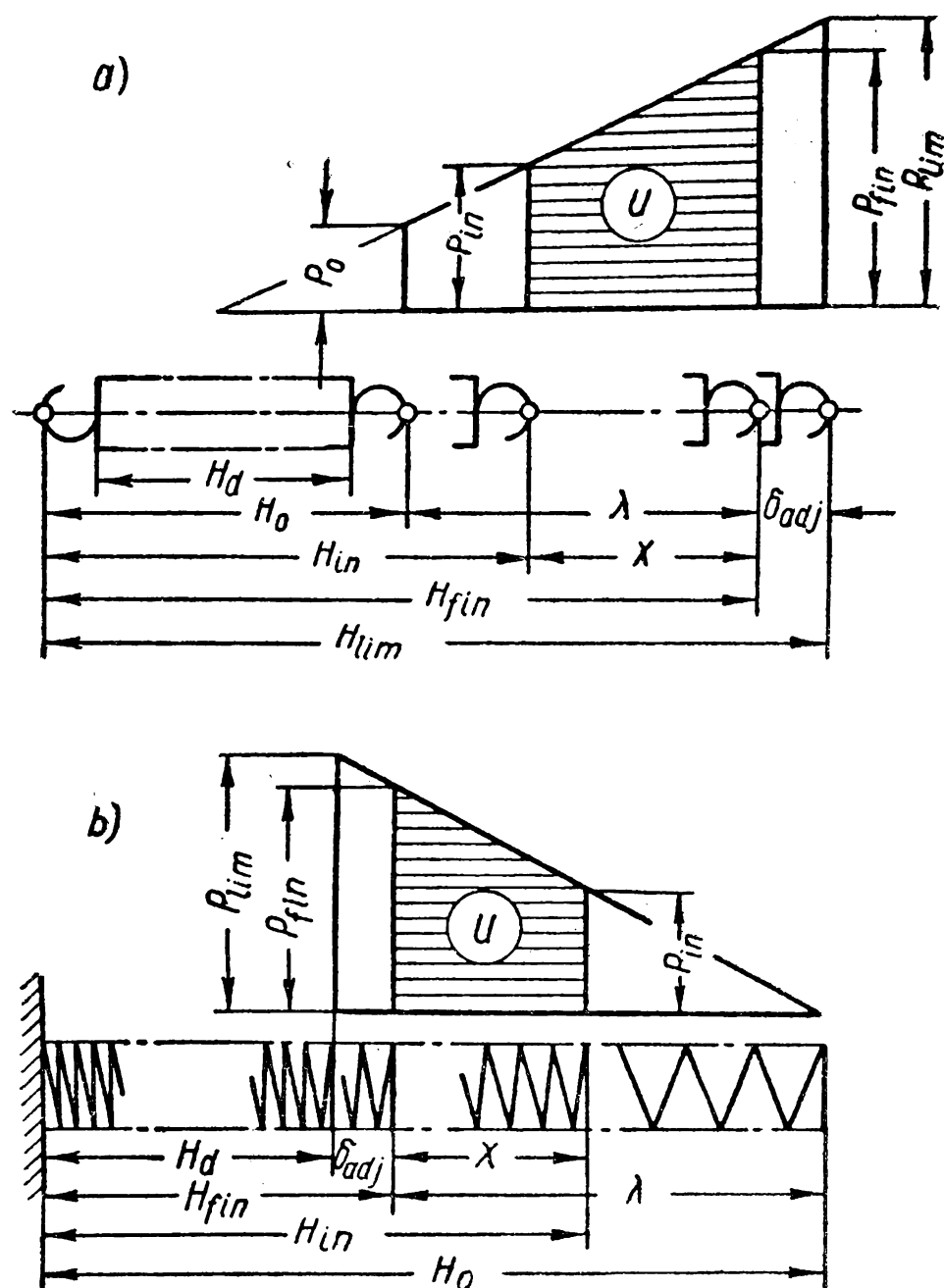


Fig. 310

The latter is understood to mean the force causing in the spring material a stress equal to the limit of elasticity.

Tentatively with wire diameter

$$\begin{aligned} d < 5 \text{ mm} & P_0 = 0.33P_{lim}; \\ d > 5 \text{ mm} & P_0 = 0.25P_{lim}. \end{aligned} \quad (496)$$

In turn  $P_{lim} = (1.1-1.2)P_{fin}$  where  $P_{fin}$  is the maximum working load corresponding to the stress  $[\tau]$  used in calculations.

The initial (adjusting) load  $P_{in}$  is determined by the purpose of the spring.

The characteristic of an extension spring is given in Fig. 310, *a*. The forces are laid off on the vertical and the corresponding spring deformations on the horizontal line. The shaded area indicates the work of deformation  $U$ .

For adjustment the final length of the spring  $H_{fin}$  is taken by 5-10% less than the limit length  $H_{lim}$ . The adjustment deflection is shown in Fig. 310, *a* as  $\delta_{adj}$ .

The total deflection of the spring is

$$\lambda = H_{fin} - H_0.$$

Since the spring is assembled in a tensed state corresponding to the length  $H_{in}$  the working deflection is

$$x = H_{fin} - H_{in}.$$

The free length of a spring  $H_0 = H_d + (1-2)D$  and more, depending on the design of the hooks—the ends of the spring by which it is secured in the assembly;  $H_d = id$  is the solid length when the spring is tightly compressed.

The length of unwound wire or bar is

$$l = \frac{\pi D_i}{\cos \alpha} + l_{hook}$$

where  $l_{hook}$  is the length left for the hooks.

The total normal stress in the section 1-1 of the hook (Fig. 309, *a*) due to the tensile force  $P$  and the bending moment  $P \frac{D}{2}$  should be less than that permitted for the given material of the spring.

**Compression Springs.** The tasks of the practical calculations of compression springs are essentially the same as for extension springs and are solved by the same design formulae.

Compression springs employ no hooks and are so wound as to provide clearance  $\delta$  between the coils (Fig. 309, *b*).

Fig. 310, *b* shows a characteristic of a compression spring. Here  $P_{lim}$  is the load compressing the spring until the adjacent coils touch.

To provide for adjustment the maximum load  $P_{fin}$  is taken by 10-15% below  $P_{lim}$ .

The initial (adjusting) load ensuring a tight contact between the spring end turns and the unit parts is chosen within

$$0.1P_{fin} \leq P_{in} \leq 0.5P_{fin}.$$

The inactive end coils of the spring should be thoroughly worked to fit tightly against the thrust surfaces.

The total thickness of the end coils is  $\approx 0.5d$ .

The solid length of the spring compressed until the coils touch is

$$H_d = (i' - 0.5)d$$

where  $i'$  is the total number of coils (both active and inactive).

The number of the active coils  $i = i' - 2$ .

The free length of the spring (see Figs 309, *b* and 310, *b*) is

$$H_0 = H_d + i(h - d).$$

The coil pitch  $h$  is from  $\frac{D}{3}$  to  $\frac{D}{2}$ .

Compression springs with  $\frac{H_0}{D} > 3$  may buckle during operation (Fig. 311, *a*). Such springs should be mounted over an arbor or placed in guide tubes (Fig. 311, *b*).

The length of unwound wire or bar for a compression spring  $l_0 = \frac{\pi D i'}{\cos \alpha}$ ;  $\alpha$  is the helix angle in a free spring determined by the relation  $\tan \alpha = \frac{h}{\pi D}$ .

*Example.* Calculate an extension spring made from round wire and operating in conditions of static loading.

Initial data:

maximum working load  $P_{fin} = 80$  kg;

initial (adjusting) load  $P_{in} = 35$  kg;

working deflection  $x = 45$  mm.

For the spring, steel wire of grade 85 with  $[\tau] = 50$  kg/mm<sup>2</sup> is chosen.

The spring index  $c = 6$  is taken; then by the formula (485)

$$k \approx \frac{4c + 2}{4c - 3} = \frac{4 \times 6 + 2}{4 \times 6 - 3} = 1.24.$$

The wire diameter by the formula (488) is

$$d = 1.6 \sqrt{\frac{P_{ch}}{[\tau]}} = 1.6 \sqrt{\frac{80 \times 6 \times 1.24}{5,000}} = 0.55 \text{ cm.}$$

From the wire standard  $d = 0.6$  cm.

The spring coil mean diameter  $D = c \times d = 6 \times 0.6 = 3.6$  cm.

The limit load is

$$P_{lim} = 1.2 P_{fin} = 1.2 \times 80 = 96 \text{ kg.}$$

The initial tension is

$$P_0 = 0.25 P_{lim} = 0.25 \times 96 = 24 \text{ kg.}$$

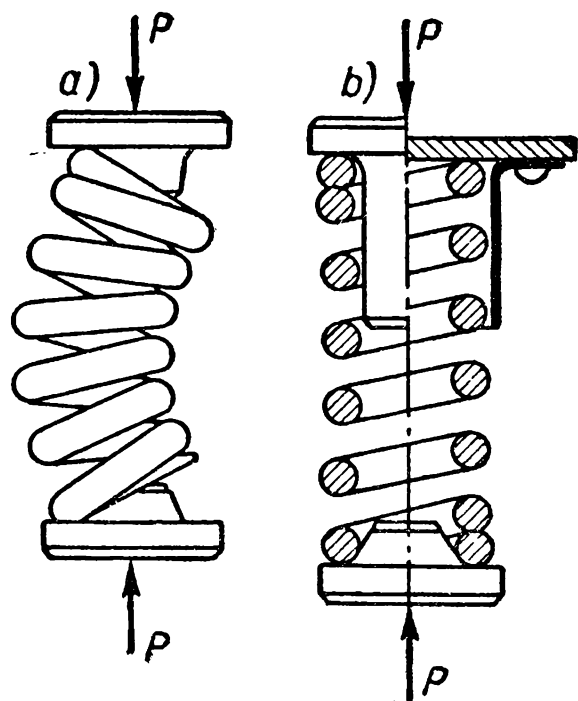


Fig. 311

The adjusting deflection is (Fig. 310, *a*)

$$\delta_{adj} = x \frac{P_{lim} - P_{fin}}{P_{fin} - P_{in}} = 4.5 \frac{96 - 80}{80 - 35} = 1.6 \text{ cm.}$$

The total deflection

$$\lambda = x \frac{P_{fin} - P_0}{P_{fin} - P_{in}} = 4.5 \frac{80 - 24}{80 - 35} = 5.6 \text{ cm.}$$

The number of coils by the formula (492)

$$i = 10^5 \frac{\lambda d}{(P_{fin} - P_{in}) c^3} = 10^5 \frac{5.6 \times 0.6}{(80 - 35) 6^3} = 35.$$

The solid length is

$$H_d = id = 35 \times 0.6 = 21 \text{ cm.}$$

The total free length is

$$H_0 = H_d + (1-2) D = 21 + 2 \times 3.6 = 28.2 \text{ cm.}$$

The characteristic of the calculated spring is represented in Fig. 312.

**Cluster Springs.** For large loads use is made of cluster springs consisting of several, usually two, concentric springs, wound in different directions.

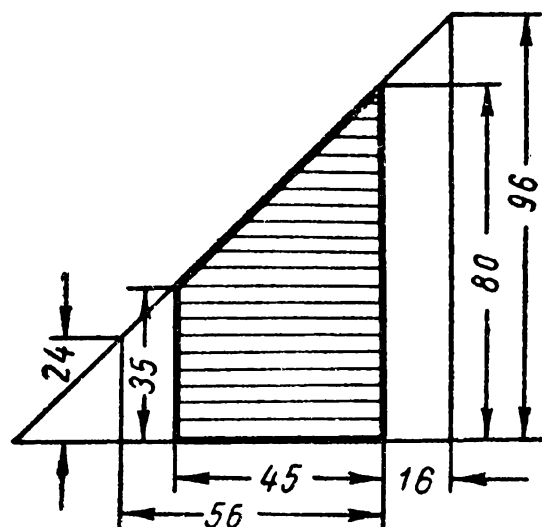


Fig. 312

Fig. 313, *a* shows a cluster spring of the valve gear mechanism in an aircraft engine.

When fitting such springs provision should be made for a clearance  $\Delta$  (Fig. 313, *b*) which will guarantee normal operation with slight misalignment. Tentatively

$$\Delta = \frac{d_1 - d_2}{2} \quad (497)$$

where  $d_1$  and  $d_2$  are the diameters of the wire of the external and internal springs respectively.

The following conditions form the basis of the calculation of cluster springs.

*The first condition*—the maximum actual stresses  $\tau$  in the materials of the springs are equal, if the springs are made from the same material, or do not exceed the minimum of the allowable stresses of both materials, i. e.,

$$\tau_1 = \tau_2 \leq \tau_{\min}.$$

This condition can be written on the basis of the relation (487) as follows

$$\frac{P_1 D_1}{d_1^3} = \frac{P_2 D_2}{d_2^3}. \quad (498)$$

The factors  $k$  which take into account the effect of the additional phenomena (see p. 547) are taken as equal for both springs.

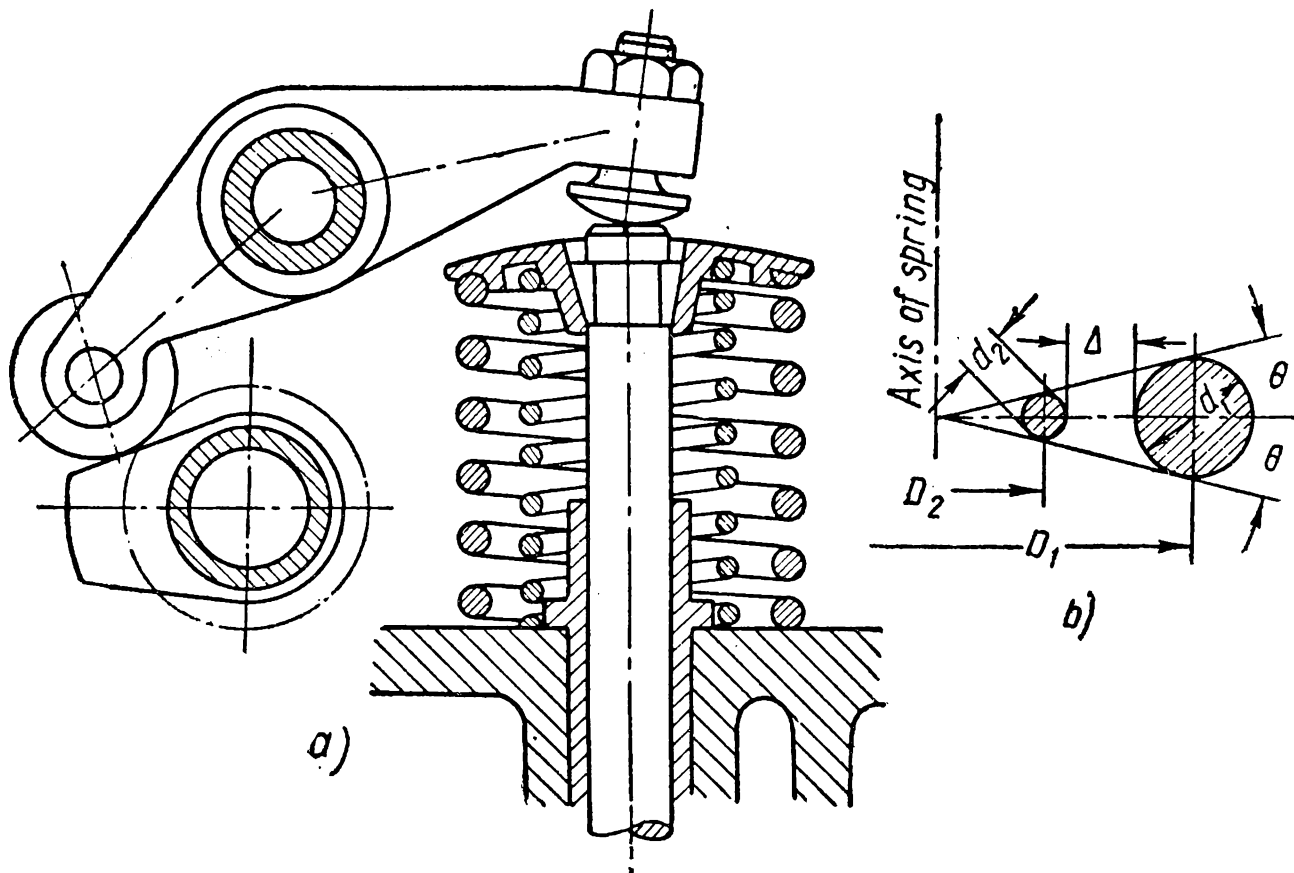


Fig. 313

The second condition—the working deflection  $x$  and the deflection  $\lambda$  are the same in both springs, i. e.,

$$x_1 = x_2 \text{ and } \lambda_1 = \lambda_2.$$

On the basis of this condition we obtain from the equation (493)

$$\frac{P_1 D_1^3 i_1}{d_1^4} = \frac{P_2 D_2^3 i_2}{d_2^4} \quad (499)$$

The third condition—both springs, when compressed until the adjacent coils meet, have the same solid height

$$H_d = i_1 d_1 = i_2 d_2.$$

Dividing, by terms, the equation (499) by (498) we shall get

$$\frac{D_1^2}{d_1} \times i_1 = \frac{D_2^2}{d_2} \times i_2.$$

It follows from this and the preceding equation that

$$\frac{D_1}{d_1} = \frac{D_2}{d_2} = c. \quad (500)$$

Thus, when designing cluster springs, their proportions should be so chosen that their indexes are the same.

In Fig. 313, *b*

$$\tan \theta = \frac{d_1}{D_1} = \frac{d_2}{D_2} = \frac{1}{c}. \quad (501)$$

Solving this equation simultaneously with the equation (495) we get

$$\tan \theta = 2 \times 10^{-3} \sqrt{\frac{H_d}{k\lambda} [\tau]}. \quad (502)$$

Bearing in mind the relation (500), we get from the equation (498)

$$\frac{P_1}{P_2} = \frac{d_1^2}{d_2^2} = \frac{F_1}{F_2}, \quad (503)$$

i. e., the efforts in cluster springs are distributed between them in proportion to the areas of the coil cross-section.

From Fig. 313, *b*

$$\Delta = \frac{(D_1 - D_2) - (d_1 + d_2)}{2}$$

and when choosing  $\Delta$  by the formula (497)

$$d_1 = \frac{D_1 - D_2}{2}.$$

After dividing both sides of this relation by  $d_2$  we obtain, after simple transformations,

$$\frac{d_1}{d_2} = \frac{c}{c-2}. \quad (504)$$

*Example.* Calculate a compression cluster spring using the following initial data:

the total load on the springs  $P=600$  kg; the total deflection  $\lambda=40$  mm; the solid length of the compressed spring (disregarding the end coils)  $H_d=50$  mm; the allowable stress  $[\tau]=85$  kg/mm<sup>2</sup>.

We take tentatively  $k=1.2$ . From the formula (502) we get

$$\tan \theta = 2 \times 10^{-3} \sqrt{\frac{H_d}{k\lambda} [\tau]} = 2 \times 10^{-3} \sqrt{\frac{5}{1.2 \times 4}} \times 8,500 \approx 0.188.$$

The spring index from the formula (501) is

$$c = \cot \theta = \frac{1}{0.188} = 5.32.$$

We take  $c=5$ .

From the relations (503) and (504) we find

$$\frac{P_1}{P_2} = \left( \frac{c}{c-2} \right)^2 = \left( \frac{5.32}{3.32} \right)^2 = 2.56$$

and since  $P=P_1+P_2=600$  kg, the loads on the springs are  $P_1 \approx 430$  kg and  $P_2 \approx 170$  kg.



The diameter of the wire for the internal spring is found by the formula (488):

$$d_2 = 1.6 \sqrt{\frac{P_2 c k}{[\tau]}} = 1.6 \sqrt{\frac{170 \times 5 \times 1.2}{85}} = 5.5 \text{ mm.}$$

The diameter of the wire for the external spring—from the equation (503):

$$d_1 = d_2 \sqrt{\frac{P_1}{P_2}} = 5.5 \sqrt{\frac{430}{170}} \approx 9 \text{ mm.}$$

From the wire standard we take  $d_2 = 5 \text{ mm}$  and  $d_1 = 10 \text{ mm}$ .

Further calculations and the plotting of the characteristic for the cluster spring can be done on the basis of the conclusions in the preceding sections.

Powerful and stiff springs are made with square or rectangular coils (Fig. 309, c).

*Conical* springs may have round (Fig. 309, d) or rectangular coils with a large height-to-thickness ratio. The latter are made from flat steel and are called *telescoping* (Fig. 309, e).

The main feature of such springs is the different diameter of adjacent coils. This circumstance also causes different values of deflection: the greater the diameter  $D$  of the coil the greater is its deflection  $\lambda$ .

At a certain value of the compressive force  $P$  the larger coils may successively be put out of action by seating on the next smaller coil.

This dropping out of action decreases not only the number of the coils  $i$  participating in the work but also the mean diameter of the entire spring. These two circumstances affect the stiffness of the spring [see formula (494)] which gradually increases.

Depending on purpose springs can be selected with a characteristic that will change in accordance with a predetermined regularity.

**Bar Springs.** For elastic elements use is sometimes made of *elastic bars* called *torsion bars* (Fig. 309, f).

The torsional stress of a bar under the action of the torque  $M_t = Pa$  is

$$\tau = \frac{16M_t}{\pi d^3} \leq [\tau]. \quad (505)$$

The angle of bar twist is

$$\varphi = \frac{32M_t l}{\pi d^4 G} \text{ radians} \quad (506)$$

where  $l$  is the working length of the bar in cm;

$d$ —its diameter in cm;

$G$ —the modulus of elasticity in shear in kg/cm<sup>2</sup>.

Solving simultaneously the equations (505) and (506) we get at  $G = 8 \times 10^5 \text{ kg/cm}^2$  the formula for determining the diameter of the

bar at the given values of  $l$ ,  $[\tau]$  and  $\varphi$ :

$$d = 25 \times 10^{-7} \frac{l}{\varphi} [\tau] \text{ cm.} \quad (507)$$

Fig. 309, *g* shows an elastic element in the form of a cylindrical rubber block in torsion.

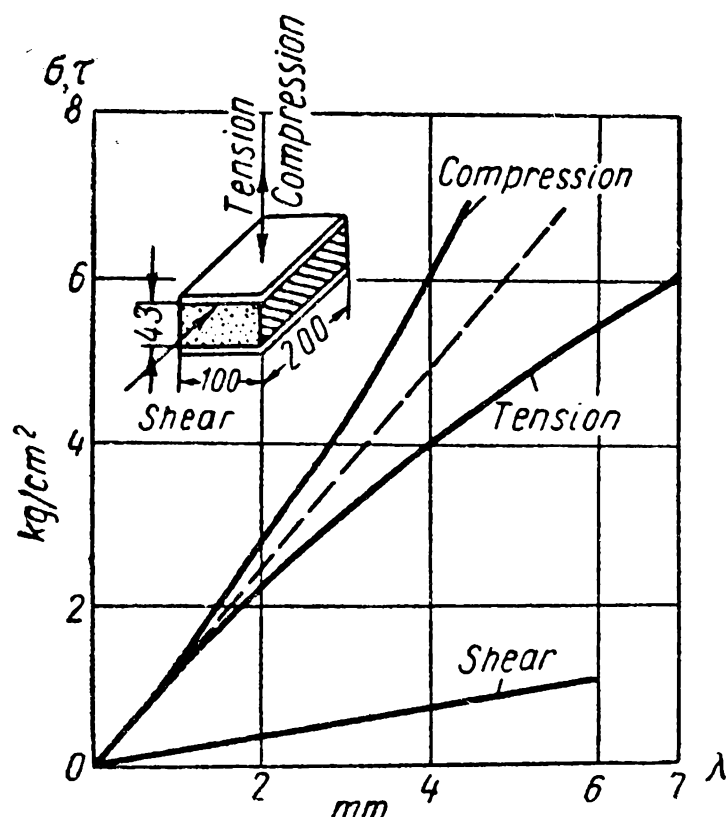


Fig. 314

Torque is transmitted through steel washers bonded to the cylinder ends. Rubber elastic elements are gaining widespread favour in assemblies of machines due to the property of rubber of allowing considerable deformations with dispersion of a great amount of energy per unit of volume.

Rubber bonded to metal plates and bushings can work in tension, compression and shear (Fig. 314).

Designs of elements where rubber works mainly in shear possess greater possibilities with respect to changing the form and the better utilisation of the elastic properties of rubber.

### FLEXURAL STRESSED SPRINGS

**Helical Springs.** This group of springs includes flexural stressed helical springs loaded by torque  $Pa$  (Fig. 309, *h*). These springs are extensively used in farm and other machinery. The work expended in such springs is transformed into the work of elastic turn of the coils around the longitudinal axis of the spring.

Such springs are wound with a helix angle of  $\alpha \leq 12^\circ$  with a certain clearance between the coils to prevent them from touching each other on twisting.

To obtain design relations, as in extension-compression springs, the effect of additional factors connected with the helix angle and the curvature of the coils is accounted for by the factor  $k_0$ .

For springs with round coils  $k_0 = \frac{4c-1}{4c-4}$ .

Analysis of the work of helical torque loaded springs shows that the torque causes a pure flexion of the coil. With account taken of  $k_0$ , the maximum stresses in the cross-section are determined from

the formula

$$\sigma_{\max} = \frac{Mk_0}{W} \leq [\sigma] \quad (508)$$

where  $W$  is the polar section modulus.

The diameter of the wire (bar) is

$$d = 2.15 \sqrt[3]{\frac{Mk_0}{[\sigma]}} \text{ cm.} \quad (509)$$

Here  $[\sigma] = (1.25-1.5)[\tau]$  is the allowable bending stress for the wire material in  $\text{kg/cm}^2$ ;

$M$  is the loading torque in  $\text{kg/cm}$ .

The deflection of a torsional spring is determined by the angle of turn  $\varphi$  (Fig. 315, *b*) between the end coils which, as is proved by the

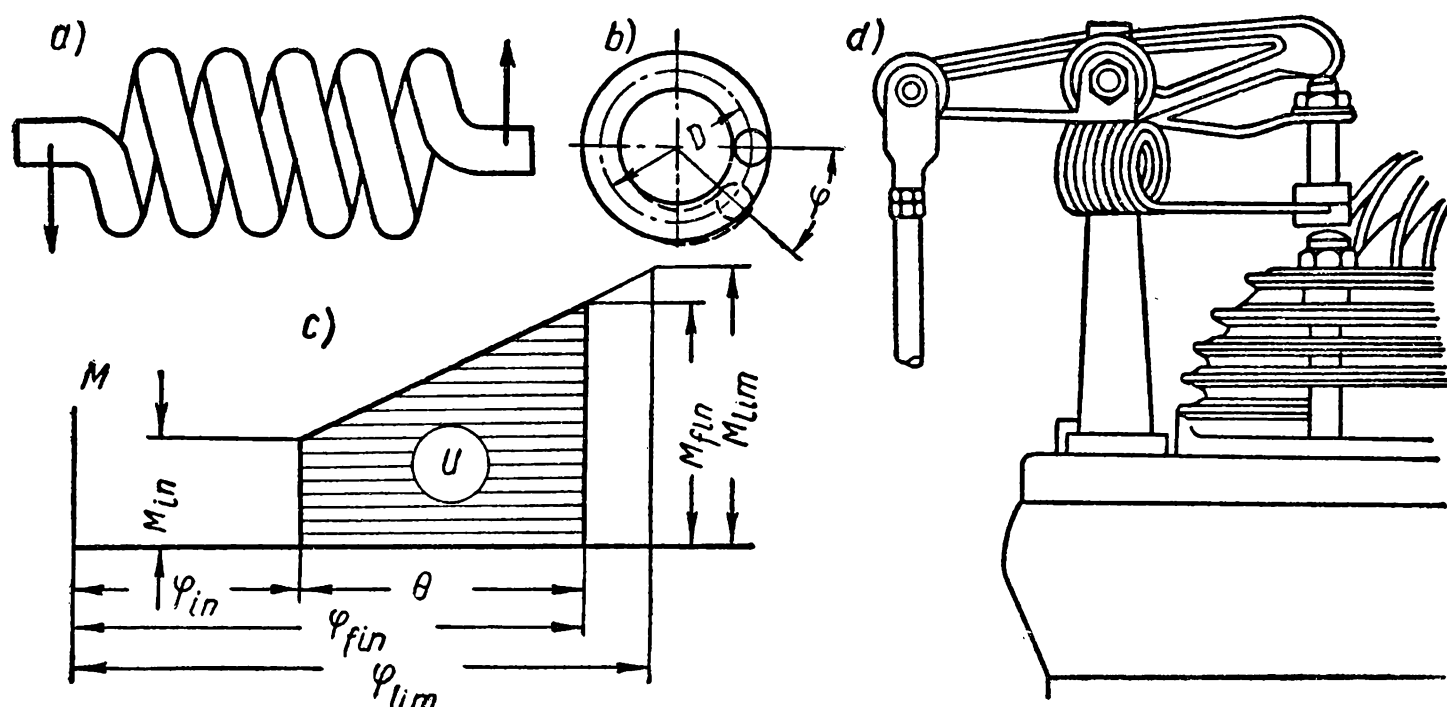


Fig. 315

theory of the strength of materials, can be found from the formula

$$\varphi = \frac{Ml}{EI} \text{ radians} \quad (510)$$

where  $E$  is the modulus of normal elasticity;

$I$ —the moment of inertia of the cross-section in bending;

$l$ —the unwound length of the wire or bar.

Since  $l = \pi Di$  (because  $\cos \alpha \approx 1$ ) then, taking for steel wire  $E = 2 \times 10^6 \text{ kg/cm}^2$ , after substitution in the formula (510) we shall obtain for a spring with round coils

$$i = 0.32 \times 10^5 \frac{\varphi}{M} \times \frac{d^4}{D} \quad (511)$$

where  $\varphi$  is the angle of twist in radians;

$M$ —the torque acting on the spring in kg/cm;  
 $D$  and  $d$ —the mean diameters respectively of the spring coils and of the wire in cm.

From the equations (509) and (511) we get the following formula for determining the number of coils with a given material and the given sizes  $D$ ,  $d$  and  $\varphi$ :

$$i = 3.2 \times 10^5 \frac{k_0}{c} \times \frac{\varphi}{[\sigma]}. \quad (512)$$

The characteristic of the spring which reflects the connection between the applied torque and the deformation is given in Fig. 315, c.

The initial torque  $M_{in}$  corresponds to the initial twisting of the spring by the angle  $\varphi_{in}$ . It preloads the spring and ensures a tight contact between the assembly parts.

Tentatively

$$0.1M_{fin} \leq M_{in} \leq 0.5M_{fin}.$$

The energy stored by the spring in the process of loading is

$$U = \frac{M_{fin} + M_{in}}{2} (\varphi_{fin} - \varphi_{in}).$$

Fig. 315, d shows a torsional spring in the valve mechanism of an aircraft engine.

If the load applied to the spring changes from  $P_{in} = P_{min}$  to  $P_{fin} = P_{max}$  and is of infinitely multiple action the spring should be calculated for endurance (springs in automatic machine tools, engine valves, etc.).

The calculation of springs for endurance is reduced to determining the safety margin by the formula (12).

Shot peening of springs considerably increases their endurance.

**Spiral Springs.** Spiral springs are loaded with torque. These springs are extensively used in clocks and watches, various instruments, firearms, etc.

The spring is loaded by turning spindle 1 (Fig. 316, a) rigidly connected to one end of spring 2.

During operation the spring gradually unwinds and rotates drum 3 with which it is connected by its other end.

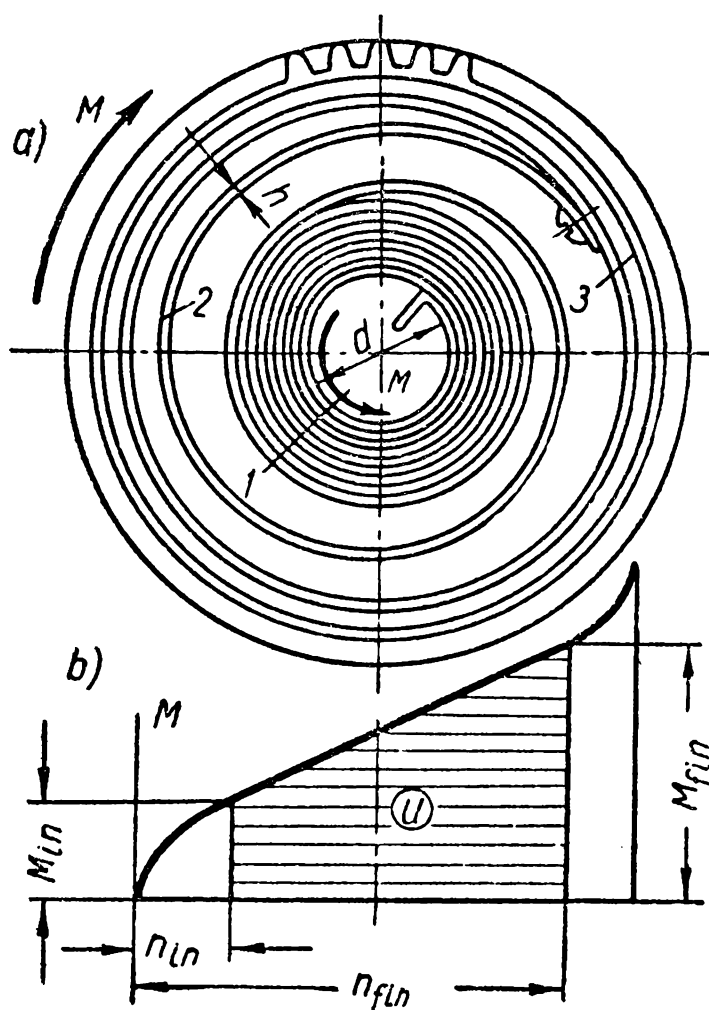


Fig. 316

These springs are made from high-carbon steel. Thermal treatment includes hardening and tempering.

After being wound the spiral spring in a coiled state is placed in a drum and kept there for a long time. This operation is similar to the presetting of coil springs.

When the spring ends are rigidly secured the applied torque  $M$  will cause flexion of the spring; its width  $b$  is found from the formula

$$b = \frac{6M}{h^2 [\sigma]} \text{ cm} \quad (512')$$

where  $M$  is the loading torque in kg/cm;

$[\sigma]$ —the allowable stress for bending for the spring material in kg/cm<sup>2</sup>;

$h$ —the thickness of the spring in cm, usually equal to  $(0.03-0.04)d$  where  $d$  is the diameter of the spindle (see Fig. 316, *a*).

The spring deformation is found from the formula (510) for a torsional helical spring. Substituting for a given case in this formula the corresponding value of  $I$ , assuming for the steel band  $E=2 \times 10^6$  kg/cm<sup>2</sup> and remembering also that at  $n$  revolutions of the drum the angle of twist  $\varphi=2\pi n$  we obtain

$$l = 10.5 \times 10^5 \frac{n}{M} b h^3 \text{ cm.} \quad (513)$$

If we substitute here instead of  $b$  its value from (512') we shall find that

$$l = 63 \times 10^5 \frac{nh}{[\sigma]} \text{ cm.} \quad (514)$$

As a rule, spiral and helical springs are preloaded with the torque  $M_{in}$  when fitted. If we assume that this torque corresponds to  $n_{in}$  of revolutions of the winding spindle then the total energy stored by the spring will be

$$U = \frac{M_{fin} + M_{in}}{4\pi} (n_{fin} - n_{in}).$$

This reasoning is true only when the spring ends are rigidly fastened. When they are hinge-jointed the calculation proceeds in a somewhat different manner.

The accurate calculation of spiral springs requires the remanent stresses of presetting to be taken into account. It becomes even more difficult when it is remembered that, during the initial and final periods of operation of the spring, not all its length  $l$  but only a portion of it takes part in the work. The rest of the spring wound around a bar or pressed against the drum is inactive. This explains why only the middle portion of the characteristic of the spiral spring is rectili-

near (Fig. 316, *b*), reflecting the linear dependence  $M=f(n)$  in conformity with the formula (513).

**Disc Springs.** Disc springs (Fig. 309, *j*) consist of a set of disc elements in the form of dishes (Fig. 317, *a*) with the angle  $\theta=2-6^\circ$  and made from sheet steel (grade 60C2A or similar) 1 to 20 mm thick. They work as compression springs.

The diameter of the base  $D$  of the element of a disc spring varies between 28 and 300 mm and the dish height  $h$  is 0.6-9 mm.

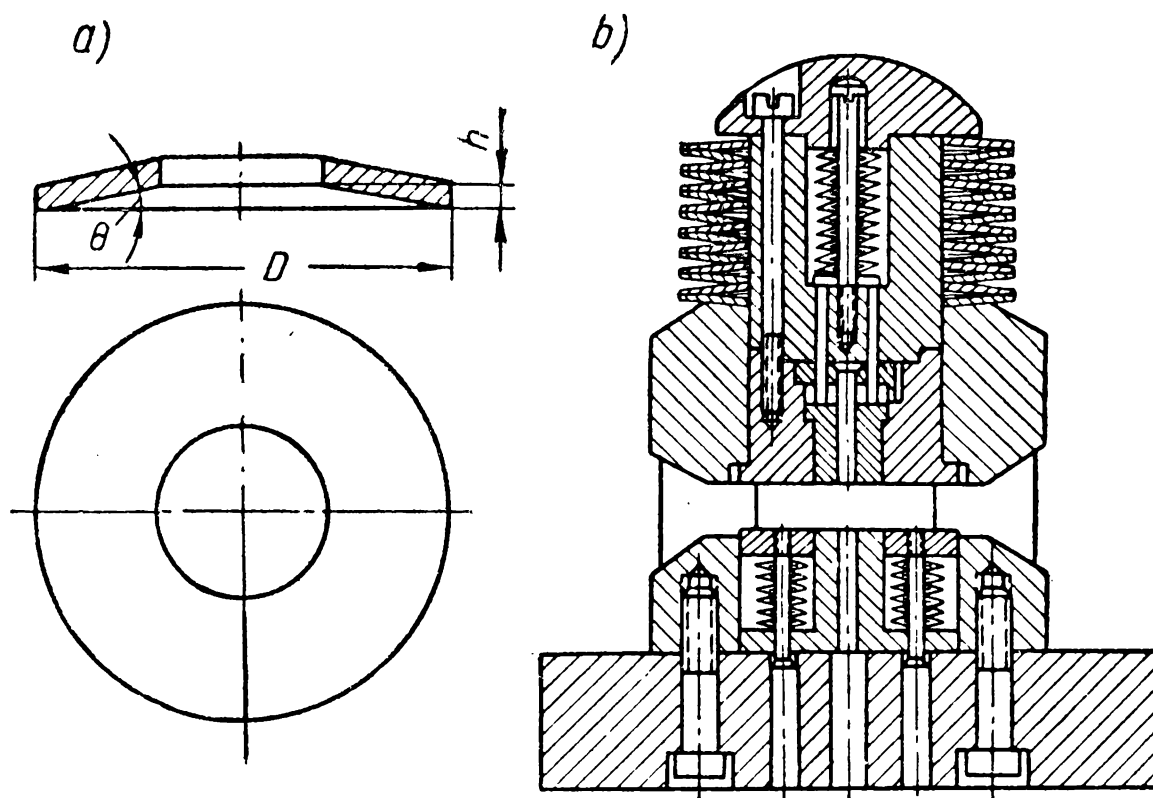


Fig. 317

When the spring is loaded on its perimeter its discs are subjected to elastic deformation. The dish height should not be reduced to less than  $0.8 h$ .

Disc springs belong to the group of stiff springs and can withstand severe loads. For this reason they are sometimes employed in construction frames for the vibrational insulation of industrial structures.

Soviet standards specify disc springs with diameters from 28 to 300 mm. These springs allow the maximum working load of 52 tons. To increase deflection they are assembled in sections. The magnitude of deflection is in this case proportional to the number of springs in the set.

Fig. 317, *b* shows a spring cushion of a metal-working die.

It is difficult to plot the characteristic of a disc spring because its calculation is very complex. In practice the values for springs of this type are selected from tables. To increase the carrying capacity of disc springs they are preset, i. e., subjected to preliminary plastic compression.

**Flat Springs.** Flat springs are extensively used in farm and other machinery. Springs of this type are usually intended for efforts acting over a short distance.

Flat springs can be supported at both ends and take the load in the middle, or be secured at one end and take the load at the other.

The stress in a cantilever spring (Fig. 309, *k*) is

$$\sigma = \frac{M}{W} \leq [\sigma] \quad (515)$$

where  $M = Pl$  is the bending moment;  $W$ —the section modulus to flexion.

The deflection is found from the formula

$$\lambda = \frac{Pl^3}{3EI} = \frac{2Ml^2}{3EW h} \quad (516)$$

Solving simultaneously (515) and (516) at  $E = 2 \times 10^6$  kg/cm<sup>2</sup> we find the thickness  $h$  of the steel spring with given values of  $l$ ,  $\lambda$  and  $[\sigma]$

$$h = 33 \times 10^{-8} \frac{l^2}{\lambda} [\sigma] \text{ cm.} \quad (517)$$

Here  $l$  is the spring length in cm,

$\lambda$ —deflection in cm;

$[\sigma]$ —the allowable stress in bending in kg/cm<sup>2</sup> (see p. 565).

The spring width is

$$b = \frac{6M}{h^2 [\sigma]} \text{ cm.} \quad (518)$$

#### TENSION-COMPRESSION STRESSED SPRINGS

**Ring Springs.** A ring spring (Fig. 309, *l*) is composed of a set of specially profiled rings. When the end rings are loaded on the perimeter the outer rings move over the inner ones. As a result the outer rings expand and the inner contract. Simultaneously, the total height of the spring decreases.

After the external load has been removed, the internal forces of elasticity again bring the rings apart. This becomes possible because the angle of taper  $\beta$  (Fig. 318, *a*) is larger than the angle of friction  $\varrho$  between the ring surfaces.

The work of friction when the ring spring is relieved from load is about 2/3 of all work done by it under load. This means that ring springs can effectively cushion shocks and jerks.

For this reason they are widely employed in shock-absorbing devices carrying severe loads.

Fig. 318, *b* shows the design of a buffer of a railway car with ring and helical springs.

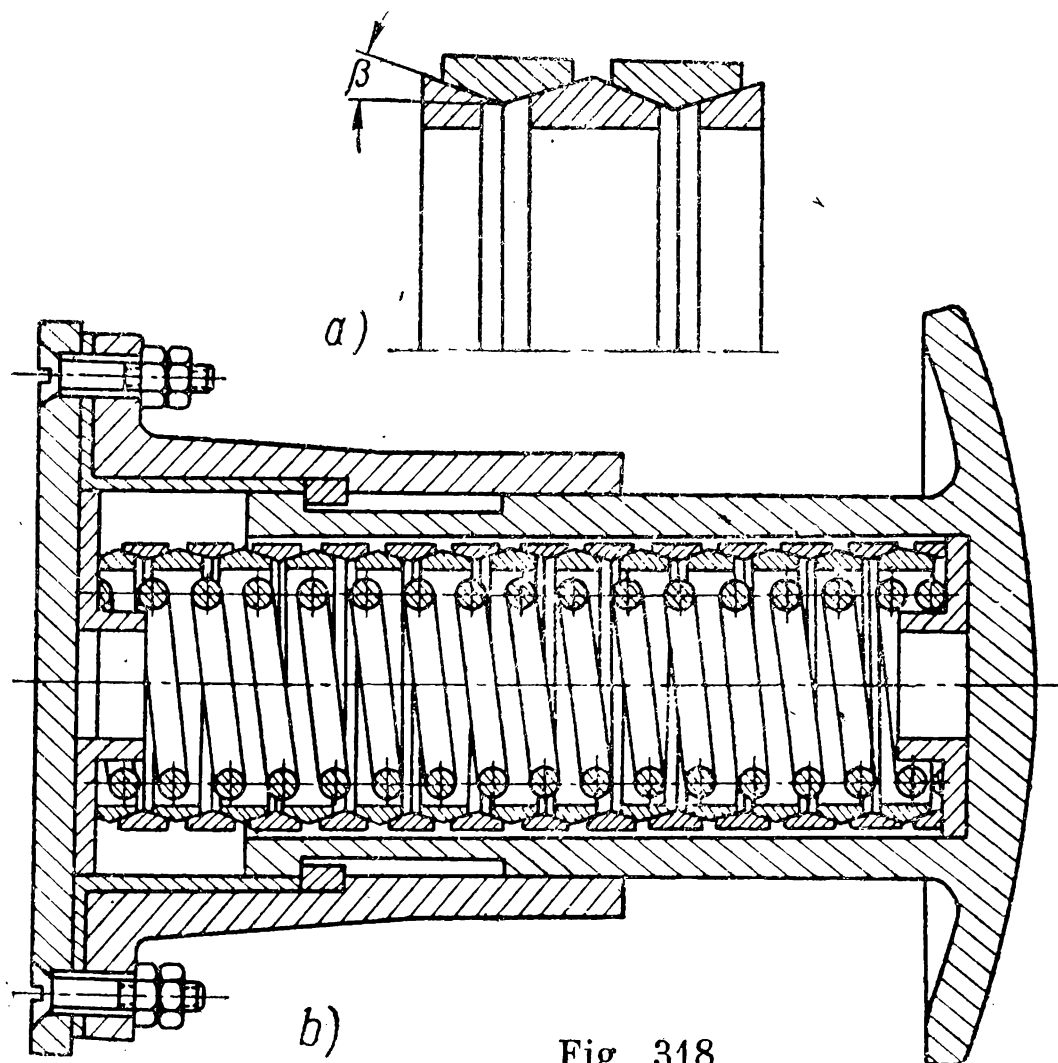


Fig. 318

The comparatively high cost of ring springs limits their application.

**Block Springs.** Block compression springs with *rubber* elastic elements (Fig. 309, *m*) in the form of blocks of various form are used mainly as shock-absorbers to cushion shocks and decrease vibration (see, for example, the compression buffer of the front suspension of the Soviet "Pobeda" car in Fig. 308).

In compression the rubber displays maximum stiffness (see Fig. 314).

The stress arising under the action of the force  $P$  (Fig. 309, *m*) is

$$\sigma = \frac{P}{F} \leq [\sigma]_c \quad (519)$$

and the deformation

$$\lambda = \frac{Ph}{EF}$$

or

$$\lambda = \frac{h [\sigma]_c}{E} \text{ cm.} \quad (520)$$

Here  $h$  is the height of the block in cm;

$[\sigma]_c = 10\text{-}50 \text{ kg/cm}^2$ —the allowable compressive stress depending on the quality of rubber and the nature of loading;

$E = 18\text{-}100 \text{ kg/cm}^2$ —the modulus of longitudinal elasticity of the rubber.



## LEAF SPRINGS

Leaf springs are employed mainly in shock-absorbing devices of automotive vehicles and in some designs of forging equipment.

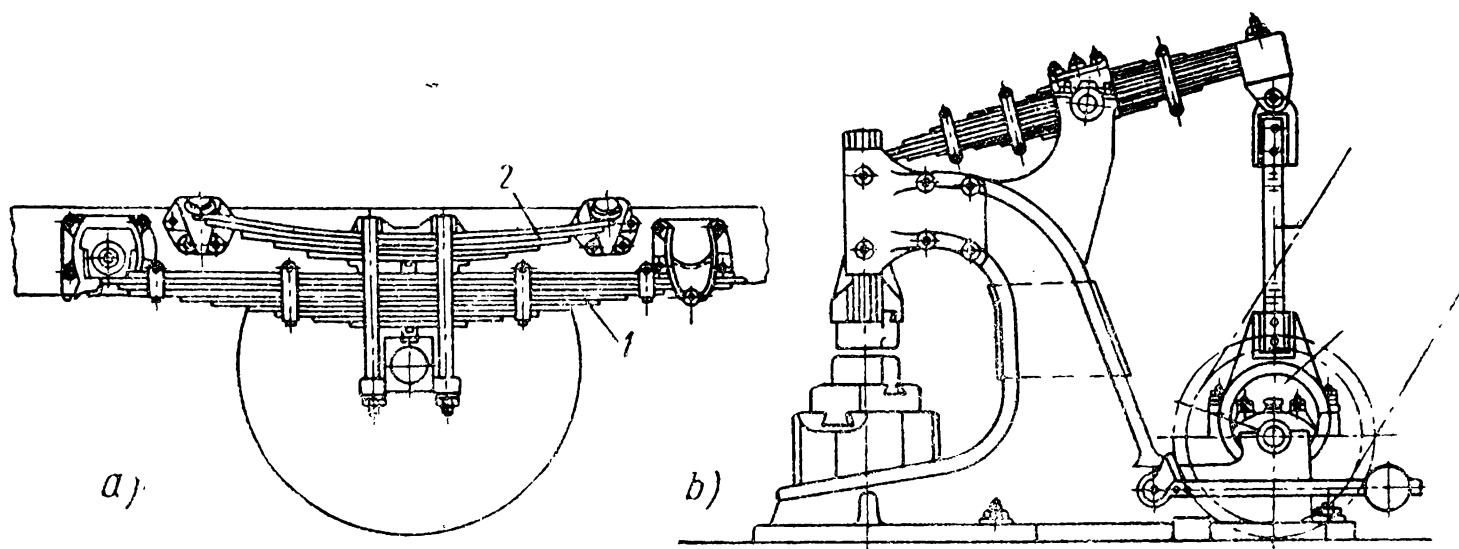


Fig. 319

Fig. 319, *a* shows the suspension of the Soviet ЯГ-6 lorry and Fig. 319, *b* — a forging hammer of the «Ajax» type.

A leaf spring is a beam of equal resistance to bending composed of steel strips (Fig. 320, *a*). To decrease stresses the leaves are given a curvilinear form (Fig. 320, *b*) so that an assembled leaf spring is subject to a preliminary deformation opposite to that caused by the forces acting upon it during operation in a machine.

Leaves are made from manganese steel of grade 50ХГ or silicon-manganese steel of grade 55С2 with the ultimate strength  $\sigma_{ul} = 130 \text{ kg/mm}^2$ . To increase the fatigue strength the leaf blanks are sometimes subjected to shot peening.

Leaf springs are calculated by the formulae for the lateral flexure of beams.

The specific conditions of leaf spring operation due to the unequal length of the leaves and the presence of friction between them during flexure are taken into account by introducing the factor  $k > 1$ . The curvature of the leaf spring is neglected in practical calculations.

Practice has confirmed the correctness of the assumption that the effort  $P$  acting upon a leaf spring is distributed uniformly between

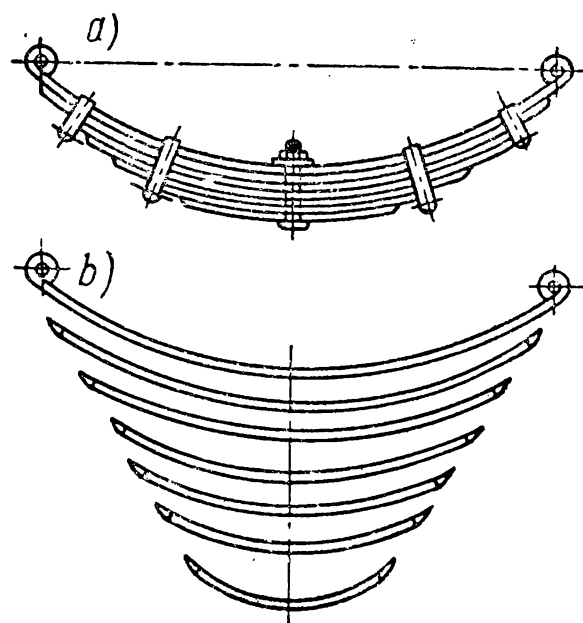


Fig. 320

the leaves, i. e., the effort acting on one leaf  $P_1 = \frac{P}{i}$  where  $i$  is the number of leaves in the spring.

The length of leaves is so selected that the spring assembled from them forms a beam of equal resistance.

Most widespread are the following three types of leaf springs: a) *quarter-elliptic*, b) *cantilever*, c) *semi-elliptic*.

For a quarter-elliptic leaf spring (Table 68) the stress in the leaf is

$$\sigma = \frac{M_b}{iW} = \frac{6Pl}{ibh^2} \ll [\sigma] \quad (521)$$

and the deflection is

$$\lambda = \frac{kPl^3}{3Ei} = \frac{4kPl^3}{Eibh^3} \quad (522)$$

In these formulae  $P$  is the load applied to the spring end;  $l$ —the leaf spring length;  $i$ —the number of leaves;  $b$  and  $h$  are the width and thickness of one leaf respectively,  $E$ —the modulus of elasticity.

As applied to design diagrams of cantilever and semi-elliptic leaf springs the formulae obtained in this manner for the value of the stress and deformation are given in Table 68.

It follows from the comparison of the formulae in Table 68 that a quarter-elliptic spring possesses the greatest flexibility. All other conditions being equal, the deflections of quarter-elliptic, cantilever and semi-elliptic leaf springs are related to one another as 16 : 4 : 1.

In existing designs the deflection of leaf springs reaches 300 mm.

As distinct from the leaf springs with a constant stiffness, there are designs in which the leaf spring stiffness is a variable magnitude. Thus, for example, in the double spring in Fig. 319, *a* only the main leaf spring 1 is in operation under small loads. As the load increases the deflection of the main spring also increases so that leaf spring 2 will participate in the work.

This design makes it possible to calculate the main spring not for full but for partial load.

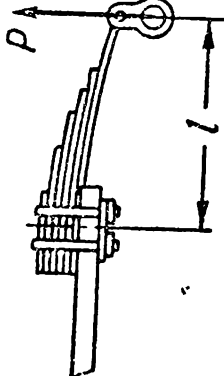

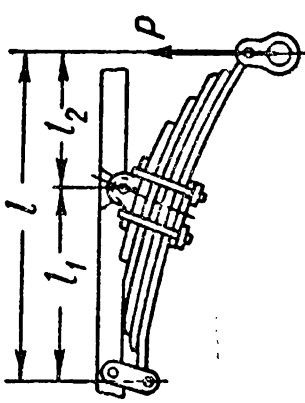
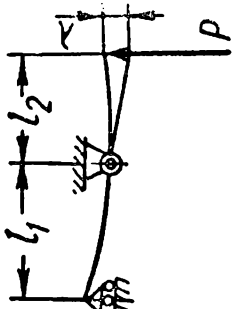
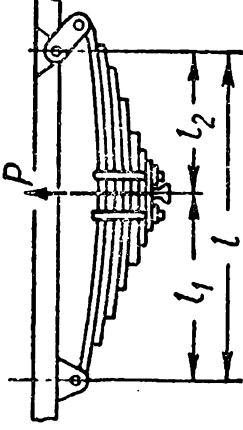
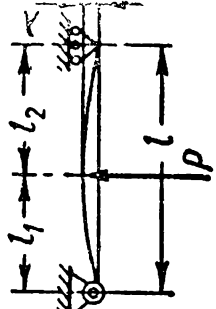
As a result, its rigidity can be less, which, in lorries for example, causes smoother movement when they carry no load.

*Calculation.* The practical calculation of leaf springs is reduced to determining the number of leaves  $i$  and their proportions  $h$  and  $b$  by the given values of the load  $P$  and the deformation  $\lambda$ .

For a quarter-elliptic leaf spring by the formulae (521) and (522) at  $E = 2 \times 10^6$  kg/cm<sup>2</sup> we obtain

$$h = \frac{1}{3} \times 10^{-6} kl^2 \frac{[\sigma]}{\lambda} \text{ cm.} \quad (523)$$

Table 68  
Formulae for Calculating the Main Types of Leaf Spring

Type of spring	Sketch	Design diagram	Stress $\sigma$ in kg/cm <sup>2</sup>	Deflection $\lambda$ in cm	Thickness of leaf $h$ in cm	Parameter $ib$ in cm
Quarter-elliptic			$\sigma = \frac{6Pl}{ibh^2}$	$\lambda = \frac{4kPl^3}{Eibh^3}$	$h = \frac{1}{3} \times 10^{-6} kl^2 \frac{[\sigma]}{\lambda}$	$ib = \frac{6Pl}{h^2 [\sigma]}$
Cantilever			$\sigma = \frac{3Pl}{ibh^2}$	$\lambda = \frac{kPl^3}{Eibh^3}$	$h = \frac{1}{6} \times 10^{-6} kl^2 \frac{[\sigma]}{\lambda}$	$ib = \frac{3Pl}{h^2 [\sigma]}$
Semi-elliptic			$\sigma = \frac{3Pl}{ibh^2}$	$\lambda = \frac{kPl^3}{4Eibh^2}$	$h = \frac{1}{24} \times 10^{-6} kl^2 \frac{[\sigma]}{\lambda}$	$ib = \frac{3Pl}{h^2 [\sigma]}$

Notes: 1. In these formulae the load  $P$  is in kg, the allowable stress  $[\sigma]=4,500-6,000$  kg/cm<sup>2</sup> (chosen depending on the operating conditions of the spring); the other dimensions are in cm.  
2. The factor  $k=1.25-1.5$ ; the nearer a spring to a beam of equal resistance to bending, the greater  $k$  is.

For the same leaf spring from the formula (521)

$$ib = \frac{6Pl}{h^2 [\sigma]} \text{ cm.} \quad (524)$$

The formulae obtained in the same way for  $h$  and  $ib$  of cantilever and semi-elliptic springs are given in Table 68.

*Example.* Calculate a quarter-elliptic leaf spring by the following initial data:  $P=750$  kg;  $l=500$  mm;  $\lambda_{\max}=60$  mm; the spring material is steel for which  $[\sigma]=6,000$  kg/cm<sup>2</sup>.

We assume tentatively  $k=1.25$ ; then by the formula (523)

$$h = \frac{1}{3} \times 10^{-6} kl^2 \frac{[\sigma]}{\lambda} = \frac{1}{3} \times 10^{-6} \times 1.25 \times 50^2 \times \frac{6,000}{6} = 1.04 \text{ cm.}$$

From the spring steel standard we find  $h=10$  mm.  
By the formula (524)

$$ib = \frac{6Pl}{h^2 [\sigma]} = \frac{6 \times 750 \times 50}{6,000} = 37.5 \text{ cm.}$$

We take  $i=5$  and  $b=75$  mm.

## CHAPTER XXV

### MACHINE FRAMES

Beds, bases and box-type housings, all of which in our further exposition we shall call *machine frames* for brevity, comprise, as a rule, a considerable part of the total weight of machines (for example, in machine tools up to 70-90%). It is obvious therefore that reduction in the weight of a machine largely depends on the material, form and dimensions of the machine frames.

Because of a great diversity of designs of machine frames we shall deal with them only in general outline.

The problems of designing and calculating machine frames should be the subject for detailed study of special courses (dealing, for example, with metal-cutting machine tools, forging and metal-working machines, steam and gas turbines, etc.).

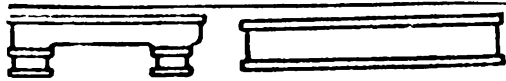
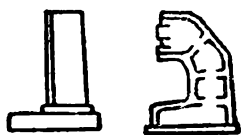
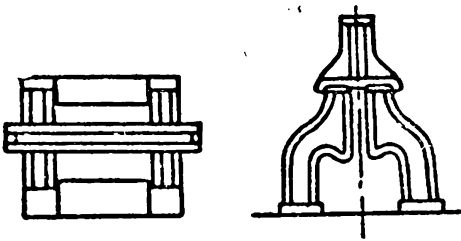
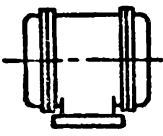
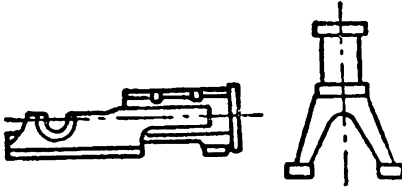

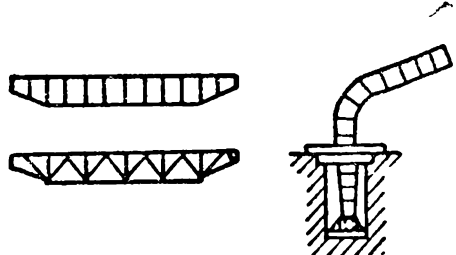

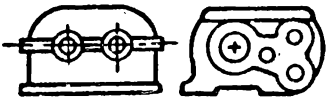
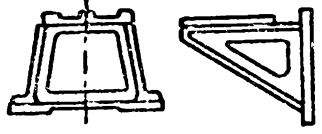
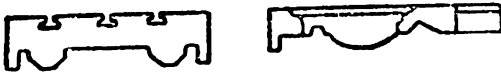

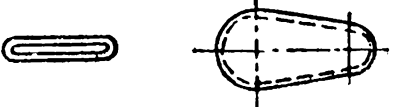
*Classification of machine frames.* Table 69 shows an enlarged classification of machine frames suggested by D. N. Reshetov.

Machine frames can be subdivided by various characteristics into the following groups.

*By purpose* into:

- 1) beds, frameworks, carrying bodies;
- 2) bases, bedplates;
- 3) housing-type components of assemblies including: a) housings, boxes; b) columns, pillars, brackets and other stationary supporting

Table 69

Machine Frames	
	Simple frames and beds of horizontal machines
	Simple frames and beds of vertical machines
	Portal frames
	Circular frames, housings
	Frames of piston machines, banks of cylinders
	Frames of conveying machines
	Crane structures
	Baseplates
	Boxes
	Pillars, brackets, pedestals, hangers, etc.
	Tables, slide blocks, carriages
	Crossheads, slides, jibs
	Lids, covers and casings

members; c) worktables, carriages, slides and other movable supporting members; d) casings and covers.

*By form into:*

1) components in which one overall size considerably exceeds the two others (machine-tool beds, crosspieces, slides);

2) components in which one overall size is considerably less than the other two (bedplates, tables);

3) components in which all three overall sizes are the same (boxes and similar parts).

*By the presence of a parting plane into:*

1) monoblock type; 2) split type.

*By operating conditions into:*

1) stationary; 2) movable.

*By the method of manufacture into:*

1) cast; 2) welded; 3) combined.

*Choice of the optimal forms of cross-section, systems of ribs and partitions.* It is typical of the majority of machine frames (beds, pillars, brackets) that they operate in conditions of complex stress and the strain of their material is simultaneously composed of bending, torsion and tensile strains.

It follows from the formulae for the strength of materials for stresses and strains that in tension and compression the strength and rigidity of an element depend, all other conditions being equal, only on the area of its cross-section and not on its form. Therefore, in these cases the consumption of material is entirely determined, on the one hand, by the acting forces and, on the other, by allowable stresses and deformations. Conversely, in bending and torsion the consumption of material can be reduced by a rational choice of form for the cross-section of the element with a view to increasing the moments of resistance and inertia while maintaining the same cross-sectional area, i.e., the same weight of this element. The effect achieved here is illustrated in Table 70.

The table shows that as far as rigidity in bending and especially in torsion is concerned, a section in the form of a hollow rectangle is the most rational. In bending strength it is slightly inferior only to an I-section and in torsional strength—to a circular section. Since design considerations, particularly with regard to the possibility of convenient conjunction with other components, also favour this form of cross-section, it underlies the design of most machine frames.

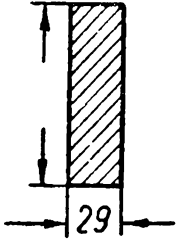
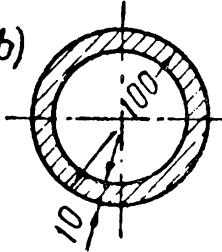
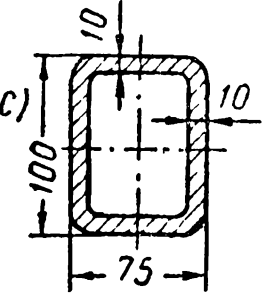
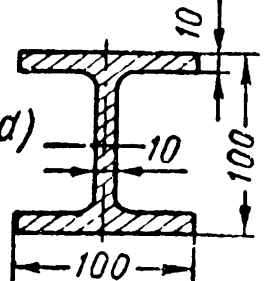
The strength and especially rigidity of hollow machine frames is increased by ribs and partitions, which are especially necessary when the operating conditions of the component do not allow it to be completely closed so that it remains open on one or two sides. This is the case with lathe bedplates. So that shavings can fall through

the bed and be easily removed, the bed in many lathes consists of two walls connected by a system of ribs and partitions.

In other cases the presence of apertures (holes) in the walls is dictated by the necessity of accommodating various mechanisms and units inside machine frames.

Table 70

Maximum Bending Moments and Torques for Cross-Sections of Various Forms

Cross-section		Weight in kg/m	Maximum allowable bending moment			Maximum allowable torque			
Form	Area in cm <sup>2</sup>		by stress		by deflection, relative value	by stress		by relative angle of twist	
			in kg/cm	relative value		in kg/cm	relative value	in kg/cm	relative value
a) 	29.0	22	$48.3 \times [\sigma]_b$	1.0	1.0	$2.7 \times [\tau]_t$	1.0	$66 \times G \times \theta$	1.0
b) 	28.3	22	$58.2 \times [\sigma]_b$	1.2	1.15	$116 \times [\tau]_t$	43	$580 \times G \times \theta$	8.8
c) 	29.5	22	$66.3 \times [\sigma]_b$	1.4	1.6	$104 \times [\tau]_t$	38.5	$2,070 \times G \times \theta$	31.4
d) 	29.5	22	$90 \times [\sigma]_b$	1.8	1.8	$12 \times [\tau]_t$	4.5	$126 \times G \times \theta$	1.9

The effectiveness of partitions and ribs largely depends on their arrangement. Sometimes, an increase in rigidity due to partitions is negligible and does not compensate for the additional consumption

of material and labour expended on the manufacture of the component. This is illustrated by Table 71 which compares for several models relative (as compared to a component of a box-like section of equal size but without partitions) values of rigidity  $S_b$  in bending and  $S_t$  in torsion, weight  $G$  and unit rigidities  $\frac{S_b}{G}$ ,  $\frac{S_t}{G}$ .

Table 71

**Characteristics of Bending and Torsional Rigidities for Models of Various Forms**

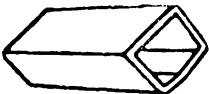
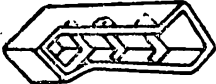



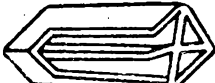
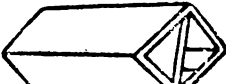
Model No.	Model form	Relative rigidity in bending $S_b$	Relative rigidity in torsion $S_t$	Weight of model $G$	$\frac{S_b}{G}$	$\frac{S_t}{G}$
1 (basic)		1.00	1.00	1.00	1.00	1.00
2a		1.10	1.63	1.10	1.00	1.48
2b		1.09	1.39	1.05	1.04	1.32
3		1.08	2.04	1.14	0.95	1.79
4		1.17	2.16	1.38	0.85	1.56
5		1.78	3.69	1.49	1.20	3.07
6		1.55	2.94	1.26	1.23	2.39

Table 71 shows the little effect all partitions have on the bending rigidity except those used in the models 5 and 6. For models 3 and 4 the relative increase in  $S_b$  is even smaller than the relative increase in weight ( $\frac{S_b}{G} < 1$ ). The question naturally arises as to whether it would not be more expedient to use the same amount of material not for partitions but to increase the thickness of the walls. The answer is provided by Table 72; the second solution is somewhat more advantageous as regards bending rigidity for all models, except 5 and 6, but it is unrational as regards torsional rigidity; therefore, generally speaking, it is more expedient to use partitions in a component subjected simultaneously to bending and torsion forces.



*Choice of the wall thickness.* With definite dimensions of machine frames assigned by design their weight is largely due to the wall thickness.

Table 72

Variations in Relative Bending and Torsional Rigidity for Models of Various Forms

Model No.	Relative weight of box-like section	Relative rigidity in bending		Relative rigidity in torsion	
		With ribs	With thicker walls	With ribs	With thicker walls
1 (basic)	1.00	1.00	1.00	1.00	1.00
2a	1.10	1.10	1.15	1.63	1.18
2b	1.05	1.09	1.10	1.39	1.10
3	1.14	1.08	1.16	2.04	1.21
4	1.38	1.17	1.29	2.16	1.40
5	1.49	1.78	1.30	3.69	1.46
6	1.26	1.55	1.19	2.94	1.24

For hollow parts the considerations of higher strength and rigidity in bending and torsion with minimum weight dictate the choice as far as possible of walls of minimum thickness. The stability of thin walls is achieved by reinforcing them with ribs.

In cast parts the minimum thickness of walls is determined mainly by the requirements of the casting processes and partly by machining. These requirements can be formulated as follows:

a) the wall thickness should ensure an adequate filling of the mould with liquid metal; the minimum thickness of walls for castings are given in Table 73.

b) the optimal thickness of the ribs and inner walls amounts to 0.6-0.8 of the thickness of the main wall;

c) the reduced wall thickness—ratio between the cross-sectional area and its perimeter—should be, as far as possible, the same in all parts of the casting; the ratio of the reduced thickness at various points of one casting should not exceed 2-2.5 since, otherwise, shrinkage stresses may arise which will exceed the ultimate strength of the metal;

d) the wall should be thick enough to withstand shocks in knocking out, cleaning and chipping the casting, in handling and also in subsequent machining;

e) the values of the wall thickness indicated above are further increased to compensate for possible inaccuracies in the manufacture and assembly of the core and mould.

To satisfy the above requirements in practice a sufficiently large wall thickness is taken—much larger than necessary to guarantee the strength and rigidity of the part in operating conditions. Thus, for example, the beds of light machine tools are made with walls 12-15 mm thick, of medium—18-22 mm thick and of heavy—23—35 mm thick.

Table 73

Minimum Allowable Wall Thickness of Castings

Metal	Minimum wall thickness of casting in mm	Notes
Carbon steel	Light 6 Medium 10-12 Heavy 15-20	When casting from acid-lined electric furnace the walls of light castings can be up to 4 mm thick, in individual cases up to 3 mm and less (precision casting).
Gray cast iron	Light 3-4 Medium 6-8-10 Heavy 15-20 and more	A 6-mm wall, 1,000 mm long. Globular graphite cast iron allows parts to be cast with the same wall thickness as from gray cast iron.
Inoculated cast iron	15-20% thicker than in castings from gray cast iron	
Malleable cast iron	3-6	When an electric furnace is used, the lower size, i. e., 3 mm is recommended.
Tin bronze	Light 3-5 Medium 6-8	Length up to 150 mm.
Aluminium-base alloys	Light 3-5 Medium 5-8	Length up to 200 mm. In die-casting up to 1.5 mm. For castings from aluminium-copper alloy minimum wall thickness 5 mm.
Magnesium-base alloys	Medium 4 Heavy 6	In die-casting thicknesses as low as to 2 mm are permitted.
Special grades of brass	Minimum 5-6	Aluminium and silicon brass minimum 6 mm.
Zinc-base alloys	Up to 3	In die-casting thicknesses may be decreased to 1.5 mm.
Alloy steel	Depending on the grade of steel but in all cases 20%-40% greater than in corresponding castings from carbon steel.	
Heat-resistant steel	As in castings from grey cast iron.	

Due to the great national importance attached to saving metal close attention should be given to assigning proper thickness to the walls of the principal heavy machine frames. Table 73 should be

used to assign minimum thicknesses on the basis of the capabilities of the foundry industry. As the cultural standard of production grows in a given foundry shop and the casting processes improve the values of wall thicknesses should be regularly reconsidered—decreased in order to approximate them to the values required to meet strength and rigidity standards.

*Cast and welded bedplates.* Machine frames are cast from cast iron, steel or light alloys or welded from rolled steel or cast or rolled steel elements.

As a rule, machine frames are cast from cast iron. In recent years welded frames have been increasingly used instead of cast-iron and all-cast steel frames.

The advantages and disadvantages of cast-iron and steel welded machine frames can be summed up as follows.

a) Ordinary grey cast iron costs less than rolled steel; the mechanical properties of cast iron are inferior to those of steel (see Table 74).

b) To cast a component, a casting pattern, a core box and other tools are required. This involves additional expenditure and more time in manufacture.

c) A weldment requires no patterns. Since the mechanical properties of steel are higher than those of ordinary cast iron a steel weldment weighs less than a cast-iron component with the same loads and margin of safety. This is illustrated by Tables 74 and 75 compiled for steel and cast-iron elements of the same arbitrary length. The figures underlined in the last line (Table 75) show that with the same rigidity the weight of the steel element is  $1/2$ - $3/4$  that of the cast-iron element.

Only in compression does cast iron prove superior in respect of weight to steel if heat-treated steel of a higher quality than 3 or 5 is not used for the manufacture of the given element.

In actual fact, the economy of metal when a cast-iron component is replaced by a steel one depends on the design of both versions.

d) When necessary a weldment can be easily corrected—its strength and rigidity can be improved and its form and dimensions altered. It is far more difficult to make such corrections in a cast component. The possibility of correction is a valuable feature of components used in experimental machines.

By comparing the advantages and disadvantages of both versions we can mark out the fields where they will be most effective.

A welded version is preferable for heavily loaded frames of special-purpose machines to be produced in limited quantity.

For parts carrying moderate loads and to be produced in quantity preference is given to a cast-iron version.

Table 74

Material	Limit of elasticity		Yield point $\sigma_y$	Ultimate strength in			
	1st class $E$	2nd class $G$		tension $\sigma_{ult}$	compression* $\sigma_{ulc}$	bending $\sigma_{ulb}$	torsion $\tau_{ult}$
kg/mm <sup>2</sup>							
Steel 5	21,000	8,000	27	50-53	50-53	50-53	40
Cast iron CY-21-40	10,000	3,800	—	21	75	40	15-25
Maximum stress due to load ( $P$ —in tension-compression, $M$ —in bending, $M_t$ —in torsion)							
				$\sigma = \frac{P}{F}$	$\sigma = \frac{P}{F}$	$\sigma = \frac{M}{W}$	$\tau = \frac{M_t}{W_0}$
Safety factor $n' = \frac{\text{ultimate strength}}{\text{maximum stress}}$				$\frac{\sigma_{ult}}{\sigma} = \sigma_{ult} \frac{F}{P}$	$\frac{\sigma_{ulc}}{\sigma} = \sigma_{ulc} \frac{F}{P}$	$\frac{\sigma_{ulb}}{\sigma} = \sigma_{ulb} \frac{W}{M}$	$\frac{\tau_{ult}}{\tau} = \tau_{ult} \frac{W_0}{M_t}$
At the same load and dimension of the elements the values of $P$ , $M$ , $M_t$ and $W$ , $W^{polar}$ for steel and cast-iron elements are the same; therefore the relation				$\frac{\sigma_{ult2}}{\sigma_{ult1}} = \frac{21}{50} = 0.4$	$\frac{\sigma_{ulc2}}{\sigma_{ulc1}} = \frac{75}{50} = 1.5$	$\frac{\sigma_{ulb2}}{\sigma_{ulb1}} = \frac{40}{50} = 0.8$	$\frac{\tau_{ult2}}{\tau_{ult1}} = \frac{15-25}{40} = 0.4-0.6^*$
$\frac{n'_2}{n'_1} = \frac{\sigma_{ult2}}{\sigma_{ult1}}$ or $\frac{\tau_{ult2}}{\tau_{ult1}}$ , i. e.,							

\* Depending on the form of the element cross-section.  
Note. In Tables 74 and 75  $P$  is the tensile or compressive force,  $M$ —bending moment;  $M_t$ —torque;  $F$ —cross-sectional area of the element;  $W$ —moment of section modulus in bending;  $W_0$ —moment of section modulus in torsion;  $I$ —moment of inertia of cross-section;  $I_0$ —polar moment of inertia of cross-section;  $V$ —volume of the element;  $Q$ —weight of the element. The index 1 is for steel, the index 2—for cast iron. To calculate the ratio  $Q_1:Q_2$  we take  $Q_1=7.8 \times V_1$ ,  $Q_2=7.25 \times V_2$ .

Table 75

Tension		Bending		Torsion	
Form of the element cross-section					
Arbitrary	Same contours, different wall thickness $\delta$	Geometrically similar sections, proportional dimensions; proportionality factor $m$	Same contours, different wall thickness $\delta$	Geometrically similar sections, proportional dimensions; proportionality factor $m$	
	$\frac{F_1}{F_2} = \frac{I_1}{I_2} = \frac{W_1}{W_2} = \frac{V_1}{V_2} = \frac{\delta_1}{\delta_2}$	$\frac{F_1}{F_2} = \frac{V_1}{V_2} = m^2; \frac{W_1}{W_2} = m^3; \frac{I_1}{I_2} = m^4$	$\frac{F_1}{F_2} = \frac{I_{p1}}{I_{p2}} = \frac{W_{p1}}{W_{p2}} = \frac{V_1}{V_2} = \frac{\delta_1}{\delta_2}$	$\frac{F_1}{F_2} = \frac{V_1}{V_2} = m^2; \frac{W_{p1}}{W_{p2}} = m^3; \frac{I_{p1}}{I_{p2}} = m^4$	
At the same margin of safety $n'$					
$\frac{F_1}{F_2} = \frac{\sigma_{ult2}}{\sigma_{ult1}} = 0.4$	$\frac{W_1}{W_2} = \frac{\sigma_{ulb2}}{\sigma_{ulb1}} = 0.8$	$\frac{W_{p1}}{W_{p2}} = \frac{\tau_{ult2}}{\tau_{ult1}} = 0.4-0.6$			
$\frac{V_1}{V_2} = \frac{F_1}{F_2} = 0.4$	$\frac{W_1}{W_2} = \frac{\sigma_{ulb2}}{\sigma_{ulb1}} = 0.8$	$\left(\frac{W_1}{W_2}\right)^{\frac{2}{3}} = 0.8^{\frac{2}{3}} = 0.86$	$\frac{W_{p1}}{W_{p2}} = 0.4-0.6$	$\left(\frac{W_{p1}}{W_{p2}}\right)^{\frac{2}{3}} = 0.4^{\frac{2}{3}} - 0.6^{\frac{2}{3}} = 0.55-0.71$	
$\frac{Q_1}{Q_2} = 1.07; \frac{V_1}{V_2} = 0.43$	$1.07 \times 0.8 = 0.86$	$1.07 \times 0.86 = 0.92$	$1.07 \times (0.4-0.6) = 0.43-0.64$	$1.07 \times (0.55-0.71) = 0.59-0.76^*$	

\* Depending on the form of the element cross-section

Tension	Bending	Torsion
At the same rigidity $S = \frac{\text{load}}{\text{deformation}}$		
$\lambda = \frac{P \times l}{E \times F};$ $S = \frac{P}{\lambda} = \frac{E \times F}{l};$ $\frac{F_1}{F_2} = \frac{E_2}{E_1} = 0.48$	$f = k \frac{P \times l^3}{EI}; S = \frac{P}{f} = \frac{E \times I}{k \times l^3}; \frac{I_1}{I_2} = \frac{E_1}{E_2} = 0.48$	$\theta = \frac{M_t l}{G \times I_p}; S = \frac{M_t}{\theta} = \frac{GI_p}{l}; \frac{I_{p1}}{I_{p2}} = \frac{G_2}{G_1} = 0.48$
$\frac{V_1}{V_2} = \frac{F_1}{F_2} = 0.48$	$\frac{I_1}{I_2} = \frac{E_2}{E_1} = 0.48$	$\left(\frac{I_{p1}}{I_{p2}}\right)^{\frac{1}{2}} = 0.48^{\frac{1}{2}} = 0.69$
$\frac{Q_1}{Q_2} = 1.07; \frac{V_1}{V_2} = 0.51$	$1.07 \times 0.48 = 0.51$	$1.07 \times 0.69 = 0.74$

When similar components are produced in quantity the cost of the patterns per one component is negligible. Under small loads the high mechanical properties of steel will not be utilised to the full advantage.

Such are the general conclusions. In especially important cases the choice of a design is determined by comparative technical and economical calculations. In this case the terms of manufacture, production capabilities of the manufacturer, cooperation and other factors are taken into account.

*Fundamentals of calculation.* Rigidity is the main criterion of the operating capacity of machine frames. In machine tools the rigidity of the bed, for example, determines the productivity and accuracy with which the parts are machined, the rigidity of the housing of a toothed reduction gear determines the correctness of the wheel engagement and hence the operating capacity of the reduction gear as a whole, etc.

As a rule, frames are most complicated parts of a machine requiring much labour and involving greater costs. A damaged frame not infrequently puts the entire machine out of commission for a long time. Therefore, the dimensions of machine frames are so assigned as to safeguard them against breakage even under the maximum possible loads.

When checking the strength of machine frames the design load is assumed to be the maximum load at which the safety device operates or the maximum load possible in the given operating conditions.

*By possible calculation schemes* machine frames can be subdivided into the following groups:

1) components regarded as beams of box-like cross-section (beds and pillars with a completely or partially closed contour of cross-section);

2) components regarded as frames (portal beds, frames of transporting machines, frames of ploughs and other agricultural machines);

3) components regarded as slabs (plates, round and rectangular tables of machine tools under the action of the load not distributed over the entire length);

4) components regarded as boxes ( housings of toothed reduction gears and gearboxes, crankcases).

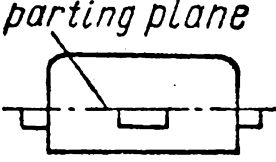
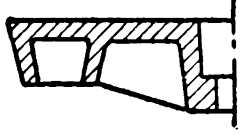
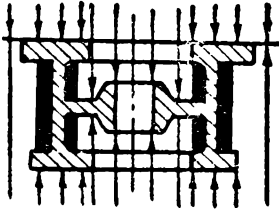
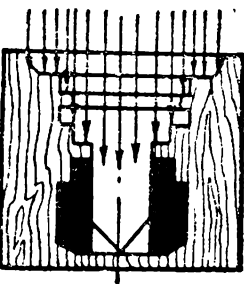
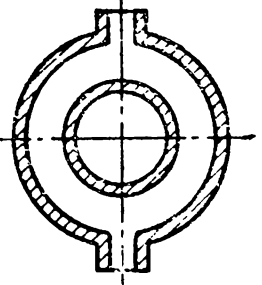
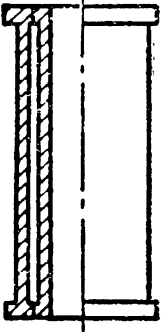

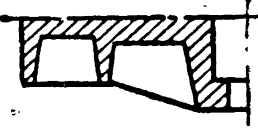
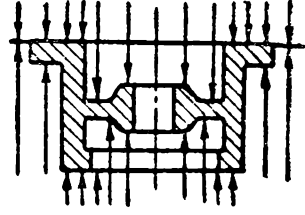
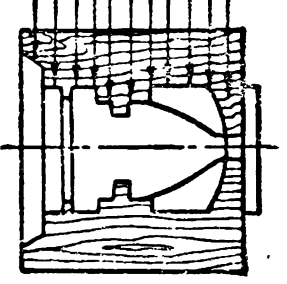
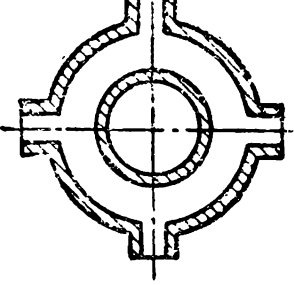
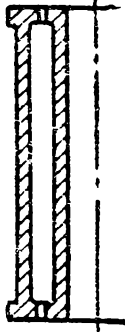
In accordance with this scheme the fundamentals of calculating machine frames are outlined in the theories of the strength of materials, construction mechanics and the theory of elasticity.

Calculations of real components are given in special courses and textbooks describing machines which employ similar components.

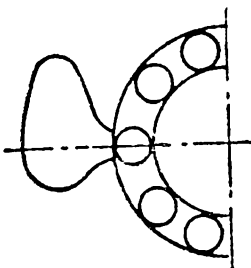
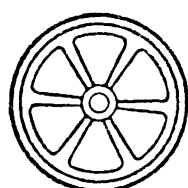
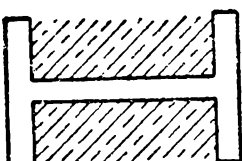
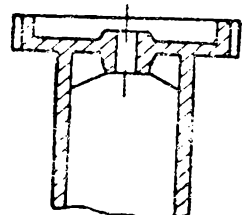
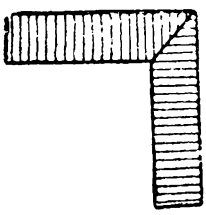
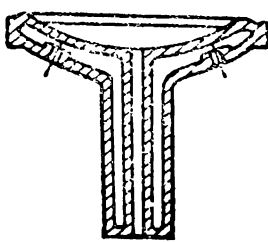
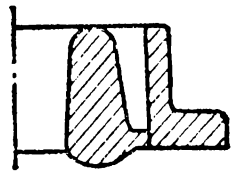
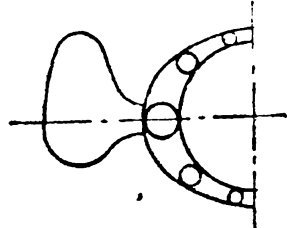
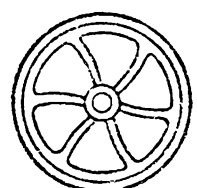
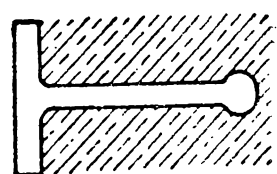
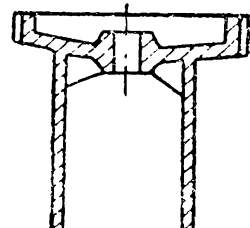
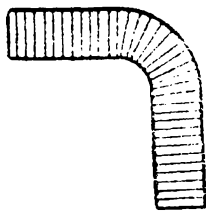
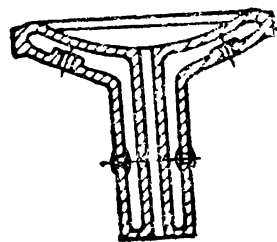
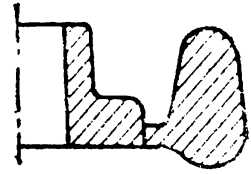
The elements of calculating the housings for toothed reduction gears were outlined above. General recommendations for designing cast components are illustrated in Table 76.

Table 76

Main Rules for Designing Components and Castings

Rules for obtaining the most adequate design	Incorrect design	Correct design
<p>A. Convenience of moulding</p> <p>As far as possible the casting should be arranged in one semi-mould or have one parting plane.</p> <p>The external and internal sides of the casting should be provided with casting draft directed from the parting plane of the mould.</p> <p>The design of the casting should ensure moulding without detachable parts on the pattern and in the boxes and with the minimum number of cores. The observance of this principle can be checked by the following method: lines drawn from the side of the parting of the mould or the core box should not encounter on their path the external and internal contours of the components more than once.</p> <p>Components with complex and closed planes should be provided with an adequate number of holes for the reliable fastening of cores without chaplets (gags).</p> <p>The thickness of the core in a double-walled casting should not be below the sum of the thicknesses of both walls to avoid the scouring of core necks.</p>	     	     



Rules for obtaining the most adequate design	Incorrect design	Correct design
<p><b>B. Obtaining a good casting</b></p> <p>In castings from white cast iron, globular-graphite cast iron and other grades of cast iron distinguished by the intensive formation of shrinkage cavities there should be ensured a gradual decrease in the rate of solidification (the increase in the diameters on inscribed circles) towards the risers.</p> <p>To prevent the formation of cracks curved spokes and discs should be used in flywheels and pulleys.</p> <p>Projections and bosses hindering shrinkage should be avoided especially in cast iron with intensive shrinkage to prevent the formation of cracks.</p> <p>Large upper horizontal surfaces should be replaced by inclined surfaces (especially for castings subjected to enamelling) to avoid the formation of gas pits and accumulation of nonmetallic inclusions.</p> <p>Corner joints of the external and internal surfaces of castings should be rounded off to prevent the formation of cracks, shrinkage cavities and burns. This is especially important for castings subjected to enamelling.</p> <p><b>C. Convenient chipping and cleaning</b></p> <p>Casting should be provided with a sufficient number of holes of appropriate dimensions for the removal of cores and skeletons (the holes may be for production purpose only).</p> <p>The design of castings should allow a supply of metal from the side of the external surfaces to facilitate the trimming of the sprues.</p>	      	      

### **TO THE READER**

*The Foreign Languages Publishing House  
would be glad to have your opinion of the  
translation and the design of the book.*

*Please send all suggestions to 21, Zubov-  
sky Boulevard, Moscow, U.S.S.R.*







